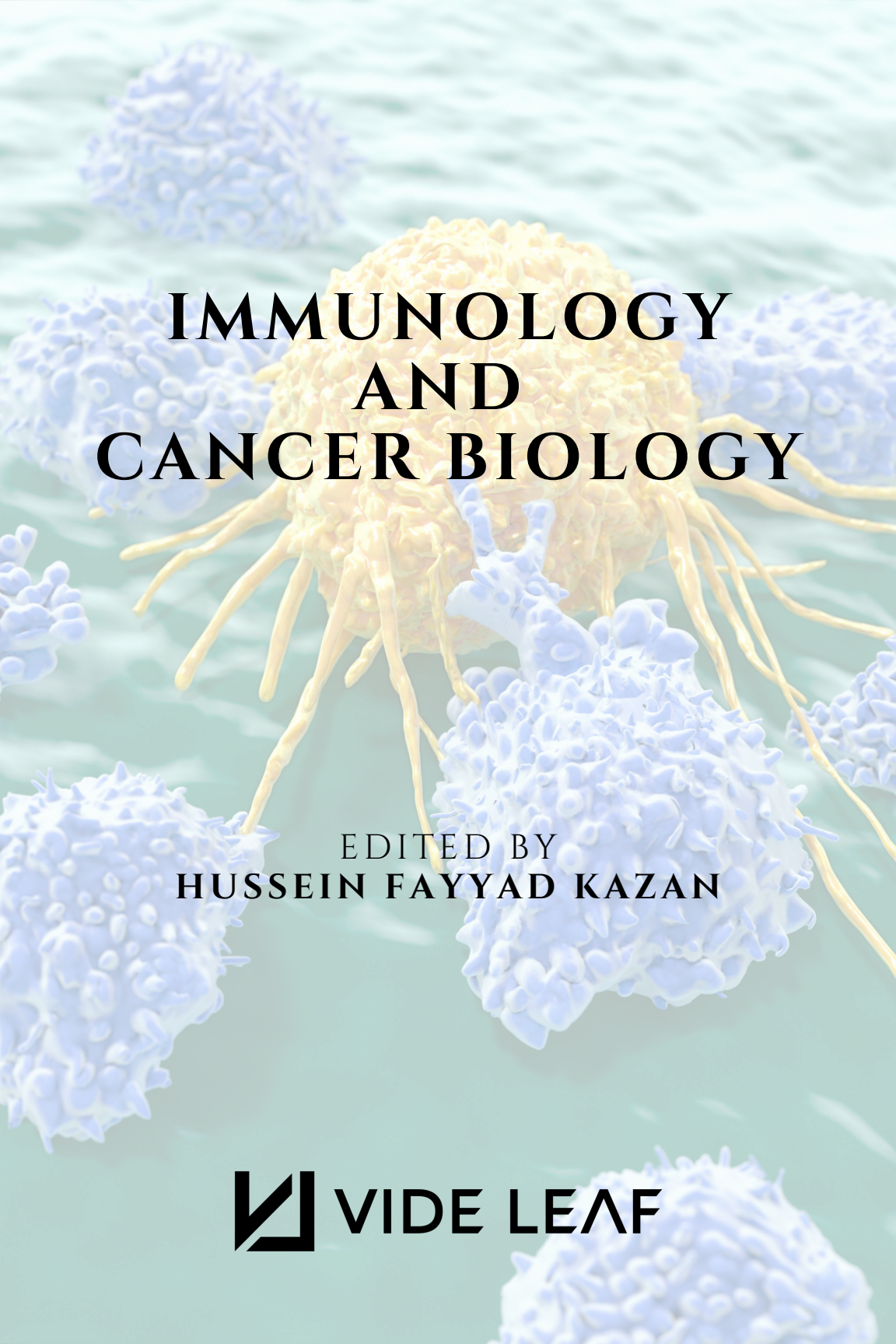

IMMUNOLOGY AND CANCER BIOLOGY

EDITED BY
HUSSEIN FAYYAD KAZAN

VIDE LEAF

Immunology and Cancer Biology

The book Immunology and Cancer Biology cover topics from different fields in Immunology and Cancer.

Editor: Hussein Fayyad Kazan

ISBN: 978-81-953047-2-1

Year Published 2024

Publisher: Vide Leaf

Electronic version of the book can be accessed online at www.videleaf.com

Table of Contents

Circulating miR-150 and miR-342 in Plasma are Novel Potential Biomarkers for Acute Myeloid Leukemia
Hussein Fayyad-Kazan, Nizar Bitar, Mohammad Fayyad-Kazan, Philippe Lewalle, Walid Rachidi, Aksam Merched, Malak Alannan, Makram Merimi, Mehdi Najar, Eva Hamade, Rim ElDirani, Luc Vanhamme, Arsène Burny, Philippe Martiat, Redouane Rouas and Bassam Badran

A microRNA Profile of Human CD8+ Regulatory T cells and Characterization of the Effects of microRNAs on Treg Cell-Associated Genes
Fadi Jebbawi, Hussein Fayyad-Kazan, Makram Merimi, Philippe Lewalle, Mohammad Fayyad-Kazan, Walid Rachidi, Aksam Merched, Malak Alannan, Jean-Christophe Verougstraete, Oberdan Leo, Pedro Romero, Arsene Burny, Bassam Badran, Philippe Martiat and Redouane Rouas

Metabolic Deregulations in Acute Myeloid Leukemia
Mossuz P, Mondet J and Chevalier S

Amino Acid Metabolism in Acute Myeloid Leukemia
Mossuz Pascal, Mondet Julie, Rajesh Christabelle

Link between Base Excision Repair (BER), Reactive Oxygen Species (ROS), and Cancer
Nour Fayyad, Farah Kobaisi, Mohammad Fayyad-Kazan, Ali Nasrallah, Hussein Fayyad-Kazan and Walid Rachidi

Implication of Ultraviolet Irradiation in Photo-carcinogenesis
Farah Kobaisi, Eric Sulpice, Mohammad Fayyad-Kazan, Ali Nasrallah, Xavier Gidrol, Hussein Fayyad-Kazan and Walid Rachidi

Melanoma Cell Adhesion Molecule, CD146: A Major Actor and Target in Physiopathology
Ahmad Joshkon, Hussein Fayyad-Kazan, Bassam Badran, Nathalie Bardin and Marcel Blot-Chabaud

Analysis of the In Vitro and In Vivo Effects of Photodynamic Therapy on Colorectal Cancer by Using New Porphyrin-Xylan-Coated Silica Nanoparticles
Ludovic Bretin, Aline Pinon, Soukaina Bouramtane, Frédérique Bregier, Vincent Sol, Vincent Chaleix, David Yannick Leger and Bertrand Liagre

The cis-enhancers 3'RR and 5'Eμ are Independent Motors of IgH Locus Remodelling
Melissa Ferrad, Nour Ghazzaui, Hussein Issaoui, Ophélie Alyssa Martin, Jeanne Cook-Moreau, François Boyer, Sandrine Le Noir and Yves Denizot

Identification of Acute Myeloid Leukemia Bone Marrow Circulating MicroRNAs
Douâa Moussa Agha, Redouane Rouas, Mehdi Najar, Fatima Bouhtit, Najib Naamane, Hussein Fayyad-Kazan, Dominique Bron, Nathalie Meuleman, Philippe Lewalle and Makram Merimi

Dihydropyrimidinase Protects from DNA Replication Stress Caused by Cytotoxic Metabolites
Jihane Basbous, Antoine Aze, Laurent Chaloin, Rana Lebdy, Dana Hodroj, Cyril Ribeyre, Marion Larroque, Caitlin Shepard, Baek Kim, Alain Pruvost, Jérôme Moreaux, Domenico Maiorano, Marcel Mechali and Angelos Constantinou

HTLV-1 Infection and Adult T Cell Leukemia: Mechanisms of Oncogenesis and Alteration of Immunity
Mariam Shallak, Greta Forlani and Roberto S Accolla

HDAC/HDACi, IgH 3'RR Enhancers, B-Cells and B-Cell Lymphomas
Melissa Ferrad, Nour Ghazzaui, Hussein Issaoui, Jeanne Cook-Moreau, Tiffany Marchiol, Justine Pollet, Sandrine Le Noir and Yves Denizot

BMP9, but Not BMP10, Acts as a Quiescence Factor on Tumor Growth, Vessel Normalization and Metastasis in a Mouse Model of Breast Cancer
Marie Ouarné, Claire Bouvard, Gabriela Boneva, Christine Mallet, Johnny Ribeiro, Agnès Desroches-Castan, Emmanuelle Soleilhac, Emmanuelle Tillet, Olivier Peyruchaud and Sabine Bailly

The BMP910-ALK1-Endoglin Pathway as a Target of Anti-Angiogenic Therapy in Cancer
Al Tabosh T, Al Tarrass M and Bailly S

Overview of NKT Type I Cells and Their Importance in Immunity
Elise Ramia

Immune Response Characteristics in SARS-CoV-2 Infection
Sally Badawi

Wnt Pathway Dysregulation and Immune System: Two Culprits of CRC Initiation & Progression
Zeinab Homayed, Guillaume Belthier and Julie Pannequin

Mechanical Forces in T cell Biology
Farah Mustapha, Kheya Sengupta and Pierre-Henri Puech

Role of Macrophages in Response to Wear Debris from Joint Replacement
Mona EL KADRI

Mitochondrial Dynamics Disturbance: Meeting Different Cancer Traits and Antitumor Immunity
Zahraa FAKIH and Ahmad CHEHAITLY

Role of DNA Repair in Genome Stability, Tumor Prevention, and Main Complications in Case of Repair Failure
Mohammad Rida Hayek and Joanna Timmins

MAGE Genes, The Cancer Tested Antigens Targeted by Immunotherapy
Aline Radi and Martin Kömhoff

Renal Involvement in Localized and Systemic Autoimmunity Diseases with Insights into the Ongoing Therapeutic Approaches
Aline Radi and Sadiq Nasrah

The Invadopodial Protein CRP2 in Breast Cancer: Molecular Pathology and Therapeutic Perspectives
Hady AL SHAMI and Fatima J BERRO

Gain-of-function Mutant P53 and Metabolomics in Lung Cancer: Novel Biomarkers for Early Detection
Hady AL SHAMI and Fatima J BERRO

Inflammasomes: Key Players in the Development of Cancer
Aline Radi and Hussein Fayyad-Kazan

Tumor Associated Macrophages (TAMs) Contribution in Melanoma Progression: Potential Molecular Pathways and Proposed Therapies
Alaa Skeyni, Hady Al Shami and Hussein Fayyad-Kazan

Liquid Biopsy in Non-Small Cell Lung Cancer (NSCLC): State of the Art and the Next Opportunity
Carl KHAWLY

Central and Peripheral Neuroinflammation: A Focus on the Macrophage
Zeina MSHEIK

The Secreted Glycoprotein PAMR1: A New Potential Tumor Suppressor in Cancer
Layla Haymour, Abderrahman Maftah and Sébastien Legardinier

Role of Extracellular Vesicles in Cancer Progression
Bailasan Haidar, Batul Kamar, Farah A Farran, Karen Moghabghab, Rayan A Assaf and Hussein Fayyad-Kazan

An iTRAQ Quantitative Proteomic Study to Reveal How Hypoxia in Tumor Micro-Environment Regulates Metabolic Reprogramming in A549 KRAS-Mutant Non-Small Cell Lung Cancer Cells upon Lysine Deacetylases Inhibitor Treatments to propose Machine-Learning-Based Drug Repositioning
Alfonso Martín-Bernabé, Josep Tarragó-Celada, Valérie Cunin, Sylvie Michelland, Roldán Cortés, Johann Poignant, Cyril Boyault, Walid Rachidi, Sandrine Bourgoin-Voillard, Marta Cascante and Michel Seve

Adoptive T-cell Therapy in Cancer
Else Marit Inderberg

Therapeutic Cancer Vaccines
Else Marit Inderberg

Role of Tumor Cell Metabolism and Immune Cells in Tumor Progression
Zeinab El Rashed, Mariangela Petito, Silvia Ravera and Ulrich Pfeffer

A Practical Introduction to Single-Cell RNA-seq in Immuno-Oncology
Benoît Aliaga, Matthieu Genais and Vera Pancaldi

Dissecting Cellular Phenotypes in the Tumour Microenvironment through Gene Regulatory Networks: Inference, Analysis and Dynamical Modelling
Malvina Marku, Hugo Chenel and Vera Pancaldi

The Dualistic Role of Macrophages in Aortic Valve Calcification
Nervana Issa, Alexandre Candellier, Cédric Boudot, Saïd Kamel and Lucie Hénaut

Skin Cancer Metabolism
Ferial KHALIFE and Hamid-Reza REZVANI

Breast Cancer Stem Cells: A Key for Breast Cancer Treatment
Rania El Majzoub, Jana Doghman, Zeinab Al Dirani, Rawan Issa, Mohammad Fayyad-Kazan, Chourouk Joumaa, Ali Hamade, Farah A. Farran, Berlant Shakra, Samah Al Zein, Mona Al Jamal, Fatima Soufan, Katia Smeha, Jana Zaraket, Jana Kourani, Mariam Hamze, Mohamad El Saheli, Sana Dheini, Fatima Fakih, Zahraa Fakih, Alaa Bishkar, Ritaj Fakih, Amal Al Kadi, Khalid Omama, Afaf El Joubaei, Douaa Khreis, Fatima Dandash, Fatima Berro, Hussein Fayyad-Kazan

Current Breast Cancer Treatment Strategies and Resistance Mechanisms

Rania El Majzoub, Zeinab Al Dirani, Rawan Issa, Samah Al Zein, Mohammad Fayyad-Kazan, Zahra Farroukh, Sana Dheini, Mona Al Jamal, Ali Hamade, Mohamad El Saheli, Leen Fadlallah, Mona Sahmarani, Jana Zaraket, Fatima Shaalan, Chourouk Joumaa, Ali Al Khatib, Belal Osman, Mariam Hamze, Jana Kourani, Farah A. Farran, Berlant Shakra, Katia Smeha, Khalid Omama, Dima Dagher, Aya El Hage Ali, Douaa Khreis, Fatima Dandash, Fatima Berro, Hussein Fayyad-Kazan

Breast Cancer Treatment in the Modern Era: A Focus on Drug Combinations

Rania El Majzoub, Zeinab Al Dirani, Chourouk Joumaa, Rawan Issa, Mohammad Fayyad-Kazan, Dima Dagher, Mariam Hamze, Samah Al Zein, Ali Bannout, Katia Smeha, Jana Zaraket, Aya El Hage Ali, Fatima Shaalan, Belal Osman, Ali Al Khatib, Mohamad El Saheli, Jana Mahmoud-Haidar, Ghinwa Itani, Ghida Temraz, Samer Krayan, Khalid Omama, Somaya Al Hallak, Mona Sahmarani, Dima Obeid, Douaa Khreis, Fatima Dandash, Fatima Berro, Hussein Fayyad-Kazan

Targeting Signaling Pathways for TNBC Treatment

Zeinab El Dor, Berlant Shakra, Zeinab Al Dirani, Zahraa Salhab, Mohammad Fayyad-Kazan, Rawan Issa, Farah A. Farran, Mariam Hamze, Chourouk Joumaa, Mohamad El Saheli, Ghinwa Osman, Samah Al Zein, Ali Bannout, Ritaj Fakih, Katia Smeha, Jana Zaraket, Zahra Farroukh, Leen Fadlallah, Ghida Temraz, Ali Al Khatib, Belal Osman, Ghinwa Itani, Marwa Bazzi, Khalid Omama, Diana El Hosni, Mohammad Shkeir, Malak El Itawi, Malak AlMazbouh, Douaa Khreis, Fatima Dandash, Hussein Fayyad-Kazan

Novel Therapies Based on Synthetic Biology to Cure a Range of Ailments

Fatima Fakih, Ghoson Albahri, Zeinab Al Dirani, Dima Dagher, Rawan Issa, Mohammad Fayyad-Kazan, Aya El Hage Ali, Fatima Shaalan, Mariam Hamze, Zahra Farroukh, Mona Al Jamal, Leen Fadlallah, Marwa Bazzi, Samer Krayan, Khalid Omama, Belal Osman, Mohamad El Saheli, Ali Hamade, Soumaya Al Hallak, Samah Al Zein, Jana Doghman, Ritaj Fakih, Jana Mahmoud-Haidar, Ghinwa Itani, Ghida Temraz, Aisha Al Sousi, Jana Zaraket, Katia Smeha, Douaa Khreis, Fatima Dandash, Hussein Fayyad-Kazan

Book Chapter

Circulating miR-150 and miR-342 in Plasma are Novel Potential Biomarkers for Acute Myeloid Leukemia

Hussein Fayyad-Kazan[1,2]*, Nizar Bitar[2], Mohammad Fayyad-Kazan[2], Philippe Lewalle[1], Walid Rachidi[3], Aksam Merched[4]*, Malak Alannan[4], Makram Merimi[1], Mehdi Najar[1], Eva Hamade[2], Rim ElDirani[2], Luc Vanhamme[5], Arsène Burny[1], Philippe Martiat[1]*, Redouane Rouas[1] and Bassam Badran[2]

[1]Laboratory of Experimental Hematology, Institut Jules Bordet, Université Libre de Bruxelles, Belgium
[2]Laboratory of Cancer Biology and Molecular Immunology, Lebanese University, Faculty of Sciences, Lebanon
[3]SYMMES/CIBEST UMR 5819 UGA-CNRS-CEA, Univ. Grenoble Alpes, Grenoble, France
[4]miRCaDe team, Univ. Bordeaux, INSERM , U1035 (Biotherapy of Genetic, Inflammatory Diseases and Cancer), F-33000 Bordeaux, France.
[5]Laboratory of Molecular Parasitology and Laboratory of Molecular Biology of Ectoparasites, IBMM (Institute for Molecular Biology and Medicine), Université Libre de Bruxelles, Belgium

***Corresponding Authors:** Philippe Martiat, Laboratory of Experimental Hematology, Institut Jules Bordet, Université Libre de Bruxelles, 121, Boulevard de Waterloo, Bruxelles 1000, Belgium

Hussein Fayyad-kazan, Laboratory of Experimental Hematology, Institut Jules Bordet, Université Libre de Bruxelles, 121, Boulevard de Waterloo, Bruxelles 1000, Belgium/[2]Laboratory of Cancer Biology and Molecular Immunology, Lebanese University, Faculty of Sciences, Lebanon

Aksam Merched, [4]miRCaDe team, Univ. Bordeaux, INSERM, BMGIC, U1035, F-33000 Bordeaux, France

Published **November 18, 2020**

This Book Chapter is mainly adapted from an article published by Philippe Martiat, et al. at Journal of Translational Medicine in February 2013. (Fayyad-Kazan, H., Bitar, N., Najar, M. et al. Circulating miR-150 and miR-342 in plasma are novel potential biomarkers for acute myeloid leukemia. J Transl Med 11, 31 (2013). https://doi.org/10.1186/1479-5876-11-31)

How to cite this book chapter: Hussein Fayyad-Kazan, Nizar Bitar, Mohammad Fayyad-Kazan, Philippe Lewalle, Walid Rachidi, Aksam Merched, Malak Alannan, Makram Merimi, Mehdi Najar, Eva Hamade, Rim ElDirani, Luc Vanhamme, Arsène Burny, Philippe Martiat, Redouane Rouas, Bassam Badran. Circulating miR-150 and miR-342 in Plasma are Novel Potential Biomarkers for Acute Myeloid Leukemia. In: Hussein Fayyad Kazan, editor. Immunology and Cancer Biology. Hyderabad, India: Vide Leaf. 2020.

Acknowledgement: This work was supported by grants from the Lebanese University- Research Group IR019, the Lebanese CNRS, the Belgian Fonds National de la Recherche Scientifique (FRSM, Télévie), the MEDIC Foundation, the International Brachet Stiftung, the Lambeau-Marteaux Foundation, les Amis de l'Institut Bordet, the Van Buuren Foundation and the Hoguet Foundation.

Competing Interests: The authors declare that they have no competing interests.

Abstract

Background: MicroRNAs (miRNAs) are small (19-22-nt) single-stranded noncoding RNA molecules whose deregulation of expression can contribute to human disease including the multistep processes of carcinogenesis in human. Circulating miRNAs are emerging biomarkers in many diseases and cancers such as type 2 diabetes, pulmonary disease, colorectal cancer, and gastric cancer among others; however, defining a plasma miRNA signature in acute myeloblastic leukemia (AML) that could serve as a biomarker for diagnosis or in the follow-up has not been done yet.

Methods: TaqMan miRNA microarray was performed to identify deregulated miRNAs in the plasma of AML patients. Quantitative real-time RT-PCR was used to validate the results. Receiver-operator characteristic (ROC) curve analysis was conducted to evaluate the diagnostic accuracy of the highly and significantly identified deregulated miRNA(s) as potential candidate biomarker(s).

Results: The plasma expression level of let-7d, miR-150, miR-339, and miR-342 was down-regulated whilst that of let-7b, and miR-523 was up-regulated in the AML group at diagnosis compared to healthy controls. ROC curve analyses revealed an AUC (the areas under the ROC curve) of 0.835 (95% CI: 0.7119– 0.9581; P<0.0001) and 0.8125 (95% CI: 0.6796–0.9454; P=0.0005) for miR-150, and miR-342 respectively. Combined ROC analyses using these 2 miRNAs revealed an elevated AUC of 0.86 (95% CI: 0.7819–0.94; P<0.0001) indicating the additive effect in the diagnostic value of these 2 miRNAs. QRT-PCR results showed that the expression level of these two miRs in complete remission AML patients resembled that of healthy controls.

Conclusions: Our findings indicated that plasma miR-150 and miR-342 are novel important promising biomarkers in the diagnosis of AML. These novel and promising markers warrant validation in larger prospective studies.

Background

Acute myeloid leukemia (AML) is a clonal disorder caused by malignant transformation of a bone marrow-derived progenitor cell, which demonstrates an enhanced proliferation as well as aberrant differentiation resulting in hematopoietic insufficiency (i.e. granulocytopenia, thrombocytopenia or anaemia)[1,2]. AML is the most common type of acute leukemia occurring in adults, with approximately 11,900 individuals diagnosed annually in the United States only [3]. Adults over age 60 comprise more than two-thirds of this group [2], with a median age of onset of about 65 [3]. The incidence of AML rises significantly with age, with 4 cases per 100,000 people annually in the sixth decade of life, to over 20 cases per 100,000 in the ninth decade of life [4]. An increased incidence of AML is seen in patients with disorders associated with excessive chromatin fragility such as Bloom syndrome, Fanconi anemia, Kostmann syndrome, Wiskott-Aldrich syndrome or ataxia telangiectasia syndrome. Other syndromes, such as Down (trisomy 21), Klinefelter (XXY and variants), and Patau (trisomy 13), have also been associated with a higher incidence of AML [5–8]. In fact, AML patients in remission frequently relapse due to the addition of new mutations [9].

In general, adults with AML show a variety of symptoms including fatigue, bruising or bleeding, fever, and infection, reflecting a state of bone marrow failure [10]. Physical findings other than bleeding and infection may include organomegaly, lymphadenopathy, sternal tenderness, retinal hemorrhages, and infiltration of gingivae, skin, soft tissues, or meninges (more common with monocytic variants M4 or M5) [10]. The diagnosis of AML is often demonstrated by an increased number of myeloblasts in the bone marrow or peripheral blood. According to the WHO criteria, acute leukemia is diagnosed when a 200-cell differential reveals the presence of 20% or more myeloblasts in a marrow aspirate or in blood [11].

MicroRNAs (miRNAs) are small (19-22-nt) single-stranded noncoding RNA molecules that are derived from hairpin-structured precursors [12]. These microRNAs function by directly binding to their potential target site in the 3′ untranslated

region (3′UTRs) of specific target mRNA, leading to the repression of mRNA translation or the degradation of target mRNAs. Small non-coding RNAs were also recently implicated in control of DNA-damage response [13]. Currently, there are 2042 mature human miRNA sequences listed in the miRNA registry (Sanger miRBase release 19; http://www.mirbase.org/). Over recent years, many miRNAs have been investigated in various human cancers [14,15]. The deregulation of expression of microRNAs has been shown to contribute to the multistep processes of carcinogenesis in human by modification either of oncogenic or suppressor gene function [16,17]. Nowadays, microRNA expression patterns are known to characterize the developmental origins of tumors more effectively than mRNA expression signatures and thus can be a useful tool for the diagnosis and prognosis of human cancer [18]. The search for non-invasive tools for the diagnosis and management of cancer that can greatly reduce its worldwide health burden has long been a goal of cancer research [19]. Recently, it has been reported that microRNAs are circulating in serum/plasma [20,21] and tumor-derived microRNAs such as miR-155, miR-21, miR-15b, miR-16 and miR-24 have been detected in the plasma and sera of tumor-bearing patients [22,23]. These circulating microRNAs can be considered as a new class of effective biomarkers where their abundance profile might reflect physiological and/or pathological conditions. Accordingly, several subsequent studies have proven that miRNAs can serve as potential biomarkers for various diseases including cancer [20,24,25].

A previous report [26] had shown that down-regulation of miR-92 is a novel marker for acute leukemia patients (AML, ALL). In our study, we investigated the profile of circulating microRNAs in the plasma of acute myeloid leukemia patients compared with healthy individuals. Our results have revealed the presence of two microRNAs (miR-150, miR-342) whose levels were very significantly downregulated in the plasma of AML patients at diagnosis compared to healthy controls. The combination of their decrease is of utmost significance using ROC curve analysis. Investigation of the expression level of these two microRNAs in complete remission (CR) AML patients by qRT-PCR revealed a similar expression level as that of healthy controls. Thus, besides

miR-92, these two microRNAs are novel candidate biomarkers of acute myeloid leukemia and potential predictors of relapse.

Methods

Patients

Patients used in this study had a newly diagnosed AML in addition to being in complete remission as determined by blood test. A total of 20 patients at the time of diagnosis in addition to other 20 patients in complete remission provided blood samples. Healthy subjects were collected as negative controls. None of these controls had previously been diagnosed with any type of malignancy or other benign disease. Informed consent, approved by the Clinical Research Ethics Committee of Jules Bordet Institute, was obtained from each participant. Details of clinical data are provided in Table 1.

Table 1: Summary of clinical details of AML patients and healthy controls used for analysis.

Sex	
Men	13
Women	7
Total	20
Control	20
French-American—British classification	
AML M0	3
AML M1	3
AML M2	2
AML M3	2
AML M4	2
AML M4E0	2
AML M5	2
AML M6	2
AML M7	2

The classification was done according to the French-American-British system[27].
M0= Undifferentiated acute myeloblastic leukemia; M1= Acute myeloblastic leukemia with minimal maturation; M2= Acute myeloblastic leukemia with maturation; M3=Acute promyelocytic leukemia (APL); M4= Acute myelomonocytic leukemia; M4E0=Acute myelomonocytic leukemia with eosinophilia; M5= Acute monocytic leukemia; M6= Acute erythroid leukemia; M7= Acute megakaryoblastic leukemia.

Plasma Sampling and RNA Extraction

At presentation, blood samples for miRNA detection were collected in EDTA-K2 tubes and processed within 1 hour of collection. Blood samples were centrifuged at 1,200 g for 10 min at 4°C to spin down the blood cells, and the supernatant was transferred into microcentrifuge tubes, followed by a second centrifugation at 12,000 g for 10 min at 4°C. The supernatant was transferred to RNase/DNase-free tubes and stored at −80°C. Total RNA was isolated from the plasma using a mirVana PARIS isolation kit (Ambion, Austin, Texas) according to the manufacturer's instructions for plasma samples. Briefly, 400 µL of human plasma was used to extract total RNA. Each sample was eluted in 100 µL of RNAse-free water and was concentrated to a final volume of 20 µL by using Eppendorf Concentrator Plus 5301 (Eppendorf, Germany).

RNA sample concentration was quantified by NanoDrop ND-1000 (Nanodrop, USA). All RNA samples were analyzed for miR-16 expression, a stable endogenous reference miRNA, to assess an approximate yield of RNA extraction and to ensure that comparable amounts of starting material were used in each reverse transcription reaction [22,28–31].

MiRNA Expression Profile

In our study, a three-step procedure was performed to profile the miRNAs in the plasma samples. First, for cDNA synthesis from the miRNAs, 30 ng of total RNA was subjected to RT (reverse transcription) using a TaqMan® microRNA Reverse Transcription Kit (#4366596; Applied Biosystems) and Megaplex RT primers (Human Pool A, #4399966; Applied Biosystems) following the manufacturer's protocol, allowing simultaneous reverse transcription of 380 mature human miRNAs to generate a miRNA cDNA library corresponding to each plasma sample. RT was performed on a Mastercycler Epgradient thermocycler (Eppendorf) with the following cycling conditions: 40 cycles at 16°C for 2 min, 42°C for 1 min and 50°C for 1 s followed by a final step of 80°C for 5 min to inactivate reverse transcriptase. Thereafter, to generate enough miRNA

cDNA template for the following real-time PCR, the cDNA libraries were pre-amplified using Megaplex PreAmp primer (Humam Pool A, #4399233; Applied Biosystems) and PreAmp Master Mix (#4384266; AppliedBiosystems) following the manufacturer's instructions. The PreAmp primer pool used here consisted of forward primers specific for each of the 380 human miRNAs and a universal reverse primer. The pre-amplification cycling conditions were as follows: 95°C for 10 min, 55°C for 2 min, 72°C for 2 min followed by 12 cycles at 95°C for 30 s and 60°C for 4 min; the samples were then held at 99.9°C for 10 min. After the preamplification step, the products were diluted with RNase-free water, combined with TaqMan gene expression Master Mix and then loaded into TaqMan Human MicroRNA Array A (#4398965; Applied Biosystems), which is a 384-well formatted plate and real-time PCR-based microfluidic card with embedded TaqMan primers and probes in each well for the 380 different mature human miRNAs; MiR-16 transcript was used as a normalization signal.

Real-time PCR was performed on an ABI PRISM 7900HT sequence detection system (Applied Biosystems) with the following cycling conditions: 50°C for 2 min, 94.5°C for 10 min followed by 40 cycles at 95°C for 30 s and 59.7°C for 1 min. The Ct (cycle threshold) was automatically given by SDS 2.3 software (Applied Biosystems) and is defined as the fractional cycle number at which the fluorescence passes the fixed threshold of 0.2. MiR-16 embedded in the TaqMan Human MicroRNA Arrays was used as an endogenous control. The relative expression levels of miRNAs were calculated using the comparative ΔΔCt method as described previously [32,33]. The fold changes in miRNAs were calculated by the equation $2^{-\Delta\Delta Ct}$.

Taqman miRNA Assay for Individual miRNAs

Gene-specific reverse transcription was performed for each miR using 10 ng of purified total RNA, 100 mM dNTPs, 50 U MultiScribe reverse transcriptase, 20 U RNase inhibitor, and 50 nM of gene-specific RT primer samples using the TaqMan MicroRNA Reverse Transcription kit (Applied Biosystems, Gent, Belgium). 15 µl reactions were incubated for 30 min at

16°C, 30 min at 42°C, and 5 min at 85°C to inactivate the reverse transcriptase. Real time RT-PCR reactions (5 µl of RT product, 10 µl TaqMan 2x Universal PCR master Mix, (Applied Biosystems, Gent, Belgium), and 1 µl TaqMan MicroRNA Assay Mix containing PCR primers and TaqMan probes) were carried out on ABI Prism 7900HT Sequence Detection System (Applied Biosystems, Gent, Belgium) at 95°C for 10 min followed by 40 cycles at 95°C for 15 s and 60°C for 1 min. The qRT-PCR reactions were performed in triplicate, and the signal was collected at the end of every cycle. Due to a lack of generally accepted standards, all qRT-PCR data on single miRNA expression were analyzed as unadjusted Ct values and standardized to miR-16. To validate miR-16 as a stable internal reference, its stability during extraction was compared to that of synthetic cel-miR-39, a miRNA of C. elegans that is not present in humans. Twenty-five fmol of synthetic cel-miR-39 were spiked in after adding the Denaturing Solution (provided in the mirVana PARIS isolation kit) to the human plasma samples to avoid degradation by endogenous RNases, and the RNA was extracted. We measured the expression of cel-miR-39, miR-16 and the validated differentially expressed microRNAs in AML patients (diagnosis and complete remission) and healthy controls. Afterwards, the expression of the validated microRNAs in AML patients and healthy controls was compared with miR-16 and cel-miR-39 normalizers, respectively.

Statistical Analysis

Data characterized by a normal distribution, determined using Kolmogorov-Smirnov and Shapiro-Wilk normality tests, were expressed as the mean and standard deviation. Widely presented using the $2^{-\Delta\Delta Ct}$ method, the relative gene expression involves the gene of interest data (Ct gene of interest) relative to an internal control gene (Ct internal control gene), named delta Ct. The calculated delta Ct ± SD for the patients was compared with the delta Ct ± SD (SD stands for the standard deviation of the average delta Ct of the group) for the healthy control group and tested for statistical significance. Sensitivity, specificity, and the area under the curve (AUC) for plasma microRNAs were determined using Receiver Operator Characteristic (ROC) analysis. Data were analyzed using Student's t test. P-values

<0.05 (*), <0.01 (**), and <0.001(***) obtained using t-test were considered statistically significant.

Results

Expression Profiles of miRNAs in the Plasma of AML Patients

RNA from twenty independent human AML patients and healthy controls was first studied using the TLDA technique. We could identify several miRs that were statistically differentially expressed between AML and healthy controls (Table 2). These microRNAs were further studied to validate their differential expression by quantitative Real Time PCR (qRT-PCR) and to investigate whether anyone could be used as a candidate biomarker of AML at the diagnosis.

Table 2: Circulating plasma microRNA expression levels in AML patients compared to healthy controls.

MicroRNA	AML/Healthy control ratio	P value
Hsa-let-7b	6.5	0.021
Hsa-let-7d	0.2	0.026
Hsa-miR-150	0.045	0.0026
Hsa-miR-335	4.5	0.041
Hsa-miR-339	0.4	0.031
Hsa-miR-342	0.07	0.0048
Hsa-miR-374	3.5	0.045
Hsa-miR-523	5	0.022

Validation of Candidate miRNAs

Differential miR expressions were validated by real-time PCR in all samples. The change in candidate miRNAs for the AML patients versus the healthy controls is shown in Figure 1. These data have been normalized by the expression level of miR-16, a widely used endogenous reference miRNA that was also confirmed to be unchanged in our experiments (TLDA cards). In addition, as cel-miR-39, miR-16 is stable (Figure 2). Moreover, we compared the difference in let-7b, let-7d, miR-150, miR-339, miR-342, and miR-523 expression between AML patients and healthy controls and obtained the same differences in their expression regardless of whether cel-miR-39 or miR-16 was

used as the normalizer (Figure 3), which further supports that miR-16 is a stable reference in this study.

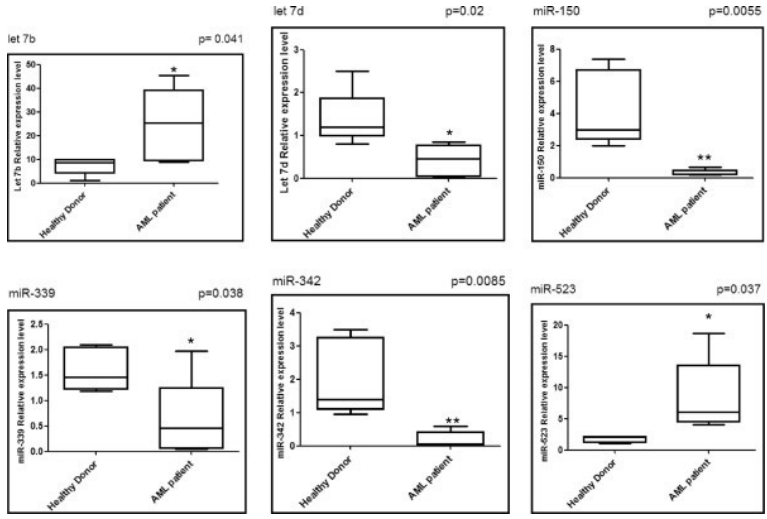

Figure 1: Relative expression levels of the six differentially expressed miRs**.** Six miRNAs are significantly differentially expressed in the plasma of AML patients when compared to healthy controls (n=20). Data obtained by quantitative RT-PCR amplification of miRs are plotted. p-values for each miRNA are shown. Boxes represent SE. Error bars represent SD; pooled data from five independent experiments. *p<0.05, **p<0.01 AML patient versus Healthy controls (Student's t-test).

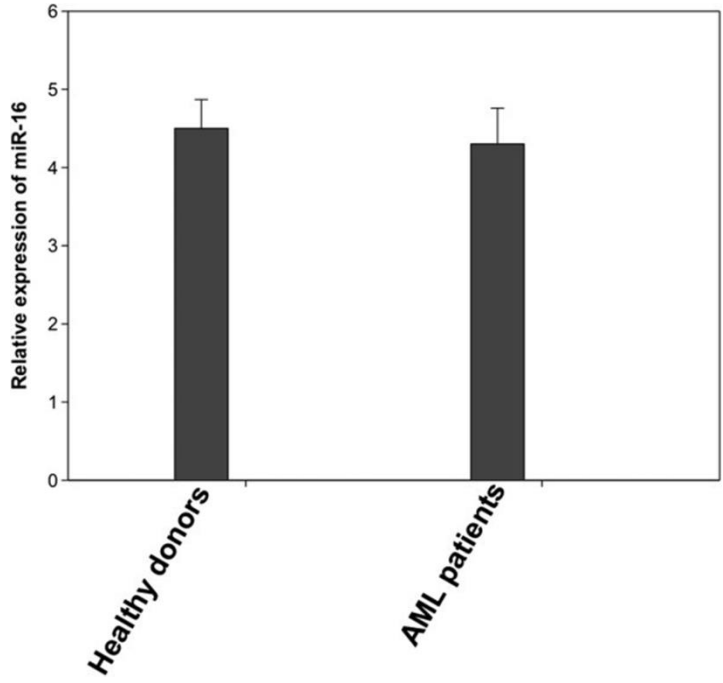

Figure 2: miR-16 expression level is stable in both healthy controls and AML patients. MiR-16 expression levels were assessed by qRT-PCR and normalized by cel-miR-39. Shown are the relative levels (mean ± S.D.) of five independent experiments performed on all participants, each done in triplicate.

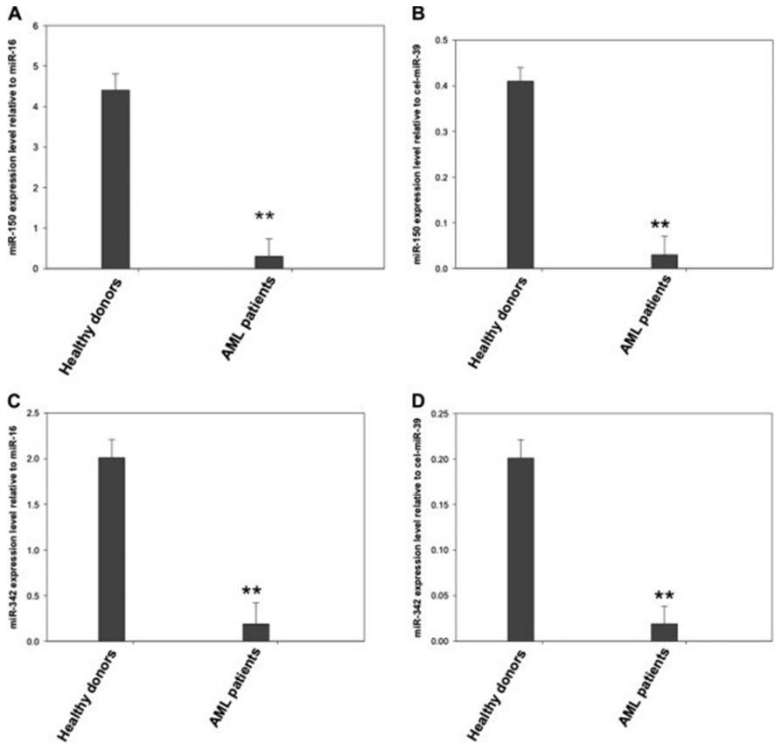

Figure 3: Relative plasma miR-150 and miR-342 expression levels normalized by cel-miR-39 and hsa-miR-16. MiR-150 **(A, B)** and miR-342 **(C, D)** expression levels were assessed by qRT-PCR and normalized by cel-miR-39 and hsa-miR-16 respectively in healthy controls and Acute Myeloid Leukemia patients. Shown are the relative levels (mean ± S.D.) of five independent experiments performed on all participants, each done in triplicate. Statistical significance was determined by Student's t test and is denoted as follows: ** $p < 0.01$ *versus* healthy donors.

The plasma expression level of let-7d, miR-150, miR-339, and miR-342 was down-regulated whilst that of let-7b, and miR-523 was up-regulated in the AML group compared to healthy controls (Figure 1). To confirm that the assay is reproducible, we also analyzed expression levels in the plasma (second sampling) collected 1 h after the first sampling of the plasma of three AML patients. No significant difference in the levels of the above mentioned microRNAs was found between the first sampling and the second sampling, which suggests that the assay is reproducible (Figure 4).

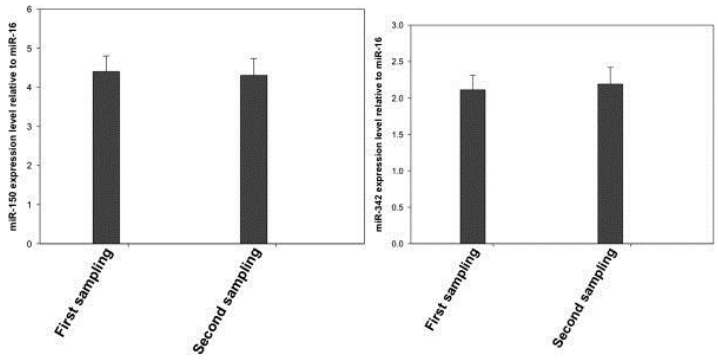

Figure 4: miR-150 and miR-342 expression levels do not vary between the first and second sampling. Plasma miR-150 and miR-342 expression levels in the first sampling and second sampling were assessed by qRT-PCR. The expression level of these two microRNAs was normalized to miR-16. Shown are the relative levels (mean ± S.D.) of five independent experiments performed on all participants, each done in triplicate.

Diagnostic Accuracy of Plasma miR-150 and miR-342 in AML

The ROC curve analysis was used to analyze the diagnostic accuracy of plasma miR-150 and miR-342. ROC curve analyses revealed that both plasma miR-150 and miR-342 could serve as valuable biomarkers for differentiating AML from controls with an AUC (the areas under the ROC curve) of 0.835 (95% CI: 0.7119– 0.9581; P<0.0001) and 0.8125 (95% CI: 0.6796–0.9454; P=0.0005), respectively (Figures 5A and5B).

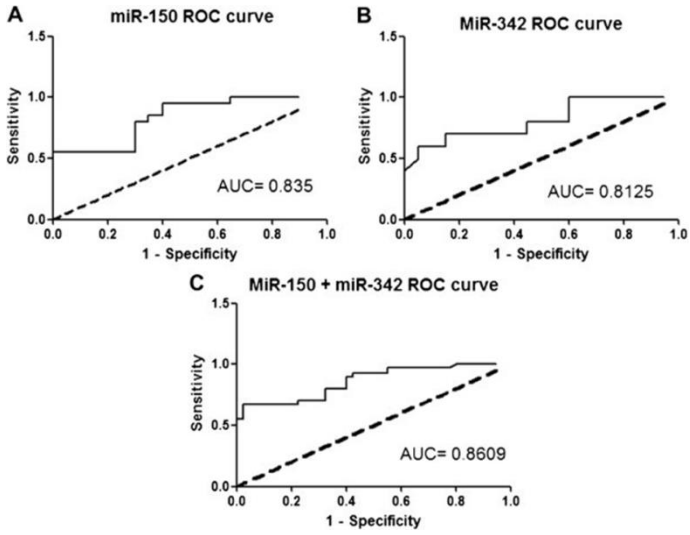

Figure 5: Receiver operating characteristics (ROC) curve analysis using plasma miR-150 and miR-342 for discriminating AML patients. Plasma miR-150 yielded an AUC (the areas under the ROC curve) of 0.835 (95% CI: 0.7119– 0.9581; P<0.0001) with 80% sensitivity and 70% specificity in discriminating AML **(A)**, and plasma miR-342 yielded AUC of 0.8125 (95% CI: 0.6796–0.9454; P=0.0005) with 70% sensitivity and 85% specificity **(B)** in discriminating AML. Elevated ROC analysis revealed an elevated AUC of 0.860 (95% CI: 0.7819–0.94; P<0.0001) with 73% sensitivity and 78% specificity in discriminating AML **(C)**.

At the cut-off value less than 2.79 for miR-150, the sensitivity and the specificity were 80% and 70%, respectively. At the cut-off value less than 1.146 for miR-342, the sensitivity and the specificity were 70% and 85%, respectively. Combination ROC analyses resulted in an increased AUC of 0.86 (95% CI: 0.7819–0.94; P<0.0001) with 73.0% sensitivity and 78% specificity indicating the additive effect in the diagnostic value of these 2 miRNAs (Figure 5C).

MiR-150 and miR-342 in CR AML Patients showed an Expression Level Similar to that of Healthy Controls

ROC curve analyses revealed that plasma miR-150 and miR-342 could serve as valuable biomarkers for differentiating AML from controls. Thus, in order to confirm that, we assessed the

expression level of these two microRNAs in CR AML patients, compared to AML patients at diagnosis and healthy controls, using qRT-PCR. Results showed that the plasma expression level of miR-150 and miR-342 was similar to that of healthy controls while it was still upregulated compared to AML patients at diagnosis (Figure 6) thus making these two microRNAs as additional novel biomarkers for AML.

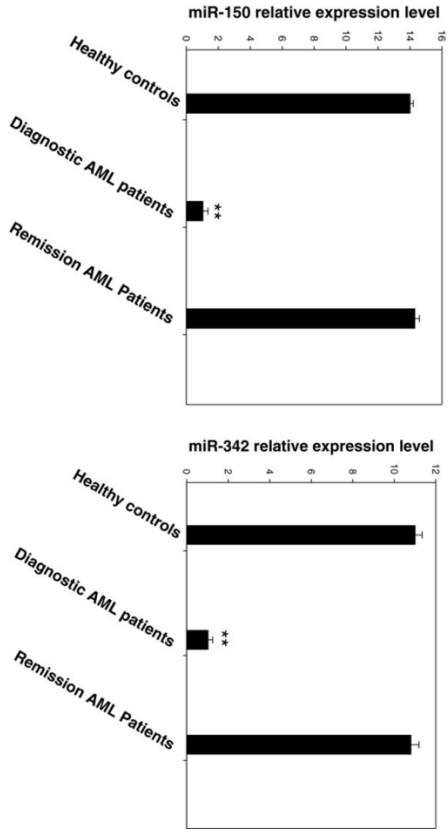

Figure 6: miR-150 and miR-342 expression levels in Remission AML patients resembles that of healthy controls. Plasma miR-150 and miR-342 expression levels in remission AML patients and healthy controls were assessed by qRT-PCR. The expression level of these two microRNAs was normalized to miR-16. Shown are the relative levels (mean ± S.D.) of five independent experiments performed on all controls, each done in triplicate. Statistical significance was determined by Student's t test and is denoted as follows: ** $p < 0.01$ *versus* healthy donors.

Discussion

In this study, we identified several microRNAs in the plasma of AML patients at diagnosis that were differentially expressed compared to healthy controls. Among these miRs, two were upregulated (Let-7b, miR-523) and four were downregulated (let-7d, miR-150, miR-339, and miR-342). Importantly, the expression level of these microRNAs didn't show any significant difference between the male and female donors implicated in this study as revealed by student's t- test statistical analysis. The latter was performed based on the Kolmogorov-Smirnov and Shapiro-Wilk normality analysis tests. Among these microRNAs, miR-150, and miR-342 were very significantly downregulated in the plasma of AML patients as confirmed using ROC curve analysis (AUC of 0.835 and 0.8125) that revealed that miR-150, and miR-342 were promising candidate biomarkers for AML at diagnosis (Figure 7). These data suggest that microRNA expression signature in plasma can serve as a valuable diagnostic and potential prognostic marker for human AML. In that respect, the rebound in CR AML patients of miR-150 and miR-342 at the healthy controls' levels is of particular significance in the perspective of their use as diagnostic and prognostic factors.

Recent studies have revealed that miRNAs are potential diagnostic biomarkers and prognostic factors in cancers [34,35]. Mitchell et al.[23] were the first to identify the presence of circulating tumor-associated miRNAs in plasma and to show that circulating microRNAs may have an important value for cancer diagnosis. Another group [24] also determined that circulating miRNA profiles in patients with lung cancer, colorectal cancer (CRC), and diabetes had a prognostic significance. Although the clinical significance of these observations has not been elucidated in detail, those findings demonstrated that circulating miRNAs could be non-invasive diagnostic or prognostic markers for cancer and in this case for AML. A recent study [35] showed that miR-150 was downregulated in sepsis, both in granulocytes and monocytes and inversely correlated with the severity of the disease. Interestingly, plasma levels of tumor necrosis factor alpha, interleukin-10, and interleukin-18, which all have a

complementary sequence to miR-150, were negatively correlated with the plasma levels of miR-150. This could impact on the immune system response to leukemia. On the other hand, an important report [36] related to miR-342 demonstrated the importance of its decreased plasma level in breast cancer, particularly in resistance to certain agents.

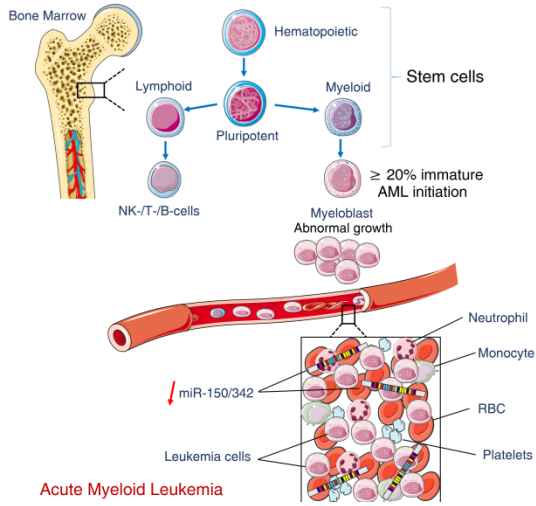

Figure 7: AML is a clonal disorder occurring in hematopoietic stem cells specifically the myeloblasts. Myeloblasts are immature precursor cells that are capable of differentiating into healthy monocytes or granulocytes. However in AML, these cells do not differentiate, but grow and multiply uncontrollably resulting in their accumulation in the bone marrow and peripheral blood (≥20%). Accordingly, the plasma of AML patients will have circulating leukemia cells and most importantly, a decreased expression in two novel potential biomarkers: miR-150 and miR-342, whose combination have a very important diagnostic value that enables the identification of AML with high sensitivity and specificity.

From a technical point of view, normalization is a key step for the accurate quantification of RNA levels with qRT-PCR. In our study, miR-16 was used as an internal control for plasma miRNA quantification as is the case of other studies carried out on different tumors, including CRC [25] breast cancer [37] ovarian cancer [38] where miR-16 was present in plasma/serum at similar levels across normal controls and patients. In addition to the normalization of qRT-PCR data, appropriate control is

also a key issue for diagnostic studies. It is therefore crucial to ensure that the control group is free of any disease, even benign, which is the case in this study. Larger sample size may also be helpful to eliminate potential sampling error.

Exosomes are small (50–90 nm) membrane vesicles of endocytic origin that are released into the extracellular environment on fusion of multivesicular bodies (MVB) with the plasma membrane [39]. Many cells including reticulocytes [40], dendritic cells [41], B cells [42], T cells [43], mast cells [44], epithelial cells [45] and tumor cells [46] have the capacity to release exosomes. Exosomes' content, notably microRNAs known to exist in a form that is resistant to plasmatic RNase activity [23], can be delivered to another cell and function in a new location [47]. These studies suggest that microRNAs are packaged inside exosomes that are secreted from cells. Thus, it might be possible that cancer cells specifically take in the exosome that contains miR-150 and miR-342 and as a result, miR-150 and miR-342 decrease in the plasma.

In the study quoted above [35], the authors determined that the level of miR-150 was independent from the number of white blood cells (WBC), but decreased both in these normal WBCs and in the plasma. However, the mechanism was not elucidated. Thus, an alternative explanation could be that leukemic process creates a decrease in the normal WBC compartment and consequently in the plasma. This is of course purely speculative, and further experiments should address the mechanisms involved.

In summary, we have shown that the expression level of miR-150 and miR-342 in plasma is associated with diagnosis of AML in human. Present knowledge does not involve circulating miR-150 and miR-342 as references in other human cancers [48,49].

Conclusions

In our study, we identified 8 miRNAs differentially expressed between plasma of AML patients and healthy controls by TLDA. Among those eight microRNAs, seven were confimed by qRT-

PCR; let-7b and miR-523 were upregulated whilst others were downregulated including the two highly significant microRNAs, miR-150, and miR-342. Combination of these miRs has diagnostic value enabling identification of AML with the sensitivity of 73%, specificity 78% and AUC = 0.86. The diagnostic value of these two microRNAs was confirmed where the expression level of these two microRNAs in AML patients at remission resembled that of healthy controls. Thus, we believe, that circulating miR-150 and −342 in plamsa are novel biomarkers in AML.

References

1. Estey E, Dohner H. Acute myeloid leukaemia. Lancet. 2006; 368: 1894-1907.
2. Lowenberg B, Downing JR, Burnett A. Acute myeloid leukemia. N Engl J Med. 1999; 341: 1051-1062.
3. Stone RM, O'Donnell MR, Sekeres MA. Acute myeloid leukemia. Hematology. Am. Soc. Hematol. Educ. Program. 2004; 98-117.
4. Craig CM, Schiller GJ. Acute myeloid leukemia in the elderly: conventional and novel treatment approaches. Blood Rev. 2008; 22: 221-234.
5. Pedersen-Bjergaard J, Christiansen DH, Andersen MK, Skovby F. Causality of myelodysplasia and acute myeloid leukemia and their genetic abnormalities. Leukemia. 2002; 16: 2177-2184.
6. Dong F, Brynes RK, Tidow N, Welte K, Lowenberg B, et al. Mutations in the gene for the granulocyte colony-stimulating-factor receptor in patients with acute myeloid leukemia preceded by severe congenital neutropenia. N Engl J Med. 1995; 333: 487-493.
7. West RR, Stafford DA, White AD, Bowen DT, Padua RA. Cytogenetic abnormalities in the myelodysplastic syndromes and occupational or environmental exposure. Blood. 2000; 95: 2093-2097.
8. Crane MM, Strom SS, Halabi S, Berman EL, Fueger JJ, et al. Correlation between selected environmental exposures and karyotype in acute myelocytic leukemia. Cancer Epidemiol Biomarkers Prev. 1996; 5: 639-644.

9. Ding L, Ley TJ, Larson DE, Miller CA, Koboldt DC, et al. Clonal evolution in relapsed acute myeloid leukaemia revealed by whole-genome sequencing. Nature. 2012; 481: 506-510.
10. Jabbour EJ, Estey E, Kantarjian HM. Adult acute myeloid leukemia. Mayo Clin Proc. 2006; 81: 247-260.
11. Vardiman JW, Harris NL, Brunning RD. The World Health Organization (WHO) classification of the myeloid neoplasms. Blood. 2002; 100: 2292-2302.
12. Bartel DP. MicroRNAs: genomics, biogenesis, mechanism, and function. Cell. 2004; 116: 281-297.
13. Francia S, Michelini F, Saxena A, Tang D, De HM, et al. Site-specific DICER and DROSHA RNA products control the DNA-damage response. Nature. 2012; 488: 231-235.
14. Croce CM. Causes and consequences of microRNA dysregulation in cancer. Nat Rev Genet. 2009; 10: 704-714.
15. Lu J, Getz G, Miska EA, Alvarez-Saavedra E, Lamb J, et al. MicroRNA expression profiles classify human cancers. Nature. 2005; 435: 834-838.
16. Esquela-Kerscher A, Slack FJ. Oncomirs - microRNAs with a role in cancer. Nat Rev Cancer. 2006; 6: 259-269.
17. Osada H, Takahashi T. MicroRNAs in biological processes and carcinogenesis. Carcinogenesis. 2007; 28: 2-12.
18. Lujambio A, Lowe SW. The microcosmos of cancer. Nature. 2012; 482: 347-355.
19. Etzioni R, Urban N, Ramsey S, McIntosh M, Schwartz S, et al. The case for early detection. Nat Rev Cancer. 2003; 3: 243-252.
20. Chim SS, Shing TK, Hung EC, Leung TY, Lau TK, et al. Detection and characterization of placental microRNAs in maternal plasma. Clin Chem. 2008; 54: 482-490.
21. Gilad S, Meiri E, Yogev Y, Benjamin S, Lebanony D, et al. Serum microRNAs are promising novel biomarkers. PLoS One. 2008; 3: e3148-
22. Lawrie CH, Gal S, Dunlop HM, Pushkaran B, Liggins AP, et al. Detection of elevated levels of tumour-associated microRNAs in serum of patients with diffuse large B-cell lymphoma. Br J Haematol. 2008; 141: 672-675.
23. Mitchell PS, Parkin RK, Kroh EM, Fritz BR, Wyman SK, et al. Circulating microRNAs as stable blood-based markers for

cancer detection. Proc Natl Acad Sci USA. 2008; 105: 10513-10518.
24. Chen X, Ba Y, Ma L, Cai X, Yin Y, et al. Characterization of microRNAs in serum: a novel class of biomarkers for diagnosis of cancer and other diseases. Cell Res. 2008; 18: 997-1006.
25. Ng EK, Chong WW, Jin H, Lam EK, Shin VY, et al. Differential expression of microRNAs in plasma of patients with colorectal cancer: a potential marker for colorectal cancer screening. Gut. 2009; 58: 1375-1381.
26. Tanaka M, Oikawa K, Takanashi M, Kudo M, Ohyashiki J, et al. Down-regulation of miR-92 in human plasma is a novel marker for acute leukemia patients. PLoS One. 2009; 4: e5532.
27. Bennett JM, Catovsky D, Daniel MT, Flandrin G, Galton DA, et al. Proposed revised criteria for the classification of acute myeloid leukemia. A report of the French-American-British Cooperative Group. Ann Intern Med. 1985; 103: 620-625.
28. Wong TS, Liu XB, Wong BY, Ng RW, Yuen AP, et al. Mature miR-184 as Potential Oncogenic microRNA of Squamous Cell Carcinoma of Tongue. Clin Cancer Res. 2008; 14: 2588-2592.
29. Huang Z, Huang D, Ni S, Peng Z, Sheng W, et al. Plasma microRNAs are promising novel biomarkers for early detection of colorectal cancer. Int J Cancer. 2010; 127: 118-126.
30. Liu CJ, Kao SY, Tu HF, Tsai MM, Chang KW, et al. Increase of microRNA miR-31 level in plasma could be a potential marker of oral cancer. Oral Dis. 2010; 16: 360-364.
31. Yamamoto Y, Kosaka N, Tanaka M, Koizumi F, Kanai Y, et al. MicroRNA-500 as a potential diagnostic marker for hepatocellular carcinoma. Biomarkers. 2009; 14: 529-538.
32. Schmittgen TD, Livak KJ. Analyzing real-time PCR data by the comparative C(T) method. Nat Protoc. 2008; 3: 1101-1108.
33. Livak KJ, Schmittgen TD. Analysis of relative gene expression data using real-time quantitative PCR and the 2(−Delta Delta C(T)) Method. Methods. 2001; 25: 402-408.

34. Schetter AJ, Leung SY, Sohn JJ, Zanetti KA, Bowman ED, et al. MicroRNA expression profiles associated with prognosis and therapeutic outcome in colon adenocarcinoma. JAMA. 2008; 299: 425-436.
35. Vasilescu C, Rossi S, Shimizu M, Tudor S, Veronese A, et al. MicroRNA fingerprints identify miR-150 as a plasma prognostic marker in patients with sepsis. PLoS One. 2009; 4: e7405.
36. Cittelly DM, Das PM, Spoelstra NS, Edgerton SM, Richer JK, et al. Downregulation of miR-342 is associated with tamoxifen resistant breast tumors. Mol Cancer. 2010; 9: 317.
37. Zhu W, Qin W, Atasoy U, Sauter ER. Circulating microRNAs in breast cancer and healthy subjects. BMC.Res.Notes. 2009; 2: 89.
38. Resnick KE, Alder H, Hagan JP, Richardson DL, Croce CM, et al. The detection of differentially expressed microRNAs from the serum of ovarian cancer patients using a novel real-time PCR platform. Gynecol Oncol. 2009; 112: 55-59.
39. Van NG, Porto-Carreiro I, Simoes S, Raposo G. Exosomes: a common pathway for a specialized function. J Biochem. 2006; 140: 13-21.
40. Pan BT, Johnstone RM. Fate of the transferrin receptor during maturation of sheep reticulocytes in vitro: selective externalization of the receptor. Cell. 1983; 33: 967-978.
41. Thery C, Regnault A, Garin J, Wolfers J, Zitvogel L, et al. Molecular characterization of dendritic cell-derived exosomes. Selective accumulation of the heat shock protein hsc73. J Cell Biol. 1999; 147: 599-610.
42. Raposo G, Nijman HW, Stoorvogel W, Liejendekker R, Harding CV, et al. B lymphocytes secrete antigen-presenting vesicles. J Exp Med. 1996; 183: 1161-1172.
43. Blanchard N, Lankar D, Faure F, Regnault A, Dumont C, Raposo G, Hivroz C: TCR activation of human T cells induces the production of exosomes bearing the TCR/CD3/zeta complex. J Immunol. 2002, 168: 3235-3241.
44. Raposo G, Tenza D, Mecheri S, Peronet R, Bonnerot C, et al. Accumulation of major histocompatibility complex class II molecules in mast cell secretory granules and their release upon degranulation. Mol Biol Cell. 1997; 8: 2631-2645.

45. Van NG, Raposo G, Candalh C, Boussac M, Hershberg R, et al. Intestinal epithelial cells secrete exosome-like vesicles. Gastroenterology. 2001; 121: 337-349.
46. Mears R, Craven RA, Hanrahan S, Totty N, Upton C, et al. Proteomic analysis of melanoma-derived exosomes by two-dimensional polyacrylamide gel electrophoresis and mass spectrometry. Proteomics. 2004; 4: 4019-4031.
47. Valadi H, Ekstrom K, Bossios A, Sjostrand M, Lee JJ, et al. Exosome-mediated transfer of mRNAs and microRNAs is a novel mechanism of genetic exchange between cells. Nat Cell Biol. 2007; 9: 654-659.
48. Qu H, Xu W, Huang Y, Yang S; Circulating miRNAs: promising biomarkers of human cancer. Asian Pac J Cancer Prev. 2011; 12: 1117-1125.
49. Reid G, Kirschner MB, Van ZN. Circulating microRNAs: Association with disease and potential use as biomarkers. Crit Rev Oncol Hematol. 2011; 80: 193-208.

Book Chapter

A microRNA Profile of Human CD^{8+} Regulatory T cells and Characterization of the Effects of microRNAs on Treg Cell-Associated Genes

Fadi Jebbawi[1], Hussein Fayyad-Kazan[1,2]*, Makram Merimi[1], Philippe Lewalle[1], Mohammad Fayyad-Kazan[2], Walid Rachidi[3], Aksam Merched[4]*, Malak Alannan[4], Jean-Christophe Verougstraete[5], Oberdan Leo[1], Pedro Romero[6], Arsene Burny[1], Bassam Badran[2], Philippe Martiat[1] and Redouane Rouas[1]*

[1]Experimental Hematology, Institut Jules Bordet, Université Libre de Bruxelles, Belgium
[2]Laboratory of Cancer Biology and Molecular Immunology, Faculty of Sciences, Lebanese University, Lebanon
[3]SYMMES/CIBEST UMR 5819 UGA-CNRS-CEA, Univ. Grenoble Alpes, Grenoble, France
[4]miRCaDe team, Univ. Bordeaux, INSERM, U1035, (Biotherapy of Genetic, Inflammatory Diseases and Cancer) F-33000 Bordeaux, France.
[5]Department of Gynecology and Obstetrics, Clinique Saint-Pierre, Belgium
[6]Ludwig Center for Cancer Research of the University of Lausanne, Switzerland

***Corresponding Authors:** Redouane Rouas, Experimental Hematology, Institut Jules Bordet, Université Libre de Bruxelles, 121, Boulevard de Waterloo, 1000 Bruxelles, Belgium

Hussein Fayyad-Kazan, Experimental Hematology, Institut Jules Bordet, Université Libre de Bruxelles, Belgium/Laboratory of Cancer Biology and Molecular Immunology, Faculty of Sciences, Lebanese University, Lebanon

Aksam Merched, miRCaDe team, Univ. Bordeaux, INSERM, BMGIC, U1035, F-33000 Bordeaux, France

Published **November 18, 2020**

This Book Chapter is mainly adapted from an article published by Redouane Rouas, et al. at Journal of Translational Medicine in August 2014. (Jebbawi, F., Fayyad-Kazan, H., Merimi, M. et al. A microRNA profile of human CD8+ regulatory T cells and characterization of the effects of microRNAs on Treg cell-associated genes. J Transl Med 12, 218 (2014). https://doi.org/10.1186/s12967-014-0218-x)

How to cite this book chapter: Fadi Jebbawi, Hussein Fayyad-Kazan, Makram Merimi, Philippe Lewalle, Mohammad Fayyad-Kazan, Walid Rachidi, Aksam Merched, Malak Alannan, Jean-Christophe Verougstraete, Oberdan Leo, Pedro Romero, Arsene Burny, Bassam Badran, Philippe Martiat, Redouane Rouas. A microRNA Profile of Human CD8+ Regulatory T cells and Characterization of the Effects of microRNAs on Treg Cell-Associated Genes. In: Hussein Fayyad Kazan, editor. Immunology and Cancer Biology. Hyderabad, India: Vide Leaf. 2020.

Acknowledgments: This work was supported by grants from les Amis de l'Institut Jules Bordet, the MEDIC Foundation, the Belgian Fonds National pour la Recherche Scientifique - TELEVIE, the Van Buuren, Lambeau Marteaux, and Hoguet Foundations.

Competing interest: The authors declare that they have no competing interest.

Abstract

Background: Recently, regulatory T (Treg) cells have gained interest in the fields of immunopathology, transplantation and oncoimmunology. Here, we investigated the microRNA expression profile of human natural $CD8^+CD25^+$ Treg cells and the impact of microRNAs on molecules associated with immune regulation.

Methods: We purified human natural $CD8^+$ Treg cells and assessed the expression of FOXP3 and CTLA-4 by flow cytometry. We have also tested the ex vivo suppressive capacity of these cells in mixed leukocyte reactions. Using TaqMan low-density arrays and microRNA qPCR for validation, we could identify a microRNA 'signature' for $CD8^+CD25^+FOXP3^+CTLA\text{-}4^+$ natural Treg cells. We used the 'TargetScan' and 'miRBase' bioinformatics programs to identify potential target sites for these microRNAs in the 3′-UTR of important Treg cell-associated genes.

Results: The human $CD8^+CD25^+$ natural Treg cell microRNA signature includes 10 differentially expressed microRNAs. We demonstrated an impact of this signature on Treg cell biology by showing specific regulation of FOXP3, CTLA-4 and GARP gene expression by microRNA using site-directed mutagenesis and a dual-luciferase reporter assay. Furthermore, we used microRNA transduction experiments to demonstrate that these microRNAs impacted their target genes in human primary Treg cells ex vivo.

Conclusions: We are examining the biological relevance of this 'signature' by studying its impact on other important Treg cell-associated genes. These efforts could result in a better understanding of the regulation of Treg cell function and might reveal new targets for immunotherapy in immune disorders and cancer.

Background

Regulatory T (Treg) cells are specialized subsets of T cells that modulate the immune system to avert unwanted immune

responses, maintain immunological self-tolerance and homeostasis, dampen inflammatory responses, and limit tissue damage. Treg cells can be divided into natural and adaptive Treg cells. Natural Treg cells develop in the thymus and express both CD25 and FOXP3. Adaptive Treg cells develop in the periphery following antigenic (by self- or foreign-antigen) stimulation in the presence of specific immunomodulatory molecules. Moreover, Treg cells can also be divided into two classes, $CD4^+$ and $CD8^+$ Treg cells [1].

$CD8^+$ T cells play a major role as adaptive effectors in several immunopathological conditions, such as autoimmune disease [2-6], transplantation [7,8], host defense and cancer [8,9]. Despite the long-held notion that $CD8^+$ T cells could mediate suppression, most reports have focused on the regulatory properties of $CD4^+$ T cell subsets and only a few studies have characterized $CD8^+$ T cell-mediated immune regulation. The main reason for the relative neglect of $CD8^+$ Treg cells by researchers is the absence of markers that allow their identification. Recently, several subsets of $CD8^+$ Treg cells have been identified based on the expression of CD25, CD56 [10], FOXP3, CXCR3, LAG-3, CD103, CD122 and/or HLA-G, as well as the absence of CD28 expression. These diverse subpopulations of $CD8^+$ Treg cells have different mechanisms of suppression and play roles in cancer, infection, transplantation and autoimmunity [11-25]. Natural $CD8^+$ Treg cells include $CD8^+CD25^+$ T cells, which share functional and phenotypic similarities with $CD4^+CD25^+$ Treg cells, such as CTLA-4, GITR and intracellular Foxp3 expression. $CD8^+CD25^+$ Treg cells can suppress $CD4^+CD25^-$ T cells in a membrane-bound TGFβ and CTLA-4-mediated contact-dependent manner that induces IL-2Rα downregulation on target T cells [19]. They can also act by producing immunosuppressive cytokines, such as TGF-β and IL-10 [26], or by inactivating dendritic cells [21]. Moreover, naturally occurring human $CD8^+CXCR3^+$ T cells have been shown to secrete IL-10 and suppress IFN-γ production, in a manner similar to murine $CD8^+CD122^+$ Treg cells [27].

FOXP3 has emerged as a marker for T cells with regulatory activity. Deletion or mutation of FOXP3 is associated with the

lymphoproliferative disorder that occurs in *scurfy* mice and immunodysregulation, polyendocrinopathy, enteropathy, X-linked (IPEX) syndrome in humans [28-30]. As a 'master transcription factor', FOXP3 is a critical regulator of $CD4^+CD25^+$ Treg cell development and function, and appears to be the best marker to identify natural $CD4^+$ Treg cells [31,32]. However, despite being the most specific marker of Treg cells, together with elevated expression of the high-affinity IL-2 receptor-α chain (CD25), FOXP3 cannot be used to isolate viable Treg cells because of its intracellular expression.

Although we still lack specific markers, many cell-surface molecules have been reported to characterize human Treg cells, such as expression of glucocorticoid-induced tumor necrosis factor receptor (GITR), CD62 ligand (CD62L), OX40 (CD134), cytotoxic T-lymphocyte antigen-4 (CTLA-4), and low expression of IL-7 receptor (CD127) [33-35] and glycoprotein A repetitions predominant (GARP) [36]. CTLA-4 is known to be a critical regulator of immune responses by reducing T cell activation and proliferation. $CD4^+$ Treg cells are known to constitutively express CTLA-4 [33]. Polymorphisms in CTLA-4 have been associated with several autoimmune diseases, including systemic lupus erythematosus and insulin-dependent diabetes mellitus; a general susceptibility to autoimmune diseases has also been described for CTLA-4 polymorphisms [37-39], emphasizing its pivotal role in immune tolerance.

GARP appears to be a crucial membrane-anchored receptor for latent TGF-β on the Treg cell surface [40,41]. GARP expression has been shown to identify selectively activated human $FOXP3^+$ Treg cells and to play a role in Treg cell-mediated immunosuppression [36].

The microRNAs (miRNAs) are an abundant class of evolutionarily conserved small non-coding RNAs that regulate gene expression post-transcriptionally by affecting the degradation and translation of target mRNA transcripts. The biogenesis of miRNAs involves several processing steps that have mostly been defined in cell-based and biochemical studies. Primary miRNA transcripts are first processed into precursor

microRNA (pre-miRNA) by the nuclear RNase III enzyme Drosha [42-45]. These pre-miRNAs are then actively transported by Exportin-5 to the cytoplasm, where they are further processed by the cytoplasmic RNase III enzyme Dicer [46-48]. The functional miRNA strand is then selectively loaded into the RNA-induced silencing complex (RISC) [49,50]. Mature miRNAs then guide the RISC to cognate target genes, and target gene expression is repressed by either destabilizing the target mRNAs or repressing their translation. To date, a rapidly growing number of miRNAs have been identified in mammalian cells and shown to be involved in a range of physiological responses, including development, differentiation and homeostasis [51-53].

Recent publications have provided compelling evidence that miRNAs are highly expressed in Treg cells, and that the expression of Foxp3 is controlled by miRNAs. Among miRNAs, miR-21, −24, −31, −95, −210 [51] and −155 [54] affect Foxp3 expression, and miR-155 is an important regulator of lymphocyte function and homeostasis. Other studies have shown that miRNAs are involved in the regulation of T cell function. For example, miR-142-3p can regulate GARP expression in $CD4^+CD25^+$ T cells [55]. Huang et al. showed an indirect effect of miR-142-3p on FOXP3 expression by targeting AC9 mRNA [56]. Moreover, miR-17-92 has been implicated in the regulation of IL-10 secretion by regulatory T cells [57]. Many studies have reported links between alterations in miRNA homeostasis and pathological conditions, such as cancer, cardiovascular disease, diabetes, psychiatric disorders and neurological diseases [58].

Here, we investigated the miRNA expression profile of human natural $CD8^+CD25^+$ Treg cells and its potential impact on Treg cell-associated functional molecules. We focused on a subset of $CD8^+$ Treg cells in human cord blood, which contains a distinct population of $CD8^+CD25^+$ Treg cells that are less heterogeneous than in adult peripheral blood. Cord blood is useful for studies aimed at understanding human natural Treg cells because, in contrast to adult blood, they are less contaminated by activated T cells that express CD25 and lack regulatory function [59]. Therefore, we investigated the miRNA expression profile of

these natural $CD8^+CD25^+$ Treg cells and compared it with that of $CD8^+CD25^-$ T cells. Additionally, we focused our study on genes that have been reported in the literature to be associated with human Treg cell biology. Interestingly, we found that some miRNAs have direct effects on FOXP3 and CTLA-4 expression, molecules that regulate Treg cell development and function, and also on GARP expression.

Materials and Methods

Collection and Preparation of Cord Blood Samples

After approval by local and academic ethic committees and informed consent, umbilical cord blood mononuclear cells (UCBMC) were isolated from the umbilical vein blood from normal full-term deliveries placenta. UCBMC were isolated by appropriate centrifugation over a lymphocyte separation medium (PAA laboratories). The study was approved by the Institut Jules Bordet scientific, and ethic committees and by the committees of Université Libre de Bruxelles.

Isolation of T-Cell Populations

Cord blood $CD8^+$ lymphocytes were purified using $CD8^+$ T cell isolation kit (Miltenyi Biotec, Bergisch Gladbach, Germany) according to the manufacturer protocol. Briefly, UCBMC were first incubated in PBS supplemented with 2% heat-inactivated fetal bovine serum and saturating amounts of biotin-conjugated antibody cocktail (anti- CD4, CD15, CD16, CD19, CD36, CD56, CD123, TCR-γ/δ and anti-Glycophorin A). Leucocytes were then incubated with anti-biotin microbeads and $CD8^+$ T cells were purified using magnetic separation columns (Miltenyi Biotec). The negatively selected cells were incubated with anti-CD25 micro-beads, and then $CD25^+$ and $CD25^-$ cells were purified from $CD8^+$ T lymphocyte fraction using magnetic columns (Miltenyi Biotec).

FOXP3 Intracellular Staining and Flow Cytometry

FOXP3 intracellular staining was performed using anti-human FOXP3-PE detection Kit (BD Biosciences) following the

manufacturer's instructions. Anti-CD3-PerCP, anti-CD8-APC, anti-CTLA-4-PE (BD Biosciences), anti-CD25-PE (Miltenyi Biotec) were used to assess cell phenotype and purity. Corresponding isotype controls served as controls. Flow cytometry analysis was performed on a FACSCalibur machine with Cell Quest software (Becton-Dickinson Biosciences).

Treg Suppressive Capacity Assessment in Mixed Leukocyte Reaction Assays

Treg suppressive capacity toward proliferation of activated allogeneic carboxyfluorescein succinimidyl ester (CFSE)-labeled T lymphocytes was assessed by flow cytometry analysis after 5 days of co-culture experiments. Briefly, cord blood and healthy adult blood samples were collected after informed consent had been obtained. T lymphocytes were immunomagnetically purified from healthy donor's peripheral blood mononuclear cells by positive selection using anti-human CD3 microbeads (Miltenyi Biotec) according to the manufacturer's instructions. These T lymphocytes were then labeled by CFDA-SE (CellTrace-CFSE cell proliferation kit, Invitrogen) by using 10 mM CFDA-SE dye to stain 10^7 cells.

$CD8^+CD25^+$ Tregs were isolated from cord blood mononuclear cells as described above. The purity of the selected cells was always above 96%, as determined by flow cytometry analysis.

Mixed leukocyte reactions (MLR) were performed by culturing irradiated allogeneic peripheral blood mononuclear cells, as stimulating cells (2×10^5), to activate CFSE-labeled allogeneic T lymphocytes responder cells (2×10^5), in a 48-well plate (control MLR).

$CD8^+CD25^+$ nTregs or $CD8^+CD25^-$ T cells were added to MLRs at a 1:1:1 ratio before culture in RPMI with 10% decomplemented FBS (both from Lonza Europe, Verviers, Belgium). After 5 days of co-culture, CFSE fluorescence dilution was measured by flow cytometry, gating on CFSE positive cells. Samples were run on a FACSCalibur (BD Biosciences) and

analyzed using Kaluza® Flow Cytometry Analysis software (Beckman Coulter Inc.).

RNA Extraction, RT and Real-Time PCR Quantification

Total RNA was extracted from cells using Trizol® total RNA isolation reagent (Invitrogen, Life Technologies, Belgium). The concentration was quantified using a NanoDrop Spectrophotometer. TaqMan microRNA assays (Applied Biosystems) were used to quantify mature microRNA (miR) expression. RNU44 (Applied Biosystems) was used as endogenous control for miR expression studies.

Thus, gene-specific RT was performed for each miR using 10 ng of purified total RNA, 100 mM dNTP, 50 U MutliScribe reverse transcriptase, 20 U RNase inhibitor, and 50 nM of gene-specific RT primer samples using the TaqMan MicroRNA Reverse Transcription kit (Applied Biosystems). Fifteen microliter reactions were incubated for 30 min at 16°C, 30 min at 42°C, and 5 min at 85°C to inactivate the reverse transcriptase. Real-time RT-PCR (5 µL of RT product, 10 µL TaqMan 2× Universal PCR master Mix, (Applied Biosystems) and 1 µL TaqMan MicroRNA Assay Mix containing PCR primers and TaqMan probes) were run in triplicates at 95°C for 10 min followed by 40 cycles at 95°C for 15 s and 60°C for 1 min.

Quantitative miR expression data were acquired and analyzed using an ABI Prism 7900HT Sequence Detection System (Applied Biosystems).

TLDA and Individual Quantitative PCR Validation

The TaqMan Low Density Array (TLDA, Applied Biosystems) technique allowed us to measure the expression of 384 miRs, in order to compare the miR expression profile of purified nTregs with their $CD25^-$ counterpart T cells originating from five different cord bloods. cDNA was synthesized from 100 ng of total cellular RNA by First Strand cDNA Synthesis System using 100 mM dNTP, 50 U MutliScribe reverse transcriptase, 20 U

RNase inhibitor, 10× RT buffer, and Multiplex RT human primer. Ten microliter reactions were incubated for 30 min at 16°C, 30 min at 42°C, 5 min at 85°C to inactivate the reverse transcriptase.

Five microliter cDNA were mixed with 307 μL nuclease free water and 50 μL of this diluted cDNA were mixed with 50 μL of TaqMan Universal PCR Master Mix (Applied Biosystems). After that, 100 μL of the sample-specific PCR mixture was loaded into one sample port, the cards were centrifuged twice for 1 min at 280 *g* and sealed to prevent well-to-well contamination. The cards were placed in the Micro Fluidic Card Sample Block of an ABI Prism 7900 HT Sequence Detection System (Applied Biosystems). The thermal cycling conditions were 2 min at 50°C and 10 min at 95°C, followed by 40 cycles of 15 s at 95°C and 1 min at 60°C.

In each sample, average cycle threshold (Ct) values for the target genes were subtracted from the average Ct value of the reference gene to yield the ΔCt value. 2-ΔCt values were calculated to indicate the relative amount of transcripts in each sample.

For each miR that was found differentially expressed, a validation by individual quantitative PCR was performed, and we retained only the miR concordant with the two techniques.

Real-Time PCR

Real-time PCR quantitative mRNA analyses were performed on the ABI Prism 7000 sequence detection system using the SYBR Green fluorescence quantification system (Applied Biosystems, Warrington, UK). The standard PCR conditions were 95°C for 10 min, 40 cycles for 1 min at 94°C, 56°C (1 min), and 72°C (2 min), followed by the standard denaturation curve. The sequences of human primers were designed in Primer3 Input software (version 0.4.0) and the primers were designed as follows (Invitrogen):

β-actin,

sense: *TGACAAAACCTAACTTGCGC*,

antisense: *ATAAAGCCATGCCAATCTCA*.

IL-10,

sense: *AGATCT-CCGAGATGCCTTCA*,

antisense: *CCGTGGAGCAGGTGAAGAAT*

TGF-β,

sense: GTGGAAACCCACAACGAAA,

antisense: TAAGGCGAAAGCCCTCAAT

Foxp3,

sense: GAGAAGCTGAGTGCCATGCA,

antisense: GGTCAGTGCCATTTTCCCAG

CTLA-4,

sense: ATCGCCAGCTTTGTGTGTGA,

antisense: GACCTCAGTGGCTTTGCCTG

FOXO1,

sense: GCAGATCTACGAGTGGATGGT,

antisense: AAACTGTGATCCAGGGCTGTC

HELIOS,

sense: TCACAACTATCTCCAGAATGTCA,

antisense: AGGCGGTACATGGTGACTCAT

ICOS,

sense: CCATAGGATGTGCAGCCTTTG,

antisense: GGTCGTGCACACTGGATGAA

CD28,

sense: ATGCTCAGGCTGCTCCTGGCTCTC,

antisense: CAGCCGGCCGGCTTCTGGATAG

GARP,

sense: CCCTGTAAGATGGTGGACAAGAA,

antisense: CAGATAGATCAAGGGTCTCAGTGTCT

CCR4,

sense: GTGGTTCTGGTCCTGTTCAAATAC,

antisense: CGTGGAGTTGAGAGAGTACTTGGTT

IL2RA,

sense: AATGCAGCCAGTGGACCAA,

antisense: TGATAAATTCTCTCTGTGGCTTCATTT

The SYBR Green PCR master mix (Applied Biosystems), 0.1–0.2 μg/μl specific primers and 2.5 ng cDNA, was used in each reaction. Threshold for positivity of real-time PCR was determined based on negative controls. Calculations to determine the relative level of gene expression were made according to the instructions from the user's bulletin (P/N 4303859) of Applied

Biosystems by reference to the β-actin in each sample, using the cycle threshold (Ct) method. Negative controls without RNA and without RT were also performed. Results show one experiment representative of three.

Cell Line Culture

The 293 T and HeLa cell lines were cultured in DMEM (Lonza, Verviers, Belgium) supplemented with 10% heat inactivated fetal bovine serum (Invitrogen Europe, Paisley, UK), 2 mM l-glutamine, 50 IU/mL Penicillin and 50 µg/mL Streptomycin (all from Lonza).

Plasmid Construction

A 249-bp fragment of *FOXP3* 3′-UTR encompassing the miR-335 potential target site and a 300-bp fragment of *CTLA-4* encompassing the miR-9 and miR-155 potential target sites were cloned downstream of the *Renilla* luciferase gene (Eco RI/Xho I sites) in the psiCHECK-1 plasmid (Promega, Mannheim, Germany) and designated as psiCHECK 3′-UTR WT. PCR primers used for amplification of the *FOXP3* and *CTLA-4* 3′-UTR were as follows (5′ to 3′):

FOXP3 primers:

GCGCCTCGAGTCACCTGTGTATCTCACGCATA (forward)

GCGCGAATTCGAGCTCGGCTGCAGTTTATT (reverse)

CTLA-4 primers:

GCGCCTCGAGAGGAGCTCAGGACACTAATA (forward)

GCGCGAATTCAATTGGGCCCATCGAACT (reverse)

QuikChange site-directed mutagenesis (deletion) of miR-9, miR-24, miR-155 and miR-335 target sites in psiCHECK 3′-UTR WT was performed according to manufacturer's protocols (Stratagene, La Jolla, CA) and designated as psiCHECK-

UTRdel. QuikChange site-directed mutagenesis were performed using the following primers (5′ to 3′):

FOXP3 (miR-335 site deleted 3′UTR):

GCCCCCCAGTGGGTGTCCCGTGCAG (forward)

CTGCACGGGACACCCACTGGGGGGC (reverse)

CTLA-4 (miR-9 site deleted 3′UTR):

GGGAATGGCACAGCAGGAAAAGGG (forward)

CCCTGCCTTTTCCTGCTGTGCCATTCCC (reverse)

CTLA-4 (miR-155 site deleted 3′UTR),

GGGATTAATATGGGGATGCTGATGTGGGTCAAGG (forward)

CCTTGACCCACATCAGCATCCCCATATTAATCCC (reverse)

GARP 3′UTR 2070-bp encompassing the miR-24 and −335 potential target sites were cloned downstream the *Firefly* luciferase gene (AsiSI/Xho1 sites) in the pEZX-MT01 plasmid (Labomics, Nivelles, Belgium) and designed as pEZX-MT01 3′-UTR WT. PCR primers used for amplification of the *FOXP3* and *CTLA-4* 3′-UTR were as follows (5′ to 3′):

GARP primers:

CTCGAGAGAAGCCGGGAGAC (forward)

CCGCGGACATTCAGGTAGG (reverse)

QuikChange site-directed mutagenesis were performed using the following primers (5′ to 3′):

GARP (miR-24 site deleted 3′UTR),

GCCCCACCTTGGCTGCAGGAGCTAAAACC (forward)
GGTTTTAGCTCCTGCAGCCAAGGTGGGGC (reverse)

GARP (miR-335 3′UTR site deleted),

GGGTTCTCCTGTTCTCTCTGTCATTCTCTCATTCCC (forward)

GGGAATGAGAGAATGACAGAGAGAACAGGAGAACCC (reverse)

The constructs were verified by sequencing (GATC Biotech, Konstanz, Germany).

Luciferase Assays

Luciferase assays were conducted in a 24-well format. Reporter plasmids (psiCHECK, psiCHECK 3′-UTR WT, psiCHECK 3′-UTR deleted, pEZX-MT01, pEZX-MT01 3′-UTR GARP WT, pEZX-MT01 GARP 3′-UTR deleted) (100 ng) were co-transfected in HEK293T and HeLa cells along with miR-9, miR-24, miR-155, and miR-335-mimic/miR-negative control-mimic at a final concentration of 10 μM (mirVana miRNA mimic, Life Technologies, Gent, Belgium) and control firefly plasmid pGL3-CMV for the psiCHECK vectors only (100 ng) using Lipofectamine 2000 (Invitrogen) according to the manufacturer's guidelines. Before proceeding to the transfection assays, the cell lines were assessed for expression of the miR of interest using quantitative RT-PCR, as described below. 24 h post-transfection, cells were harvested, and luciferase levels were measured using the Dual-Luciferase reporter assay system (Promega Benelux BV, Leiden, The Netherlands) according to the manufacturer's guidelines. Relative protein levels were expressed as *Renilla*/firefly luciferase ratios. Relative protein levels were expressed as *Renilla*/firefly luciferase ratios in case of co-transfections with psiCHECK and PGL3-CMV vectors and firefly/Renilla for transfections with pEZX-MT01 vectors.

Lentiviral Vector Production

VSV-G pseudotyped lentiviral particles were generated by polyethyleneimine (Sigma) co-transfection of HEK293T cells with three plasmids, pMIRNA, pCMVΔR8.91, and pMD.G [60].

pCMVΔR8.91 is an HIV-derived packaging construct that encodes the HIV-1 Gag and Pol precursors as well as the regulatory proteins Tat and Rev [61]. VSV-G was expressed from pMD.G [62]. pMIRNA, provided by System Biosciences, is a lentivirus-based vector in which a microRNA precursor molecule has been cloned downstream of the CMV promoter and contains *copGFP* as a reporter gene. 24 h after transient transfection of HEK293T cells, viral supernatants were collected, filtered through 0.45-μm low protein-binding filters (Nalgene, Rochester, NY), and concentrated as described previously [63]. The viral pellets were then resuspended in 1/100 volume of PBS. Viral stocks were stored in aliquots at −80°C, and the titers were determined by transducing HeLa cells in a limiting dilution assay. Lentiviral vector preparations collected 24 h post-transfection, and after concentration, displayed titers of 10^8–10^9 transducing units/ml in HeLa cells. No replication-competent virus was detected in the concentrated lentiviral stocks. A second production cycle was repeated after 24 h, routinely generating lentiviral vector preparations of 5×10^7 to 5×10^8 transducing units/ml.

Lentiviral Transduction

Tregs were plated at a density of 10^6 cells/well in 12-well tissue culture plates in 1 ml of RPMI 1640 supplemented with 10% heat-inactivated fetal bovine serum, 2 mM L-glutamine, 50 units/ml penicillin, 50 μg/ml streptomycin (Lonza), in the presence of 5 μg/ml phytohemagglutinin (PHA-L, Sigma) and 20 units/ml IL-2.

24 h after Treg isolation, cells were exposed to lentiviral vector preparation at a multiplicity of infection of 5 in a volume of 500 μl in the presence of 8 μg/ml polybrene (Sigma). GFP-

positive cells were sorted by flow cytometry at day 7 after transduction.

MiR-9, miR-24, miR-155 and miR-335 Detection by TaqMan Real-time PCR

TaqMan miRNA assays (Applied Biosystems) used the stem loop method [64,65] to detect the expression level of mature miR-9, miR-24 miR-155 and miR-335. For RT reactions, 10 ng of total RNA was used in each reaction (15 µl) and mixed with the RT primer (3 µl). The RT reaction was carried out under the following conditions: 16°C for 30 min, 42°C for 30 min, 85°C for 5 min, and then holding at 4°C. After the RT reaction, the cDNA products were diluted at 5×, and 9 µl of the diluted cDNA was used for PCR along with the TaqMan microarray assay (1 µl) and PCR master mix (10 µl). The PCR was conducted at 95°C for 10 min, followed by 40 cycles of 95°C for 15 s and 60°C for 60 s in the ABI 7900 real-time PCR system. The real-time PCR results were analyzed and expressed as relative miRNA expression of *Ct* value, which was then converted to -fold changes. RT primer, PCR primers, and TaqMan probe for miR-9, miR-24, miR-155 and miR-335 were purchased from ABI. RNU48 was used for normalization.

Quantitative PCR for FOXP3, CTLA-4 and GARP Expression

Total RNA was extracted with Trizol reagent according to the manufacturer's guidelines (Invitrogen), and first-strand cDNAs were synthesized by reverse transcription (Superscript First-strand Synthesis System for RT-PCR kit, Invitrogen) Quantitative mRNA expression was measured by real-time PCR with the PRISM 7900 sequence detection system (Applied Biosystems), and the TaqMan master mix kit; EF1-α mRNA was used as an internal control. Human TaqMan gene expression assay for *FOXP3* (Hs01085834-m1), *CTLA-4* (Hs03044418-m1), GARP (Hs0019436-m1) and EF1-α (Hs01024875-m1) were purchased from Applied Biosystems. The program used for amplification was as follows: 10 min at 95°C followed by 40 cycles of 15 s at 95°C, 1 min at 60°C.

Statistical Analysis

Data are presented as means ± SD of at least three independent experiments and analyzed using Student's *t* test. *p* values of <0.05 (*), <0.01 (**), and <0.001 (***) were considered significant.

Results

$CD8^+CD25^+$ Natural Treg Cells Express FOXP3 and CTLA-4

$CD8^+CD25^+$ and $CD8^+CD25^-$ T cells were immunomagnetically purified from fresh human cord blood by negative selection of $CD8^+$ T cells, followed by CD25-based positive selection (Miltenyi Biotec, Bergisch Gladbach, Germany). To confirm the purity of the separated cell fractions, $CD8^+CD25^+$ and $CD8^+CD25^-$ T cells were analyzed by flow cytometry. Purity was always >96%. $CD8^+$ natural Treg cells expressed more intracellular FOXP3 and cell-surface CTLA-4 proteins compared with $CD8^+$ $CD25^-$ T cells (Figure 1).

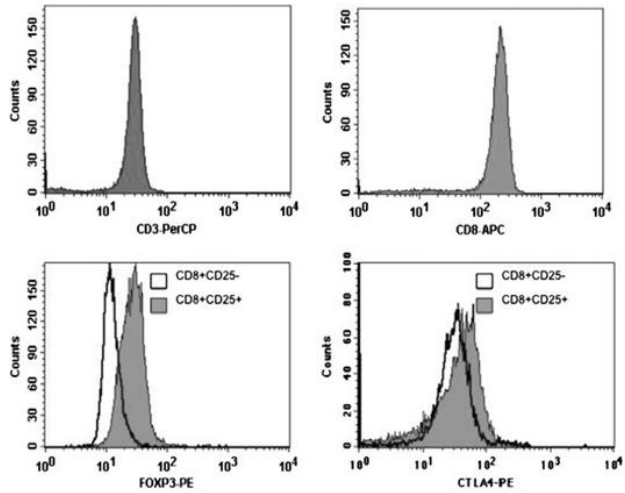

Figure 1: Purified human CD8 $^+$ CD25 $^+$ natural Tregs express FOXP3 and CTLA-4. Separated cell fractions, $CD8^+CD25^+$ and $CD8^+CD25^-$ T cells, were analyzed by multicolor FACS using the following antibodies: anti-CD3 PerCP, anti-CD8-APC (BD biosciences) and anti-CD25-PE (Miltenyi Biotec) to assess

purity for each isolation. Intracellular FOXP3 and cell-surface CTLA-4 were assessed using human anti-FOXP3-PE detection kit and anti-CTLA-4-PE (BD biosciences). Flow cytometry was performed using a FACSCalibur applying CellQuest software (BD Biosciences). CD3 and CD8 purity was above 97% among isolated $CD8^+$ T cells. $CD8^+CD25^+$ nTregs express FOXP3 and CTLA-4 when compared to $CD8^+CD25^-$ T cells.

$CD8^+CD25^+$ Natural Treg Cells are Suppressive

In vitro Treg cell suppression assays were performed to assess the functional impact of the isolated Treg cells on activated T cell proliferation. $CD8^+CD25^+$ natural Treg cells suppressed allogeneic mixed leukocyte reactions when measured at day 5, as indicated by CFSE dilution of $CD3^+$ T cells. Our analysis (Figure 2) indicated that $CD8^+CD25^+$ natural Treg cells could inhibit allogeneic T cell proliferation.

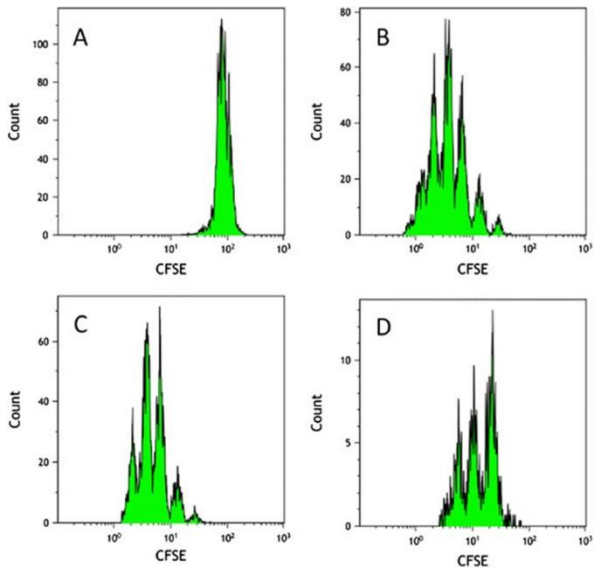

Figure 2: Functional assessment of CD8 $^+$ CD25 $^+$ nTreg cell suppressive capacity toward proliferation of allogeneically activated CFSE-labeled T lymphocytes. CFSE dilution analysis shows $CD8^+CD25^+$ nTreg-mediated suppression of allogeneic T cell proliferation in 5 days mixed leukocyte reaction (MLR) compared to control MLR and compared to MLR with $CD8^+CD25^-$ non-Tregs. CFSE dilution histograms are shown for 1:1 suppressor/responder cell ratio. Shown is one representative experiment out of four independent experiments performed. **(A)** CFSE-labeled allogeneic T cells alone at d0 before MLR. **(B)** Proliferation of CFSE-labeled allogeneic T cells

after 5 days of allo-MLR (control MLR). **(C)** Allo-MLR in presence of $CD8^+CD25^-$ non-Treg cells, at day 5. **(D)** Allo-MLR in presence of $CD8^+CD25^+$ nTregs, at day 5.

Assessment of Treg Cell-Related Gene Expression in $CD8^+CD25^+$ and $CD8^+CD25^-$ T Cells qPCR

The mRNA transcript levels were analyzed by qPCR to compare $CD8^+CD25^+$ with $CD8^+CD25^-$ T cells using SYBR green detection. Importantly, we showed (Table 1) that IL-2RA, FOXP3, CTLA-4, CCR4, GARP, IL-10 and TGF-β were upregulated in $CD8^+CD25^+$ natural Treg cells compared with $CD8^+CD25^-$ T cells, whereas CD28, ICOS, FOXO1 and HELIOS were downregulated in $CD8^+CD25^+$ natural Treg cells compared with $CD8^+CD25^-$ T cells.

Table 1: Relative regulatory T cell-associated gene expression for $CD8^+CD25^+/CD8^+CD25^-$ by individual qPCR (SYBR Green).

Relative Treg-associated gene expression							
Gene	**IL2RA**	**FOXP3**	**CTLA-4**	**CCR4**	**GARP**	**IL10**	**TGF-B**
CD8 + CD25+/CD8 + CD25-	65 ± 1,414	11,5 ± 4,9	3.19 ± 1,73	13.43 ± 4,69	13,66 ± 4,12	4.86 ± 2,68	4.57 ± 2,61
Gene	**CD28**	**ICOS**	**FOXO1**	**HELIOS**			
CD8 + CD25+/CD8 + CD25-	0,05 ± 0,019	0,342 ± 0,125	0,18 ± 0,078	0,288 ± 0,13			

Gene mRNA levels were evaluated using quantitative RT-PCR of $CD8^+CD25^+/CD8^+CD25^-$ T cells. Data represent the mean ± SD of five independent experiments, each done in triplicate.

The $CD8^+CD25^+$ Natural Treg Cell microRNA Signature

We first studied miRNAs from five independent $CD8^+CD25^+$ natural Treg cell and $CD8^+CD25^-$ T cell samples using the TLDA technique. We could identify several miRNAs that were differentially expressed between $CD8^+CD25^+$ natural Treg cells and $CD8^+CD25^-$ T cells. Differentially expressed miRNAs were validated by real-time PCR (Figure 3). A Treg cell miRNA signature was identified that included 10 significantly differentially expressed miRNAs: miR-9, −24, −31, −155, −210, −335 and −449 were downregulated in $CD8^+$ natural Treg cells, whereas miR-214, −205 and −509 were overexpressed.

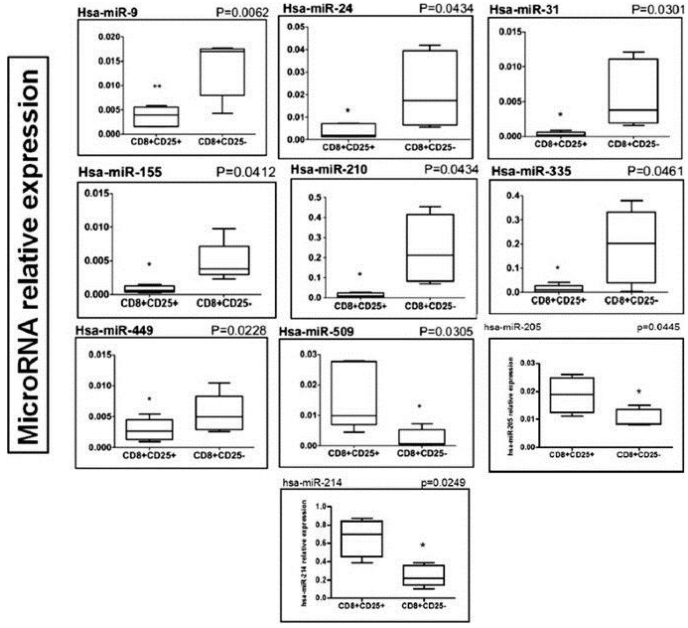

Figure 3: Differential expression of miR-24, −335, −155, −31, −210, −449, −509, −214, −205 and −9 between $CD8^+CD25^+$ nTregs and $CD8^+CD25^-$ T cells. Data obtained by qRT-PCR amplification of miRs are plotted. *p* values for each miRNA relative expression are presented. *Boxes* represent SE; and Error bars SD Pooled data from five independent experiments are shown. ($^*p < 0.05$; $^{**}p < 0.01$ $CD8^+CD25^+$ nTregs versus $CD8^+CD25^-$ T cells (Student's *t* test).

Target Prediction for miR-9, −24, −155 and −335

Computer-based programs were used to predict potential targets sites for the miRNAs that were associated with downregulation in the *FOXP3* and *CTLA-4* 3′-UTRs. We searched miRBase [66] and TargetScan 4.2 [67]. We could identify putative miRNA target sites in the *FOXP3* and *CTLA-4* 3′-UTRs by both programs—miR-335 in the *FOXP3* 3′-UTR and both miR-9 and −155 in the *CTLA-4* 3′-UTR. Furthermore, miR-31, −24, −210 and −335 have target sites in the *FOXP3* 3′-UTR but not in the *CTLA-4* 3′-UTR, while miR-9 and −155 have target sites in the *CTLA-4* 3′-UTR but not in the *FOXP3* 3′-UTR [68,69].

FOXP3 is Directly Regulated by miR-335

A 249-bp fragment of the 3′-UTR of *FOXP3* containing the miR-335 target sequence was cloned into a psiCHECK-1 vector downstream of the *Renilla* luciferase gene (psiCHECK-UTRwt). In parallel, in the same way we cloned this *FOXP3* 3′-UTR fragment with a deleted miR-335 target site (psiCHECK-UTRdel). Transient transfections of psiCHECK-UTRwt or psiCHECK-UTRdel in HEK293T cells led to no significant change in reporter luciferase activity when compared with the psiCHECK control vector (Figure 4A). By contrast, co-transfection of HEK293T cells with miR-335 and psiCHECK-UTRwt led to a significant reduction (~47%) in relative reporter luciferase activity, and also for activity compared with the co-transfection of HEK293 T cells with miR-Ctrl and psiCHECK-UTRwt.

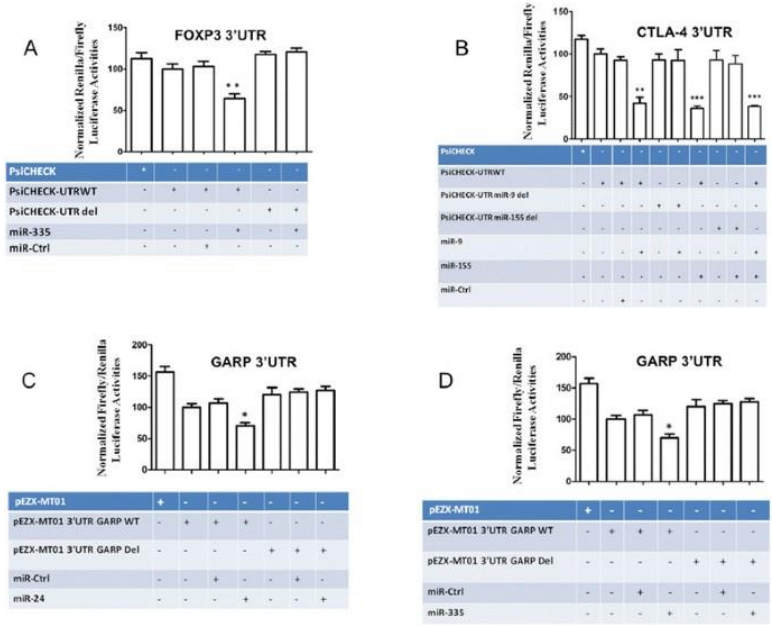

Figure 4: MicroRNA specific activities. **(A)** MiR-335 negatively regulates luciferase expression in a plasmid coupling its coding sequence with FOXP3 3′UTR. *Renilla* luciferase reporter assays with constructs holding *FOXP3* 3′-UTR sequences from the indicated genes were co-transfected into HEK293T cells along with a firefly luciferase transfection control plasmid either alone or together with miR-335. **(B)** MiR-9 and miR-155 negatively regulate luciferase expression in a plasmid coupling its coding sequence with CTLA-4 3′UTR. *Renilla* luciferase reporter assays with constructs holding *CTLA-4* 3′-UTR sequences, wild type or miR-site deleted, were co-transfected into HEK293T cells along with a firefly luciferase transfection control plasmid either alone or together with miR-9, −155. MiR-24 **(C)** and miR-335 **(D)** specifically targets GARP 3′UTR and negatively regulate luciferase reporter expression. *Renilla* and *firefly* luciferase reporter assays with constructs holding *GARP* 3′-UTR sequences, wild type or miR-site deleted, were co-transfected into HEK293T cells along with miR-24, −335. Relative luciferase values normalized to transfections without miRNA are shown. Data represent mean ± SD (*error bars*) of three independent experiments, each performed in triplicate. (*p < 0.05; **, p < 0.01, Student's *t* test).

Together, these results demonstrate a specific role for miR-335 in the regulation of *FOXP3* expression through direct binding to its target site.

CTLA-4 is Directly Regulated by miR-9 and miR-155

We next investigated whether *CTLA-4* could be directly targeted by miR-9 and −155. We engineered luciferase reporter plasmids containing either the wild-type 3′-UTR of this gene (psiCHECK-UTRwt) or a 3′-UTR with deleted miR-9 and −155 target sites (psiCHECK-UTRdel). We found that co-transfection of HEK293 T cells with miR-9 and psiCHECK-UTRwt led to a reduction (~52%) in reporter luciferase activity compared with the co-transfection of HEK293 T cells with miR-9 and psiCHECK-UTRdel or the co-transfection of HEK293 T cells with miR-Ctrl and either psiCHECK-UTRwt or psiCHECK-UTRdel (Figure 4B).

Similarly, the co-transfection of HEK293 T cells with miR-155 and psiCHECK-UTRwt led to a significant reduction (~65%) in reporter luciferase activity, while there was no difference observed for the co-transfection of HEK293 T cells with miR-155 and psiCHECK-UTRdel or for the co-transfection of miR-Ctrl and either psiCHECK-UTRwt or psiCHECK-UTRdel. Moreover, the co-transfection of HEK293 T cells with psiCHECK-UTRwt and both miR-9 and −155 led to a reduction (~65%) in reporter luciferase activity, but this reduction was not greater than that achieved using miR-155 alone, suggesting that either miR-155 or −9 alone could achieve robust downregulation of CTLA-4.

Altogether, these results demonstrate the roles of miR-9 and −155 in the regulation of CTLA-4 expression through direct and specific binding to their target sites.

The *GARP* 3′-UTR is Directly Targeted by miR-24 and −335

Analysis of reporter luciferase activity in HEK293 T cells co-transfected with the *GARP* 3′-UTR, wild-type or miRNA site-deleted, and either miR-24 (Figure 4C) or miR-335 (Figure 4D), showed a direct and specific targeting of the *GARP* 3′-UTR by these miRNAs, leading to reduced luciferase expression.

Lentiviral Expression of miR-335 in fresh Treg Cells Significantly Reduces *FOXP3* Transcription

To study the effect of over-expression of miR-335 in Treg cells, specifically on FOXP3 expression, lenti-miR-335 was used to transduce Treg cells (Figure 5); transduced Treg cells were FACS-sorted based on GFP positivity. The miR-335 levels in lenti-miR-335-transduced Treg cells were significantly higher than in lenti-miR-ctrl transduced cells, whereas the levels of miR-335 were two-fold lower in Treg cells compared with their negative counterparts (Figure 6A). The control for each miRNA transduction was a scrambled miR sequence. Clearly, the expression levels of miR-335 in transduced Treg cells were higher than the physiological level observed in non-Treg cells, but this resulted from our inability to adjust the levels of expression of the transgene. Nevertheless, this finding indicates that miR-335 can down-regulate FOXP3 expression, although not to the level of non-Treg cells, demonstrating that FOXP3 expression must be controlled by combined inputs from several pathways, including miR-335. Additionally, the levels of FOXP3 were 3.19-fold lower in lenti-miR-31 transduced cells compared with lenti-miR-ctrl and non-transduced cells [68]. These results demonstrate that FOXP3 expression is controlled by miR-335.

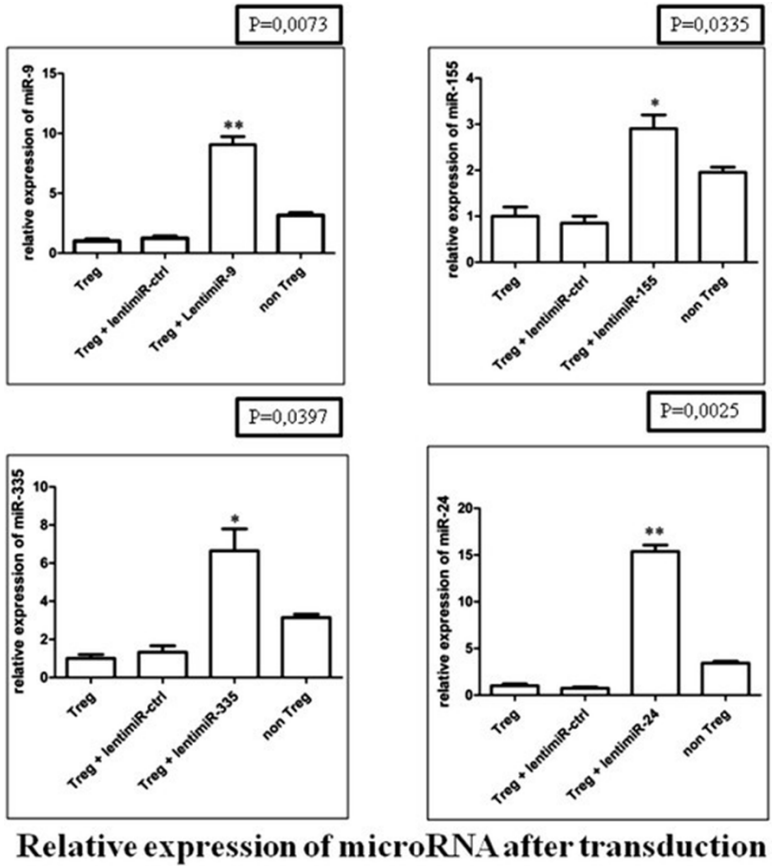

Figure 5: Differential expression of miR-24, −335, −155 and −9 in CD8 $^{+}$ CD25 $^{+}$ natural Treg cells after transduction by lenti-miR-24, −335, −155 and −9. Data obtained by qRT-PCR amplification of miRs are plotted for $CD8^{+}CD25^{+}$nTregs versus non-transduced $CD8^{+}CD25^{+}$ nTregs. *p* values for each miRNA relative expression are presented. *Boxes* represent SE; and Error bars SD. Pooled data from five independent experiments are shown. (*$p < 0.05$; **$p < 0.01$ Student's *t* test).

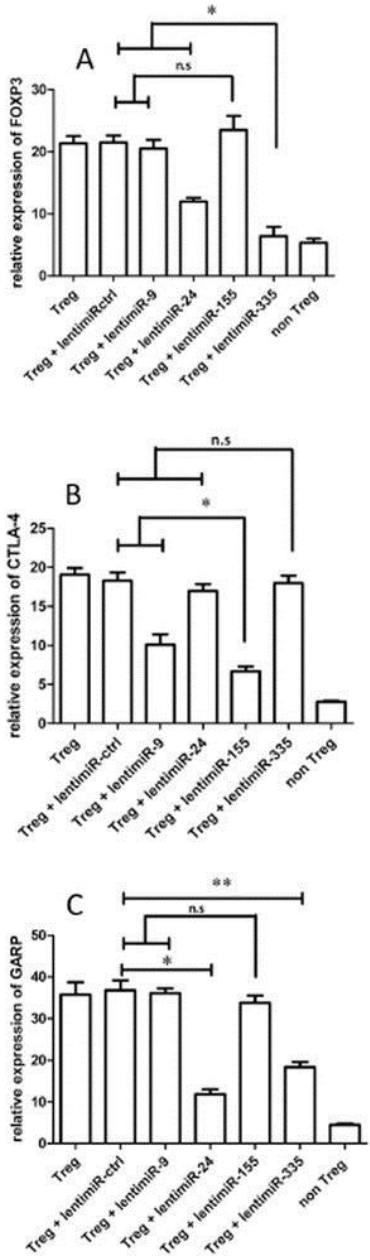

Figure 6: MicroRNA specific activities. **(A)** In primary human Treg cells, miR-335 specifically regulates FOXP3 expression. Relative miR-335 and FOXP3 expression in $CD8^{+}CD25^{+}$ Treg cells transduced by lenti-miR-335

compared with $CD8^+CD25^+$ Treg cells transduced by lenti-miR-Ctrl, as determined by relative qRT-PCR. **(B)** In primary human Treg cells, miR-9 and −155 specifically regulate CTLA-4 expression. Relative miR-9, miR-155 and CTLA-4 expression in $CD8^+CD25^+$ Treg cells transduced by lenti-miR-9 or lenti-miR-155 compared with $CD8^+CD25^+$ Treg cells transduced by lenti-miR-Ctrl, as determined by relative qRT-PCR. **(C)** In primary human Treg cells, miR-24 and −335 specifically regulate GARP expression. Relative miR-24 and GARP expression in $CD8^+CD25^+$ Treg cells transduced by lenti-miR-24 compared with $CD8^+CD25^+$ Treg cells transduced by lenti-miR-Ctrl, as determined by relative qRT-PCR. Relative miR-335 and GARP expression in $CD8^+CD25^+$ Treg cells transduced by lenti-miR-335 compared with $CD8^+CD25^+$ Treg cells transduced by lenti-miR-Ctrl. as determined by relative qRT-PCR. $CD8^+CD25^-$ T cells were considered to be non-Tregs; *p < 0.05, **p < 0.01, ***p < 0.001 (as determined by Student's *t*-test).

Lentiviral Transduction of miR-9 and −155 in Treg Cells Significantly Reduces CTLA-4 Expression

To study the effect of miR-9 and −155 on the mRNA expression levels of *CTLA-4*, we increased miR-9 and −155 levels by expressing the miR-9 and −155 precursors from a lentiviral vector (lenti-miR-9 and −155). After lenti-miR-9 and −155 viral transduction (Figure 5), we found that the mRNA levels of *CTLA-4* decreased (2.02-fold) in the lenti-miR-9-transduced Treg cells compared with the lenti-miR-ctrl transduced cells and the mRNA levels of *CTLA-4* decreased (2.79-fold) in the lenti-miR-155 transduced Treg cells compared with the lenti-miR-ctrl transduced cells (Figure 6B).

Lentiviral Transduction of miR-24 and −335 in Treg Cells Significantly Reduces GARP Expression

Efficient ex vivo transduction of Treg cells using lenti-miR-24 and lenti-miR-335 (Figure 5) showed that miR-24 and −335 expression significantly reduced GARP expression levels by 3.21- and 1.96-fold, respectively (Figure 6C).

Discussion

We previously described a miRNA signature in human natural $CD4^+$ Treg cells. We could also identify a miRNA signature in $CD4^+CD25^+CD127^{low}$ Treg cells from peripheral blood.

Importantly, for both signatures, we could show how the described miRNAs specifically regulate genes associated with Treg cell function in human primary T cells [68,69].

Here, we purified $CD8^+CD25^+$ natural Treg cells from human cord blood, assessed FOXP3 and CTLA-4 expression by flow cytometry and measured mRNA levels using quantitative PCR. As expected, FOXP3 and CTLA-4 protein and mRNA levels were increased in the $CD8^+CD25^+$ natural Treg cells compared with $CD8^+CD25^-$ T cells. Importantly, those cells showed suppressive properties ex vivo in a mixed T cell reaction in which irradiated allogeneic PBMCs were used as stimulators.

Reviewing the Treg cell literature, we identified a list of genes known to play an important role in the regulation of Treg cell function and development. We investigated the relative expression of these genes in $CD8^+CD25^+$ natural Treg cells compared with $CD8^+CD25^-$ T cells using qPCR. We found that expression of the *FOXP3*, *CTLA-4*, *CCR4*, *GARP*, *IL-10* and *TGF-β* genes was upregulated in $CD8^+CD25^+$ natural Treg cells, whereas the *CD28*, *ICOS*, *FOXO1* and *HELIOS* genes were underexpressed. Obviously, *IL2RA* (CD25) was found to be overexpressed by these Treg cells. Overall, these results further support the regulatory features and potential of these cells.

Using TaqMan low-density arrays and quantitative PCR confirmation of selected transcripts, we could define the first miRNA 'signature' for human purified $CD8^+CD25^+$ natural Treg cells. This 'signature' included 10 significantly differentially expressed miRs: miR-214, −205 and −509 were overexpressed, whereas miR-9, −24, −31, −155, −335, −210 and −449 were underexpressed in $CD8^+CD25^+$ natural Treg cells compared with $CD8^+CD25^-$ T cells.

Next, we investigated the potential role of the miRNAs from this signature on the expression of genes related to Treg cell function and development. We found that the 3′-UTR of FOXP3 contained miRNA target sites for miR-24, −31, −210 and −335, which were all underexpressed in $CD8^+CD25^+$ natural Treg cells compared with $CD8^+$CD25- T cells. Scanning the 3′-UTR of

CTLA-4 revealed that miR-9 and −155 (both underexpressed in Treg cells) contained a target site. Similarly, we found miR-24 and miR-335 target sites in the *GARP* 3′-UTR (Figure 7).

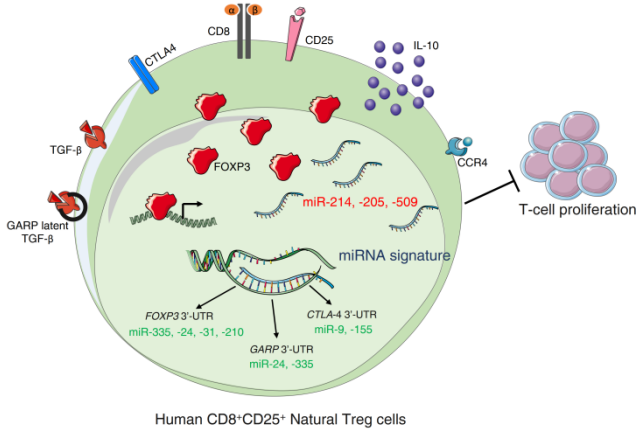

Figure 7: miRNA signature of human $CD8^{+}CD25^{+}$ Natural Treg cells and its impact on Treg-cell associated genes**.** Human $CD8^{+}CD25^{+}$ nTreg cells are characterized by their high expression of CD25 (IL2Rα), FOXP3, CTLA-4, CCR4, GARP, IL-10 and TGF-β in comparison to $CD8^{+}CD25^{-}$ T cells. The former cells have a specific miRNA signature that included 10 deregulated miRNAs: (red) miRNAs that are overexpressed and (green) miRNAs that are underexpressed. Interestingly, the underexpressed miRNAs can directly regulate the expression of important genes like FOXP3, CTLA-4 and GARP by binding to their respective 3'-UTR.

Although not Treg cell-specific, FOXP3 remains the best-known transcription factor that specifically orchestrates a transcriptional program that is required for the establishment, maintenance and function of the Treg cell lineage.

Importantly, we have previously shown that miR-24, miR-210 and miR-31 [68,69] negatively regulate the expression of FOXP3 in human T cells. Interestingly, using 3′-UTR cloning, site-directed mutagenesis and miRNA co-transfection experiments, we demonstrated that miR-335 negatively regulates FOXP3 expression in a direct and specific manner. Moreover, transducing lenti-miR-335 in natural Treg cells leads to the negative regulation of FOXP3 expression compared with lenti-

miR-Ctrl transduced cells. Importantly, four out of the seven underexpressed miRNAs in the $CD8^+$ natural Treg cell miRNA 'signature' can regulate FOXP3 expression in primary Treg cells (Figure 7).

Many studies have focused on the role of CTLA-4 expression in Treg cells. Kolar et al. showed that CTLA-4 had an important function in Treg cell homeostasis and also highlighted the importance of CTLA-4 in the in vivo suppressive mechanism employed by Treg cells. These findings have identified CTLA-4 as a crucial costimulator of Treg cells by demonstrating its role in mediating the resistance of Treg cells to activation-induced cell death [70]. Additionally, CTLA-4 expression and signaling are essential for Treg cells to execute their suppressive function in vivo. Moreover, CTLA-4 has been described to play a negative role in tumor progression or persistence. These findings have brought several groups, including Jim Allison's group, to work on anti-CTLA-4 antibodies for cancer immunotherapy that have already shown very promising clinical results [70]. Considering the important role of CTLA-4 in Treg cell biology, we decided to investigate the effect of miR-9 and −155 (underexpressed in $CD8^+$ natural Treg cells) on CTLA-4 expression. Using the same strategy as we did for FOXP3, we carried out *CTLA-4* 3′-UTR cloning, site-directed mutagenesis and miRNA co-transfection experiments with a reporter luciferase activity assay and lentiviral-mediated microRNA transduction of primary natural Treg cells. We could show that both miR-9 and −155 negatively regulate CTLA-4 expression in a direct and specific way. Recently, miR-155 was shown to be overexpressed in tissues of patients with atopic dermatitis, associated with inflammatory $CD4^+$ T cells and capable of targeting *CTLA-4*. This study supports our findings by suggesting that miR-155 underexpression in $CD8^+$ natural Treg cells contributes to the regulation of CTLA-4 expression.

GARP received significant attention from the immune regulation field, as it is naturally produced by Treg cells and has the capacity to present latent TGF-β on the Treg cell surface. Very recently, Skapenko's group showed that miR-142-3p targeted GARP in $CD4^+CD25^+$ T cells [55] and Sophie Lucas' group

described that GARP is regulated by microRNAs (miR-142-3p, −181a and −185) and controls latent TGF-β production by human $CD4^+$ Treg cells [71]. Our experiments show that miR-24 and −335 specifically bind to the *GARP* 3′-UTR and directly regulate GARP expression in primary human $CD8^+$ natural Treg cells.

With great interest, we noticed the relatively high number of potential target sites for miRNAs in the signature that were found in many genes relevant to Treg cell biology. However, additional work will be required to prove that these miRNAs effectively regulate these genes.

In parallel, it is also interesting to note that the majority of miRNAs in the $CD8^+CD25^+$ natural Treg cell signature are also found to be differentially expressed in either the $CD4^+CD25^+$ natural Treg cell (miR-31) or the circulating peripheral blood $CD4^+CD25^+CD127^{low}$ Treg cell (miR-9, −24, −210, −335 and −509) signatures, which may suggest that a limited number of miRNAs control the expression of major features of Treg cells. While subpopulations of Treg cells that our group has studied do not encompass all human Treg cells described, they likely cover the vast majority of them.

Conversely, the miRNAs that are not shared by several Treg cell subpopulations could condition, or be conditioned by, phenotypic or functional differences between types of regulatory cells. In this sense, miR-155 appears in our miRNA signature to be more closely linked to $CD8^+$ natural Treg cells. It appears that miR-155 has an important role in the immune system. Romero's group described a specific important role for miR-155, in mice and humans, in the maturation of $CD8^+$ T cells from a naive to effector state and in their further acquisition of cytolytic properties; both processes correlated with high expression of miR-155 [72]. Our observation that miR-155 targets CTLA-4 in $CD8^+$ T cells can extend the insights provided by this group, suggesting an additional role for miR-155 that not only coordinates the expression of the machinery elements needed for cytotoxicity, but also controls some immunosuppressive

molecules during the effector phase of the cellular immune response.

Another observation shows that in a single subtype of human Treg cells, different microRNAs can target the 3′-UTR of the same gene (*FoxP3* is targeted by miR-24, −31, −210 and −335, *CTLA-4* is targeted by miR-9 and −155, and *GARP* is targeted by miR-24 and −335). Furthermore, a defined miRNA can target several genes important for Treg cells, suggesting a high level of coordination between miRNAs for the efficient regulation of a target gene or function. Our findings also suggest the existence of a 'program' carried out by a single miRNA that targets a set of genes associated with a type of activity.

All of these observations emphasize the importance of miRNA-mediated regulation of complex biological processes.

Caution should be taken when comparing miRNA signatures because they are always generated by relative comparisons to a cell type that is chosen and described as the negative counterpart of the cell population studied. This implies that a signature may vary when one swaps the cell taken as a 'counterpart'. Therefore, it is crucial not to limit oneself to the study of how miRNAs affect the expression of a reporter gene transfected in a cell line, but rather to look at the biological relevance of the signature in the corresponding fresh primary Treg cells using transduction by a vector expressing the miRNA of interest compared with a control vector.

Conclusions

We have identified an easy and convenient source of human $CD8^+CD25^+$ natural Treg cells and confirmed they share key known features of Treg cells. We reported for the first time the microRNA signature of these cells. Moreover, we found an essential role for six miRNAs out of 10 found in the signature, suggesting that this signature is directly relevant for Treg biology (Figure 7). The hypothesis that different signatures modulate distinct aspects of regulatory function should be explored. We are currently studying the role of these under- and

overexpressed miRNAs to identify new target genes implicated in the direct or indirect control of Treg cell biology. While much work still needs to be done to better understand the overall regulation of Treg cell functions, this study underlines the importance of miRNAs in this area and the chance that they offer to explore new therapeutic targets in immune disorders, infectious diseases and cancers.

References

1. Dinesh RK, Skaggs BJ, La Cava A, Hahn BH, Singh RP: CD8+ Tregs in lupus, autoimmunity, and beyond. Autoimmun Rev. 2010; 9: 560-568.
2. Daniele N, Scerpa MC, Landi F, Caniglia M, Miele MJ, et al. T(reg) cells: collection, processing, storage and clinical use. Pathol Res Pract. 2011; 207: 209-215.
3. Huseby ES, Liggitt D, Brabb T, Schnabel B, Ohlen C, et al. A pathogenic role for myelin-specific CD8(+) T cells in a model for multiple sclerosis. J Exp Med. 2001; 194: 669-676.
4. Liblau RS, Wong FS, Mars LT, Santamaria P. Autoreactive CD8 T cells in organ-specific autoimmunity: emerging targets for therapeutic intervention. Immunity. 2002; 17: 1-6.
5. Miller A, Lider O, Roberts AB, Sporn MB, Weiner HL. Suppressor T cells generated by oral tolerization to myelin basic protein suppress both in vitro and in vivo immune responses by the release of transforming growth factor beta after antigen-specific triggering. Proc Natl Acad Sci U S A. 1992; 89: 421-425.
6. Zhang GX, Ma CG, Xiao BG, Bakhiet M, Link H, et al. Depletion of CD8+ T cells suppresses the development of experimental autoimmune myasthenia gravis in Lewis rats. Eur J Immunol. 1995; 25: 1191-1198.
7. Martin PJ. Donor CD8 cells prevent allogeneic marrow graft rejection in mice: potential implications for marrow transplantation in humans. J Exp Med. 1993; 178: 703-712.
8. Fowler DH, Breglio J, Nagel G, Eckhaus MA, Gress RE. Allospecific CD8+ Tc1 and Tc2 populations in graft-versus-leukemia effect and graft-versus-host disease. J Immunol. 1996; 157: 4811-4821.

9. Prezzi C, Casciaro MA, Francavilla V, Schiaffella E, Finocchi L, et al. Virus-specific CD8(+) T cells with type 1 or type 2 cytokine profile are related to different disease activity in chronic hepatitis C virus infection. Eur J Immunol. 2001; 31: 894-906.
10. Hu D, Weiner HL, Ritz J. Identification of cytolytic Cytolytic CD161^{-}CD56^{+} Regulatory CD8 T Cells in Human Peripheral Blood. PLoS One. 2013; 8: e59545
11. Xystrakis E, Dejean AS, Bernard I, Druet P, Liblau R, et al. Identification of a novel natural regulatory CD8 T-cell subset and analysis of its mechanism of regulation. Blood. 2004; 104: 3294-3301.
12. Uss E, Rowshani AT, Hooibrink B, Lardy NM, van Lier RA, et al. CD103 is a marker for alloantigen-induced regulatory CD8+ T cells. J Immunol. 2006; 177: 2775-2783.
13. Tilburgs T, Roelen DL, van der Mast BJ, van Schip JJ, Kleijburg C, et al. Differential distribution of CD4(+)CD25(bright) and CD8(+)CD28(−) T-cells in decidua and maternal blood during human pregnancy. Placenta. 2006; 27: S47-S53.
14. Tennakoon DK, Mehta RS, Ortega SB, Bhoj V, Racke MK, et al. Therapeutic induction of regulatory, cytotoxic CD8+ T cells in multiple sclerosis. J Immunol. 2006; 176: 7119-7129.
15. Shao L, Jacobs AR, Johnson VV, Mayer L. Activation of CD8+ regulatory T cells by human placental trophoblasts. J Immunol. 2005; 174: 7539-7547.
16. Popescu I, Macedo C, Abu-Elmagd K, Shapiro R, Hua Y, et al. EBV-specific CD8+ T cell reactivation in transplant patients results in expansion of CD8+ type-1 regulatory T cells. Am J Transplant. 2007; 7: 1215-1223.
17. Joosten SA, van Meijgaarden KE, Savage ND, de Boer T, Triebel F, et al. Identification of a human CD8+ regulatory T cell subset that mediates suppression through the chemokine CC chemokine ligand 4. Proc Natl Acad Sci U S A. 2007; 104: 8029-8034.
18. Filaci G, Fenoglio D, Fravega M, Ansaldo G, Borgonovo G, et al. CD8+ CD28- T regulatory lymphocytes inhibiting T cell proliferative and cytotoxic functions infiltrate human cancers. J Immunol. 2007; 179: 4323-4334.

19. Cosmi L, Liotta F, Lazzeri E, Francalanci M, Angeli R, et al. Human CD8+CD25+ thymocytes share phenotypic and functional features with CD4+CD25+ regulatory thymocytes. Blood. 2003; 102: 4107-4114.
20. Colovai AI, Mirza M, Vlad G, Wang S, Ho E, et al. Regulatory CD8+CD28- T cells in heart transplant recipients. Hum Immunol. 2003; 64: 31-37.
21. Chang CC, Ciubotariu R, Manavalan JS, Yuan J, Colovai AI, et al. Tolerization of dendritic cells by T(S) cells: the crucial role of inhibitory receptors ILT3 and ILT4. Nat Immunol. 2002; 3: 237-243.
22. Cai J, Lee J, Jankowska-Gan E, Derks R, Pool J, et al. Minor H antigen HA-1-specific regulator and effector CD8+ T cells, and HA-1 microchimerism, in allograft tolerance. J Exp Med. 2004; 199: 1017-1023.
23. Brimnes J, Allez M, Dotan I, Shao L, Nakazawa A, et al. Defects in CD8+ regulatory T cells in the lamina propria of patients with inflammatory bowel disease. J Immunol. 2005; 174: 5814-5822.
24. Bisikirska B, Colgan J, Luban J, Bluestone JA, Herold KC. TCR stimulation with modified anti-CD3 mAb expands CD8+ T cell population and induces CD8+CD25+ Tregs. J Clin Invest. 2005; 115: 2904-2913.
25. Billerbeck E, Blum HE, Thimme R. Parallel expansion of human virus-specific FoxP3- effector memory and de novo-generated FoxP3+ regulatory CD8 T cells upon antigen recognition in vitro. J Immunol. 2007; 179: 1039-1048.
26. Gilliet M, Liu YJ. Generation of human CD8 T regulatory cells by CD40 ligand-activated plasmacytoid dendritic cells. J Exp Med. 2002; 195: 695-704.
27. Shi Z, Okuno Y, Rifa'i M, Endharti AT, Akane K, et al. Human CD8+CXCR3+ T cells have the same function as murine CD8+CD122+ Treg. Eur J Immunol. 2009; 39: 2106-2119.
28. Yagi H, Nomura T, Nakamura K, Yamazaki S, Kitawaki T, et al. Crucial role of FOXP3 in the development and function of human CD25+CD4+ regulatory T cells. Int Immunol. 2004; 16: 1643-1656.
29. Wildin RS, Ramsdell F, Peake J, Faravelli F, Casanova JL, et al. X-linked neonatal diabetes mellitus, enteropathy and

endocrinopathy syndrome is the human equivalent of mouse scurfy. Nat Genet. 2001; 27: 18-20.
30. Bennett CL, Christie J, Ramsdell F, Brunkow ME, Ferguson PJ, et al. The immune dysregulation, polyendocrinopathy, enteropathy, X-linked syndrome (IPEX) is caused by mutations of FOXP3. Nat Genet. 2001; 27: 20-21.
31. Khattri R, Cox T, Yasayko SA, Ramsdell F. An essential role for Scurfin in CD4+CD25+ T regulatory cells. Nat Immunol. 2003; 4: 337-342.
32. Buckner JH, Ziegler SF. Functional analysis of FOXP3. Ann NY Acad Sci. 2008; 1143: 151-169.
33. Kolar P, Knieke K, Hegel JK, Quandt D, Burmester GR, et al. CTLA-4 (CD152) controls homeostasis and suppressive capacity of regulatory T cells in mice. Arthritis Rheum. 2009; 60: 123-132.
34. Hori S, Nomura T, Sakaguchi S. Control of regulatory T cell development by the transcription factor Foxp3. Science. 2003; 299: 1057-1061.
35. Fontenot JD, Gavin MA, Rudensky AY. Foxp3 programs the development and function of CD4+CD25+ regulatory T cells. Nat Immunol. 2003; 4: 330-336.
36. Wang R, Kozhaya L, Mercer F, Khaitan A, Fujii H, et al. Expression of GARP selectively identifies activated human FOXP3+ regulatory T cells. Proc Natl Acad Sci U S A. 2009; 106: 13439-13444.
37. Ariyan C, Salvalaggio P, Fecteau S, Deng S, Rogozinski L, et al. Cutting edge: transplantation tolerance through enhanced CTLA-4 expression. J Immunol. 2003; 171: 5673-5677.
38. Kavvoura FK, Ioannidis JP. CTLA-4 gene polymorphisms and susceptibility to type 1 diabetes mellitus: a HuGE Review and meta-analysis. Am J Epidemiol. 2005; 162: 3-16.
39. Ribas A, Camacho LH, Lopez-Berestein G, Pavlov D, Bulanhagui CA, et al. Antitumor activity in melanoma and anti-self responses in a phase I trial with the anti-cytotoxic T lymphocyte-associated antigen 4 monoclonal antibody CP-675,206. J Clin Oncol. 2005; 23: 8968-8977.
40. Tran DQ, Andersson J, Wang R, Ramsey H, Unutmaz D, et al. GARP (LRRC32) is essential for the surface expression

of latent TGF-beta on platelets and activated FOXP3+ regulatory T cells. Proc Natl Acad Sci U S A. 2009; 106: 13445-13450.
41. Stockis J, Colau D, Coulie PG, Lucas S. Membrane protein GARP is a receptor for latent TGF-beta on the surface of activated human Treg. Eur J Immunol. 2009; 39: 3315-3322.
42. Han J, Lee Y, Yeom KH, Nam JW, Heo I, et al. Molecular basis for the recognition of primary microRNAs by the Drosha-DGCR8 complex. Cell. 2006; 125: 887-901.
43. Lee Y, Ahn C, Han J, Choi H, Kim J, et al. The nuclear RNase III Drosha initiates microRNA processing. Nature. 2003; 425: 415-419.
44. Lee Y, Han J, Yeom KH, Jin H, Kim VN. Drosha in primary microRNA processing. Cold Spring Harb Symp Quant Biol. 2006; 71: 51-57.
45. Yeom KH, Lee Y, Han J, Suh MR, Kim VN. Characterization of DGCR8/Pasha, the essential cofactor for Drosha in primary miRNA processing. Nucleic Acids Res. 2006; 34: 4622-4629.
46. Bohnsack MT, Czaplinski K, Gorlich D. Exportin 5 is a RanGTP-dependent dsRNA-binding protein that mediates nuclear export of pre-miRNAs. RNA. 2004; 10: 185-191.
47. Chendrimada TP, Gregory RI, Kumaraswamy E, Norman J, Cooch N, et al.TRBP recruits the Dicer complex to Ago2 for microRNA processing and gene silencing. Nature. 2005; 436: 740-744.
48. Lund E, Guttinger S, Calado A, Dahlberg JE, Kutay U. Nuclear export of microRNA precursors. Science. 2004; 303: 95-98.
49. Liu J, Carmell MA, Rivas FV, Marsden CG, Thomson JM, et al. Argonaute2 is the catalytic engine of mammalian RNAi. Science. 2004; 305: 1437-1441.
50. Lingel A, Simon B, Izaurralde E, Sattler M. Structure and nucleic-acid binding of the Drosophila Argonaute 2 PAZ domain. Nature. 2003; 426: 465-469.
51. Stefani G, Slack FJ. Small non-coding RNAs in animal development. Nat Rev Mol Cell Biol. 2008; 9: 219-230.
52. Williams AE. Functional aspects of animal microRNAs. Cell Mol Life Sci. 2008; 65: 545-562.

53. Tili E, Michaille JJ, Gandhi V, Plunkett W, Sampath D, et al. miRNAs and their potential for use against cancer and other diseases. Future Oncol. 2007; 3: 521-537.
54. Lu LF, Thai TH, Calado DP, Chaudhry A, Kubo M, et al. Foxp3-dependent microRNA155 confers competitive fitness to regulatory T cells by targeting SOCS1 protein. Immunity. 2009; 30: 80-91.
55. Zhou Q, Haupt S, Prots I, Thummler K, Kremmer E, et al. miR-142-3p is involved in CD25+ CD4 T cell proliferation by targeting the expression of glycoprotein A repetitions predominant. J Immunol. 2013; 190: 6579-6588.
56. Huang B, Zhao J, Lei Z, Shen S, Li D, et al. miR-142-3p restricts cAMP production in CD4+ CD25- T cells and CD4+CD25+ TREG cells by targeting AC9 mRNA. EMBO Rep. 2009; 10: 180-185.
57. de Kouchkovsky D, Esensten JH, Rosenthal WL, Morar MM, Bluestone JA, et al. microRNA-17-92 regulates IL-10 production by Tregs and control of experimental autoimmune encephalomyelitis. J Immunol. 2013; 191: 1594-1605.
58. Ha TY. The Role of MicroRNAs in Regulatory T Cells and in the Immune Response. Immun Netw. 2011; 11: 11-41.
59. Bresatz S, Sadlon T, Millard D, Zola H, Barry SC. Isolation, propagation and characterization of cord blood derived CD4+ CD25+ regulatory T cells. J Immunol Methods. 2007; 327: 53-62.
60. Naldini L, Blomer U, Gallay P, Ory D, Mulligan R, et al. In vivo gene delivery and stable transduction of nondividing cells by a lentiviral vector. Science. 1996; 272: 263-267.
61. Zufferey R, Nagy D, Mandel RJ, Naldini L, Trono D. Multiply attenuated lentiviral vector achieves efficient gene delivery in vivo. Nat Biotechnol. 1997; 15: 871-875.
62. Yeung ML, Bennasser Y, Le SY, Jeang KT. siRNA, miRNA and HIV: promises and challenges. Cell Res. 2005; 15: 935-946.
63. Johnston JC, Gasmi M, Lim LE, Elder JH, Yee JK, et al. Minimum requirements for efficient transduction of dividing and nondividing cells by feline immunodeficiency virus vectors. J Virol. 1999; 73: 4991-5000.

64. Abbas-Terki T, Blanco-Bose W, Deglon N, Pralong W, Aebischer P. Lentiviral-mediated RNA interference. Hum Gene Ther. 2002; 13: 2197-2201.
65. Cobb BS, Hertweck A, Smith J, O'Connor E, Graf D, et al. A role for Dicer in immune regulation. J Exp Med. 2006; 203: 2519-2527.
66. Krek A, Grun D, Poy MN, Wolf R, Rosenberg L, et al. Combinatorial microRNA target predictions. Nat Genet. 2005; 37: 495-500.
67. Grimson A, Farh KK, Johnston WK, Garrett-Engele P, Lim LP, et al. MicroRNA targeting specificity in mammals: determinants beyond seed pairing. Mol Cell. 2007; 27: 91-105.
68. Rouas R, Fayyad-Kazan H, El Zein N, Lewalle P, Rothe F, et al. Human natural Treg microRNA signature: role of microRNA-31 and microRNA-21 in FOXP3 expression. Eur J Immunol. 2009; 39: 1608-1618.
69. Fayyad-Kazan H, Rouas R, Fayyad-Kazan M, Badran R, El Zein N, et al. MicroRNA profile of circulating CD4+ regulatory T cells in human adults and impact of differentially expressed microRNAs on expression of two genes essential to their function. J Biol Chem. 2012; 287: 9910-9922.
70. Pandiyan P, Gartner D, Soezeri O, Radbruch A, Schulze-Osthoff K, et al. CD152 (CTLA-4) determines the unequal resistance of Th1 and Th2 cells against activation-induced cell death by a mechanism requiring PI3 kinase function. J Exp Med. 2004; 199: 831-842.
71. Gauthy E, Cuende J, Stockis J, Huygens C, Lethe B, et al. GARP Is Regulated by miRNAs and Controls Latent TGF-beta1 Production by Human Regulatory T Cells. PLoS One. 2013; 8: e76186
72. Dudda JC, Salaun B, Ji Y, Palmer DC, Monnot GC, et al. MicroRNA-155 is required for effector CD8+ T cell responses to virus infection and cancer. Immunity. 2013; 38: 742-753.

Book Chapter

Metabolic Deregulations in Acute Myeloid Leukemia

Mossuz P[1,3]*, Mondet J[2,3] and Chevalier S[1,3]

[1]Department of biological hematology, Institut of Biology and Pathlogy, University Hospital of Grenoble, France
[2]Department of molecular pathology, Institut of Biology and Pathlogy, University Hospital of Grenoble, France
[3]Institute for Advanced Bioscience UMR1209 Inserm University of Grenoble Alpes (UGA), France

***Corresponding Author:** Mossuz Pascal, Department of biological hematology, Institut of Biology and Pathlogy, University Hospital of grenoble, CS 10217 38043 Grenoble cedex 9, France

Published **January 20, 2021**

How to cite this book chapter: Mossuz P, Mondet J, Chevalier S. Metabolic Deregulations in Acute Myeloid Leukemia. In: Hussein Fayyad Kazan, editor. Immunology and Cancer Biology. Hyderabad, India: Vide Leaf. 2021.

Introduction

Acute myeloid leukemia (AML) is a bone marrow cancer affecting the myeloïd compartment of hematopoietic cells, leading to the accumulation of immature cells called leukemic blasts in the bone marrow and the peripheral blood. The leukemic population comprises stem cells and cells at a very

early stage of differentiation. Consequently, the prognosis of AML is very poor, with a 5-year survival rate(excluding AML3)of about 35-40% for patients until 60 years, and decreasing to 5-15% for patients over 60 years of age [1].

Molecular genetic, abnormalities associated with the emergence and development of leukemic clones, revealed that many cellular functions are deregulated [2]. Mutations occurring in the *FLT3*, *RAS* or *KIT* genes result in hyperactivation of signaling pathways [3,4] providing a proliferative advantage to the transformed cells. Oncogenic fusion genes, such as *PML-RARA* or *AML1-ETO* [5] are responsible for cell differentiation blockage, and mutations in genes involved in epigenetic control of gene expression, such as *ASXL1*, *DNMT3A*, *IDH* or *TET2*, lead to deregulation of the chromatin structure (via chemical changes in histones) or abnormalities in DNA methylation [1]. Finally, it is now well documented that these abnormalities can also lead to alterations in metabolism that play a critical role in leukemogenesis and in the phenotypic characteristics of leukemic cells [6]. The most described example in AML are the *IDH1* and *IDH2* mutations, which lead to production of an oncometabolite, the 2-Hydroxy-Glutarate (2HG), instead of α-Ketoglutarate (α-KG) [7]. The increase in 2-HG directly impacts the metabolic functions of leukemic cells promoting their proliferation at the expense of normal hematopoietic stem cells (see below for more details of impact of *IDH* mutations).

I-Metabolic Deregulation in AML

Like most cancer cells, AML cells are characterized by a rapid and uncontrolled proliferation that requires nutrients and energy. To achieve this, several mechanisms are put into play. The best known is the Warburg effect, described in the 1920s by Otto Heinrich Warburg, who showed that regardless of oxygenation conditions, cancer cells preferentially use aerobic glycolysis, which converts glucose into lactate, to produce energy and maintain cancer proliferation [8]. Despite poor energy efficiency (in terms of the production of ATP molecules), cancer cells maintain aerobic glycolysis to favor the production of intermediate products from glycolysis, mandatory for generating

nucleotides, lipids or amino acids. This allows a rapid supply of the components essential to the formation of future daughter cells, and thus a more effective cell proliferation [9]. Beyond the Warburg effect, many metabolic pathways are involved in the leukemic process.

Mutations of Genes Encoding the Isocitrate Dehydrogenase (IDH)

Isocitrate dehydrogenase (IDH) catalyzes the decarboxylation of isocitrate leading to the production of alpha-ketoglutarate (KG) and NAdPH/NADH. IDH1, located in the cytoplasm, promotes the generation of NADPH but also, thanks to the carboxylation of the α-KG in isocitrate, the acetylCoA and lipid generation after conversion of citrate into acetyl-coA. IDH2 regulates the concentration of α-KG and isocitrate in the mitochondria using NAD to oxidize isocitrate in α-KG in the Tri-carboxylic acid (TCA) cycle [10]. Finally, there is a third isoform, the IDH3, which is NAD-dependent and which promotes the production of α-KG required for the generation of succinate and then ATP [11].

In AML, *IDH* gene mutations are found in about 15-20% of patients. Only the two isoforms IDH1 and IDH2 can be mutated but the two mutations are mutually exclusive. Mutations affect arginine residues critical for the IDH function, codon R132 for *IDH1* and codons R140 and R172 for *IDH2*. They are "gain of function" mutations that both result in the production of a new metabolite, the 2-Hydroxy-Glutarate (2HG) instead of KG in tumor cells [7]. It should be noted that the mutation does not cause any change in the concentration of α-KG in the serum, nor other intermediary metabolites of the TCA cycle, such as succinate, malate or fumarate [12]. In addition, 2-HG is the only product of the transformation of the α-KG by mutated IDH [13]. Interestingly, the amount of 2-HG produced by tumor cells negatively correlates with the prognosis of the disease [14].

2HG behaves as a competitive inhibitor for many enzymes using KG as a cofactor, such as prolyl hydroxylases, histone demethylases, JmjC or 5-methyl hydroxylase of the TET family.

Thereby, the production of 2HG impacts the methylation level of DNA and histones resulting in a hypermethylated DNA, responsible for altering the epigenetic regulation of gene expression [15]. This phenomenon contributes to the differentiation blockage in leukemic cells and thus to the initiation and progression of AML [16]. On the other hand, alterations of prolyl hydroxylase function increase the expression levels of the HIF factor promoting the proliferation of leukemic cells under hypoxic conditions. Concurrently to *IDH* mutations, glutathione concentration is reduced, secondary to the increased NADPH consumption, decreasing the anti-oxidant capacity of cells [17].

Deregulation of Glucose Metabolism

Very intense glucose consumption and very high absorption of this metabolite into the bone marrow have been widely described in AML. AML bone marrow cells display high levels of glucose uptake and high levels of aerobic glycolysis at diagnosis that are correlated with survival and response to chemotherapy. NMR analysis of 443 AML patients showed a specific signature of glucose metabolism, based on the levels of a panel of six metabolites involved in glycolysis (glycerol-3-phosphate, pyruvate, lactate) and in the TCA cycle (citrate, α-KG, 2-HG). This signature confers an adverse prognosis to normal karyotype AMLs, which results in a weak response to aracytin treatment [18]. Similarly, high levels of serum LDH at diagnosis are highly negative prognostic markers in AML [10].

Given the high rate of glucose use by leukemic cells, they can improve their glucose absorption, specifically in case of too low intake levels, by positively regulating the gene *SLC2A5*, which encodes for the trans-membrane glucose transporter, GLUT5. Indeed, *GLUT5* over-expression was associated with a poor prognosis, and conversely, inhibition of this carrier increased the susceptibility of leukemic cells to Ara-C. Similarly, overexpression of mRNA coding for GLUT1, another member of GLUT family, has been associated with poor responsiveness to chemotherapy [19,20].

The PI3K/AKT/mTOR pathway is frequently implicated in deregulation of glycolytic activity. The hexokinase HK2 which catalyzes the first step of glycolysis could be activated by PI3K/AKT dependent mechanisms. mTOR plays an important role in leukemic cell addiction to glucose, through regulation of G6PD (Glucose-6-Phosphate Dehydrogenase), which is an important source of NADPH and which intervenes in the maintenance of the energy metabolism of leukemic cells. In addition, overexpression of G6PD is strongly correlated with an adverse prognosis in AML patients [21]. Indeed, inhibition of G6PD by nicotinamide induces AML blast apoptosis while non affecting normal hematopoiesis. mTORC1 plays also an important regulatory role in the pentose phosphate pathway that is an important pathway for cell survival in AML and all cancers. MAP kinase, a serine/threonine kinase, also promotes the use of glucose and glycolysis by leukemic cells. Its deletion leads to inhibition of leukemic stem cells by decreasing glucose flow and oxidative stress in the hypoglycemic medullary microenvironment [22] through reducing the expression of GLUT1.

Finally, it has been shown that leukemic cells can induce complex variations of the metabolic homeostasis of the host, in order to ensure high glucose concentrations in the bone marrow. In particular, leukemic cells cause increase of insulin resistance and inhibition of insulin secretion by tissues [23]. Such modifications result from an increased production of IGFBP1 by adipose tissue.

Deregulations of Glutamine Metabolism

Glutamine, which is *either produced in* the cell or imported by the glutamine transporter SLC1A5, plays a particular role in normal cells. It fuels the TCA cycle, through regulation of glutathione production and impacts on mTORC1 activity, via regulation of leucine export [24].

Glutamine is particularly involved in the metabolic reprogramming of cancer and leukemic cells [25]. Leukemic cells use glutamine as a source of carbon for energy production

via the TCA cycle. Therefore, leukemic cells have developed an addiction to glutamine [26] on which they depend for survival and proliferation. Consequently, plasma glutamine concentrations in AML patients are much lower than those found in healthy individuals and that KO of *SLC1A5* leads to apoptosis of AML cell lines. Similarly, glutaminase (GLS) is found to be strongly expressed in AML, making it a critical factor for TCA cycle activity [27].

Indeed, many studies have shown that targeting glutaminolysis in AML is a good strategy in the search for new therapeutic agents. This is particularly the case in mutated *FLT3-ITD* AML, which are highly dependent on glutamine to produce energy [28,29]. Targeting glutamine absorption leads to efficient anti-leukemia responses, which may be related to the impact of Glutamine levels on mTORC1 activity [30]. The balance between glutaminolysis and TCA cycle activity therefore appears to be essential in the survival of leukemic cells [10,31]. Moreover, it has been shown that L-Asparaginase which could catalyze the degradation of glutamine suppresses mTORC1 activity leading to AML cell apoptosis. Thereby, this agent well known for its antileukemic activity in ALL, has been proposed for the treatment of AML and recently, an impact on refractory AML has been reported.

Finally, glutamine plays an essential role to control redox homeostasis in AML cells, through its impact on glutathione synthesis and on oxidative phosphorylation in the mitochondria. Blockade of glutathione production through a specific inhibitor provokes accumulation of mitochondrial ROS in multiple AML types and subsequently apoptotic cell death.

Deregulations of Lipid Metabolism

Lipids play a particularly important role in energy production as well as the synthesis of signaling macromolecules for cells. The lipid balance depends on the balance between the lipid intakes and their consumption by oxidation (fatty acid oxidation-FAO) which feed the TCA. As a result, the absorption and consumption of fatty acid (FA) impacts important aspects of the

biology of cancer cells [32]. Indeed, overexpression of FASN (Fatty Acid Synthase), which is a key metabolic enzyme for the final stage of FA synthesis, provides a growth and survival benefit for cancer cells. Interestingly, FASN expression is affected by certain components that play a critical role in cancer metabolism such as PI3K/AKT/mTOR and MAPK signaling pathways [33,34]. Moreover, under metabolic stress conditions, in addition to the increase in lipogenesis, tumor cells can acquire FA *via* lipolysis to support their growth. They will also tend to recover extracellular lipids to maintain their proliferation and survival [35,36]. This lipolysis is mediated by a key enzyme: Lipoprotein Lipase (LPL).Its high activity has been described in lung cancers. LPL has been also identified as a marker of poor prognosis in chronic lymphoid leukemias [37].

In AMLs, absorption and consumption of FA influence the fate of Leukemic Stem Cells (LSC), their adaptation to the microenvironment and their resistance to drugs [10]. The consumption of FA is increased in leukemic cells in order to meet their needs of lipid biosynthesis [38-40]. In promyelocytic AML, the division of HSCs is regulated by FAO and FAO lowers the threshold for apoptosis and promotes the quiescence of leukemic cells. Several lipid profiles representative of different types of AML have recently been identified by mass spectrometry. Significant differences in the modulation of ceramides and sphingolipid synthesis were found in patients with t(8;21) compared to those with inv(16) or normal karyotype [41]. Also, *Stuani et al.* highlighted deregulations of lipid metabolism in a IDH1 mutated cell model of AML, compared to the un-mutated model. These differences are mainly characterized by an increase in phosphatidylinositol, sphingolipids, free cholesterol and monounsaturated FA in mutated IDH cells [42]. This, once again, highlights the impact of cytogenetic characteristics and mutational status of AML patients on cellular metabolism. Finally, a recent study showed a decrease in total FA in plasma of AML patients as well as a reduction in phosphocholine, triglycerides and plasma ester cholesterol. Conversely, arachidonic acid appears to be increased in AML plasma, suggesting its involvement in the cancer phenotype [43].

The critical role of FA metabolism in AML is underlined by its impact on patient prognosis and the subsequent therapeutic interest of targeting this metabolism. A recent study showed that patients with rapidly progressing AML and who did not respond to treatment, had alterations in lipid metabolism compared to other patients [39]. ATP Citrate Lyase (ACL), the enzyme that catalyzes the production of acetyl-coA causes a blockade in cell growth when inhibited in leukemic cell models [44] and has also been shown to be associated with a favorable prognosis in AML patient with low levels of ACL.

In this context, several teams have tested different molecules to inhibit FAO. Among them, etomoxir sensitizes leukemic cells to apoptosis and decreases the number of quiescent progenitors [45]. Also, the molecule Avocatin B combined with a standard chemotherapy agent (AraC) induces apoptosis of AML cells and inhibition of cell growth [46]. Finally, *Picou et al* tested the impact of polyunsaturated FA on AML cell lines and on patient blasts [47]. This type of FA inhibited mitochondrial oxidative phosphorylation and increased glycolysis and oxidative stress, resulting in death of cancer cells. On the other hand, CPT1A, a sub-unit of the mitochondrial enzyme on which FAO relies, was found overexpressed in bone marrow samples from AML patients compared to normal bone marrow. This overexpression was strongly associated with an unfavorable prognosis [48]. FAO could therefore contribute to a mechanism promoting resistance to therapies. Indeed, resistant AML cells showed overexpression of the FA transporter, CD36, and a very intense FAO [49,50]. FAO-derived NADPH can be a decisive electron donor for leukemic cells under therapy, which then allows them to combat oxidative stress, and can be used in the anabolic processes necessary for cell division [10,51]. In addition, a new element, PHD3 (Prolyl Hydroxylase Domain 3), has been discovered as potentially interesting in the metabolism of AML. It is part of a class of enzymes capable of coordinating metabolism in response to changing cellular conditions. The normal function of this KG-dependent enzyme is to suppress FAO activity under conditions of nutrient abundance in the cellular environment. However, it has been shown that in AML, this enzyme is present at a low level, which leads to the

persistence of FAO regardless of external nutrient conditions. This could make PHD3 a very good biomarker of AML [52].

Deregulation of Phospholipid Metabolism

Very little information is available regarding the potential links between the deregulation of phospholipid metabolism and leukemogenesis. A team recently studied the plasma phospholipid profile of AML patients, and showed a decrease in free total FA, including phosphocholine, which is likely due to increase FA oxidation in AML cells [39]. This would have an adverse prognosis. Moreover, Wang *et al* showed lower phosphocholine (PC) levels in sera of AML patients, probably linked to the excessive need for this metabolite for leukemic proliferating cells. Interestingly, they also observed that this metabolite was expressed at a higher level in the serum of intermediate prognosis patients compared to favorable prognosis ones. This argues in favor of an adverse prognosis of the PC [39]. On the other hand, a significant decrease in phosphatidylserine (PS) and sphingomyelin (SM) have been described in the blood mononuclear cells of AML patients compared to healthy donors [53].

Finally, a much more recent study highlighted the involvement of an enzyme, the Taffarazine (TAZ) not yet described in AML [54,55]. TAZ is a mitochondrial enzyme that catalyzes the maturation of cardiolipin, and is therefore a key enzyme for phospholipid biosynthesis. TAZ suppression leads to a decrease in cancerous cell proliferation, inhibition of clonogenic growth and induction of leukemic cell differentiation, while preserving normal hematopoiesis. Interestingly, the study of the phospholipid profile of AML cells when TAZ is suppressed shows that, in addition to an expected decrease in cardiolipin, a decrease in phosphatidyl-ethanolamine and an increase in phosphatidylserine. Targeting phospholipid metabolism therefore appears to be a promising hypothesis for targeting LSC [54,55].

II-The Particular Role ok LKB1 in Pathogenesis of AML

One of the major controllers of adequacy between the energy production level and proliferation signals is the mTOR kinase (target of rapamycine). mTOR integrates mitogenic signals from PI3K/AKT that are based on the nutrient or energy reserves enabling synthesis of proteins, amino acids and lipids necessary for cell proliferation. Effectors modulate mTOR activation state via phosphorylation of the TSC1-TSC2 complex [56,57].

PI3K/AKT/mTOR pathway is one of the most frequently altered in tumors and in particular in AML [58], by mutation or due to deregulation of tumor suppressor genes such as *PTEN* [59]. These deregulations induce signals of proliferation and cell growth, but also have a significant impact on metabolic activity. AKT can induce an increase in glycolysis through increased glucose captation, FOXO inhibition or activation of protein glycosylation enzymes [60]. In addition, AKT strongly stimulates mTOR activity by inhibiting its degradation, thus promoting protein and lipid synthesis even in energy deficiency conditions. Similarly, the p53 protein, whose gene is frequently mutated or inhibited in tumors, is an important regulator of metabolism highlighting the close links between proliferation and metabolic changes in tumor cells [61].

One of the major signals detected by mTOR is the level of ATP (thus the energy level of the cell). When the intra-cellular ATP concentration decreases, the AMP/ATP ratio is modified resulting in the recruitment of AMPK that will inhibit mTOR signaling [62]. The phosphorylation of AMPK is performed by LKB1 which is a serine threonine kinase encoded by the STK11 gene located on chromosome 19p13.3 in humans [63,64]. This enzyme is involved in the regulation of cellular metabolism, while also governing important processes such as cell proliferation, polarity and migration, all of which being crucial in carcinogenesis [65]. Previous studies have identified several effectors regulated by LKB1. Some of them include major proteins in carcinogenesis, implicated in several cancers such as p53 [66] and the tumor suppressor gene PTEN (Phosphatase and

TENsin homolog) [67]. However, one of the most important targets of LKB1 is the AMP-dependent kinase protein (AMPK) activated by phosphorylation of threonine 172 [68], demonstrating the major role of the LKB1/AMPK axis in detecting cell energy levels. It has also been discovered that 14 other AMPK-like kinases are activated by LKB1, but of these, only AMPK 1 and 2 (catalytic components of AMPK) appear to be activated under low-nutrient conditions [69].

LKB1 was identified as a tumor suppressor when it was discovered that germ mutations occurring in the gene encoding for *LKB1* were responsible for a rare disease called Peutz-Jeghers syndrome (SPJ), which causes a predisposition to cancer [70]. In addition, LKB1 mutations or 19p chromosome losses are also implicated in sporadic pulmonary adenocarcinomas and somatic mutations of *LKB1* have been shown to synergize with human papillomavirus infections and promote disease progression in approximately 20% of cervical cancer patients [71].

Recent studies have shown that LKB1 may play a role in the pathophysiology of several hematological cancers, including AML [72]. However, in AML, unlike to what is observed in many solid tumors, the tumor suppressor role of LKB1 is controversial. LKB1 appears strongly expressed in leukemic stem cell population. Inhibition of LKB1 activity in these cells appears to stop their proliferation and make them more sensitive to chemotherapy. By studying gene expression profiles in a leukemic cell line (KG1a) expressing LKB1, it was found that the MAPK pathway was activated by LKB1 but independently of AMPK [73]. Therefore, unlike its tumor suppressor role in most cancers, in AML LKB1, via mechanisms independent of AMPK can act as a tumor promoting factor, even if this mechanism remains to be confirmed. Conversely, the LKB1 pathway through AMPK-dependent mTOR inhibition, is responsible for inhibiting protein translation and thus cell proliferation [72], in favor of a tumor suppressor action. In addition, in 7% of a cohort of 54 patients, a polymorphism in LKB1 was found in position 354 causing an amino acid change from leucine to phenylalanine (Leu354Phe) in the C-terminal

protein domain. This polymorphism would cause a decrease in AMPK activation mediated by LKB1 [74] and could have an unfavorable prognostic value in AML.

Another set of effector kinases activated by LKB1 are the SIK2 and 3 (Salt-Inducible Kinase) [75]. This LKB1-SIK2/3 axis has been very recently involved in the progression of AML. The activation of SIK2 and SIK3 following LKB1-mediated phosphorylation, promotes activation of the histone deacetylases (HDACs), which include HDAC 4, 5, 7 and 9 [73] Of these, HDAC4 is specifically involved in the progression of AML. Normally, when HDAC4 is active, it inhibits a repressive factor called MEF2C (Myocyte Enhancer Factor 2C), which has been found to be highly overexpressed in leukemias [72,74]. SIK2 and 3 by phosphorylating HDAC4 inhibit its deacetylation activity and therefore, HDAC4 cannot inhibit MEF2C leading to de-repression and expression of genes that promote the proliferation of AML cells. Thus, seen from this side, LKB1 seems to be pro-tumoral with regard to AML The treatment of these leukemic cells with SIK2/3 inhibitors confers sensitivity to drugs and death of these cells, giving rise to a potential therapeutic value for SIK inhibitors in AML cases positive with an activation of the LKB1-SIK axis [74].

III-Deregulation of Redox Balance

Reactive oxygen species (ROS) are the products of molecular oxygen metabolism by cells. They include superoxide anion O_2^- hydrogen peroxide H_2O_2, hydroxyl radicals and NO nitrogen monoxide. They can be generated by the electron transport system in the mitochondria and by the NADPH Oxydase (NOX) complexes at the membrane level [76]. Within the hematopoietic niche, hematopoietic stem cells (HSCs) proliferate in the most hypoxic part of the bone marrow and their differentiation roughly follows the oxygen gradient (from 6 to 1%) present in this hematopoietic niche [77]. The redox balance which reflects the balance between oxidizing and anti-oxidant (reducing) species, acts as a specific effector of certain regulatory effectors, and therefore directly impacts the cellular fate of the HSC. Hypoxia in the hematopoietic niche regulates NOX by keeping

ROS levels low, which helps to keep HSCs in quiescence [78], while protecting them from DNA damage, which can be induced by ROS [79]. Conversely, an increase in ROS can lead to changes in the phenotype of HSCs and promote their differentiation to progenitors [80]. Indeed, reactive oxygen species levels regulate transcription factors such as FOXO3, GATA-1, NFE2 and therefore play a decisive role in the engagement or progress of the maturation and differentiation processes of hematopoietic stem cells [81].

Redox-Dependent Changes in Leukemogenesis and AML

Excessive production of Reactive Oxygen Species has long been described in malignant hemopathies and in particular in acute myeloid leukemia (AML) or chronic myeloid leukemia (CML) [82]. Oxygenated radical levels are higher in AML blasts compared to normal leukocytes [83].

However, the mechanisms between ROS production and leukemia progression are still incompletely understood. Disturbances in anti-oxidant activities, particularly those dependent on FOXO transcription factors, can lead to an environment conducive to the generation of tumor clones. An excess of ROS production via the activation of NOX2 [84] has been shown in CD34 cells expressing the *RAS* mutation. The same is true with the *FLT3-ITD* and *NOX4* mutation [85]. Among other possibilities, inactivation of PTEN phosphatase by H_2O_2 may promote activation of the AKT pathway observed in AMLs.

AKT and *FLT3* are consistently activated in the majority of AML, suggesting inhibition of FOXO function and an increase in ROS levels compared to normal HSC [86], as well as regulation of leukemic cell survival, associated with resistance to chemotherapy [87]. Indeed, it appears that the aggressiveness and poor prognosis associated with *FLT3-ITD* mutated AML is due to the increase in endogenous ROS, which is produced by STAT5 transcription factor signaling and the activation of RAC1, which is an essential component of ROS-producing NOX

[88]. The expression of the *RUNX1-RUNX1T1* protein, associated with t(8;21), leads to a ROS-dependent increase in the survival and proliferation of hematopoietic precursors [78]. Finally, *IDH1/2* mutations are accompanied by a reduction in the synthesis of glutathione, secondary to the decline in NADPH production, which could increase the deleterious effect of ROS induced by the overproduction of 2HG [16]. Thus, significantly pro-oxidant conditions generally lead to cell death, but genetic changes in leukemic clones allow for survival and proliferation. Blast development could therefore be the result of a deficiency in the detection, response and/or integration of signals induced by partial oxygen pressure and redox potential.

Conversely, ROS-inducing chemotherapy selectively eradicates leukemia stem cells. Thus, inter-individual variations (SNP) of the gene coding for NADPH oxidase, the key enzyme in ROS emission, appear to influence the effectiveness of chemotherapy in AML [89]. In that meaning, a correlation between oxidative stress and the incidence of AML relapses was found as well as the therapeutic value of molecules targeting iron homeostasis and ROS production in chemotherapy-resistant AMLs [90]. Finally, our team recently showed that AML patients had a deregulated redox balance related to their molecular status, involving leukemia cells, non-tumor cells and the antioxidant system, which play a major role in the prognosis of patients [91]. In particular we showed that depending on the capacity of mitochondria to mobilize their spare capacity, we can identify different prognosis sub groups and that both high reduced/oxydative glutathione ratio and high thiol levels at diagnosis were associated with a lower risk of death.

The other major source of ROS is mitochondria. This production participates in redox signaling in normal cells but can also promote the tumor process. Although most tumor cells switch their metabolism to aerobic glycolysis (Warburg effect), mitochondria appear to remain functional and above all capable of producing ROS during the tumor process. In particular, in hypoxic conditions that normally decrease the production of mitochondrial ROS, leukemic cells can increase this production of ROS [92]. This increase promotes the proliferation of tumor

cells in a hypoxic environment, and the progression of the disease by their potential to damage DNA.

Mitochondrial ROS can also promote the tumor process by inducing damage to nuclear or mitochondrial DNA [93]. In addition, mutations in mitochondrial DNA cause a deficit in the activity of the mitochondrial respiratory chain and are associated with the overproduction of ROS [94]. Numerous studies have observed an increase in mitochondrial ROS induced by anti-leukemic treatments during apoptosis [95] but few studies have studied the pathophysiological role of mitochondrial ROS in leukemia. Mitochondrial ROS emitted by CD34 blasts appear to be weaker than those produced by normal CD34s [82]. However, a recent study also showed that blasts showed increased sensitivity to mitochondrial oxidative stress. These blast cells were characterized by an increase in mitochondrial mass, but without a concomitant increase in their respiratory activity [96].

Indeed, mitochondria play a key role in metabolism as well as in many processes such as apoptosis, calcium homeostasis and more recently in phospholipid metabolism (see above). Thus, dysfunctional mitochondria are highly involved in carcinogenesis and directly or indirectly in tumor cell replication, insensitivity to antiproliferative signals, sustained angiogenesis, invasiveness, avoidance of immune response [97,98]. Leukemic cells are characterized by an increase in mitochondrial mass, but without a concomitant increase in respiratory activity [96,99]. Although some tumor cells switch their metabolism to aerobic glycolysis (Warburg effect) most AML use oxidative phosphorylation to meet their energy needs. The microenvironment in particular stromal cells plays a role as a donor of mitochondria through the creation of nanotubes [100,101]. Thus, chemotherapy resistant leukemic cells have high levels of ROS and a high mitochondrial mass, which seems to be related to the transfer of mitochondria from the bone marrow to the blasts, which requires the activity of NOX2 that stimulates the release of mitochondria by stromal cells [100]. Aracytin-resistant leukemic cells show high use of oxidative phosphorylation, increased β-oxidation and hyperexpression of CD36 [51]. Therefore, targeting the synthesis of mitochondrial

proteins or the oxidation of fatty acids appears to be a promising way to improve therapeutic efficiency.

References

1. Döhner H, Weisdorf DJ, Bloomfield CD. Acute Myeloid Leukemia. N Engl J Med. 2015; 373: 1136–1152.
2. Grimwade D, Ivey A, Huntly BJP. Molecular landscape of acute myeloid leukemia in younger adults and its clinical relevance. Blood. 2016; 127: 29–41.
3. Sami SA, Darwish NHE, Barile ANM, Mousa SA. Current and Future Molecular Targets for Acute Myeloid Leukemia Therapy. Curr Treat Options Oncol. 2020; 21: 3.
4. Gaidzik V, Döhner K. Prognostic Implications of Gene Mutations in Acute Myeloid Leukemia With Normal Cytogenetics. Semin Oncol. 2008; 35: 346–355.
5. Chan WI, Huntly BJP. Leukemia Stem Cells in Acute Myeloid Leukemia. Semin Oncol. 2008; 35: 326–335.
6. Lo Presti C, Fauvelle F, Mondet J, Mossuz P. The differential activation of metabolic pathways in leukemic cells depending on their genotype and micro-environmental stress. Metabolomics Off J Metabolomic Soc. 2020; 16: 13.
7. Ward PS, Patel J, Wise DR. The Common Feature of Leukemia-Associated IDH1 and IDH2 Mutations Is a Neomorphic Enzyme Activity Converting α-Ketoglutarate to 2-Hydroxyglutarate. Cancer Cell. 2010; 17: 225–234.
8. Vander Heiden MG, Cantley LC, Thompson CB. Understanding the Warburg effect: the metabolic requirements of cell proliferation. Science. 2009; 324: 1029–1033.
9. DeBerardinis RJ, Chandel NS. Fundamentals of cancer metabolism. Sci Adv. 2016; 2: e1600200.
10. Kreitz, Schönfeld, Seibert. Metabolic Plasticity of Acute Myeloid Leukemia. Cells. 2019; 8: 805.
11. Castelli G, Pelosi E, Testa U. Emerging Therapies for Acute Myelogenus Leukemia Patients Targeting Apoptosis and Mitochondrial Metabolism. Cancers. 2019; 11: 260.
12. Janin M, Mylonas E, Saada V. Serum 2-hydroxyglutarate production in IDH1- and IDH2-mutated de novo acute myeloid leukemia: a study by the Acute Leukemia French

Association group. J Clin Oncol Off J Am Soc Clin Oncol. 2014; 32: 297–305.
13. Gross S, Cairns RA, Minden MD. Cancer-associated metabolite 2-hydroxyglutarate accumulates in acute myelogenous leukemia with isocitrate dehydrogenase 1 and 2 mutations. J Exp Med. 2010; 207: 339–344.
14. DiNardo CD, Propert KJ, Loren AW. Serum 2-hydroxyglutarate levels predict isocitrate dehydrogenase mutations and clinical outcome in acute myeloid leukemia. Blood. 2013; 121: 4917–4924.
15. Lu C, Ward PS, Kapoor GS. IDH mutation impairs histone demethylation and results in a block to cell differentiation. Nature. 2012; 483: 474–478.
16. Figueroa ME, Abdel-Wahab O, Lu C. Leukemic IDH1 and IDH2 Mutations Result in a Hypermethylation Phenotype, Disrupt TET2 Function, and Impair Hematopoietic Differentiation. Cancer Cell. 2010; 18: 553–567.
17. Montalban-Bravo G, DiNardo CD. The role of IDH mutations in acute myeloid leukemia. Future Oncol Lond Engl. 2018; 14: 979–993.
18. Chen W-L, Wang J-H, Zhao A-H. A distinct glucose metabolism signature of acute myeloid leukemia with prognostic value. Blood. 2014; 124: 1645–1654.
19. Song K, Li M, Xu X, Xuan LI, Huang G, Liu Q. Resistance to chemotherapy is associated with altered glucose metabolism in acute myeloid leukemia. Oncol Lett. 2016; 12: 334–342.
20. Song K, Li M, Xu X-J. HIF-1α and GLUT1 gene expression is associated with chemoresistance of acute myeloid leukemia. Asian Pac J Cancer Prev APJCP. 2014; 15: 1823–1829.
21. Stuani L, Sabatier M, Sarry J-E. Exploiting metabolic vulnerabilities for personalized therapy in acute myeloid leukemia. BMC Biol. 2019; 17: 57.
22. Saito Y, Chapple RH, Lin A, Kitano A, Nakada D. AMPK Protects Leukemia-Initiating Cells in Myeloid Leukemias from Metabolic Stress in the Bone Marrow. Cell Stem Cell. 2015; 17: 585–596.

23. Ye H, Adane B, Khan N. Subversion of Systemic Glucose Metabolism as a Mechanism to Support the Growth of Leukemia Cells. Cancer Cell. 2018; 34: 659-673.e6.
24. Dang CV. Glutaminolysis: supplying carbon or nitrogen or both for cancer cells? Cell Cycle Georget Tex. 2010; 9: 3884–3886.
25. Jin L, Alesi GN, Kang S. Glutaminolysis as a target for cancer therapy. Oncogene. 2016; 35: 3619–3625.
26. Jacque N, Ronchetti AM, Larrue C. Targeting glutaminolysis has antileukemic activity in acute myeloid leukemia and synergizes with BCL-2 inhibition. Blood. 2015; 126: 1346–1356.
27. Darmaun D, Matthews DE, Bier DM. Glutamine and glutamate kinetics in humans. Am J Physiol. 1986; 251: E117-126.
28. Jones CL, Stevens BM, D'Alessandro A. Inhibition of Amino Acid Metabolism Selectively Targets Human Leukemia Stem Cells. Cancer Cell. 2018; 34: 724-740.e4.
29. Gallipoli P, Giotopoulos G, Tzelepis K. Glutaminolysis is a metabolic dependency in FLT3 ITD acute myeloid leukemia unmasked by FLT3 tyrosine kinase inhibition. Blood. 2018; 131: 1639–1653.
30. Willems L, Jacque N, Jacquel A. Inhibiting glutamine uptake represents an attractive new strategy for treating acute myeloid leukemia. Blood. 2013; 122: 3521–3532.
31. Stäubert C, Bhuiyan H, Lindahl A. Rewired metabolism in drug-resistant leukemia cells: a metabolic switch hallmarked by reduced dependence on exogenous glutamine. J Biol Chem. 2015; 290: 8348–8359.
32. Maan M, Peters JM, Dutta M, Patterson AD. Lipid metabolism and lipophagy in cancer. Biochem Biophys Res Commun. 2018; 504: 582–589.
33. Currie E, Schulze A, Zechner R, Walther TC, Farese RV. Cellular fatty acid metabolism and cancer. Cell Metab. 2013; 18: 153–161.
34. Menendez JA, Lupu R. Fatty acid synthase and the lipogenic phenotype in cancer pathogenesis. Nat Rev Cancer. 2007; 7: 763–777.
35. Louie SM, Roberts LS, Mulvihill MM, Luo K, Nomura DK. Cancer cells incorporate and remodel exogenous palmitate

into structural and oncogenic signaling lipids. Biochim Biophys Acta BBA - Mol Cell Biol Lipids. 2013; 1831: 1566–1572.
36. Liu Q, Luo Q, Halim A, Song G. Targeting lipid metabolism of cancer cells: A promising therapeutic strategy for cancer. Cancer Lett. 2017; 40139–44015.
37. Maan M, Peters JM, Dutta M, Patterson AD. Lipid metabolism and lipophagy in cancer. Biochem Biophys Res Commun. 2018; 504: 582–589.
38. Pabst T, Kortz L, Fiedler GM, Ceglarek U, Idle JR, et al. The plasma lipidome in acute myeloid leukemia at diagnosis in relation to clinical disease features. BBA Clin. 2017; 7105–7114.
39. Wang Y, Zhang L, Chen W-L. Rapid diagnosis and prognosis of de novo acute myeloid leukemia by serum metabonomic analysis. J Proteome Res. 2013; 12: 4393–4401.
40. Kuliszkiewicz-Janus M, Tuz MA, Kiełbiński M, Jaźwiec B, Niedoba J, et al. 31P MRS analysis of the phospholipid composition of the peripheral blood mononuclear cells (PBMC) and bone marrow mononuclear cells (BMMC) of patients with acute leukemia (AL). Cell Mol Biol Lett. 2009; 14: 35–45.
41. Stefanko A, Thiede C, Ehninger G, Simons K, Grzybek M. Lipidomic approach for stratification of acute myeloid leukemia patients. PLOS ONE. 2017; 12: e0168781.
42. Stuani L, Riols F, Millard P. Stable Isotope Labeling Highlights Enhanced Fatty Acid and Lipid Metabolism in Human Acute Myeloid Leukemia. Int J Mol Sci. 2009; 19: 3325.
43. Loew A, Köhnke T, Rehbeil E, Pietzner A, Weylandt KH. A Role for Lipid Mediators in Acute Myeloid Leukemia. Int J Mol Sci. 2019; 20: 2425.
44. Wang J, Ye W, Yan X. Low expression of ACLY associates with favorable prognosis in acute myeloid leukemia. J Transl Med. 2019; 17: 149.
45. Samudio I, Harmancey R, Fiegl M. Pharmacologic inhibition of fatty acid oxidation sensitizes human leukemia cells to apoptosis induction. J Clin Invest. 2010; 120: 142–156.

46. Tabe Y, Saitoh K, Yang H. Inhibition of FAO in AML co-cultured with BM adipocytes: mechanisms of survival and chemosensitization to cytarabine. Sci Rep. 2018; 8: 16837.
47. Picou F, Debeissat C, Bourgeais J. n-3 Polyunsaturated fatty acids induce acute myeloid leukemia cell death associated with mitochondrial glycolytic switch and Nrf2 pathway activation. Pharmacol Res. 2018; 13645–13655.
48. Shi J, Fu H, Jia Z, He K, Fu L, et al. High Expression of CPT1A Predicts Adverse Outcomes: A Potential Therapeutic Target for Acute Myeloid Leukemia. EBioMedicine. 2016; 1455–1464.
49. Maher M, Diesch J, Casquero R, Buschbeck M. Epigenetic-Transcriptional Regulation of Fatty Acid Metabolism and Its Alterations in Leukaemia. Front Genet. 2018; 9405.
50. Ye H, Adane B, Khan N. Leukemic Stem Cells Evade Chemotherapy by Metabolic Adaptation to an Adipose Tissue Niche. Cell Stem Cell. 2016; 19: 23–37.
51. Farge T, Saland E, de Toni F. Chemotherapy-Resistant Human Acute Myeloid Leukemia Cells Are Not Enriched for Leukemic Stem Cells but Require Oxidative Metabolism. Cancer Discov. 2017; 7: 716–735.
52. German NJ, Yoon H, Yusuf RZ. PHD3 Loss in Cancer Enables Metabolic Reliance on Fatty Acid Oxidation via Deactivation of ACC2. Mol Cell. 2016; 63: 1006–1020.
53. Kuliszkiewicz-Janus M, Tuz M, Kiełbiński M, Jaźwiec B, Niedoba J, et al. 31P MRS analysis of the phospholipid composition of the peripheral blood mononuclear cells (PBMC) and bone marrow mononuclear cells (BMMC) of patients with acute leukemia (AL). Cell Mol Biol Lett. 2009; 14: 35-45.
54. Xu M, Seneviratne AK, Schimmer AD. Phospholipid metabolism regulates AML growth and stemness. Aging. 2019; 11: 3895–3897.
55. Seneviratne AK, Xu M, Henao JJA. The Mitochondrial Transacylase, Tafazzin, Regulates AML Stemness by Modulating Intracellular Levels of Phospholipids. Cell Stem Cell. 2019; 24: 621-636.e16.
56. Mossmann D, Park S, Hall MN. mTOR signalling and cellular metabolism are mutual determinants in cancer. Nat Rev Cancer. 2018; 18: 744–757.

57. Gwinn DM, Shackelford DB, Egan DF. AMPK phosphorylation of raptor mediates a metabolic checkpoint. Mol Cell. 2008; 30: 214–226.
58. Green AS, Chapuis N, Lacombe C, Mayeux P, Bouscary D, et al. LKB1/AMPK/mTOR signaling pathway in hematological malignancies: from metabolism to cancer cell biology. Cell Cycle Georget Tex. 2011; 10: 2115–2120.
59. Counihan JL, Grossman EA, Nomura DK. Cancer Metabolism: Current Understanding and Therapies. Chem Rev. 2018; 118: 6893–6923.
60. Bose S, Le A. Glucose Metabolism in Cancer. Adv Exp Med Biol. 2018; 10633–10612.
61. Lago CU, Sung HJ, Ma W, Wang P, Hwang PM. p53, aerobic metabolism, and cancer. Antioxid Redox Signal. 2011; 15: 1739–1748.
62. Saito Y, Chapple RH, Lin A, Kitano A, Nakada D. AMPK Protects Leukemia-Initiating Cells in Myeloid Leukemias from Metabolic Stress in the Bone Marrow. Cell Stem Cell. 2015; 17: 585–596.
63. Kullmann L, Krahn MP. Controlling the master-upstream regulation of the tumor suppressor LKB1. Oncogene. 2018; 37: 3045–3057.
64. Reference GH. STK11 gene. Genetics Home Reference. Available Online at: https://ghr.nlm.nih.gov/gene/STK11.
65. Shackelford DB, Shaw RJ. The LKB1-AMPK pathway: metabolism and growth control in tumour suppression. Nat Rev Cancer. 2009; 9: 563–575.
66. Zeqiraj E, Filippi BM, Deak M, Alessi DR, van Aalten DMF. Structure of the LKB1-STRAD-MO25 complex reveals an allosteric mechanism of kinase activation. Science. 2009; 326: 1707–1711.
67. Deng L, Yao P, Li L. p53-mediated control of aspartate-asparagine homeostasis dictates LKB1 activity and modulates cell survival. Nat Commun. 2020; 11: 1755.
68. Zeqiraj E, Filippi BM, Goldie S. ATP and MO25alpha regulate the conformational state of the STRADalpha pseudokinase and activation of the LKB1 tumour suppressor. PLoS Biol. 2009; 7: e1000126.

69. Alessi DR, Sakamoto K, Bayascas JR. LKB1-dependent signaling pathways. Annu Rev Biochem. 2006; 75137–75163.
70. Jansen M, Ten Klooster JP, Offerhaus GJ, Clevers H. LKB1 and AMPK family signaling: the intimate link between cell polarity and energy metabolism. Physiol Rev. 2009; 89: 777–798.
71. Wingo SN, Gallardo TD, Akbay EA. Somatic LKB1 mutations promote cervical cancer progression. PloS One. 2009; 4: e5137.
72. Green AS, Chapuis N, Trovati Maciel T. The LKB1/AMPK signaling pathway has tumor suppressor activity in acute myeloid leukemia through the repression of mTOR-dependent oncogenic mRNA translation. Blood. 2010; 116: 4262–4273.
73. Wang H, Wang X, Xin N. Live kinase B1 maintains CD34+CD38− AML cell proliferation and self-renewal. Mol Cell Biochem. 2017; 434: 25–32.
74. Yang MY, Hsiao HH, Liu YC, Hsu CM, Lin SF, et al. Phe354Leu Polymorphism of LKB1 Is a Potential Prognostic Factor for Cytogenetically Normal Acute Myeloid Leukemia. Vivo Athens Greece. 2017; 31: 841–847.
75. Gwinn DM, Shackelford DB, Egan DF. AMPK phosphorylation of raptor mediates a metabolic checkpoint. Mol Cell. 2008; 30: 214–226.
76. Kamata H, Hirata H. Redox Regulation of Cellular Signalling. Cell Signal. 1999; 11: 1–14.
77. Sánchez-Aguilera A, Méndez-Ferrer S. The hematopoietic stem-cell niche in health and leukemia. Cell Mol Life Sci CMLS. 2017; 74: 579–590.
78. Hole PS, Darley RL, Tonks A. Do reactive oxygen species play a role in myeloid leukemias? Blood. 2011; 117: 5816–5826.
79. Piccoli C, D'Aprile A, Ripoli M. Bone-marrow derived hematopoietic stem/progenitor cells express multiple isoforms of NADPH oxidase and produce constitutively reactive oxygen species. Biochem Biophys Res Commun. 2007; 353: 965–972.
80. Yahata T, Takanashi T, Muguruma Y. Accumulation of oxidative DNA damage restricts the self-renewal capacity of

human hematopoietic stem cells. Blood. 2011; 118: 2941–2950.
81. Eliasson P, Jönsson JI. The hematopoietic stem cell niche: Low in oxygen but a nice place to be. J Cell Physiol. 2010; 222: 17–22.
82. Hole PS, Zabkiewicz J, Munje C. Overproduction of NOX-derived ROS in AML promotes proliferation and is associated with defective oxidative stress signaling. Blood. 2013; 122: 3322–3330.
83. Adane B, Ye H, Khan N. The Hematopoietic Oxidase NOX2 Regulates Self-Renewal of Leukemic Stem Cells. Cell Rep. 2019; 27: 238-254.e6.
84. Hole PS, Pearn L, Tonks AJ. Ras-induced reactive oxygen species promote growth factor-independent proliferation in human CD34+ hematopoietic progenitor cells. Blood. 2010; 115: 1238–1246.
85. Jayavelu AK, Müller JP, Bauer R. NOX4-driven ROS formation mediates PTP inactivation and cell transformation in FLT3ITD-positive AML cells. Leukemia. 2016; 30: 473–483.
86. Xu Q. Survival of acute myeloid leukemia cells requires PI3 kinase activation. Blood. 2003; 102: 972–980.
87. Zeng Z, Samudio IJ, Zhang W. Simultaneous Inhibition of PDK1/AKT and Fms-Like Tyrosine Kinase 3 Signaling by a Small-Molecule KP372-1 Induces Mitochondrial Dysfunction and Apoptosis in Acute Myelogenous Leukemia. Cancer Res. 2006; 66: 3737–3746.
88. Sallmyr A, Fan J, Datta K. Internal tandem duplication of FLT3 (FLT3/ITD) induces increased ROS production, DNA damage, and misrepair: implications for poor prognosis in AML. Blood. 2008; 111: 3173–3182.
89. Megías-Vericat JE, Montesinos P, Herrero MJ. Impact of NADPH oxidase functional polymorphisms in acute myeloid leukemia induction chemotherapy. Pharmacogenomics J. 2018; 18: 301–307.
90. Callens C, Coulon S, Naudin J. Targeting iron homeostasis induces cellular differentiation and synergizes with differentiating agents in acute myeloid leukemia. J Exp Med. 2010; 207: 731–750.

91. Mondet J, Presti CL, Garrel C. Adult patients with de novo acute myeloid leukemia show a functional deregulation of redox balance at diagnosis which is correlated with molecular subtypes and overall survival. Haematologica. 2019; 104: e393–e397.
92. Mattes K, Vellenga E, Schepers H. Differential redox-regulation and mitochondrial dynamics in normal and leukemic hematopoietic stem cells: A potential window for leukemia therapy. Crit Rev Oncol Hematol. 2019; 144102814.
93. Sabharwal SS, Schumacker PT. Mitochondrial ROS in cancer: initiators, amplifiers or an Achilles' heel? Nat Rev Cancer. 2014; 14: 709–721.
94. Ishikawa K, Takenaga K, Akimoto M. ROS-generating mitochondrial DNA mutations can regulate tumor cell metastasis. Science. 2008; 320: 661–664.
95. Lee EA, Angka L, Rota SG. Targeting Mitochondria with Avocatin B Induces Selective Leukemia Cell Death. Cancer Res. 2015; 75: 2478–2488.
96. Sriskanthadevan S, Jeyaraju DV, Chung TE. AML cells have low spare reserve capacity in their respiratory chain that renders them susceptible to oxidative metabolic stress. Blood. 2015; 125: 2120–2130.
97. Galluzzi L, Morselli E, Kepp O. Mitochondrial gateways to cancer. Mol Aspects Med. 2010; 31: 1–20.
98. Wallace DC. Mitochondria and cancer. Nat Rev Cancer. 2012; 12: 685–698.
99. Liyanage SU, Hurren R, Voisin V. Leveraging increased cytoplasmic nucleoside kinase activity to target mtDNA and oxidative phosphorylation in AML. Blood. 2017; 129: 2657–2666.
100. Marlein CR, Zaitseva L, Piddock RE. NADPH oxidase-2 derived superoxide drives mitochondrial transfer from bone marrow stromal cells to leukemic blasts. Blood. 2017; 130: 1649–1660.
101. Lapalombella R. Mitochondria on the move: BMSCs fuel AML energy. Blood. 2017; 130: 1603–1604.

Book Chapter

Amino Acid Metabolism in Acute Myeloid Leukemia

Mossuz Pascal[1,3]*, Mondet Julie[2,3], Rajesh Christabelle[1,3]

[1]Department of biological hematology, Institut of Biology and Pathlogy, University Hospital of Grenoble, France
[2]Department of molecular pathology, Institut of Biology and Pathlogy, University Hospital of Grenoble, France
[3]Institute for Advanced Bioscience UMR1209 Inserm University of Grenoble Alpes (UGA), France

***Corresponding Author:** Pr Mossuz Pascal, Department of biological hematology, Institut of Biology and Pathlogy, University Hospital of grenoble, CS 10217 38043 Grenoble cedex 9, France

Published **January 20, 2021**

How to cite this book chapter: Mossuz Pascal, Mondet Julie, Rajesh Christabelle. Amino Acid Metabolism in Acute Myeloid Leukemia. In: Hussein Fayyad Kazan, editor. Immunology and Cancer Biology. Hyderabad, India: Vide Leaf. 2021.

Abstract

The role of metabolic alterations in cancer cells has been discussed and clarified over the years. Researchers focused on key metabolites and the mechanisms they initiate in cancer. Acute myeloid leukemia (AML) is one such cancer that is dependent on certain metabolites and the pathways they trigger.

Even though several advances have been made in understanding the mechanisms underlying the initiation and progression of AML, therapies targeted toward these mechanisms, although potent, do not always achieve the desired effect. Hence, studying the metabolic alterations in AML is one of the many approaches researchers currently employ in order to glean a deeper understanding of the intricacies that govern this cancer. Amino acids are crucial players in AML. They trigger several cell survival and replication processes, as well as modulate key epigenetic processes – all of which are critical in carcinogenesis. Moreover, several amino acids have been found to play a role in the maintenance of leukemic stem cells, which are correlated to poor prognosis in AML. The role of a few amino acids in AML are highlighted in this review.

Introduction

Almost a century ago, Otto Warburg proposed the first metabolism-related alteration in cancer when he showed that cancer cells selectively prefer aerobic glycolysis for their propagation [1]. This led to a revolutionary development in the field of metabolic reprogramming in cancers. Metabolic pathways involved in carbohydrate, fatty acid and amino acid metabolism have been explored. More specifically, glycolysis and the tricarboxylic acid cycle (TCA) and their alterations in cancer have been largely studied. Much attention was also focused on amino acids and their role in cancer metabolism [2]. All these studies established that tumors differ metabolically from normal counterpart tissues [3]. Glucose and amino acids are important substrates used by cancer cells. Glutamine has been deemed a "super nutrient" as it participates to various signalling pathways including the TCA via anaplerosis and also contributes to redox homeostasis, a critical regulator of proliferation in cancer [4]. Moreover, in 2016 a study revealed that other amino acids which are consumed at slower rates than glutamine and glucose are major fuels for proliferating mammalian cells [5]. This is a major incentive to further investigate the role of amino acids in cancer cell metabolism. Acute myeloid leukemia (AML) is a highly heterogeneous bone marrow cancer characterized by uncontrolled proliferation of

immature myeloblasts (referred to as 'AML blasts') in the bone marrow and peripheral blood, causing failure in erythropoiesis [6]. This leukemia is most common in adults about 65 years of age and fairly uncommon in people less than 45 years, and has an overall five years survival rate after diagnosis of 28.7% [6,7]. Like most cancers, the role of metabolic reprogramming has been established in AML [8]. In this review, we discuss the role of certain amino acids, mostly non-essential ones, in cancer and more specifically in AML.

Synthesis of Amino Acids and its Link to Other Metabolic Pathways

A total of 20 amino acids are the known building blocks for proteins and are categorized into two major groups on the basis of dietary requirements as essential amino acids (EAAs) and non-essential amino acids (NEAAs) [9]. Of these 20 amino acids, 9 are thought to be essential and include Valine, Leucine, Isoleucine, Histidine, Methionine, Tryptophan, Phenylalanine, Lysine and Threonine. The remaining 11 are non-essential and consists of Glutamic acid, Glutamine, Proline, Glycine, Tyrosine, Alanine, Serine, Arginine, Asparagine, Cysteine and Aspartic acid [10]. As metabolism is a highly dynamic process, amino acid metabolism is interconnected with several other cellular pathways. Amino acids are building blocks of proteins. Furthermore they are degraded to provide energy or consume energy for their own biosynthesis.The metabolic fate of various amino acids is called anaplerosis or cataplerosis of amino acids, which represents the replenishing or removal of TCA cycle intermediates, respectively [11]. Glucogenic amino acids are those that are ultimately channelled into gluconeogenesis via intermediate conversions into TCA cycle products oxaloacetate, pyruvate, succinyl-CoA, fumarate or α-ketoglutarate (α-KG); while ketogenic amino acids form ketone bodies through intermediate conversions into acetyl-CoA [12]. The glucogenic amino acids include alanine, glycine, serine, cysteine, asparagine, aspartic acid, proline, glutamine, glutamic acid, arginine, methionine, valine and histidine; while the ketogenic amino acids comprise of leucine and lysine. The remaining five which include threonine, tryptophan, tyrosine, phenylalanine and

isoleucine are both – glucogenic and ketogenic. [11]. Overall, the cataplerotic and anaplerotic metabolism of amino depends on the metabolic and nutritional condition of the body [11]. The above mentioned reactions utilize the carbon skeleton of amino acids, however, the nitrogen of amino acids is removed first through various transamination reactions, all using the coenzyme pyridoxal phosphate. This nitrogen is ultimately funnelled into the urea cycle for its removal from the body [13]. Thus, the breakdown and utilisation of amino acids comprises a number of enzymes and forms a highly dynamic and intricate metabolic network.

Role of Amino Acids in Cancer Manifestation

A variety of processes that suggest amino acids to be crucial players in cancer progression and disease manifestation have been discovered. One widely accepted theory is that as cancer cells proliferate profusely, they have a higher demand of amino acids. Cancer cells glean the required amino acids by mechanisms like protein scavenging, but can also depend on their environment for a supply of NEAAs [14]. Another mechanism for cancer cells to meet the high requirement of amino acids is to increase the number of amino acid transporters on the cell membrane [15]. For example, the SLC7A5 transporter, belonging to the System Leucine-preferring amino acid transporters, also known as L-amino acid transporter 1 (LAT1)is overexpressed on the metastatic lesions of various cancers as compared to their primary site of origin [16]. Another transporter of neutral amino acids called ASCT2 (or SLC1A5) has been specifically implicated in AML [17]. ASCT2 mediates transport of Glutamine, Alanine, Cysteine, Serine, Valine and Threonine [18,19]. The constitutive deletion and thus loss of ASCT2 function has been shown to disrupt the influx of leucine (that is dependent on glutamine; discussed further under glutamine metabolism) is responsible for mammalian target of rapamycin (mTOR) signalling and induces apoptotic cell death in AML cells [17]. Moreover, factors controlling oncogenesis like the suppressive microRNAs miR-126 and the activation of the c-myc gene (an important regulator of cell proliferation) are also responsible for the downstream expression of LAT1 [20,21].

This suggests that amino acid uptake and metabolism are crucial mechanisms in carcinogenesis.

Glutamine and its Metabolism in Cancers and AML

According to a study published by Kroemer et al in 2008, glucose and glutamine are two necessary ingredients for the uncontrolled proliferation and propagation of cancer [22]. Glutamine is abundantly present in human plasma (0.6 – 0.9 mM) as well as inside cells (~20 mM). These concentrations are beneficial to cell physiology and to carcinogenesis [23]. Glutamine contributes to a number of important processes like generation of NEAAs , DNA replication via purine and pyrimidine biosynthesis, metabolite generation to sustain mitochondrial metabolism, synthesis of fatty acids for cell proliferation, redox homeostasis by supplying antioxidants to eliminate reactive oxygen species (ROS)-induced damages and activation of various pro-tumoral signalling mechanisms. Glutamine is so crucial in cancer cell metabolism that the process of anaplerosis by which glutamine provides TCA cycle metabolites and upholds the metabolic prowess of cancer cells has been called another "hallmark of cancer metabolism" [24-26]. In acute myeloid leukemia the bidirectional amino acid transporter SLC1A5 takes up leucine while simultaneously exporting glutamine. Leucine activates mammalian target of rapamycin complex 1 (mTORC1) stimulating protein synthesis, thus sustaining AML [27,28]. Hence, removal of glutamine supply to these AML cells leads to the inhibition of mTORC1 and subsequent hindrance in protein synthesis, and ultimately death of AML cells via apoptosis [29]. The enzyme glutaminase is encoded by two different genes: GLS1 which produces two splice variants – the kidney-type glutaminase and glutaminase C; and GLS2 which encodes the liver-type glutaminase [30]. Of these two genes, the products encoded by GLS1 are highly expressed in cancer, including AML [28,31]. Proper functioning of glutaminase, that causes glutamine deamination to glutamate, which is then converted to α-KG to enter the TCA cycle, has been found to be elevated and essential to various cancers [32,33]. Hence, using a glutaminase inhibitor CB-839 led to an instable level of ROS in the mitochondria of AML cells due to

impaired generation of the antioxidant glutathione (GSH), which culminated in the mitochondrial apoptotic death of these AML cells [34]. As the mitochondrial apoptotic pathway is induced, glutaminase inhibitor treatment in combination with BCL-2 inhibitors confers a synergistic effect in eliminating AML blasts [35]. Moreover, in AML cases with isocitrate dehydrogenase (IDH) mutations, use of this CB-839 GLS inhibitor also led to a decrease in the production of 2-hydroxyglutarate, an onco-metabolite. This further emphasizes the importance of glutamine metabolism in AML [31,36].

Targeting the Linked Asparagine and Glutamine Metabolisms in AML

Asparagine is one of the eleven NEAAs and hence, is produced by the body itself in a reaction catalysed by the enzyme asparagine synthetase (ASNS), which uses aspartate and glutamine as substrates to produce asparagine and glutamine in a transamination reaction utilizing ATP [9,37]. However, if cells are unable to produce asparagine by this mechanism, they can be targeted and killed upon treatment with L-asparaginase (ASNase), an enzyme that hydrolyses glutamine and asparagine resulting in their subsequent depletion in the bone marrow and peripheral blood [23,38,39]. Such treatment with ASNase has been potent in haematological malignancies like lymphomas and acute lymbhoblastic leukemia (ALL), as the cancer cells in these cases lack ASNS and hence cannot replenish the lost asparagine post ASNase administration [40,41]. These low levels of asparagine and glutamine ultimately trigger certain downstream mechanisms like – (a.) activation of GCN2, a kinase that phosphorylates eIF2α, which causes a decrease in cellular protein synthesis [42]; (b.) induction of apoptosis to deplete lymphoma cells [43]; (c.) inhibition of mTOR – an effect specific to the glutamine-depleting function of ASNase, which also leads to a decrease in protein synthesis and disrupts cell survival mechanisms [29,44]. Hence, glutamine reduction is a crucial process that accompanies the anti-cancer effects of ASNase [23]. As compared to ALL, AML blasts are heterogeneous for ASNS expression and are generally more responsive to glutamine deprivation [38]. Heterogeneity could

contribute to AML resistance to asparaginase-based treatments. Interestingly, a study published in 2019 suggested that the $CD34^{+}CD38^{+/-}$ leukemic stem cells (LSCs) from AML patients show an intrinsic sensitivity to L-asparaginase treatment, but the microenvironment in the bone marrow has monocytic cells that can produce a lysosomal protease called cathepsin B, that is capable of degrading the ASNase. The AML cells (belonging to the FAB M5 category in this case) themselves may also produce this protease to inactivate ASNase and reduce treatment efficacy [45]. Moreover, ASNase with intrinsic glutaminase activity has been shown to be more effective in treating AML. One such ASNase, called Erwinase (derived from *Erwinia chrysanthemi*), has a glutaminase activity that is ten times superior to that of *E. coli* [46]. Of note, combination of ASNase with cytarabine in AML therapy led to an improved survival length, the administration sequence of the two drugs being critically important [47,48].

Targeting Arginine Metabolism in AML

Arginine has been deemed "semi-essential" as under normal physiological conditions, the body is capable of generating arginine from other amino acids like proline, glutamine and glutamate [49]. However, in pathologic conditions like cancer, cells become auxotrophic for arginine [50]. Cancer cells rely on arginine as it generates polyamines, components of chromatin necessary for cell growth, proliferation and metastasis [51,52]. Arginine is also important for the generation of nitric oxide (NO), low levels of which seem to be pro-tumoral whereas high NO levels lead to cell death [53-55]. The enzyme argininosuccinate synthetase 1 (ASS1) of the urea cycle uses aspartate, citrulline and ATP to form argininosuccinate, which is converted to arginine by another enzyme called argininosuccinate lyase (ASL) [56]. Immunohistochemical analysis of AML samples confirmed that most cases did not stain positively for ASS1, while expressing ASL normally – making these AML cells dependent on extracellular sources of arginine [57,58]. Further analysis revealed that methylation of the ASS1 gene promoter in AML samples as well as other lymphoma samples was the cause for arginine dependence in these cancers

[57,59]. Moreover, it was found that cancer cells deficient in arginine undergo apoptosis or autophagy, or both when deprived of arginine [60]. It was shown that a pegylated form of arginine deiminase called ADI-PEG, derived from *Mycoplasma,* converts arginine to citrulline, thereby depleting AML cells from arginine to. AML cells lacking ASS1 enzyme showed activation of caspases, whilst cells with functional ASS1 were resistant to ADI-PEG 20 induced arginine deprivation. The same investigations showed that in patients deficient for ASS1, combination therapy using cytarabine and ADI-PEG 20 proved to be more potent than either single treatment [58]. Another enzyme arginase (ARGase) also participates in the urea cycle by converting arginine to ornithine [56]. In 2015, researchers showed that along with ASS1, another enzyme of arginine metabolism – ornithine transcarbamylase (OTC) was also deficient in AML blasts, with the simultaneous upregulation of cationic amino acid transporters CAT-1 and CAT-2B, which helped in the uptake of arginine from the extracellular milieu to make up for loss of functional ASS1 and OTC. They formulated the pegylated recombinant human arginase called BCT-100, which like ADI-PEG 20 depleted the arginine supply from AML blasts along with the intracellular arginine reserves, but unlike ADI-PEG 20 did not treat only ASS1-deficient AML, but both – ASS1 and OTC-lacking AML. BCT-100 also showed synergy with cytarabine treatment in AML [61]. This lead to development of "arginine deprivation therapy" in cancers like AML, wherein the enzymes ASS1 and OTC served as biomarkers for response or resistance to such treatment.

Alanine Metabolism in Cancers

The production of alanine in the cell is regulated by the enzyme alanine aminotransferase (ALT), also known as glutamate-pyruvate transaminase (GPT) – which uses glutamate and pyruvate to generate alanine and α-KG in a reversible reaction [62]. Two isoforms of ALT encoded by two different genes on two chromosomes exist – ALT1 (or GPT1) is encoded from chromosome 8q24.3 and represents the cytosolic protein, whilst ALT2 (or GPT2) is encoded from chromosome 16q11.2 and generates the mitochondrial protein [63]. The role of ALT has

been described in lung carcinoma cells. ALT inhibition using cycloserine and chloroalanine was found to disrupt alanine production and glucose intake by these cells, followed by a subsequent activation of mitochondrial metabolism - all of which ultimately led to a decline in proliferation and acquisition of a malignant potential [64]. Moreover, ALT function appeared to play a role in the development of extracellular matrix (ECM) through the formation of α-KG, which causes collagen hydroxylation by increasing certain enzymatic activities and thus acting as a crucial contributor to metastatic breast cancer [65]. Another instance of alanine metabolism has been described in pancreatic ductal adenocarcinoma (PDAC). In this case, the pancreatic stellate cells (PSCs) in the stroma around the tumor secrete alanine (via an autophagic mechanism induced by the tumor), which is then taken up by the PDAC tumor itself and fuelled into the TCA cycle via anaplerotic reactions that generate pyruvate. It is interesting to note that this secreted alanine is the major carbon source for the TCA cycle in these tumors, even beating the carbon derived from glutamine and glucose, which are the two main cancer promoting and cell survival carbon providers (66). This allows the use of glucose and glutamine for other reactions, depending on the demand of the cancerous tissue [66,67]. When it comes to AML, no direct link between alanine metabolism and cancer progression has been described yet. However, the liver kinase B1 (LKB1) is an important “master kinase” of metabolism in various cancers, and is thought, for the most part, to act as a tumor suppressor in AML by downregulating the mTOR pathway and subsequently decreasing cell growth and survival [68]. Recently, it was found that LKB1 regulates ALT activity and thus the pyruvate-alanine conversion in neural crest cells, in a pathway that relies on mTOR [69]. As LKB1 is highly active under nutrient-deficient conditions in AML, it could potentially affect alanine metabolism by regulating ALT activity in a similar manner, although this premise remains hypothetical.

Role of Amino Acids in "Stemness" and Leukemia Progression

It has been established that for hematopoietic stem cell (HSC) sustenance, valine is essential, and depriving these HSCs of valine supplementation leads to a decrease in their overall numbers. More specifically, valine is necessary for the self-renewal of HSCs [70]. Valine is a branched-chain amino acid (BCAA) – along with leucine and isoleucine [71]. BCAAs are involved in nutrient sensing (especially via leucine) and play a role in modulating the overall metabolism of cells, cell proliferation and protein synthesis via the AMPK and mTOR signalling pathways [72,73]. Catabolism of BCAAs takes place in two steps: the first is catalysed by the transaminases BCAT1 (cytosolic) and BCAT2 (mitochondrial), which use a BCAA and transfer nitrogen to α-KG leading to glutamate and the corresponding branched-chain keto acid [74]. The latter and final step is catalysed by a common branched-chain α-ketodehydrogenase (BCKDH) complex, which ultimately generates TCA cycle metabolites succinyl-CoA or acetyl-CoA [75]. This BCKDH has three subunits (E1, E2, E3-ligase) and a phosphatase activity called PPM1K. It dephosphorylates the E3-ligase component and activates BCKDH activity to promote BCAAs breakdown [76]. As BCAAs are crucial to maintain HSCs, PPM1K functioning is important to maintain a certain threshold of these BCAAs and has been found to sustain "stemness" of not only HSCs, but also leukemia initiating cells (LICs) by ubiquitination-mediated regulation of p21 and MEIS1 [77]. Moreover, PPM1K was found to promote AML development, thus highlighting the involvement of BCAAs in AML [77]. The role of BCAAs has now been sufficiently investigated to postulate that AML cells are "addicted" to these amino acids for their stemness and propagation [78]. Leukemic stem cells (LSCs) are known to have a low level of OXPHOS (on which they rely for metabolism, as opposed to glycolysis-dependent metabolism) as compared to other AML blasts, which have a relatively high OXPHOS signature [79]. However, LSCs seem to rely on BCL-2 (anti-apoptotic) and glutathione in order to sustain the low level of their mitochondrial output and avoid cell death [80]. Hence, using venetoclax (a BCL-2 inhibitor) has

been proposed to selectively target LSCs in AML [81]. LSCs harvested from primary AML tissue are enriched in amino acids, which sustain the aforementioned OXPHOS in these LSCs and hence promote their survival [82]. Azacitidine (a hypomethylation drug) in combination with venetoclax has been previously used in clinical trials to treat *de novo* AML and show a relatively strong response by mechanisms which target LSCs [83]. Jones et al used this combination therapy and saw that it lowered the amino acids load in LSCs, which could be another mechanism to decrease leukemogenesis and propagation of AML [82]. Overall, research has identified amino acids to sustain LSCs and hence given incentive to study the role of amino acids in blood cancers like AML.

Amino Acid-Mediated Epigenetic Regulation in AML

The role of metabolic pathways in the regulation of epigenetic processes has been established in recent years [84]. It is known that epigenetic alterations can modify expression of various metabolic genes (like those governing amino acid metabolism) Conversely, many epigenetic enzymes depend on and interact with various metabolites [85]. As discussed above, α-KG is produced through various transamination reactions involving the amino acids glutamate and alanine, and also through the enzymes glutamate dehydrogenase and IDH [63,84]. Epigenetic enzymes TET (ten-eleven translocation) and JHDM (Jumonji-C domain containing histone demethylase) rely on this α-KG and iron (Fe^{2+}) in the nucleus [86]. In AML, the IDH1 and IDH2 mutations lead to production of the onco-metabolite 2-hydroxyglutarate (2-HG), which competitively inhibits enzymes dependent on α-KG like TET2 (a DNA demethylase), leading to global or specific DNA hypermethylation, which ultimately disrupts HSC differentiation and seems to confer an overall pro-leukemic effect [87,88]. EGL-9 family of hypoxia inducible factor 1 (EGLN1) is another DNA demethylase that uses α-KG as a cofactor and targets HIF-1α for proteasomal-mediated degradation [89]. The enzyme BCAT1 which is involved in BCAAs catabolism regulates the intracellular α-KG reservoir, as discussed above. A proteomic analysis of stem and non-stem cell

groups in AML samples showed enrichment of BCAT1 in LSCs [90]. The role of hypoxia-inducible factor 1α (HIF-1α) plays a major role to maintain LSC populations in AML [91]. AML stem cells that highly express BCAT1 have decreased α-KG concentrations, which hinder EGLN1activity and promote leukemia onset via HIF-1α in LSCs. This mimics the pro-leukemic DNA hypermethylation effect observed in IDH mutant AML cells [90,92]. Hence, depletion of BCAT1 leads to an increase in the α-KG levels and thereby, an increase in EGLN1-mediated degradation of HIF-1α, which disrupts the leukemia-initiating ability of AML stem cells [90]. In conclusion, amino acids are important metabolites that affect cancer onset and propagation through various mechanisms, including epigenetic modifications.

Conclusion

A large amount of research and metabolic networking tools have been able to establish the pivotal role of amino acid metabolism in an array of cancers. Amino acids can be either pro-tumoral or tumor-suppressing, depending on the pathways they trigger in cancer cells [2]. The role of glutamine is well established in various cancers, including AML, and glutamine starvation has been a highly debated area in terms of anti-cancer therapy [15,29]. Even though glutamine evidently affects cancer progression and growth, other amino acids discussed in this review have also been shown to be significant in promoting or disrupting carcinogenesis. The role of asparagine has been highlighted in blood cancers, especially ALL, and hence treatment with L-asparaginase was an important milestone in ALL treatment, but was considered as subpar against AML [23]. However, the discovery of a mechanistic link between glutamine and asparagine in AML made it reasonable to use asparaginases with high glutaminase activit [38]. This provided a much needed boost to asparaginase-based anti-AML therapy. Arginine is another amino acid which has been shown to be an important tumor-promoting metabolite to cancer cells, including AML blasts [57]. The finding of intricate mechanisms that are based on enzymes like argininosuccinate lyase (ASL), that normally function in the urea cycle, led to the development of arginine-

metabolism targeting anti-cancer drugs like ADI-PEG 20 [58]. Researchers were also able to increase the efficacy of standard cytarabine therapy by combining it with ADI-PEG 20, which appears as a success story in AML therapy, especially in cases that are 'auxotrophic' for arginine [58]. Furthermore, the role of alanine has been highlighted in cancer [66]. Although there is no solid evidence of its role in promoting AML, it is supposed to act in tandem wilth the liver kinase LKB1 [69]. Leukemic stem cells (LSCs) are an essential area of research that has been discussed over the years with regard to AML [93]. Not surprisingly, the role of BCAAs and others in maintaining these LSC populations and thus being an important mediator in AML manifestation has been another key discovery [77,82]. Lastly, targeting the role of amino acids and the enzymes modulating amino acid metabolism in epigenetic regulation of gene expression in AML is a more recent and novel approach [89]. The importance of amino acids in regulating cancer metabolism in conjunction with several other metabolic pathways is emerging as an important hallmark that has led to the development of various drugs targeting amino acid metabolism, some of which are in clinical trials [2]. Studies highlighting various aspects of amino acids in cancer are an important pillar of metabolomics research that will certainly shape the future of therapeutic action against cancer. Finally, it did not escape the reader's attention that amino acids are major players in the normal landscape of physiology. It follows that anti-cancer interventions will require a high specificity.

References

1. Otto Warburg B, Wind F, Negelein N. The Metabolism of Tumors in the Body. J Gen Physiol. 1927; 8: 519-523.
2. Lieu EL, Nguyen T, Rhyne S, Kim J. Amino acids in cancer. Vol. 52, Experimental and Molecular Medicine. Berlin: Springer Nature. 2020; 15–30.
3. Hanahan D, Weinberg RA. Hallmarks of cancer: The next generation. Vol. 144, Cell. Cell. 2011; 646–674.
4. Hensley CT, Wasti AT, DeBerardinis RJ. Glutamine and cancer: Cell biology, physiology, and clinical opportunities.

Vol. 123, Journal of Clinical Investigation. J Clin Invest. 2013; 3678–3684.
5. Hosios AM, Hecht VC, Danai LV, Johnson MO, Rathmell JC, et al. Amino Acids Rather than Glucose Account for the Majority of Cell Mass in Proliferating Mammalian Cells. Dev Cell. 2016; 36: 540–549.
6. Vakiti A, Mewawalla P. Cancer, Acute Myeloid Leukemia (AML, Erythroid Leukemia, Myelodysplasia-Related Leukemia, BCR-ABL Chronic Leukemia) StatPearls: StatPearls Publishing. 2019. Available Online at: http://www.ncbi.nlm.nih.gov/pubmed/29939652
7. Acute Myeloid Leukemia — Cancer Stat Facts 2020. 2020 Available Online at: https://seer.cancer.gov/statfacts/html/amyl.html
8. Castro I, Sampaio-Marques B, Ludovico P. Targeting Metabolic Reprogramming in Acute Myeloid Leukemia. Cells. 2019; 8: 967.
9. Reeds PJ. Dispensable and indispensable amino acids for humans. J Nutr. 2000; 130: 1835S-1840S.
10. Wu G. Amino acids: biochemistry and nutrition. 2013. Available Online at: https://books.google.com/books?hl=en&lr=lang_en&id=Sj6Xrc78LKUC&oi=fnd&pg=PP1&ots=xJS1i9SyE_&sig=2MufwjxnYjIlGiHSvyhpR8SvwQ4
11. Owen OE, Kalhan SC, Hanson RW. The Key Role of Anaplerosis and Cataplerosis for Citric Acid Cycle Function*. 2002. Available Online at: http://www.jbc.org/
12. D'Andrea G. Classifying amino acids as gluco(glyco)genic, ketogenic, or both. Biochem Educ. 2000; 28: 27–28.
13. Biochemistry - NCBI Bookshelf. 2000. Available Online at: https://www.ncbi.nlm.nih.gov/books/NBK21154/
14. Finicle BT, Jayashankar V, Edinger AL. Nutrient scavenging in cancer. Vol. 18, Nature Reviews Cancer. Germany: Nature Publishing Group. 2018. p. 619–33.
15. Bhutia YD, Babu E, Ramachandran S, Ganapathy V. Amino acid transporters in cancer and their relevance to "glutamine addiction": Novel Targets for the design of a new class of anticancer drugs. Vol. 75, Cancer Research. USA: American Association for Cancer Research Inc. 2015; 1782–1788.

16. Kaira K, Oriuchi N, Imai H, Shimizu K, Yanagitani N, et al. L-type amino acid transporter 1 and CD98 expression in primary and metastatic sites of human neoplasms. Cancer Sci. 2008; 99: 2380–2386.
17. Ni F, Yu WM, Li Z, Graham DK, Jin L, Kang S, et al. Critical role of ASCT2-mediated amino acid metabolism in promoting leukaemia development and progression. Nat Metab. 2019; 1: 390–403.
18. Kekuda R, Prasad PD, Fei YJ, Torres-Zamorano V, Sinha S, et al. Cloning of the sodium-dependent, broad-scope, neutral amino acid transporter B(o) from a human placental choriocarcinoma cell line. J Biol Chem. 1996; 271: 18657–18661.
19. Fuchs BC, Bode BP. Amino acid transporters ASCT2 and LAT1 in cancer: Partners in crime? Vol. 15, Seminars in Cancer Biology. Cambridge: Academic Press. 2005. p. 254–66.
20. Miko E, Margitai Z, Czimmerer Z, Várkonyi I, Dezs B, et al. MiR-126 inhibits proliferation of small cell lung cancer cells by targeting SLC7A5. FEBS Lett. 2011; 585: 1191–1196.
21. Gao P, Tchernyshyov I, Chang TC, Lee YS, Kita K, et al. C-Myc suppression of miR-23a/b enhances mitochondrial glutaminase expression and glutamine metabolism. Nature. 2009; 458: 762–765.
22. Kroemer G, Pouyssegur J. Tumor Cell Metabolism: Cancer's Achilles' Heel. Vol. 13, Cancer Cell. Amsterdam: Elsevier. 2008; 472–82.
23. Emadi A, Zokaee H, Sausville EA. Asparaginase in the treatment of non-ALL hematologic malignancies. Vol. 73, Cancer Chemotherapy and Pharmacology. Germany: Springer Verlag. 2014; 875–83.
24. Yang L, Venneti S, Nagrath D. Glutaminolysis: A Hallmark of Cancer Metabolism. Annu Rev Biomed Eng. 2017; 19: 163–164.
25. Yang L, Moss T, Mangala LS, Marini J, Zhao H, et al. Metabolic shifts toward glutamine regulate tumor growth, invasion and bioenergetics in ovarian cancer. Mol Syst Biol. 2014; 10.
26. Suzuki S, Tanaka T, Poyurovsky MV, Nagano H, Mayama T, et al. Phosphate-activated glutaminase (GLS2), a p53-

inducible regulator of glutamine metabolism and reactive oxygen species. Proc Natl Acad Sci U S A. 2010; 107: 7461–7466.
27. Nicklin P, Bergman P, Zhang B, Triantafellow E, Wang H, et al. Bidirectional Transport of Amino Acids Regulates mTOR and Autophagy. Cell. 2009; 136: 521–534.
28. Jacque N, Bouscary D. Targeting glutamine uptake in AML. Vol. 1, Oncoscience. New York: Impact Journals LLC. 2014; 1–2.
29. Willems L, Jacque N, Jacquel A, Neveux N, Maciel TT, et al. Inhibiting Glutamine uptake represents an attractive new strategy for treating acute myeloid leukemia. Blood. 2013; 122: 3521–3532.
30. Elgadi KM, Meguid RA, Qian M, Souba WW, Abcouwer SF. Cloning and analysis of unique human glutaminase isoforms generated by tissue-specific alternative splicing. Physiol Genomics. 1999; 1999: 51–62.
31. Matre P, Velez J, Jacamo R, Qi Y, Su X, et al. Inhibiting glutaminase in acute myeloid leukemia: Metabolic dependency of selected AML subtypes. Oncotarget. 2016; 7: 79722–79735.
32. Wang J Bin, Erickson JW, Fuji R, Ramachandran S, Gao P, et al. Targeting mitochondrial glutaminase activity inhibits oncogenic transformation. Cancer Cell. 2010; 18: 207–219.
33. Choi BH, Coloff JL. The Diverse Functions of Non-Essential Amino Acids in Cancer. Cancers (Basel). 2019; 11.
34. Gregory MA, Nemkov T, Park HJ, Zaberezhnyy V, Gehrke S, et al. Targeting glutamine metabolism and redox state for leukemia therapy. Clin Cancer Res. 2019; 25: 4079–4090.
35. Jacque N, Ronchetti AM, Larrue C, Meunier G, Birsen R, et al. Targeting glutaminolysis has antileukemic activity in acute myeloid leukemia and synergizes with BCL-2 inhibition. Blood. 2015; 126: 1346–1356.
36. Dang L, Yen K, Attar E. IDH mutations in cancer and progress toward development of targeted therapeutics. 2016.
37. Lomelino CL, Andring JT, McKenna R, Kilberg MS. Asparagine synthetase: Function, structure, and role in disease. Vol. 292, Journal of Biological Chemistry. USA: American Society for Biochemistry and Molecular Biology Inc. 2017; 19952–9958.

38. Kaspers GJL. Acute myeloid leukaemia niche regulates response to L□asparaginase. Br J Haematol. 2019; 186: bjh.15924.
39. Hermanova I, Arruabarrena-Aristorena A, Valis K, Nuskova H, Alberich-Jorda M, et al. Pharmacological inhibition of fatty-acid oxidation synergistically enhances the effect of l-asparaginase in childhood ALL cells. Leukemia. 2016; 30: 209–218.
40. Broome JD. Evidence that the L-asparaginase of guinea pig serum is responsible for its antilymphoma effects. II. Lymphoma 6C3HED cells cultured in a medium devoid of L-asparagine lose their susceptibility to the effects of guinea pig serum in vivo. J Exp Med. 1963; 118: 121–148.
41. Capizzi RL, Bertino JR, Skeel RT, Creasey WA, Zanes R, et al. L-asparaginase: clinical, biochemical, pharmacological, and immunological studies. Ann Intern Med. 1971; 74: 893–901.
42. Shan J, Lopez MC, Baker HV, Kilberg MS. Expression profiling after activation of amino acid deprivation response in HepG2 human hepatoma cells. Artic Press Physiol Genomics. 2010; 41: 315–327.
43. Story MD, Voehringer DW, Stephens LC, Meyn RE. L-asparaginase kills lymphoma cells by apoptosis. Cancer Chemother Pharmacol. 1993; 32: 129–133.
44. Covini D, Tardito S, Bussolati O, R Chiarelli L, V Pasquetto M, et al. Expanding Targets for a Metabolic Therapy of Cancer: L-Asparaginase. Recent Pat Anticancer Drug Discov. 2012; 7: 4–13.
45. Michelozzi IM, Granata V, De Ponti G, Alberti G, Tomasoni C, et al. Acute myeloid leukaemia niche regulates response to L-asparaginase. Br J Haematol. 2019; 186: 420–430.
46. Emadi A, Law JY, Strovel ET, Lapidus RG, Jeng LJB, et al. Asparaginase Erwinia chrysanthemi effectively depletes plasma glutamine in adult patients with relapsed/refractory acute myeloid leukemia. Cancer Chemother Pharmacol. 2018; 81: 217–222.
47. Capizzi RL, Davis R, Powell B, Cuttner J, Ellison RR, et al. Synergy between high-dose cytarabine and asparaginase in the treatment of adults with refractory and relapsed acute

myelogenous leukemia - a cancer and leukemia group B study. J Clin Oncol. 1988; 6: 499–508.
48. Wells RJ, Woods WG, Lampkin BC, Nesbit ME, Lee JW, et al. Impact of high-dose cytarabine and asparaginase intensification on childhood acute myeloid leukemia: A report from the childrens cancer group. J Clin Oncol. 1993; 11: 538–545.
49. Morris SM. Arginine: Beyond protein. In: American Journal of Clinical Nutrition. 2006.
50. Feun LG, Marini A, Walker G, Elgart G, Moffat F, et al. Negative argininosuccinate synthetase expression in melanoma tumours may predict clinical benefit from arginine-depleting therapy with pegylated arginine deiminase. Br J Cancer. 2012; 106: 1481–1485.
51. Patil MD, Bhaumik J, Babykutty S, Banerjee UC, Fukumura D. Arginine dependence of tumor cells: Targeting a chink in cancer's armor. Vol. 35, Oncogene. Germany: Nature Publishing Group. 2016; 4957–4972.
52. Weiger TM, Hermann A. Cell proliferation, potassium channels, polyamines and their interactions: A mini review. Vol. 46, Amino Acids. Germany: Springer-Verlag Wien. 2014; 681–688. Available Online at: http://www.ncbi.nlm.nih.gov/pubmed/23820618
53. Lind DS. Arginine and Cancer. J Nutr. 2004; 134: 2837S-2841S.
54. Pervin S, Singh R, Hernandez E, Wu G, Chaudhuri G. Nitric oxide in physiologic concentrations targets the translational machinery to increase the proliferation of human breast cancer cells: Involvement of mammalian target of rapamycin/eIF4E pathway. Cancer Res. 2007; 67: 289–299.
55. Tabe Y, Lorenzi PL, Konopleva M. Amino acid metabolism in hematologic malignancies and the era of targeted therapy. Vol. 134, Blood. USA: American Society of Hematology. 2019; 1014–23.
56. Mitchell S, Ellingson C, Coyne T, Hall L, Neill M, et al. Genetic variation in the urea cycle: A model resource for investigating key candidate genes for common diseases. Hum Mutat. 2009; 30: 56–60.
57. Plunkett W. Arginine addiction in AML. Vol. 125, Blood. USA: American Society of Hematology. 2015; 3971–3972.

58. Miraki-Moud F, Ghazaly E, Ariza-McNaughton L, Hodby KA, Clear A, et al. Arginine deprivation using pegylated arginine deiminase has activity against primary acute myeloid leukemia cells in vivo. Blood. 2015; 125: 4060–4068.
59. Delage B, Luong P, Maharaj L, O'Riain C, Syed N, et al. Promoter methylation of argininosuccinate synthetase-1 sensitises lymphomas to arginine deiminase treatment, autophagy and caspase-dependent apoptosis. Cell Death Dis. 2012; 3: e342.
60. Changou CA, Chen YR, Xing L, Yen Y, Chuang FYS, et al. Arginine starvation-associated atypical cellular death involves mitochondrial dysfunction, nuclear DNA leakage, and chromatin autophagy. Proc Natl Acad Sci U S A. 2014; 111: 14147–14152.
61. Mussai F, Egan S, Higginbotham-Jones J, Perry T, Beggs A, et al. Arginine dependence of acute myeloid leukemia blast proliferation: A novel therapeutic target. Blood. 2015; 125: 2386–2396.
62. Liu Z, Que S, Xu J, Peng T. Alanine aminotransferase-old biomarker and new concept: A review. Vol. 11, International Journal of Medical Sciences. Sydney: Ivyspring International Publisher. 2014; 925–35.
63. Rafter I, Gråberg T, Kotronen A, Strömmer L, Mattson CM, et al. Isoform-specific alanine aminotransferase measurement can distinguish hepatic from extrahepatic injury in humans. Int J Mol Med. 2012; 30: 1241–1249.
64. Beuster G, Zarse K, Kaleta C, Thierbach R, Kiehntopf M, et al. Inhibition of alanine aminotransferase in Silico and in vivo promotes mitochondrial metabolism to impair malignant growth. J Biol Chem. 2011; 286: 22323–22330.
65. Elia I, Rossi M, Stegen S, Broekaert D, Doglioni G, et al. Breast cancer cells rely on environmental pyruvate to shape the metastatic niche. Vol. 568, Germany: Nature. Nature Publishing Group. 2019; 117–121.
66. Sousa CM, Biancur DE, Wang X, Halbrook CJ, Sherman MH, et al. Pancreatic stellate cells support tumour metabolism through autophagic alanine secretion. Nature. 2016; 536: 479–483.

67. Vettore L, Westbrook RL, Tennant DA. New aspects of amino acid metabolism in cancer. Vol. 122, British Journal of Cancer. Berlin: Springer Nature. 2020; 150–156.
68. Green AS, Chapuis N, Maciel TT, Willems L, Lambert M, et al. The LKB1/AMPK signaling pathway has tumor suppressor activity in acute myeloid leukemia through the repression of mTOR-dependent oncogenic mRNA translation. Blood. 2010; 116: 4262–4273.
69. Radu AG, Torch S, Fauvelle F, Pernet-Gallay K, Lucas A, et al. LKB1 specifies neural crest cell fates through pyruvate-alanine cycling. Sci Adv. 2019; 5: 1–18.
70. Taya Y, Ota Y, Wilkinson AC, Kanazawa A, Watarai H, et al. Depleting dietary valine permits nonmyeloablative mouse hematopoietic stem cell transplantation. Science (80-). 2016; 354: 1152–1155.
71. Wilkinson AC, Morita M, Nakauchia H, Yamazaki S. Branched-chain amino acid depletion conditions bone marrow for hematopoietic stem cell transplantation avoiding amino acid imbalance-associated toxicity. Exp Hematol. 2018; 63: 12-16.e1.
72. Kimball SR, Ravi S, Gordon BS, Dennis MD, Jefferson LS. Amino Acid–Induced Activation of mTORC1 in Rat Liver Is Attenuated by Short-Term Consumption of a High-Fat Diet. J Nutr. 2015; 145: 2496–2502.
73. Saha AK, Xu XJ, Lawson E, Deoliveira R, Brandon AE, et al. Downregulation of AMPK accompanies leucine- and glucose-induced increases in protein synthesis and insulin resistance in rat skeletal muscle. Diabetes. 2010; 59: 2426–2434.
74. Harper AE, Miller RH, Block KP. Branched-Chain Amino Acid Metabolism. Annu Rev Nutr. 1984; 4: 409–454.
75. White P, McGarrah R, Grimsrud P, metabolism ST-C, 2018 undefined. The BCKDH kinase and phosphatase integrate BCAA and lipid metabolism via regulation of ATP-citrate lyase. Elsevier. 2020. Available Online at: https://www.sciencedirect.com/science/article/pii/S1550413118302584
76. Lu G, Sun H, She P, Youn JY, Warburton S, et al. Protein phosphatase 2Cm is a critical regulator of branched-chain

amino acid catabolism in mice and cultured cells. J Clin Invest. 2009; 119: 1678–1687.
77. Liu X, Zhang F, Sun H, Chen GQ, Correspondence JZ. PPM1K Regulates Hematopoiesis and Leukemogenesis through CDC20-Mediated Ubiquitination of MEIS1 and p21. CellReports. 2018; 23: 1461–1475.
78. Kikushige Y, Miyamoto T, Maeda T, Akashi K. Human Acute Leukemia Is Addicted to Branched-Chain Amino Acid Metabolism to Maintain Leukemia Stemness. Blood. 2019; 134: 2516–2516.
79. Mattes K, Vellenga E, Schepers H. Differential redox-regulation and mitochondrial dynamics in normal and leukemic hematopoietic stem cells: A potential window for leukemia therapy. Vol. 144, Critical Reviews in Oncology/Hematology. Ireland: Elsevier Ireland Ltd. 2019; 102814.
80. Lagadinou ED, Sach A, Callahan K, Rossi RM, Neering SJ, et al. BCL-2 inhibition targets oxidative phosphorylation and selectively eradicates quiescent human leukemia stem cells. Cell Stem Cell. 2013; 12: 329–341.
81. Pollyea DA. BCL-2 Inhibition in Acute Myeloid Leukemia. Clin Lymphoma Myeloma Leuk. 2017; 17: S112–114.
82. Jones CL, Stevens BM, Alessandro AD, Degregori J, Pollyea DA, et al. Inhibition of Amino Acid Metabolism Selectively Targets Human Leukemia Stem Cells. Cancer Cell. 2018; 34.
83. DiNardo CD, Pratz KW, Letai A, Jonas BA, Wei AH, et al. Safety and preliminary efficacy of venetoclax with decitabine or azacitidine in elderly patients with previously untreated acute myeloid leukaemia: a non-randomised, open-label, phase 1b study. Lancet Oncol. 2018; 19: 216–228.
84. Lu C, Thompson CB. Metabolic regulation of epigenetics. Vol. 16, Cell Metabolism. Cell Metab. 2012; 9–17.
85. Yun J, Johnson JL, Hanigan CL, Locasale JW. Interactions between epigenetics and metabolism in cancers. Front Oncol. 2012; 2.
86. Teperino R, Schoonjans K, Auwerx J. Histone methyl transferases and demethylases; Can they link metabolism and transcription? Vol. 12, Cell Metabolism. Cell Press. 2010; 321–327.

87. Dang L, White DW, Gross S, Bennett BD, Bittinger MA, et al. Cancer-associated IDH1 mutations produce 2-hydroxyglutarate. Nature. 2009; 462: 739–744.
88. Figueroa ME, Abdel-Wahab O, Lu C, Ward PS, Patel J, et al. Leukemic IDH1 and IDH2 Mutations Result in a Hypermethylation Phenotype, Disrupt TET2 Function, and Impair Hematopoietic Differentiation. Cancer Cell. 2010; 18: 553–567.
89. Gutierrez SE, Romero-Oliva FA. Epigenetic changes: a common theme in acute myelogenous leukemogenesis. J Hematol Oncol. 2013; 61: 1–14.
90. Raffel S, Falcone M, Kneisel N, Hansson J, Wang W, et al. BCAT1 restricts αkG levels in AML stem cells leading to IDHmut-like DNA hypermethylation. Nature. 2017; 551: 384–388.
91. Peng G, Liu Y. Hypoxia-inducible factors in cancer stem cells and inflammation. Vol. 36, Trends in Pharmacological Sciences. New York: Elsevier Ltd. 2015; 374–383.
92. High BCAT1 Expression Mimics IDH Mutations in Acute Myeloid Leukemia. Cancer Discov. 2018; 8: OF12–OF12.
93. Hanekamp D, Cloos J, Schuurhuis GJ. Leukemic stem cells: identification and clinical application. Int J Hematol. 2017; 105: 549–557.

Book Chapter

Link between Base Excision Repair (BER), Reactive Oxygen Species (ROS), and Cancer

Nour Fayyad[1], Farah Kobaisi[2,3], Mohammad Fayyad-Kazan[3], Ali Nasrallah[2], Hussein Fayyad-Kazan[3] and Walid Rachidi[2]*

[1]University of Grenoble Alpes, CEA/IRIG/CIBEST, France
[2]University of Grenoble Alpes, CEA/IRIG/Biomics, France
[3]Laboratory of Cancer Biology and Molecular Immunology, Faculty of Sciences I, Lebanese University, Lebanon

***Corresponding Author:** Walid Rachidi, University of Grenoble Alpes, CEA/IRIG/Biomics, 38000 Grenoble, France

Published **February 25, 2021**

How to cite this book chapter: Nour Fayyad, Farah Kobaisi, Mohammad Fayyad-Kazan, Ali Nasrallah, Hussein Fayyad-Kazan, Walid Rachidi. Link between Base Excision Repair (BER), Reactive Oxygen Species (ROS), and Cancer. In: Hussein Fayyad Kazan, editor. Immunology and Cancer Biology. Hyderabad, India: Vide Leaf. 2021.

ROS: Sources, Targets, Cancer, and Defense Mechanisms

Different cellular organelles contribute to the production of free electron-radical and stable non-radical ROS (Reactive Oxygen Species). This includes lysosomes, cytoplasm, peroxisomes, and

endoplasmic reticulum [1]. Most importantly, eukaryotic mitochondrial membrane (complex I, complex II, complex III, inner membrane components) produces ROS through the electron transport chain. As shown in Reaction 1, it reduces oxygen into superoxide ($O_2^{\bullet-}$) that can further be converted into hydrogen peroxide (H_2O_2) via dismutation [2].

Reaction 1: The Conversion of Oxygen (O_2) into different ROS due to mitochondrial enzymes and processes.

At physiological levels, ROS have a vital role in fertilization, intra/intercellular signaling pathways, and inflammatory immune responses against infections [3,4]. For instance, upon pathogen invasion, T-lymphocytes and phagocytes (eosinophils, neutrophils, and macrophages) release hydrogen peroxide, NADPH oxidase-dependent superoxide anion, and its derivatives [3]. Other cell types (fibroblasts, keratinocytes, endothelial, and muscle cells) produce ROS as a regulator of cellular signaling pathways, including growth, differentiation, progression, and cell death [3,5]. ROS can stimulate NFκB-pathway, a cell-cycle and pro-inflammatory pathway, directly by inhibiting its cysteine residues' phosphorylation and oxidation or indirectly by inactivating and degrading I$\kappa B\alpha$ through inducing (1) phosphorylation of its tyrosine residues, (2) Cysteine-179 residue's S-glutathionylation, (3) and ubiquitination. NFκB-pathway can also regulate ROS by inducing the expression of antioxidants as superoxide dismutase (SOD) and glutathione peroxidase (GPx) [6]. Similarly, mitogen-activated protein kinase (MAPK) pathway is regulated by ROS via (1) kinases [extracellular signal-regulated kinases (ERK), and c-JUN N-terminal kinases (JNK)], and/or (2) p38 activation. Keap1-Nrf2-ARE signaling pathway is regulated through inhibiting Keap1 (Nrf2 inhibitor), increasing Ca^{2+} influx, or activating kinases (protein kinase C and MAPK…) that will activate Nrf2. Such a process detoxifies ROS by upregulating antioxidants. It is worth mentioning that high level of ROS can induce Nrf2 phosphorylation and degradation through GSK3β. Other regulated pathways include ubiquitination/proteasome,

mitochondrial permeability transition pore (mPTP), and protein kinase pathways [6,7].

Elevated ROS level induces oxidative stress, a misbalance in the redox homeostasis that causes uncontrolled proliferation and damages to all cellular components, including proteins, lipids, and DNA. This could lead to aging and various pathologies (neurological, cardiovascular diseases, obesity, Fanconi anemia, cancer…). Zabłocka-Słowińska, K. et al. found that lipid peroxidation is higher in lung cancer patients compared to control subjects. This may be due to the direct/indirect antioxidant role of some components involved in lipid metabolism that are altered by the misbalanced redox state. Peroxidized products [4-hydroxynonenal (4-HNE), Malondialdehyde (MDA)…] downregulate antioxidants' serum level (vitamin E, α-tocopherols) and generate point mutations in tumor suppressor genes that will trigger the necessary inflammatory response for cancer [8]. Similarly, protein and DNA high oxidation levels have been proven to contribute to gastric and colorectal carcinoma mechanism [9,10].

Furthermore, oxidative stress is involved in most cancerogenesis steps. As presented in Figure 1., it acts as the hallmark of cancer initiation, promotion, progression, and metastasis via inducing a prime tumor-microenvironment [11,12]. These cancers could be internal (breast, lung, liver, colon, prostate, ovary, and brain) or skin cancers [non-melanoma (NMSC) and melanoma skin cancers (MSC)] [13].

In addition to genomic instability, ROS induce the upregulation and stabilization of hypoxia-inducible transcription factors (HIFs) that will orchestrate expression of oncogenes , glycolytic enzymes, and proteins (GLUT1, GLUT3, hexokinases), and trigger angiogenesis [12,14]. HIF upregulates expression of vascular endothelial growth factor (VEGF) that will induce endothelial cell proliferation via the stimulation of several signaling cascades, including extracellularly regulated kinase/mitogen-activated protein kinase (ERK/MAPK) pathway [12]. Endothelial cell proliferation could also be triggered by CAFs (cell-associated fibroblasts). Chan et al. proved that H_2O_2

triggers the transformation of normal fibroblasts into CAFs, *invivo*, and *invitro*, through the NFκB signaling pathway. Then, CAFs will produce more ROS and promote the onset, propagation, and metastasis of tumors [15].

Such a ROS-dependent microenvironment also induces immunosuppression. Despite that, as mentioned before, a low level of ROS does not impede immune cells; a high level prevents them to act. Both T-cell and natural killer cell proliferation and function are impaired. For example, ROS induced undifferentiated myeloid-derived suppressor cells and regulatory T cells (Tregs) inhibiting T-lymphocytes and inducing their apoptosis [16]. ROS can also inhibit T-lymphocytes activation and metabolism by inhibiting the mTOR signaling pathway and inducing Granzyme B-dependent cell death [16]. It is noteworthy to point out that this ROS-induced apoptotic mechanism varies in sensitivity amongst the different T-lymphocytes subsets as follows: effector T cells > regulatory T cells > naive T cells > memory T cells. This shows that effector T cells are the least sensitive to ROS-induced apoptosis, while memory T cells are the most sensitive [16].

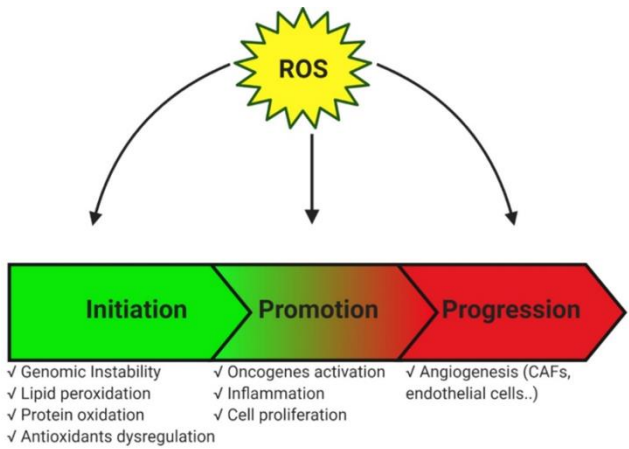

Figure 1: ROS induce cancer's initiation, promotion, and progression. (1) Initiation of cancer occurs upon genomic instability, accumulation of mutations, and protein and lipids damage. (2) Then ROS trigger promotion upon inflammation (activation of immunological cells), oncogenes activations, and uncontrolled cellular proliferation. (3) Finally, metastasis/progression

occurs due to angiogenesis, tumor-environment, and activation of several signaling cascades.

As shown in Figure 2., the antioxidants defense system is present to neutralize such an upregulation. This could be done via antioxidant proteins like superoxide dismutases (SOD1, SOD2…), glutathione peroxidase (GPx) that induce protective intracellular mechanisms, or through synthetic/natural consumable products (strawberry, pomegranate, carotenoids..). Such products include ROS scavengers that could strengthen the defense against oxidative stress [6,17].

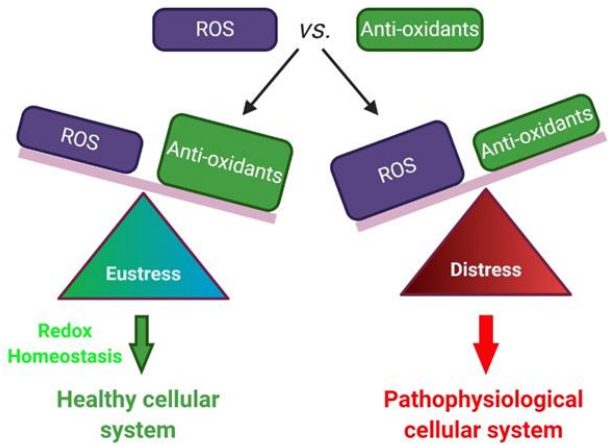

Figure 2: The balance between ROS and antioxidants. At the physiological state, the antioxidant defense mechanism can induce redox homeostasis by preventing ROS's upregulation. However, once an imbalance between ROS and antioxidants occurs in favor of the former, disruption of signaling mechanisms and molecular damages induce a pathophysiological state (pathologies and cancer).

Base Excision Repair (BER) and ROS

Overview of BER

One of the primary DNA repair pathways involved in genome integrity is base excision repair (BER). It is responsible for repairing single-strand breaks or small DNA base damages, including oxidized, deaminated, and alkylated DNA damage

[18]. Such damages occur numerously each day, and their repair failure leads to highly mutagenic risk, pathologies, aging, and cancer [19]. As shown in Figure 3., it is divided into 2 sub-pathways: short-patch BER (SP-BER) that repairs a single nucleotide and long-patch BER (LP-BER) that repairs 2 or more nucleotides. At least 11 different substrate specific-DNA glycosylases are known to be involved in the lesion splicing [18]. OGG1(8-oxoGuanine glycosylase) and MYH (MutY DNA glycosylase) are the most studied nuclear glycosylases due to their role in recognizing and removing ROS-induced oxidative DNA lesions, including 8-oxoGuanine.

Contrary to OGG1, MYH does not directly identify the lesion but rather recognizes the adenine nucleotide opposing 8-oxoGuanine [18]. Such an excision process will form an apurinic/apyrimidinic site (AP) site where APE1 (apurinic/apyrimidinic endonuclease 1) will cleave the 5'phosphodiester bond generating a single-strand break with 3′ hydroxyl and 5′ dRP termini. This will prepare the intermediate for the DNA polymerase that will insert the correct nucleotides followed by nick ligation via DNA ligase and its scaffold protein, X-ray repair cross-complementing protein 1 (XRCC1) [18].

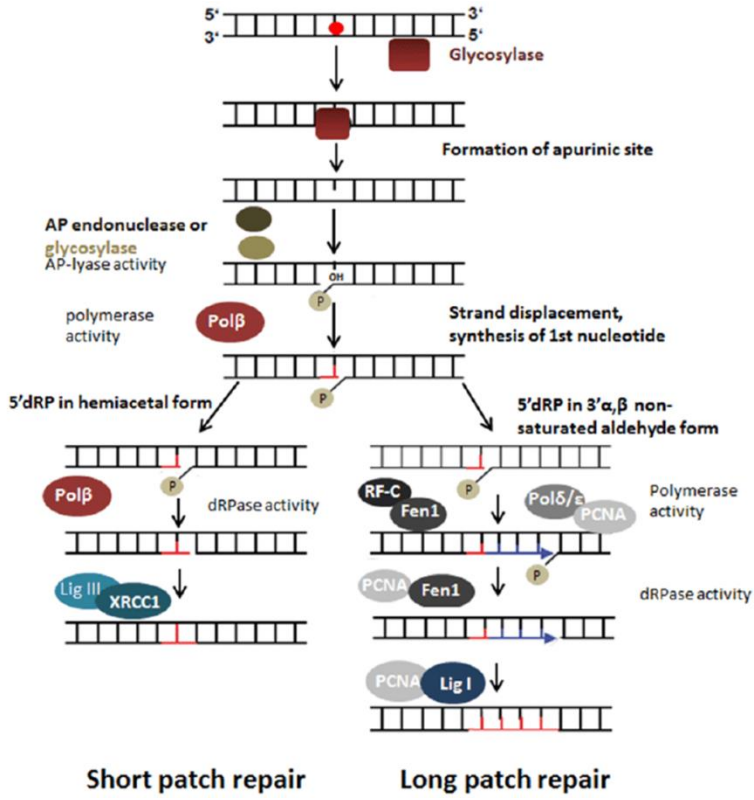

Figure 3: Schematic representation of base excision repair (BER) mechanism [20]. BER involves two sub-pathways (short patch repair and long patch repair). Both involve lesion recognition and incision through glycosylases and/or AP endonuclease, polymerization through polymerase activity, and ligation.Polβ (Polymerase-Beta), Polδ (Polymerase-Delta), Polε (Polymerase-Epsilon), Lig III (Ligase III), XRCC1 (X-ray repair cross-complementing protein 1), RF-C (Replication factor-C), PCNA (Proliferating cell nuclear antigen), Fen1 (Flap-endonuclease 1), Lig I (ligase I).

BER and Human Disorders

Since BER repairs oxidative DNA damage, its dysregulation is the main driver of ROS-dependent pathologies due to an accumulation of point mutations. Such a dysfunction is cytotoxic and could be the cause of aging and its consequences: stress, genomic instability, and appearance of variants [21]. This could be seen in various neurodegenerative diseases such as in

Alzheimer-patients were ligases, polymerases, endonuclease (APE1), and glycosylases (OGG1, MYH, NEIL1) were shown to be downregulated [22]. Meanwhile, APE1 was shown to be dysregulated in amyotrophic lateral sclerosis (ALS) patients [21,23]. Similarly, OGG1's glycosylase activity is downregulated in Parkinson disease, another neurodegenerative disease [24]. Another type of disorders linking BER, oxidative stress, and oxidative DNA damage is currently observed in diabetes, where studies showed a decreased OGG1 protein expression [25]. In addition, recently, BER deficiency at expression and activity level was linked to Gorlin and Xeroderma Pigmentosum C diseases [26,27].

Unfortunately, BER's dysregulation could generate dramatic consequences such as cell transformation. 8-oxoGuanine is the most common oxidative DNA damage that is induced upon oxidative stress [28]. If left unrepaired, it can pair with adenine forming G: C to T: A transversion and induce double-strand breaks during replication [28]. Such a damage is found in numerous internal cancers (prostate, lung, liver, esophageal, and kidney cancers) and skin cancer [29-33].

BER Variants/Mutations and Cancer (Skin and Internal)

As mentioned previously, studies have shown a link between BER alterations and cancerogenesis [34].

Loss of OGG1 protein has been studied by many researchers who shared a similar conclusion, linking OGG1's absence to tumorigenesis. Upon OGG1 knockout, lung adenocarcinoma, and skin tumors (squamous cell carcinoma and sarcoma) developed in mice [35,36]. A double knockout in OGG1 and MYH induces a high frequency (65.7%) of lung and ovarian tumors and lymphomas [37-40]. Missense mutations in OGG1 at codons 85, 131, and 232 were linked to lung and kidney cancers [41]. Also, missense and nonsense mutations in OGG1 (Cys326Ser, Val159Gly; Gly221Arg; and Trp375STOP) were related to breast cancer [42] Moreover, single nucleotide variations in OGG1 have been shown to be linked to an increase in cancer risk. This may be due to a lower activity level

compared to the wild type. Benitez-Buelga et al. showed that the rs2304277 variant downregulates its transcriptional expression, thereby contributing to ovarian cancer risk in BRCA1 mutation carriers [43]. Similarly, Tayyaba et al. showed that such a variant contributes to urothelial bladder carcinoma [44]. In parallel, rs1052133 *OGG1* variant was linked to various cancers as breast, colon, stomach, kidney, orolaryngeal, bladder, colorectal cancers, and leukemia [45-50]. Rs113561019 *OGG1* was suggested as a low penetrance contributor to colorectal cancer [51].

Surprisingly, an upregulation in OGG1 protein is seen in various cancers as esophageal squamous carcinoma and ulcerative colitis-associated cancer [52]. This may indicate a persistence of oxidative stress and the inefficiency in OGG1's activity despite its high expression.

Studies have also shown a dramatic increase in cancer in the absence of MYH. A study involving MYH knockout in mice revealed significantly higher spontaneous tumorigeneses compared to control. Upon treatment with $KBrO_3$, an oxidizing agent, small intestinal tumor incidences were substantially higher in MYH's absence compared to its presence [53]. P.Tyr179Cys *MYH* variant showed a breast cancer risk while *MYH* Gln324His polymorphism showed a direct link with lung cancer risk in the Japanese population [54,55]. *MYH* monoallelic mutations, including Y179C and G396D, have been shown to have a higher risk in colorectal, endometrial, gastric, and liver cancers, while biallelic *MYH* mutations increase urinary bladder and ovarian cancer [56,57].

Other BER factors' variants/mutations were also linked to increased cancer occurrence. For example, APE1 Asp148Glu (rs3136820) is associated with breast and lung cancer [48,58]. XRCC1 Arg194Trp, Arg280His, and Arg399Gln were linked to various cancers like lung, stomach, bladder, and breast cancers [48]. Additionally, PARP-1 Ala762Ala and P53 Arg72Pro are significantly associated with cervical cancer [34]. While T889C Polβ point mutation increases membrane progesterone receptors, consequently, gastric cancer [59]. Polymerase mutations could

inhibit its expression/activity, thereby triggering the aggressiveness of cancer as breast cancer [60].

On the other hand, BER's overexpression (as APE1 and/or XRCC1) has also been detected in solid tumors and poor survival [61]. APE1's overexpression promotes ovarian cancer, and polymerase's overexpression (particularly Polβ) induces ovary, stomach, and prostate cancers [63,64].

Base Excision Repair Targeted Treatment

Cancer therapy is a modified chemotherapy that involves ionizing radiations or other types of DNA damaging cytotoxic process in addition to molecules that could augment the tumor-killing and reduce resistance to therapy. Since base excision repair is an essential pathway in repairing DNA, targeting its factors could be interesting to kill tumor cells selectively.

Methoxyamine is a small molecule that targets apurinic sites (AP) sites to block their repair by APE1. It is used as a potential targeting molecule in parallel to other chemotherapeutic agents as temozolomide (TMZ) or 1,3-bis-(2-chloroethyl)-1-nitrosourea (BCNU) that induce such sites in the DNA. This leads to the accumulation of DNA cytotoxic damages, thereby an induction of apoptosis. An important discovery about methoxyamine was its p53-independence, where usually loss of p53 is a common cancer resistance trait. Another strength point is its ability to target APE1 that plays an essential role in BER and regulating redox signaling. A phase 1 clinical trial has been conducted studying the combination of methoxyamine and TMZ in targeting solid tumors [65,66]. Other phase 1 and phase 2 studies are ongoing [63]. In 2019, Khoei et al. showed that methoxyamine enhances colon cancer cell lines' sensitization to the modified combined chemo- and radiation therapy. Such therapy included gamma radiation and 5-fluorouracil (5-FU), a cytotoxic molecule targeting DNA and RNA. Methoxyamine was shown to improve the efficacy of such a combined treatment by increasing the cytotoxicity and genotoxicity without increasing the gamma radiation dose [65]: **CRT0044876** was conducted as another APE1-inhibitor that reduced the survival of

fibrosarcoma cells in combination with TMZ. Unfortunately, this was not the case in combination with ionizing radiation. It had a poor potentiation [63]. Two interesting agents, **E3330** and **Gossypol/AT101**, NFκB and BCL2 inhibitors, respectively, were shown to bind to APE1 and inhibit its redox activity. Such agents could induce cytotoxicity solely or in combination with other cancer therapies in lung, lymphoma, prostate, adrenocortical, and glioblastoma cancers. More than 20 clinical trials are currently ongoing [63].

Loss of OGG1's activity has also been registered as a potential process towards sensitizing cells to chemo- and radiotherapy [67]. After screening almost 25975 potential compounds, Tahara et al. found a promising new compound, **SU0268**, that could bind specifically to OGG1 in HEK293T and HeLa cells and inhibit its activity [67]. Similarly, **SU0383** was developed to target MTH1, another 8-oxoguanine glycosylase. By inhibiting both glycosylases, oxidized bases will accumulate, forcing cancer cells to apoptosis. The effect of such inhibitors on animal cancer models is in progress [63]. **TH5487**, a recent OGG1 inhibitor that prevents its binding to oxidized purines and prevents inflammatory responses, seems promising but needs further experimental studies within cancer cell models [63].

Researchers have also targeted PARP1 due to its role in activating OGG1's expression and regulating oncogenes and tumor suppressors expression. Some PARP1 inhibitors are already on the market as **talazoparib** and **niraparib,** targeting BRCA-deficient cancer cells (breast, ovarian, and peritoneal cancers) [63,68]. However, drug resistance through increasing PARP1 levels and activation of repair pathways as homologs recombination has emerged. Hence, researchers are trying to develop other inhibitors that could have better efficacy [63]. Other dual anti-cancer molecules, **PD0332991** and **LEE011**, had shown a promising efficiency in targeting lung cancer cells by reducing PARP1 transcriptional expression and impairing OGG1-dependent BER, consequently inducing oxidative-cell death. Such treatment has its drawbacks. It depends on a link between RB1 (retinoblastoma protein), PARP1, and OGG1. However, RB1 is mutated in some cancer types as

retinoblastomas and small cell lung cancers. This may interfere with its efficacy. Therefore, further genomic and transcriptomic screenings are required before administration of this dual treatment as a potential PARP1 inhibitor can be foreseen [68].

Conclusion

Base excision repair plays a significant role in protecting cells against oxidative DNA damage, single-strand breaks, and ROS-cancerogenesis. Any variation/mutation or expression dysregulation in BER could alter its function in favor of cancerogenesis. However, targeting such a repair system to induce massive oxidative DNA damage in cancer cells could be a potential therapeutic process forcing cancers to cell death. Nevertheless, such an advanced targeted therapy seems challenging and needs further studies to avoid targeting normal cells and compensating their inhibition by activating other repair systems [63]. Immunotherapy and BER inhibitors combination could be one of the solutions to target cancer cells specifically by targeting specific cancer cell receptors and inhibiting repair to induce cancer apoptosis. Such combinatorial therapy has already resulted in intriguing and exciting findings.

References

1. Di Meo S, Reed TT, Venditti P, Victor VM. Role of ROS and RNS Sources in Physiological and Pathological Conditions. Oxidative Medicine and Cellular Longevity. 2016; 2016: 1–44.
2. Murphy MP. How mitochondria produce reactive oxygen species. Biochem J. 2009; 417: 1–13.
3. Ahmad G, Almasry M, Dhillon AS, Abuayyash MM, Kothandaraman N, et al. Overview and Sources of Reactive Oxygen Species (ROS) in the Reproductive System. In: Agarwal A, Sharma R, Gupta S, Harlev A, Ahmad G, et al, editors. Oxidative Stress in Human Reproduction: Shedding Light on a Complicated Phenomenon. Cham: Springer International Publishing. 2017; 1–16.
4. Finkel T. Signal transduction by reactive oxygen species. J Cell Biol. 2011; 194: 7–15.

5. Hirobe T. Keratinocytes regulate the function of melanocytes. Dermatologica Sinica, Special Issue: Pigmentary Disorders-Bringing Colors to Our Specialty. 2014; 32: 200–204.
6. Zhang J, Wang X, Vikash V, Ye Q, Wu D, et al. ROS and ROS-Mediated Cellular Signaling [WWW Document]. Oxidative Medicine and Cellular Longevity. 2016.
7. Rottenberg H, Hoek JB. The path from mitochondrial ROS to aging runs through the mitochondrial permeability transition pore. Aging Cell. 2017; 16: 943–955.
8. Zabłocka-Słowińska K, Płaczkowska S, Skórska K, Prescha A, Pawełczyk K, et al. Oxidative stress in lung cancer patients is associated with altered serum markers of lipid metabolism. PLoS One. 2019; 14.
9. Kondo S, Toyokuni S, Iwasa Y, Tanaka T, Onodera H, et al. Persistent oxidative stress in human colorectal carcinoma, but not in adenoma. Free Radic Biol Med. 1999; 27: 401–410.
10. Ma Y, Zhang L, Rong S, Qu H, Zhang Y, et al. Relation between Gastric Cancer and Protein Oxidation, DNA Damage, and Lipid Peroxidation. Oxid Med Cell Longev. 2013; 2013.
11. Liu Z, Ren Z, Zhang J, Chuang CC, Kandaswamy E, et al. Role of ROS and Nutritional Antioxidants in Human Diseases. Front Physiol. 2018; 9.
12. Weinberg F, Ramnath N, Nagrath D. Reactive Oxygen Species in the Tumor Microenvironment: An Overview. Cancers (Basel). 2019; 11.
13. Saha SK, Lee SB, Won J, Choi HY, Kim K, et al. Correlation between Oxidative Stress, Nutrition, and Cancer Initiation. Int J Mol Sci. 2017; 18.
14. Jun JC, Rathore A, Younas H, Gilkes D, Polotsky VY. Hypoxia-Inducible Factors and Cancer. Curr Sleep Med Rep. 2017; 3: 1–10.
15. Chan JSK, Tan MJ, Sng MK, Teo Z, Phua T, et al. Cancer-associated fibroblasts enact field cancerization by promoting extratumoral oxidative stress. Cell Death Dis. 2017; 8: e2562.

16. Chen X, Song M, Zhang B, Zhang Y. Reactive Oxygen Species Regulate T Cell Immune Response in the Tumor Microenvironment. Oxid Med Cell Longev. 2016; 2016.
17. Amaro-Ortiz A, Yan B, D'Orazio JA. Ultraviolet radiation, aging and the skin: prevention of damage by topical cAMP manipulation. Molecules. 2014; 19: 6202–6219.
18. Krokan HE, Bjørås M. Base Excision Repair. Cold Spring Harb Perspect Biol. 2013; 5.
19. Rolseth V, Luna L, Olsen AK, Suganthan R, Scheffler K, et al. No cancer predisposition or increased spontaneous mutation frequencies in NEIL DNA glycosylases-deficient mice. Scientific Reports. 2017; 7: 4384.
20. Leyns L, Gonzalez L. Genomic Integrity of Mouse Embryonic Stem Cells. Embryogenesis. 2012.
21. Sidler C. Chapter 29 - Genomic Instability and Aging: Causes and Consequences, in: Kovalchuk, I., Kovalchuk, O. (Eds.), Genome Stability. Boston: Academic Press. 2016; 511–525.
22. Weissman L, Jo DG, Sørensen MM, de Souza-Pinto NC, Markesbery WR, et al. Defective DNA base excision repair in brain from individuals with Alzheimer's disease and amnestic mild cognitive impairment. Nucleic Acids Res. 2017; 35: 5545–5555.
23. Sliwinska A, Sitarek P, Toma M, Czarny P, Synowiec E, et al. Decreased expression level of BER genes in Alzheimer's disease patients is not derivative of their DNA methylation status. Progress in Neuro-Psychopharmacology and Biological Psychiatry. 2017; 79: 311–316.
24. Canugovi C, Misiak M, Ferarelli LK, Croteau DL, Bohr VA. The role of DNA repair in brain related disease pathology. DNA Repair (Amst). 2013; 12: 578–587.
25. Simone S, Gorin Y, Velagapudi C, Abboud HE, Habib SL. Mechanism of Oxidative DNA Damage in Diabetes: Tuberin Inactivation and Downregulation of DNA Repair Enzyme 8-Oxo-7,8-Dihydro-2′-Deoxyguanosine-DNA Glycosylase. Diabetes. 2008; 57: 2626–2636.
26. Charazac A, Fayyad N, Beal D, Bourgoin-Voillard S, Seve M, et al. Impairment of Base Excision Repair in Dermal Fibroblasts Isolated From Nevoid Basal Cell Carcinoma Patients. Front Oncol. 2020; 10: 1551.

27. Fayyad N, Kobaisi F, Beal D, Mahfouf W, Ged C, et al. Xeroderma Pigmentosum C (XPC) Mutations in Primary Fibroblasts Impair Base Excision Repair Pathway and Increase Oxidative DNA Damage. Front. Genet. 2020; 11.
28. Aguiar PHN, Furtado C, Repolês BM, Ribeiro GA, Mendes IC, et al. Oxidative Stress and DNA Lesions: The Role of 8-Oxoguanine Lesions in Trypanosoma cruzi Cell Viability. PLoS Negl Trop Dis. 2013; 7.
29. Bendesky A, Michel A, Sordo M, Calderón-Aranda ES, Acosta-Saavedra LC, et al. DNA damage, oxidative mutagen sensitivity, and repair of oxidative DNA damage in nonmelanoma skin cancer patients. Environ Mol Mutagen. 2006; 47: 509–517.
30. Cooke MS, Evans MD, Dizdaroglu M, Lunec J. Oxidative DNA damage: mechanisms, mutation, and disease. The FASEB Journal. 2003; 17: 1195–1214.
31. Gackowski D, Speina E, Zielinska M, Kowalewski J, Rozalski R, et al. Products of oxidative DNA damage and repair as possible biomarkers of susceptibility to lung cancer. Cancer Res. 2003; 63: 4899–4902.
32. Kubo N, Morita M, Nakashima Y, Kitao H, Egashira A, et al. Oxidative Dna damage in human esophageal cancer: clinicopathological analysis of 8-hydroxydeoxyguanosine and its repair enzyme. Dis Esophagus. 2014; 27: 285–293.
33. Oberley TD. Oxidative Damage and Cancer. Am J Pathol. 2002; 160: 403–408.
34. Chen H, Wang H, Liu J, Cheng Q, Chen X, et al. Association of Base Excision Repair Gene hOGG1 Ser326Cys Polymorphism with Susceptibility to Cervical Squamous Cell Carcinoma and High-Risk Human Papilloma Virus Infection in a Chinese Population. Genetic Testing and Molecular Biomarkers. 2019; 23: 138–144.
35. Kunisada M, Sakumi K, Tominaga Y, Budiyanto A, Ueda M, et al. 8-Oxoguanine Formation Induced by Chronic UVB Exposure Makes Ogg1 Knockout Mice Susceptible to Skin Carcinogenesis. Cancer Res. 2005; 65: 6006–6010.
36. Smith CG, West H, Harris R, Idziaszczyk S, Maughan TS, et al. Role of the Oxidative DNA Damage Repair Gene OGG1 in Colorectal Tumorigenesis. J Natl Cancer Inst. 2013; 105: 1249–1253.

37. Lee TH, Kang TH. DNA Oxidation and Excision Repair Pathways. Int J Mol Sci. 2019; 20.
38. Tahara YK, Auld D, Ji D, Beharry AA, Kietrys AM, et al. Potent and Selective Inhibitors of 8-Oxoguanine DNA Glycosylase. J. Am. Chem. Soc. 2018; 140: 2105–2114.
39. Wallace SS, Murphy DL, Sweasy JB. Base Excision Repair and Cancer. Cancer Lett. 2012; 327: 73–89.
40. Xie Y, Yang H, Cunanan C, Okamoto K, Shibata D, et al. Deficiencies in Mouse Myh and Ogg1 Result in Tumor Predisposition and G to T Mutations in Codon 12 of the K-Ras Oncogene in Lung Tumors. Cancer Res. 2004; 64: 3096–3102.
41. Chevillard S, Radicella JP, Levalois C, Lebeau J, Poupon MF, et al. Mutations in OGG1, a gene involved in the repair of oxidative DNA damage, are found in human lung and kidney tumours. Oncogene. 1998; 16: 3083–3086.
42. Ali K, Mahjabeen I, Sabir M, Mehmood H, Kayani MA. OGG1 Mutations and Risk of Female Breast Cancer: Meta-Analysis and Experimental Data [WWW Document]. Disease Markers. 2015.
43. Benitez-Buelga C, Vaclová T, Ferreira S, Urioste M, Inglada-Perez L, et al. Molecular insights into the OGG1 gene, a cancer risk modifier in BRCA1 and BRCA2 mutations carriers. Oncotarget. 2016; 7: 25815–25825.
44. Ahmed T, Nawaz S, Noreen R, Bangash KS, Rauf A, et al. A 3' untranslated region polymorphism rs2304277 in the DNA repair pathway gene OGG1 is a novel risk modulator for urothelial bladder carcinoma. Ann Hum Genet. 2018; 82: 74–87.
45. Elahi A, Zheng Z, Park J, Eyring K, McCaffrey T, et al. The human OGG1 DNA repair enzyme and its association with orolaryngeal cancer risk. Carcinogenesis. 2002; 23: 1229–1234.
46. Habib SL, Danial E, Nath S, Schneider J, Jenkinson CP, et al. Genetic polymorphisms in OGG1 and their association with angiomyolipoma, a benign kidney tumor in patients with tuberous sclerosis. Cancer Biology & Therapy. 2008; 7: 23–27.

47. Hassan FM. OGG1 rs1052133 Polymorphism and Genetic Susceptibility to Chronic Myelogenous Leukaemia. Asian Pac J Cancer Prev. 2019; 20: 925–928.
48. Hung RJ, Hall J, Brennan P, Boffetta P. Genetic Polymorphisms in the Base Excision Repair Pathway and Cancer Risk: A HuGE Review. Am J Epidemiol. 2005; 162: 925–942.
49. Smal MP, Kuzhir TD, Savina NV, Nikitchenko NV, Rolevich AI, et al. BER gene polymorphisms associated with key molecular events in bladder cancer. Exp. Oncol. 2018; 40: 288–298.
50. Su Y, Xu A, Zhu J. The effect of oxoguanine glycosylase 1 rs1052133 polymorphism on colorectal cancer risk in Caucasian population. Tumor Biol. 2014; 35: 513–517.
51. Ogg G, Tumorigenesis C, Smith CG, Maughan TS, Kaplan R, et al. Role of the Oxidative DNA Damage Repair gene OGG1 in colorectal tumorigenesis. J Natl Cancer Inst. 2013; 105: 1249-1253.
52. Kumagae Y, Hirahashi M, Takizawa K, Yamamoto H, Gushima M, et al. Overexpression of MTH1 and OGG1 proteins in ulcerative colitis-associated carcinogenesis. Oncol Lett. 2018; 16: 1765–1776.
53. Sakamoto K, Tominaga Y, Yamauchi K, Nakatsu Y, Sakumi K, et al. MUTYH-Null Mice Are Susceptible to Spontaneous and Oxidative Stress–Induced Intestinal Tumorigenesis. Cancer Res. 2007; 67: 6599–6604.
54. Miyaishi A, Osawa K, Osawa Y, Inoue N, Yoshida K, et al. MUTYH Gln324His gene polymorphism and genetic susceptibility for lung cancer in a Japanese population. J Exp Clin Cancer Res. 2009; 28: 10.
55. Rizzolo P, Silvestri V, Bucalo A, Zelli V, Valentini V, et al. Contribution of MUTYH Variants to Male Breast Cancer Risk: Results From a Multicenter Study in Italy. Front. Oncol. 2018; 8.
56. Win AK, Cleary SP, Dowty JG, Baron JA, Young JP, et al. Cancer risks for monoallelic MUTYH mutation carriers with a family history of colorectal cancer. Int J Cancer. 2011; 129: 2256–2262.
57. Win AK, Reece JC, Dowty JG, Buchanan DD, Clendenning M, et al. Risk of extracolonic cancers for people with

biallelic and monoallelic mutations in MUTYH. International Journal of Cancer. 2016; 139: 1557–1563.
58. Hsieh WC, Lin C, Chen DR, Yu WF, Chen GJ, et al. Genetic polymorphisms in APE1 Asp148Glu(rs3136820) as a modifier of the background levels of abasic sites in human leukocytes derived from breast cancer patients and controls. Breast Cancer. 2017; 24: 420–426.
59. Tan X, Wu X, Ren S, Wang H, Li Z, et al. A Point Mutation in DNA Polymerase β (POLB) Gene Is Associated with Increased Progesterone Receptor (PR) Expression and Intraperitoneal Metastasis in Gastric Cancer. J Cancer. 2016; 7: 1472–1480.
60. Abdel-Fatah TMA, Russell R, Agarwal D, Moseley P, Abayomi MA, et al. DNA polymerase β deficiency is linked to aggressive breast cancer: A comprehensive analysis of gene copy number, mRNA and protein expression in multiple cohorts. Molecular Oncology. 2014; 8: 520–532.
61. Yuan CL, He F, Ye JZ, Wu HN, Zhang JY, et al. APE1 overexpression is associated with poor survival in patients with solid tumors: a meta-analysis. Oncotarget. 2017; 8: 59720–59728.
62. Albertella MR, Lau A, O'Connor MJ. The overexpression of specialized DNA polymerases in cancer. DNA Repair. 2005; 4: 583–593.
63. Grundy GJ, Parsons JL. Base excision repair and its implications to cancer therapy. Essays Biochem. 2020; 64: 831–843.
64. Wen X, Lu R, Xie S, Zheng H, Wang H, et al. APE1 overexpression promotes the progression of ovarian cancer and serves as a potential therapeutic target. Cancer Biomark. 2016; 17: 313–322.
65. Khoei S, Poorabdollahi R, Mostaar A, Faeghi F. Methoxyamine Enhances 5-Fluorouracil-Induced Radiosensitization in Colon Cancer Cell Line HT29. Cell J. 2017; 19: 283–291.
66. Sharma RA, Dianov GL. Targeting base excision repair to improve cancer therapies. Molecular Aspects of Medicine, DNA Base Excision Repair and Human Pathology. 2007; 28: 345–374.

67. Tahara YK, Auld D, Ji D, Beharry AA, Kietrys AM, et al. Potent and Selective Inhibitors of 8-Oxoguanine DNA Glycosylase. J. Am. Chem. Soc. 2018; 140: 2105–2114.
68. Tempka D, Tokarz P, Chmielewska K, Kluska M, Pietrzak J, et al. Downregulation of PARP1 transcription by CDK4/6 inhibitors sensitizes human lung cancer cells to anticancer drug-induced death by impairing OGG1-dependent base excision repair. Redox Biol. 2017; 15: 316–326.

Book Chapter

Implication of Ultraviolet Irradiation in Photo-carcinogenesis

Farah Kobaisi[1,2], Eric Sulpice[1], Mohammad Fayyad-Kazan[2], Ali Nasrallah[1], Xavier Gidrol[1], Hussein Fayyad-Kazan[2] and Walid Rachidi[1]*

[1]University of Grenoble Alpes, CEA/IRIG/Biomics, France
[2]Laboratory of Cancer Biology and Molecular Immunology, Faculty of Sciences I, Lebanese University, Lebanon

***Corresponding Author:** Walid Rachidi, University of Grenoble Alpes, CEA/IRIG/Biomics, 38000 Grenoble, France

Published **February 25, 2021**

How to cite this book chapter: Farah Kobaisi, Eric Sulpice, Mohammad Fayyad-Kazan, Ali Nasrallah, Xavier Gidrol, Hussein Fayyad-Kazan, Walid Rachidi. Implication of Ultraviolet Irradiation in Photo-carcinogenesis. In: Hussein Fayyad Kazan, editor. Immunology and Cancer Biology. Hyderabad, India: Vide Leaf. 2021.

Abstract

Human skin is exposed, on a daily basis, to various exogenous threats including ultra violet (UV) solar rays. Long-term UV exposure can lead to serious consequences such as photo ageing, freckles as well as formation of either malignant or benign skin tumors. Such exposure activates distinct signaling pathways and triggers the formation of lesions whose regulation and repair are

fine-tuned and can determine the cell's fate (survival, apoptosis or carcinogenesis).

UV Radiation, Skin Penetration and Resulting Damage

Solar UV radiation is sub-classified into UVA (320-400nm), UVB (280-320nm) and UVC (200-280nm). UVC is absorbed by the ozone layer rendering the UV spectrum reaching earth restricted to 95% UVA and 5% UVB. These two solar rays allow the induction of DNA lesions, thus playing a critical role in skin carcinogenesis. The more energetic UVB can be absorbed by the epidermis and superficial dermis; whereas the less energetic more penetrating UVA can reach deep into the dermis.

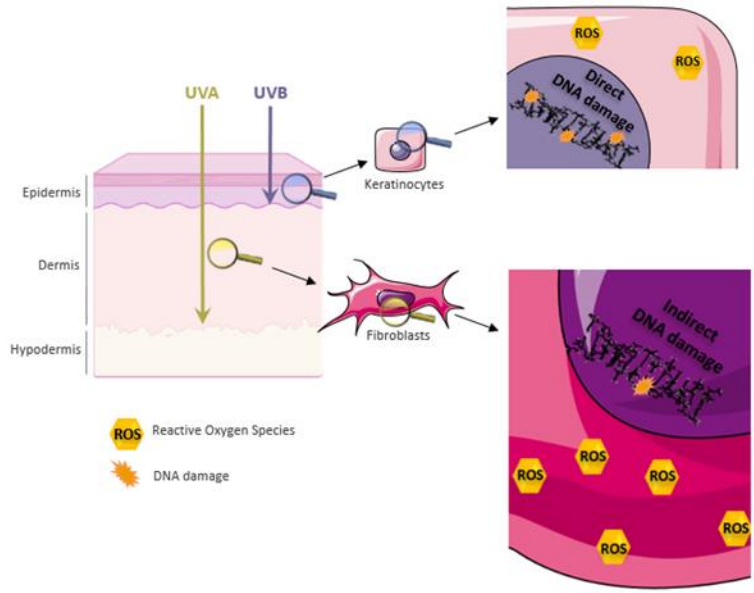

Figure 1: UV skin penetration and molecular outcomes.
Out of solar rays, UVA and UVB can penetrate the skin to reach deep into the dermis or be restricted to the epidermis respectively. UVB rays induce direct damages to the DNA and the formation of reactive oxygen species (ROS). UVA's damage to the DNA is indirect via photosensitization reactions by ROS produced at a high rate.

On one hand, UVB irradiation generates direct damages to the DNA in the form of dimeric pyrimidine photoproducts including Cyclobutane pyrimidine dimers (CPDs), 6-4 pyrimidine-pyrimidone photoproducts (6-4PPs) and Dewar isomers [3]. The latter are formed between two adjacent pyrimidine sites TT, CT, TC or CC. The 6-4 PPs are readily repaired in faster kinetics compared to CPDs where the TC and CC-CPD are the most mutagenic ones [4]. UVB also contributes to the generation of double-strand breaks via collapsing the replication forks at dimer sites and formation of reactive oxygen species (ROS) [5]. The generation of 8-hydroxy-2-deoxyguanosines (8-OHdG) was reported post UVB irradiation that leads to G→T transversion. The majority of UVB-induced mutations are C→T or CC→TT transitions designated as the UVB signature mutation [6]. On the other hand, UVA damage to the DNA is indirect via reactive oxygen species that are generated at bigger amounts than UVB-induced ROS. The most common UVA-induced lesion is 8-oxo guanine. CPDs' indirect formation post UVA are mediated by chemically generated excited electronic states [7]. In addition to DNA damage, ROS can also contribute to lipid peroxidation and protein oxidation (figure 1).

UV-Induced Apoptosis

Apoptosis is triggered in irradiated cells by three different mechanisms. UV-induced DNA damage favors the activation of ataxia telangiectasia and rad3 related (ATR), ataxia telangiectasia mutated (ATM) and DNA-PK kinases that ultimately activates p53 via checkpoint kinase ChK1/2 as part of the DNA damage response. p53 regulates the transcription of cell cycle protein p21 and several pro-apoptotic factors including APAF1, NOXA, PUMA, Bax and Bak. This contributes to the arrest of the cell cycle. If damage repair fails, P53 via downstream effectors the modulation of mitochondrial permeability to allow the release of cytochrome c. APAF1, procaspase 9 and cytochrome c favor the formation of the apoptosome leading to the activation of caspase 9 then caspase 3 [2]. Moreover, the production of reactive oxygen species post UV induces, in addition to DNA damage, lipid peroxidation, protein oxidation and the release of cytochrome c to mediate

another intrinsically triggered apoptotic pathway. One final mechanism of apoptosis is mediated via the extrinsic effect of UV in clustering death receptors, includng the tumor necrosis factor (TNF) receptor superfamily members the CD95 (Fas/APO-1) or TRAIL, leading to the activation of a cascade of caspases from caspase 8 till caspase 3 [8] (figure 2).

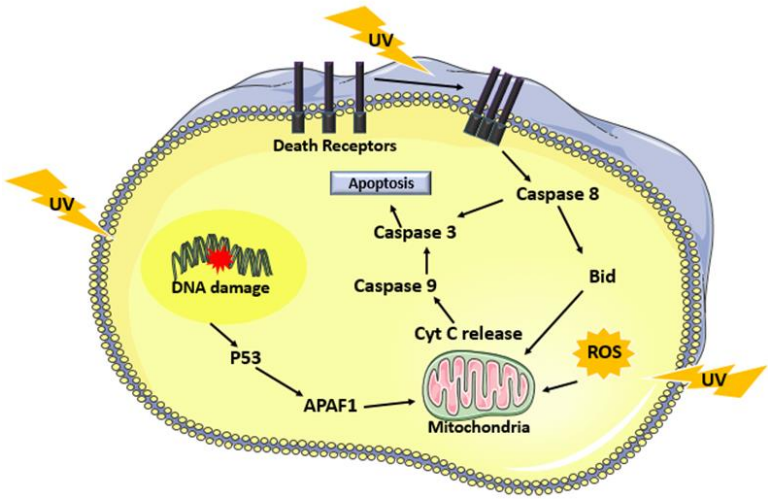

Figure 2: Mechanisms of UV induced apoptosis.
UV irradiation triggers cell apoptosis by three different mechanisms. The first is mediated by p53 activation due to DNA damage that ultimately leads to the activation of caspase 9 followed by caspase 3. Reactive oxygen species generated by UV also induce apoptosis by enabling the release of cytochrome c from the mitochondria. One final mechanism is via UV mediated clustering of death receptors leading to the activation of caspase 8.

UV-Induced Signal Transduction

AKT Pathway

The full kinase activity of Akt is achieved on one hand by its phosphorylation at two distinct sites, Thr308 phosphorylation via receptor tyrosine kinase activated PI3K and Ser473 by mTOR complex 2 (mTOR/Rictor; mTORC2) [9]. Its inhibition, on the other hand, is achieved by the tumor suppressor PTEN [10]. UV triggers tyrosine kinase receptors as well as the inhibition of PTEN to enable Akt activation post-irradiation [11]. This further

permits the activation of anti-apoptotic transcription factor NFκB [10] and p53 negative regulator MDM2 [12]. The latter together with Akt mediated inhibition of FOXO [13], pro-apoptotic forkhead transcription factor, and apoptotic proteins Bad and caspase 9 [14] infers an anti-apoptotic Akt mediated signal. Cell cycle progression is also achieved via the inhibition of nuclear translocation of cell cycle inhibitors p21 and p27 [15]. Akt also increases metabolic activity via the phosphorylation and thus inhibition of glycogen synthase kinase (GSK3) [16]. The outcome involves the modulation of protein synthesis and autophagy. The Akt-mediated inhibition of TSC2, tuberous sclerosis protein 2, leads to activation of mTOR/Raptor (mTORC1) that promotes translation via phosphorylation of eukaryotic initiation factor 4E (eIF-4E) binding protein-1 (4E-BP1) and p70/p85 S6 kinase (S6K) [17] (figure 3).

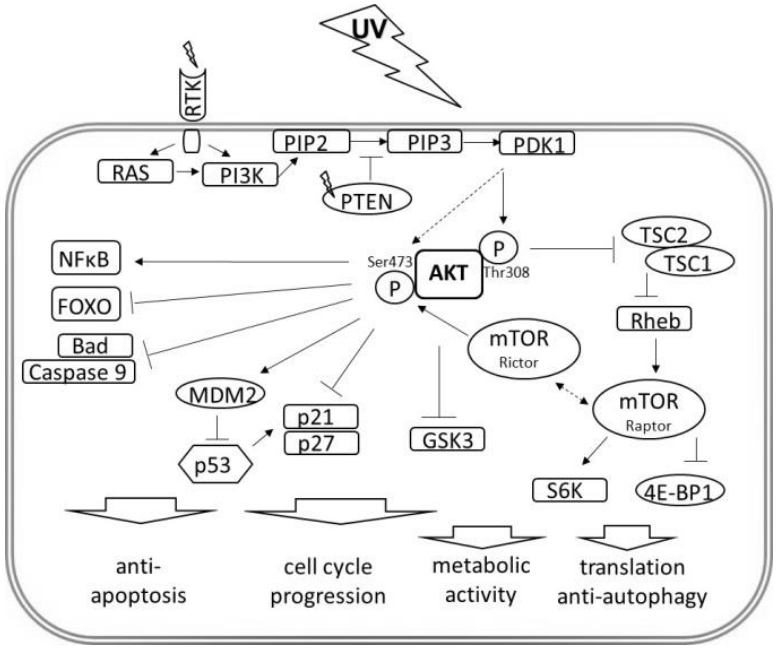

Figure 3: Physiological functions triggered by UV induced Akt signaling.
UV induced Akt activation can induce the activation of several downstream cellular functions including inhibition of apoptosis, cell cycle progression, metabolic activity inductions and translation. Detailed description available in the text [2].

MAPK Pathway

Another UV-activated pathway is the mitogen-activated protein kinase (MAPK) pathway with final effectors including the c-JUN NH2 terminal kinases (JNKs), the extracellular signal-regulated kinases (ERKs) and p38 kinases that regulate the activity of transcription factors NFκB and AP-1. The different forms of UV irradiation (UVA, UVB, UVC) explicit different modes of MAPK activation that is dose-dependent.

UVA induced MAPK signaling

UVA induces the activation of epidermal growth factor receptor (EGFR) that then leads to the phosphorylation of the 40*S* ribosomal protein S6 by $p70^{S6K}$ (70-kD ribosomal S6 kinase) and $p90^{RSK}$ (90-Kd ribosomal S6 kinase, also known as MAPKAP-K1) [18,19]. The activation of $p70^{S6K}$, on one hand, is achieved by different MAPK pathways phosphorylating four distinct sites.

PI3K activation induces the phosphorylation at Ser411, Thr421 and Ser424 while mTOR phosphorylates the Thr389 site. These four sites are phosphorylated by ERK1/2. P38 phosphorylates Thr389 and JNK added phosphate groups on both Ser411 and Thr389 [20]. On the other hand, ERK and JNK but not p38 enable the phosphorylation/activation of p90RSK at Ser381 [21]. It should be noted that the inhibition of EGFR abrogated the UV induced phosphorylation of ERK but not p38 and JNK implying that EGFR mediated signaling to p90RSK and p70S6K is ERK [22] and PI3K dependent. These ribosomal kinases regulate various cellular functions like proliferation and differentiation. Moreover, UVA irradiation can direct cellular decision towards apoptosis triggered by p53 and JNK [23]. The latter being activated by sphingomyelinase (SMase) and thus ceramide hydrolysis [24] (figure 4).

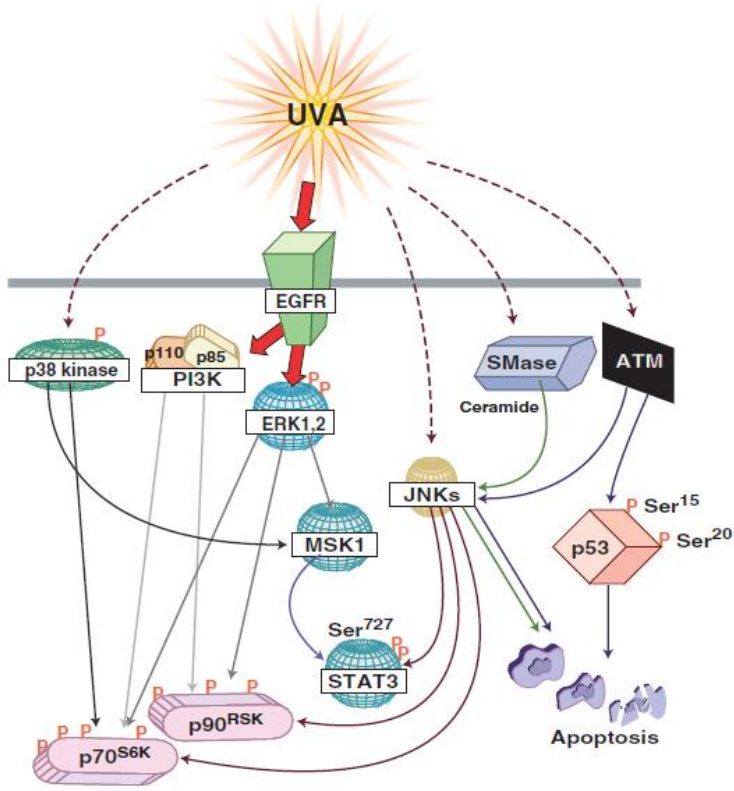

Figure 4: UVA induced MAPK signaling.
UVA activates EGFR that leads to the phosphorylation/activation of several downstream effectors including $p70^{S6K}$ and $p90^{RSK}$. UVA mediated apoptosis is mediated by the activation of JNK, ATM, or SMase [1].

UVB induced MAPK signaling

MAPK mediated UVB induced activation of AP-1 via PKC

UVB-induced activation of AP-1 implicates protein kinase C (PKC) that favors activation of JNK and ERK [25]. ERK further on mediates activation of AP-1 [26]. P38, however, was shown to be activated in EGFR dependent mechanism post UVB and that it further on led to apoptosis [27] (figure 5A).

MAPK-mediated UVB Induced Apoptosis

UVB-induced p53 dependent apoptosis is mediated via the phosphorylation of the latter at Ser20 by JNK [28]. Nonetheless, p38 and ERK phosphorylate p53 at Ser15 [29] (figure 5B). Apoptosis is also mediated by the activation of the pro-apoptotic protein BAD. The phosphorylation of BAD is carried out by several kinases including JNK1, ERK downstream kinases RSK1 and MSK1 and by p38 kinase allowing BAD's dissociation from the anti-apoptotic Bcl-XL [30] (figure 5C).

MAPK mediated UVB Induced Chromatin Remodeling

The phosphorylation of nucleosome structural protein histone H3 regulates its role in enabling gene expression and chromatin remodeling. Two phosphorylation sites are present on histone H3 which are the Ser10 and Ser28. Ser10 phosphorylation is mediated via ERK and p38 [29] whereas Ser28's phosphorylation is mediated by JNK, ERK and p38 kinases together with ERK and p38 downstream kinase MSK1 [31,32] (figure 5D).

MAPK mediated UVB Induced Growth Control

Growth control regulation can be mediated at either the transcriptional level via ribosomal kinases or at the translational level by translation initiation factors. UVB activates PI3K pathway triggering the phosphorylation of several downstream effectors like Akt and p70S6K [33]. Akt UVB-induced activation is mediated via MSK1 [34] (figure 5E). Moreover, the p38 kinase through its downstream effector MSK1 phosphorylates eukaryotic initiation factor 4E (eIF-4E)-binding protein (4E-BP1) allowing its dissociation from eIF-4F, relieving the translational block and allowing cap-dependent translation initiation [35] (figure 5F).

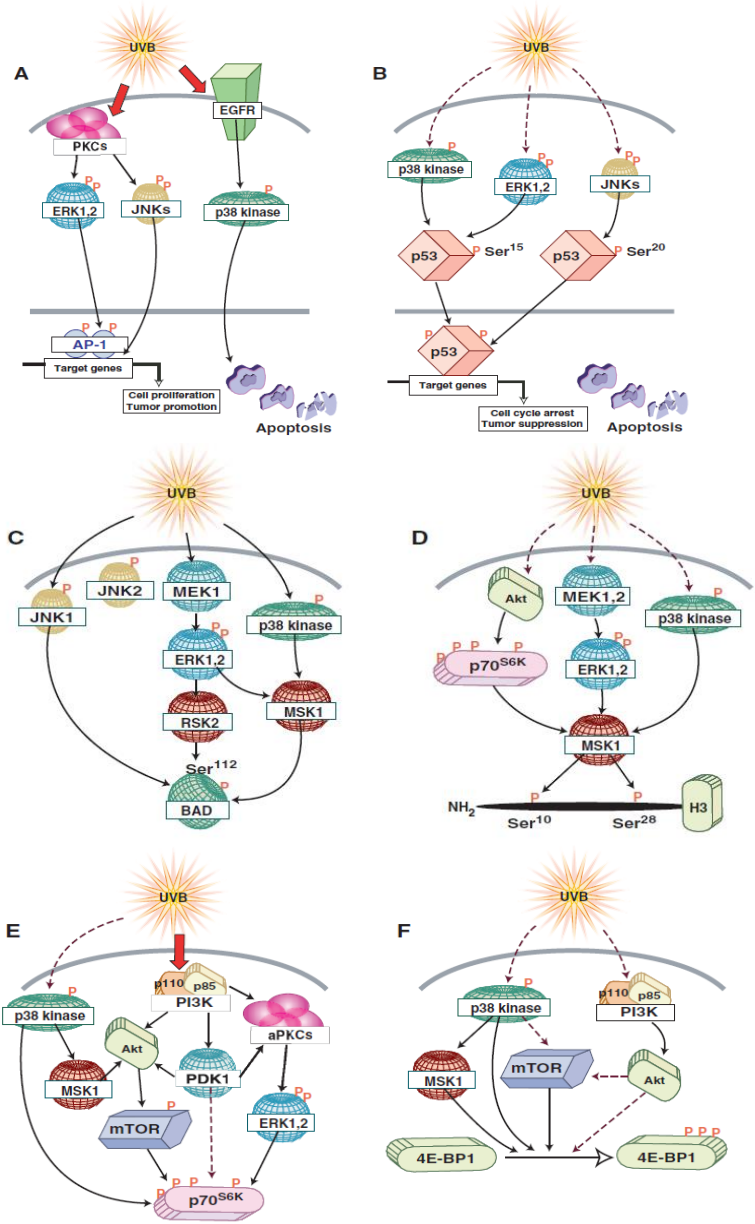

Figure 5: UVB induced MAPK signaling.
UVB can trigger different cellular functions via the activation of the diverse MAPK effectors. (A) UVB can, on one hand, activate PKC leading to the activation of AP-1 and, on the other hand, mediate the activation of p38 via EGFR that leads to apoptosis. (B) P53 phosphorylation is achieved by both

ERK and p38 at Ser15 and by JNK on Ser15. (C) BAD phosphorylation at Ser112 is facilitated by JNK1, RSK2 and MSK1. (D) Histone H3 is phosphorylated at two sites: Ser10 by ERK and p38 kinase and at Ser28 by ERK, p38 and JNK. MSK1, a downstream effector of ERK and p38, also favors the phosphorylation at Ser28. (E) UVB mediated activation of Akt is PI3K dependent and MSK1 can also be involved in such activation. (F) 4EBP1 phosphorylation by the p38 kinase to MSK1 pathway favors its activation and dissociation from eIF-4E [1].

UV-Induced Mutations and Carcinogenesis

p53

p53 plays a critical role in the cell cycle arrest post-stress induction. It activates cell cycle checkpoints halting cycle progression allowing enough time for DNA damage repair. If the repair was unsuccessful, p53 aids in the commitment of the cell to apoptosis by the expression of several pro-apoptotic proteins. UV-induced activation of p53 is mainly mediated via (ATR) that phosphorylates checkpoint kinases (chk1/2) ultimately leading to p53 phosphorylation at Ser15 and Ser20 [36]. Mutations in p53 can be mainly detected in squamous cell carcinoma and less in basal cell carcinoma. Such mutations carry the UV fingerprint C → T transition [37]. Such mutations hinder the pro-apoptotic activity of p53 resulting in amplification of DNA damage accumulating cells. That combined with UVR-induced upregulation of heat shock proteins poses a combined effect on carcinogenesis evident via their co-localization with mutant p53 in squamous cell carcinoma [38].

PTEN

Phosphate tensin homolog is a known inhibitor of the PI3K/Akt leading to the deregulation of cell proliferation and induction of apoptosis. Besides, PTEN also has a role in the regulation of DNA damage repair of NER and DSB. In the course of NER, Ming et al. showed that downregulation of PTEN expression in the epidermis of mice predisposes them to skin tumorigenesis upon UV irradiation [39]. One hypothesis involves the reduction of xeroderma pigmentosum C (XPC) expression upon PTEN downregulation via the Akt/p38 pathway. XPC is a DNA damage recognition protein in the nucleotide excision repair

pathway required for the identification of the UV induced DNA damages. The decrease of XPC thus allows the accumulation of CPDs and 6-4PPs. In DSB, PTEN downregulation leads to decreased Rad51 expression [40].

PTCH

PTCH gene encodes for a membrane receptor in the sonic hedgehog (Shh) pathway. The later plays an important role in regeneration and re-differentiation of adult tissue. The canonical signaling in the Shh pathway starts with the biding of the Shh ligand to the transmembrane receptor Patched (PTCH) inactivating it. This will relieve the PTCH-mediated inhibition of smoothened (SMO). SMO will further on activate the downstream signaling to result in the translocation of the Glioma zinc finger transcriptions factors (Gli) to the nucleus to initiate transcription [41]. Some of the downstream expressed genes are involved in tumorigenesis and they include BCL2 for apoptosis resistance, SNAIL for epithelial-mesenchymal transition, Wnt2 for cell stemness, and TGFβ for immune suppression among others [42]. PTCH mutations bear the UV signature C→T or CC→TT transitions. The latter allows the inactivation of PTCH and its role in the inhibition of smoothened (SMO) expression. Therefore, SMO can then mediate the activation of Gli1 transcriptional factor resulting in tumor formation [43]. Such deficiency was recorded in 85% of BCC [44]. Gorlin syndrome is characterized with an increased predisposition to basal cells carcinomas due to a mutation in PTCH1 tumor suppressor gene. Charazac et al. reported that fibroblasts from Gorlin patients exhibit high radio-sensitivity. These cells appeared to manifest low expression and activity of base excision repair pathway proteins thus linking Gorlin clinical manifestations to possible defects in DNA damage response or repair capacity [45].

NRAS and BRAF

NRAS and BRAF play a major role in the mitogen-activated protein kinase (MAPK) pathway. The binding of growth factor to their respective tyrosine kinase receptor activates this pathway. RAS GTPase then conveys the intracellular signaling.

Active Ras bound to GTP allows the recruitment of effectors including the RAF family of serine/threonine kinases that regulate cell proliferation. RAF further on activates MAP kinase kinase (MEK1/2) and then MAP kinase (ERK1/2). The latter promotes cell proliferation [46]. Activating mutations in these genes are mainly found in melanoma. Only a single mutation in either gene can exist at a time [47]. Mutations in either are of the activating type enhancing the MAPK signaling. BRAF most frequent mutation is a T→A transversion.[48]. NRAS most frequent mutation is either a C→A transversion or A→G transitions in sun-exposed areas [49]. These mutations are not exactly a C→T UV signature mutation, however, their comparison with the mutagenic profile in bacteria reveals that they may be derived from UVA mediated oxidative DNA damage [50].

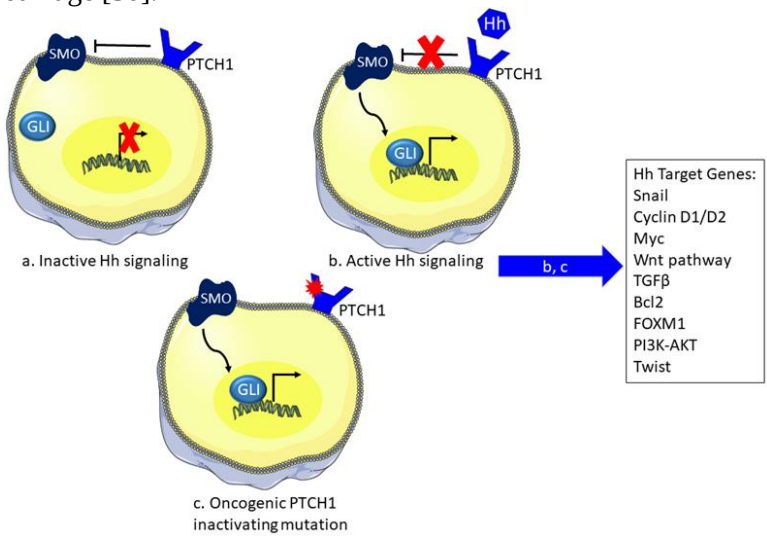

Figure 6: The sonic hedgehog pathway and the effect of UV irradiation.
The SHH pathway controls the expression of several downstream effectors. a) In the inactive state, PTCH receptor inhibits SMO and thus preventing the translocation of Gli to the nucleus blocking transcription of underlying genes. b) However, in the presence of the Hh ligand the PTCH receptor becomes inactive losing its inhibitory effect on SMO favoring the activity of Gli in transcription. c) Inactivating mutation of PTCH induced by UV irradiation relieve SMO inhibition and activates the pathway to express downstream genes via Gli. SHH: sonic hedgehog, PTCH: patched receptor, SMO: smoothened, Gli: glioma transcription factor

RAC1 and PREX2

PREX2 is a GTP/GDP exchange factor that can promote tumorigenesis via the inhibition of PTEN, a known regulator of the PI3K signaling pathway [51]. PREX2 also mediates the activation of the GTPase RAC involved in cell migration [52]. Large scale cancer genomic profiling revealed the involvement of mutations in these two genes with the melanoma oncogenesis [53, 54]. These genes interact to promote the PI3K/Akt [52, 55]. Mutations in the RAC1 gene possess the typical UV signature C→T transition mutation in sun-exposed areas that allows the activation of RAC1 and the underlying signaling pathways [56]. PREX2 mutations are also mainly found in sun-exposed areas [54] where it inhibits PTEN annulling its effect in the inhibition of the PI3K pathway.

Although other genes have been recorded to be involved in skin carcinogenesis, they do not possess a UV signature mutation profile signifying a different origin other than UV as their carcinogenesis initiator. The latter includes mutations in the cell cycle genes found in both basal and squamous cell carcinoma [57]. In addition, loss of p16INK4A was also identified in melanoma leading to the enhancement of CDK4 activity promoting proliferation [58].

UV-Irradiation Induced Immunosuppression

Genetic mutations alone do not represent the only initiators of skin tumorigenesis. An intricate signaling network interplays with such mutations leading ultimately to tumor generation one of which is the UV irradiation-induced immune suppression. The first form of suppression is mediated via the defective antigen presentation activity of Langerhans cells. UVR leads to the elevation of IL6, IL10 and TNFα levels thus inhibiting the skin immune response by downregulating Langerhans cells activity [59]. Moreover, UV irradiation was found to have a negative effect on the number of natural killer cells in a UV dose-dependent manner. The latter cells are implicated in anti-tumor and anti-viral infection [60]. UVB exposure also increases the expression of cyclooxygenase (COX-2) enzyme that catalyzes

the first step for the conversion of arachidonic acid to active prostaglandin involved in the inflammatory response. COX-2 is implicated in the development of several types of tumors [61]. Finally, one last activator of immune suppression is urocanic acid (UCA), a histamine deamination product highly available in the skin [62]. The inhibition of UCA with an antibody against it enabled the delay of tumor formation in irradiated skin [63].

Conclusion

Despite the filtration of the harmful UVC radiation by the ozone layer, the two remaining solar ultraviolet rays reaching the earth's surface are proving to be hazardous. UVB radiation can directly damage the DNA of exposed cells while UVA can indirectly create such damage via the generation of reactive oxygen species. After such induced stress, the cells that fail to repair the damage can either be committed to apoptosis or persist where their damaged DNA progresses to the UV signature C→T transition. These mutations have been identified in several genes correlated with skin carcinogenesis signifying a link between UV exposure and tumorigenesis. Moreover, UV irradiation activates several downstream signaling pathways including the Akt and MAPK pathways implicated in the regulation of cell proliferation, apoptosis and tumor promotion among many others. Finally, an additional instigator of tumor formation can be the UV-induced immune suppression where the inhibition of the action of some immune cells allows the cells' harboring damage and tumors escape from the surveillance of the body. For that, possessing an active repair system is essential to eliminate such dangerous UV-induced lesions where any defect will give rise to diseases like Xeroderma Pigmenstosum and others with increased risks of skin cancers and neurodegeneration.

References

1. Bode A, AM, Z Dong. Mitogen-activated protein kinase activation in UV-induced signal transduction. Sci STKE. 2003; 2003: Re2.
2. Strozyk E, D Kulms. The role of AKT/mTOR pathway in stress response to UV-irradiation: implication in skin carcinogenesis by regulation of apoptosis, autophagy and senescence. Int. J. Mol. Sci. 2013; 14: 15260-15285.
3. Ravanat JL, T Douki, J Cadet. Direct and indirect effects of UV radiation on DNA and its components. J Photochem Photobiol B. 2001; 63: 88-102.
4. Seebode C, J Lehmann, S Emmert. Photocarcinogenesis and Skin Cancer Prevention Strategies. Anticancer Res. 2016; 36: 1371-1378.
5. Rajesh P Rastogi, Shailendra P Singh, Donat-P Häder, Rajeshwar P Sinha. Detection of reactive oxygen species (ROS) by the oxidant-sensing probe 2',7'-dichlorodihydrofluorescein diacetate in the cyanobacterium Anabaena variabilis PCC 7937. Biochem Biophys Res Commun. 2010; 397: 603-607.
6. Armstrong JD, BA Kunz. Site and strand specificity of UVB mutagenesis in the SUP4-o gene of yeast. Proc Natl Acad Sci U S A. 1990; 87: 9005-9009.
7. George J Delinasios, Mahsa Karbaschi, Marcus S Cooke, Antony R Young. Vitamin E inhibits the UVAI induction of "light" and "dark" cyclobutane pyrimidine dimers, and oxidatively generated DNA damage, in keratinocytes. Sci Rep, 2018; 8: 423.
8. Chih-Hung Lee, Shi-Bei Wu, Chien-Hui Hong, Hsin-Su Yu, Yau-Huei Wei. Molecular Mechanisms of UV-Induced Apoptosis and Its Effects on Skin Residential Cells: The Implication in UV-Based Phototherapy. Int J Mol Sci, 2013; 14: 6414-6435.
9. Mihail S Iordanov, Remy J Choi, Olga P Ryabinina, Thanh-Hoai Dinh, Robert K Bright,et al. The UV (Ribotoxic) stress response of human keratinocytes involves the unexpected uncoupling of the Ras-extracellular signal-regulated kinase signaling cascade from the activated epidermal growth factor receptor. Mol Cell Biol, 2002; 22: 5380-5394.

10. Ichiro Yajima, Mayuko Y Kumasaka, Nguyen Dinh Thang, Yuji Goto, Kozue Takeda, et al. RAS/RAF/MEK/ERK and PI3K/PTEN/AKT Signaling in Malignant Melanoma Progression and Therapy. Dermatol Res Pract, 2012; 2012: 354191.
11. M Ming, W Han, J Maddox, K Soltani, CR Shea, et al. UVB-induced ERK/AKT-dependent PTEN suppression promotes survival of epidermal keratinocytes. Oncogene. 2010; 29: 492-502.
12. Tanya M Gottlieb, Juan Fernando Martinez Leal, Rony Seger, Yoichi Taya, Moshe Oren. Cross-talk between Akt, p53 and Mdm2: possible implications for the regulation of apoptosis. Oncogene. 2002; 21: 1299-1303.
13. Pascale F Dijkers, Kim U Birkenkamp, Eric W-F Lam, N Shaun B Thomas, Jan-Willem J Lammers, et al. FKHR-L1 can act as a critical effector of cell death induced by cytokine withdrawal: protein kinase B-enhanced cell survival through maintenance of mitochondrial integrity. J Cell Biol. 2002; 156: 531-542.
14. SR Datta, H Dudek, X Tao, S Masters, H Fu, et al. Akt phosphorylation of BAD couples survival signals to the cell-intrinsic death machinery. Cell. 1997; 91: 231-241.
15. Franke TF. PI3K/Akt: getting it right matters. Oncogene. 2008; 27: 6473-6488.
16. Naihan Xu, Yuanzhi Lao, Yaou Zhang, David A Gillespie. Akt: a double-edged sword in cell proliferation and genome stability. J.Oncol. 2012; 2012: 951724.
17. Ma XM, J Blenis. Molecular mechanisms of mTOR-mediated translational control. Nat Rev Mol Cell Biol. 2009; 10: 307-318.
18. Dufner A, G Thomas. Ribosomal S6 kinase signaling and the control of translation. Exp Cell Res. 1999; 253: 100-109.
19. Frodin M, S Gammeltoft. Role and regulation of 90 kDa ribosomal S6 kinase (RSK) in signal transduction. Mol Cell Endocrinol. 1999; 151: 65-77.
20. Y Zhang, Z Dong, M Nomura, S Zhong, N Chen, et al. Signal transduction pathways involved in phosphorylation and activation of p70S6K following exposure to UVA irradiation. J Biol Chem. 2001; 276: 20913-20923.

21. Y Zhang, S Zhong, Z Dong, N Chen, AM Bode, et al. UVA induces Ser381 phosphorylation of p90RSK/MAPKAP-K1 via ERK and JNK pathways. J Biol Chem. 2001; 276: 14572-14580.
22. Y Zhang, Z Dong, AM Bode, WY Ma, N Chen, et al. Induction of EGFR-dependent and EGFR-independent signaling pathways by ultraviolet A irradiation. DNA Cell Biol. 2001; 20: 769-779.
23. Yiguo Zhang, Wei-Ya Ma, Akira Kaji, Ann M Bode, Zigang Dong. Requirement of ATM in UVA-induced signaling and apoptosis. J Biol Chem. 2002; 277: 3124-3131.
24. Y Zhang, P Mattjus, PC Schmid, Z Dong, S Zhong, et al. Involvement of the acid sphingomyelinase pathway in uva-induced apoptosis. J Biol Chem, 2001; 276: 11775-11782.
25. N Chen, Wy Ma, C Huang, Z Dong. Translocation of protein kinase Cepsilon and protein kinase Cdelta to membrane is required for ultraviolet B-induced activation of mitogen-activated protein kinases and apoptosis. J Biol Chem. 1999; 274: 15389-15394.
26. C Huang, J Li, N Chen, W Ma, GT Bowden, et al. Inhibition of atypical PKC blocks ultraviolet-induced AP-1 activation by specifically inhibiting ERKs activation. Mol Carcinog. 2000; 27: 65-75.
27. S Nakamura, H Takahashi, M Kinouchi, A Manabe, A Ishida-Yamamoto, et al. Differential phosphorylation of mitogen-activated protein kinase families by epidermal growth factor and ultraviolet B irradiation in SV40-transformed human keratinocytes. J Dermatol Sci. 2001; 25: 139-149.
28. She QB, WY Ma, Z Dong. Role of MAP kinases in UVB-induced phosphorylation of p53 at serine 20. Oncogene. 2002; 21: 1580-1589.
29. She QB, N Chen, Z Dong. ERKs and p38 kinase phosphorylate p53 protein at serine 15 in response to UV radiation. J Biol Chem. 2000; 275: 20444-20449.
30. Qing-Bai She, Wei-Ya Ma, Shuping Zhong, Zigang Dong. Activation of JNK1, RSK2, and MSK1 is involved in serine 112 phosphorylation of Bad by ultraviolet B radiation. J Biol Chem. 2002; 277: 24039-24048.

31. S Zhong, Y Zhang, C Jansen, H Goto, M Inagaki,et al. MAP kinases mediate UVB-induced phosphorylation of histone H3 at serine 28. J Biol Chem. 2001; 276: 12932-12937.
32. S Zhong, C Jansen, QB She, H Goto, M Inagaki,et al. Ultraviolet B-induced phosphorylation of histone H3 at serine 28 is mediated by MSK1. J Biol Chem. 2001; 276: 33213-33219.
33. M Nomura, A Kaji, Z He, WY Ma, K Miyamoto, et al. Inhibitory mechanisms of tea polyphenols on the ultraviolet B-activated phosphatidylinositol 3-kinase-dependent pathway. J Biol Chem. 2001; 276: 46624-46631.
34. M Nomura, A Kaji, WY Ma, S Zhong, G Liu, et al. Mitogen- and stress-activated protein kinase 1 mediates activation of Akt by ultraviolet B irradiation. J Biol Chem. 2001; 276: 25558-25567.
35. Guangming Liu, Yiguo Zhang, Ann M Bode, Wei-Ya Ma, Zigang Dong. Phosphorylation of 4E-BP1 is mediated by the p38/MSK1 pathway in response to UVB irradiation. J Biol Chem. 2002; 277: 8810-8816.
36. Masaoki Kawasumi, Bianca Lemos, James E Bradner, Renee Thibodeau, Yong-son Kim, et al. Protection from UV-induced skin carcinogenesis by genetic inhibition of the ataxia telangiectasia and Rad3-related (ATR) kinase. Proceedings of the National Academy of Sciences. 2011; 108: 13716-13721.
37. Kumar R, G Deep, R Agarwal. An Overview of Ultraviolet B Radiation-Induced Skin Cancer Chemoprevention by Silibinin. Curr Pharmacol Rep. 2015; 1: 206-215.
38. Ingela Kindas-Mügge, Constanze Rieder, Ilse Fröhlich, Michael Micksche, Franz Trautinger. Characterization of proteins associated with heat shock protein HSP27 in the squamous cell carcinoma cell line A431. Cell Biology International. 2002; 26: 109-116.
39. Mei Ming, Li Feng, Christopher R Shea, Keyoumars Soltani, Baozhong Zhao, et al. PTEN positively regulates UVB-induced DNA damage repair. Cancer Res. 2011; 71: 5287-5295.
40. Wen Hong Shen, Adayabalam S Balajee, Jianli Wang, Hong Wu, Charis Eng,et al. Essential role for nuclear PTEN in

maintaining chromosomal integrity. Cell. 2007; 128: 157-170.
41. Gabriela Basile Carballo, Jéssica Ribeiro Honorato, Giselle Pinto Farias de Lopes, Tania Cristina Leite de Sampaio E Spohr et al. A highlight on Sonic hedgehog pathway. Cell Commun Signal. 2018; 16: 11.
42. Jia Y, Y Wang, J Xie. The Hedgehog pathway: role in cell differentiation, polarity and proliferation. Arch Toxicol. 2015; 89: 179-191.
43. Fahimeh Rahnama, Takashi Shimokawa, Matthias Lauth, Csaba Finta, Priit Kogerman,et al. Inhibition of GLI1 gene activation by Patched1. Biochem J. 2006; 394: 19-26.
44. Terumi Mizuno, Shoji Tokuoka, Masao Kishikawa, Eiji Nakashima, Kiyohiko Mabuchi, et al. Molecular basis of basal cell carcinogenesis in the atomic-bomb survivor population: p53 and PTCH gene alterations. Carcinogenesis. 2006; 27: 2286-2294.
45. Aurélie Charazac, Nour Fayyad, David Beal, Sandrine Bourgoin-Voillard, Michel Seve, et al. Impairment of Base Excision Repair in Dermal Fibroblasts Isolated From Nevoid Basal Cell Carcinoma Patients. Front Oncol. 2020; 10: 1551.
46. Nicolas Dumaz, Fanélie Jouenne, Julie Delyon, Samia Mourah, Armand Bensussan, et al. Atypical BRAF and NRAS Mutations in Mucosal Melanoma. Cancers (Basel). 2019; 11.
47. Marcia S Brose, Patricia Volpe, Michael Feldman, Madhu Kumar, Irum Rishi, et al. BRAF and RAS mutations in human lung cancer and melanoma. Cancer Res. 2002; 62: 6997-7000.
48. John A Curtin, Jane Fridlyand, Toshiro Kageshita, Hetal N Patel, Klaus J Busam, et al. Distinct sets of genetic alterations in melanoma. N Engl J Med. 2005; 353: 2135-2147.
49. Katarina Omholt, Anton Platz, Lena Kanter, Ulrik Ringborg, Johan Hansson. NRAS and BRAF mutations arise early during melanoma pathogenesis and are preserved throughout tumor progression. Clin Cancer Res. 2003; 9: 6483-6488.
50. KC Cheng, DS Cahill, H Kasai, S Nishimura, LA Loeb. 8-Hydroxyguanine, an abundant form of oxidative DNA

damage, causes G----T and A----C substitutions. J Biol Chem. 1992; 267: 166-172.
51. Barry Fine, Cindy Hodakoski, Susan Koujak, Tao Su, Lao H Saal, et al. Activation of the PI3K pathway in cancer through inhibition of PTEN by exchange factor P-REX2a. Science. 2009; 325: 1261-1265.
52. Sarah M Mense, Douglas Barrows, Cindy Hodakoski, Nicole Steinbach, David Schoenfeld, et al. PTEN inhibits PREX2-catalyzed activation of RAC1 to restrain tumor cell invasion. Sci Signal. 2015; 8: ra32.
53. Eran Hodis, Ian R Watson, Gregory V Kryukov, Stefan T Arold, Marcin Imielinski, et al. A landscape of driver mutations in melanoma. Cell. 2012; 150: 251-263.
54. Michael F.Berger, Eran Hodis, Timothy P Heffernan, Yonathan Lissanu Deribe, Michael S Lawrence, et al. Melanoma genome sequencing reveals frequent PREX2 mutations. Nature. 2012; 485: 502-506.
55. Douglas Barrows, Sarah M Schoenfeld, Cindy Hodakoski, Antonina Silkov, Barry Honig, et al. p21-activated Kinases (PAKs) Mediate the Phosphorylation of PREX2 Protein to Initiate Feedback Inhibition of Rac1 GTPase. J Biol Chem. 2015; 290: 28915-28931.
56. Halaban R. RAC1 and melanoma. Clin Ther. 2015; 37: 682-685.
57. Isabelle Conscience, Nicolas Jovenin, Christelle Coissard, Marianne Lorenzato, Anne Durlach, et al. P16 is overexpressed in cutaneous carcinomas located on sun-exposed areas. European Journal of Dermatology. 2006; 16: 518-522.
58. Amaya Viros, Berta Sanchez-Laorden, Malin Pedersen, Simon J Furney, Joel Rae, et al. Ultraviolet radiation accelerates BRAF-driven melanomagenesis by targeting TP5. Nature. 2014; 511: 478-482.
59. C Petit-Frère, P H Clingen, M Grewe, J Krutmann, L Roza, et al. Induction of interleukin-6 production by ultraviolet radiation in normal human epidermal keratinocytes and in a human keratinocyte cell line is mediated by DNA damage. J Invest Dermatol. 1998; 111: 354-359.
60. Hiroko Miyauchi-Hashimoto, Akira Sugihara, Kiyoji Tanaka, Takeshi Horio. Ultraviolet radiation-induced

impairment of tumor rejection is enhanced in xeroderma pigmentosum a gene-deficient mice. J Invest Dermatol. 2005; 124: 1313-1317.

61. M Athar, KP An, KD Morel, AL Kim, M Aszterbaum, et al. Ultraviolet B(UVB)-induced cox-2 expression in murine skin: an immunohistochemical study. Biochem Biophys Res Commun. 2001; 280: 1042-1047.
62. De Fabo EC, FP Noonan. Mechanism of immune suppression by ultraviolet irradiation in vivo. I. Evidence for the existence of a unique photoreceptor in skin and its role in photoimmunology. J Exp Med. 1983; 158: 84-98.
63. S Beissert, D Rühlemann, T Mohammad, S Grabbe, A El-Ghorr, et al. IL-12 prevents the inhibitory effects of cis-urocanic acid on tumor antigen presentation by Langerhans cells: implications for photocarcinogenesis. J Immunol. 2001; 167: 6232-6238.

Book Chapter

Melanoma Cell Adhesion Molecule, CD146: A Major Actor and Target in Physiopathology

Ahmad Joshkon[1,2]*, Hussein Fayyad-Kazan[2], Bassam Badran[2], Nathalie Bardin[1] and Marcel Blot-Chabaud[1]

[1]Center for CardioVascular and Nutrition Research C2VN, INSERM1263, INRAE1260, Aix-Marseille University, Faculty of Pharmacy, France
[2]Laboratory of Cancer Biology and Molecular Immunology, Faculty of Science, Lebanese University, Lebanon

***Corresponding Author:** Ahmad Joshkon, Center for CardioVascular and Nutrition Research C2VN, INSERM1263, INRAE1260, Aix-Marseille University, Faculty of Pharmacy, Timone Campus, 27 Bd. Jean Moulin, 13005 Marseille, France

Published **March 17, 2021**

How to cite this book chapter: Ahmad Joshkon, Hussein Fayyad-Kazan, Bassam Badran, Nathalie Bardin, Marcel Blot-Chabaud. Melanoma Cell Adhesion Molecule, CD146: A Major Actor and Target in Physiopathology. In: Hussein Fayyad Kazan, editor. Immunology and Cancer Biology. Hyderabad, India: Vide Leaf. 2021.

CD146: Generalities

CD146, also referred to as Melanoma Cell Adhesion Molecule (MCAM), Hemopoietic Cell Adhesion Molecule (HEMCAM),

MUC18, S-Endo1, or A32 antigen, is a cell adhesion molecule essentially expressed on the entire vascular tree that belongs to the immunoglobulin superfamily [1]. It plays a significant role in regulating vascular permeability, cell-cell cohesion, leukocyte transmigration, angiogenesis, and tumor progression [2–4]. The extracellular domain of this single-pass membrane glycoprotein is composed of two variable regions (V) and three constant regions (C2) V-V-C2-C2-C2, while the intracellular domain is relatively short, containing a single tyrosine residue that may become phosphorylated [5,6]. Two membrane isoforms of CD146 exist, short and long, generated by alternative splicing of the transcript in exon 15, leading to a shift of the reading frame. Despite expressing identical extracellular and transmembrane domains, these two isoforms differ by their cytoplasmic tail. The short isoform (shCD146) displays a shorter cytoplasmic domain encompassing one phosphorylation site for protein kinase C (PKC) and an interaction site with proteins containing a PDZ domain. In contrast, the long isoform (lgCD146) displays two phosphorylation sites by PKC and a dileucine motif for protein targeting to the basolateral membrane [5,7]. Of interest, the expression of these isoforms is spatially selective. The long isoform is located at the cell junction and is involved in structural functions while the short isoform is essentially expressed at the apical membrane of the cell and contributes to angiogenesis [8] (figure 1). Also, shedding of membrane CD146 proteins, as induced by matrix metalloproteinases, generates a soluble form (sCD146) that is detected in the sera of healthy people at a concentration around 260 ±60 ng/ml [9]. Of interest, CD146 is conserved among species [10,11]. Homologous proteins with similar sequences are found in mice, rats, chicken and zebrafish, hinting to its fundamental role in physiological development.

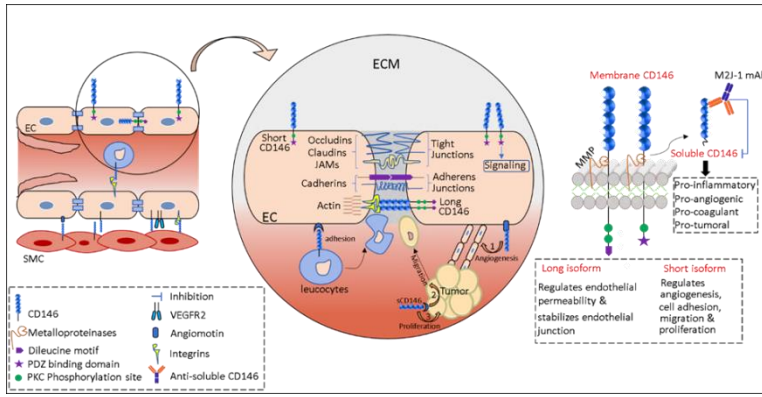

Figure 1: CD146 expression pattern and functions.

CD146 is a transmembrane glycoprotein consisting of 5 immunoglobulin like-domains. Two membrane isoforms for CD146 exists which differ in the intracellular domain: a short form with only 1 protein kinase C (PKC) phosphorylation site in addition to 1 PDZ binding domain and a long form containing 2 PKC phosphorylation sites and 1 dileucine motif. The long isoform is primary expressed at the cellular junction but not in the tight or adherens junction, while the short isoform is located at the apical side of the cells and involved in signaling and trafficking. In addition to membrane CD146, soluble form of CD146 is generated by the action of matrix metalloproteinases (MMP) which shed the extracellular portion of protein. The membrane and soluble CD146 regulate endothelial permeability, leucocytes trafficking, and vessel formation and integrity. Besides, soluble CD146 induce tumor angiogenesis, metastasis, epithelial-mesenchymal transition, and growth. The use of the monoclonal anti-sCD146 M2J1 drastically reduces these effects and lowered tumor-associated coagulative events. JAM: Junction adhesion molecule

CD146 Expression Pattern and Functions

CD146 is expressed all along the vascular tree regardless of the vessel size and anatomical location, including endothelial cells, smooth muscle cells, and pericytes [12]. This distribution pattern is important for maintaining vessel architecture through

heterotypic interaction among these cells via CD146 and its binding partners. As mentioned earlier, the long and the short membrane isoforms have different localizations on endothelial cells. lgCD146 is mainly stored intracellularly when the cells are not confluent. However, at confluency lgCD146 is redistributed to inter-cellular junctions, outside the tight or adherens junctions, and regulate cell-cell cohesion, paracellular permeability, and monocyte transmigration. shCD146 is involved in regulating endothelial cells adhesion, migration, proliferation, and consequently angiogenesis [8]. Of remark, CD146 was first identified on melanoma cells as a poor prognostic marker correlating with disease progression, but was later found to be expressed on various cancer cell lines such as breast, kidney, gastric, ovarian, and prostate cancers [1,7,13]. The mechanisms underlying CD146 upregulation on cancer cells remain to be found. Elevated membrane CD146 expression and high soluble CD146 concentration in plasma are associated with increased cancer cell proliferation, motility, metastatic dissemination and tumor angiogenesis along with a decrease in patients' overall survival [14]. Moreover, CD146 is also expressed on several immune cell subsets, in particular on T lymphocytes [15,16]. Along this line, it was demonstrated that soluble factors in the tumor microenvironment induce CD146 expression on tumor infiltrating T lymphocytes. Indeed, the density of CD146 expressed on tumor-infiltrating CD4+ T cells is higher than that on peripheral T cells [15,17]. Analysis of the RNA profile of CD4+ CD146+ T cells from peripheral blood shows high levels of genes associated with Th17 cells (IL-17A, ROR-γ, IL-22, IL-26, IL-23R, CXCL-13, IL1-β, GM-CSF) which exacerbate inflammatory reactions and indirectly promote tumor progression [16]. Also, Th17 cells contribute to auto-immune diseases progression as in multiple sclerosis (MS) and systemic sclerosis (SS). In fact, CD146+Th17 cells constitute the principal T-cell subset in the cerebrospinal fluid of MS patients and is considered as a poor prognostic marker [18]. Finally, CD146 was found to be expressed on the intermediate and extra-villous trophoblasts [19,20].

CD146 Ligands and Signaling

Initially considered as an orphan receptor, successive studies have identified new ligands for CD146 (table 1). Most of the newly discovered ligands emphasize the role of CD146 in angiogenesis as these ligands were found to promote angiogenic effects on endothelial cells. For example, in one study, authors showed that netrin-1, a neuronal guidance molecule, induces HUVEC cell proliferation, migration, and tube formation by interacting with CD146 but not VEGFR2 [21]. They also showed that netrin-1 binds to the domain IV of CD146 to induce activation of P38 and Erk1/2, a characteristic signaling pathway implicated in VEGFR2 signaling, and relied this effect to the fact that CD146 also acts as a co-receptor for VEGFR2. Indeed, siRNA experiment targeting CD146 abolished the angiogenic effects of netrin-1 on HUVECs while the knock-down of VEGFR2 barely induced similar results. In the same study, the authors used a monoclonal anti-CD146 antibody, AA98, which blocks CD146. They showed that netrin-1 lost its angiogenic effects after treating HUVECs with AA98. Consistently, AA98 efficiently reduced the number of blood vessels in Matrigel plugs conditioned with netrin-1 and grafted in mice, when compared to the group treated with netrin-1 without the antibody. Likewise, in a zebrafish embryo model, antisense morpholino oligonucleotides (MO) targeting CD146 inhibited netrin-1-induced angiogenesis and blocked the development of parachordal vessels. These data underscore the relevance of CD146 as a potent angiogenic molecule both in vitro and in vivo and highlight the capability of CD146 to mediate angiogenic signals even in the absence of conventional pro-angiogenic molecules like VEGF or b-FGF.

Galectins are a family of soluble carbohydrate-binding lectins which mediate cell-to-cell and cell-to-ECM adhesions. As glycosylation accounts for nearly 35% of CD146 apparent molecular weight, it was tempting to speculate that CD146 could interact with sugar-binding proteins such as lectins. In particular, galectin-1, a protein produced by vascular, interstitial, epithelial, and immune cells, was found to interact readily with N-linked oligosaccharides of membrane CD146 and signal to protect

endothelial cells from apoptosis as well as to regulate angiogenesis [22]. In this study, Jouve et al. evidenced that CD146 is mainly N-glycosylated and validated its interaction with galectin-1. They showed that galectin-1, by binding CD146, was protecting endothelial cells from apoptosis. In addition, in vivo experiments in zebrafish showed impaired vascular network formation and poorly developed intersomitic vessels upon knocking down galectin-1 [23] and CD146 [2] respectively. Moreover, in a galectin-1 knockout (KO) mouse model [23], tumor growth was markedly impaired and this effect was attributed to a weak tumor angiogenesis. In the same way, administration of anti-CD146 monoclonal antibody, AA98, potently reduced tumor vessel formation in nude mice xenografted with human tumor cells (SMMC7721, SK-LMS-1, SW1990). Another study by Thijssen et al. [24] showed that galectin-1 is significantly upregulated on activated endothelium and positively correlates with strong angiogenesis by augmenting VEGF receptors and H-RAS signaling and phosphorylation. Thus, galectin-1 effect on angiogenesis could be, at least in part, mediated by CD146, which is indeed a coreceptor for VEGFR2. Importantly, it was recently described that endothelial CD146 binds platelet-derived growth factor receptor-β (PDGFR-β) on pericyte and regulates the PDGF-induced activation of PDGFR-β signaling [25]. By this mechanism, CD146 appears to have a crucial role in recruiting adjacent pericytes in the endothelium and hence stabilizing the developing vessels. All other ligands that are documented in the literature to interact directly with CD146 are summarized in table 1 along with the consequent biological significance.

Table 1: CD146 binding partners and ligands. A summary of proteins validated to interact with membrane CD146 and the consequent biological effects.

	Interaction	Type of Interaction	Biological significance	Reference
CD146	Vegf-c	Ligand	Lymphatic system development	[26]
	FGF4	Ligand	Regulate morphogenesis/ Mediate cellular polarity	[27]
	Netrin1	Ligand	Enhance VEGF-a signaling/ Pro-angiogenic	[21]
	Wnt1	Ligand	Induce fibroblasts activation and proliferation	[28]
	Wnt5a	Ligand	Cytoskeleton remodeling/ Increase cell migration	[29]
	VEGFR2	Co-receptor	Enhance VEGFR2 signaling/ Pro-angiogenic	[30]
	PDGFR-β	Co-receptor	Pericytes recruitment/ Vessel stabilization	[25]
	Laminin 421	Ligand	Cancer metastasis/ Retina development	[31]
	Laminin 411	Ligand	Lymphocytes extravasation in to CNS	[32]
	Galectin 1	Ligand	Endothelial cells survival/ Vascular development	[22]
	Galectin 3	Ligand	Cancer progression and metastasis	[33]
	S100A8/A9	Ligand	Chemotactic effect on cancer cells/ Pro-metastatic	[34]
	Matriptase	Ligand	Stimulate neuron differentiation/ Cancer invasion	[35]

CD146 Mechanism of Action

CD146 is mainly a monomeric protein. However, it can dimerize and multimerize in response to physiological stimuli [35]. Indeed, the stimulation of endothelial cells with VEGF or by means of anti-CD146 AA98 antibody results in receptor dimerization as revealed by FRET (fluorescence resonance energy transfer) technology. This dimerization leads to conformational changes in CD146 structure and induces changes in ligand binding. However, whether this dimerization causes receptor auto-activation and -phosphorylation is not elucidated yet.

Indeed, CD146 can interact with diverse ligands that mediate and alter endothelial functions (figure 2). In fact, CD146 activation induces the phosphorylation of p125FAK and paxillin along with p59fyn recruitment in cultured endothelial cells, leading to actin cytoskeleton reorganization and activation of transcription factors that modulate cell migration and survival [36]. Moreover, the intracellular domain of CD146 interacts physically with actin linked proteins of the ERM (ezrin-radixin-moesin) family, bringing them to the level of membrane protrusions. This CD146-mediated formation of microvilli like extensions will then allow the activation of RhoA by sequestering RhoGDI1 (Rho guanine nucleotide dissociation inhibitory factor 1), leading to an increase in cell motility. In addition, the stimulation of

melanoma cells with Wnt5a induces CD146 redistribution within polarized structures known as W-RAMP (Wnt5a-mediated Receptor-Actin-Myosin Polarity), leading to membrane retraction and cell migration in a RhoA-mediated mechanism [37]. Finally, a defect in CD146 expression is associated with an upregulation of the canonical Wnt pathway and a downregulation of the non-canonical pathway [38].

On endothelial cells, both VEGFR2 and CD146 extracellular domains were found to interact physically even without VEGF binding [30]. A study showed that CD146 dimerizes upon VEGF-A stimulation in a mechanism involving RAC1, Nox4, and ROS production [39]. The inhibition of CD146 using siRNAs, miRNAs, or inhibitory antibodies as AA98 decreased VEGF-A-induced VEGFR2, p38/MAPK, and AKT phosphorylation and reduced NFκB activation in HUVECs [30]. Similarly, in lung vascular endothelial cells from CD146KO mice, VEGF-A stimulation resulted in decreased VEGFR2 and FAK phosphorylation [40]. Also, by regulating further junctional proteins such as VE-cadherin and PECAM, CD146 mediates VEGF-induced permeability in endothelial cells.

As mentioned earlier, CD146 can interact with netrin-1 and mediate angiogenesis [21]. Indeed, silencing CD146 in Zebrafish inhibits netrin-1-induced vascularization. However, netrin-1 does not always stimulate angiogenesis. The controversy about its angiogenic role is attributed to the binding partner, as netrin-1 preferentially binds CD146 at low concentrations but UNC5B at high concentrations. Indeed, netrin-1 has higher affinity for CD146 as compared to its cognate ligand UNC5B. By binding UNC5B, signals will be triggered to counteract those of CD146 and thus inhibit angiogenesis [21]. On the other hand, netrin-1 can induce CD146 dimerization and VEGFR2 phosphorylation, and the inhibition of CD146 decreases netrin-1 effect on HUVEC migration, proliferation, and tube formation in vitro by reducing VEGFR2, ERK1/2, and p38 activation.

Soluble CD146 is also involved in activating several signaling pathways. Stalin et al. showed that soluble CD146 binds angiomotin P80 on endothelial progenitor cells and HUVECs

and regulates vessel formation and cell migration [9]. Mechanistically, soluble CD146 triggers a signalosome constituted of angiomotin, short CD146, VEGFR1, VEGFR2, and presenilin-1 in lipid rafts and phosphorylates VEGF receptors 1 and 2 on endothelial cells [41]. Within this signalosome, soluble CD146 promotes the proteolytic cleavage of short CD146 extracellular domain through matrix metalloproteinases /a disintegrin and metalloproteinase (MMP/ADAM), followed by intracellular cleavage of the cytoplasmic domain by presenilin-1. The generated so-called short CD146 intracellular fragment (shCD146 IC) will be then translocated to the nucleus where it associates with the transcription factor CSL to regulate the transcription of FADD, Bcl-xl and eNOS genes that are involved in cell survival and angiogenesis [41].

Soluble CD146 also significantly contributes to tumor progression in different manners. This form, by associating with its cognate binding partners on cancer cells, activates the oncogene c-myc which in turn activates signaling pathways leading to increased cell proliferation and migration [42].

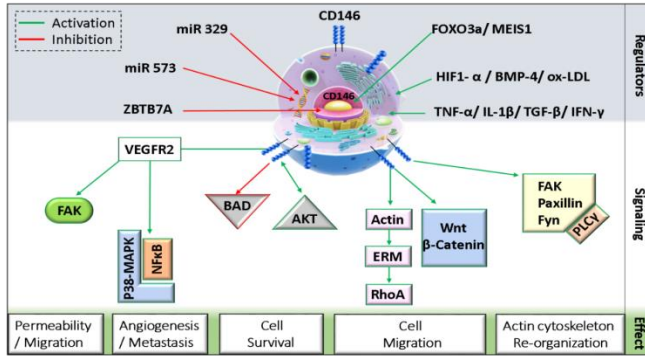

Figure 2: Schematic representation of CD146 cellular localization and regulation.(MEIS1: Myeloid Ecotropic Viral Integration Site 1; HIF1-α: Hypoxia-inducible factor 1 alpha; TGF-β: Transforming growth factor-beta; IFN-γ: interferon-gamma; BMP-4: Bone morphogenetic protein 4; ox-LDL: oxidized low density lipoprotein; ZBTB7A: Zinc finger and BTB domain-containing protein 7A; FAK: focal adhesion kinase; BAD: Bcl-2 associated agonist of cell death; ERM: Ezrin, radixin, and moesin; PLC-γ: Phospholipase C-gamma).

CD146 in Physiological Angiogenesis

CD146 in Embryonic Angiogenesis

The first direct evidence highlighting the significance of CD146 in physiological angiogenesis came from in vivo experiments in Zebrafish [43]. Gicerin, the chicken homologue of human CD146, was overexpressed in zebrafish embryos to assess its impact on vascular development. Multiple gicerin constructs were designed to code for either the full-length receptor, the extracellular domain, the cytoplasmic domain, or constructs devoid of cytoplasmic domain. These experiments showed that mRNA encoding the extracellular domain of gicerin or gicerin lacking the cytoplasmic domain abrogate intersegmental vessels (ISVs) sprouting and inhibit angiogenic vessels development as confirmed by microangiography 55 hours' post-fertilization. Constructs solely encoding immunoglobulin domain I of gicerin's extracellular segment led to vascular anomalies in the embryos. At variance, overexpression of domains II to IV didn't impact vascularization. Thus, the first immunoglobulin domain of gicerin is highly relevant for efficient angiogenesis in zebrafish. Similarly, knocking-down gicerin in zebrafish embryos using antisense morpholino that disrupt protein translation resulted in anomalies in blood circulation 48 hours' post-fertilization but also abnormal phenotype linked to pericardial edema. Alongside, microangiography in gicerin morphants revealed incomplete formation of ISVs with no sprouting, while in situ hybridization technique validated the absence of vascular markers as kdrl and fli1a in the ISVs 24 hours' post-fertilization without any detectable changes in VEGFR2 expression. Of interest, both the hemangioblast and angioblast specific markers, scl and fli-1a, were not altered in the gicerin morphants, suggesting that gicerin selectively inhibits angiogenesis with no effects on vasculogenesis. Expectedly, the angiogenic defect in gicerin morphants was rescued upon injecting synthetic gicerin mRNA. Concomitant with these results, gicerin was also found to be essential for VEGF-A signaling. In fact, induced expression of VEGF-A in zebrafish embryos resulted in ectopic vessel formation in common cardinal vein (CCV), a phenomenon that was abolished when embryos received gicerin-morpholino together with VEGF-A mRNA.

This suggests that gicerin is indispensable for VEGF-A-induced angiogenesis. In another study by Chan et al. [4], CD146 was found to have a critical role in ISV development specifically by modulating the lumen size in blood vessels. Intriguingly, whole mount in situ hybridization experiments in 24 hour-old zebrafish embryos revealed the localization of CD146 in the dorsal aorta, caudal artery, caudal vein, and the sprouting ISVs, thereby highlighting the fundamental role of CD146 in vascular development. In accordance with the aforementioned results, disrupting CD146 protein sequence using morpholino oligonucleotide (MO) that deletes the amino-terminus region (V32 to T57) or totally abrogates protein expression resulted in a circulation shunt that led to partially bypass the caudal artery-vein system. Moreover, microangiography revealed that while both control and CD146 morphants expressed similar ISVs density, the vessels were narrower in the latter and the blood circulation was reduced. Moreover, Halt et al. elucidated the function of CD146 in mouse embryonic kidney development ex vivo [44]. This study unraveled a heterogenous population of endothelial cells in the embryonic kidney that variably stained for the markers CD31, VEGFR2, and CD146. Of interest, despite depleting CD31+ ECs from embryonic kidneys, regeneration of the endothelial cell network took place. On the contrary, the depletion of CD146+ ECs abolished this phenomenon. Additionally, it was found that CD146+/CD31- ECs potently regenerate a pool of CD31+ ECs following their depletion which then incorporate into the developing vessels of the embryonic kidneys. Hence, CD146+/CD31- cells exhibit a pivotal role during embryonic kidney development as they prove to act as progenitors for CD31+ ECs. From a therapeutic perspective, these findings raise the interest of using CD146+ EC progenitors in the treatment of endothelial injury in adult kidneys owing to their fundamental role in maintaining and stabilizing renal vasculature. In general, CD146 appears to be an indispensable factor in vascular development and structure (lumen size, morphology) by mediating a series of cellular events that ultimately lead to dynamic changes in the cytoskeleton during development. This conclusion is strongly supported by the fact that CD146 interacts with actin cytoskeleton in HUVECs and modulates the expression of

several integrins of the β1 family on these cells [45]. Several studies have emphasized that sCD146 concentration is significantly increased in sera of patients with chronic kidney failure compared to healthy controls [46]. Concomitantly, serum sCD146 was found to be elevated in patient with diabetic nephropathy with a gradual increase in this concentration relative to the stages of the disease (stage IIIb: 558.6 ±87.5, stage IV: 519.3 ±80.8, stage V: 619.7 ±32.5 versus control: 268.0 ±45.0 ng/ml), a phenomenon which is also seen in patients with chronic renal failure. Indeed, sCD146 is a hallmark of endothelial damage, explaining the positive correlation between its serum concentration and disease progression.

CD146 in Pregnancy

The sustainability of many animal species is guaranteed by sexual reproduction. During this process, genetic material carried by a motile gamete fuses with that of a stationary gamete to give rise to a zygote. Afterwards, cells undergo mitotic divisions to form a blastocyst which will be implanted into the endometrium of the uterine wall. In fact, implantation is considered to be the most critical step in pregnancy and any factor perturbing this phenomenon will ultimately leads to miscarriage. Recently, several studies have addressed the physiological role of CD146 for successful pregnancies. For instance, Liu et al. showed that CD146 is uniquely upregulated on both receptive maternal uteri and invasive embryonic trophoblasts during early stages of pregnancy but not on non-pregnant uterus [19]. Indeed, a harmonized cascade of events occurs prior to blastocyst implantation. This includes a potent increase in the expression of adhesion molecules on the receptive endometrium like L-selectin and integrins which facilitates embryo implantation. Meanwhile, embryonic trophoblasts secrete matrix metalloproteinases and upregulate the expression of several adhesion molecules (VE-cadherin, α4β1) to enhance their invasive capabilities for reaching the spiral arteries. Of interest, a positive correlation exists between trophoblastic invasive potential and CD146 expression. It was found that CD146 is preferentially expressed on invasive trophoblasts, intermediate trophoblasts, but absent on the non-invasive ones, cytotrophoblasts and

syncytiotrophoblasts [20]. In accordance, women suffering from pre-eclampsia expressed significantly lower CD146 levels on intermediate trophoblasts which hinders their invasive capabilities. Noteworthy, CD146 expression on the endometrium was found to be stringently specific and temporal; highly upregulated in early stages of pregnancy but totally lost afterwards and mostly absent in non-pregnant uterine endothelium [19]. Moreover, in vitro experiments using the antibody AA98 revealed a potent decrease in trophoblast attachment to uterine endothelial cells along with remarkable reduction in trophoblast outgrowth as compared to isotype matched mouse IgG-treated cells, hence validating the significance of CD146 in mediating proper embryo implantation. Similarly, in vivo administration of blocking anti-CD146, AA98, into the left uterine horn of pregnant mice (3.5 days post coitum) resulted in no or few poorly developed embryos while well-developed embryos were found in the right uterine horn that received isotype-matched control IgG [19]. Also, immunohistochemical analysis using anti-CD31 validated the poor neovascularization in the AA98-treated uterine horn, which suggests and reinforces the fundamental role of CD146 not only in early embryonic attachment and development but also in inducing adequate neovascularization leading to a successful pregnancy. Of note, CD146KO mice were found to be fertile, which suggests that other adhesion molecules may functionally compensate the loss of CD146 in vivo or some of CD146 functions may be operated, at least in part, by some other protein(s).

Of putative clinical importance, sCD146 is regarded as an important factor during pregnancy and is detected in sera of pregnant women. Its concentration fluctuates according to the embryonic developmental stage and can reflect several pregnancy-associated malignancies [47]. Notably, sCD146 is potentially a biomarker for selecting the optimal embryos during in vitro fertilization (IVF). In fact, Bardin et al. showed that the concentration of sCD146 was elevated in the culture supernatants from blastocysts that failed to implant into the uterine wall while those that successfully embedded into the endometrium produced significantly lower amounts (1310 vs

845 pg. mL-1) [48]. Given the bright expression of CD146 on early embryonic blastocyst and building on the aforementioned data, it is tempting to speculate that the increase of sCD146 in the supernatant of the in vitro fertilized embryos is the result of MMPs-mediated shedding of membrane CD146. This will decrease CD146 surface expression and subsequently diminish the potential of a successful uterine implantation. Thus, high membrane CD146 and low concentration of sCD146 contribute to an effective embryonic attachment, placental vascularization, and embryonic development. This could thus represent an innovative method for selecting embryos during in vitro fertilization.

CD146 in Adult Angiogenesis

Angiogenesis is a vital physiological process that ensures adequate delivery of blood and nutrients to all body parts. Several studies have highlighted the central role of CD146 in the development of the vascular system and other postnatal biological processes. Postnatally, the expression of CD146 becomes stringently regulated and shows tissue selectivity [12]. Wang et al. showed that the physiological expression of CD146 is restricted to limited normal tissues in adults and that its adhesive strength is relatively weak as compared to other cell adhesion molecules [49]. CD146 expression was found to be spatiotemporally regulated, increased under circumstances such as inflammation for a period of time and then returned back to its basal expression levels. Indeed, the alternating mode of expression of CD146 in adult is not a random process but on the contrary finely tuned by various factors in response to body changes and stimuli. Unlike the prenatal life, species are more exposed to environmental and developmental changes postnatally. In fact, one of the mechanisms by which the body adapts to changes is by modifying the expression of adhesion molecules as CD146. For instance, from the onset of puberty and menstrual cycles in females, CD146 expression on the endometrial endothelial cells becomes elevated which in turn sensitizes the cells to angiogenic stimuli thus facilitating the repair phase [50]. Investigations focusing on the role of CD146 in organogenesis revealed its significance in kidney, liver, and

retina development and vascularization [44,51]. Moreover, rapid proliferation of cells, a phenomenon typically occurring during wound healing and normal body growth, is characterized by a robust increase in CD146 expression which allows active interaction between cells themselves as well as with the surrounding microenvironmental structures. So, CD146 helps transmitting signals inside the cells to accordingly modify their proliferative, migrative, and invasive potentials. Simultaneously, CD146 mediates and regulates a series of events leading to angiogenic responses. In particular, CD146 activates NF-κB in endothelial cells, a feature relevant to tip stalk-cell selection [52]. In the same way, sCD146 was shown to be indispensable in the vascular repair mechanism and to be an inducer of post-ischemic neovascularization [53].

CD146 in Pathological Angiogenesis

CD146 in Miscarriage

Approximately 10 to 15 % of fertile women experience unexplained pregnancy loss, of which 5% suffer from consecutive spontaneous abortion [54]. The first evidence highlighting the implication of CD146 and its soluble form in pregnancy complications, precisely miscarriage, came from a study initiated by Pasquier et al. In this clinical study involving one hundred women with unexplained pregnancy loss versus 100 age-matched control women, the authors revealed that sCD146 plasma concentration significantly correlates with cases of pregnancy loss [47]. Indeed, the plasma concentration of sCD146 was significantly elevated in patients as compared to healthy subjects (279.2 ±61.2 vs 241.1 ±46.7 ng/ml). Of interest, sCD146 plasma concentration was shown to be potently upregulated in the group of patients suffering from early pregnancy loss upon stratifying patients according to the gestation time at which spontaneous abortion occurs. The increase in sCD146 parallels endothelial damages and vascular anomalies. This result is in accordance with other studies demonstrating sCD146 as a molecule impeding trophoblast invasiveness and consequently placenta vascular development. For instance, sCD146 inhibited extravillous trophoblast (EVT) outgrowth and tube like-structure formation in vitro by

negatively regulating their migratory and invasive properties [55]. In humans, these results are reflected by downregulation of sCD146 plasma concentration during physiological pregnancy, hence allowing trophoblasts to invade the endometrium to reach the spiral arteries. A study on 50 pregnant women also showed that sCD146 levels decrease in plasma as compared to non-gestational women. Indeed, repetitive systemic injection of recombinant sCD146 into pregnant rats reduced fertility and hampered embryos implantation by inhibiting glycogen cell (analogous to human cytotrophoblast) migration into the decidua. Alongside, another study showed that CD146 is strictly required during the implantation window (time at which the blastocyst adheres to the uterine wall) where its expression robustly increases on both the endometrium and the extravillous trophoblasts after which it starts to progressively faint [56]. Undoubtedly, abnormal expression of CD146 during this critical period or external interference with CD146 expression using blocking antibodies such as AA98 led to either fetus anomalies due to irregular vascularization or pregnancy miscarriage. In view of these results, sCD146 can be considered as a novel biomarker to predict obstetric anomalies and endometrial vascular development problems.

CD146 in Ocular Diseases

The retina is regarded as a physiological model for studying and analyzing angiogenesis. It is considered as an accessible organ relative to other parts of the body, and given its well-organized vascular anatomy, multiple animal models have been developed to study different vascular anomalies associated with ocular diseases. In fact, the retina is well compartmentalized into vascular and avascular regions as the human central retina is devoid of vessels. This characteristic mode of vascularization is extremely important for preserving healthy vision. In fact, aberrant retinal angiogenesis is linked to several retinal diseases that ultimately lead to blindness such as retinopathy of prematurity, diabetic retinopathy, and age-related macular degeneration (AMD). Recently, it has been evidenced that oxygen is a key factor regulating retinal angiogenesis and vessel maturity [57]. Indeed, under physiological hypoxic conditions

created during late embryogenesis as a result of increased cell differentiation and metabolic activity, HIF1-α becomes active, which in turn induces VEGF expression. This temporal expression of VEGF enhances angiogenesis in the retina. Intriguingly, CD146 gene expression was also found to be activated by HIF1-α. And since CD146 acts as a co-receptor for VEGFR2, it is tempting to speculate that VEGF and CD146, both HIF1-α inducible factors, act in a coordinated manner to regulate angiogenic responses and stabilize newly formed vessels in the retina. In pathological conditions, the increase in CD146 expression is associated with increased angiogenic responses which ultimately extend vascularization to the retinal avascular regions and consequently cause vision anomalies. Strikingly, sCD146 was found to act as a biomarker in exudative age-related macular degeneration (AMD), a chronic disease that progressively leads to irreversible loss of central vision in elder people [51]. In this study, Liu et al. showed that the plasma level of sCD146 was significantly higher in 88 AMD patients in comparison with sex- and age-matched healthy controls (171.88 ±65 vs 125.52 ±61 ng/ml). In fact, when AMD patients were further sub-categorized into patients with classic choroidal neovascularization (CNV) or occult CNV, the serum concentration of sCD146 was found to be significantly higher in the former cases than the latter. Likewise, the authors discovered that the soluble form of VEGFR2 was also significantly increased in the sera of AMD patients as compared to healthy subjects. Indeed, multiple clinical studies unveiled the role of VEGFR2 in the progression of exudative AMD and correlated it to the disease pathogenesis. Of notice, Harhouri et al. succeeded to show that sCD146 acts on endogenous endothelial cells to promote the expression of VEGFR2 and VEGF by these cells. They showed that both sCD146 and VEGF synergistically induce endothelial progenitor cell recruitment, proliferation, migration, and vascular-like structure formation in Matrigel plugs [53]. These results present sCD146 as a novel biomarker in various pathological diseases not limited to exudative AMD. As the secretion of sCD146 become relevant upon vascular damage, and since most of the clinical pathologies are manifested by vascular malformations, it would be of relevance to use a reliable biological marker that is easily quantifiable in human biopsies.

Accordingly, sCD146 represents an appealing biomarker for the early detection of various diseases but also other physiological processes.

CD146 in Skin and Autoimmune Pathologies

The expression of CD146 has been identified on primary cultures of keratinocytes but was absent on healthy epidermis [58]. Indeed, CD146 increases in response to different skin pathologies such as psoriasis, Kaposi's sarcomas, lichen planus, in the epidermis covering skin neoplasm, or in chronic or acute dermatitis. Of remark, Bardin et al. discovered that TNF-α, a key inflammatory cytokine, vigorously induces CD146 expression on the endothelium [2]. They validated that TNF-α augments sCD146 secretion from endothelial cells which facilitates leucocytes trans-endothelial migration and propagation toward inflammatory sites. Thus, in addition to mediating endothelial integrity and vascular permeability, CD146 also mediates cell recruitment and trafficking.

Besides, Mehta et al. showed that CD146 is a major contributor to psoriasis pathogenesis [59]. In fact, IL-17A which is mainly produced by Th17 cells drives inflammatory reactions and intensifies psoriatic lesions. The authors distinguished a unique population of CD3+CD4+ T cells which was primarily present in both the skin lesions and sera of psoriatic patients, the CD146+ Th17 cells. These CD3+CD4+CD146+ Th17 cells produced significantly higher amount of IL-17 than CD146 negative cells. Likewise, PMA / ionomycin stimulation of cells from peripheral blood and skin lesions showed that CD146+ CD4+ and CD146+ CD8+ T cells produced much more IL-17A than the CD146- subset as demonstrated by flow cytometry and immunohistochemistry. Noteworthy, when compared to healthy subjects, circulating CD3+CD146+ T cells were found to be significantly elevated in peripheral blood of patients with various inflammatory autoimmune diseases such as sarcoidosis, inflammatory bowel disease, multiple sclerosis, connective tissue disease, and Behcet's disease. In the same way, Gabsi et al. evidenced that both sCD146 and IL-17A concentrations as well as CD146+ Th17 cells were significantly higher in the sera of

fifty patients with systemic sclerosis (SSC) as compared to control subjects [16]. Impressively, low concentrations of sCD146 were correlated with pulmonary fibrosis, a life-threatening complication associated with the disease. A strong positive correlation was observed between sCD146 serum concentration and the abundance of CD146+Th17 cells. Indeed, 24-hour treatment of peripheral blood mononuclear cells (PBMCs) from SSC patients with sCD146 significantly augmented the number of CD146+Th17 cells and increased the expression density of CD146 on CD146+Th17 subset. This result is extremely significant in inflammatory and autoimmune diseases given that these pathologies are characterized by vascular damages which will subsequently boost sCD146 levels in serum and thus contribute to a poor disease prognosis. So far, sCD146 has been demonstrated to act both on endothelial cells and leucocytes (Th17 cells) in response to inflammatory cytokines and increases the ratio of CD146+Th17 subset which will facilitate the patrolling of these cells on the endothelium and their subsequent extravasation. sCD146 can also exert a chemotactic effect on the recruited immune cells to guide them toward inflammatory sites, thereby exacerbating inflammatory responses. Excessive inflammatory reaction can lead to sepsis, induces coagulation factors, activate oncogenes, or permanently damage nearby tissues and organs [60]. More recently, Bardin et al. revealed that the levels of sCD146 in patients with systemic sclerosis is much higher than that in healthy subjects, 870 ±30 ng/ml versus 495 ±16 ng/ml. Besides, they validated the correlation existing between low levels of sCD146 and digital gangrene or pulmonary fibrosis, two severe manifestations of the disease [45]. Indeed, in vivo experiments using non-immunocompromised CD146-deficient mice showed an increased sensitivity to develop fibrotic lesions in bleomycin-treated animals as compared to wild type mice. This effect was reversed by injecting sCD146 which protects mice from severe fibrotic lesions. Thus, CD146 appears to be an active mediator between autoimmune diseases such as systemic sclerosis and fibrotic events through signaling pathways that involve the Wnt cascade and probably others that are not defined yet. Similarly, in neurodegenerative diseases, sCD146 was elevated in the cerebrospinal fluid (CSF) of patients with active multiple

sclerosis (MS), as compared to patients with inactive MS or non-demyelinating diseases [61]. The pathological increase in sCD146 in CSF was positively correlated with levels of pro-inflammatory cytokines as IL-2, IFN-γ, TNF-α, and IL-17A. Unfortunately, the abnormally elevated sCD146 levels in CSF negatively impact the blood brain barrier (BBB) integrity, increase permeability, damage vessels, and recruit inflammatory leucocytes, all factors promoting disease progression. In atherosclerosis, a process in which vessels are progressively clogged, as plaques enlarge in size, vessel's intima thickens and oxygen supply from the arterial lumen to this area declines [62]. This creates a hypoxic state, a phenomenon that activates CD146 gene expression in addition to other inflammatory cytokines [63,64]. The newly induced inflammatory microenvironment potentiates the release of angiogenic factors that stimulate sprouting angiogenesis from the vasa vasorum [62]. Neovascularization and CD146 expression on macrophages carrying LDL facilitate the infiltration of these cells into the atherosclerotic plaque. This enhances lipid deposition into the arterial wall and exacerbates inflammation which drive atherosclerosis lesion progression. In view of these results, the urge to therapeutically target CD146/ sCD146 raises for the sake of easing its adverse effects in various autoimmune diseases but also other pathologies such as in cancer.

CD146 in Cancer

Initially described by Johnson and colleagues in 1987 as a tumor antigen expressed on advanced primary melanoma and metastatic lesions, CD146 was later found to be overexpressed in a broad range of cancer cell lines not limited to pancreatic, breast, prostate, ovarian, lung, kidney cancers, osteosarcoma, Kaposi sarcoma, angiosarcoma, glioblastoma, and leiomyosarcoma [1,7,13]. In fact, how cancer cells preferentially upregulate the adhesion molecule CD146 is not yet fully elucidated. A study by Liu et al. revealed an increase in the methylation status of the gene promoter in prostate cancer cells. The authors showed that the ATG upstream sequence of CD146 gene promoter becomes hypermethylated during malignant transformation of the cells which in part mediates CD146

expression [65]. Clinically, CD146 surface expression positively correlates with resistance to some chemotherapies. For instance, it has been shown that the 786-O renal cell carcinoma robustly increases membrane CD146 expression together with the soluble form of this protein in the culture media as the cultured cells become resistant to Sunitinib, a tyrosine kinase inhibitor [66]. These resistant cells, referred to as 786-R, showed higher metastatic and invasive potentials as compared to 786-O cells. Another study linked CD146 expression to cancer progression while others demonstrated higher expression during the vascularization phase of the tumor. Likewise, Liang et al. showed that CD146 expression conferred tamoxifen resistance to breast cancer cells and chemo-resistance to small-cell lung cancer cells [67,68]. Undoubtedly, all solid tumors rely primarily on angiogenesis to support the high demanding metabolic activity, growth, and metastasis. Of interest, most of the ligands that have been so far described in the literature to interact with membrane CD146 on cancer cells belong to a family of proangiogenic growth factors such as Netrin1, Wnt5a, VEGF-c, Wnt1, and FGF4 which induce angiogenic responses [49]. Indeed, the tumor microenvironment comprises a cocktail of inflammatory cytokines, growth factors, chemokines, matrix metalloproteinases, and leucocytes. Accordingly, it has been demonstrated that most of the tumor infiltrating lymphocytes (TILs) and tumor-associated macrophages (TAM) are in situ reprogrammed to promote tumor growth essentially by initiating angiogenesis [69–71]. Stalin et al. succeeded to assess sCD146 concentration in the tumor microenvironment and confirmed the potent elevation of this factor in CD146+ tumors. Indeed, their work showed that sCD146 exerts autocrine effects on cancer cells to induce the expression of mesenchymal markers such as vimentin, N-cadherin, and the transcription factors Snail and Slug, thus inducing epithelial to mesenchymal transition (EMT) beside its effect on activating cancer stem cell markers that enhance cancer metastatic potential [14]. Also, sCD146, via its paracrine effect on tumor endothelial cells, induces the upregulation of membrane CD146, integrins, and other adhesion molecules which all together facilitate cancer cell metastasis and leucocyte transmigration [42]. Surprisingly, it was found that most of cancer cell lines producing the angiogenic cytokine

VEGF also produced sCD146 almost equally to or higher than that produced by endothelial cells HUVECs. A comparative study elucidated the direct effect of sCD146 and VEGF on cancer cells of different origin and proved to induce proliferation, migration, and invasion in in vitro assays while protecting cells from apoptosis in response to endogenous oxidative stress [42]. Indeed, in vivo experiments on nude mice xenografted with Matrigel plugs containing luciferase-expressing Panc-1 cells showed that plugs that were injected with recombinant sCD146, unlike those treated with PBS, have higher fluorescence intensity at day 15 post injection signifying enhanced cell survival in vivo. Moreover, the density of vascularization in these plugs was also increased in those ones treated with sCD146 as observed by doppler ultrasound imaging and isolectin B4 labelling. To illustrate the paracrine effect exerted by cancer cells on the endothelium, conditioned media (CM) from different cultured cancer cells, UACC1273, Panc-1, and C81-61, were used to treat HUVECs. These media stimulated ECs proliferation, an effect totally abolished upon depleting the CM from sCD146 or VEGF using S-Endo-1 or bevacizumab, respectively. Thus, beside its pro-tumoral effects, sCD146 proved to be a pro-angiogenic molecule critically relevant in tumor angiogenesis. Furthermore, induced expression of CD146 on hepatocellular carcinoma and ovarian cancer cells significantly increased their invasive and metastatic potentials whilst the inhibition of this molecule impeded tumor spread and metastasis by enhancing apoptosis [72,73]. These effects were attributed to CD146-mediated activation of Rho GTPases which are directly linked to the induction of cancer cells invasion, proliferation, and metastasis. Likewise, CD146 expression was more prominent on osteosarcomas as compared to non-pathological osteoblasts [74]. Altogether, CD146 is regarded as a poor prognostic marker in most solid tumors, not only being pro-angiogenic, pro-tumoral, pro-survival, and pro-coagulant [75] but also conferring resistance to chemotherapies (table 2).

Table 2: Biological consequences of CD146 expression on various cancer cells. Cancers are grouped according to their classification; Genito-urinary and gynecologic (yellow), Gastrointestinal (blue), and Skin, Bone, Breast, and Lungs (Green).

	Cancer Type	Biological consequences	Reference
CD146 / sCD146	Cervical	Increase cell migration/ Tumor metastasis	[76]
	Endometrial	Tumor angiogenesis/ Tumor metastasis	[76]
	Ovarian	Cell survival/ Tumor metastasis/ Poor prognosis	[77], [78]
	Prostate	Increase cell invasiveness/ Tumor metastasis	[65], [79]
	Renal cell carcinoma	Tumor recurrence/ Chemotherapy resistance	[66], [80]
	Breast	Increase cell migration/ Induce EMT/ Chemotherapy resistance	[81], [82]
	Melanoma	Cell survival/ Tumor angiogenesis/ Tumor metastasis	[1], [83]
	Non small cell Lung cancer	Poor prognosis/ Poor overall survival rate	[83], [84]
	Osteosarcoma	Tumor metastasis/ Poor prognosis	[85]
	Colon	Immune escape/ Induce EMT	[86]
	Gastric	Induce EMT/ Tumor metastasis	[87]
	Gallbladder adenocarcinoma	Increase cell invasiveness/ Tumor metastasis/ Poor prognosis	[88]
	Hepatocellular carcinoma	Increase cell invasiveness/ Tumor metastasis/ Poor prognosis	[73]
	Pancreatic carcinoma	Tumor growth and progression/ Poor prognosis	[42]

Interest of using Anti-CD146/ sCD146 mAb to Block Pathological Angiogenesis

Angiogenesis appears to be critically important for mediating physiological development and contributes to homeostasis. However, this biological phenomenon can have deleterious consequences if occurring randomly or becoming uncontrollable as is the case with most solid tumors. Thus, angiogenesis acts as a dual edge-sword, justifying an effective therapeutic intervention. To this end, several blocking and neutralizing antibodies have been developed to target membrane CD146 and its soluble form. The AA98 monoclonal anti-CD146 antibody generated in 2003 and targeting tumor-endothelial cells was among the first antibodies to be developed for therapeutic applications [89]. This antibody displays an efficient inhibitory effect on tumor growth and angiogenesis. In fact, the CD146-blocking antibody AA98 was designed to recognize CD146 on tumor vasculature with minimal reactivity for healthy tissue vasculature. Using HUVECs previously stimulated for 3 weeks with SMMC7721 hepatocellular carcinoma conditioned media as an immunogen, the authors injected these cells into BALB/c mice and finally selected the IgG2a/κ AA98 antibody. In vitro, AA98 was able to inhibit CD146+ endothelial cells proliferation

in a concentration dependent manner but failed to induce similar effects on cancer cell lines, including melanoma A375, hepatocarcinoma SMMC7221, cervical Hela cells, and ovarian SKOV3. Similarly, AA98 reduced HUVECs migration by 75% as compared to those treated with an isotype-matched control IgG. In vivo, the injection of AA98 into chicken chorioallantoic membrane (CAM) robustly decreased vascularization almost by 7-folds as compared to IgG control CAMs. Likewise, AA98 reduced tumor angiogenesis in nude mice xenografted with leiomyosarcoma, pancreatic, and hepatocellular carcinoma to an extent reaching 50%, 41%, and 72% respectively. Of remark, AA98 inhibitory effect on angiogenesis was attributed to the inhibition of NFκB activity in targeted cells which also decreased the expression of adhesion molecules as ICAM-1 and MMP-9, thus hampering cell migration and metastatic potentials. Also, among the different antibodies targeting CD146, the ABX-MA1 antibody recognized both tumor and endothelial CD146 molecules [90]. This antibody inhibited the formation of melanoma cell spheroids in vitro but had no effect on their proliferative capabilities. However, the authors showed that, in vivo, the antibody was able to inhibit growth of melanoma xenografts in nude mice, an effect being essentially related to impaired tumor angiogenesis. In addition, tumor metastasis was reduced thanks to the inhibitory effect on MMP-2 expression, an enzyme strongly related to metastatic processes. Unfortunately, as AA98 and ABX-MA1 do not specifically target tumor CD146 molecule, these antibodies seem to alter normal vascularization beside the inhibitory effect on tumor vascularization. Therefore, it was mandatory to develop an antibody to precisely target cancer-CD146 while maintaining minimal reactivity to endothelial CD146. This approach would allow maintaining vascular integrity while specifically blocking pathological CD146 expression on cancer cells. To this end, a tumor specific anti-CD146 (TsCD146) monoclonal antibody was generated [7]. Via immunofluorescence and flow cytometry experiments, the TsCD146 mAb was validated to target CD146+ tumor cells while failing or only faintly labeling endothelial cells, HUVECs and HMEC-1, and smooth muscle cells HUA-SMC. Of interest, TsCD146 mAb reduced CD146+ tumor cells proliferation as well as CD146 surface expression by internalizing the molecule.

Indeed, animal model of xenograft revealed that TsCD146 mAb diminished CD146+ tumors growth by inhibiting proliferation while inducing apoptosis. Imaging validated that this mAb specifically detects CD146+ tumors both in vivo and in human biopsies. Furthermore, it was able to detect cancer CD146+ microparticles in sera from patients, making it an excellent biomarker for the diagnosis and early detection of human CD146+ cancers for personalized therapy.

Noteworthy, sCD146 has also been regarded as a poor prognostic factor in nearly all solid tumors and most autoimmune diseases. In fact, sCD146 has been detected in the sera of cancer patients but also in the interstitial fluid of patients with autoimmune diseases and chronic inflammation. Besides, the pro-thrombotic effects of sCD146 in cancers are now well-acknowledged. Accordingly, an anti-soluble CD146 monoclonal antibody known as M2J-1 was generated. This neutralizing anti-sCD146 mAb attested its therapeutic efficacy by inhibiting both tumor growth and angiogenesis in xenografted nude mice with either human melanoma cells or pancreatic carcinoma. Moreover, it enhances cancer cells' susceptibility to undergo apoptosis in vivo. Importantly, M2J-1 mAb abolished tumor-induced endothelial cell proliferation and vascularization both in vivo and ex-vivo as evidenced by doppler ultrasound imaging in nude mice implanted with Matrigel plugs pre-conditioned with either irrelevant IgG or M2J-1. Of remark, a key feature of this antibody relies in its ability to interact with sCD146 while maintaining no/ low affinity to bind membrane CD146, thus limiting the adverse effects seen with other anti-CD146 antibodies that can interact with any cell expressing this protein. Thus, in view of the major role of CD146/sCD146 in numerous pathologies related to angiogenesis, different anti-CD146/sCD146 antibodies have been generated that are currently tested for diagnostic purposes but also for therapeutic objectives (Figure 3). These newly generated anti-CD146/sCD146 antibodies will pave the way for a better targeted therapy and more relevant personalized treatment in the context of angiogenic diseases and cancers.

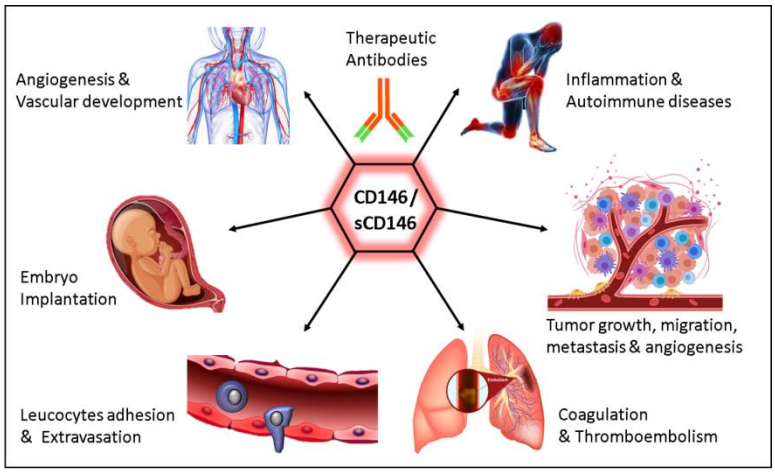

Figure 3: Illustration summarizing the multifaceted role of CD146/sCD146 in physiology and pathology.

CD146/ sCD146 in Coagulation and Thrombosis

Role of Tissue Factor in Hemostasis and Thrombosis

Hemostasis is a process that allows blood to form a clot to prevent blood loss as a result of a vessel injury, followed by a repair[91]. During this process, platelets are recruited to the site of injury, where they become a major component of the developing thrombus [92]. Concomitantly, blood coagulation, after a cascade of proteolytic events, culminated in the generation of thrombin and fibrin [93]. When pathologic processes, as those found in cancers, overwhelm the regulatory mechanism of hemostasis, excessive quantities of thrombin form, initiating thrombosis. Both in physiological (hemostasis) and pathological (thrombosis) processes, an initiating factor plays a major role, the tissue factor (TF) [94].

Tissue factor, factor III, thromboplastin, or CD142 is a single-pass type I membrane glycoprotein constitutively expressed on sub-endothelial tissues as well as many nonvascular cells including various cancer cells depending upon their stage and the therapeutic approaches employed in the treatment [95,96]. It is also exposed at the surface of monocytes and endothelial cells

upon stimulation [96]. This 47 kDa membrane protein consists of an extracellular, transmembrane, and cytoplasmic domain. As a member of cytokine-receptor class II family, this receptor is activated by various inflammatory cytokines such as IFN-α, IFN-β, IFN-γ, TNF- α, interleukin-1 and -10 [97]. Its activation is also induced by endotoxin and the stimulation of T cells by PMA was shown to potently induce TF expression [98]. It binds with high affinity to activated FVII, forming a surface complex that catalyzes in a co-factor independent mechanism a cascade of coagulation events, ultimately leading to fibrin clot. During the last decades, it has been clearly demonstrated that TF plays a major role in the etiology of cancer-related thrombosis [99]. Remarkably, the intracellular domain of TF is involved in signaling functions [100]. In addition, a soluble form of TF exists and is generated by alternative splicing of the mRNA transcript whereby exon 4 is spliced directly to exon 6, skipping exon 5 and liberating most of the extracellular domain. This alternatively spliced TF lacks important residues, reducing its procoagulant activity but playing a major role in cancer biology by promoting angiogenesis and proliferation of tumor cells. Of interest, Szotowski et al. showed that the pro-inflammatory cytokine TNF-α is able to induce soluble TF in endothelial cells within 10 minutes of stimulation [101]. Finally, in addition to the effects of TF and sTF, it has been shown that cancer cells are able to generate microvesicles that are involved in thromboembolism. Thus, these microvesicles are able to induce thrombosis through different factors they convey at their surface, as TF, but also polyphosphates or phosphatidylethanolamine [102,103].

Role of Tissue Factor in Cancer Dissemination

In addition to its well-documented expression on cancer cells and the positive correlation existing between its expression density and cancers' metastatic potential, a new role of TF has emerged as a potent inducer of cancer stem cell phenotype in various cancer cell lines including breast cancer, squamous cell carcinoma (SCC) and pancreatic cancers [104,105]. This effect was demonstrated after treating SCC with TF neutralizing antibody and injecting cells into mice tail which shows an

impaired ability to develop tumors. In addition, the fact that TF expression on SCC was correlated with the expression of CD133, a cancer stem cell marker, further supports this idea. In breast cancer, it was validated that cells expressing TF have higher ability to form spheres in vitro, and up-regulate the expression of stem-cell markers. Another study showed that TF represents a therapeutic target for eradicating CSCs in lungs, breast, and ovarian cancers [104]. A positive correlation was demonstrated between CD133 and TF expressed in various cancer cells although the ratio TF over CD133 was not constant among the different cells. On the contrary, a study initiated by Clouston HW et al. evidenced that colorectal cancer cells DLD-1, which intrinsically express higher TF level than SW620, has lower cancer stem cell activity as assessed by a decrease in colony-sphere forming efficiency and aldehyde dehydrogenase (ALDH) activity [106]. Moreover, they showed that upon knocking down TF by shRNA, both SW620 and DLD-1 cell lines exhibit enhanced ability to form sphere colonies and ALDH activity was potentiated, indicating an overall increase in cancer stem cell phenotype. Hence, the therapeutic interest of targeting TF is highly dependent on the type of solid tumor as well as the stage of the tumor. In all cases, TF was found to be associated with enhanced cancer cell viability and proliferation. Likewise, soluble TF (sTF) was found to induce angiogenesis, survival and cell growth. In breast cancer patients, the plasma concentration of sTF was found to be correlated with the tumor growth and membrane TF and has been used as a biomarker for detecting tumor prognosis, metastasis and patients' overall survival [107].

CD146 and TF are induced by the Same Molecules and Activate Common Signaling Pathways

Recent studies showed that hypoxia, proinflammatory cytokines and vascular endothelial growth factor potently induce TF expression on cancer cells [108–110]. Interestingly, these factors also induce CD146 expression via a common signaling pathways, the mitogen activated-protein kinase (MAPK), P38 signaling, PI3K, PKC, and AKT/PKB [111,112]. Luo et al. confirmed that CD146 induces HIF1-α expression, while other study showed that HIF1-α induces TF overexpression on MDA-

MB-231 cells. Alongside, Yu et al. validated that loss of P53 tumor suppressor enhanced TF expression, and another study by Jin et al. showed that overexpression of CD146 in mesenchymal stem cells (MSC) caused significant decrease in P53 marker. Finally, both CD146 and TF expression were found to be correlated in surface expression and both receptors can induce tumor metastasis, invasion, and angiogenesis [100,113] (figure 2). As mentioned earlier, CD146 and TF activate common signaling pathways but no relationship between these two molecules has been described before. Recent publication suggested that soluble CD146 can induce effects on endothelial cells permeability through integrin beta 1 [114]. Likewise, soluble TF has been recognized to signal through integrins beta 1 on cancer cells, such as integrin alpha6 beta 1, to induce cell proliferation, migration, and angiogenesis [115]. Besides, similar signaling pathways have been shown to be activated by both sCD146 and sTF, including the PKC, ERK1/2, P44/42 MAPK, and AKT signaling pathways (figure 3). Finally, thrombin-mediated activation of PAR1 receptor was shown to upregulate CD146 on melanoma cells [116]. In view of these results, it was proposed that sCD146 and sTF share and activate common signaling pathways.

CD146/sCD146 and Venous Thromboembolism: Therapeutic Interest of an anti-sCD146 Antibody

Stalin et al. revealed the direct impact of CD146/soluble CD146 on TF expression and their interrelated consequences on tumor metastasis and venous thromboembolism [113]. Using two highly metastatic CD146-positive cell lines, the ovarian HEY and melanoma A375, they showed that sCD146, which is secreted by the cells, was able to upregulate TF expression, increasing their procoagulant activity alongside with an enhanced epithelial to mesenchymal transition and overexpression of cancer stem cells genes. To this end, two experimental tumor models were used to demonstrate the in-vivo effect of sCD146 in inducing cancer cell metastasis and pro-coagulant effects. As a first model, luciferase expressing cancer cells, HEY and A373, were injected subcutaneously before peritumoral treatment with recombinant sCD146 (rsCD146). In a

second model, cells expressing luciferase were injected intracardially after in vitro treatment with rsCD146. At the endpoint, organs with potential tumor metastasis were isolated and bioluminescence was measured. Results confirmed that rsCD146 treatment increased tumor cells metastasis, in particular to the liver and lungs, induced cancer cell growth, and drastically decreased mice overall survival as compared to control PBS treated group. These effects were closely associated with an increase in coagulation cascade and subsequent thrombosis. Besides, sCD146 upregulates the surface expression of TF by cancer cell lines HEY and A375, and induced a robust increase in soluble TF in the cells' culture supernatant along with an increase in factor Xa, the substrate of membrane TF.

Of interest, a therapeutic antibody targeting only human sCD146 was introduced. This antibody, named M2J-1, fail to detect membrane CD146 which is present on the whole vascular system and displays major physiological functions. RNA profiling analysis of cancer cells treated with M2J-1 mAb as compared to control IgG, showed that M2J-1 antibody potently neutralizes the adverse effect of sCD146, by decreasing the expression of genes implicated in EMT, cancer stem cells generation, and pro-oncogenes while increasing tumor suppressors. Also, M2J-1 mAb reduces the expression of coagulation-related proteins such as TF, factor X, and thrombin receptor PAR1. Finally, M2J-1 mAb significantly reduced the number of cancer microparticles detected in the plasma of mice. This strongly emphasizes the interest of M2J-1 mAb as a therapeutic approach in treating cancers overexpressing CD146 due to its anti-metastatic and anti-thrombosis effects.

References

1. Lehmann JM, Riethmüller G, Johnson JP. MUC18, a Marker of Tumor Progression in Human Melanoma, Shows Sequence Similarity to the Neural Cell Adhesion Molecules of the Immunoglobulin Superfamily. Proc. Natl. Acad. Sci. U. S. A. 1989; 86: 9891–9895.
2. Bardin Nathalie, Blot-Chabaud Marcel, Despoix Nicolas, Kebir Abdeldjalil, Harhouri Karim, et al. CD146 and Its

Soluble Form Regulate Monocyte Transendothelial Migration. Arterioscler. Thromb. Vasc. Biol. 2009; 29: 746–753.
3. Chen J, Luo Y, Hui H, Cai T, Huang H, et al. CD146 Coordinates Brain Endothelial Cell-Pericyte Communication for Blood-Brain Barrier Development. Proc. Natl. Acad. Sci. U. S. A. 2017; 114: E7622–E7631.
4. Chan B, Sinha S, Cho D, Ramchandran R, Sukhatme VP. Critical Roles of CD146 in Zebrafish Vascular Development. Dev. Dyn. Off. Publ. Am. Assoc. Anat. 2005; 232: 232–244.
5. Guezguez B, Vigneron P, Alais S, Jaffredo T, Gavard J, et al. A Dileucine Motif Targets MCAM-l Cell Adhesion Molecule to the Basolateral Membrane in MDCK Cells. FEBS Lett. 2006; 580: 3649–3656.
6. Xu W, Hua H, Chiu YH, Li G, Zhi H, et al. CD146 Regulates Growth Factor-Induced MTORC2 Activity Independent of the PI3K and MTORC1 Pathways. Cell Rep. 2019 ; 29 : 1311–1322.e5.
7. Nollet M, Stalin J, Moyon A, Traboulsi W, Essaadi A, et al. A Novel Anti-CD146 Antibody Specifically Targets Cancer Cells by Internalizing the Molecule. Oncotarget. 2017; 8: 112283–112296.
8. Kebir A, Harhouri K, Guillet B, Liu JW, Foucault-Bertaud A, et al. CD146 Short Isoform Increases the Proangiogenic Potential of Endothelial Progenitor Cells in Vitro and in Vivo. Circ. Res. 2010; 107: 66–75.
9. Stalin J, Harhouri K, Hubert L, Subrini C, Lafitte D, et al. Soluble Melanoma Cell Adhesion Molecule (SMCAM/SCD146) Promotes Angiogenic Effects on Endothelial Progenitor Cells through Angiomotin. J. Biol. Chem. 2013; 288: 8991–9000.
10. Stalin J, Nollet M, Dignat-George F, Bardin N, Blot-Chabaud M. Therapeutic and Diagnostic Antibodies to CD146: Thirty Years of Research on Its Potential for Detection and Treatment of Tumors. Antibodies. 2017; 6.
11. Yang H, Wang SW, Liu Z, Wu MWH, McAlpine B, et al. Isolation and Characterization of Mouse MUC18 CDNA Gene, and Correlation of MUC18 Expression in Mouse

Melanoma Cell Lines with Metastatic Ability. Gene. 2001; 265: 133–145.
12. Wang Z, Yan X. CD146, a Multi-Functional Molecule beyond Adhesion. Cancer Lett. 2013; 330: 150–162.
13. Zeng P, Li H, Lu PH, Zhou LN, Tang M, et al. Prognostic Value of CD146 in Solid Tumor: A Systematic Review and Meta-Analysis. Sci. Rep. 2017 ; 7 : 4223.
14. Stalin J, Traboulsi W, Vivancos-Stalin L, Nollet M, Joshkon A, et al. Therapeutic Targeting of Soluble CD146/MCAM with the M2J-1 Monoclonal Antibody Prevents Metastasis Development and Procoagulant Activity in CD146-Positive Invasive Tumors. Int. J. Cancer. 2020; 147: 1666–1679.
15. Elshal MF, Khan SS, Takahashi Y, Solomon MA, McCoy JP. CD146 (Mel-CAM), an Adhesion Marker of Endothelial Cells, Is a Novel Marker of Lymphocyte Subset Activation in Normal Peripheral Blood. Blood. 2005; 106: 2923–2924.
16. Gabsi A, Heim X, Dlala A, Gati A, Sakhri H, et al. TH17 Cells Expressing CD146 Are Significantly Increased in Patients with Systemic Sclerosis. Sci. Rep. 2019; 9.
17. Dagur PK, Tatlici G, Gourley M, Samsel L, Raghavachari N, et al. CD146+ T Lymphocytes Are Increased in Both the Peripheral Circulation and in the Synovial Effusions of Patients with Various Musculoskeletal Diseases and Display Pro-Inflammatory Gene Profiles. Cytometry B Clin. Cytom. 2010; 78: 88–95.
18. Brucklacher-Waldert V, Stuerner K, Kolster M, Wolthausen J, Tolosa E. Phenotypical and Functional Characterization of T Helper 17 Cells in Multiple Sclerosis. Brain J. Neurol. 2009; 132: 3329–3341.
19. Liu Q, Zhang B, Zhao X, Zhang Y, Liu Y, et al. Blockade of Adhesion Molecule CD146 Causes Pregnancy Failure in Mice. J. Cell. Physiol. 2008; 215: 621–626.
20. Liu Q, Yan X, Li Y, Zhang Y, Zhao X, et al. Pre-Eclampsia Is Associated with the Failure of Melanoma Cell Adhesion Molecule (MCAM/CD146) Expression by Intermediate Trophoblast. Lab. Investig. J. Tech. Methods Pathol. 2004; 84: 221–228.
21. Tu T, Zhang C, Yan H, Luo Y, Kong R, et al. CD146 Acts as a Novel Receptor for Netrin-1 in Promoting Angiogenesis and Vascular Development. Cell Res. 2015; 25: 275–287.

22. Jouve N, Despoix N, Espeli M, Gauthier L, Cypowyj S, et al. The Involvement of CD146 and Its Novel Ligand Galectin-1 in Apoptotic Regulation of Endothelial Cells. J. Biol. Chem. 2013; 288: 2571–2579.
23. Thijssen VLJL, Postel R, Brandwijk RJMGE, Dings RPM, Nesmelova I, et al. Galectin-1 Is Essential in Tumor Angiogenesis and Is a Target for Antiangiogenesis Therapy. Proc. Natl. Acad. Sci. U. S. A. 2006; 103: 15975–15980.
24. Thijssen VL, Barkan B, Shoji H, Aries IM, Mathieu V, et al. Tumor Cells Secrete Galectin-1 to Enhance Endothelial Cell Activity. Cancer Res. 2010; 70: 6216–6224.
25. Chen J, Luo Y, Huang H, Wu S, Feng J, et al. CD146 Is Essential for PDGFRβ-Induced Pericyte Recruitment. Protein Cell. 2018; 9: 743–747.
26. Yan H, Zhang C, Wang Z, Tu T, Duan H, et al. CD146 Is Required for VEGF-C-Induced Lymphatic Sprouting during Lymphangiogenesis. Sci. Rep. 2017; 7: 7442.
27. Gao Q, Zhang J, Wang X, Liu Y, He R, et al. The Signalling Receptor MCAM Coordinates Apical-Basal Polarity and Planar Cell Polarity during Morphogenesis. Nat. Commun. 2017 ; 8 : 15279.
28. Zhang L, Luo Y, Teng X, Wu Z, Li M, et al. CD146: A Potential Therapeutic Target for Systemic Sclerosis. Protein Cell. 2018; 9: 1050–1054.
29. Ye Z, Zhang C, Tu T, Sun M, Liu D, et al. Wnt5a Uses CD146 as a Receptor to Regulate Cell Motility and Convergent Extension. Nat. Commun. 2013 ; 4 : 2803.
30. Jiang T, Zhuang J, Duan H, Luo Y, Zeng Q, et al. CD146 Is a Coreceptor for VEGFR-2 in Tumor Angiogenesis. Blood. 2012; 120: 2330–2339.
31. Ishikawa T, Wondimu Z, Oikawa Y, Gentilcore G, Kiessling R, et al. Laminins 411 and 421 Differentially Promote Tumor Cell Migration via A6β1 Integrin and MCAM (CD146). Matrix Biol. J. Int. Soc. Matrix Biol. 2014; 38: 69–83.
32. Flanagan K, Fitzgerald K, Baker J, Regnstrom K, Gardai S, et al. Laminin-411 Is a Vascular Ligand for MCAM and Facilitates TH17 Cell Entry into the CNS. PloS One. 2012; 7: e40443.

33. Colomb F, Wang W, Simpson D, Zafar M, Beynon R, et al. Galectin-3 Interacts with the Cell-Surface Glycoprotein CD146 (MCAM, MUC18) and Induces Secretion of Metastasis-Promoting Cytokines from Vascular Endothelial Cells. J. Biol. Chem. 2017; 292: 8381–8389.
34. Tung HH, Lee SL. Physical Binding of Endothelial MCAM and Neural Transmembrane Protease Matriptase—Novel Cell Adhesion in Neural Stem Cell Vascular Niche. Sci. Rep. 2017; 7: 4946.
35. Bu P, Zhuang J, Feng J, Yang D, Shen X, et al. Visualization of CD146 Dimerization and Its Regulation in Living Cells. Biochim. Biophys. Acta. 2007; 1773: 513–520.
36. Anfosso F, Bardin N, Francès V, Vivier E, Camoin-Jau L, et al. Activation of Human Endothelial Cells via S-Endo-1 Antigen (CD146) Stimulates the Tyrosine Phosphorylation of Focal Adhesion Kinase P125FAK. J. Biol. Chem. 1998; 273: 26852–26856.
37. Luo Y, Zheng C, Zhang J, Lu D, Zhuang J, et al. Recognition of CD146 as an ERM-Binding Protein Offers Novel Mechanisms for Melanoma Cell Migration. Oncogene. 2012; 31: 306–321.
38. Liu D, Du L, Chen D, Ye Z, Duan H, et al. Reduced CD146 Expression Promotes Tumorigenesis and Cancer Stemness in Colorectal Cancer through Activating Wnt/β-Catenin Signaling. Oncotarget. 2016; 7: 40704–40718.
39. Zhuang J, Jiang T, Lu D, Luo Y, Zheng C, et al. NADPH Oxidase 4 Mediates Reactive Oxygen Species Induction of CD146 Dimerization in VEGF Signal Transduction. Free Radic. Biol. Med. 2010; 49: 227–236.
40. Zeng Q, Wu Z, Duan H, Jiang X, Tu T, et al. Impaired Tumor Angiogenesis and VEGF-Induced Pathway in Endothelial CD146 Knockout Mice. Protein Cell. 2014 ; 5 : 445–456.
41. Stalin J, Harhouri K, Hubert L, Garrigue P, Nollet M, et al. Soluble CD146 Boosts Therapeutic Effect of Endothelial Progenitors through Proteolytic Processing of Short CD146 Isoform. Cardiovasc. Res. 2016 ; 111 : 240–251.
42. Stalin J, Nollet M, Garigue P, Fernandez S, Vivancos L, et al. Targeting Soluble CD146 with a Neutralizing Antibody

Inhibits Vascularization, Growth and Survival of CD146-Positive Tumors. Oncogene. 2016; 35: 5489–5500.
43. So JH, Hong SK, Kim HT, Jung SH, Lee MS, et al. Gicerin/Cd146 Is Involved in Zebrafish Cardiovascular Development and Tumor Angiogenesis. Genes Cells Devoted Mol. Cell. Mech. 2010; 15: 1099–1110.
44. Halt KJ, Pärssinen HE, Junttila SM, Saarela U, Sims-Lucas S, et al. CD146+ Cells Are Essential for Kidney Vasculature Development. Kidney Int. 2016; 90: 311–324.
45. Bardin N, Anfosso F, Massé JM, Cramer E, Sabatier F, et al. Identification of CD146 as a Component of the Endothelial Junction Involved in the Control of Cell-Cell Cohesion. Blood. 2001; 98: 3677–3684.
46. Fan Y, Fei Y, Zheng L, Wang J, Xiao W, et al. Expression of Endothelial Cell Injury Marker Cd146 Correlates with Disease Severity and Predicts the Renal Outcomes in Patients with Diabetic Nephropathy. Cell. Physiol. Biochem. 2018; 48: 63–74.
47. Pasquier E, Bardin N, De Saint Martin L, Le Martelot MT, Bohec C, et al. The First Assessment of Soluble CD146 in Women with Unexplained Pregnancy Loss. A New Insight? Thromb. Haemost. 2005; 94:1280–1284.
48. Bouvier S, Paulmyer-Lacroix O, Molinari N, Bertaud A, Paci M, et al. Soluble CD146, an Innovative and Non-Invasive Biomarker of Embryo Selection for in Vitro Fertilization. PLoS ONE. 2017; 12.
49. Wang Z, Xu Q, Zhang N, Du X, Xu G, et al. CD146, from a Melanoma Cell Adhesion Molecule to a Signaling Receptor. Signal Transduct. Target. Ther. 2020; 5.
50. Chaudhari-Kank MS, Zaveri K, Antia V, Hinduja I. Comparison of CD9 & CD146 Markers in Endometrial Stromal Cells of Fertile & Infertile Females. Indian J. Med. Res. 2018; 147: 552–559.
51. Liu YY, Bin Y, Wang X, Peng H. Increased Serum Levels of Soluble CD146 and Vascular Endothelial Growth Factor Receptor 2 in Patients with Exudative Age-Related Macular Degeneration. Int. J. Ophthalmol. 2019; 12: 457–463.
52. Chen W, Xia P, Wang H, Tu J, Liang X, et al. The Endothelial Tip-Stalk Cell Selection and Shuffling during Angiogenesis. J. Cell Commun. Signal. 2019; 13: 291–301.

53. Harhouri K, Kebir A, Guillet B, Foucault-Bertaud A, Voytenko S, et al. Soluble CD146 Displays Angiogenic Properties and Promotes Neovascularization in Experimental Hind-Limb Ischemia. Blood. 2010; 115: 3843–3851.
54. Lucas ES, Vrljicak P, Muter J, Diniz-da-Costa MM, Brighton PJ, et al. Recurrent Pregnancy Loss Is Associated with a Pro-Senescent Decidual Response during the Peri-Implantation Window. Commun. Biol. 2020, 3, 1–14.
55. Kaspi E, Guillet B, Piercecchi-Marti MD, Alfaidy N, Bretelle F, et al. Identification of Soluble CD146 as a Regulator of Trophoblast Migration: Potential Role in Placental Vascular Development. Angiogenesis. 2013; 16: 329–342.
56. Staun-Ram E, Shalev E. Human Trophoblast Function during the Implantation Process. Reprod. Biol. Endocrinol. RBE. 2005; 3: 56.
57. Gariano RF, Gardner TW. Retinal Angiogenesis in Development and Disease. Nature. 2005; 438: 960–966.
58. Weninger W, Rendl M, Mildner M, Mayer C, Ban J, et al. Keratinocytes Express the CD146 (Muc18/S-Endo) Antigen in Tissue Culture and during Inflammatory Skin Diseases. J. Invest. Dermatol. 2000; 115: 219–224.
59. Mehta NN, Dagur PK, Rose SM, Naik HB, Stansky E, et al. IL-17A Production in Human Psoriatic Blood and Lesions by CD146+ T Cells. J. Invest. Dermatol. 2015; 135: 311–314.
60. Bosmann M, Ward PA. The Inflammatory Response in Sepsis. Trends Immunol. 2013; 34: 129–136.
61. Wang D, Duan H, Feng J, Xiang J, Feng L, et al. Soluble CD146, a Cerebrospinal Fluid Marker for Neuroinflammation, Promotes Blood-Brain Barrier Dysfunction. Theranostics. 2020; 10: 231–246.
62. Camaré C, Pucelle M, Nègre-Salvayre A, Salvayre R. Angiogenesis in the atherosclerotic Plaque. Redox Biol. 2017; 12: 18–34.
63. Rytkönen KT, Heinosalo T, Mahmoudian M, Ma X, Perheentupa A, et al. Transcriptomic Responses to Hypoxia in Endometrial and Decidual Stromal Cells. Reprod. Camb. Engl. 2020; 160: 39–51.

64. Imtiyaz HZ, Simon MC. Hypoxia-Inducible Factors as Essential Regulators of Inflammation. Curr. Top. Microbiol. Immunol. 2010; 345: 105–120.
65. Liu JW, Nagpal JK, Jeronimo C, Lee JE, Henrique R, et al. Hypermethylation of MCAM Gene Is Associated with Advanced Tumor Stage in Prostate Cancer. The Prostate. 2008; 68: 418–426.
66. Dufies M, Nollet M, Ambrosetti D, Traboulsi W, Viotti J, et al. Soluble CD146 Is a Predictive Marker of Pejorative Evolution and of Sunitinib Efficacy in Clear Cell Renal Cell Carcinoma. Theranostics. 2018; 8: 2447–2458.
67. Liang YK, Zeng D, Xiao YS, Wu Y, Ouyang YX, et al. MCAM/CD146 Promotes Tamoxifen Resistance in Breast Cancer Cells through Induction of Epithelial-Mesenchymal Transition, Decreased ERα Expression and AKT Activation. Cancer Lett. 2017; 386: 65–76.
68. Tripathi SC, Fahrmann JF, Celiktas M, Aguilar M, Marini KD, et al. A Novel Mechanism of Chemoresistance in Small Cell Lung Cancer Mediated by MCAM via PI3K/AKT/SOX2 Signaling Pathway. Cancer Res. 2017; 77: 4414–4425.
69. Dandekar RC, Kingaonkar AV, Dhabekar GS. Role of Macrophages in Malignancy. Ann. Maxillofac. Surg. 2011; 1: 150–154.
70. Bremnes RM, Busund LT, Kilvær TL, Andersen S, Richardsen E, et al. The Role of Tumor-Infiltrating Lymphocytes in Development, Progression, and Prognosis of Non-Small Cell Lung Cancer. J. Thorac. Oncol. Off. Publ. Int. Assoc. Study Lung Cancer. 2016; 11: 789–800.
71. Kataki A, Scheid P, Piet M, Marie B, Martinet N, et al. Tumor Infiltrating Lymphocytes and Macrophages Have a Potential Dual Role in Lung Cancer by Supporting Both Host-Defense and Tumor Progression. J. Lab. Clin. Med. 2002; 140: 320–328.
72. Imbert AM, Garulli C, Choquet E, Koubi M, Aurrand-Lions M, et al. CD146 Expression in Human Breast Cancer Cell Lines Induces Phenotypic and Functional Changes Observed in Epithelial to Mesenchymal Transition. PLOS ONE. 2012; 7: e43752.

73. Jiang G, Zhang L, Zhu Q, Bai D, Zhang C, et al. CD146 Promotes Metastasis and Predicts Poor Prognosis of Hepatocellular Carcinoma. J. Exp. Clin. Cancer Res. CR. 2016; 35.
74. Schiano C, Grimaldi V, Casamassimi A, Infante T, Esposito A, et al. Different Expression of CD146 in Human Normal and Osteosarcoma Cell Lines. Med. Oncol. Northwood Lond. Engl. 2012; 29: 2998–3002.
75. Joshkon A, Stalin J, Traboulsi W, Vivancos-Stalin L, Nollet M, et al. CD146-Positive Tumors Are Associated with Venous Thromboembolism. J. Cell. Immunol. 2020; 2.
76. Zhang H, Zhang J, Wang Z, Lu D, Feng J, et al. CD146 Is a Potential Marker for the Diagnosis of Malignancy in Cervical and Endometrial Cancer. Oncol. Lett. 2013; 5: 1189–1194.
77. Wu Z, Wu Z, Li J, Yang X, Wang Y, et al. MCAM Is a Novel Metastasis Marker and Regulates Spreading, Apoptosis and Invasion of Ovarian Cancer Cells. Tumour Biol. J. Int. Soc. Oncodevelopmental Biol. Med. 2012; 33: 1619–1628.
78. Aldovini D, Demichelis F, Doglioni C, Di Vizio D, Galligioni E, et al. M-CAM Expression as Marker of Poor Prognosis in Epithelial Ovarian Cancer. Int. J. Cancer. 2006; 119: 1920–1926.
79. Wu GJ, Peng Q, Fu P, Wang SW, Chiang CF, et al. Ectopical Expression of Human muc18 Increases Metastasis of Human Prostate Cancer Cells. Gene. 2004; 327: 201–213.
80. Feng G, Fang F, Liu C, Zhang F, Huang H, et al. CD146 Gene Expression in Clear Cell Renal Cell Carcinoma: A Potential Marker for Prediction of Early Recurrence after Nephrectomy. Int. Urol. Nephrol. 2012; 44: 1663–1669.
81. Zabouo G, Imbert AM, Jacquemier J, Finetti P, Moreau T, wet al. CD146 Expression Is Associated with a Poor Prognosis in Human Breast Tumors and with Enhanced Motility in Breast Cancer Cell Lines. Breast Cancer Res. BCR. 2009; 11: R1.
82. Zeng Q, Li W, Lu D, Wu Z, Duan H, et al. CD146, an Epithelial-Mesenchymal Transition Inducer, Is Associated with Triple-Negative Breast Cancer. Proc. Natl. Acad. Sci. U. S. A. 2012; 109: 1127–1132.

83. Oka S, Uramoto H, Chikaishi Y, Tanaka F. The Expression of CD146 Predicts a Poor Overall Survival in Patients with Adenocarcinoma of the Lung. Anticancer Res. 2012 ; 32 : 861–864.
84. Ilie M, Long E, Hofman V, Selva E, Bonnetaud C, et al. Clinical Value of Circulating Endothelial Cells and of Soluble CD146 Levels in Patients Undergoing Surgery for Non-Small Cell Lung Cancer. Br. J. Cancer. 2014; 110: 1236–1243.
85. McGary EC, Heimberger A, Mills L, Weber K, Thomas GW, et al. A Fully Human Antimelanoma Cellular Adhesion Molecule/MUC18 Antibody Inhibits Spontaneous Pulmonary Metastasis of Osteosarcoma Cells in Vivo. Clin. Cancer Res. Off. J. Am. Assoc. Cancer Res. 2003; 9: 6560–6566.
86. Kato K, Shimizu Y, Yamazaki T. CD146 Contributes the Metastatic Properties and Antitumor Immunity of Human Colon Adenocarcinoma Cells. J. Immunol. 2019; 202.
87. Liu WF, Ji SR, Sun JJ, Zhang Y, Liu ZY, et al. CD146 Expression Correlates with Epithelial-Mesenchymal Transition Markers and a Poor Prognosis in Gastric Cancer. Int. J. Mol. Sci. 2012; 13: 6399–6406.
88. Wang W, Yang Z, Liu J, Jiang S, Miao X. Identification of CD146 Expression, Angiogenesis, and Lymphangiogenesis as Progression, Metastasis, and Poor-Prognosis Related Markers for Gallbladder Adenocarcinoma. Tumor Biol. 2012; 33: 173–182.
89. Yan X, Lin Y, Yang D, Shen Y, Yuan M, et al. A Novel Anti-CD146 Monoclonal Antibody, AA98, Inhibits Angiogenesis and Tumor Growth. Blood. 2003; 102: 184–191.
90. Mills L, Tellez C, Huang S, Baker C, McCarty M, et al. Fully Human Antibodies to MCAM/MUC18 Inhibit Tumor Growth and Metastasis of Human Melanoma. Cancer Res. 2002; 62: 5106–5114.
91. LaPelusa A, Dave HD. Physiology, Hemostasis. In StatPearls. Treasure Island: StatPearls Publishing. 2020.
92. Kattula S, Byrnes JR, Wolberg AS. Fibrinogen and Fibrin in Hemostasis and Thrombosis. Arterioscler. Thromb. Vasc. Biol. 2017; 37: e13–e21.

93. Gale AJ. Current Understanding of Hemostasis. Toxicol. Pathol. 2011; 39: 273–280.
94. Furie B, Furie BC. Mechanisms of Thrombus Formation. N. Engl. J. Med. 2008; 359: 938–949.
95. Cole M, Bromberg M. Tissue Factor as a Novel Target for Treatment of Breast Cancer. The Oncologist. 2013; 18: 14–18.
96. Grover SP, Mackman N. Tissue Factor: An Essential Mediator of Hemostasis and Trigger of Thrombosis. Arterioscler. Thromb. Vasc. Biol. 2018; 38: 709–725.
97. Poll T. van der, Jonge, E. de, An, H. ten C. Cytokines as Regulators of Coagulation. Landes Bioscience. 2013,
98. De Palma R, Cirillo P, Ciccarelli G, Barra G, Conte S, et al. Expression of Functional Tissue Factor in Activated T-Lymphocytes in Vitro and in Vivo: A Possible Contribution of Immunity to Thrombosis? Int. J. Cardiol. 2016; 218: 188–195.
99. van den Berg YW, Osanto S, Reitsma PH, Versteeg HH. The Relationship between Tissue Factor and Cancer Progression: Insights from Bench and Bedside. Blood. 2012; 119: 924–932.
100. Versteeg HH, Spek CA, Peppelenbosch MP, Richel DJ. Tissue Factor and Cancer Metastasis: The Role of Intracellular and Extracellular Signaling Pathways. Mol. Med. 2004; 10: 6–11.
101. Szotowski B, Antoniak S, Poller W, Schultheiss HP, et al. Procoagulant Soluble Tissue Factor Is Released from Endothelial Cells in Response to Inflammatory Cytokines. Circ. Res. 2005; 96: 1233–1239.
102. Lacroix R, Vallier L, Bonifay A, Simoncini S, Mege D, et al. Microvesicles and Cancer Associated Thrombosis. Semin. Thromb. Hemost. 2019; 45: 593–603.
103. Date K, Ettelaie C, Maraveyas A. Tissue Factor-Bearing Microparticles and Inflammation: A Potential Mechanism for the Development of Venous Thromboembolism in Cancer. J. Thromb. Haemost. JTH. 2017; 15: 2289–2299.
104. Hu Z, Xu J, Cheng J, McMichael E, Yu L, et al. Targeting Tissue Factor as a Novel Therapeutic Oncotarget for Eradication of Cancer Stem Cells Isolated from Tumor

Cell Lines, Tumor Xenografts and Patients of Breast, Lung and Ovarian Cancer. Oncotarget. 2016; 8: 1481–1494.
105. Shaker H, Harrison H, Clarke R, Landberg G, Bundred NJ, et al. Tissue Factor Promotes Breast Cancer Stem Cell Activity in Vitro. Oncotarget. 2017; 8: 25915–25927.
106. Clouston HW, Rees PA, Lamb R, Duff SE, Kirwan CC. Effect of Tissue Factor on Colorectal Cancer Stem Cells. Anticancer Res. 2018; 38: 2635–2642.
107. Ueno T, Toi M, Koike M, Nakamura S, Tominaga T. Tissue Factor Expression in Breast Cancer Tissues: Its Correlation with Prognosis and Plasma Concentration. Br. J. Cancer. 2000; 83: 164–170.
108. Bluff JE, Brown NJ, Reed MW, Staton CA. Tissue Factor, Angiogenesis and Tumour Progression. Breast Cancer Res. BCR. 2008; 10: 204.
109. Poon RTP, Lau CPY, Ho JWY, Yu WC, Fan ST, et al. Tissue Factor Expression Correlates with Tumor Angiogenesis and Invasiveness in Human Hepatocellular Carcinoma. Clin. Cancer Res. 2003; 9: 5339–5345.
110. Hu Z, Cheng J, Xu J, Ruf W, Lockwood CJ. Tissue Factor Is an Angiogenic-Specific Receptor for Factor VII-Targeted Immunotherapy and Photodynamic Therapy. Angiogenesis. 2017; 20: 85–96.
111. Luo Y, Teng X, Zhang L, Chen J, Liu Z, et al. CD146-HIF-1α Hypoxic Reprogramming Drives Vascular Remodeling and Pulmonary Arterial Hypertension. Nat. Commun. 2019; 10.
112. Yoshioka S, Fujiwara H, Higuchi T, Yamada S, Maeda M, et al. Melanoma Cell Adhesion Molecule (MCAM/CD146) Is Expressed on Human Luteinizing Granulosa Cells: Enhancement of Its Expression by HCG, Interleukin-1 and Tumour Necrosis Factor-Alpha. Mol. Hum. Reprod. 2003 ; 9 : 311–319.
113. Stalin J, Traboulsi W, Vivancos-Stalin L, Nollet M, Joshkon A, et al. Therapeutic Targeting of Soluble CD146/MCAM with the M2J-1 Monoclonal Antibody Prevents Metastasis Development and Procoagulant Activity in CD146-Positive Invasive Tumors. Int. J. Cancer. 2020; 147: 1666-1679.

114. Wang D, Duan H, Feng J, Xiang J, Feng L, et al. Soluble CD146, a Cerebrospinal Fluid Marker for Neuroinflammation, Promotes Blood-Brain Barrier Dysfunction. Theranostics. 2020; 10: 231–246.
115. Berg YW, van den, Hengel LG, van den Myers HR, Ayachi O, et al. Alternatively Spliced Tissue Factor Induces Angiogenesis through Integrin Ligation. Proc. Natl. Acad. Sci. 2009; 106: 19497–19502.
116. Melnikova VO, Balasubramanian K, Villares GJ, Dobroff AS, Zigler M, et al. Crosstalk between Protease-Activated Receptor 1 and Platelet-Activating Factor Receptor Regulates Melanoma Cell Adhesion Molecule (MCAM/MUC18) Expression and Melanoma Metastasis. J. Biol. Chem. 2009; 284: 28845–28855.

Book Chapter

Analysis of the *In Vitro* and *In Vivo* Effects of Photodynamic Therapy on Colorectal Cancer by Using New Porphyrin-Xylan-Coated Silica Nanoparticles

Ludovic Bretin[1], Aline Pinon[1], Soukaina Bouramtane[2], Frédérique Bregier[2], Vincent Sol[2], Vincent Chaleix[2], David Yannick Leger[1] and Bertrand Liagre[1]*

[1]Laboratoire PEIRENE EA 7500, Faculté de Pharmacie, Université de Limoges, France
[2]Laboratoire PEIRENE EA 7500, Faculté des Sciences & Techniques, Université de Limoges, France

***Corresponding Author:** Bertrand Liagre, Laboratoire PEIRENE EA 7500, Faculté de Pharmacie, Université de Limoges, 2, rue du Docteur Raymond Marcland, 87025 Limoges cedex, France

Published **April 16, 2021**

This Book Chapter is a republication of an article published by Bertrand Liagre, et al. at Cancers in September 2019. (Bretin, L.; Pinon, A.; Bouramtane, S.; Ouk, C.; Richard, L.; Perrin, M.-L.; Chaunavel, A.; Carrion, C.; Bregier, F.; Sol, V.; Chaleix, V.; Leger, D.Y.; Liagre, B. Photodynamic Therapy Activity of New Porphyrin-Xylan-Coated Silica Nanoparticles in Human Colorectal Cancer. Cancers 2019, 11, 1474. https://doi.org/10.3390/cancers11101474)

How to cite this book chapter: Ludovic Bretin, Aline Pinon, Soukaina Bouramtane, Frédérique Bregier, Vincent Sol, Vincent Chaleix, David Yannick Leger, Bertrand Liagre. Analysis of the *In Vitro* and *In Vivo* Effects of Photodynamic Therapy on Colorectal Cancer by Using New Porphyrin-Xylan-Coated Silica

Nanoparticles. In: Hussein Fayyad Kazan, editor. Immunology and Cancer Biology. Hyderabad, India: Vide Leaf. 2021.

Author Contributions: S.B., F.B., V.S. and V.C. synthesized and characterized free TPPOH and TPPOH-X SNPs. L.B. performed, analyzed the experiments and wrote the paper. A.P., D.Y.L. and B.L. provided technical assistance for the experiments and corrected the paper. All authors approved the final version of the manuscript.

Funding: The expenses of this work were defrayed in part by the Ministère de l'Enseignement Supérieur, de la Recherche et de l'Innovation through the European Fund of Regional Development FEDER 2014-2020 and by the Conseil Régional Nouvelle Aquitaine.

Acknowledgments: Authors are grateful to histopathology platform (Histolim - Research Institute GEIST) of the University of Limoges especially Carine Guillot and Sandrine Robert for a major part of histopathological staining and Mathilde Duchesne for cytopathology. Authors acknowledge Mickael Meyrand and Nicolas Roy for their assistance for IncuCyte analysis. Authors also thank Alexis Desmoulière for providing histopathological supplies and Laetitia Vignaud for providing technical assistance in histopathological staining. The authors are indebted to Jeanne Cook-Moreau for help in manuscript editing.

Conflicts of Interest: The authors declare no conflict of interest.

Abstract

Photodynamic therapy (PDT) using porphyrins has been approved for treatment of several solid tumors due to the generation of cytotoxic reactive oxygen species (ROS).

However, low physiological solubility and lack of selectivity towards tumor sites are the main limitations of their clinical use. Nanoparticles are able to spontaneously accumulate in solid tumors through an enhanced permeability and retention (EPR) effect due to leaky vasculature, poor lymphatic drainage, and increased vessel permeability. Herein, we proved the added value of nanoparticle vectorization on anticancer efficacy and tumor-targeting by 5-(4-hydroxyphenyl)-10,15,20-triphenylporphyrin (TPPOH). Using 80 nm silica nanoparticles (SNPs) coated with xylan-TPPOH conjugate (TPPOH-X), we first showed very significant phototoxic effects of TPPOH-X SNPs mediated by post-PDT ROS generation and stronger cell uptake in human colorectal cancer cell lines compared to free TPPOH. Additionally, we demonstrated apoptotic cell death induced by TPPOH-X SNPs-PDT and the interest of autophagy inhibition to increase anticancer efficacy. Finally, we highlighted in vivo, without toxicity, elevated anticancer efficacy of TPPOH-X SNPs through improvement of tumor-targeting compared to a free TPPOH protocol. Our work demonstrated for the first time the strong anticancer efficacy of TPPOH in vitro and in vivo and the merit of SNPs vectorization.

Keywords

Anticancer Drug; Porphyrin; Silica Nanoparticles; Drug Delivery; Photodynamic Therapy

Abbreviations

3-MA- 3-methyladenine; APTES- (3-aminopropyl) triethoxysilane; Ce6- Chlorin e6; CRC- Colorectal Cancer; DCFDA- 2',7'-dichlorofluorescein diacetate; ELISA- Enzyme-Linked Immunosorbent Assay; EPR effect- Enhanced Permeability and Retention Effect; FBS- Fetal Bovine Serum; HES- Hematoxylin/Eosin/Saffron; HRP- Horseradish Peroxidase; JC-1- 5,5′,6,6′-tetrachloro-1,1′,3,3′-tetraethylbenzimidazolocarbocyanine Iodide; LC3- light chain 3; LD_{50}- lethal dose 50; MTT- 3-(4,5-dimethylthiazol-2-yl)-2,5-diphenyltetrazolium Bromide; NAC- N-acetyl-L-cysteine; NPs- Nanoparticles; PBS- Phosphate Buffered Saline; PDT-

Photodynamic Therapy; PI- Propidium Iodide; Protoporphyrin IX- PpIX; PS- Photosensitizer; ROI- Region of Interest; ROS- Reactive Oxygen Species; SEM- Standard Error of the Mean; SNPs- Silica Nanoparticles; TBHP- tert-butyl hydrogen peroxide; TEM- Transmission Electron Microscopy; TPP- Tetraphenylporphyrin; TPPOH-X- xylan-TPPOH Conjugate; TPPOH- 5-(4-hydroxyphenyl)-10,15,20-Triphenylporphyrin; TUNEL- Terminal Deoxynucleotidyl Transferase dUTP Nick-End Labeling

Introduction

In 2018, colorectal cancer (CRC) was the third most common cancer with 1.8 million cases globally, and the second leading cause of death for oncological reasons with 862,000 deaths [1]. The conventional treatment options for patients with CRC are surgery, chemotherapy, and/or radiotherapy, which unfortunately has many side effects and long recovery periods. Over the past decade, significant progress in CRC treatment has been achieved through the development of novel drugs and treatment protocols. However, the increasing resistance of tumor cells toward these novel drugs and persistent side effects due to toxicity on healthy tissues make it imperative to find other methods of CRC therapy [2–6].

Photodynamic therapy (PDT), an alternative cancer treatment, appears to be a promising option [7]. The molecular mechanism of PDT involves simultaneous interaction between a photosensitizer (PS), a light source with an appropriate wavelength, and molecular oxygen. Relative to traditional therapies, PDT has several advantages including non-invasive therapy, non-cytotoxic molecules without light activation, and site-specific light treatment which decreases the side effects, thus accelerating the healing process [8,9]. PDT is based on the generation of reactive oxygen species (ROS) which mediate cellular toxicity. Upon light irradiation, the PS is activated from a ground to an excited state. The excited PS is very unstable and loses its excess energy either directly or via the excited triplet state. The excited triplet state is generated by intersystem crossing. In this long-lived excited triplet state, the PS slowly

returns to the ground state through type I or type II photochemical reactions. In the first reaction, the excited PS reacts with a biological substrate via hydrogen or electron transfer, producing free radical species. These species can react with molecular oxygen producing ROS such as the superoxide radical anion ($O_2^{\bullet -}$) and hydrogen peroxide (H_2O_2). In the second reaction, the excited PS transfers its energy directly to molecular oxygen to form singlet oxygen ($^1O_2$). These highly cytotoxic ROS can oxidize a variety of biomolecules, induce an acute stress response, and trigger a series of redox signaling pathways, leading to cell death frequently through apoptosis [10–13]. At present, tetrapyrrole compounds such as porphyrins, chlorins, bacteriochlorins, and phthalocyanines are the most commonly used PS in PDT [14]. However, the main disadvantages of these PS are their poor solubility in water, which limits intravenous administration, their low photo-physical properties due to the aggregation of PS, and their poor tumor selectivity limiting their use in clinical protocols.

In order to increase the selectivity and bioavailability of PS, new drug delivery systems are emerging. Nanotechnology using nanocarriers appears to be the most promising strategy. Nanoparticles (NPs) are able to spontaneously accumulate in solid tumors through passive targeting: the enhanced permeability and retention (EPR) effect occurs due to a combination of leaky vasculature, poor lymphatic drainage, and increased vessel permeability. Vectorizing NPs through encapsulation or attachment of PS not only enhances tumor-targeting through the EPR effect but also increases the hydrophilicity and tissue lifetime of PS [15–18]. Recently, various nanocarriers have been developed using organic and inorganic strategies. Organic drug delivery systems suffer from intrinsic instability and low drug-loading capacity/efficiency, restricting their further clinical potential. However, inorganic NPs show high chemical stability and resistance to corrosion under physiological conditions. Among these inorganic NPs, silica nanoparticles (SNPs) have been recognized as promising nanocarriers for PDT. SNPs have numerous advantages such as their easy synthesis, stability, controllable size, modifiable surface potential and easy functionalization. One of the major

issues of inorganic NPs is biocompatibility. SNPs are one of the most biocompatible materials, thereby increasing interest in their use for medical applications [19–22].

One of the biggest challenges in controlled drug delivery systems is blood circulation half-life due to mononuclear phagocyte sequestration. To delay opsonization and increase nanocarrier lifetimes in the bloodstream, coating NPs with hydrophilic groups appears to be a promising strategy. This strategy involves grafting long chain polymers such as polyethylene glycol or polysaccharides on NPs. These polymers create a protective hydrophilic layer around the NPs which prevents the binding of opsonins via steric repulsion forces, thus delaying opsonization and phagocytosis of NPs [23–25]. Xylan, a hemicellulose, is defined as a group of cell wall polysaccharides. Xylan is a natural, biodegradable, and non-toxic biomaterial which has been reported to stabilize magnetic NPs in biological media with improvement of their biocompatibility and biodistribution [26,27]. Xylan has been also demonstrated to play an important function in drug delivery. Esterification of xylan via activation of carboxylic acid with N,N'-carbonyldiimidazole produces prodrugs for the controlled release of ibuprofen [28].

In the current paper, we investigated the anticancer efficacy of the PS 5-(4-hydroxyphenyl)-10,15,20-triphenylporphyrin (TPPOH). According to our research program on polysaccharide modifications with PS for PDT applications, we explored the newly synthesized core-shell hybrid SNPs based on xylan for the targeted delivery of TPPOH [29]. First, we showed a strong anticancer efficacy of TPPOH in human CRC cell lines, which has not been described before. Then, we demonstrated that vectorizing SNPs enhances TPPOH anticancer efficacy through increased uptake and ROS production due to optimal hydrophilicity and no aggregation of TPPOH. Subsequently, like other PDT studies, our results indicated that TPPOH achieves its anticancer efficacy through apoptosis. Because autophagy is frequently involved in PDT and plays a role in resistance to anticancer treatment [30,31], we established that inhibition of PDT-induced autophagy by pharmacological inhibitor markedly

increases apoptosis. Finally, we highlighted that SNPs vectorization enhances TPPOH tumor cytotoxicity in a CRC xenograft mice model through better tumor-targeting due to the EPR effect. Together, the in vitro and in vivo results revealed the strong anticancer efficacy of TPPOH-X SNPs and showed strong potential for possible clinical use in further PDT therapies.

Results

SNPs Vectorization Enhanced TPPOH-PDT Phototoxic Effects Mediated by ROS Production

To examine the phototoxicity of TPPOH-PDT in vitro, we treated three human CRC cell lines: HT-29, HCT116, and SW620 with free TPPOH or TPPOH-X SNPs. Then, cells were exposed or not to PDT with red irradiation and phototoxic effects were determined 48 h post-PDT, using 3-(4,5-dimethylthiazol-2-yl)-2,5-diphenyltetrazolium bromide (MTT) assay. Free TPPOH and TPPOH-X SNPs had no toxic effects on HT-29 cells when cells were kept in the dark (Figure 1A). When photoactivated, free TPPOH or TPPOH-X SNPs induced a strong decrease in cell viability in a dose-dependent manner (Figure 1A). However, TPPOH-X SNPs-PDT was more effective than free TPPOH-PDT. SNPs alone had no toxic effect with or without photoactivation regardless of the concentrations tested (Figure 1B). The same results were seen in HCT116 (Figure S1A,B) and SW620 (Figure S2A,B) cell lines.

IC_{50} values were calculated in order to compare free TPPOH-PDT vs. TPPOH-X SNPs-PDT. We observed that TPPOH-X SNPs-PDT was much more effective than free TPPOH-PDT in HT-29 cells with 10.8-fold more cytotoxicity with IC_{50} values of 550.2 nM for TPPOH-X SNPs-PDT and around 6 μM for free TPPOH-PDT [29]. Similar results were observed in HCT116 (40.5-fold) and SW620 (39.5-fold) cell lines with respective IC_{50} values of 72.6 and 75.4 nM for TPPOH-X SNPs-PDT and around 3 μM for free TPPOH-PDT. HT-29 cells appeared to be the most resistant as IC_{50} values for free TPPOH-PDT and TPPOH-X SNPs-PDT were higher than those found for HCT116 and SW620 cell lines (2- and 7-fold respectively). For the

following experiments, compounds were used at IC_{50} values except for during uptake and localization experiments.

PDT-induced cell death generally occurs through generation of intracellular ROS. Therefore, we measured intracellular ROS levels using 2',7'-dichlorofluorescein diacetate (DCFDA) staining 4 h post-PDT. Flow cytometry analyses indicated that exposure of cells to free TPPOH enhanced intracellular ROS levels only after photoactivation (Figure 1C). The median fluorescence intensity of 2',7'-dichlorofluorescein (DCF) after photoactivated free TPPOH treatment was increased compared to free TPPOH and control and was decreased after pretreatment with the ROS scavenger: NAC. After SNPs vectorization, TPPOH-X SNPs also enhanced intracellular ROS levels only after photoactivation. Pretreatment with NAC decreased further the median fluorescence intensity of DCF (Figure 1D). Free TPPOH-PDT was more effective on ROS generation than TPPOH-X SNPs (Figure 1E). In fact, it is well-known complexation of PS to NPs often leads to a decrease of ROS generation through PS quenching [32,33]. TBHP was used as a positive control. The same results were observed in HCT116 (Figure S1C–E) and SW620 (Figure S2C–E) cell lines

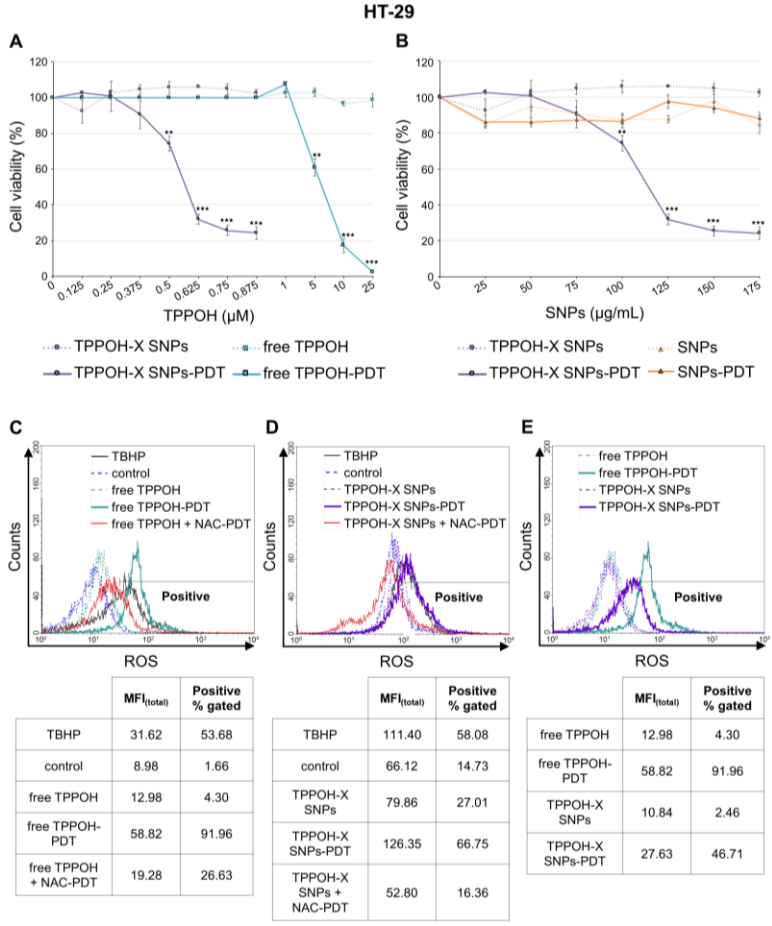

	$MFI_{(total)}$	Positive % gated
TBHP	31.62	53.68
control	8.98	1.66
free TPPOH	12.98	4.30
free TPPOH-PDT	58.82	91.96
free TPPOH + NAC-PDT	19.28	26.63

	$MFI_{(total)}$	Positive % gated
TBHP	111.40	58.08
control	66.12	14.73
TPPOH-X SNPs	79.86	27.01
TPPOH-X SNPs-PDT	126.35	66.75
TPPOH-X SNPs + NAC-PDT	52.80	16.36

	$MFI_{(total)}$	Positive % gated
free TPPOH	12.98	4.30
free TPPOH-PDT	58.82	91.96
TPPOH-X SNPs	10.84	2.46
TPPOH-X SNPs-PDT	27.63	46.71

Figure 1: In vitro phototoxic effects of 5-(4-hydroxyphenyl)-10,15,20-triphenylporphyrin (TPPOH)-X silica nanoparticles (SNPs)- Photodynamic therapy (PDT) and reactive oxygen species (ROS) production. (**A**) HT-29 cells were treated or not treated with free TPPOH and TPPOH-X SNPs based on TPPOH concentration. Then, cells were exposed or were not exposed to PDT. Phototoxic effects were determined 48 h post-PDT using the MTT assay. Cell viability, expressed as a percentage of each condition, was compared to controls. IC_{50} values were calculated using 550.2 nM for TPPOH-X SNPs-PDT and around 6 µM for free TPPOH-PDT. (**B**) HT-29 cells were treated or not treated with TPPOH-X SNPs and SNPs based on nanoparticles concentration. Then, cells were exposed or not exposed to PDT. Phototoxic effects were determined 48 h post-PDT using the MTT assay. Cell viability, expressed as a percentage of each condition, was compared to controls. (**C**) HT-29 cells were treated or not treated with free TPPOH or (**D**) TPPOH-X SNPs with or without NAC co-treatment and then photoactivated or not photoactivated. (**E**)

Comparison of free TPPOH and TPPOH-X SNPs on ROS generation in HT-29 cells. Intracellular ROS levels using DCFDA staining were measured 4 h post-PDT by flow cytometry. A greater right shift implied higher fluorescence intensity resulting from higher amounts of 2',7'-dichlorofluorescein (DCF) formation and thus greater ROS generation. Data are shown as mean ± SEM (n = 3). ** $p < 0.01$ and *** $p < 0.001$.

SNPs Vectorization Increased TPPOH Accumulation in Lysosomes

To explore the large difference in IC_{50} values between TPPOH-X SNPs-PDT and free TPPOH-PDT, we studied the uptake of these compounds through a kinetics study in human CRC cell lines by using AMNIS® imaging flow cytometry analysis. The results demonstrated that, used at the same concentration (1 μM), TPPOH-X SNPs uptake was much higher in HT-29 cells than that of free TPPOH with 98.8% vs. 2.32%, respectively, 24 h post-treatment (Figure 2A). The same results were observed at 2, 6, and 12 h post-treatment (data not shown). TPPOH fluorescence (red) was clearly observed in cell cytoplasm, indicating cellular internalization. The same results were demonstrated in HCT116 (Figure S3A) and SW620 (Figure S4A) cell lines for TPPOH-X SNPs and free TPPOH with 99.9% vs. 0.53% and 99.8% vs. 0.9%, respectively.

To visualize uptake on a single cell level, TEM analysis was used to evaluate the localization of TPPOH-X SNPs (Figure 2B). Images showed TPPOH-X SNPs uptake without cellular morphological changes. TPPOH-X SNPs seemed to be internalized by lysosomes probably by endocytosis and/or diffusion through cell membranes. TPPOH-X SNPs internalization seemed to be the same for HCT116 (Figure S3B) and SW620 (Figure S4B) cell lines.

Then cells were co-treated with TPPOH-X SNPs and LysoTracker or MitoTracker. Results demonstrated that TPPOH-X SNPs co-localized preferentially with lysosomes (50.8%) compared to mitochondria (12%) in HT-29 cells (Figure 2C). TPPOH-X SNPs co-localized similarly in HCT116 (Figure S3C) and SW620 (Figure S4C) cell lines with lysosomes at 49.7% and 59.3% compared to mitochondria at 15% and 5.4%, respectively. TPPOH-X SNPs fluorescence co-localized preferably with

LysoTracker fluorescence, as indicated by yellow fluorescence. TPPOH-X SNPs lysosomal localization was confirmed by confocal microscopy in HT-29 (Figure S5A), HCT116 (Figure S6A) and SW620 (Figure S7A) cell lines. In addition, confocal microscopy analysis revealed no co-localization between TPPOH-X SNPs and mitochondria in HT-29 (Figure S5B), HCT116 (Figure S6B), and SW620 (Figure S7B) cell lines. These data showed that SNPs vectorization enhanced cellular uptake and lysosome internalization compared to free TPPOH.

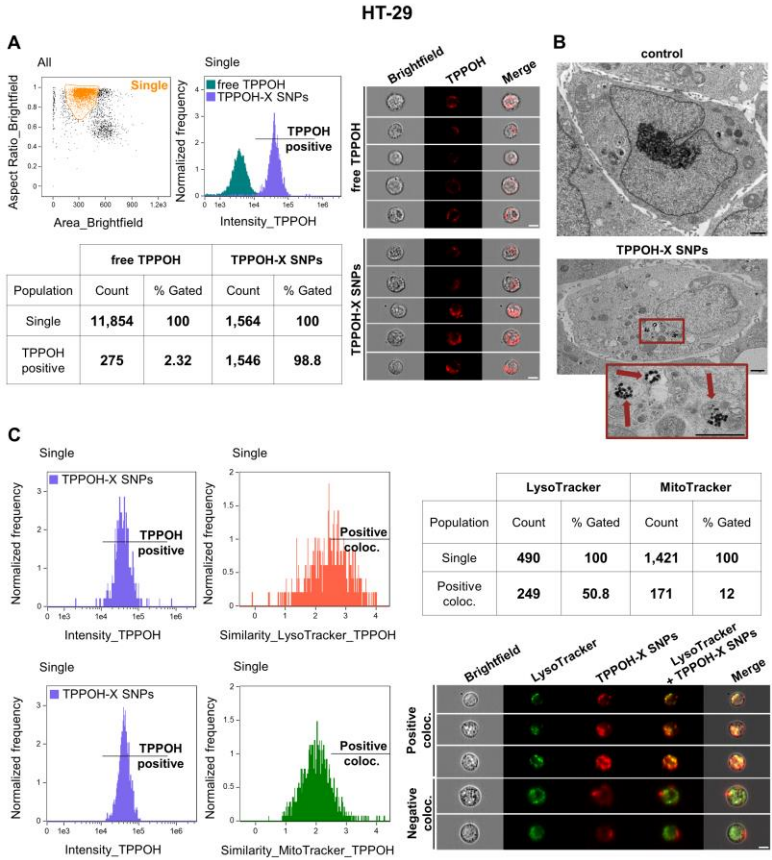

	free TPPOH		TPPOH-X SNPs	
Population	Count	% Gated	Count	% Gated
Single	**11,854**	**100**	**1,564**	**100**
TPPOH positive	**275**	**2.32**	**1,546**	**98.8**

	LysoTracker		MitoTracker	
Population	Count	% Gated	Count	% Gated
Single	**490**	**100**	**1,421**	**100**
Positive coloc.	**249**	**50.8**	**171**	**12**

Figure 2: Cell uptake of TPPOH-X SNPs by HT-29 cells. (**A**) HT-29 cells were treated with free TPPOH and TPPOH-X SNPs at 1 µM and cell uptake of these compounds was studied 24 h post-treatment by AMNIS® imaging flow cytometry. The first graph highlights the size/structure of HT-29 cells. After selection of the cell population, TPPOH intensity in HT-29 cells was shown in

the second graph and in representative images. The table summarizes the amount of positive TPPOH cells relative to all cells compared to free TPPOH and TPPOH-X SNPs treatments. White scale bar = 10 μm. (**B**) Representative TEM images of HT-29 cells treated or not treated with TPPOH-X SNPs 24 h post-treatment are shown. Red arrows indicate intracellular nanoparticles. Black scale bar = 1 μm. (**C**) HT-29 cells were co-treated with TPPOH-X SNPs and LysoTracker or MitoTracker and co-localization was studied 24 h post-treatment by using AMNIS® imaging flow cytometry analysis. The first graph shows TPPOH intensity in HT-29 cells and the second graph shows similarity of TPPOH positive cells compared to LysoTracker or MitoTracker. The table summarizes the amount of TPPOH positive cells co-localized with LysoTracker or MitoTracker. Representative images of co-localization of TPPOH-X SNPs and LysoTracker in HT-29 cells are shown. White scale bar = 10 μm. Data are shown as three independent experiments.

TPPOH-X SNPs-PDT Induced Apoptosis

To determine the mechanism of the decrease in cell viability induced by TPPOH-X SNPs-PDT on human CRC cell lines, mitochondrial membrane potential was evaluated by flow cytometry using the cationic dye JC-1. In control cells, JC-1 forms J-aggregates in mitochondria. In apoptotic cells, JC-1 accumulates in the cytoplasm as monomers due to collapse of the mitochondrial membrane potential. Mitochondria predominantly exhibited accumulation of J-aggregates in HT-29 cells after light control or TPPOH-X SNPs treatment (Figure 3A). TPPOH-X SNPs-PDT disrupted mitochondrial membrane potential as revealed by an increase in monomer rates: 14.4% compared to 6.6% and 7.3% for light control and TPPOH-X SNPs, respectively. The same increase in monomer rates were demonstrated in HCT116 cells (Figure S8A) with 42.6% compared to 6.3% and 7.2% and SW620 cells (Figure S9A) with 22.7% compared to 0.8% and 1.1% for TPPOH-X SNPs-PDT relative to light control and TPPOH-X SNPs treatments, respectively.

Consequently, the rate of apoptosis induced by TPPOH-X SNPs-PDT was determined by dual staining with Annexin V-FITC and PI by flow cytometry. In HT-29 cells, light control and TPPOH-X SNPs treated cells were mostly viable, whereas the rate of early and late apoptosis simultaneously increased with TPPOH-X SNPs-PDT to 20.7% compared to 12.8% and 12% for light control and TPPOH-X SNPs, respectively (Figure 3B). HCT116

and SW620 cells were more sensitive than HT-29 cells. TPPOH-X SNPs-PDT increased the rate of early and late apoptosis to 33.8% compared to 15% and 14% in HCT116 cells (Figure S8B) and to 30.4% compared to 12.1% and 15.1% in SW620 cells (Figure S9B) for TPPOH-X SNPs-PDT relative to light control and TPPOH-X SNPs, respectively.

To further confirm that TPPOH-X SNPs-PDT induced apoptosis, we characterized the effects of TPPOH-X SNPs-PDT on activity of the key apoptosis executioner caspase-3/7 by IncuCyte imaging live cell analysis. HT-29 cells submitted to TPPOH-X SNPs-PDT showed a significant increase in caspase-3/7 activity in a time-dependent manner compared to light control or TPPOH-X SNPs (Figure 3C). At 48h, TPPOH-X SNPs-PDT induced a significant increase in caspase-3/7 activity by 4.6-fold ± 0.2-fold compared to light control. The same results were observed in HCT116 (Figure S8C) and SW620 (Figure S9C) cell lines with a significant increase in caspase-3/7 activity by 4.1-fold ± 0.1-fold and by 4.4-fold ± 0.1-fold, respectively, compared to light control.

Furthermore, to study the nuclear changes in apoptosis caused by TPPOH-X SNPs-PDT, DNA fragmentation was evaluated by ELISA. TPPOH-X SNPs-PDT treatment induced a significant increase in DNA fragmentation by 2.9-fold ± 0.2-fold compared to light control or TPPOH-X SNPs in HT-29 cells (Figure 3D). The same results were seen in HCT116 (Figure S8D) and SW620 (Figure S9D) cell lines with a significant increase in DNA fragmentation by 2.5-fold ± 0.1-fold and by 2.4-fold ± 0.1-fold, respectively, compared to light control.

TEM was also used to assess the apoptotic effects of TPPOH-X SNPs-PDT. The results showed that HT-29 (Figure 3E), HCT116 (Figure S8E) and SW620 cells (Figure S9E) treated with light control and TPPOH-X SNPs exhibited normal morphology with intact cell structures and undamaged nuclei. However, human CRC cell lines submitted to TPPOH-X SNPs-PDT showed a complete breakdown of intracellular structures. These cells exhibited morphological features such as cell membrane shrinkage, nuclear condensation and formation of

phagocytic vesicles, or apoptotic bodies, which are hallmarks of apoptosis. These results demonstrated that TPPOH-X SNPs-PDT induced death of human CRC cell lines through apoptosis.

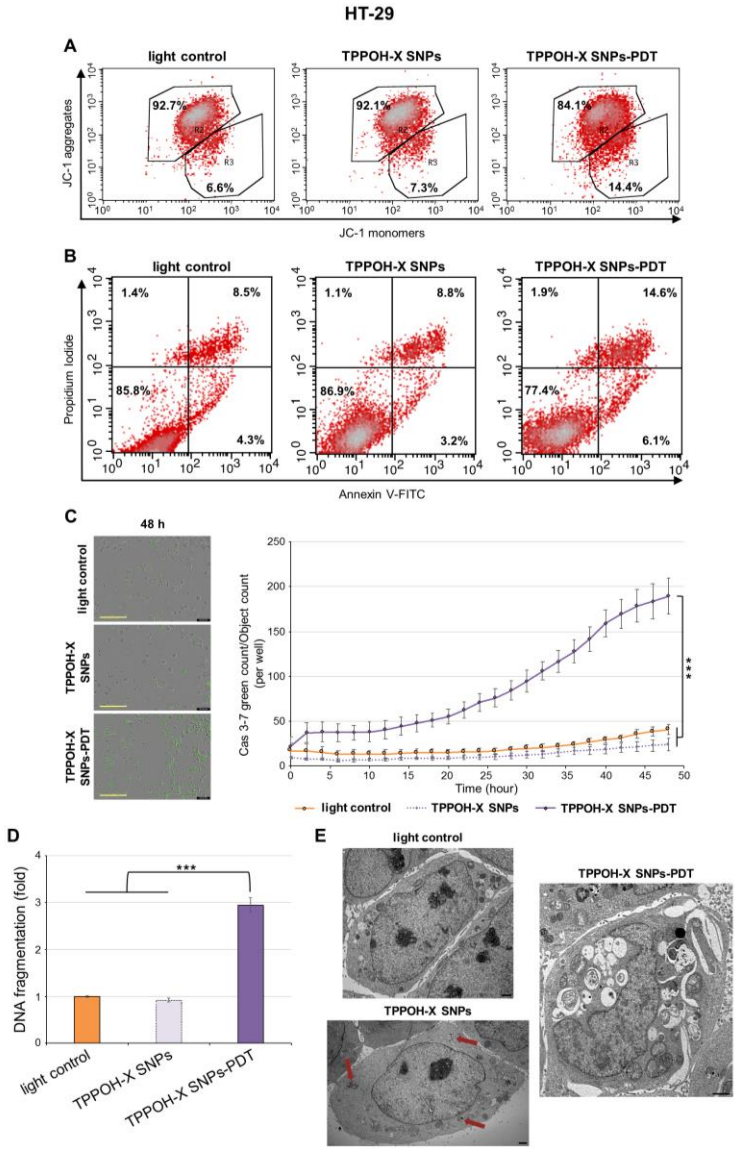

Figure 3: Effects of TPPOH-X SNPs-PDT on HT-29 cell line apoptosis. (**A**) HT-29 cells were treated or not treated with TPPOH-X SNPs and then

photoactivated or not photoactivated. The mitochondrial membrane potential was analyzed by flow cytometry with JC-1 at 48 h post-PDT. R2 represents the aggregate ratio and R3 represents the monomer ratio. (**B**) HT-29 cells were also stained, 48 h post-PDT, with Annexin V-FITC and PI, and apoptosis was analyzed by flow cytometry. The upper right quadrant represents the percentage of late apoptosis, and the lower right quadrant represents early apoptosis. (**C**) Caspase-3/7 activity, with the same conditions in HT-29 cells, was evaluated every 2 h during 48 h post-PDT by IncuCyte imaging live cell analysis and green count/cell count/well are shown. Representative images at 48 h post-PDT are shown. Yellow scale bar = 400 µm. (**D**) DNA fragmentation in HT-29 cells 48 h post-PDT was quantified from cytosol extracts by ELISA. Results are reported as n-fold compared to light control. (**E**) Representative TEM images of HT-29 cells treated or not treated with TPPOH-X SNPs and photoactivated or not 48 h post-PDT were shown. Red arrows indicate intracellular nanoparticles. Black scale bar = 1 µm. Data are shown as mean ± SEM (n = 3). *** $p < 0.001$.

Autophagy Inhibition Enhanced TPPOH-X SNPs-PDT-Induced Apoptosis

For all Western blot figures, please include densitometry readings/intensity ratio of each band; please include the whole blot showing all the bands with all molecular weight markers on the Western area in the Supplemental Materials section.

Because autophagy is often involved during PDT-treatments, we studied TPPOH-X SNPs-PDT effects on autophagy. Western blotting was performed on autophagy-related proteins, Beclin-1, and Atg5, two key regulators of autophagy and light chain 3 (LC3) forms which are involved in autophagosome formation. The results demonstrated that HT-29 cells expressed a slight increase in Beclin-1 and Atg5 protein levels and induced a higher conversion of LC3-I into LC3-II after TPPOH-X SNPs-PDT compared to light control, resulting in autophagy activation (Figure 4A). Then we used a pharmacological inhibitor of autophagy as co-treatment: 3-MA, which can block the early steps of autophagy. Cells treated with TPPOH-X SNPs + 3-MA-PDT expressed lower levels of autophagy-related proteins compared to cells exposed to TPPOH-X SNPs-PDT without co-treatment with 3-MA. Similar results were obtained in HCT116 (Figure S10A) and SW620 cells (Figure S11A).

Next, to confirm the induction of autophagy, cells were examined by TEM. Light control cells had an integrated cell nucleus and discrete organelles. However, HT-29 (Figure 4B), HCT116 (Figure S10B), and SW620 cells (Figure S11B) exposed to TPPOH-X SNPs-PDT were seriously damaged with clear cytoplasm vacuolization, with many membrane-bound vesicles containing organelles, cellular fragments, and double-membrane autophagosomes.

To determine whether this autophagy induction is a key mediator in resistance to TPPOH-X SNPs-PDT in human CRC cells, we examined whether inhibition of autophagy by 3-MA enhanced TPPOH-X SNPs-PDT-induced apoptosis. First, effects of co-treatment with 3-MA on the rate of apoptosis were evaluated by dual staining with Annexin V-FITC and PI by flow cytometry. In HT-29 cells, TPPOH-X SNPs + 3-MA-PDT increased the rate of early and late apoptosis simultaneously compared to TPPOH-X SNPs-PDT by 33.3% vs. 20.7%, respectively. Moreover, HT-29 cells treated with TPPOH-X SNPs + 3-MA without irradiation were mostly viable, as were light control cells with 84.6% and 85.8% live cells, respectively (Figure 4C). The same results were obtained for HCT116 (Figure S10C) and SW620 cells (Figure S11C) with 52.1% vs. 33.8% and 37.8% vs. 30.4% increases for the rate of early and late apoptosis simultaneously after TPPOH-X SNPs + 3-MA-PDT and TPPOH-X SNPs-PDT, respectively. Similarly to HT-29 cells, HCT116 and SW620 cells co-treated with 3-MA were mostly viable with 83.4% and 83.7% increases compared to 82.7% and 86.4% for light control cells, respectively.

In addition to these results, in HT-29 cells, co-treatment with 3-MA with TPPOH-X SNPs-PDT induced a significant increase in caspase-3/7 activity in a time-dependent manner (Figure 4D) and enhanced DNA fragmentation (Figure 4E) compared to TPPOH-X SNPs-PDT. Furthermore, co-treatment by 3-MA without PDT neither increased caspase-3/7 activity nor DNA fragmentation. The same results were found in HCT116 (Figure S10D,E) and SW620 (Figure S11D,E) cell lines. These data demonstrated in our study that autophagy acts as a resistance pathway of apoptosis.

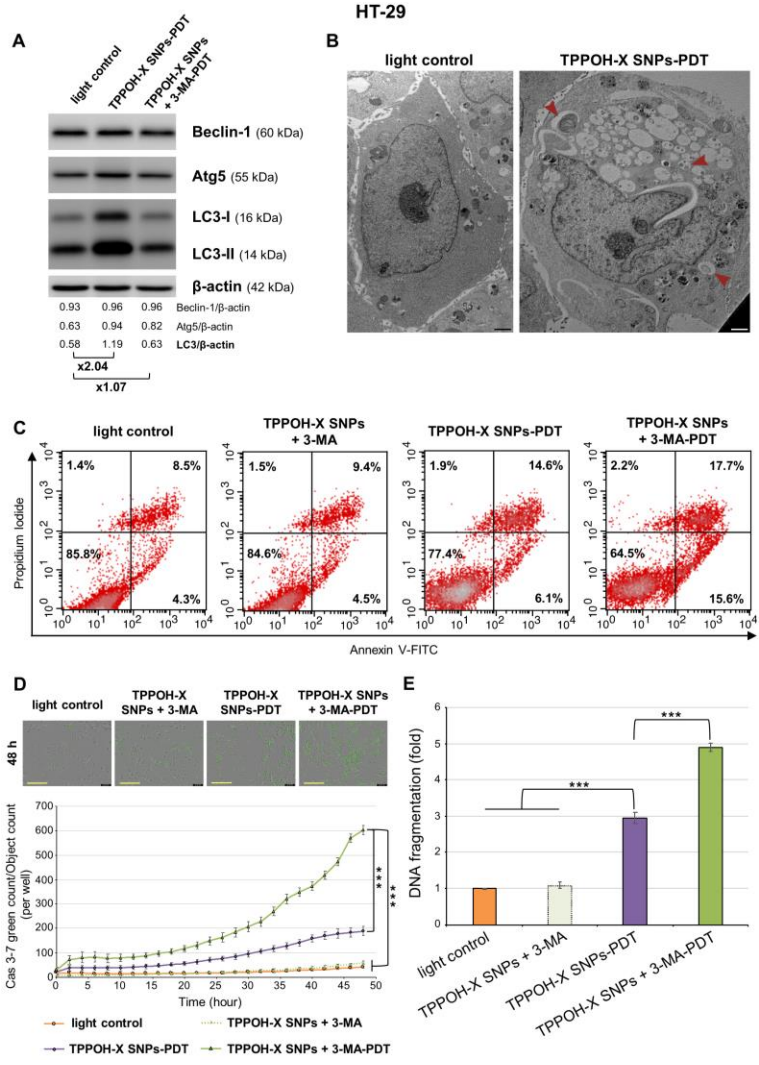

Figure 4: Effects of autophagy inhibition on HT-29 apoptosis. (**A**) HT-29 cells were treated or not with TPPOH-X SNPs in the presence or absence of 3-MA for 24 h. Expression of autophagy-related proteins was analyzed by Western blotting 48 h post-PDT. β-actin was used as a loading control. Representative images were shown. (**B**) Representative TEM images of HT-29 cells treated or not with TPPOH-X SNPs 48 h post-PDT protocol are shown. Red arrowheads indicate autophagosomes in the treated cells. Scale bar = 1 μm. (**C**) HT-29 cells were treated or not with TPPOH-X SNPs with or without 3-MA co-treatment and then were photoactivated or not photoactivated. At 48 h post-PDT, cells were stained with Annexin V-FITC and PI, and apoptosis was analyzed by flow

cytometry. Upper right quadrant represents the percentage of late apoptosis, and the lower right quadrant represents early apoptosis. (**D**) With the same conditions of treatment, caspase-3/7 activity was evaluated each 2 h during 48 h post-PDT protocol by IncuCyte imaging live cell analysis and green count/cell count/well were shown. Representative images at 48 h post-PDT protocol were shown. Yellow scale bar = 400 μm. (**E**) With the same conditions of treatment, DNA fragmentation was quantified from cytosol extracts with ELISA. Results were reported as n-fold compared to light control. Data are shown as mean ± SEM (n = 3). *** $p < 0.001$.

SNPs Vectorization and Autophagy Inhibition Enhanced TPPOH-PDT Effects on Suppressing CRC Tumor Growth In Vivo

To test TPPOH-PDT phototoxic effects on tumor growth, we used a xenograft CRC tumor model. HT-29 cells, the most resistant cell line in our study, were injected subcutaneously into both flanks of Balb/c nude mice. When tumor volume reached 100–150 mm^3, treatments were conducted by intravenous injection, at 1/100e LD_{50} for all TPPOH groups. After 24 h incubation, one tumor from each mouse was irradiated by laser. For the TPPOH-X SNPs multi group, the same protocol was conducted every 5 days. Tumor growth was recorded every 2 days during a period of 20 days (Figure 5A). In the control group, tumors exhibited rapid growth after seeding and no significant difference in tumor volume between light and non-light tumors was detected. This result indicated that light protocol did not suppressed tumorigenicity in vivo. However, TPPOH-PDT reduced tumor growth compared to TPPOH non-photoactivated treatments in all groups at the end point but with significant differences. TPPOH-PDT groups exhibited a slowing of tumor growth after approximately 2–4 days post-PDT. At the end point, free TPPOH-PDT induced a significant reduction in tumor growth by 22.5% ± 1.8% compared to free TPPOH non-PDT. TPPOH-X SNPs-PDT also induced a significant reduction of tumor growth by 37.7% ± 1.4% compared to non-photoactivated TPPOH-X SNPs. However, TPPOH-X SNPs-PDT was significantly more effective than free TPPOH-PDT. Moreover, tumor growth inhibition was significantly enhanced by 3-MA co-treatment. TPPOH-X SNPs + 3-MA-PDT significantly decreased tumor growth by 49% ± 1.7% vs. TPPOH-X SNPs + 3-MA non-PDT. However, TPPOH-X SNPs

+ 3-MA-PDT was significantly more efficient than TPPOH-X SNPs-PDT, with a significant reduction in tumor growth by 19.9% ± 0.3% compared to TPPOH-X SNPs-PDT. In addition, multi TPPOH-X SNPs-PDT were also efficient, with a significant reduction in tumor growth by 54.5% ± 3.2% vs. non-photoactivated multi TPPOH-X SNPs. Unfortunately, multi TPPOH-X SNPs-PDT did not induce the slowing of tumor growth but instead significantly increased tumor growth inhibition by 22.1% ± 1.3% compared to mono TPPOH-X SNPs treatment. Mouse body weight showed no significant difference between groups over the course of treatment (Figure S12A) indicating no systemic toxicity of free TPPOH or TPPOH-X SNPs. Mice were then sacrificed, and tumors were collected, recorded, and weighed. Tumor weights were consistent with tumor volumes. The tumor weight of TPPOH-PDT groups was in each case significantly decreased compared to the control or non-photoactivated TPPOH tumor groups (Figure S12B). These results were in agreement with the representative images showed for mouse and ex-vivo tumors from each group at the end point (Figure 5B).

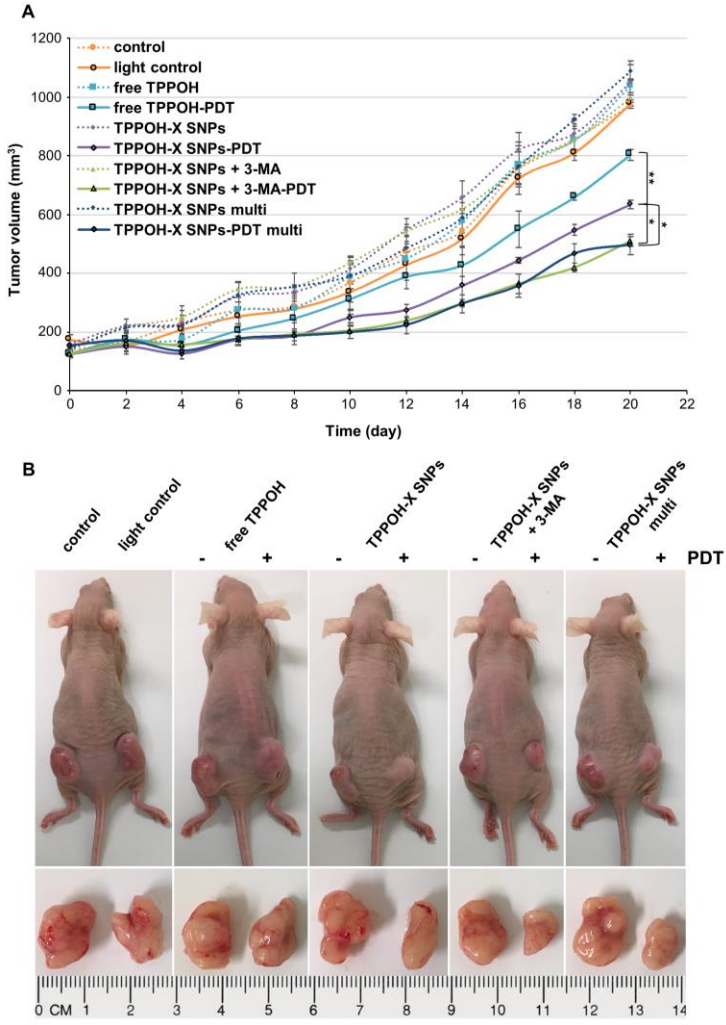

Figure 5: In vivo phototoxic effects on tumor growth. (**A**) Tumor growth curves of different groups over the treatment period until mouse sacrifice. (**B**) Representative images of HT-29 tumor-bearing nude mice and ex-vivo tumors after the mice being sacrificed on day 20. Data are shown as mean ± SEM (n = 5). * $p < 0.05$ and ** $p < 0.01$.

TPPOH-X SNPs-PDT Induced Apoptosis In Vivo

To estimate in vivo antitumor efficacy, histological analyses of tumors were performed 24 h post-PDT. One mouse from each

group was sacrificed to determine the mechanism of cell death induced by our treatments. HES staining showed decreased cell density and increased tumor fibrosis after TPPOH-PDT, especially after TPPOH-X SNPs-PDT with or without 3-MA, which are evidence of tissue injury caused by oxidative damage (Figure 6A). Terminal deoxynucleotidyl transferase dUTP nick-end labeling (TUNEL)staining to assess the number of apoptotic cells, revealed apoptosis in tumors harvested from mice exposed to TPPOH-PDT. TPPOH-X SNPs-PDT with or without 3-MA induced the highest levels of apoptosis in tumors compared to free TPPOH-PDT which exhibited weak staining, indicating slight apoptosis. LC3 staining revealed 3-MA co-treatment efficacy, with a decrease in LC3 staining after TPPOH-X SNPs + 3-MA-PDT compared to TPPOH-PDT without 3-MA. According to precedent in vitro results, TPPOH-X SNPs + 3-MA-PDT induced the best antitumor response, revealed by strong levels of apoptosis in tumors compared to all TPPOH-PDT. Moreover, the comparison of PDT and non-PDT tumors, where almost all tumor cells were viable, validated the importance of laser irradiation as a trigger of apoptosis.

At the end point, histological analyses of tumors were also performed. Consistent with the early HES staining, TPPOH-PDT induced a decrease in cell density and an increase in tumor fibrosis especially in TPPOH-X SNPs + 3-MA-PDT and multi TPPOH-X SNPs-PDT groups (Figure 6B). Ki-67 staining, a nuclear cell proliferation marker, showed that the number of cancer cells with a positively stained nucleus was markedly decreased after TPPOH-PDT compared to the control or non-PDT tumor groups. Consistent with the tumor growth results, SNPs vectorization of TPPOH showed a larger decrease in Ki-67 staining compared to the free TPPOH group. In addition, autophagy inhibition or multi TPPOH-X SNPs-PDT showed a marked decrease in Ki-67 staining compared to mono TPPOH-X SNPs-PDT. All these results demonstrating increased apoptosis and cell proliferation inhibition after TPPOH-PDT confirmed the in vivo antitumor efficacy of TPPOH-X SNPs.

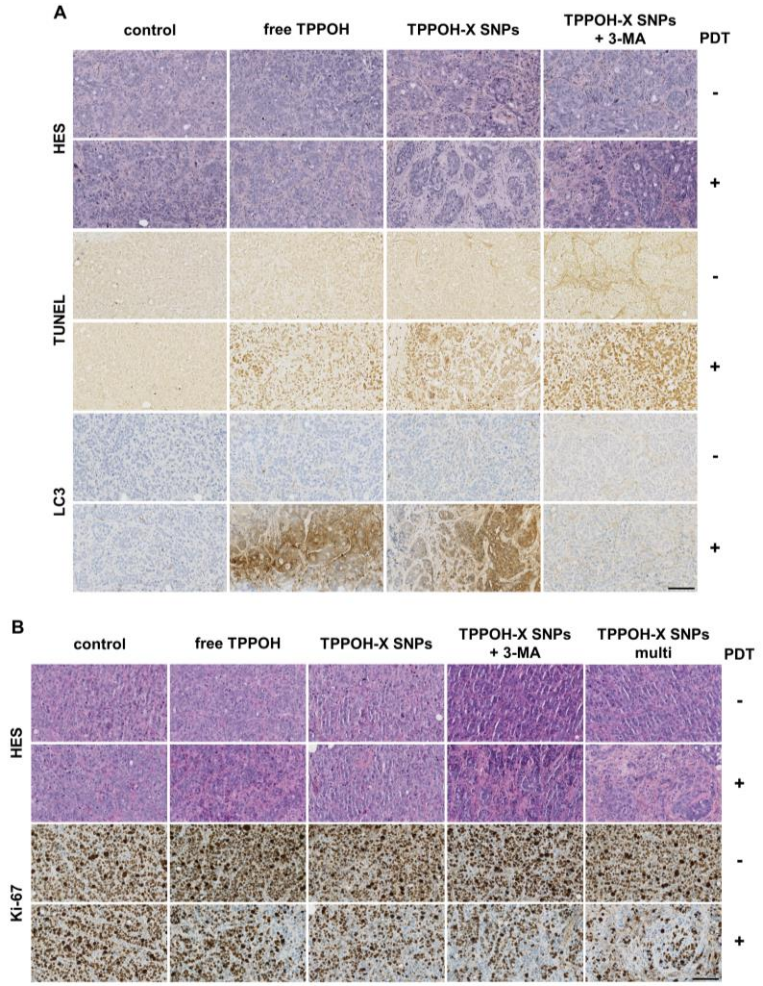

Figure 6: In vivo antitumor efficacy. (**A**) Tumors sections from treatment groups at 24 h post-PDT were stained with hematoxylin/eosin/saffron (HES), terminal deoxynucleotidyl transferase dUTP nick-end labeling (TUNEL) or LC3 staining. (**B**) Tumors sections from treatment groups after sacrifice were stained with HES and Ki-67. Representative images of each condition are shown. Black scale bar = 100 μm.

SNPs Vectorization Enhanced Tumor-Targeting without Systemic Toxicity

In comparison with free drugs, tumor-specific accumulation through the EPR effect is a key characteristic of nano-scale drugs. Therefore, we explored the biodistribution of TPPOH-X SNPs in our HT-29 cell xenograft tumor model using the IVIS Lumina quantitative fluorescence imaging system. Cy5.5-labeled free TPPOH and TPPOH-X SNPs were administered intravenously at 1/100e LD_{50} for each group. As shown in Figure 7A, a strong TPPOH-X SNPs fluorescence signal was observed at tumor sites 24 h post injection. In contrast, free TPPOH displayed minimal accumulation at tumor sites and had a highly diffuse fluorescence pattern. To further verify the tumor-specific accumulation properties of TPPOH-X SNPs, ex-vivo fluorescence imaging of tumors and major organs was performed at 24 h post-injection (Figure 7B). In both cases, liver and kidney fluorescence intensities were higher than other organs or tumors. However, tumor fluorescence intensity of TPPOH-X SNPs was higher compared to other organs than that of free TPPOH. These observations were confirmed by quantitative ROI analysis (Figure 7C) which demonstrated that TPPOH-X SNPs displayed significantly better tumor-targeting than free TPPOH.

To evaluate the potential systemic toxicity of our drug delivery system, sections of the major organs were stained with HES. In each case, including the TPPOH-X SNPs multi group, no damage was detected compared to the control group (Figure 7D). Pathological observations of SNPs treatments did not reveal significant differences, especially for hepatic inflammation or regeneration and renal impairment. These results highlighted the efficacy of TPPOH-X SNPs as having no toxic effects on the liver and kidneys, despite the high accumulation of SNPs on these organs at this dose.

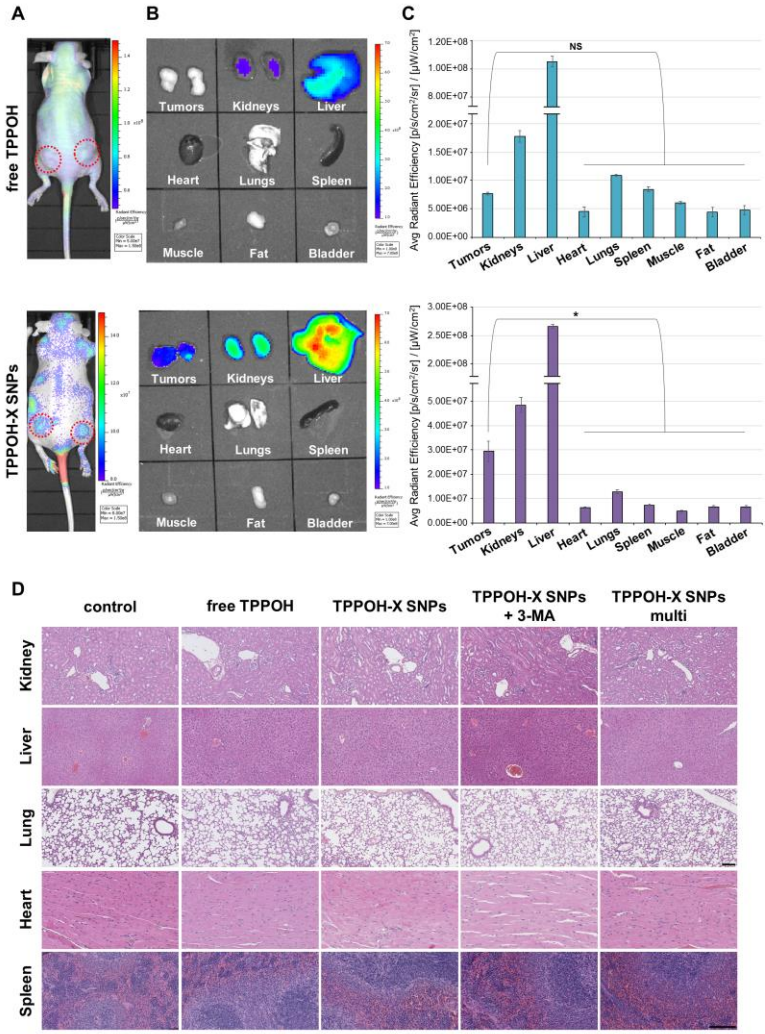

Figure 7: In vivo and ex vivo fluorescence imaging for biodistribution and safety evaluation. (**A**) In vivo fluorescence imaging of HT-29 tumor-bearing mice at 24 h post-intravenous injection of Cy5.5-labeled free TPPOH and TPPOH-X SNPs, at 1/100^{e} LD_{50} for each group. The red circles indicate tumor sites. (**B**) Ex-vivo fluorescence imaging of tumors and organs at 24 h post-injection. (**C**) ROI analysis of fluorescence intensity of tumors and organs at 24 h post-injection. (**D**) Representative images of histological analyses of major organ (kidney, liver, lung, heart and spleen) sections by HES staining. Black scale bar = 100 μm. Data are shown as mean ± SEM (n = 3). *p < 0.05 and NS: not significant.

Discussion

To increase the delivery of hydrophobic porphyrins to target sites, nanotechnology using nanocarriers appears to be the most promising strategy. NPs vectorization through encapsulation or attachment of PS not only enhances tumor-targeting through the EPR effect, but also increases PS hydrophilicity and tissue lifetime. Roy et al. entrapped the 2-devinyl-2-(1-hexyloxyethyl) pyropheophorbide (HPPH) into SNPs [34]. They reported efficient uptake, therefore significant cell death, after light irradiation compared to free drug in ovarian and cervical cancer cell lines. Secret et al. demonstrated similar results using anionic porphyrin-grafted porous silicon nanoparticles in breast cancer cells [35]. Other studies using chlorins as PS reported enhanced uptake using Chlorin e6 (Ce6) SNPs compared to Ce6 free carrier and also a stronger decrease in cell viability after Ce6 SNPs PDT compared to Ce6 alone in glioblastoma cancer cells [36] and breast cancer cells [37]. In addition, Brezániová et al. demonstrated that temoporfin SNPs enhanced uptake and cell death in breast cancer cells but also in MDA-MB-231 tumor bearing mice. They reported efficient antitumor responses using SNPs vectorization of temoporfin compared to free drug usage due to better tumor targeting through the EPR effect [38]. Furthermore, Simon et al. highlighted that protoporphyrin IX (PpIX) SNPs have better uptake and significantly enhanced cell death compared to free PpIX, which was confirmed by a strong fluorescence signal of ROS in HCT116 and HT-29 CRC cell lines. They reported that PpIX SNPs resulted in better tumor accumulation in HCT116 tumor bearing mice than the control alone, highlighting a greater selectivity for tumor tissues with SNPs vectorization [39]. Moreover, xylan could probably play an important role in controlled drug release. Sauraj et al. reported increased anticancer efficacy of xylan-stearic acid/5-fluorouracil NPs [40] and xylan-curcumin NPs [41] in HT-29 and HCT-15 CRC cell lines compared to free drugs. Xylan appears to be an efficient system for the delivery of hydrophobic anticancer drugs in cancer therapy. In our study, we compared the interest of TPPOH-X SNPs compared to free TPPOH. We demonstrated very significant phototoxic effects of TPPOH-X SNPs mediated by ROS generation post-PDT compared to free TPPOH in CRC

cell lines. This improvement in anticancer activity shown by the decreased IC_{50} dose after SNPs vectorization was due to efficient cell uptake compared to free carrier TPPOH. In vivo, we improved antitumor efficacy using TPPOH-X SNPs-PDT compared to free TPPOH due to better tumor targeting through the EPR effect, as shown by increased accumulation of TPPOH-X SNPs in tumors compared to free TPPOH. These findings demonstrated a strong interest in SNPs vectorization for hydrophobic drug delivery in vitro and mainly in vivo with efficient tumor targeting.

The major issues of inorganic SNPs are biosafety and toxicity. SNPs are one of the most biocompatible materials. However, diverse results have been reported about the safety of SNPs. The adverse effect depends on cell type and NPs size. Liu et al. demonstrated that 20 nm SNPs significantly induced apoptosis in a dose dependent manner from 100 μg/mL in human umbilical vein endothelial cells [42]. In contrast, Sergent et al. reported no cytotoxicity for 25 nm SNPs and limited cytotoxicity for 100 nm SNPs in HT-29 cells [43]. Cho et al. investigated the effect of the particle size on tissue distribution and tissue injury in vivo. They showed an accumulation in liver and spleen for 50 nm, 100 nm, and 200 nm SNPs, and observed a hepatic inflammatory response after injection of 100 and 200 nm SNPs. However, this effect was not reported for the smaller particles [44]. Moreover, Kumar et al. reported that 20 nm SNPs accumulated in all organs without signs of organ toxicity [45]. Although NPs size is important, the predominant issue is the dose injected. Chan et al. found no toxic effect in vivo after 150 nm SNPs intravenous injection up to 300 mg/kg [46]. Liu et al. demonstrated no side effects in vivo after up to 500 mg/kg of 110 nm SNPs intravenously. Repeated doses of 20, 40, and 80 mg/kg by continuous intravenous administration for 14 days have shown no toxicity. Nevertheless, for single dose toxicity, the LD_{50} was higher than 1 g/kg [47]. In our study, we did not detect any cytotoxicity for our 80 nm SNPs in HT-29 cells up to 175 μg/mL and in HCT116 and SW620 cell lines up to 35 μg/mL. We also explored the effect of 80 nm SNPs on apoptosis. Administration of 80 nm SNPs did not induce apoptosis in CRC cell lines and CRC cells exhibited normal morphology with intact cellular

structures and undamaged nuclei on TEM (data not shown). In vivo, we did not observe any toxicity of mono or multi intravenous administration of SNPs at 270 mg/kg. SNPs accumulated especially in the liver and kidneys but with no signs of hepatic inflammation or renal impairment (data not shown). These results attest to the low toxicity of SNPs in vitro and in vivo when intravenous injection at single dose or repeated administrations.

The mode of cellular photodamage that occurs after PDT often involves death pathways such as necrosis or apoptosis. Necrosis is generally accompanied by a loss of membrane integrity and metabolic homeostasis due to uncontrolled and immediate cellular disintegration. This death pathway is associated with characteristic morphologic changes including cell swelling and membrane rupture. In general, necrosis may occur in cells when high fluence and PS concentrations are being applied [48]. Cell death described after PDT is usually through apoptosis. Apoptosis involves controlled cell destruction and packaging of cell components in apoptotic bodies, which can be phagocytized. Apoptosis is characterized morphologically by cell shrinkage and other distinctive changes such as nuclear chromatin condensation, fragmentation of the nucleus, and segregation of the cell into apoptotic bodies [49]. ROS generated either in mitochondria or in the cytoplasm have been shown to be a potent inducer of apoptosis. PDT-induced ROS-generation triggers mitochondrial pore-opening leading to caspase activation and thus induces apoptotic cell death [50,51]. Some authors have shown that tetraphenylporphyrin (TPP) derivatives triggered PDT-induced apoptosis. Costa et al. reported that 5,10,15,20-Tetra (quinolin-2-yl) porphyrin (2-TQP) decreased cell viability after PDT in HT-29 CRC cells [52]. Baldea et al. demonstrated the meso-5,10,15,20-tetrakis (4-hydroxyphenyl) porphyrin (THOPP) induced apoptosis through caspase activation after PDT [53]. Liao et al. reported TPP derivatives possessing piperidine groups induced cell death after PDT in the QBC-939 cholangiocarcinoma cell line and antitumor efficacy in QBC-939 tumor-bearing mice [54]. Roby et al. described TPP free and TPP-loaded PEG-PE micelles induced apoptosis in murine Lewis lung carcinoma [55]. Wu et al. highlighted apoptosis

induction after PDT using POCL treatment composed in part of TPP in HeLa cervical cancer cells or HeLa tumor-bearing mice [56]. In our study, we demonstrated that TPPOH-X SNPs-PDT induced in vitro and in vivo cell death through the apoptosis pathway due to ROS generation in CRC cell lines. We have shown that TPPOH-X SNPs-PDT triggered mitochondrial pore-opening by the increase in JC-1 monomer rates. We highlighted apoptosis was due to caspase-3/7 involvement leading to DNA fragmentation. In addition, we demonstrated by TEM that CRC cells exhibited morphological features such as cell membrane shrinkage, nuclear condensation and formation of phagocytic vesicles or apoptotic bodies, hallmark events of apoptosis. We also reported that TPPOH-X SNPs induced apoptosis in our HT-29 tumor-bearing mice, as shown by the TUNEL assay.

Numerous studies have indicated that autophagy is activated after PDT as a result of ROS generation. Autophagy is an essential physiological process that functions to maintain cell homeostasis by removing dysfunctional or impaired cellular components and organelles [57]. There are some controversies regarding autophagy functions: autophagy plays a critical role both in programmed cell death and in survival processes. Several reports have demonstrated that PDT-induced autophagy significantly improved cytoprotective effects. Xue et al. showed that Ce6-mediated PDT induced significant apoptosis and autophagy, as indicated by the increased expression of cleaved caspase-3 and enhanced conversion of LC3-I/II forms. Autophagy inhibition by the pharmacological inhibitor: 3-MA, markedly increased PDT-induced cell death in SW620 cells [58]. Xiong et al. demonstrated the same results with also an increased number of autophagic vacuoles using Photosan-mediated PDT in HCT116 and SW620 cells. Combined treatment with the autophagy inhibitor: chloroquine, aggravated apoptosis. This combined strategy also resulted in a greater killing effect in a xenograft model, in which tumor volume decreased faster in the combined group than in the group treated with PDT alone [59]. Wei et al. reported same data in vitro and in vivo using PpIX-mediated PDT and autophagy pharmacological inhibitors or Atg5 depletion in CRC cells [60]. However, autophagy can also act as a pro-death process. Some studies showed that applying an

autophagy inhibitor significantly decreased cytotoxicity and apoptosis in osteosarcoma cells [61] or in breast cancer cells [62] treated with PDT. In our study, autophagy was involved after TPPOH-X SNPs-PDT in vitro as shown by the overexpression of autophagy-related proteins (Beclin-1, Atg5 and LC3) and the increased number of autophagic vacuoles. Autophagy is also enhanced in vivo as shown by the increased LC3 immunohistochemistry staining. Pharmacological autophagy inhibition by 3-MA markedly increased PDT-induced cell death in CRC cell lines. Moreover, in vivo autophagy inhibition induced a significant decrease in tumor volume compared to TPPOH-X SNPs-PDT without 3-MA co-treatment. Taken together, these findings suggest that PDT-stimulated autophagy acts as a PDT-resistance mechanism in our CRC model.

Materials and Methods

Materials

DMEM medium, DMEM red-phenol-free medium, RPMI 1640 medium, RPMI 1640 red-phenol-free medium, fetal bovine serum (FBS), L-glutamine and penicillin-streptomycin were purchased from Gibco BRL (Cergy-Pontoise, France). 3-(4,5-dimethylthiazol-2-yl)-2,5-diphenyltetrazolium bromide (MTT), N-acetyl-L-cysteine (NAC), 3-methyladenine (3-MA), anti-β-actin antibody, 5,5′,6,6′-tetrachloro-1,1′,3,3′-tetraethylbenzimidazolocarbocyanine iodide (JC-1) and cell death detection enzyme-linked immunosorbent assay^{PLUS} (ELISA) were obtained from Sigma-Aldrich (Saint-Quentin-Fallavier, France). Beclin-1, Atg5 and LC3 antibodies were acquired from Cell Signaling Technology—Ozyme (Saint-Quentin-en-Yvelines). 2',7'-dichlorofluorescein diacetate (DCFDA) cellular ROS detection assay kit and goat anti-rabbit IgG H&L horseradish peroxidase (HRP) secondary antibody were purchased from Abcam (Paris, France). LysoTracker, MitoTracker, rabbit anti-mouse IgG-IgM H&L HRP secondary antibody, TO-PRO-3, annexin V-FITC and propidium iodide (PI) were obtained from Invitrogen—Thermo Fisher Scientific (Villebon-sur-Yvette, France). Immobilon Western Chemiluminescent HRP Substrate was acquired from Merck

(Lyon, France). Caspase-3/7 green reagent was purchased from Sartorius (Göttingen, Germany).

Synthesis of Free TPPOH and TPPOH-X SNPs

The synthesis and characterization of free TPPOH and TPPOH-X SNPs were recently published by our research team [29]. SNPs were synthesized with an 80 nm average diameter following the modified Stöber method. Free TPPOH was synthesized and was conjugated with xylan via an esterification reaction forming TPPOH-X which was used in the surface modification of SNPs. The presence of glucuronic acid groups on xylan results in the formation of ionic bonds on the surface of SNPs which is made cationic by (3-aminopropyl) triethoxysilane (APTES). SNPs vectorization did not induced changes in the TPPOH spectrum (supplementary data [29]). Stock solutions of free TPPOH (5 mg/mL) and TPPOH-X SNPs (20 mg/mL) were prepared in ethanol.

Cell Culture

Human CRC cell lines (HT-29, HCT116 and SW620) were purchased from the American Type Culture Collection (ATCC—LGC Standards, Molsheim, France). Cells were grown in DMEM medium for HT-29 cells and RPMI 1640 medium for HCT116 and SW620 cells. Cells were supplemented with 10% FBS, 1% L-glutamine and 100 U/mL penicillin and 100 µg/mL streptomycin. Cultures were maintained in a humidified atmosphere containing 5% CO_2 at 37 °C. For all experiments, cells were seeded at 2.1×10^4, 1.2×10^4 and 1.5×10^4 cells/cm^2 for HT-29, HCT116 and SW620 cells respectively and culture medium was replaced by red phenol-free appropriate culture medium before PDT. Stock solutions of free TPPOH and TPPOH-X SNPs were diluted in culture medium to obtain the appropriate final concentrations. The same amount of vehicle (percentage of ethanol did not exceed 0.6%) was added to control cells.

In Vitro Phototoxicity of TPPOH-PDT

Phototoxicity was determined using MTT assay. Cells were seeded in 96-well culture plates and grown for 24 h in appropriate culture medium prior to exposure or not to TPPOH or SNPs. After 24 h incubation, cells were irradiated or not with 630–660 nm CURElight lamp at 75 J/cm^2 (PhotoCure ASA, Oslo, Norway). MTT assay were performed 48 h after irradiation and cell viability was expressed as a percentage of each treatment condition by normalizing to untreated cells.

Intracellular ROS Generation by TPPOH-PDT

ROS generation was quantified using a cellular reactive oxygen species detection assay which uses the cell permeant reagent DCFDA. Cells were seeded in 6-well culture plates and were grown for 24 h prior to exposure or not to TPPOH at respective IC_{50} values. After 24 h incubation, cells were stained with DCFDA for 30 min at 37 °C. After washing, cells were irradiated or not. To confirm ROS inhibition, cells were pretreated with ROS scavenger NAC 1 h before PDT at 10 mM. ROS generation was examined by flow cytometry 4 h post-PDT. Tert-Butyl Hydrogen Peroxide (TBHP) was used as a positive control at 250 μM.

TPPOH Cellular Uptake and Localization

Cells were seeded in 6-well culture plates and were grown for 24 h prior to exposure to free TPPOH or TPPOH-X SNPs at the same concentration (1 μM TPPOH). After 24 h incubation, TPPOH fluorescence (excitation/emission: 405/650 nm) was determined by AMNIS® imaging flow cytometry analysis and studied with IDEAS software (Merck). To determine TPPOH-X SNPs localizations, cells were seeded and treated as described above and co-treated at 37 °C with 75 nM LysoTracker during 2 h or 150 nM MitoTracker during 45 min. TPPOH-X SNPs localizations were determined by AMNIS® imaging flow cytometry and studied with IDEAS software using TPPOH fluorescence (excitation/emission: 405/650 nm) with LysoTracker fluorescence (excitation/emission: 578/603 nm) or

MitoTracker fluorescence (excitation/emission: 490/516 nm). The same protocol was conducted for confocal microscopy analysis and photos were taken with a confocal microscope (laser Zeiss LSM 510 Meta—×1000)

Transmission Electron Microscopy (TEM)

Cells were seeded in 6-well culture plates and were grown for 24 h prior to exposure or not to TPPOH-X SNPs treatment. After 24 h of incubation, cells were recovered for uptake experiment. For apoptosis and autophagy experiments, cells were irradiated or not. 48 h post-PDT protocol or immediately after 24 h of incubation for uptake experiment, cells were then incubated in 1% osmium tetroxide solution for 30 min at room temperature, dehydrated with increasing ethanol concentrations, and embedded in epon. Cells were polymerized over 48 h at 60 °C and ultrathin sections (80–100 nm) were prepared. Grids were stained with uranyl acetate and lead citrate and examined with TEM JEM-1011 (JEOL, Croissy-sur-Seine, France) operated at 80 KeV.

Autophagy Detection and Inhibition

Cells were seeded in 25 cm^2 tissue culture flasks and were grown for 24 h prior to exposure or not to TPPOH-X SNPs at the IC_{50} value. After 24 h incubation, cells were treated or not with the autophagy pharmacological inhibitor: 3-MA at 2 mM and were irradiated. 48 h post-PDT, cells were recovered and lysed in RIPA lysis buffer. Protein levels were determined using the Bradford method. Western blotting was performed on autophagy-related proteins, anti-Beclin-1 (1:1000), anti-Atg5 (1:1000) and anti-LC3 (1:1000). Anti-β-actin (1:5000) was used as a loading control. After incubation with the appropriate secondary antibodies, blots were developed using the Immobilon Western Chemiluminescent HRP Substrate and G:BOX system (Syngene, Cambridge, UK).

In vitro Apoptosis by TPPOH-X SNPs

Cells were seeded in 25 cm^2 tissue culture flasks and were grown for 24 h prior to exposure or not to TPPOH-X SNPs at the IC_{50} value. After 24 h incubation, cells were treated or not with 3-MA and were irradiated. Cells were recovered 48 h post-PDT and divided in three groups. The first group was used to estimate mitochondrial membrane potential using JC-1. Cells were treated with JC-1 (1 μg/mL) for 30 min at 37 °C and then with TO-PRO-3 (1 μM) and mitochondrial membrane potential was immediately evaluated by flow cytometry. The second group of cells was used to determine apoptosis by dual staining with Annexin V-FITC and PI. Cells were treated with Annexin V-FITC and PI (1.5 μM) for 15 min at room temperature and cell viability was determined by flow cytometry. The last group was used to assess DNA fragmentation. Histone release from the nucleus during apoptosis was analyzed using the Cell Death Detection ELISA^{PLUS} as previously described [63]. Cytosol extracts were obtained according to the manufacturer's protocol. DNA fragmentation was measured and results were reported as n-fold compared to control.

Cells were seeded in 96-well culture plates and were grown for 24 h prior to exposure or not to TPPOH-X SNPs at the IC_{50} value. After 24 h incubation, cells were treated or not with 3-MA and were irradiated. Then, cells were treated with caspase-3/7 green reagent (5 μM) and were placed in the IncuCyte S3 live cell analysis system (Sartorius). Cells were imaged every 2 h with 4 images/well in phase contrast and green fluorescence modes using a ×10 objective to detect apoptotic cells. Apoptotic level was quantified by the IncuCyte software (Sartorius) as caspase-3/7 green count/cell count/well.

Heterotopic CRC Model

To establish a subcutaneous xenograft model of human CRC, human CRC HT-29 cells ($5x10^6$ cells in 100 μL of 50/50 PBS-matrigel) were subcutaneously injected in each side of the dorsal region of four-week-old female Balb/c nude mice (≈20 g). At these sites, the tumors were easily accessible for treatment and

assessment of response. We measured tumor dimensions every other day by a caliper and calculated the volume with the formula ($V = 4\pi/3 \times LW^2/8$, where L is tumor length and W is tumor width) [64].

In Vivo Antitumor Efficacy and Biosafety Evaluation of TPPOH-PDT

To confirm antitumor efficacy, HT-29 tumor-bearing mice were established as described above and anticancer treatments were administered when the tumors were approximately 100–150 mm^3. Mice were randomly divided into five groups (n = 6): control, free TPPOH, TPPOH-X SNPs, TPPOH-X SNPs + 3-MA and TPPOH-X SNPs multi. Mice were injected in the tail vein with 100 μL phosphate buffered saline (PBS) or $1/100^e$ lethal dose 50 (LD_{50}) (Log LD_{50} = 0.435 log IC_{50} (mM) + 0.625) [65] for all TPPOH groups: free TPPOH (3.26 mg/kg), TPPOH-X SNPs with or without 3-MA and multi group (1.16 mg/kg TPPOH and 334 mg/kg SNPs). Mice from the TPPOH-X SNPs + 3-MA group received a 100 μL IP injection of 24 mg/kg 3-MA [66]. Then, 24 h post-injection, only one tumor per mouse was subjected to light irradiation to compare intra-individual irradiation effects. Consequently, 10 conditions were studied: each of the 5 groups was divided in 2 conditions (no irradiation: PDT—and red irradiation: PDT +). Irradiation was performed with a 660 nm red laser (Z-LASER, Freiburg, Germany). PDT was performed by 2 sequences of 5 min irradiation separated by 5 min (at 660 nm with 100 mW, for a 200 J/cm^2 fluence as previously described [67]. For the TPPOH-X SNPs multi group, the same protocol was conducted every 5 days. At 24 h post-PDT, one mouse from each group except for the TPPOH-X SNPs multi group was sacrificed and tumors were harvested and fixed in 4% paraformaldehyde to prepare paraffin sections. Hematoxylin/eosin/saffron (HES) staining was used for histological analyses, while TUNEL assay and LC3 staining were performed to assess apoptosis and autophagy levels in the tumors, respectively. For other mice, tumor size and mouse body weight were recorded every 2 days. HT-29 tumor-bearing mice were sacrificed on day 20 after initial drug treatment and tumor weight was recorded. Tumors and major organs including

kidneys, liver, lungs, heart and spleen were harvested and fixed in 4% paraformaldehyde to prepare paraffin sections. HES staining was used for histological analysis and Ki-67 staining was used to assess tumor cell proliferation and growth. HES staining was performed with Tissue Tek (Sakura, Alphen aan den Rijn, Netherlands), Ki-67 staining with BenchMark Ultra Ventana (Roche Diagnostics, Meylan, France), TUNEL assay with the cell death detection kit POD (Roche Diagnostics) and LC3 staining with LC3 antibody (1:200) and revealed with Acuity Advanced Biotin Free Polymer Detection System DAB (BioLegend, London, UK). All histological analyses were scanned under the NanoZoomer RS2 optical microscope scanner (Hamamatsu Photonics, Massy, France) and studied with NDPView software.

In Vivo Biodistribution of TPPOH-X SNPs

To determine the biodistribution of TPPOH treatments, free TPPOH and TPPOH-X SNPs were labeled with Cyanine 5.5 (Lumiprobe, Hannover, Germany) to allow tracking because the TPPOH emission spectrum overlaps with that of blood. HT-29 tumor-bearing mice, established as described above, were randomly divided into two groups (n = 3) and intravenously injected with $1/100^{e}$ LD_{50} for both group: Cy5.5-free TPPOH (3.26 mg/kg) and Cy5.5-TPPOH-X SNPs (1.16 mg/kg TPPOH and 334 mg/kg SNPs). Then 24 h post-injection, the biodistribution was determined using IVIS Lumina quantitative fluorescence imaging system (PerkinElmer, Villepinte, France). Subsequently, the mice were sacrificed and ex vivo biodistribution images of the tumors and major organs were immediately taken. Relative signal intensity in tumors and organs was calculated, using Living Image software (PerkinElmer), as radiant efficiency ([photons/s/cm^2/sr]/[μW/cm^2]) per pixel of the region of interest (ROI), which was drawn around the respective organ.

Ethical Statement

Institutional review board approval was obtained from the Regional Animal Experimentation Ethics Committee (approval

number: #16335-2018073009499570 v3). All animal experiments and experimental protocols were in accordance with the recommendations of the European Directive of 22 September 2010 (2010/63/EU) on the protection of animals used for scientific purposes. All efforts were made to reduce the number of animals used and to ensure their optimal conditions of well-being before, during, and after each experiment.

Statistical Analysis

All quantitative results are expressed as the mean ± standard error of the mean (SEM) of separate experiments. Statistical significance was evaluated by the two-tailed unpaired Student's t-test and expressed as: * $p < 0.05$; ** $p < 0.01$ and *** $p < 0.001$.

Conclusions

In this study, we evaluated for the first time the anticancer efficacy of the new TPPOH-X SNPs synthesized by our research team in human CRC cell lines and on HT-29 tumor-bearing mice. According to our hypothesis concerning the interest of SNPs vectorization, we demonstrated the strong anticancer efficacy of TPPOH in vitro and in vivo, and the additional benefit of vectorized SNPs. As shown by the strong antitumor efficacy on HT-29 tumor-bearing mice with both multi TPPOH-X SNPs-PDT or co-treatment with an autophagy inhibitor, our new TPPOH-X SNPs seem to be a promising PDT agent for further clinical protocols.

References

1. Globocan. Estimated Cancer Incidence, Mortality and Prevalence Worldwide in 2018. Information and Online Prediction. WHO International Agency for Research of Cancer. 2018. Available online at: http://gco.iarc.fr/today/home.
2. Xue L, Williamson A, Gaines S, Andolfi C, Paul-Olson T, et al. An Update on Colorectal Cancer. Curr. Probl. Surg. 2018; 5555: 76–116.

3. Matsuda T, Yamashita K, Hasegawa H, Oshikiri T, Hosono M, et al. Recent updates in the surgical treatment of colorectal cancer. Ann. Gastroenterol. Surg. 2018; 22: 129–136.
4. Wolpin BM, Mayer RJ. Systemic Treatment of Colorectal Cancer. Gastroenterology. 2008; 134134: 1296–1310.
5. Lee YT, Tan YJ, Oon CE. Molecular targeted therapy: Treating cancer with specificity. Eur. J. Pharmacol. 2018; 834: 188–196.
6. Van der Jeught K, Xu HC, Li YJ, Lu XB, Ji G. Drug resistance and new therapies in colorectal cancer. World J. Gastroenterol. 2018; 2424: 3834–3848.
7. Kawczyk-Krupka A, Bugaj AM, Latos W, Zaremba K, Wawrzyniec K, et al. Photodynamic therapy in colorectal cancer treatment-The state of the art in preclinical research. Photodiagnosis Photodyn. Ther. 2016; 13: 158–174.
8. Kwiatkowski S, Knap B, Przystupski D, Saczko J, Kędzierska E, et al. Photodynamic therapy–mechanisms, photosensitizers and combinations. Biomed. Pharmacother. 2018; 106: 1098–2107.
9. Hamblin MR, Mroz P. Advances in Photodynamic Therapy: Basic, Translational and Clinical, 1st ed, Boston, Mass. Norwood: Artech House Publishers. 2008.
10. Dolmans DEJGJ, Fukumura D, Jain RK. Photodynamic therapy for cancer. Nat. Rev. Cancer. 2003; 33: 380–387.
11. DeRosa MC, Crutchley RJ. Photosensitized singlet oxygen and its applications. Coord. Chem. Rev. 2002; 233: 351–371.
12. Mroz P, Yaroslavsky A, Kharkwal GB, Hamblin MR. Cell Death Pathways in Photodynamic Therapy of Cancer. Cancers. 2011; 33: 2516–2539.
13. Plaetzer K, Kiesslich T, Verwanger T, Krammer B. The Modes of Cell Death Induced by PDT: An Overview. Med. Laser Appl. 2003; 1818: 7–19.
14. Abrahamse H, Hamblin MR. New photosensitizers for photodynamic therapy. Biochem. J. 2016; 473: 347–364.
15. Saini RK, Chouhan R, Bagri LP, Bajpai AK. Strategies of Targeting Tumors and Cancers. J. Cancer Res. Updates. 2012; 1: 129–152.

16. Huang YY, Sharma SK, Dai T, Chung H, Yaroslavsky A, et al. Can nanotechnology potentiate photodynamic therapy? Nanotechnol. Rev. 2012; 11: 111–146.
17. Iyer AK, Khaled G, Fang J, Maeda H. Exploiting the enhanced permeability and retention effect for tumor targeting. Drug. Discov. Today. 2006; 11: 812–818.
18. Zhou Y, Liang X, Dai Z. Porphyrin-loaded nanoparticles for cancer theranostics. Nanoscale. 2016; 8: 12394–12405.
19. Debele TA, Peng S, Tsai HC. Drug Carrier for Photodynamic Cancer Therapy. Int. J. Mol. Sci. 2015; 16: 22094–22136.
20. Wu X, Wu M, Xiaojun Zhao J. Recent Development of Silica Nanoparticles as Delivery Vectors for Cancer Imaging and Therapy. Nanomedicine. 2014; 10: 297–312.
21. Couleaud P, Morosini V, Frochot C, Richeter S, Raehm L, et al. Silica-based nanoparticles for photodynamic therapy applications. Nanoscale. 2010; 2: 1083–1095.
22. Chen Y, Chen H, Shi J. In Vivo Bio-Safety Evaluations and Diagnostic/Therapeutic Applications of Chemically Designed Mesoporous Silica Nanoparticles. Adv. Mater. 2013; 25: 3144–3176.
23. Lemarchand C, Gref R, Couvreur P. Polysaccharide-decorated nanoparticles. Eur. J. Pharm. Biopharm. 2004; 58: 327–341.
24. Gref R. Surface-engineered nanoparticles as drug carriers. In: Baraton MI, editor. Synthesis, Functionalization and Surface Treatment of Nanoparticles, 1st ed. California: American Scientific Publishers. 2002; 233–256.
25. Owens DE, Peppas NA. Opsonization, biodistribution, and pharmacokinetics of polymeric nanoparticles. Int. J. Pharm. 2006; 307: 93–102.
26. Shrotri A, Kobayashi H, Fukuoka A. Chapter Two-Catalytic Conversion of Structural Carbohydrates and Lignin to Chemicals. Adv. Catal. 2017; 60: 59–123.
27. Ma J, Li D, Zhong L, Du F, Tan J, et al. Synthesis and characterization of biofunctional quaternized xylan-Fe2O3 core/shell nanocomposites and modification with polylysine and folic acid. Carbohydr. Polym. 2018; 199: 382–389.
28. Daus S, Heinze T. Xylan-based nanoparticles: Prodrugs for ibuprofen release. Macromol. Biosci. 2010; 10: 211–220.

29. Bouramtane S, Bretin L, Pinon A, Leger D, Liagre B, et al. Porphyrin-xylan-coated silica nanoparticles for anticancer photodynamic therapy. Carbohydr. Polym. 2019; 213: 168–175.
30. Lai K, Killingsworth MC, Lee CS. The significance of autophagy in colorectal cancer pathogenesis and implications for therapy. J. Clin. Pathol. 2014; 67: 854–858.
31. Duan X, Chen B, Cui Y, Zhou L, Wu C, et al. Ready player one? Autophagy shapes resistance to photodynamic therapy in cancers. Apoptosis. 2018; 23: 587–606.
32. Hackbarth S, Horneffer V, Wiehe A, Hillenkamp F, Röder B. Photophysical properties of pheophorbide-a-substituted diaminobutane poly-propylene-imine dendrimer. Chem. Phys. 2001; 269: 339–346.
33. Li Y, Jang WD, Nishiyama N, Kishimura A, Kawauchi S, et al. Dendrimer Generation Effects on Photodynamic Efficacy of Dendrimer Porphyrins and Dendrimer-Loaded Supramolecular Nanocarriers. Chem. Mater. 2007; 19: 5557–5562.
34. Roy I, Ohulchanskyy TY, Pudavar HE, Bergey EJ, Oseroff AR, et al. Ceramic-based nanoparticles entrapping water-insoluble photosensitizing anticancer drugs: A novel drug-carrier system for photodynamic therapy. J. Am. Chem. Soc. 2003; 125: 7860–7865.
35. Secret E, Maynadier M, Gallud A, Gary-Bobo M, Chaix A, et al. Anionic porphyrin-grafted porous silicon nanoparticles for photodynamic therapy. Chem. Commun. (Camb.). 2013; 49: 4202–4204.
36. Youssef Z, Jouan-Hureaux V, Colombeau L, Arnoux P, Moussaron A, et al. Titania and silica nanoparticles coupled to Chlorin e6 for anti-cancer photodynamic therapy. Photodiagnosis Photodyn. Ther. 2018; 22: 115–126.
37. Bharathiraja S, Moorthy MS, Manivasagan P, Seo H, Lee KD, et al. Chlorin e6 conjugated silica nanoparticles for targeted and effective photodynamic therapy. Photodiagnosis Photodyn. Ther. 2017; 19: 212–220.
38. Brezániová I, Záruba K, Králová J, Adámková H, Ulbrich P, et al. Silica-based nanoparticles are efficient delivery systems for temoporfin. Photodiagnosis Photodyn. Ther. 2018; 21: 275–284.

39. Simon V, Devaux C, Darmon A, Donnet T, Thiénot E, et al. Pp IX silica nanoparticles demonstrate differential interactions with in vitro tumor cell lines and in vivo mouse models of human cancers. Photochem. Photobiol. 2010; 86: 213–222.
40. Kumar V, Kumar B, Deeba F, Bano S, Kulshreshtha A, et al. Lipophilic 5-fluorouracil prodrug encapsulated xylan-stearic acid conjugates nanoparticles for colon cancer therapy. Int. J. Biol. Macromol. 2019; 128: 204–213.
41. Sauraj Kumar SU, Kumar V, Priyadarshi R, Gopinath P, Negi YS. pH-responsive prodrug nanoparticles based on xylan-curcumin conjugate for the efficient delivery of curcumin in cancer therapy. Carbohydr. Polym. 2018; 188: 252–259.
42. Liu X, Sun J. Endothelial cells dysfunction induced by silica nanoparticles through oxidative stress via JNK/P53 and NF-kB pathways. Biomaterials. 2010; 31: 8198–8209.
43. Sergent JA, Paget V, Chevillard S. Toxicity and genotoxicity of nano-SiO_2 on human epithelial intestinal HT-29 cell line. Ann. Occup. Hyg. 2012; 56: 622–630.
44. Cho M, Cho WS, Choi M, Kim SJ, Han BS, et al. The impact of size on tissue distribution and elimination by single intravenous injection of silica nanoparticles. Toxicol. Lett. 2009; 189: 177–183.
45. Kumar R, Roy I, Ohulchanskky TY, Vathy LA, Bergey EJ, et al. In vivo biodistribution and clearance studies using multimodal organically modified silica nanoparticles. ACS Nano. 2010; 4: 699–708.
46. Chan WT, Liu CC, Chiau JSC, Tsai ST, Liang CK, Cheng ML, et al. In vivo toxicologic study of larger silica nanoparticles in mice. Int. J. Nanomedicine. 2017; 12: 3421–3432.
47. Liu T, Li L, Teng X, Huang X, Liu H, et al. Single and repeated dose toxicity of mesoporous hollow silica nanoparticles in intravenously exposed mice. Biomaterials. 2011; 32: 1657–1668.
48. Zhou CN. Mechanisms of tumor necrosis induced by photodynamic therapy. J. Photochem. Photobiol. B. 1989; 3: 299–318.

49. Elmore S. Apoptosis: A review of programmed cell death. Toxicol. Pathol. 2007; 35: 495–516.
50. Li X, Zhu F, Jiang J, Sun C, Wang X, et al. Synergistic antitumor activity of withaferin A combined with oxaliplatin triggers reactive oxygen species-mediated inactivation of the PI3K/AKT pathway in human pancreatic cancer cells. Cancer Lett. 2015; 357: 219–230.
51. Skulachev VP. Mitochondrial physiology and pathology, concepts of programmed death of organelles, cells and organisms. Mol. Asp.S Med. 1999; 20: 139–184.
52. Costa LD, e Silva J de A, Fonseca SM, Arranja CT, Urbano AM, et al. Photophysical Characterization and in Vitro Phototoxicity Evaluation of 5,10,15,20-Tetra (quinolin-2-yl) porphyrin as a Potential Sensitizer for Photodynamic Therapy. Molecules. 2016; 21: 439.
53. Baldea I, Olteanu DE, Bolfa P, Ion RM, Decea N, et al. Efficiency of photodynamic therapy on WM35 melanoma with synthetic porphyrins: Role of chemical structure, intracellular targeting and antioxidant defense. J. Photochem. Photobiol. B 2015; 151: 142–152.
54. Liao PY, Gao YH, Wang XR, Bao LL, Bian J, et al. Tetraphenylporphyrin derivatives possessing piperidine group as potential agents for photodynamic therapy. J. Photochem. Photobiol. B 2016; 165: 213–219.
55. Roby A, Erdogan S, Torchilin VP. Enhanced in vivo antitumor efficacy of poorly soluble PDT agent, meso-tetraphenylporphine, in PEG-PE-based tumor-targeted immunomicelles. Cancer Biol. Ther. 2007; 6: 1136–1142.
56. Wu M, Wu L, Li J, Zhang D, Lan S, et al. Self-Luminescing Theranostic Nanoreactors with Intraparticle Relayed Energy Transfer for Tumor Microenvironment Activated Imaging and Photodynamic Therapy. Theranostics. 2019; 9: 20–33.
57. Janku F, McConkey DJ, Hong DS, Kurzrock R. Autophagy as a target for anticancer therapy. Nat. Rev. Clin. Oncol. 2011; 8: 528–539.
58. Xue Q, Wang X, Wang P, Zhang K, Liu Q. Role of p38MAPK in apoptosis and autophagy responses to photodynamic therapy with Chlorin e6. Photodiagnosis Photodyn. Ther. 2015; 12: 84–91.

59. Xiong L, Liu Z, Ouyang G, Lin L, Huang H, et al. Autophagy inhibition enhances photocytotoxicity of Photosan-II in human colorectal cancer cells. Oncotarget. 2017; 8: 6419–6432.
60. Wei MF, Chen MW, Chen KC, Lou PJ, Lin SYF, et al. Autophagy promotes resistance to photodynamic therapy-induced apoptosis selectively in colorectal cancer stem-like cells. Autophagy. 2014; 10: 1179–1192.
61. Tu P, Huang Q, Ou Y, Du X, Li K, et al. Aloe-emodin-mediated photodynamic therapy induces autophagy and apoptosis in human osteosarcoma cell line MG-63 through the ROS/JNK signaling pathway. Oncol. Rep. 2016; 35: 3209–3215.
62. Zhu J, Tian S, Li KT, Chen Q, Jiang Y, et al. Inhibition of breast cancer cell growth by methyl pyropheophenylchlorin photodynamic therapy is mediated though endoplasmic reticulum stress-induced autophagy in vitro and vivo. Cancer Med. 2018; 7: 1908–1920.
63. Lepage C, Léger DY, Bertrand J, Martin F, Beneytout JL, et al. Diosgenin induces death receptor-5 through activation of p38 pathway and promotes TRAIL-induced apoptosis in colon cancer cells. Cancer Lett. 2011; 301: 193–202.
64. Lu J, Liong M, Li Z, Zink JI, Tamanoi F. Biocompatibility, Biodistribution, and Drug-Delivery Efficiency of Mesoporous Silica Nanoparticles for Cancer Therapy in Animals. Small. 2010; 6: 1794–1805.
65. Guidance Document on Using In Vitro Data to Estimate In Vivo Starting Doses for Acute Toxicity. NIH Publication No. 01–4500. 2001. Available online at: https://ntp.niehs.nih.gov/iccvam/docs/acutetox_docs/guidance0801/iv_guide.pdf.
66. Li J, Hou N, Faried A, Tsutsumi S, Kuwano H. Inhibition of autophagy augments 5-fluorouracil chemotherapy in human colon cancer in vitro and in vivo model. Eur. J. Cancer. 2010; 46: 1900–1909.
67. Fidanzi-Dugas C, Liagre B, Chemin G, Perraud A, Carrion C, et al. Analysis of the in vitro and in vivo effects of photodynamic therapy on prostate cancer by using new photosensitizers, protoporphyrin IX-polyamine derivatives. Biochim. Biophys. Acta. 2017; 1861: 1676–1690.

Supplementary Materials

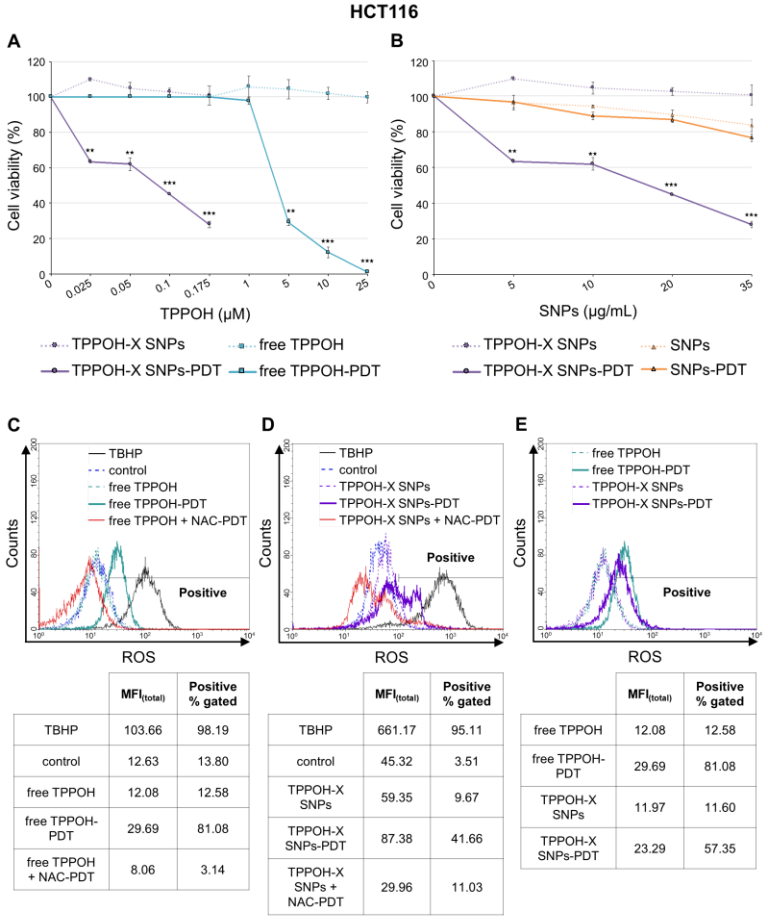

	$MFI_{(total)}$	Positive % gated
TBHP	103.66	98.19
control	12.63	13.80
free TPPOH	12.08	12.58
free TPPOH-PDT	29.69	81.08
free TPPOH + NAC-PDT	8.06	3.14

	$MFI_{(total)}$	Positive % gated
TBHP	661.17	95.11
control	45.32	3.51
TPPOH-X SNPs	59.35	9.67
TPPOH-X SNPs-PDT	87.38	41.66
TPPOH-X SNPs + NAC-PDT	29.96	11.03

	$MFI_{(total)}$	Positive % gated
free TPPOH	12.08	12.58
free TPPOH-PDT	29.69	81.08
TPPOH-X SNPs	11.97	11.60
TPPOH-X SNPs-PDT	23.29	57.35

Figure S1: In vitro phototoxic effects of TPPOH-X SNPs-PDT and ROS production. (A) HCT116 cells were treated or not with free TPPOH and TPPOH-X SNPs based on TPPOH concentration. Then, cells were exposed or not to PDT. Phototoxic effects were determined 48 h post-PDT using the MTT assay. Cell viability, expressed in percentage of each condition, was compared to controls. IC50 values were calculated of 72.6 nM for TPPOH-X SNPs-PDT and around 3 µM for free TPPOH-PDT. (B) HCT116 cells were treated or not with TPPOH-X SNPs and SNPs based on nanoparticles concentration. Then, cells were exposed or not to PDT. Phototoxic effects were determined 48 h post-PDT using the MTT assay. Cell viability, expressed in percentage of each condition, was compared to controls. (C) HCT116 cells were treated or not with

free TPPOH or (D) TPPOH-X SNPs with or without NAC co-treatment and then photoactivated or not. (E) Comparison of free TPPOH and TPPOH-X SNPs on ROS generation in HCT116 cells. Intracellular ROS levels using DCFDA staining were measured 4 h post-PDT by flow cytometry. Greater right shift implied higher fluorescence intensity resulting from higher amounts of DCF formation and thus greater ROS generation. Data are shown as mean ± SEM (n = 3). **p < 0.01 and ***p < 0.001.

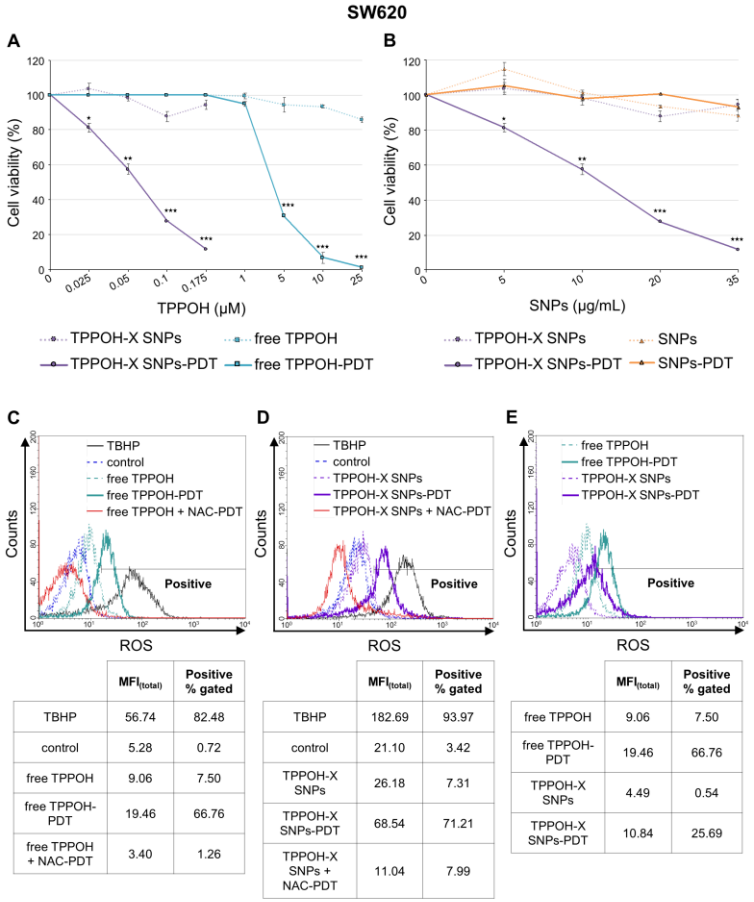

	MFI(total)	Positive % gated
TBHP	56.74	82.48
control	5.28	0.72
free TPPOH	9.06	7.50
free TPPOH-PDT	19.46	66.76
free TPPOH + NAC-PDT	3.40	1.26

	MFI(total)	Positive % gated
TBHP	182.69	93.97
control	21.10	3.42
TPPOH-X SNPs	26.18	7.31
TPPOH-X SNPs-PDT	68.54	71.21
TPPOH-X SNPs + NAC-PDT	11.04	7.99

	MFI(total)	Positive % gated
free TPPOH	9.06	7.50
free TPPOH-PDT	19.46	66.76
TPPOH-X SNPs	4.49	0.54
TPPOH-X SNPs-PDT	10.84	25.69

Figure S2: In vitro phototoxic effects of TPPOH-X SNPs-PDT and ROS production. (A) SW620 cells were treated or not with free TPPOH and TPPOH-X SNPs based on TPPOH concentration. Then, cells were exposed or not to PDT. Phototoxic effects were determined 48 h post-PDT using the MTT assay. Cell viability, expressed in percentage of each condition, was compared to controls. IC50 values were calculated of 75.4 nM for TPPOH-X SNPs-PDT and around 3 µM for free TPPOH-PDT. (B) SW620 cells were treated or not

with TPPOH-X SNPs and SNPs based on nanoparticles concentration. Then, cells were exposed or not to PDT. Phototoxic effects were determined 48 h post-PDT using the MTT assay. Cell viability, expressed in percentage of each condition, was compared to controls. (C) SW620 cells were treated or not with free TPPOH or (D) TPPOH-X SNPs with or without NAC co-treatment and then photoactivated or not. (E) Comparison of free TPPOH and TPPOH-X SNPs on ROS generation in SW620 cells. Intracellular ROS levels using DCFDA staining were measured 4 h post-PDT by flow cytometry. Greater right shift implied higher fluorescence intensity resulting from higher amounts of DCF formation and thus greater ROS generation. Data are shown as mean ± SEM (n = 3). **p < 0.01 and ***p < 0.001.

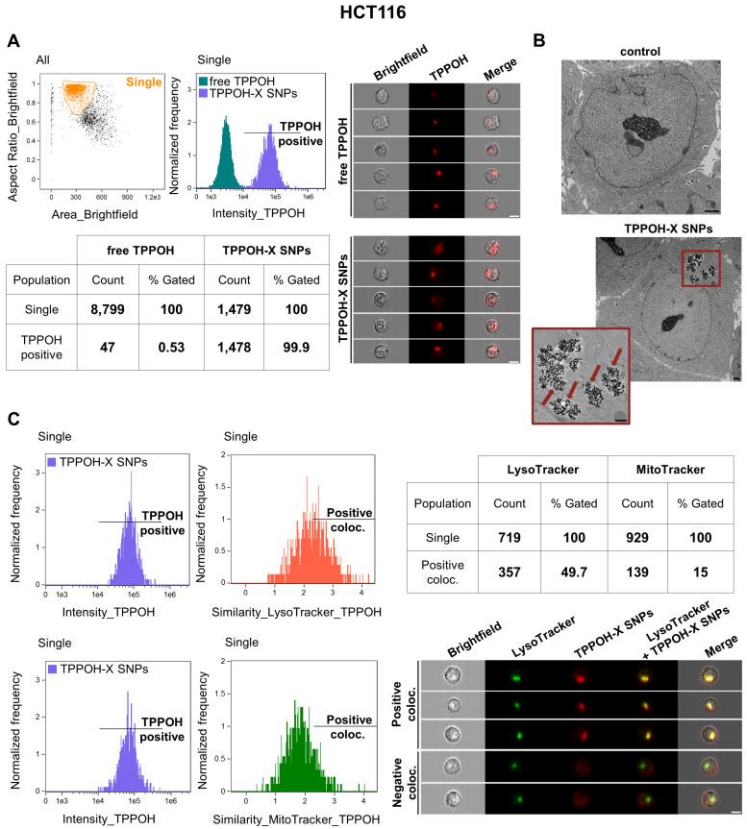

	free TPPOH		TPPOH-X SNPs	
Population	Count	% Gated	Count	% Gated
Single	8,799	100	1,479	100
TPPOH positive	47	0.53	1,478	99.9

	LysoTracker		MitoTracker	
Population	Count	% Gated	Count	% Gated
Single	719	100	929	100
Positive coloc.	357	49.7	139	15

Figure S3: Cell uptake of TPPOH-X SNPs by HCT116 cells. (A) HCT116 cells were treated with free TPPOH and TPPOH-X SNPs at 1 µM and cell uptake of these compounds was studied 24 h post-treatment by AMNIS imaging flow cytometry. The first graph highlights the size/structure of HCT116 cells. After selection of the cell population, TPPOH intensity in

HCT116 cells was shown in the second graph and in representative images. The table summarizes the amount of positive TPPOH cells relative to all cells compared to free TPPOH and TPPOH-X SNPs treatments. White scale bar = 10 µm. (B) Representative TEM images of HCT116 cells treated or not with TPPOH-X SNPs 24 h post-treatment are shown. Red arrows indicate intracellular nanoparticles. Black scale bar = 1 µm. (C) HCT116 cells were co-treated with TPPOH-X SNPs and LysoTracker or MitoTracker and co-localization was studied 24 h post-treatment by AMNIS imaging flow cytometry analysis. The first graph shows TPPOH intensity in HCT116 cells and the second graph shows similarity of TPPOH positive cells compared to LysoTracker or MitoTracker. The table summarizes the amount of TPPOH positive cells co-localized with LysoTracker or MitoTracker. Representative images of colocalization of TPPOH-X SNPs and LysoTracker in HCT116 cells are shown. White scale bar = 10 µm. Data are shown as three independent experiments.

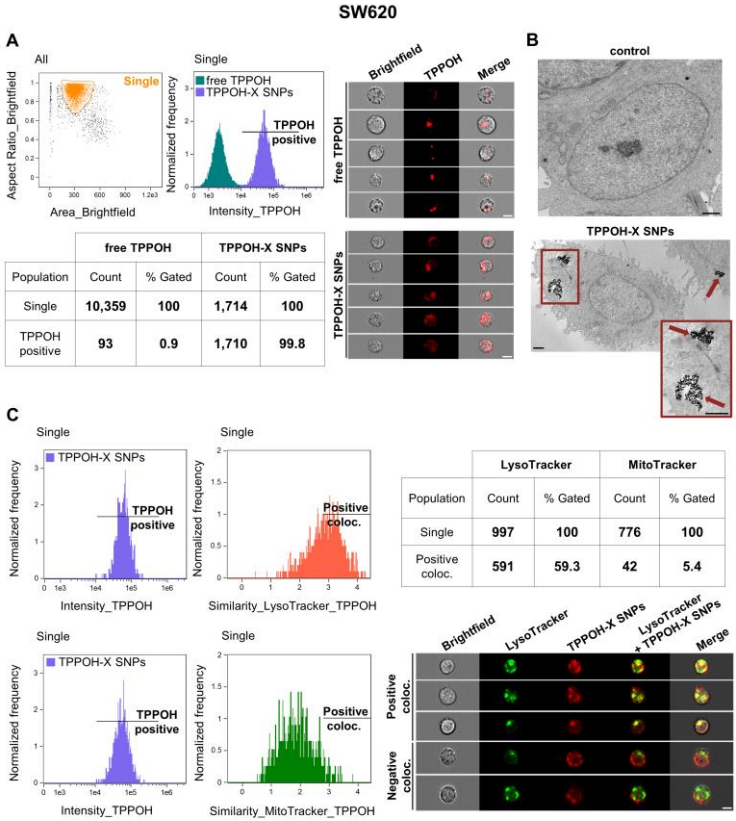

Figure S4: Cell uptake of TPPOH-X SNPs by SW620 cells. (A) SW620 cells were treated with free TPPOH and TPPOH-X SNPs at 1 µM and cell uptake of these compounds was studied 24 h post-treatment by AMNIS imaging flow

cytometry. The first graph highlights the size/structure of SW620 cells. After selection of the cell population, TPPOH intensity in SW620 cells was shown in the second graph and in representative images. The table summarizes the amount of positive TPPOH cells relative to all cells compared to free TPPOH and TPPOH-X SNPs treatments. White scale bar = 10 μm. (B) Representative TEM images of SW620 cells treated or not with TPPOH-X SNPs 24 h post-treatment are shown. Red arrows indicate intracellular nanoparticles. Black scale bar = 1 μm. (C) SW620 cells were co-treated with TPPOH-X SNPs and LysoTracker or MitoTracker and co-localization was studied 24 h post-treatment by AMNIS imaging flow cytometry analysis. The first graph shows TPPOH intensity in SW620 cells and the second graph shows similarity of TPPOH positive cells compared to LysoTracker or MitoTracker. The table summarizes the amount of TPPOH positive cells co-localized with LysoTracker or MitoTracker. Representative images of co-localization of TPPOH-X SNPs and LysoTracker in SW620 cells are shown. White scale bar = 10 μm. Data are shown as three independent experiments.

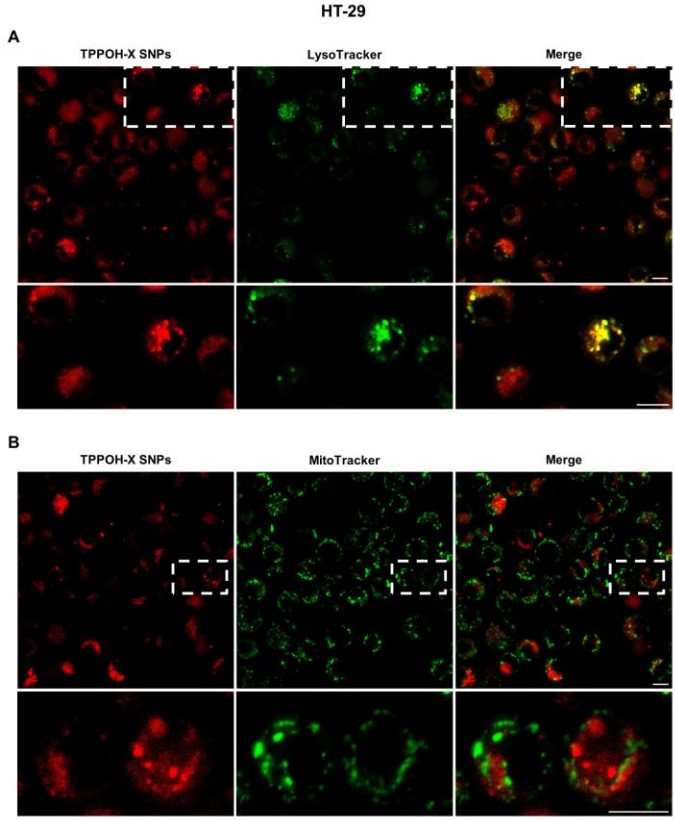

Figure S5: TPPOH-X SNPs localization in HT-29 cells. (A) HT-29 cells were co-treated with TPPOH-X SNPs and LysoTracker or (B) MitoTracker and co-

localization was studied 24 h post-treatment by confocal microscopy. Representative images of co-localization of TPPOH-X SNPs with LysoTracker or MitoTracker in HT-29 cells are shown. White scale bar = 10 μm. Data are shown as three independent experiments.

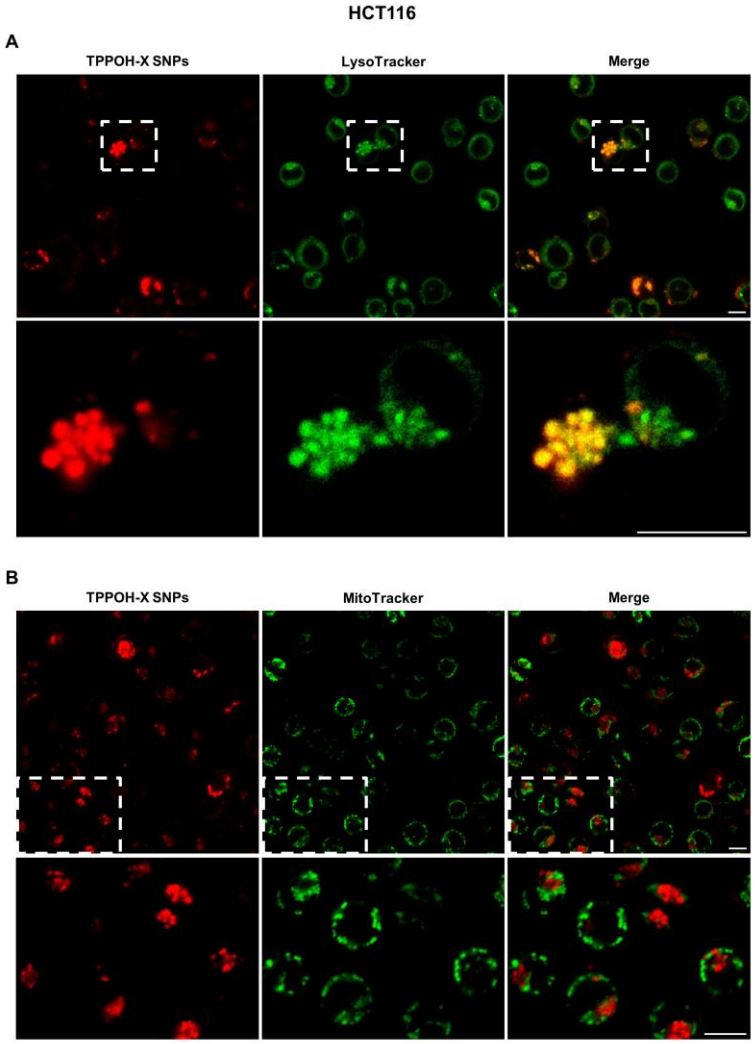

Figure S6: TPPOH-X SNPs localization in HCT116 cells. (A) HCT116 cells were co-treated with TPPOH-X SNPs and LysoTracker or (B) MitoTracker and co-localization was studied 24 h post-treatment by confocal microscopy. Representative images of co-localization of TPPOH-X SNPs with LysoTracker or MitoTracker in HCT116 cells are shown. White scale bar = 10 μm. Data are shown as three independent experiments.

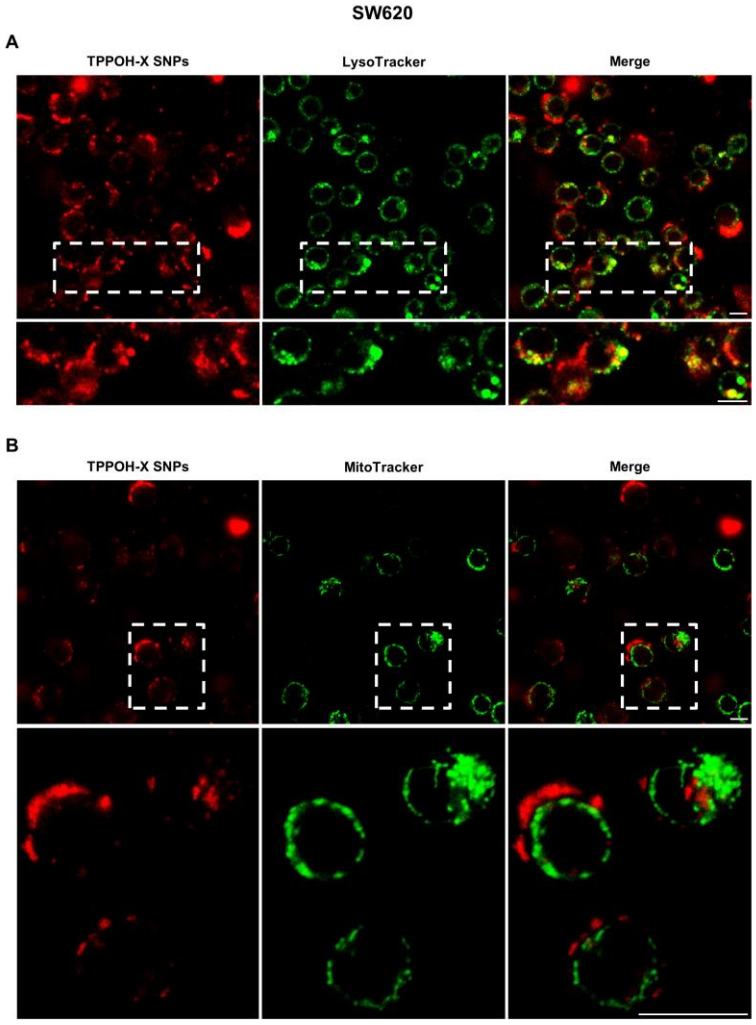

Figure S7: TPPOH-X SNPs localization in SW620 cells. (A) SW620 cells were co-treated with TPPOH-X SNPs and LysoTracker or (B) MitoTracker and co-localization was studied 24 h post-treatment by confocal microscopy. Representative images of co-localization of TPPOH-X SNPs with LysoTracker or MitoTracker in SW620 cells are shown. White scale bar = 10 μm. Data are shown as three independent experiments.

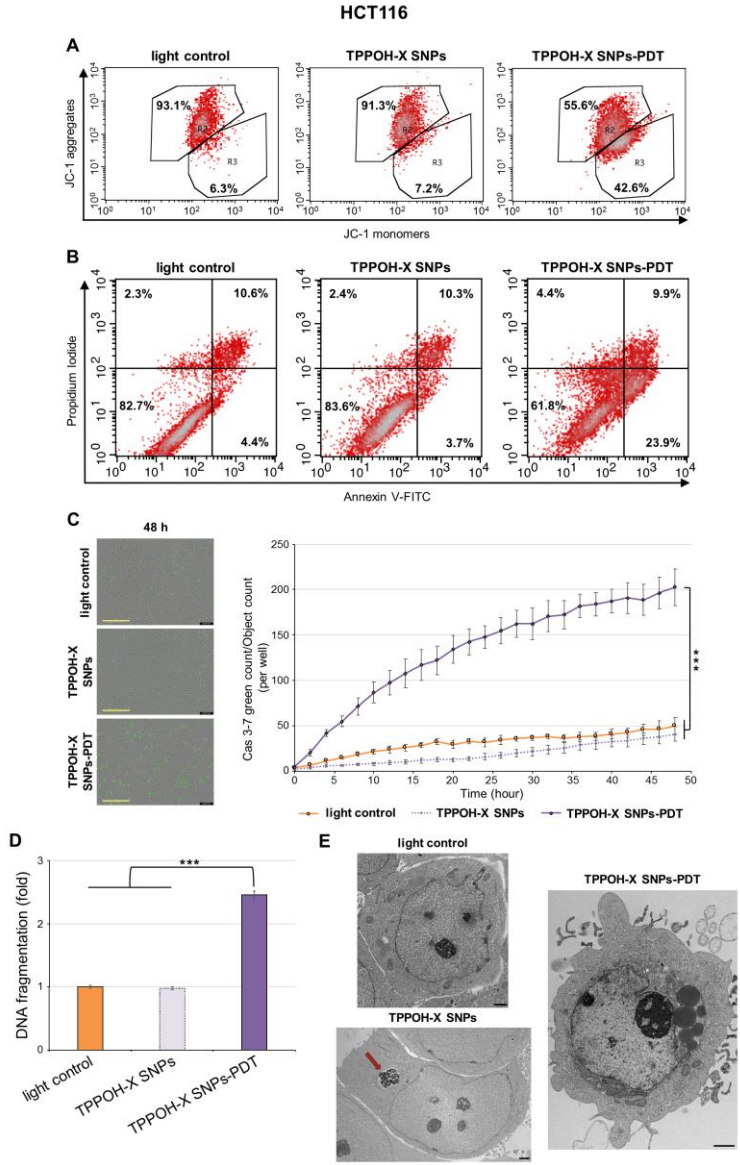

Figure S8: Effects of TPPOH-X SNPs-PDT on HCT116 cell line apoptosis. (A) HCT116 cells were treated or not with TPPOH-X SNPs and then photoactivated or not. The mitochondrial membrane potential was analyzed by flow cytometry with JC-1 at 48 h post-PDT. R2 represents the aggregate ratio and R3 the monomer ratio. (B) HCT116 cells were also stained, 48 h post-PDT, with Annexin V-FITC and PI, and apoptosis was analyzed by flow cytometry.

Upper right quadrant represents the percentage of late apoptosis, and the lower right quadrant represents early apoptosis. (C) Caspase-3/7 activity, with the same conditions in HCT116 cells, was evaluated every 2 h during 48 h post-PDT by IncuCyte imaging live cell analysis and green count/cell count/well are shown. Representative images at 48 h post-PDT are shown. Yellow scale bar = 400 μm. (D) DNA fragmentation in HCT116 cells 48 h post-PDT was quantified from cytosol extracts by ELISA. Results are reported as n-fold compared to light control. (E) Representative TEM images of HCT116 cells treated or not with TPPOH-X SNPs and photoactivated or not 48 h post-PDT were shown. Red arrows indicate intracellular nanoparticles. Black scale bar = 1 μm. Data are shown as mean ± SEM (n = 3). ***$p < 0.001$.

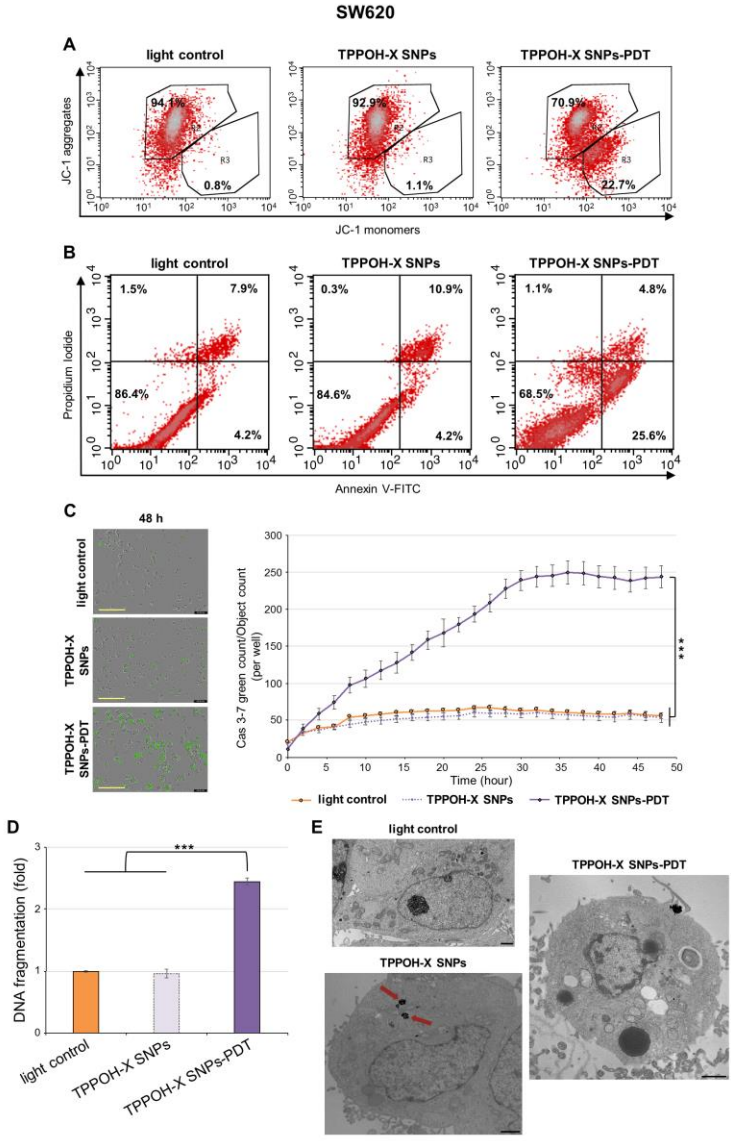

Figure S9: Effects of TPPOH-X SNPs-PDT on SW620 cell line apoptosis. (**A**) SW620 cells were treated or not with TPPOH-X SNPs and then photoactivated or not. The mitochondrial membrane potential was analyzed by flow cytometry with JC-1 at 48 h post-PDT. R2 represents the aggregate ratio and R3 the monomer ratio. (**B**) SW620 cells were also stained, 48 h post-PDT, with Annexin V-FITC and PI, and apoptosis was analyzed by flow cytometry. Upper right quadrant represents the percentage of late apoptosis, and the lower right

quadrant represents early apoptosis. (**C**) Caspase-3/7 activity, with the same conditions in SW620 cells, was evaluated every 2 h during 48 h post-PDT by IncuCyte imaging live cell analysis and green count/cell count/well are shown. Representative images at 48 h post-PDT are shown. Yellow scale bar = 400 µm. (**D**) DNA fragmentation in SW620 cells 48 h post-PDT was quantified from cytosol extracts by ELISA. Results are reported as n-fold compared to light control. (**E**) Representative TEM images of SW620 cells treated or not with TPPOH-X SNPs and photoactivated or not 48 h post-PDT were shown. Red arrows indicate intracellular nanoparticles. Black scale bar = 1 µm. Data are shown as mean ± SEM (n = 3). ***p < 0.001.

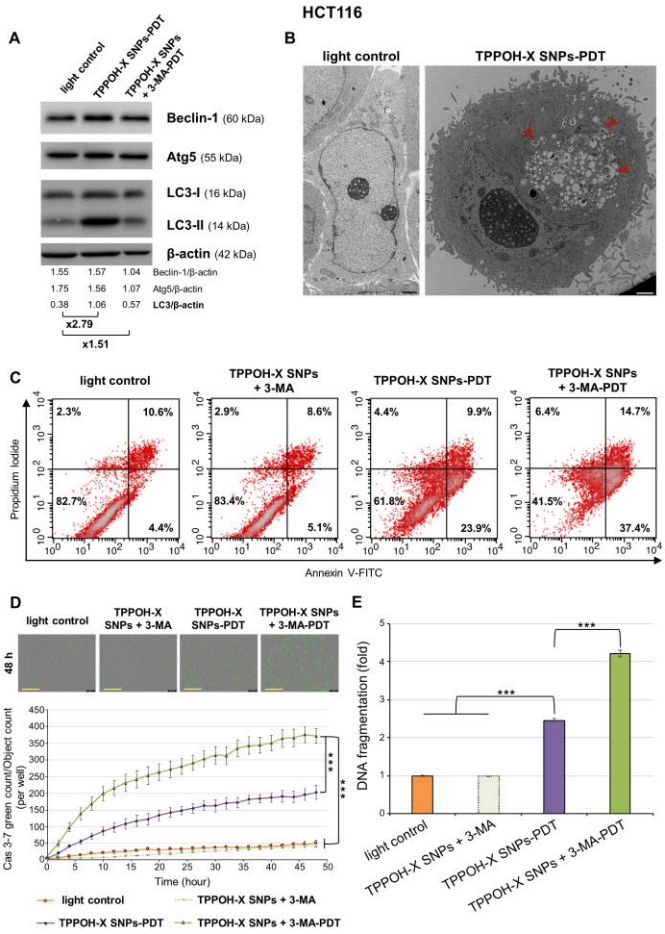

Figure S10: Effects of autophagy inhibition on HCT116 apoptosis. (**A**) HCT116 cells were treated or not with TPPOH-X SNPs in the presence or absence of 3-MA for 24 h. Expression of autophagy-related proteins was

analyzed by Western blotting 48 h post-PDT. β-actin was used as a loading control. Representative images were shown. (**B**) Representative TEM images of HCT116 cells treated or not with TPPOH-X SNPs 48 h post- PDT protocol are shown. Red arrowheads indicate autophagosomes in the treated cells. Scale bar = 1 μm. (**C**) HCT116 cells were treated or not with TPPOH-X SNPs with or without 3-MA co-treatment and then photoactivated or not. At 48 h post-PDT, cells were stained with Annexin V-FITC and PI, and apoptosis was analyzed by flow cytometry. Upper right quadrant represents the percentage of late apoptosis, and the lower right quadrant represents early apoptosis. (**D**) With the same conditions of treatment, caspase-3/7 activity was evaluated each 2 h during 48 h post-PDT protocol by IncuCyte imaging live cell analysis and green count/cell count/well were shown. Representative images at 48 h post-PDT protocol were shown. Yellow scale bar = 400 μm. (**E**) With the same conditions of treatment, DNA fragmentation was quantified from cytosol extracts with ELISA. Results were reported as n-fold compared to light control. Data are shown as mean ± SEM (n = 3). ***$p < 0.001$.

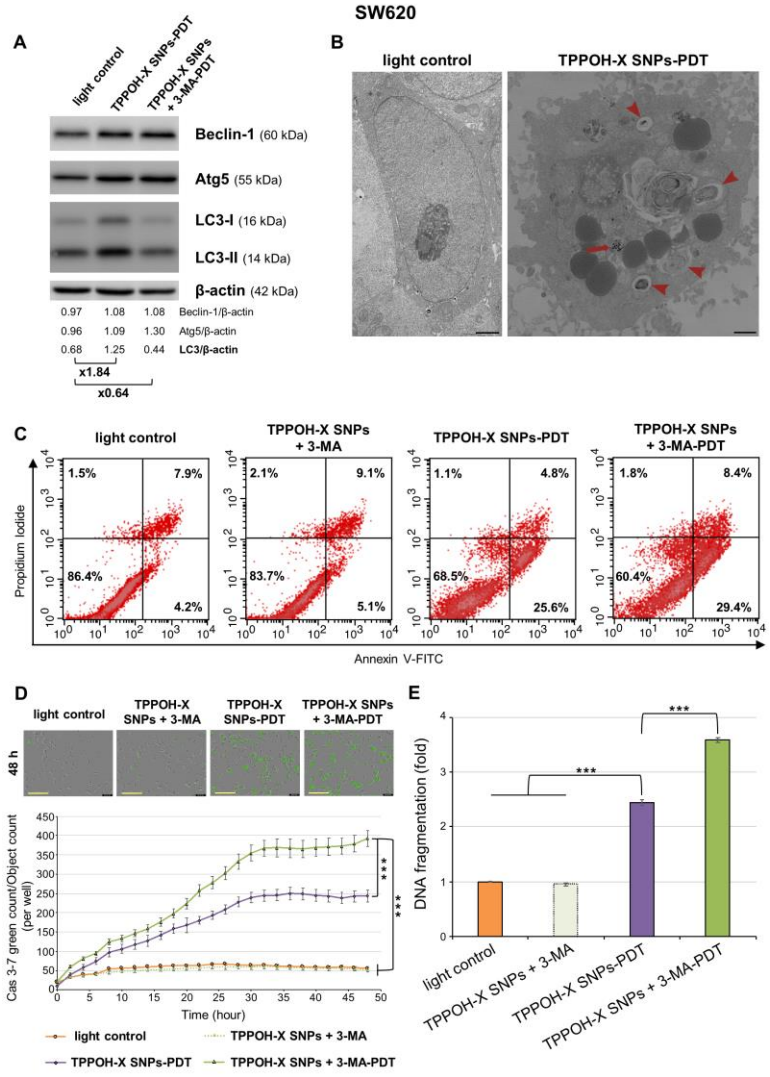

Figure S11: Effects of autophagy inhibition on SW620 apoptosis. (**A**) SW620 cells were treated or not with TPPOH-X SNPs in the presence or absence of 3-MA for 24 h. Expression of autophagy-related proteins was analyzed by Western blotting 48 h post-PDT. β-actin was used as a loading control. Representative images were shown. (**B**) Representative TEM images of SW620 cells treated or not with TPPOH-X SNPs 48 h post- PDT protocol are shown. Red arrowheads indicate autophagosomes in the treated cells. Scale bar = 1 μm. (**C**)

SW620 cells were treated or not with TPPOH-X SNPs with or without 3-MA co-treatment and then photoactivated or not. At 48 h post-PDT, cells were stained with Annexin V-FITC and PI, and apoptosis was analyzed by flow cytometry. Upper right quadrant represents the percentage of late apoptosis, and the lower right quadrant represents early apoptosis. (**D**) With the same conditions of treatment, caspase-3/7 activity was evaluated each 2 h during 48 h post-PDT protocol by IncuCyte imaging live cell analysis and green count/cell count/well were shown. Representative images at 48 h post-PDT protocol were shown. Yellow scale bar = 400 μm. (**E**) With the same conditions of treatment, DNA fragmentation was quantified from cytosol extracts with ELISA. Results were reported as n-fold compared to light control. Data are shown as mean ± SEM (n = 3). ***$p < 0.001$.

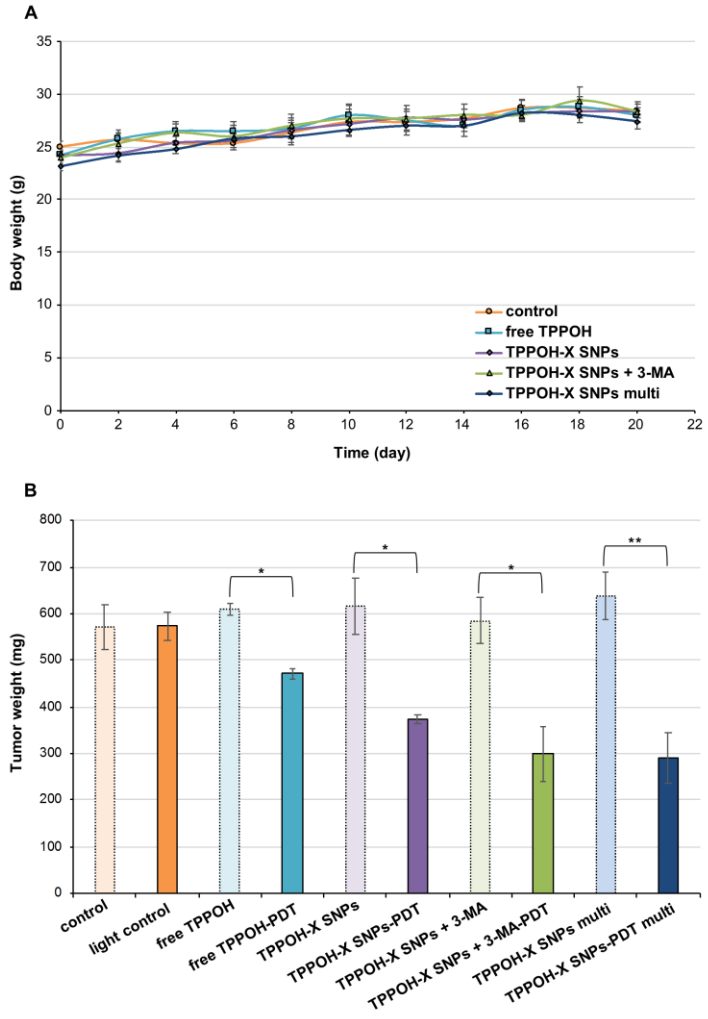

Figure S12*:* *In vivo* phototoxic effects on tumor growth. (**A**) Body weight variations of HT-29 tumor-bearing nude mice over the treatment period. (**B**) Tumor weight of the treatment groups after mice sacrifice. Data are shown as mean ± SEM (n = 5). *p < 0.05 and **p < 0.01**.**

Book Chapter

The *cis*-enhancers 3'RR and 5'Eμ are Independent Motors of IgH Locus Remodelling

Melissa Ferrad[#], Nour Ghazzaui[#], Hussein Issaoui[#], Ophélie Alyssa Martin, Jeanne Cook-Moreau, François Boyer, Sandrine Le Noir and Yves Denizot*

CNRS UMR 7276, Inserm U1262, Equipe Labellisée LIGUE 2018, Université de Limoges, France

[#]Equal contributors

***Corresponding Author:** Yves Denizot, CNRS UMR 7276, Inserm U1262, Equipe Labellisée LIGUE 2018, Université de Limoges, France

Published **July 05, 2021**

How to cite this book chapter: Melissa Ferrad, Nour Ghazzaui, Hussein Issaoui, Ophélie Alyssa Martin, Jeanne Cook-Moreau, François Boyer, Sandrine Le Noir, Yves Denizot. The *cis*-enhancers 3'RR and 5'Eμ are Independent Motors of IgH Locus Remodelling. In: Hussein Fayyad Kazan, editor. Immunology and Cancer Biology. Hyderabad, India: Vide Leaf. 2021.

Author Contributions: MF, HI, NG, FB, OAM, JCM, SLN and YD designed and performed experiments and wrote the manuscript. YD obtained financial grants.

Conflicts of Interest: Authors declare no conflict of interest.

Acknowledgements: This work was supported by grants from Ligue Contre le Cancer (Equipe labellisée LIGUE 2018) and Agence Nationale de la Recherche (ANR: projet EpiSwitch-3'RR 2016). N. Ghazzaui was supported by a grant from Association de Spécialisation et d'Orientation Scientifique (Lebanon), the municipality of Khiam (Lebanon) and the Société Française d'Hématologie. H. Issaoui is supported by a fellowship of the University of Limoges. F.B. is supported by Fondation Partenariale de l'Université de Limoges and ALURAD. We thank the genomics platform of Nice Sophia Antipolis for RNAseq experiments and the animal facility of University of Limoges for mice housing.

Abstract

B-cell development is spatially and temporally regulated with the Ig heavy chain (IgH) locus as a conductor. Starting with the first steps of B-cell development, IgH DNA remodeling constantly occurs under the control of the two *cis*-regulatory elements 5'E_μ (during early stages of B-cell development) and 3'RR (during late stages of B-cell development). These enhancers are reported to physically interact via IgH DNA loops of still unclear functional significance at the pro-B cell stage. We thus investigated if 5'E_μ and 3'RR were independent drivers of locus remodelling or if their functions were more intimately intermingled during B-cell ontogeny. RNAseq experiments reported that these two *cis*-enhancers are independent motors of IgH locus remodelling with no mutual *cis*-transcriptional interactions within the IgH locus and no *trans*-transcriptional interaction with the Ig light chain kappa (Igκ) locus. These results validate the hypothesis that the two major enhancers of the IgH locus are independent engines of locus remodelling; the activation of one does not depend on the activation of the other (and vice versa).

Keywords

IgH 3' Regulatory Region; 5'E_μ Enhancer; IgL Locus; Transcriptional Enhancer; Knock-out Mice; RAG-Deficient Mice

Introduction

By their impact on nuclear organisation, enhancers are master regulators of cell fate [1]. The immunoglobulin heavy chain (IgH) locus undergoes numerous changes throughout B-cell differentiation. Among them, transcription and accessibility for V(D)J recombination, class switch recombination (CSR) and somatic hypermutation (SHM) are the most notable [2]. The IgH locus carries two potent enhancers separated by 200 kb (Figure 1A). 5'E_μ and the 3' regulatory region (3'RR), located at both ends of the constant gene cluster, control locus remodelling during B-cell differentiation [2]. Several studies have reported long-range interactions between 5'E_μ and 3'RR enhancers during B-cell maturation [3-5]. The question of mutual transcriptional cross-talk between these two enhancer entities remains open. During B-cell development, the heavy and light chain (IgL) loci are poised for their VDJ and VJ rearrangements, respectively [2]. The IgH locus first rearranges with D-J segments at the pro-B-cell stage followed by V-DJ joining at the pre-B-cell stage. The Ig*k* locus is poised for VJ rearrangements at the pre-B cell stage. A transient association (*trans*-mediated by Igκ enhancer elements) between IgH and Ig*k* loci has been demonstrated at the pre-B cell stage [6,7]. The question of a *trans*-mediated effect of IgH enhancer elements (5'E_μ and 3'RR) on Igκ locus remains open. In this study we examined whether 5'E_μ and 3'RR enhancers were independent motors of locus remodelling or if their functions were more intimately intermingled during B-cell ontogeny. We thus developed ΔE_μ-RAG-deficient and Δ3'RR-RAG-deficient mice to investigate potential transcriptional cross-talk between 5'E_μ and 3'RR enhancers at the immature B-cell stage. We also analysed transcriptomic data in order to identify a putative *trans*-transcriptional effect beyond the Ig*k* locus in IgH enhancer-deficient mice.

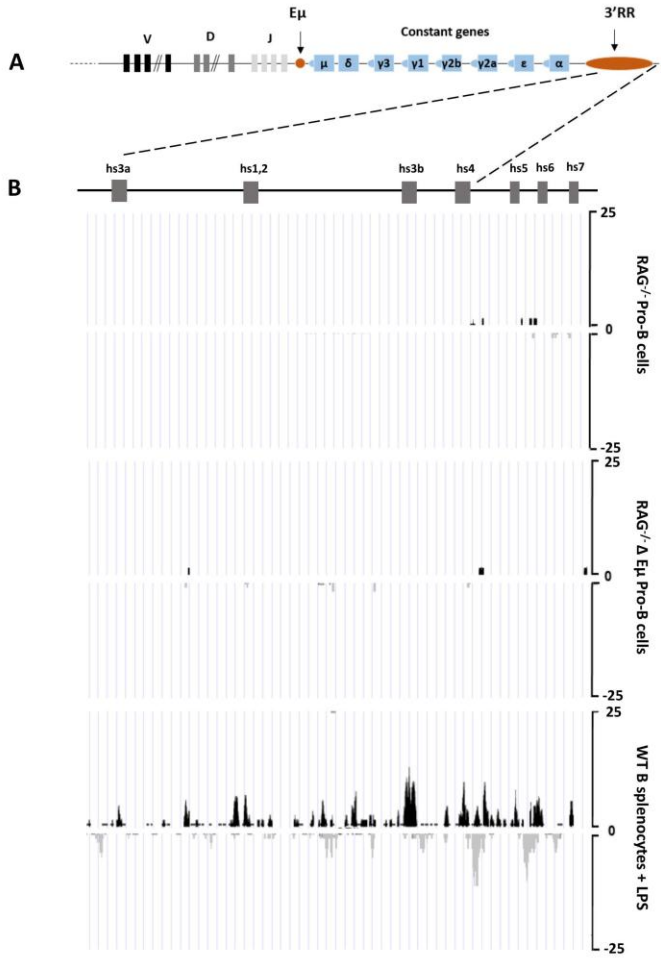

Figure 1: 3'RR eRNA in pro-B cells.
A: Schematic representation of the IgH locus (not to scale). V (variable), D (diversity), J (junctional) and C (constant) segments are located as well as the 5'E_μ element and the 3'RR. The 3'RR contains 4 transcriptional enhancers. Three of them are encompassed in a 25kb palindromic structure. B: Detection of 3'RR eRNAs. Lower panel: *Wt* B-cell splenocytes were stimulated 2 days with 5 μg/ml LPS (8-12 weeks old, males and females). RNAseq experiments were done after depletion of rRNA. One representative experiment out of two is reported with 3 mice per sample. Upper and medium panels: Pro-B cells of RAG-deficient (upper panel) and ΔEμ-RAG-deficient (medium panel) mice. One representative experiment out of two is reported with 4 to 5 mice per genotype.

Material and Methods

Mice

RAG-deficient mice (Janvier Labs, France), ΔE_{μ} [8] -RAG-deficient mice and Δ3'RR [9] -RAG-deficient mice were housed in the EOPS facility of the University of Limoges (France) and procedures were conducted in agreement with European Directive 2010/63/EU on animals used for scientific purposes. The APAFiS≠13855 projet was authorized by the French « Ministère de l'Education Nationale, de l'Enseignement Supérieur et de la Recherche ».

Cells for RNAseq Experiments

Femoral pro-B cells were recovered with the EasySep™ mouse B-cell isolation Kit (STEMCELL Technologies, France) designed to isolate B cells from single-cell suspensions by negative selection. Unwanted cells were targeted for removal with biotinylated antibodies directed against non-B cells and streptavidin-coated magnetic particles (RapidSpheres™). Labeled cells were separated using an EasySep™ magnet without the use of columns. Desired cells were collected into a new tube. Cells of RAG-deficient, ΔEμ-RAG-deficient and Δ3'RR-RAG-deficient mice (8-12 weeks old, males and females) were used. In another set of experiments, *wt* B-splenocytes were stimulated with 5μg/ml LPS for two days as a positive control of 3'RR eRNA detection.

RNAseq Experiments

Pro-B cells were obtained from 10 RAG-deficient, 10 Δ3'RR-RAG-deficient mice and 10 ΔE_{μ}-RAG-deficient mice. RNA was extracted using miRNeasy kit from QIAGEN, according to the manufacturer's instructions. Two RNA pools (five samples each) were obtained for each genotype. RNA libraries were prepared using TruSeq Stranded Total RNA with Ribo-Zero Gold (Illumina), according to the manufacturer's instructions. Libraries were sequenced on a NextSeq500 sequencer, using NextSeq 500/550 High Output Kit (Illumina). Illumina

NextSeq500 paired-end 2x150nt reads were mapped with STAR release v2.4.0a versus mm10 with a gene model from Ensembl release 77 with default parameters.10-12 RNAseq experiments were done by the genomics platform of Nice Sophia Antipolis (France). Data were deposited in Gene Expression Omnibus under the accession number GSE117449, GSE169690 and GSE169691.

Results and Discussion

Femoral pro-B cells were isolated from RAG-deficient, ΔE_{μ}-RAG-deficient and Δ3'RR-RAG-deficient mice to investigate the potential transcriptional cross-talk between 5'E_{μ} and 3'RR enhancers in immature B-cells. A schematic representation of the IgH locus is reported in Figure 1A. Non coding RNAs (ncRNAs) contribute to chromosomal looping.13 Among these ncRNAs, enhancer RNAs (eRNAs) are transcribed from DNA sequences of enhancers including the 3'RR and contribute to their enhancer function [14,15]. As a positive control of 3'RR eRNA detection, LPS-stimulated *wt* B-splenocytes were used (Figure 1B, lower panel). RNAseq experiments did not highlight any 3'RR eRNAs in pro-B cells of RAG and ΔE_{μ}-RAG-deficient mice (Figure 1B, upper and middle panel, respectively) confirming results from a previous study with specific RT-QPCR [16]. The absence of 3'RR eRNAs in pro-B cells is in agreement with studies reporting that 3'RR has no direct role on V(D)J recombination [17,18].

The 5'E_{μ} enhancer is implicated during DJ recombination [8]. A schematic representation of the variable part of the IgH locus is shown in Figure 2A. Genomic deletion of the 5'E_{μ} enhancer abrogated transcription around its location including J_H and C_{μ} transcription as well as peaks of transcription specifically found to originate from the D_{Q52} promotor ($D_{4\text{-}1}$) and the 5'E_{μ} enhancer (known as μo and I_{μ} sense transcripts, respectively) (Figure 2B, upper and middle panels). As previously reported by Braikia and coll, [16] genomic deletion of the 3'RR had no effect on both μo and I_{μ} transcripts (Figure 2B, lower panel). A small increase in D antisense transcription was found in 3'RR-deficient mice

supporting a 3'RR-mediated transcriptional DJ silencing activity as previously suggested by Braikia and coll, [16] with RT-QPCR analysis. Together with the absence of 3'RR eRNA (Figure 1B), these results strongly suggest no transcriptional interaction of the 3'RR with the 5'E_μ element that transcriptionally control DJ recombination at the pro-B cell stage.

A *trans*-mediated transcriptional effect of the Igκ locus (mediated by Igκ enhancer elements) on the IgH locus has been demonstrated at the pre-B cell stage [6,7]. We next explored the potential transcriptional cross-talk between IgH enhancers on the Igκ locus (schematized in Figure 3A) in pro-B cells. Deletion of 5'E_μ did not affect Igκ locus transcription (Figure 3B, middle panel). Deletion of 3'RR enhancers slightly affected Igκ locus sense and antisense transcription (Figure 3B, lower panel) but this effect was weak and its relevance (if any) remains obscure. In mature B-cells, deletion of 3'RR and 5'E_μ had no *trans* effect on Igκ transcription in LPS-stimulated splenocytes (Figure 3C, middle and lower panels, respectively). These results are expected since no close association between the Ig*k* and IgH loci has been reported in mature B-cells.

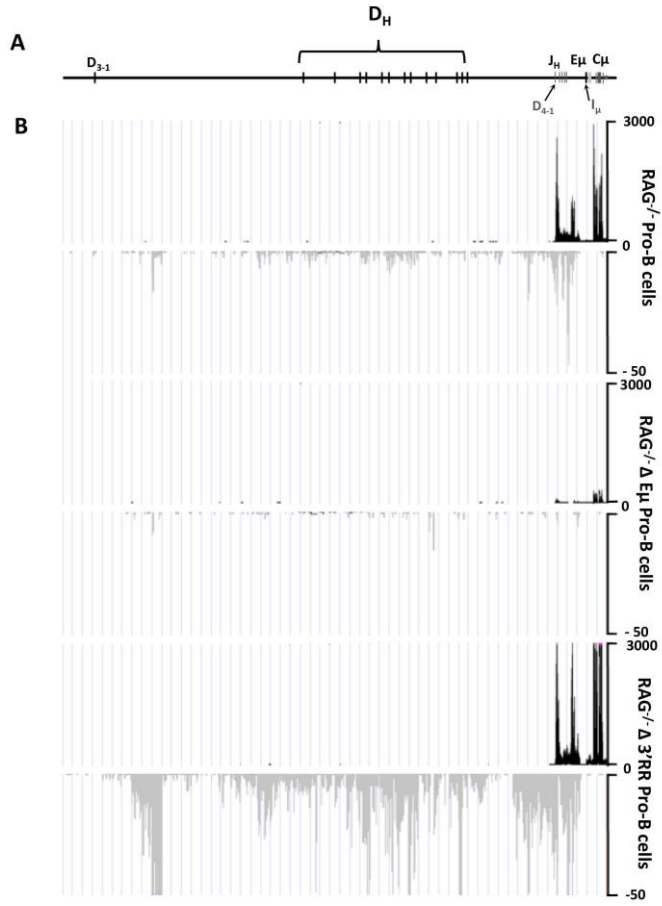

Figure 2: Influence of 5'E_μ and 3'RR deletion on pro-B cell DJ transcription. A: Schematic representation of the IgH locus (not to scale). V, D, J and C_μ segments are located as well as the 5'E_μ element and the 3'RR. B: D, J, 5'E_μ, and C_μ sense and antisense transcription in pro-B cells of RAG-deficient, ΔEμ-RAG-deficient and Δ3'RR-RAG-deficient mice. One representative experiment out of two is reported with 4 to 5 mice per genotype. Locations of D_{4-1} (also known as D_{Q52}) and I_μ promotors are indicated.

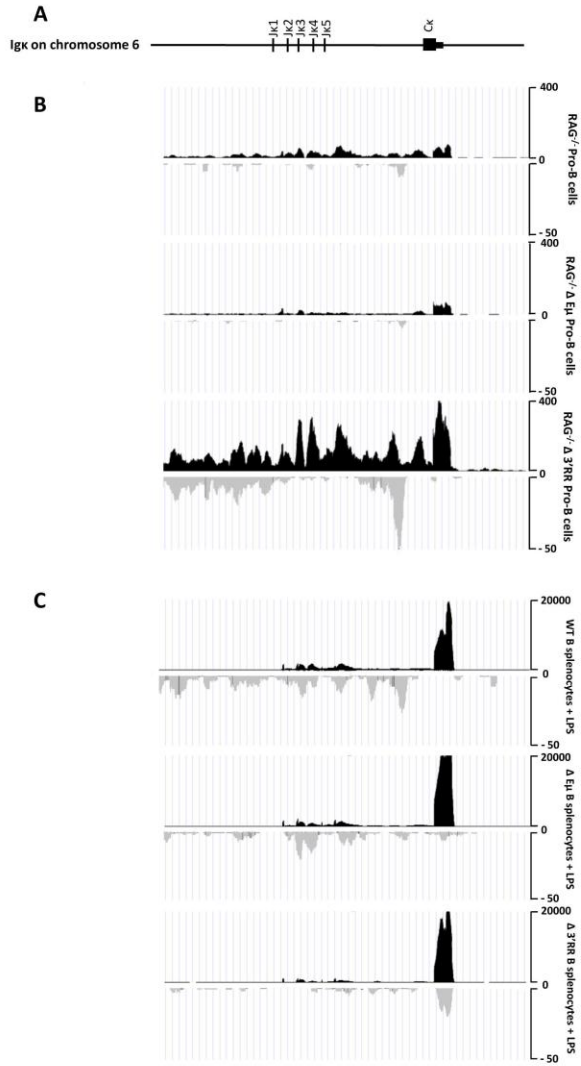

Figure 3: Influence of 5'E_μ and 3'RR deletion on Igκ transcription.
A: Schematic representation of the Igκ locus (not to scale). B: Igκ transcription in pro-B cells of RAG-deficient, ΔEμ-RAG-deficient and Δ3'RR-RAG-deficient mice. One representative experiment out of two is shown with 4 to 5 mice per genotype. C: Igκ transcription in B-cell splenocytes from *wt*, ΔEμ and Δ3'RR mice. B-cell splenocytes were stimulated 2 days with 5 μg/ml LPS (8-12 weeks old, males and female). One representative experiment out of two is shown with 3 mice per sample.

Concluding Remarks

Studies have reported the role of 5'Eμ and 3'RR enhancers during B-cell fate and maturation. Deletion of the 5'Eμ enhancer markedly lowered B-cell V(D)J recombination with no effect on SHM and CSR [8,19]. In contrast, deletion of the 3'RR enhancer affected B-cell fate, [20] SHM, [21] and CSR [9,11,12]. If studies reported the independent roles of 5'E_μ and 3'RR in B-cell maturation, few data were available concerning their synergy, cooperation and transcriptional cross-talk. This study shows that despite strong physical interactions during IgH locus DNA looping at the pro-B cell stage, [4,5] 5'E_μ and 3'RR enhancers are independent drivers of locus remodelling. Their function is not intimately intermingled and their optimal activation does not require physical contact with each other. Analysis of IgH locus transcription in 5'E_μ- and 3'RR-deficient mice reveals unilateral dependence of this pair of enhancers: 5'E_μ and 3'RR autonomously in immature B-cells and mature B-cells, respectively. These results obtained with knock-out (KO) mice are in agreement with previous results obtain with 5'E_μ-GFP, GFP-3'RR and 5'Eμ-GFP-3'RR transgenics [22-24].

References

1. Qian J, Wang Q, Dose M, Pruett N, Kieffer-Kwon KR, et al. B cell super-enhancers and regulatory clusters recruit AID tumorigenic activity. Cell. 2014; 159: 1524-1537.
2. Pinaud E, Marquet M, Fiancette R, Péron S, Vincent-Fabert C, et al. The IgH locus 3' regulatory region: pulling the strings from behind. Adv Immunol. 2011; 110: 27-70.
3. Wuerffel R, Wang L, Grigera F, Manis J, Selsing E, et al. S-S synapsis during class switch recombination is promoted by distantly located transcriptional elements and activation-induced deaminase. Immunity. 2007; 27: 711-722.
4. Medvedovic J, Ebert A, Tagoh H, Tamir IM, Schwickert TA, et al. Flexible long-range loops in the VH gene region of the IgH locus facilitate the generation of a diverse antibody repertoire. Immunity. 2013; 39: 229-244.

5. Guo C, Yoon HS, Franklin A, Jain S, Ebert A, et al. CTCF-binding elements mediate control of V(D)J recombination. Nature. 2011; 477: 424-430.
6. Xiang Y, Zhou X, Hewitt SL, Skok JA, Garrard WT. A multifunctional element in the mouse Igκ locus that specifies repertoire and Ig loci subnuclear location. J Immunol. 2011; 186: 5356-5366.
7. Hewitt SL, Farmer D, Marszalek K, Cadera E, Liang HE, et al. Association between the Igκ and Igh immunoglobulin loci mediated by the 3' Igκ enhancer induces "decontraction" of the Igh locus in pre-B cells. Nat Immunol. 2008; 9: 396-404.
8. Marquet M, Garot A, Bender S, Carrion C, Rouaud P, et al. The Eμ enhancer region influences H chain expression and B cell fate without impacting IgVH repertoire and immune response in vivo. J Immunol. 2014 ; 193: 1171-1183.
9. Vincent-Fabert C, Fiancette R, Pinaud E, Truffinet V, Cogné N, et al. Genomic deletion of the whole IgH 3' regulatory region (hs3a, hs1,2, hs3b, hs4) dramatically affects class switch recombination and Ig secretion to all isotypes. Blood. 2010; 116: 1895-1898.
10. Saintamand A, Vincent-Fabert C, Marquet M, Ghazzaui N, Magnone V, et al. Eμ and 3'RR IgH enhancers show hierarchic unilateral dependence in mature B-cells. Sci Rep. 2017; 7: 442.
11. Saintamand A, Rouaud P, Saad F, Rios G, Cogné M, et al. Elucidation of IgH 3' region regulatory role during class switch recombination via germline deletion. Nature Commun. 2015 ; 6: 7084.
12. Saintamand A, Vincent-Fabert C, Garot A, Rouaud P, Oruc Z, et al. Deciphering the importance of the palindromic architecture of the immunoglobulin heavy-chain 3' regulatory region. Nat Comm. 2016; 7: 10730.
13. Pefanis E, Wang J, Rothschild G, Lim J, Kazadi D, et al. RNA exosome-regulated long non-coding RNA transcription controls super-enhancer activity. Cell. 2015; 161: 774-789.
14. Péron S, Laffleur B, Denis-Lagache N, Cook-Moreau J, Tinguely A, et al. AID-driven deletion causes immunoglobulin heavy chain locus suicide recombination in B cells. Science. 2012; 336: 931-934.

15. Lam MT, Li W, Rosenfeld G, Glass CK. Enhancer RNAs and regulated transcriptional programs. Trends Biochem Sci. 2014; 39: 170-182.
16. Braikia FZ, Conte C, Moutahir M, Denizot Y, Cogné M, et al. Developmental switch in the transcriptional activity of a long range regulatory element. Mol Cell Biol. 2015; 35: 3370-3380.
17. Rouaud P, Vincent-Fabert C, Fiancette R, Cogné M, Pinaud E, et al. Enhancers located in heavy chain regulatory region (hs3a, hs1,2, hs3b and hs4) are dispensable for diversity of VDJ recombination. J Biol Chem. 2012; 287: 8356-8360.
18. Ghazzaui N, Issaoui H, Saintamand A, Oblet C, Carrion C, et al. The immunoglobulin heavy chain 3' regulatory region super-enhancer controls mouse B1 B-cell fate and late VDJ repertoire diversity. Blood Adv. 2018; 2: 252-262.
19. Perlot T, Alt FW, Bassing CH, Suh H, Pinaud E. Elucidation of IgH introninc enhancer functions via germ-line deletion. Proc Natl Acad Sci USA. 2005; 102: 14362-14367.
20. Saintamand A, Rouaud P, Garot A, Saad F, Carrion C, et al. The IgH 3' regulatory region governs μ chain transcription in mature B lymphocytes and the B cell fate. Oncotarget. 2015; 6: 4845-4852.
21. Rouaud P, Vincent-Fabert C, Saintamand A, Fiancette R, Marquet M, et al. The IgH 3' regulatory region controls AID-induced somatic hypermutation in germinal centre B-cells in mice. J Exp Med. 2013; 210: 1501-1507.
22. Guglielmi L, Le Bert M, Truffinet V, Cogné M, Denizot Y. Insulators to improve expression of a 3'IgH LCR-driven reporter gene in transgenic mouse models. Biochem Biophys Res Commun. 2003; 307: 466-471.
23. Guglielmi L, Le Bert M, Comte I, Dessain ML, Drouet M, et al. Combination of 3' and 5' IgH regulatory elements mimics the B-specific endogenous expression pattern of IgH genes from pro-B cells to mature B cells in a transgenic mouse model. Biochim Biophys Acta. 2003; 1642: 181-190.
24. Guglielmi L, Truffinet V, Carrion C, Le Bert M, Cogné N, et al. The 5'HS4 insulator element is an efficient tool to analyse the transient expression of an Em-GFP vector in a transgenic mouse model. Transgenic Res. 2005; 14: 361-364.

Book Chapter

Identification of Acute Myeloid Leukemia Bone Marrow Circulating MicroRNAs

Douâa Moussa Agha[1†], Redouane Rouas[1†], Mehdi Najar[2,3], Fatima Bouhtit[1,3], Najib Naamane[4], Hussein Fayyad-Kazan[1], Dominique Bron[1], Nathalie Meuleman[5], Philippe Lewalle[1] and Makram Merimi[1,3]*

[1]Laboratory of Experimental Hematology, Department of Haematology, Jules Bordet Institute, Université Libre de Bruxelles, Belgium
[2]Osteoarthritis Research Unit, University of Montreal Hospital Research Center (CRCHUM), Department of Medicine, University of Montreal, Canada
[3]Genetics and Immune Cell Therapy Unit, Faculty of Sciences, University Mohammed Premier, Morocco
[4]Translational and Clinical Research Institute, Newcastle University, UK
[5]Laboratory of Clinical Cell Therapy, Jules Bordet Institute, Université Libre de Bruxelles, Belgium

[†]These authors contributed equally to this work.

***Corresponding Author:** Makram Merimi, Laboratory of Experimental Hematology, Department of Haematology, Jules Bordet Institute, Université Libre de Bruxelles, 1000 Brussels, Belgium

Published **June 16, 2021**

This Book Chapter is a republication of an article published by Makram Merimi, et al. at International Journal of Molecular Sciences in September 2020. (Moussa Agha, D.; Rouas, R.; Najar, M.; Bouhtit, F.; Naamane, N.; Fayyad-Kazan, H.; Bron, D.; Meuleman, N.; Lewalle, P.; Merimi, M. Identification of Acute Myeloid Leukemia Bone Marrow Circulating

MicroRNAs. Int. J. Mol. Sci. 2020, 21, 7065. https://doi.org/10.3390/ijms21197065)

How to cite this book chapter: Douâa Moussa Agha, Redouane Rouas, Mehdi Najar, Fatima Bouhtit, Najib Naamane, Hussein Fayyad-Kazan, Dominique Bron, Nathalie Meuleman, Philippe Lewalle, Makram Merimi. Identification of Acute Myeloid Leukemia Bone Marrow Circulating MicroRNAs. In: Hussein Fayyad Kazan, editor. Immunology and Cancer Biology. Hyderabad, India: Vide Leaf. 2021.

Author Contributions: Conceptualization, D.M.A., R.R., M.N., PL and M.M.; investigation, D.M.A., R.R., M.N., N.N., H.F.K, and F.B.; resources, P.L., and M.M.; writing-original/draft preparation, D.M.A., M.N., N.N., H.F.K, F.B. and M.M.; review and editing, D.M.A., M.N., and M.M.; supervision, M.M.; project administration, D.B., N.M., P.L., and M.M.; funding acquisition, PL and M.M.

Funding: This work was supported by Les Amis de l'Institut Bordet, Le Fonds National de la Recherche Scientifique (FNRS, Télévie).

Conflicts of Interest: The authors have no conflicts of interest to declare. They confirm that there are no conflicts of interest associated with this publication. The manuscript has been read and approved by all named authors.

Abstract

Background: In addition to their roles in different biological processes, microRNAs in the tumor microenvironment appear to be potential diagnostic and prognostic biomarkers for various malignant diseases, including acute myeloid leukemia (AML).

To date, no screening of circulating miRNAs has been carried out in the bone marrow compartment of AML. Accordingly, we investigated the circulating miRNA profile in AML bone marrow at diagnosis (AMLD) and first complete remission post treatment (AMLPT) in comparison to healthy donors (HD).

Methods: Circulating miRNAs were isolated from AML bone marrow aspirations, and a low-density TaqMan miRNA array was performed to identify deregulated miRNAs followed by quantitative RT-PCR to validate the results. Bioinformatic analysis was conducted to evaluate the diagnostic and prognostic accuracy of the highly and significantly identified deregulated miRNA(s) as potential candidate biomarker(s).

Results: We found several deregulated miRNAs between the AMLD vs HD vs AMLPT groups, which were involved in tumor progression and immune suppression pathways. We also identified significant diagnostic and prognostic signatures with the ability to predict AML patient treatment response.

Conclusions: This study provides a possible role of enriched circulating bone marrow miRNAs in the initiation and progression of AML and highlights new markers for prognosis and treatment monitoring.

Keywords

Acute Myeloid Leukemia; Bone Marrow; Biomarkers; Circulating microRNAs; Oncogene; Tumor Suppressor; Immune Regulation; Tumor Microenvironment

Introduction

Acute myeloid leukemia (AML) is a common myelogenous malignancy in adults that is often characterized by disease relapse. It is caused by the acquisition of cytogenetic and molecular abnormalities by a hematopoietic stem cell, which transforms it into a leukemic stem cell that self-renews and proliferates [1]. Although many researchers are interested in improving our understanding of AML disease evolution [2], its pathogenesis, resistance to treatments and escape from immune

surveillance have not yet been fully elucidated [3]. Despite recent advances in understanding the molecular basis of this cancer, allowing the development of target-specific therapies, more than 50% of patients with AML relapse and die [4]. They develop resistance to treatment caused by different genetic and immunosuppressive mechanisms. These mechanisms include changes in the expression levels of both intracellular and circulating microRNAs (miRNAs) [3,5–7]. Moreover, AML has been proven to be a heterogeneous disease, and to date, the cytogenetic classification fails to predict the clinical outcome for a large group of patients and therefore fails to guide the continuation of treatment in almost one-third of the patients [8]. The prognostic factors currently used remain unsatisfactory, and it is necessary to explore new biomarkers for the diagnosis, prognosis, and therapeutic targets of AML to develop more effective surveillance and treatment programs [3].

Small (19- to 22-nucleotide long) noncoding RNAs called microRNAs are crucial for the posttranscriptional regulation of gene expression. They play an integral role in numerous biological processes, including the immune response, cell-cycle control, metabolism, stem cell self-renewal and differentiation [9]. Aberrant miRNA expression is associated with many diseases, including cancer, and miRNA-based drugs represent a novel and potentially powerful therapeutic approach [10,11,12]. Several studies have proposed using miRNAs as biomarkers for diagnosis, prediction and prognosis in cancer diseases, including AML [13,14]. Extracellular miRNAs, namely, those circulating in peripheral blood, seem to be attracting increasing attention from researchers. Given the ease with which miRNAs can be isolated and their structural stability under different conditions of treatment and sample isolation, they are also proposed as diagnostic, prognostic or predictive biomarkers in several cancers [15,16].

In AML, peripheral blood circulating miRNAs have been detected and could be useful as noninvasive biomarkers for the detection of leukemia at the time of diagnosis and prognosis [3,7,14,17]. In our laboratory, we previously identified eight plasma miRs differentially expressed between healthy donors and AML patients, showing that miR-150 and miR-342 are

downregulated in the plasma of AML patients at diagnosis, and their expression levels in complete remission AML patients resembled those in healthy controls [18]. Zhi et al. performed an analysis using AML serum samples and showed a significant increase in six miRNAs (miR-10a-5p, miR-93-5p, miR-129-5p, miR-155-5p, miR-181b-5p and miR-320d) [19]. The level of miR-181b-5p in serum, on the other hand, is significantly associated with an increased survival rate [19]. Yan J. and his team have shown that miR-217, a tumor suppressor, [17] is deregulated in patients with AML and more importantly in patients with low genetic risk. Other circulating miRNAs also seem of great interest for AML prognosis, namely, miR-210, whose deregulation was observed in patients in complete remission (CR) [20]. Patients expressing miR-210 have a significantly worse overall survival (OS), and those with weak expression of miR-328 have a shorter OS [20,21]. A significantly reduced expression of miR-638 has been shown in AML patients and increased in CR [22]. Another study carried out by Tian C et al. showed that the plasma expression of miR-192 is also increased in AML patients with favorable cytogenetic risk and high OS [23].

Several studies have focused on the profile of peripheral blood circulating miRNAs in acute myeloblastic leukemia. To date, no study has been published on miRNAs in the main microenvironment of AML development, namely, the bone marrow. It remains unknown how miRNAs released in the bone marrow niche in which AML arises are subverted to support leukemic cells and protect them from immunosurveillance. The contribution of the tumor microenvironment (TME) to the survival, spread, and relapse of AML in the bone marrow is crucial in the development, progression, immune response escape, and therapy failure in leukemia. Therefore, the aim of this study was to investigate, for the first time, whether circulating miRNAs display differential expression profiles in the bone marrow of AML patients at diagnosis and first complete remission after treatment in comparison with healthy donors. Such screening will highlight the crucial role of enriched circulating bone marrow miRNAs in AML diagnosis and prognosis and their impact on both disease progression and response to treatment.

Results

Bone Marrow Circulating miRNAs Expression Profile in Newly Diagnosed AML Patients

A few studies have focused on circulating peripheral blood miRNAs, but at this time, no studies have characterized them in the principal compartment of AML disease, namely, the bone marrow. We detected miRNA expression in bone marrow body fluid of AML patients at diagnosis (AMLD) (n = 27), and we compared their profile to that in healthy donors (HD) (n = 11). Moreover, miRNAs with a Ct value > 35 in either the AML group or the control group were excluded from further analysis. Differentially expressed (DE) miRNAs between AMLD and HD samples, of which 61 were upregulated and 37 were downregulated, were identified with a threshold of $p < 0.05$ and a 1,5-fold change (Table 1).

Table 1: Bone marrow circulating miRNAs differentially expressed in AML newly diagnosed compared to healthy donors.

Up regulated miRNAs in AMLD v.s. HD		
MiR Connotation	***p* Value**	**FC AMLD1 v.s. HD**
hsa-miR-520a-3p	0.0000004	103.59
hsa-miR-548b-5p	0.0000187	15.35
hsa-miR-651	0.0007066	13.01
hsa-miR-449b	0.0029965	7.84
hsa-miR-520f	0.0012403	7.19
hsa-miR-330-5p	0.0476803	6.55
hsa-miR-34c-5p	0.0300460	5.10
hsa-miR-9	0.0030388	15.45
hsa-miR-34a	0.0008391	14.22
hsa-miR-548d-5p	0.0000390	13.09
hsa-miR-655	0.0061917	8.55
hsa-miR-548c-5p	0.0002937	7.99
hsa-miR-135a	0.0225966	6.95
hsa-miR-502-5p	0.0028352	6.68
hsa-miR-576-3p	0.0008681	5.99
hsa-miR-449a	0.0003304	5.97
hsa-miR-518f	0.0015237	5.88
hsa-miR-21	0.0000118	5.61
hsa-miR-629	0.0000000	5.60
hsa-miR-195	0.0000050	5.32
hsa-miR-517c	0.0011033	5.02

hsa-miR-597	0.0026663	4.94
hsa-miR-199b-5p	0.0421635	4.85
hsa-miR-548d-3p	0.0203888	4.76
hsa-miR-181a	0.0039392	4.76
hsa-miR-570	0.0180477	4.75
hsa-miR-660	0.0000101	4.56
hsa-miR-202	0.0100613	4.24
hsa-miR-24	0.0225184	4.24
hsa-miR-375	0.0016871	4.18
hsa-miR-130b	0.0000115	3.81
hsa-miR-361-5p	0.0020377	3.65
hsa-miR-451	0.0019980	3.58
hsa-miR-181c	0.0131902	3.49
hsa-miR-579	0.0002417	3.49
hsa-miR-362-3p	0.0106066	3.22
hsa-miR-25	0.0005764	3.15
hsa-miR-29c	0.0095014	3.00
hsa-miR-511	0.0103669	2.90
hsa-miR-146b-3p	0.0096730	2.88
hsa-miR-532-5p	0.0014276	2.70
hsa-miR-106a	0.0012818	2.62
hsa-miR-874	0.0089434	2.61
hsa-miR-212	0.0012351	2.50
hsa-miR-598	0.0046231	2.48
hsa-miR-221	0.0144840	2.47
hsa-miR-18a	0.0052162	2.46
hsa-miR-27a	0.0160879	2.45
hsa-miR-590-5p	0.0015733	2.40
hsa-miR-20b	0.0471303	2.36
hsa-miR-101	0.0162702	2.23
hsa-miR-146a	0.0174218	2.22
hsa-miR-142-3p	0.0246946	2.21
hsa-miR-146b-5p	0.0305051	2.14
hsa-miR-93	0.0175670	1.97
hsa-miR-140-5p	0.0362266	1.96
hsa-miR-18b	0.0224577	1.90
hsa-miR-423-5p	0.0088564	1.87
hsa-miR-92a	0.0443479	1.71
hsa-miR-210	0.0429423	1.68
hsa-miR-483-5p	0.0423541	1.62
Downregulated miRNAs in AMLD vs HD		
MiR Connotation	***p* Value**	**FC AMLD1 vs HD**
hsa-miR-326	0.00663326	0.103
hsa-miR-198	0.00282623	0.078
hsa-miR-518d-3p	0.00001285	0.018
hsa-miR-107	0.00000130	0.012
hsa-miR-215	0.00082673	0.009

hsa-miR-504	0.00000004	0.006
hsa-miR-890	0.00000995	0.001
hsa-miR-448	0.00007498	0.001
hsa-miR-532-3p	0.05245365	0.616
hsa-miR-342-3p	0.04884326	0.602
hsa-miR-200c	0.04994680	0.547
hsa-miR-491-5p	0.01187570	0.543
hsa-miR-28-3p	0.00718598	0.531
hsa-miR-99b	0.00686813	0.444
hsa-miR-574-3p	0.01232231	0.432
hsa-miR-744	0.00082444	0.358
hsa-miR-190	0.05420973	0.353
hsa-miR-150	0.00317263	0.322
hsa-miR-197	0.00005892	0.270
hsa-miR-125a-5p	0.00614751	0.262
hsa-miR-203	0.02014882	0.258
hsa-miR-891a	0.02627127	0.248
hsa-miR-485-3p	0.05481495	0.247
hsa-miR-489	0.00938728	0.245
hsa-miR-204	0.00027158	0.207
hsa-miR-193b	0.00487572	0.203
hsa-miR-184	0.01694239	0.203
hsa-miR-484	0.00012474	0.173
hsa-miR-618	0.03435969	0.152
hsa-miR-134	0.01390311	0.145
hsa-miR-433	0.04689247	0.135
hsa-miR-145	0.00000042	0.120
hsa-miR-149	0.02704296	0.119
hsa-miR-328	0.00004261	0.105
hsa-miR-654-5p	0.03086797	0.079
hsa-miR-365	0.00000686	0.066
hsa-miR-518b	0.00169071	0.063

The clustering of the pretreated AML patients and HD based on the highly significant DE miRNAs (21 up and 18 down $p < 0.005$ and 2 FC) showed a high separation between the two groups (Figure 1A,B). Interestingly, 16 of these DE miRNAs were undetectable or expressed at very low levels in one of the two groups (miR-520a-3p, miR-548d, miR-449b, miR-49-3p, miR-520f, miR-330-5p, and miR-34c-5p in HD patients and miR-326, miR-198, miR-miR-518d, miR-107, miR-215, miR-504, miR-890, and miR-448 in AML), suggesting their important role in the progression of AML disease.

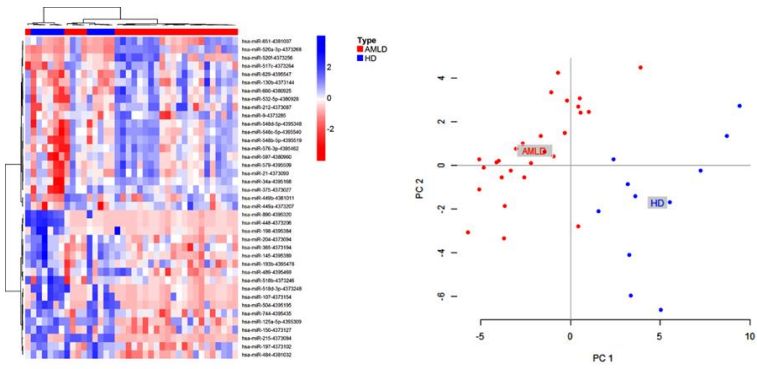

A B

Figure 1: Differentially expressed bone marrow circulating miRNAs in newly diagnosed AML patients compared to healthy donors. (**A**) Hierarchical clustering and heatmap of microRNA (miRNA) expression profile in acute myeloid leukemia (AML) (n = 27) versus healthy donors (n = 11). The list of miRNAs was filtered with a p-value < 0.005 and fold change ≤ 0,5 or ≥ 2. A total of 39 miRNAs (21 up- and 18 downregulated) were significant differentially expressed. The color key indicates centred and standardized miRNA expression levels (Z-scores). Upper color bar labels samples by baseline diagnosis. (**B**) Principal Component Analysis (PCA) showing the grouping of AML patients (red) and HD (blue) based on the 39 DEmiRNAs profile.

To validate our data analysis, the levels of the top 46 differentially expressed miRNAs with very high statistical significance were quantified by RT-qPCR in a second independent cohort including 15 AML patient bone marrow aspiration samples. The results showed that 30 of the 46 miRNAs tested and identified as DE in the first cohort were confirmed in the second cohort (Table 2), while 14 were also DE in the same way as in the first cohort but were statistically insignificant. Only two miRNAs out of the 46 tested showed a different profile between the first and second cohorts, suggesting the need to increase the number of patients in our second cohort.

Table 2: Confirmed differentially expressed microRNAs between AML patients and HD in a second cohort.

MiRNAs connotation	*p* value AMLD1	FC AMLD1	*p* value AMLD2	FC AMLD2	*p* value AMLDtotal	FC. AMLD total
hsa-miR-520a-3p	4.08 10^{-07}	103.58	0.016	3.724	9.22 10^{-05}	31.587
hsa-miR-9	0.003	15.451	3.20 10^{-05}	41.678	0.0002	22.022
hsa-miR-548b-5p	1.87 10^{-05}	15.354	0.22	2.003	0.0026	7.418
hsa-miR-34a	0.0008	14.221	0.006	13.443	6.19 10^{-05}	13.938
hsa-miR-548d-5p	3.89 10^{-05}	13.091	0.021	5.268	7.85 10^{-05}	9.458
hsa-miR-651	0.0007	13.011	0.004	7.129	0.0006	10.496
hsa-miR-548c-5p	0.0002	7.993	0.150	1.961	0.0031	4.839
hsa-miR-449b	0.0029	7.843	0.007	6.301	0.0019	7.253
hsa-miR-520f	0.0012	7.190	0.001	3.562	0.0011	5.594
hsa-miR-502-5p	0.0028	6.676	0.132	2.898	0.0109	4.955
hsa-miR-576-3p	0.0008	5.989	2.11 10^{-05}	8.364	2.68 10^{-05}	6.748
hsa-miR-449a	0.0003	5.972	0.078	2.814	0.0021	4.565
hsa-miR-21	1.17 10^{-05}	5.611	1.76 10^{-07}	8.913	8.07 10^{-08}	6.619
hsa-miR-629	2.98 10^{-08}	5.600	2.23 10-^{07}	3.693	3.41 10^{-09}	4.826
hsa-miR-195	5.006 10^{-06}	5.315	0.20	1.546	0.002	3.419
hsa-miR-517c	0.0011	5.019	0.35	1.264	0.020	3.068
hsa-miR-597	0.0026	4.941	0.0008	8.215	0.0001	5.925
hsa-miR-181a	0.0039	4.760	0.0161	2.755	0.0044	3.916
hsa-miR-660	1.00 10^{-05}	4.558	0.0590	1.536	0.0003	3.091
hsa-miR-375	0.001	4.177	0.0009	9.544	0.0001	5.611
hsa-miR-130b	1.14 10^{-05}	3.815	0.1794	1.766	0.0077	2.897
hsa-miR-361-5p	0.002	3.651	0.0168	1.920	0.0025	2.902
hsa-miR-451	0.0019	3.584	0.0128	2.659	0.0016	3.221
hsa-miR-579	0.0002	3.487	0.0290	1.927	0.0006	2.821
hsa-miR-25	0.0005	3.154	5.15 10^{-05}	4.060	2.71 10^{-05}	3.451
hsa-miR-106a	0.0012	2.616	0.07	1.558	0.0050	2.174
hsa-miR-212	0.0012	2.501	0.49	1.003	0.0251	1.805
hsa-miR-598	0.0046	2.482	0.24	1.346	0.0280	1.994
hsa-miR-18a	0.0052	2.459	0.0008	3.101	0.0011	2.671
hsa-miR-744	0.0008	0.358	3.03 10^{-05}	0.201	8.80 10^{-05}	0.291
hsa-miR-150	0.0031	0.322	1.10 10^{-05}	0.116	0.0001	0.223
hsa-miR-197	5.8910-05	0.270	0.19	0.734	0.0041	0.386
hsa-miR-204	0.0002	0.207	1.39 10^{-05}	0.113	8.73 10^{-06}	0.167
hsa-miR-193b	0.0048	0.203	9.67 10^{-07}	0.052	0.0001	0.125
hsa-miR-484	0.0001	0.173	0.11	0.552	0.0023	0.262
hsa-miR-145	4.21 10^{-07}	0.120	4.47 10^{-06}	0.112	3.11 10^{-09}	0.117
hsa-miR-328	4.26 10^{-05}	0.105	0.42	1.135	0.014	0.245
hsa-miR-198	0.0028	0.078	0.22	0.409	0.013	0.141
hsa-miR-365	6.86 10^{-06}	0.066	0.0005	0.132	3.58 10^{-06}	0.084
hsa-miR-518b	0.001	0.063	4.28 10^{-05}	0.007	5.05 10^{-05}	0.028
hsa-miR-518d-3p	1.28 10^{-05}	0.018	0.37	0.656	0.005	0.066
hsa-miR-107	1.30 10^{-06}	0.012	0.11	0.174	0.0004	0.031
hsa-miR-215	0.0008	0.009	0.06	0.083	0.0024	0.019
hsa-miR-504	3.50 10^{-08}	0.006	5.70 10^{-06}	0.012	1.70 10^{-10}	0.008
hsa-miR-890	9.94 10^{-06}	0.001	0.0001	0.001	9.74 10^{-08}	0.001
hsa-miR-448	7.49 10^{-05}	0.001	0.0007	0.001	1.63 10^{-06}	0.001

The 46 miRNAs identified in the first cohort were confirmed in a second cohort. The list of miRNAs from first cohort was filtered with a p-value < 0.005 and fold change ≤ 0.5 or ≥ 2.0. FC: fold change.

Our results permit us to establish an AML bone marrow circulating miRNA signature consisting of downregulated miR-448, miR-890, miR-504, miR-145, and miR-365 (Figure 2A) and upregulated miR-9, miR-21, miR-629 and miR-449b (Figure 2 B), with highly significant AUCs (Figure 2C) and highly differentially expressed fold changes (p-value < 0,005; FC > 2). The combination of these miRNAs has diagnostic value, enabling the identification of AML with high sensitivity and specificity (AUC = 0.98; p-value < 0,0001) (Figure 2D).

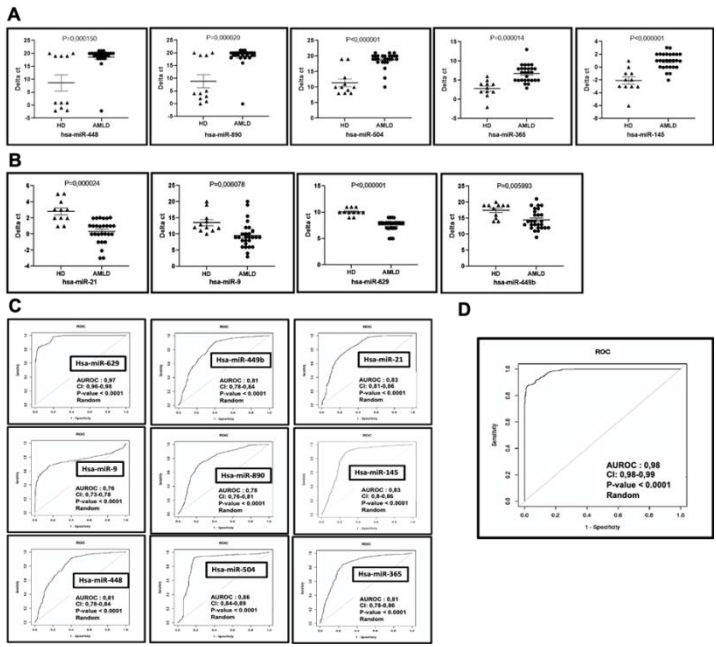

Figure 2: AML bone marrow circulating miRNA signature. The dot blot (A,B) and receiver operating characteristic (ROC) curves (C,D) reflecting the ability of the bone marrow circulating miRNA expression signature to differentiate the AML cases (n = 27) from the controls (n = 11). (**A**) Downregulated miRNAs: miR-448, 890, 504, 145, 365 and. (**B**) Upregulated miRNAs: miR-9; 21, 629 and 449b. (**C**) ROC curves reflecting the performance of the individual features of the 9 miRNA signature in discriminating AML patients from healthy donors. (**D**) Combined ROC showing the overall discriminatory power of the 9-miRNA signature. AUROC: Area Under ROC; CI: 95% Confidence Intervals; p-value: correspond to a Mann-Whitney U test addresses testing the null hypothesis of the AUROC is 0.5 (i.e., the classifier is random).

This miRNAs signature was also confirmed in the second cohort (Figure 3A–C).

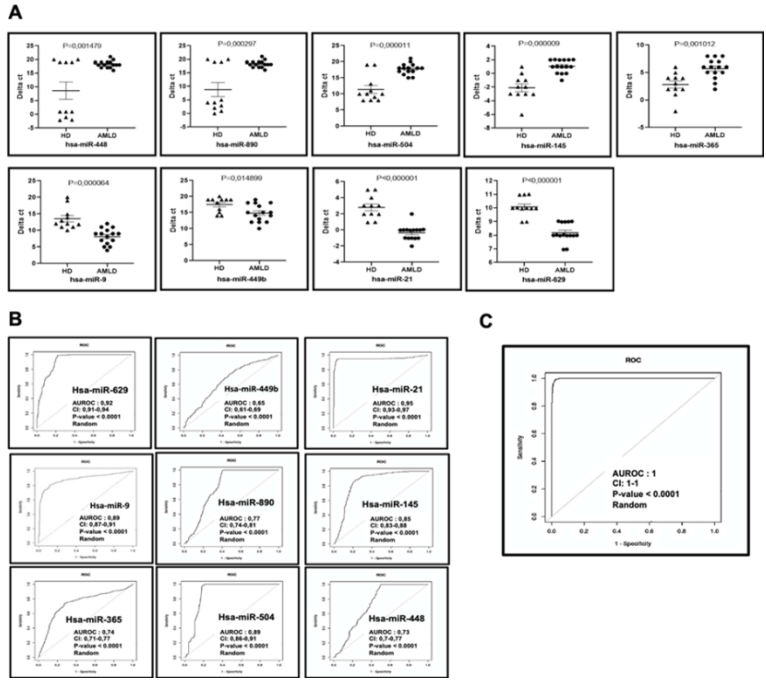

Figure 3: Confirmation of differentially expressed miRNAs in a second cohort (n = 15).(**A**) The dot plots of Downregulated and Upregulated AML miRNA signature in a second cohort of AML patients at diagnosis compared to HD (**B**) ROC curves reflecting the performance of the individual features of the 9 miRNA signature in discriminating AML patients from healthy donors. (**C**) ROC plot showing the discriminatory value of the 9-miRNA signature in the second cohort. AUROC: Area Under ROC; CI: 95% Confidence Intervals; *p*-value: correspond to a Mann-Whitney U test addresses testing the null hypothesis of the AUROC is 0.5 (i.e., the classifier is random).

Functional Analysis of the Pathways of AML Bone Marrow Circulating miRNAs

GO classification and KEGG pathway analyses were used to identify the biological functions of miRNA pathways, including oncogenic processes, cell death pathways, immune functions and proliferation signaling pathways. The threshold of GO and KEGG classification was set as $p < 0.05$. MicroRNAs in cancer

(hsa:05206, $p = 6.05 \times 10^{-11}$), acute myeloid leukemia apoptosis (hsa:05221, $p = 3.98 \times 10^{-5}$), Ras signaling pathway (hsa:05221, $p = 2.29 \times 10^{-5}$) and PI3K-Akt signaling pathway (hsa:04151, $p = 1.82 \times 10^{-4}$) were the most significantly enriched miRNA target gene pathways. We also observed miRNAs implicated in apoptosis, chemokine and T cell receptor signaling pathways (Table 3A). GO classification analysis of DE miRNAs also showed several biological processes, cellular components, and molecular functions implicated in the regulation of macromolecule metabolic processes, positive cell proliferation, negative regulation of cell death, regulation of apoptosis and immune processes (Table 3B). This suggests the implication of these deregulated circulating miRNAs both in malignant cell proliferation and the immune tumor microenvironment of AML.

Table 3: Gene Ontology classification and Kyoto Encyclopedia of Genes and Genomes (KEGG) pathway enrichment analysis of differentially expressed circulating bone marrow miRNAs in AML. A) KEGG Pathway Enrichment Analysis of differentially expressed bone marrow circulating miRNAs in AML. A. GO annotation of differentially expressed bone marrow circulating miRNAs in AML.B) GO annotation of differentially expressed bone marrow circulating miRNAs in AML.

A		
KEGG ID and Term	**Count**	**pvalue**
hsa05206: MicroRNAs in cancer	60	$6.05\ 10^{-11}$
hsa05200: Pathways in cancer	62	$1.51\ 10^{-10}$
hsa04014: Ras signaling pathway	48	$2.29\ 10^{-05}$
hsa05221:Acute myeloid leukemia	45	$3.98\ 10^{-05}$
hsa04068: FoxO signaling pathway	52	0.000106
hsa04151: PI3K-Akt signaling pathway	54	0.000182
hsa04012: ErbB signaling pathway	46	0.00181
hsa05202: Transcriptional misregulation in cancer	49	0.003887
hsa04066: HIF-1 signaling pathway	47	0.003892
hsa05231: Choline metabolism in cancer	42	0.00457
hsa04520: Adherens junction	50	0.004866
hsa04210: Apoptosis	35	0.005405
hsa04620: Toll-like receptor signaling pathway	37	0.005751
hsa04010: MAPK signaling pathway	52	0.009669
hsa04672: Intestinal immune network for IgA production	16	0.010748
hsa04064: NF-kappa B signaling pathway	37	0.012295
hsa04150: mTOR signaling pathway	30	0.014025

hsa04650: Natural killer cell mediated cytotoxicity	34	0.014803
hsa04062: Chemokine signaling pathway	48	0.01481
hsa04550: Signaling pathways regulating pluripotency of stem cells	45	0.016837
hsa04660: T cell receptor signaling pathway	32	0.031392
hsa04115: p53 signaling pathway	37	0.045474
hsa04330: Notch signaling pathway	26	0.047169
hsa04110: Cell cycle	44	0.049139
B		
Gene Ontology: GO ID and Term	**Count**	**pvalue**
Biological Process		
GO:0010604~positive regulation of macromolecule metabolic process	70	$2.52384\ 10^{-16}$
GO:0010628~positive regulation of gene expression	68	$1.05757\ 10^{-12}$
GO:0042127~regulation of cell proliferation	69	$1.97068\ 10^{-11}$
GO:0008219~cell death	68	$3.48089\ 10^{-10}$
GO:0006915~apoptotic process	66	$4.40894\ 10^{-10}$
GO:0002682~regulation of immune system process	65	$6.91088\ 10^{-10}$
GO:0045595~regulation of cell differentiation	68	$1.57355\ 10^{-09}$
GO:0060548~negative regulation of cell death	62	$1.0149\ 10^{-08}$
GO:0008284~positive regulation of cell proliferation	62	$1.04\ 10^{-08}$
GO:0097190~apoptotic signaling pathway	54	$1.20513\ 10^{-08}$
GO:0043410~positive regulation of MAPK cascade	56	$2.1753\ 10^{-06}$
GO:0050776~regulation of immune response	57	$4.45138\ 10^{-06}$
GO:0070489~T cell aggregation	57	$6.58436\ 10^{-06}$
GO:0051726~regulation of cell cycle	58	$8.80856\ 10^{-06}$
GO:0043408~regulation of MAPK cascade	60	$1.07104\ 10^{-05}$
GO:0045596~negative regulation of cell differentiation	65	$1.11453\ 10^{-05}$
GO:0097191~extrinsic apoptotic signaling pathway	47	$1.20729\ 10^{-05}$
GO:0002819~regulation of adaptive immune response	33	$9.06477\ 10^{-05}$
GO:0007219~Notch signaling pathway	43	$9.88879\ 10^{-05}$
GO:0046651~lymphocyte proliferation	45	0.000115119
GO:0006955~immune response	62	0.000124958
GO:0002683~negative regulation of immune system process	45	0.000299385
GO:0001959~regulation of cytokine-mediated signaling pathway	37	0.00094784

GO:0030099~myeloid cell differentiation	54	0.001058782
GO:0097194~execution phase of apoptosis	31	0.00363619
GO:0070227~lymphocyte apoptotic process	32	0.008369403
GO:0097300~programmed necrotic cell death	13	0.011048278
Molecular Function		
GO:0019899~enzyme binding	67	$2.15784\ 10^{-07}$
GO:0000981~RNA polymerase II transcription factor activity. SSB	65	$1.2604\ 10^{-05}$
GO:0044212~transcription regulatory region DNA binding	64	$3.84654\ 10^{-05}$
GO:0000975~regulatory region DNA binding	64	$5.11725\ 10^{-05}$
GO:0044877~macromolecular complex binding	62	$5.44329\ 10^{-05}$
GO:0019900~kinase binding	62	$6.77415\ 10^{-05}$
GO:0008134~transcription factor binding	64	0.000131465
GO:0003690~double-stranded DNA binding	62	0.000142272
GO:0003682~chromatin binding	52	0.00091488
GO:0016301~kinase activity	61	0.001966828
GO:0001077~transcriptional activator activity. RNA polymerase II SSB	49	0.002467546
GO:0050839~cell adhesion molecule binding	45	0.007658872
GO:0001085~RNA polymerase II transcription factor binding	40	0.01087498
GO:0005126~cytokine receptor binding	49	0.010986866
GO:0071837~HMG box domain binding	16	0.012673444
GO:0019838~growth factor binding	42	0.021399477
GO:0042826~histone deacetylase binding	40	0.02268476
GO:0008327~methyl-CpG binding	15	0.039968845
GO:0005125~cytokine activity	37	0.04028971
GO:0070851~growth factor receptor binding	38	0.046274794
Cellular Component		
GO:0000785~chromatin	55	0.000142352
GO:0000790~nuclear chromatin	51	0.000199439
GO:0005829~cytosol	68	0.001232442
GO:0044454~nuclear chromosome part	52	0.002342868
GO:0000792~heterochromatin	25	0.002647328
GO:0000791~euchromatin	20	0.003993973
GO:0005578~proteinaceous extracellular matrix	42	0.004102668
GO:0044427~chromosomal part	56	0.00606402
GO:0005794~Golgi apparatus	50	0.006148438
GO:0005741~mitochondrial outer membrane	32	0.010046195

GO:0005576~extracellular region	61	0.010189067
GO:0005667~transcription factor complex	47	0.017135475
GO:0016604~nuclear body	42	0.017270393
GO:0019867~outer membrane	32	0.018716537
GO:0098857~membrane microdomain	51	0.020024305
GO:0045121~membrane raft	40	0.024624821
GO:0005739~mitochondrion	58	0.027721756
GO:0005912~adherens junction	51	0.02781721
GO:0070161~anchoring junction	36	0.028521889

The analysis of signaling pathways related to the published data (see the discussion section) showed the involvement of several of these confirmed DE miRNAs, such as miR-21, miR-24 and miR-9, in T cell activation, proliferation and Th2 and Treg polarization. Some of these DE miRNAs are considered oncogenes and are expressed in AML tumor cells, suggesting their role in tumor protection and T cell dysfunction.

Prognosis Value of Bone Marrow Circulating miRNAs in AML Based on Genetic Risk

We compared the miRNA profiles of newly diagnosed patients based on their genetic risk classification to highlight the correlation between circulating bone marrow miRNAs and the prognostic value of classical genetic risk. Given the experimental limits and the limited number of patients, we compared two groups of patients, those considered favorable (FAV) (n = 9) and those considered adverse (ADV) (n = 10), according to their prognosis of molecular and genetic risk. The list of miRNAs was filtered with a p-value < 0.05 and fold change ≥ 1.5. Our analysis identified 19 downregulated miRNAs in the favorable group compared to the adverse group, and only miRNA-222 was upregulated (FC = 30; p = 0.04) (Table 4). Interestingly, six of these downregulated miRNAs in the FAV group were also downregulated in all AML patients at diagnosis compared to HD. However, miR-196b and 490-3p were downregulated in both the FAV group and the HD group compared to all AML patients (Table 4). This suggests a link between some DE BM circulating miRNAs and classical genetic risk classification.

Table 4: Differentially expressed miRNAs based on genetic risk AML Good prognosis (FAV) compared to Adverse risk (ADV).

MiRNAs connotation	pvalue FAV v.s. ADV	FC FAV v.s. ADV
hsa-miR-886-3p	0.003362062	0.242595592
hsa-miR-671-3p	0.003550766	0.533445656
hsa-miR-187	0.00401137	0.071572526
hsa-miR-886-5p	0.007422418	0.36174907
hsa-miR-99b	0.011423156	0.405734354
hsa-miR-337-5p	0.016909231	0.147489611
hsa-miR-501-5p	0.019700757	0.515368965
hsa-miR-125a-5p	0.019760174	0.252095185
hsa-miR-532-3p	0.023040754	0.49492166
hsa-miR-636	0.024538272	0.436038555
hsa-miR-196b	0.02857687	0.210572395
hsa-miR-363	0.030540457	0.459860525
hsa-miR-152	0.037124343	0.44325062
hsa-miR-125a-3p	0.045392856	0.277844263
hsa-miR-616	0.046918254	0.557903991
hsa-miR-184	0.04693333	0.148403457
hsa-miR-328	0.046990145	0.315492217
hsa-miR-490-3p	0.049822819	0.075649011
hsa-miR-222	0.049940917	3.023869496

The list of miRNAs was filtered with a p-value < 0.05 and fold change ≥ 1.5.

Correlation between Bone Marrow Circulating miRNA Expression Profiles and Overall Survival Rate of Patients with AML

Regarding cytogenetic risk, the AML circulating bone marrow miRNA profile revealed a set of differentially expressed miRNAs between the unfavorable and favorable groups. Regardless of the classic classification factors, we compared patients only on the basis of their overall survival 4 years after diagnosis. Comparison of the two groups of patients at the time of diagnosis showed that 4 miRNAs (miR-328; miR-671-3p; miR-636 and miR-363) were downregulated in patients who remained in remission 4 years after treatment (n = 12) compared to those who died during the first three years after treatment (n = 15) (Figure 4A). We confirmed these downregulated miRNAs in a small second cohort (12 AML patients at diagnosis: 6 AMLDCR vs 6 AMLDR) (Figure 4B). These miRNAs could be

used as independent prognostic factors for overall survival. In particular, the prognostic relevance of miR-328 and miR-671-3p expression was more statistically significant in separating the patient group based on their OS than based on their genetic risk, and the combined ROC analyses revealed an AUC of 0.7 in first and 0.92 in second cohort ($p < 0.0001$), indicating a prognostic value of these 2 miRNAs (Figure 4C). In conclusion, our analysis showed that the expression of circulating bone marrow miRNAs appears to be associated with overall survival risk.

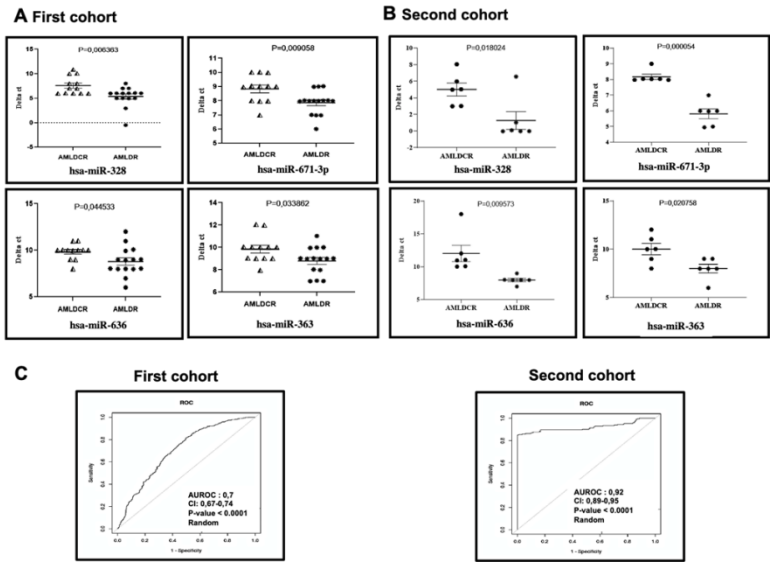

Figure 4: Prognosis value of AML bone marrow circulating miRNAs. The expression dot blot and receiver operating characteristic (ROC) curves reflecting the representative bone marrow circulating miRNAs (4 miRNAs) differentially expressed between the AML patients based on their overall survival at diagnosis (**A**) and validated in an independent second cohort of patients (**B**). (**C**) Receiver Operating Characteristic (ROC) plot validating the combined prognosis power of miR-671-3p and miR-328 in the first and second cohorts. AMLDCR: AML at diagnosis samples in which the patients have complete remission 4 years post diagnosis. AMLDR: AML at diagnosis samples in which the patients relapsed and died during the 4 years post diagnosis.

Bone Marrow Circulating miRNAs Profile of First Complete Remission AML Patients (AMLPT)

To understand the importance of these DE miRNAs described previously in defining the response to treatment, we analyzed and compared the miRNA profiles of twelve paired patients at diagnosis to their profiles during first complete remission (CR1) three months post treatment (PT). Our results showed that 19 miRNAs were upregulated and 69 were downregulated in CR1 AML patients after treatment (AMLPT) compared to newly diagnosed patients (AMLD) ($p < 0.05$ and 1,5-fold change) (Table 5).

Table 5: Differentially expressed bone marrow circulating miRNAs between newly diagnosed (AMLD) and first complete remission post-treated (AMLPT) AML patients.

MIRNAs connotation	*p* value	FC AMLD v.s. AMLPT
hsa-miR-10b	0.01421971	47.195
hsa-miR-22	0.02777678	30.223
has-miR-155	$2.1736\ 10^{-06}$	15.886
hsa-miR-29c	$7.6596\ 10^{-07}$	11.930
hsa-miR-181a	0.00018836	11.307
hsa-miR-181c	0.00060928	10.557
hsa-miR-31	0.04346473	9.674
hsa-miR-193a-3p	0.0017743	9.137
hsa-miR-542-5p	0.00255845	9.027
hsa-miR-24	0.0202524	8.248
hsa-miR-517a	0.00148494	7.944
hsa-miR-205	0.03307049	7.550
hsa-miR-146b-5p	$2.0118\ 10^{-07}$	7.488
hsa-miR-32	0.01163137	7.056
hsa-miR-150	0.00052394	6.297
hsa-miR-196b	0.01001577	6.294
hsa-miR-29a	0.00499311	6.213
hsa-miR-95	0.00012723	5.918
hsa-miR-140-3p	$2.4156\ 10^{-06}$	5.603
hsa-miR-503	0.03701134	5.591
hsa-miR-616	0.00153298	5.563
hsa-miR-345	$1.9647\ 10^{-05}$	5.303
hsa-miR-324-3p	0.00632634	5.086
hsa-miR-627	0.00796799	5.039
hsa-miR-523	0.04255625	4.853
hsa-miR-574-3p	0.05035657	4.795
hsa-miR-362-3p	0.01189798	4.470

hsa-miR-339-3p	0.00211171	4.439
hsa-miR-518f	0.01914946	4.261
hsa-miR-548b-5p	0.03672825	4.166
hsa-miR-652	0.00221981	3.952
hsa-miR-489	0.01868762	3.762
hsa-miR-708	0.04542188	3.758
hsa-miR-362-5p	0.00066885	3.745
hsa-miR-324-5p	0.0004552	3.737
hsa-miR-146b-3p	0.00350397	3.544
hsa-miR-212	9.932810^{-05}	3.541
hsa-miR-106b	0.00022376	3.533
hsa-miR-628-5p	0.00724292	3.350
hsa-miR-138	0.00521557	3.343
hsa-miR-342-3p	0.00134169	3.336
hsa-miR-146a	0.0132347	3.315
hsa-miR-140-5p	0.0013407	3.143
hsa-miR-374b	0.00172676	2.978
hsa-miR-548c-5p	0.04039887	2.967
hsa-miR-361-5p	0.0093724	2.963
hsa-miR-200c	0.00275003	2.961
hsa-miR-340	0.03578044	2.952
hsa-miR-200b	$1.0495\ 10^{-05}$	2.810
hsa-miR-126	0.00102753	2.638
hsa-miR-744	0.01146915	2.633
hsa-miR-502-5p	0.02889317	2.510
hsa-miR-590-5p	0.00094189	2.509
hsa-miR-28-5p	0.01105795	2.491
hsa-miR-142-5p	0.00951069	2.371
hsa-let-7g	0.00883628	2.368
hsa-miR-374a	0.01189576	2.338
hsa-miR-199b-5p	0.04657583	2.248
hsa-miR-532-5p	0.01865158	2.236
hsa-miR-27a	0.02344286	2.230
hsa-miR-186	0.01390867	2.225
hsa-miR-15b	0.01605429	2.115
hsa-miR-195	0.02292656	2.105
hsa-miR-26a	0.02280752	2.101
hsa-miR-106a	0.00925626	2.099
hsa-miR-26b	0.03471509	1.985
hsa-miR-30c	0.03123522	1.869
hsa-miR-30b	0.04525501	1.765
hsa-miR-491-5p	0.0305936	1.652
hsa-miR-375	0.03634904	0.393
hsa-miR-99b	0.00549437	0.391
hsa-miR-365	0.04837696	0.373
hsa-miR-92a	0.00974346	0.371
hsa-miR-671-3p	$2.371\ 10^{-05}$	0.312

hsa-miR-450a	0.04665015	0.232
hsa-miR-484	0.00424698	0.187
hsa-miR-885-5p	0.00758973	0.185
hsa-miR-190	0.00698937	0.154
hsa-miR-654-3p	0.01975562	0.123
hsa-miR-328	0.01366178	0.121
hsa-miR-211	0.02452068	0.099
hsa-miR-296-5p	0.00035013	0.078
hsa-miR-486-5p	$4.0707\ 10^{-05}$	0.075
hsa-miR-490-3p	0.02091499	0.055
hsa-miR-485-3p	0.00378225	0.039
hsa-miR-23a	0.01913452	0.015
hsa-miR-518d-3p	0.00055143	0.008
hsa-miR-326	$8.7126\ 10^{-07}$	0.003

Differentially expressed bone marrow circulating miRNAs between AML patients at diagnosis (AMLD) and first complete remission post treatment (AMLPT), consisting of 69 upregulated and 19 downregulated miRNAs, were identified with a threshold of p value < 0.05 and 1,5-fold change.

To determine the prognostic value of these miRNAs in determining posttreatment remission, we compared the profiles of miRNAs differentiating AML patients in CR1 (AMLPT) and healthy donors (HD) from those of newly diagnosed patients (AMLD). The results showed that 14 miRNAs are upregulated, and four miRNAs were downregulated in AMLD compared to both AMLPT patients and healthy donors.

Interestingly, the results showed that the bone marrow expression level of miR-518d-3p was also still undetectable in CR1 patients after treatment similar to HD (Figure 5). Overall, this correlation allowed us to establish promising bone marrow circulating miRNA biomarkers for AML remission post treatment, suggesting their possible role in the response of AML patients to chemotherapy treatment.

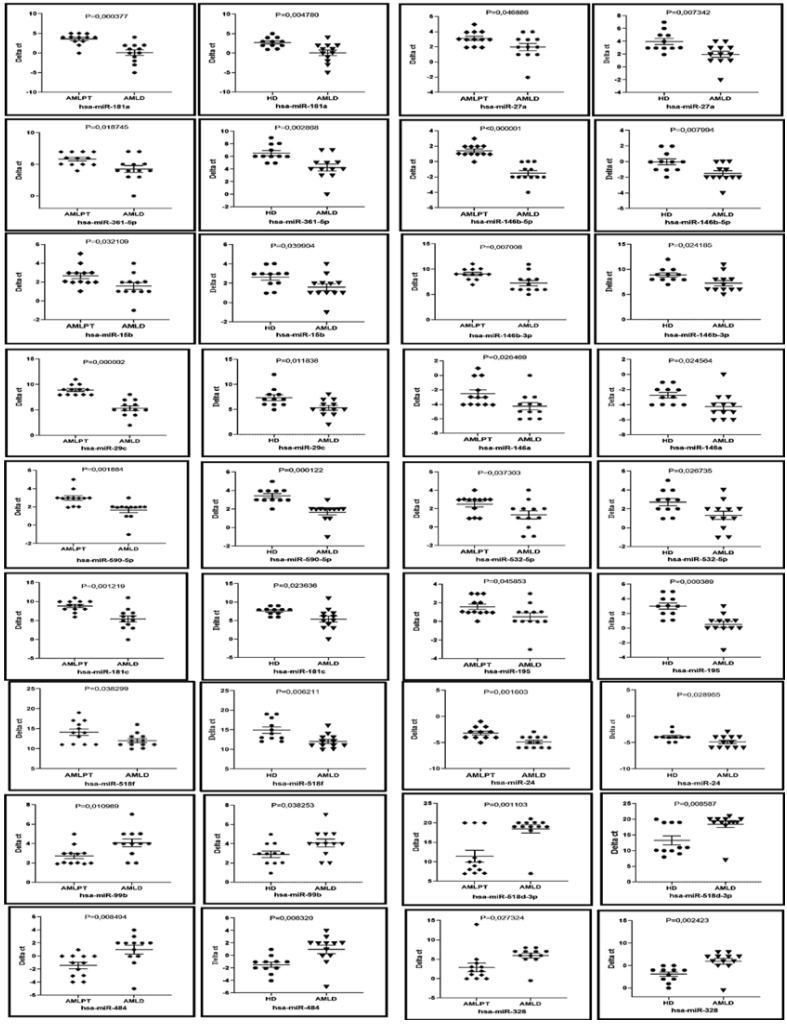

Figure 5: Prognosis value of AML bone marrow circulating miRNAs related to remission after treatment. Correlated differentially expressed miRNAs between AMLD vs AMLPT patients and AMLD patients v.s. HD. The expression dot plot curves reflecting the correlated differentially expressed bone marrow circulating miRNAs in AML patients at diagnosis (n = 12) compared to both healthy donors (n = 11) and the same patients in relative remission (blast < 5%) post treatment (n = 12). AMLD: AML patients at diagnosis. HD: Healthy donors. AMLPT: AML first complete remission post treatment patients.

Discussion

Despite advances in the search for new optimal therapeutic approaches, including targeted immunotherapy, only a minority of patients are cured, especially in the elderly population. The identification of new therapeutic targets is necessary to design new or improve existing therapeutic protocols. This is only possible through understanding the different players that drive the pathogenesis of this disease, especially those related to TME. In addition, the search for new diagnostic and prognostic markers of AML is necessary, given the heterogeneity of the disease and the inadequacy of current genetic markers in predicting survival. MiRNAs circulating free or contained in microvesicles (MVs) can be secreted by a wide variety of cells in the TME and are increasingly seen as potential future markers for the diagnosis and prognosis of various malignant diseases.

In this work, we have for the first time analyzed the profile of enriched miRNAs circulating in the bone marrow, which is considered the main location of the initiation and development of acute myeloid leukemia. The results demonstrated a consistent number of differentially expressed miRNAs between AML patients and healthy donors. This allowed us to establish a miRNA signature at the time of diagnosis that provided good separation between the patients and healthy donors. More than thirty of these miRNAs were validated in a second independent cohort of patients. However, two DE miRNAs in the first cohort did not give similar results in the second cohort, of which 14 were similarly DE but statistically insignificant. This could be due to the limited number of patients in the second cohort, which suggests the need to increase the number of patients in the future. Interestingly, some of these DE miRNAs were undetectable or expressed at very low levels either in patients or in HD, suggesting their role in the development of AML. Among the miRNAs that were expressed in HD but undetectable in patients, we found miR-448, miR-890 and miR-504. These miRNAs have been shown to be downregulated and function as tumor suppressors in several types of cancer [24,25]. Recently, miR-504 was shown to be significantly downregulated in the serum of AML patients and cell lines, and its overexpression inhibits cell

growth and induces apoptosis in leukemic cells [26]. MiR-448 is downregulated in T-cell acute lymphoblastic leukemia (T-ALL) and seems to target the principal proto-oncogene (TAL1) of this disease [27]. To date, no publication has shown a link between miR-448 and miR-890 in AML, suggesting that their deregulation in bone marrow fluid may be associated with cells other than leukemic blasts. Their deregulation in the TME following the development of the disease must be elucidated for their direct impact not only on the proliferation of malignant cells but also on immune TME cells. Interestingly, it was reported that in human colon cancer, miR-448 could suppress CD8+ T-cell apoptosis and enhance the CD8+ T-cell response by inhibiting indoleamine 2,3-dioxygenase 1 enzyme function [28]. In our results, we also observed other differentially expressed miRNAs, including miR-520a, 651, 520f and 449, that were upregulated in patients and undetectable or expressed at very low levels in HD. Among these, only miR-520a was described to be DE in AML blasts and was associated with a poor prognosis in AML [29], and miR-520f has been reported as an oncogene in human melanoma and promotes malignant cell proliferation [30].

Our results also allowed us to detect miRNAs that are strongly DE but are expressed in both the AML and HD groups. Some, such as miR-9, miR-548d and miR-21, are highly deregulated and are known to be oncogenes in AML or other types of cancer. An increased level of miR-9 has been observed in the bone marrow and peripheral blood of 200 AML patients compared to HD [31]. Chen Tian et al. showed that the knockdown of miR-9 suppressed the proliferation of AML cells by the induction of G0 arrest and apoptosis in vitro, resulting in decreased circulating leukemic cells and prolonged survival in a xenotransplant mouse model [32]. In addition, overexpression of miR-9 enhances the suppressive function of MDSCs, while its knockdown impairs them and inhibits the tumor growth of Lewis lung carcinoma in mice. [33]. MiRNA-548d-5p was shown to be upregulated in metastatic colorectal cancer tumor-derived exosomes [34]. There was no association between these miRNAs and AML in the literature, suggesting that upregulation of AML in bone marrow fluid is due to a cell origin other than leukemic cells. Certain studies have shown its role in promoting osteogenic

differentiation of mesenchymal stem cells [35,36]. Surprisingly, we also observed that some AML-upregulated bone marrow circulating miRNAs are reported in the literature as tumor suppressors, including miR-34a, miR-375, miR-576-3p, and miR-597. For example, miR-34a is strongly expressed in AML patient bone marrow fluid and is known to be downregulated in leukemia cells in the marrow and peripheral blood serum of patients [37,38] and appears to play an important role as a tumor suppressor and immunotherapeutic agent [39,40]. The expression of miR-375 was also downregulated in leukemic cell lines and primary AML blasts compared to normal controls, and its overexpression decreased proliferation and colony formation, reduced xenograft tumor size and prolonged the survival time in a leukemia xenograft mouse model [41]. MiR-576-3p was shown to be downregulated in colorectal [42] and bladder cancer [43], to inhibit the migration and invasion of lung adenocarcinoma [44] and to significantly inhibit the migration and pro-angiogenic abilities of glioma cells under hypoxic conditions [45]. Additionally, miR-597 inhibits breast and colon cancer cell proliferation, migration and invasion [46,47]. These findings strengthen our previous hypothesis for a cell origin other than leukemia cells for these miRNAs and suggest their dual function according to the type of cancer or the tumor focus. Interestingly, recent analyses of the regulatory network of CD19-CAR-T immunotherapy for B acute lymphocyte leukemia revealed that microRNA miR-375 could regulate the crosstalk between the genes encoding transcription factors and histones involved in CD19-CAR-T therapy [48].

Our results also showed that some miRNAs were expressed in both the AML and HD groups but were significantly downregulated in AML patients compared to HD, among which we found miR-145, 150, 204, 365 and 518b. MiR-145 has been increasingly identified as a critical suppressor of carcinogenesis and therapeutic resistance in several cancers [49]. Recent data showed that the level of this miRNA in serum and bone marrow mononuclear cells of AML patients was significantly lower than that of HD and was related to poor prognosis [50]. MiR-145 seems to play an important role in the immune response against leukemic cells. It was reported to enhance host antitumor

immunity by altering the cytokine milieu, metastatic microenvironment and reprogramming tumor-associated myeloid cells [51]. Recent work revealed that miR-145, which is known to be downregulated by cisplatin in cisplatin-resistant ovarian cancer cells, also represses PD-L1 gene expression and induces T cell apoptosis in vitro [52]. It is known that the level of miR-150 is decreased in the plasma and blast cells of AML patients at diagnosis and that reintroducing miR-150 expression induces myeloid differentiation and inhibits the proliferation of AML cells [18,53]. Xi et al. developed a novel targeted therapeutic strategy using FLT3L-guided miR-150-based nanoparticles to treat FLT3-overexpressing AML in an animal model with high efficacy and minimal side effects [54]. MiR-204 expression in AML patients was decreased and was associated with shorter patient survival. Higher expression of this miR was observed in patients after induction therapy and was correlated with complete remission [55], and its targeting promotes the viability and invasion of AML cells [56]. Wang et al. demonstrated that overexpression of these miRNAs potentiates the sensitivity of AML cells to arsenic trioxide [57]. In addition, recent work showed that in breast cancer, miR-204 regulated the expression of key cytokines in tumor cells and reprogrammed immune cells by shifting myeloid and lymphocyte populations, suggesting that this miRNA suppresses tumor metastasis and remodeling the immune microenvironment [58]. MiR-518b was also reported to function as a tumor suppressor in glioblastoma [56], esophageal and squamous cell carcinoma [59].

Based on these results, we also established an AML signature at diagnosis, consisting of nine miRNAs with an AUC greater than 0.77. Combined ROC analyses using these nine miRNAs revealed an elevated AUC of 0.98 ($p < 0.0001$), indicating an additive effect on the diagnostic value of these miRNAs. This signature, as well as more than thirty DE miRNAs, was validated in a second cohort of patients and provided good separation between AML patients and HD. Our patient group comparison at diagnosis based on their overall survival showed that miR-328, miR-671-3p, miR-636 and miR-363 are upregulated in relapsed patients. These miRs are described in the literature as promising prognostic biomarkers in AML or other malignant diseases

[21,60–75]. Interestingly, all the patients involved in this comparison were not grafted, which suggests that these four miRs could constitute a signature to guide the choice of the best treatment strategy, especially the utility of grafting patients at diagnosis. A recent study using a TCGA dataset identified a set of miRNAs, including miR-363, that could predict clinical outcome in a heterogeneous AML population [76]. This study confirms our results showing the high expression of circulating bone marrow miR-363 in nontransplanted patients with shorter OS and suggests that its high expression may help to identify patients recommended for an early allo-HSCT regimen. Interestingly, this miRNA seems to play an important role in the immune response against leukemic cells. An enrichment of specific cellular miRNAs, including miR-363, in EVs derived from CD40/IL-4-stimulated chronic lymphoblastic leukemia cells was observed, and autologous patient CD4(+) T cells were found to be capable of internalizing the CLL-EVs that target the immunomodulatory molecule CD69 [77].

Our comparison of patients before and after three months of treatment (first complete remission (CR1)) allowed us to identify a set of miRNAs that were differentially expressed (4 downregulated and 14 upregulated) in the same way as when comparing patients at diagnosis with HD. However, other analyses are underway on a larger cohort of patients to study the long-term prognostic value (four years after treatment) of these miRNAs. It should also be noted that an analysis of the profile of relapsing patients during the first months is also necessary to validate these miRNAs, which we could not obtain in our study. These miRNAs, in addition to their value in monitoring posttreatment remission, may also play a role in the elimination of blasts directly or indirectly by improving the antileukemia response. Among these DE in AML CR1, miR-484, miR-518d and miR-99b are upregulated in addition to the previously described miR-328. MiR-99b was also showed as being responsible for the conversion of monocytes into MDSCs and to be associated with resistance to treatment with immune checkpoint inhibitors in melanoma patients [78]. MiR-518d may be an interesting target due to its low or undetectable level in HD and post treatment. It was reported to be implicated in the

inhibition of cervical cancer cell proliferation, migration and invasion [79] and in the regulation of advanced small cell lung cancer cell proliferation, migration and chemotherapy response [80]. To date, little work has focused on this miRNA, and none of the studies have reported its involvement in AML, which makes it a good avenue for future investigation. For the downregulated miRNAs in AML CR1, miR-24 appear to be involved in AML evolution an immune response. High expression of miR-24 has been observed in AML leukemia patients and is associated with the risk of relapse and poor survival [81], and its role in nasopharyngeal carcinoma pathogenesis by mediating T-cell suppression has been demonstrated [82]. In a previous study, we demonstrated that this miRNA negatively regulates IFN-γ expression in T lymphocytes [83], and recently, we showed its direct impact on AML T lymphocyte fragility and dysfunction (in preparation). Furthermore, other downregulated miRNAs in CR1, such as miR-15b [84], miR-27a [85], miR-29c [86], miR-106a [87] and miR-181a [88], have been described as being implicated in AML pathogenesis or drug resistance.

As reported, high expression of miR-181a in AML blasts, cell lines and serum has been observed [89,90], and its overexpression significantly enhanced cell proliferation and increased the ratio of S-phase cells by regulating the tumor suppressor ATM [91,92]. Inhibition of this miR in mice implanted with AML CD34+ hematopoietic progenitor cells (HSPCs) increased myeloid differentiation, inhibited engraftment and infiltration of leukemic CD34+ cells into the bone marrow and spleen, and finally reduced leukemic symptoms [93]. However, miR-181a also plays a role in the sensitization of leukemic resistant cells to daunorubicin and NK cells and may provide a promising option for AML immunotherapy treatment of chemoresistant blasts [94]. MiR-181a appears to play an important role in T cell activation [95] and CAR-T cell immunotherapy [96]. A recent study showed that inhibition of DOT1L reduces the expression of miR-181a, which in turn selectively enhances low-avidity T cell responses and attenuates graft versus host development, suggesting that this would allow the safe and effective use of allogeneic

antitumor T cells [97]. In melanoma patients, the plasma levels of miR-181a were higher in patients at diagnosis compared to controls, and the development of metastasis has been associated with changes in immune effector and regulatory cells with changes in plasma and cellular levels of immune regulatory miRNA [98]. Melanoma-derived exosomes decrease TNFα secretion in CD8+ cells and are enriched for hsa-miR-181a, which is capable of interacting directly with the 3′-UTR sequence of TNFα and driving immune escape in melanoma [99]. We have previously shown in our laboratory that overexpression of miR-181a negatively regulates IFN-γ expression in activated PB CD4+ T cells by directly binding to its target sites in the mRNA and increases the expression of IL4 [83]. MiR-181c also seems to play a dual role similar to miR-181a in both malignant and immune cells. A study conducted by R Su et al. compared patients with AML blasts with normal controls, and most AML patients showed significantly increased expression levels of all miR-181 members, including miR-181c [100]. MiR-181c is important in T cell activation, and the overexpression of miR-181c results in inhibition of T cell activation and actin polymerization coupled with defective immunological synapse formation [101]. Interestingly, R. Le Dieu et al. showed that the ability of AML T cells to form immune synapses was significantly impaired [102]. It was identified as a novel miRNA that promotes Th17 cell differentiation and autoimmunity [103]. In addition, circulating miR-181c can be of a cell origin other than cancer cells. Xiao Li et al. showed that exosomes derived from human umbilical cord mesenchymal stem cells are enriched for miR-181c, which in turn attenuates burn-induced excessive inflammation [104].

MiR-532 was reported as an oncogene in breast [105], colorectal [106] and human gastric cancers [107]. In recent published work, Lin et al. concluded that plasma exosome-derived miR-532 can be used as a novel survival predictor for acute myeloid leukemia [108]. This miRNA has also been implicated in the immune inflammatory response [109]. In addition to its function as a tumor suppressor and/or oncogene [110], miR-146a was shown to play a critical role in regulating T cell functions by providing a general brake on proliferation and activation of immune cells

and was able to limit immune responses linked to the TH1 and TH17 subsets. Mice lacking this miRNA developed more severe TH17 responses in murine models of autoimmunity, with increased production of IFN-γ and IL-17 and reduced secretion of IL-4 [111]. Furthermore, miR-146a is also a key regulator of Treg cell biology, as deficiency of miR-146a leads to impaired function of Treg cells and consequently to the breakdown of immunological tolerance and to the development of fatal immune-mediated lesions depending on IFN-γ. Indeed, in addition to their role in the proliferation of cancer cells, many of these downregulated miRNAs, including miR-15 [112,113], miR-27a [114,115] and miR-29c [116,117,118], appear to play a role in immune regulation, T regulatory and inflammatory responses and TIL dysfunction.

Together, these results suggest that enriched circulating bone marrow miRNAs are key regulators of AML blast proliferation and affect immune cell functions in the TME. Our GO classification and KEGG pathway analyses confirmed that these DE circulating miRNAs could play a role not only in the oncogenic process, cell death and proliferation signaling pathways but also in immune function. Further research may elucidate their role in the malignant cells and TME. Studies are currently underway in our laboratory to investigate the impact of these miRNAs on the antileukemic immune response with the aim of establishing new immunotherapeutic targets of AML.

Materials and Methods

Patients

Patients used in this study had a newly diagnosed AML in addition to being in complete remission after the first treatment (three months after first induction) as determined by bone marrow test. A total of 46 patients at the time of diagnosis, 12 of them in complete remission post treatment, provided bone marrow samples. Healthy subjects (n =11) were enrolled as negative controls. None of these controls had been previously diagnosed with any type of malignancy or other benign disease. Informed consent, approved by the Clinical Research Ethics Committee of Jules Bordet Institute (approval code:

B079201214544, approval date: 05/07/2012) was obtained from each participant. Details of the clinical data are provided in Table 6.

Table 6: Summary of AML patient clinical details used for the analysis.

Clinical Details of AML Patients (42)	**Number**
Sex and age	
Males	20
Females	22
Age < 55y	17
Age ≥ 55y	25
Classification of AML Patients	
Cytogenetic abnormalities	
Normal Karyotype	10
Chromosome 9 deletion	4
Inversion (16) MYH11-CBFB	4
Translocation (t8;21)	4
Translocation (t15;17)	6
Translocation (X:21) (p11;q22)	2
trisomy 8 complex Karyotype	1 3
WHO 2016 System AML with recurrent genetic abnormalities (t8;21) AML with recurrent genetic abnormalities (inv 16)	 4 4
AML with recurrent genetic abnormalities (t15;17) Acute monoblastic/monocytic leukemia Pure erythroid leukemia AML not otherwise specified (NOS) AML with myelodysplasia-related changes **ELN 2017 Genetic Risk Stratification**	*6* *2* *2* *20* 6
Favorable	14
Intermediate	7
Adverse	16
unkown	5

The classification of AML patients was performed according to WHO 2016. The genetic risk stratification of AML patients was performed according to the 2017 European LeukemiaNet genetic risk stratification [1]: Favorable = Good prognosis; IT = Intermediate prognosis; Adverse = adverse risk.

Bone Marrow Aspiration Sampling and RNA Extraction

At presentation, bone marrow aspiration samples for miRNA detection were collected in EDTA-K2 tubes and processed within 1 h of collection. Bone marrow body fluid samples were centrifuged at 1200× *g* for 10 min at 4 °C to pellet the hematopoietic cells, and the supernatant was transferred into microcentrifuge tubes, followed by a second centrifugation at 12,000× *g* for 10 min at 4 °C. The supernatant was transferred to RNase/DNase-free tubes and stored at −80 °C. Total RNA was isolated from the plasma using a mirVana PARIS isolation kit (Ambion, Austin, TX, USA) according to the manufacturer's instructions for plasma samples. Briefly, 400 µL of human bone marrow plasma was used to extract total RNA. Each sample was eluted in 100 µL of RNase-free water and concentrated to a final volume of 20 µL by using an Eppendorf Concentrator Plus 5301 (Eppendorf, Aarschot, Belgium). The RNA sample concentration was quantified by a NanoDrop ND-1000 (Thermo Fisher Scientific, Waltham, MA, USA).

miRNA Expression Profile

Thirty nanograms of total bone marrow fluid extracted RNA was used for cDNA synthesis from the miRNAs using a TaqMan® microRNA Reverse Transcription Kit (#4366596; Applied Biosystems, Waltham, MA, USA) and Megaplex RT primers (Human Pool A, #4399966; Applied Biosystems) following the manufacturer's protocol described previously [18]. After the preamplification step, the products were amplified and then loaded into TaqMan Human MicroRNA Array A (#4398965; Applied Biosystems), which contains the TaqMan primers and probes in each well for the 380 different mature human miRNAs; miR-425 transcript was used as a normalization signal. The relative expression levels of miRNAs were calculated using the comparative ΔΔ*C*t method as described previously [18]. The fold changes in miRNAs were calculated by the equation $2^{-\Delta\Delta Ct}$.

TaqMan miRNA Assay for Individual miRNAs

The expression of individual miRs was determined using the TaqMan miRNA assay as described previously [18]. The expression levels of miRNAs were calculated as described previously, and miR-425 was used as an internal reference. The predesigned TaqMan assay primers and probes corresponding to the ones used in TLDA card A were purchased from Thermo Fisher Scientific. The calculated delta Ct ± SD for the patients was compared with the delta Ct ± SD (SD stands for the standard deviation of the average delta *C*t of the group for the healthy control group and tested for statistical significance).

Statistical Analysis

Data analysis was performed in R version 3.5.3 using packages of the Bioconductor project (DOI: 10.1186/gb-2004-5-10-r80). Raw cycle threshold (*C*t) values were loaded into R using the HTqPRC package (doi:10.1093/bioinformatics/btp578) and flagged as "Undetermined" if they were above 35. miRNAs that are expressed in at least one sample group (i.e., *C*t > 35 in at least X samples) were retained for further analysis. To normalize the data, delta *C*t (Δ*C*t) values were calculated for each sample by subtracting the *C*t value of miR-425 from its other values. miR-425 was selected as the best reference candidate by both the geNorm and NormFinder methods implemented in the NormqPCR package (https://rdrr.io/bioc/NormqPCR/man/NormqPCR-package.html) accessed on 01 August 2020. Testing for differential expression between sample groups was performed using empirical Bayes moderated t-statistics computed by the limma package (https://bioconductor.org/packages/release/bioc/html/limma.html). miRNAs with an absolute fold change > 1.5 and a p value < 0.05 were considered differentially expressed (DEmiRNAs). The ability of the selected signatures and miRNAs to accurately discriminate between different patient groups was estimated by constructing and assessing the performance of ensemble-based classifiers (DOI 10.1007/s10462-009-9124-7). These are stacked classifiers that combine the predictions of several classification algorithms in order to predict the outcome. The Area Under

Receiver Operating Characteristic Curve (AUC) was calculated by a bootstrapping procedure with 100 iterations. Enrichment analysis of Gene Ontology (GO) terms and Kyoto Encyclopedia of Genes and Genomes (KEGG) pathways (https://www.genome.jp/kegg/pathway.html) was performed using the Database for Annotation, Visualization, and Integrated Discovery (DAVID) tool (http://david.abcc.ncifcrf.gov/) accessed on 13 August 2020.

Conclusions

In our study, for the first time, we highlight circulating miRNAs in the bone marrow of AML patients and provide important insight into the possible role of these miRNAs in the TME. We have shown that the main TME of AML is well enriched in molecules that have variable expression according to the progression of the disease as well as the predisposition to the treatment response. In addition to the value that these circulating miRNAs can provide for the diagnosis of AML or its confirmation, their contribution could extend to the prognostic level by guiding, at diagnosis, the choice of transplants for certain patients. Some of these miRNAs appear to be of malignant origin, and their impact on resistance to treatment or evasion of immune system surveillance has been described in other types of cancer. Other miRNAs that to date have never been described in AML could have another cellular origin (immune cells, MSCS and stromal cells) and could be at the origin of the promotion of the proliferation of blasts while directing the immune response to a protumoral phenotype. Further in vitro and in vivo investigations are necessary to confirm these hypotheses, which open a wide door to new immunotherapeutic targets for the eradication of AML.

References

1. Thomas D, Majeti R. Biology and relevance of human acute myeloid leukemia stem cells. Blood. 2017; 129: 1577–1585.
2. Shysh AC, Nguyen LT, Guo M, Vaska M, Naugler C, et al. The incidence of acute myeloid leukemia in Calgary,

Alberta, Canada: A retrospective cohort study. BMC Public Health. 2017; 18: 94.
3. Liu Y, Cheng Z, Pang Y, Cui L, Qian T, et al. Role of microRNAs, circRNAs and long noncoding RNAs in acute myeloid leukemia. J. Hematol. Oncol. 2019; 12: 51.
4. Watts J, Nimer S. Recent advances in the understanding and treatment of acute myeloid leukemia. F1000Research. 2018; 7: 1196.
5. Marcucci G, Mrozek K, Radmacher MD, Garzon R, Bloomfield CD. The prognostic and functional role of microRNAs in acute myeloid leukemia. Blood. 2011; 117: 1121–1129.
6. He C, Luo B, Jiang N, Liang Y, He Y, Zeng J, et al. OncomiR or antioncomiR: Role of miRNAs in Acute Myeloid Leukemia. Leuk. Lymphoma. 2019; 60: 284–294.
7. Trino S, Lamorte D, Caivano A, Laurenzana I, Tagliaferri D, et al. MicroRNAs as New Biomarkers for Diagnosis and Prognosis, and as Potential Therapeutic Targets in Acute Myeloid Leukemia. Int. J. Mol. Sci. 2018; 19: 460.
8. Dohner H, Estey E, Grimwade D, Amadori S, Appelbaum FR, et al. Diagnosis and management of AML in adults: 2017 ELN recommendations from an international expert panel. Blood. 2017; 129: 424–447.
9. Christopher AF, Kaur RP, Kaur G, Kaur A, Gupta V, et al. MicroRNA therapeutics: Discovering novel targets and developing specific therapy. Perspect. Clin. Res. 2016; 7: 68–74.
10. Ling H, Fabbri M, Calin GA. MicroRNAs and other non-coding RNAs as targets for anticancer drug development. Nat. Rev. Drug Discov. 2013; 12: 847–865.
11. Si W, Shen J, Zheng H, Fan W. The role and mechanisms of action of microRNAs in cancer drug resistance. Clin. Epigenet. 2019; 11: 25.
12. Slaby O, Laga R, Sedlacek O. Therapeutic targeting of non-coding RNAs in cancer. Biochem. J. 2017; 474: 4219–4251.
13. Ferreira P, Roela RA, Lopez RVM, Del Pilar Estevez-Diz M. The prognostic role of microRNA in epithelial ovarian cancer: A systematic review of literature with an overall survival. Oncotarget. 2020; 11: 1085–1095.

14. Buhagiar A, Borg J, Ayers D. Overview of current microRNA biomarker signatures as potential diagnostic tools for leukaemic conditions. Noncoding RNA Res. 2020; 5: 22–26.
15. Hamam R, Hamam D, Alsaleh KA, Kassem M, Zaher W, et al. Circulating microRNAs in breast cancer: Novel diagnostic and prognostic biomarkers. Cell Death Dis. 2017; 8: e3045.
16. Dufresne S, Rebillard A, Muti P, Friedenreich CM, Brenner DR. A Review of Physical Activity and Circulating miRNA Expression: Implications in Cancer Risk and Progression. Cancer Epidemiol. Biomark. Prev. 2018; 27: 11–24.
17. Yan J, Wu G, Chen J, Xiong L, Chen G, et al. Downregulated miR-217 expression predicts a poor outcome in acute myeloid leukemia. Cancer Biomark. 2018; 22: 73–78.
18. Fayyad-Kazan H, Bitar N, Najar M, Lewalle P, Fayyad-Kazan M, et al. Circulating miR-150 and miR-342 in plasma are novel potential biomarkers for acute myeloid leukemia. J. Transl. Med. 2013; 11: 31.
19. Zhi F, Cao X, Xie X, Wang B, Dong W, et al. Identification of circulating microRNAs as potential biomarkers for detecting acute myeloid leukemia. PLoS ONE. 2013; 8: e56718.
20. Tang X, Chen L, Yan X, Li Y, Xiong Y, et al. Overexpression of miR-210 is Associated with Poor Prognosis of Acute Myeloid Leukemia. Med. Sci. Monit. 2015; 21: 3427–3433.
21. Liu L, Chen R, Zhang Y, Fan W, Xiao F, et al. Low expression of circulating microRNA-328 is associated with poor prognosis in patients with acute myeloid leukemia. Diagn. Pathol. 2015; 10: 109.
22. Liu X, Li P, Yun Y, Zhang D, Ma H, et al. Prognostic value of plasma miR-638 in patients with acute myeloid leukemia. Int. J. Clin. Exp. Pathol. 2017; 10: 550–555.
23. Tian C, Zhang L, Li X, Zhang Y, Li J, et al. Low miR-192 expression predicts poor prognosis in pediatric acute myeloid leukemia. Cancer Biomark. 2018; 22: 209–215.

24. Li B, Ge L, Li M, Wang L, Li Z. miR-448 suppresses proliferation and invasion by regulating IGF1R in colorectal cancer cells. Am. J. Transl. Res. 2016; 8: 3013–3022.
25. Wang C, Xu C, Niu R, Hu G, Gu Z, et al. MiR-890 inhibits proliferation and invasion and induces apoptosis in triple-negative breast cancer cells by targeting CD147. BMC Cancer. 2019; 19: 577.
26. Li SM, Zhao YQ, Hao YL, Liang YY. Upregulation of miR-504-3p is associated with favorable prognosis of acute myeloid leukemia and may serve as a tumor suppressor by targeting MTHFD2. Eur. Rev. Med. Pharm. Sci. 2019; 23: 1203–1213.
27. Correia NC, Melao A, Povoa V, Sarmento L, Gomez de Cedron M, et al. microRNAs regulate TAL1 expression in T-cell acute lymphoblastic leukemia. Oncotarget. 2016; 7: 8268–8281.
28. Lou Q, Liu R, Yang X, Li W, Huang L, et al. miR-448 targets IDO1 and regulates CD8(+) T cell response in human colon cancer. J. Immunother. Cancer. 2019; 7: 210–214.
29. Gao HY, Wang W, Luo XG, Jiang YF, He X, et al. Screening of prognostic risk microRNAs for acute myeloid leukemia. Hematology. 2018; 23: 747–755.
30. Sun MX, An Q, Chen LM, Guo L. MIR-520f Regulated Itch Expression and Promoted Cell Proliferation in Human Melanoma. Cells. Dose Response. 2020; 18: 1559325820918450.
31. Zheng HZ, Sun YB, Zhan T, Zeng KD, Liu CZ, et al. miR-9-5p prompts malignancies of acute myeloid leukemia cells mainly by targeting p27. Int. J. Clin. Exp. Med. 2018; 11: 2076–2083.
32. Chen L, Hu W, Li G, Guo Y, Wan Z, et al. Inhibition of miR-9-5p suppresses prostate cancer progress by targeting StarD13. Cell Mol. Biol. Lett. 2019; 24: 20.
33. Tian J, Rui K, Tang X, Ma J, Wang Y, et al. MicroRNA-9 Regulates the Differentiation and Function of Myeloid-Derived Suppressor Cells via Targeting Runx1. J. Immunol. 2015; 195: 1301–1311.
34. Tang Y, Zhao Y, Song X, Song X, Niu L, et al. Tumor-derived exosomal miRNA-320d as a biomarker for

metastatic colorectal cancer. J. Clin. Lab. Anal. 2019; 33: e23004.
35. Zhang W, Zhang L, Zhou Y, Ji X, Liu J, et al. Synergistic Effects of BMP9 and miR-548d-5p on Promoting Osteogenic Differentiation of Mesenchymal Stem Cells. Biomed. Res. Int. 2015; 2015: 309747.
36. Sun J, Wang Y, Li Y, Zhao G. Downregulation of PPARgamma by miR-548d-5p suppresses the adipogenic differentiation of human bone marrow mesenchymal stem cells and enhances their osteogenic potential. J. Transl Med. 2014; 12: 168.
37. Liu X, Li H. Diagnostic Value of miR-34a in Bone Marrow Mononuclear Cells of Acute Myeloid Leukemia Patients. Clin. Lab. 2020; 66.
38. Huang Y, Zou Y, Lin L, Ma X, Chen H. Identification of serum miR-34a as a potential biomarker in acute myeloid leukemia. Cancer Biomark. 2018; 22: 799–805.
39. Liu L, Ren W, Chen K. MiR-34a Promotes Apoptosis and Inhibits Autophagy by Targeting HMGB1 in Acute Myeloid Leukemia Cells. Cell Physiol. Biochem. 2017; 41: 1981–1992.
40. Wang X, Li J, Dong K, Lin F, Long M, et al. Tumor suppressor miR-34a targets PD-L1 and functions as a potential immunotherapeutic target in acute myeloid leukemia. Cell Signal. 2015; 27: 443–452.
41. Bi L, Zhou B, Li H, He L, Wang C, et al. A novel miR-375-HOXB3-CDCA3/DNMT3B regulatory circuitry contributes to leukemogenesis in acute myeloid leukemia. BMC Cancer. 2018; 18: 182.
42. Eldaly MN, Metwally FM, Shousha WG, El-Saiid AS, Ramadan SS. Clinical Potentials of miR-576-3p, miR-613, NDRG2 and YKL40 in Colorectal Cancer Patients. Asian Pac. J. Cancer Prev. 2020; 21: 1689–1695.
43. Meng FM, Meng FM, Song XL. MiR-576-3p is a novel marker correlated with poor clinical outcome in bladder cancer. Eur. Rev. Med. Pharmacol. Sci. 2017; 21: 973–977.
44. Greenawalt EJ, Edmonds MD, Jain N, Adams CM, Mitra R, et al. Targeting of SGK1 by miR-576-3p Inhibits Lung Adenocarcinoma Migration and Invasion. Mol. Cancer Res. 2019; 17: 289–298.

45. Hu Q, Liu F, Yan T, Wu M, Ye M, et al. MicroRNA5763p inhibits the migration and proangiogenic abilities of hypoxiatreated glioma cells through hypoxiainducible factor1alpha. Int. J. Mol. Med. 2019; 43: 2387–2397.
46. He J, Mai J, Li Y, Chen L, Xu H, et al. miR-597 inhibits breast cancer cell proliferation, migration and invasion through FOSL2. Oncol Rep. 2017; 37: 2672–2678.
47. Li S, Liu Z, Fang XD, Wang XY, Fei BY. MicroRNA (miR)-597-5p Inhibits Colon Cancer Cell Migration and Invasion by Targeting FOS-Like Antigen 2 (FOSL2). Front. Oncol. 2019; 9: 495.
48. Zhang Q, Hu H, Chen SY, Liu CJ, Hu FF, et al. Transcriptome and Regulatory Network Analyses of CD19-CAR-T Immunotherapy for B-ALL. Genom. Proteom. Bioinform. 2019; 17: 190–200.
49. Xu W, Hua Y, Deng F, Wang D, Wu Y, et al. MiR-145 in cancer therapy resistance and sensitivity: A comprehensive review. Cancer Sci. 2020; 111: 3122–3131.
50. Shi Q, Xing G, Qi M, Xing Y. Lower Serum miR-145 Predicts Poor Prognosis in Patients with Acute Myeloid Leukemia. Clin. Lab. 2020; 66: 7754.
51. Ishii H, Vodnala SK, Achyut BR, So JY, Hollander MC, et al. miR-130a and miR-145 reprogram Gr-1+CD11b+ myeloid cells and inhibit tumor metastasis through improved host immunity. Nat. Commun. 2018; 9: 2611.
52. Sheng Q, Zhang Y, Wang Z, Ding J, Song Y, et al. Cisplatin-mediated down-regulation of miR-145 contributes to up-regulation of PD-L1 via the c-Myc transcription factor in cisplatin-resistant ovarian carcinoma cells. Clin. Exp. Immunol. 2020; 200: 45–52.
53. Morris VA, Cummings CL, Korb B, Boaglio S, Oehler VG. Deregulated KLF4 Expression in Myeloid Leukemias Alters Cell Proliferation and Differentiation through MicroRNA and Gene Targets. Mol. Cell. Boil. 2016; 36: 559–573.
54. Jiang X, Bugno J, Hu C, Yang Y, Herold T, et al. Eradication of acute myeloid leukemia with FLT3 ligand-targeted miR-150 nanoparticles. Cancer Res. 2016; 76: 4470–4480.
55. Butrym A, Rybka J, Baczynska D, Tukiendorf A, Kuliczkowski K, et al. Low expression of microRNA-204

(miR-204) is associated with poor clinical outcome of acute myeloid leukemia (AML) patients. J. Exp. Clin. Cancer Res. 2015; 34: 68.
56. Xue F, Che H. The long non-coding RNA LOC285758 promotes invasion of acute myeloid leukemia cells by down-regulating miR-204-5p. FEBS Open Bio. 2020; 10: 734–743.
57. Xu X, Zhang F, Chen X, Ying Q. MicroRNA-518b functions as a tumor suppressor in glioblastoma by targeting PDGFRB. Mol. Med. Rep. 2017; 16: 5326–5332.
58. Hong BS, Ryu HS, Kim N, Kim J, Lee E, et al. Tumor suppressor microRNA-204-5p regulates growth, metastasis, and immune microenvironment remodeling in breast cancer. Cancer Res. 2019; 79: 1520–1534.
59. Zhang M, Zhou S, Zhang L, Zhang J, Cai H, et al. miR-518b is down-regulated, and involved in cell proliferation and invasion by targeting Rap1b in esophageal squamous cell carcinoma. FEBS Lett. 2012; 586: 3508–3521.
60. Di Meo A, Brown MD, Finelli A, Jewett MA, Diamandis EP, et al. Prognostic urinary miRNAs for the assessment of small renal masses. Clin. Biochem. 2020; 75: 15–22.
61. Xia W, Gong D, Qin X, Cai Z. MicroRNA-671-3p suppresses proliferation and invasion of breast cancer cells by targeting DEPTOR. Nan Fang Yi Ke Da Xue Xue Bao. 2020; 40: 42–48.
62. Yao Y, Zhou Y, Fu X. miR-671-3p is downregulated in non-small cell lung cancer and inhibits cancer progression by directly targeting CCND2. Mol. Med. Rep. 2019; 19: 2407–2412.
63. Li Z, Zhang Z, Bi H, Zhang Q, Zhang S, et al. Upregulated microRNA-671-3p promotes tumor progression by suppressing forkhead box P2 expression in non-small-cell lung cancer. Mol. Med. Rep. 2019; 20: 3149–3159.
64. Lu GF, You CY, Chen YS, Jiang H, Zheng X, et al. MicroRNA-671-3p promotes proliferation and migration of glioma cells via targeting CKAP4. OncoTargets Ther. 2018; 11: 6217–6226.
65. Zhu Z, Wen Y, Xuan C, Chen Q, Xiang Q, et al. Identifying the key genes and microRNAs in prostate cancer bone metastasis by bioinformatics analysis. FEBS Open Bio. 2020; 10: 674–688.

66. Hu QL, Xu ZP, Lan YF, Li B. miR-636 represses cell survival by targeting CDK6/Bcl-2 in cervical cancer. Kaohsiung J. Med. Sci. 2020; 36: 328–335.
67. Erdogan B, Facey C, Qualtieri J, Tedesco J, Rinker E, et al. Diagnostic microRNAs in myelodysplastic syndrome. Exp. Hematol. 2011; 39: 915–926.e2.
68. Zhao YJ, Song X, Niu L, Tang Y, Song X, et al. Circulating Exosomal miR-150-5p and miR-99b-5p as Diagnostic Biomarkers for Colorectal Cancer. Front. Oncol. 2019; 9: 1129.
69. Wang Z, Zhao Z, Yang Y, Luo M, Zhang M, et al. MiR-99b-5p and miR-203a-3p Function as Tumor Suppressors by Targeting IGF-1R in Gastric Cancer. Sci. Rep. 2018; 8: 10119.
70. Liu CJ, Huang FZ, Yang JH, Liu CP, Mao XH, et al. The role of miR-99b in mediating hepatocellular carcinoma invasion and migration. Eur. Rev. Med Pharmacol. Sci. 2018; 22: 2273–2281.
71. Chen S, Chen Y, Zhu Z, Tan H, Lu J, et al. Identification of the key genes and microRNAs in adult acute myeloid leukemia with FLT3 mutation by bioinformatics analysis. Int. J. Med Sci. 2020; 17: 1269–1280.
72. Ma X, Jin L, Lei X, Tong J, Wang R. MicroRNA-363-3p inhibits cell proliferation and induces apoptosis in retinoblastoma cells via the Akt/mTOR signaling pathway by targeting PIK3CA. Oncol. Rep. 2020; 43: 1365–1374.
73. Zhang L, Wang L, Lu N, Wang J, Yan R, et al. Micro RNA-363 inhibits esophageal squamous cell carcinoma progression by directly targeting sperm-associated antigen 5. J. Int. Med Res. 2020; 48.
74. Xie Y, Chen L, Gao Y, Ma X, He W, et al. miR-363 suppresses the proliferation, migration and invasion of clear cell renal cell carcinoma by downregulating S1PR1. Cancer Cell Int. 2020; 20: 227.
75. Zhang R, Li Y, Dong X, Peng L, Nie X. MiR-363 sensitizes cisplatin-induced apoptosis targeting in Mcl-1 in breast cancer. Med Oncol. 2014; 31: 347.
76. Zhang H, Zhang N, Wang R, Shao T, Feng Y, et al. High expression of miR-363 predicts poor prognosis and guides

treatment selection in acute myeloid leukemia. J. Transl. Med. 2019; 17: 106.
77. Smallwood DT, Apollonio B, Willimott S, Lezina L, Alharthi A, et al. Extracellular vesicles released by CD40/IL-4-stimulated CLL cells confer altered functional properties to CD4+ T cells. Blood. 2016; 128: 542–552.
78. Huber V, Vallacchi V, Fleming V, Hu X, Cova A, et al. Tumor-derived microRNAs induce myeloid suppressor cells and predict immunotherapy resistance in melanoma. J. Clin. Investig. 2018; 128: 5505–5516.
79. Liu J, Wang D, Long Z, Liu J, Li W. CircRNA8924 Promotes Cervical Cancer Cell Proliferation, Migration and Invasion by Competitively Binding to MiR-518d-5p /519-5p Family and Modulating the Expression of CBX8. Cell Physiol. Biochem. 2018; 48: 173–184.
80. Huang J, Cao D, Sha J, Zhu X, Han S. DLL3 is regulated by LIN28B and miR-518d-5p and regulates cell proliferation, migration and chemotherapy response in advanced small cell lung cancer. Biochem. Biophys. Res. Commun. 2019; 514: 853–860.
81. Organista-Nava J, Gómez-Gómez Y, Illades-Aguiar B, Alarcón-Romero LDC, Saavedra-Herrera MV, et al. High miR-24 expression is associated with risk of relapse and poor survival in acute leukemia. Oncol. Rep. 2015; 33: 1639–1649.
82. Ye S, Zhang H, Cai TT, Liu YN, Ni JJ, et al. Exosomal miR-24-3p impedes T-cell function by targetingFGF11and serves as a potential prognostic biomarker for nasopharyngeal carcinoma. J. Pathol. 2016; 240: 329–340.
83. Fayyad-Kazan H, Hamade E, Rouas R, Najar M, Fayyad-Kazan M, et al. Downregulation of microRNA-24 and -181 parallels the upregulation of IFN-gamma secreted by activated human CD4 lymphocytes. Hum. Immunol. 2014; 75: 677–685.
84. Lovat F, Nigita G, Distefano R, Nakamura T, Gasparini P, et al. Combined loss of function of two different loci of miR-15/16 drives the pathogenesis of acute myeloid leukemia. Proc. Natl. Acad. Sci. USA 2020; 117: 12332–12340.
85. Sun YP, Lu F, Han XY, Ji M, Zhou Y, et al. MiR-424 and miR-27a increase TRAIL sensitivity of acute myeloid

leukemia by targeting PLAG1. Oncotarget. 2016; 7: 25276–25290.
86. Tang LJ, Sun GK, Zhang TJ, Wu DH, Zhou JD, et al. Down-regulation of miR-29c is a prognostic biomarker in acute myeloid leukemia and can reduce the sensitivity of leukemic cells to decitabine. Cancer Cell Int. 2019; 19: 177.
87. Lim EL, Trinh DL, Ries RE, Wang J, Gerbing RB, et al. MicroRNA Expression-Based Model Indicates Event-Free Survival in Pediatric Acute Myeloid Leukemia. J. Clin. Oncol. 2017; 35: 3964–3977.
88. Han YX, You LS, Liu H, Mao LP, Ye X, et al. Apoptosis of acute myeloid leukemia HL-60 cells induced by CDK inhibitor SNS-032 and its molecular mechanisms. Zhejiang Da Xue Xue Bao Yi Xue Ban. 2015; 44: 174–178.
89. Xu P, Zhou D, Yan G, Ouyang J, Chen B. Correlation of miR-181a and three HOXA genes as useful biomarkers in acute myeloid leukemia. Int. J. Lab. Hematol. 2020; 42: 16–22.
90. Ma Y, Yan MX, Luo ZY. Expression of miR-181a in Acute Myeloid Leukaemia and Its Effect on Cell Proliferation. Zhongguo Shi Yan Xue Ye Xue Za Zhi. 2016; 24: 985–989.
91. Liu X, Liao W, Peng H, Luo X, Luo Z, et al. miR-181a promotes G1/S transition and cell proliferation in pediatric acute myeloid leukemia by targeting ATM. J. Cancer Res. Clin. Oncol. 2016; 142: 77–87.
92. Hua JY, Feng Y, Pang Y, Zhou XH, Xu B, et al. MiR-181a Promotes Proliferation of Human Acute Myeloid Leukemia Cells by Targeting ATM. Zhongguo Shi Yan Xue Ye Xue Za Zhi. 2016; 24: 347–351.
93. Guo Q, Luan J, Li N, Zhang Z, Zhu X, et al. MicroRNA-181 as a prognostic biomarker for survival in acute myeloid leukemia: a meta-analysis. Oncogene. 2017; 8: 89130–89141.
94. Nanbakhsh A, Visentin G, Olive D, Janji B, Mussard E, et al. miR-181a modulates acute myeloid leukemia susceptibility to natural killer cells. OncoImmunology. 2015; 4: e996475.
95. Okada H, Kohanbash G, Lotze MT. MicroRNAs in immune regulation—Opportunities for cancer immunotherapy. Int. J. Biochem. Cell Boil. 2010; 42: 1256–1261.

96. Papapetrou EP, Kovalovsky D, Beloeil L, Sant'Angelo D, Sadelain M. Harnessing endogenous miR-181a to segregate transgenic antigen receptor expression in developing versus post-thymic T cells in murine hematopoietic chimeras. J. Clin. Investig. 2009; 119: 157–168.
97. Kagoya Y, Nakatsugawa M, Saso K, Guo T, Anczurowski M, et al. DOT1L inhibition attenuates graft-versus-host disease by allogeneic T cells in adoptive immunotherapy models. Nat. Commun. 2018; 9: 1915.
98. Achberger S, Aldrich W, Tubbs R, Crabb JW, Singh AD, et al. Circulating immune cell and microRNA in patients with uveal melanoma developing metastatic disease. Mol. Immunol. 2014; 58: 182–186.
99. Vignard V, Labbé M, Marec N, André-Grégoire G, Jouand N, et al. MicroRNAs in Tumor Exosomes Drive Immune Escape in Melanoma. Cancer Immunol. Res. 2020; 8: 255–267.
100. Su R, Lin HS, Zhang XH, Yin XL, Ning HM, et al. MiR-181 family: Regulators of myeloid differentiation and acute myeloid leukemia as well as potential therapeutic targets. Oncogene. 2014; 34: 3226–3239.
101. Lim SP, Ioannou N, Ramsay AG, Darling D, Gäken J, et al. miR-181c -BRK1 axis plays a key role in actin cytoskeleton-dependent T cell function. J. Leukoc. Boil. 2018; 103: 855–866.
102. Le Dieu R, Taussig DC, Ramsay AG, Mitter R, Miraki-Moud F, et al. Peripheral blood T cells in acute myeloid leukemia (AML) patients at diagnosis have abnormal phenotype and genotype and form defective immune synapses with AML blasts. Blood. 2009; 114: 3909–3916.
103. Zhang Z, Xue Z, Liu Y, Liu H, Guo X, et al. MicroRNA-181c promotes Th17 cell differentiation and mediates experimental autoimmune encephalomyelitis. Brain Behav. Immun. 2018; 70: 305–314.
104. Li X, Liu L, Yang J, Yu Y, Chai J, et al. Exosome Derived From Human Umbilical Cord Mesenchymal Stem Cell Mediates MiR-181c Attenuating Burn-induced Excessive Inflammation. EBio Medicine. 2016; 8: 72–82.

105. Huang L, Tang X, Shi X, Su L. miR-532-5p promotes breast cancer proliferation and migration by targeting RERG. Exp. Ther. Med. 2019; 19: 400–408.
106. Zhang J, Zhou W, Liu Y, Liu T, Li C, et al. Oncogenic role of microRNA-532-5p in human colorectal cancer via targeting of the 5'UTR of RUNX3. Oncol. Lett. 2018; 15: 7215–7220.
107. Xu X, Zhang Y, Liu Z, Zhang X, Jia J. miRNA-532-5p functions as an oncogenic microRNA in human gastric cancer by directly targeting RUNX3. J. Cell. Mol. Med. 2016; 20: 95–103.
108. Lin X, Ling Q, Lv Y, Ye W, Huang J, et al. Plasma exosome-derived microRNA-532 as a novel predictor for acute myeloid leukemia. Cancer Biomarkers. 2020; 28: 151–158.
109. Ibrahim S, Szóstek-Mioduchowska A, Skarzynski DJ. Expression profiling of selected miRNAs in equine endometrium in response to LPS challenge in vitro: A new understanding of the inflammatory immune response. Veter. Immunol. Immunopathol. 2019; 209: 37–44.
110. Shomali N, Mansoori B, Mohammadi A, Shirafkan N, Ghasabi M, et al. MiR-146a functions as a small silent player in gastric cancer. Biomed. Pharmacother. 2017; 96: 238–245.
111. Emming S, Chirichella M, Monticelli S. MicroRNAs as modulators of T cell functions in cancer. Cancer Lett. 2018; 430: 172–178.
112. Gagnon JD, Kageyama R, Shehata HM, Fassett MS, Mar DJ, et al. miR-15/16 Restrain Memory T Cell Differentiation, Cell Cycle, and Survival. Cell Rep. 2019; 28: 2169–2181e4.
113. Singh Y, Garden OA, Lang F, Cobb BS. MicroRNA-15b/16 Enhances the Induction of Regulatory T Cells by Regulating the Expression of Rictor and mTOR. J. Immunol. 2015; 195: 5667–5677.
114. Yao X, Tu Y, Xu Y, Guo Y, Yao F, et al. Endoplasmic reticulum stress-induced exosomal miR-27a-3p promotes immune escape in breast cancer via regulating PD-L1 expression in macrophages. J. Cell. Mol. Med. 2020; 24: 9560-9573.

115. Fan X, Wang J, Qin T, Zhang Y, Liu W, et al. Exosome miR-27a-3p secreted from adipocytes targets ICOS to promote antitumor immunity in lung adenocarcinoma. Thorac. Cancer. 2020; 11: 1453–1464.
116. Wang Y, Zhang X, Li H, Yu J, Ren X. The role of miRNA-29 family in cancer. Eur. J. Cell Boil. 2013; 92: 123–128.
117. Schmitt M, Margue C, Behrmann I, Kreis S. MiRNA-29: A microRNA Family with Tumor-Suppressing and Immune-Modulating Properties. Curr. Mol. Med. 2013; 13: 572–585.
118. Chandiran K, Lawlor R, Pannuti A, Perez GG, Srinivasan J, et al. Notch1 primes CD4 T cells for T helper type I differentiation through its early effects on miR-29. Mol. Immunol. 2018; 99: 191–198.

Book Chapter

Dihydropyrimidinase Protects from DNA Replication Stress Caused by Cytotoxic Metabolites

Jihane Basbous[1]*, Antoine Aze[1], Laurent Chaloin[2], Rana Lebdy[1], Dana Hodroj[1,3], Cyril Ribeyre[1], Marion Larroque[1,4], Caitlin Shepard[5], Baek Kim[5], Alain Pruvost[6], Jérôme Moreaux[1], Domenico Maiorano[1], Marcel Mechali[1] and Angelos Constantinou[1]*

[1]Institute of Human Genetics (IGH), CNRS, Universit´e de Montpellier, France
[2]Institut de Recherche en Infectiologie de Montpellier, CNRS, Universit´e de Montpellier, France
[3]Cancer Research Center of Toulouse (CRCT), France
[4]Institut du Cancer de Montpellier (ICM), France
[5]School of Medicine, Emory University, USA
[6]Service de Pharmacologie et Immunoanalyse (SPI), Plateforme SMArt-MS, CEA, INRA, Universit´e Paris-Saclay, France

***Corresponding Authors:** Jihane Basbous, Institute of Human Genetics (IGH), CNRS, Universit ´e de Montpellier, 34396 Montpellier Cedex 5, France

Angelos Constantinou, Institute of Human Genetics (IGH), CNRS, Universit ´e de Montpellier, 34396 Montpellier Cedex 5, France

Published **July 05, 2021**

This Book Chapter is a republication of an article published by Angelos Constantinou, et al. at Nucleic Acids Research in February 2020. (Jihane Basbous, Antoine Aze, Laurent Chaloin, Rana Lebdy, Dana Hodroj, Cyril Ribeyre, Marion Larroque, Caitlin Shepard, Baek Kim, Alain Pruvost, Jérôme Moreaux, Domenico Maiorano, Marcel Mechali, Angelos Constantinou, Dihydropyrimidinase protects from DNA replication stress

caused by cytotoxic metabolites, Nucleic Acids Research, Volume 48, Issue 4, 28 February 2020, Pages 1886–1904, https://doi.org/10.1093/nar/gkz1162. License Number: 5070940465272)

How to cite this book chapter: Jihane Basbous, Antoine Aze, Laurent Chaloin, Rana Lebdy, Dana Hodroj, Cyril Ribeyre, Marion Larroque, Caitlin Shepard, Baek Kim, Alain Pruvost, Jérôme Moreaux, Domenico Maiorano, Marcel Mechali, Angelos Constantinou. Dihydropyrimidinase Protects from DNA Replication Stress Caused by Cytotoxic Metabolites. In: Hussein Fayyad Kazan, editor. Immunology and Cancer Biology. Hyderabad, India: Vide Leaf. 2021.

Data Availability: Mendeley
data: https://data.mendeley.com/datasets/dssp4hdnw3/draft?a=7e48f805-d946-43bd-bd2d-f6cb080797b2.

Acknowledgements: We thank Helena Sapede, Julie Devin, Touffic Kassouf, Lucile Broseus and Olivier Ganier for technical help, Ketan J Patel, Bruno Vaz and Kristijan Ramadan for helpful discussion and members of the laboratory for critical reading of the manuscript.

Funding: Fondation ARC pour la recherche sur le cancer [PGA1 RF20180206787 to A.C]; l'Institut National du Cancer [INCa121770 to J.M., A.C.]; MSD Avenir (to A.C., D.M., M.M.); SIRIC Montpellier Cancer Grant [INCa_Inserm_DGOS_12553 to A.C.]; USA NIH Grants [AI136581, NIH AI150451USA to B.K.]; INSERM Plan Cancer (to D.M.); French National Research Agency [ANR-10-INBS-04; «Investments for the future» (to the Imaging facility MRI). Funding for open access charge: Fondation ARC pour la recherche sur le cancer [PGA1 RF20180206787].

Conflict of Interest Statement: None declared.

Abstract

Imbalance in the level of the pyrimidine degradation products dihydrouracil and dihydrothymine is associated with cellular transformation and cancer progression. Dihydropyrimidines are degraded by dihydropyrimidinase (DHP), a zinc metalloenzyme that is upregulated in solid tumors but not in the corresponding normal tissues. How dihydropyrimidine metabolites affect cellular phenotypes remains elusive. Here we show that the accumulation of dihydropyrimidines induces the formation of DNA–protein crosslinks (DPCs) and causes DNA replication and transcriptional stress. We used Xenopus egg extracts to recapitulate DNA replication *invitro*. We found that dihydropyrimidines interfere directly with the replication of both plasmid and chromosomal DNA. Furthermore, we show that the plant flavonoid dihydromyricetin inhibits human DHP activity. Cellular exposure to dihydromyricetin triggered DPCs-dependent DNA replication stress in cancer cells. This study defines dihydropyrimidines as potentially cytotoxic metabolites that may offer an opportunity for therapeutic-targeting of DHP activity in solid tumors.

Introduction

Adjustments in metabolic activities are required to satisfy high metabolic demands associated with cancer cell proliferation [1]. Alterations in nucleotide metabolisms are emerging as distinctive features of cancers cells. While nucleotide bases may be limiting for cancer cells proliferation [2], accumulating evidence suggests that carcinogenesis is associated with metabolic rewiring of the pyrimidine catabolic pathway [3–6]. Whether and how rewiring of the pyrimidine catabolic pathway supports tumor progression, however, remains poorly defined.

In humans, the pyrimidines uracil and thymine are degraded in three enzymatic steps (Figure 1A). First, dihydropyrimidine dehydrogenase (DPD) reduces the pyrimidine ring of uracil and thymine with hydrogen and yields 5, 6-dihydrouracil and 5, 6-

dihydrothymine (dihydropyrimidines). Second, the saturated rings between position 3 and 4 are opened by dihydropyrimidinase (DHP). Third, β-ureidopropionase (BUP-1) degrades the β-ureidopropionic acid and β-ureidoisobutyric acid products formed by DHP into β-alanine and β-aminoisobutyric acid. DPD activity has been detected in all tissues examined, but the activity of DHP and BUP-1 is essentially restricted to the liver and the kidney [7]. In cancer cells, however, the level of pyrimidine degradation activities is considerably altered. Increased expression of DPD has been observed in human hepatocellular carcinoma [8]. Human skin cutaneous melanomas progressing toward metastatic tumors accumulate mutations in DPD and up-regulate the expression of the genes encoding DPD and DHP [6]. The accumulation of 5, 6-dihydrouracil is a distinct metabolic feature of early lung adenocarcinoma [5]. Intriguingly, an increase in the concentration of dihydropyrimidines in epithelial breast cancer cells supports the acquisition of aggressive mesenchymal characteristics [4]. How dihydropyrimidines affect cellular phenotypes, however, remains elusive. Pioneering studies have identified DHP activity as a good marker of tumorigenicity and a target for cancer therapy [3]. Whereas hardly detectable in normal extrahepatic and kidney tissues (van Kuilenburg *et al.*, [7]), the activity of DHP is strikingly high in human carcinomas of the lung, colon, pancreas, salivary gland and stomach [3].

Another hallmark of cancer is DNA replication stress causing genomic instability [1,9]. Stress in the context of DNA replication is defined as the slowing or stalling of DNA chain elongation [10]. Known sources of DNA replication stress include nucleotides insufficiency [11], misincorporated nucleotides [12,13], replication/transcription conflicts [14–16] and DNA lesions caused by reactive metabolic products such as reactive oxygen species and aldehydes [17–19]. Furthermore, cellular metabolites can yield structurally diverse DNA–protein crosslinks (DPCs) that precipitate the loss of cellular functions [20].

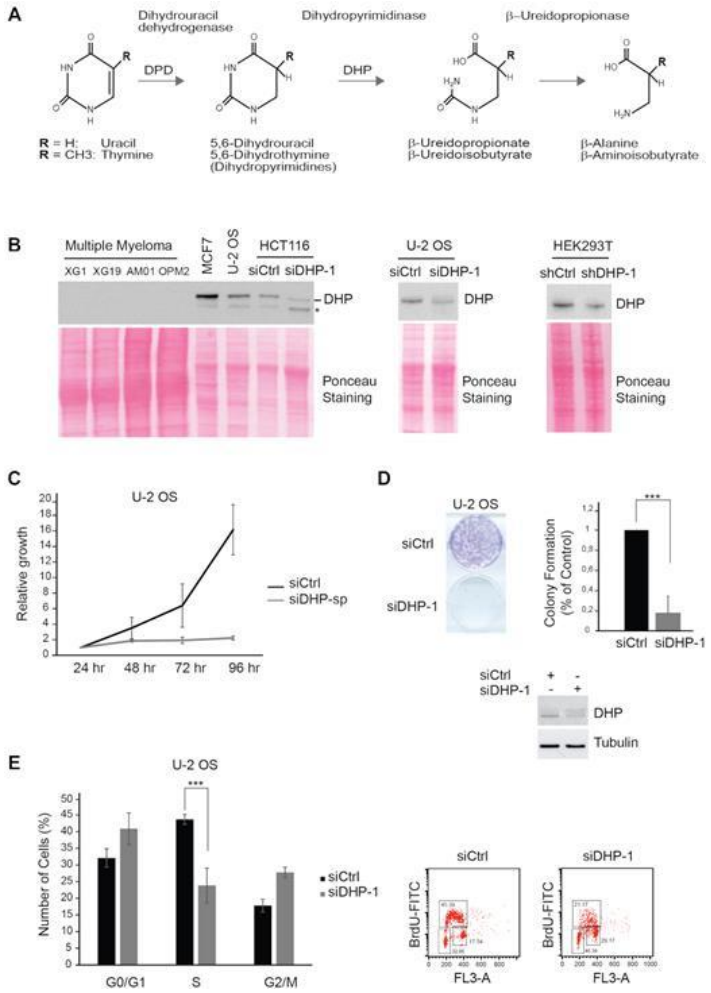

Figure 1: Depletion of DHP impairs the proliferation of epithelial cancer cells. (**A**) Schematic representation of the pyrimidine degradation pathway. (**B**) DHP was probed by western blotting in the indicated transformed cells. When indicated, DHP was knocked down using anti-DHP siRNA or shRNA molecules with distinct target sequences. Ponceau staining was used as loading control. * non-specific signal. One representative experiment is shown from three to six biological replicates. (**C**) U-2 OS cells were transfected with control or anti-DHP siRNA (siDHP-sp) and their viability was assessed during 4 days using the MTT cell growth assay. Mean viability is representative of three independent biological replicates. Error bars represent ±S.D. (**D**) Colony-forming assay of U-2 OS cells after transfection with control or anti-DHP siRNA (siDHP-1). A representative image is shown. An histogram represents the quantification of colony formation. Data shown are averages over three

independent biological replicates with two technical replicates for each. Error bars represent ±S.D. *P*-values were calculated using a regression model with Poisson distribution: ***$P < 0.0001$. Bottom panel: the efficiency of DHP knockdown was assessed by western blotting. (**E**) Histogram representing the percentage of U-2 OS cells, 72 h after transfection with control or anti-DHP siRNA (siDHP-1) in G0/G1, S and G2/M phases. Data shown are averages over three independent biological replicates. Error bars represent ±S.D. *P*-values were calculated using a regression model with Poisson distribution: ***$P < 0.0001$.

DNA replication stress in cancer cells is exploited therapeutically with the use of inhibitors of the DNA damage response [21,22]. DNA replication stress induces the accumulation of 70–500 long nucleotide stretches of single-stranded DNA [23–25], which trigger a protein kinase cascade orchestrated by the checkpoint kinase ATR and its effector kinase Chk1 [26–29]. ATR signaling promotes cell and organismal survival through coordination of DNA repair and DNA replication with cell physiological processes including cell-cycle progression and transcription [30].

We show here that suppression of DHP in cancer cell lines induces DNA replication stress, as revealed by the accumulation of single-stranded DNA, by the induction of ATR/Chk1 signaling and by the slowing of replication fork progression. Depletion of DHP also attenuates transcription activity, stabilizes p53 and eventually blocks cell proliferation. The addition of dihydropyrimidines to Xenopus egg-extracts induces the formation of abnormal DNA replication products. In DHP-depleted cells, DNA replication and transcriptional stress correlate with the accumulation of DPCs. Thus, we suggest that dihydropyrimidines yield DPCs that directly interfere with DNA-templated processes. We found that the flavonoid dihydromyricetin inhibits the activity of purified human DHP. Addition of dihydromyricetin in the cell culture medium induces the accumulation of DPCs and interferes with the progression of replication forks. These findings indicate that unless degraded by dihydropyimidinase, the amount of dihydropyrimidines produced in cancer cell cultures is sufficient to block DNA templated processes.

Materials and Methods

Cell Lines, Plasmids and Chemicals

U-2 OS, HEK293T and MCF7 were grown under standard conditions in Dulbecco's modified Eagle's medium (DMEM) (Invitrogen) supplemented with 10% fetal bovine serum (FBS) and 1% penicillin/streptomycin (P/S). HCT116 (Horizon Discovery Ltd.) were cultured in McCoy's 5A modified Medium (Sigma-Aldrich) supplemented with 10% FBS and 1% P/S. HEK293 cells were cultured in RPMI (Invitrogen) supplemented with 10% FBS and 1% P/S. HEK293 cells expressing wild-type and the translocase dead FANCM mutant protein are as described previously [31]. XG1 and XG19 IL6 dependent human myeloma cell lines (HMCLs) were obtained as previously described [32]. AMO-1 and OPM2 were purchased from DSMZ (Braunsweig, Germany). These HMCLs were routinely maintained in RPMI 1640 and 10% fetal calf serum (FCS; Biowittaker, Walkersville, MD), supplemented with 3 ng/ml IL-6 (Peprotech, Rocky Hill, NJ, USA) for IL6 dependent cell lines. HMCLs were authenticated according to their short tandem repeat profiling and their gene expression profiling using Affymetrix U133 plus 2.0 microarrays deposited in the ArrayExpress public database under accession numbers E-TABM-937 and E-TABM-1088. Dihydrouracil, Uracil, Dihydromyricetin, Aphidicolin and Roscovitine were purchased from Sigma-Aldrich. Formaldehyde was purchased from VWR chemicals. Embryomax nucleosides (100X) (cytidine, 0.73 g/l; guanosine, 0.85 g/l; uridine, 0.73 g/l; adenosine, 0.8 g/l; thymidine, 0.24 g/l) was purchased from Millipore. pDONR223-DPYS was obtained through MGC Montpellier Genetic Collections and cloned into destination vectors using gateway technology (Invitrogen).

Antibodies

Primary antibodies were purchased from Abcam (Histone H3, p53, DNA polymerase eta, nucleolin, FANCD2), Bethyl Laboratories (RPA32-Ser33, RPA32-Ser4/S8, DNA polymerase kappa, XPA, ERCC5/XPG), Calbiochem (RPA32), Cell Signaling Technology (Chk1-Ser345, Ubiquityl-PCNA

(Lys164)), ElabScience (SPRTN, UPP1), ProteinTech Group (DPYS), Santa Cruz Biotechnology (Chk1, HA), Sigma-Aldrich (α-Tubulin, DPYD, PCNA). Xenopus polymerase η antibody was previously described [33]. The Mouse anti-RNA-DNA hybrid S9.6 hybridoma was purchased from ATCC. Orc2 antibodies were kindly provided by Dr Marcel Mechali (Institute of Human Genetics). The FANCA antibody was a gift from the Fanconi anemia research fund and the anti-FANCM antibody was a gift from Weidong Wang (NIH). Secondary antibodies (anti-rabbit-HRP and anti-mouse-HRP) were from Promega

DHP Bacterial Protein Expression and Purification

DPYS was cloned into the pET-28a (+) (Novagen) vector containing an N-terminal 6×His tag. The protein was overexpressed in *Escherichia coli* BL21(DE3) host cells and induced by 1 mM Isopropyl β-D-1-thiogalactopyranoside (IPTG) (Sigma-Aldrich) for 3 h in presence of 1 mM ZnCl2. Cells were lysed with Buffer A (50 mM Potassium Phosphate pH 7.5, 150 mM NaCl, 0.1% NP40, 15 mM Imidazol (Sigma-Aldrich)) and protease inhibitors (Roche). Extracts were incubated for 30 min at 4°C and harvested at 28 000 rpm for 1 h. The soluble supernatant fraction was purified on a 5 ml HisTrap HP column (GE Healthcare) using the AKTA protein purification system (GE Healthcare). The column was washed with 10 column volumes of Buffer A with 60 mM Imidazol. Bound protein was eluted from the column using Buffer A with 250 mM Imidazol. The fractions corresponding to each peak in the chromatogram were dialysed against buffer containing 50 mM Tris HCl pH 7.5, 150 mM NaCl, 1 mM DTT and 10% glycerol.

RNA Interference and Transfection

ON-TARGET plus siRNA Human DPYS siRNA SMARTpool (siDHP-SP) (L-008455-00), ON-TARGET plus siRNA Human DPYS (siDHP-1) (J-008455-07) (GCACAGAUGGCACUCACUA), siGENOME SMARTpool Human DPYD (M-008376-02), ON-TARGETplus FANCM siRNA (L-021955-00), siGENOME SMARTpool Human FANCD2 (M-016376-02), siGENOME SMARTpool Human

FANCA (M-019283-02), siGENOME SMARTpool Human SPRTN (M-015442-02), siGENOME SMARTpool Human XPA (M-005067-01), siGENOME SMARTpool Human ERCC5 (M-006626-01), siGENOME SMARTpool Human UPP1 (M-006647-01), siGENOME Non-targeting Control siRNA pool 2 (D-001206-14) and ON-TARGET plus Non-Targeting Pool (D-001810-10), were purchased from Dharmacon. siDHP-2 (GAAUAGCUGUAGGAUCAGATT) was purchased from Eurofins MWG. shDHP-3: DPYS MISSION plasmid (Sigma Aldrich, TRC0000046747), target sequence (TGTGGCAGTTACCAGCACAAA) and shDHP-4: DPYS MISSION plasmid (Sigma-Aldrich, TRC0000046744), target sequence (CTAATGATGATCTAACCACAA). Puro-shRNA FANCM used was described in [34]. SiRNAs were transfected with INTERFERin (Polyplus), shRNA with Lipofectamine 2000 (Invitrogen). Plasmids encoding cDNAs were transfected using jetPEI or jetPRIME reagent (Polyplus).

Small-Scale Chromatin Fractionation Assay and Western Blotting

As described [35], cells were collected, washed with phosphate-buffered saline (PBS), and resuspended in buffer A (10 mM HEPES [pH 7.9], 10 mM KCl, 1.5 mM $MgCl_2$, 0.34 M sucrose, 10% glycerol, 1 mM dithiothreitol (DTT), and protease inhibitors (Roche)). Triton X-100 was added (0.1% final concentration), the cells were incubated on ice for 5 min, and nuclei were collected by centrifugation (5 min, 1300 × *g*, 4°C). The supernatant (Cytosolic fraction) was clarified by high-speed centrifugation (5 min, 20 000 × *g*, 4°C), and the supernatant (Cytosolic fraction) was collected. The nuclei were then washed once in buffer A and lysed for 30 min in buffer B (3 mM ethylenediaminetetraacetic acid (EDTA), 0.2 mM Ethylene Glycol Tetraacetic Acid (EGTA), 1 mM DTT and protease inhibitor (Roche)), and insoluble chromatin and soluble fractions (Nucleosolic fraction) were separated by centrifugation (5 min, 17 000 × *g*, 4°C). The insoluble chromatin fraction was washed twice with buffer B and resuspended in sodium dodecyl sulphate (SDS)-Laemmli buffer and boiled for 10 min. Western blotting was performed using the ECL procedure according to the

manufacturer's instructions (Amersham Bioscience, Inc) using anti-mouse or rabbit-HRP secondary antibodies (Promega)

Immunofluorescence Staining and ssDNA Detection

Cells grown on coverslips were fixed with 3.7% paraformaldehyde (PFA) in PBS for 15 min at RT followed by a 0.5% Triton X-100-PBS permeabilization step for 10 min. Cells were then blocked in PBS containing 3% bovine serum albumin (BSA) for 30 min and incubated in the primary antibody and then in the appropriate secondary antibodies Alexa Fluor 488 or Alexa Fluor 555 (Invitrogen), diluted in blocking solution for 1 h in a humidified chamber at RT. DNA was stained with Hoechst (Invitrogen) and coverslips were mounted on glass slides with Prolong (Sigma-Aldrich).

For ssDNA detection, cells were grown on microscopic slides in 20 μM BrdU for 24 hr. Primary mouse antibody against BrdU in ssDNA was used (BD). All the Microscopic analysis was performed using Zeiss Z2 Axioimager with ApoTome. ImageJ was used for picture processing and quantification of S9.6 mean intensity.

DNA Fiber Labeling

DNA fiber spreads were prepared as described previously [36]. Cells were labeled with 25 μM IdU (5-iodo-2′-deoxyuridine), washed with warm media and then exposed to 50 μM CldU (5-Chloro-2′-deoxyuridine). Cells were lysed with the spreading buffer (200 mM Tris–HCl pH 7.5, 50 mM EDTA and 0.5% SDS) and DNA fiber were stretched onto glass slides. The DNA fibers were denatured with 2.5 M HCl for 1 h, washed with PBS and blocked with 2% BSA in PBS-Tween 20 for 60 min. IdU replication tracts were revealed with a mouse anti-BrdU/IdU antibody (BD Bioscience) and CldU tracts with a rat anti-BrdU/CldU antibody (Abcam). DNA fibers were uniformly labeled with a mouse anti-human single-stranded DNA antibody (Millipore). The secondary antibodies used for the assay were: alexa fluor 488 anti-mouse antibody (Life technologies), alexa fluor 647 anti-mouse antibody (Life technologies) and Cy3 anti-

rat antibody (Jackson Immunoresearch). Replication tracts were analyzed with ImageJ software. The probability that two datasets stem from the same distribution was assayed by a non-parametrical Mann–Whitney test (Prism Software).

Fluorescence-Activated Cell Sorting (FACS)

Cells were pulse labeled with 10 μM BrdU for 15 min before fixation with ice-cold 100% ethanol. Then cells were incubated with PBS and 50 μg/ml of RNase A for 1 h at 37°C. After treatment with 2N HCl for 30 min, cells were incubated with an anti-BrdU antibody (BD) for 1 h at RT and then with an FITC-conjugated anti-mouse IgG (Life Technologies) at RT for 30 min. Cells were stained with 25 μg/ml of propidium iodide in PBS and analyzed using a FACSCalibur machine (BD).

Enzyme Assay

5, 6-Dihydrouracil (DHU) was used as the substrate in the standard assay of DHP. Briefly, 2.5 μg of purified His-tagged DHP was added to 200 μl of 5, 6-dihydrouracil (50 μM) solution containing 50 mM Tris, 50 μM DTT, pH 8.0 in presence of several concentrations of dihydromyricetin, the samples were then incubated at 37°C for 1 h. An aliquot (100 μl) from each point was taken before incubation as a control without enzymatic reaction. DHU decomposition was monitored by HPLC using a Waters Alliance system connected to a C18 reversed phase Symmetry column (4.6 × 150 mm, 5 μm, Waters). Elution of DHU was achieved by applying an isocratic flow of H_2O/TFA 0.1% as mobile phase for 15 min using a flow rate of 1 ml/min. For each sample, the column was first washed with 20% CH_3CN/TFA 0.1% to remove any residual dihydromyricetin and equilibrated again with elution phase for 10 min. Under these conditions DHU was eluted at 2.8 min and detected by absorbance at 230 nm. Quantification of DHU was performed by integration of the corresponding HPLC peak using Empower Pro software. IC_{50} calculation was performed using Grafit-7 (Erithacus Software).

Intracellular dNTP Measurement

For dNTP analysis and quantification, siRNA or shRNA transfected cells were harvested and lysed in iced cold 65% methanol, and vigorously vortexed for 2 min. Extracts were incubated at 95°C for 3 min. Supernatants were collected and dried in a speed vacuum. Samples were processed in Kim Baek laboratory for the single nucleotide incorporation assay as described [37].

Metabolite Extraction

Cells pellet (1 million cells) were extracted on dry ice in 0.5 ml cold 70% methanol. The cell mixtures were shaken vigorously on a Vortex mixer for 10 min. These extracts were then centrifuged at 20 000 g at +4°C for 10 min, and the supernatants were transferred into polypropylene tubes for evaporation with a turbovap evaporator (Biotage, France). Dried extracts were reconstituted in 50 µl of mobiles phases A/B; 9/1. Five microliter of this sample was injected in the LC-MS/MS system. For LC Analysis: An UPLC Acquity I Class (Waters, France) was used for this study. The chromatographic separation was perform onto an Acquity UPLC BEH HSS T3 column (150 × 2.1 mm, 1.8 µm) using a gradient from 0.5%formic acid in water/0.5% formic acid in acetonitrile; 9/1; v/v as initial conditions to 6/4; v/v from 0.5 min to 3 min at a flow rate of 0.3 ml/min. The run time was 5 min allowing the system to reach 100% of 0.5% formic acid in acetonitrile to rinse the column and return to initial mobile phase conditions. The autosampler and the column compartment were held at 4°C and 30°C, respectively. Under these conditions, uracil and dihydrouracil displayed a mean retention time of 1.33 and 1.34 min, respectively. For MS Analysis, the UPLC system was coupled to a Waters XEVO™ TQ-XS mass spectrometer (Waters, France) operating in positive ion mode. For pyrimidine detection, the capillary voltage was set to 2.5 kV. The source and desolvation temperatures were held at 150°C and 600°C, respectively. The cone and desolvation gas flow were set at 150 and 800 l/h, respectively. The MS data acquisition was performed in multiple reaction monitoring (MRM) mode. Monitored MRM transitions were m/z 112.93 > 69.96 and

114.98 > 72.91 for uracil and dihydrouracil, respectively. Range of calibration curves were 0.28–108 and 0.27–110 nmol/cell pellet for uracil and dihydrouracil, respectively.

Cell Viability and Colony Forming Assay

The effect of siRNA on cell proliferation was measured using the CellTiter-Glo® Luminescent Cell Viability Assay Kit (Promega) according to the manufacturer's protocol or using the MTT cell growth assay. Briefly, siRNA transfected cells were seeded in 96-well plate and 4 days later, 100 µl CellTiter-Glo® reagent was added to each well that contained 100 µl cell culture medium. Cells were then lysed by shaking in an orbital shaker for 2 min, followed by incubation at room temperature for 10 min to stabilize the luminescent signal. The luminescent intensity was recorded on a Tristar LB 941 Multimode Microplate Reader (Berthold Technologies). For the MTT assay, siRNA-transfected cells were seeded into 24-well plates and cell growth was documented every 24 h via a colorimetric assay using a 3-(4,5-dimethylthiazol-2-yl)-2,5-diphenyltetrazolium bromide (MTT) assay (Sigma-Aldrich). Absorbance values were collected at 600 nm using a BioPhotometer (Eppendorf). In each individual experiment, proliferation was determined in triplicate and the overall experiment was repeated three times. For colony formation analysis, cells were seeded in 6-well plates at a density of 5000 cells per well. The medium was changed every 3 days for 10 days until visible colonies formed. Colonies were fixed in methanol for 10 min and stained with crystal violet.

Transcription Assay

siRNA transfected cells were grown on cover slips and incubated with EU for 20 min. Cells were fixed with 4% paraformaldehyde for 15 min and permeabilized for 20 min in 0.1% Triton X-100 in PBS. EU incorporation were detected by staining with the Click-it Edu Alexa Fluor 555 azide Imaging Kit (Invitrogen) according to the manufacturer's instructions and DNA was stained with Hoechst (Invitrogen). The intensity of staining within individual nuclei was quantified using Image J software.

X. laevis Egg Extracts Preparation and DNA Replication Kinetics

Low Speed Egg extracts (LSE) were prepared as previously described [38]. M13 replication kinetics was assessed using 500 ng of M13mp18 single-stranded DNA (New England BioLabs) per 50 µl of LSE supplemented with cyclohexymide (250 µg/ml), an energy regeneration system (1 mM ATP, 2 mM $MgCl_2$, 10 mM creatine kinase, 10 mM creatine phosphate) and α-[^{32}P]-dCTP (0.37 MBq). Chromosomal DNA replication was assessed by adding 1000 demembranated *Xenopus laevis* sperm nuclei per microliters of extract. The mixtures were incubated at 23°C for the indicated time, then samples were neutralized in 10 mM Tris-HCl pH 8.0, 10 mM EDTA, 0.5% SDS, 200 µg/ml Proteinase K (Sigma-Aldrich) and incubated at 52°C for 1 h. Incorporation of radiolabeled deoxynucleotides in DNA was monitored using a Phosphor Imager Typhoon TriO+ (Amersham Biosciences) following agarose gel electrophoresis or alkaline agarose gel electrophoresis of purified DNA.

Sperm chromatin purification was performed as previously described [39]. Briefly, egg extracts supplemented with demembranated sperm nuclei were diluted 10-fold in ice cold XB (10 mM Hepes-KOH pH 7.7, 100 mM KCl, 2 mM $MgCl_2$, 50 mM sucrose and protease inhibitor) and pelleted at 1500 *g* for 5 min. Nuclei were washed once in XB buffer and then detergent extracted with 0.1% NP40 for 5 min on ice. Chromatin was recovered after centrifugation and ressuspended in Laemmli buffer for western blot analysis. For the chromatin transfer experiments, chromatin samples were incubated for 30 min in the first extract with the indicated drugs (Figure 4D). Purification for chromatin transfers and isolation of nuclei were performed following the protocol detailed in [40]. Isolated nuclei integrity was verified by microscopy and then transferred into fresh extract supplemented with geminin and Roscovitine (to inhibit new replication events) together with α-[^{32}P]-dCTP. After 2 h, dCTP incorporation was monitored by autoradiography on neutral gel as described previously.

DNA–Protein Crosslinks Isolation and Detection

DPCs isolation DPCs were prepared as described in [41]. In brief, 1.5 to 2 × 10^6 cells were lysed in 1 ml of M buffer (MB), containing 6 M GTC, 10 mM Tris–HCl (pH 6.8), 20 mM EDTA, 4% Triton X-100, 1% Sarkosyl and 1% DTT. DNA was precipitated by adding 1 ml of 100% ethanol and was washed three times in wash buffer (20 mM Tris–HCl pH 6.8, 150 mM NaCl and 50% ethanol) and DNA was solubilized in 1 ml of 8 mM NaOH. A small aliquot of the recovered DNA was digested with 50 µg/ml proteinase K (Invitrogen) for 3 h at 50°C and quantified using Qubit dsDNA HS Assay Kit (Invitrogen) according to manufacturer instructions. DNA concentration was further confirmed by slot-blot where the proteinase K digested samples were diluted in TBS buffer and applied to nylon membrane (Hybond N+) followed by immunodetection with antibody against dsDNA.

The remaining solubilized DNA was digested with Benzonase (Sigma-Aldrich) for 30 min at 37°C. Proteins were precipitated by standard Trichloroacetic Acid (TCA) protocol. At last, the crosslinked-proteins were resuspended with the appropriate buffer and total DPCs were analyzed by Silver Staining (Invitrogen) as recommended by the manufacturer after electrophoretic separation on polyacrylamide gels and specific crosslinked-proteins were immunodetected using western blot assay. Signals were quantified using Image J software. Alternatively, proteins recovered by RADAR were analyzed by mass spectrometry as described previously [42]. Analysis of raw files were performed using MaxQuant [43] version 1.6.3.3 using default settings with label-free quantification option enabled. Raw file spectra were searched against the human UniProt reference database. Protein, peptide, and site false discovery rate (FDR) were adjusted to 0.01.

Statistical Analysis

Biological replicates were experiments performed independently of each other to test biological variation. Technical replicates

were performed during one biological replicate to test variation of the measuring equipment and protocols.

For replication tracks analyses, the probability that two data sets stem from the same distribution was assayed by a non-parametrical Mann–Whitney test using the GraphPad Prism 5 software Prism software. To determine whether an siRNA treatment significantly increased or decreased the percentage of events by comparing the siRNA-treated cells to siRNA-control cells, p values were calculated with the open-source R software package (www.r-project.org) using a generalized linear model with Poisson distribution. The test used and p values are indicated in figure legends.

Results

Suppression of DHP Induces DNA Replication Stress and Inhibits Cell Proliferation

DHP is mainly expressed in the liver and the kidney [7]. Yet, we detected DHP in the epithelial cancer cells MCF7 (breast adenocarcinoma), U-2 OS (osteosarcoma), HCT116 (colorectal carcinoma) and HEK293T (embryonic kidney) (Figure 1B). We also detected DHP in hTERT-immortalized retinal pigment epithelial cells (hTERT RPE-1) and in primary human dermal fibroblasts (HDF) (Supplementary Figure S1A), suggesting that regardless of their transformation status, certain types of cells express DHP when cultured *in vitro*. By contrast, DHP was not detectable in multiple myeloma cells (Figure 1B), consistent with the absence of DHP activity in hematopoietic malignant cells [3]. The knockdown of DHP by means of siRNA in HCT116, U-2 OS and HEK293T cells confirmed the specificity of the anti-DHP signal (Figure 1B).

As DHP is produced in different epithelial cancer cells, we set out to explore the phenotypic consequences of DHP depletion. Depletion of DHP in U-2 OS cells blocked cell proliferation measured by colorimetric and by colony forming assays (Figure 1C and D). In addition, suppression of DHP by either one of two anti-DHP siRNAs with different target sequences impaired the growth of HCT116 cells (Supplementary Figure

S1B), but not of the multiple myeloma cell line AMOI, that does not express DHP (Supplementary Figure S1C). We used also two plasmids encoding shRNAs with different target sequences to exclude potential off-target effects caused by the seed region of siRNAs [44]. Using this strategy, we suppressed DHP in HEK293T cells and observed severely compromised cell viability and proliferation (Supplementary Figure S1D and E). Together, these observations confirm that growth inhibition induced by DHP depletion is not a singular property of U-2 OS cells. Because DHP is essential for the proliferation of these cancer cell lines, we surmised that it was not possible to generate *DPYS* (encodes DHP) knockouts cell lines by CRISPR/CAS9 genome editing to explore the function of DHP.

Flow cytometry cell-cycle analyses 72-h post-transfection revealed alterations in the cell-cycle distribution of osteosarcoma U-2 OS cells treated with an anti-DHP siRNA (Figure 1E). In comparison with control cells, suppression of DHP reduced the fraction of U-2 OS cells in S phase. The impact of DHP depletion was less pronounced in the transformed HEK293T cell line (Supplementary Figure S1F), perhaps reflecting differences in the dependency on DHP activity or in the efficiency of DHP depletion. To evaluate further the capacity of DHP-depleted HEK293T cells to proceed through the cell cycle, we performed pulse-chase experiments with the nucleotide analog BrdU. Cells were labeled with BrdU for 30 min and sorted by two-dimensional flow cytometry at the indicated time of incubation in BrdU free medium. After 6-h incubation in BrdU-free medium, the majority of control cells had completed S phase and a significant proportion proceeded to the G1 phase (9.27%), whereas the proportion of DHP-depleted HEK293T cells to reach G1 was reduced by half (Supplementary Figure S2A).

To explore the cause of the cell cycle delays, we analyzed DNA replication tracks at the single molecule level by DNA fiber labeling. Replication tracks were dually labeled with two consecutive pulses of fluorescent nucleotide analogues iodo-deoxyuridine (IdU) and chloro-deoxyuridine (CldU) for 30 min each. We assessed the progression of isolated replication forks by measuring the length of CldU tracks adjacent to IdU tracks.

The knockdown of DHP by siRNA or shRNA molecules with different target sequences reduced the length of replication tracts in U-2 OS or HEK293T cells (Figure 2A and Supplementary Figure S2B). Re-expression of a siRNA-resistant myc-tagged DHP protein in DHP knockdown U-2 OS cells partially rescued replication progression (Figure 2A). This confirms that the DNA replication defect is a direct consequence of DHP depletion.

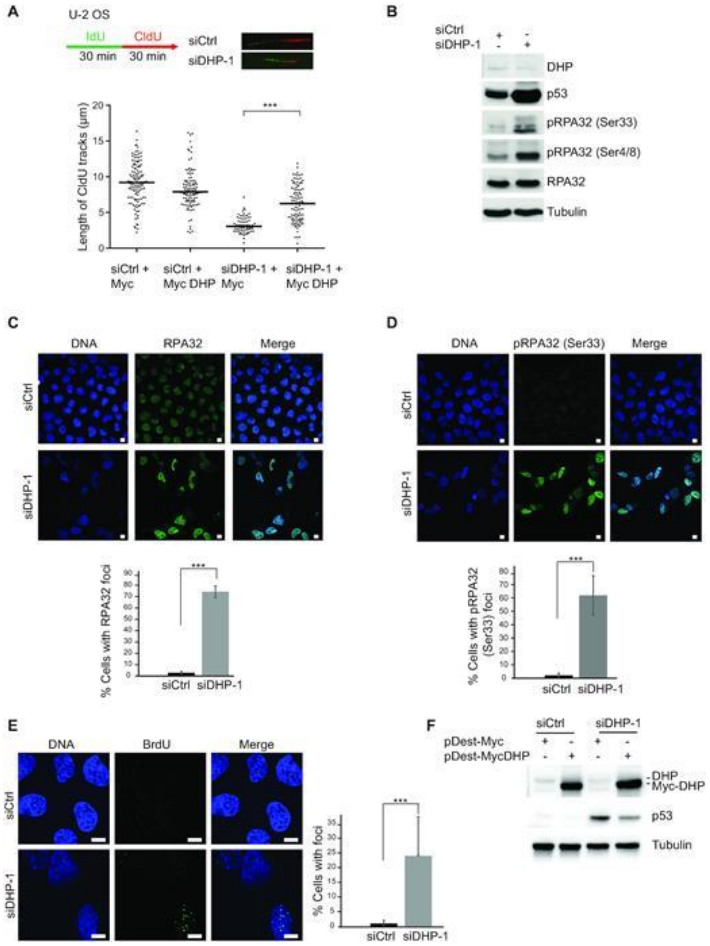

Figure 2: Suppression of DHP interferes with replication fork progression and induces activation of DNA damage responses. (**A**) Experimental scheme: 72 h after transfection with control or anti-DHP siRNA (siDHP-1), cells were labeled with two consecutive pulses of 30 min with CldU and IdU, as indicated. DNA was stretched out on glass slides and newly synthesized DNA was

revealed by immunofluorescence. Graphic representation of replication track lengths in U-2 OS cells co-transfected with control or anti-DHP siRNA (siDHP-1) along with control plasmid or a plasmid encoding siRNA-resistant DHP. The bar dissecting the data points represents the median of 100 tracts length from one biological replicate. Differences between distributions were assessed with the Mann–Whitney rank sum test. *P*-values: *** < 0.0001. (**B**) Whole-cell extracts from control and DHP knockdown U-2 OS cells (siDHP-1) were analyzed by western blotting with the indicated antibodies. One representative experiment is shown from more than three biological replicates (**C**) RPA32 immunofluorescence staining of control and DHP knockdown U-2 OS cells (siDHP-1). DNA was stained by Hoechst. Bars indicate 10 μm. Bottom panel: Quantification of the percentage of RPA32 foci positive cells in a population of 100 cells. Data from three independent biological replicates are represented as mean ± S.D. *P*-values were calculated using a regression model with Poisson distribution: ****P* < 0.0001. (**D**) Immunofluorescence staining of Ser33 phospho RPA32 in control and DHP knockdown U-2 OS cells (siDHP-1). DNA was stained by Hoechst. Bars indicate 10 μm. Bottom panel: Histogram representing the percentage of Ser33 pRPA32 foci positive cells in a population of 100 cells. Data from three independent biological replicates are represented as mean ± S.D. (100 cells were counted per experiment). *P*-values were calculated using a regression model with Poisson distribution: ****P* < 0.0001. (**E**) Control and DHP knockdown U-2 OS cells (siDHP-1) were uniformly labeled with BrdU before immunofluorescence staining in native conditions with an anti-BrdU antibody. DNA was stained by Hoechst. Bars indicate 10 μm. Right panel: Histogram representation of the percentage of ssDNA positive cells. Values are the mean ± S.D of three independent biological replicates (100 cells were counted per experiment). *P*-values were calculated using a regression model with Poisson distribution: ****P* < 0.0001. (**F**) Western blotting analysis with the indicated antibodies of whole-cell extracts from control and DHP knockdown U-2 OS cells (siDHP-1) complemented or not with a siRNA-resistant DHP cDNA, as indicated. One representative experiment is shown from three biological replicates.

Next, we probed cells for indicators of DNA replication stress by monitoring ATR/Chk1 signaling. We observed spontaneous accumulation of Chk1 phosphorylated on Ser345 in the soluble fraction and of RPA32 phosphorylated on Ser 4/8 and Ser33 in the chromatin fraction of DHP-depleted HEK293T and U-2 OS cells (Supplementary Figure S2C and D). Phospho RPA32 (Ser33 and/or Ser4/8) accumulated in U-2 OS whole cell extracts (Figure 2B) and in HEK293T cells transfected with a different anti-DHP shRNA (Supplementary Figure S2E). To confirm this observation, we visualized RPA foci and phospho RPA signals by means of immunofluorescence microscopy. RPA32 and phospho RPA32 (ser33) signals accumulated in U-2 OS cells transfected with anti-DHP siRNA (Figure 2C and D), and in

HEK293T cells transfected with a distinct anti-DHP shRNA (Supplementary Figure S2F). To verify that the formation of RPA32 foci correlates with the accumulation of single-stranded DNA (ssDNA), we probed ssDNA by immunofluorescence microscopy using uniform BrdU labeling and BrdU detection in native conditions [45]. Nearly 30% of DHP-depleted cells exhibited multiple and distinct BrdU signals indicative of severe replication-associated defects (Figure 2E). Last, we monitored the level of p53 that is stabilized in response to genotoxic stress. Depletion of DHP markedly increased the level of p53 in U-2 OS cells (Figure 2B and F). Expression of a siRNA-resistant cDNA encoding DHP reduced the level of p53, confirming that the stabilization of p53 results, at least in part, from the depletion of DHP (Figure 2F). Collectively, these data indicate that suppression of DHP induces DNA replication stress, at least in a subset of cancer cell lines.

Accumulation of Dihydropyrimidines Induces DNA Replication Stress

Next, we sought to investigate how suppression of DHP inhibits fork progression. The rate of DNA chain elongation is dependent on the pool of available deoxyribonucleotides. Thus, we measured the impact of DHP depletion on dNTPs levels using a single nucleotide incorporation assay [37]. The level of dNTPs increases in proliferating cells and fluctuates during the cell cycle [46]. Since the suppression of DHP has consequences on cell growth and cycle progression, cells lacking DHP may exhibit altered dNTPs levels. Consistent with this, the suppression of DHP in HEK293T and U-2 OS cells led to a reduction in the global level of dNTPs (Supplementary Figure S3A and B). To test if alterations of dNTPs levels were responsible for the defect in fork progression observed in DHP-depleted cells, we complemented the cell culture medium with saturating concentrations of nucleosides and measured the length of CldU-labeled replication tracks from isolated replication forks. Addition of nucleosides in the cell culture medium markedly increased the length of replication tracks in shControl HEK293T cells (Supplementary Figure S3C), with a median fold stimulation of 1.7×. This data indicate that nucleosides are

limiting in these cells. By contrast, saturation of DHP-depleted cells with a cocktail of nucleosides did not markedly increase the length of replication tracks (Supplementary Figure S3C). Therefore, changes in dNTPs levels are not the primary cause of replication stress in these cells. Consistent with this interpretation, addition of an excess of nucleosides in the cell culture medium of DHP-depleted cells did not attenuate the accumulation of p53 and the phosphorylation of RPA32 on Ser33 (Supplementary Figure S3D).

It is noteworthy that measurements of the global pool of dNTPs does not give insights into local levels of dNTPs available to the DNA replication machinery [47], and that the rate of replication fork progression is primarily determined by the amount of DNA damage and the level of activated p53, not by the global concentrations of dNTPs [47]. Thus, we considered the possibility that DNA replication stress in DHP-depleted cells was caused by the accumulation of dihydropyrimidines. To test this, we measured the cellular concentration of uracil and its breakdown product dihydrouracil by liquid chromatography and mass spectrometry (LC-MS). DHP-depletion in U-2 OS cells yielded a 4-fold increase in the molar ratio of intracellular dihydrouracil/uracil (Figure 3A). This indicate that the transient knockdown of DHP is sufficient to raise the intracellular concentration of dihydropyrimidines. To counteract the accumulation of dihydropyrimidines in DHP-knockdown cells, we co-depleted DPD, the first enzyme in the pyrimidine catabolic pathway that produces dihydropyrimidines (Figure 1A). We tried to measure the dihydrouracil/uracil ratio in DPD-depleted cells co-transfected with control and anti-DHP siRNAs. In the absence of DPD, however, the cellular concentration of dihydrouracil decreased below quantification levels. Suppression of DPD in DHP-depleted cells rescued the rate of fork progression to the level of control cells (Figure 3B). Consistent with this result, the levels of p53, of Ser33 phosphorylated RPA32 and the intensity of RPA32 foci were close to normal when both DPD and DHP enzymes were depleted (Figure 3C and D). To test if the genotoxic consequences of dihydropyrimidines was dependent on the salvage pathway, we knocked-down uridine phosphorylase

(UPP1) by means of RNA interference. Suppression of UPP1 in DHP-depleted cells had no impact on markers of DNA replication stress (Supplementary Figure S3E). Altogether, these observations suggest that the DNA replication stress phenotype of DHP-depleted cells is the consequence of the accumulation of dihydropyrimidines.

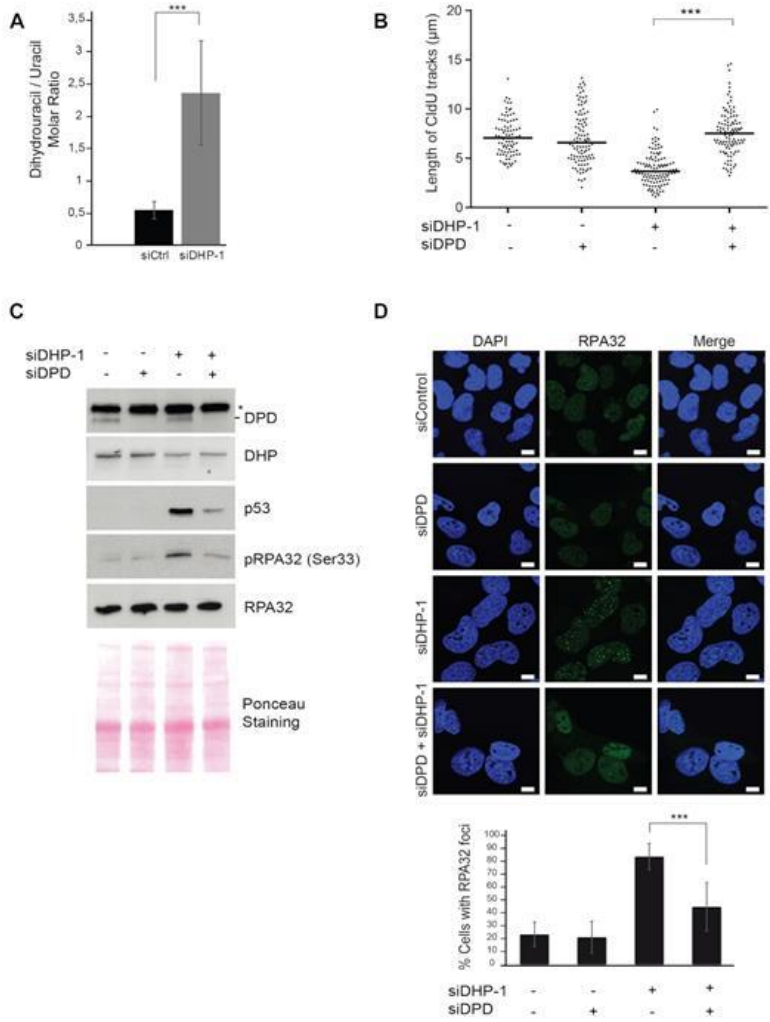

Figure 3: Accumulation of dihydropyrimidines induces DNA replication stress. (**A**) The concentrations of dihydrouracil and uracil were measured in U-2 OS cells transfected with control or anti-DHP siRNA (siDHP-1). The ratio of

molar concentrations between the two metabolites in each sample is presented. Data from three independent biological replicates, with three technical replicates for each, are represented as mean ± S.E.M. *P*-values were calculated using a regression model with Poisson distribution: ***$P < 0.0001$. (**B**) Replication tracks were labeled with two consecutive pulses of 30 min with CldU and IdU in U-2 OS cells transfected with the indicated siRNAs. Graphic representations of replication track lengths measured in µm (y-axis). The bar dissecting the data points represents the median of 100 tracts length from one biological replicate. Differences between distributions were assessed with the Mann–Whitney rank sum test. *P*-values: *** < 0.0001. (**C**) Western blot analysis with the indicated antibodies of whole cell extracts from U-2 OS transfected with anti-DHP and anti-DPD siRNAs, as indicated, Ponceau staining was used as control of protein loading and transfer. * non-specific band. One representative experiment is shown from two biological replicates. (**D**) RPA32 immunofluorescence staining of U-2 OS cells transfected with the indicated siRNAs. Bars indicate 10 µm. DNA was stained by Hoechst. Bottom panel: Histogram representation of the percentage of RPA32 foci-positive cells in a population of 100 cells. Data from three independent biological replicates are represented as mean ± S.D. *P*-values were calculated using a regression model with Poisson distribution: ***$P < 0.0001$.

Dihydropyrimidine Accumulation Induces Transcriptional Stress

The data thus far indicate that dihydropyrimidine metabolites induce DNA replication stress. We reasoned that dihydropyrimidines could induce directly or indirectly the formation of DNA adducts and interfere with DNA-templated processes including transcription. Thus, we explored the effect of DHP loss on global transcription activity. Nascent RNA were pulse labeled for 20 min with the modified RNA precursor 5-ethynyluridine (EU) and overall transcription activity was evaluated via fluorescent-based quantification. In comparison with control cells, we observed a drop of EU incorporation in DHP-depleted U-2 OS cells (Figure 4A). Next, we used the anti-RNA:DNA hybrids S9.6 antibody to visualize R-loops by immunofluorescence staining. R-loops are induced by defects in the processing of nascent pre-mRNAs or by the accumulation of negative supercoiling behind RNA polymerases [15,48]. Immunofluorescence staining experiments revealed a significant increase in the level of nuclear RNA:DNA hybrids in DHP-depleted cells compared to control cells after excluding nucleolar signals from the analysis (Figure 4B). R-loops and nucleolin immunofluorescence staining revealed alterations in the

morphology of nucleoli, which appeared more condensed and rounded (Figure 4B). These observations indicate that the accumulation of dihydropyrimidine metabolites in DHP-depleted cells induces transcriptional stress.

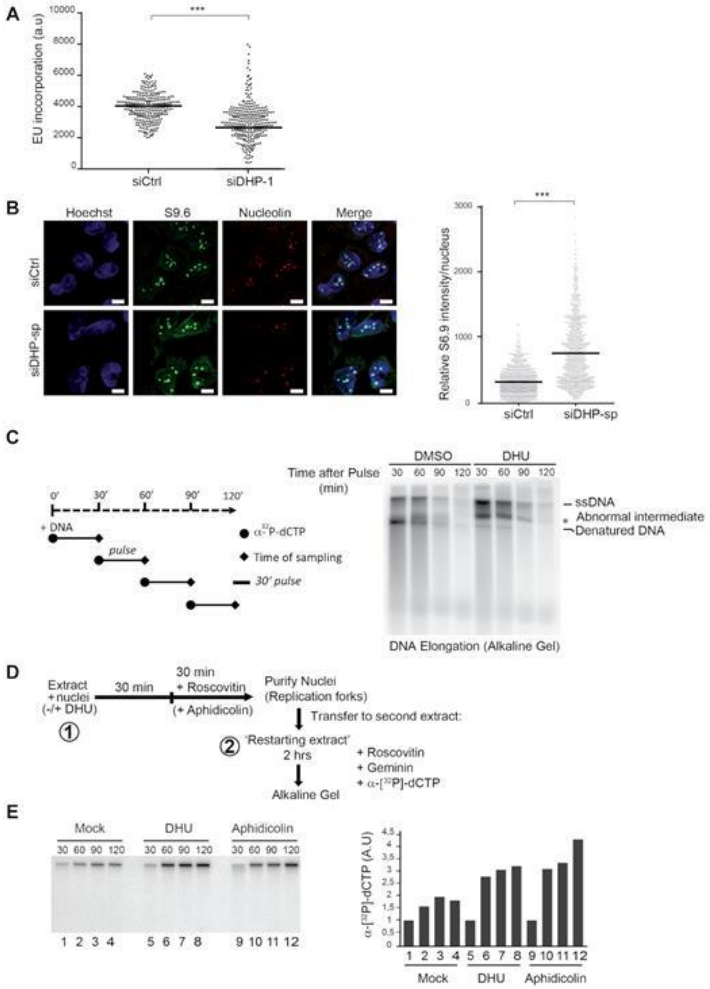

Figure 4: Dihydropyrimidines induce transcriptional stress and yield abnormal DNA replication intermediates. (**A**) Graphic representation of global transcriptional activity visualized by 5-ethynyl uridine (EU) incorporation. U-2 OS cells transfected with control and anti-DHP siRNA (siDHP-1) were labeled with EU for 20 min before fixation. The EU intensity of 100 cells from two independent biological replicates was measured by fluorescence microscopy.

The bar dissecting the data points represents the median of EU intensity. Differences between distributions were assessed with the Mann–Whitney rank sum test. *P*-values: *** < 0.0001. (**B**) Immunofluorescence staining with S9.6 and nucleolin antibodies of DHP-depleted or control U-2 OS cells (siDHP-sp). DNA was stained by Hoechst. Bars indicate 10 μm. Right panel: The graph shows the median of S9.6 signal intensity par nucleus after nucleolar signal removal. More than 1000 cells from two independent biological replicates were considered. Differences between distributions were assessed with the Mann–Whitney rank sum test. *P*-values: *** < 0.0001. (**C**) Left panel: Experimental scheme. DNA synthesis reactions (control: DMSO; DHU: 15 mM) were pulse-labeled for 30 min with α-[^{32}P]-dCTP at the indicated times during the course of a 2-h reaction. Replication products were purified and resolved by electrophoresis through a 1.2% agarose gel in denaturing conditions. (*) abnormal replication intermediate. One representative experiment is shown from two biological replicates. (**D**) Experimental scheme: Sperm nuclei were added to Xenopus egg-extract (in presence or not of 7.5 mM DHU dissolved in water) and incubated at 23°C to allow origins firing and replication initiation. After 30 min incubation, the firing of new replication origins was blocked with roscovitine (0.5 mM). Replicating nuclei were then isolated after 60 min of incubation and transferred to a second extract (restarting extract) supplemented with roscovitine (0.5 mM) and Geminin (60 mM) to block the firing and the assembly of novel origins, respectively. DNA synthesis reactions were pulse-labeled with α-[^{32}P]-dCTP during incubation in the second extract. (**E**) Replication products were resolved by 1% alkaline agarose gel electrophoresis and revealed by autoradiography. Lanes 1–4: Mock treated extracts; Lanes 5–8: incubation in the first extract was performed in the presence of 7.5 mM DHU. Lanes 10–12 serve as positive controls: after 30 min incubation in the first extract, DNA synthesis was blocked with aphidicolin (100 ng/μl). Right panel: Histogram representing the quantification of the gel by image J of replication products (arbitrary unit). One representative experiment is shown from two biological replicates (See Supplementary Figure S4A).

Dihydropyrimidine Accumulation Induces Abnormal DNA Replication Products Independently of Transcription

Because interference between transcription and DNA replication is an important endogenous source of DNA replication stress (Tuduri *et al.*, [15]), we wanted to know if dihydropyrimidine metabolites can directly interfere with the process of DNA replication, independently of transcription activity. To test this, we used a *cell-free* DNA replication system derived from Xenopus eggs in which transcription is inactive. In this system, a circular single-stranded DNA is converted into a double-stranded DNA via priming and elongation of DNA chains in a semiconservative manner. The replicated DNA is then assembled

into chromatin leading to the formation of supercoiled DNA [49]. DNA replication was measured by the incorporation of the radioactive nucleotide precursor α^{32}P-dCTP.

First, we labeled DNA during the course of a 2-h reaction with 30 min pulses of α^{32}P-dCTP, as indicated (Figure 4C, left panel), and analyzed DNA replication products by alkaline agarose gel electrophoresis. In these denaturing conditions, irreversibly denatured DNA produced in control extracts was replaced by an abnormal replication intermediate in extracts supplemented with 5, 6-dihydrouracil (Figure 4C). This novel replication product was visible from the earliest stages of the replication reaction (Figure 4C). This observation indicate that dihydropyrimidines interfere directly with the process of DNA chain elongation in Xenopus egg-extracts. Moreover, the dNTPs pool is not limiting during DNA replication in Xenopus egg extracts. Therefore, in this system, the possibility that DHU may imbalance the pool of dNTP pool is eliminated.

We designed a multistep chromatin transfer experiment to verify if 5, 6-dihydrouracil directly interferes with chromosomal DNA synthesis (Figure 4D). First, we performed a standard chromatin DNA replication reaction in Xenopus egg-extracts using demembranated sperm nuclei [50–52]. Interference with the progression of replication forks, for example using the replicative DNA polymerase inhibitor aphidicolin, is expected to yield incomplete DNA replication intermediates that can prime DNA synthesis during the course of a second DNA replication reaction. To obtain evidence for the formation of aborted replication intermediates in extracts supplemented with 5, 6 dihydrouracil, we purified and transferred the replicated, or partially replicated, chromatin to a second extract supplemented with both Geminin, to block the licensing of new origins of replication, and the CDK2 inhibitor roscovitine, to block the firing of new origins. In this situation, DNA synthesis is the result of priming of pre-existing replication intermediates. The transfer of nuclei from a replication reaction carried out in the presence of aphidicolin to a second extract unable to fire new origins led to a significant increase in α^{32}P-dCTP incorporation in comparison with mock-treated nuclei

(Figure 4E and Supplementary Figure S4A, compare lanes 1–4 with lanes 9–12), indicative of replication fork restart and/or DNA repair activities. Likewise, in comparison with mock-treated nuclei, addition of 5,6-dihydrouracil during the first replication reaction yielded an increased incorporation of α^{32}P-dCTP in the restarting extract (Figure 4E and Supplementary Figure S4A, lane 5–9), indicating that DNA replication in the presence of 5,6-dihydrouracil generates DNA intermediates that prime DNA synthesis. Collectively, these data indicate that dihydropyrimidine metabolites directly interfere with the process of DNA replication.

Dihydromyricetin Induces DNA Replication Stress

We noticed a report suggesting that the plant flavonoid dihydromyricetin is a competitive inhibitor of a putative DHP from *Pseudomonas aeruginosa* [53] (Figure 1A). Human and *P. aeruginosa* DHPs are predicted to fold into a similar structure [53]. Since DHP activity is a good marker of tumorigenicity and a candidate target for cancer therapy [3], we wanted to test if dihydromyricetin also inhibits the human DHP. We expressed and purified recombinant human DHP to near homogeneity (Supplementary Figure S4B) and assessed its activity by measuring the decomposition of 5, 6-dihydrouracil using high performance liquid chromatography. In an experimental system containing purified DHP (0.2 μM) and 5, 6 dihydrouracil as a substrate (50 μM), dihydromyricetin inhibited DHP activity with a half maximal inhibitory concentration (IC_{50}) value of about 6 μM (Figure 5A). Next, we analyzed the phenotypic consequences of acute exposure of U-2 OS cells to dihydromyricetin, and observed an increased intracellular molar ratio of dihydrouracil/uracil (Figure 5B), the induction of RPA32 and Chk1 phosphorylation (Figure 5C and Supplementary Figure S4C), the formation of RPA32 nuclear foci (Figure 5D), and the slowing of DNA replication forks (Figure 5E). In addition, DPD-depleted U-2 OS cells were more resistance to dihydromyricetin treatment and rescued the DNA replication stress markers induced by dihydromyricetin (Figure 5F and G). By contrast, suppression of the salvage pathway enzyme UPP1 had no impact on DNA replication stress markers induced by dihydromyricetin

(Supplementary Figure S4D). These data indicate that the treatment of cells with dihydromyricetin induces replication stress phenotypes that are similar to the phenotypes of DHP-knockdown cells.

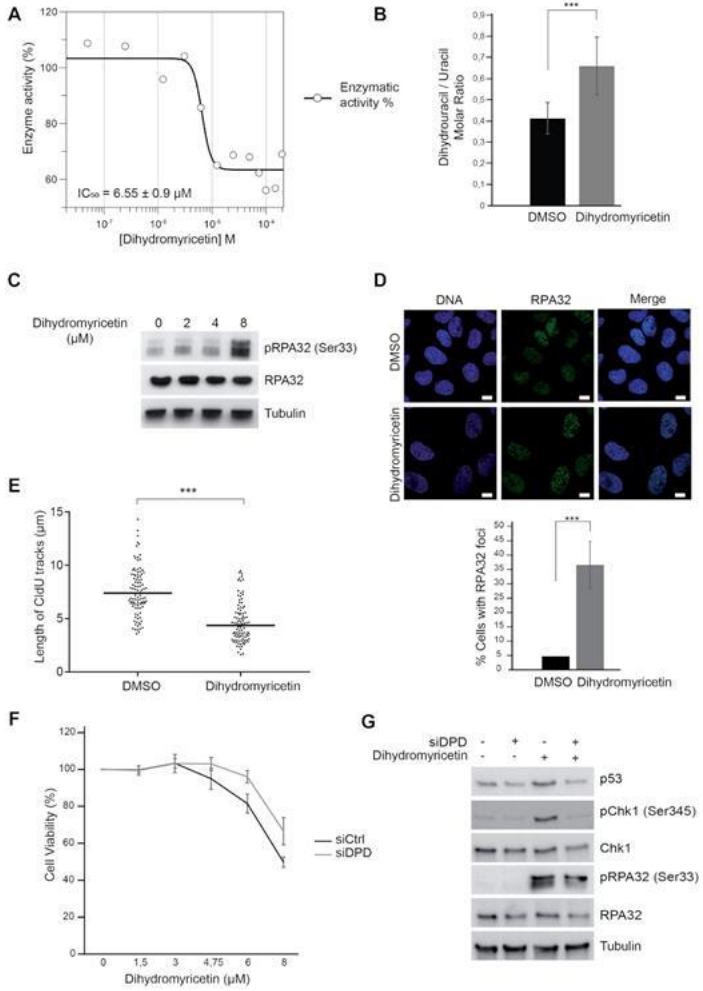

Figure 5: Dihydromyricetin induces DNA replication stress. (**A**) IC_{50} determination of dihydromyricetin for DHP (0.2 µM) using dihydrouracil (50 µM) as a substrate. One representative experiment is shown from three biological replicates. (**B**) Molar ratios of dihydrouracil versus uracil measured in U-2 OS cells treated with 20 µM dihydromyricetin for 16 h. Data from three independent biological replicates, with three technical replicates for each, are

represented as mean ± S.E.M. *P*-values were calculated using a regression model with Poisson distribution: ***$P < 0.0001$. (**C**) Western blot analysis with the indicated antibodies of U-2 OS whole-cell extracts treated with dihydromyricetin for 48 h at the indicated concentrations. One representative experiment is shown from three biological replicates. (**D**) RPA32 immunofluorescence staining of U-2 OS cells treated with DMSO or 20 μM dihydromyricetin for 16 h. Bars indicate 10 μm. DNA was stained by Hoechst. Bottom panel: Histogram representation of the percentage of RPA32 foci-positive cells in a population of 100 cells. Data from three independent biological replicates are represented as mean ± S.D. *P*-values were calculated using a regression model with Poisson distribution: ***$P < 0.0001$. (**E**) Graphic representation of replication track lengths measured in μm (y-axis) in control and U-2 OS cells treated with 20 μM of dihydromyricetin for 16 h. The bar dissecting the data points represents the median of 100 tracts length from one biological replicate. Differences between distributions were assessed with the Mann-Whitney rank sum test. *P*-values: *** < 0.0001. (**F**) U-2 OS cells were transfected with control or anti-DPD siRNA and exposed to increasing concentrations of dihydromyricetin for 2 days. Cell viability was estimated using Cell Titer-Glo assay. Mean viability is representative of experiments performed in triplicate. Error bars represent ± S.E.M. (**G**) Western blot analysis with the indicated antibodies of whole cell extracts from U-2 OS transfected with anti-DPD siRNA and treated or not with 20 μM of dihydromyricetin for 24 h. One representative experiment is shown from two biological replicates.

Suppression of Dihydropyrimidinase Activity Induces DNA–Protein Crosslinks

Next, we sought to evaluate whether dihydropyrimidines inhibit DNA-templated processes via the formation of DNA adducts. First, we asked if the accumulation of these metabolites triggers the recruitment of translesion DNA polymerases to chromatin. Suppression of DHP induced chromatin recruitment of the translesion DNA polymerase η that can bypass replication-blocking lesions such as UV photoproducts and oxidized bases [54,55], but not DNA polymerase κ, which has a different specificity for DNA lesions than polymerase η (Figure 6A and Supplementary Figure S5A). We also observed monoubiquitinated PCNA in the chromatin fraction of DHP-depleted cells (Figure 6A), a posttranslational modification that facilitates the interaction of TLS polymerases with PCNA [56]. Consistent with this observation, addition of 5, 6-dihydrouracil in Xenopus eggs extracts induced a pronounced accumulation of TLS pol η on chromatin after 2 h of incubation, when the replication process was completed (Figure 6B). In light of these

observations, we propose that the accumulation of dihydropyrimidines or their decomposition products may induce bulky DNA adducts.

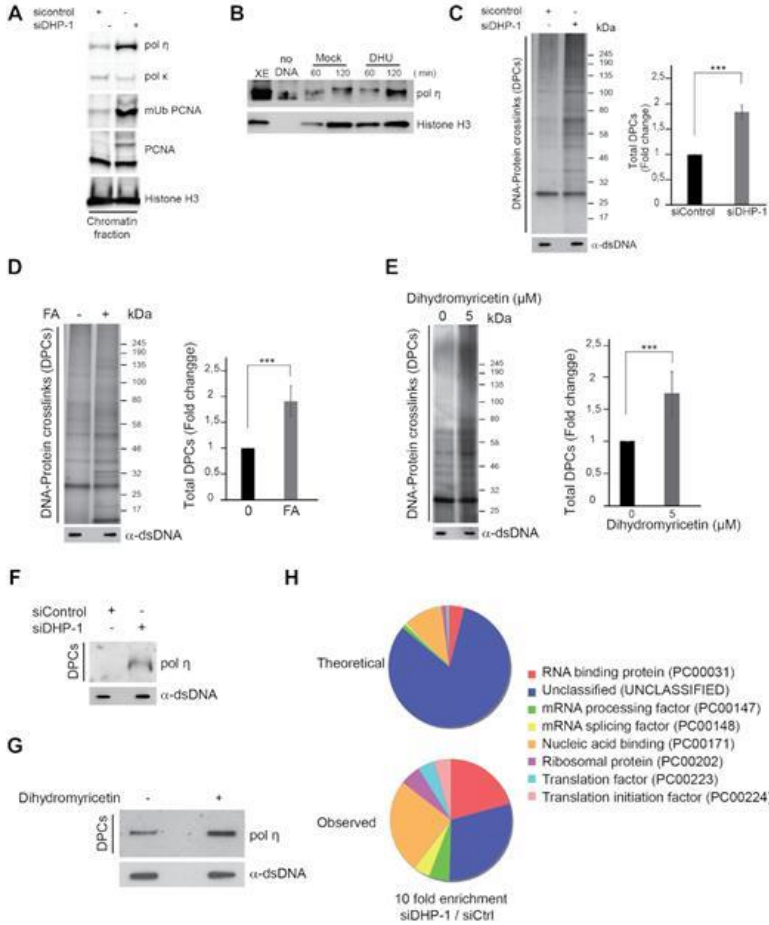

Figure 6: Dihydropyrimidines metabolites induce DPCs. (**A**) The chromatin fraction of control and DHP knockdown U-2 OS cells (siDHP-1) was subjected to western blot analysis with the indicated antibodies. *Histone H3* was used as *loading control*. One representative experiment is shown from two biological replicates. (**B**) Chromatin extracts from nuclei incubated in control and DHU (7.5 mM) containing extracts for 60 and 120 min were subjected to western blot analysis with the indicated antibodies. Histone H3 was used as loading control. One representative experiment is shown from two biological

replicates. (**C**) Total DPC levels in U-2 OS cells transfected with control or anti-DHP siRNA (siDHP-1) visualized by silver staining. Right panel: Histogram representing the quantification of DPC levels normalized to total DNA amount by image J. Three independent biological replicates are averaged in the bar graphs. Error bars represent ± S.D. *P*-values were calculated using a regression model with Poisson distribution: ***$P < 0.0001$. (**D**) Total DPC levels in U-2 OS cells treated or not with 1 mM FA for 2 h visualized by silver staining. Right panel: Histogram representing the quantification of DPC levels normalized to total DNA amount by image J. Three independent biological replicates are averaged in the bar graphs. Error bars represent ± S.D. *P*-values were calculated using a regression model with Poisson distribution: ***$P < 0.0001$. (**E**) Total DPC levels after U-2 OS cells treatment with DMSO or 5 μM of Dihydromyricetin for 16 h visualized by silver staining. Right panel: Histogram representing the quantification of DPC levels normalized to total DNA amount by image J. Three independent biological replicates are averaged in the bar graphs. Error bars represent ± S.D. *P*-values were calculated using a regression model with Poisson distribution: ***$P < 0.0001$. (**F**) Western blot analysis of crosslinked DNA polymerase η in total DPC extracts from U-2 OS cells transfected with control or anti-DHP siRNA (siDHP-1) and the corresponding DNA quantification. One representative experiment is shown from two biological replicates. (**G**) Slot-blot showing crosslinked DNA polymerase η in total DPC extracts from U-2 OS cells treated with 20 μM dihydromyricetin for 16 h and the corresponding DNA quantification. (**H**) Pie chart representation of gene ontology analyses using the panther Classification system (http://www.pantherdb.org/on). Theoretical relates to gene ontology classification expected from random sampling of the proteome. Observed is the classification of proteins enriched at least 10-folds in DHP-depleted cells versus control cells. Proteins selected for the analysis were identified in three independent experiments.

A variety of endogenous metabolites, environmental and chemotherapeutic DNA damaging agents induce covalent DPCs [20]. We use the RADAR assay (rapid approach to DNA-adduct recovery) to test if the suppression of DHP activity yields DPCs. We isolated genomic DNA and quantified it using Qubit fluorometric quantitation to ensure that DPC analyses were performed using equal amounts of material. Next, we digested DNA with benzonase, resolved DPC by SDS-polyacrylamide gelelectrophoresis and detected them by silver staining. An increase in total DPCs was consistently detected after suppression of DHP using distinct siRNA and shRNA molecules, in U-2 OS and in HEK293T cells (Figure 6C and Supplementary Figure S5B). The level of DPCs in DHP-depleted cells was comparable to that of U-2 OS cells exposed to formaldehyde (Figure 6D). In addition, treatment of U-2 OS cells with dihydromyricetin increased by 2-folds the

amount of total DPCs (Figure 6E). The proteolysis of DPCs is coupled to DNA replication via at least two independent mechanisms, one mediated by the DNA-dependent metalloprotease Spartan (DVC1) [41,57], and one mediated by the proteasome (58). Given the importance of DNA replication in DPC repair, we analyzed if the slowing of replication forks *per se* influences the overall level of DPCs measured by RADAR. Low dose aphidicolin (0.1 μM) reduced the length of replication tracks, as expected, but did not increase the overall level of DPCs (Supplementary Figure S5C). Thus, the formation DPCs in DHP-depleted cells is unlikely a consequence of replication-fork slowing. The data suggest that dihydropyrimidines metabolites induce the formation of covalent bonds between proteins and DNA.

A large diversity of proteins can be crosslinked to DNA. As the TLS polymerase η functions at blocked replication forks and accumulates in the chromatin fraction of DHP-depleted cells, we examined if DNA polymerase η was crosslinked to DNA. The level of covalently trapped DNA polymerase η increased in DHP-depleted cells (Figure 6F) and in cells exposed to dihydromyricetin (Figure 6G), but not in presence of low dose of aphidicolin (Supplementary Figure S5D), suggesting that dihydropyrimidines covalently trap DNA polymerase η on DNA. To gain a panoramic view of covalently trapped proteins in DHP-depleted cells, we performed RADAR assay and analyzed protein–DNA complexes by mass spectrometry. We used the MaxQuant computational platform for label free quantification of proteins identified by RADAR-MS. We selected proteins identified in three independent experiments that were enriched by at least 10-folds in samples prepared from DHP-depleted cells in comparison with control cells. Next, we used PANTHER Classification System (http://pantherdb.org/) to perform Gene Ontology analyses. We observed a strong and non-random enrichment in nucleic acid binding, mRNA processing and splicing proteins, consistent with the crosslinking of chromatin-associated proteins (Figure 6H).

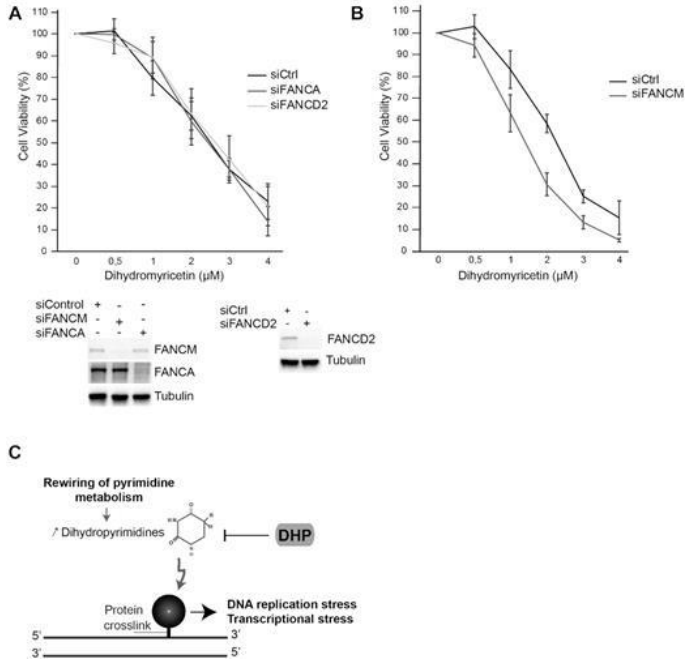

Figure 7: FANCM promotes cellular tolerance to dihydromyricetin. (**A**) U-2 OS cells were transfected with the indicated siRNAs and exposed to increasing concentrations of dihydromyricetin for 2 days. Cell viability was estimated using Cell Titer-Glo assay. Mean viability is representative of experiments preformed in triplicate. Error bars represent ±S.D. Bottom panel: the efficiency of FANCM, FANCD2 or FANCA knockdown was assessed by western blotting. (**B**) U-2 OS cells were transfected with FANCM siRNA and cell viability was assessed as described in A. Mean viability representative of quadruplicates. Error bars represent ±S.D. (**C**) Model: The accumulation of Dihydropyrimidines in cancer cells induces DNA replication and transcriptional stress via the formation of DPCs.

To begin to understand how cells process DNA lesions induced by dihydromyricetin, we used siRNAs to suppress a subset of DNA repair factors. Surprisingly, depletion of Spartan did not sensitize U-2 OS cells to dihydromyricetin, nor did the depletion of the nucleotide excision repair factors XPA, ERCC5/XPG, nor the Fanconi anemia proteins FANCA and FANCD2 (Supplementary Figure S6A and Figure 7A). By contrast, depletion of the DNA translocase FANCM sensitized cells to dihydromyricetin (Figure 7B). We confirmed this observation using an anti-FANCM shRNA with a different target sequence in

HEK293T cells (Supplementary Figure S6B). To assess the role of FANCM translocase activity in cellular protection against dihydromyricetin-induced DNA replication stress, we measured the impact of dihydromyricetin on the viability of HEK293 cell lines that stably express an anti-FANCM siRNA and that are complemented either with recombinant WT FANCM or with the translocase dead mutant K117R FANCM [31]. Cells expressing the ATPase-dead mutant K117R were more sensitive to dihydromyricetin than cells expressing WT FANCM (Supplementary Figure S6C). These data suggest that the DNA translocase FANCM promotes cellular tolerance to dihydromyricetin.

Discussion

The activity of DHP is high in the liver and in the kidney [7], absent in the majority of healthy human tissues and re-expressed in a variety of human carcinomas [3]. In this study, we show that DHP activity is necessary to prevent transcriptional and DNA replication stress in transformed cell lines.

Suppression of DHP induced the slowing of DNA replication forks, the accumulation of single-stranded DNA, the activation of ATR signaling, the accumulation of RNA:DNA hybrid structures and the inhibition of transcription. Multiple lines of evidence obtained using orthogonal experimental methods lead us to conclude that dihydropyrimidines are potentially cytotoxic metabolites: (i) depletion of DHP by RNA interference impeded DNA replication and transcription; (ii) DNA replication stress in DHP-depleted cells was reversed by suppression of DPD, the enzyme that produces dihydropyrimidines and by expression of a siRNA resistant cDNA encoding Myc-DHP; (iii) Inhibition of DHP activity with dihydromyricetin phenocopied the defects of DHP-depleted cells; (iv) Dihydropyrimidines directly altered DNA replication products synthesized in Xenopus egg extracts.

We reproduced the DNA replication stress phenotypes in different cell lines with different siRNA and shRNA targeting sequences. We failed, however, to rescue the long-term viability of DHP-depleted cells using retrovirus or lentivirus to transduce

siRNA-resistant DHP cDNAs. Although we cannot exclude that the anti-DHP siRNA has other target(s) that affect cellular viability, we believe it is unlikely. It is noteworthy that an anti-DHP siRNA did not alter the viability of multiple myeloma cells (AMOI) that do not express DHP. The complexity of nucleotide metabolism and the need to regulate tightly the activity and the level of DHP protein may compromise the rescue of cell viability with unregulated recombinant DHP.

The observed reduction of dNTPs levels may contribute to the DNA replication stress phenotype of DHP-depleted cells. However, the pool of dNTPs increases in S phase. Thus, the apparent reduction of the pool of dNTPs may simply reflect the reduction of the proportion DHP-depleted cells in S phase. Furthermore, previous studies have shown that the rate of replication fork progression does not correlate directly with the global concentration of dNTPs [47,59], as the latter does not reflect the amount of nucleotides available to the replication machinery. By contrast, the length of replication tracks is determined directly by the accumulation of DNA lesions in the template DNA and by p53 activation [47]. Several lines of evidence suggest that it is unlikely that alterations of the pool of dNTPs determine the phenotypes of DHP-depleted cells. First, the length of replication tracks in DHP-depleted cells remain shorter than in control cells after saturation of the cell culture medium with exogenous nucleotides. Second, the pool of dNTPs is not limiting in Xenopus egg extracts, yet supplementation of Xenopus egg extracts with dihydropyrimidines interfered with DNA replication. Third, transcription does not depend on dNTPs precursors, yet, the accumulation of dihydropyrimidines also inhibited RNA synthesis. The accumulation of dihydropyrimidines induced p53 stabilization and DNA damage, two parameters that determine directly the length of replication tracks [47].

Cellular metabolites and environmental agents generate a range of structurally diverse protein–DNA crosslink that precipitate the loss of cellular functions, including transcription and DNA replication [20]. During DNA replication, DPCs are degraded either by the DNA-dependent metalloprotease Spartan/DVC1

[41,57] or by the proteasome [58]. Proteasomal degradation requires DPC ubiquitylation whereas SRTN requires nascent strand extension within a few nucleotides from the lesion [58]. Recent evidence indicates that DPC proteolysis occurs only after the DNA replicative helicase CMG (CDC45/MCM2-7/GINS) has bypassed the intact DPC adduct [60], thereby protecting the replication machinery against promiscuous proteolysis.

The data presented here reveal that dihydropyrimidines are cytotoxic metabolites that induce DNA replication and transcriptional stress, and that the accumulation of dihydropyrimidines is linked with the accumulation of DPCs. Yet, we did not elucidate the chemical and structural identity of the damage (s) induced by dihydropyrimidines. Suppression of DHP did not yield any detectable increase in apurinic/apyrimidinic sites nor ribonucleotides incorporation into genomic DNA (data not shown). Some evidence suggests that dihydrouracil and its derivatives could be incorporated into ribonucleic acids [61,62], but it is not clear whether salvage pathways can convert 5,6-dihydrouracil and 5,6-dihydrothymine into nucleosides or deoxynucleosides. Suppression of the salvage pathway UPP1, however, did not attenuate the replication stress phenotype of cells treated with anti-DHP siRNAs or with dihydromyricetin. During the course of this study, we did not detect any direct evidence of dihydropyrimidines incorporation into DNA. Dihydropyrimidines are non-coding bases that have lost their planar structure as a consequence of the saturation of the C5-C6 double bound [17]. Above physiological pH, and more slowly at physiological pH, these saturated bases can further decompose into fragments of bases [63]. Some decomposition products could be genotoxic. Alternatively, metabolites alterations by chemical side reactions are widespread [64]. Dihydropyrimidines may react with oxidants or other metabolites to form potent DNA damaging agents [65].

We report that dihydromyricetin inhibits the activity of recombinant human DHP. Dihydromyricetin is a versatile flavonoid from the Chinese pharmacopeia. It scavenges reactive oxygen species and has a variety of biological activities [66]. Although dihydromyricetin is not a specific inhibitor of DHP,

the latter is likely a target. Indeed, U-2 OS cells exposed to dihydromyricetin exhibited cellular phenotypes similar to that of DHP-depleted cells: (i) accumulation of protein-DNA crosslinks; (ii) replication forks slowing; and (iii) induction of markers of DNA replication stress. Consistent with the later observation, dihydromyricetin elicits p53 stabilization in hepatocellular carcinoma and activates the G2/M checkpoint via ATM/ATR signaling [67].

Suppression of NER factors, Spartan, or the Fanconi anemia proteins FANCA and FANCD2 did not sensitize cells to dihyromyricetin. The DNA translocase FANCM, however, promoted cellular tolerance to dihydromyricetin. This observation does not contradict the fact that the Fanconi anemia (FA) pathway is not involved in the repair of DPCs [57,68]. The clinical symptoms of patients with biallelic inactivation of *FANCM* are distinct from Fanconi anemia [69–71]. FANCM facilitates the FA pathway and exerts many FA-independent functions [72]. Further studies will be required to understand exactly how FANCM mitigates the toxicity of dihydromyricetin.

A deficiency in DHP activity yields clinical symptoms that are consistent with dihydropyrimidines exerting toxic effects. Individuals carrying bi-allelic mutations in DHP accumulate high levels of 5, 6-dihydrouracil and 5, 6-dihydrothymine in urine, blood and cerebrospinal fluids. DHP deficiency can remain asymptomatic, but most patients present neurological abnormalities including mental retardation, hypotonia and seizures [73–76]. DHP deficiency also manifests with growth retardation, dysmorphic features and gastrointestinal abnormalities [77–79].

In the context of carcinogenesis, the rewiring of the pyrimidine degradation pathway appears as a metabolic adaptation that supports tumor progression. Most cultured cells require glutamine for TCA cycle anaplerosis that yields precursors for several biosynthetic pathways, including nucleotides, which are necessary for tumor growth [2,80]. The accumulation of the pyrimidine degradation products dihydropyrimidines facilitate directly the epithelial mesenchymal transition (EMT) (4). The

role of dihydropyrimidines in cancer progression toward metastasis could be linked with the genotoxic potential of these metabolites. Endogenous DNA damage and DNA replication stress induce genomic instability and thereby accelerate the acquisition of growth promoting properties. Furthermore, key sensors and mediators of the DNA damage response regulate the EMT-associated transcription factor ZEB1 [81–83]. An overload of DNA lesions, however, will trigger cell death. The previously unrecognized cytotoxicity of dihydropyrimidines described here implies that a tight equilibrium between pyrimidine synthetic and pyrimidine degradation activities is required for the proliferation of some cancer cells. We propose that DHP fulfills the function of a sanitization enzyme required for epithelial cancer cells to mitigate the toxicity of dihydropyrimidines (Figure 7C). DHP is a potential target for cancer chemotherapy [3]. This study shows that DHP activity is a cellular target of dihydromyricetin. Dihydromyricetin induces cell cycle arrest and apoptosis in human gastric cancer cells, hepatocellular carcinoma and melanoma cells, without cytotoxicity to normal cells [67,84–86]. It inhibits the growth of prostate cancer in mice [87]. The model discussed here offers a conceptual framework for further exploring the potential therapeutic utility of targeted inhibition of DHP.

References

1. Hanahan D, Weinberg RA. Hallmarks of cancer: the next generation. Cell. 2011; 144: 646–674.
2. Vander Heiden MG, DeBerardinis RJ. Understanding the intersections between metabolism and cancer biology. Cell. 2017; 168: 657–669.
3. Naguib FN, el Kouni MH, Cha S. Enzymes of uracil catabolism in normal and neoplastic human tissues. Cancer Res. 1985; 45: 5405–5412.
4. Shaul YD, Freinkman E, Comb WC, Cantor JR, Tam WL, et al. Dihydropyrimidine accumulation is required for the epithelial-mesenchymal transition. Cell. 2014; 158: 1094–1109.
5. Wikoff WR, Grapov D, Fahrmann JF, DeFelice B, Rom WN, et al. Metabolomic markers of altered nucleotide metabolism

in early stage adenocarcinoma. Cancer Prev. Res. 2015; 8: 410–418.
6. Edwards L, Gupta R, Filipp FV. Hypermutation of DPYD deregulates pyrimidine metabolism and promotes malignant progression. Mol. Cancer Res. 2016; 14: 196–206.
7. van Kuilenburg AB, van Lenthe H, van Gennip AH. Activity of pyrimidine degradation enzymes in normal tissues. Nucleosides Nucleotides Nucleic Acids. 2006; 25: 1211–1214.
8. Yoo BK, Gredler R, Vozhilla N, Su ZZ, Chen D, et al. Identification of genes conferring resistance to 5-fluorouracil. Proc. Natl. Acad. Sci. U.S.A. 2009; 106: 12938–12943.
9. Macheret M, Halazonetis TD. DNA replication stress as a hallmark of cancer. Annu. Rev. Pathol. 2015; 10: 425–448.
10. Zeman MK, Cimprich KA. Causes and consequences of replication stress. Nat. Cell Biol. 2013; 16: 2–9.
11. Bester AC, Roniger M, Oren YS, Im MM, Sarni D, et al. Nucleotide deficiency promotes genomic instability in early stages of cancer development. Cell. 2011; 145: 435–446.
12. Huang SN, Williams JS, Arana ME, Kunkel TA, Pommier Y. Topoisomerase I-mediated cleavage at unrepaired ribonucleotides generates DNA double-strand breaks. EMBO J. 2017; 36: 361–373.
13. Lazzaro F, Novarina D, Amara F, Watt DL, Stone JE, et al. RNase H and postreplication repair protect cells from ribonucleotides incorporated in DNA. Mol. Cell. 2012; 45: 99–110.
14. Macheret M, Halazonetis TD. Intragenic origins due to short G1 phases underlie oncogene-induced DNA replication stress. Nature. 2018; 555: 112–116.
15. Tuduri S, Crabbe L, Conti C, Tourriere H, Holtgreve-Grez H, et al. Topoisomerase I suppresses genomic instability by preventing interference between replication and transcription. Nat. Cell Biol. 2009; 11: 1315–1324.
16. Castellano-Pozo M, Santos-Pereira JM, Rondon AG, Barroso S, Andujar E, et al. R loops are linked to histone H3 S10 phosphorylation and chromatin condensation. Mol. Cell. 2013; 52: 583–590.

17. Lindahl T. Instability and decay of the primary structure of DNA. Nature. 1993; 362: 709–715.
18. Langevin F, Crossan GP, Rosado IV, Arends MJ, Patel KJ. Fancd2 counteracts the toxic effects of naturally produced aldehydes in mice. Nature. 2011; 475: 53–58.
19. Pontel LB, Rosado IV, Burgos-Barragan G, Garaycoechea JI, Yu R, et al. Endogenous formaldehyde is a hematopoietic stem cell genotoxin and metabolic carcinogen. Mol. Cell. 2015; 60: 177–188.
20. Tretyakova NY, Groehler At, Ji S. DNA-protein cross-links: formation, structural identities, and biological outcomes. Acc. Chem. Res. 2015; 48: 1631–1644.
21. Luo J, Solimini NL, Elledge SJ. Principles of cancer therapy: oncogene and non-oncogene addiction. Cell. 2009; 136: 823–837.
22. Jackson SP, Helleday T. DNA REPAIR. Drugging DNA repair. Science. 2016; 352: 1178–1179.
23. Zellweger R, Dalcher D, Mutreja K, Berti M, Schmid JA, et al. Rad51-mediated replication fork reversal is a global response to genotoxic treatments in human cells. J. Cell Biol. 2015; 208: 563–579.
24. Hashimoto Y, Chaudhuri AR, Lopes M, Costanzo V. Rad51 protects nascent DNA from Mre11-dependent degradation and promotes continuous DNA synthesis. Nat. Struct. Mol. Biol. 2010; 17: 1305–1311.
25. Sogo JM, Lopes M, Foiani M. Fork reversal and ssDNA accumulation at stalled replication forks owing to checkpoint defects. Science. 2002; 297: 599–602.
26. Guo Z, Kumagai A, Wang SX, Dunphy WG. Requirement for Atr in phosphorylation of Chk1 and cell cycle regulation in response to DNA replication blocks and UV-damaged DNA in Xenopus egg extracts. Genes Dev. 2000; 14: 2745–2756.
27. Hekmat-Nejad M, You Z, Yee MC, Newport JW, Cimprich KA. Xenopus ATR is a replication-dependent chromatin-binding protein required for the DNA replication checkpoint. Curr. Biol. 2000; 10: 1565–1573.
28. Liu Q, Guntuku S, Cui XS, Matsuoka S, Cortez D, et al. . Chk1 is an essential kinase that is regulated by Atr and

required for the G(2)/M DNA damage checkpoint. Genes Dev. 2000; 14: 1448–1459.
29. Zhao H, Piwnica-Worms H. ATR-mediated checkpoint pathways regulate phosphorylation and activation of human Chk1. Mol. Cell Biol. 2001; 21: 4129–4139.
30. Ciccia A, Elledge SJ. The DNA damage response: making it safe to play with knives. Mol. Cell. 2010; 40: 179–204.
31. Collis SJ, Ciccia A, Deans AJ, Horejsi Z, Martin JS, et al. FANCM and FAAP24 function in ATR-mediated checkpoint signaling independently of the Fanconi anemia core complex. Mol. Cell. 2008; 32: 313–324.
32. Moreaux J, Klein B, Bataille R, Descamps G, Maïga S, et al. A high-risk signature for patients with multiple myeloma established from the molecular classification of human myeloma cell lines. Haematologica. 2011; 96: 574–582.
33. Kermi C, Prieto S, van der Laan S, Tsanov N, Recolin B, et al. RAD18 Is a Maternal Limiting Factor Silencing the UV-Dependent DNA Damage Checkpoint in Xenopus Embryos. Dev. Cell. 2015; 34: 364–372.
34. Luke-Glaser S, Luke B, Grossi S, Constantinou A. FANCM regulates DNA chain elongation and is stabilized by S-phase checkpoint signalling. EMBO J. 2010; 29: 795–805.
35. Wysocka J, Reilly PT, Herr W. Loss of HCF-1-chromatin association precedes temperature-induced growth arrest of tsBN67 cells. Mol. Cell Biol. 2001; 21: 3820–3829.
36. Jackson DA, Pombo A. Replicon clusters are stable units of chromosome structure: evidence that nuclear organization contributes to the efficient activation and propagation of S phase in human cells. J. Cell Biol. 1998; 140: 1285–1295.
37. Diamond TL, Roshal M, Jamburuthugoda VK, Reynolds HM, Merriam AR, et al. Macrophage tropism of HIV-1 depends on efficient cellular dNTP utilization by reverse transcriptase. J. Biol. Chem. 2004; 279: 51545–51553.
38. Lutzmann M, Méchali M. MCM9 binds Cdt1 and is required for the assembly of prereplication complexes. Mol. Cell. 2008; 31: 190–200.
39. Recolin B, Van der Laan S, Maiorano D. Role of replication protein A as sensor in activation of the S-phase checkpoint in Xenopus egg extracts. Nucleic Acids Res. 2012; 40: 3431–3442.

40. Gillespie PJ, Gambus A, Blow JJ. Preparation and use of Xenopus egg extracts to study DNA replication and chromatin associated proteins. Methods. 2012; 57: 203–213.
41. Vaz B, Popovic M, Newman JA, Fielden J, Aitkenhead H, et al. Metalloprotease SPRTN/DVC1 Orchestrates Replication-Coupled DNA-Protein crosslink repair. Mol. Cell. 2016; 64: 704–719.
42. Kumbhar R, Vidal-Eychenie S, Kontopoulos DG, Larroque M, Larroque C, et al. Recruitment of ubiquitin-activating enzyme UBA1 to DNA by poly(ADP-ribose) promotes ATR signalling. Life Sci. Alliance. 2018; 1: e201800096.
43. Cox J, Mann M. MaxQuant enables high peptide identification rates, individualized p.p.b.-range mass accuracies and proteome-wide protein quantification. Nat. Biotechnol. 2008; 26: 1367–1372.
44. Adamson B, Smogorzewska A, Sigoillot FD, King RW, Elledge SJ. A genome-wide homologous recombination screen identifies the RNA-binding protein RBMX as a component of the DNA-damage response. Nat. Cell Biol. 2012; 14: 318–328.
45. Raderschall E, Golub EI, Haaf T. Nuclear foci of mammalian recombination proteins are located at single-stranded DNA regions formed after DNA damage. Proc. Natl. Acad. Sci. U.S.A. 1999; 96: 1921–1926.
46. Lane AN, Fan TW. Regulation of mammalian nucleotide metabolism and biosynthesis. Nucleic Acids Res. 2015; 43: 2466–2485.
47. Techer H, Koundrioukoff S, Carignon S, Wilhelm T, Millot GA, et al. Signaling from Mus81-Eme2-Dependent DNA Damage elicited by Chk1 deficiency modulates replication fork speed and origin usage. Cell Rep. 2016; 14: 1114–1127.
48. Li X, Manley JL. Inactivation of the SR protein splicing factor ASF/SF2 results in genomic instability. Cell. 2005; 122: 365–378.
49. Mechali M, Harland RM. DNA synthesis in a cell-free system from Xenopus eggs: priming and elongation on single-stranded DNA in vitro. Cell. 1982; 30: 93–101.
50. Aze A, Fragkos M, Bocquet S, Cau J, Mechali M. RNAs coordinate nuclear envelope assembly and DNA replication

through ELYS recruitment to chromatin. Nat. Commun. 2017; 8: 2130.
51. Errico A, Costanzo V, Hunt T. Tipin is required for stalled replication forks to resume DNA replication after removal of aphidicolin in Xenopus egg extracts. Proc. Natl. Acad. Sci. U.S.A. 2007; 104: 14929–14934.
52. Trenz K, Smith E, Smith S, Costanzo V. ATM and ATR promote Mre11 dependent restart of collapsed replication forks and prevent accumulation of DNA breaks. EMBO J. 2006; 25: 1764–1774.
53. Huang CY. Inhibition of a putative dihydropyrimidinase from pseudomonas aeruginosa PAO1 by Flavonoids and substrates of cyclic amidohydrolases. PLoS One. 2015; 10: e0127634.
54. Kannouche PL, Wing J, Lehmann AR. Interaction of human DNA polymerase eta with monoubiquitinated PCNA: a possible mechanism for the polymerase switch in response to DNA damage. Mol. Cell. 2004; 14: 491–500.
55. Zlatanou A, Despras E, Braz-Petta T, Boubakour-Azzouz I, Pouvelle C, et al. The hMsh2-hMsh6 complex acts in concert with monoubiquitinated PCNA and Pol eta in response to oxidative DNA damage in human cells. Mol. Cell. 2011; 43: 649–662.
56. Sale JE, Lehmann AR, Woodgate R. Y-family DNA polymerases and their role in tolerance of cellular DNA damage. Nat. Rev. Mol. Cell Biol. 2012; 13: 141–152.
57. Stingele J, Bellelli R, Alte F, Hewitt G, Sarek G, et al. Mechanism and regulation of DNA-Protein crosslink repair by the DNA-Dependent metalloprotease SPRTN. Mol. Cell. 2016; 64: 688–703.
58. Larsen NB, Gao AO, Sparks JL, Gallina I, Wu RA, et al. Replication-coupled DNA-protein crosslink repair by SPRTN and the proteasome in Xenopus egg extracts. Mol. Cell. 2019; 73: 574–588.
59. Kumar D, Viberg J, Nilsson AK, Chabes A. Highly mutagenic and severely imbalanced dNTP pools can escape detection by the S-phase checkpoint. Nucleic Acids Res. 2010; 38: 3975–3983.

60. Sparks JL, Chistol G, Gao AO, Raschle M, Larsen NB, et al. The CMG helicase bypasses DNA-protein cross-links to facilitate their repair. Cell. 2019; 176: 167–181.
61. Mokrasch LC, Grisolia S. Incorporation of hydropyrimidine derivatives in ribonucleic acid with liver preparations. Biochim. Biophys. Acta. 1958; 27: 226–227.
62. Mokrasch LC, Grisolia S. Some enzymic actions on hydrouracil derivatives. Biochim. Biophys. Acta. 1960; 39: 361–363.
63. Lin G, Jian Y, Dria KJ, Long EC, Li L. Reactivity of damaged pyrimidines: DNA cleavage via hemiaminal formation at the C4 positions of the saturated thymine of spore photoproduct and dihydrouridine. J. Am. Chem. Soc. 2014; 136: 12938–12946.
64. Lerma-Ortiz C, Jeffryes JG, Cooper AJ, Niehaus TD, Thamm AM, et al.'Nothing of chemistry disappears in biology': the Top 30 damage-prone endogenous metabolites. Biochem. Soc. Trans. 2016; 44: 961–971.
65. Wang M, Cheng G, Khariwala SS, Bandyopadhyay D, Villalta PW, et al. Evidence for endogenous formation of the hepatocarcinogen N-nitrosodihydrouracil in rats treated with dihydrouracil and sodium nitrite: a potential source of human hepatic DNA carboxyethylation. Chem. Biol. Interact. 2013; 206: 83–89.
66. Li H, Li Q, Liu Z, Yang K, Chen Z, et al. The versatile effects of dihydromyricetin in health. Evid Based Complement Alternat. Med. 2017; 2017: 1053617.
67. Huang H, Hu M, Zhao R, Li P, Li M. Dihydromyricetin suppresses the proliferation of hepatocellular carcinoma cells by inducing G2/M arrest through the Chk1/Chk2/Cdc25C pathway. Oncol. Rep. 2013; 30: 2467–2475.
68. Duxin JP, Dewar JM, Yardimci H, Walter JC. Repair of a DNA-protein crosslink by replication-coupled proteolysis. Cell. 2014; 159: 346–357.
69. Neidhardt G, Hauke J, Ramser J, Gross E, Gehrig A, et al. Association between Loss-of-Function mutations within the FANCM Gene and Early-Onset familial breast cancer. JAMA Oncol. 2016; 3: 1245–1248.
70. Bogliolo M, Bluteau D, Lespinasse J, Pujol R, Vasquez N, et al. Biallelic truncating FANCM mutations cause early-onset

cancer but not Fanconi anemia. Genet. Med. 2017; 20: 458–463.
71. Catucci I, Osorio A, Arver B, Neidhardt G, Bogliolo M, et al. Individuals with FANCM biallelic mutations do not develop Fanconi anemia, but show risk for breast cancer, chemotherapy toxicity and may display chromosome fragility. Genet. Med. 2017; 20: 452–457.
72. Basbous J, Constantinou A. A tumor suppressive DNA translocase named FANCM. Crit. Rev. Biochem. Mol. Biol. 2019; 54: 27–40.
73. Sumi S, Kidouchi K, Hayashi K, Ohba S, Wada Y. Dihydropyrimidinuria without clinical symptoms. J. Inherit. Metab. Dis. 1996; 19: 701–702.
74. van Kuilenburg AB, Dobritzsch D, Meijer J, Meinsma R, Benoist JF, et al. Dihydropyrimidinase deficiency: Phenotype, genotype and structural consequences in 17 patients. Biochim. Biophys. Acta. 2010; 1802: 639–648.
75. Putman CW, Rotteveel JJ, Wevers RA, van Gennip AH, Bakkeren JA, et al. Dihydropyrimidinase deficiency, a progressive neurological disorder. Neuropediatrics. 1997; 28: 106–110.
76. van Kuilenburg AB, Meijer J, Dobritzsch D, Meinsma R, Duran M, et al. Clinical, biochemical and genetic findings in two siblings with a dihydropyrimidinase deficiency. Mol. Genet. Metab. 2007; 91: 157–164.
77. Hamajima N, Kouwaki M, Vreken P, Matsuda K, Sumi S, et al. Dihydropyrimidinase deficiency: structural organization, chromosomal localization, and mutation analysis of the human dihydropyrimidinase gene. Am. J. Hum. Genet. 1998; 63: 717–726.
78. Assmann B, Hoffmann GF, Wagner L, Brautigam C, Seyberth HW, et al. Dihydropyrimidinase deficiency and congenital microvillous atrophy: coincidence or genetic relation. J. Inherit. Metab. Dis. 1997; 20: 681–688.
79. Henderson MJ, Ward K, Simmonds HA, Duley JA, Davies PM. Dihydropyrimidinase deficiency presenting in infancy with severe developmental delay. J. Inherit. Metab. Dis. 1993; 16: 574–576.
80. Lunt SY, Muralidhar V, Hosios AM, Israelsen WJ, Gui DY, et al. Pyruvate kinase isoform expression alters nucleotide

synthesis to impact cell proliferation. Mol. Cell. 2015; 57: 95–107.
81. Park SY, Korm S, Chung HJ, Choi SJ, Jang JJ, et al. RAP80 regulates epithelial-mesenchymal transition related with metastasis and malignancy of cancer. Cancer Sci. 2016; 107: 267–273.
82. Liu X, Dong R, Jiang Z, Wei Y, Li Y, et al. MDC1 promotes ovarian cancer metastasis by inducing epithelial-mesenchymal transition. Tumour Biol. 2015; 36: 4261–4269.
83. Zhang P, Wei Y, Wang L, Debeb BG, Yuan Y, et al. ATM-mediated stabilization of ZEB1 promotes DNA damage response and radioresistance through CHK1. Nat. Cell Biol. 2014; 16: 864–875.
84. Ji FJ, Tian XF, Liu XW, Fu LB, Wu YY, et al. Dihydromyricetin induces cell apoptosis via a p53-related pathway in AGS human gastric cancer cells. Genet. Mol. Res. 2015; 14: 15564–15571.
85. Zeng G, Liu J, Chen H, Liu B, Zhang Q, et al. Dihydromyricetin induces cell cycle arrest and apoptosis in melanoma SK-MEL-28 cells. Oncol. Rep. 2014; 31: 2713–2719.
86. Zhang Q, Liu J, Liu B, Xia J, Chen N, et al. Dihydromyricetin promotes hepatocellular carcinoma regression via a p53 activation-dependent mechanism. Sci. Rep. 2014; 4: 4628.
87. Ni F, Gong Y, Li L, Abdolmaleky HM, Zhou JR. Flavonoid ampelopsin inhibits the growth and metastasis of prostate cancer in vitro and in mice. PLoS One. 2012; 7: e38802.

Supplementary data

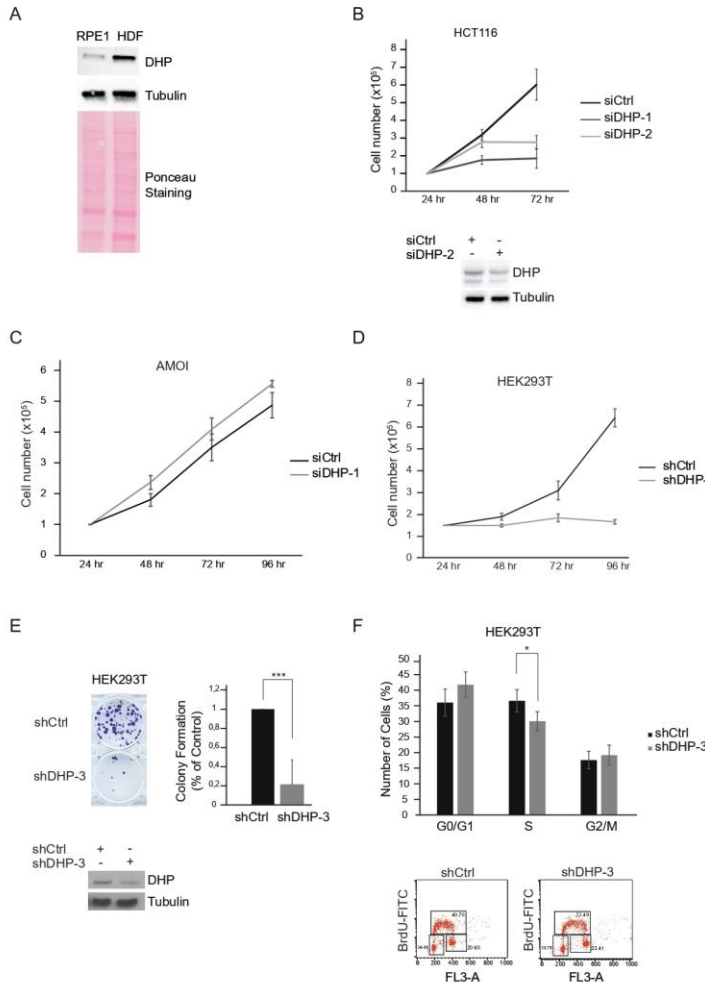

Figure S1:

(A) DHP was probed by Western blotting in hTERT-immortalized retinal pigment epithelial cells (hTERT RPE-1) and in primary human dermal fibroblasts (HDF). Tubulin and Ponceau staining were used as loading control.

(B) HCT116 cells were transfected with control or two distinct anti-DHP siRNAs (siDHP-1 and siDHP-2). At the indicated times, viable cells were identified via trypan blue exclusion and counted. Mean viability is

representative of three independent biological replicates. Error bars represent +/- S.D. Bottom panel: The efficiency of DHP knockdown was assessed by western blotting.

(C) AMOI cells were transfected with control or anti-DHP siRNAs. At the indicated times, viable cells were identified via trypan blue exclusion and counted. Mean viability is representative of three independent biological replicates. Error bars represent +/- S.D.

(D) HEK239T cells were transfected with shControl or shDHP-3. At the indicated times, viable cells were counted by trypan blue staining. Mean viability is representative of three independent biological replicates. Error bars represent +/- S.D.

(E) Colony-forming assay of HEK293T cells after transfection with control or anti-DHP shRNA (shDHP-3). A representative image is shown. An histogram represents the quantification of colony formation. Data shown are averages over three independent biological replicates with two technical replicates for each. Error bars represent +/- S.D. p-values were calculated using a regression model with Poisson distribution: *** $P < 0.0001$. Bottom panel: The efficiency of DHP knockdown was assessed by western blotting.

(F) Histogram representing the cell cycle distribution of HEK293T cells 72 hours after transfection with control or anti-DHP shRNA. Data shown are averages over three independent biological replicates. Error bars represent +/- S.D. p-values were calculated using a regression model with Poisson distribution: * $P < 0.05$.

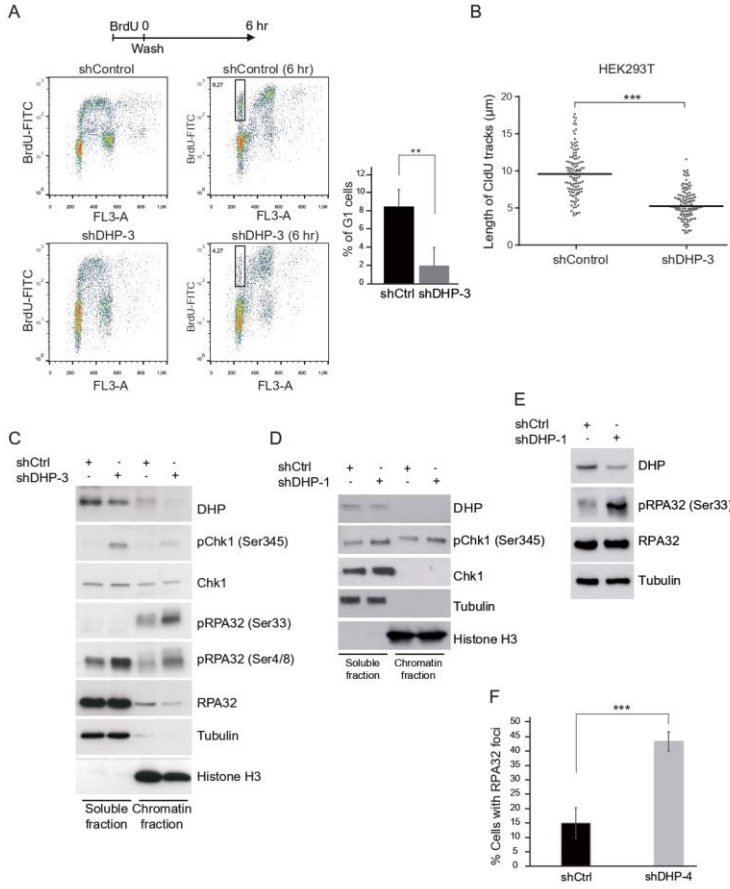

Figure S2:

(A) Upper panel: Experimental scheme. HEK293T cells transfected with control or anti-DHP shRNA were pulse-labeled with 20 µM BrdU for 30 min, washed (W) and incubated for 6 hours in BrdU-free medium before analysis of the cell cycle distribution by two-dimensional (BrdU/DNA) flow cytometry. Right panel: Histogram representing the percentage of G1 cells that were in S phase (incorporating BrdU) 6 hours before the flow cytometry analysis. Data from three independent biological replicates are represented as mean +/- S.D. p-values were calculated using a regression model with Poisson distribution: ** $P < 0.001$.

(B) Graphic representation of replication track lengths in control and HEK293T cells for DHP using a shRNA molecule with a distinct target sequence in DHP. The bar dissecting the data points represents the median of 100 tracts length from one biological replicate. Differences between

distributions were assessed with the Mann-Whitney rank sum test. p-values: *** < 0.0001.

(C) DHP knockdown HEK293T cells were subjected to subcellular fractionation and probed by western blotting with the indicated antibodies. *Tubulin and histone H3* were used as *loading controls* for the cytoplasmic and chromatin *fractions*, respectively. One representative experiment is shown from two biological replicates.

(D) DHP-depleted U-2 OS cells were subjected to subcellular fractionation and probed by western blotting with the indicated antibodies. *Tubulin and histone H3* were used as *loading controls* for the cytoplasmic and chromatin *fractions*, respectively. One representative experiment is shown from two biological replicates.

(E) Whole-cell extracts from control and DHP knockdown HEK293T cells (shDHP-4) were analyzed by western blotting with the indicated antibodies. One representative experiment is shown from two biological replicates.

(F) Quantification of the percentage of RPA32 foci positive cells in a population of 100 cells of DHP-depleted HEK293T cells (shDHP-4). Data from three independent biological replicates are represented as mean +/- S.D. p-values were calculated using a regression model with Poisson distribution: *** $P < 0.0001$.

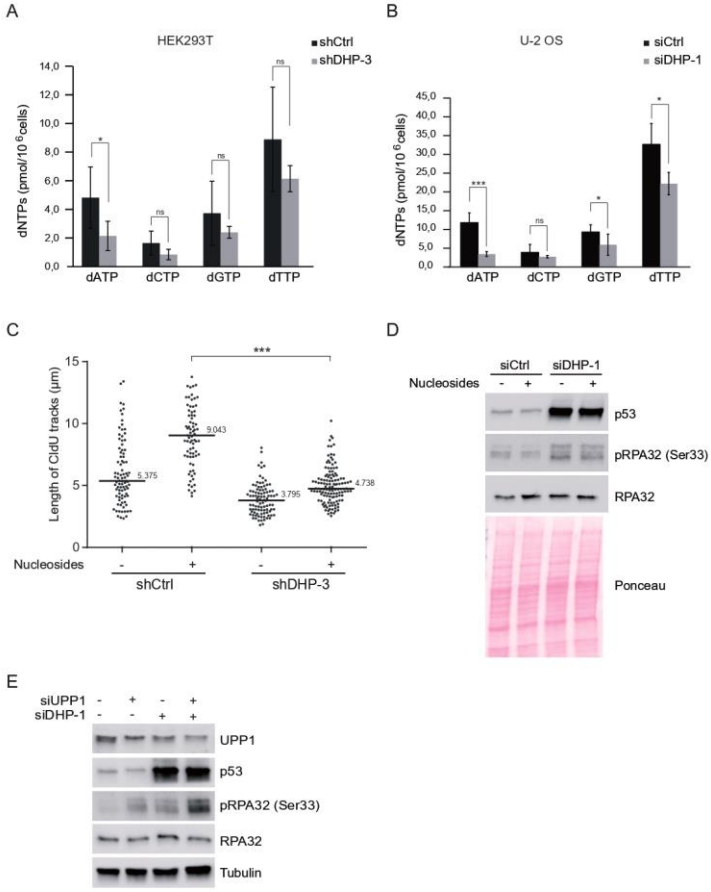

Figure S3:

(A) Analysis of dNTP concentrations in control and DHP knockdown HEK293T cells. Data from three independent biological replicates, with three technical replicates for each, are represented as mean +/- S.D. Cellular dNTPs were measured by HIV-RT based dNTP assay (Diamond TL et al, 2004). p-values were calculated using a regression model with Poisson distribution: * $P < 0.05$, ns: not significant.

(B) Analysis of dNTP concentrations in control and DHP knockdown U-2 OS cells. Data from three independent biological replicates, with three technical replicates for each, are represented as mean +/- S.D. p-values were calculated using a regression model with Poisson distribution: *** $P < 0.0001$, * $P < 0.05$, ns: not significant.

(C) Control and DHP knockdown HEK293T cells were supplemented with nucleosides and incubated for 18 hours before DNA fiber analysis of the length of CldU labeled replication tracks, in µm (y axis). The bar dissecting the data points represents the median of 100 tracts length from one biological replicate. Differences between distributions were assessed with the Mann-Whitney rank sum test. p-values: *** < 0.0001.

(D) Control and DHP knockdown U-2 OS cells (siDHP-1) were supplemented with nucleosides and incubated for 18 hours before western blot analysis with the indicated antibodies. Ponceau staining was used as loading control.

(E) Western blot analysis with the indicated antibodies of whole cell extracts from U-2 OS transfected with anti-DHP and anti-UPP1 siRNAs. One representative experiment is shown from two biological replicates.

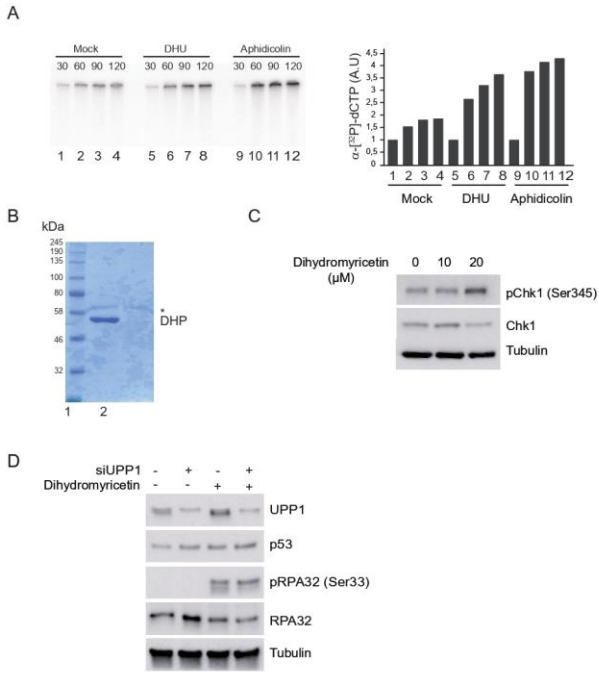

Figure S4:

(A) Replicate of chromatin transfer as described in Figure 4D. Replication products were resolved by 1 % alkaline agarose gel electrophoresis and revealed by autoradiography. Lanes 1-4: Mock treated extracts; Lanes 5-8: incubation in the first extract was performed in the presence of 7.5 mM DHU. Lanes 10-12 serve as positive controls: after 30 min incubation in the first extract, DNA synthesis was blocked with aphidicolin (100 ng/µl). Right panel: Histogram representing the quantification of the gel by image J of replication products (arbitrary unit).

(B) Purified His-tagged DHP was resolved by SDS/PAGE and stained with Coomassie (lane 2). Size marker (lane 1). * non-specific band.
(C) Western blot analysis with the indicated antibodies of U-2 OS whole-cell extracts treated with dihydromyricetin for 12 hr at the indicated concentrations. One representative experiment is shown from three biological replicates.
(D) Western blot analysis with the indicated antibodies of whole cell extracts from U-2 OS transfected with anti-UPP1 siRNA and treated or not with 20 μM of dihydromyricetin for 24 hr. One representative experiment is shown from two biological replicates.

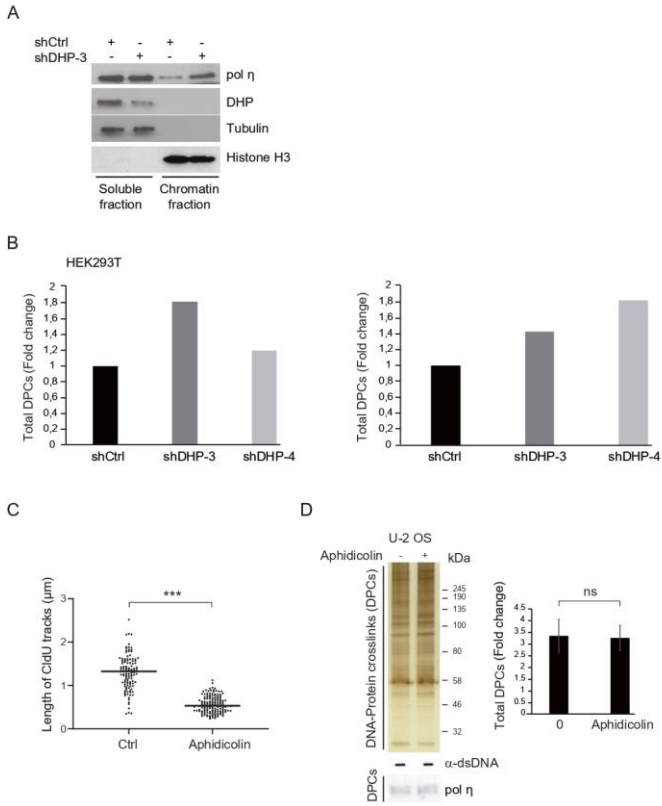

Figure S5:

(A) DHP knockdown HEK293T cells were subjected to subcellular fractionation and probed by western blotting with the indicated antibodies. *Tubulin and histone H3* were used as *loading controls* for the cytoplasmic and chromatin *fractions,* respectively.
(B) Histogram representing the quantification of DPC levels of HEK293T cells transfected with control or two anti-DHP shRNAs (shDHP-3 and

shDHP-4) normalized to total DNA. Two independent biological replicates are represented. p-values were calculated using a regression model with Poisson distribution: *** $P < 0.0001$.

(C) Graphic representation of replication track lengths in U-2 OS cells treated or not with 0.1 µM Aphidicolin for 30 min. The bar dissecting the data points represents the median of 100 tracts length from one biological replicate. Differences between distributions were assessed with the Mann-Whitney rank sum test. p-values: *** < 0.0001.

(D) Total DPC levels in U-2 OS cells treated or not with 0.1 µM Aphidicolin for 30 min visualized by silver staining. Right panel: Histogram representing the quantification of DPC levels normalized to total DNA amount by image J. Three independent biological replicates are averaged in the bar graphs. Error bars represent +/- S.D. p-values were calculated using a regression model with Poisson distribution: ns; not significant. Bottom panel: Western blot analysis of crosslinked DNA polymerase η in total DPC extracts from the experiment above. One representative experiment is shown from three biological replicates.

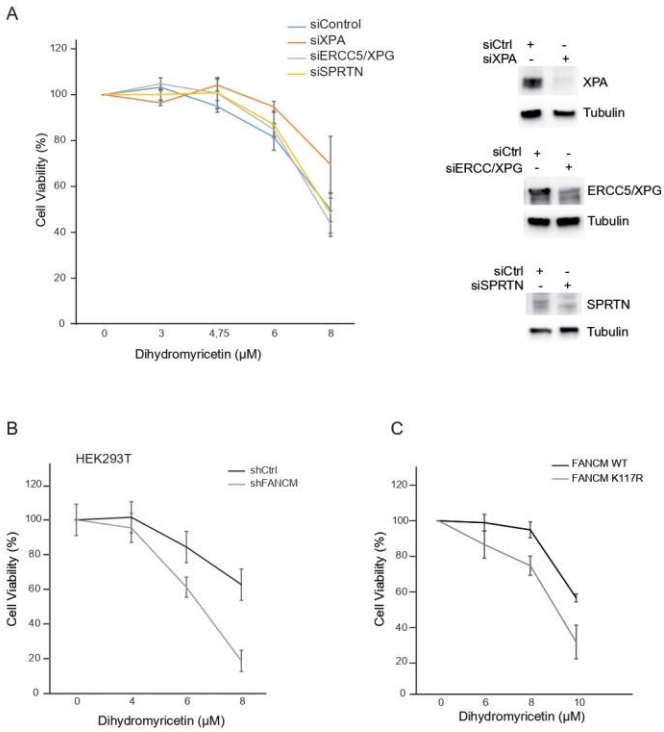

Figure S6:

(A) U-2 OS cells were transfected with the indicated siRNAs and exposed to increasing concentrations of dihydromyricetin for two days. Cell viability

was estimated using Cell Titer-Glo assay. Mean viability is representative of experiments preformed in triplicate. Error bars represent +/- S.E.M. Right panel: the efficiency of XPA, SPRTN and ERCC5/XPG knockdown was assessed by western blotting.

(B) HEK293T cells were transfected with control or anti-FANCM shRNA and, after 36 hours, exposed to increasing doses of dihydromyricetin for 48 hours. Cell viability was assessed by Cell Titer-Glo. Mean viability is representative of experiments preformed in duplicate. Error bars represent +/- S.E.M.

(C) HEK293 FANCM WT and FANCM K117R cells were exposed to increasing doses of dihydromyricetin for 48 hours. Cell viability assessed by Cell Titer-Glo. Mean viability is representative of experiments preformed in triplicate. Error bars represent +/- S.D.

Book Chapter

HTLV-1 Infection and Adult T Cell Leukemia: Mechanisms of Oncogenesis and Alteration of Immunity

Mariam Shallak*, Greta Forlani and Roberto S Accolla

Laboratories of General Pathology and Immunology "Giovanna Tosi", Department of Medicine and Surgery, University of Insubria, Italy

*PhD program in Experimental and Translational Medicine

***Corresponding Author:** Mariam Shallak, Laboratories of General Pathology and Immunology "Giovanna Tosi", Department of Medicine and Surgery, University of Insubria, 21100 Varese, Italy

Published **August 06, 2021**

How to cite this book chapter: Mariam Shallak, Greta Forlani, Roberto S Accolla. HTLV-1 Infection and Adult T Cell Leukemia: Mechanisms of Oncogenesis and Alteration of Immunity. In: Hussein Fayyad Kazan, editor. Immunology and Cancer Biology. Hyderabad, India: Vide Leaf. 2021.

Abstract

HTLV-1 is the first discovered human oncogenic retrovirus leading to an aggressive malignancy known as Adult T cell Leukemia/Lymphoma (ATL) or to a neuroinflammatory disease defined as HTLV-1 associated myelopathy/tropic spastic

paraparesis (HAM/TSP). ATL development occurs in 2–5% of infected individuals 30–50 years after initial exposure. HTLV-1 mainly targets CD4+ T cells resulting in the dysregulation of the host immune response. HTLV-1 oncogenesis is generally accompanied by genomic instability, clonal proliferation of the infected cells, and immune evasion. Among the various proteins encoded by HTLV-1, Tax and HBZ play a crucial role in initiation of cellular transformation and maintenance of cell proliferation, respectively, and as such they are operatively considered as viral oncogenes. Nevertheless, the complete picture underlying cellular transformation and persistence of the leukemic state after infection remain mostly unexplained. This review highlights the interactions between HTLV-1 viral oncogenes and the host immune system, which may help to better understand HTLV-1 mediated leukemogenesis.

Background

Human T-cell leukemia virus (HTLV-1) is the first oncogenic retrovirus identified in humans [1]. It is estimated that HTLV-1 infects at least 10-15 million people worldwide. Large endemic areas are mainly identified in Southern Japan, the Caribbean, Central and South America, the Middle East, Melanesia, and equatorial regions of Africa [2]. Most HTLV-1 infected individuals remain asymptomatic carriers (AC) for lifelong. About 3–5% of them develop, after many years of clinical latency, a severe malignancy of CD4+ T cells, known as Adult T-cell Leukemia/lymphoma (ATL) or a severe neuropathological inflammatory syndrome defined as HTLV-1-associated myelopathy/tropical spastic paraparesis (HAM/TSP) [3].

HTLV-1 belongs to the family of deltaretroviruses that, similarly to other retroviruses, harbors *gag*, *pol*, *pro*, and *env* genes flanked by long terminal repeats (LTR). The *gag* gene provides the main constituent of the viral capsid. The *pol* and *pro* region encode the reverse transcriptase, protease, and integrase. The *env* gene codes for a glycoprotein that mediates viral entry. In addition, HTLV-1 genome contains between *env* and the 3′-LTR a region designated pX region that encodes for Tax, Rex, and additional accessory proteins p12, p13, p21, and p30. Tax is a

viral transactivator that activates transcription from the LTR. Rex mediates nuclear export of viral RNA. At variance to other retroviruses, HTLV-1 encodes an antisense open reading frame encoding the helix-basic loop zipper protein HBZ. Tax and HBZ are two major viral regulatory proteins that cooperate to mediate HTLV-1 leukemogenesis [4].

HTLV-1 transmission mainly occurs through three routes: from mother to child by breastfeeding; during sexual intercourse and after exposure to contaminated blood products [5]. HTLV-1 is mainly transmitted by cell-to-cell contact, as cell-free HTLV-1 viral particles are not efficient for infection. Three cellular factors were identified to favor the viral entry, namely glucose transporter (GLUT1), heparan sulfate proteoglycan (HSPG), and neuropilin-1. These molecules are crucial for the interaction between the HTLV-1 envelope and the cell membrane. It has been suggested that the virus may first contact HSPG and then form complexes with neuropilin-1, followed by GLUT1 association on the cell surface prior to membrane fusion and entry into the cell [6]. After penetration into target cells, reverse transcription of HTLV-1 genomic RNA into DNA occurs followed by its integration at random sites within the host genome. Interestingly, however, in leukemic cells integrated proviral DNA is preferentially found near the transcriptional start sites of host genes, a feature indicating positive selection of cells during leukemogenesis [7].

ATL is a heterogeneous disease with four clinical subtypes: acute, lymphoma, chronic, and smoldering. Acute and lymphoma subtypes are known as aggressive ATL with large tumor burden, blood and lymph node involvement, and hypercalcemia. Chronic and smoldering subtypes are indolent ATL characterized by rash and minimal blood involvement. The leukemic cells are characterized often by unusual morphology with ovulated nuclei that confer to the cell a characteristic “flower-like” aspect. Despite the progress achieved in the clinical treatment of the disease, prognosis remains poor with an average survival rate of only a few months [8].

HTLV-1 Oncoproteins Tax-1 and HBZ

The basic molecular mechanism behind HTLV-1 infection progressing towards ATL is not yet fully understood although various studies point to the involvement of Tax-1 and HBZ.

Tax-1 is a 40-kDa transactivator protein serving as the master regulator of HTLV-1 proviral expression from the LTR. Activation of viral gene expression depends on Tax-1 interaction with CREB. Tax-1 also recruits co-transcriptional activators including p300/CREB- binding protein (CBP) and CREB-regulating transcriptional coactivators (CRTCs) to the core TATAA promoter of HTLV-1 in order to favor its optimal activity [9]. Tax-1 attracts other regulatory enzymes to modulate the process of the viral transcription. p21-activated kinases increase Tax-mediated LTR-dependent transcription [10]. On the other hand, LKB1 and salt-inducible kinases, protein deacetylases SIRT1, as well as T cell- specific transcription factors TCF1 and LEF1 are recruited to exert negative regulation of proviral transcription [4].

Tax-1 activates constitutively the nuclear factor kappa B (NF-κB) pathway [11]. The oncogenic capacity of Tax-1 is highly correlated to its capability to modulate this particular signaling pathway. In addition, the alteration of NF-κB signaling pathway could also be associated with the inflammatory state observed in HAM/TSP [12]. Interestingly, at protein level, we have demonstrated that Tax-1 is found in 100% of HTLV-1 AC, and in 75% of HAM/TSP cases but rarely in ATL cases.[13] It is of note that Tax expression alone is capable to transform murine fibroblasts, immortalize T lymphocytes, and induce tumor formation in nude mice and transgenic mice. Tax-1 contribution to transformation necessitates the activation of both CREB and NF-κB signaling pathways along with the assistance of Tax-1 activated host cellular genes [4]. It is also of note that Tax-1 induces significant mitogenic activity at the G1–S-phase transition, by stimulating the upregulation of G1 D cyclins, activation of cyclin-dependent kinases (CDKs), and downregulation of CDK inhibitors (CKIs) [14]. Moreover, Tax-1 can induce direct DNA damage through elevated reactive oxygen

species. Tax-1 inactivates p53, CHK1 and CHK2 kinases, and perturbs DNA repair by suppression of base excision repair (BER), and nucleotide excision repair (NER), leading to the accumulation of DNA damage [15]. Tax-1 is highly immunogenic and a major target for cytotoxic T cell effectors (see below), this may partially explains the fact that loss of Tax-1 expression is frequently observed in ATL cells [16]. Genetic and epigenetic modifications in the proviral genome are also responsible of Tax-1 silencing [17]. Taken together, these observations support the role of Tax-1 in the oncogenic process leading to ATL particularly in the triggering and much less in the persistence of the oncogenic phenotype.

Besides Tax-1, HBZ has become a crucial hotspot in HTLV-1 research. HTLV-1 infected individuals and ATL patients express constantly HBZ both at RNA [18] and protein levels [19]. Experimental animal models have shown that HBZ-transgenic animals develop chronic inflammatory diseases and, importantly, various forms of lymphomas [20], thus suggesting that HBZ is important not only for cellular transformation but also for the maintenance of neoplastic state. HBZ is encoded by the negative strand of the HTLV-1 genome [21]. Three major HBZ transcriptional isoforms have been identified: the unspliced (usHBZ) form and two alternative spliced forms (SP1 and SP2). SP1 is more frequent than SP2 [22]. The unspliced and SP1 spliced HBZ transcripts are translated into polypeptides of 209 and 206 amino acids, respectively, and they have almost identical sequences except for a stretch of seven amino acids at the N-terminus of the protein (MAAS for SP1 HBZ and MVNFVSA for usHBZ). Both proteins are characterized by their N-terminal activation domain, a central domain and a C-terminal basic ZIP domain. HBZ was reported to interact with CREB/CREB-2 through its bZIP domain, and this association was indispensable to abolish Tax-mediated HTLV-1 viral transcription [21]. Various findings have proven that HBZ exerts opposite effects with respect to Tax-1 on signaling pathways. HBZ interaction with p300/CBP impairs their binding to Tax-1 leading to the suppression of Tax-1 mediated HTLV-1 transactivation [23]. HBZ inhibits classical NF-κB pathway, which is activated by Tax-1, by preventing the recruitment of

p65-RelA to its consensus DNA sequence and inducing its degradation [24]. HBZ protein has poor immunogenicity due to the poor presentation of HBZ epitopes on MHC-I [25]. The low immunogenicity of HBZ favors the viral immune escape, thus promoting the spreading of infection and the persistence of viral latency. Moreover, HBZ establishes viral latency by preventing Rex-mediated export of nuclear RNA transcripts thus, abolishing the viral particles production [26]. HBZ promotes ATL cell proliferation by inhibiting apoptosis. It impairs the binding of AFT3 to p53, thus affecting the activation of p53-mediated apoptosis signaling [27]. It inhibits the transcriptional activation of pro-apoptotic genes as Bim and Fas Ligand, by interfering with FoxO3 [28]. HBZ binds to NFAT and suppresses the production of Th1 cytokines, thus impairing anti-viral immune responses [29]. Collectively, these findings highlight the importance of HBZ in promoting cellular proliferation and the persistence of the viral infection.

Subcellular Localization of Tax-1 and HBZ during HTLV-1 Pathogenesis

While Tax-1 can be found both in the cytoplasm and nucleus in AC, HAM/TSP and, when expressed, in ATL leukemic patients, the subcellular distribution of HBZ appears quite distinct. Historically, most of HBZ biochemical and functional studies were performed in artificial overexpressing transfected cells that hardly mimic the physiological state of HBZ within HTLV-1 infected individuals. More recently, the isolation of the anti-HBZ monoclonal antibody, 4D4-F3, in our laboratory, provided us with the possibility to assess the endogenous HBZ expression, localization and interaction *in vivo* in HTLV-1 infected individuals, HAM/TSP and ATL patients. We have demonstrated that endogenous HBZ is 20- to 50- fold lower in ATL patients as compared to HBZ transfected cells. Extensive confocal microscopy studies have been performed to verify some reported HBZ interactions. Indeed, endogenous HBZ interacts and co-localizes with p300 and JunD. Partial colocalization was observed also for CBP and CREB2. Regarding the level of HBZ expression, it was observed that almost 100% of ATL cells express HBZ protein, around 0.4 to 11% of peripheral

mononuclear cells (PBMC) of HAM/TSP patients, and rare PBMC of asymptomatic HTLV-1 carriers [19].

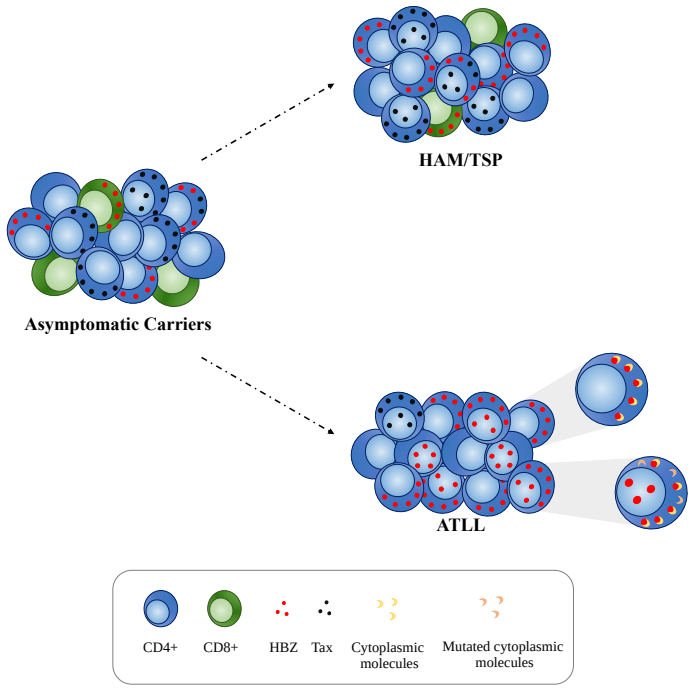

Figure 1: Hypothetical model of disease progression in HTLV-1 infected people based on the expression and localization of Tax-1 and HBZ proteins at the single cell level. Upon infection of T cells by HTLV-1, asymptomatic carriers are characterized by the exclusive cytoplasmic expression and localization of HBZ protein, at variance with Tax-1 that can be found both in the cytoplasm and nucleus. This feature is conserved during the progression to chronic neurologic inflammatory syndrome (HAM/TSP). Leukemogenesis, on the other hand, is marked by the progressive translocation of HBZ from the cytoplasm to the nucleus. It is likely that HBZ cytoplasmic localization in ATL is mediated by the same retention mechanism present in asymptomatic carriers and HAM/TSP that is gradually lost during neoplastic transformation allowing HBZ protein to dislocate into the nucleus.

Previous studies had suggested a specific nuclear localization of HBZ. Unexpectedly, instead, our findings have demonstrated an exclusive cytoplasmic localization of naturally expressed endogenous HBZ in the PBMCs of asymptomatic carriers (ACs) and HAM/TSP patients [30], which was not modified by

treatment of the cells with Leptomycin B, a compound that blocks the CRM1-dependent nuclear protein export, indicating that the viral protein does not shuttle between the nucleus and the cytoplasm. The majority of cytoplasmic HBZ-expressing cells were exclusively found in CD4+ T cells and very rarely in CD8+ T cells. Interestingly, the HBZ-positive CD4+ cells did not express the CD25 T cell activation marker [13]. This suggests that the infected cells do not belong to the category of regulatory T cells and are not under rapid proliferative state. Of relevance, very recent studies of our group showed that in leukemic cells of ATL patients, HBZ localizes both in the cytoplasm and in the nucleus irrespective of patient's clinical status, with a strong preference for the cytoplasmic localization. (Figure 1) It is likely that there is a retention mechanism of HBZ within the cytoplasm which is gradually lost during neoplastic transformation. Taken together, these studies strongly suggests a cytoplasmic-to-nuclear unidirectional translocation in HTLV-1-mediated oncogenesis [31].

Preferential Clonal Expansion of HTLV-1 infected CD4+ T Cells and the Immune response against the Virus

HTLV-1 can infect various cell types *in vitro* such as dendritic cells, macrophages, B cells and T cells [32]; however, the preferential targets of HTLV-1 infection *in vivo* are the CD4+ T cells [33]. It is believed that the clonal proliferation induced by the virus is crucial for establishing the biological conditions for the transformation of infected CD4+ T cells in some HTLV-1 carriers. Once they are infected, CD4+ T cells become the target of the cellular immune response against the virus which is highly dominated by the CD8+ T cells with cytolytic function (CTL).

As previously mentioned, a major target of CTL response is Tax-1. Indeed, Tax-1-derived peptides are presented by HLA-class I molecules expressed on infected cells with high frequency and certain HLA class I alleles have been found to be associated to stronger response against the virus. For example, the *HLA-A*02* allele is associated with both a reduction in the provirus load of HTLV-1 as well as with protection against HAM/TSP

[34]. However, in ATL patients, anti-Tax-1 CTL response appears relatively weak, mostly as result of the selection of HTLV-1 infected clones with silenced Tax-1 expression, as outlined previously. In addition, a significant proportion of CD8+ T lymphocytes are found to be HTLV-1 infected *in vivo*. The susceptibility of CTLs to HTLV-1 infection might be explained by the cell contact between CTLs and HTLV-1 infected APCs resulting in the spread of HTLV-1 *in vivo*. CTL response can be also down modulated by Foxp3+ Treg cells. Tregs suppress the functions of APCs and CTLs through direct cell contact via CTLA-4. Also, Tregs secret inhibitory cytokines IL-10 and TGF-β that maintain an immunosuppressive microenvironment. The rate of CTL-mediated lysis of autologous HTLV-1 infected cells is negatively correlated to the frequency of Treg cells *ex vivo* [35].

Interestingly, upon the transplantation of allogeneic bone marrow (HSCT), an improvement in ATL outcome has been noticed but only in those who were in remission. Donor-derived T-cells endowed the recipients with de novo immune response mediated by Tax-1-specific CTL. This observation led to the designation of the first anti-ATL therapeutic vaccine to activate CD8+ Tax-specific CTLs by using Tax peptides as antigen and autologous DCs as adjuvant [36]. The three ATL patients that have undergone the vaccination showed clear proliferative responses of Tax-specific CTLs without severe adverse effects. These favorable clinical outcomes of the Tax-DC vaccine indicate the significance of Tax-specific CTLs in maintenance of remission in those ATL cases in which Tax-1 is still expressed that, as outlined above, are unfortunately 50-60%.

Immune Suppression Mechanism in ATL Patients

In general, ATL patients are under immunosuppressive conditions [37]. The dominant production of IL-10 and TGF-β in ATL patients may contribute to this state. Both Tax and HBZ induce IL-10 production [38,39] which in turn, decreases the antigen presenting capacity of dendritic cells predisposing to viral persistence in these patients. In the complex picture of immune suppression generated by HTLV-1 infection the peculiar

epidemiology and pathophysiology of infection should also be taken into account.

Based on epidemiological studies, one of the risk factors of ATL development is the vertical route of transmission that is accompanied with impaired HTLV-1 specific CTL responses due to immune tolerance. Breastfeeding from an HTLV-1-infected mother may potentially induce newborn tolerance where IL-10 producing regulatory T cells (T regs) may play a role, possibly contributing to immune suppression [15]. In addition, induction of immune checkpoint molecules may lead to the virus specific immune suppression. Programmed cell death protein 1 (PD1) expression on Tax-1-specific CTL is elevated in both HTLV-1 carriers and ATL patients [40] and this may influence the activity of HTLV-1-specific CTL in a negative fashion In fact, blockade of the PD1/PD-Ligand 1 (PD-L1) has been found to improve the Tax-1-specific CTL function [41]. Hence, reestablishment of the host CTL function would be a possible way to complement strategies of therapeutic intervention in ATL.

In infected CD4+ T cells, the HTLV-1 auxiliary protein p12 interacts with the MHC-I heavy chain, preventing its maturation and resulting in proteasomal degradation, leading to downregulation of MHC-I on the surface and this may contribute to immune escape from CTL recognition. On the other hand, MHC-I cell surface molecules act as NK cell inhibitory ligands and protect the cell from NK killing. Thus, if MHC-I is absent, the cell becomes a target for NK cell activity, in this case p12-mediated downregulation of MHC-I alone would be detrimental to the survival of an HTLV-1 infected cell. However, p12 expression also leads to reduced surface expression of intercellular adhesion molecules ICAM-1 and ICAM-2, as well as ligands for the NK cell activating receptors NCR and NKG2D, and thus limits the adhesion of NK cells to infected cells resulting in diminished ability of NK cells to kill HTLV-1-infected cells [42].

CIITA as an HTLV-1 Restriction Factor

Besides adaptive immunity that act as a major pathogen-specific way of defense, intrinsic immunity is considered as an additional mechanism of host protection against pathogens. Intrinsic immunity depends on intracellular molecules known as restriction factors (RFs). They are either constitutively expressed or induced by innate immunity mediators. Their main function is the inhibition of viral infection by counteracting various phases of viral life cycle, from capsid uncoating, viral genome integration, replication, virus particle formation to viral budding [43].

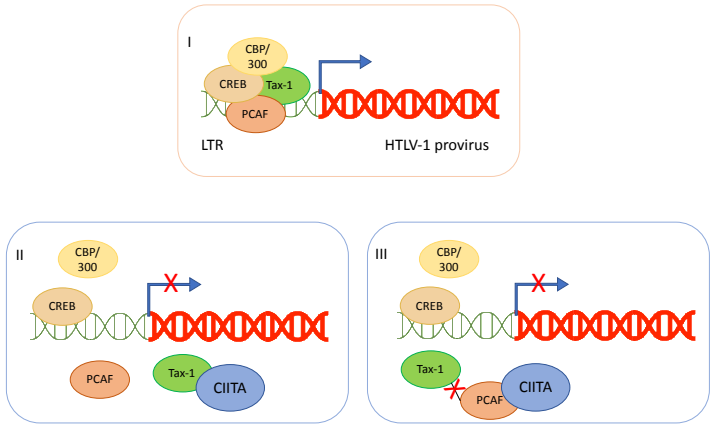

Figure 2: Possible strategies by which CIITA mediates inhibition of Tax-1-mediated LTR transactivation. **I-** In the absence of CIITA, Tax-1 induces the formation of a multiprotein complex containing CREB, CBP and PCAF on the viral LTR promoter, activating HTLV-1 proviral genome transcription. **II-** In the presence of CIITA, Tax-1 is bound by the MHC class II transactivator, preventing the physical formation and assembling of the multiprotein complex on the viral promoter, resulting in inhibition of LTR transcription. **III-** CIITA competitively bind to PCAF, rendering the binding of Tax-1 to PCAF insufficient to promote the transcription of HTLV-1 provirus.

A recently described potent anti-HTLV-1 RF is the MHC class II transcriptional activator, designated as CIITA, originally discovered in our laboratory as the major coordinator of expression of all MHC II genes [44]. In this original role, CIITA is crucial for triggering the adaptive immune responses against

various pathogenic antigens presented by MHC-II molecules. Beside its leading role in the adaptive immune response, the first evidence that CIITA may act as an RF in the context of HTLV-1 infection has arisen when we have demonstrated that CIITA acts as a potent transcriptional repressor for HTLV-1. HTLV-1 replicated in the CIITA-negative U937 cells but not in the CIITA-positive isogenic cells, [45] suggesting that physiological levels of CIITA efficiently inhibited HTLV-1 replication. Ectopic expression of CIITA in CIITA-negative U937 clones led to HTLV-1 replication inhibition. Regarding the basic molecular mechanism behind CIITA-mediated HTLV-1 restriction, we have demonstrated that CIITA targets Tax-1 in a rather complex mode. First, CIITA inhibits the physical and functional interaction between the viral transactivator and crucial cellular factors, such as PCAF, needed to promote Tax-1-mediated HTLV-1 LTR transactivation either by a direct binding to Tax-1 itself or by competitive binding to PCAF. (Figure 2). Of particular interest is the action of CIITA on the Tax-1-mediated activation of the NF-kB pathway. It is widely accepted this Tax-1 mediated function is of primary importance for HTLV-1 mediated oncogenic transformation. We have demonstrated that the CIITA-Tax-1 interaction blocks the activation of NF-kB both at cytoplasmic and at nuclear level [46]. Within this frame, the inhibitory effects exerted by CIITA may counteract the initial phases of Tax-1-mediated HTLV-1 oncogenic transformation.

Conclusion

ATL prevention and treatment have witnessed a noteworthy improvement in recent years. *De novo* HTLV-1 infection has been diminished after the identification of the mother-to-child vertical route of transmission via breastfeeding. Moreover, the prognosis of ATL has enhanced significantly upon allogeneic bone marrow transplantation. Hence, the stimulation of immune response against HTLV-1 might be a possible strategy to combat HTLV-1 associated diseases. Thus, deciphering the function of the host immune response in the context of HTLV-1 infection would further our knowledge and consequently improve immune strategies of intervention. Identification of biomarkers would be beneficial to predict the disease progression. Within this frame

the recently described distinct subcellular distribution of HBZ during the various phases of infection and progression toward ATL may certainly be of help not only as a specific marker but also as a possible causative event favoring oncogenic transformation. Development of preventive and therapeutic vaccines and screening of new drugs would also improve ATL therapy.

References

1. BJ Poiesz, FW Ruscetti, AF Gazdar, PA Bunn, JD Minna,et al. Detection and isolation of type C retrovirus particles from fresh and cultured lymphocytes of a patient with cutaneous T-cell lymphoma. Proc. Natl. Acad. Sci. U. S. A. 1980; 77: 7415–7419.
2. A Gessain, O Cassar. Epidemiological Aspects and World Distribution of HTLV-1 Infection. Front. Microbiol. 2012; 3.
3. E Matsuura, Y Yamano, S Jacobson. Neuroimmunity of HTLV-I Infection, J. Neuroimmune Pharmacol. Off. J. Soc. NeuroImmune Pharmacol. 2010; 5: 310–325.
4. CP Chan, KH Kok, DY Jin. Human T-Cell Leukemia Virus Type 1 Infection and Adult T-Cell Leukemia. In: Q Cai, Z Yuan, K Lan, editors. Infectious Agents Associated Cancers: Epidemiology and Molecular Biology. Singapore: Springer. 2017; 147–166.
5. H Take, M Umemoto, K Kusuhara, K Kuraya. Transmission Routes of HTLV-I: An Analysis of 66 Families. Jpn. J. Cancer Res. Gann. 1993; 84: 1265–1267.
6. H Hoshino. Cellular Factors Involved in HTLV-1 Entry and Pathogenicit. Front. Microbiol. 2012; 3.
7. K Doi. Preferential selection of human T-cell leukemia virus type I provirus integration sites in leukemic versus carrier states. Blood. 2005; 106: 1048–1053.
8. O Hermine, JC Ramos, K Tobinai. A Review of New Findings in Adult T-cell Leukemia–Lymphoma: A Focus on Current and Emerging Treatment Strategies. Adv. Ther. 2018; 35: 135–152.
9. RPS Kwok. Control of cAMP-regulated enhancers by the viral transactivator Tax through CREB and the co-activator CBP. 1996; 380: 5.

10. CP Chan, YT Siu, KH Kok, YP Ching, HMV Tang, et al. Group I p21-activated kinases facilitate Tax-mediated transcriptional activation of the human T-cell leukemia virus type 1 long terminal repeats. Retrovirology. 2013; 10: 47.
11. L Petropoulos, R Lin, J Hiscott. Human T Cell Leukemia Virus Type 1 Tax Protein Increases NF-κB Dimer Formation and Antagonizes the Inhibitory Activity of the IκBα Regulatory Protein. Virology. 1996; 225: 52–64.
12. JM Peloponese, ML Yeung, KT Jeang. Modulation of nuclear factor-kappaB by human T cell leukemia virus type 1 Tax protein: implications for oncogenesis and inflammation. Immunol. Res. 2006; 34: 1–12.
13. M Baratella. Cytoplasmic Localization of HTLV-1 HBZ Protein: A Biomarker of HTLV-1-Associated Myelopathy/Tropical Spastic Paraparesis (HAM/TSP). PLoS Negl. Trop. Dis. 2017; 11: e0005285.
14. I Schmitt, O Rosin, P Rohwer, M Gossen, R Grassmann. Stimulation of Cyclin-Dependent Kinase Activity and G1- to S-Phase Transition in Human Lymphocytes by the Human T-Cell Leukemia/Lymphotropic Virus Type 1 Tax Protein. J. Virol. 1998; 72: 633–640.
15. SJ Marriott, OJ Semmes. Impact of HTLV-I Tax on cell cycle progression and the cellular DNA damage repair response. Oncogene. 2005; 24.
16. M Nomura. Repression of Tax Expression Is Associated both with Resistance of Human T-Cell Leukemia Virus Type 1-Infected T Cells to Killing by Tax-Specific Cytotoxic T Lymphocytes and with Impaired Tumorigenicity in a Rat Model. J. Virol. 2004; 78: 3827–3836.
17. Y Taniguchi. Silencing of human T-cell leukemia virus type I gene transcription by epigenetic mechanisms. Retrovirology. 2005; 2: 64.
18. M Matsuoka, PL Green. The HBZ gene, a key player in HTLV-1 pathogenesis. Retrovirology. 2009; 6: 71.
19. GU Raval, C Bidoia, G Forlani, G Tosi, A Gessain, et al. Localization, quantization and interaction with host factors of endogenous HTLV-1 HBZ protein in infected cells and ATL. Retrovirology. 2015; 12: P60.
20. Y Higuchi. HTLV-1 induces T cell malignancy and inflammation by viral antisense factor-mediated modulation

of the cytokine signaling. Proc. Natl. Acad. Sci. 2020; 117: 13740–13749.
21. G Gaudray, F Gachon, J Basbous, M Biard-Piechaczyk, C Devaux, et al. The Complementary Strand of the Human T-Cell Leukemia Virus Type 1 RNA Genome Encodes a bZIP Transcription Factor That Down-Regulates Viral Transcription. J. Virol. 2002; 76: 12813–12822.
22. MH Cavanagh. HTLV-I antisense transcripts initiating in the 3'LTR are alternatively spliced and polyadenylated. Retrovirology. 2006; 3: 15.
23. I Clerc. An Interaction between the Human T Cell Leukemia Virus Type 1 Basic Leucine Zipper Factor (HBZ) and the KIX Domain of p300/CBP Contributes to the Down-regulation of Tax-dependent Viral Transcription by HBZ*. J. Biol. Chem. 2008; 283: 23903–23913.
24. T Zhao. Human T-cell leukemia virus type 1 bZIP factor selectively suppresses the classical pathway of NF-κB. Blood. 2009; 113: 2755–2764.
25. AG Rowan. Cytotoxic T lymphocyte lysis of HTLV-1 infected cells is limited by weak HBZ protein expression, but non-specifically enhanced on induction of Tax expression. Retrovirology. 2014; 11: 116.
26. S Philip, MA Zahoor, H Zhi, YK Ho, CZ Giam. Regulation of Human T-Lymphotropic Virus Type I Latency and Reactivation by HBZ and Rex. PLOS Pathog. 2014; 10: e1004040.
27. K Hagiya, J Yasunaga, Y Satou, K Ohshima, M Matsuoka. ATF3, an HTLV-1 bZip factor binding protein, promotes proliferation of adult T-cell leukemia cells. Retrovirology. 2011; 8: 19.
28. A Tanaka-Nakanishi, J Yasunaga, K Takai, M Matsuoka. HTLV-1 bZIP Factor Suppresses Apoptosis by Attenuating the Function of FoxO3a and Altering Its Localization. Cancer Res. 2014; 74: 188–200.
29. K Yasuma. HTLV-1 bZIP Factor Impairs Anti-viral Immunity by Inducing Co-inhibitory Molecule, T Cell Immunoglobulin and ITIM Domain (TIGIT). PLOS Pathog. 2016; 12: e1005372.
30. G Forlani, M Baratella, A Tedeschi, C Pique, S Jacobson, et al. HTLV-1 HBZ Protein Resides Exclusively in the

Cytoplasm of Infected Cells in Asymptomatic Carriers and HAM/TSP Patients. Front. Microbiol. 2019; 10: 819.
31. G Forlani. Dual cytoplasmic and nuclear localization of HTLV-1-encoded HBZ protein is a unique feature of adult T cell leukemia. Haematologica. 2021.
32. Y Koyanagi. In Vivo Infection of Human T-Cell Leukemia Virus Type I in Non-T Cells. Virology. 1993; 196: 25–33.
33. JH Richardson, AJ Edwards, JK Cruickshank, P Rudge, AG Dalgleish. In vivo cellular tropism of human T-cell leukemia virus type 1. J. Virol. 1990; 64: 5682–5687.
34. KJM Jeffery. HLA alleles determine human T-lymphotropic virus-I (HTLV-I) proviral load and the risk of HTLV-I-associated myelopathy. Proc. Natl. Acad. Sci. U. S. A. 1999; 96: 3848–3853.
35. F Toulza, A Heaps, Y Tanaka, GP Taylor, CRM Bangham. High frequency of CD4+FoxP3+ cells in HTLV-1 infection: inverse correlation with HTLV-1–specific CTL response. Blood. 2008; 111: 5047–5053.
36. Y Suehiro. Clinical outcomes of a novel therapeutic vaccine with Tax peptide-pulsed dendritic cells for adult T cell leukaemia/lymphoma in a pilot study. Br. J. Haematol. 2015; 169: 356–367.
37. T Tashiro, T Yamasaki, H Nagai, H Kikuchi, M Nasu. Immunological Studies on Opportunistic Infection and the Development of Adult T-cell Leukemia. Intern. Med. 1992; 31: 1132–1136.
38. N Mori, PS Gill, T Mougdil, S Murakami, S Eto, et al. Interleukin-10 gene expression in adult T-cell leukemia. Blood. 1996; 88: 1035–1045.
39. Y Higuchi. HTLV-1 induces T cell malignancy and inflammation by viral antisense factor-mediated modulation of the cytokine signaling. Proc. Natl. Acad. Sci. 2020; 117: 13740–13749.
40. T Kozako. PD-1/PD-L1 expression in human T-cell leukemia virus type 1 carriers and adult T-cell leukemia/lymphoma patients. Leukemia. 2009; 23.
41. T Kozako. PD-1/PD-L1 expression in human T-cell leukemia virus type 1 carriers and adult T-cell leukemia/lymphoma patients. Leukemia. 2009; 23: 375–382.

42. P Banerjee, G Feuer, E Barker. Human T-cell leukemia virus type 1 (HTLV-1) p12I down-modulates ICAM-1 and -2 and reduces adherence of natural killer cells, thereby protecting HTLV-1-infected primary CD4+ T cells from autologous natural killer cell-mediated cytotoxicity despite the reduction of major histocompatibility complex class I molecules on infected cells. J. Virol. 2007; 81: 9707–9717.
43. PD Bieniasz. Intrinsic immunity: a front-line defense against viral attack. Nat. Immunol. 2004; 5: 1109–1115.
44. RS Accolla, M Jotterand-Bellomo, L Scarpellino, A Maffei, G Carra, et al. aIr-1, a newly found locus on mouse chromosome 16 encoding a trans-acting activator factor for MHC class II gene expression. J. Exp. Med. 1986; 164: 369–374.
45. G Tosi. Major Histocompatibility Complex Class II Transactivator CIITA Is a Viral Restriction Factor That Targets Human T-Cell Lymphotropic Virus Type 1 Tax-1 Function and Inhibits Viral Replication. J. Virol. 2011; 85: 10719–10729.
46. G Forlani, R Abdallah, RS Accolla, G Tosi. The Major Histocompatibility Complex Class II Transactivator CIITA Inhibits the Persistent Activation of NF-κB by the Human T Cell Lymphotropic Virus Type 1 Tax-1 Oncoprotein. J. Virol. 2016; 90: 3708–3721.

Book Chapter

HDAC/HDACi, IgH 3'RR Enhancers, B-Cells and B-Cell Lymphomas

Melissa Ferrad[1#], Nour Ghazzaui[1#], Hussein Issaoui[1#], Jeanne Cook-Moreau[1], Tiffany Marchiol[1], Justine Pollet[2], Sandrine Le Noir[1] and Yves Denizot[1]*

[1]UMR CNRS 7276, INSERM U1262, Equipe Labellisée LIGUE 2018, Université de Limoges, CBRS, France
[2]BISCEm - Pôle analyses moléculaires, France

[#]Equal contributors

***Corresponding Author:** Yves Denizot, UMR CNRS 7276, INSERM U1262, Equipe Labellisée LIGUE 2018, Université de Limoges, CBRS, rue Pr. Descottes, 87025 Limoges, France

Published **September 15, 2021**

How to cite this book chapter: Melissa Ferrad, Nour Ghazzaui, Hussein Issaoui, Jeanne Cook-Moreau, Tiffany Marchiol, Justine Pollet, Sandrine Le Noir, Yves Denizot. HDAC/HDACi, IgH 3'RR Enhancers, B-Cells and B-Cell Lymphomas. In: Hussein Fayyad Kazan, editor. Immunology and Cancer Biology. Hyderabad, India: Vide Leaf. 2021.

Acknowledgments: Authors are "Equipe Labellisée LIGUE 2018". This work was in part supported by ANR (projet EpiSwitch-3'RR 2016). N.G. and H.I were supported by a grant from ANR (projet EpiSwitch-3'RR 2016). M.F. is supported by University of Limoges and "Région Nouvelle Aquitaine". We

thank the animal facility of Limoges University (France) for housing mice and the Nice/Sophia Antipolis Microarray Facility (France) for RNAseq experiments.

For readers: Some of these results were previously published in the following article: Nour Ghazzaui, Mélissa Ferrad, Hussein Issaoui, Sandrine Lecardeur, Jeanne Cook-Moreau, Justine Pollet, Sandrine Le Noir & Yves Denizot (2021) HDAC recruitment in the IgH locus 3' regulatory region is different between mature B-cells and mature B-cell lymphomas, Leukemia & Lymphoma, DOI: 10.1080/10428194.2021.1961239

Conflict of interest: The authors declare no conflict of interest.

Author contributions: Nour Ghazzaui, Melissa Ferrad, Hussein Issaoui and Tiffany Marchiol performed experiments. Sandrine Le Noir, Jeanne Cook-Moreau and Yves Denizot analysed data and wrote the paper. Justine Pollet, Sandrine Le Noir and Yves Denizot analyzed transcriptomic data. Yves Denizot obtained financial grants.

Abstract

Numerous B-cell lymphomas feature translocations linking oncogenes with the immunoglobulin heavy chain (IgH) locus. Epigenetic drugs such as histone deacetylase inhibitors (HDACi) have been approved to treat certain T-cell and B-cell lymphomas. Transcription, accessibility and remodelling of the IgH locus are under the control of the potent *cis*-acting 3' regulatory region (3'RR) suggesting that its targeting would be of therapeutic interest to reduce oncogenicity *in vivo*. We thus investigated HDAC recruitment and HDACi effects on 3'RR activation in normal mature mouse B-cells and whether or not results paralleled those obtained with mature mouse B-cell lymphomas. HDAC1 was recruited to the hs1,2 enhancer element in the centre of the 3'RR palindromic structure during mouse B-cell activation. The HDACi SAHA (suberanilohydroxamic acid) reduced B-cell growth and affected B-cell class switch recombination (CSR) in an isotype-dependent

manner (decreased IgG_3 and increased IgG_1) without any obvious effect on complete IgH locus transcription (including 3'RR eRNA production). Results were markedly different in mature mouse B-cell lymphomas with no HDAC1 recruitment to the 3'RR but recruitment of the CBP histone acetyl transferase (HAT) to hs3a and hs3b elements bordering the 3'RR palindromic structure. No corresponding effect of SAHA on *in vitro* growth of freshly isolated B-cell lymphomas was found. In conclusion, differences in HDAC recruitment and HDACi effects exist between normal mature B-cells and mature B-cell lymphomas. The precise mechanism underlining beneficial use of HDACi to treat several B-cell lymphoid malignancies remains to be elucidated but is clearly not mediated by direct action on IgH 3'RR enhancers.

Introduction

After encountering antigen, B-cells undergo class switch recombination (CSR) that substitutes the constant $(C)_\mu$ gene with C_γ, C_ε or C_α, thereby generating IgG, IgE and IgA antibodies with new effector functions but the same antigenic specificity [1]. CSR is controlled in *cis* by the immunoglobulin heavy chain (IgH) 3'regulatory region (3'RR) that is essential to target the DNA-editing enzyme activation-induced deaminase (AID) onto DNA switch (S) acceptor regions [2,3]. The 3'RR is a complex element with four transcriptional enhancers (namely hs3a, hs1,2, hs3b and hs4) encompassed in a unique and functional 3D palindromic architecture [4,5]. The 3'RR has transcriptional activator activity from immature to mature B-cell stages [6,7] and is the conductor for Ig production [8]. Histone deacetylase inhibitors (HDACi) are a class of compounds reported to modulate gene expression by remodelling chromatin accessibility. HDACi are reported to affect *in vivo* and *in vitro* B-cell responses [9,10]. HDACi are approved for treating certain T-cell and B-cell lymphomas [11,12]. Deciphering the molecular events or mechanisms that underlie the B-cell HDACi-induced effect is of interest not only for basic B-cell immune responses but also for a better understanding of the rationale for the use of HDACi in B-cell lymphoma treatment. HDAC1 has been previously reported to bind to the IgH 3'RR during B-cell

activation suggesting a direct role for HDAC recruitment on 3'RR regulatory functions [9]. The aim of this study was to determine if the effect of the HDACi SAHA on B-cell responses is mediated by a direct effect on the IgH locus through a repressive effect on 3'RR enhancer activation or to a more pleiotropic effect on all cell proliferation/activation/survival pathways.

Material and Methods

Mice - 129 *wt* mice and ΔIRIS mice [4] were used. Mice were housed and procedures were conducted in agreement with European Directive 2010/63/EU on animals used for scientific purposes applied in France as the « Décret n°2012-118 du 1er février 2013 relatif à la protection des animaux utilisés à des fins scientifiques ». Accordingly, the present project (APAFiS≠13855) was authorized by the « Ministère de l'Education Nationale, de l'Enseignement Supérieur et de la Recherche ».

Spleen Cell Cultures for Growth, CSR and Ig Determinations - Single-cell suspensions of $CD43^-$ spleen cells of *wt* mice (8-12 week old, males and females) were cultured 3 days at $1x10^6$ cells/ml in RPMI 1640 with 10% foetal calf serum (FCS), 5μg/ml LPS with or without 20ng/ml IL4 (PeproTech, Rocky Hill, NJ) in the presence or not of various concentrations of SAHA. At day 3, cell proliferation (six replicates) was evaluated using the MTS assay. At day 4, CSR was evaluated by incubating cultured spleen B-cells with anti-B220-SpectralRed (PC5)-labelled antibodies (Biolegend, ref: 103212), anti-IgG_1- (ref: 107020) and anti-IgG_3- (ref: 110002) fluorescein-isothiocyanate (FITC)-labelled antibodies (Southern Biotechnologies) and analyzed on a Fortessa LSR2 (Beckton-Dickinson). At day 3, $1x10^6$ cells were cultured for 24 hours in growth medium without LPS/cytokine/SAHA. Supernatants were recovered and stored at -20°C until used for Ig quantification (ELISA assays specific for IgG_1 and IgG_3) [3,13]. In a separate set of experiments spleen B-cells were directly labelled with anti-B220-, anti-CD19-, anti-IgM-, anti-IgD- and anti-CD138- antibodies to assess the percentage of transitional

B-cells ($B220^+CD19^+IgM^+IgD^-$), mature B-cells ($B220^+CD19^+IgM^+IgD^+$) and plasma B-cells ($B220^+CD19^+CD138^+$) in our experimental conditions.

ChIP Experiments - Single-cell suspensions of $CD43^-$ spleen cells from *wt* mice and ΔIRIS mice were cultured 2 days at $1x10^6$ cells/ml in RPMI 1640 with 10% FCS and 5μg/ml LPS. ChIP experiments were done as previously described [3] with HDAC1 (ab7028, Abcam), HDAC2 (ab7030), HDAC3 (ab7029), CBP (ab2832) and PCAF (ab12188) specific antibodies. PCR primers for quantitative PCR were the following: hs4-Fw-ChIP 5'-CCATGGGACTGAAACTCAGGGAACCAGAAC-3'; hs4-Rev-ChIP 5'-CTCTGTGACTCGTCCTTAGC-3'; hs3b-Fw-ChIP 5'-TGGTTTGGGCCACCTGTGCTGAG-3'; hs3b-Rev-ChIP 5'-GGGTAGGGCAGGGATGTTCA CAT-3'; hs3a-Fw-ChIP 5'-GGGTAGGGCAGGGATGCTCACAT-3'; hs3a-Rev-ChIP 5'-GCTCTGGTTTGGGGCACCTGTGC-3'; hs1,2-Fw-ChIP 5'-AGCATACACTGGGACTGG-3'; hs1,2-Fw-ChIP 5'-CTCTCACTTCCCTGGGGTGTT-3'.

RNAseq Experiments - $CD43^-$ splenocytes were obtained from *wt* mice after 48h of *in vitro* stimulation ($1x10^6$ cells/ml in RPMI 1640 with 10% FCS) with 5μg/ml LPS ± 200 ng/ml SAHA. RNA was extracted using miRNeasy kit from QIAGEN, according to the manufacturer's instructions. Two pooled RNAs (each with three samples) were obtained for each stimulatory condition. RNA libraries were obtained using TruSeq Stranded Total RNA with Ribo-Zero Gold (Illumina), according to the manufacturer's instructions. Libraries were sequenced on a NextSeq500 sequencer, using NextSeq 500/550 High Output Kit (Illumina) (Nice Sophia-Antipolis Functional Genomics Platform, France). Illumina NextSeq500 paired-end 2x150nt reads were mapped with STAR release v2.4.0a versus mm10 with gene model from Ensembl release 77 with default parameters. RNAseq data were deposited with the accession number GSE169690 (https://www.ncbi.nlm.nih.gov/geo/query/acc.cgi?acc=GSE169690) and GSE169691 (https://www.ncbi.nlm.nih.gov/geo/query/acc.cgi?acc=GSE169691).

Mature B-Cell Lymphomas - Freshly isolated $B220^+IgM^+IgD^+$ mature B-cell lymphomas were obtained from i*Myc*C_μ, i*Myc*E_μ and i*Myc*C_α mice [14-18]. ChIP experiments and proliferation studies were performed as for mature *wt* B-cells.

Results

HDAC1 is Recruited to the 3'RR hs1,2 Enhancer - A schematic representation of the IgH locus (not to scale) is shown in Figure 1A. The IgH 3'RR palindromic structure (to scale) with its four enhancer elements (hs3a, hs1,2, hs3b and hs4) and the IRIS sequences are represented. In this study we investigated $CD43^-$ mature spleen B-cells (*i.e.*, depleted $CD43^+$ T-cells and monocytes). About 90% of spleen B-cells had a mature $B220^+CD19^+IgM^+IgD^+$ phenotype. The remaining cells consisted of transitional B-cells (IgM^+IgD^-). Less than 1% expressed the CD138 plasmocyte antigen (Figure 1B). Confirming a previous study [9], ChIP assays indicated that HDAC1 binds to the 3'RR hs1,2 enhancer in LPS-stimulated mature B-cell splenocytes (Figure 2A). No significant HDAC1 binding was found for the 3 other 3'RR enhancers (*i.e.*, hs3a, hs3b and hs4). No hs1,2 HDAC1 binding was found in resting B-cell splenocytes (data not shown). In similar LPS-stimulated conditions no significant HDAC2 and HDAC3 binding to hs1,2 was found (Figure 2A). Deconstructing the palindromic 3'RR structure by deleting the 5'IRIS [4] precluded hs1,2 HDAC1 binding in mature B-cell (Figure 2B).

SAHA Effect on In Vitro Mature B-Cell Proliferation, CSR and Ig Synthesis - SAHA selectively inhibits HDAC I (such as HDAC1) and II classes. We thus investigated the role of SAHA on mature B-cell growth, CSR and Ig synthesis. As shown in Figure 3A, MTS assay indicated that SAHA decreased B-cell growth in a dose-dependent manner in two experimental conditions (LPS ± IL4). Flow cytometry analysis indicated that SAHA decreased IgG_3 CSR (LPS stimulation) and increased IgG_1 CSR (LPS+IL4 stimulation) (Figure 3B). ELISA experiments indicated that SAHA effects on IgG_3 and IgG_1 CSR paralleled those on IgG_3 and IgG_1 secretion (Figure 3C)

suggesting that levels of Ig productions depend on the number of switched cells.

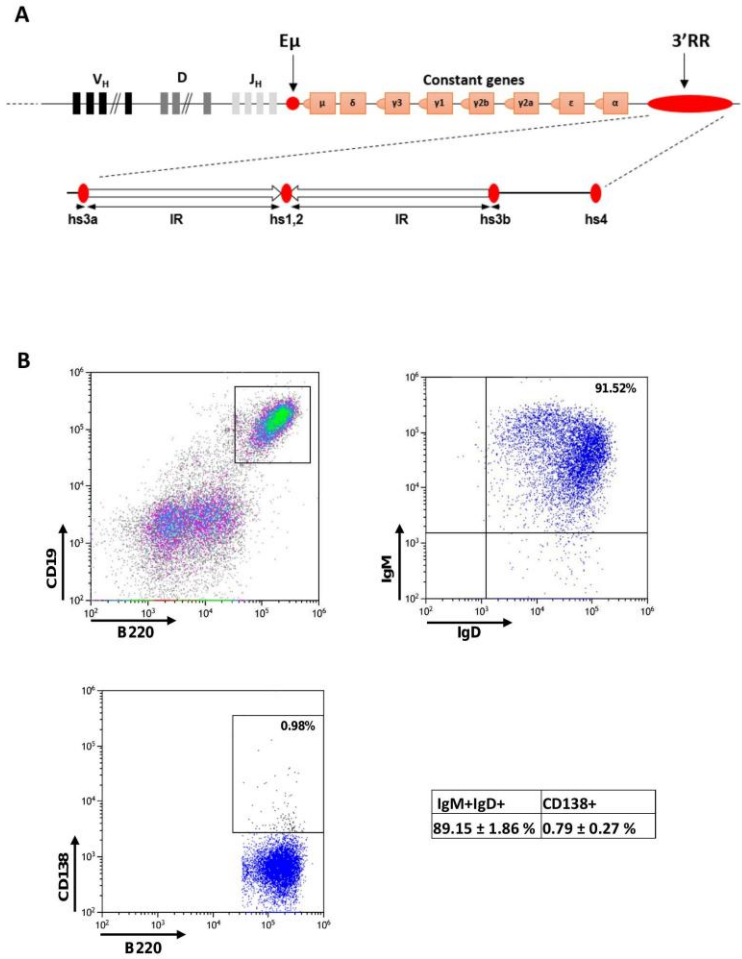

Figure 1: IgH locus and mature spleen B-cells. A: IgH locus (not to scale). The locations of variability (V), diversity (D), junction (J) and constant segments are indicated as well as 5'Eμ and 3'RR enhancers. The palindromic structure of the IgH 3'RR (to scale) with its four enhancer elements (hs3a, hs1,2, hs3b and hs4) and the IRIS sequences are represented.
B: Surface phenotype of $CD43^-$ spleen B-cells. % of IgM^+IgD^+ and IgM^+IgD^- cells were determined after gating on $B220^+CD19^+$ cells. The following labelled antibodies were used: B220-bv510, CD19-PE, IgM-FITC, IgD-bv421 and CD138-APC. Results are representative of 4 mice. Results are reported as mean ± SEM of 4 experiments.

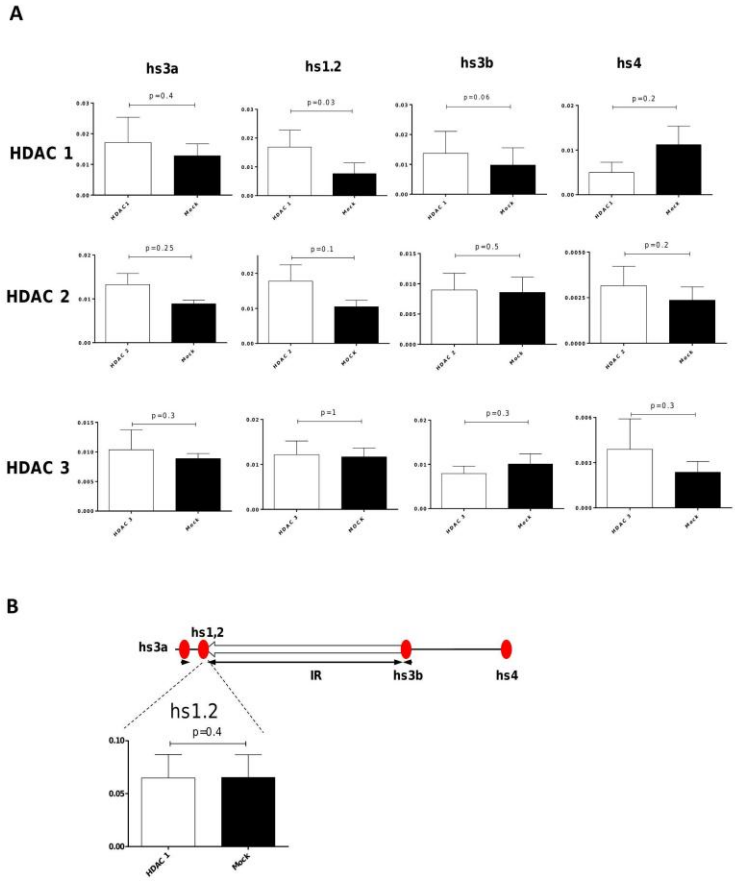

Figure 2: HDAC and 3'RR enhancers. A: HDAC1, HDAC2 and HDAC3 fixation on enhancer elements of the 3'RR. ChIP experiments were performed on 2-day LPS-stimulated spleen B-cells. Mean ± SEM of 5 experiments (significance with the student-*t*-test for paired data). The mock IP during ChIP is the control IP to avoid nonspecific antigen-antibody reactions. Another antibody (anti mouse rabbit IgG) which does not specifically bind HDAC was used. Quantitative PCR experiments were compared between samples treated with HDAC antibodies (white bars) and unspecific antibodies (mock, black bars). B: The 3'RR in ΔIRIS mice (to scale). HDAC1 fixation on the hs1,2 enhancer was studied on 2-day LPS-stimulated spleen ΔIRIS B-cells. Mean ± SEM of 6 experiments (significance with the student-*t*-test for paired data).

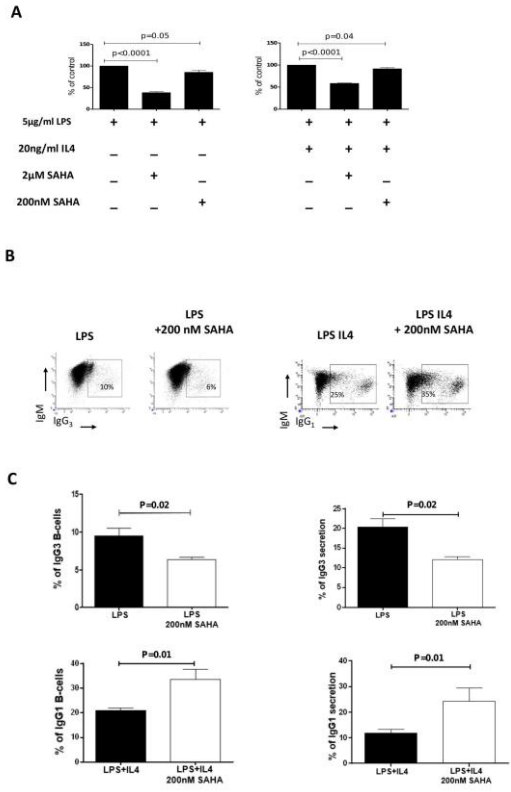

Figure 3: Influence of SAHA on *in vitro* mature B-cell growth, CSR and Ig secretion. A: Influence of SAHA on *in vitro* mature B-cell growth. Proliferation (six replicates) was evaluated by the MTS assay after 3 days stimulation with LPS (5 µg/ml) ± IL-4 (20 ng/ml) in the presence of various SAHA concentrations. Results (mean ± SEM of 4 independent experiments) are reported as % of variations as compared to stimulated cells without SAHA. Mann-Whitney *U*-test for significance. B: Influence of SAHA on *in vitro* mature B-cell CSR. Spleen B-cells were stimulated as in A. IgG_3 CSR (LPS stimulation) and IgG_1 CSR (LPS+IL4 stimulation) were evaluated by flow cytometry. Cells gated on $B220^+$ and/or $CD138^+$ cells were labelled with anti-IgM, anti-IgG_3 and anti-IgG_1 antibodies. A typical flow cytometry phenotyping was reported for each stimulatory condition. Results are reported as mean ± SEM of 4 and 5 independent experiments for IgG_3 and IgG_1, respectively. Mann-Whitney *U*-test for significance. C: Influence of SAHA on *in vitro* Ig secretion. Spleen B-cells were stimulated as in A and Ig secretion was evaluated at day 4 by specific ELISAs. Results are reported as mean ± SEM of 4 and 5 independent experiments for IgG_3 and IgG_1, respectively. Mann-Whitney *U*-test for significance.

SAHA Effect on IgH Locus Transcription - CSR and Ig synthesis are controlled through IgH locus transcription with 3'RR as a conductor [8, 13]. We then determined if the effect of SAHA on B-cell responses was mediated through an overall down regulation of IgH locus transcription and/or a specific targeting of 3'RR activation assessed through generation of enhancer RNA (eRNA). RNAseq experiments indicated that SAHA treatment had no effect on 3'RR activation judging by the expression of 3'RR eRNA (both sense and antisense) (Figure 4). Since the 3'RR controls IgH locus transcription, the lack of SAHA effect on 3'RR activation was consistent with the absence of obvious effects of SAHA on $I_{\gamma 3}$-$C_{\gamma 3}$ transcription (LPS stimulation) and $I_{\gamma 1}$-$C_{\gamma 1}$ transcription (LPS+IL4 stimulation) of the IgH locus (Figure 4). We next analyzed genome-wide gene expression between LPS- and LPS+SAHA-treated mature spleen B-cells. Data indicated 112 down-regulated genes by SAHA (log2 fold change threshold > 1, adjusted p value <0.05) (Table 1). Numerous genes were implicated in growth processes, in epigenetic-related processes (Smyd2, Nek2, Trmt10a, Rnmtl1) and histone markers (Hist1h2ai/2an/2ah/2ag/2af/2ab/3b/3g) highlighting efficiency of SAHA treatment. Seventy seven genes were up-regulated in response to SAHA but without evident links to HDAC/AID pathways and switch processes (Table 2).

Table 1: Down-regulated genes in response to SAHA. $CD43^-$ spleen B-cells were stimulated for 2-day with LPS ± SAHA. Genes implicated in growth processes are colored in yellow. Genes implicated in epigenetic-related processes and histone markers are colored in bleu. Log2 fold change threshold > 1 and adjusted p value <0.05.

Down regulated genes								
Genes	log2 fold change	P adjusted	Genes	log2 fold change	P adjusted	Genes	log2 fold change	P adjusted
Hspd1	-1.11	4.15e-6	Cdca8	-1.05	7.90e-4	Kpna2	-1.07	4.63e-6
Sgol2a	-1.03	0.001	Rcc1	-1.05	3.07e-5	Birc5	-1.07	9.03e-5
Ctla4	-1.71	0.004	Sesn2	-1.27	0.006	Idi1	-1.03	1.99e-4
Il10	-1.28	3.07e-5	Hmgn2	-1.10	5.94e-5	Hist1h2ai	-1.00	0.002
Aspm	-1.08	6.00e-5	Alpl	-1.15	0.001	Hist1h2an	-1.18	8.18e-4
Nuf2	-1.01	0.001	Cldn12	-1.10	0.036	Hist1h2ah	-1.29	1.89e-4
Cenpf	-1.06	1.55e-4	Dbf4	-1.00	1.45e-4	Hist1h2ag	-1.12	0.002
Smyd2	-1.26	0.001	Ncapg	-1.10	6.00e-5	Hist1h2af	-1.34	6.22e-6
Nek2	-1.01	0.001	Adap1	-1.01	0.002	Hist1h3g	-1.00	0.001
Suv39h2	-1.12	0.011	Asns	-1.41	9.08e-8	Hist1h2ab	-1.21	1.14e-4
Sapcd2	-1.07	0.034	RP23-5D6.6	-1.59	0.048	Hist1h3b	-1.25	3.07e-5
Snora17	-1.00	0.047	Ptgir	-1.35	4.06e-4	Eef1e1	-1.15	1.64e-4
Pkp4	-1.26	0.008	Slco3a1	-1.24	0.001	Cenpp	-1.13	0.011
Kif18a	-1.12	1.06e-4	Prc1	-1.19	2.51e-5	Nfil3	-1.64	0.001
Aven	-1.05	0.013	Lrrc32	-1.22	0.025	Trip13	-1.13	9.03e-5
Chac1	-2.14	1.14e-4	Plk1	-1.09	0.001	Ccnb1	-1.33	2.09e-8
Oip5	-1.03	0.010	Fbxo5	-1.13	4.94e-4	Ppap2a	-1.03	0.021
Nusap1	-1.09	3.07e-5	Prdm1	-1.43	1.65e-5	Rrm2	-1.05	8.49e-5
Bub1	-1.13	2.03e-5	Ppa1	-1.22	1.31e-6	Id2	-1.10	0.033
Eif2s2	-1.00	9.03e-5	Dna2	-1.06	0.002	Mis18bp1	-1.25	2.03e-5
Fam83d	-1.16	0.013	Cdk1	-1.21	4.72e-7	Cdc45	-1.05	2.79e-4
Mybl2	-1.08	3.18e-4	Hsp90b1	-1.04	1.08e-4	Tfrc	-1.03	3.07e-5
Ube2c	-1.10	4.20e-5	Parpbp	-1.01	0.016	Sgol1	-1.32	7.60e-5
Pfdn4	-1.08	0.005	Nup37	-1.05	0.001	Kif20a	-1.15	7.85e-4
Aurka	-1.21	9.24e-5	Hmgb2	-1.11	6.66e-4	Tubb6	-1.33	0.014
Cfp	-1.48	4.44e-6	Neto2	-1.09	0.031	Ska1	-1.07	0.006
Kif4	-1.01	4.10e-4	Cenpn	-1.07	0.009	Kif11	-1.09	1.03e-5
Slc7a3	-1.60	3.73e-6	Slc7a5	-1.11	0.001	Slc35g1	-1.16	0.036
Siah1b	-1.15	0.015	Cdkn3	-1.24	0.010	Psmc3ip	-1.15	0.003

Fabp5	-1.19	0.002	Ska3	-1.22	0.001	Mfsd2a	-1.18	0.004
Ect2	-1.15	2.39e-5	Pbk	-1.08	0.001			
Ccna2	-1.06	8.66e-6	Spc24	-1.08	2.79e-4			
Plk4	-1.02	1.48e-4	H2afx	-1.06	2.66e-4			
Fam46c	-1.60	9.08e-8	Kif23	-1.24	1.01e-5			
Slc16a1	-1.04	3.54e-5	Ccnb2	-1.01	4.67e-4			
Cenpe	-1.02	3.40e-4	Traip	-1.01	0.006			
Trmt10a	-1.00	0.006	Pno1	-1.02	4.68e-4			
Depdc1a	-1.05	0.002	Hmmr	-1.07	9.03e-5			
Ccne2	-1.02	0.001	Rnmtl1	-1.10	0.013			
Kif2c	-1.08	0.001	Tmem97	-1.13	2.06e-4			
Cdc20	-1.37	4.19e-6	Top2a	-1.02	8.66e-6			

Table 2: Up-regulated genes in response to SAHA treatment. Same cells as in Table 1. Log2 fold change threshold > 1 and adjusted p value <0.05.

Up-regulated genes					
Genes	log2 fold change	P adjusted	genes	log2 fold hange	P adjusted
Dst	1.51	0.012	Tsc22d1	1.45	0.006
Bmpr2	1.75	0.015	Ddx25	1.45	0.036
Mroh2a	2.35	0.010	Cyp4f18	1.50	2.72e-7
Mr1	1.11	0.047	Lpcat2	1.78	0.004
Pbx1	2.23	0.026	Fam65a	1.53	0.023
Cr2	1.22	9.08e-8	Cbfa2t3	1.32	0.045
Ralgps1	1.29	0.037	Zfhx2	1.26	0.025
Gsn	1.53	6.22e-6	Slc9a9	2.54	2.796e-4
Cers6	1.06	0.015	Abhd14b	1.63	0.045
Ttn	2.20	0.023	Fbxw10	1.87	0.048
Accs	1.10	0.033	Cacnb1	1.83	0.041
Slpi	1.52	0.005	Kif19a	2.55	0.004
Arhgap6	1.28	0.033	Rab37	1.56	0.030
Maml3	1.13	0.033	Sox4	1.29	0.049
Cd1d1	1.22	0.001	Pdlim7	1.09	0.037

Tspan2	1.02	0.008	Naip5	1.20	0.016
Rwdd3	1.29	0.037	Zfp36l1	1.02	8.89e-5
Sit1	1.19	0.031	Ift43	2.29	0.037
Mir5120	1.43	0.032	Lifr	2.35	0.040
Whrn	1.52	0.001	Mapk11	1.03	0.005
Rnu11	1.11	0.005	Iglc4	1.99	0.048
Ahdc1	1.13	0.031	Lamp3	1.70	0.035
Padi2	1.50	0.044	Bcl6	1.15	9.493e-4
Tnfrsf18	1.94	0.003	BC051142	1.61	0.026
Gsap	1.33	8.52e-4	Msh5	1.24	0.035
Afap1	2.09	0.018	Tnf	1.12	7.90e-4
Antxr2	1.02	0.034	Lta	1.24	0.041
Rasgef1b	1.13	7.46e-4	Gabbr1	1.23	0.028
Gbp8	2.32	3.99e-4	Crisp3	1.49	7.90e-4
Clip2	1.65	0.018	Cxxc5	1.01	0.006
Hip1	1.48	0.002	Clcf1	1.03	0.002
Vamp5	1.40	0.032	Ifit1bl1	1.06	0.017
Pex26	1.30	0.048	Grk5	1.26	0.044
Tmem147os	1.49	0.043	mt-Tq	1.39	0.016
Arrb1	1.13	0.001	Evi5l	1.21	0.032
Trim3	1.29	0.048			
Sbf2	1.12	0.003			
Rassf7	1.35	0.040			
Marcks	1.24	2.03e-5			
Smpdl3a	1.07	0.012			
Gdf11	1.04	0.001			
Fcer2a	1.17	1.67e-6			

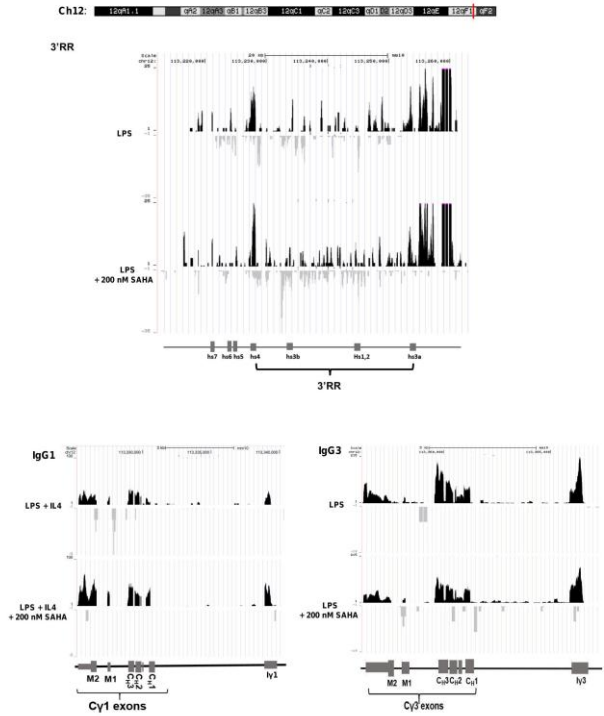

Figure 4: Influence of SAHA on IgH locus transcription. Upper panel: Effect of SAHA on 3'RR eRNA. Sense (in black) and antisense (in grey) transcription in two-day LPS (5μg/ml) ± SAHA (200 nM) stimulated mature B-cell splenocytes from *wt* mice. One representative experiment out of 2 is reported (pooled cells from three mice per group). The locations of hs3a, hs1,2, hs3b and hs4 enhancer elements of the 3'RR are shoxn. Lower panels: Effect of SAHA on $I_{\gamma 3}$-$C_{\gamma 3}$ transcription (LPS stimulation) and $I_{\gamma 1}$-$C_{\gamma 1}$ transcription (LPS+IL4 stimulation). One representative experiment out of 2 is reported.

SAHA and in vitro B-Cell Lymphoma Proliferation - Convincing demonstrations of the essential contributions of the 3'RR in mature B-cell lymphomagenesis have been provided by knock-in (KI) animal models which bring the oncogene *c-myc* under 3'RR transcriptional control (such as for i*Myc*C_{μ}, i*Myc*E_{μ} and i*Myc*C_{α} mice) [14-18]. We next examined the effect of SAHA on growth of mature mouse B-cell lymphomas ($B220^{+}CD19^{+}IgM^{+}IgD^{+}$) induced after c-myc insertion into the IgH locus. As shown in Figure 5A, and in contrast to normal mature B-cells, results clearly indicated an inconsistent SAHA

effect on mature B-cell lymphoma growth; some lymphoma samples increased their LPS stimulated growth in response to SAHA, some had unchanged growth and some reduced their growth (despite the same $IgM^{+}IgD^{+}$ mature B-cell phenotype). ChIP assays indicated no HDAC1 binding to the 3'RR hs1,2 enhancer in these freshly isolated mature mouse B-cell lymphomas (Figure 5B).

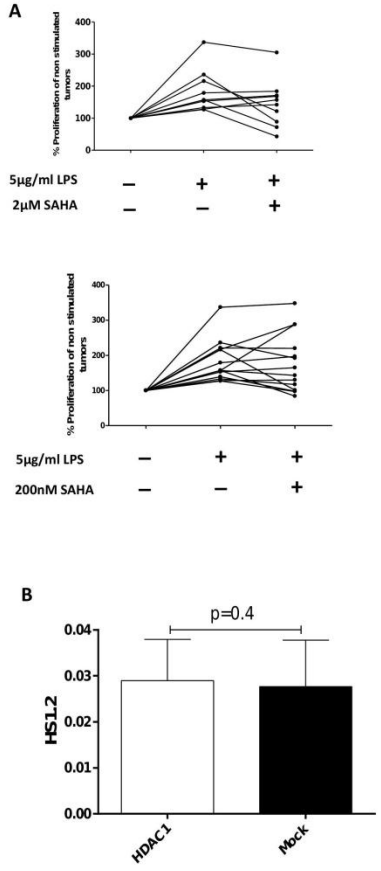

Figure 5: Influence of SAHA on proliferation of c-myc-induced mature B-cell lymphomas. A: Freshly isolated mature B-cell lymphomas from $iMycE_{\mu}$, $iMycC_{\mu}$ and $iMycC_{\alpha}$ mice were used. Each line represents one B-cell lymphoma. Each point represents the % proliferation in response to LPS with or without SAHA (10 and 14 different mouse B-cell lymphomas for 2mM SAHA and 200 nM SAHA, respectively). Each point is the mean of six

replicates. Proliferation of $B220^{+}IgM^{+}IgD^{+}$ B-cell lymphomas was evaluated with the MTS assay The first part of each graph shows the effect of LPS on B-cell lymphoma proliferation (to ensure that B-cell lymphomas remain alive after 3 days of *in vitro* growth). Thus all tested lymphomas had a percentage of proliferation higher than their controls without LPS (indicated as 100%). Only B-cells lymphomas with a higher proliferation in response to LPS were investigated for SAHA treatment to withdraw lymphomas unable to survive under the experimental conditions. B: hs1,2 HDAC1 binding in mature mouse B-cell lymphomas. ChIP experiments were performed on freshly isolated B-cell lymphomas from $iMycE_{\mu}$, $iMycC_{\mu}$ and $iMycC_{\alpha}$ mice. Mean ± SEM of 10 experiments (no significance with the Wilcoxon matched paired test). See legend to Figure 1 for mock explanation.

CPB is recruited to the hs3a and hs3b Enhancer in Freshly Isolated Mature Mouse B-Cell Lymphomas - Histone acetyl transferases (HATs) and HDACs act in concert to remodel chromatin and alter gene expression. CBP HAT binding to the hs3 enhancer was reported in Raji cells (a human Burkitt's cell line) [19]. As reported in Figure 6A, CBP was recruited to hs3a and hs3b in freshly isolated B-cell lymphomas. However, PCAF, another HAT, was not (data not shown). In contrast to B-cell lymphomas, no significant CBP binding was found in normal resting B-cell splenocytes or after 2-days LPS-stimulation (Figure 6B).

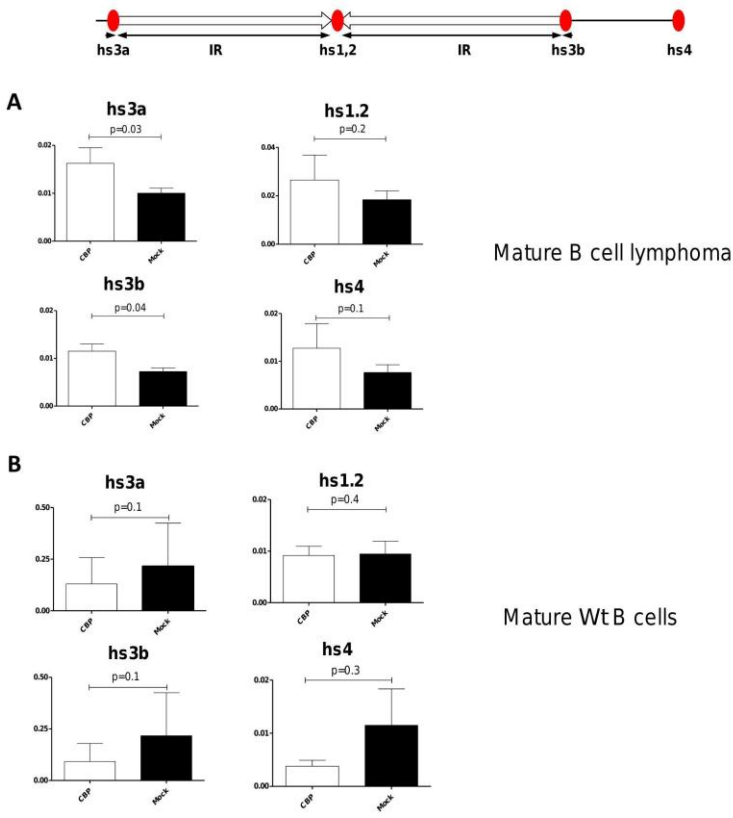

Figure 6: CBP fixation on 3'RR in freshly isolated mature B-cell lymphomas and *wt* B-cells. A: CBP ChIP experiments were performed on freshly isolated B-cell lymphomas from transgenic mice bearing c-myc in various locations of the IgH locus (iMycE$_\mu$, iMycC$_\mu$ and iMycC$_\alpha$ mice). Mean ± SEM of 4 experiments. Significance with the student-*t*-test for paired data. B: CBP ChIP experiments were performed on 2-day LPS-stimulated spleen B-cells. Mean ± SEM of 5 experiments (significance with the student-*t*-test for paired data). See legend to Figure 1 for mock explanation.

Discussion

The balance between acetylation and deacetylation of chromatin histone proteins and non-histone proteins controls gene expression regulation. HATs and HDACs are chromatin-modifying enzymes. Their interplay regulates the action of numerous signal transducers and activators of transcription with,

in the end, potent effects on a wide range of cell processes such as cell cycle, cell death, differentiation, immune response and cancer. HDACi have been approved as additional treatment for lymphomas [11,12]. HDACi are reported to affect B-cell responses both *in vivo* and *in vitro.* We studied the relationship between the HAT/HDAC pathway and 3'RR enhancers of the IgH locus during normal mature B-cell responses and mature B-cell lymphoma growth.

As previously reported [9], we observed that in LPS-activated mature B-cell splenocytes HDAC1 was recruited to the hs1,2 element of the 3'RR as determined by ChIP assays. In similar experimental conditions, other members of HDAC class I with ubiquitous tissue distribution such as HDAC2 and HDAC3 were not recruited to the 3'RR. The mouse 3'RR contains four enhancer elements with hs1,2 flanked by IRIS sequences and the center of a 25-kb palindrome bordered by two hs3 enhancer inverted copies (hs3a and hs3b). Evolution maintained this unique palindromic arrangement in mammals suggesting that it is functionally significant [20]. Deconstructing the palindromic IgH 3'RR in ΔIRIS mice strongly impacts its function [4]. In agreement with this latter result we report that HDAC1 is not efficiently recruited to the hs1,2 enhancer in LPS-stimulated ΔIRIS mature spleen B-cells.

Histone acetylation has been associated with key remodelling events of the IgH locus including CSR [21]. We examined the role of the HDACi SAHA in B-cell growth, CSR, Ig production and IgH locus transcription. SAHA decreased *in vitro* mature B-cell growth in a dose dependent manner and in response to various stimulatory conditions. In contrast, SAHA decreased CSR toward IgG_3 and stimulated CSR toward IgG_1. The effect of SAHA on Ig production (stimulation for IgG_1 and inhibition for IgG_3) paralleled its effect on CSR. Thus the elevated production of IgG_1 in response to SAHA was due to an increased level of IgG_1 switched cells. In turn, reduced production of IgG_3 in response to SAHA was due to decreased amounts of IgG_3 switched cells. This result differs markedly from previously reported results with primary spleen B-cells from MRL-lpr mice (a mouse strain prone to develop an autoimmune disease

resembling systemic lupus erythematosus) where the HDACi Trichostatin A (TSA) inhibited both germline and post-switch γ1 and γ2a transcription suggesting that inhibition of HDAC activity can downregulate gene transcription [9]. RNAseq analysis of transcription at the IgH locus of *wt* mature spleen B-cells in response to LPS revealed no evident effect of SAHA on transcription at the IgH locus in $I_{\gamma 3}$-$C_{\gamma 3}$ regions (nor in $I_{\gamma 1}$-$C_{\gamma 1}$ regions in response to LPS+IL4 stimulation). Furthermore, 3'RR eRNAs were not affected by SAHA treatment suggesting no direct effect on 3'RR activation. The effect of SAHA on CSR and Ig production is thus not through a direct effect on 3'RR activation but through another mechanism (such as isotype-dependent acetylation/deacetylation of S regions) that remains to be determined. Genome-wide gene expression analysis in response to SAHA indicated several down-regulated genes implicated in growth processes, a result that fitted well with the effect of SAHA as an inhibitor of cell proliferation. Similarly several down-regulated genes linked to epigenetic-related processes were found highlighting efficiency of SAHA treatment on mature B-cell responses.

Deciphering the mechanism that underpins the B-cell HDACi-induced effect is also of interest for a better understanding of the rationale for use of HDACi to treat B-cell lymphomas. Our results indicated that HDC1 does not bind to the hs1,2 enhancer element in freshly isolated mature mouse B-cell lymphomas with a c-myc insertion in the IgH locus; a major difference compared to results of stimulated normal mature B-cells. Another major difference was the binding of the HAT CBP to hs3a and hs3b enhancers that bounder the 3'RR palindrome indicating that the HAT/HDAC pathway is not identically regulated in stimulated normal mature B-cells and freshly isolated mature B-cell lymphomas. Furthermore if normal mature B-cell growth was consistently down regulated *in vitro* by SAHA, this was not the case in freshly isolated mature B-cell lymphomas where SAHA sometimes had no effect or a decreased/stimulatory effect without evident links to a B-cell lymphoma phenotype. This effect is consistent with the fact that despite similar "primom movens" (the insertion of c-myc in the IgH locus) B-cell lymphomas arise with different kinetics, various KI67 indices

and different locations due to the numerous different oncogenic hits favouring lymphoma emergence. Our results clearly indicated that even though SAHA affects normal mature B-cell growth, this effect is not consistently found in mature B-cell lymphomas and that trying to use HDACi to down regulate 3'RR activation in order to down regulate its effect on oncogene transcription (c-myc in our animal models) is utopic.

Important differences thus exist concerning the effect of SAHA on proliferation of *wt* mature B-cells *vs* mature B-cell lymphomas. Differences are also documented concerning the recruitment of CBP/HDAC1 to the IgH 3'RR. We report an isotype-effect of SAHA on B-cell CSR and no effect of SAHA on IgH locus transcription. SAHA effects are not mediated by down-regulation of 3'RR transcriptional activity in normal mature B-cells. Previous studies with transgenic mice bearing an IgH with an inserted c-myc (*i.e.* under transcriptional dependence of the 3'RR) have suggested that targeting the 3'RR would be of interest in order to down regulate c-myc deregulated transcripts leading to B-cell lymphomagenesis [14,18,22]. Our present results argue against this hypothesis. Translocations in B-cell lymphomas undoubtedly induce epigenetic changes [23] and epigenetic drugs targeting histone acetylation (HDACi) and histone methylation (EZH2 inhibitors) are already used to treat several B-cell lymphoid malignancies [11,12]. The precise mechanism underlining their beneficial use remains to be elucidated but is clearly not mediated by direct action on IgH 3'RR enhancers.

Only one HDACi (*i.e.*, SAHA, a pan-HDACi) was investigated in this study, which might limit the generalization of our results across different HDACi (particularly pan-HDACi *vs* class I-specific inhibitors). HDACi are approved for treatment of certain lymphomas but their narrow therapeutic index limits their use. Inconsistent effects of HDACi treatments have been reported [12] and HDACi are found to synergize with other treatments such as PD1 blockade [24]. As the HAT CBP, rather than HDAC1, was recruited to the 3'RR in mature B-cell lymphomas but not normal mature B cells, it will be interesting to see whether targeting CBP would be active against mature B-cell

lymphomas. It is possible that recruitment of CBP, instead of HDAC1, causes the intrinsic resistance to HDACi in some types of B-cell lymphomas.

In this study only *wt* mature spleen IgM^+IgD^+ B-cells were specifically considered because the 3'RR is the major driver of CSR and Ig synthesis. It is also why we explored HDAC binding and HDACi effects only in mature B-cell lymphomas ($B220^+IgM^+IgD^+$). It is evident that similar studies on the entire spectrum of B-cell subsets (from pro-B cells to plasmocytes) and B-cell lymphomas would be of interest. Finally, despite wide functional/structural similarities between mouse and human 3'RRs [20], our results cannot be directly translated into human counterparts requiring further studies to clarify this point.

References

1. Oudinet C, Braikia FZ, Dauba A, Khamlichi AA. Mechanism and regulation of class switch recombination by IgH transcriptional control elements. Adv Immunol. 2020; 147: 89-137.
2. Rouaud P, Saintamand A, Saad F, Carrion C, Lecardeur S, et al. Elucidation of the enigmatic IgD class-switch recombination via germline deletion of the IgH 3' regulatory region. J Exp Med. 2014; 211: 975-985.
3. Saintamand A, Rouaud P, Saad F, Rios G, Cogné M, et al. Elucidation of IgH 3' region regulatory role during class switch recombination via germline deletion. Nat Commun. 2015; 6: 7084.
4. Saintamand A, Vincent-Fabert C, Garot A, Rouaud P, Oruc Z, et al. Deciphering the importance of the palindromic architecture of the immunoglobulin heavy chain 3' regulatory region. Nat Commun. 2016; 7: 10730.
5. Le Noir S, Boyer F, Lecardeur S, Brousse M, Oruc Z, et al. Functional anatomy of the immunoglobulin heavy chain 3' super-enhancer needs not only core enhancer elements but also their unique DNA context. Nucleic Acids Res. 2017; 45: 5829-5837.
6. Saintamand A, Vincent-Fabert C, Marquet M, Ghazzaui N, Magnone V, et al. E□ and 3'RR IgH enhancers show

hierarchic unilateral dependence in mature B-cells. Sci Rep. 2017; 7: 442.
7. Guglielmi L, Le Bert M, Truffinet V, Cogné M, Denizot Y. Insulators to improve expression of a 3'IgH LCR-driven reporter gene in transgenic mouse models. Biochem Biophys Res Commun. 2003; 307: 466-471.
8. Saintamand A, Rouaud P, Garot A, Saad F, Carrion C, et al. The IgH 3' regulatory region governs μ chain transcription in mature B lymphocytes and the B cell fate. Oncotarget. 2015; 6: 4845-4852.
9. Lu ZP, Ju ZL, Shi GY, Zhang JW, Sun J. Histone deacetylase inhibitor trichostatin A reduces anti-DNA autoantibody production and represses IgH gene transcription. Biochem Biophys Res Comm. 2005; 330: 204-209.
10. Waibel M, Christiansen AJ, Hibbs ML, Shortt J, Jones SA, et al. Manipulation of B-cell responses with histone deacetylase inhibitors. Nat Comm. 2015; 6: 6838.
11. Cheng T, Grasse L, Shah J, Chandra J. Panobinostat, a pan-histone deacetylase inhibitor: Rationale for and application to treatment of multiple myeloma. Drugs Today. 2015; 51: 491-504
12. Sborov DW, Canella A, Hade EM, Mo X, Khountham S, et al. A phase 1 trial of the HDAC inhibitor AR-42 in patients with multiple myeloma and T- and B-cell lymphomas. Leuk Lymphoma. 2017; 58: 2310-1218.
13. Vincent-Fabert C, Fiancette R, Pinaud E, Truffinet V, Cogné N, et al. Genomic deletion of the whole IgH 3' regulatory region (hs3a, hs1,2, hs3b, hs4) dramatically affects class switch recombination and Ig secretion to all isotypes. Blood. 2010; 116: 1895-1898.
14. Ferrad M, Ghazzaui N, Issaoui H, Cook-Moreau J, Denizot Y. Mouse models of c-myc deregulation driven by IgH locus enhancers as models of B-cell lymphomagenesis. Front Immunol. 2020; 11: 1564.
15. Rosean TR, Holman CJ, Tompkins VS, Jing X, Krasowski MD, et al. KSHV-encoded vIL6 collaborates with deregulated c-MYC to drive plasmablastic neoplasm in mice. Blood Cancer J. 2016; 6: e398.
16. Cheung WC, Kim JS, Linden M, Peng L, Ness BV, et al. Novel targeted deregulation of c-myc cooperates with Bcl-

XL to cause plasma cell neoplasms in mice. J Clin Invest. 2004; 113: 1763-1773.
17. Park SS, Kim JS, Tessarollo L, Owens JD, Peng L, Han SS, et al. Insertion of c-Myc into IgH induces B-cell and plasma-cell neoplasms in mice. Cancer Res. 2005; 65: 1306-1315.
18. Ghazzaui N, Issaoui H, Ferrad M, Carrion C, Cook-Moreau J, et al. Eμ and 3'RR transcriptional enhancers of the IgH locus cooperate to promote c-myc-induced mature B-cell lymphomas. Blood Adv. 2020; 4: 28-39.
19. Hu HM, Kanda K, Zhang L, Boxer LM. Activation of the c-myc P1 promoter in Burkitt's lymphoma by the hs3 immunoglobulin heavy-chain gene enhancer. Leukemia. 2007; 21: 747-753.
20. D'addabbo P, Scascitelli M, Giambra V, Rocchi M, Frezza D. Position and sequence conservation in Amniota of polymorphic enhancer HS1,2 within the palindrome of IgH 3' regulatory region. BMC Evol Biol. 2011; 11: 71.
21. Nambu Y, Sugai M, Gonda H, Lee CG, Katakai T, et al. Transcription-coupled events associating with immunoglobulin switch region chromatin. Science. 2003; 302: 2137-40.
22. Saintamand A, Saad F, Denizot Y. 3'RR targeting in lymphomagenesis: a promising strategy? Cell Cycle. 2015; 14: 789-790.
23. Lindström MS, Wiman KG. Role of genetic and epigenetic changes in Burkitt lymphoma. Semin Cancer Biol. 2002; 12: 381-387.
24. Wang X, Waschke BC, Woolaver RA, Chen Z, Zhang G, et al. Histone Deacetylase Inhibition Sensitizes PD1 Blockade-Resistant B-cell Lymphomas. Cancer Immunol Res. 2019; 7: 1318-1331.

Book Chapter

BMP9, but Not BMP10, Acts as a Quiescence Factor on Tumor Growth, Vessel Normalization and Metastasis in a Mouse Model of Breast Cancer

Marie Ouarné[1], Claire Bouvard[1], Gabriela Boneva[1], Christine Mallet[1], Johnny Ribeiro[2,3,4], Agnès Desroches-Castan[1], Emmanuelle Soleilhac[5], Emmanuelle Tillet[1], Olivier Peyruchaud[2,3,4] and Sabine Bailly[1]*

[1]Université Grenoble Alpes, Inserm, CEA, BIG-Biologie du Cancer et de l'Infection, France
[2]Inserm, U1033, France
[3]Université Claude Bernard Lyon 1, France
[4]Faculté de Médecine de Lyon Est, France
[5]Université Grenoble Alpes, Inserm, CEA, BIG-Biologie à Grande Echelle, France

***Corresponding Author:** Sabine Bailly, Université Grenoble Alpes, Inserm, CEA, BIG-Biologie du Cancer et de l'Infection, 38000 Grenoble, France

Published **October 07, 2021**

This Book Chapter is a republication of an article published by Sabine Bailly, et al. at Journal of Experimental & Clinical Cancer Research in August 2018. (Ouarné, M., Bouvard, C., Boneva, G. et al. BMP9, but not BMP10, acts as a quiescence factor on tumor growth, vessel normalization and metastasis in a mouse model of breast cancer. J Exp Clin Cancer Res 37, 209 (2018). https://doi.org/10.1186/s13046-018-0885-1)

How to cite this book chapter: Marie Ouarné, Claire Bouvard, Gabriela Boneva, Christine Mallet, Johnny Ribeiro, Agnès Desroches-Castan, Emmanuelle Soleilhac, Emmanuelle Tillet, Olivier Peyruchaud, Sabine Bailly. BMP9, but Not BMP10, Acts

as a Quiescence Factor on Tumor Growth, Vessel Normalization and Metastasis in a Mouse Model of Breast Cancer. In: Hussein Fayyad Kazan, editor. Immunology and Cancer Biology. Hyderabad, India: Vide Leaf. 2021.

Acknowledgements: We thank Dr. S.J. lee (Johns Hopkins University School of Medicine, Baltimore, MD, USA) and Dr. T. Zimmers (Thomas Jefferson University, Philadelphia, PA, USA) for providing *Gdf2*$^{-/-}$ mice and Dr. D Metzger (IGBMC, Illkirch, France) for providing us the Rosa26-CreER^{T2} mouse, and the animal facility staff at Institut de Biosciences et Biotechnologies de Grenoble (BIG, Grenoble, France) for animal husbandry.

Funding: M.O. was supported by the PhD program of CEA/DRF (IRTELIS). This work was supported by INSERM (Institut National de la Santé et de la Recherche Médicale, U1036), CEA (Commissariat à l'Energie Atomique et aux Energies Alternatives, DRF/BIG/BCI), UGA (University Grenoble-Alpes, BCI), the Ligues Départementales contre le Cancer de la Loire et de la Savoie, the association Maladie de Rendu-Osler (AMRO-HHT France), the Association pour la Recherche sur le Cancer (ARC), the Fondation Recherche Médicale (FRM) and the Labex GRAL. We thank the Fondation Maladies Rares (FMR) for the generation of *Bmp10* $^{lox/lox}$ mice.

Availability of Data and Materials: All data generated or analyzed during this study are included in this publication.

Author Contributions: MO and CB performed, analyzed and participated in the writing of the manuscript. GB, CM, JR, ADC, ET performed some experiments. ES helped in the analysis of the data. OP helped in the design of the experiments and the writing. SB designed the experiments and wrote the manuscript. All authors read and approved the final manuscript.

Ethics Approval and Consent to Participate: All animal studies were approved by the institutional guidelines and those formulated by the European Community for the Use of Experimental Animals. The ethical approval for these experiments was given by the French ministry under the number APAFIS#7345–2016102512011432 v2.

Competing Interests: The authors declare that they have no competing interests.

Abstract

Background: Angiogenesis has become an attractive target for cancer therapy. However, despite the initial success of anti-VEGF (Vascular endothelial growth factor) therapies, the overall survival appears only modestly improved and resistance to therapy often develops. Other anti-angiogenic targets are thus urgently needed. The predominant expression of the type I BMP (bone morphogenetic protein) receptor ALK1 (activin receptor-like kinase 1) in endothelial cells makes it an attractive target, and phase I/II trials are currently being conducted. ALK1 binds with strong affinity to two ligands that belong to the TGF-ß family, BMP9 and BMP10. In the present work, we addressed their specific roles in tumor angiogenesis, cancer development and metastasis in a mammary cancer model.

Methods: For this, we used knockout (KO) mice for BMP9 (constitutive *Gdf2-deficient*), for BMP10 (inducible *Bmp10-deficient*) and double KO mice (*Gdf2* and *Bmp10*) in a syngeneic immunocompetent orthotopic mouse model of spontaneous metastatic breast cancer (E0771).

Results: Our studies demonstrate a specific role for BMP9 in the E0771 mammary carcinoma model. *Gdf2* deletion increased tumor growth while inhibiting vessel maturation and tumor perfusion. *Gdf2* deletion also increased the number and the mean size of lung metastases. On the other hand, *Bmp10* deletion did not significantly affect the E0771 mammary model and the double deletion (*Gdf2* and *Bmp10*) did not lead to a stronger phenotype than the single *Gdf2* deletion.

Conclusions: Altogether, our data show that in a tumor environment BMP9 and BMP10 play different roles and thus blocking their shared receptor ALK1 is maybe not appropriate. Indeed, BMP9, but not BMP10, acts as a quiescence factor on tumor growth, lung metastasis and vessel normalization. Our results also support that activating rather than blocking the BMP9 pathway could be a new strategy for tumor vessel normalization in order to treat breast cancer.

Abbreviations

ActR2-Activin type 2 Receptor; *ALK1*-Activin Receptor-like Kinase 1; *BMP*-Bone Morphogenetic Protein; *BMPR2*-BMP type 2 Receptor; *GDF*-Growth and Differentiation Factor; *PCNA*-Proliferating Cell Nuclear Antigen; *SMA*-Smooth Muscle Actin; *VEGF*-Vascular Endothelial Growth Factor; *WT*-Wild type

Background

Neovascularization is one of the hallmarks of cancer as it is a necessary process to provide tumor with its metabolic requirements, while simultaneously creating an escape route by which cancer cells will disseminate [1,2]. Thus, several angiogenesis inhibitors have been developed and most of them target vascular endothelial growth factor (VEGF) signaling [3]. Today, VEGF inhibitors are included in first-line therapies against advanced and metastatic cancers [4]. However, the lack of substantial improvements of overall survival and resistance issues clearly support the crucial need for identification of alternative and/or complementary targets for drug development [5].

The transforming growth factor (TGF)-β family type I receptor ALK1 (activin receptor-like kinase 1), which is mainly expressed on endothelial cells, has been identified as a potential target for anti-angiogenic cancer treatment [6,7]. ALK1 is indeed an essential receptor in vascular development, as genetic ablation of *Acvrl1* (encoding ALK1) in mice results in embryonic lethality due to vasculogenic or angiogenic defects [8,9]. In addition, mutations of the genes *ACVRL1* and *ENG*, encoding

the co-receptor endoglin, are responsible of the Rendu-Osler syndrome also known as hereditary hemorrhagic telangiectasia (HHT) [10,11]. The discovery of the high affinity binding of BMP9 (bone morphogenetic protein) and BMP10 to ALK1 has revealed the key role of these two ligands in vascular development [12,13]. BMP9 and BMP10 are very similar at the amino-acids levels but they differ in several ways. First, the site of expression is different, as BMP9 is mainly produced by the liver [14] while BMP10 is mostly produced by the heart [15], although they are both detected in blood [16,17]. Second, although BMP9 and BMP10 both bind to the type I receptor ALK1 with high affinity, only BMP9 binds to ALK2 [18] and their affinities for the type II receptors differ [19]. Knockout mice for *Gdf2* (encoding BMP9) are viable and fertile with no overt defect in blood vessel development [20] while *Bmp10*$^{-/-}$ mice die during embryonic development due to heart defects [21]. Still, we could show that *Gdf2*-deficient mice present defects in lymphatic valve formation and lymph drainage, supporting a specific role for BMP9 in lymphatic maturation [22]. Moreover, it was recently shown that BMP9 and BMP10 play redundant roles in retinal vascularization and ductus arteriosus closure [17,20,23]. Together, these data clearly demonstrate, in vivo, the crucial roles of ALK1 and its two ligands, BMP9 and BMP10, in vascular development. However, their precise role during the complex process of physiological angiogenesis has proven difficult to pinpoint from in vitro studies, as their actions appear highly concentration- and context-dependent [24].

Still, due to the key role of this pathway in angiogenesis, ALK1 has been identified as an interesting target in tumor angiogenesis [6,25]. Pharmacological targeting of ALK1 has been evaluated using either a neutralizing anti-ALK1 antibody (PF-03446962) or a soluble form of ALK1 (Dalantercept) that will trap the biological ligands of ALK1, BMP9 and BMP10 [26,27]. Most of the published preclinical studies, using these neutralizing tools, reported a decrease in tumor volume, tumor angiogenesis and metastasis [28-30]. Thus, several phase I/II studies using these agents are currently being conducted. However, despite being

generally well tolerated, no efficacy of ALK1 blockade has been demonstrated to date [5,25,31,32].

Little is known about the respective roles of BMP9 and BMP10 in tumor angiogenesis, cancer development and metastatic dissemination. BMP9 has been shown to play, via ALK2, a direct role on tumor growth as an autocrine growth factor in hepatocarcinoma [33]. The roles of BMP9 and BMP10 have also been studied in different cancers using tumor cells overexpressing either BMP9 or BMP10 [34-37], although BMP9 and BMP10 are not or moderately expressed in most of the tumors that have been studied so far. In these studies, BMP9 and BMP10 were described as tumor suppressors acting directly on cancer cells but their roles in tumor angiogenesis have not been investigated.

Herein, we studied the respective roles of BMP9 and BMP10 in tumor growth, tumor angiogenesis and metastatic dissemination using the murine syngeneic orthotopic mammary cancer model (E0771) [38,39]. To understand the contribution of BMP9 and BMP10 ligands, we made use of *Gdf2*-deficient mice, inducible *Bmp10*-deficient mice and double *Gdf2- and Bmp10*-deficient mice. Our study demonstrates a specific role for BMP9 in tumor growth, tumor angiogenesis and lung metastasis in the E0771 model. *Bmp10* deletion did not significantly affect this mammary model, and the double deletion did not lead to a stronger phenotype than the single deletion of *Gdf2*.

Methods

Cell Lines

E0771 (Tebu-Bio) breast cancer mouse cells were maintained in culture in RPMI-1640 (Life Technologies) supplemented with 10% fetal calf serum (FCS) and were used below passage 5. Mouse endothelial cells H5V (gift from Dr. A. Mantovani) were maintained in culture in DMEM 4.5 g/L glucose (Life Technologies) supplemented with 10% FCS. Breast epithelial cells EpH4 (Clone J3B1A, a gift from Dr. P. Soulie) were maintained in culture in DMEM/F12 (Life Technologies)

supplemented with 10% FCS. All cells were tested for Mycoplasma (MycoAlert™ PLUS, Lonza).

Gdf2 $^{-/-}$, *Bmp10*-cKO and double-KO (*Gdf2* $^{-/-}$ *and Bmp10*) Mice

Gdf2$^{-/-}$mice generation was previously described [20]. To circumvent the early embryonic lethality of *Bmp10*-KO mice [21], the Institut Clinique de la Souris (Illkirch, France) generated for us a *Bmp10*$^{lox/lox}$ mice by flanking loxP sites around exon2. These mice were then crossed with the Rosa26CreER^{T2} mice provided by Pr. P. Chambon (IGBMC, Illkirch, France) [40] to generate conditional knockout mice for *Bmp10* (*Bmp10*-cKO mice). Intraperitoneal injections of tamoxifen (1 mg) were performed for five days in 3-week-old control (*Bmp10*$^{lox/lox}$) and *Bmp10*-cKO (Rosa26CreER^{T2};*Bmp10*$^{lox/lox}$) in order to delete *Bmp10*. Rosa26CreER^{T2};*Bmp10*-cKO mice were crossed with *Gdf2*$^{-/-}$ mice to generate *Gdf2*$^{-/-}$*;Bmp10*$^{lox/lox}$ that will be referred to as double-KO mice. The same protocol as for *Bmp10*-cKO mice was used to delete *Bmp10*. *Bmp10*-cKO mice were maintained in the C57BL/6 background. All mice described were viable and fertile.

Orthotopic Syngeneic Mammary Tumor Models

For the E0771 model, 10^5 cells were injected orthotopically into the fourth mammary fat pad of isofluran-anesthesized C57BL/6 CTL and KO females at 6 weeks of age. Mice were euthanized at 9 weeks of age 10 min after intravenous injection of 50 µL of tomato lectin (DyLight 488 *Lycopersicon esculentum*, DL-1174, Vector Laboratories, 1 mg/mL). Tumor size was measured with calipers, and the volume was calculated according to the formula $(L*w^2)/2$ where L and w stand for length and width respectively.

Tissue Preparation and Immunostainings

Tumors were fixed in 4% paraformaldehyde over night at 4 °C and embedded in Tissue-Tek^R OCT™ compound (optimum cutting temperature) (Sakura) for frozen sections or in paraffin.

For immunohistochemistry, paraffin-embedded sections were deparaffinized and rehydrated followed by citrate antigen retrieval. Blocking was performed in 2% BSA in TBS. Sections were stained using antibodies to PCNA (dilution 1:6000; Abcam [PC10] Ab29) and active pase-3 (dilution 1:1000; R&D Systems AF835). Appropriate biotinylated secondary antibodies were used (Vector Laboratories). Sections were incubated with an avidin-biotin complex (Vectastain ABC kit; Vector Laboratories) and staining revealed by addition of 3.3′-diaminobenzidine (Liquid DAB+ Substrate Chromogen System; Dako). Counterstaining was performed using hematoxylin or fast nuclear red. Images were acquired with a Zeiss Axioplan microscope and analyzed using Axiovision 4.8 software.

For immunofluorescence, frozen sections were fixed in 4% paraformaldehyde and permeabilized in 0.5% triton in PBS. Blocking was performed in 2% BSA in PBS. Sections were stained using antibodies to podocalyxin (dilution 1:50; R&D Systems AF1556), FITC (dilution 1:100; Alexa Fluor 488 conjugated; Jackson Immunoresearch Laboratories [1F8-1E4] 200–542-037), α-SMA (dilution 1:200; Cy3 conjugated; Sigma Aldrich [1A4] C6198) and LYVE-1 (dilution 1:100; R&D Systems MAB2125). Appropriate secondary antibodies conjugated with fluorochromes were used (Jackson Immunoresearch Laboratories). Apoptosis was analyzed by the indirect TUNEL (Terminal deoxynucleotidyl transferase dUTP nick end labeling) method (ApopTag® Red In Situ Apoptosis Detection Kit from Millipore). Nucleus were stained using Hoechst blue (33,342, Sigma). Images were acquired with a Zeiss ApoTome microscope, treated using Zen Blue software and analyzed using ImageJ software.

For necrosis quantification, paraffin-embedded sections were stained with hematoxylin and eosin. Images were acquired using AxioScan Z1 (Zeiss) slide scanner and analyzed using Zen Blue software.

All quantifications were performed by assessing 3 to 5 images per tumor using ImageJ software.

Quantification of Lung Metastases

After being inflated using 4% paraformaldehyde, lungs were embedded in paraffin upon tissue fixation in 4% paraformaldehyde. The metastatic burden was assessed by serial sectioning of the entire lungs. Hematoxylin and eosin staining was performed on sections every 200 μm. Images were acquired using AxioScan Z1 (Zeiss) slide scanner and analyzed using Zen Blue software.

Western Blot Analysis

Cells were stimulated in 0% FCS with recombinant BMP9 (R&D Systems) at the concentration indicated for 1 h after 1 h30 of serum deprivation. Cell extracts were lysed in 50 mmol/L Tris-HCl pH 7.4, 0.5 mol/L NaCl and a cocktail of protease inhibitors (Sigma) by sonication. 20 μg of proteins from cell lysates were separated on a SDS/PAGE, 4–20% (Bio-Rad) and analyzed by immunoblotting with anti-pSmad1/5/9 antibody (Cell Signaling #9511). The same membrane was reprobed with a monoclonal antibody against β-actin (clone AC-15; Sigma) to confirm equal protein loading.

RT-PCR Analyses

Total RNAs were extracted at the indicated times using the Nucleospin RNA XS kit (Macherey-Nagel). First-strand cDNAs were synthesized from 1 μg of total RNA by reverse transcription using the reverse transcriptase iScript system from Bio-Rad according to the manufacturer's instructions. Quantitative RT-PCR was performed using a Bio-Rad CFX96 apparatus and qPCR Master Mix (Promega). Relative quantification of gene expression was normalized to the RPL13a mRNA expression level. Sequences of the PCR primers were as follows:

ALK1: F-CCTCACGAGATGAGCAGTCC, R-GGCGATGAAGCCTAGGATGTT;

ALK2: F-GTCATGGTTCAGGGAGACGG, R-CCAGAGTAGTGAGCTGAAGGT;

ALK3: F-ATGCAAGGATTCACCGAAAGC, R-AACAACAGGGGGCAGTGTAG;

BMPRII: F-TGGCAGTGAGGTCACTCAAG, R-TTGCGTTCATTCTGCATAGC;

ActRIIA: F-AGCAAGGGGAAGATTTGGTT, R-GGTGCCTCTTTTCTCTGCAC;

ActRIIB: F-CTGTGCGGACTCCTTTAAGC, R-TCTTCACAGCCACAAAGTCG;
BMP9: F-CAGATACACAACGGACAAATCGTC, R-TTGGCAGGAGACATAGAGTCGG;

BMP10: F- CCATGCCGTCTGCTAACATCATC, R-ACATCATGCGATCTCTCTGCACCA;

RPL13a: F- CCCTCCACCCTATGACAAGA, R-TTCTCCTCCAGAGTGGCTGT.

Enzyme-linked Immunosorbent Assay (ELISA)

BMP9 and BMP10 ELISAs were performed with commercially available assays (R&D Systems). VEGF-A ELISA was performed with a commercially available assay (Mouse VEGF Quantikine ELISA Kit, R&D Systems).

Cell Proliferation, Migration, Viability and Apoptosis

Cells were treated with 10 ng/mL of BMP9 or BMP10 in 0% FCS RPMI-1064 medium. Cell proliferation was assessed by counting cells every 24 h using an automated cell counter (TC20, Bio-Rad). Cell migration was assessed after wounding with a plastic pipette tip, placed back at 37 °C in the incubator and photographed at indicated times (0, 24, 48 and 72 h). Quantitation of monolayer closure was performed using Zen Blue software. Results are expressed as % of wound closure.

Cell viability was assessed using the cell titer-Glo luminescent assay (Promega) at 24 h and 48 h after BMP9 addition. Cell apoptosis was assessed using the pase-Glo 3/7 assay from Promega at 24 h and 48 h after BMP9 addition.

Statistical Analysis

Statistical data analysis was performed using the Mann-Whitney test except for tumor growth analysis, and in vitro proliferation and migration which were performed by the two-way Anova test using GraphPad Prism6.

Results

Loss of BMP9 Increases Tumor Growth in the E0771 Mammary Carcinoma Model

To understand the contribution of BMP9 in tumor growth, we used the syngeneic orthotopic mouse mammary carcinoma models (E0771) [38]. The E0771 mammary cancer cell line is derived from a spontaneous adenocarcinoma recently described as claudin-low [39]. E0771 cancer cells were orthotopically injected into the fourth mammary gland of 6-week-old WT and *Gdf2*-deficient mice in the C57BL/6 background. We observed that *Gdf2*$^{-/-}$ mice presented significantly larger and heavier tumors than WT mice (Fig. 1a and b). We next investigated whether these effects could be due to a direct effect of BMP9 on these cells. We first analyzed by quantitative RT-PCR the expression levels of the different type I and type II BMP receptors (Additional file 1: Fig. S1A and B). We found that both the mammary tumor cells (E0771) or the non-tumoral primary mammary epithelial cells (EpH4) expressed very low amount of ALK1, while, as expected, the endothelial cell line (H5V) expressed high levels of ALK1. All cells expressed ALK2 at a similar level, while ALK3 was expressed in E0771 and EpH4 cells but not in H5V cells. All cell types also expressed BMPRII and ActRIIA, whereas ActRIIB was below detectable level. None of these cells expressed BMP9 or BMP10 mRNA, which were also not detected in E0771 tumors (data not shown). In accordance with this receptor profile, we found that only high doses of BMP9 (5 ng/mL) induced Smad1/5/9 phosphorylation

(Additional file 1: Fig. S1C), suggesting that this phosphorylation is not mediated by the high affinity receptor ALK1, in accordance with the low amount of the high affinity receptor ALK1 in these cells (Additional file 1: Fig. S1A), but by either ALK2 or ALK3. However, addition of high doses of BMP9 (10 ng/mL) did not affect E0771 cell growth, migration, viability or apoptosis (Additional file 1: Fig. S1D, E, F and G). In vivo, we also analyzed tumor necrosis and found that the percentage of necrosis was significantly higher in *Gdf2*$^{-/-}$ mice than WT mice (Fig. 1c). Finally, we analyzed E0771 tumor sections to assess whether BMP9 affected tumor cell proliferation and apoptosis, in vivo, by counting the number of PCNA-, cleaved pase 3- and TUNEL-positive cells and found no significant differences between WT and *Gdf2*$^{-/-}$ mice (Fig. 1d, e, f, g, h and i).

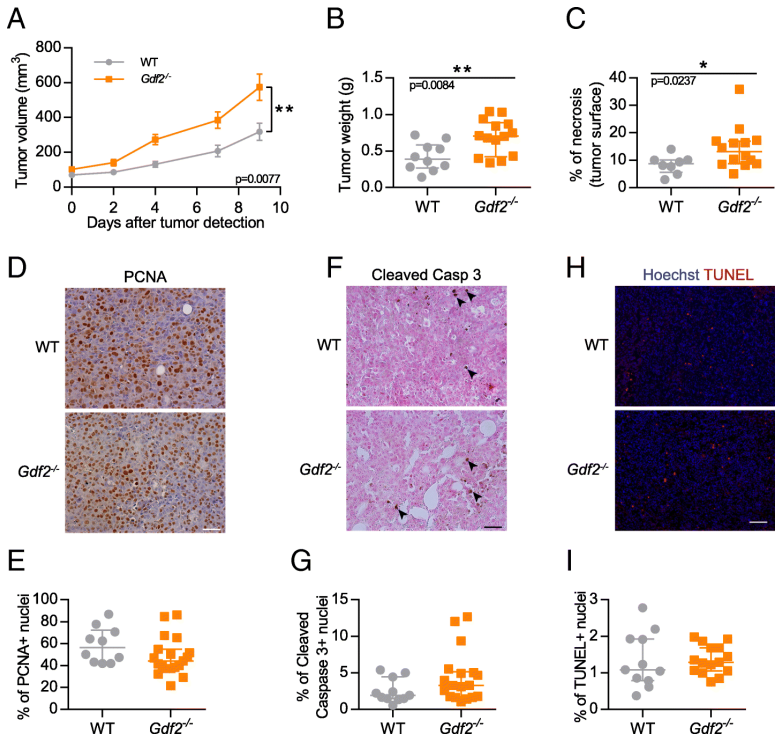

Figure 1: *Gdf2* deletion increases tumor growth in the E0771 mammary cancer model. E0771 cells were injected in the 4th mammary gland and tumor growth

was assessed by caliper measurement every 2 to 3 days after tumor detection (**a**) and tumor weight measured (**b**) at the end of the experiment, 9 days after tumor detection (WT $n = 10$, *Gdf2*$^{-/-}$ $n = 14$, 1 representative experiment out of 4). **c** Tumor necrosis area quantification (% of total tumor area) (WT $n = 8$, *Gdf2*$^{-/-}$ $n = 14$, 2 experiments). **d-i** Representative images and quantitative analysis of the tumors stained for PCNA (**d**, **e**), cleaved-pase 3 (black arrowheads **f**, **g**), (WT $n = 11$, *Gdf2*$^{-/-}$ $n = 18$, 2 experiments). Scale bar 50 μm), and TUNEL (**h**, **i**) (WT $n = 11$, *Gdf2*$^{-/-}$ $n = 15$, 1 experiment. Scale bar 100 μm) (**a**) Data are the mean ± SEM. Statistical analysis: Two-way matched ANOVA. (**b**, **c**, **e**, **g**, **i**) Data are the median ± interquartile range. Statistical analysis: Mann-Whitney test. *$p \leq 0.05$ and **$p \leq 0.01$ significantly different

Loss of BMP9 Decreases Vessel Perfusion in the Mouse E0771 Mammary Carcinoma Model

As we could not observe any effect of BMP9 on tumor cell proliferation that could explain the increase in tumor size in *Gdf2*$^{-/-}$ mice, we next addressed whether the loss of BMP9 could be due to an effect on tumor angiogenesis. For this purpose, tumor sections were stained for the luminal endothelial cell marker podocalyxin [28,30,41], that we found to be the most suitable for automated vessel density quantification (this marker was validated by CD31 and von Willebrand Factor co-stainings, data not shown). Podocalyxin staining showed a slight but significant increase in vessel density in *Gdf2*$^{-/-}$ mice versus WT mice (Fig. 2a and b) while there were no differences in vessel diameter (Fig. 2c), supporting that this increase in vessel density is due to an increase in vessel number rather than vessel size. VEGF-A being the main actor involved in tumor neovascularization, we analyzed circulating and tumor levels of VEGF-A by ELISA. We found no differences between *Gdf2*$^{-/-}$ and WT mice (Additional file 2: Fig. S2A and B), supporting that the *Gdf2*$^{-/-}$ phenotype is not directly linked to modifications of the VEGF-A pathway.

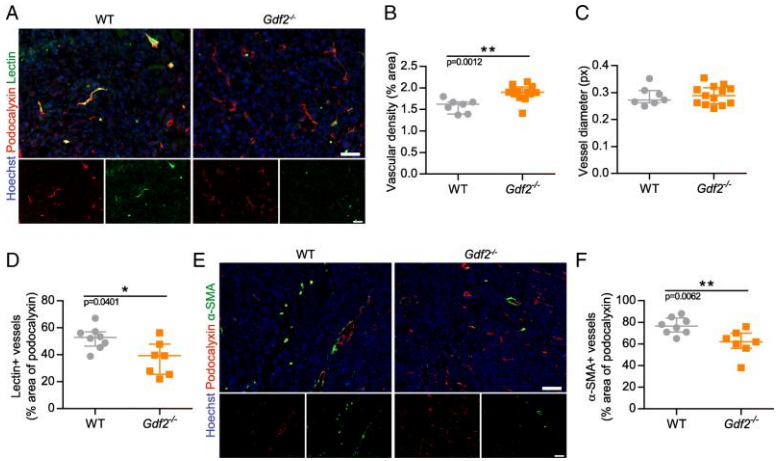

Figure 2: *Gdf2* deletion decreases tumor perfusion and maturation in the E0771 mammary cancer model. E0771 cells were injected in the 4th mammary gland of WT and $Gdf2^{-/-}$ mice and tumor vascularization was analyzed 9 days after tumor detection. **a** Representative images of the tumors stained for podocalyxin (red), lectin (green) and cell nuclei (blue, Hoechst). Scale bar 50 µm. **b** Vascular density quantified by podocalyxin positive area (% of tumor area) and (**c**) assessment of vessel diameter using Ferret's theorem (WT $n = 7$, $Gdf2^{-/-}$ $n = 13$, 1 representative experiment out of 2). **d** Quantification of vessel perfusion by lectin staining (% area of lectin/podocalyxin) (WT $n = 8$, $Gdf2^{-/-}$ $n = 7$, 1 representative experiment out of 3). **e** Representative images of the tumors stained for podocalyxin (red), α-smooth muscle actin (α-SMA) (green) and cell nuclei (blue, Hoechst). Scale bar 100 µm. **f** α-SMA staining quantification (% area of α-SMA/podocalyxin) (WT $n = 8$, $Gdf2^{-/-}$ $n = 7$, 1 representative experiment out of 3). **b**, **c**, **d**, **f** Data are the median ± interquartile range. Statistical analysis: Mann-Whitney test. $*p \leq 0.05$ and $**p \leq 0.01$ significantly different

We next analyzed whether tumor vessels were functional by performing intravenous injection of FITC-conjugated tomato lectin that has a strong affinity for endothelial cells. We found that the percentage of tumor vessels perfused by lectin was significantly reduced in $Gdf2^{-/-}$ versus WT mice (Fig. 2a and d), supporting a defect in vessel perfusion in absence of BMP9. To test if this defect could be due to a lack of vessel maturation, we determined the presence of vessel-associated mural cells by performing immunostaining for α-smooth muscle actin (α-SMA). We found that the percentage of vessel coverage by α-SMA was also significantly reduced in $Gdf2^{-/-}$ versus WT mice (Fig. 2e and f).

Loss of BMP9 Increases the Number and the Size of Lung Metastases in the Mouse E0771 Mammary Carcinoma Model

We next asked whether the loss of BMP9 could affect metastatic dissemination. The E0771 mammary cancer model has been shown to spontaneously disseminate in lungs [38]. We thus looked for lung metastases and found that the incidence of metastasis was similar in *Gdf2*$^{-/-}$ compared to WT animal (72% vs 71%). However, the total area of lung metastases was significantly increased in *Gdf2*$^{-/-}$ versus WT mice (Fig. 3a and b), which was linked to both an increase in the number and in the mean size of metastases (Fig. 3c and d). We next studied tumor lymphangiogenesis, an important route for lung metastases. Using LYVE-1 staining, we were able to detect lymphatic vessels in most of the E0771 tumors (respectively 61% and 72% of WT and *Gdf2*$^{-/-}$ mice) but found no differences in lymphatic vessel density between *Gdf2*$^{-/-}$ and WT mice (Additional file 3: Fig. S3A and B).

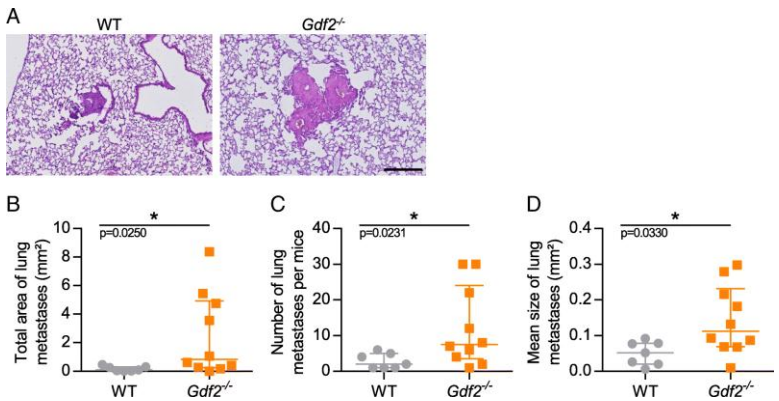

Figure 3: *Gdf2* deletion increases metastatic burden in the E0771 mammary cancer model. E0771 cells were injected in the 4th mammary gland of WT and *Gdf2*$^{-/-}$ mice and lung metastases were analyzed 9 days after tumor detection. **a** Representative hematoxylin eosin colorations of metastases within WT and *Gdf2*$^{-/-}$ lungs. Scale bar 250 µm. **b** Total area, (**c**) number and (**d**) mean size of lung metastases per mice bearing metastases (WT n = 7, *Gdf2*$^{-/-}$ n = 10, 1 representative experiment out of 3). **b**, **c**, **d** Data are the median ± interquartile range. Statistical analysis: Mann-Whitney test. *$p \leq 0.05$ significantly different

Loss of BMP10 does not affect Tumor Growth, Tumor Angiogenesis and Metastasis in the Mouse E0771 Mammary Carcinoma Model

We next addressed the role of BMP10, the other ALK1's ligand, in the E0771 mammary cancer model. As *Bmp10* deletion is embryonic lethal due to cardiac defects [21], we generated a conditional Rosa26 CreER^{T2};*Bmp10*$^{lox/lox}$ mice that allowed deletion of *Bmp10* after tamoxifen injection. Both Cre-positive (*Bmp10*-cKO) and Cre-negative (CTL) mice were injected with tamoxifen when three-week-old (Fig. 4a). At the age of six weeks, E0771 cells were injected into the fourth mammary gland. On the day of euthanasia, blood was collected and circulating BMP10 levels were measured by ELISA. As expected, tamoxifen treatment significantly decreased BMP10 circulating levels (64 and 7 pg/mL, in CTL and *Bmp10*-cKO mice, respectively, Fig. 4b). We found that loss of BMP10 did not significantly modify tumor volume (Fig. 4c). We next analyzed tumor vascularization but could not detect any differences in tumor vessel density (podocalyxin staining), nor in vessel perfusion (lectin injection) between CTL and *Bmp10*-deleted mice (Fig. 4d-f). We also studied lung metastasis in these mice and could not detect any differences in the total area, number or mean size of lung metastases between CTL and *Bmp10*-cKO mice (Fig. 4g-i).

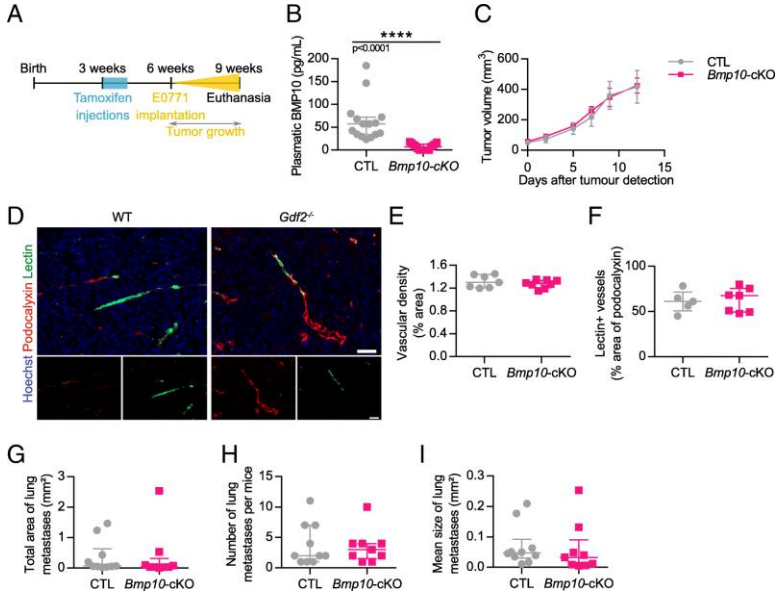

Figure 4: *Bmp10* conditional deletion has no impact on tumor growth, angiogenesis and lung metastasis in the E0771 mammary cancer model. **a** Schematic representation of the experimental protocol for *Bmp10* specific deletion and E0771 cells implantation. Tamoxifen was injected in all 3-week-old mice; 3 weeks later, E0771 cells were injected and tumor growth was analyzed for 3 weeks. **b** Plasmatic levels of BMP10 in control (CTL, n = 15) and *Bmp10* conditional KO (*Bmp10*-cKO, n = 15) mice assessed by ELISA at the end of the experiment. **c** Tumor growth was assessed by caliper measurement every 2 to 3 days after tumor detection (CTL n = 7, *Bmp10*-cKO n = 8, 1 representative experiment out of 3). **d** Representative images of the tumors stained for podocalyxin (red), lectin (green) and cell nuclei (blue, Hoechst). Scale bar 50 µm. **e** Vascular density quantified by podocalyxin surface area (% of tumor area) and (**f**) Quantification of vessel perfusion by lectin staining (% area of lectin/podocalyxin) (CTL n = 7, *Bmp10*-cKO n = 8, 1 representative experiment out of 3). **g** Total area, (**h**) number and (**i**) mean size of lung metastases per mice bearing metastases (CTL n = 10, *Bmp10*-cKO *n* = 9, 2 experiments). **c** Data are the mean ± SEM. Statistical analysis: Two-way matched ANOVA. **b**, **e**, **f**, **g**, **h**, **i** Data are the median ± interquartile range. Statistical analysis: Mann-Whitney test. ****$p \leq 0.001$ significantly different

We tested whether this absence of effect in the *Bmp10*-cKO mice could be due to a compensation by BMP9. However, we found similar levels of BMP9 mRNA in the liver of CTL and *Bmp10*-cKO mice (Additional file 4: Fig. S4).

The loss of BMP9 and BMP10 in Double Knockout Mice does not lead to a Stronger Effect on Mouse E0771 Mammary Carcinoma Tumor Growth and Angiogenesis than the Single Loss of BMP9

We next addressed whether the loss of both BMP9 and BMP10 within the same mice would have a more pronounced effect on the E0771 mammary cancer model. These mice were generated by crossing *Gdf2*$^{-/-}$mice with Rosa26 CreER^{T2};*Bmp10*$^{lox/lox}$ mice. Both Cre-positive (*Gdf2*$^{-/-}$;*Bmp10*$^{lox/lox}$, referred as double-cKO) and Cre-negative (*Gdf2*$^{+/+}$;*Bmp10*$^{lox/lox}$, referred as CTL) mice were injected with tamoxifen at the age of three weeks. As expected, the circulating levels of BMP9 and BMP10 measured after euthanasia by ELISA were strongly reduced in double-KO mice as compared to CTL mice (Fig. 5a and b). These double-KO mice were viable during the eight weeks of the experimental procedure. At the age of six weeks, E0771 cells were injected as described in Fig. 4a. We found that double-KO mice developed larger tumors than CTL mice (Fig. 5c). They also presented a slight increase in vessel density and a decrease in perfused vessels (Fig. 5d and e). Together these data showed that the double-KO mice, in this experimental model of E0771 mammary cancer, behaved as *Gdf2*$^{-/-}$*mice.*

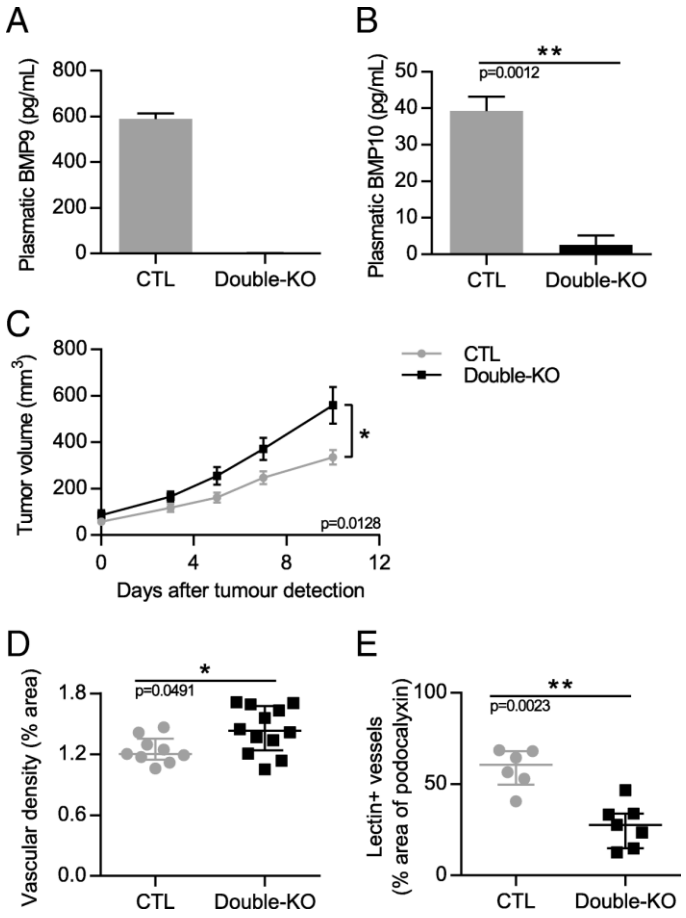

Figure 5: Double deletion of *Gdf2* and *Bmp10* increases tumor growth and decreases tumor perfusion in the E0771 mammary cancer model. Tamoxifen was injected in all 3-week-old mice; 3 weeks later E0771 cells were injected and tumor growth was analyzed for 3 weeks. **a**, **b** BMP9 and BMP10 circulating levels in CTL and double-KO mice assessed by ELISAs at the end of the experiment. **c** Tumor growth was assessed by caliper measurement every 2 to 3 days after tumor detection (CTL n = 13, Double-KO $n = 11$, 2 experiments). **d** Vascular density quantified by podocalyxin surface area (% of tumor area) (CTL n = 9, Double-KO $n = 12$, 1 representative group out of 4) and (**e**) Quantification of vessel perfusion by lectin staining (% area of lectin/podocalyxin) (CTL $n = 6$, Double-KO n = 7, 1 representative group out of 4). **a**, **b** Data are the mean ± SEM. Statistical analysis: Mann-Whitney. **c** Data are the mean ± SEM. Statistical analysis: Two-way matched ANOVA. **d**, **e** Data are the median ± interquartile range. Statistical analysis: Mann-Whitney test. *$p \leq 0.05$, and **$p \leq 0.01$ significantly different

Discussion

Several clinical trials targeting ALK1 or its co-receptor endoglin are ongoing although the role of these two receptors in a tumor context are not yet understood and, so far present limited beneficial results [25]. Since both ALK1's ligands, BMP9 and BMP10 circulate in blood, there is an urgent need to understand the respective contribution of each ligand in tumor development and metastasis. Contrary to what we expected from many preclinical studies aiming at blocking ALK1, we found that loss of BMP9 led to an increase in tumor growth, combined with decreased tumor vessel maturation and increased lung metastasis in the E0771 model. On the other hand, loss of BMP10 did not seem to affect the E0771 mammary cancer model and the double deletion of BMP9 and BMP10 did not lead to a stronger phenotype than the single deletion of BMP9. Together these results demonstrate, for the first time, that BMP9 and BMP10 exhibit distinct roles in tumor growth, angiogenesis and metastatic dissemination.

We show that the loss of BMP9 led to a small but statistically significant increase in tumor volume. However, this result does not seem to be a consequence of a direct effect of BMP9 on tumor cell proliferation since BMP9 did not affect E0771 cell proliferation, cell viability nor apoptosis in vitro. In accordance, we could not observe any significant differences in PCNA staining nor on activated pase-3 or TUNEL stainings on tumors that were harvested at the end of the study. This is in contrast to other studies that have shown that overexpression of BMP9 using adenoviruses inhibit the growth, invasion and migration of the breast cancer cell lines MDA-MB-231, SK-BR-3 and 4 T1 [35,42,43]. This could be due to differences in breast cancer models or in the doses of BMP9 used. On the other hand, we found that loss of BMP9 affected tumor neovascularization. Indeed, we found that the loss of BMP9 increased tumor vessel density, and decreased tumor vessel perfusion and coverage by mural cells as illustrated by α-SMA staining, indicating decreased vessel maturation. This is in accordance with the current hypothesis that BMP9 is a maturation or "normalization" factor [44]. The tumor vasculature has been described as a dense

but chaotic and heterogeneous network of structurally and functionally abnormal vessels with a compromised blood flow, a lack of pericyte coverage and a high permeability with non-specific extravasation of blood components [45]. "Normalization" of the tumor vasculature through the Angiopoietin-Tie2 axis, for example, decreases vessel density, increases vessel coverage and perfusion while decreasing permeability. As a consequence of this vessel normalization, tumor growth is decreased as well as tumor necrosis and metastasis [46]. Our results on E0771 tumor growth, necrosis, metastasis and tumor perfusion are in accordance with this concept. Together, our data support that BMP9 is a circulating vascular quiescence factor in both physiological and tumoral contexts.

Most cancer patients die of their metastases rather than of their primary tumor so therapeutic strategies have recently focused on metastasis. In the E0771 model, we found that *Gdf2*$^{-/-}$ mice developed more and larger metastases. This supports the normalization theory where heterogeneity, leakage and lack of perfusion leads to hypoxia and aggravates tumor progression and metastasis (which is hindered upon normalization) [47]. It is also possible that, as for the primary tumor, the growth of the metastases would be favored in *Gdf2*$^{-/-}$ mice. Differences in lymphangiogenesis could also be an explanation as we have previously shown that *Gdf2* deletion in the C57BL/6 background leads to lymphatic drainage deficiency [22]. However, although we detected lymphatic vessels in these tumors, we found no differences in tumor lymphatic vessel density between WT and *Gdf2*$^{-/-}$ mice.

It was recently shown, in another preclinical study, that blocking BMP9, using a neutralizing anti-BMP9 antibody, significantly reduced renal tumor growth and reduced tumor vascular permeability [48] suggesting potential differences between different tumor types. The role of BMP9, using a similar approach of *Gdf2* knockdown, has recently been described in the pancreatic RIP1-TAg2 PanNETS cancer model [49]. However, in this model, *Bmp9* ablation led to a reduced tumor volume, no effect in vessel density but an increase in vessel branching and

pericyte coverage and an increase in metastasis. These results, apart for the increase in metastasis, differ from our results. This might be due to differences between cancer types. However, in this paper, using the same pancreatic model, the authors obtained different and even opposite results with mice deleted within this signaling pathway (*Eng*$^{+/-}$, *Acvrl1*$^{+/-}$ and *Gdf2*$^{-/-}$ mice) [49], highlighting the difficulties of understanding the role of this pathway in cancer and tumor angiogenesis. Nevertheless, their results [49] and ours show that, in these two cancers, the loss of BMP9 leads to an increase in metastasis and thus cautions against blockade of this BMP9/ALK1 pathway in cancer treatments.

We found that, in contrast to the loss of BMP9, the loss of BMP10 had no significant effect in the E0771 mammary carcinoma model and the loss of both BMP9 and BMP10 in the double-Knockout mice did not lead to a stronger phenotype than the single loss of BMP9. This was not due to tamoxifen injection as *Gdf2*-KO mice injected with tamoxifen also showed significantly increased tumor growth (data not shown). Tamoxifen injection led to a 90% decrease in BMP10 circulating levels. It is unlikely, that the remaining 10% of BMP10 could explain the lack of effect. Our results rather support that BMP10 does not play an important role in this breast tumor model. It is interesting to note that loss of BMP9 is sufficient to affect tumor development in this mammary carcinoma model. This supports that, in contrast to post-natal model of angiogenesis or vascular remodeling [17,20,23], there is no redundancy between BMP9 and BMP10 in this tumor context. This absence of redundancy could be due to differences between physiological and tumor angiogenesis or due to the fact that the role of BMP9 and BMP10 might be different in newborns and adults. Indeed, we have previously shown that blocking BMP10 with a neutralizing antibody in newborn *Gdf2*$^{-/-}$ mice led to the death of these pups within few days [23], which is not the e here in adult mice.

Conclusions

There are currently several anticancer drugs targeting ALK1 or its ligands in phase I/II of clinical development although with

limited beneficial results so far [5,25]. Our present work highlights the need of performing detailed mechanistic studies prior to pursuing clinical testing of drugs impinging this pathway. Our studies show that targeting BMP9 or BMP10 differently affect tumor growth, angiogenesis and metastatic dissemination. These data also support that targeting specifically BMP9 rather than ALK1 or endoglin, that will affect both ligands, could be more appropriate. It also addresses the question whether blocking this pathway is relevant in cancer treatments as, at least in this mammary mouse model, loss of BMP9 increases tumor growth and lung metastasis. Anti-angiogenic treatments have slightly changed optic recently and it is not clear whether drugs should block angiogenesis, sustain vessel normalization or promote vascularization [50]. Thus, BMP9 might be an interesting quiescence factor in the context of vessel normalization but in this e, we might want to activate this pathway by giving recombinant BMP9 in cancer than rather blocking it and to combine it with current chemotherapies or immunotherapies.

References

1. Hanahan D, Weinberg RA. Hallmarks of cancer: the next generation. Cell. 2011; 144: 646–674.
2. Ronca R, Benkheil M, Mitola S, Struyf S, Liekens S. Tumor angiogenesis revisited: regulators and clinical implications. Med Res Rev. 2017; 37: 1231–1274.
3. Ferrara N, Hillan KJ, Novotny W. Bevacizumab (Avastin), a humanized anti-VEGF monoclonal antibody for cancer therapy. Biochem Biophys Res Commun. 2005; 333: 328–335.
4. Jain RK. Antiangiogenesis strategies revisited: from starving tumors to alleviating hypoxia. Cancer Cell. 2014; 26: 605–622.
5. Viallard C, Larrivee B. Tumor angiogenesis and vascular normalization: alternative therapeutic targets. Angiogenesis. 2017; 20: 409–426.
6. Cunha SI, Pietras K. ALK1 as an emerging target for antiangiogenic therapy of cancer. Blood. 2011; 117: 6999–7006.

7. Bhatt RS, Atkins MB. Molecular pathways: can Activin-like kinase pathway inhibition enhance the limited efficacy of VEGF inhibitors? Clin Cancer Res. 2014; 20: 2838–2845.
8. Oh SP, Seki T, Goss KA, Imamura T, Yi Y, et al. Activin receptor-like kinase 1 modulates transforming growth factor-beta 1 signaling in the regulation of angiogenesis. Proc Natl Acad Sci U S A. 2000; 97: 2626–2631.
9. Urness LD, Sorensen LK, Li DY. Arteriovenous malformations in mice lacking activin receptor-like kinase-1 [in process citation]. Nat Genet. 2000; 26: 328–331.
10. Johnson DW, Berg JN, Baldwin MA, Gallione CJ, Marondel I, et al. Mutations in the activin receptor-like kinase 1 gene in hereditary haemorrhagic telangiectasia type 2. Nat Genet. 1996; 13: 189–195.
11. McAllister KA, Grogg KM, Johnson DW, Gallione CJ, Baldwin MA, et al. Endoglin, a TGF-beta binding protein of endothelial cells, is the gene for hereditary haemorrhagic telangiectasia type 1. Nat Genet. 1994; 8: 345–351.
12. Brown MA, Zhao Q, Baker KA, Naik C, Chen C, et al. Crystal structure of BMP-9 and functional interactions with pro-region and receptors. J Biol Chem. 2005; 280: 25111–25118.
13. David L, Mallet C, Mazerbourg S, Feige JJ, Bailly S. Identification of BMP9 and BMP10 as functional activators of the orphan activin receptor-like kinase 1 (ALK1) in endothelial cells. Blood. 2007; 109: 1953–1961.
14. Miller AF, Harvey SA, Thies RS, Olson MS. Bone morphogenetic protein-9. An autocrine/paracrine cytokine in the liver. J Biol Chem. 2000; 275: 17937–17945.
15. Neuhaus H, Rosen V, Thies RS. Heart specific expression of mouse BMP-10 a novel member of the TGF-beta superfamily. Mech Dev. 1999; 80: 181–184.
16. Bidart M, Ricard N, Levet S, Samson M, Mallet C, et al. BMP9 is produced by hepatocytes and circulates mainly in an active mature form complexed to its prodomain. Cellular and molecular life sciences : CMLS. 2012; 69: 313–324.
17. Chen H, Brady Ridgway J, Sai T, Lai J, Warming S, et al. Context-dependent signaling defines roles of BMP9 and BMP10 in embryonic and postnatal development. Proc Natl Acad Sci U S A. 2013; 110: 11887–11892.

18. Olsen OE, Wader KF, Misund K, Vatsveen TK, Ro TB, et al. Bone morphogenetic protein-9 suppresses growth of myeloma cells by signaling through ALK2 but is inhibited by endoglin. Blood cancer journal. 2014; 4: e196.
19. Townson SA, Martinez-Hackert E, Greppi C, Lowden P, Sako D, et al. Specificity and structure of a high affinity activin receptor-like kinase 1 (ALK1) signaling complex. J Biol Chem. 2012; 287: 27313–27325.
20. Ricard N, Ciais D, Levet S, Subileau M, Mallet C, et al. BMP9 and BMP10 are critical for postnatal retinal vascular remodeling. Blood. 2012; 119: 6162–6171.
21. Chen H, Shi S, Acosta L, Li W, Lu J, et al. BMP10 is essential for maintaining cardiac growth during murine cardiogenesis. Development. 2004; 131: 2219–2231.
22. Levet S, Ciais D, Merdzhanova G, Mallet C, Zimmers TA, et al. Bone morphogenetic protein 9 (BMP9) controls lymphatic vessel maturation and valve formation. Blood. 2013; 122: 598–607.
23. Levet S, Ouarne M, Ciais D, Coutton C, Subileau M, et al. BMP9 and BMP10 are necessary for proper closure of the ductus arteriosus. Proc Natl Acad Sci U S A. 2015; 112: E3207–3215.
24. Goumans MJ, Zwijsen A, Ten Dijke P, Bailly S. Bone morphogenetic proteins in vascular homeostasis and disease. Cold Spring Harb Perspect Biol. 2018; 10.
25. de Vinuesa AG, Bocci M, Pietras K, Ten Dijke P. Targeting tumour vasculature by inhibiting activin receptor-like kinase (ALK)1 function. Biochem Soc Trans. 2016; 44: 1142–1149.
26. Mitchell D, Pobre EG, Mulivor AW, Grinberg AV, tonguay R, et al. ALK1-fc inhibits multiple mediators of angiogenesis and suppresses tumor growth. Mol Cancer Ther. 2010; 9: 379–388.
27. van Meeteren LA, Thorikay M, Bergqvist S, Pardali E, Stampino CG, et al. Anti-human activin receptor-like kinase 1 (ALK1) antibody attenuates bone morphogenetic protein 9 (BMP9)-induced ALK1 signaling and interferes with endothelial cell sprouting. The J Biol Chem. 2012; 287: 18551–18561.
28. Cunha SI, Pardali E, Thorikay M, Anderberg C, Hawinkels L, et al. Genetic and pharmacological targeting of activin

receptor-like kinase 1 impairs tumor growth and angiogenesis. J Exp Med. 2010; 207: 85–100, S101-105.
29. Hu-Lowe DD, Chen E, Zhang L, Watson KD, Mancuso P, et al. Targeting Activin receptor-like kinase 1 inhibits angiogenesis and tumorigenesis through a mechanism of action complementary to anti-VEGF therapies. Cancer Res. 2011; 71: 1362–1373.
30. Cunha SI, Bocci M, Lovrot J, Eleftheriou N, Roswall P, et al. Endothelial ALK1 is a therapeutic target to block metastatic dissemination of breast Cancer. Cancer Res. 2015; 75: 2445–2456.
31. Jimeno A, Posner MR, Wirth LJ, Saba NF, Cohen RB, et al. A phase 2 study of dalantercept, an activin receptor-like kinase-1 ligand trap, in patients with recurrent or metastatic squamous cell carcinoma of the head and neck. Cancer. 2016; 122: 3641–3649.
32. Wheatley-Price P, Chu Q, Bonomi M, Seely J, Gupta A, et al. A phase II study of PF-03446962 in patients with advanced malignant pleural mesothelioma. CCTG trial IND.207. J Thorac Oncol. 2016; 11: 2018–2021.
33. Herrera B, Garcia-Alvaro M, Cruz S, Walsh P, Fernandez M, et al. BMP9 is a proliferative and survival factor for human hepatocellular carcinoma cells. PLoS One. 2013; 8: e69535.
34. Wan S, Liu Y, Weng Y, Wang W, Ren W, et al. BMP9 regulates cross-talk between breast cancer cells and bone marrow-derived mesenchymal stem cells. Cell Oncol (Dordr). 2014; 37: 363–375.
35. Wang K, Feng H, Ren W, Sun X, Luo J, et al. BMP9 inhibits the proliferation and invasiveness of breast cancer cells MDA-MB-231. J Cancer Res Clin Oncol. 2011; 137: 1687–1696.
36. Ren W, Sun X, Wang K, Feng H, Liu Y, et al. BMP9 inhibits the bone metastasis of breast cancer cells by downregulating CCN2 (connective tissue growth factor, CTGF) expression. Mol Biol Rep. 2014; 41: 1373–1383.
37. Ye L, Bokobza S, Li J, Moazzam M, Chen J, et al. Bone morphogenetic protein-10 (BMP-10) inhibits aggressiveness of breast cancer cells and correlates with poor prognosis in breast cancer. Cancer Sci. 2010; 101: 2137–2144.

38. Ewens A, Mihich E, Ehrke MJ. Distant metastasis from subcutaneously grown E0771 medullary breast adenocarcinoma. Anticancer Res. 2005; 25: 3905–3915.
39. Yang Y, Yang HH, Hu Y, Watson PH, Liu H, et al. Immunocompetent mouse allograft models for development of therapies to target breast cancer metastasis. Oncotarget. 2017; 8: 30621–30643.
40. Imayoshi I, Ohtsuka T, Metzger D, Chambon P, Kageyama R. Temporal regulation of Cre recombinase activity in neural stem cells. Genesis. 2006; 44: 233–238.
41. Depner C, Zum Buttel H, Bogurcu N, Cuesta AM, Aburto MR, et al. EphrinB2 repression through ZEB2 mediates tumour invasion and anti-angiogenic resistance. Nat Commun. 2016; 7: 12329.
42. Varadaraj A, Patel P, Serrao A, Bandyopadhay T, Lee NY, et al. Epigenetic regulation of GDF2 suppresses Anoikis in ovarian and breast epithelia. Neoplasia. 2015; 17: 826–838.
43. Ren W, Liu Y, Wan S, Fei C, Wang W, et al. BMP9 inhibits proliferation and metastasis of HER2-positive SK-BR-3 breast cancer cells through ERK1/2 and PI3K/AKT pathways. PLoS One. 2014; 9: e96816.
44. David L, Mallet C, Keramidas M, Lamande N, Gasc JM, et al. Bone morphogenetic protein-9 is a circulating vascular quiescence factor. Circ Res. 2008; 102: 914–922.
45. Fukumura D, Duda DG, Munn LL, Jain RK. Tumor microvasculature and microenvironment: novel insights through intravital imaging in pre-clinical models. Microcirculation. 2010; 17: 206–225.
46. Park JS, Kim IK, Han S, Park I, Kim C, et al. Normalization of tumor vessels by Tie2 activation and Ang2 inhibition enhances drug delivery and produces a favorable tumor microenvironment. Cancer Cell. 2016; 30: 953–967.
47. Cooke VG, LeBleu VS, Keskin D, Khan Z, O'Connell JT, et al. Pericyte depletion results in hypoxia-associated epithelial-to-mesenchymal transition and metastasis mediated by met signaling pathway. Cancer Cell. 2012; 21: 66–81.
48. Brand V, Lehmanna C, Umkehrera C, Bissingera S, Thierb M, et al. Impact of selective anti-BMP9 treatment on tumor

cells and tumor angiogenesis. Mol Oncol. 2016; 10: 1603–1620.
49. Eleftheriou NM, Sjolund J, Bocci M, Cortez E, Lee SJ, et al. Compound genetically engineered mouse models of cancer reveal dual targeting of ALK1 and endoglin as a synergistic opportunity to impinge on angiogenic TGF-beta signaling. Oncotarget. 2016; 7: 84314–84325.
50. Rivera LB, Bergers G. CANCER. Tumor angiogenesis, from foe to friend. Science. 2015; 349: 694–695.

Additional files

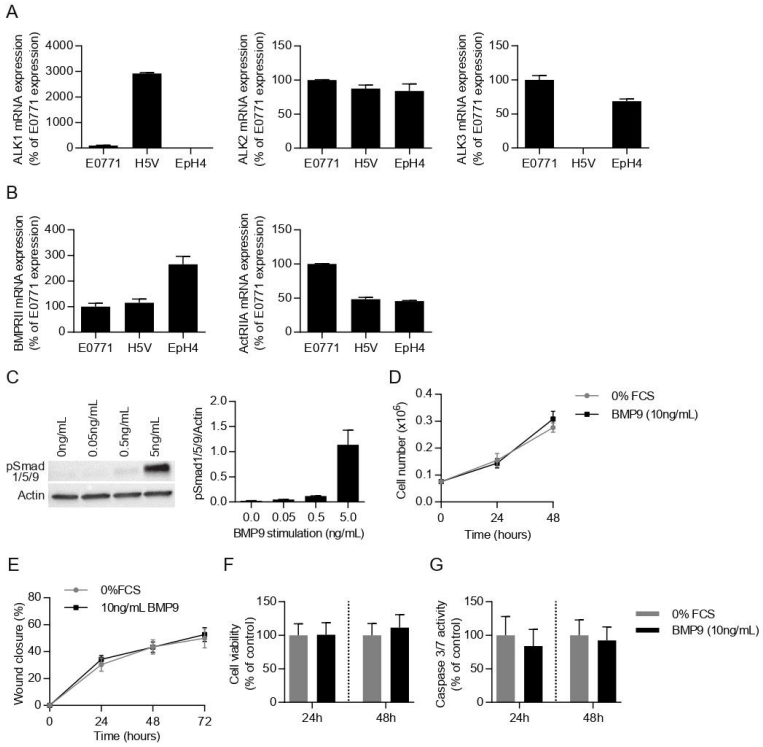

Figure S1. Characterization of E0771 cells in vitro and their response to BMP9.

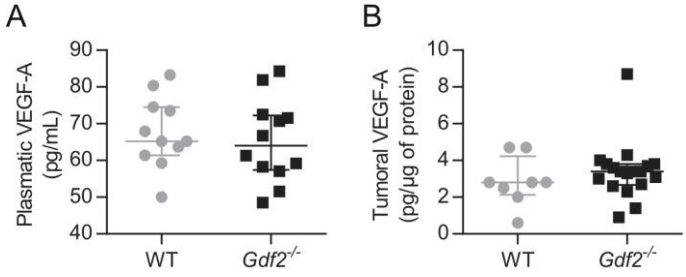

Figure S2. VEGF-A levels in the E0771 mammary cancer model.

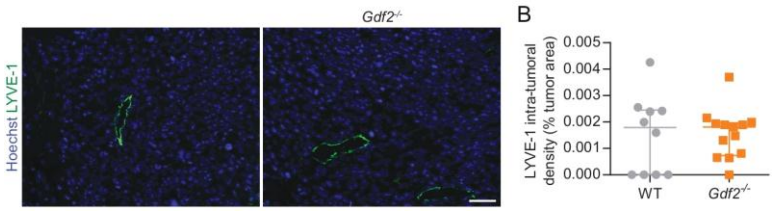

Figure S3. *Gdf2* deletion has no impact on tumor lymphangiogenesis in the E0771 breast cancer model.

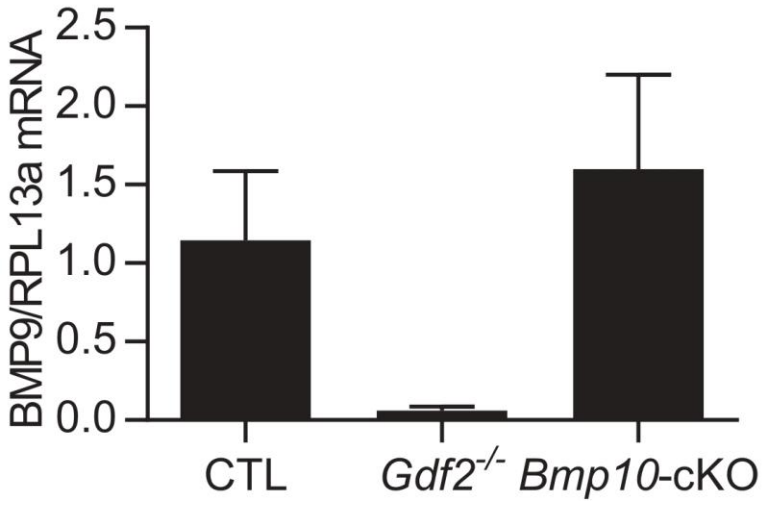

Figure S4. BMP9 mRNA levels in liver of *Bmp10*-cKO mice.

Book Chapter

The BMP9/10-ALK1-Endoglin Pathway as a Target of Anti-Angiogenic Therapy in Cancer

Al Tabosh T[#], Al Tarrass M[#] and Bailly S*

Universite Grenoble Alpes, Inserm, CEA, Biology of Cancer and Infection Laboratory, France

[#]These authors contributed equally to this work

***Corresponding Author:** Bailly S, Universite Grenoble Alpes, Inserm, CEA, Biology of Cancer and Infection Laboratory, F-38000 Grenoble, France

Published **November 26, 2021**

How to cite this book chapter: Al Tabosh T, Al Tarrass M, Bailly S. The BMP9/10-ALK1-Endoglin Pathway as a Target of Anti-Angiogenic Therapy in Cancer. In: Hussein Fayyad Kazan, editor. Immunology and Cancer Biology. Hyderabad, India: Vide Leaf. 2021.

Abstract

The growth and dissemination of solid tumors heavily relies on angiogenesis, making it an attractive therapeutic target in cancer. Tumor angiogenesis is orchestrated by a plethora of secreted factors and signaling pathways. The initial inhibition of the VEGF-pathway, despite successful preclinical studies, yielded only modest clinical benefits in patients, promoting the search

for other anti-angiogenic targets. The BMP9/10-ALK1-endoglin pathway is an important regulator of vascular development. This pathway has been investigated by multiple groups as a therapeutic target for tumor angiogenesis inhibition. For that, various pharmacological and genetic means were used to target different components of this pathway. Here, we recapitulate the outcome of most cellular, preclinical and clinical studies targeting BMP9/10-ALK1-endoglin pathway as an attempt to block tumor angiogenesis.

Introduction

Angiogenesis, the formation of new blood vessels from pre-existing ones, is active during physiological development to provide the growing tissues with an adequate supply of oxygen and nutrients while removing metabolic wastes. In adulthood, the vascular tree generally reaches a quiescent state, with few exceptions including wound healing and the female menstrual cycle. This vascular quiescence is tightly regulated by a variety of pro-angiogenic and anti-angiogenic factors that coordinate angiogenic processes in a spatiotemporal manner [1]. Vascular endothelial growth factor (VEGF), basic fibroblastic growth factor (bFGF), angiogenin, thrombospondin (TSP), angiopoietins, and transforming growth factor-β (TGF-β) are all examples of angiogenic factors that control the ON-OFF angiogenic switch [2]. In solid malignancies, dysregulation of the angiogenic switch towards the pro-angiogenic phenotype promotes the development of a highly vascularized niche that supports tumor growth and provides an escape route for metastatic dissemination [3]. Therefore, inhibition of tumor angiogenesis is considered an important therapeutic strategy in cancer treatment [4].

The main goal of anti-angiogenic therapies is to abrogate the formation of new blood vessels within the tumor, in an attempt to deprive cancer cells from oxygen and nutrients, and consequently inhibit tumor growth and progression. Moreover, tumor induced angiogenesis is associated with the formation of aberrant vascular network characterized by acidosis, interstitial hypertension and hypoxia. This abnormal microenvironment

endangers the efficacy and proper delivery of therapeutics to solid tumors [5]. Therefore, the development of anti-angiogenic therapies and combining them with cytotoxic drugs constitutes an important aspect in cancer therapies.

Targeting VEGF signaling has been demonstrated as the prime antiangiogenic target in the clinic for the last two decades. Anti-VEGF therapies, including blocking antibodies against VEGF (bevacizumab), kinase inhibitors (sunitinib, imatinib, sorafenib, axitinib and regorafenib), and decoy receptors, have been included in the first line therapies against advanced and metastatic cancers [6]. Unfortunately, in contrast to the promising results from preclinical studies, the use of this monotherapy has yielded only modest therapeutic benefit in some tumor types, failed in others and was associated with the generation of resistant and more aggressive tumors [7,8]. Hence, alternative and/or complementary therapeutics directed at novel targets of vascular development are urgently needed.

Members of the Transforming growth β (TGF-β) superfamily of signaling molecules have been previously described as important modulators of vasculogenic and angiogenic processes. Among them, BMP9 and BMP10, which bind with high affinity to a signaling complex of receptors composed of activin receptor-like-kinase-1 (ALK1) and endoglin [9] which are mostly expressed on endothelial cells, play an essential role in vascular development [10]. This signaling complex is composed of two type I receptors (ALK1), two type II receptors (BMPRII, ActRIIA or ActRIIB) and the co-receptor endoglin. Both type I and type II receptors possess Serine/Threonine kinase activities. Binding of BMP9/10 to this receptor complex leads to the phosphorylation of ALK1 by the constitutively active type II receptor. Consequently, activated ALK1 phosphorylates transcription factors known as Smads that modulate target gene expression [9,11,12]. Endoglin is a homodimeric cell-surface co-receptor that lacks enzymatic activity and functions as a co-receptor in association with ALK1, enhancing ALK1 signaling [13]. ALK1 and endoglin display highly similar expression patterns, being mostly restricted to endothelial cells. Complete genetic ablation of either ALK1 or endoglin in mice results in

embryonic lethality due to impairment of blood vessel development [14]. In addition, heterozygous loss-of-function mutations in either gene in humans give rise to two closely related forms of the vascular disorder hereditary hemorrhagic telangiectasia (HHT) [15].

Interestingly, an elevated expression level of both ALK1 and endoglin was reported in the angiogenic tumor endothelium [16,17] and the BMP9/10-ALK1-endoglin pathway was proposed to be involved in resistance to anti-VEGF therapy in tumors [18]. In addition, BMP9 is known to regulate the development of lymphatic vessels [19,20], which has implications for metastatic spread of tumor cells through lymphatic vasculature [21]. As a result, the BMP9/10-ALK1-endoglin signaling pathway emerged as an interesting candidate target for anti-angiogenic cancer therapies. Consequently, extensive *in vitro* and *in vivo* studies have been performed in the past two decades to investigate the implication of this pathway in tumor angiogenesis, using multiple cancer models. Most preclinical studies revealed promising anti-angiogenic responses, giving rise to several clinical trials aiming to improve the overall survival of cancer patients. Here, we provide a brief overview of the cellular, preclinical and clinical studies targeting BMP9/10-ALK1-endoglin pathway as an attempt to block tumor angiogenesis.

Targeting ALK1 as an Anti-Angiogenic Therapy in Cancer

Different biological compounds have been designed/identified to interfere with ALK1 signaling including the BMP type-I receptor inhibitors LDN-193189 [22], OD16 and OD29 [23], and the miRNA miR-199b-5p [24], all of which have demonstrated effective inhibition of ALK1 signaling. However, the specificity of designed drugs and crosstalk with other pathways make it difficult to predict the final outcome of such inhibitors. For this reason, targeting ALK1 have been majorly studied in the context of tumor angiogenesis through highly specific designed products such as ALK1-Fc fusion ligand trap (dalantercept/ACE-041) developed by Acceleron Pharma Inc [25], and PF-03446962

(fully human antibody that targets extracellular domain of ALK1) developed by Pfizer [26], both of which have been implicated in independent clinical trials.

Preclinical Studies

ALK1 Ligand Trap

The characterization of the ALK1-Fc fusion protein has demonstrated its ability to specifically trap BMP9 and BMP10, but not any other ligand of the TGF-β family [27]. In vitro studies showed that dalantercept, and its mouse counterpart RAP-041, inhibited BMP9 and BMP10 induced Smad1/5 phosphorylation and downstream signaling (e.g, id1 gene expression), without affecting TGF-β induced Smad2 phosphorylation [27,28]. Moreover, functional assays showed that dalantercept blocks cord formation and endothelial sprouting *in vitro* in human umbilical vein endothelial cells (HUVEC), as well as FGF induced neovascularization and VEGF-induced vessel formation *in vivo* in a chick chorioallantoic membrane (CAM) assay [27]. The anti-tumor effects of ALK-1 Fc were primarily investigated through the application of RAP-041 in rat insulin promoter – SV40 large T antigen (RIP1-Tag2) model of pancreatic neuroendocrine tumorigenesis. Results showed an impaired tumor growth already after 2 weeks [28] and a decrease in the number of hepatic micro metastasis compared to the control cohort after a prolonged 4-week treatment [29]. Similar results have been obtained by blocking metastatic dissemination in the transgenic spontaneous mouse mammary tumor virus (MMTV)-polyoma middle T antigen (PyMT) and the syngeneic transplantable E0771 breast cancer models [30]. Likewise, dalantercept reduced tumor burden in MCF-7 mammary adenocarcinoma orthotopic model [27]. On the other hand, in another study of poorly/non-metastatic melanoma, breast, head and neck cancer, no effect was observed on primary tumor growth at the experimental endpoint following the use of RAP-041 as a monotherapy [31].

ALK1 Antibody

The ALK1 antibody (PF-03446962) directly binds to the extracellular domain of ALK1 (residues 42-56) with a high affinity, but doesn't bind to other closely related ALKs, such as ALK2/3/4/5/or ALK7, thus reducing potential off-target effects. *In vitro* studies demonstrated that PF-03446962 prevented binding of BMP9 to endothelial cells (ECs), inhibited BMP9-induced Smad1 phosphorylation, and BMP responsive element (BRE)-luciferase transcriptional reporter activity [32]. Moreover, the monoclonal antibody efficiently blocked serum-induced Smad1 phosphorylation, migration, endothelial sprouting, as well as tube formation in HUVECs [32,33]. Similarly, a reduction in tumor growth and inhibition of both microvascular and lymphatic vessel density has been reported in MDA-MB-231 human breast cancer xenografts when using PF-03446962 [33].

Although both strategies are directed to block the signaling through ALK1, the modes of action of dalantercept and PF-03446962 are distinct, one blocking the ligands the other blocking the receptor. Both approaches demonstrated that ALK1-targeting induces changes in the vascular network and subsequent alterations in the tumor microenvironment, described through in-depth vasculature characterization using several approaches such as monitoring pericyte coverage, vascular perfusion, as well as sprouting and leakiness of the vessels [30-34], all of which are critical factors that describe what is known by "vascular normalization". In the context of tumor anti-angiogenic therapies, the vascular normalization hypothesis states that antiangiogenic therapy aims to restore the balance between pro- and antiangiogenic factors back towards equilibrium. As a result, vessel structure and function become more normal: vessels are more mature with enhanced perivascular coverage, blood flow is more homogeneous, vessel permeability and hypoxia are reduced, and importantly the delivery of systemically administered anticancer therapies into tumors is more uniform [35]. Nevertheless, contradicting data have been described when assessing the functionality of the tumor-associated vasculature following administration of either RAP-041 or PF-03446962. For instance, PF-03446962

quantitatively disrupted vascular normalization in M24met/R xenograft tumors [33], while ALK1-Fc treatment that increased coverage of tumor endothelial cells by NG2-expressing cells (i.e. pericytes) [31]. Hu-lowe et al [33] displayed that flow rates were only affected in large, functional blood vessels, whereas smaller ones were unaffected. Contradictory to this result, Hawinkels et al [31] described a slight increase in perfusion. These results demonstrate that targeting the same receptor by two different approaches in different tumor models yields different results, and suggests more investigation of the underlying mechanisms following ALK1 activation.

Alk1+/- Mice

Other means of targeting ALK1 signaling as a therapeutic approach in cancer angiogenesis include genetic approaches using heterozygote mice. Cunha et al reported that blunted ALK1 expression using RIP1-Tag2; $Alk1^{+/-}$ mice showed a significant retardation in tumor progression through the angiogenic switch, reduced de novo tumor growth, and impaired angiogenesis in comparison to RIP1-Tag2; $Alk1^{+/+}$ mice, consistent with results of using RAP-041 which has been addressed in this same work [28,29].

Combinatory Treatments

Combinatorial treatments of ALK1-blocking agents with other targeted therapies have also shown promising results in targeting both tumor angiogenesis and progression. For instance, combined use of ALK1-Fc fusion along with chemotherapy (Doxorubicin or Cisplatin) has shown increased cytotoxic effect and impaired tumor growth in melanoma, head and neck cancer, and breast cancer models [31]. Likewise, in experimental breast carcinomas, RAP-041-induced blunted vessel density was further diminished in combined therapy group (RAP-041 + Docetaxel), accompanied by a significant reduction in the metastatic count in the lungs [30]. Moreover, Dual targeting of VEGF and BMP9/10 signals using a newly designed ALK1FLT1-Fc (ALK-Fc fused to VEGFR1-Fc) trap significantly inhibited both angiogenesis and growth of human

BxPC3 pancreatic tumor xenografts [36]. Of note, co-administration of RAP-041 and VEGFR2 neutralizing antibody DC101 showed no additional therapeutic benefit in MMTV-PyMT breast cancer model [30]. Interestingly, tumors described previously as resistant to VEGF inhibitors showed a significant decrease in tumor burden and associated vasculature when exposed to PF-03446962, through a mechanism suggesting disruption of vascular normalization phenotype induced by bevacizumab [33]. It was also shown that combinatorial use of dalantercept with the VEGFR2 tyrosine kinase inhibitor sunitinib leads to tumor stasis in renal cell carcinoma [37].

Clinical Trials

The results obtained from preclinical studies of the two ALK1 targeting agents in different cancer models prompted several clinical trials to assess safety, pharmacokinetics, pharmacodynamics, and anti-tumor efficacy in patients with advanced cancer, either as monotherapy or in combination with other antiangiogenic approaches. Phase I clinical trials in patients with different tumors, including non-small lung cancer carcinoma, hepatocellular carcinoma (HCC), persistent or recurrent ovarian carcinoma and related malignancies, as well as relapsed/refractory multiple myeloma showed that both dalantercept and PF-03446962 were generally well tolerated, gave promising and motivating responses, and had a manageable safety profile distinct from that of anti-VEGF therapy [26,38-40]. None of the patients enrolled in these clinical trials displayed the most severe adverse events (AE) reported following bevacizumab treatment (gastrointestinal perforation, impaired wound healing, and serious bleeding). Commonly observed AE upon dalantercept administration were peripheral oedema, fatigue and anemia, whilst fatigue, nausea and thrombocytopenia (not associated with bleeding) were typical of PF-03446962 infusion [25,26]. Moreover, several patients enrolled in these trials developed telangiectases, which are often observed in HHT patients, demonstrating an on-target effect of blocking ALK1 receptor signaling. Though safe, independent phase II clinical trials utilizing dalantercept as monotherapy in patients with recurrent/persistent endometrial carcinoma, ovarian

carcinoma, and squamous cell carcinoma of the head and neck revealed insufficient single agent activity with limited efficacy that did not reach the intended primary endpoint [41-43]. Similarly, phase II clinical trials assessing the efficacy of PF-03446962 in pre-treated patients with refractory urothelial cancer and advanced malignant pleural mesothelioma demonstrated no or limited activity as single drug [44,45].

Acceleron Pharma Inc has recruited patients to test efficacy of combining dalantercept with sorafenib and axitinib in advanced HCC and renal cell carcinoma (RCC), respectively. Results from the dose-escalation and expansion cohorts evaluating the combination of dalantercept plus axitinib in advanced RCC showed that the combination of these two therapies is well tolerated and associated with a clinical response [46]. However, the phase II trial of this combination in RCC patients showed that the addition of dalantercept to axitinib did not appear to improve treatment-related outcomes in previously treated patients with advanced RCC reporting 1 treatment related death and a lower objective response rate in the combination group (19%) in comparison to placebo plus axitinib (24.6%). Likewise, combinatorial phase Ib study of dalantercept and sorafenib showed no improvement in antitumor activity in patients with HCC [47]. In a similar fashion, Pfizer also tested the combination of PF-03446962 with regorafenib in patients with refractory metastatic colorectal cancer, however the combined therapy was associated with unacceptable toxicity and did not demonstrate notable clinical activity in these patients [48].

Targeting Endoglin as an Anti-Angiogenic Therapy in Cancer

Another proposed anti-tumorigenic target within the ALK1 signaling pathway is endoglin (CD105). Several lines of evidence support the rationale for targeting endoglin as a novel anti-angiogenic therapy in cancer. Endoglin is highly expressed on the tumor-associated vascular and lymphatic endothelium, and its expression holds prognostic significance in certain tumors [17]. In addition, gene expression profiling of circulating endothelial cells (CEC), which are elevated in the blood of

cancer patients and are thought to contribute to tumor angiogenesis, revealed an increase of endoglin expression of CEC-enriched samples from metastatic patients compared to healthy subjects [49]. Moreover, a soluble form of endoglin, which is shed following cleavage of the membrane-bound form by matrix metalloproteinase 14 [50], is detected in the serum of patients with different solid tumors [17]. Last but not least, anti-VEGF was shown to increase endoglin expression on tumor-endothelial cells [51], in line with suggestions implicating the ALK1 signaling pathway in resistance to anti-VEGF therapies.

With that, several groups focused on targeting endoglin to suppress tumor angiogenesis, either by directly blocking endoglin using an antibody raised against it or by sequestering its ligands through an endoglin ligand trap composed of the extracellular region of endoglin fused to an immunoglobulin Fc domain (Eng-Fc).

Preclinical Studies

Endoglin Antibody

In vitro, TRC105, a chimeric antibody that binds human endoglin with high avidity, triggered the apoptosis of HUVECs through antibody-dependent cellular cytotoxity [52]. Preclinically, SN6j, a parental antibody of TRC105, showed promising anti-tumorigenic effects without significant side effects. Antibody treatment reduced microvessel density and angiogenesis in multiple metastatic tumor models and suppressed tumor metastasis, leading to prolonged survival of the tumor-bearing mice [53]. In addition, combination of SN6j with the chemotherapeutic agent cyclophosphamide synergistically enhanced antitumor efficacy [54].

Endoglin Ligand Trap and Genetic Targeting

Endoglin ligand traps also triggered anti-angiogenic responses both *in vitro* and *in vivo*. Exogenous treatment or expression of HUVECs with Eng-Fc efficiently inhibited spontaneous and VEGF-induced sprouting on matrigel and in 3D collagen matrices [50]. *In vivo*, Eng-Fc blocked angiogenesis by

suppressing VEGF-induced vessel formation or sprouting in CAM assay and angioreactors respectively. The ligand trap also successfully decreased tumor burden in a colon-26 adenocarcinoma model [55]. Contrary to these findings, one group exploring the impact of single or dual genetic targeting of ALK1 and endoglin on tumor angiogenesis reported no effect of genetic ablation of one copy of the *Eng* gene on tumor angiogenesis and growth in a mouse model of pancreatic neuroendocrine tumors [56]. On the other hand, reducing Acvrl1 gene dosage in the same model decreased tumor vasculature and delayed tumor growth. Interestingly, dual targeting of Acvrl1 and Eng, through genetic ablation of one copy of each gene, resulted in a synergistic reduction of overall tumor burden, suggesting a beneficial impact of combinatorial targeting of ALK1 and endoglin. The different effects of endoglin targeting on tumor angiogenesis could be explained by the different levels of target inhibition when using antibodies versus genetic ablation of a single *Eng* allele or by inherent differences between disease models rendering some more responsive to therapy than others.

Clinical Trials

The encouraging preclinical results led to some phase I clinical studies assessing TRC105 safety, pharmacokinetics and anti-tumor efficacy in patients with advanced or metastatic solid tumors [57,58]. In these studies, TRC105 resulted in a short-term stable disease in some patients with two showing exceptional ongoing responses after 18 and 48 months. The safety assessment of TRC105 identified well-tolerated adverse events at clinically relevant doses mostly comprising infusion reactions, low-grade headaches and anemia that is probably caused by suppression of endoglin-expressing proerythroblasts. Interestingly, some patients receiving TRC105 developed mucocutaneous telangiectases [58] or epistaxis [57], well known symptoms of the vascular disorder HHT caused by endoglin or ALK1 mutations, demonstrating on-target effect of TRC105. Finally, TRC105 treatment induced a significant induction of VEGF levels in patients of one study, which could be a potential compensatory mechanism for the anti-angiogenic effect of TRC105 [57]. This further encouraged combination therapies

comprising TRC105 and anti-VEGF treatments, which is feasible due to the distinct identified safety profile of TRC105 compared to anti-VEGF therapies.

These studies were followed by a phase II clinical trial assessing the tolerability and efficacy of TRC105 administration on 13 heavily pre-treated patients with urothelial carcinoma. TRC105 was once again well-tolerated, but its anti-tumor activity was not satisfactory with only 2 patients achieving stable disease for 4 months and a median overall survival of 8.3 months [59]. However, in this study TRC105 seemed to have a positive impact on immune subsets, notably regulatory T cells, suggesting potential benefit for combining TRC105 with immunotherapy. In support of that, enhanced therapeutic effects were recently reported when combining TRC105 with PD1 inhibition in four preclinical cancer models [60].

Another phase II study aimed to investigate the efficacy of TRC105 administration in HCC patients that have previously progressed on sorafenib. Evidence of clinical activity was not enough to proceed [61], but combination therapy with sorafenib in HCC was tested in a following phase I trial [61]. The combination of both agents was well-tolerated using the recommended single agent doses and encouraging activity triggered the launch of a phase II study. A few other clinical trials assessed the combination of TRC105 with other VEGF-targeting agents such as bevacizumab [62,63] and axitinib [64]. The combination of TRC105 with bevacizumab was well-tolerated [62]. Despite initial reports showing clinical response, TRC105 addition to bevacizumab failed to improve progression-free survival in patients with refractory metastatic RCC [63]. Following this trial, TRC105's efficacy was assessed with axitinib instead of bevacizumab in metastatic RCC patients. This combination therapy was also well-tolerated and provided encouraging evidence of activity leading to further investigations [64].

Targeting BMP9 and BMP10 as an Anti-Angiogenic Therapy in Cancer

Most preclinical studies addressing the role of the ALK1 signaling pathway in tumor angiogenesis relied on the pharmacological targeting of ALK1 or endoglin, either using neutralizing antibodies or soluble forms of ALK1 or endoglin. However, these approaches globally suppress the signaling pathway without considering potential specific roles of BMP9 versus BMP10 in tumor angiogenesis. By following tumor growth and dissemination in a syngeneic orthotopic mammary cancer model genetically deficient in *Bmp9*, *Bmp10* or both, we showed that deletion of *Bmp9*, but not *Bmp10*, increases tumor vascular density and decreases vessel normalization, leading to enhanced tumor growth and metastasis [65]. In addition, mice deficient in both *Bmp9* and *Bmp10* did not show any added therapeutic benefit compared to *Bmp9*-deficient mice. These results suggest that BMP10 targeting can be omitted, and specific targeting of BMP9 rather than ALK1 or endoglin could be more suitable in this model. Interestingly, this study also highlighted BMP9 as an angiogenic quiescence factor that promotes vessel normalization. In this case, activating the BMP9 pathway rather than blocking it can provide new means for cancer therapy, especially when combined with chemo- or immunotherapies [65]. In line with the role of BMP9 as a vascular quiescence factor, Bmp9 deficiency in a pancreatic neuroendocrine tumor model led to hyperbranching and increased metastases, despite a contradictory decrease in tumor growth [56]. On the other hand, blocking BMP9 through a monoclonal anti-BMP9 antibody showed anti-tumor activity and an increase in the normalization of tumor blood vessels in a model of RCC [66]. All in all, targeting different components, and sometimes even the same element, within a signaling pathway can yield different or opposing outcomes in different models.

Conclusion

The BMP9/10-ALK1-endoglin pathway is an important regulator of vascular development that recently captivated the attention of

the scientific and medical community as a target for inhibiting tumor angiogenesis and growth [67]. Several groups attempted to block different components of this pathway (ALK1, endoglin or BMP9) using distinct pharmacological and genetic means either alone or in combination with chemo- or antiangiogenic therapy. Despite the encouraging reported effects of blocking this pathway on tumor angiogenesis and growth in most preclinical models tested, single agent therapies in patients with different solid malignancies generated only modest effects. In this regard, combinatorial clinical trials integrating BMP9/10-ALK1-endoglin and other pathways targeting agents are still ongoing with the hope of better potential.

Targeting the tumor vasculature to "starve a tumor to death" instead of targeting tumor cells with chemotherapeutic drugs was conceived over four decades ago and has led to the development of antiangiogenic drugs approved in cancer since now two decades. However, antiangiogenic therapies so far have not fulfilled expectations and provide only transitory improvements. More recent work is now proposing the opposite, that is to promote angiogenesis in order to increase influx of chemotherapeutic drugs into tumor cells [68]. It will be interesting in the future to see how the BMP9/10-ALK1-endoglin pathway will fit into this new hypothesis.

References

1. Ricard N, Bailly S, Guignabert C, Simons M. The quiescent endothelium: signalling pathways regulating organ-specific endothelial normalcy. Nat Rev Cardiol. 2021; 18: 565–580.
2. Ribatti D, Nico B, Crivellato E, Roccaro AM, Vacca A. The history of the angiogenic switch concept. Leukemia. 2007; 21: 44–52.
3. Bergers G, Benjamin LE. Tumorigenesis and the angiogenic switch. Nat Rev Cancer. 2003; 3: 401–410.
4. Marmé D. Tumor Angiogenesis: A Key Target for Cancer Therapy. Oncol Res Treat. 2018; 41: 164.
5. Munn LL. Aberrant vascular architecture in tumors and its importance in drug-based therapies. Drug Discov Today. 2003; 8: 396–403.

6. Meadows KL, Hurwitz HI. Anti-VEGF Therapies in the Clinic. Cold Spring Harbor Perspectives in Medicine. 2012; 2: a006577–a006577.
7. Crawford Y, Ferrara N. Tumor and stromal pathways mediating refractoriness/resistance to anti-angiogenic therapies. Trends in Pharmacological Sciences. 2009; 30: 624–630.
8. Kieran MW, Kalluri R, Cho YJ. The VEGF pathway in cancer and disease: responses, resistance, and the path forward. Cold Spring Harb Perspect Med. 2012; 2: a006593.
9. David L, Mallet C, Mazerbourg S, Feige JJ, Bailly S. Identification of BMP9 and BMP10 as functional activators of the orphan activin receptor-like kinase 1 (ALK1) in endothelial cells. Blood. 2007; 109: 1953–1961.
10. Desroches-Castan A, Tillet E, Bouvard C, Bailly S. BMP9 and BMP10 : Two close vascular quiescence partners that stand out. Developmental Dynamics. 2021.
11. Townson SA. Specificity and Structure of a High Affinity Activin Receptor-like Kinase 1 (ALK1) Signaling Complex. Journal of Biological Chemistry. 2012; 287: 27313–27325.
12. Shi Y, Massagué J. Mechanisms of TGF-β Signaling from Cell Membrane to the Nucleus. Cell. 2003; 113: 685–700.
13. Kim SK, Henen MA, Hinck AP. Structural biology of betaglycan and endoglin, membrane-bound co-receptors of the TGF-beta family. Exp Biol Med (Maywood). 2019; 244: 1547–1558.
14. Tual-Chalot S, Oh SP, Arthur HM. Mouse models of hereditary hemorrhagic telangiectasia: recent advances and future challenges. Front. Genet. 2015; 6.
15. Dupuis-Girod S, Bailly S, Plauchu H. Hereditary hemorrhagic telangiectasia: from molecular biology to patient care: Hereditary hemorrhagic telangiectasia. Journal of Thrombosis and Haemostasis. 2010; 8: 1447–1456.
16. Seki T, Yun J, Oh SP. Arterial endothelium-specific activin receptor-like kinase 1 expression suggests its role in arterialization and vascular remodeling. Circ Res. 2003; 93: 682–689.
17. Bernabeu C, Lopez-Novoa JM, Quintanilla M. The emerging role of TGF-β superfamily coreceptors in cancer. Biochimica

et Biophysica Acta (BBA) - Molecular Basis of Disease. 2009; 1792: 954–973.
18. Hu-Lowe DD. Targeting Activin Receptor-Like Kinase 1 Inhibits Angiogenesis and Tumorigenesis through a Mechanism of Action Complementary to Anti-VEGF Therapies. Cancer Res. 2011; 71: 1362–1373.
19. Niessen K, Zhang G, Ridgway JB, Chen H, Yan M. ALK1 signaling regulates early postnatal lymphatic vessel development. Blood. 2010; 115: 1654–1661.
20. Levet S. Bone morphogenetic protein 9 (BMP9) controls lymphatic vessel maturation and valve formation. Blood. 2013; 122: 598–607.
21. Duong T, Koopman P, Francois M. Tumor lymphangiogenesis as a potential therapeutic target. J Oncol. 2012; 2012: 204946.
22. Cuny GD. Structure-activity relationship study of bone morphogenetic protein (BMP) signaling inhibitors. Bioorg Med Chem Lett. 2008; 18: 4388–4392.
23. Ma J. Inhibiting Endothelial Cell Function in Normal and Tumor Angiogenesis Using BMP Type I Receptor Macrocyclic Kinase Inhibitors. Cancers (Basel). 2021; 13: 2951.
24. Lin X. MiR-199b-5p Suppresses Tumor Angiogenesis Mediated by Vascular Endothelial Cells in Breast Cancer by Targeting ALK1. Front Genet. 2019; 10: 1397.
25. Bendell JC. Safety, pharmacokinetics, pharmacodynamics, and antitumor activity of dalantercept, an activin receptor-like kinase-1 ligand trap, in patients with advanced cancer. Clin Cancer Res. 2014; 20: 480–489.
26. Simonelli M. Phase I study of PF-03446962, a fully human monoclonal antibody against activin receptor-like kinase-1, in patients with hepatocellular carcinoma. Ann Oncol. 2016; 27: 1782–1787.
27. Mitchell D. ALK1-Fc inhibits multiple mediators of angiogenesis and suppresses tumor growth. Mol Cancer Ther. 2010; 9: 379–388.
28. Cunha SI. Genetic and pharmacological targeting of activin receptor-like kinase 1 impairs tumor growth and angiogenesis. J Exp Med. 2010; 207: 85–100.

29. Eleftheriou NM. Compound genetically engineered mouse models of cancer reveal dual targeting of ALK1 and endoglin as a synergistic opportunity to impinge on angiogenic TGF-β signaling. Oncotarget. 2016; 7: 84314–84325.
30. Cunha SI. Endothelial ALK1 Is a Therapeutic Target to Block Metastatic Dissemination of Breast Cancer. Cancer Res. 2015; 75: 2445–2456.
31. Hawinkels LJAC. Activin Receptor-like Kinase 1 Ligand Trap Reduces Microvascular Density and Improves Chemotherapy Efficiency to Various Solid Tumors. Clin Cancer Res. 2016; 22: 96–106.
32. van Meeteren LA. Anti-human activin receptor-like kinase 1 (ALK1) antibody attenuates bone morphogenetic protein 9 (BMP9)-induced ALK1 signaling and interferes with endothelial cell sprouting. J Biol Chem. 2012; 287: 18551–18561.
33. Hu-Lowe DD. Targeting activin receptor-like kinase 1 inhibits angiogenesis and tumorigenesis through a mechanism of action complementary to anti-VEGF therapies. Cancer Res. 2011; 71: 1362–1373.
34. Cunha SI, Pietras K. ALK1 as an emerging target for antiangiogenic therapy of cancer. Blood. 2011; 117: 6999–7006.
35. Goel S, Wong AHK, Jain RK. Vascular Normalization as a Therapeutic Strategy for Malignant and Nonmalignant Disease. Cold Spring Harb Perspect Med. 2012; 2: a006486.
36. Akatsu Y. Dual targeting of vascular endothelial growth factor and bone morphogenetic protein-9/10 impairs tumor growth through inhibition of angiogenesis. Cancer Sci. 2017; 108: 151–155.
37. Wang X. Inhibition of ALK1 signaling with dalantercept combined with VEGFR TKI leads to tumor stasis in renal cell carcinoma. Oncotarget. 2016; 7: 41857–41869.
38. Goff LW. A Phase I Study of the Anti-Activin Receptor-Like Kinase 1 (ALK-1) Monoclonal Antibody PF-03446962 in Patients with Advanced Solid Tumors. Clin Cancer Res. 2016; 22: 2146–2154.

39. Doi T. A phase I study of the human anti-activin receptor-like kinase 1 antibody PF-03446962 in Asian patients with advanced solid tumors. Cancer Med. 2016; 5: 1454–1463.
40. Bendell JC. Safety, pharmacokinetics, pharmacodynamics, and antitumor activity of dalantercept, an activin receptor-like kinase-1 ligand trap, in patients with advanced cancer. Clin Cancer Res. 2014; 20: 480–489.
41. Burger RA. Phase II evaluation of dalantercept in the treatment of persistent or recurrent epithelial ovarian cancer: An NRG Oncology/Gynecologic Oncology Group study. Gynecol Oncol. 2018; 150: 466–470.
42. Makker V. Phase II evaluation of dalantercept, a soluble recombinant activin receptor-like kinase 1 (ALK1) receptor fusion protein, for the treatment of recurrent or persistent endometrial cancer: an NRG Oncology/Gynecologic Oncology Group Study 0229N. Gynecol Oncol. 2015; 138: 24–29.
43. Jimeno A. A phase 2 study of dalantercept, an activin receptor-like kinase-1 ligand trap, in patients with recurrent or metastatic squamous cell carcinoma of the head and neck. Cancer. 2016; 122: 3641–3649.
44. Necchi A. PF-03446962, a fully-human monoclonal antibody against transforming growth-factor β (TGFβ) receptor ALK1, in pre-treated patients with urothelial cancer: an open label, single-group, phase 2 trial. Invest New Drugs. 2014; 32: 555–560.
45. Wheatley-Price P. A Phase II Study of PF-03446962 in Patients with Advanced Malignant Pleural Mesothelioma. CCTG Trial IND.207. J Thorac Oncol. 2016; 11: 2018–2021.
46. Voss MH. The DART Study: Results from the Dose-Escalation and Expansion Cohorts Evaluating the Combination of Dalantercept plus Axitinib in Advanced Renal Cell Carcinoma. Clin Cancer Res. 2017; 23: 3557–3565.
47. Abou-Alfa GK. A Phase Ib, Open-Label Study of Dalantercept, an Activin Receptor-Like Kinase 1 Ligand Trap, plus Sorafenib in Advanced Hepatocellular Carcinoma. Oncologist. 2019; 24: 161-e170.
48. Clarke JM. A phase Ib study of the combination regorafenib with PF-03446962 in patients with refractory metastatic

colorectal cancer (REGAL-1 trial). Cancer Chemother Pharmacol. 2019; 84: 909–917.
49. Smirnov DA. Global Gene Expression Profiling of Circulating Endothelial Cells in Patients with Metastatic Carcinomas. Cancer Res. 2006; 66: 2918–2922.
50. Hawinkels LJAC. Matrix Metalloproteinase-14 (MT1-MMP)–Mediated Endoglin Shedding Inhibits Tumor Angiogenesis. Cancer Res. 2010; 70: 4141–4150.
51. Bockhorn M. Differential vascular and transcriptional responses to anti-vascular endothelial growth factor antibody in orthotopic human pancreatic cancer xenografts. Clin Cancer Res. 2003; 9: 4221–4226.
52. Seon BK. Endoglin-targeted cancer therapy. Curr Drug Deliv. 2011; 8: 135–143.
53. Uneda S. Anti-endoglin monoclonal antibodies are effective for suppressing metastasis and the primary tumors by targeting tumor vasculature. Int J Cancer. 2009; 125: 1446–1453.
54. Takahashi N, Haba A, Matsuno F, Seon BK. Antiangiogenic therapy of established tumors in human skin/severe combined immunodeficiency mouse chimeras by anti-endoglin (CD105) monoclonal antibodies, and synergy between anti-endoglin antibody and cyclophosphamide. Cancer Res. 2001; 61: 7846–7854.
55. Castonguay R. Soluble Endoglin Specifically Binds Bone Morphogenetic Proteins 9 and 10 via Its Orphan Domain, Inhibits Blood Vessel Formation, and Suppresses Tumor Growth. Journal of Biological Chemistry. 2011; 286: 30034–30046.
56. Nikolas M Eleftheriou, Jonas Sjölund, Matteo Bocci, Eliane Cortez, Se-Jin Lee. et al. Compound genetically engineered mouse models of cancer reveal dual targeting of ALK1 and endoglin as a synergistic opportunity to impinge on angiogenic TGF-β signaling. Oncotarget. 2016; 7: 84314–84325.
57. Karzai FH. A phase I study of TRC105 anti-endoglin (CD105) antibody in metastatic castration-resistant prostate cancer. BJU Int. 2015; 116: 546–555.

58. Rosen LS. A Phase I First-in-Human Study of TRC105 (Anti-Endoglin Antibody) in Patients with Advanced Cancer. Clinical Cancer Research. 2012; 18: 4820–4829.
59. Apolo AB. A Phase II Clinical Trial of TRC105 (Anti-Endoglin Antibody) in Adults With Advanced/Metastatic Urothelial Carcinoma. Clin Genitourin Cancer. 2017; 15: 77–85.
60. Schoonderwoerd MJA. Targeting Endoglin-Expressing Regulatory T Cells in the Tumor Microenvironment Enhances the Effect of PD1 Checkpoint Inhibitor Immunotherapy. Clin Cancer Res. 2020; 26: 3831–3842.
61. Duffy AG. Phase I and Preliminary Phase II Study of TRC105 in Combination with Sorafenib in Hepatocellular Carcinoma. Clin Cancer Res. 2017; 23: 4633–4641.
62. Gordon MS. An open-label phase Ib dose-escalation study of TRC105 (anti-endoglin antibody) with bevacizumab in patients with advanced cancer. Clin Cancer Res. 2014; 20: 5918–5926.
63. Dorff TB. Bevacizumab alone or in combination with TRC105 for patients with refractory metastatic renal cell cancer. Cancer. 2017; 123: 4566–4573.
64. Toni K Choueiri, M Dror Michaelson, Edwin M Posadas, Guru P Sonpavde, David F McDermott, et al. An Open Label Phase Ib Dose Escalation Study of TRC105 (Anti-Endoglin Antibody) with Axitinib in Patients with Metastatic Renal Cell Carcinoma. Oncologist. 2019; 24: 202–210.
65. Marie Ouarné, Claire Bouvard, Gabriela Boneva, Christine Mallet, Johnny Ribeiro, et al. BMP9, but not BMP10, acts as a quiescence factor on tumor growth, vessel normalization and metastasis in a mouse model of breast cancer. J Exp Clin Cancer Res. 2018; 37: 209.
66. Verena Brand, Christian Lehmann, Christian Umkehrer, Stefan Bissinger, Martina Thier, et al. Impact of selective anti-BMP9 treatment on tumor cells and tumor angiogenesis. Molecular Oncology. 2016; 10: 1603–1620.
67. Sherwood LM, Parris EE, Folkman J. Tumor Angiogenesis: Therapeutic Implications. New England Journal of Medicine. 1971; 285: 1182–1186.
68. Rivera LB, Bergers G. CANCER. Tumor angiogenesis, from foe to friend. Science. 2015; 349: 694–695.

Book Chapter

Overview of NKT Type I Cells and Their Importance in Immunity

Elise Ramia

Experimental Immunology Unit, Division of Immunology, Transplantation, and Infectious Diseases, IRCCS San Raffaele Scientific Institute, Italy

***Corresponding Author:** Elise Ramia, Experimental Immunology Unit, Division of Immunology, Transplantation, and Infectious Diseases, IRCCS San Raffaele Scientific Institute, 20132 Milano, Italy

Published **February 10, 2022**

How to cite this book chapter: Elise Ramia. Overview of NKT Type I Cells and Their Importance in Immunity. In: Hussein Fayyad Kazan, editor. Immunology and Cancer Biology. Hyderabad, India: Vide Leaf. 2022.

Acknowledgments: I would like to express my gratitude to Dr. Giulia Casorati and Dr. Paolo Dellabona, who read and provided suggestions to this review.

Funding: The project is supported by the WWCR (worldwide cancer research) Grant ref. number: 19-0133.

Abstract

iNKT cells are a subpopulation of T lymphocytes with a characteristic semi-invariant TCR that recognizes lipid antigens displayed in CD1d molecules. Their maturation and differentiation into different subsets occur in the thymus. While only a small population remains in the thymus, iNKT cells reside in tissues and scarce quantity are detected in the periphery. Upon activation, they can promptly secrete high levels of cytokines and interact with several types of immune cells of both the innate and adaptive immunity rendering them the bridge between both immunities. iNKT cells can have a direct cytotoxic effect which allows them to respond strongly against several pathogenic infections, where they have shown to be responsible for bacterial clearance. Outstandingly, iNKT cells have demonstrated a crucial role in tumor immunosurveillance in both murine and human studies. They are able to modify the tumor microenvironment, directly target CD1d positive tumor cells, and activate immune cells of both the innate and adaptive immunities designating them an aim for immunotherapy. Indeed, various groups are working on activating iNKT cells or retargeting them against cancers to use them as anti-tumor therapy and they have demonstrated a beneficial outcome.

Introduction

NKT (Natural Killer T) cells were first described back in the 1990s as a T cell subset expressing a semi-invariant TCR (T cell Receptor) and having a memory-like phenotype that express the NK (Natural Killer) surface marker NK1.1 [1,2]. The TCR is comprised, in mice, of a canonical Vα14 and Jα18 TCR α chains combined with a TCR β chain of either Vβ8, Vβ7 or Vβ2. Human NKT cells express a homologous TCR composed of Vα24-Jα18 TCR α chains combined with a Vβ11 TCR β chain. The TCR recognizes lipid antigens presented by the non-polymorphic MHC (major histocompatibility complex) class I-related molecule CD1d [3]. The CD1d-restricted NKT cells form two major types: type I NKT also referred to as iNKT (invariant NKT) due to their expression of the formerly described semi-invariant TCR and type II NKT cells that display a more diverse

TCR with different antigen specificity [4]. Due to the larger TCR diversity in type II NKT cells and the lack of a specific marker that is capable of identifying them, they are not as excessively studied as NKT type I cells. Moreover, while they both play important roles in immunity, in this review the focus will be on type I NKT cells regarding their development and differentiation into different subtypes, activation, and function in immunity in general and anti-tumor immunity specifically.

Overview of iNKT Cell

The initial description of NKT cells is considered a simplified definition and not entirely accurate. A more advanced definition was later established based on their function in being a bridge between the innate and the adaptive immune system since they retain features from both. As it will be detailed later on in the review, iNKT cells are capable of rapidly secreting high levels of cytokines and interacting with other cells in the immune system.

iNKT cells are distributed all along the body and can be found in the blood, bone marrow, lungs, gastrointestinal tract, spleen, and skin of mice as well as the liver which has the highest frequency for up to 30%. In humans, iNKT cells distribution in the periphery seems similar to that of mice but at lower frequencies. For example, in the liver the iNKT cells constitute a much lower percentage than in mice for a maximum of 1%. In peripheral blood, their range varies among individuals from undetectable to a maximum of 3% [5].

iNKT cells express semi-invariant TCR and NK cells markers, such as NK1.1, NKG2D and Ly49. They are CD69+, $CD62L^{low}$, $CD44^{high}$, and $CD122^{high}$ rendering their phenotype as memory/ activated-like phenotype. iNKT cells in mice can either express CD4+ or be DN (double negative), CD4 and CD8 negative. On the other hand, in humans iNKT cells can express CD8 molecules [6]. The semi-invariant TCR recognizes lipid antigens that can be cell endogenous or derived from bacteria. αGalCer (α galactosylceramide) is a prototypical glycolipid widely used to activate iNKT cells. It comprises an αgalactosyl head and a ceramide base and was originally extracted from marine sponge,

Agelas mauritianus, based on its anti-tumor activity [7]. The endogenous lipids can be α- linked glycosylceramides [8], while the bacterial lipids share a common structure of that could be either ceramide or glycerol. In addition, it has been reported also that CD1d can bind cell endogenous phospholipids [9,10]. Both acyl chains bind inside the CD1d grove and the polar head emerge out of CD1d that binds to the TCR of iNKT.

The lipid antigens are represented to iNKT cells in a CD1d restricted manner. CD1d belongs to the CD1 family which is similar to the MHC class I in structure consisting of 3 extracellular domains α1, α2, and α3 binding to a β2 microglobulin. Unlike MHC class I, CD1 molecules are non-polymorphic and display high degree of similarity. The members of the CD1 family can be divided into 3 groups: group 1 consisting of CD1a, CD1b, and CD1c, group 2 comprising CD1d, and group 3 including CD1e. Group 1 CD1 is expressed in humans and not in mice, preferentially on APC (antigen presenting cells). On the other hand, CD1d is present in both mice and humans, and its expression is not limited to APC but also on hematopoietic and non-hematopoietic cells, such as epithelial cells and keratinocytes. [11,12]. CD1e is also present only in humans, and it localize in lysosomes where it facilitates the loading of lipid antigens on group 1 and 2 CD1 molecules [13].

Thymic Selection and development of iNKT Cells

iNKT cells differentiation and development occur in the thymus. iNKT cells develop from DP (double positive) precursors that stochastically rearrange the semi-invariant TCR and are positively selected by homotypic interaction with other immature DP thymocytes expressing CD1d. This is in sharp contrast with the conventional MHC-restricted T cells that are selected at the DP stage by thymic epithelial cells. Furthermore, and again unlike T cells, thymic iNKT cells undergo activation and expansion, leading to the acquisition of an effector/memory phenotype before emigrating into the periphery [14–16]. The expression of the semi-invariant TCR and other additional phenotypic markers has divided iNKT cell development in

different stages. Stage 0, which is referred to as the positive selection of iNKT cells, the semi-invariant TCR expressed on the DP thymocyte recognizes endogenous-glycolipids bound to CD1d molecules expressed on another DP thymocytes. The expression of CD1d on DP thymocytes, specifically, is crucial for iNKT cells development [6,15]. As shown by experiments with CD1d knockout mice, iNKT cells did not develop and were not detected [17]. However, when the expression of CD1d on DP thymocytes was restored iNKT cells developed normally and proved to be functional in ex-vivo assays [18]. In addition, the interaction of SLAM (signaling lymphocytic activation molecules) family (SLAMf1 and SLAMf6) between the DP thymocytes generates another signal, which together with the signal arising from the TCR-CD1d interaction lead to the recruitment of SAP (SLAM-associated protein) and Src Kinase Fyn that are crucial for NKT development [19] and trigger the downregulation of HSA (Heat Stable Antigen or CD24) and the upregulation of CD44 and DX5 [15]. Stage 1 comprises CD44-NK1.1- iNKT precursors that are defined naive. Stage 2 comprises CD44+NK1.1- iNKT precursors that acquire an effector/memory phenotype. Stage 3 defines CD44+NK1.1+ iNKT cells that have reached the terminal maturation stage. In parallel, maturing thymic iNKT cells also acquire effector cytokine expression, dividing them into IFNγ iNKT1, IL-4 iNKT2 and IL-17 iNKT17 subsets [20]. iNKT cells may also undergo negative selection in the thymus; however, much less is known about this phase. The negative selection depends on the recruitment of SAP and Fyn Kinase as well as many downstream signaling pathways, such as that of NKκB, T-bet, and RORγ [15]. It has also been indicated that CD80 and CD86 co-stimulatory molecules have important roles in thymic iNKT cells selections and maturation and that in their absence iNKT cells fail to mature thus resulting in a reduced thymic and peripheral iNKT count [21]. Thymic iNKT cells can become long resident, or emigrate to the peripheral compartment at stage 2, acquiring distinct phenotypic markers in different tissues and becoming tissue-resident cells. The iNKT cells in the periphery can either be positive for NK1.1 or negative. Nonetheless, studies have shown that the NK1.1- population has distinct features from its NK1.1+ counterparts and from the NK1.1+ iNKT that underwent

maturation in the thymus [22,23]. In addition, it has been shown that IL-15 has a critical role in the development, homeostasis and maintenance of the cytotoxic function of mature iNKT cells, in the periphery as well as in the thymus [24].

The different Subtypes of iNKT

In the thymus, iNKT cells differentiate into several subtypes, which are similar to those of CD4+ T cells. Three different subsets have been distinctly identified: iNKT1, iNKT2, and iNKT17.

Similar to CD4 Th1 (T helper) cells, iNKT1 profile is driven by the high expression of T-bet transcription factor, which is encoded by TBX21. Once activated, iNKT1 cells are able to secrete high amounts of IFNγ; however, unlike Th1 cells, they can also produce a notable amount of IL-4. These features permitted iNKT1 cells to have a cytotoxic function superior to all the other subtypes [25]. iNKT1 are mostly NK1.1+ and can be either positive or negative for CD4. They mostly reside in the liver and spleen [26,27]. iNKT2 cells are similar to Th2 cells in their secretion of IL-4 and IL-13 as well as IL-9 and IL-10. They are regulated by the high level of expression of PLZF transcription factor. iNKT2 are also abundant in the spleen, mesenteric lymph nodes, intestine and lungs. In the latter, iNKT2 have been reported to produce airway hyperreactivity in an IL-25 dependent manner [26,27]. It's noteworthy to mention that CD4+ iNKT cells can differentiate into Th1 and Th2 cytokine-producing phenotype, whereas CD4- iNKT cells can mainly produce Th1 cytokines [28]. iNKT17 cell are similar to Th17 cells by their secretion of high level of IL-17 and are regulated by RORγt. They also express a considerable amount of PLZF transcription factor. They mostly reside in the lymph nodes, lungs, skin and in the spleen, but to lesser extent compared to other iNKT subtypes [26,27]. Recently, another iNKT subset that is capable of interacting with B cells has been described. These iNKT cells exhibit a phenotype similar to the classic Tfh (follicular helper T) cells expressing CXCR5 and PD-1 which required the expression of Bck-6 transcription factor. Therefore, they were referred to as iNKTfh. They have been shown to

provide help to B cells in an IL-21 dependent manner and lead to the formation of early germinal center [29,30]. However, unlike NKT1-2-17 subsets, the iNKTfh one is only detected in periphery and not in the thymus, suggesting that it is generated by the differentiation of mature cells.

iNKT Cells Activation

The activation on iNKT cells can occur in two different mechanisms, either antigen independent/ cytokine mediated or antigen dependent mechanism. Unlike T cells, whose activation is merely dependent on the antigen presented in MHC molecules, iNKT cells possessing innate characteristics can become activated upon infection and inflammation through a strong release of IL-12 and IL-18 produced by myelomonocytic cells [31]. Once a DC (dendritic cells) recognizes foreign molecules through the PRR (pattern recognition receptor) and becomes activated, the subsequent release of cytokines leads to the activation of iNKT cells. IL-12 was shown to be a crucial cytokine released by APCs in order to properly activate iNKT cells in vivo and in vitro and in its absence iNKT cells fail to be activated [32]. This is due to the fact that iNKT cells are especially sensitive to IL-12 due to the high expression level of IL-12 receptor on their surface. As mentioned earlier, iNKT cells express NKG2D receptor that recognizes stress-induced ligands MIC (MHC class I chain related) A and B protein families. NKG2D ligands have a restricted expression on normal cells but are overly expressed in cancerous and infected cells [33]. It has been demonstrated that iNKT cells can be activated through the engagement of NKG2D receptor on its surface in the absence of CD1d stimulation [34]. In addition, studies have demonstrated a role of the relatively new cytokine IL-33 in iNKT cells activation. It has been shown that IL-33, in combination with either TCR activation by αGalCer or IL-12, is capable of activating iNKT cells and induce consequent IFNγ release. IL-33 was first described to be the ligand of a receptor expressed on mast cells and Th2 effector T cells and able to promote Th2 immunity [35].

The antigen dependent mechanism involves a strong lipid antigen presented to iNKT cells by CD1d molecules expressed on APC, with some reliance on cytokine release depending on the antigenic strength [32]. Several microbial lipids have been indicated to stimulate iNKT cells such as α-linked glycosphingolipids and diacylglycerol that are expressed by certain bacteria as *Sphingomonas*, *Ehrlichia*, and *Borrelia burgdorferi* [36]. Upon activation, iNKT cells release a wide range of cytokines which include IFNγ, TNFα, IL-2, IL-4, IL-10 and several others. iNKT cells can exert their cytotoxic function through the release of perforin and granzymes and through the interactions of Fas/FasL [6]. Activated iNKT cells were noted to be short lived and can become anergic after prolonged exposure to the antigen [37,38]. However, a recent study demonstrated the presence of a long lived memory-like iNKT cells in the lungs of mice, capable of recognizing the antigen displayed in CD1d molecules and becoming activated within months after their first encounter [39]. These iNKT cells exhibit features found on memory T cells [40], such as the expression of KLRG1 (killer cell lectin-like receptor subfamily G, member 1).

iNKT Cell Function in Immunity

As previously mentioned, iNKT cells upon stimulation and activation can directly kill infected cells and promptly secrete high levels of cytokines and chemokines that in turn affect the functions of other immune cells. In fact, the rapid release of cytokines by iNKT cells, and in particular IFNγ and IL-4, could be traced to their high levels of pre-formed mRNAs that are normally expressed in a resting state [41], resulting in the secretion of IFNγ and IL-4 by most of the iNKT cells in the liver within couple of hours after antigen exposure [42]. This feature allows the crosstalk of iNKT cells with cells of both the adaptive and the innate immunity. Through IFNγ secretion, iNKT cells can recruit neutrophils to the site of infection contributing to an inflammatory response [31]. Studies have shown that iNKT cells-derived cytokines can activate CD4+ and CD8+ T cells. Together with IFNγ, the interaction between CD40 and CD40L on iNKT cells and APCs, such as DCs and macrophages, results in their potent activation, upregulation of costimulatory

molecules, and cytokine release. iNKT cells can also trigger the activation of NK cells through the release of IFNγ and IL-12 [43]. In addition, through the release of several cytokines, iNKT cells can trigger a strong antibody release from B cells and aid in their memory formation through different approaches [44]. Furthermore, iNKT cells play a role in immunosurveillance by modulating the role of CD4+CD25+ T reg (regulator T) cells in an IL-2 dependent manner. The latter's secretion by iNKT cells promote the proliferation of T regs [39].

Nonetheless, iNKT cells can exhibit direct cytotoxic function through their expression of FasL and secretion of high levels of granzymes and perforin. Studies have revealed that iNKT cells are capable of controlling bacterial infections through controlling their growth and elimination. During *Brucella suis* infection, for instance, which is a bacterium that can cause fever, arthritis and osteomyelitis, CD4+ iNKT cells are activated by lipid antigens bound to CD1d molecules expressed on macrophages and able to impair the growth of *Brucella suis* to subsequently trigger its clearance. This mechanism is achieved through Fas/ FasL interaction and the release of lytic granules by activated iNKT cells [46]. In addition, studies have shown that iNKT cells are also involved in the elimination of *Borrelia burgdorferi*, which is a bacterium that causes Lyme borreliosis. Liver iNKT cells become activated in the blood vessels by CD1d on macrophages expressing glycolipids of the joint-homing bacteria. Successively, the activated iNKT cells disrupt the bacterial spreading in the joints and lead to its elimination via their cytotoxic function mediated by granzymes release [47].

Besides bacterial clearance, iNKT cells have an important role during viral infections as well. During HBV (Hepatitis B virus) infection, the levels of Tim3 (T cell immunoglobulin and mucin domain 3), a negative immune checkpoint regulator, were upregulated on iNKT cells. These Tim3+ iNKT cells showed reduced cytotoxic function, which was successively reversed by Tim3 blockage. Subsequently, iNKT cells were able to inhibit the viral replication through the release of cytotoxic granules in addition to the expression of IFNγ and TNFα [48].

The Role of iNKT Cells in Antitumor Immunity

The discovery of immunity governed by iNKT cells against cancer goes back to the point where treatment with αGalCer granted protection from tumor progression [49]. This tumor immunosurveillance role of iNKT cells has been further validated in mouse models deficient in iNKT cells, where the tumor progressed compared to that of the wild type mice [50–55]. Furthermore, iNKT cell count and functional activity have been found to be impaired in cancer patients of several types as compared to healthy donors [56], supporting the importance of iNKT cells in anti-tumor immunity. Moreover, infiltrating iNKT cells in primary colorectal cancers were correlated with better prognosis [57]. Similar findings were observed in children neuroblastoma, in which infiltrating iNKT cells were associated with long term disease free survival [47].

iNKT cells exhibit an indirect effect on tumor's growth via IFNγ-dependent activation of anti-tumor CD8+ CTL and NK responses (50) and modulation of suppressive myeloid populations in the TME (tumor microenvironment). iNKT cells, preferentially iNKT1 cells, have been shown to modify the TME through their interaction with TAM (tumor associated macrophages) exhibiting M2 phenotype, which promotes tumor growth and progression. One method utilized by iNKT1 cells is the direct killing of TAM through the recognition of tumor-derived glycolipids loaded on CD1d molecules. Correspondingly, co-transferring of monocytes and iNKT cells to tumor bearing mice suppressed tumor growth through the killing of monocytes [59]. Besides, iNKT cells exhibit other tactics regarding TME modification, in which the production of GM-CSF (granulocyte monocyte – colony stimulating factor) skew the M2 phenotype towards a functional M1 polarized phenotype [60]. In addition, through IFNγ dependent mechanism, iNKT1 cells have been shown to inhibit tumor angiogenesis through the repression of M2 differentiation [61]. In fact, it has been shown that iNKT cells can control prostate cancer progression through interacting with pro-angiogenic M2 macrophages in a CD1d, Fas and CD40 dependent manner and inducing their killing, while sustaining and promoting the survival of M1 macrophages, thus remodeling the aggressive

TME of prostate cancer [62]. In patients with CLL (chronic lymphocytic leukemia) it was shown that the increased expression of CD1d on the tumor cells correlated to the disease progression and that iNKT cells in vivo, in CLL mouse models, were able to control initial expansion of the tumor but were rendered dysfunctional upon disease progression. This control was not dependent on the direct recognition of leukemic cells but rather on the interaction of iNKT cells with the CLL-specific TAM, designated as NLC (nurse-like cells), which in vitro can differentiate to CLL. It was shown that iNKT cells restricted NLC differentiation in vitro in a CD1d dependent manner which consequently impaired CLL survival [55]. Another population of myeloid suppressive cells are neutrophils. Immunosuppressive IL-10 secreting neutrophils have been found in the blood of patients with melanoma with an increased frequency correlated to the stage of the cancer. It has also been shown that a promoted crosstalk between iNKT cells and neutrophils in a CD1d dependent manner can reverse their immunosuppressive role by reducing IL-10 and promoting IL-12 secretion instead [63].

Additionally, iNKT cells can affect tumor growth through direct targeting. The cytotoxic activity of iNKT cells in tumors has been extensively verified in hematopoietic tumors due to the fact that these cells express CD1d molecules on their surface that are capable of directly activating iNKT cells. In AML (acute myeloid leukemia) and JMML (juvenile myelomonocytic leukemia) the cytotoxicity of iNKT cells was shown to be mediated mostly by perforin/ granzyme B pathway and to a lesser extend through TNFα, FASL and TRAIL (TNF-related apoptosis inducing ligand). Moreover, this cytotoxicity was enhanced when iNKT cells were pulsed with αGalCer and inhibited when treated with anti-CD1d antibodies [64]. In patients with progressive MM (multiple myeloma), iNKT cells were found to reside in the tumor beds and circulating in the blood. These iNKT cells were rendered dysfunctional, since when stimulated they exhibited a deficiency in IFNγ production, which lead to the progression of the disease form precursor to clinical MM. However, iNKT cell function was restored in vitro upon treatment with αGalCer-pulsed DCs leading to the killing of CD1d+ myeloma cells [65].

CD1d expression has also been detected on B cell malignancies such as B-CLL (B cell chronic lymphocytic leukemia). In a study where B-CLL were loaded with αGalCer in vitro, iNKT cells became activated and exhibited a significant CD1d-dependent cytotoxicity towards the tumor [66]. Also in B cell lymphoma tumor bearing mice, iNKT cells controlled disease progression in a CD1d dependent manner. Notably, while iNKT cells promoted tumor control, type II NKT cells were correlated with poor prognosis and an increase mortality rate [67].

Despite the wide improvement in cancer immunotherapy, allo-HSCT (allogeneic hematopoietic stem cell transplantation) remains the only curative treatment for hematological malignancies. However, the success in allo-HSCT is determined by the occurrence of GVHD (graft-versus-host disease), in which the donor's T cells recognize antigens on the host cells and attack them. GVHD is one of the major complications encountered by allo-HSCT and is responsible for high morbidity and mortality in patients [68]. It has been shown that the recovery of iNKT cells in patients who underwent allo- HSCT is able to predict the occurrence of GVHD and improve overall survival [69]. Nonetheless, patients who received allo-HSCT and had high levels of CD4- iNKT cells in their peripheral blood had a better prognosis and exhibited protection from GVHD [70]. In addition, in pediatric leukemia patients, failure to reconstitute iNKT cells correlated to the leukemic relapse [71].

iNKT cells' anti-tumoral role is not just limited to CD1d+ hematopoietic malignancies, but was also demonstrated in several other CD1d positive and even negative solid tumors. It was found that in CD1d negative lung cancer patients, the number of iNKT cells were lower than in healthy individuals and that they had a lower activation status when stimulated by αGalCer. However, αGalCer- stimulated iNKT cells from healthy individuals were able to recognize 2 lung tumor cell lines out of 7 in vitro and eliminate them through the release of perforin. This cytotoxic activity by iNKT cells was found to be dependent on ICAM-1 (intracellular adhesion molecule 1) expression on tumor cells [72]. In addition, iNKT cells were also found to be depleted from the blood and lungs of patients

with NSCLC (non-small cell lung cancer). Furthermore, the expression of CD1d in patients with adenocarcinoma and squamous cell carcinoma was significantly lower than that in healthy individuals, which was due to the low expression of CD1d mRNA. The latter was associated with poor prognosis in patients, while high CD1d expression in NSCLC correlated to a significant overall survival. Treatment of NSCLS with epigenetic modulators triggered chromatin remodeling and induced a dose-dependent expression of CD1d molecule that was capable of activating iNKT cells, resulting in their degranulation [73]. Nonetheless, iNKT cells purified from patients with OS (osteosarcoma) were cytotoxic against CD1d+ OS cells in a perforin/ granzyme B and Fas/FasL dependent manner while showing no cytotoxicity towards CD1d- osteoblast or CD1d+ mesenchymal stem cells. In addition, treating the OS cells with iNKT cells and an increasing dose of chemotherapeutic drugs enhanced tumor cell death. This effect was eliminated in the absence of CD1d [74]. iNKT cells have also been found effective against brain tumors. Functional iNKT cells were detected in patients with glioma. Upon treatment with αGalCer-pulsed DC, iNKT cells readily secrete IFNγ and expand. Moreover, CD1d expression was detected on primary glioma cells as well as endothelial cells in blood vessels. Consequently, iNKT cells were able to recognize the ligand loaded on CD1d molecules expressed on the glioma cells and effectively lead to their killing [75]. All of these studies highlight the importance of iNKT cells in anti-tumor immunity in both directly targeting malignant cells and activating other immune effectors.

Immunotherapeutic Approaches using NKT Cells

As iNKT cells have effectively been proven to have anti-tumor activities through direct cytotoxic killing of tumor cells, modulating the TME, and through the activation of innate and adaptive immunities, while harnessing protection from GVHD, in the case of allo-HSCT, iNKT cell-based immunotherapies have been the target in the fight against cancer. Many studies relied on targeting iNKT cells activation through the administration of αGalCer loaded monocyte-derived DC, which led to clinically significant anti-tumor immune response. In the first described clinical trial that was carried out on 12 patients

with different malignancies, the results obtained were rapid and highly reproducible. It was shown that after therapy the levels of IL-12 and IFNγ in the serum of the patients increased. Nonetheless, this study provided the first clinical evidence that iNKT cells act as bridge between the innate and the adaptive immunity, since following the activation of iNKT cells, NK, T and B cells were shown to be activated. This activation was even faster and greater after administering the second dose of therapy as regards to the number of activated cells and their sustainability. In addition, IFNγ serum levels were higher after the second dose. It is worth mentioning that some patients suffered mild side effects, such as fever and headache, that were associated with the activation of the immune system and the release of the cytokines, since these symptoms were reproducible, appeared at the same stage of the treatment cycle, and were absent outside the study timing [76]. Other phase I-II clinical studies were also able to demonstrate the safety and efficacy of iNKT cell-based immunotherapy. In 5 patients with advanced MM, the levels of iNKT cells were expanded by a 100 fold increase following the αGalCer-pulsed DCs treatment. This increase was still detected in the patients even after 6 months of the initial injection. In addition, vaccinated patients showed a significant increase in several cytokines and an increase in a distinct memory CD8+ T cells specific for CMV (cytomegalovirus) [77]. In another study where twenty-three patients with NSCLC were treated with αGalCer pulsed PBMC and cultured with IL-2 and GM-CSF, there were no adverse side effects recorded. Furthermore, 10 out of the 23 patients showed an increase in the levels of IFNγ in the blood following iNKT cells activation which was correlated with prolonged median survival time of the patients [78]. Nonetheless, combinational therapy that targets iNKT cells activation with chemotherapeutic drugs also showed to be both safe and effective. Six MM patients were treated with αGalCer-loaded monocyte-derived DC and lenalidomide, an immunomodulatory drug that in previous studies correlated with better outcome in patients. The patients demonstrated an expansion of iNKT cells and NK cells expressing NKG2D on their surface. The treatment also led to the increase in serum IL-12 receptor and antitumor T cell

immunity, which was either pre-existing or treatment induced. Consequently, all these factors lead to tumor regression [79].

Currently, CAR (chimeric antigen receptor) T cells have gained wide popularity especially after the observed success in treating patients with B-ALL using CD19.CAR T cells. However, the risk of the generation of GVHD caused by the endogenous TCR of the transferred CAR T cells cannot be overshadowed particularly since the orientation is moving towards finding an "off-the-shelf" allogeneic CAR T cells for immunotherapy [80]. While on the other hand, the iNKT cells endogenous CD1d-targeted TCR has proven to be useful in anti-tumor immunity, and since many pre-clinical and clinical studies have validated the significant role of iNKT cells in controlling GVHD without having any negative effect on the GVL (graft-versus-leukemia) function [81], iNKT cells would make the ideal platform for the CAR immunotherapy. In fact, CAR iNKT cells were generated against GD2 (ganglioside), which is highly expressed in NB (neuroblastoma). GD2.CAR iNKT cells exhibited a specific and potent cytotoxicity against NB expressing GD2, while still maintaining the function of the endogenous CD1d-TCR. When injected in vivo, GD2.CAR iNKT cells were localized in the tumor sites and had potent antitumor activity skewing the response towards Th1 cytokine profile with high levels of IFNγ and GM-CSF. In addition, repeated injections resulted in a better long-term survival in mice with metastatic NB. Most importantly, unlike CAR T cells, GD2.CAR iNKT cells did not induce GVHD [82]. These results provided evidence for the safety and efficient role of using CAR iNKT cells in immunotherapy. Nonetheless, the same group worked on generating a CAR iNKT that co-express both GD2 and IL-15, which is important for iNKT homeostasis and maturation [17]. They showed that GD2.CAR.IL-15 iNKT cells enhanced the iNKT cells survival and reduced the expression of exhaustion markers such as PD-1, TIM3 and LAG3 of both in vitro and in vivo cells. Nonetheless, these GD2.CAR.IL-15 iNKT cells were able to infiltrate solid tumor tissues and exhibit a cytotoxic activity in mice in vivo without showing any signs of toxicity [83]. These results paved the way for the first clinical trial in humans using CAR iNKT cells as anti-tumor immunotherapeutic approach. The ongoing phase I clinical trial has an estimate

enrollment of 24 NB patients, whose ages vary from 1 till 21 years old, to be treated with GD2.CAR.IL-15 iNKT cells. So far, two 12 years-old and one 6 years-old males were enrolled and subjected to the treatment. Prior to CAR iNKT cells injection at day 0, the patients were treated at days -4, -3, and -2 with cyclophosphamide and fludarabine which would cause lymphodepletion. The patients exhibited minor side effects that were mostly linked to the cyclophosphamide/ fludarabine treatment, since the adverse effects were witnessed before the injection of iNKT cells, and no dose-limiting toxicities such as cytokine release syndrome or neurotoxicities were observed following the CAR iNKT injections. In addition, all the patients exhibited an increase in the peripheral iNKT cell frequency as well as CAR iNKT cells that lasted up until week 4 of the evaluation period. These iNKT cells were detected at the tumor site and in one patient were able to cause a regression in the bone marrow metastatic lesion. CAR iNKT cells were well tolerated in patients suggesting a safety measure for treatment. More results are needed to assess the cytotoxicity of the treatment [84].

Conclusion

In conclusion knowing and understanding the functions of iNKT cells, most importantly the bridge they implement between the 2 arms of the immune system have opened a new array of studies that aim in activating iNKT cells. In this review, the summarized preclinical and clinical studies provide promising evidence in targeting iNKT for innovative immunotherapies against several types of cancers, such as hematological malignancies or other previously mentioned types that express CD1d and serve as direct targets for iNKT cells recognition and cytotoxicity. Nonetheless, murine and human studies have well demonstrated the safety and tolerance in administering such treatment and in some cases a significant amelioration in the final outcome. Furthermore, the lack of polymorphism by the CD1d gene renders the iNKT cell transfer more applicable and provide several advantages over T cell therapies. Most importantly, the transfer of iNKT cell for cancer immunotherapy has shown to limit the GVHD while still governing protection to the recipient. However, better understanding of iNKT cells reconstitution, survival and effector function in humans is required in order to

completely benefit from their full potential as an immunotherapeutic approach against cancer.

References

1. P Dellabona, E Padovan, G Casorati, M Brockhaus, A Lanzavecchia. An invariant V alpha 24-J alpha Q/V beta 11 T cell receptor is expressed in all individuals by clonally expanded CD4-8- T cells. J. Exp. Med. 1994; 180: 1171–1176.
2. Lantz, A Bendelac. An invariant T cell receptor alpha chain is used by a unique subset of major histocompatibility complex class I-specific CD4+ and CD4-8- T cells in mice and humans. J. Exp. Med. 1994; 180: 1097–1106.
3. S Porcelli, CE Yockey, MB Brenner, SP Balk. Analysis of T cell antigen receptor (TCR) expression by human peripheral blood CD4-8- alpha/beta T cells demonstrates preferential use of several V beta genes and an invariant TCR alpha chain. J. Exp. Med. 1993; 178: 1–16.
4. P Arrenberg, R Halder, V Kumar. Cross-regulation between distinct natural killer T cell subsets influences immune response to self and foreign antigens. J. Cell. Physiol. 2009; 218: 246–250.
5. D Slauenwhite, B Johnston. Regulation of NKT Cell Localization in Homeostasis and Infection. Front. Immunol. 2015; 6: 255.
6. JL Matsuda, T Mallevaey, J Scott-Browne, L Gapin. CD1d-restricted iNKT cells, the ‘Swiss-Army knife’ of the immune system. Curr. Opin. Immunol. 2008; 20: 358–368.
7. Tetsu Kawano, Junqing Cui, Yasuhiko Koezuka, Isao Toura, yoshikatsu Kaneko et al., CD1d-restricted and TCR-mediated activation of valpha14 NKT cells by glycosylceramides. Science. 1997; 278: 1626–1629.
8. Lisa Kain, Bill Webb, Brian L Anderson, Shenglou Deng, Marie Holt, et al. The Identification of the Endogenous Ligands of Natural Killer T Cells Reveals the Presence of Mammalian α-Linked Glycosylceramides. Immunity. 2014; 41: 543– 554.
9. J López-Sagaseta, LV Sibener, JE Kung, J Gumperz, EJ Adams. Lysophospholipid presentation by CD1d and

recognition by a human Natural Killer T-cell receptor. EMBO J. 2012; 31: 2047–2059.
10. Federica Facciotti, Gundimeda S Ramanjaneyulu, Marco Lepore, Sebastiano Sansano, Marco Cavallari, et al. Peroxisome-derived lipids are self antigens that stimulate invariant natural killer T cells in the thymus. Nat. Immunol. 2012; 13: 474–480.
11. PA Sieling. CD1-Restricted T cells: T cells with a unique immunological niche. Clin. Immunol. Orlando Fla. 2000; 96: 3–10.
12. M Brigl, MB Brenner. CD1: antigen presentation and T cell function, Annu. Rev. Immunol. 2004; 22: 817–890.
13. Federica Facciotti, Marco Cavallari, Catherine Angénieux, Luis F Garcia-Alles, François Signori, et al. Fine tuning by human CD1e of lipid-specific immune responses. Proc. Natl. Acad. Sci. U. S. A. 2011; 108: 14228–14233.
14. H Spits. Development of alphabeta T cells in the human thymus. Nat. Rev. Immunol. 2002; 2: 760–772.
15. T Hu, I Gimferrer, J Alberola-Ila. Control of early stages in invariant natural killer T- cell development. Immunology. 2011; 134: 1–7.
16. DG Pellicci, HF Koay, SP Berzins. Thymic development of unconventional T cells: how NKT cells, MAIT cells and γδ T cells emerge. Nat. Rev. Immunol. 2020; 20: 756–770.
17. H Xu, T Chun, A Colmone, H Nguyen, CR Wang. Expression of CD1d under the control of a MHC class Ia promoter skews the development of NKT cells, but not CD8+ T cells. J. Immunol. Baltim. Md 1950. 2003; 171: 4105–4112.
18. J Schümann, P Pittoni, E Tonti, HR Macdonald, P Dellabona, et al. Targeted expression of human CD1d in transgenic mice reveals independent roles for thymocytes and thymic APCs in positive and negative selection of Valpha14i NKT cells. J. Immunol. Baltim. Md 1950. 2005; 175: 7303–7310.
19. DI Godfrey, SP Berzins. Control points in NKT-cell development. Nat. Rev. Immunol. 2007; 7: 505–518.
20. SH Krovi, L Gapin. Invariant Natural Killer T Cell Subsets-More Than Just Developmental Intermediates. Front. Immunol. 2018; 9: 1393.
21. Yeonseok Chung, Roza Nurieva, Eiji Esashi, Yi-Hong Wang,

Dapeng Zhou, et al. A critical role of costimulation during intrathymic development of invariant NK T cells. J. Immunol. Baltim. Md 1950. 2008; 180: 2276–2283.
22. Finlay W McNab, Daniel G Pellicci, Kenneth Field, Gurdyal Besra, Mark J Smyth, et al. Peripheral NK1.1 NKT cells are mature and functionally distinct from their thymic counterparts. J. Immunol. Baltim. Md 1950. 2007; 179: 6630–6637.
23. SP Berzins, FW McNab, CM Jones, MJ Smyth, DI Godfrey. Long-term retention of mature NK1.1+ NKT cells in the thymus. J. Immunol. Baltim. Md 1950. 2006; 176: 4059–4065.
24. Laura E Gordy, Jelena S Bezbradica, Andrew I Flyak, Charles T Spencer, Alexis Dunkle, et al. IL-15 regulates homeostasis and terminal maturation of NKT cells. J. Immunol. Baltim. Md 1950. 2011; 187: 6335–6345.
25. You Jeong Lee, Gabriel J Starrett, Seungeun Thera Lee, Rendong Yang, Christine M Henzler, et al. Lineage-Specific Effector Signatures of Invariant NKT Cells Are Shared amongst γδ T, Innate Lymphoid, and Th Cells. J. Immunol. 2016; 197: 1460–1470.
26. YJ Lee, H Wang, GJ Starrett, V Phuong, SC Jameson, et al. Tissue- Specific Distribution of iNKT Cells Impacts Their Cytokine Response. Immunity. 2015; 43: 566–578.
27. Hiroshi Watarai, Etsuko Sekine-Kondo,Tomokuni Shigeura,Yasutaka Motomura,Takuwa Yasuda, et al. Development and Function of Invariant Natural Killer T Cells Producing TH2- and TH17-Cytokines. PLOS Biol. 2012; 10: e1001255.
28. JE Gumperz, S Miyake, T Yamamura, MB Brenner. Functionally distinct subsets of CD1d-restricted natural killer T cells revealed by CD1d tetramer staining. J. Exp. Med. 2002; 195: 625–636.
29. Pheh-Ping Chang, Patricia Barral, Jessica Fitch, Alvin Pratama, Cindy S Ma, et al. Identification of Bcl-6-dependent follicular helper NKT cells that provide cognate help for B cell responses. Nat. Immunol. 2012; 13: 35–43.
30. Irah L King, Anne Fortier, Michael Tighe, John Dibble, Gerald FM Watts, et al. Invariant natural killer T cells direct B cell responses to cognate lipid antigen in an IL-21-

dependent manner. Nat. Immunol. 2011; 13: 44–50.
31. PJ Brennan, M Brigl, MB Brenner. Invariant natural killer T cells: an innate activation scheme linked to diverse effector functions. Nat. Rev. Immunol. 2013; 13: 101–117.
32. Manfred Brigl, Raju VV Tatituri, Gerald FM Watts, Veemal Bhowruth, Elizabeth A Leadbetter, et al. Innate and cytokine-driven signals, rather than microbial antigens, dominate in natural killer T cell activation during microbial infection. J. Exp. Med. 2011; 208: 1163–1177.
33. S González, A López-Soto, B Suarez-Alvarez, A López-Vázquez, C López-Larrea. NKG2D ligands: key targets of the immune response. Trends Immunol. 2008; 29: 397– 403.
34. Carlotta Kuylenstierna, Niklas K Björkström, Sofia K Andersson, Peter Sahlström, Lidija Bosnjak, et al. NKG2D performs two functions in invariant NKT cells: direct TCR-independent activation of NK-like cytolysis and co-stimulation of activation by CD1d. Eur. J. Immunol. 2011; 41: 1913–1923.
35. Elvire Bourgeois, Linh Pham Van, Michel Samson, Séverine Diem, Anne Barra, et al. The pro-Th2 cytokine IL-33 directly interacts with invariant NKT and NK cells to induce IFN-gamma production. Eur. J. Immunol. 2009; 39: 1046–1055.
36. M Brigl, MB Brenner. How invariant natural killer T cells respond to infection by recognizing microbial or endogenous lipid antigens. Semin. Immunol. 2010; 22: 79–86.
37. S Fujii, K Shimizu, M Kronenberg, RM Steinman. Prolonged IFN-gamma-producing NKT response induced with alpha-galactosylceramide-loaded DCs. Nat. Immunol. 2002; 3: 867–874.
38. Vrajesh V Parekh, Michael T Wilson, Danyvid Olivares-Villagómez, Avneesh K Singh, Lan Wu, et al. Glycolipid antigen induces long-term natural killer T cell anergy in mice. J. Clin. Invest. 2005; 115: 2572–2583.
39. Kanako Shimizu, Yusuke Sato, Jun Shinga, Takashi Watanabe, Takaho Endo, et al. KLRG+ invariant natural killer T cells are long-lived effectors. Proc. Natl. Acad. Sci. 2014; 111: 12474–12479.
40. NB Beyersdorf, X Ding, K Karp, T Hanke. Expression of inhibitory ‘killer cell lectin- like receptor G1’ identifies

unique subpopulations of effector and memory CD8 T cells. Eur. J. Immunol. 2001; 31: 3443–3452.
41. Daniel B Stetson, Markus Mohrs, R Lee Reinhardt, Jody L Baron, Zhi-En Wang, et al. Constitutive cytokine mRNAs mark natural killer (NK) and NK T cells poised for rapid effector function. J. Exp. Med. 2003; 198: 1069–1076.
42. JL Matsuda, OV Naidenko, L Gapin, T Nakayama, M Taniguchi, et al. Tracking the response of natural killer T cells to a glycolipid antigen using CD1d tetramers. J. Exp. Med. 2000; 192: 741–754.
43. M Kronenberg, L Gapin. The unconventional lifestyle of NKT cells. Nat. Rev. Immunol. 2002; 2: 557–568.
44. L Clerici, G Casorati, P Dellabona. B Cell Help by CD1d-Rectricted NKT Cells. Antibodies. 2015; 4.
45. A La Cava, L Van Kaer, null Fu-Dong-Shi. CD4+CD25+ Tregs and NKT cells: regulators regulating regulators. Trends Immunol. 2006; 27: 322–327.
46. S Bessoles, S Dudal, GS Besra, F Sanchez, V Lafont. Human CD4+ invariant NKT cells are involved in antibacterial immunity against *Brucella suis* through CD1d-dependent but CD4-independent mechanisms. Eur. J. Immunol. 2009; 39: 1025–1035.
47. Woo-Yong Lee, Maria-Jesus Sanz, Connie H Y Wong, Pierre-Olivier Hardy, Aydan Salman-Dilgimen, et al. Invariant natural killer T cells act as an extravascular cytotoxic barrier for joint-invading Lyme Borrelia. Proc. Natl. Acad. Sci. U. S. A. 2014; 111: 13936–13941.
48. Yong Xu, Zehua Wang, Xianhong Du, Yuan Liu, Xiaojia Song, et al. Tim-3 blockade promotes iNKT cell function to inhibit HBV replication. J. Cell. Mol. Med. 2018; 22: 3192–3201.
49. E Kobayashi, K Motoki, T Uchida, H Fukushima, Y Koezuka. KRN7000, a novel immunomodulator, and its antitumor activities. Oncol. Res. 1995; 7: 529–534.
50. RM McEwen-Smith, M Salio, V Cerundolo. The regulatory role of invariant NKT cells in tumor immunity. Cancer Immunol. Res. 2015; 3: 425–435.
51. MJ Smyth, KY Thia, SE Street, E Cretney, JA Trapani, et al. Differential tumor surveillance by natural killer (NK) and NKT cells. J. Exp. Med. 2000; 191: 661–668.

52. Jeremy B Swann, Adam P Uldrich, Serani van Dommelen, Janelle Sharkey, William K Murray, et al. Type I natural killer T cells suppress tumors caused by p53 loss in mice. Blood. 2009; 113: 6382–6385.
53. Matteo Bellone, Monica Ceccon, Matteo Grioni, Elena Jachetti, Arianna Calcinotto, et al. iNKT cells control mouse spontaneous carcinoma independently of tumor- specific cytotoxic T cells. PloS One. 2010; 5: e8646.
54. Naveena B Janakiram, Altaf Mohammed, Taylor Bryant, Rebekah Ritchie, Nicole Stratton, et al. Loss of natural killer T cells promotes pancreatic cancer in LSL- KrasG12D/+ mice. Immunology. 2017; 152: 36–51.
55. Francesca Gorini, Laura Azzimonti, Gloria Delfanti, Lydia Scarfò, Cristina Scielzo, et al. Invariant NKT cells contribute to chronic lymphocytic leukemia surveillance and prognosis. Blood. 2017; 129: 3440–3451.
56. K Yanagisawa, K Seino, Y Ishikawa, M Nozue, T Todoroki, et al. Impaired proliferative response of V alpha 24 NKT cells from cancer patients against alpha- galactosylceramide. J. Immunol. Baltim. Md 1950. 2002; 168: 6494–6499.
57. Tsuyoshi Tachibana, Hisashi Onodera, Tatsuaki Tsuruyama, Akira Mori, Satoshi Nagayama, et al. Increased intratumor Valpha24-positive natural killer T cells: a prognostic factor for primary colorectal carcinomas. Clin. Cancer Res. Off. J. Am. Assoc. Cancer Res. 2005; 11: 7322–7327.
58. Leonid S Metelitsa, Hong-Wei Wu, Hong Wang, Yujun Yang, Zamir Warsi,et al. Natural killer T cells infiltrate neuroblastomas expressing the chemokine CCL2. J. Exp. Med. 2004; 199: 1213–1221.
59. Liping Song, Shahab Asgharzadeh, Jill Salo, Kelly Engell, Hong-wei Wu, et al. Valpha24-invariant NKT cells mediate antitumor activity via killing of tumor-associated macrophages. J. Clin. Invest. 2009; 119: 1524–1536.
60. Amy N Courtney, Gengwen Tian, Daofeng Liu, Ekaterina Marinova, Andras Heczey, et al. Cross-talk between NKT cells and tumor associated macrophages in the tumor microenvironment. J. Immunol. 2016; 196:142.7-142.7.
61. Tao Sun, Ye Yang, Xiaoguang Luo, Ying Cheng, Mingyu Zhang, et al. Inhibition of Tumor Angiogenesis by Interferon-γ by Suppression of Tumor- Associated

Macrophage Differentiation. Oncol. Res. Featur. Preclin. Clin. Cancer Ther. 2014; 21: 227–235.
62. Filippo Cortesi, Gloria Delfanti, Andrea Grilli, Arianna Calcinotto, Francesca Gorini, et al. Bimodal CD40/Fas-Dependent Crosstalk between iNKT Cells and Tumor-Associated Macrophages Impairs Prostate Cancer Progression. Cell Rep. 2018; 22: 3006–3020.
63. Carmela De Santo, Ramon Arscott, Sarah Booth, Ioannis Karydis, Margaret Jones, et al. Invariant NKT cells modulate the suppressive activity of Serum Amyloid A-differentiated IL-10-secreting neutrophils. Nat. Immunol. 2010; 11: 1039–1046.
64. LS Metelitsa, KI Weinberg, PD Emanuel, RC Seeger. Expression of CD1d by myelomonocytic leukemias provides a target for cytotoxic NKT cells. Leukemia. 2003; 17: 1068–1077.
65. Madhav V Dhodapkar, Matthew D Geller, David H Chang, Kanako Shimizu, Shin-Ichiro Fujii, et al. A reversible defect in natural killer T cell function characterizes the progression of premalignant to malignant multiple myeloma. J. Exp. Med. 2003; 197: 1667–1676.
66. Franco Fais, Fortunato Morabito, Caterina Stelitano, Vincenzo Callea, Sabrina Zanardi, et al. CD1d is expressed on B-chronic lymphocytic leukemia cells and mediates alpha-galactosylceramide presentation to natural killer T lymphocytes. Int. J. Cancer. 2004; 109: 402–411.
67. GJ Renukaradhya, MA Khan, M Vieira, W Du, J Gervay-Hague, et al. Type I NKT cells protect (and type II NKT cells suppress) the host's innate antitumor immune response to a B-cell lymphoma. Blood. 2008; 111: 5637–5645.
68. JLM Ferrara, JE Levine, P Reddy, E Holler. Graft-versus-Host Disease. Lancet. 2009; 373: 1550–1561.
69. Marie-Thérèse Rubio, Lucia Moreira-Teixeira, Emmanuel Bachy, Marie Bouillié, Pierre Milpied, et al. Early posttransplantation donor-derived invariant natural killer T-cell recovery predicts the occurrence of acute graft-versus-host disease and overall survival. Blood. 2012; 120: 2144–2154.
70. Aristeidis Chaidos, Scott Patterson, Richard Szydlo, Mohammed Suhail Chaudhry, Francesco Dazzi, et al. Graft

invariant natural killer T-cell dose predicts risk of acute graft-versus- host disease in allogeneic hematopoietic stem cell transplantation. Blood. 2012; 119: 5030–5036.
71. Claudia de Lalla, Anna Rinaldi, Daniela Montagna, Laura Azzimonti, Maria Ester Bernardo, et al. Invariant NKT cell reconstitution in pediatric leukemia patients given HLA-haploidentical stem cell transplantation defines distinct CD4+ and CD4- subset dynamics and correlates with remission state. J. Immunol. Baltim. Md 1950. 2011; 186: 4490– 4499.
72. J Konishi, K Yamazaki, H Yokouchi, N Shinagawa, K Iwabuchi, et al. The characteristics of human NKT cells in lung cancer--CD1d independent cytotoxicity against lung cancer cells by NKT cells and decreased human NKT cell response in lung cancer patients. Hum. Immunol. 2004; 65: 1377–1388.
73. Éilis Dockry, Seónadh O'Leary, Laura E Gleeson, Judith Lyons, Joseph Keane, et al. Epigenetic induction of CD1d expression primes lung cancer cells for killing by invariant natural killer T cells. Oncoimmunology. 2018; 7: e1428156.
74. S Fallarini, T Paoletti, N Orsi Battaglini, G Lombardi. Invariant NKT cells increase drug-induced osteosarcoma cell death. Br. J. Pharmacol. 2012; 167: 1533–1549.
75. Kavita M Dhodapkar, Barbara Cirignano, Francesca Chamian, David Zagzag, Douglas C Miller, et al. Invariant natural killer T cells are preserved in patients with glioma and exhibit antitumor lytic activity following dendritic cell-mediated expansion. Int. J. Cancer. 2004; 109: 893–899.
76. Mie Nieda, Miki Okai, Andrea Tazbirkova, Henry Lin, Ayako Yamaura, et al. Therapeutic activation of Valpha24+Vbeta11+ NKT cells in human subjects results in highly coordinated secondary activation of acquired and innate immunity. Blood. 2 0 0 4; 103: 383–389.
77. David H Chang, Keren Osman, John Connolly, Anjli Kukreja, Joseph Krasovsky, et al. Sustained expansion of NKT cells and antigen-specific T cells after injection of alpha-galactosyl-ceramide loaded mature dendritic cells in cancer patients. J. Exp. Med. 2005; 201: 1503–1517.
78. Shinichiro Motohashi, Kaoru Nagato, Naoki Kunii, Heizaburo Yamamoto, Kazuki Yamasaki, et al. A phase I-II

study of alpha-galactosylceramide-pulsed IL-2/GM-CSF-cultured peripheral blood mononuclear cells in patients with advanced and recurrent non-small cell lung cancer. J. Immunol. Baltim. Md 1950. 2009; 182: 2492–2501.
79. Joshua Richter, Natalia Neparidze, Lin Zhang, Shiny Nair, Tamara Monesmith, et al. Clinical regressions and broad immune activation following combination therapy targeting human NKT cells in myeloma. Blood. 2013; 121: 423–430.
80. K Sanber, B Savani, T Jain. Graft-versus-host disease risk after chimeric antigen receptor T-cell therapy: the diametric opposition of T cells. Br. J. Haematol. 2021; 195: 660–668.
81. P Guan, H Bassiri, NP Patel, KE Nichols, R Das. Invariant natural killer T cells in hematopoietic stem cell transplantation: killer choice for natural suppression. Bone Marrow Transplant. 2016; 51: 629–637.
82. Andras Heczey, Daofeng Liu, Gengwen Tian, Amy N Courtney, Jie Wei, et al. Invariant NKT cells with chimeric antigen receptor provide a novel platform for safe and effective cancer immunotherapy. Blood. 2014; 124: 2824–2833.
83. Xin Xu, Wei Huang, Andras Heczey, Daofeng Liu, Linjie Guo, et al. NKT Cells Coexpressing a GD2-Specific Chimeric Antigen Receptor and IL15 Show Enhanced In Vivo Persistence and Antitumor Activity against Neuroblastoma. Clin. Cancer Res. Off. J. Am. Assoc. Cancer Res. 2019; 25: 7126–7138.
84. Andras Heczey, Amy N Courtney, Antonino Montalbano, Simon Robinson, Ka Liu, et al. Anti-GD2 CAR-NKT cells in patients with relapsed or refractory neuroblastoma: an interim analysis. Nat. Med. 2020; 26: 1686–1690.

Book Chapter

Immune Response Characteristics in SARS-CoV-2 Infection

Sally Badawi*

Department of Genetics and Genomics, College of Medicine and Health Sciences, United Arab Emirates University, Al-Ain, UAE

***Corresponding Author:** Sally Badawi, Department of Genetics and Genomics, College of Medicine and Health Sciences, United Arab Emirates University, Al-Ain, UAE

Published **August 06, 2021**

How to cite this book chapter: Sally Badawi. Immune Response Characteristics in SARS-CoV-2 Infection. In: Hussein Fayyad Kazan, editor. Immunology and Cancer Biology. Hyderabad, India: Vide Leaf. 2021.

Introduction

Corona virus disease (COVID-19), reported in December 2019 and declared a pandemic in March 2020, represents a serious unprecedent health and economic burden globally leading to more than 180 million infection cases and almost 4 million deaths worldwide (as of 4 July 2021). COVID-19 is caused by the novel severe acute respiratory syndrome coronavirus 2, SARS-CoV-2, which belongs to a family of coronaviruses of zoonotic origin and infects humans causing mild to severe respiratory and intestinal infections [1]. Phylogenic analysis and genomic characterization of SARS-CoV-2 have shown that it

shares around 79% and 50% genome sequence with its predecessors coronaviruses the SARS-CoV and the Middle East respiratory syndrome coronavirus (MERS-CoV), respectively [2]. The similarity between these viruses has greatly contributed to the understanding of the origin, the infection and the associated reaction of COVID-19.

SARS-CoV-2 is a single stranded RNA virus bound to nucleocapsid protein (N) and covered by a lipid membrane constituting the membrane protein (M), the envelope protein (E) and importantly, the spike protein (S) as shown in Figure.1 [1]. Similarly to SARS-CoV, SARS-CoV-2 uses its spike protein as mediator for viral attachment and entry into the host cells via the angiotensin converting enzyme 2 (ACE2) receptor [3,4]. Upon binding to ACE2 on the surface epithelial cells in the lungs, the virus starts replicating rapidly. In the early infectious phase, no symptoms are observed. 2-14 days post infection, symptoms start to appear including fever, dry cough, fatigue and shortness of breath. As the viral replication and propagation continues in the lungs, immune response is strongly activated accompanied by respiratory failure and acute respiratory distress syndrome in some patients causing their death [5]. Moreover, the underlying machinery causing respiratory failure and the extensive activation of the immune response post-infection is not fully elucidated yet.

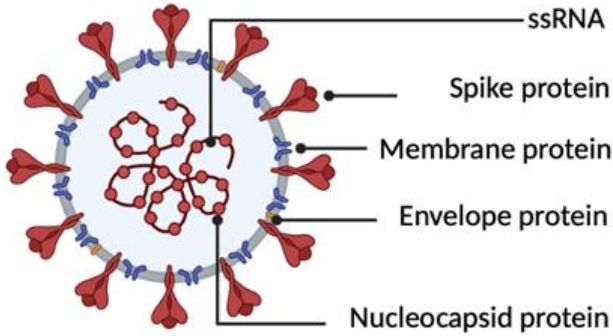

Figure 1: Severe acute respiratory syndrome corona virus structure. A schematic drawing representing the structure of SARS-CoV-2 virus including its proteins and genomic material.

Innate Immunity in SARS-CoV-2

Virus Recognition and Immune Evasion

During viral infections, pathogen recognition receptors (PPRs) like the toll-like receptors 3,7 and 8, that are usually present in the cytosolic compartment of immune cells [6], are the first to recognize and identify the pathogen associated molecular patterns (PAMPs) of the virus [7]. Upon interaction, the viral particles are endocytosed and further identified by intracellular cytosolic PPRs like the Retinoic Acid-Inducible Gene I protein (RIG-1) and Mitochondrial antiviral-signaling proteins (MAVs) leading to the activation of signaling cascades and stimulation of NF-κB. In a similar fashion to SARS-CoV and MERS-CoV, several inflammatory cytokines are activated by the transcriptional factor role played by NF-κB [8]. NF-κB pathway activation leads to enhanced production of the antiviral Type I Interferon (IFN-1) which activates neighboring cells including the natural killer cells, through the IFN α/β receptor and stimulating the transcription of inflammatory factors (interferon-stimulated genes, ISGs) and stimulates the antigen phagocytosis by macrophages [9]. Interestingly, among the stimulated ISGs is ACE2 which suggests that SARS-CoV-2 utilizes the IFN upregulation in the lungs to enhance its infection [10]. Additionally, unlike SARS-CoV, SARS-CoV-2 replication was found to be more sensitive and can be inhibited invitro in response to IFN-1 pretreatment, which could present a potent therapeutic targeting for tackling the virus [11].

Inflammatory Cytokine Production

SARS-CoV-2 infected patients were shown to experience a strong inflammatory reaction and rapid production of cytokines as a defense mechanism against the virus. Cytokines and chemokine production were found to play a crucial role in SARS-CoV-2 development and progression. The induced cytokine production acts as a double-edged sword; although it is firstly regraded as the body's defense mechanism, it could also lead to autoinflammation, organ failure and consequently death in several cases [12]. Pro-inflammatory cytokines like IL-6, TNF-α, IL-2, MIP-α and IFN α along with CCL2, CXCL1,

CXCL5 and CXCL10 chemokines have displayed an significantly elevated profile during SARS infections [13,14]. Although delayed, this increased profile was also detected in MERS-CoV infected patients as well [15,16]. Among these cytokines, IL-6 is suggested to be a diagnostic marker that plays a major role during the disease, in which it is significantly increased in symptomatic and critically ill COVID-19 patients [17]. These inflammatory factors are secreted through variety of cells including immune cells like the monocytes, macrophages, dendritic cells (DCs) and natural killer cells and other non-immune cells like the fibroblasts and the endothelial cells [18]. Moreover, not only these cells play a role in the innate immunity but also contribute to the activation of the adaptive immune response. Among these cells are the dendritic cells that represent the major antigen-presenting cells in the body. Both immature and mature forms of DCs contribute to the inflammatory process, where immature DCs effectively migrate to the site of infection and mature DCs can activate the naive T cells of the cell mediated immune response [19]. Several studies have reported that DCs can be infected by SARS-CoV leading to enhanced inflammatory reaction and decreased antiviral response [20]. Interestingly, SARS-CoV-2 was also shown to directly infect DCs and limit their maturation and consequently delay/impair the activation of T cells [21], suggesting that reduced or loss of DCs function in SARS-CoV-2 patients would significantly delay their immune response [22].

SARS-CoV-2 Induced Cell Death

During viral infections, neutrophils are the first to infiltrate to the site of infection, however, it is not yet well clear to which extent these cells contribute to the pathology and progression of SARS-CoV-2. Recently, it has been shown that neutrophil to lymphocyte ratio could present a simple phenotyping tool to assess the severity of SARS-CoV-2 in infected patients and a prediction tool for their clinical outcome [23]. Not only through their infiltration neutrophils contribute to the disease's pathology, but also through their extracellular traps (NET) that constitute DNA, histones, and proteases and are released from neutrophils in response to infections [24]. Excessive availability

of NETs is well known to play a pathogenic role in respiratory diseases and were found to contribute to tissue damage in several organs including lung, heart and kidney during infections [24–26]. Interestingly, these NETs have also contributed to mortality and organ damage in SARS-CoV-2 patients [27] where sera of COVID-19 patients have been shown to trigger the release of NET from neutrophils during invitro studies [28]. The whole process of releasing the condensed granular content from the neutrophils is called NETosis which represent a unique cell death process triggered in COVID-19 patients mainly by the release of inflammatory cytokines and chemokines including Il-6,IL-1β, CXCL2 and CXCL8 and consequently lead to further cytokine production [29–31]. Aside from NETtosis, recent studies have shown increased activation of caspase-8 which is a hallmark for apoptotic cell death. Moreover, caspase-8 activation in the lung epithelial cells was shown to trigger the activation of a dual cell death pathways including the apoptotic and the necroptotic death in COVID-19 patients [32,33]. Necroptosis represents a form of immunogenic programmed cell death that activates the immune response through the associated release of inflammatory cytokines and the damage associated molecular patterns (DAMPs) [32]. Necroptotic cell death pathway is mainly triggered by different stimulators, including TLRs, TNFR and IFNRs. It is mediated by the phosphorylation of mixed lineage kinase domain like protein (MIKL) mediated by receptor-interacting protein kinase 3 (RIPK3) [34]. To date, few are the studies that display clear evidence of necroptosis during SARS-CoV-2 infection however, a recent study suggests elevated serum levels of RIPK3 in SARS-CoV-2 infected patients [35], where in another invitro study SARS-CoV-2 is shown to induce RIPK3 phosphorylation suggesting the activation of necroptotic cell death [32], moreover further investigations are required to understand how exactly SARS-CoV-2 activates necroptosis.

Furthermore, as shown in Figure 2. SARS-CoV-2 has been also reported to induce pyroptotic cell death in monocytes and macrophages [36,37]. Pyroptosis is another form of cell death that is Caspase-1 dependent and is found to amplify the immune response during SARS infection. Caspase-1 is mainly activated

by the inflammasome complex and consequently leads to the maturation of some cytokines like the IL-1β and IL-18. In addition, caspase-1 activation leads to the cleavage of Gasdermin D (GSDMD) which translocate to the plasma membrane and forms a pore causing the release of the cellular content including the activated cytokines and consequently causing cell death [38]. This form of cell death has been reported in the lung tissue of COVID-19 patients along with increased infiltration of proinflammatory macrophages [37].

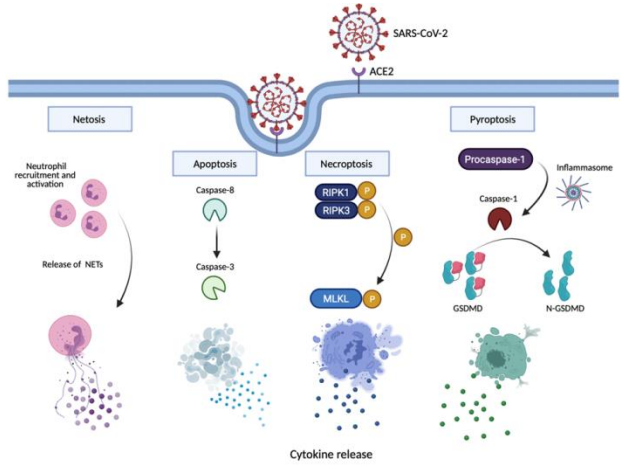

Figure 2: SARS-CoV-2 mediated cell death. A schematic representation of the various types of cell death induced by SARS-CoV-2 infection, including the neutrophils' NET mediated death (NETosis), the apoptotic cell death mediated by caspase-8, the necroptotic cell death via the RIPK/MLKL activated pathway and the pyroptotic cell death caused by GSDMD pore formation on the cellular membrane. Membrane rupture caused by all forms of death is associated with the release of cell content along with massive release of inflammatory cytokines. Image made using Biorender.com.

Cell Mediated Immune Response against SARS-CoV-2

T-cells Mediated Immunity

Lymphopenia, defined as low lymphocyte count in the blood, has been strongly observed in COVID-19 patients and mainly in non-survivor ones [17,39,40]. This decrease has been also

observed in SARS-CoV and MERS-CoV infections that has been also associated with a decrease in T lymphocyte subtypes that persisted until recovery [41,42]. Interestingly, T Helper CD4+ cells and cytotoxic T lymphocytes CD8+ were found decreased in severe cases compared to mild ones [40]. During SARS-CoV-2 infection, both B cells and T cells were detected during the first week post symptomatic infections [43]. Aside from the humoral role played mainly by the different subtypes of B lymphocytes, T cells were shown to tackle SARS-CoV-2 directly through interacting with viral infected cells and indirectly through regulating the humoral immune response [44]. In the blood, CD4 and CD8 T cell populations were found reduced but in a hyperactivated status proven by high HLA-DR along with high toxicity of CD8 T cells assessed by the granulysin cytotoxic concentration [45]. This decrease was also shown to be associated with the severity of the infection, in which severe cases displayed an enhanced decrease compared to moderate ones [46]. Moreover, the peripheral blood decrease was explained by the infiltration of T cells to the infection site which was evidenced by the increased mononuclear cells mainly lymphocytes in lung autopsies of COVID-19 patients [45]. Among T cells population, CD8+ cells are known to control respiratory viruses via attacking viral infected cells and preventing viral replication [47]. On the other hand, CD4+ cells are required for priming CD8+ and B cells that in turn are responsible for recruiting immune cells to the infection site via cytokine production and mediating the humoral immune response via producing viral-specific antibodies [48].

Previous data from studies on SARS coronavirus have highlighted the importance of CD4+ cells in controlling the viral infection where both CD4+ and CD8+ T cells subtypes were present in the lungs and contributed to increased protection and survival in SARS-CoV infected immunodeficient mice [49,50]. Furthermore Interestingly, recovered patients from SARS-CoV infections have developed memory T cells that lasted around two years post infections [51,52]. Similarly, insufficiency of CD4+ T cells in aged or impaired adaptive immune response in COVID-19 patients leads to uncoordinated immune response that fails to control the progression of the disease [53]. Recently, a preprint

study shows that CD8+ cells from COVID-19 patients recognizes different SARS-CoV-2 variants [54], which along with all the precedents suggests T cells as a putative therapeutic target that can be used to tackle coronavirus.

B cells Mediated Immunity

Similar to T cells, antibody-secreting cells (ASCs) that differentiate from activated B cells peak approximately one week post symptoms onset in COVID-19 patients [43]. B cells response including memory cells , binding and neutralizing antibodies depends greatly on the CD4+ T cells subtype [55]. Evidently, immunoglobulin (Ig) G titers against SARS-CoV-2 were shown to strongly correlate with CD4+ cells in COVID-19 patients [43,56-58]. Interestingly the development of anti-SARS-CoV-2 titers were developed at a faster rate compared to SARS-CoV infections [59] and produced antibodies from convalescent serum samples were efficient in treating both coronaviruses, SARS-CoV and SARS-CoV-2 [60,61]. It is worth noting that not all SARS-CoV-2 recovered patients have displayed a long-lasting immunity which could probably explain the SARS-CoV-2 reinfections.

Aside from the binding antibodies that are secreted by B cells firstly against the N protein then against the viral S protein 4-8 days post infection, main protection against SARS-CoV-2 is contributed to the neutralizing antibodies that are also secreted by B cells after 2 to 3 weeks with the help of CD4+ cells [55]. Similar to SARS-CoV, the receptor binding domain (RBD) of the spike protein represents the major target of neutralizing antibodies [62]. The latter are monoclonal antibodies with viral neutralizing potency that compete with ACE2 to block RBD-ACE2 interaction and viral entry to host cell [62]. Antibodies developed against RBD, S and N proteins display a correlated pattern where IgG and IgA were detected in almost all SARS-CoV-2 patients and IgM detected in fewer cases [53,62]. Unlike the availability of T cells subtypes, the titers of the neutralizing antibodies are not used as a predictive tool of COVID-19 severity. Moreover, understanding the pharmacokinetics of the neutralizing antibodies along with the coordination with T cells

subtypes represent a powerful tool for a wide therapeutic range that can be used in treating SARS-CoV-2 infections.

Immuno-based Therapy in SARS-CoV-2 Treatment

As we have previously displayed the pathophysiology of SARS-CoV-2 infection and its downstream immunological features that efficiently contribute to the disease progression, several therapeutic interventions in this context have been introduced to target the dysfunction in the immunoregulation or the viral infection directly. Aside from the approaches that aim to block viral entry via blocking ACE2 receptor using the soluble humanized ACE2 or other drugs that are tested clinically [63–65], several immunosuppressive strategies have been assessed in treating SARS-CoV-2 infections. Among these strategies are the use of corticosteroids that were found to suppress immune cells in COVID-19 patients despite the deleterious effect it was thought to have [66,67]. In this regard, a novel anti-inflammatory therapeutic approach aiming to absorb cytokines has been also assessed on COVID-19 patients experiencing cytokines storm This strategy involves the use of a filter device called the Cytosorb that has successfully contributed to the survival of critically ill patient [68]. Additionally, antibody-based therapies have been also studied like the use of human monoclonal antibodies including sarilumab and tocilizumab to inhibit IL-6 and prevent its binding to its receptor [69–71] and the granulocyte–macrophage colony-stimulating factor (GM-CSF) targeting antibodies like gimsilumab [72] and lenzilumab [73] to limit the inflammatory reaction during infection. Besides, COVID-19 patients have successfully gained passive immunity through the infusion of neutralizing antibodies from convalescent plasma, also called the convalescent plasma therapy, of recovered COVID-19 patients. CPT mainly contains IgG and IgM that play a major role in binding to SARS-CoV-2 and restricting its progression [74-76]. The antibodies acquired immunity in the context of SARS-CoV-2 can either be achieved passively as discussed earlier, or actively using antiviral vaccines. Most successful SARS-CoV-2 vaccines to date have mainly targeted the spike glycoprotein of the virus despite the various approaches that included inactivated and attenuated

virus, RNA and DNA based vaccines or adenovirus vectors introducing viral antigens [77].

Furthermore, a cell-based therapeutic approach has recently gained attention during SARS-CoV-2 infections, after it's been highlighted in cancer treatments. Interestingly, different clinical trials have been conducted to assess the effectiveness of treating COVID-19 with various immune cells including the natural killer cells [78,79], dendritic cells and macrophages [80]. In addition to T lymphocytes based therapy that are transferred from convalescent donor to newly infected patients in a process called adoptive transfer [81]. On top of the cell-based therapy comes the role of the mesenchymal stem cells that have an immunomodulatory effect through inhibiting cytokine production and reducing immune cells activation, where several clinical studies have been designed in this regard [82–85].

Conclusion

Throughout this chapter, we review the underlying immunopathogenesis during SARS-CoV-2 infection. Based on the precedent, understanding the immunological features in COVID-19 patients plays a crucial role in controlling the infection and limiting its progression. So far, different vaccines have shown encouraging results and high efficiency in clinical trials, moreover, no effective treatment has been reported yet, the fact that highlights the importance of extensive research efforts to test the safety and efficacy of immune-based therapy in treating SARS-CoV-2 infections and preventing its progress.

References

1. J Cui, F Li, ZL Shi. Origin and evolution of pathogenic coronaviruses. Nat. Rev. Microbiol. 2019; 17: 181–192.
2. R Lu. Genomic characterisation and epidemiology of 2019 novel coronavirus: implications for virus origins and receptor binding. Lancet Lond. Engl. 2020; 395: 565–574.
3. M Letko, A Marzi, V Munster. Functional assessment of cell entry and receptor usage for SARS-CoV-2 and other lineage B betacoronaviruses. Nat. Microbiol. 2020; 1–8.
4. S Badawi, BR Ali. ACE2 Nascence, trafficking, and SARS-CoV-2 pathogenesis: the saga continues. Hum. Genomics.

2021; 15: 8.
5. P Mehta, DF McAuley, M Brown, E Sanchez, RS Tattersall, et al. COVID-19: consider cytokine storm syndromes and immunosuppression. Lancet Lond. Engl. 2020; 395: 1033–1034.
6. K Vijay. Toll-like receptors in immunity and inflammatory diseases: Past, present, and future. Int. Immunopharmacol. 2018; 59: 391–412.
7. R Baccala. Sensors of the innate immune system: their mode of action. Nat. Rev. Rheumatol. 2009; 5: 448–456.
8. VK Shah, P Firmal, A Alam, D Ganguly, S Chattopadhyay. Overview of Immune Response During SARS-CoV-2 Infection: Lessons From the Past. Front. Immunol. 2020; 11.
9. LB Ivashkiv, LT Donlin. Regulation of type I interferon responses. Nat. Rev. Immunol. 2014; 14: 36–49.
10. CGK Ziegler. SARS-CoV-2 Receptor ACE2 Is an Interferon-Stimulated Gene in Human Airway Epithelial Cells and Is Detected in Specific Cell Subsets across Tissues. Cell. 2020; 181: 1016-1035.
11. KG Lokugamage. Type I Interferon Susceptibility Distinguishes SARS-CoV-2 from SARS-CoV. J. Virol. 2020; 94.
12. M Buszko. Lessons learned: new insights on the role of cytokines in COVID-19. Nat. Immunol. 2021; 22.
13. MJ Cameron, JF Bermejo-Martin, A Danesh, MP Muller, DJ Kelvin. Human immunopathogenesis of severe acute respiratory syndrome (SARS). Virus Res. 2008; 133: 13–19.
14. CK Wong. Plasma inflammatory cytokines and chemokines in severe acute respiratory syndrome. Clin. Exp. Immunol. 2004; 136: 95–103.
15. SKP Lau. Delayed induction of proinflammatory cytokines and suppression of innate antiviral response by the novel Middle East respiratory syndrome coronavirus: implications for pathogenesis and treatment. J. Gen. Virol. 2013; 94: 2679–2690.
16. J Zhou. Active replication of Middle East respiratory syndrome coronavirus and aberrant induction of inflammatory cytokines and chemokines in human macrophages: implications for pathogenesis. J. Infect. Dis. 2014; 209: 1331–1342.

17. Q Ruan, K Yang, W Wang, L Jiang, J Song. Clinical predictors of mortality due to COVID-19 based on an analysis of data of 150 patients from Wuhan, China. Intensive Care Med. 2020; 1–3.
18. S Sherwani, MWA Khan. Cytokine Response in SARS-CoV-2 Infection in the Elderly. J. Inflamm. Res. 2020; 13: 737–747.
19. E Stephenson. Single-cell multi-omics analysis of the immune response in COVID-19. Nat. Med. 2021; 1–13.
20. HKW Law. Chemokine up-regulation in SARS-coronavirus-infected, monocyte-derived human dendritic cells. Blood. 2005; 106: 2366–2374.
21. R Zhou. Acute SARS-CoV-2 Infection Impairs Dendritic Cell and T Cell Responses. Immunity. 2020; 53: 864-877.
22. VUS Rao. COVID-19: Loss of bridging between innate and adaptive immunity? Med. Hypotheses. 2020; 144: 109861.
23. B Zhang. Immune Phenotyping Based on the Neutrophil-to-Lymphocyte Ratio and IgG Level Predicts Disease Severity and Outcome for Patients With COVID-19. Front. Mol. Biosci. 2020; 7.
24. SH Twaddell, KJ Baines, C Grainge, PG Gibson. The Emerging Role of Neutrophil Extracellular Traps in Respiratory Disease. Chest. 2019; 156: 774–782.
25. KW Chen. Noncanonical inflammasome signaling elicits gasdermin D-dependent neutrophil extracellular traps. Sci. Immunol. 2018; 3.
26. MJ Kaplan, M Radic. Neutrophil extracellular traps: double-edged swords of innate immunity. J. Immunol. Baltim. Md 1950. 2012; 189: 2689–2695.
27. BJ Barnes. Targeting potential drivers of COVID-19: Neutrophil extracellular traps. J. Exp. Med. 2020; 217.
28. Y Zuo. Neutrophil extracellular traps in COVID-19. JCI Insight. 2020; 5.
29. P Sil, H Wicklum, C Surell, B Rada. Macrophage-derived IL-1β enhances monosodium urate crystal-triggered NET formation. Inflamm. Res. Off. J. Eur. Histamine Res. Soc. Al. 2017; 66: 227–237.
30. AK Meher. Novel Role of IL (Interleukin)-1β in Neutrophil Extracellular Trap Formation and Abdominal Aortic Aneurysms. Arterioscler. Thromb. Vasc. Biol. 2018; 38: –

853.
31. Y Xiong. Transcriptomic characteristics of bronchoalveolar lavage fluid and peripheral blood mononuclear cells in COVID-19 patients. Emerg. Microbes Infect. 2020; 9: 761–770.
32. S Li. SARS-CoV-2 triggers inflammatory responses and cell death through caspase-8 activation. Signal Transduct. Target. Ther. 2020; 5.
33. A Donia, H Bokhari. Apoptosis induced by SARS-CoV-2: can we target it? Apoptosis. 2021; 26: 7–8.
34. F Yang, Y He, Z Zhai, E Sun. Programmed Cell Death Pathways in the Pathogenesis of Systemic Lupus Erythematosus. J. Immunol. Res. 2019; 2019.
35. H Nakamura, T Kinjo, W Arakaki, K Miyagi, M Tateyama, et al. Serum levels of receptor-interacting protein kinase-3 in patients with COVID-19. Crit. Care. 2020; 24.
36. AC Ferreira. SARS-CoV-2 induces inflammasome-dependent pyroptosis and downmodulation of HLA-DR in human monocytes. medRxiv. 2020.
37. J Zhang. Pyroptotic macrophages stimulate the SARS-CoV-2-associated cytokine storm. Cell. Mol. Immunol. 2021; 18.
38. DR Miller, SD Cramer, A Thorburn. Chapter Five - The interplay of autophagy and non-apoptotic cell death pathways. In: JKE Spetz, L Galluzzi, editors. International Review of Cell and Molecular Biology, vol. 352. London: Academic Press. 2020; 159–187.
39. I Huang, R Pranata. Lymphopenia in severe coronavirus disease-2019 (COVID-19): systematic review and meta-analysis. J. Intensive Care. 2020; 8: 36.
40. G Zhang. Clinical features and short-term outcomes of 221 patients with COVID-19 in Wuhan. China, J. Clin. Virol. 2020; 127: 104364.
41. J Gu. Multiple organ infection and the pathogenesis of SARS. J. Exp. Med. 2005; 202: 415–424.
42. A Assiri. Epidemiological, demographic, and clinical characteristics of 47 cases of Middle East respiratory syndrome coronavirus disease from Saudi Arabia: a descriptive study. Lancet Infect. Dis. 2013; 13: 752–761.
43. I Thevarajan. Breadth of concomitant immune responses prior to patient recovery: a case report of non-severe

COVID-19. Nat. Med. 2020; 1–3.
44. X Wang, J Gui. Cell-mediated immunity to SARS-CoV-2. Pediatr. Investig. 2020; 4: 281–291.
45. Z Xu. Pathological findings of COVID-19 associated with acute respiratory distress syndrome. Lancet Respir. Med. 2020; 8: 420–422.
46. R Liu. Decreased T cell populations contribute to the increased severity of COVID-19. Clin. Chim. Acta Int. J. Clin. Chem. 2020; 508: 110–114.
47. ME Schmidt, SM Varga. The CD8 T Cell Response to Respiratory Virus Infections. Front. Immunol. 2018; 9.
48. MZ Tay, CM Poh, L Rénia, PA MacAry, LFP Ng. The trinity of COVID-19: immunity, inflammation and intervention. Nat. Rev. Immunol. 2020; 20.
49. A Roberts. A Mouse-Adapted SARS-Coronavirus Causes Disease and Mortality in BALB/c Mice. PLOS Pathog. 2007; 3: e5.
50. J Zhao, J Zhao, S Perlman. T Cell Responses Are Required for Protection from Clinical Disease and for Virus Clearance in Severe Acute Respiratory Syndrome Coronavirus-Infected Mice. J. Virol. 2010; 84: 9318–9325.
51. DH Libraty, KM O'Neil, LM Baker, LP Acosta, RM Olveda. Human CD4+ memory T-lymphocyte responses to SARS coronavirus infection. Virology. 2007; 368: 317–321.
52. LT Yang. Long-lived effector/central memory T-cell responses to severe acute respiratory syndrome coronavirus (SARS-CoV) S antigen in recovered SARS patients. Clin. Immunol. Orlando Fla. 2006; 20: 171–178.
53. C Rydyznski Moderbacher. Antigen-Specific Adaptive Immunity to SARS-CoV-2 in Acute COVID-19 and Associations with Age and Disease Severity. Cell. 2020; 183: 996-1012.
54. AD Redd. CD8+ T cell responses in COVID-19 convalescent individuals target conserved epitopes from multiple prominent SARS-CoV-2 circulating variants. MedRxiv Prepr. Serv. Health Sci. 2021.
55. S Crotty. T Follicular Helper Cell Biology: A Decade of Discovery and Diseases. Immunity. 2019; 50: 1132–1148.
56. A Grifoni. Targets of T Cell Responses to SARS-CoV-2 Coronavirus in Humans with COVID-19 Disease and

Unexposed Individuals. Cell. 2020; 181: 1489-1501.
57. QX Long. Antibody responses to SARS-CoV-2 in patients with COVID-19. Nat. Med. 2020; 26: 845–848.
58. L Ni. Detection of SARS-CoV-2-Specific Humoral and Cellular Immunity in COVID-19 Convalescent Individuals. Immunity. 2020; 52: 971-977.
59. J Peiris. Clinical progression and viral load in a community outbreak of coronavirus-associated SARS pneumonia: a prospective study. Lancet Lond. Engl. 2003; 361: 1767–1772.
60. Y Cheng. Use of convalescent plasma therapy in SARS patients in Hong Kong, Eur. J. Clin. Microbiol. Infect. Dis. 2005; 24: 44–46.
61. YOY Soo. Retrospective comparison of convalescent plasma with continuing high-dose methylprednisolone treatment in SARS patients. Clin. Microbiol. Infect. 2004; 10: 676–678.
62. B Ju. Human neutralizing antibodies elicited by SARS-CoV-2 infection. Nature. 2020; 584.
63. G Wang. Dalbavancin binds ACE2 to block its interaction with SARS-CoV-2 spike protein and is effective in inhibiting SARS-CoV-2 infection in animal models. Cell Res. 2021; 31.
64. M Vaduganathan, O Vardeny, T Michel, JJV McMurray, MA Pfeffer, et al. Renin–Angiotensin–Aldosterone System Inhibitors in Patients with Covid-19. N. Engl. J. Med. 2020.
65. H Kai, M Kai. Interactions of coronaviruses with ACE2, angiotensin II, and RAS inhibitors—lessons from available evidence and insights into COVID-19. Hypertens. Res. 2020; 43.
66. X Tang. Early Use of Corticosteroid May Prolong SARS-CoV-2 Shedding in Non-Intensive Care Unit Patients with COVID-19 Pneumonia: A Multicenter, Single-Blind, Randomized Control Trial. Respir. Int. Rev. Thorac. Dis. 2021; 100: 116–126.
67. S Huanzhong. Efficacy and Safety of Corticosteroids in COVID-19: A Prospective Randomized Controlled Trails. clinicaltrials.gov, Clinical trial registration NCT04273321. 2020. Available online at: https://clinicaltrials.gov/ct2/show/NCT04273321
68. S Rizvi, M Danic, M Silver, V LaBond. Cytosorb filter: An

adjunct for survival in the COVID-19 patient in cytokine storm? A case report. Heart Lung. 2021; 50: 44–50.
69. FX Lescure. Sarilumab in patients admitted to hospital with severe or critical COVID-19: a randomised, double-blind, placebo-controlled, phase 3 trial. Lancet Respir. Med. 2021; 9: 522–532.
70. IO Rosas. Tocilizumab in Hospitalized Patients with Severe Covid-19 Pneumonia. N. Engl. J. Med. 2021; 384: 1503–1516.
71. O Abani. Tocilizumab in patients admitted to hospital with COVID-19 (RECOVERY): a randomised, controlled, open-label, platform trial. The Lancet. 2021; 397: 1637–1645.
72. Kinevant Sciences GmbH, A Multi-Center, Adaptive, Randomized, Double-blind, Placebo-controlled Study to Assess the Efficacy and Safety of Gimsilumab in Subjects With Lung Injury or Acute Respiratory Distress Syndrome Secondary to COVID-19 (BREATHE), clinicaltrials.gov, Clinical trial registration NCT04351243. 2021. Available online at: https://clinicaltrials.gov/ct2/show/NCT04351243
73. Humanigen, Inc., A Phase 3 Randomized, Placebo-Controlled Study of Lenzilumab in Hospitalized Patients With Severe and Critical COVID-19 Pneumonia, clinicaltrials.gov, Clinical trial registration NCT04351152. 2021. Available online at: https://clinicaltrials.gov/ct2/show/NCT04351152
74. AM Cheraghali, H Abolghasemi, P Eshghi. Management of COVID-19 Virus Infection by Convalescent Plasma. Iran. J. Allergy Asthma Immunol. 2020; 19: 3–6.
75. C Shen. Treatment of 5 Critically Ill Patients With COVID-19 With Convalescent Plasma. JAMA. 2020; 323: 1582–1589.
76. EM Bloch. Deployment of convalescent plasma for the prevention and treatment of COVID-19. J. Clin. Invest. 2020; 130: 2757–2765.
77. A Esmaeilzadeh, R Elahi. Immunobiology and immunotherapy of COVID-19: A clinically updated overview. J. Cell. Physiol. 2020; 236: 2519-2543.
78. Xinxiang medical university, Clinical Investigation of Natural Killer Cells Treatment in Pneumonia Patients Infected With 2019 Novel Coronavirus, clinicaltrials.gov,

Clinical trial registration NCT04280224. 2021. Available online at: https://clinicaltrials.gov/ct2/show/NCT04280224
79. CAP Lopez. Phase I / II Clinical Study of Immunotherapy Based on Adoptive Cell Transfer as a Therapeutic Alternative for Patients With COVID-19 in Colombia, clinicaltrials.gov, Clinical trial registration NCT04344548. 2021. Available online at: https://clinicaltrials.gov/ct2/show/NCT04344548
80. S Lega, S Naviglio, S Volpi, A Tommasini. Recent Insight into SARS-CoV2 Immunopathology and Rationale for Potential Treatment and Preventive Strategies in COVID-19, Vaccines. 2020; 8.
81. KK Women's and Children's Hospital, Novel Adoptive Cellular Therapy With SARS-CoV-2 Specific T Cells in Patients With Severe COVID-19, clinicaltrials.gov, Clinical trial registration NCT04351659. 2020. Available online at: https://clinicaltrials.gov/ct2/show/NCT04351659
82. Q Zhou. Safety and Efficacy Study of Human Embryonic Stem Cells Derived M Cells (CAStem) for the Treatment of Severe COVID-19 Associated With or Without Acute Respiratory Distress Syndrome (ARDS). clinicaltrials.gov, Clinical trial registration NCT04331613. 2020. Available online at: https://clinicaltrials.gov/ct2/show/NCT04331613
83. S Li. Safety and Efficacy of Intravenous Infusion of Bone Marrow-Derived Mesenchymal Stem Cells in Severe Patients With Coronavirus Disease 2019 (COVID-19): A Phase 1/2 Randomized Controlled Trial. clinicaltrials.gov, Clinical trial registration NCT04346368. 2020. Available online at: https://clinicaltrials.gov/ct2/show/NCT04346368
84. SBÜ Dr. Sadi Konuk Eğitim ve Araştırma Hastanesi, What is the Effect of Mesenchymal Stem Cell Therapy on Seriously Ill Patients With Covid 19 in Intensive Care? (Prospective Double Controlled Study). clinicaltrials.gov, Clinical trial registration NCT04392778. 2021. Available online at: https://clinicaltrials.gov/ct2/show/NCT04392778
85. E Bari, I Ferrarotti, L Saracino, S Perteghella, ML Torre, et al. Mesenchymal Stromal Cell Secretome for Severe COVID-19 Infections: Premises for the Therapeutic Use. Cells. 2020; 9.

Book Chapter

Wnt Pathway Dysregulation and Immune System: Two Culprits of CRC Initiation & Progression

Zeinab Homayed[#], Guillaume Belthier[#] and Julie Pannequin*

Montpellier University - Institute for Functional Genomics: Department of Physiology and Cancer UMR5203 CNRS U1191 INSERM, France

[#]These authors have contributed equally.

***Corresponding Author:** Julie Pannequin, Montpellier University - Institute for Functional Genomics: Department of Physiology and Cancer UMR5203 CNRS U1191 INSERM, Montpellier, France

Published **October 07, 2021**

How to cite this book chapter: Zeinab Homayed, Guillaume Belthier, Julie Pannequin. Wnt Pathway Dysregulation and Immune System: Two Culprits of CRC Initiation & Progression. In: Hussein Fayyad Kazan, editor. Immunology and Cancer Biology. Hyderabad, India: Vide Leaf. 2021.

Intestinal Homeostasis

The gastrointestinal tract is one of the largest exposed and challenged organ in the human body. It is constantly in contact with the outside microenvironment. Thus, it must constitute an obstacle in front of external pathogens and toxic substances but

in the meantime, it should allow the absorbance of nutrients coming from food processing. This mechanism is finely tuned by many cell types that interact not only with each other, but also with the immune system in order to preserve the host defense and to maintain the intestinal homeostasis. Any abnormal activation of the immune system can lead to the development of several inflammatory diseases such as inflammatory bowel disease (IBD) and Crohn disease that make patients more prone to develop colorectal cancer (CRC) [1].

Structure and Organization of the Intestinal Tract

The intestinal tract can be described as a tube whose wall is assembled by three tissue layers: 1) the outer layer is mainly composed of smooth muscle connected with the nervous system and permitting the peristaltic movement of the intestine; 2) stroma, the connective tissue between the outer muscle layer and the inner epithelial part, filled by numerous immune cells; and 3) the luminal surface termed also the mucosa formed by a continuous monolayer of epithelial cells that is characterized by an immense turnover capacity.

The architecture as well as the cellular composition of this epithelium differs between the small and the large intestine.

In the small intestine, the epithelium forms two spatially defined partitions: an invaginated part called the crypt also known as gland of Lieberkühn and a projection into the lumen part called the villi. The villus epithelium is entirely composed of differentiated cells mainly enterocytes with an absorptive role, Goblet cells specialized with the secretion of mucin and tuft cells dedicated to immunity. The crypts are the main site of cellular proliferation and differentiation. Paneth cells are the only fully differentiated cells localized specifically at the base of the crypt and surrounding intestinal stem cells from both sides [2]. The intestinal stem cells give rise to transient proliferative progenitor cells along the crypt-villus axis which in turn differentiate and mature while migrating apically along the crypt. As the cells migrate apically, they acquire properties enabling them to exert a

specific function. Once intestinal epithelial cells arrive at the apex of the crypts, , two scenarios can be observed: they can either undergo apoptosis to be further shed into the lumen or they detach from the underlying extracellular matrix and activate a cell death program termed anoikis [3]. In homeostatic conditions, the entire intestinal crypt is estimated to be replaced every 4-5 days in mice and approximately every week in human [4].

In the large intestine, the colonic epithelium is organized into crypt structures only. The apical part contains the same differentiated cells found in the villi of the small intestine. Except the absence of Paneth cells, the bottom of the crypt contains also stem cells that give rise to progenitors in order to regenerate the colonic epithelium.

Intestinal Stem Cells

Residing at the basal compartment of crypts, intestinal stem cells (ISC) are multipotent adult stem cells with a continuous self-renew capacity throughout life. ISC can give rise to either another stem cell to maintaining the self-renew or to a progenitor cell that will rapidly divide and differentiate into specialized intestinal epithelial cells.

Using elegant lineage tracing, the laboratory of Hans Clever has demonstrated that leucine-rich-repeat-containing G-protein-coupled receptor 5 expression (Lgr5) was a reliable ISC marker [5]. Using a 3-dimensional culture condition, single Lgr5 positive cells isolated from the intestine were able to sufficiently form intestinal organoids with a crypt/villus resembling architecture and recapitulating all epithelial intestinal cell types [6]. Another study has reported that Lgr5 was a targeted gene of the canonical Wnt/ β-catenin signaling pathway that actively catalyze stem cell self-renewal [7].

Physiologically, this self-renewal capacity is finely regulated by a specialized microenvironment called the stem cell niche maintaining a balance between proliferation and differentiation. This microenvironment in closed proximity with ISC contains

non-epithelial stromal cells such as immune cells (lymphocytes, macrophages, neutrophils), neural cells, endothelial cells as well as the intestinal epithelial cell secretome (i.e., Paneth cells secreted factors). These different cell types produce distinct niche ligands such as Wnt, R-spondin, bone morphogenic protein (BMP), epidermal growth factor (EGF), all crucial for the maintenance of ISC behavior and to limit an excessive stem cell production leading to cancer development [8].

Signaling Pathways Regulating Intestinal Homeostasis

Wnt/ β-Catenin Signaling Pathway

The canonical Wnt signalling pathway is considered as a major trigger of intestinal stem cells proliferation. It is activated through the binding of Wnt ligands to their core receptors Frizzled (FZD) as well as to the low-density lipoprotein receptor-related protein 5/6 (LRP5/6) co-receptors. Simultaneously, this complex will inhibit the β-catenin ubiquitination dependent degradation complex composed of adenomatous polyposis coli (APC), Axin, casein Kinase 1 (CK1) and glycogen synthase kinase 3β (GSK3β) leading to β-catenin nuclear translocation, its association with LEF/TCF factors and consequently the transcriptional activation of Wnt target genes regulating stemness, cell proliferation and differentiation and cell cycle progression [9].

Genetic studies have highlighted the pivotal role of the Wnt signalling in maintaining the self-renewal capacity of ISCs where a drastic impact on intestinal proliferation had been observed after the knock-out of Tcf4 or the overexpression of a secreted Wnt antagonist Dickkopf-1 (DKK1) [10-12].

The source of Wnt proteins in the ISC niche has been the focus of many studies. Nineteen different Wnt genes are expressed in a distinct pattern in diverse cell types of the epithelial as well as the stromal layer of the intestine [13]. The essential role of stromal cells in the Wnt secretion was demonstrated by the fact that Wnt3a deletion, mainly secreted by Paneth cells, does not affect intestinal regeneration post-injuries [14]. However, the

deletion of a subpopulation of mesenchymal stromal cells expressing forkhead box l1 (Foxl1) prompted a loss of Wnt2b, Wnt4 and Wnt5a expression in the crypt and a loss of Lgr5+ ISC along with severe crypt loss and shortening of the gut tube [15]. Moreover, blocking Wnt secretion specifically in Gli1 positive sub-epithelial stromal cells prevents ISC self-renewal and consequently the destruction of the epithelium leading to death [16].

In addition to its role in maintaining intestinal homeostasis, Wnt signaling pathway also play a major role in intestinal regeneration following injuries. It is largely known that the intestinal epithelium can regenerate in response to damaging stress that disrupt the tissue. This regeneration is assured by an increase of cellular proliferation within the crypt compartment [17]. Several studies have demonstrated that the activation of Wnt signaling is a key event for intestinal regeneration induction. In respond to DNA damage, Ashton et al., have demonstrated that the activation of c-Myc, a Wnt target, is essential in inducing intestinal regeneration via focal adhesion and Akt/mTor signaling [18]. Moreover, following wound injury, an expansion of mesenchymal cells expressing Wnt5a in the stroma was observed. This Wnt Ligand was required for crypt regeneration mediated by activation of TGF-beta signaling [19]. Interestingly, blocking Wnt secretion by macrophages, major constituent of intestinal stroma, resulted an impaired recovery from radiation injury along with loss of Lgr5 positive cells and a decrease of survival. These results suggest that macrophage-derived Wnt are critical for intestinal regeneration following injuries [20].

Finally, aging is a complex process where a decrease in the capacity of tissue regeneration is observed. Indeed, in an ageing intestine, a decrease of Wnt3 in the stem cell compartment and in its niche was seen [21].This phenomenon was accompanied by an alteration of ISCs function, with a decrease in the expression of cell proliferation and extracellular matrix production related genes. This aging-related occurrence leads to an overall reduction in ISCs regenerative capacity but in the other hand it

might play a protective role to counter a hyper activation of age-related mutations that could cause intestinal hyperplasia.

TGF/BMP Signalling Pathway

Bone morphogenic proteins (BMPs) are signaling proteins that belong to the transforming growth factor β (TGFβ) family of morphogenic proteins. They were first known for their role in bone and cartilage formation but nowadays, studies have demonstrated an important role of BMPs in organ development and tissue homeostasis [22]. In the intestine, the BMP signalling pathway is a negative regulator of intestinal cellular proliferation and it limits the number of ISCs in the crypt [23]. The BMPs signal by binding to BMP type I and II receptors which in turn will phosphorylate SMADs 1, 5, and 8 receptors (SMAD1/5/8). This will allow the formation of a complex with SMAD4 and therefore its translocation into the nucleus to regulate the transcription pattern of target genes [24]. BMP is expressed in a decreasing gradient along the crypt-villus axis, where the apical cells have the highest BMP signalling activity. Both differentiated intestinal epithelial and mesenchymal cells express BMP ligands. These BMPs will act on differentiated cells that express BMP receptors mediating their apoptosis, suggesting a tumor suppressive role of BMPs [25]. BMP antagonists are mainly present in the ISCs niche. A genomic analysis has demonstrated that myofibroblasts and smooth muscle cells localized at the bottom of the crypts express BMP antagonists inhibiting the differentiation of surrounding basal crypt cells and contributing to the stem cell niche [26].

Behind its role in maintain tissue homeostasis, a dysregulation of BMP signaling is associated with several diseases including colorectal cancer. Mutations in the BMP pathway were found in patients with juvenile polyposis that have an increased risk of developing CRC [27]. In addition, Knocking out Smad4 in mice leads to gastric and duodenal polyp formation [28]. Furthermore, mice with an inducible BMP type 1 receptor mutation develop intestinal polyps with an abnormal extended mesenchymal stroma [23]. These studies link the BMP signalling disruption with the initiation of adenomas in both humans and mice.

EGFR Signaling Pathway

Epidermal growth factor (EGF) is an extracellular ligand mediating cellular proliferation, migration and differentiation through binding to its epidermal growth factor tyrosine kinase receptor (EGFR) also known as ErbB1/HER1. Once EGFR is activated by EGF, it forms an active homodimer with an auto-phosphorylation activity which drives the activation of downstream effectors by phosphorylating their SH2 domains. EGFR can activate many signaling pathways including the mitogen-activated protein kinase MAPK/ERK, phosphatidylinositol 3-kinase (PI3K), phospholipase C (PLC) and Jun N-terminal kinases (JNK) [29]. EGF is highly secreted by the mesenchyme and Paneth cells in the ISC niche. In addition, using an EGFR reporter mice, a study has demonstrated a strong expression pattern of EGFR in the villus compartment compared to the crypt and more precisely, a stronger expression in the transit-amplifying cells (TA) and ISCs [30]. Importantly, a strong control of this signalling pathway is needed to maintain a balance between a quiescent and proliferative state in ISCs. This control is maintained by a negative regulator transmembrane protein Lrig1, also described as a ISC marker, that will induce the ubiquitination of the EGFR receptor and thus its degradation. Furthermore, Lrig1 knock out mice presented enlarged crypt morphology associated with a drastic expansion of the stem cell compartment [31].

Notch Signalling Pathway

The Notch pathway is a highly-conserved cascade that signals via direct cell to cell contact. In the intestine, Notch controls several aspects of homeostasis by regulating the differentiation of progenitor cells into enterocytes, regulating the intestinal cell fate between absorptive and secretory cell types and finally regulating the proliferation of intestinal epithelial cells [32,33]. The Notch family comprises four transmembrane receptors (Notch1-4) and five transmembrane ligands (Jagged 1-2, Delta-like 1,3 and 4). Out of these 4 Notch receptors, Notch1 has been reported to be expressed in ISC and transit-amplifying TA cells, whereas, Notch2 is expressed by some crypt cells [34,35]. The

ligands Delta-like 1 and 4 are expressed by secretory cells, markedly by Paneth cells localized in proximity with ISC. In addition, Jagged 1 and 2 ligands were reported to be co-expressed by Notch1+ cells. All these ligands enrich the stem cell niche in Notch signals to activate the Notch pathway in ISCs [36]. Once Notch ligand binds to its Notch receptor, γ-secretase protein complex will cleave the Notch receptor resulting in an active form of Notch which is the Notch intracellular domain (NICD). Subsequently, NICD will be translocated into the nucleus to form a complex with the central transcription factor (CSL) and other co-activators to drive the expression of target genes [37].

An ectopic activation of Notch signaling promotes ISC proliferation at the bottom of the crypt along with a preferential differentiation of progenitor cells toward absorptive cells but not secretory cells [33,38]. Furthermore, Notch signalling pathway inhibition in mice using Dibenzazepine (DBZ) was associated with a decrease of LGR5+ cell number and reduction of stem cell proliferation [39].

Signaling Pathway Dysregulation and CRC Tumorigenesis

According to GLOBOCAN 2020 study, CRC is the second most deadly cancer in both sexes and the third commonly diagnosed cancer worldwide. The CRC usually starts with non-cancerous proliferation of epithelial cells leading to polyp or adenoma formation that can gradually grow for multiple years before becoming cancerous. The risk of cancer increases when the polyp gets bigger. A small percentage of adenomas can progress to an invasive cancer known as adenocarcinoma, when cancer cells invade nearby lymph nodes or tissue and finishing with a metastasis to distant organs mainly to the liver and the lung.

Various genes associated with Wnt, EGFR/MAPK, Notch and TGF-β signalling pathways have been frequently reported to be mutated in CRC. These mutations will cause a dysregulation of signalling pathways leading to an increase in cell proliferation, apoptosis inhibition and a gain invasion capacities, thus, to CRC progression.

According to the multistep carcinogenesis theory of Fearon and Vogelstein [40], intestinal epithelial cells accumulate a number of molecular alterations leading to malignant cell formation. It starts with an activating mutation of Wnt pathway, most frequently due to APC inactivation, leading to benign adenoma initiation. An advanced adenoma stage can be driven by an activating mutation of K-ras, an oncogenic component of mitogen activated protein kinase (MAPK) signalling pathway which is a member of EGFR signaling cascade. The transition to malignancy can be induced by a bi-allelic inactivating mutation of the "guardian of the genome" p53 involved in multiple essential cellular processes such as cell cycle arrest, apoptosis and senescence [40–42].

Initially, during the transition between normal intestinal epithelial and pre-cancerous lesions, the bi-allelic inactivating mutation of the adenomatous polyposis coli (APC), a tumor-suppressor gene is believed to cause the transformation of normal intestinal epithelial cells to a benign adenoma at early stage of CRC [43]. APC is a key negative regulator of the Wnt signaling pathway. In normal condition, the APC control the cellular proliferation and differentiation processes in the gastrointestinal tract, by promoting β–catenin exports from the nucleus [44]. APC mutations lead to a constitutive activation of the Wnt signaling pathway translated by a nuclear accumulation of β-catenin, thus, an upregulation of its downstream target such as Myc and cyclinD1, the main drivers of tumor formation due to their key roles in cell cycle progression and proliferation [45]. In 2012, The Cancer Genome Atlas consortium has estimated that more than 93% of sporadic CRC harbored at least one mutation in a key regulator of the Wnt signalling pathway suggesting that an uncontrolled Wnt signalling pathway is a hallmark of colorectal cancer [46]. Considerably, many model systems have been used to improve our knowledge on the Wnt pathway in CRC including transgenic animal models and organoids. To detail some, the earliest genetically engineered mouse model, generated in early 1990s, was the Apc^{Min} where 1 allele of the APC gene encodes for a nonsense truncating mutation at the 850 codon. Additionally, using homologous recombination in embryonic stem cells, several APC mutant mice have been

generated: $APC^{\Delta 14}$ which contains a frame shift mutation at the codon 580 [47]; $APC^{\Delta 1309}$ also containing a frame shift at codon 1309 [48]; $APC^{\Delta 716}$ which contains a truncating mutation at codon 716 and many other mutant forms [49]. All these germline mutations predispose mice to intestinal adenoma formation and all the adenomas are histologically indistinguishable between mice model but the only difference is the number of adenomas formation. For exemple, $APC^{\Delta 716}$ mouse forms ~ 300 polyps however, $APC^{\Delta 14}$ develops ~65 [50]. Conversely, all these mice will predominantly develop adenomas in the intestine rather than in the colon like in humans [51]. In order to specifically localize tumor development in the colon, scientist have developed inducible tissue-specific Cre mice, such as Cdx2-CreER [52], Car1-CreER [53] that when crossed with loxP targeted APC allele develop adenomas in the colon [54]. The use of these mice has demonstrated that the loss of APC is highly sufficient for tumorigenesis initiation. Indeed, hyper-proliferative adenomas where observed 12-16 weeks following doxycycline treatment in shAPC/Lgr5 mouse model, where a conditional loss of APC is induced specifically in LGR5+ cells. More interestingly, the restoration of APC after doxycycline withdrawal was associated with rapid regression of intestinal adenomas, and no macroscopic polyps were visible 2 weeks after APC restoration. Moreover, the addition of Kras and P53 mutations in this mouse model resulted in a drastic acceleration of tumour progression into adenocarcinoma and importantly the APC restoration still induced a sustained tumor regression. This study has demonstrated a clear association between a hyper activated Wnt signalling pathway and adenoma initiation confirming the initial essential role of the constitutively activated Wnt/B-cat pathway described by Fearon & Volgelstein. Nevertheless, activation of additional signaling pathways are needed to promote carcinogenesis [55].

With the development of innovative culture technologies, stem cell-derived organoids also known as organ-like cultures have led to remarkable advances in regenerative biology and human diseases. The definition of organoid is a three-dimensional 3D structure established from stem cells that will self-organize, proliferate and differentiate in order to obtain a tissue like

structure. There are two main types of stem cells initiating organoids: 1) pluripotent stem cells that combine embryonic stem cells (ES) and their synthetic induced pluripotent cells (iPS) and 2) adult stem cells that are organ restricted (aSCs). These two methods have demonstrated a potent potential to infinitely expand normal stem cells in culture [56].

As previously mentioned, Clevers and colleagues in 2009 were the first to establish "mini-guts" 3D culture starting from single LGR5 positive ISC. This breakthrough was based on years of *lineage tracing* studies that unraveled the factors needed to maintain a homeostatic intestinal tissue. From theses required factors for *in-vitro* propagation and differentiation of ISC: R-spondin (Rspo) an agonist of the Wnt Pathway also known as LGR5 ligand, EGF and Noggin which is an inhibitor of the BMP signaling pathway [6]. In addition, along with the recent advances in CRISPR/Cas9 technology, the introduction of plasmids expressing Cas9 and single guide RNAs targeting APC allowed the growth of cystic organoids in a medium lacking Wnt and Rspo. These organoids presented a constitutive activity of Wnt pathway analyzed by an elevated expression of Axin2 mRNA, a Wnt target gene, confirming the importance of APC in suppressing the Wnt signalling pathway [57]. Furthermore, based on the theory of Vogelstein previously detailed, the additional introduction of sequential inactivating mutations of P53, KRAS and SMAD4 in APC knock-out intestinal organoids made the growth of organoids independent of any stem-cell niche factors. Additionally, to mimic the cancer onset, these quadruple mutants organoids were able to grow as invasive carcinomas when they have been injected subcutaneously in immunodeficient mice emphasizing the importance of the use of organoids as a promising in vitro cancer model [58].

Tumor- Infiltrating Cells and Cancer Progression

The immune system is a crucial player in the tissue homeostasis maintenance. However, in a tumorigenic state, the immune system constitutes a main actor during tumor development. It is currently well known that every organ contains resident immune

cells and frequently new ones arrive through the blood or lymphatic system. Moreover, some organs, especially when they are in constant interaction with external pathogens, like the intestine, contain their own second lymphoid organs as the gut associated lymphoid tissue. The most representative lymph nodes of these latter ones are the Payer's patches, small follicles inserted between the mucosa and submucosa layer of the small intestine and mainly composed of T and B cells. Nevertheless, immune cells can be distributed along all the different layers of the intestine. Indeed, many publications reviewed by Viola and Boeckxstaens [59] describe different macrophage subtypes according to their origin and their localization into the intestine. Once a tumor starts to grow, immune cells immediately react with a local infiltration to surround the tumor in order to eliminate these cancer cells [60,61]. However, during tumor progression, cancer cells try to corrupt a part of immune system, especially the myeloid cells, to counteract cytotoxic lymphoid cells. In addition, they also benefit from ECM remodeling and many released immune cytokines to grow and disseminate [62–64]. Following sections will summarize the current general knowledge with some CRC specificities, on the two myeloid cells, macrophages and neutrophils mainly known for their ability to switch from an anti-tumoral to a pro-tumoral phenotype.

Tumor Associated Macrophages

By educating stromal and immune cells to further produce inflammatory mediators, cancer cells induce a chronical moderate inflamed environment. This prolonged inflammation is not only confined within the primary tumour microenvironment but it spreads to distant tissues or organs, as the bone marrow and the spleen, where it stimulates myeloid cell development and mobilization. This results in an accumulation and polarization of myeloid cells systemically and within solid tumors. Indeed, monocytes, precursors of macrophages, proliferate into the bone marrow and go into the blood circulation to finally reach their target destination. Some will never differentiate into macrophages but will actively participate in tumor immune escape. However, many studies have detected the presence of

these immunosuppressive monocytes into the blood or the spleen, indicating that their polarization as immunosuppressive monocytes is already induced distantly by the primary tumor [65–67]. The other part of monocytes will differentiate into macrophages once they reach the tissue or the tumor in response to various chemo-attractant factors such as: damage-associated molecular patterns (DAMPs), pro-inflammatory signalling molecules and chemokines [68,69]. A known example of tumor-derived chemo-attractants is the colony-stimulating factor 1 (CSF1; named also M-CSF), that stimulates the differentiation and maturation of monocytes into tumour-associated macrophages (TAMs).

Macrophages are myeloid cells with a strong phagocytic potential but not with the strongest antigen presentation ability when compared to dendritic cells. However, they often represent a major part of the tumor immune infiltration and they are associated with poor patient outcome [68,70]. This correlation between macrophages and poor prognosis is the consequence of an acquisition or persistence of an immunosuppressive phenotype of these macrophages. However, many studies have shown that an increased density of macrophages in CRC is correlated with a better prognosis [71–74] and in some others, it is correlated with a poor prognosis [75–77]. This discrepancy indicates that macrophages can play opposites roles accordingly to the tissue and cancer type but also along tumor evolution. It is generally accepted that initially the tumor recruited macrophages exhibit pro-inflammatory activity and then, during tumor progression, they switch to a pro-tumor phenotype.

Indeed, the majority of the literature classify macrophages into two types: the ‘classically activated’ or ‘alternatively activated’ macrophages, usually called M1 or M2 macrophages. M1 macrophages are defined as anti-tumorigenic and M2 macrophages as pro-tumorigenic (i.e. TAMs) [78,79]. These polarizations are also found in CRC, with a strong plasticity and intermediate states according to the tumor microenvironment (TME) [80].

The literature has described some main function of M2 macrophages within tumor evolution such as angiogenesis stimulation, extracellular matrix (ECM) remodeling, release and production of growth factors or cytokines to directly boost the tumor growth and modulate other immune cells. Indeed, in human breast cancer and lymphomas, a strong TAM concentration is frequently associated with an increased vascularization [81–83]. This phenomenon was also confirmed in a transgenic mouse model for breast cancer, where CSF1 inactivation leads as expected, to a macrophages deficiency but interestingly, leads also to a decrease in vascularization [84]. Other studies in mouse cancer models had intensively deciphered the TAM pro-angiogenic role by examining how endothelial cell (ED) survival, activation and proliferation are promoted by TAM secretions. Markedly, the well-known vascular endothelial growth factor A (VEGFA), was found as an important macrophage-secreted factor in both human and mouse tumors [85–88]. Furthermore, VEGFA was not only described as a growth factor for EDs but also contributes to facilitating tumor cell intravasation and dissemination by increasing vascular permeability [89]. In addition to the VEGFA and two other VEGF-family members (the placental growth factor (PlGF) and the VEGFC), several other pro-angiogenic factors secreted by TAMs were characterized such as interleukin-1β (IL-1β) and IL-6, fibroblast growth factor 2 (FGF2), tumor necrosis factor (TNF) and inflammatory factor CXC-chemokine ligand 8 (CXCL8; also known as IL-8) [90–92]. TAMs are also a source of some members of the WNT family. Using once again a transgenic mouse model for breast cancer, Wnt7b deletion in TAMs reduced the WNT– β catenin pathway activation in EDs. The consequence is a decrease of the expression of mitogenic β catenin target genes in tumor EDs and a tumor vasculature reduction [93]. In addition, hypoxia induces the expression of CXCL12 (also known as SDF1) and Angiopoetin2 (ANGPT2) by tumor cells and EDs, respectively. Both factors stimulate the recruitment of TAMs that express the respective cognate receptors CXC-chemokine receptor 4 (CXCR4) and TIE2 and lead to their perivascular accumulation. his subpopulation of TAMs called perivascular TAMs, is implicated in tumor angiogenesis [94–96] and positively correlates with a higher

microvascular density and an increase in the dissemination ability in different types of cancer [89,97]. Finally, TAMs express semaphorins, a family of vascular guidance molecules, some of which were described as impacting EDs sur¬vival and migration [98]. However, being one of the M2 characteristics, the pro-angiogenic capacity of TAMs may depend on the specific TME in which they reside and the cytokine medium to which they are exposed [68,90].

The second aspect of the M2 phenotype is the ability to remodel the ECM favoring tumor progression. ECM encompasses 1) the interstitial matrix that forms porous three-dimensional networks around stromal cells, connecting these cells to the basement membrane and 2) the basement membrane that represents a thin but extremely dense ECM, acting as a mechanical frontier between epithelial cells and the interstitial matrix. ECM fibers can be rearranged by an array of secreted enzymes, such as proteases and oxidases. Furthermore, the ECM represents a major source of soluble factors due to its ability to bind growth factors and other ECM-associated proteins. Thereby cell surface receptors can interact with ECM components mediating a broad range of cell behavior like apoptosis, proliferation, differentiation and migration [99]. Noticeably during cancer progression, i.e. once the basement membrane is broken and the tumor become invasive [100], the remodeling of the interstitial ECM induces a large range of changes affecting ECM stiffness, cell signalling, tumor progression (differentiation or CSC trait acquisition) and cell migration. Both in healthy and pathological context, interstitial ECM components production and ECM remodeling are essentially made by fibroblasts, especially once they are activated into myofibroblasts. [101]. However, many other cell types could also induce an ECM remodeling including tumoral and immune cells.

TAMs polarized into an M2-like phenotype and tumor-associated neutrophils (TANs) that we will discuss latter, are important sources of proteases in the tumor microenvironment. The matrix metalloproteinases (MMPs), disintegrin and metalloproteinases with thrombospondin motifs (ADAMTS) and the disintegrin and metalloproteinases (ADAMs) are among the

most well-known and described proteases. These metalloproteinases are counterbalanced by protease inhibitors called tissue inhibitor of metalloproteinases (TIMPs) [102–104]. Indeed, TAMs induce interstitial collagen degradation through MMP overexpression, including proangiogenic TIMP-1-free MMP-9, accompanied by increased endocytosis and lysosomal degradation of collagen [105,106]. Interestingly, macrophages are also able to deposit the glycoprotein osteonectin, which is known to promote stromal invasion in a mouse model of breast cancer [107]. Recently, in a mouse orthotopic colorectal cancer model, TAMs where shown to contribute to ECM deposition. This study highlighted that TAMs are the major cell type to upregulate synthesis, deposition, cross-linking and linearization of collagens, especially collagen types I, VI and XIV around invasive tumoral cells [108]. These data add evidences that immune cells participate not only to ECM degradation but also to ECM deposition.

ECM remodeling by TAMs has a strong impact on cancer cell motility [109]. In addition, due to ECM degradation, some inactive growth factors can be released. For example, fibronectin, binds insulin like growth factor binding-protein-3, FGF-2 and VEGF-A with high affinity [110]. Another example, secreted by cancer and stromal cells, VEGF can bind to the ECM [111] but also can be released through macrophages-produced MMP9, driving angiogenesis and invasiveness [112–114]. Additionally, MMPs can alter tumor progression by a non-proteolytic function. For example, MMP-3 binds and inhibits non-canonical Wnt5b, resulting in a Wnt signaling increase [100].

CRC cells take advantage from pro-tumoral polarized macrophages. Thereby, this crosstalk between both cell types initiates and maintains a positive feed-back loop supporting tumor progression and dissemination. Though publications describing M2 macrophages in CRC remain still rare, some start to decipher this crosstalk. Indeed, CRC cells carrying a missense mutant P53 (but not an inactivating mutation) were shown to release exosomes leading to an M2 polarization. A study, where authors have used patient samples for *ex vivo* experiments as

well as for *in vivo* subcutaneous and intrasplenic CRC cell injections, they have found that macrophages induce an immunosuppressive environment demonstrated by a higher production of ECM remodeling enzymes, pro-angiogenic factors, and factors acting directly on tumor cell growth and mobility as TGF-β and TGF-βi [77]. Additionally to its immune suppressive potential [115], TGF-β is a potent EMT inducer in many cancer types including CRC [116] but only on cancer cells still responsiveness to TGFβ signaling through TGFβ-receptor and SMAD4. However, it is interesting to note that M2 macrophages can produced TGF-βi because this factor was recently described as an enhancer of tumor vascularization and CRC cell migration despite SMAD4 mutation [117]. A series of studies from the same lab described another crosstalk between a specific M2 macrophage subtype and CRC cells. Wnt5a, a member of the Wnt family, was originally observed to be secreted by TAMs in CRC [118]. Based on this observation, Xiong's lab confirmed this observation in CRC patient samples. Additionally, the number of Wnt5a positive TAM correlates with TNM state and is associated with a poor recurrence-free survival (RFS) and overall survival (OS). Behind these effects, CRC cells through their IL-4 secretion, were able to induce Wnt5a TAM expression. Wnt5a acts then as an autocrine factor on the other TAMs, inducing their CCL2 and IL-10 production. Thereby, these cytokines enhance macrophage recruitment, macrophage motility and M2 polarization. Finally, even if a direct or an indirect effect on CRC cells is not yet well deciphered, CCL2 and IL-10 increase also tumor growth, cell migration and circulating tumor cell (CTC) number. Among the diversity of factors secreted by M2 macrophages, some are known for their immunosuppressive potential such as IL-10, TGF-b, VEGF, CCL18, CCL21, CXCL12 that are implicated in tumor evolution and others as IL-6 and TGF- β, play a role in EMT transition [119,120].

TAMs also modulate directly or indirectly T cell activity. Using ovarian carcinoma patient samples, Curiel *et al.,* have found that TAMs constitute an important source of CCL17 and CCL22 that act on directing T reg into the TME [121]. A similar observation was done in CRC mouse models either induced by N-methyl-N-

nitrosourea (MNU) and H. *Pilory* infection or by subcutaneous CRC cell line injection. CCR6 positive T reg cells were strongly attracted into the tumor due to the macrophages-CCL20 production (the sole ligand of CCR6) and this attraction was lost when macrophages were depleted [122]. Additionally, it was also observed in human renal carcinoma that isolated TAMs were able to induce CD4+ T cells differentiation into Treg cells *in vitro* [123]. CD4+ T cell differentiation into Treg and their proliferation could be induced by TGF-β production by myeloids cells like DCs and M2 macrophages [124–127]. Moreover, TAMs can also themselves inactivate CD8+ T cells by either upregulating the ligands PDL1 and PDL2, which actively inhibit TCR signaling on T cells, or by releasing inducible nitric oxide synthase (iNOS) [65,66,128] or TGF-β [115,125,129,130], preventing cytotoxic CD8+ T lymphocytes (CTL) function [131]. Finally, TAMs can also impact CTL function by acting on the initial step of T cell priming into lymph nodes. Indeed, TAM-derived IL-10 can induce lipid accumulation into dendritic cells, suppressing antigen presentation by DCs but also it could reduce IL-12 secretion by DCs. Both decreased significantly DCs ability to prime CTL [132–134]. Together, these different T cell modulations by TAM highlight that blocking TAM recruitment in spontaneous breast cancer mouse model can increase CD8 positive T cell infiltration and CTL activity in the primary tumor [135].

However, recent single-cell RNA sequencing studies unveiled that TAM are distributed along a large range from M1 to M2 phenotype [136–138], reflecting the complexity to attribute a pro or anti-tumoral role of a macrophage population. Macrophages polarization should be defined by several M1 and M2 markers and always interpreted according to the tissue and tumor state. Moreover, the macrophage origin (resident population or monocyte derived) should be further considered. In the future, deciphering intestinal macrophage role during CRC initiation and development could highly help to better understand CRC progression especially since resident breast and lung macrophages were shown to induce early cancer cell dissemination and EMT [139,140].

Neutrophils

Neutrophils, another myeloid cell type of the bone marrow, play a crucial role during acute inflammation especially when an infection occurs. In homeostatic conditions, around 1% of mature neutrophils are circulating [141], and the rest is retained in the bone marrow. Upon infection or during tumor development, factors are produced and transported through the blood until the bone marrow to allow Neutrophil proliferation and recruitment. Indeed, primary tumor cells and their microenvironment induce an elevated systemic level of cytokines, chemokines and growth factors, such as CCL2, CCL15, IL-17, IL-1β, IL-8 and granulocyte colony stimulating factor (G- CSF also called CFS3), contributing to systemic myeloid expansion by two mechanisms. These factors alter hematopoietic lineages in favor of the myeloid lineage, especially toward neutrophil differentiation and then, force the bone marrow to release them into the blood [141]. For example, once CSF3 binds to its receptor (CSF3R) expressed by neutrophil precursors, it activates the Janus kinase (JAK)–signal transducer and activator of transcription 3 (STAT3) pathway, promoting neutrophil proliferation and expansion. Then, the recruitment of neutrophils to the tumors (but also other organs), is in part mediated by CXCL chemokines through CXCR1 and CXCR2 [142]. In the case of CRC, SMAD4 mutated cancer cells are not only unresponsiveness to the cytostatic effect of TGF-β but they also overexpress the myeloid chemokines CCL2 and CCL15 [143,144] involved in neutrophil expansion and recruitment. Interestingly, patient sample analysis indicated that tumor-bearing patients with a high neutrophil to-lymphocyte ratio (NLR) in the circulation is associated with a poor clinical outcome in many different types of cancer including CRC [145–148] especially because they facilitate metastatic spread [149–151]. However, opposing functions of neutrophils have been described, and some evidences suggest that intratumoral neutrophils can have anti-tumor functions. Thereby, it has been suggested that neutrophils may be classified like macrophages as either N1, ‘anti-tumorigenic’, or N2, ‘pro-tumorigenic’ with also differential states of activation and differentiation [152–154]. These latter studies highlighted that the use of binary

classification systems is not yet perfect to fully understand the complexity of the tumor microenvironment. Indeed, neutrophil polarization range is difficult to study because their short half-life complexes their study *in vitro*.

However, some factors inducing a M2 phenotype as TGF-β, induces also a N2 phenotype [152]. This finding has allowed to repeat TGF- β, /macrophages experiments with neutrophils instead. Interestingly, evidences emerged that tumor- derived cytokines and chemokines can prolong neutrophil survival [155,156]. In a CRC mouse model, the cancer stem cell population is particularly responsible of the release of chemokines and exosomes systemically to attract neutrophils. Interestingly, these exosomes contain short RNAs able to induce an N2 phenotype and prolong neutrophils survival, thus, N2 neutrophils can survive for a sufficient amount of time to reach the primary tumor and exert their pro-tumorigenic role [157].

Among N2 markers, the literature had described globally the same four different types of markers previously described for M2 markers. To avoid redundancy, less details will be given for these shared mechanisms between M2 macrophages and N2 neutrophils but emphasize on recent literature describing specific aspects of N2 neutrophils.

Attracted by hypoxic conditions [114], neutrophils are among the most important culprits of pro-angiogenic factors release, especially due to their ability to remodel TME [158]. Indeed, following STAT3 signaling pathway activation by CFS3, N2 neutrophils express several pro-angiogenic proteins such as VEGF-A, FGF2 and MMP9 [159] and it has been shown in human, that exposure to TNF, stimulates rapidly their VEFG-A granule-release [160]. Furthermore, CSF3-STAT3 axis also induces prokineticin-2 over-expression (also called BV8) [129] ; a factor previously described as promoting EC proliferation and angiogenesis in tumors [130]. Concomitant with angiogenic factor release, ECM remodeling proteases produced by neutrophils exacerbate the tumor angiogenesis. The better example is the MMP9, a strong releaser of ECM-bound VEGF-A [163–165]. In addition, compared with TAMs production,

neutrophils are the main source of TIMP-free pro-MMP9 [165–168]. Moreover, like M2 macrophages, N2 neutrophils can directly or indirectly prevent CTL function [169]. Indeed, theyare also a main source of MMP9, known to fully process latent TGF-β into its active form [170], participating to inactivate CTL in CRC [171–173]. Additionally, N2 neutrophils prevents directly or indirectly CTL function also by ROS [142,150] and arginase 1 (Arg1) production [174].

Recently, the major neutrophils' weapon against bacteria, the neutrophil extra-cellular trap (NET), was also described as a key process favoring cancer dissemination through different mechanisms. This neutrophil death program called NETosis is the expel of modified chromatin decorated with bactericidal proteins, acting like a spider web that can catch and kill pathogens [175–177]. Interestingly, circulating tumor cells (CTCs) could take advantages of this NETosis to facilitate their fixation and extravasation in distant target organs. Indeed, many studies, with mouse models and CRC patient data, observed that bacterial infections or exposure to lipopolysaccharides (LPS), a bacterial compound, generates a better CTC fixation on capillary vessel due to the neutrophil NETosis [178–182]. Briefly, this CTC fixation is helped by β-integrin interaction with NET[182]. Furthermore, the literature described that CTCs induce and bring with them N2 neutrophils from the primary tumor to travel in cluster into the blood vasculature. These breast CTCs exhibit a higher proliferation potential than their single or other type of cluster counterparts explaining the poor prognosis of the patient for whom only one of this cluster type is detected in the blood [183]. But the potential of these neutrophils clustered with CTCs to enter into NETosis is unfortunately still unknown. However, it is describe in metastatic sites for breast cancer and CRC, that for example, IL-8 secretion by disseminated cancer cells (DTCs) activate neutrophils NETosis in order to first, create a shield against CTL [172], secondly, to locally facilitate the extravasation/migration capacity of CTCs/DTCs [151] and thirdly, to act also as a chemo-attractant on colorectal and breast CTCs [173]. Finally, a recent study highlighted a side effect of lung inflammation on DTC awaken. Indeed, breast patients without detectable lung metastasis are more prone to develop

metastasis if they have a history of smoking. Using mouse models, this poor prognosis was explained by NETosis activation releasing ECM remodeling proteases as neutrophil-elastase (NE) and MMP9. Thereby, these proteases cleaved the basement membrane laminin. Once cleaved, the laminin products bind the β-integrin of the dormant DTCs and activate an awaken program [186]. The same mechanism could explain CRC metastatic recurrence after liver surgery where significant NETosis is observed after the surgery [187].

Primary tumor in different cancer types appears also to be able of initiating a pre-metastatic niche through secretion of soluble factors/ exosomes into the blood to reach distant sites. This process strongly implicates neutrophil bone-marrow expansion and recruitment in the future distant targeted organs. Indeed, clinical datas and mouse model for ovarian cancer showed that neutrophils are recruited before any detected dissemination and more importantly, that the NETosis will help the future CTC extravasation and their proliferation [188]. As previously discussed above, exosomes can be systemically released to polarize and recruit bone-marrow derived N2 neutrophils into the primary tumor but some evidences start also to demonstrate that exosomes can indirectly recruit neutrophils in the pre-metastatic niche [189]. For example, TIMP-1, produced by the primary tumor and its TME, reaches the liver through the blood and changes hepatocyte expression profile. Among these changes, potent neutrophil chemokines like fibronectin, TGF-β, SDF-1 and urokinase plasminogen activator (uPA) are overexpressed allowing bone-marrow derived neutrophil recruitment into the liver to initiate a pre-metastatic niche [190]. In a specific CRC subtype, using patient data accompanied with mouse models, Jackstadt et al., showed that tumor cells induce bone-marrow derived neutrophil expansion notably through CXCL5 secretion and neutrophil recruitment by TGF-β2 not only into the primary tumor but also into the liver before metastasis formation. This recruitment leads to an immunosuppressive environment orchestrated by a reduction of T cell liver infiltration [191].

Conclusion

The Wnt signaling pathway has emerged as one of the main key biological pathway in regulating intestinal stem cell homeostasis and determining cell fate. In tumorigenic state, since its first association with human FAP and the development of Apc^{Min} mouse model, the Wnt pathway has been highly described as involved in intestinal tumor formation in humans and mice. New technologies such as CRISPR/Cas9 are being used to successfully create innovative and elegant mammalian CRC models. This includes generating transgenic mouse models with multiple genetic mutations mimicking CRC initiation and progression [58], metastatic CRC models [192,193],tools for tracking cancer stem cells in vivo [194], and xenografts from organoids biobank derived from a range of CRC tumors with different clinical stage s [195,196]. These complementary mouse models coupled to organoid culture have greatly improved our knowledge on mechanisms involved in cancer. The impact of aberrant Wnt signaling is not restricted to cancer cells since it dynamically interacts as well with the surrounding microenvironment including the immune system. This latter appears in each cancer type as a potent partner of tumor progression [146,197,198]. However, immunotherapies like immune checkpoint inhibitors represent a promising hope to act in synergy with chemotherapies [199–203]. Initially, CRC tumors were thought as poorly immunologic and immunotherapy failure was expected. However, several studies reported that lymphocyte activation is, indeed, associated with a good prognostic [204]. In addition, some CRC subtypes (Lynch syndrome or microsatellite instability-high (MSI-H) tumors), were more prone to respond to the combination of chemotherapy and immunotherapy [205]. For other subgroups, including sporadic CRC without mutations in DNA mismatch repair (MMR) genes, fundamental research on resident macrophages and other myeloid and lymphoid cells should be done in order to better decipher the role of the immune system along the CRC progression. Thereby, as in breast cancers, potential new targets should be found in order to re-educate the immune system against tumor cells.

References

1. DD Weedon, RG Shorter, DM Ilstrup, KA Huizenga, WF Taylor. Crohn's disease and cancer. N. Engl. J. Med. 1973; 289: 1099–1103.
2. T Sato. Paneth cells constitute the niche for Lgr5 stem cells in intestinal crypts. Nature. 2011; 469: 415–418.
3. JM Williams, CA Duckworth, MD Burkitt, AJM Watson, BJ Campbell, et al. Epithelial Cell Shedding and Barrier Function. Vet. Pathol. 2015; 52: 445–455.
4. LG van der Flier, H Clevers. Stem Cells, Self-Renewal, and Differentiation in the Intestinal Epithelium. Annu. Rev. Physiol. 2009; 71: 241–260.
5. N Barker. Identification of stem cells in small intestine and colon by marker gene Lgr5. Nature. 2007; 449: 1003–1007.
6. T Sato. Single Lgr5 stem cells build crypt-villus structures in vitro without a mesenchymal niche. Nature. 2009; 459: 262–265.
7. W de Lau. Lgr5 homologues associate with Wnt receptors and mediate R-spondin signaling. Nature. 2011; 476: 293–297.
8. BS Sailaja, XC He, L Li. The regulatory niche of intestinal stem cells. J. Physiol. 2016; 594: 4827–4836.
9. BT MacDonald, K Tamai, X He. Wnt/β-catenin signaling: components, mechanisms, and diseases. Dev. Cell. 2009; 17: 9–26.
10. V Muncan. Rapid Loss of Intestinal Crypts upon Conditional Deletion of the Wnt/Tcf-4 Target Gene c-Myc. Mol. Cell. Biol. 2006; 26: 8418–8426.
11. D Pinto, A Gregorieff, H Begthel, H Clevers. Canonical Wnt signals are essential for homeostasis of the intestinal epithelium. Genes Dev. 2003; 17: 1709–1713.
12. F Kuhnert. Essential requirement for Wnt signaling in proliferation of adult small intestine and colon revealed by adenoviral expression of Dickkopf-1. Proc. Natl. Acad. Sci. U. S. A. 2004; 101: 266–271.
13. A Gregorieff, D Pinto, H Begthel, O Destrée, M Kielman, et al.Expression Pattern of Wnt Signaling Components in the Adult Intestine. Gastroenterology. 2005; 129: 626–638.

14. Z Kabiri. Stroma provides an intestinal stem cell niche in the absence of epithelial Wnts. Dev. Camb. Engl. 2014; 141: 2206–2215.
15. R Aoki. Foxl1-Expressing Mesenchymal Cells Constitute the Intestinal Stem Cell Niche, Cell. Mol. Gastroenterol. Hepatol. 2015; 2: 175–188.
16. B Degirmenci, T Valenta, S Dimitrieva, G Hausmann, K Basler. GLI1-expressing mesenchymal cells form the essential Wnt-secreting niche for colon stem cells. Nature. 2015; 558: 449–453.
17. NP Bernal, W Stehr, Y Zhang, S Profitt, CR Erwin, et al. Evidence for active Wnt signaling during postresection intestinal adaptation. J. Pediatr. Surg. 2005; 40: 1025–1029; discussion 1029.
18. GH Ashton. Focal adhesion kinase is required for intestinal regeneration and tumorigenesis downstream of Wnt/c-Myc signaling. Dev. Cell. 2010; 19: 259–269.
19. H Miyoshi, R Ajima, CTY Luo, TP Yamaguchi, TS Stappenbeck. Wnt5a Potentiates TGF-β Signaling to Promote Colonic Crypt Regeneration after Tissue Injury. Science. 2012; 338: 108–113.
20. S Saha. Macrophage-derived extracellular vesicle-packaged WNTs rescue intestinal stem cells and enhance survival after radiation injury. Nat. Commun. 2016; 7: 13096.
21. K Nalapareddy. Canonical Wnt Signaling Ameliorates Aging of Intestinal Stem Cells. Cell Rep. 2017; 18: 2608–2621.
22. RN Wang. Bone Morphogenetic Protein (BMP) signaling in development and human diseases. Genes Dis. 2014; 1: 87–105.
23. XC He. BMP signaling inhibits intestinal stem cell self-renewal through suppression of Wnt-beta-catenin signaling. Nat. Genet. 2004; 36: 1117–1121.
24. CH Heldin, K Miyazono, P ten Dijke. TGF-beta signalling from cell membrane to nucleus through SMAD proteins. Nature. 1997; 390: 465–471.
25. JCH Hardwick. Bone morphogenetic protein 2 is expressed by, and acts upon, mature epithelial cells in the colon. Gastroenterology. 2004; 126: 111–121.
26. C Kosinski. Gene expression patterns of human colon tops and basal crypts and BMP antagonists as intestinal stem cell

niche factors. Proc. Natl. Acad. Sci. 2007; 104: 15418–15423.
27. JR Howe. Germline mutations of the gene encoding bone morphogenetic protein receptor 1A in juvenile polyposis. Nat. Genet. 2001; 28: 184–187.
28. K Takaku, H Miyoshi, A Matsunaga, M Oshima, N Sasaki, et al. Gastric and duodenal polyps in Smad4 (Dpc4) knockout mice. Cancer Res. 1999; 59: 6113–6117.
29. P Wee, Z Wang. Epidermal Growth Factor Receptor Cell Proliferation Signaling Pathways. Cancers. 2017; 9, Art. no. 5.
30. YP Yang. A Chimeric Egfr Protein Reporter Mouse Reveals Egfr Localization and Trafficking in Vivo. Cell Rep. 2017; 19: 1257–1267.
31. VWY Wong. Lrig1 controls intestinal stem cell homeostasis by negative regulation of ErbB signaling. Nat. Cell Biol. 2012; 14: 401–408.
32. J Milano. Modulation of notch processing by gamma-secretase inhibitors causes intestinal goblet cell metaplasia and induction of genes known to specify gut secretory lineage differentiation. Toxicol. Sci. Off. J. Soc. Toxicol. 2004; 82: 341–358.
33. S Fre, M Huyghe, P Mourikis, S Robine, D Louvard, et al. Notch signals control the fate of immature progenitor cells in the intestine. Nature. 2005; 435: 964–968.
34. AJ Carulli, TM Keeley, ES Demitrack, J Chung, I Maillard, et al. Notch receptor regulation of intestinal stem cell homeostasis and crypt regeneration. Dev. Biol. 2015; 402: 98–108.
35. S Fre. Notch Lineages and Activity in Intestinal Stem Cells Determined by a New Set of Knock-In Mice. PLOS ONE. 2011; 6: e25785.
36. GR Sander, BC Powell. Expression of notch receptors and ligands in the adult gut. J. Histochem. Cytochem. Off. J. Histochem. Soc. 2004; 52: 509–516.
37. T Borggrefe, F Oswald. Setting the Stage for Notch: The Drosophila Su(H)-Hairless Repressor Complex. PLoS Biol. 2016; 14: e1002524.

38. BZ Stanger, R Datar, LC Murtaugh, DA Melton. Direct regulation of intestinal fate by Notch. Proc. Natl. Acad. Sci. U. S. A. 2005; 102: 12443–12448.
39. KL VanDussen. Notch signaling modulates proliferation and differentiation of intestinal crypt base columnar stem cells. Dev. Camb. Engl. 2012; 139: 488–497.
40. ER Fearon, B Vogelstein. A genetic model for colorectal tumorigenesis. Cell. 1990; 61: 759–767.
41. KM Sullivan, PS Kozuch. Impact of KRAS Mutations on Management of Colorectal Carcinoma. Pathol. Res. Int. 2011; 2011: 219309.
42. XL Li, J Zhou, ZR Chen, WJ Chng. p53 mutations in colorectal cancer- molecular pathogenesis and pharmacological reactivation. World J. Gastroenterol. WJG. 2015; 21: 84–93.
43. H Nagase, Y Nakamura. Mutations of the APC (adenomatous polyposis coli) gene. Hum. Mutat. 1993; 2: 425–434.
44. A Klaus, W Birchmeier. Wnt signalling and its impact on development and cancer. Nat. Rev. Cancer. 2008; 8: 387–398.
45. L Zhang, JW Shay. Multiple Roles of APC and its Therapeutic Implications in Colorectal Cancer. JNCI J. Natl. Cancer Inst. 2017; 109.
46. Comprehensive molecular characterization of human colon and rectal cancer. Nature. 2012; 487: 330–337.
47. S Colnot. Colorectal cancers in a new mouse model of familial adenomatous polyposis: influence of genetic and environmental modifiers. Lab. Investig. J. Tech. Methods Pathol. 2004; 84: 1619–1630.
48. CF Quesada, H Kimata, M Mori, M Nishimura, T Tsuneyoshi, et al. Piroxicam and acarbose as chemopreventive agents for spontaneous intestinal adenomas in APC gene 1309 knockout mice. Jpn. J. Cancer Res. Gann. 1998; 89: 392–396.
49. M Oshima, H Oshima, K Kitagawa, M Kobayashi, C Itakura, et al. Loss of Apc heterozygosity and abnormal tissue building in nascent intestinal polyps in mice carrying a truncated Apc gene. Proc. Natl. Acad. Sci. U. S. A. 1995; 92: 4482–4486.

50. AE McCart, NK Vickaryous, A Silver. Apc mice: models, modifiers and mutants. Pathol. Res. Pract. 2008; 204: 479–490.
51. AR Moser, HC Pitot, WF Dove. A dominant mutation that predisposes to multiple intestinal neoplasia in the mouse. Science. 1990; 247: 322–324.
52. Y Feng. Sox9 Induction, Ectopic Paneth Cells, and Mitotic Spindle Axis Defects in Mouse Colon Adenomatous Epithelium Arising From Conditional Biallelic Apc Inactivation. Am. J. Pathol. 2013; 183: 493–503.
53. PW Tetteh. Generation of an inducible colon-specific Cre enzyme mouse line for colon cancer research. Proc. Natl. Acad. Sci. U. S. A. 2016; 113: 11859–11864.
54. T Hinoi. Mouse model of colonic adenoma-carcinoma progression based on somatic Apc inactivation. Cancer Res. 2007; 67: 9721–9730.
55. LE Dow. Apc restoration promotes cellular differentiation and reestablishes crypt homeostasis in colorectal cancer. Cell. 2015; 161: 1539–1552.
56. H Clevers. Modeling Development and Disease with Organoids. Cell. 2016; 165: 1586–1597.
57. D Yamazaki, O Hashizume, S Taniguchi, Y Funato, H Miki. Role of adenomatous polyposis coli in proliferation and differentiation of colon epithelial cells in organoid culture. Sci. Rep. 2021; 11: 3980.
58. J Drost. Sequential cancer mutations in cultured human intestinal stem cells. Nature. 2015; 521: 43–47.
59. MF Viola, G Boeckxstaens. Intestinal resident macrophages: Multitaskers of the gut. Neurogastroenterol. Motil. Off. J. Eur. Gastrointest. Motil. Soc. 2020; 32: e13843.
60. LM Coussens, Z Werb. Inflammation and cancer. Nature. 2002; 420: 860–867.
61. R Virchow. An Address on the Value of Pathological Experiments. Br. Med. J. 1881; 2: 198–203.
62. TL Whiteside. The tumor microenvironment and its role in promoting tumor growth. Oncogene. 2008; 27: 5904–5912.
63. JA Joyce, JW Pollard. Microenvironmental regulation of metastasis. Nat. Rev. Cancer. 2009; 9: 239–252.
64. T Kitamura, BZ Qian, JW Pollard. Immune cell promotion of metastasis. Nat. Rev. Immunol. 2015; 15: 73–86.

65. JI Youn, S Nagaraj, M Collazo, DI Gabrilovich. Subsets of myeloid-derived suppressor cells in tumor-bearing mice. J. Immunol. Baltim. Md 1950. 2008; 181: 5791–5802.
66. K Movahedi. Identification of discrete tumor-induced myeloid-derived suppressor cell subpopulations with distinct T cell-suppressive activity. Blood. 2008; 111: 4233–4244.
67. E Schlecker. Tumor-infiltrating monocytic myeloid-derived suppressor cells mediate CCR5-dependent recruitment of regulatory T cells favoring tumor growth. J. Immunol. Baltim. Md 1950. 2012; 189: 5602–5611.
68. BZ Qian, JW Pollard. Macrophage diversity enhances tumor progression and metastasis. Cell. 2010; 141: 39–51.
69. Q Lahmar, J Keirsse, D Laoui, K Movahedi, E Van Overmeire, et al. Tissue-resident versus monocyte-derived macrophages in the tumor microenvironment. Biochim. Biophys. Acta. 2016; 1865: 23–34.
70. L Bingle, NJ Brown, CE Lewis. The role of tumour-associated macrophages in tumour progression: implications for new anticancer therapies. J. Pathol. 2002; 196: 254–265.
71. A Algars. Type and location of tumor-infiltrating macrophages and lymphatic vessels predict survival of colorectal cancer patients. Int. J. Cancer. 2012; 131: 864–873.
72. J Forssell, A Oberg, ML Henriksson, R Stenling, A Jung, et al. High macrophage infiltration along the tumor front correlates with improved survival in colon cancer. Clin. Cancer Res. Off. J. Am. Assoc. Cancer Res. 2007; 13: 1472–1479.
73. C Lackner. Prognostic relevance of tumour-associated macrophages and von Willebrand factor-positive microvessels in colorectal cancer. Virchows Arch. Int. J. Pathol. 2004; 445: 160–167.
74. Q Zhou. The density of macrophages in the invasive front is inversely correlated to liver metastasis in colon cancer. J. Transl. Med. 2010; 8: 13.
75. JC Kang, JS Chen, CH Lee, JJ Chang, YS Shieh. Intratumoral macrophage counts correlate with tumor progression in colorectal cancer. J. Surg. Oncol. 2010; 102: 242–248.

76. Q Liu. Wnt5a-induced M2 polarization of tumor-associated macrophages via IL-10 promotes colorectal cancer progression. Cell Commun. Signal. CCS. 2020; 18.
77. T Cooks. Mutant p53 cancers reprogram macrophages to tumor supporting macrophages via exosomal miR-1246. Nat. Commun. 2018; 9: 771.
78. A Mantovani, S Sozzani, M Locati, P Allavena, A Sica. Macrophage polarization: tumor-associated macrophages as a paradigm for polarized M2 mononuclear phagocytes. Trends Immunol. 2002; 23: 549–555.
79. A Mantovani, A Sica, S Sozzani, P Allavena, A Vecchi, et al. The chemokine system in diverse forms of macrophage activation and polarization. Trends Immunol. 2004; 25: 677–686.
80. R Braster, M Bögels, RHJ Beelen, M van Egmond. The delicate balance of macrophages in colorectal cancer; their role in tumour development and therapeutic potential. Immunobiology. 2017; 222: 21–30.
81. RD Leek, CE Lewis, R Whitehouse, M Greenall, J Clarke, et al. Association of macrophage infiltration with angiogenesis and prognosis in invasive breast carcinoma. Cancer Res. 1996; 56: 4625–4629.
82. YW Koh, CS Park, DH Yoon, C Suh, J Huh. CD163 Expression Was Associated with Angiogenesis and Shortened Survival in Patients with Uniformly Treated Classical Hodgkin Lymphoma. PLOS ONE. 2014; 9: e87066.
83. AJ Clear. Increased angiogenic sprouting in poor prognosis FL is associated with elevated numbers of CD163+ macrophages within the immediate sprouting microenvironment. Blood. 2010; 115: 5053–5056.
84. EY Lin. Macrophages regulate the angiogenic switch in a mouse model of breast cancer. Cancer Res. 2006; 66: 11238–11246.
85. SJ Priceman. Targeting distinct tumor-infiltrating myeloid cells by inhibiting CSF-1 receptor: combating tumor evasion of antiangiogenic therapy. Blood. 2010; 115: 1461–1471.
86. JS Lewis, RJ Landers, JC Underwood, AL Harris, CE Lewis. Expression of vascular endothelial growth factor by

macrophages is up-regulated in poorly vascularized areas of breast carcinomas. J. Pathol. 2000; 192: 150–158.
87. C Stockmann. Deletion of vascular endothelial growth factor in myeloid cells accelerates tumorigenesis. Nature. 2008; 456: 814–818.
88. R Hughes. Perivascular M2 Macrophages Stimulate Tumor Relapse after Chemotherapy. Cancer Res. 2015; 75: 3479–3491.
89. AS Harney. Real-Time Imaging Reveals Local, Transient Vascular Permeability, and Tumor Cell Intravasation Stimulated by TIE2hi Macrophage-Derived VEGFA. Cancer Discov. 2015; 5: 932–943.
90. ML Squadrito, M De Palma. Macrophage regulation of tumor angiogenesis: implications for cancer therapy. Mol. Aspects Med. 2011; 32: 123–145.
91. C Baer, ML Squadrito, ML Iruela-Arispe, M De Palma. Reciprocal interactions between endothelial cells and macrophages in angiogenic vascular niches. Exp. Cell Res. 2013; 319: 1626–1634.
92. C Murdoch, M Muthana, SB Coffelt, CE Lewis. The role of myeloid cells in the promotion of tumour angiogenesis. Nat. Rev. Cancer. 2008; 8: 618–631.
93. EJ Yeo. Myeloid WNT7b mediates the angiogenic switch and metastasis in breast cancer. Cancer Res. 2014; 74: 2962–2973.
94. CE Lewis, AS Harney, JW Pollard. The Multifaceted Role of Perivascular Macrophages in Tumors. Cancer Cell. 2016; 30: 18–25.
95. M De Palma, MA Venneri, C Roca, L Naldini. Targeting exogenous genes to tumor angiogenesis by transplantation of genetically modified hematopoietic stem cells. Nat. Med. 2003; 9: 789–795.
96. M De Palma. Tie2 identifies a hematopoietic lineage of proangiogenic monocytes required for tumor vessel formation and a mesenchymal population of pericyte progenitors. Cancer Cell. 2005; 8: 211–226.
97. T Matsubara. TIE2-expressing monocytes as a diagnostic marker for hepatocellular carcinoma correlates with angiogenesis. Hepatol. Baltim. Md. 2013; 57: 1416–1425.

98. L Tamagnone. Emerging role of semaphorins as major regulatory signals and potential therapeutic targets in cancer. Cancer Cell. 2012; 22: 145–152.
99. JF Hastings, JN Skhinas, D Fey, DR Croucher, TR Cox. The extracellular matrix as a key regulator of intracellular signalling networks. Br. J. Pharmacol. 2019; 176: 82–92.
100. K Kessenbrock, V Plaks, Z Werb. Matrix metalloproteinases: regulators of the tumor microenvironment. Cell. 2010; 141: 52–67.
101. B Hinz. Recent developments in myofibroblast biology: paradigms for connective tissue remodeling. Am. J. Pathol. 2012; 180: 1340–1355.
102. C Bonnans, J Chou, Z Werb. Remodelling the extracellular matrix in development and disease. Nat. Rev. Mol. Cell Biol. 2014; 15: 786–801.
103. P Lu, K Takai, VM Weaver, Z Werb. Extracellular matrix degradation and remodeling in development and disease. Cold Spring Harb. Perspect. Biol. 2011; 3: a005058.
104. S Saw. Metalloprotease inhibitor TIMP proteins control FGF-2 bioavailability and regulate skeletal growth. J. Cell Biol. 2019; 218: 3134–3152.
105. DH Madsen. Tumor-Associated Macrophages Derived from Circulating Inflammatory Monocytes Degrade Collagen through Cellular Uptake. Cell Rep. 2017; 21: 3662–3671.
106. E Zajac. Angiogenic capacity of M1- and M2-polarized macrophages is determined by the levels of TIMP-1 complexed with their secreted proMMP-9. Blood. 2013; 122: 4054–4067.
107. S Sangaletti. Macrophage-derived SPARC bridges tumor cell-extracellular matrix interactions toward metastasis. Cancer Res. 2008; 68: 9050–9059.
108. R Afik. Tumor macrophages are pivotal constructors of tumor collagenous matrix. J. Exp. Med. 2016; 213: 2315–2331.
109. F Kai, AP Drain, VM Weaver. The Extracellular Matrix Modulates the Metastatic Journey. Dev. Cell. 2019; 49: 332–346.
110. MM Martino, JA Hubbell. The 12th-14th type III repeats of fibronectin function as a highly promiscuous growth

factor-binding domain. FASEB J. Off. Publ. Fed. Am. Soc. Exp. Biol. 2010; 24: 4711–4721.
111. KA Houck, DW Leung, AM Rowland, J Winer, N Ferrara. Dual regulation of vascular endothelial growth factor bioavailability by genetic and proteolytic mechanisms. J. Biol. Chem. 1992; 267: 26031–26037.
112. D Belotti. Matrix metalloproteinases (MMP9 and MMP2) induce the release of vascular endothelial growth factor (VEGF) by ovarian carcinoma cells: implications for ascites formation. Cancer Res. 2003; 63: 5224–5229.
113. EI Deryugina, JP Quigley. Tumor angiogenesis: MMP-mediated induction of intravasation- and metastasis-sustaining neovasculature. Matrix Biol. J. Int. Soc. Matrix Biol. 2015; 44–46: 94–112.
114. R Du. HIF1alpha induces the recruitment of bone marrow-derived vascular modulatory cells to regulate tumor angiogenesis and invasion. Cancer Cell. 2008; 13: 206–220.
115. DA Thomas, J Massagué. TGF-beta directly targets cytotoxic T cell functions during tumor evasion of immune surveillance. Cancer Cell. 2005; 8: 369–380.
116. J Cai, L Xia, J Li, S Ni, H Song, et al. Tumor-Associated Macrophages Derived TGF-β–Induced Epithelial to Mesenchymal Transition in Colorectal Cancer Cells through Smad2,3-4/Snail Signaling Pathway. Cancer Res. Treat. 2019; 51: 252–266.
117. B Chiavarina. Metastatic colorectal cancer cells maintain the TGFβ program and use TGFBI to fuel angiogenesis. Theranostics. 2021; 11: 1626–1640.
118. K Smith, TD Bui, R Poulsom, L Kaklamanis, G Williams, et al. Up-regulation of macrophage wnt gene expression in adenoma-carcinoma progression of human colorectal cancer. Br. J. Cancer. 1999; 81: 496–502.
119. A Sica, T Schioppa, A Mantovani, P Allavena. Tumour-associated macrophages are a distinct M2 polarised population promoting tumour progression: potential targets of anti-cancer therapy. Eur. J. Cancer Oxf. Engl. 1990. 2006; 42: 717–727.
120. J Chen. CCL18 from tumor-associated macrophages promotes breast cancer metastasis via PITPNM3. Cancer Cell. 2011; 19: 541–555.

121. TJ Curiel. Specific recruitment of regulatory T cells in ovarian carcinoma fosters immune privilege and predicts reduced survival. Nat. Med. 2004; 10: 942–949.
122. J Liu. Tumor-associated macrophages recruit CCR6+ regulatory T cells and promote the development of colorectal cancer via enhancing CCL20 production in mice. PloS One. 2011; 6: e19495.
123. I Daurkin. Tumor-associated macrophages mediate immunosuppression in the renal cancer microenvironment by activating the 15-lipoxygenase-2 pathway. Cancer Res. 2011; 71: 6400–6409.
124. F Ghiringhelli. Tumor cells convert immature myeloid dendritic cells into TGF-beta-secreting cells inducing CD4+CD25+ regulatory T cell proliferation. J. Exp. Med. 2005; 202: 919–929.
125. JA Trapani. The dual adverse effects of TGF-beta secretion on tumor progression. Cancer Cell. 2005; 8: 349–350.
126. K Nakamura, A Kitani, W Strober. Cell contact-dependent immunosuppression by CD4(+)CD25(+) regulatory T cells is mediated by cell surface-bound transforming growth factor beta. J. Exp. Med. 2001; 194: 629–644.
127. EM Shevach. Mechanisms of foxp3+ T regulatory cell-mediated suppression. Immunity. 2009; 30: 636–645.
128. L Dolcetti. Hierarchy of immunosuppressive strength among myeloid-derived suppressor cell subsets is determined by GM-CSF. Eur. J. Immunol. 2010; 40: 22–35.
129. L Gorelik, RA Flavell. Immune-mediated eradication of tumors through the blockade of transforming growth factor-beta signaling in T cells. Nat. Med. 2001; 7: 1118–1122.
130. L Gorelik, RA Flavell. Transforming growth factor-beta in T-cell biology. Nat. Rev. Immunol. 2002; 2: 46–53.
131. R Noy, JW Pollard. Tumor-associated macrophages: from mechanisms to therapy. Immunity. 2014; 41: 49–61.
132. B Ruffell. Macrophage IL-10 blocks CD8+ T cell-dependent responses to chemotherapy by suppressing IL-12 expression in intratumoral dendritic cells. Cancer Cell. 2014; 26: 623–637.

133. DL Herber. Lipid accumulation and dendritic cell dysfunction in cancer. Nat. Med. 2010; 16: 880–886.
134. JR Cubillos-Ruiz. ER Stress Sensor XBP1 Controls Anti-tumor Immunity by Disrupting Dendritic Cell Homeostasis. Cell. 2015; 161: 1527–1538.
135. DG DeNardo. Leukocyte complexity predicts breast cancer survival and functionally regulates response to chemotherapy. Cancer Discov. 2011; 1: 54–67.
136. A Mantovani, M Locati. Tumor-associated macrophages as a paradigm of macrophage plasticity, diversity, and polarization: lessons and open questions. Arterioscler. Thromb. Vasc. Biol. 2013; 33: 1478–1483.
137. E Azizi. Single-Cell Map of Diverse Immune Phenotypes in the Breast Tumor Microenvironment. Cell. 2018; 174: 1293-1308.e36.
138. S Müller. Single-cell profiling of human gliomas reveals macrophage ontogeny as a basis for regional differences in macrophage activation in the tumor microenvironment. Genome Biol. 2017; 18: 234.
139. N Linde. Macrophages orchestrate breast cancer early dissemination and metastasis. Nat. Commun. 2018; 9: 21.
140. M Casanova-Acebes. Tissue-resident macrophages provide a pro-tumorigenic niche to early NSCLC cells. Nature. 2021; 1–7.
141. CL Semerad, F Liu, AD Gregory, K Stumpf, DC Link. G-CSF is an essential regulator of neutrophil trafficking from the bone marrow to the blood. Immunity. 2002; 17: 413–423.
142. SB Coffelt, MD Wellenstein, KE de Visser. Neutrophils in cancer: neutral no more. Nat. Rev. Cancer. 2016; 16: 431–446.
143. S Inamoto. Loss of SMAD4 Promotes Colorectal Cancer Progression by Accumulation of Myeloid-Derived Suppressor Cells through the CCL15-CCR1 Chemokine Axis. Clin. Cancer Res. Off. J. Am. Assoc. Cancer Res. 2016; 22: 492–501.
144. E Chun. CCL2 Promotes Colorectal Carcinogenesis by Enhancing Polymorphonuclear Myeloid-Derived Suppressor Cell Population and Function. Cell Rep. 2015; 12: 244–257.

145. B Azab. Usefulness of the neutrophil-to-lymphocyte ratio in predicting short- and long-term mortality in breast cancer patients. Ann. Surg. Oncol. 2012; 19: 217–224.
146. AJ Templeton. Prognostic role of neutrophil-to-lymphocyte ratio in solid tumors: a systematic review and meta-analysis. J. Natl. Cancer Inst. 2014; 106: dju124.
147. FCM Cananzi, A Dalgleish, S Mudan. Surgical management of intraabdominal metastases from melanoma: role of the neutrophil to lymphocyte ratio as a potential prognostic factor. World J. Surg. 2014; 38: 1542–1550.
148. W Fan, Y Zhang, Y Wang, X Yao, J Yang, et al. Neutrophil-to-lymphocyte and platelet-to-lymphocyte ratios as predictors of survival and metastasis for recurrent hepatocellular carcinoma after transarterial chemoembolization. PloS One. 2015; 10: e0119312.
149. SK Wculek, I Malanchi. Neutrophils support lung colonization of metastasis-initiating breast cancer cells. Nature. 2015; 528: 413–417.
150. SB Coffelt. IL-17-producing γδ T cells and neutrophils conspire to promote breast cancer metastasis. Nature. 2015; 522: 345–348.
151. J Park. Cancer cells induce metastasis-supporting neutrophil extracellular DNA traps. Sci. Transl. Med. 2016; 8: 361ra138.
152. ZG Fridlender. Polarization of tumor-associated neutrophil phenotype by TGF-beta: 'N1' versus 'N2' TAN. Cancer Cell. 2009; 16: 183–194.
153. A Mantovani, MA Cassatella, C Costantini, S Jaillon. Neutrophils in the activation and regulation of innate and adaptive immunity. Nat. Rev. Immunol. 2011; 11: 519–531.
154. R Zilionis. Single-Cell Transcriptomics of Human and Mouse Lung Cancers Reveals Conserved Myeloid Populations across Individuals and Species. Immunity. 2019; 50: 1317-1334.e10.
155. F Colotta, F Re, N Polentarutti, S Sozzani, A Mantovani. Modulation of granulocyte survival and programmed cell death by cytokines and bacterial products. Blood. 1992; 80: 2012–2020.

156. Y Sawanobori. Chemokine-mediated rapid turnover of myeloid-derived suppressor cells in tumor-bearing mice. Blood. 2008; 111: 5457–5466.
157. WL Hwang, HY Lan, WC Cheng, SC Huang, MH Yang. Tumor stem-like cell-derived exosomal RNAs prime neutrophils for facilitating tumorigenesis of colon cancer. J. Hematol. Oncol.J Hematol Oncol. 2019; 12: 10.
158. W Liang, N Ferrara. The Complex Role of Neutrophils in Tumor Angiogenesis and Metastasis, Cancer Immunol. Res. 2016; 4: 83–91.
159. M Kujawski, M Kortylewski, H Lee, A Herrmann, H Kay, et al. Stat3 mediates myeloid cell-dependent tumor angiogenesis in mice. J. Clin. Invest. 2008; 118: 3367–3377.
160. M Gaudry, O Brégerie, V Andrieu, J El Benna, MA Pocidalo, et al. Intracellular pool of vascular endothelial growth factor in human neutrophils. Blood. 1997; 90: 4153–4161.
161. X Qu, G Zhuang, L Yu, G Meng, N Ferrara. Induction of Bv8 expression by granulocyte colony-stimulating factor in CD11b+Gr1+ cells: key role of Stat3 signaling. J. Biol. Chem. 2012; 287: 19574–19584.
162. F Shojaei. Bv8 regulates myeloid-cell-dependent tumour angiogenesis. Nature. 2007; 450: 825–831.
163. G Bergers. Matrix metalloproteinase-9 triggers the angiogenic switch during carcinogenesis. Nat. Cell Biol. 2016; 2: 737–744.
164. W Liang, N Ferrara. The Complex Role of Neutrophils in Tumor Angiogenesis and Metastasis. Cancer Immunol. Res. 2016; 4: 83–91.
165. H Nozawa, C Chiu, D Hanahan. Infiltrating neutrophils mediate the initial angiogenic switch in a mouse model of multistage carcinogenesis. Proc. Natl. Acad. Sci. U. S. A. 2006; 103: 12493–12498.
166. EI Deryugina, E Zajac, A Juncker-Jensen, TA Kupriyanova, L Welter, et al. Tissue-infiltrating neutrophils constitute the major in vivo source of angiogenesis-inducing MMP-9 in the tumor microenvironment. Neoplasia N. Y. N. 2014; 16: 771–788.

167. S Huang. Contributions of stromal metalloproteinase-9 to angiogenesis and growth of human ovarian carcinoma in mice. J. Natl. Cancer Inst. 2002; 94: 1134–1142.
168. VC Ardi, TA Kupriyanova, EI Deryugina, JP Quigley. Human neutrophils uniquely release TIMP-free MMP-9 to provide a potent catalytic stimulator of angiogenesis. Proc. Natl. Acad. Sci. U. S. A. 2007; 104: 20262–20267.
169. T Chao, EE Furth, RH Vonderheide. CXCR2-Dependent Accumulation of Tumor-Associated Neutrophils Regulates T-cell Immunity in Pancreatic Ductal Adenocarcinoma. Cancer Immunol. Res. 2016; 4: 968–982.
170. Q Yu, I Stamenkovic. Cell surface-localized matrix metalloproteinase-9 proteolytically activates TGF-beta and promotes tumor invasion and angiogenesis. Genes Dev. 2000; 14: 163–176.
171. S Mariathasan. TGFβ attenuates tumour response to PD-L1 blockade by contributing to exclusion of T cells. Nature. 2018; 554: 544–548.
172. DVF Tauriello. TGFβ drives immune evasion in genetically reconstituted colon cancer metastasis. Nature. 2018; 554: 538–543.
173. M Germann. Neutrophils suppress tumor-infiltrating T cells in colon cancer via matrix metalloproteinase-mediated activation of TGFβ. EMBO Mol. Med. 2020; 12: e10681.
174. PC Rodriguez. Arginase I production in the tumor microenvironment by mature myeloid cells inhibits T-cell receptor expression and antigen-specific T-cell responses. Cancer Res. 2004; 64: 5839–5849.
175. V Brinkmann. Neutrophil extracellular traps kill bacteria. Science. 2004; 303: 1532–1535.
176. CF Urban. Neutrophil extracellular traps contain calprotectin, a cytosolic protein complex involved in host defense against Candida albicans. PLoS Pathog. 2009; 5: e1000639.
177. B McDonald, R Urrutia, BG Yipp, CN Jenne, P Kubes. Intravascular neutrophil extracellular traps capture bacteria from the bloodstream during sepsis. Cell Host Microbe. 2012; 12: 324–333.
178. B McDonald, J Spicer, B Giannais, L Fallavollita, P Brodt, et al. Systemic inflammation increases cancer cell

adhesion to hepatic sinusoids by neutrophil mediated mechanisms. Int. J. Cancer. 2009; 125: 1298–1305.
179. JD Spicer. Neutrophils promote liver metastasis via Mac-1-mediated interactions with circulating tumor cells. Cancer Res. 2012; 72: 3919–3927.
180. JK Lin. The influence of fecal diversion and anastomotic leakage on survival after resection of rectal cancer. J. Gastrointest. Surg. Off. J. Soc. Surg. Aliment. Tract. 2011; 15: 2251–2261.
181. SG Farid. Correlation between postoperative infective complications and long-term outcomes after hepatic resection for colorectal liver metastasis. Ann. Surg. 2010; 251: 91–100.
182. S Najmeh. Neutrophil extracellular traps sequester circulating tumor cells via β1-integrin mediated interactions. Int. J. Cancer. 2017; 140: 2321–2330.
183. BM Szczerba. Neutrophils escort circulating tumour cells to enable cell cycle progression. Nature. 2019; 566: 553–557.
184. Álvaro Teijeira, Saray Garasa, María Gato, Carlos Alfaro, Itziar Migueliz, et al. CXCR1 and CXCR2 Chemokine Receptor Agonists Produced by Tumors Induce Neutrophil Extracellular Traps that Interfere with Immune Cytotoxicity. Immunity. 2020; 52: 856-871.e8.
185. Linbin Yang, Qiang Liu, Xiaoqian Zhang, Xinwei Liu, Boxuan Zhou,et al. DNA of neutrophil extracellular traps promotes cancer metastasis via CCDC25, Nature. 2020; 583: 133–138.
186. Jean Albrengues, Mario A Shields, David Ng, Chun Gwon Park, Alexandra Ambrico, et al. Neutrophil extracellular traps produced during inflammation awaken dormant cancer cells in mice. Science. 2018; 361: eaao4227.
187. Samer Tohme, Hamza O Yazdani, Ahmed B Al-Khafaji, Alexis P Chidi, Patricia Loughran, et al. Neutrophil Extracellular Traps Promote the Development and Progression of Liver Metastases after Surgical Stress. Cancer Res. 2016; 76: 1367–1380.
188. W Lee, SY Ko, MS Mohamed, HA Kenny, E Lengyel, et al. Neutrophils facilitate ovarian cancer premetastatic niche

formation in the omentum. J. Exp. Med. 2019; 216: 176–194.

189. M Lafitte, C Lecointre, S Roche. Roles of exosomes in metastatic colorectal cancer. Am. J. Physiol. Cell Physiol. 2019; 317: C869–C880.

190. Bastian Seubert, Barbara Grünwald, Julia Kobuch, Haissi Cui, Florian Schelter, et al. Tissue inhibitor of metalloproteinases (TIMP)-1 creates a premetastatic niche in the liver through SDF-1/CXCR4-dependent neutrophil recruitment in mice. Hepatol. Baltim. Md. 2015; 61: 238–248.

191. Rene Jackstadt, Sander R van Hooff, Joshua D Leach, Xabier Cortes-Lavaud, Jeroen O Lohuis, et al. Epithelial NOTCH Signaling Rewires the Tumor Microenvironment of Colorectal Cancer to Drive Poor-Prognosis Subtypes and Metastasis. Cancer Cell. 2019; 36: 319-336.e7.

192. Kevin P O'Rourke, Evangelia Loizou, Geulah Livshits, Emma M Schatoff, Timour Baslan, et al. Transplantation of engineered organoids enables rapid generation of metastatic mouse models of colorectal cancer. Nat. Biotechnol. 2017; 35: 577–582.

193. Jatin Roper, Tuomas Tammela, Naniye Malli Cetinbas, Adam Akkad, Ali Roghanian, et al. In vivo genome editing and organoid transplantation models of colorectal cancer and metastasis. Nat. Biotechnol. 2017; 35: 569–576.

194. Mariko Shimokawa, Yuki Ohta, Shingo Nishikori, Mami Matano, Ai Takano, et al. Visualization and targeting of LGR5+ human colon cancer stem cells. Nature. 2017; 545: 187–192.

195. Masayuki Fujii, Mariko Shimokawa, Shoichi Date, Ai Takano, Mami Matano, et al. A Colorectal Tumor Organoid Library Demonstrates Progressive Loss of Niche Factor Requirements during Tumorigenesis. Cell Stem Cell. 2016; 18: 827–838.

196. Marc van de Wetering, Hayley E Francies, Joshua M Francis, Gergana Bounova, Francesco Iorio, et al. Prospective derivation of a living organoid biobank of colorectal cancer patients. Cell. 2015; 161: 933–945.

197. C Jochems, J Schlom. Tumor-infiltrating immune cells and prognosis: the potential link between conventional

cancer therapy and immunity. Exp. Biol. Med. Maywood NJ. 2011; 236: 567–579.
198. Qiong-wen Zhang, Lei Liu, Chang-yang Gong, Hua-shan Shi, Yun-hui Zeng, et al. Prognostic Significance of Tumor-Associated Macrophages in Solid Tumor: A Meta-Analysis of the Literature. PLOS ONE. 2012; 7: e50946.
199. DM Pardoll. The blockade of immune checkpoints in cancer immunotherapy. Nat. Rev. Cancer. 2012; 12: 252–264.
200. MK Callahan, JD Wolchok, At the bedside: CTLA-4- and PD-1-blocking antibodies in cancer immunotherapy. J. Leukoc. Biol. 2013; 94: 41–53.
201. Richard R Furman, Jeff P Sharman, Steven E Coutre, Bruce D Cheson, John M Pagel, et al. Idelalisib and Rituximab in Relapsed Chronic Lymphocytic Leukemia. N. Engl. J. Med. 2014; 370: 997–1007.
202. Kenneth J Pienta, Jean-Pascal Machiels, Dirk Schrijvers, Boris Alekseev, Mikhail Shkolnik, et al. Phase 2 study of carlumab (CNTO 888), a human monoclonal antibody against CC-chemokine ligand 2 (CCL2), in metastatic castration-resistant prostate cancer. Invest. New Drugs. 2013; 31: 760–768.
203. Giovanni Germano, Roberta Frapolli, Cristina Belgiovine, Achille Anselmo, Samantha Pesce, et al. Role of macrophage targeting in the antitumor activity of trabectedin. Cancer Cell. 2013; 23: 249–262.
204. Shuji Ogino, Katsuhiko Nosho, Natsumi Irahara, Jeffrey A Meyerhardt, Yoshifumi Baba, et al. Lymphocytic Reaction to Colorectal Cancer Is Associated with Longer Survival, Independent of Lymph Node Count, Microsatellite Instability, and CpG Island Methylator Phenotype. Clin. Cancer Res. 2009; 15: 6412–6420.
205. G Golshani, Y Zhang. Advances in immunotherapy for colorectal cancer: a review. Ther. Adv. Gastroenterol. 2020; 13: 1756284820917527.

Book Chapter

Mechanical Forces in T cell Biology

Farah Mustapha[1,2,3,4,5], Kheya Sengupta[4,5]* and Pierre-Henri Puech[1,2,3,4]*

[1]Aix Marseille University, France
[2]Inserm, UMR_S 1067, France
[3]CNRS, UMR 7333, France
[4]CENTURI, Turing Center for Living Systems, France
[5]Centre Interdisciplinaire de Nanoscience de Marseille (CINAM), CNRS - AMU UMR 7325, France

***Corresponding Authors:** Pierre-Henri Puech, Aix Marseille University, LAI UM 61, Marseille, F-13288, France

Kheya Sengupta, CENTURI, Turing Center for Living systems, Marseille, France

Published **March 31, 2022**

How to cite this book chapter: Farah Mustapha, Kheya Sengupta, Pierre-Henri Puech. Mechanical Forces in T cell Biology. In: Hussein Fayyad Kazan, editor. Immunology and Cancer Biology. Hyderabad, India: Vide Leaf. 2022.

Acknowledgments: Part of this work was supported by institutional grants from INSERM, CNRS and Aix-Marseille University to the LAI and CINAM.

FM was supported by a PhD grant from the European Union's Horizon 2020 research and innovation programme under the Marie Skłodowska-Curie grant agreement No713750, with the

financial support of the Regional Council of Provence- Alpes-Côte d'Azur and with of the A*MIDEX (n° ANR- 11-IDEX-0001-02), funded by the Investissements d'Avenir project funded by the French Government, managed by the French National Research Agency (ANR).

Author Contributions: F.M.; writing- original draft preparation. K.S.; review and editing. P.H.P.; figure preparation, review and editing. All authors have read and agreed to the published version of the manuscript.

Conflict of Interest: The authors declare no conflict of interest.

Abstract

The fate of the adult human body, in terms of tissue development and homeostasis, is governed by how well its cells interact with one another, and with their environment. While the biochemical aspect of such interactions has been extensively studied for decades, their mechanical features, have only more recently captured the attention of cell biologists. Such an over sight becomes particularly notable when studying immune cells that experience different mechanical milieus during their life cycles- from primary/secondary/tertiary lymphoid organs and peripheral tissues displaying variable substrate rigidities, to the blood and lymphatic circulatory systems presenting complex hydrodynamic forces- and that are capable of exerting a substantial amount of force against their interacting surfaces. Indeed, mechanical cues, both dynamic forces and spatial features, have been shown to regulate the development, activation, differentiation and expansion of immune cells. T cells in specific, however, depict a unique paradigm of mechano-immunomodulation as the T cell receptor (TCR) itself has been shown to both sense and convert forces into biochemical signals, as well as induce force exertion following triggering. Consequently, it is only reasonable to imagine that incorporating mechanical cues into our "classical" view of T cell biology will help us better understand and manipulate their behavior, and more importantly, address the still unresolved mystery of their activation. In this chapter, we will review the existing body of knowledge showcasing the influence

of mechanical forces on certain T cell surface and cytoplasmic proteins, the process of force generation during T cell interactions, how these forces come into play in T cell biology, and finally the ability of T cells to sense and respond to substrate stiffness and ligand mobility.

Keywords

Immune Cells; T Cells; Mechanical Cues; TCR; Forces; Substrate Stiffness; Ligand Mobility

Looking Back on History

In all forms of life, survival depends on the ability to adapt to environmental stresses, including mechanical stimuli such as external physical forces. It is a requirement so fundamental that it is at the core of all biological designs; virtually all organisms have evolved structures from the macro (organs, tissues) to the micro (cells) and even down to the nanoscale (molecular assemblies, single proteins) that are not only sensitive, but also responsive to forces.

The biological effects of these forces are perhaps most evident in the context of physical structure and activity- the skeleton provides structural support to sustain the force of gravity. The skin provides a protective barrier that is maintained upon the application of external stretch. Even the simplest of physiological functions, such as respiration and circulation, require the generation of forces. This could explain why the earliest understanding and quantifications of these forces were focused on the organism and organ levels. In 1917, biologist D'Arcy Thompson published his book 'On Growth and Form', in which he discussed how mechanical forces contribute to the shape and size of living organisms [1]. Near contemporaries of Thompson, Cecil Murray and Julius Wolff, proved respectively that shear stress controls the size of blood vessels [2] and that mechanical loading increases the thickness and density of bone [3].

This goes to show that the study of the interplay between physical forces and biological function dates back to well before the term ‘mechanobiology’ was even coined. Today, there is a general consensus that cells constantly sense the various mechanical cues (e.g. force, stress, strain, rigidity, topology and adhesiveness) of their micro-environment, *via* a process called ‘mechanosensing’. They then translate these cues into biochemical signals such as modified binding affinity, altered phosphorylation state, and/or a conformational change; a process called ‘mechanotransduction’.

These features are ubiquitous among different cell types and find themselves at the core of many physiological functions; in particular, it has been demonstrated that they are instrumental for key moments of immune cell life and function [4]. For decades, immunological research had focused on identifying the networks of secreted ligands, cell surface receptors, intracellular signaling pathways, and transcriptional factors mediating the immune response [5]. These networks have been predominantly regarded as chemical in nature, largely because the individual molecules that make them up have been characterized by their non-covalent molecular interactions and/or enzymatic activity. Though this chemical description may not be incorrect, it neglects the influence of physical cues, in particular mechanical forces, on signaling networks, as well as the influence of signaling networks on the mechanical environment within and outside of the cell. Such an oversight becomes particularly relevant when studying immune cells whose lives are intensely “physical”: regularly deforming, migrating through tight interstitial spaces, adhering under shear flow, and forming stable interfaces (known as immunological synapses; ISs) with other cells [6] (Figure1). Effectively, this means that the receptor-ligand interactions that govern immune cell function are likewise being subjected to and influenced by the same mechanically tempestuous microenvironment. And, given that several cell surface proteins (e.g. integrins) are known to be strongly connected to the actin cytoskeleton, which is in turn connected to other intracellular proteins, this makes the molecular machinery involved in signal transduction ideal for relaying physical information about the extracellular environment into the cell, as well as translating

biochemical signals inside the cell into physical forces exerted against that environment [7,8].

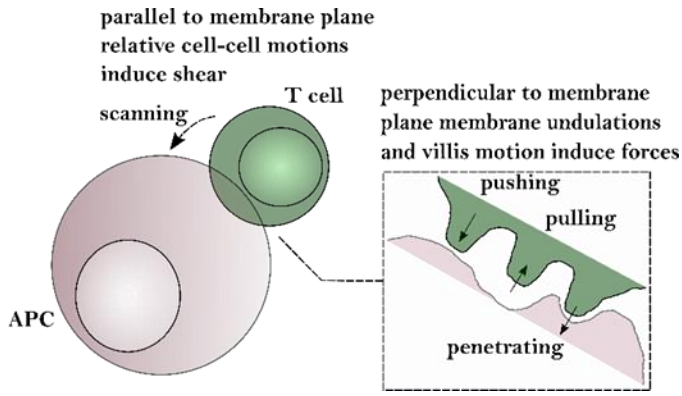

Figure 1: Origins and orientations of forces at the cellular and molecular scales in T cell recognition and function.

Exemplifying the importance of mechanosensing and mechanotransduction in their development and function are T cells, key players of the adaptive immune system [9]. Broadly speaking, T cells can be divided into three categories; Cytotoxic T cells that directly kill virally infected cells and cancer cells, and Helper and Regulatory T cells that activate and tune the effector functions of other cells in the immune system. In either case, T cells carry out the formidable task of identifying a particular cognate peptide bound to the major histocompatibility complex (pMHC) (Figure 2A), against a very noisy environmental background of endogenous self-peptides MHCs, many of which involve the same MHC molecule [10]. They do so even though the T cell receptors (TCRs) are cross-reactive and typically low in affinity when measured in isolation. One would expect that such high-fidelity decisions would be time consuming, however, T cells scan numerous antigen presenting cells (APCs) in a very short time (~ a few minutes) so that the immune system can react fast enough and avoid any potential significant damage to the body. The ability of T cells to perform their function properly while simultaneously abiding by all these constraints has baffled the scientific community for many years. Over the last decade, mechano-sensing/transduction has been

proposed to be the missing puzzle piece in our understanding of T cell function [11,12]. Different players may have different roles, as we will exemplify further on.

Integrins: The Prototypic Mechanoreceptors

As in any architectural structure, if mechanical load is to be transmitted across the cell surface into the cell, the simplest manner to do so would be through pliable structural elements that are physically interconnected [13]. Given that integrins link either the ECM or integrin ligands on other cells (through their extracellular domains) to the actin-cytoskeleton (through their cytoplasmic tails and adapter molecules) (Figure 2B), they represent excellent candidates for both mechanosensing and mechanotransduction. In fact, the demonstration that integrins are indeed mechanoreceptors was made almost three decades ago in a series of elegant experiments using magnetic twisting cytometry, where twisting ligand-bearing beads bound to β1 integrins caused endothelial cells to stiffen [14].

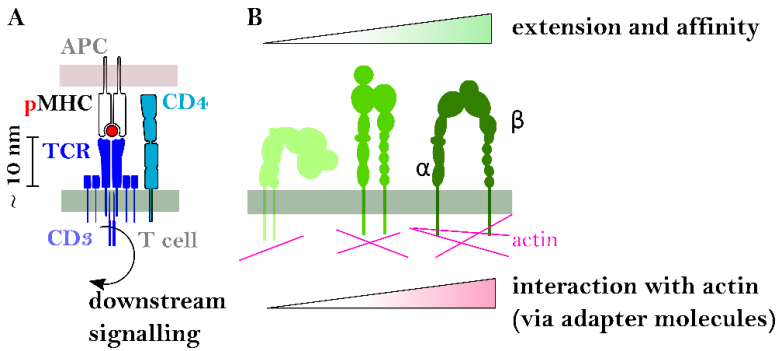

Figure 2: Key mechanosensory molecules for T cells. A: TCR interacts with peptide bearing MHC of an APC and directs the specificity of the adaptive immune response through signaling via the phosphorylation of CD3 cytoplasmic tails. B: Integrins can modulate their extension and interaction with the cytoskeleton depending on forces acting on them (outside-in signaling) or in response to e.g. T cell activation through the TCR (inside-out signaling) [15].

T cells specifically rely heavily on integrins, whether it is for adhesion during trafficking from the bloodstream, migration within tissues, immune synapse formation, or for signaling and

cell polarization [16]. Lymphocyte function-associated antigen-1 (LFA-1) is the predominant integrin on T cells, binding intercellular adhesion molecule-1 and -2 (ICAM-1 and ICAM-2) on partner cells (APCs or endothelial cells) [5]. Like other members of the integrin family, LFA-1 is a heterodimer comprising one α and one β chain, each containing a long, stalk-like extracellular domain, a transmembrane helix, and a short intracellular tail responsible for interacting with cytoplasmic signaling and cytoskeletal proteins [17].

The affinity of LFA-1 to ICAMs, however, is intimately coupled to its conformation, which is in turn set by the cell activation status [18]. In the cell resting state, LFA-1 exhibits a low affinity, bent conformation in which its ligand binding pockets are oriented towards the plasma membrane. In the presence of activating TCR signals during immune synapse formation, specific protein complexes (e.g. talin and kindlins) assemble on the cytoplasmic tails of the α and β chains and drive them apart [19]. The conformational change induces the extension of the extracellular domain, thus allowing ligand recognition. Although this extended conformation is capable of ligand binding, it can only do so at intermediate affinity. In fact, TCR signaling alone is insufficient to unlock the full binding potential of LFA-1 [20].

Only under applied tangential force, originating from the actin cytoskeleton (further elaborated later on), and transferred to integrins via interactions between cytoskeletal adaptors, such as talin, and the tail of the β subunit, does LFA-1 reach peak binding affinity (~ 100 fold increase) [21,22], a clear signature of catch-bond behavior. Catch bonds are an unusual kinetic behavior of ligand receptor interactions where the exertion of a physical force on a molecular complex counter-intuitively prolongs its bond lifetime, in contrast to the so called ‘ordinary’ slip bonds, where force intuitively shortens bond lifetime. Indeed, similar to other integrins [23], LFA-1 binding with ICAM-1 behaves as a catch bond [24].

Interestingly enough, the engagement of LFA-1 alone does not generate any measurable forces or intracellular signaling [25]. This observation suggests that the mechano-sensing/transduction

capacity of T cells could not be limited to conventional adhesion molecules such as integrins.

The TCR as a Mechanosensor

In the event that a cognate pMHC on an APC is encountered, TCR signaling will rapidly convert the ligand-binding event to the phosphorylation of up to 10 immunoreceptor tyrosine-based activation motif elements (ITAMS) in the cytoplasmic tails of the associated CD3 complexes. The ensuing signaling cascade ultimately results in developmental decisions, effects, or functions [26]. Unfortunately, our current knowledge of this signaling cascade far exceeds our limited understanding of how it is initiated upon TCR-pMHC binding.

The TCR-pMHC interaction is probably among the weakest protein-protein interactions that can initiate an effective biological response [27]. The affinity of a TCR binding to a pMHC is only around 10^{-4}-10^{-6}M [28], about 1000 times weaker than a typical antigen-antibody binding (10^{-6}-10^{-10}M [29]). Aside, shape-complementarity at the TCR-pMHC interface has been shown to be extremely poor [30]. Despite that, the TCR is still capable of discriminating as few as one to ten non-self antigens in a sea of endogenous self antigens that are presented by the same self-MHC molecule on the APC surface, and even a single pMHC is thought to be sufficient to trigger efficient TCR signaling and subsequent T cell activation [31]. All of this begs the question: How can a seemingly weak interaction simultaneously achieve such levels of specificity and sensitivity?

In an attempt to answer this question, in 2008, Ma and colleagues proposed a ‘receptor deformation model’ for TCR signaling. In this model, TCR signaling is initiated by significant conformational changes in the TCR/CD3 complex, induced by a pulling force originating from the cytoskeleton of the T cell and transmitted through pMHC-TCR binding interactions with enough strength to resist rupture [32]. Essentially, providing a mechanistic explanation to the specificity and sensitivity of the TCR.

A year later, Kim and colleagues provided the first concrete proof that the TCR behaves as a mechanosensor [19]. They used optical tweezers (OT) and nuclear magnetic resonance (NMR) techniques to characterize the distinct functional consequences of several anti-CD3 monoclonal antibodies (mAbs) binding to T cells. In parallel, they quantified Ca^{2+} levels as a measure of T cell activation. The NMR cross-correlation analysis showed that agonist Abs (i.e. those capable of triggering calcium fluxes) bind CD3 in a *diagonal* fashion, in comparison to CD3 Abs that do not trigger downstream signaling which bind CD3 in an upright mode (perpendicular to cell membrane plane). Interestingly enough, perpendicularly binding Abs were still capable of activating T cells but only when a significant *tangential* force, of ~50 piconewtons (pN), i.e. ~10-12 times the thermal agitation limit, was applied by OT. Based on these observations, the authors proposed a model in which external tangential forces generated following pMHC ligation during the scanning of the APC by the T cell, allow TCRs to mechanically sense and then transduce the first activation signals.

The TCR-pMHC Bond can Exhibit Complex Behaviors: The Catch Bond Proposition

In 2014, Liu and colleagues connected yet another piece of the puzzle [33]. Using biomembrane force probes (BFPs), they showed that the lifetime of the bond between a TCR and its specific pMHC was *prolonged* by the application of a ~ 10pN force, indicative of catch-bond behavior. Such a complex response was also associated with more robust and long-lived cellular calcium fluxes, suggesting that catch bond formation may be required for stronger T cell activation. By contrast, the affinity of non-specific TCR-pMHC bonds peaked at zero force, indicative of slip-bond behavior. OT experiments using DNA tethers further revealed that it is in fact the FG loop of the constant domain of the β chain that allosterically controls the V domain modules' catch bond lifetime and peptide discrimination, through a force-driven conformational transition [34]. Collectively, these findings demonstrated that by eliciting antigen-specific catch bonds, external forces may amplify the power of T cell antigen discrimination by separating agonist

pMHCs that induce catch bonds from non-specific pMHCs that exhibit only slip bonds.

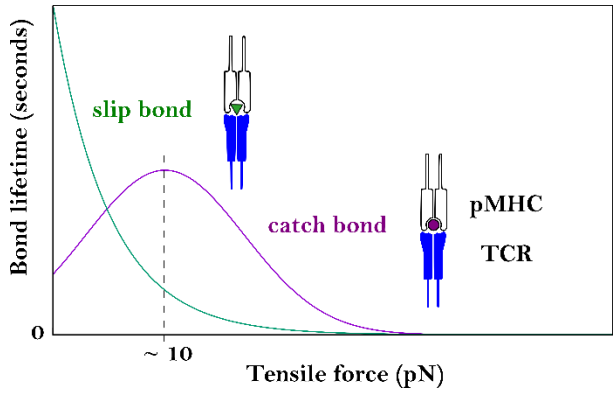

Figure 3: Different bond behaviors that have been proposed to play a role in antigen discrimination during the TCR-pMHC interaction. Slip bonds, whose lifetime only decreases when subjected to increasing forces, vs. catch bonds whose lifetime increases when subjected to increasing forces, up to a certain maximum limit (which has been estimated to be ~ 10pN for TCR/pMHC), beyond which the lifetime decreases as a function of force, similar to slip bond behavior [33].

While catch bonds have been observed in a broad range of molecules, TCR-pMHC catch bonds are still enigmatic, as their origin is still a matter of debate; numerous reports employing purely acellular systems have demonstrated that, outside the cellular context, the TCR does not exhibit catch bond behavior [35]. Aside, how can a tangential (to the membrane) force applied to the TCR-pMHC bond make it stronger? The same group attempted to answer this question using an integrated approach of steered molecular dynamics (SMD) simulation, MTs, and BFPs [36]. Their results showed that forces acting on the TCR-agonist pMHC complex induced a conformational change in the MHC that subsequently increased the length of the complex. Specifically, the increased force experienced by the TCR-agonist pMHC bond uncoupled the α-chain β2-microglobulin (β2m) interdomain interaction, resulting in a 5–10 nm extension of the MHC. They proposed that such pronounced extension would not only stabilize the TCR- agonist pMHC bond but also promote the formation of new interactions after forces

rupture the preexisting ones. Based on these results, the authors hypothesized that, in the case of agonist pMHCs, the forces acting on the TCR-agonist pMHC complex would induce a conformational change in the MHC, ultimately stabilizing the complex and creating a catch bond. The catch bond would then endow the TCR with the power to sensitively discriminate between peptides (self and non-self), plus, the increased chance of bond formation would make T cell activation easier. Nevertheless, this still does not explain the discrepancy observed by [35] and more work will be needed to clarify (i) if the catch bond behavior is indeed essential for T cell activation and (ii) if it is in fact a hallmark of TCR-cognate pMHC bonds, where is it originating from.

Mechanosensitivity Feature of the TCR Conserved at the Pre-TCR Level

Even before the TCR, force-based discrimination, is thought to be conserved in its developmental precursor, the pre-TCR, for the selection of efficient TCRs. Early thymic progenitors (ETPs; uncommitted thymic cells retaining some myeloid, NK and little if any B lineage potential) enter the corticomedullary junction of the thymus as double-negative cells (DN, stages DN1 to 4), lacking the expression of both CD4 and CD8, as well as the full T cell receptor (whether TCRαβ or TCRγδ). For the αβ T cell lineage, a surrogate preT-α chain (denoted pTα, which lacks Vα of final TCRαβ) is expressed on the surface of DN2 cells in place of the α chain seen in the final αβTCR. Shortly after, the cells enter the DN3 stage where they synthesize the TCRβ chain and express it on their surface in association with the pTα chain, forming what is known as the pre-TCR receptor [37]. Signaling through this pre-TCR marks the first major checkpoint in early thymic development, referred to as β-selection, whereby only DN cells with productive TCRβ are selected to continue their development. The question here is how does pre-TCR signaling occur?

Initially, pre-TCR signaling was thought to be ligand-autonomous [38,39] and purely dependent on pTα charge-based receptor oligomerization [40]. That theory was readily

discredited by Mallis and colleagues [41] who showed through NMR and BFP experiments that the pre-TCR, just like its mature form, and through the βchain alone, is capable of recognizing its respective pMHC (albeit with a broader specificity than its final TCRαβ form), as well as triggering calcium fluxes. Using OT, the same group later showed that this pre-TCR-pMHC recognition occurs specifically through the Vβ hydrophobic patch, in partnership with the Cβ FG loop of the TCRβ, and that the recognition is in-fact force-sensitive [42]. Indeed, the pre-TCR-pMHC interaction, similar to the TCR-pMHC one, was shown to exhibit features of catch bond behavior. Diminishing bond strength and/or bond lifetime (through mutating either the Vβ or the Cβ FG loop) negatively impacted pre-TCR ligand discrimination and ultimately reduced post-DN3 thymocyte proliferation and developmental progression (Li et al. 2021).

These observations show that only under force is pre-TCR signaling induced during β-selection. In this sense, the β repertoire is tuned prior to the αβ repertoire final tuning, with mechanotransduction through the β subunit serving as the first checkpoint towards ensuring a functional TCR. As for the diminished ligand specificity of the pre-TCR in comparison with that of the final αβTCR, it is possible that the broader ligand focus allows the β chain to interact with multiple self-pMHC ligands in the pMHC-rich stromal environment, affording DN3 growth/survival advantage to pMHC binding competent preTCRs and imprinting self-reactivity in the developing repertoire. Thus, DN progression selects for a self-reactive repertoire early in development. The Vβ patch may contribute to this behavior, relaxing peptide specificity requirements and functioning as a surrogate Vα domain whose replacement at the double positive (DP) stage (signaling through the pre-TCR marks the end of DN3 stage and the transition into the DP stage where the cells stop β chain rearrangement, undergo a period of proliferation, and begin to express both CD4 and CD8) where by an actual Vα domain then imposes more precise peptide recognition. Negative selection, that corresponds to the final selection before T cells leave the thymus where only DP T cells that bind self antigens at low affinity survive, therein purges high pMHC self-reactivity while maintaining a low self-pMHC bias.

Sensing and Exerting Forces on the Cellular Level: The Role of the Actomyosin Cytoskeleton

Moving up from the molecular to the cellular level, mechanical forces play a very important role in T cell function. However, before diving into that, one should first address how forces are generated and sensed on the cellular scale. Ultimately, mechanosensing/transduction, on any scale, and force exertion are tightly linked processes. Mechanically induced conformational changes, just as those described for activating the pMHC-TCR and LFA-1-ICAM bonds, only occur under the influence of force. Ergo, mechanotransduction necessitates that the cell exerts and receives forces from its environment. Conversely, force exertion is itself regulated by feedback from mechanosensing pathways, as we will see later on.

Cells exert forces against their environments via dynamic cytoskeletal remodeling; the cytoskeleton is a polymer network composed of three distinct biopolymers: actin, microtubules, and intermediate filaments. Typically, it is the filamentous actin (F-actin) cytoskeleton that bears the brunt of the mechanical load; It is a highly dynamic structure that undergoes continuous reorganization in response to external mechanical cues. This feature is what enables the cell to rapidly change its elastic properties and what consequently endows it with the capacity to apply forces against a substrate and move [44]. The classical model for F-actin dependent force exertion involves myosin motors consuming chemical energy in the form of ATP and walking on actin filaments in a general three-step process of binding, power stroke, and unbinding. This process is continuously repeated and leads to the generation of a contractile force (actomyosin contractile force) [44]. Although actomyosin contractility was initially characterized in muscle cells, it is now clear that it is a universal mechanism for force generation in most eukaryotic cells, fueling a wide range of processes including adhesion, division and motility. With that being said, it is important to note that actin polymerization alone, in the absence of myosin motors, does also generate force. However, such protrusive forces are far less characterized, most likely

because they are easily masked by the long-lasting, contractile ones [43].

Whether it is protrusive or contractile, in order for forces to propagate from the cytoskeleton onto the extracellular environment (substrate or cell), both parties have to be linked through *adhesive* contact points. The most characterized of such contact points are focal adhesions (FAs); FAs constitute large protein assemblies in which transmembrane adhesion receptors (e.g. integrins) and F-actin are bridged via a specialized layer of cytoplasmic scaffolding proteins (e.g. paxillin, vinculin, talin…) [45]. The size, composition, and structure of such adhesion sites are directly dependent on the mechanical forces that they are subjected to, whether it is from actomyosin contractility or from the extracellular environment. This explains why FAs are readily observed for fibroblasts cultured on stiff supports, while similar prominent contacts are harder to detect in-vivo, where the extracellular matrix (ECM) is much more compliant [46]. Interestingly, the process of building FAs from initial adhesion receptors is intricately coupled to the activity of intracellular signaling cascades, not through their possession of enzymatic activity, rather, their capacity to recruit specific, "classical" adhesome signaling components to the growing FAs [47]. For example, in the case of integrin mediated adhesions, the focal adhesion kinase (FAK) recruited to the FA site regulates diverse downstream signaling pathways, including those promoting cell growth and survival [48].

It has to be underlined that, unlike large adherent cells such as the fibroblasts mentioned above, many immune cells, among which the T cells, do *not* form distinct FAs-like structures in vitro or in vivo. Rather, they form *transient* adhesive contacts that contain cell surface receptors, F-actin, and cytoplasmic proteins such as the ones typically found in FAs. These contacts likely serve as sites for force exertion during migration and cell-cell interactions [4].

The most straightforward way in which cellular forces could contribute to T cell function is through enabling their migration and trafficking. Typically, as a cell moves on a substrate

(whether it is the ECM or simply a cover slide), it experiences external forces, mainly the viscous force/resistance from the surrounding medium and cell-substrate interaction forces, as well as internal forces that are generated by the cytoskeleton. In T cells, as in most animal cells, the cytoskeleton is the essential component in creating these motility-driving forces, and in coordinating the entire process of movement: First, a cell propels the membrane forward by growing the actin network at its leading edge, creating an F-actin rich lamellipodium. Second, it adheres to the substrate (for example through integrin adhesions in T cells) at the leading edge and deadheres (releases) at the cell body and rear of the cell (also known as uropod). Finally, the cell propels forward by the F-actin retrograde flow generated against the adhesive contacts present at the base of the leading edge of the cell; retrograde flow describes the variable movement of actin filaments rearward with respect to the substrate, generally in the direction opposite to cell movement [43] and it is caused by actin polymerization against the plasma membrane, which drives the growing fibers backwards, and myosin contractility, which collapses the leading edge F-actin network into linear bundles [4].

Aside from motility, cellular forces come into play at different time points in T cell activation. To begin with, the most basic requirement for T cell activation is for the TCR to interact with the pMHC. This may seem trivial to point out, however, there are physical barriers that make this interaction not as straightforward; The TCR-pMHC bonds (10-15 nm) are much smaller than individual TCR and APC glycocalyx proteins, such as the T cell receptor tyrosine phosphatases CD45 (28-50 nm) and CD148 (47-55 nm), and even LFA-ICAM bonds (45-50 nm for the couple). Though models such as the kinetic segregation one [49] were originally put forth to explain how the T cell overcomes these barriers, there still remains several key issues that the model does not account for [50]. Recently, Cai et al. combined time-resolved lattice light-sheet microscopy and quantum dot–enabled synaptic contact mapping microscopy to show how highly dynamic T cell F-actin-rich microvilli colocalized with TCR microclusters (MCs; upon ligand binding, TCRs coalesce into signaling microclusters containing >10

receptors each), and in the absence of external stimulus, scanned the entire area of opposing cells and surfaces (coated with antagonist/agonist pMHCs and ICAM-1) before and during antigen recognition, at a time frame (≃ 1 min) similar to that recorded for T cell–APC contacts in vivo [51]. These observations, coherent with earlier ones [52], suggest that T cell microvilli, with an average length of 380 nm, can promote TCR signaling by surpassing the size-related restrictions, penetrating the glycocalyx, and bringing the TCR into close proximity with the pMHCs. Additionally, one could imagine that the applied F-actin protrusive forces would further stabilize low affinity TCR-pMHC bonds, and with the microvilli containing pre-clustered TCRs, it would provide an easy access platform for signal amplification, explaining the high sensitivity of T-cells to low numbers of pMHC antigens.

After TCR engagement, actin polymerization at the T cell-APC contact zone commences. The membrane deformation resulting from such polymerization forces allows the T cell to spread over the APC. This spreading process is critical as it not only allows the T cell to scan a larger area of the APC and thus increases the efficiency of antigen sampling [53], but it also exerts force on the receptor-ligand pairs engaged, such as the mechanosensitive TCR-pMHC and LFA-1-ICAM-1/2 bonds, further enhancing peptide discrimination and TCR activation.

As the T cell reaches its maximal spreading area, the same actin polymerization forces, combined with myosin contractility, create retrograde flow. Forces originating from this retrograde flow organize the various TCR MCs and signaling molecules present at the T cell-APC contact zone, and order them into the infamous spatially symmetric bullseye structure of the IS [54]. To be more specific, the TCR MCs are swept towards the center of the contact by retrograde F-actin centripetal flow at the periphery and then by myosin II dependent actin arcs closer to the center, leading to the formation of the cSMAC (central supramolecular activation cluster) surrounded by a ring of integrins (LFA-1/ICAM bonds) in the pSMAC (peripheral supramolecular activation cluster). The interruption of F-actin centripetal flow eradicates TCR MC signaling within seconds,

further confirming that force exertion is imperative for maintaining proper TCR activation. Interestingly enough though, the same actin machinery described above may also break TCR-pMHC bonds, allowing the serial engagement of the same pMHC with the other TCRs present in the TCR MC, consequently augmenting TCR signaling.

Once the IS is established, it has to be maintained for a long enough period of time (up to hours) to enable the proper activation of the T cell. This is a particularly difficult task as T cells are already highly motile cells and the T cell-APC interaction occurs in non-static conditions. By monitoring the T cell cytoskeletal organization during their interaction with both APCs and APC mimetic surfaces, Kumari et al. found that antigen recognition triggered the formation of actin foci (by the help of Wiskott–Aldrich syndrome protein) at the T cell-APC-substrate contact that, with the assistance of myosin II contractility, generated and sustained intracellular tension within the T cell that maintained the stability and symmetry of the IS for the activation time frame [55].

Finally, in an elegant series of experiments combining pMHC and ICAM-1 coated on beads bared by deformable micropipettes and on micropillar arrays, Basu et al. demonstrated that mechanical forces at the IS potentiate cytotoxic T cell (CTL) cytotoxicity: CTLs destroy target cells by secreting a mixture of the protein perforin and granzyme proteases, where perforin forms pores in the target cell membrane that enable granzymes to access the cytoplasm and induce apoptosis [56]. Specifically, their study revealed that altering the membrane tension of the CTLs using pharmacological drugs or osmotic shock strongly perturbed the pore-forming activity of perforin. Similarly, altering the membrane tension of the target cell by changing substrate stiffness modulated CTL killing, with cells on stiffer substrates exhibiting a higher sensitivity to perforin-induced pore formation. Taken together, these results point towards a model in which forces at the IS promote CTL killing by straining the target cell membrane, thus facilitating the formation of perforin pores. Considering that several reports have correlated transformation and malignancy with cellular softening, this work

puts forth a very compelling hypothesis in which tumor cells modulate their mechanical properties to relief forces at the IS and thus evade the immune system [4,57].

T Cells can Sense and React to Substrate Stiffness

Just as we do when we use our fingers to apply pressure on an object, T cells exert forces to test their mechanical environment, particularly stiffness. Pioneering work by Judokusumo et al. initially documented this property by stimulating naïve CD4+ mouse T cells with polyacrylamide gels of different rigidities, and functionalized with activating antibodies against CD3 and CD28 [58]. Their experiments revealed that T cells exhibited stronger activation, quantified as IL-2 secretion, with increasing substrate rigidities (over the range of 10-200 KPa), and that this mechano-sensing/transduction ability was largely affiliated with the TCR/CD3 complex rather than CD28. Intriguingly, this "stiffness sensitivity" property was observed only when the anti-CD3 antibody was immobilized onto the surface of the gel, rather than added as a soluble solution, and it was lost upon myosin inhibition. These observations are in accordance with the now commonly accepted idea that antigen receptors pull against their ligands for optimal signaling. Conversely, similar experiments done by O'Connor et al. on polydimethylsiloxane substrates with the same functionalization but using a different rigidity range (100-200 KPa), showed that naïve CD4+ human T cells were stimulated and proliferated more on softer substrates in comparison to stiffer ones [59]. Taken together, these studies suggest a possible biphasic response to stiffness sensitivity. Another crucial piece of information came from Tabdanov et al. who employed a combination of activating anti-CD3 antibody and ICAM-1 functionalized flat micropatterned PDMS substrates (5 KPa- 2000 KPa) and micropillar arrays to delineate the contributions of both the TCR/CD3 complex and LFA-1 in stimulated CD4+ human T cell activation [60]. In these experiments, early T cell activation, measured by the total phosphor-tyrosine levels, was weaker on soft substrates than on rigid ones. Though this stiffness sensitivity was observed in the absence of LFA-1 engagement, it was enhanced by its presence.

Even more interestingly, their results also highlighted a mechanical cooperation between the TCR/CD3 and LFA-1-ICAM-1 systems, whereby actin nucleation downstream of TCR signaling sustained the growth of the LFA-1 dependent actin network, which in turn provided the cytoskeletal tension to allow mechanical sensing, T-cell spreading and enhanced TCR activation.

Similar experiments were later repeated but on substrates with stiffnesses of more physiologic relevance in terms of T cell function, considering that APCs display a stiffness range between ≃ 200 Pa and 2 KPa [61]. Notable of which were those performed by Hui et al. [62,63] who used poly-l-lysine-antiCD3-coated soft polyacrylamide gels (1- 5 KPa) to demonstrate the contributions of actin polymerization and myosin contractility, as well as dynamic microtubules, to force generation and maintenance during enhanced green fluorescent protein (eGFP)–actin expressing Jurkat T cell activation (quantified as phosphotyrosine signaling). Their results, similar to what was originally documented by Judokusumo et al., showed that T cells exhibited higher levels of activation on stiffer gels in comparison to softer ones.

Though these studies are difficult to directly compare because they differ in substrate chemistry, antibody/protein immobilization, stiffness ranges, and more importantly the T cell types/subtypes used, they do overall reveal that T cells possess the inherent ability to sense stiffness. This, at least partly, explains their modified behaviors in mechanically distinct interactions, whether it is different APCs that have been activated by different stimuli and present a varying repertoire of agonist/non-agonist pMHCs, or endothelial cells in blood vessels, or infected/tumor cells inside tissues. Even if the change in stiffness between these surfaces may seem quite modest and inconsequential, it is nevertheless sensed and responded to by T cells. Wahl et al. recently proposed a model in which increased substrate stiffness heightens the TCR-pMHC resistance to cytoskeletal forces and thus increases T cell spreading and activation, that is to a certain limit, beyond which the tension on the bonds becomes too high and breaks them, which

consequently decreases spreading and weakens T cell activation [64].

T Cells can Sense and React to Ligand Mobility

Aside from stiffness sensitivity, T cells have also been shown to be sensitive to ligand mobility [65]. The interaction between a T cell and an APC necessitates extensive cytoskeletal and lipid membrane composition changes for both cells, as to allow for the spatial ligand/receptor re-ordering mentioned above. In an innovative approach, Mossman et al. investigated the impact of ligand mobility on T cell signaling by creating "artificial APCs" where nanofabricated 10–20 nm high chromium barriers were assembled on pMHC and ICAM-1 coated supported lipid bilayers [66]; set up as is, the bilayer would allow for free lipid diffusion, however, the barriers would block the movement of proteins with larger cytoplasmic domains, and more importantly, TCR MCs. Interestingly, trapping the TCR clusters in the in the IS periphery (as opposed to their natural position in the cSMAC of the IS) augmented early TCR-associated phosphotyrosine signaling and cytoplasmic Ca2+ levels in the spatially constrained IS in comparison to the native ones. In a similar approach, but playing on the lipid bilayer composition instead of using chromium barriers for limiting ligand mobility, Hsu et al. revealed that tyrosine phosphorylation and persistent elevation of cytoplasmic Ca2+ was in fact more pronounced for T cells (Jurkat and naïve or stimulated CD4+ murine) on mobile membranes than on less mobile ones [67]. Though these two studies seem contradictory, the immobilization of the TCRs differed between the two systems; in the former, the chromium barriers completely trapped the TCR clusters in the periphery, on the other hand, the latter still permitted the diffusion of TCRs but at a slower rate. This could underline a complex mechanism, potentially reliant on the spatial and temporal parameters of ligand constriction, by which T cell sensitivity to ligand mobility impacts T cell activation. However, this would require further experimentation to decipher.

More recently, pioneering work done by Bukhardt and colleagues [30,68] revealed that dendritic cell (DC) maturation-

a process characterized by an increase in DC cortical stiffness-induced a dramatic actin-dependent decrease in ICAM-1 mobility. The reported decrease in ICAM-1 mobility helped generate a counterforce that drove the centripetal flow of the actomyosin network in the T cells spreading over the APC. This flow, in turn, recruited LFA-1 to the IS, maintained it in a high affinity conformation, and consequently promoted efficient binding to ICAM-1. One could imagine that since LFA-1 connects the extra- and intra-cellular compartments, similar to other integrins, the tension on LFA-1 will also affect the dynamics of the underlying T cell actin network [69]; since the TCR is thought to be interacting with said network, this will indirectly influence tension on the TCR, potentially modulating TCR signaling [13]. This work is of particular importance as firstly, it explains how LFA-1 reaches peak binding affinity necessary for proper T cell activation, and secondly, it suggests that cells can regulate intercellular communication by altering the physical status of the signaling molecules in question, rather than just their expression level or spatial localization.

How to Relay the Message?

Although the influence of mechanical forces on the specificity and sensitivity of antigen recognition by the TCR is coming to light, how information regarding TCR-antigen binding is relayed into the cell still remains unclear [70].

As mentioned above, TCR signaling propagates across the membrane through the CD3 intracellular domains, specifically through ITAM phosphorylation. In their unphosphorylated state, ITAM chains have been shown to be buried in the hydrophobic interior of the membrane, hence inaccessible to Src kinases. Ligand binding by the TCR has been recently proposed to induce conformational change in the CD3 chains, extending them and exposing their ITAMs to phosphorylation [71]. Although there are currently no definitive studies directly linking mechanical forces applied onto the TCR protein to this CD3ζ conformational change (e.g. are the forces needed pushing/pulling on the complex to unlock it, similar to an umbrella?), a recent study using fluorescence resonance energy transfer (FRET) showed

that the TCR, under force, is able to decipher structural subtle differences between peptides by different bond conformations, independent of binding affinity and kinetics. Peptide potency then appears to directly regulate the amount of conformational change, which in turn dictates the degree of dissociation of the CD3 (ζ chain) from the inner membrane leaflet and consequently the exposure of its ITAMs to phosphorylation [72].

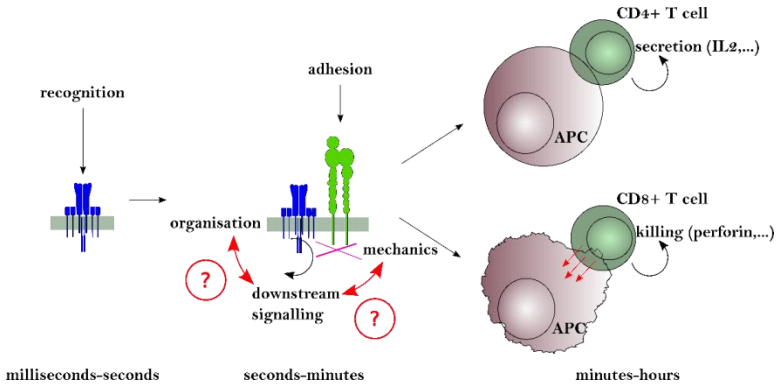

Figure 4: Typical times scales for signal propagation and consequences. The question marks indicate the interactions between different cell biology "modules" [73] that still need clarification in order to fully understand the entire process of T cell mechanotransduction and activation.

Another important question to address is the link between the different scales (Figure 4), particularly the TCR and the actin cytoskeleton. As mentioned previously, in adherent cells, the maintenance, growth and signaling through FAs are completely dependent on cytoskeletal forces. As such, FAs act as mechano-sensors/transducers bridging transmembrane adhesion receptor binding and actin flow with cell signaling. It is intriguing to imagine that the TCR MCs serve similar purposes. Using novel ratiometric tension probes, Ma et al. have demonstrated that TCRs undergoing clustering within the first few minutes of stimulation experience tension in the pN range [74,75]. It is thus highly likely that TCR clustering is stabilized by the underlying F-actin network or even through direct tethering of the TCR complex to cortical actin. Interestingly, the force-sensing protein lymphocyte-specific Crk-associated substrate (Cas-L) has recently been proposed by Santos et al. to mechanically link

TCR MCs to the underlying actin network [76]. Their experiments showed that Cas-L participates in a positive feedback loop whereby, upon TCR triggering, Cas-L localized to the TCR MCs undergoes actin-polymerization dependent activation (through phosphorylation), leading to Ca2+ signal amplification, regulation of TCR MC transport, inside-out integrin signaling, as well as actomyosin contraction [76].

Concluding Remarks

Besides the mechano-sensitive/transducive abilities of the TCR and integrins, there are several other membrane receptors, ion channels, cytoskeletal proteins, and transcriptional factors that are thought to be also affected by mechanical forces. For example, pulling forces on bound Notch receptors during endocytosis of Notch ligands induce a conformational change in Notch that ultimately drives early thymic progenitors to commit to the T cell lineage [77,78] and mechanical stretch of the membrane during IS formation activates Piezo channels, thereby triggering Ca2+ flux and regulating TCR signaling [79].

What is truly interesting is that these different elements do not function in isolation, but rather as parts of a complex mechanical signaling network with cross-talks and feedback loops, that ultimately regulates T cell mechanics, gene expression, and behavior. The challenge, now that some of the key elements have been described separately, is to understand how these mechano-signaling components and pathways are intertwined and integrated across time and length scales, and in different intra-cellular compartments, to shape the T cell response [7,73]. To take the TCR and LFA-1 as an example, Bernard and colleagues attempted to decipher the mechanical link between these two molecules by imaging T cells on anti-TCR Ab micropatterned soluble lipid bilayers (SLBs) [80]. Their results showed that the TCRs do in fact aggregate into MCs that colocalize with the anti-TCR Ab patterns, however, the clusters do not move (by the means of retrograde actin flow) to the center of the contact area, as seen during the formation of the central supramolecular activating complex of the IS. Only upon the addition of ICAM-1 to the SLBs, do the TCR MCs centralize with the actin and form

a peripheral ring around them. This study, in addition to many others [60,81,82], supports a model in which the actin cytoskeleton couples the TCR and LFA-1 in a positive feedback loop that coordinates IS formation and growth. It also puts forward a very exciting concept of the actin cytoskeleton acting as a mechanical intermediate that integrates force-dependent signals coming from different receptor-ligand interactions, and then coordinates outgoing responses over large distances [50].

Over the last decade, a sturdy foundation has emerged for measuring and interpreting mechanical forces in T cells. Nevertheless, the field remains in its infancy, we still don't know much- for example, how are mechanical forces transferred and integrated across different molecules, different scales, different time intervals, and different partner cells- however, what is becoming more and more apparent is that forces represent a fundamental component of the T cell response that can no longer be ignored. It is our hope that the literature and arguments presented in this review raise awareness to this emerging area of research in T-cell biology. It is also worth noting that the concepts presented here for T cells apply to all immune cell types, with basic similar phenomena and subtle differences for other lymphocytes such as B cells and NK cells, but also APCs such as dendritic cells, macrophages and neutrophils [4,6].

References

1. Thompson, D'Arcy Wentworth. On Growth and Form. Revised ed. édition. New York: Dover Publications Inc. 1992.
2. Murray CD. 'The Physiological Principle of Minimum Work: I. The Vascular System and the Cost of Blood Volume'. Proceedings of the National Academy of Sciences of the United States of America. 1926; 12: 207–214.
3. Teichtahl, Andrew J, Anita E Wluka, Pushpika Wijethilake, Yuanyuan Wang, et al. 'Wolff's Law in Action: A Mechanism for Early Knee Osteoarthritis'. Arthritis Research & Therapy. 2015; 17: 207.
4. Huse, Morgan. 'Mechanical Forces in the Immune System'. Nature Reviews Immunology. 2017; 17: 679–690.

5. Murphy, Ken, Paul Travers, Mark Walport. Janeway's Immunobiology 7th Edition. Edited by Garland Science. 2008.
6. Zhang, Xuexiang, Tae-Hyung Kim, Timothy J Thauland, Hongjun Li, et al. 'Unraveling the Mechanobiology of Immune Cells'. Current Opinion in Biotechnology. 2020; 66: 236–245.
7. Limozin, Laurent, Pierre-Henri Puech. 'Membrane Organization and Physical Regulation of Lymphocyte Antigen Receptors: A Biophysicist's Perspective'. The Journal of Membrane Biology. 2019; 252: 397–412.
8. Malissen, Bernard, Pierre Bongrand. 'Early T Cell Activation: Integrating Biochemical, Structural, and Biophysical Cues'. Annual Review of Immunology. 2015; 33: 539–561.
9. Rossy, Jérémie, Julia M Laufer, Daniel F Legler. Role of Mechanotransduction and Tension in T Cell Function'. Frontiers in Immunology. 2018; 9.
10. Huppa, Johannes B, Mark M Davis. 'The Interdisciplinary Science of T-Cell Recognition'. In Advances in Immunology. 2013; 119: 1–50.
11. Pageon, Sophie V, Matt A Govendir, Daryan Kempe, Maté Biro. 'Mechanoimmunology : Molecular-Scale Forces Govern Immune Cell Functions'. 2018; 29: 1919–1926.
12. Rushdi, Muaz, Kaitao Li, Zhou Yuan, Stefano Travaglino, et al. 'Mechanotransduction in T Cell Development, Differentiation and Function'. Cells. 2020; 9.
13. He, Hai-Tao, Pierre Bongrand. 'Membrane Dynamics Shape TCR-Generated Signaling'. Frontiers in Immunology. 2012; 3: 90.
14. Wang N, JP Butler, DE Ingber. 'Mechanotransduction across the Cell Surface and through the Cytoskeleton'. Science (New York, N.Y.). 1993; 260: 1124–1127.
15. Springer, Timothy A, Michael L Dustin. 'Integrin Inside-out Signaling and the Immunological Synapse'. Current Opinion in Cell Biology. 2012; 24: 107–115.
16. Gérard, Audrey, Andrew P Cope, Claudia Kemper, Ronen Alon, et al. 'LFA-1 in T Cell Priming, Differentiation, and Effector Functions'. Trends in Immunology. 2021; 42: 706–722.

17. Luo, Bing-Hao, Christopher V Carman, Timothy A Springer. ‘Structural Basis of Integrin Regulation and Signaling’. Annual Review of Immunology. 2007; 25: 619–647.
18. Dustin ML, TA Springer. ‘T-Cell Receptor Cross-Linking Transiently Stimulates Adhesiveness through LFA-1.’ Nature. 1989; 341: 619–624.
19. Kim, Sun Taek, Koh Takeuchi, Zhen-Yu J Sun, Maki Touma, et al. ‘The Alphabeta T Cell Receptor Is an Anisotropic Mechanosensor’. J Biol Chem. 2009; 284: 31028–31037.
20. Feigelson, Sara W, Ronit Pasvolsky, Saso Cemerski, Ziv Shulman, et al. ‘Occupancy of Lymphocyte LFA-1 by Surface-Immobilized ICAM-1 Is Critical for TCR- but Not for Chemokine-Triggered LFA-1 Conversion to an Open Headpiece High-Affinity State.’ Journal of Immunology (Baltimore, Md.: 1950). 2010; 185: 7394–7404.
21. Astrof, Nathan S, Azucena Salas, Motomu Shimaoka, JianFeng Chen, et al. Springer. ‘Importance of Force Linkage in Mechanochemistry of Adhesion Receptors’. Biochemistry. 2006; 45: 15020–15028.
22. Friedland, Julie C, Mark H Lee, David Boettiger. ‘Mechanically Activated Integrin Switch Controls Alpha5beta1 Function’. Science (New York, N.Y.). 2009; 323: 642–644.
23. Kong, Fang, A Paul Mould, Martin J Humphries, Cheng Zhu. ‘Demonstration of Catch Bonds between an Integrin and Its Ligand’. Cell. 2009; 185: 1275–1284.
24. Chen, Wei, Jizhong Lou, Cheng Zhu. ‘Forcing Switch from Short- to Intermediate- and Long-Lived States of the AA Domain Generates LFA-1/ICAM-1 Catch Bonds’. Journal of Biological Chemistry. 2010; 285: 35967–35978.
25. Husson, Julien, Karine Chemin, Armelle Bohineust, Claire Hivroz, et al. ‘Force Generation upon T Cell Receptor Engagement’. Edited by Javed N. Agrewala. PLoS ONE. 2011; 6: e19680.
26. Smith-Garvin, Jennifer E, Gary A Koretzky, Martha S Jordan. ‘T Cell Activation’. Annu Rev Immunol. 2009; 27: 591–619.
27. Chakraborty, Arup K, Arthur Weiss. ‘Insights into the Initiation of TCR Signaling.’ Nature Immunology. 2014; 15: 798–807.

28. Rudolph, Markus G, Robyn L Stanfield, Ian A Wilson. ‘How TCRs Bind MHCs, Peptides, and Coreceptors.’ Annu Rev Immunol. 2006; 24: 419–466.
29. Sundberg, Eric J, Roy A Mariuzza. ‘Molecular Recognition in Antibody-Antigen Complexes’. Advances in Protein Chemistry. 2002; 61: 119–160.
30. Rossjohn, Jamie, Stephanie Gras, John J Miles, Stephen J Turner, et al. ‘T Cell Antigen Receptor Recognition of Antigen-Presenting Molecules’. Annual Review of Immunology. 2015; 33: 169–200.
31. Huang, Jun, Mario Brameshuber, Xun Zeng, Jianming Xie, et al. ‘A Single Peptide-Major Histocompatibility Complex Ligand Triggers Digital Cytokine Secretion in CD4(+) T Cells.’ Immunity. 2013; 39: 846–857.
32. Ma, Zhengyu, Paul A Janmey, Terri H Finkel. ‘The Receptor Deformation Model of TCR Triggering’. The FASEB Journal. 2008; 22: 1002–1008.
33. Liu, Baoyu, Wei Chen, Brian D Evavold, Cheng Zhu. ‘Accumulation of Dynamic Catch Bonds between TCR and Agonist Peptide-MHC Triggers T Cell Signaling’. Cell. 2014; 157: 357–368.
34. Das, Dibyendu Kumar, Yinnian Feng, Robert J Mallis, Xiaolong Li, et al. ‘Force-Dependent Transition in the T-Cell Receptor β-Subunit Allosterically Regulates Peptide Discrimination and PMHC Bond Lifetime’. Proceedings of the National Academy of Sciences. 2015; 112: 1517–1522.
35. Limozin, Laurent, Marcus Bridge, Pierre Bongrand, Omer Dushek, et al. ‘TCR-PMHC Kinetics under Force in a Cell-Free System Show No Intrinsic Catch Bond, but a Minimal Encounter Duration before Binding’. Proceedings of the National Academy of Sciences of the United States of America. 2019; 116: 16943–16948.
36. Wu, Peng, Tongtong Zhang, Baoyu Liu, Panyu Fei, et al. ‘Mechano-Regulation of Peptide-MHC Class I Conformations Determines TCR Antigen Recognition’. Molecular Cell. 2019; 73: 1015-1027.e7.
37. Carpenter, Andrea C, Rémy Bosselut. ‘Decision Checkpoints in the Thymus’. Nature Immunology. 2010; 11: 666–673.
38. Irving BA, FW Alt, N Killeen. ‘Thymocyte Development in the Absence of Pre-T Cell Receptor Extracellular

Immunoglobulin Domains'. Science (New York, N.Y.). 1998; 280: 905–908.
39. Yamasaki, Sho, Takashi Saito. 'Molecular Basis for Pre-TCR-Mediated Autonomous Signaling'. Trends in Immunology. 2007; 28: 39–43.
40. Smelty, Philippe, Céline Marchal, Romain Renard, Ludivine Sinzelle, et al. 'Identification of the Pre-T-Cell Receptor Alpha Chain in Nonmammalian Vertebrates Challenges the Structure-Function of the Molecule'. Proceedings of the National Academy of Sciences of the United States of America. 2010; 107: 19991–19996.
41. Mallis, Robert J, Ke Bai, Haribabu Arthanari, Rebecca E Hussey, et al. 'Pre-TCR Ligand Binding Impacts Thymocyte Development before AβTCR Expression'. Proceedings of the National Academy of Sciences. 2015; 112: 201504971–201504971.
42. Das, Dibyendu Kumar, Robert J Mallis, Jonathan S Duke-Cohan, Rebecca E Hussey, et al. 'Pre-TCRs Leverage Vβ CDRs and Hydrophobic Patch in Mechanosensing Thymic Self-Ligands'. Journal of Biological Chemistry. 2016; 291: jbc.M116.752865-jbc.M116.752865.
43. Ananthakrishnan, Revathi, Allen Ehrlicher. 'The Forces behind Cell Movement'. International Journal of Biological Sciences. 2007; 3: 303–317.
44. Salvi, Alicia M, Kris A DeMali. 'Mechanisms Linking Mechanotransduction and Cell Metabolism'. Current Opinion in Cell Biology. 2018; 54: 114–120.
45. Chen, Christopher S, John Tan, Joe Tien. 'Mechanotransduction at Cell-Matrix and Cell-Cell Contacts'. Annual Review of Biomedical Engineering. 2004; 6: 275–302.
46. Prager-Khoutorsky, Masha, Alexandra Lichtenstein, Ramaswamy Krishnan, Kavitha Rajendran, et al. 'Fibroblast Polarization Is a Matrix-Rigidity-Dependent Process Controlled by Focal Adhesion Mechanosensing'. Nature Cell Biology. 2011; 13: 1457–1465.
47. Welf, Erik S, Christopher E Miles, Jaewon Huh, Etai Sapoznik, et al. 'Actin-Membrane Release Initiates Cell Protrusions'. Developmental Cell. 2020; 55: 723-736.e8.
48. Schlaepfer, David D, Steven K Hanks, Tony Hunter, Peter

van der Geer. ‘Integrin-Mediated Signal Transduction Linked to Ras Pathway by GRB2 Binding to Focal Adhesion Kinase’. Nature. 1994; 372: 786–791.
49. Davis, Simon J, P Anton van der Merwe. ‘The Kinetic-Segregation Model: TCR Triggering and Beyond.’ Nat Immunol. 2006; 7: 803–809.
50. Comrie, William A, Janis K Burkhardt. ‘Action and Traction: Cytoskeletal Control of Receptor Triggering at the Immunological Synapse’. Frontiers in Immunology. 2016; 7.
51. Cai, En, Kyle Marchuk, Peter Beemiller, Casey Beppler, et al. ‘Visualizing Dynamic Microvillar Search and Stabilization during Ligand Detection by T Cells’. Science. 2017; 356: eaal3118–eaal3118.
52. Brodovitch, Alexandre, Pierre Bongrand, Anne Pierres. ‘T Lymphocytes Sense Antigens within Seconds and Make a Decision within One Minute’. Journal of Immunology (Baltimore, Md.: 1950). 2013; 191: 2064–2071.
53. Brodovitch, Alexandre, Eugene Shenderov, Vincenzo Cerundolo, Pierre Bongrand, et al. ‘T Lymphocytes Need Less than 3 Min to Discriminate between Peptide MHCs with Similar TCR-Binding Parameters’. European Journal of Immunology. 2015.
54. Blumenthal, Daniel, Janis K Burkhardt. ‘Multiple Actin Networks Coordinate Mechanotransduction at the Immunological Synapse’. The Journal of Cell Biology. 2020; 219.
55. Kumari, Sudha, Michael Mak, Yeh-Chuin Poh, Mira Tohme, et al. ‘Cytoskeletal Tension Actively Sustains the Migratory T-cell Synaptic Contact’. The EMBO Journal. 2020; 39.
56. Basu, Roshni, Benjamin M Whitlock, Julien Husson, Judy Lieberman, et al. ‘Cytotoxic T Cells Use Mechanical Force to Potentiate Target Cell Killing Cytotoxic T Cells Use Mechanical Force to Potentiate Target Cell Killing’. Cell. 2016; 165: 100–110.
57. Basu, Roshni, Morgan Huse. ‘Mechanical Communication at the Immunological Synapse’. Trends in Cell Biology. 2017; 27: 241–254.
58. Judokusumo, Edward, Erdem Tabdanov, Sudha Kumari, Michael L Dustin, et al. ‘Mechanosensing in T Lymphocyte Activation’. Biophysical Journal. 2012; 102: L5-7.

59. O'Connor, Roddy S, Xueli Hao, Keyue Shen, Keenan Bashour, et al. 'Substrate Rigidity Regulates Human T Cell Activation and Proliferation.' Journal of Immunology (Baltimore, Md. : 1950). 2012; 189: 1330–1339.
60. Tabdanov, Erdem, Sasha Gondarenko, Sudha Kumari, Anastasia Liapis, et al. 'Micropatterning of TCR and LFA-1 Ligands Reveals Complementary Effects on Cytoskeleton Mechanics in T Cells'. Integrative Biology (United Kingdom). 2015; 7: 1272–1284.
61. Bufi, Nathalie, Michael Saitakis, Stéphanie Dogniaux, Oscar Buschinger, et al. 'Human Primary Immune Cells Exhibit Distinct Mechanical Properties That Are Modified by Inflammation'. Biophysical Journal. 2015; 108: 2181–2190.
62. Hui, King Lam, Lakshmi Balagopalan, Lawrence E. Samelson, Arpita Upadhyaya. 'Cytoskeletal Forces during Signaling Activation in Jurkat T-Cells'. Molecular Biology of the Cell. 2015; 26: 685–695.
63. Hui, King Lam, Arpita Upadhyaya. 'Dynamic Microtubules Regulate Cellular Contractility during T-Cell Activation'. Proceedings of the National Academy of Sciences. 2017; 114: E4175–4183.
64. Wahl, Astrid, Céline Dinet, Pierre Dillard, Aya Nassereddine, et al. 'Biphasic Mechanosensitivity of T Cell Receptor-Mediated Spreading of Lymphocytes'. Proceedings of the National Academy of Sciences. 2019; 116: 5908–5913.
65. Dillard, Pierre, Rajat Varma, Kheya Sengupta, Laurent Limozin. 'Ligand-Mediated Friction Determines Morphodynamics of Spreading T Cells'. Biophysical Journal. 2014; 107: 2629–2638.
66. Mossman, Kaspar D, Gabriele Campi, Jay T Groves, Michael L Dustin. 'Altered TCR Signaling from Geometrically Repatterned Immunological Synapses.' Science. 2005; 310: 1191–1193.
67. Hsu, Chih-Jung, Wan-Ting Hsieh, Abraham Waldman, Fiona Clarke, et al. 'Ligand Mobility Modulates Immunological Synapse Formation and T Cell Activation'. PloS One. 2012; 7: e32398.
68. Comrie, William A, Shuixing Li, Sarah Boyle, Janis K Burkhardt. 'The Dendritic Cell Cytoskeleton Promotes T Cell Adhesion and Activation by Constraining ICAM-1

Mobility'. The Journal of Cell Biology. 2015; 208: 457–473.
69. Jankowska, Katarzyna I, Edward K Williamson, Nathan H Roy, Daniel Blumenthal, et al. 'Integrins Modulate T Cell Receptor Signaling by Constraining Actin Flow at the Immunological Synapse'. Frontiers in Immunology. 2018; 9.
70. Harrison, Devin L, Yun Fang, Jun Huang. 'T-Cell Mechanobiology: Force Sensation, Potentiation, and Translation'. Frontiers in Physics. 2019; 7.
71. Lee, Mark S, Caleb R Glassman, Neha R Deshpande, Hemant B Badgandi, et al. 'A Mechanical Switch Couples T Cell Receptor Triggering to the Cytoplasmic Juxtamembrane Regions of CD3ζζ'. Immunity. 2015; 43: 227–239.
72. Sasmal, Dibyendu K, Wei Feng, Sobhan Roy, Peter Leung, et al. 'TCR–PMHC Bond Conformation Controls TCR Ligand Discrimination'. Cellular & Molecular Immunology. 2019.
73. Puech, Pierre-Henri, Pierre Bongrand. 'Mechanotransduction as a Major Driver of Cell Behaviour: Mechanisms, and Relevance to Cell Organization and Future Research'. Open Biology. 2021; 11: 210256.
74. Ma, Victor Pui-Yan, Yang Liu, Lori Blanchfield, Hanquan Su, et al. 'Ratiometric Tension Probes for Mapping Receptor Forces and Clustering at Intermembrane Junctions'. Nano Letters. 2016; 16: 4552–4559.
75. Liu, Yang, Lori Blanchfield, Victor Pui-Yan Ma, Rakieb Andargachew, Kornelia Galior, et al. 'DNA-Based Nanoparticle Tension Sensors Reveal That T-Cell Receptors Transmit Defined PN Forces to Their Antigens for Enhanced Fidelity'. Proceedings of the National Academy of Sciences. 2016; 113: 5610–5615.
76. Santos, Luís C, David A Blair, Sudha Kumari, Michael Cammer, et al. 'Actin Polymerization-Dependent Activation of Cas-L Promotes Immunological Synapse Stability'. Immunology and Cell Biology. 2016; 94: 981–993.
77. Wang X, T Ha. 'Defining Single Molecular Forces Required to Activate Integrin and Notch Signaling'. Science. 2013; 340: 991–994.
78. Luca, Vincent C, Byoung Choul Kim, Chenghao Ge, Shinako Kakuda, et al. 'Notch-Jagged Complex Structure Implicates a Catch Bond in Tuning Ligand Sensitivity'.

Science. 2017; 355: 1320–1324.
79. Liu, Chinky Shiu Chen, Deblina Raychaudhuri, Barnali Paul, Yogaditya Chakrabarty, et al. ‘Cutting Edge: Piezo1 Mechanosensors Optimize Human T Cell Activation’. The Journal of Immunology. 2018; 200: 1255–1260.
80. Benard, Emmanuelle, Jacques A Nunès, Laurent Limozin, Kheya Sengupta. ‘T Cells on Engineered Substrates: The Impact of TCR Clustering Is Enhanced by LFA-1 Engagement’. 2018; 9: 1–12.
81. Chen, Yunfeng, Lining Ju, Muaz Rushdi, Chenghao Ge, et al. ‘Receptor-Mediated Cell Mechanosensing’. Molecular Biology of the Cell. 2017; 28: 3134–3155.
82. Verma, Navin Kumar, Dermot Kelleher, Email Alerts. ‘Not Just an Adhesion Molecule: LFA-1 Contact Tunes the T Lymphocyte Program’. 2018.

Book Chapter

Role of Macrophages in Response to Wear Debris from Joint Replacement

Mona EL KADRI

Lebanese University, Faculty of Sciences I, Lebanon

***Corresponding Author:** Mona EL KADRI, Lebanese University, Faculty of Sciences I, Hadath- Beirut, Lebanon

Published **August 02, 2022**

How to cite this book chapter: Mona EL KADRI. Role of Macrophages in Response to Wear Debris from Joint Replacement. In: Hussein Fayyad Kazan, editor. Immunology and Cancer Biology. Hyderabad, India: Vide Leaf. 2022.

Abstract

Aseptic loosening secondary to periprosthetic osteolysis has been reported as the major cause of failure of total joint arthroplasties (TJAs) in the long-term. Wear particulate debris, mainly ultra-high molecular weight polyethylene (UHMWPE) particles released from the implant, are considered the main contributors to periprosthetic osteolysis. These particles can activate macrophages to release cytokines and pro-inflammatory mediators that stimulate osteoclastogenesis, leading to bone resorption, implant failure, and therefore, revision surgery. This chapter explains in details how macrophages may play an important role in periprosthetic osteolysis, and suggests new

approaches that have the potential to be future therapeutics for this condition.

Introduction to Joint Replacement

Total joint replacements (TJRs) of the lower extremity has achieved great success in orthopedics in the twentieth century. They are considered the most effective surgical treatment for alleviating pain and improving ambulation and function for patients with various end-stage hip and knee diseases [1]. TJRs are being prescribed to a growing number of youthful and physically demanding patients due to their clinical success and increasing acceptance in the surgical population. According to Kurtz et al. (2009), more than half of all hip and knee TJRs in the United States are performed on patients under the age of 65 [2]. However, long-term studies of TJRs have shown a finite failure rate and a need for revision surgery; furthermore, studies suggest that the need for revision surgeries might double over the next decades [3].

Implant failure can be caused by a variety of factors, including implant design, surgical technique, fixation method, infection, and aseptic loosening [4]. Aseptic loosening secondary to periprosthetic osteolysis is a long-term complication that may require revision surgery to excise loose implants and re-implant new ones. The more severe the bone defects, the more challenging the revision technique is, and the less predictable the outcomes are [5].

In the context of joint replacement, osteolysis is defined as the process of progressive destruction of periprosthetic bony tissue caused by osteoclasts. Routinely, osteolysis of the bone around TJRs is usually evaluated using sequential conventional radiographs and is characterized by radiolucency in the bone near the implant/cement mantle [6]. Osteolysis has been reported in up to 24% of total hip arthroplasty (THA) cases in the first 10 years of the procedure [7], and in 5% to 20% of total knee arthroplasty (TKA) cases at follow-up times ranging from less than 5 years to 15 years [8].

Wear Particles in Periprosthetic Osteolysis

Today, it is widely accepted that the major contributors to the development of periprosthetic osteolysis are the wear debris released continually from a TJR's articulating surface [6]. Materials used in surgical reconstruction can vary from polymers such as Polyethylene (PE) and Polymethylmethacrylate (PMMA) to metals and ceramics [3]. Conventional hip replacement systems generally include an acetabular cup made of ultra-high molecular weight polyethylene (UHMWPE) articulated with a rigid femoral head consisting of either metal or ceramic. The joint replacement system is either impacted i.e. (uncemented arthroplasty) or cemented with (PMMA) cement. For knee replacement surgery, the material of choice is UHMWPE tibial tray, hinged with highly polished metal femoral components [6].

Analyses of periprosthetic tissues retrieved during revision surgeries revealed that the most common type of debris surrounding failed hip, knee, and shoulder TJRs is the (UHMWPE) wear debris, regardless to whether the implants were cemented or not [9]. Hundreds of thousands of UHMWPE particles can be released during a single gait cycle. Those particles vary greatly in size and morphology, from large platelet-like particles up to 250 µm in length, to fibrils and sub-micrometer globule-shaped spheroids between 0.1 and 0.5µm in diameter. However, 90% of the reactive particles are reported to be less than 1 µm with a mean 0.5 µm diameter [10].

The Monocyte/Macrophage Lineage Cells

Blood monocytes are circulating phagocytic cells of the innate immunity, originating from the myeloid lineage of the multipotent hematopoietic stem cells (HSCs) in the bone marrow. These cells use chemokine receptors and pathogen recognition receptors (PRRs) to execute immunological effector activities. During inflammation, monocytes migrate into solid tissues where they can differentiate into resident macrophages or dendritic cells (DCs) with the help of the macrophage-colony stimulating factor (M-CSF), and the local microenvironment [4].

Macrophages, which are a key component of innate cellular immunity, have a wide range of activities that include host defense and immunity against foreign microorganisms such as bacteria, viruses, fungi, and parasites. They have a diverse set of cell surface receptors, intracellular mediators, and critical secretory chemicals that allow them to recognize, engulf, and destroy invading pathogens, as well as regulate other immune cells [11].

Tissue-resident macrophages have pattern recognition receptors (PRRs) which are necessary for the host's response to pathogens. Innate immunity relies on PRRs as the first line of defense for recognizing microbial patterns (pathogen-associated molecular patterns, or PAMPs). The most common PRRs are the Toll-like receptors (TLRs). These PRRs stimulate the synthesis and release of proinflammatory cytokines such as IL-6, TNF-α, and IL-1 [4].

Macrophages can adopt one of the two different phenotypes, the M1 and M2 phenotypes, depending on different phenotypical and functional activation stages in response to their local micro environment. The M1 phenotype is characterized by a high capacity of antigen presentation and high production of proinflammatory cytokines (TNF-α, IL-1β, IL-6, etc.), while the M2 phenotype is characterized by the suppression of proinflammatory cytokines, intracellular killing, antigen presentation, and increased production of IL-10 [12].

Macrophage Response to Wear Particles in-Vivo

Many evidences have shown that UHMWPE particles promote the presence and activity of macrophages in the periprosthetic tissues surrounding joint replacements. Analyses of periprosthetic membranes around joint replacements from patients indicated the presence of many biochemical mediators of inflammation, cellular recruitment and bone resorption such as TNF-a, IL-1, IL-6, and PGE2 [13]. Al-Saffar et al. (1995) [14] have shown that these mediators are produced by particle-activated macrophages and contribute to the enhancement of the

inflammatory response by activating endothelial cells and attracting more macrophage precursors to the interfacial membrane. Moreover, Kim et al. (1998) [15] conducted a study on rats carried where they were subjected to continuous infusion of polyethylene particles to the knee joint via an osmotic pump showed an elevation in the TNF-α mRNA in the granulomatous tissue, and its absence in the control tissue. This study was the first to note the importance of TNF-α produced by macrophages in particle induced osteolysis in vivo.

Macrophage Response to Wear Particles in-Vitro

The response of macrophages to polyethylene particles is most relevant to wear particle-induced osteolysis in vivo. However, wear particles are difficult to manipulate in vitro due to their low density compared to culture medium which causes them to float in simple systems. This fact has made research of therapeutically relevant polyethylene wear particles restricted. Furthermore, it is considered a challenge to synthesize endotoxin-free polyethylene particles that are similar in size and shape to clinical particles.

Successful in vitro studies have clearly demonstrated that particle-stimulated macrophages produce a range of potentially osteolytic mediators (IL-1, IL-6, TNF-α, GM-CSF, PGE2) with TNF-α being the key osteolytic cytokine generated [16]. This was also corroborated by Algan et al. (1997), [17] who showed that the addition of anti-TNF-α antibody can dramatically limit bone resorption by supernatants from particle-stimulated macrophages.

Regulation of Osteoclast Differentiation

In order to understand the role of macrophages and their cytokines in osteolysis, it is important to understand the relationship between macrophages and the cells involved in both normal bone metabolism and bone resorption. Osteoclasts are the main bone-resorptive cells derived from the haematopoietic cells of the mononuclear phagocyte lineage [18]; their capacity to polarize and resorb bone depends mainly on the expression of

the c-src proto-oncogene [19]. On the other hand, osteoblasts are stromal cells of mesenchymal origin concerned in bone formation [20]. Both types of cells play an equally important role in the regulation of bone mass, and it is the activity of osteoclasts relative to osteoblasts that determines the degree of osteolysis in TJR.

Osteoclast precursors express on their surface a receptor for activation of NFkB (RANK), while osteoblasts/bone marrow stromal cells express on their surface a receptor for activation of NFkB ligand (RANKL). The binding of RANKL to RANK on osteoclast precursors was shown to stimulate osteoclast differentiation (osteoclastogenesis), and RANKL was shown to activate bone resorption by mature osteoclasts [21].

On the other hand, osteoprotegerin (OPG), which is a stromal cell-secreted glycoprotein, binds to RANKL on osteoblasts/stromal cells and inhibits the interaction between RANK on osteoclast precursors and RANKL, thereby inhibiting osteoclastogenesis [6]. (Figure 1)

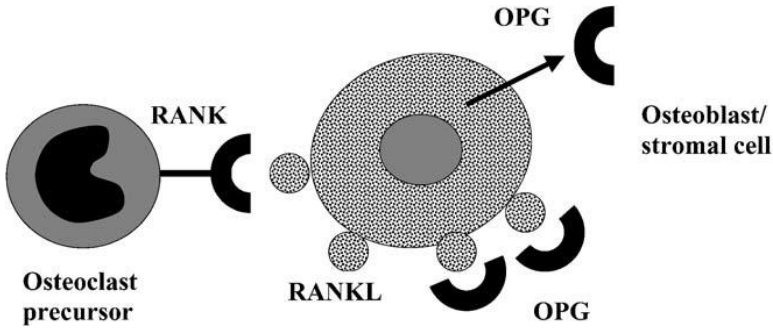

Figure 1: Relationship between RANK, RANKL and OPG [6].

RANK: receptor for activation of NFkB; RANKL: receptor for activation of NFkB ligand; OPG: osteoprotegerin

Role of Macrophages in Osteoclast Differentiation

The biological reaction to wear debris is complicated, and it frequently leads to periprosthetic tissue damage and implant loosening. While there is significant evidence that diverse cell types such as osteoblasts, fibroblasts, lymphocytes, and others are involved in the process of osteolysis, the inflammatory response to prosthetic wear debris is mainly driven by cells of the monocyte/macrophage lineage [4].

Macrophages adhere to and effectively phagocytose small foreign particles (<10 μm), while for larger particles (20–100 μm) that cannot be effectively phagocytosed by a single macrophage, foreign body granulomas will be formed. However, particles ranging between 0.1 and 1.0 μm are thought to be the most biologically active [5]. In addition to phagocytosis, contact between particles and cell membrane receptors such as CD-14, TLR, and scavenger receptors (MARCO) can also lead to the proliferation, differentiation, and activation of macrophages. These events result in intracellular signal transduction via the activation of the transcription factor NFkB and nuclear translocation, which in turn up-regulate pro-inflammatory/pro-osteoclastic cytokines gene expression [4,22].

There are different methods by which macrophages, activated by particles in the periprosthetic membrane, can contribute to osteolysis. (1) The produced inflammatory cytokines and chemotactic factors result in increased recruitment of haematopoeitic osteoclast precursors from the vasculature. (2) TNF-α and IL-1 produced by macrophages cause an increase in M-CSF and RANKL expression by osteoblasts/ stromal cells, thereby, leading to the proliferation and differentiation of osteoclast precursors into mature osteoclasts. Moreover, TNF-α may (3) accelerate the differentiation of osteoclast precursors in the presence of basal levels of RANKL-signaling by stromal cells, and (4) stimulate mature osteoclasts to resorb bone [6]. (Figure 2)

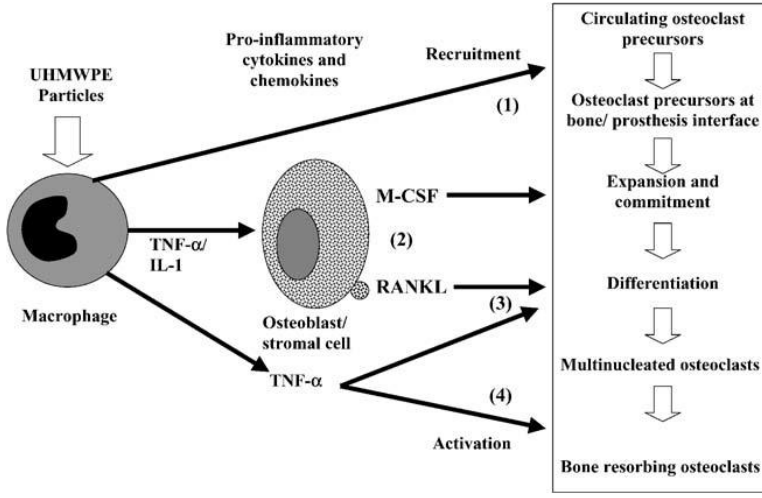

Figure 2: Potential mechanisms whereby UHMWPE particle-stimulated macrophages may stimulate osteolysis in total joint replacement [6].

UHMWPE: ultra-high molecular weight polyethylene; TNF-α: tumor necrosis factor α; IL-1: interleukin 1; M-CSF: macrophage colony stimulating factor; RANKL: receptor for activation of NFkB ligand

Treatment/Prevention of Osteolysis in Total Joint Replacement

Understanding the sequence of events that occur during wear particle osteolysis has led to the development of novel treatment approaches.

For instance, Osteoprotegerin (OPG) has displayed an ability to block RANK signaling and inhibit osteoclastogenesis in animal models of wear debris-induced osteolysis [23]. This raised the idea of gene therapy for life-long delivery of therapeutic agents such as OPG. The idea was then investigated by single intra-muscular injection of an adenoviral vector co-expressing OPG in the murine calvarial model of particle-induced osteolysis, which showed a complete inhibition of osteolysis [24].

Another recent approach suggested for the treatment of osteolysis uses the human beta-defensin 3 (HBD3). HBD3 is a cationic peptide predominantly secreted from leukocytes and epithelial tissues in response to an external stimulus such as TNF-α secreted by macrophages in the presence of a microbe. Previous studies on a mouse periodontitis model have demostrated that HBD3 can decrease the levels of TNF-α in periodontium exposed to *Porphyromonas gingivalis* (P.g) as well as to reduce osteoclast formation and lower alveolar bone loss [25]. The mechanism of HBD3 anti-inflammatory activity appeared to involve specific targeting of TLR signaling pathways resulting in transcriptional repression of pro-inflammatory genes [26]. HBD3 induces serial inhibition of IκB phosphorylation, p65 nuclear translocation, and, finally, NF-κB-dependent inflammatory responses, thereby, inhibiting pro-inflammatory cytokine release [27] (Figure3). Due to this anti-inflammatory mechanism, HBD3 is thought to be a promising therapy for reducing the TNF-α expression by macrophages, which is the main cause for the fail of TJR surgeries in patients with periprosthetic osteolysis.

However, these suggested strategies are still under study and no applicable treatments for periprosthetic osteolysis are yet available. Further studies are still needed to be done in-vivo in order to ensure the efficacy of the new approaches.

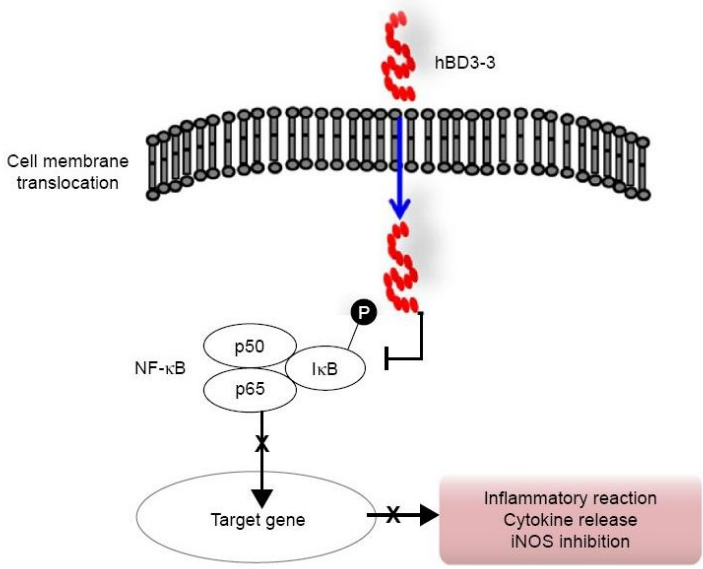

Figure 3: The anti-inflammatory mechanism of HBD3 [27].
hBD3: human beta defensin 3; NFKB: nuclear factor kappa light chain enhancer of activated B cells; IKB: inhibitor for KB; iNOS: inducible nitric oxide synthase

Conclusion

In conclusion, aseptic loosening secondary to periprosthetic osteolysis is caused by particulate debris, mainly UHMWPE particles, released from the implant. These particles of critical size can activate macrophages in the periprosthetic tissue to produce an array of cytokines and other mediators of inflammation. Specifically, macrophage-derived TNF-α stimulates osteoblast expression of RANKL and M-CSF, which are the essential factors needed for the proliferation and differentiation of osteoclast precursors into mature osteoclasts. Those events lead to the activation of mature osteoclasts to resorb bone, causing aseptic loosening. Different approaches have been suggested for the treatment of osteolysis such as gene therapy or using the anti-inflammatory peptide HBD3. However, efficacious biologic treatments of periprosthetic osteolysis are not yet available. Further research is needed to develop

preventative and therapeutic methods for particle-induced osteolysis to mitigate the need for revision surgery.

References

1. SB Goodman, E Gómez Barrena, M Takagi, YT Konttinen. Biocompatibility of total joint replacements: A review. J. Biomed. Mater. Res. A. 2009; 90; 603–618.
2. SM Kurtz, E Lau, K Ong, K Zhao, M Kelly, et al. Future young patient demand for primary and revision joint replacement: national projections from 2010 to 2030. Clin. Orthop. 2009; 467: 2606–2612.
3. SB Goodman, E Gibon, J Pajarinen, TH Lin, M Keeney, et al. Novel biological strategies for treatment of wear particle-induced periprosthetic osteolysis of orthopaedic implants for joint replacement. J. R. Soc. Interface. 2014; 11: 20130962.
4. Christophe Nich, Yuya Takakubo, Jukka Pajarinen, Mari Ainola, Abdelhakim Salem, et al. Macrophages-Key cells in the response to wear debris from joint replacements: Macrophage Response to Wear Debris. J. Biomed. Mater. Res. A. 2013; 101: 3033–3045.
5. J Rao, E Gibon, T Ma, Z Yao, RL Smith, et al. Revision joint replacement, wear particles, and macrophage polarization. Acta Biomater. 2012; 8: 2815–2823.
6. E Ingham, J Fisher. The role of macrophages in osteolysis of total joint replacement. Biomaterials. 2005; 26: 1271–1286.
7. Lübbeke, G Garavaglia, C Barea, R Stern, R Peter, et al. Influence of patient activity on femoral osteolysis at five and ten years following hybrid total hip replacement. J. Bone Joint Surg. Br. 2011; 93-B: 456–463.
8. TK Fehring, JA Murphy, TD Hayes, DW Roberts, DL Pomeroy, et al. The Coventry Award Paper: Factors Influencing Wear and Osteolysis in Press-Fit Condylar Modular Total Knee Replacements. Clin. Orthop. vol. 2004; 40–50.
9. JM Mirra, RA Marder, HC Amstutz. The pathology of failed total joint arthroplasty. Clin. Orthop. no. 1982; 170: 175–183.
10. K Hirakawa, TW Bauer, BN Stulberg, AH Wilde, M Secic. Characterization and Comparison of Wear Debris from

Failed Total Hip Implants of Different Types*. J. Bone Jt. Surg. 1996; 78: 1235–1243.
11. L Zhang, CC Wang. Inflammatory response of macrophages in infection. Hepatobiliary Pancreat. Dis. Int. 2014; 13: 138–152.
12. Mantovani, A Sica, S Sozzani, P Allavena, A Vecchi, et al. The chemokine system in diverse forms of macrophage activation and polarization. Trends Immunol. 2004; 25: 677–686.
13. J Chiba, HE Rubash, KJ Kim, Y Iwaki. The characterization of cytokines in the interface tissue obtained from failed cementless total hip arthroplasty with and without femoral osteolysis. Clin. Orthop. no. 1994; 300: 304–312.
14. N al-Saffar, JT Mah, Y Kadoya, PA Revell. Neovascularisation and the induction of cell adhesion molecules in response to degradation products from orthopaedic implants. Ann. Rheum. Dis. 1995; 54: 201–208.
15. KJ Kim, Y Kobayashi, T Itoh. Osteolysis model with continuous infusion of polyethylene particles. Clin. Orthop. no. 1998; 352: 46–52.
16. TR Green, J Fisher, M Stone, BM Wroblewski, E Ingham. Polyethylene particles of a ‘critical size’ are necessary for the induction of cytokines by macrophages in vitro. Biomaterials. 1998; 19: 2297–2302.
17. SM Algan, M Purdon, SM Horowitz. Role of tumor necrosis factor alpha in particulate-induced bone resorption. J. Orthop. Res. Off. Publ. Orthop. Res. Soc. 1996; 14: 30–35.
18. EH Burger, JW Van der Meer, JS van de Gevel, JC Gribnau, GW Thesingh, et al. In vitro formation of osteoclasts from long-term cultures of bone marrow mononuclear phagocytes. J. Exp. Med. 1982; 156: 1604–1614.
19. BF Boyce, T Yoneda, C Lowe, P Soriano, GR Mundy. Requirement of pp60c-src expression for osteoclasts to form ruffled borders and resorb bone in mice. J. Clin. Invest. 1992; 90: 1622–1627.
20. P Ducy, T Schinke, G Karsenty. The osteoblast: a sophisticated fibroblast under central surveillance. Science. 2000; 289: 1501–1504.

21. DL Lacey, E Timms, HL Tan, MJ Kelley, CR Dunstan, et al. Osteoprotegerin ligand is a cytokine that regulates osteoclast differentiation and activation. Cell. 1998; 93: 165–176.
22. J Gallo, P Kamínek, V Tichá, P Řiháková, R Ditmar. Particle disease. A comprehensive theory of periprosthetic osteolysis: a review. Biomed. Pap. 2002; 146: 21–28.
23. JJ Goater, RJ O'Keefe, RN Rosier, JE Puzas, EM Schwarz. Efficacy of ex vivo OPG gene therapy in preventing wear debris induced osteolysis. J. Orthop. Res. Off. Publ. Orthop. Res. Soc. 2002; 20: 169–173.
24. M Ulrich-Vinther, EE Carmody, JJ Goater, KS balle, RJ O'Keefe, et al. Recombinant adeno-associated virus-mediated osteoprotegerin gene therapy inhibits wear debris-induced osteolysis. J. Bone Joint Surg. Am. 2002; 84: 1405–1412.
25. Di Cui, Jinglu Lyu, Houxuan Li, Lang Lei, Tianying Bian, et al. Human β-defensin 3 inhibits periodontitis development by suppressing inflammatory responses in macrophages. Mol. Immunol. 2017; 91: 65–74.
26. Fiona Semple, Heather MacPherson, Sheila Webb, Sarah L Cox, Lucy J Mallin, et al. Human β-defensin 3 affects the activity of pro-inflammatory pathways associated with MyD88 and TRIF. Eur. J. Immunol. 2011; 41: 3291–3300.
27. Jue Yeon Lee, Jin Sook Suh, Jung Min Kim, Jeong Hwa Kim, Hyun Jung Park, et al. Identification of a cell-penetrating peptide domain from human beta-defensin 3 and characterization of its anti-inflammatory activity. Int. J. Nanomedicine. 2015; 5423.

Book Chapter

Mitochondrial Dynamics Disturbance: Meeting Different Cancer Traits and Antitumor Immunity

Zahraa FAKIH[1] and Ahmad CHEHAITLY[2]*

[1]Lebanese university, Faculty of sciences (Section 1), Hadath, Beirut, Lebanon
[2]INSERM U1179 END-ICAP, Université Paris-Saclay, UVSQ, 78000 Versailles, France

***Corresponding Author:** Ahmad CHEHAITLY, INSERM U1179 END-ICAP, Université Paris-Saclay, UVSQ, 78000 Versailles, France

Published **October 06, 2022**

How to cite this book chapter: Zahraa FAKIH, Ahmad CHEHAITLY. Mitochondrial Dynamics Disturbance: Meeting Different Cancer Traits and Antitumor Immunity. In: Hussein Fayyad Kazan, editor. Immunology and Cancer Biology. Hyderabad, India: Vide Leaf. 2022.

Abstract

Cancer is amongst the foremost reasons of mortality worldwide, and the number of new cases remains to rise. In spite of new improvements in diagnosis and therapeutic approaches, millions of cancer-related deaths happen, representing the necessity for improved therapies and diagnostic strategies. Mitochondria have been recognized as critical factors in numerous characteristics of

cancer biology, including cancer growth, metastasis, and drug resistance. Though, the modification of mitochondrial dynamics was thought to disturb the regulation of cancer cells. Mitochondria responsibilities in dynamic nets comprise variations in size and distribution of sub-cellular components, and these dynamics are upheld by two chief contrasting processes: fission and fusion. Mitochondrial fusion is facilitated by dynamin-like proteins, including mitofusin 1 (MFN1), mitofusin 2 (MFN2), and optic atrophy 1 protein (OPA1). On the other hand, mitochondrial fission outcomes in a great number of small fragments, which is mediated mainly by dynamin-related protein 1 (DRP1). As disturbed mitochondrial fission or fusion dysregulates the cellular processes that subsidize to tumorigenesis, then understanding how mitochondrial dynamics machinery is involved in cancer would present the basics to manipulate mitochondria-related processes for cancer therapy in the future. Herein, we review current advances linking mitochondrial dynamics to tumor progression at different stages and at meeting different cancer cell traits from uncontrolled proliferation, angiogenesis to invasion and metastasis, as well as on metabolic reprogramming, being a novel cancer cell trait. Additionally, this review will also cover the latest findings on the implication of mitochondrial dynamics on cancer cell extrinsic regulator, in other words the immune system.

Keywords

Cancer; Mitochondrial Dynamics; Mitochondrial Fusion; Mitochondrial Fission; Metabolic Reprogramming

Introduction

Cancer is a group of over thousand diseases characterized by abnormal uncontrolled cell growth [1]. In a healthy body, cells grow, die and are replaced in a highly controlled mechanism [1]. Damage or change in the genetic material of cells by environmental or internal factors sometimes result in cells that do not undergo apoptosis and continue to multiply until a mass of cancer or tumor develop [2]. Most cancer-related deaths are due to metastasis, malignant cells that penetrate into the

circulatory system and establish colonies in other parts of the body [3]. Great advancements have been made, but cancer is still the leading cause of death for people under the age of 85 years. In US, 1 in every 40 people die from cancer [3]. Regardless of the advancements in diagnosing and treatment strategies, millions of cancer-related deaths are still occurring, implying for better therapeutic strategies. Taking into account the essential role played by the mitochondria from cellular energy metabolism, free radical production (ROS, NOS), to apoptosis, it is not surprising that mitochondrial function failings has been assumed to contribute to the development and progression of cancer [4]. Mitochondrial stress has been chatted widely in the context of cancer. Although couple of studies investigated the effect of mitochondrial dynamics disturbance on cancer biology, it has not been reviewed much in the setting of cancer biology meeting different traits and stages of cancer. Mitochondrial dynamics are wisely delimited by dedicated proteins and lipids [5]. Under extracellular stimulations, mitochondria experience constant fission and fusion dynamics to encounter cellular demands [5]. The fact that the molecular players in these mechanisms are known to interact with various factors including tumor suppressors [6], regulators of cell cycle among others [7], allowed us to discuss in this review the role played by disturbed mitochondrial fission and fusion mechanisms on different traits of cancer during its development and progression. We will also cover recent findings on the effect of mitochondrial dynamics on the cancer cell extrinsic regulators, i.e. the immune system.

Insight into the Cancer Field

Cancer is well thought-out as a highly assorted and complex disease caused by the intricate interaction between the individual's genetic makeup predisposition and environmental stressors that drives the advanced transformation of normal cells into malignancy by a transition-state and a stepwise process [2]. Tremendous studies aimed at unravelling the genetic modifications occurring in tumors, but these have limited relevance for the build out of efficient therapies [2]. It is suggested that the development of an effective antitumor therapy will demand targeting of the biological tracks modified in tumor

cells [2]. Indeed, endless proliferative potential, ceaseless angiogenesis, escaping apoptosis, tissue attacks and metastasis are all well-known cancer cell traits [3]. However, quiet lately, the commonly named "metabolic reprogramming" of tumor cells is now documented as a trademark of cancer [8]. This later refers to the competence of tumor cells to modify their own metabolism in order to uphold the increased energy demand due to the ongoing growth, hasty proliferation of such cells, and to rapidly adapt for stress such as hypoxia and limited nutrient conditions [9]. The outcome of accumulated aberrations in a number of supervisory systems within cancer cells allow them to answer differently to these environmental stressors where these changes act as stimulators of cancer cells, introducing signals allowing them to adapt to these changes and survive, thereby, imitating many aspects of cancer cell behavior differentiating them from their normal counterparts [2]. Tumors can either be benign or malignant and are both classified based on the type of cell from which they arise [10]. On the mainstream, there exist three main sets of cancers, carcinomas, sarcomas, and lymphomas [11]. As carcinomas account for more than 90% of human cancers [11], so it will be the one of focus in this review.

The foremost step in the process of cancer is tumor initiation, this step is believed to be a result of genetic changes or alterations in indispensable genes regulating cell cycle such as proto-oncogenes and tumor suppressor genes (TSGs) leading to atypical proliferation of a single cell, forming clonally-derived tumor cells [11]. The formed proliferative cell population is benign and alone it's not adequate for them to attack the surrounding tissue and thus they form a benign adenoma (Epithelial-derived cancer) [11]. Then clonal selection promotes further growth of such adenomas giving rise to malignant carcinomas capable of invading the surrounding tissue through basal lamina into the underlying connective tissue, they also spread into other parts of the body through the circulatory and lymphatic vessels (metastasis) [11]. As cancer cell rapidly grow, they require more nutrients and oxygen supply to meet their elevated demands, hence, this is reached when cancer cells release growth factors allowing new blood vessel formation (angiogenesis) which is needed for cancer to grow [12].

Additionally, epithelial mesenchymal transition (EMT), invasion and metastasis are all well-known properties of cancer cells that affect their interaction with the tissue components and influence the progression of cancer [13]. Such hallmarks are shown in Figure 1.

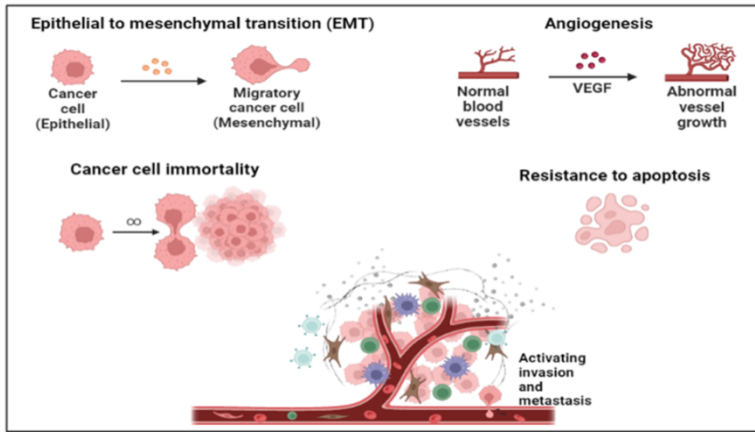

Figure 1: Cancer cell hallmarks. The Hallmarks of Cancer were planned as a set of functional competences developed by human cells as they make their way from normalcy to abnormal growth states, more precisely competences that are critical for their aptitude to form malignant tumors. These hallmarks comprise resisting cell death, enabling replicative immortality, inducing angiogenesis, and activating invasion and metastasis (EMT). [3].

Mechanism of Tumor-Induced Angiogenesis

Angiogenesis, growth of vascular network from existing vasculature, is necessary to supply nutrients, oxygen and to upkeep the growth of the proliferating tumor [12]. Such blood vessels are made in response to growth factors (GFs) secreted by tumor cells, which in turn pushes the proliferation of endothelial cells in the walls of capillaries in the immediate tissue, resulting in the extension of new capillaries into the tumor [12]. This process doesn't merely support tumor's amplified demand to nutrients and oxygen, but also support cancer metastasis [12]. Over the past decade, our understanding of the molecular mechanism of angiogenesis has augmented and lead to the agreement of anti-angiogenic drugs for cancer [12]. But

inadequate efficacy and resistance remain an issue to be fixed. Tumors release and persuade angiognic and antiangiogenic factors which play fundamental roles in regulating endothelial cell (ECs) proliferation, migration, apoptosis, cell-cell or cell-matrix interaction and adhesion through diverse intracellular signaling, which are assumed to be critical mechanisms during this process [12]. Well, the steps of angiogenesis are acknowledged which comprise: degradation of the basement membrane by proteases, migration of ECs, lumen formation and formation of a new basement membrane among other completing steps of the process [12]. The epithelial progenitor cells (EPCs) are thought to be the ones in charge for angiogenesis [14]. The furthermost frequently found angiogenic factors are vascular endothelial growth factors (VEGF) and Basic fibroblast growth factor (bFGF), which when meeting ECs, they bind to the Tyrosine kinase receptors (TKRs) on EC membranes, causing the activation of numerous signaling proteins comprising src, PI3-Kinase, signal transducers and activators of transcriptions (STAT), which in turn initiates pathways provoking the cell cycle machinery [15]. VEGF triggers ECs to yield urokinase-like plasminogen activator (uPA), proteolytic enzymes and interstitial collagenase [15]. Plasminogen activators activate plasminogen to plasmin which can break down extracellular matrix (ECM) components [15]. Tang et al have demonstrated that Urokinase-type Plasminogen Activator Receptor (uPAR) occupancy on ECs results in phosphorylation of focal adhesion proteins and the activation of MAP kinase through thus influencing EC migration and proliferation [16]. Actually, liberal growth of tumors generates continuing hypoxia, which upregulates numerous proangiogenic factors comprising VEGF, bFGF and TGF-β among others [15].

Tumor Cell Migration and EMT: The Road for Metastasis

Cancer cells are less strictly controlled than normal cells by cell-cell and cell-matrix interactions. Generally, cancer cells are less adhesive than normal cells, often as a result of reduced expression of cell surface adhesion molecules (CAMs) [17]. E-cadherin, is encoded by CDH1 gene, it is localized within the

adherens junctions at the baso-lateral membrane, it is a principle adhesion molecule of ECs, and it is important in the development of carcinomas [18]. Reduced expression of CAMs in cancer cells permit them to be unrestrained by the cell-cell and cell-matrix interactions, in that way, contributing to their aptitude to invade and metastasize [17]. Moreover, the reduced adhesiveness of cancer cells to the other cells or to their matrix, also outcomes in changes in their cytoskeletal protein arrangements, giving such cells a mesenchymal cell shape, being a stage in epithelial mesenchymal transition (EMT) [19]. EMT, a significant biological process over which epithelium-derived malignant tumor cells obtain the skill to migrate and invade, acts as a crucial role in cancer development and metastasis [20]. Several oncogenic pathways act to induce EMT and this include TGF-β, Wnt, and Notch pathways [20]. These pathways have been revealed to trigger transcription factors such as snail and slug which in turn act as transcription repressors of E-cadherin expression [20]. During EMT, ECs loose tight and adhesion junction proteins such as E-cadherin and α-catenin and up-regulate the mesenchymal cell specific marker proteins, N-cadherin, Vimentin, and Fibronectin [20]. Afterwards, ECs lose cell-cell adhesion structures and polarity, they then attain the motility and invasive features allowing them to enter the blood or lymphatic vessels and colonize distant tissues [20].

Metabolic Reprogramming of Cancer Cells: A Novel Cancer Cell Trait

"Metabolic reprogramming" refers to the talent of cancer cells to adjust their metabolism in order to support the augmented energy demand owing to continuous growth, rapid proliferation among others [21]. It encompasses some vital changes in bioenergetics and thus involves the mitochondria in this actual setting [21]. Uncontrolled proliferation is one of the most relevant characteristic of cancer cells, and not only does this feature lead to the de-regulated control of cell proliferation, but also corresponds to the adjustment of energy metabolism to meet the increase in cellular energy demands [22]. That's to say that cancer cells get used to this condition by skewing its metabolism towards aerobic glycolysis, glutaminolysis, and mitochondrial

biogenesis and activities, all of which are prominent in the majority of cancers [22]. Inhibition of glycolysis has been shown to hinder cancer growth in vivo and in vitro [23]. Under normoxic circumstances (i.e. aerobic conditions), the metabolic activity of cells predominantly relies on the mitochondrial oxidative phosphorylation (OXPHOS) to generate ATP [24]. Whereas cancer cells become desirous for glucose as they favorably undergo glycolysis even under aerobic conditions [24]. As aerobic glycolysis produces only 2 ATP/ glucose molecule, amplified uptake of glucose is encountered by cancer cells via the up-regulation of glucose transporter expression [24]. Cancer cells does this so by regulating the equilibrium between oncogenes and TSGs, MYC and HIFA, being oncogenes have been revealed to induce cancer glycolysis, however, P53, being a TSGs that is down-regulated in many cancer cells, has been shown to impede cancer glycolysis via downregulating glucose transporters [24]. This shift of cellular metabolism from OXPHOS to aerobic glycolysis even under totally functional mitochondria is designated the "Warburg effect" [24]. The purpose of the Warburg effect for tumor growth remains mysterious. Nevertheless, hypothetical calculations by means of evolutionary game model support that cells at an advanced rate, but lesser yield of ATP might gain a discerning benefit when challenging for shared and inadequate energy incomes [25]. In reality, the tumor microenvironment have restricted availability of glucose and accordingly tumor cells must contest with stromal and immune cells for the glucose [26]. Additionally, it has been suggested that the Warburg effect may represent an advantage for the cell growth in the tumor microenvironment. The aerobic glycolysis of cancer cells creates lactic acid which gets secreted to the extracellular space, in this manner, creating an acidic microenvironment [24]. It is suggested that elevated H^+ ions within the tumor surroundings modifies the tumor-stroma border, allowing for heightened invasiveness [27]. Backing up this suggestion, it has been thought that the higher rates of glycolysis within the tumor cells limit the accessibility of glucose required by infiltrating tumor lymphocytes to sustain their effector function [28], thereby, supporting pro-tumor immunity.

Mitochondrial Dynamics: Insight into Fission and Fusion Processes

The mitochondria are highly dynamic organelles experiencing fission and fusion in a highly controlled manner. Thus, they can divide, combine, and traffic along the cytoskeleton in order to meet cell metabolic needs, where the morphology of the mitochondria is linked to its functions, including the production of ATP through OXPHOS, apoptosis, and regulation of oxidative stress [29]. The role of mitochondrial dynamics is to control the morphology, quantity, and quality of the mitochondria [29]. Besides, mitochondrial dynamics is involved in mitochondrial biogenesis, cell cycle, immunity, and apoptosis [29]. Mutations in the main apparatus constituents and flaws in mitochondrial dynamics have been linked with frequent human diseases [29]. Mitochondrial fission is a multistep procedure permitting the partition of one mitochondrion into two daughter mitochondria, whilst mitochondrial fusion is the union of two mitochondria resulting in one mitochondrion [29]. The chief proteins constituting the basic machinery are large GTPase proteins fitting to the Dynamin family (Figure 1) [30]. These factors can oligomerize and modify conformation to cause membrane remodeling, contraction, scission and/or fusion [30]. Mitochondrial fission is delimited by the recruitment of the GTPase Dynamin-related protein 1 (Drp1), a cytosolic protein, to mediate mitochondrial constriction and Dynamin2 (Dnm2) which carriers out mitochondrial scission [30]. However, mitochondrial fusion is guaranteed by mitofusins 1 and 2 (Mfn1 and Mfn2) and optic atrophy 1 (OPA1), which arbitrate outer mitochondrial membrane and inner mitochondrial membrane fusion, correspondingly [30]. Mitochondrial dynamics proteins are not merely focused in the process of fusion and fission; though they cooperate with other proteins either to accomplish their functions or to participate in other cellular processes [30]. For instance, both mitochondrial fusion and fission proteins are implicated in mitophagy, a selective mitochondrial autophagy. In contrast, mitochondrial fusion proteins are implicated in other processes like cell apoptosis, endoplasmic reticulum/mitochondrial tethering, and ensuring the alignment of the respiratory chain complexes [30].

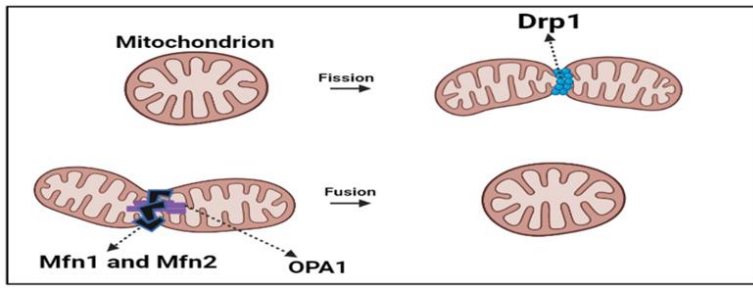

Figure 2: Mitochondrial dynamics main machinery. Mitochondrial fission is a multistep procedure permitting the partition of one mitochondrion into two daughter mitochondria. This process is mediated by Drp1. whilst mitochondrial fusion is the union of two mitochondria resulting in one mitochondrion. This process occurs due to the action of OPA1 and the mitofusins Mfn1/2. [30].

Mitochondrial Dynamics Disturbance: at Crossroads with Cancer

Mitochondrial dysfunction is a trademark of several diseases. Mitochondria and metabolic alterations have been documented as significant for cancer evolution [31]. However, a more detailed understanding of how to operate mitochondria-related procedures for cancer therapy remains to be recognized. Mitochondria are extremely dynamic organelles which constantly fuse and divide in response to miscellaneous stimuli [30]. Contribution in the above-mentioned procedures requires an accurate regulation at many points that permits the cell to connect mitochondrial activity to nutrient availability, biosynthetic demands, proliferation rates, and external incentives [32]. The altered fission/ fusion ratio is thought to correlate with different types of cancers [33]. Current studies demonstrate that augmented mitochondrial fission is a pro-tumorigenic phenotype [33]. Although much more studies point towards a link between increased fission and cancer progression, some studies demonstrated increased fusion processes during cancer evolution. Multiple factors could influence mitochondrial dynamics and this include severe stress (hypoxia, high glucose etc.) [34]. Tumor hypoxia progresses owing to irrepressible cell proliferation, altered metabolism, and irregular tumor blood vessels causing reduced transport of oxygen and nutrients [35].

Hypoxia is one of the chief characteristic of solid tumors and was revealed to associate with poor prognosis of cancer patients [35]. It has been shown to elevate the expression of some oncogenes including HIF1-α [35]. Many cancer cells showed elevated expression of HIF1-α including human prostate cancer cell lines, thyroid carcinomas, breast cancers, and liver cancers [36]. HIF1-α has been shown to promote mitochondrial fission via a process involving cyclin B1/ CDK1-dependant phosphorylation of Drp1 at s-616, allowing its translocation to the mitochondria to induce fission [37]. The expression level of Drp1 was found raised in hepatocellular carcinoma (HCC) tissues [38], glioblastoma U251 cells [39], oncocytic thyroid tumors [40], and in lung adenocarcinoma cell lines among others [41]. In human pancreatic cancer, the expression of oncogenic Ras or activation of MAP kinase pathway was associated with erk2-mediated phosphorylation of Drp1 at S-616 leading to Drp1 mitochondrial translocation and thus increased mitochondrial fission (Fragmentation) [42]. Interestingly, inhibition of this phosphorylation has been revealed as sufficient to chunk tumor growth [42]. This phosphorylation was also observed as increased in some lung cancers [43]. In contrast, a study by li et al discovered that raised mitochondrial fusion supports liver cancer and fuels tumor cell growth via shifting their metabolism [44]. Different studies have stated that the knockdown of the fusion machinery factors, chiefly OPA1 and Mfn1/2 lead to the blocking of the mitochondrial fusion process and was linked with the inhibition of cell growth in vitro and tumor creation in vivo [44].

Mitochondrial Dynamics and Tumor Cell Proliferation

In normal cells, hundreds of genes complicatedly regulate the procedure of cell division [2]. Normal growth necessitates an equilibrium between the action of those genes that encourage cell proliferation and those that suppress it [2]. Cells come to be cancerous after mutations accumulate in the numerous genes that regulate cell proliferation [2]. However, it is not surprising that defects in the expression of genes inhibiting or activating cell cycle inducers and suppressors also play an action in the process

[2]. Additionally, a normal equilibrium in fission/fusion of mitochondria is important in cell cycle progression [45]. Mitochondrial fission is an extremely controlled process that, when disturbed, can modify metabolism, proliferation and apoptosis. Interestingly, the role of Drp1 that controls mitochondrial fission has been gaining lately an interest as it has been increasingly associated with tumorigenesis via its interaction with cell cycle proteins and TSGs [46]. Theory determined study on epithelial ovarian cancer (EOC) exposed that Drp1 co-expresses exactly with the cell-cycle module accountable for mitotic evolution [46]. Shinya et al. examined cell proliferation and cell cycle utilizing the cutaneous SCC A431 and DJM1 cells that were actually transfected with shRNA vectors targeting Drp1 [47]. The study revealed that the MAP kinase signaling trail is involved in the process where MEK inhibitor PD325901 repressed cell proliferation, plus inhibited the phosphorylation of ERK1/2 and Drp1Ser616 [47]. Indicating that MEK which is activated in many cell cancers acts upstream of drp1 promoting cancer cell proliferation possibly via phosphorylation of Drp1 at serine 616. Noting that Drp1 S616 phosphorylation is essential for mitochondrial fission and even though cancer cells can survive without the energy from the mitochondria [48], they simply can't grow without mitochondria as they need it to form new strands of DNA, which we know well that it plays a key role in the process [48]. This could explain the association between increase mitochondrial fission and cancer enhanced proliferation. In addition to that, Qichao Huang et al conclusions proved that augmented mitochondrial fission plays a serious role in the regulation of HCC cell survival [49]. Where the treatment by mitochondrial division inhibitor-1 meaningfully repressed tumor development in an in vivo xenograft nude mice model [49]. Though, mitochondrial fusion has been shown to protect against cell proliferation [50]. The mitofusin Mfn2 has been presented to inhibit the ERK/MAPK signaling trail [50]. Additionally, Drp1/Mfn expression inequity has also been shown to cause additional mitochondrial fission and reduced mitochondrial fusion in human lung cancer cell lines, which is a significant process for cell cycle [51].

Mitochondrial Dynamics Implication in Apoptosis during and Outdoor of Cancer

Mitochondria play crucial roles in triggering apoptosis in mammalian cells [52]. In healthy cells, mitochondria constantly split and fuse to form an active intersecting network [53]. This network breaks during apoptosis at the time of cytochrome C release and preceding to caspase activation, producing abundant and smaller mitochondria [53]. New work shows that proteins tangled in mitochondrial fission and fusion also vigorously meet and contribute in apoptosis pathways. It remains controversial whether fission is absolutely for the progression of apoptosis. On majority, most of the studies mentioned in the literature points for the implication of mitochondrial fission in the process of apoptosis. The study by J Estaquire et al. demonstrated that Drp1-mediated mitochondrial fission inhibition prevents apoptosis via hindering the release of cytochrome C during the process of apoptosis [54]. Numerous models elucidating the mechanisms of cytochrome release have been recommended. One recommends that it rests on the activation of Drp1-mediated mitochondrial fission [55]. It is noteworthy that elevated mitochondrial fission generate more ROS which activates CD95L which further activates CD95 and mediate T cell apoptosis [56]. It has also been witnessed that the apoptotic executioner protein BAX and Drp1 has been revealed to actually interact and that this interaction is improved during apoptosis [57]. It has been noticed that upon BAX activation, Drp1 firmly associates with the mitochondrial outer membrane (MOM) through BAX/ Bak-dependent SUMO alteration of Drp1 [58]. The augmented mitochondrial fission ties up with the release of cytochrome C, where fission inhibition via RNAi targeting Drp1 slows down the release of cyto-C [54]. Martirou and colleagues lately confirmed that Drp1 encourages the formation of a nonbilayer hemifussion intermediate wherein the triggered and oligomerized BAX makes a hole, leading to MOMP [59]. Though, the procedure of fission can happen even helplessly of apoptosis processes. Consequently, in what way Drp1 contributes to apoptosis is a significant concern for upcoming studies. Not much studies for now investigating mitochondrial fusion in cancer apoptosis yet, but more fresh indication

designates that inhibiting mitochondrial fusion encourages apoptosis [60]. Qichao Huang and coworker's experiment of MFN1 knockdown was associated with the encouragement the of HCC cells survival both in vitro and in vivo largely via enabling autophagy and hindering mitochondria-dependent apoptosis [49]. The overexpression of the mitochondrial fusion machinery Mfn1/2 outcomes in slowed Bax activation, cyto-C release, and apoptosis, signifying a role for Mfn1/2 in cell death [61]. A mutant form of mfn2, which has an alteration in one of the 3 preserved residues exposed to the IMS, was incapable to protect cells from undergoing apoptosis induced by the treatment with staurosporine [62]. Moreover, since Mfn2 is recognized to inhibit ERK1/2 activation [63], and since ERK activation has been shown to encourage apoptosis [64], then Mfn2 may defend cells against apoptosis. OPA1, another fusion machinery protein, has also been revealed to be obligatory as a guard of cells from apoptosis. Olichon et al. discovered that OPA1 loss persuades unprompted apoptosis of cells. OPA1i-mediated cell death has been shown to be overcome via overexpression of bcl2 (anti-apoptotic), pointing for the likely action of mitochondrial fusion in cell death upstream of MOMP [65]. In fact, OPA1 is known to regulate normal cristae structure [65]. The majority of cyto-C is known to localize within the cristae in healthy cells, for this it has been suggested that the complete release of cyto-C from mitochondria could be a result of cristae remodeling [66]. As it appears that OPA1 oligomers seems to hold cristae at junctions together. Interestingly, the overexpression of OPA1 prevented tBid-induced cyto-C release to the IMS, which further supports mitochondrial fusion protects cells against apoptosis [67]. A recent study by Sheng-Teng Huang et al evaluated the mechanism by which Tanshinone IIA (Tan IIA) induces apoptosis in osteosarcoma cells [68]. They demonstrated that Tan IIA treatment and administration caused a noteworthy reduction in the mitochondrial fusion proteins, Mfn1/2 and Opa1, along with an elevation in the fission protein Drp1 [68]. Which further support that mitochondrial dynamic change is involved in apoptosis and that Tan IIA could represent a possible candidate to inhibit tumor progression. Hence, further studies investigating the implication of fusion blocking on apoptosis during cancer progression as a possible therapy are needed, as

well as investigating the possibility of combing the targeting both fission and fusion processes during cancer.

Mitochondrial Dynamics and Tumor Angiogenesis

Even though ECs function is influenced by mitochondrial metabolism [69], the role of mitochondrial dynamics in angiogenesis is unidentified. As tumors experience unrestrained, extreme proliferation leading to hypoxic microenvironment, such settings encourage angiogenesis to achieve cancer cell's demand for oxygen and nutrients [9]. Yet, as mitochondrial fission has been demonstrated to increase during hypoxia [70], the mechanisms encouraging angiogenesis in the context of mitochondrial fission remains foggy. The role of Drp1 in Epithelial Progenitor Cell (EPC)-mediated angiogenesis has been evaluated by Kim et al, where inhibiting Drp1 either via siRNA or treatment with Mdivi1 (Drp1 inhibitor) lead to intense drop in EPC migration, invasion, and tube formation, highlighting a role of mitochondrial fission arbitrated by Drp1 in tumor angiogenesis [70]. It is noteworthy to add that mitochondrial fission protein Fis1 has also been shown to shape EPCs and influence angiogenesis [71]. Hsueh-Hsiao Wang and colleagues overexpressed Fis1 in senescent EPCs, which lead to augmented proliferation, and restored the angiogenic potential [71].

In addition, a recent study by Stéphanie et al showed that the IMM mitochondrial fusion protein OPA1 is obligatory for tumor angiogenesis [72]. They discovered that in response to angiogenic stimuli, OPA1 levels quickly rise and that endothelial Opa1 is certainly essential in a nuclear factor kappa-light-chain-enhancer of activated B cell (NFκB)-dependent pathway crucial for tumor angiogenesis [72]. As the exact signaling involving both drp1 and opa1 in tumor angiogenesis remains unexplained, further studies into such topic is needed to unveil possible targets in the context of cancer therapy.

Mitochondrial Dynamics Meeting EMT during Cancer

Other features to be well-thought-out are cross-links with mitochondrial dysfunction and elevation of tumor cells metastasis. Epithelial–mesenchymal transition (EMT) allows

cancer cells to acquire the migration skills to traffic out of the primary tumor and translocate to new target organs. EMT coverts the EC to mesenchymal phenotypes in many epithelial tumor cells that are influenced by mitochondrial dysfunction [73]. Based on the literature, it turns out that mitochondrial dysfunction initiates EMT via EMT signaling pathways. TGF-β is recognized as a main growth factor regulates EMT development through TGF-β/SMAD/SNAIL, phosphatidylinositol-3-kinase (PI3K)/AKT signaling pathways. TGF-β phosphorylates TGF-β receptor-regulated Smad2 and Smad3, then elevate the expression of their downstream gene, Snail-1, being a positive regulator of EMT and metastasis [74]. Activated PI3K/AKT signaling can also elevate the expression of Snail, thus persuading the EMT [74]. In the tumor microenvironment, the hypoxia-induced accumulation of HIF-1 α triggers the expression of TWIST which eventually persuades EMT [75]. Additional connection with mitochondria in cancer cell metastasis is epidermal growth factor receptor (EGFR). EGFR was found highly expressed in the mitochondria of highly invasive non-small cell lung cancer (NSCLC) cells [76]. EGF is a growth factor that initiates the EMT by activating the RAS/RAF/MEK/ERK MAPK signaling cascade [76]. The activated ERK1/2-MAPK induces EMT, promoting the regulation of cell motility and invasion [76]. EGF turns on the mitochondrial translocation of EGFR, mitochondrial fission, and enhances cancer cell motility in vitro and in vivo [77]. Likewise, EGFR can regulate mitochondrial dynamics by disturbing Mfn1 polymerization, consequently, overexpression of Mfn1 opposes the phenotypes consequential from EGFR mitochondrial translocation to induce mitochondrial fission [77]. These observations indicate a possible implication of mitochondrial fusion machinery against EMT. Though encouraging mitochondrial fusion, MFN1 hinders cell proliferation, invasion and migration capability in vitro and in vivo [78]. However, mitochondrial fission has been shown to correlate with EMT during cancer progression. In breast cancer, augmented mitochondrial fragmentation or fission strengthens the capabilities of breast cancer cells to metastasize by triggering Drp1 or silencing Mfn [79]. Which indicates that elevated fission/ fusion ratio possibly associates with tumor metastasis.

The study by Jing Guoet al revealed that Drp1 elevated expression owing to high glucose resulted in augmented EMT, migration and invasion in the endometrial cancer context [80]. Where all these changes produced by high glucose could be somewhat lessened by Drp1 knockdown. Additionally, Seung-Wook Ryu et al established that TGF-β action caused in elongation of mitochondria escorted by the instruction of N-cadherin, vimentin, and F-actin in retinal pigment epithelial cells [81]. They similarly presented that Drp1 reduction augmented cell length and persuaded reorganization of F-actin [81]. In this study the authors also showed that the exhaustion of Mfn1 blocked the upsurge in cell length throughout TGF-β-mediated EMT. The results of their study together validate the participation of mitochondrial dynamics in TGF-β-induced EMT.

Mitochondrial Dynamics and Cancer Metabolic Reprograming

Metabolic reprogramming generally occurs in cancer. Mitochondrial dynamics plays a significant part in tumor evolution [31]. Though, how these dynamics mix tumor metabolism in cancer progression is quiet foggy. A study involving HCC showed that MFN1 controls metastasis through metabolic switch from aerobic glycolysis to OXPHOS [82]. Where the treatment by glycolytic inhibitor 2-Deoxy-D-glucose meaningfully suppressed the possessions persuaded by reduction of MFN1. Tian Gao et al revealed that Salt-inducible kinase 2 (SIK2), which belongs to the AMP-activated protein kinase family, encourages reprogramming of glucose metabolism via PI3K/AKT/HIF-1α pathway and Drp1-mediated mitochondrial fission in ovarian cancer [83]. As improved mitochondrial fission is established to be positively controlled through certain triggering oncogenic mutations; such as B- rapidly accelerated fibrosarcoma (BRAF), thus improving tumor progression, Rayees Ahmad et al revealed that BRAF-**V600E** induced colorectal cancers shows fragmented mitochondria which deliberates glycolytic phenotype and growth benefit to these tumors as their findings demonstrate that BRAF-**V600E** Colorectal cancer cells have higher protein levels of pDRP1-**S616** leading to a further fragmented mitochondrial state as

compared to those having a wild type BRAF [84]. Moreover, Androgen-induced expression of DRP1 has been shown to control mitochondrial metabolic reprogramming in prostate cancer [85]. Carmela Guido et al showed that mitochondrial fission encourages glycolytic reprogramming in cancer-associated myofibroblasts, inducing stromal lactate construction, and tumor growth in early stages. Where the recombinant over-expression of MFF (mitochondrial fission factor) lead to metabolic re-programming towards glycolytic metabolism [86]. As the metabolic reprogramming underlying the DRP1 inhibition is quiet undecided in cancer cells, Wenting Dai et al found that cancer cells treated with Drp1 inhibitor shows less enrichment in TCA cycle intermediates indicating less oxidative metabolism leading to reduced cell proliferation [87]. Additionally, the knockdown of the fusion regulator genes, OPA1 or MFN1, repressed the fusion process in HCC cell lines and CCA tumors [88]. This was accompanied by an inhibition in cell growth in vitro and tumor creation in vivo as well as lessened oxygen ingesting and cellular ATP manufacture of tumor cells [88]. As metabolic reprogramming represents a good way for cancer to progress, further understanding of mitochondrial dynamics in this process is warranted.

Mitochondrial Dynamics Machinery Disturbance on Anti-Tumor Immunity: A Possible Target in Immunotherapy

The innate and adaptive immune responses evoked against tumors to control them is termed “antitumor immunity” [89]. Though, the immune system has a hard time eliminating cancer cells [89]. This is due to the fact that cancer twitches when normal cells develop aberrations and begin to grow irrepressibly. Perhaps that’s why the immune system doesn’t continuously identify them as foreign [89]. For this, immunotherapy, utilizing the immune system to drive away cancer, has been planned as one of the main innovations in cancer biology [89]. This includes vaccines, cytokines, CAR T cell therapy, and monoclonal antibodies among others [89]. However, regardless of these intense advances, the effectiveness of such methods is not common and difficulties remains for the field of cancer immunotherapy. In the current years, numerous investigators

have acknowledged the possibly serious roles of mitochondrial dynamics in both innate and adaptive immunity [90]. Well, mitochondrial dynamics has been shown to influence the differentiation, activation, and cytokine construction of immune cells [91]. Immune cells, especially T cells, play a key role in immunotherapy [92]. The regulation of mitochondrial dynamics could influence T cells at different stages from clonal expansion, migration, and differentiation, thereby, affecting their effector function [93]. As it has been detected experimentally that Drp1 knockout is linked with abridged number of mature T cells, and decreased T cell proliferation even after antigen encountering [93]. Interestingly, this reduction in clonal expansion rate could be reversed by the overexpression of the phosphorylated form of Drp1 at serine 616 (Drp1-S616) [93]. Throughout the differentiation of naïve T cells into effector T cells, the metabolic manner goes from OXPHOS and fatty acid oxidation to glycolysis [94]. This procedure rest on the exact adjustment of the calcium current at immune synapses by Drp1, which encourages the transcription of genes involved in glycolysis by maintaining the activation of mTOR/cMyc [95]. It has been observed fragmented mitochondria were mostly detected in effector T cells, and this phenotype be determined by the phosphorylation of Drp1 at Ser616 to facilitate mitochondrial fission [96]. Either inhibiting glycolysis or knocking out drp1, encourages the change of T cells to a memory-like phenotype owing to the powerlessness of mitochondria to split [95]. Additionally, due to the absence of T cells or the existence of nonfunctional T cells in the tumor microenvironment, a substantial number of patients display no answer to immunotherapy [97]. As the tumor microenvironment is characterized by hypoxia and nutrient deficiency where cells compete and tumor cells mainly win, T cells experience constant TCR stimulation and grieve from nutritional shortage and hypoxia, leading to T cell exhaustion [98]. Exhausted T cells are described by reduced proliferation and functional position with co-inhibitory molecules expression [99]. Fascinatingly, exhausted T cells presented impaired mitochondria and irregular ROS production paralleled with normal T cells [100]. These observations points that mitochondrial dynamics are altered

throughout the course of T cell exhaustion, or perhaps these mitochondrial dynamic alteration causes T cell exhaustion.

Programed cell death-1 (PD-1) upregulation is one of the features of exhausted T cells, which mediates immunosuppression [99]. Simula and coworkers demonstrated that the PD-1 signal hinders the division of mitochondria in T cells by hindering the phosphorylation of Ser616 sites of Drp1, and this inhibition is achieved through the ERK and mTOR pathways [101]. In this study PD-1 inhibitors significantly improved the anti-tumor outcome of wild-type mice. It's noteworthy that reliable with the outcome of Drp1 on T cell migration defined previously, Simula and colleagues established that the density of tumor-infiltrating T cells in wild-type mice was greater than those with Drp1 Knockout, which was linked to Drp1-mediated division and reorganization of the mitochondria situated in the hind part or uropod of T cells [101].

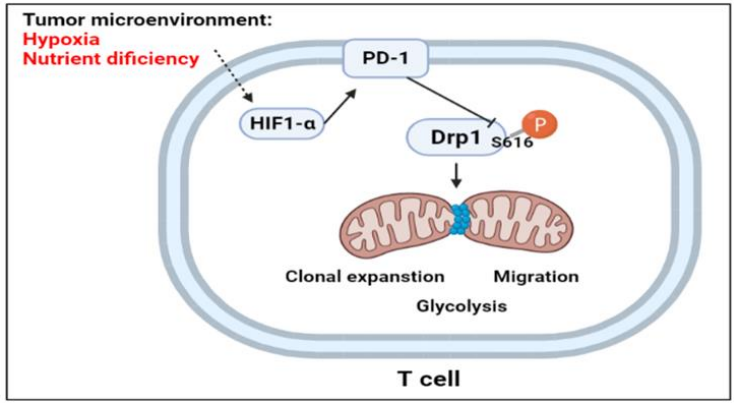

Figure 3: Involvement of mitochondrial fission in T cell activity in the tumor microenvironment. Under hypoxic condition of the tumor environment, HIF1-α becomes activated which in turn activates PD-1. PD-1 enhance T cell exhaustion via inhibiting the phosphorylation of Drp1 at S616, hence preventing mitochondrial fission-mediated processes including clonal expansion, glycolysis encouragement and migration in T cells. [102,103].

Natural killer (NK) cells have vital actions in tumor surveillance [104]. Xiaohu Zheng et al established that tumor-infiltrating NK cells in human liver cancers showed fragmented mitochondria in their cytoplasm, while liver NK cells external to tumors

presented normal large mitochondria [105]. This fragmentation was correlated with NK cell loss, causing tumor avoidance of NK cell-mediated surveillance, which expected poor survival in patients with liver cancer. They also demonstrated that hindering mitochondrial fragmentation was associated with the persistence and the antitumor capacity of NK cells. Hence, mitochondrial fission seems to play an essential role during the antitumor immunity and thus represents a potential target to enhance the antitumor immunity and fight off cancer.

Conclusion

In summary, mitochondrial dynamic disturbance seems to interfere during cancer progression by working for the favor of different cancer traits including tumor growth, angiogenesis, metabolic reprogramming, EMT and invasion (metastasis). Mitochondrial fission/ fusion ratio seems to be higher in the majority of cancers, yet the increased fusion process has been observed in some cancers as well as it leads to the inhibition of apoptosis in tumors. Fission seems to be more involved in proliferation, angiogenesis and EMT but it seems to induce apoptosis, yet increased fission is more likely to induce cancer traits wins over inducing apoptosis. As Drp1 S616 is responsible for mitochondrial fission, regulating its phosphorylation state represents a potential target to fight off tumor itself. However, mitochondrial dynamics also seems to influence the antitumor immunity. But in contrast to the negative effect of increased fission on tumor progression, increased mitochondrial fission or elevated levels of Drp1-S616 has mainly a positive influence on the antitumor immunity.

Future Directions

Further studies investigating the outcomes of combining the inhibition Drp1 phosphorylation at S616 in tumors and the effect of this Drp1 phosphorylation in antitumor immunity on the overall tumor progression in different cancers is warranted. Indicating the need of cell type specific targeting approaches. For this, also approaches aiming at easy screening patient specific cancers for the state of Drp1 phosphorylation will be of interest.

References

1. Roy PS, BJ Saikia. Cancer and cure: A critical analysis. Indian journal of cancer. 2016; 53: 441-442.
2. Wellenstein, Max D, Karin E de Visser. Cancer-Cell-Intrinsic Mechanisms Shaping the Tumor Immune Landscape. Immunity. 2018; 48: 399-416.
3. Fouad, Yousef Ahmed, Carmen Aanei. Revisiting the hallmarks of cancer. American journal of cancer research. 2017; 7: 1016-1036.
4. Wallace, Douglas C. Mitochondria and cancer. Nature reviews. Cancer. 2012; 12: 685-698.
5. Lisa Tilokani, Shun Nagashima, Vincent Paupe, Julien Prudent. Mitochondrial dynamics: overview of molecular mechanisms. Essays in biochemistry. 2018; 62: 341-360.
6. David E Moulder, Diana Hatoum, Enoch Tay, Yiguang Lin Eileen M McGowan. The Roles of p53 in Mitochondrial Dynamics and Cancer Metabolism: The Pendulum between Survival and Death in Breast Cancer? Cancers. 2018; 10: 189.
7. B Spurlock, Jma Tullet, JL Hartman, K Mitra. Interplay of mitochondrial fission-fusion with cell cycle regulation: Possible impacts on stem cell and organismal aging. Experimental gerontology. 2020; 135: 110919.
8. Faubert, Brandon et al. Metabolic reprogramming and cancer progression. Science (New York, N.Y.) vol. 368,6487 (2020): eaaw5473.
9. Ma, Yawen et al. The role of mitochondrial dynamics in human cancers. American journal of cancer research vol. 10,5 1278-1293.
10. Patel, Aisha. Benign vs Malignant Tumors. JAMA oncology. 2020; 6: 1488.
11. Cooper GM. The Cell: A Molecular Approach. 2nd edition. The Development and Causes of Cancer. Sunderland: Sinauer Associates. 2000. Available online at: https://www.ncbi.nlm.nih.gov/books/NBK9963/
12. Naoyo Nishida, Hirohisa Yano, Takashi Nishida, Toshiharu Kamura, Masamichi Kojiro. Angiogenesis in cancer. Vascular health and risk management. 2006; 2: 213-219.
13. Roche, Joëlle. The Epithelial-to-Mesenchymal Transition in

Cancer. Cancers. 2018; 10: 52.
14. Marçola, Marina, Camila Eleuterio Rodrigues. Endothelial progenitor cells in tumor angiogenesis: another brick in the wall. Stem cells international. 2015; 2015: 832649.
15. Gupta, Manoj Kumar, Ren-Yi Qin. Mechanism and its regulation of tumor-induced angiogenesis. World journal of gastroenterology. 2003; 9: 1144-1155.
16. H Tang, DM Kerins, Q Hao, T Inagami, DE Vaughan l. The urokinase-type plasminogen activator receptor mediates tyrosine phosphorylation of focal adhesion proteins and activation of mitogen-activated protein kinase in cultured endothelial cells. The Journal of biological chemistry. 1998; 273: 18268-18272.
17. Roche, Joëlle. The Epithelial-to-Mesenchymal Transition in Cancer. Cancers. 2018; 10: 52.
18. Pećina-Slaus, Nives. Tumor suppressor gene E-cadherin and its role in normal and malignant cells. Cancer cell international. 2018; 3: 17.
19. Susan E. Leggett, Alex M Hruska, Ming Guo, Ian Y Wong. The epithelial-mesenchymal transition and the cytoskeleton in bioengineered systems. Cell communication and signaling: CCS. 2018; 19: 32.
20. Voulgari, Angeliki, Alexander Pintzas. Epithelial-mesenchymal transition in cancer metastasis: mechanisms, markers and strategies to overcome drug resistance in the clinic. Biochimica et biophysica acta. 2009; 1796: 75-90.
21. Brandon Faubert, Ashley Solmonson, Ralph J DeBerardinis. Metabolic reprogramming and cancer progression. Science (New York, N.Y.). 2020; 368: eaaw5473.
22. Matthew G Vander Heiden, Lewis C Cantley, Craig B Thompson. Understanding the Warburg effect: the metabolic requirements of cell proliferation. Science (New York, N.Y.). 2009; 324: 1029-1033.
23. Qiyin Zhou, Hua Li, Yuanyuan Li, Mingjia Tan, Shaohua Fan, et al. Inhibiting neddylation modification alters mitochondrial morphology and reprograms energy metabolism in cancer cells. JCI insight. 2018; 4: e121582.
24. Zheng, Jie. Energy metabolism of cancer: Glycolysis versus oxidative phosphorylation (Review). Oncology letters. 2012; 4: 1151-1157.

25. T Pfeiffer, S Schuster, S Bonhoeffer. Cooperation and competition in the evolution of ATP-producing pathways. Science (New York, N.Y.). 2001; 292: 504-507.
26. Chih-Hao Chang, Jing Qiu, David O'Sullivan, Michael D Buck, Takuro Noguchi, et al. Metabolic Competition in the Tumor Microenvironment Is a Driver of Cancer Progression. Cell. 2015; 162: 1229-1241.
27. Gatenby, Robert A, Robert J Gillies. A microenvironmental model of carcinogenesis. Nature reviews. Cancer. 2008; 8: 56-61.
28. Ho, Ping-Chih, Susan M Kaech. Reenergizing T cell anti-tumor immunity by harnessing immunometabolic checkpoints and machineries. Current opinion in immunology. 2017; 46: 38-44.
29. Michela Di Nottia, Daniela Verrigni, Alessandra Torraco, Teresa Rizza, Enrico Bertini, et al. Mitochondrial Dynamics: Molecular Mechanisms, Related Primary Mitochondrial Disorders and Therapeutic Approaches. Genes. 2018; 12: 247.
30. Wallace, Douglas C. Mitochondria and cancer. Nature reviews. Cancer. 2012; 12: 685-698.
31. Valeria Gabriela Antico Arciuch, María Eugenia Elguero, Juan José Poderoso, María Cecilia Carreras. Mitochondrial regulation of cell cycle and proliferation. Antioxidants & redox signaling. 2012; 16: 1150-1180.
32. Yawen Ma, Lihua Wang, Renbing Jia. The role of mitochondrial dynamics in human cancers. American journal of cancer research. 2018; 10: 1278-1293.
33. Naima Zemirli, Etienne Morel, Diana Molino. Mitochondrial Dynamics in Basal and Stressful Conditions. International journal of molecular sciences. 2018; 19: 564.
34. Barbara Muz, Pilar de la Puente, Feda Azab, Abdel Kareem Azab. The role of hypoxia in cancer progression, angiogenesis, metastasis, and resistance to therapy. Hypoxia (Auckland, N.Z.). 2018; 3: 83-92.
35. Balamurugan, Kuppusamy. HIF-1 at the crossroads of hypoxia, inflammation, and cancer. International journal of cancer. 2016; 138: 1058-1066.
36. Mitra, Kasturi. Mitochondrial fission-fusion as an emerging key regulator of cell proliferation and differentiation.

BioEssays: news and reviews in molecular, cellular and developmental biology. 2013; 35: 955-964.
37. Xia-Hui Lin, Bai-Quan Qiu, Min Ma, Rui Zhang, Shu-Jung Hsu, et al. Suppressing DRP1-mediated mitochondrial fission and mitophagy increases mitochondrial apoptosis of hepatocellular carcinoma cells in the setting of hypoxia. Oncogenesis. 2020; 9: 67.
38. Yu-Ying Wan, Jian-Feng Zhang, Zhang-Jian Yang, Li-Ping Jiang, Yong-Fang Wei, et al. Involvement of Drp1 in hypoxia-induced migration of human glioblastoma U251 cells. Oncology reports. 2014; 32: 619-626.
39. André Ferreira-da-Silva, Cristina Valacca, Elisabete Rios, Helena Pópulo, Paula Soares, et al. Mitochondrial dynamics protein Drp1 is overexpressed in oncocytic thyroid tumors and regulates cancer cell migration. PloS one. 2015; 10: e0122308.
40. Lingling Yu, Zuke Xiao, Hongying Tu, Bo Tong, Shengsong Chen. The expression and prognostic significance of Drp1 in lung cancer: A bioinformatics analysis and immunohistochemistry. Medicine. 2019; 98: e18228.
41. Jennifer A Kashatus, Aldo Nascimento, Lindsey J Myers, Annie Sher, Frances L Byrne, et al. Erk2 phosphorylation of Drp1 promotes mitochondrial fission and MAPK-driven tumor growth. Molecular cell. 2015; 57: 537-551.
42. Ana Rita Lima, Liliana Santos, Marcelo Correia, Paula Soares, Manuel Sobrinho-Simões, et al. Dynamin-Related Protein 1 at the Crossroads of Cancer. Genes. 2018; 9: 115.
43. Meng Li, Ling Wang, Yijin Wang, Shaoshi Zhang, Guoying Zhou, et al. Mitochondrial Fusion Via OPA1 and MFN1 Supports Liver Tumor Cell Metabolism and Growth. Cells. 2020; 9: 121.
44. B Spurlock, Jma Tullet, JL Hartman, K Mitra. Interplay of mitochondrial fission-fusion with cell cycle regulation: Possible impacts on stem cell and organismal aging. Experimental gerontology. 2020; 135: 110919.
45. Deepak Kumar Tanwar, Danitra J Parker, Priyanka Gupta, Brian Spurlock, Ronald D Alvarez, et al. Crosstalk between the mitochondrial fission protein, Drp1, and the cell cycle is identified across various cancer types and can impact survival of epithelial ovarian cancer patients. Oncotarget.

2016; 7: 60021-60037.
46. Shinya Kitamura, Teruki Yanagi, Keisuke Imafuku, Hiroo Hata, Riichiro Abe, et al. Drp1 regulates mitochondrial morphology and cell proliferation in cutaneous squamous cell carcinoma. Journal of dermatological science. 2017; 88: 298-307.
47. Wallace, Douglas C. Mitochondria and cancer. Nature reviews. Cancer. 2012; 12: 685-698.
48. Qichao Huang, Lei Zhan, Haiyan Cao, Jibin Li, Yinghua Lyu, et al. Increased mitochondrial fission promotes autophagy and hepatocellular carcinoma cell survival through the ROS-modulated coordinated regulation of the NFKB and TP53 pathways. Autophagy. 2016; 12: 999-1014.
49. Nagdas, Sarbajeet, David F Kashatus. The Interplay between Oncogenic Signaling Networks and Mitochondrial Dynamics. Antioxidants (Basel, Switzerland). 2017; 6: 33.
50. Jalees Rehman, Hannah J Zhang, Peter T Toth, Yanmin Zhang, Glenn Marsboom, et al. Inhibition of mitochondrial fission prevents cell cycle progression in lung cancer. FASEB journal: official publication of the Federation of American Societies for Experimental Biology. 2012; 26: 2175-2186.
51. Wang, Chunxin, Richard J Youle. The role of mitochondria in apoptosis*. Annual review of genetics. 2009; 43: 95-118.
52. Der-Fen Suen, Kristi L Norris, Richard J Youle. Mitochondrial dynamics and apoptosis. Genes & development. 2008; 22: 1577-1590.
53. Estaquier J, D Arnoult. Inhibiting Drp1-mediated mitochondrial fission selectively prevents the release of cytochrome c during apoptosis. Cell death and differentiation. 2007; 14: 1086-94.
54. C Garrido, L Galluzzi, M Brunet, PE Puig, C Didelot, et al. Mechanisms of cytochrome c release from mitochondria. Cell death and differentiation. 2006; 13: 1423-1433.
55. Daniel Röth, Peter H Krammer, Karsten Gülow. Dynamin related protein 1-dependent mitochondrial fission regulates oxidative signalling in T cells. FEBS letters. 2014; 588: 1749-1754.
56. Andreas Jenner, Aida Peña-Blanco, Raquel Salvador-Gallego, Begoña Ugarte-Uribe, Cristiana Zollo, et al. DRP1

interacts directly with BAX to induce its activation and apoptosis. The EMBO journal. 2022; 41: e108587.
57. Sylwia Wasiak, Rodolfo Zunino, Heidi M McBride. Bax/Bak promote sumoylation of DRP1 and its stable association with mitochondria during apoptotic cell death. The Journal of cell biology. 2007; 177: 439-450.
58. Sylvie Montessuit, Syam Prakash Somasekharan, Oihana Terrones, Safa Lucken-Ardjomande, Sébastien Herzig, et al. Membrane remodeling induced by the dynamin-related protein Drp1 stimulates Bax oligomerization. Cell vol. 2010; 142: 889-901.
59. Der-Fen Suen, Kristi L Norris, Richard J Youle. Mitochondrial dynamics and apoptosis. Genes & development. 2008; 22: 1577-1590.
60. Rie Sugioka, Shigeomi Shimizu, Yoshihide Tsujimoto. Fzo1, a protein involved in mitochondrial fusion, inhibits apoptosis. The Journal of biological chemistry. 2004; 279: 52726-52734.
61. Margaret Neuspiel, Rodolfo Zunino, Sandhya Gangaraju, Peter Rippstein, Heidi McBride. Activated mitofusin 2 signals mitochondrial fusion, interferes with Bax activation, and reduces susceptibility to radical induced depolarization. The Journal of biological chemistry. 2005; 280: 25060-25070.
62. Kuang-Hueih Chen, Xiaomei Guo, Dalong Ma, Yanhong Guo, Qian Li, et al. Dysregulation of HSG triggers vascular proliferative disorders. Nature cell biology. 2004; 6: 872-883.
63. Cheung, Eric CC, Ruth S Slack. Emerging role for ERK as a key regulator of neuronal apoptosis. Science's STKE: signal transduction knowledge environment. 2004; 2004: PE45.
64. Aurélien Olichon, Laurent Baricault, Nicole Gas, Emmanuelle Guillou, Annie Valette, et al. Loss of OPA1 perturbates the mitochondrial inner membrane structure and integrity, leading to cytochrome c release and apoptosis. The Journal of biological chemistry. 2003; 278: 7743-7746.
65. Luca Scorrano, Mona Ashiya, Karolyn Buttle, Solly Weiler, Scott A Oakes, et al. A distinct pathway remodels mitochondrial cristae and mobilizes cytochrome c during apoptosis. Developmental cell. 2002; 2: 55-67.

66. Ryuji Yamaguchi, Lydia Lartigue, Guy Perkins, Ray T Scott, Amruta Dixit, et al. Opa1-mediated cristae opening is Bax/Bak and BH3 dependent, required for apoptosis, and independent of Bak oligomerization. Molecular cell. 2008; 31: 557-569.
67. Sheng-Teng Huang, Chao-Chun Huang, Wen-Liang Huang, Tsu-Kung Lin, Pei-Lin Liao, et al. Tanshinone IIA induces intrinsic apoptosis in osteosarcoma cells both in vivo and in vitro associated with mitochondrial dysfunction. Scientific reports. 2017; 7: 40382.
68. Caja, Sergio, Jose Antonio Enríquez. Mitochondria in endothelial cells: Sensors and integrators of environmental cues. Redox biology. 2017; 12: 821-827.
69. Da Yeon Kim, Seok Yun Jung, Yeon Ju Kim, Songhwa Kang, Ji Hye Park, et al. Hypoxia-dependent mitochondrial fission regulates endothelial progenitor cell migration, invasion, and tube formation. The Korean journal of physiology & pharmacology: official journal of the Korean Physiological Society and the Korean Society of Pharmacology. 2018; 22: 203-213.
70. Hsueh-Hsiao Wang, Yih-Jer Wu, Ya-Ming Tseng, Cheng-Huang Su, Chin-Ling Hsieh, et al. Mitochondrial fission protein 1 up-regulation ameliorates senescence-related endothelial dysfunction of human endothelial progenitor cells. Angiogenesis. 2019; 22: 569-582.
71. Herkenne, Stéphanie. Developmental and Tumor Angiogenesis Requires the Mitochondria-Shaping Protein Opa1. Cell metabolism. 2020; 31: 987-1003.e8.
72. Dudas, József. Epithelial to Mesenchymal Transition: A Mechanism that Fuels Cancer Radio/Chemoresistance. Cells. 2017; 9: 428.
73. In the tumor microenvironment, the hypoxia-induced accumulation of HIF-1 α triggers the expression of TWIST which eventually persuades EMT.
74. Hapke, Robert Y, Scott M Haake. Hypoxia-induced epithelial to mesenchymal transition in cancer. Cancer letters. 2020; 487: 10-20.
75. Sarah Sayed Hassanein, Sherif Abdelaziz Ibrahim, Ahmed Lotfy Abdel-Mawgood. Cell Behavior of Non-Small Cell Lung Cancer Is at EGFR and MicroRNAs Hands.

International journal of molecular sciences. 2021; 22: 12496.
76. Che, Ting-Fang. Mitochondrial translocation of EGFR regulates mitochondria dynamics and promotes metastasis in NSCLC. Oncotarget. 2015; 6: 37349-37366.
77. Ze Zhang, Tian-En Li, Mo Chen, Da Xu, Ying Zhu, et al. MFN1-dependent alteration of mitochondrial dynamics drives hepatocellular carcinoma metastasis by glucose metabolic reprogramming. British journal of cancer. 2020; 122: 209-220.
78. J Zhao, J Zhang, M Yu, Y Xie, Y Huang, et al. Mitochondrial dynamics regulates migration and invasion of breast cancer cells. Oncogene. 2013; 32: 4814-4824.
79. Jing Guo, Feng Ye, Xiaoping Jiang, Hui Guo, Wenli Xie, et al. Drp1 mediates high glucose-induced mitochondrial dysfunction and epithelial-mesenchymal transition in endometrial cancer cells. Experimental cell research. 2020; 389: 111880.
80. Seung-Wook Ryu, Eun Chun Han, Jonghee Yoon, Chulhee Choi et al. The mitochondrial fusion-related proteins Mfn2 and OPA1 are transcriptionally induced during differentiation of bone marrow progenitors to immature dendritic cells. Molecules and cells. 2015; 38: 89-94.
81. Ze Zhang, Tian-En Li, Mo Chen, Da Xu, Ying Zhu, et al. MFN1-dependent alteration of mitochondrial dynamics drives hepatocellular carcinoma metastasis by glucose metabolic reprogramming. British journal of cancer. 2020; 122: 209-220.
82. Tian Gao, Xiaohong Zhang, Jing Zhao, Feng Zhou, Yaya Wang, et al. SIK2 promotes reprogramming of glucose metabolism through PI3K/AKT/HIF-1α pathway and Drp1-mediated mitochondrial fission in ovarian cancer. Cancer letters. 2020; 469: 89-101.
83. Rayees Ahmad Padder, Zafar Iqbal Bhat, Zaki Ahmad, Neetu Singh, Mohammad Husain. DRP1 Promotes BRAFV600E-Driven Tumor Progression and Metabolic Reprogramming in Colorectal Cancer. Frontiers in oncology. 2021; 10: 592130.
84. Yu Geon Lee, Yeji Nam, Kyeong Jin Shin, Sora Yoon, Weon Seo Park, et al. Androgen-induced expression of DRP1 regulates mitochondrial metabolic reprogramming in prostate cancer. Cancer letters. 2020; 471: 72-87.

85. Carmela Guido, Diana Whitaker-Menezes, Zhao Lin, Richard G Pestell, Anthony Howell, et al. Mitochondrial fission induces glycolytic reprogramming in cancer-associated myofibroblasts, driving stromal lactate production, and early tumor growth. Oncotarget. 2012; 3: 798-810.
86. Wenting Dai, Guan Wang, Jason Chwa, Myung Eun Oh, Tharindumala Abeywardana, et al. Mitochondrial division inhibitor (mdivi-1) decreases oxidative metabolism in cancer. British journal of cancer. 2020; 122: 1288-1297.
87. Meng Li, Ling Wang, Yijin Wang, Shaoshi Zhang, Guoying Zhou, et al. Mitochondrial Fusion Via OPA1 and MFN1 Supports Liver Tumor Cell Metabolism and Growth. Cells. 2020; 9: 121.
88. Hugo Gonzalez, Catharina Hagerling, Zena Werb. Roles of the immune system in cancer: from tumor initiation to metastatic progression. Genes & development. 2018; 32: 1267-1284.
89. Abhishek Mohanty, Rashmi Tiwari-Pandey, Nihar R Pandey. Mitochondria: the indispensable players in innate immunity and guardians of the inflammatory response. Journal of cell communication and signaling. 2019; 13: 303-318.
90. Angajala A, Lim S, Phillips JB, Kim JH, Yates C, et al. Diverse Roles of Mitochondria in Immune Responses: Novel Insights Into Immuno-Metabolism. Front Immunol. 2018; 9: 1605.
91. Pierpaolo Ginefra, Girieca Lorusso, Nicola Vannini et al. Innate Immune Cells and Their Contribution to T-Cell-Based Immunotherapy. International journal of molecular sciences. 2020; 21: 4441.
92. Jun Song, Xiaofang Yi, Ruolin Gao, Li Sun, Zhixuan Wu, et al. Impact of Drp1-Mediated Mitochondrial Dynamics on T Cell Immune Modulation. Frontiers in immunology. 13 873834.
93. Jiaokui Xie, Yi-yuan Li, Jin Jin. The essential functions of mitochondrial dynamics in immune cells. Cellular & molecular immunology. 2020; 17: 712-721.
94. Luca Simula, Ilenia Pacella, Alessandra Colamatteo, Claudio Procaccini, Valeria Cancila, et al. Drp1 Controls Effective T Cell Immune-Surveillance by Regulating T Cell Migration,

Proliferation, and cMyc-Dependent Metabolic Reprogramming. Cell reports. 2018; 25: 3059-3073.e10.
95. Michael D Buck, David O'Sullivan, Ramon I Klein Geltink, Jonathan D Curtis, Chih-Hao Chang, et al. Mitochondrial Dynamics Controls T Cell Fate through Metabolic Programming. Cell vol. 2016; 166: 63-76.
96. Zhang, Yu, Lieping Chen. Classification of Advanced Human Cancers Based on Tumor Immunity in the MicroEnvironment (TIME) for Cancer Immunotherapy. JAMA oncology. 2016; 2: 1403-1404.
97. Wherry E John. T cell exhaustion. Nature immunology. 2011; 12: 492-499.
98. Wherry E John, Makoto Kurachi. Molecular and cellular insights into T cell exhaustion. Nature reviews. Immunology. 2015; 15: 486-499.
99. Nicole E Scharping, Ashley V Menk, Rebecca S Moreci, Ryan D Whetstone, Rebekah E Dadey, et al. The Tumor Microenvironment Represses T Cell Mitochondrial Biogenesis to Drive Intratumoral T Cell Metabolic Insufficiency and Dysfunction. Immunity. 2016; 45: 701-703.
100. Simula, Luca. PD-1-induced T cell exhaustion is controlled by a Drp1-dependent mechanism. Molecular oncology. 2022; 16: 188-205.
101. Shurin, Michael R, Viktor Umansky. Cross-talk between HIF and PD-1/PD-L1 pathways in carcinogenesis and therapy. The Journal of clinical investigation. 2022; 132: e159473.
102. Patsoukis, Nikolaos. Selective effects of PD-1 on Akt and Ras pathways regulate molecular components of the cell cycle and inhibit T cell proliferation. Science signaling. 2018; 5: 230 ra46.
103. Meza Guzman, Lizeth G. Natural Killer Cells: Tumor Surveillance and Signaling. Cancers. 2018; 12: 952.
104. Zheng, Xiaohu. Mitochondrial fragmentation limits NK cell-based tumor immunosurveillance. Nature immunology. 2019; 20: 1656-1667.

Book Chapter

Role of DNA Repair in Genome Stability, Tumor Prevention, and Main Complications in Case of Repair Failure

Mohammad Rida Hayek* and Joanna Timmins

University of Grenoble Alpes, CEA, CNRS, IBS, F-38000 Grenoble, France

***Corresponding Author:** Mohammad Rida Hayek, University of Grenoble Alpes, CEA, CNRS, IBS, F-38000 Grenoble, France

Published **October 26, 2022**

How to cite this book chapter: Mohammad Rida Hayek, Joanna Timmins. Role of DNA Repair in Genome Stability, Tumor Prevention, and Main Complications in Case of Repair Failure. In: Hussein Fayyad Kazan, editor. Immunology and Cancer Biology. Hyderabad, India: Vide Leaf. 2022.

DNA Repair Systems

A preserved genome is essential for the preservation and continuation of life. DNA, however, is known to be an intrinsically reactive molecule and is highly susceptible to chemical modifications from endogenous or exogenous agents; exogenous factors include environmental hazards such as toxic heavy metals and radiation, whereas endogenous factors comprise molecules or reactive species released by cellular metabolism inside the body or after cell damage and the loss of cell membrane integrity [1]. For example, naturally occurring

reactive oxygen species (ROS) inside cells can thus lead to various types of endogenously caused-DNA damage, which can be in the form of deamination, methylation, or oxidation of bases, but also as single- or double-strand breaks. Similarly, exposure to exogenous agents such as ultraviolet (UV) light, ionizing radiation, benzopyrene, or alkylating agents can also lead to the accumulation of various types of lethal DNA lesions [2].

DNA damage caused by either endogenous or exogenous sources can ultimately lead to DNA mutations. Mutations refer to changes in the DNA sequence, which can occur due to either exposure to DNA damaging agents (in this case mutagens) or to errors during DNA replication. Some mutations are beneficial and in fact play an important role in evolution and development of life, while others are associated with diseases, tumorigenesis, and aging. Because the accumulation of mutations can be unfavorable and lead to drastic carcinogenic consequences, cells have evolved complex DNA repair, damage tolerance, cell cycle checkpoints, and cell death pathways to maintain the integrity of the genome [2].

There are several types of mutations, ranging from single base-pair alterations to multi base-pair deletions, insertions, duplications, and inversions [3]. Depending on the type and location of the mutation, the effect can be classified as beneficial, neutral, detrimental, or lethal. However, recent research has shown that several other factors might play a role in determining the effect of a certain mutation, as in the case of "Epistasis" where the effect of a gene mutation is dependent on the presence or absence of other mutations in a manner that the environmental genetic background of such a particular DNA mutation might play a role in changing its effect [4]. Mutations that cause death or reduced life expectancy of individuals are referred to as lethal mutations, as in the case of Tay Sachs disease, where life expectancy is around 4-5 years of age [5].

Preserving one's genome after such genomic attacks and mutations is thus vital for an organism. For this purpose, the DNA repair machinery efficiently localizes and eliminates DNA

lesions to maintain genomic integrity and stability, and minimize the formation of mutations. The cell cycle includes four different stages and three checkpoints; upon detection of DNA damage, the cell cycle halts, and the DNA damage response (DDR) is activated; depending on the type of lesion, different DNA repair pathways can be initiated. There are at least six major DNA repair pathways, including direct reversal/repair (DR), base excision repair (BER), nucleotide excision repair (NER), mismatch repair (MMR), homologous recombination (HR), and non-homologous end joining (NHEJ) repair pathways [2,4] (Figure 1). Normally, if the damage is unrepairable, the cell undergoes apoptosis or necrosis [6].

Certain DNA lesions can be directly repaired. The O6-alkylguanine (O6-AG)-DNA methyltransferase (*MGMT*) also known as O6-alkylguanine-DNA alkyltransferase (AGT) can indeed repair DNA damage by removing alkyl groups from thymine or guanine bases without removing the base itself [7]. Other DNA repair pathways include multi-enzyme complexes that work together or sequentially to remove specific types of damaged bases. For example, the BER pathway involves numerous proteins that aid in maintaining genome integrity by repairing small single base DNA lesions caused by DNA alkylation or oxidation [8] including 8oxoGuanine (8oxoG), the most abundant BER substrate, which results from the oxidation of guanine, and if left unrepaired can lead to transversion mutations [9]. The NER pathway plays an important role in repairing UV-induced photoproducts, bulkier DNA lesions such as base adducts created by genotoxic agents like cisplatin, and DNA crosslinks [10]. In these two excision repair pathways, the damaged nucleotide and in some cases the neighboring DNA is excised and replaced with newly synthesized DNA using the normal DNA replication machinery. The MMR pathway plays a role in correcting single base-pair mismatches and misaligned short nucleotide repeats introduced accidently by the DNA polymerase during DNA replication; if left unrepaired they can lead to point or frameshift mutations [11]. MLH-1, MSH-2, MSH-6, and PMS-2 are the most clinically relevant MMR proteins, which participate in the repair of such errors by excising the DNA harboring the mismatch site and re-

synthesizing the correct DNA. Both HR and NHEJ are DNA repair pathways involved in repairing double-strand breaks (DSB). Proteins encoded by BRCA1, BRCA2, RAD51, and PALB2 genes mediate HR, which functions by resecting part of the DNA sequence around the DSB, after which the homologous sister chromatid is used as a template for the synthesis of the new non-damaged DNA. HR can thus only operate during the S and G2 phases of the cell cycle during which the sister chromatids are present. NHEJ, in contrast, repairs DSBs by directly ligating the loose ends of the DSBs and can therefore function throughout the cell cycle, but is more error-prone [12].

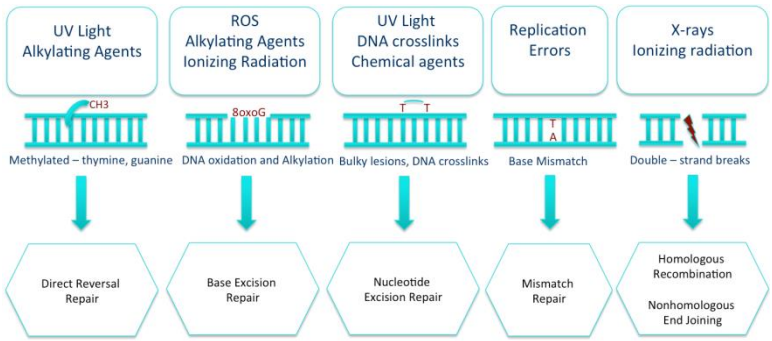

Figure 1: DNA damage and the associated DNA repair pathways.

Defects in DDR Genes and Cancer

Cancer is a disease that develops gradually. According to the mutator phenotype hypothesis, the ability of cancer cells to divide, invade, and metastasize is due to mutations in driver genes that regulate DNA repair and genetic stability. Such mutations result in deficiencies in DNA repair pathways leading to an increased mutation rate; those mutations can take place in other DNA repair genes thereby initiating a cascade of mutations in the genes that maintain genomic stability [13-15]. Eventually, this leads to genomic instability which is believed to be the main cause of tumorigenesis [16-18]. Thus, such deficiencies in DNA repair genes are the hallmark behind genomic and epi-genomic instability in case of cancer development [14].

The cancer cell genome has been shown to include several mutation classes such as substitutions, insertions, or deletions of small or large DNA segments, rearrangements, gene amplifications, copy number reduction, etc [19-22]. Several epigenetic changes that alter both chromatin structure and gene expression have also been identified in cancer cells [23,24]. Furthermore, some cancer cells have acquired exogenous DNA sequences from tumorigenic viruses such as Epstein Barr virus, hepatitis B virus, human T lymphotropic virus-1, and human herpes virus-8 [25].

DNA damage and mutations play an important role in cancer development; this is particularly obvious in case of genetic defects in the DNA repair machinery [26]. For instance, individuals with somatic or inherited germline mutations affecting DNA repair genes typically exhibit an increased risk of developing cancer. In what follows, is a list of the most commonly occurring cancer-related DNA repair defects.

Cancer-Related Defects in HR Genes: BRCA1 and 2 are tumor suppressor genes that control cell growth and differentiation. Besides their role in the regulation of gene expression, they are also known to take part in the repair of DSBs in the HR pathway. Upon HR activation, DSBs are resected into a 3'-single-stranded DNA (ssDNA) overhang, which is directly coated with the high affinity ssDNA-binding protein, RPA. After that, BRCA1, BRCA2, and PALB2 form a crucial network of proteins to mediate the replacement of RPA by RAD51, which is the main effector protein in the subsequent steps of the HR pathway [27,28]. Lung, ovarian, breast, pancreatic, and prostate carcinoma are now known to be associated with mutations in HR genes, particularly BRCA1 and BRCA2 [29-32]. A recent analysis estimated the lifetime risk of developing prostate cancer by age 85 to be 29% and 60% for BRCA1 and BRCA2 carriers, respectively, and that the risk of developing male breast cancer is 18- and 80-fold higher in BRCA1 and BRCA2 carriers, respectively [31,32]. Besides that, it was estimated that breast cancer families with BRCA2 mutations have a 10-fold higher risk of developing pancreatic cancer than families without such mutation [29,34].

Cancer-Related Defects in BER Genes: MUTYH gene encodes for the MYH DNA glycosylase enzyme, a BER protein that functions in repairing oxidative DNA damage resulting from exposure to various carcinogens. In particular, MYH is known to bind the mismatched 8oxoG:A base-pair resulting from misincorporation of adenine opposite 8oxoG during replication of 8oxoG-containing DNA, after which it excises the mismatched adenine, thereby preventing T:A transversion mutations in the following rounds of DNA replication [35]. Somatic and germline MUTYH gene mutations are known to be associated with a high risk of developing polyposis and colorectal cancer [36]. Furthermore, recent studies to understand the role of the mutated MUTYH gene in the development of extracolonic cancer estimated that biallelic MUTYH carriers have a 19- and 17-fold increased risk of developing urinary bladder and ovarian cancer, respectively, compared with the general population, and that monoallelic MUTYH carriers are at increased risk of developing gastric, liver, breast, and endometrial cancer [37]. Another study suggests that monoallelic MUTYH carriers may progress to ovarian cancer if somatic MUTYH mutations co-occur, leading to a homozygous somatic state [38]. Both mutated MUTYH related-cancer types can occur due to the failure of MUTYH driven-BER mechanism in MUTYH-mutated individuals [38].

Cancer-Related Defects in NER Genes: ERCC1 is a multifunctional protein that plays an essential role in the NER pathway. Together with XPF, it forms the structure-specific endonuclease XPF/ERCC1 complex which is known to be essential for repairing various bulky DNA lesions, pyrimidine dimers, DNA crosslinks, and DSBs. ERCC1 has been identified as the most frequently deficient DNA repair protein in non-small-cell lung cancer (NSCLC). Besides that, mammalian cells with mutated ERCC1 and XPF genes develop various genetic disorders, which result from deficient NER pathway, including Xeroderma pigmentosum (XP), trichothiodystrophy (TTD), and Cockayne syndrome (CS) [39-42]. In the same context, studies published by the Cancer Genome Atlas (TCGA) and others, demonstrate that somatic mutations in ERCC2, a DNA helicase

that also plays an important role in NER, were identified in approximately 12% of bladder cancer [43-46].

Cancer-Related Defects in MMR genes: MSH2, MSH6, MLH1, and PMS2 play an essential role in mediating the MMR pathway, which aids in repairing base-base mismatches, insertions, and deletions generated during DNA replication and recombination. Several types of cancer are associated with a deficient MMR pathway, including colorectal, endometrial, gastrointestinal, and ovarian cancers. A deficient MMR pathway is known to occur in 15-20% of colon and 10% of rectal cancers [47-50]. For instance, mutations in MLH1, MSH2, and MSH6 are the cause behind the occurrence of hereditary nonpolyposis colorectal cancer (HNPCC), the latter being characterized by colorectal, endometrial, and other cancer clusters [51,52]. Several studies have also demonstrated the existence of MMR mutations in ovarian cancer, one of which noted that the incidence of germline MMR mutations in ovarian cancer is 2%, while other inactivated gene forms occur in up to 29% of the cases [53-55].

Cancer-Related Defects in DR Genes: As previously mentioned, MGMT functions as an alkyl-acceptor that irreversibly transfers the methyl group from the O^6-methylguanine and O^4-methylthymine into its internal acceptor site (the sulfur atom of its active site cysteine), thereby repairing such alkylated adducts. Loss of MGMT function, mainly due to hyper-methylation-mediated silencing of its promoter, or mutation, has been associated with various tumor types, including glioma, gastrointestinal, esophageal, breast, and prostate cancer [56-58]. A recent analysis demonstrated the loss of MGMT protein expression in 44.5% (65/137) of gastrointestinal stromal tumors, with 10.9% (15/137) exhibiting MGMT promoter methylation [57]. Besides that, loss of MGMT protein occurs frequently in esophageal cancer patients from north India, where the absence of such protein is associated with 65% of the cases (52/80), together with a significant hyper-methylation of the MGMT promoter region [58].

Cancer-Related Defects in the tp53 Gene: tp53 is a tumor suppressor gene that encodes for the p53 protein, which in turn plays an important role in protecting the cell from DNA damage. It is a transcription factor that facilitates the DDR by halting the cell cycle to allow for the repair machinery to restore genome stability. It controls genes involved in the regulation of the cell cycle and/or apoptosis [59]. Under normal conditions, it is expressed at low levels; upon detecting DNA lesions, a series of post-translational modifications including phosphorylation and acetylation take place leading to the accumulation and activation of p53. As a transcriptional activator, p53 regulates and activates several genes involved in various DNA repair pathways (NER, BER, MMR, NHEJ, and HR) and induces either cell cycle arrest or apoptosis depending on the extent of DNA damage [59,60]. As such, p53 plays a central role in maintaining genomic integrity. It is thus no surprise that over 50% of human cancers are indeed associated with loss of function p53 mutations [61,62]. Some cancers with p53 mutations are in addition chemo-resistant, which reinforces the critical role of p53 in cancer progression [59].

Cancer-Related Defects in the PTEN Gene: PTEN is also a tumor suppressor gene that encodes for the PTEN (phosphatase and tensin homolog) protein, a lipid phosphatase that plays a major role in the regulation of the phosphatidylinositol 3 kinase (PI3K)/AKT cascade, one of the most important signaling pathways activated in response to DNA damage. PI3K/AKT regulates cell cycle progression, induction of cell death, transcription, translation, stimulation of angiogenesis, and stem cell self-renewal [63-65]. By dephosphorylating phosphoinositide signaling molecules like PIP3, PTEN can inhibit signal transduction [66] and thereby block cell migration and cell-cycle arrest [67,68]. New evidence also suggests that PTEN can regulate DDR factors such as Chk1 and p53, therefore playing an indirect role in maintaining genomic integrity [69]. PTEN loss of function mutations are associated with genetic mutations, epigenetic mutations, and gene silencing mechanisms; this loss of function is present in several cancers such as gastric cancer [70] and breast cancer [71]; loss of PTEN causes the increase in PIP3 levels and the persistent activation of PI3K

effectors which causes uncontrolled cell proliferation, apoptosis resistance, angiogenesis, genomic instability, stem cell self-renewal, cellular senescence, and cell migration [72].

When loss of function in direct or indirect DNA repair proteins occurs, more genomic alterations ranging from point mutations to chromosomal alterations are bound to occur. This is referred to as "genomic instability" [73] and is proving to be one of the major hallmarks of cancer, since it also affects other hallmarks such as oxidative stress, proteotoxic stress, metabolic stress, DNA damage and DNA replication, and mitotic stress [74].

DNA Repair Deficiency Disorders and Increased Risks of Cancer

DNA repair deficiency disorders are caused by germline mutations in DNA repair genes. Several hereditary diseases characterized by genetic defects in DNA repair mechanisms are known to be associated with increased risk of cancer [75]. This is the case of Bloom's Syndrome, Xeroderma Pigmentosum, Lynch Syndrome, Ataxia telangiectasia, and several other disorders described in this section.

Bloom's Syndrome (HR-deficient)

Bloom's syndrome is an autosomal recessive disease that occurs due to a loss of function mutation in BLM [76]. BLM encodes for the RecQ helicase, a DNA helicase that functions in HR repair of DSBs. BLM has also been shown to have a function in the early sensing of DNA damage, where it assembles with p53 and hRAD1 at sites of stalled replication and DSBs. It interacts with several other proteins to promote survival in response to DNA damage, DNA blockage, chromatin remodeling, etc. Thus, BLM has a significant role in maintaining genomic integrity and stability [76,77].

Previous *in vivo* studies have shown that the loss of function of BLM plays a significant role in enhancing the tumorigenesis of both basal cell carcinoma (BCC) (a type of skin cancer) and rhabdomyosarcomas (RMS) [78]. Not only that, but it has also

been demonstrated that any deficiency in the levels of BLM induces hyper-recombination in epithelial cells [79] and promotes tumorigenesis [80]. This evidence further proves that BLM is necessary for maintaining genomic stability.

Xeroderma Pigmentosum (NER-deficient)

Xeroderma pigmentosum (XP) is an autosomal recessive disorder that is characterized by increased sensitivity to sunlight. Individuals with XP present freckle-like pigmentation and lesions in the areas where the skin was exposed to the sunlight. XP patients are at high risk of developing skin cancer, both non-melanoma and melanoma, before the age of 10. XP patients are 10,000 times more likely to develop non-melanoma skin tumors and 2,000 times more likely to have melanoma before the age of 20 as compared to healthy people [81].

The disorder is the consequence of genetic defects in XP repair proteins, the latter being involved in mediating various steps in the NER pathway, thereby leading to a defective NER system. For instance, XP cells are unable to perform unscheduled DNA synthesis (UDS) after UV irradiation. UDS is a part of the NER pathway; it refers to the DNA synthesis that occurs after the removal of the DNA damage during the repair process. There are different classifications of XP; Classical XP (XP-A to XP-G) which is characterized by a deficiency in the removal of DNA damage through NER, and XP-V cells which are characterized by the ability to tolerate DNA lesions by replicating damaged templates through TLS. Due to their inability to remove mutations effectively and their ability to tolerate lesions, XP cells have an increased level of mutagenesis [81,82]. In addition to that, mutagenesis in XP can also be increased due to UV-induced signature mutations in tumor suppressor genes such as p53 [81,83].

Lynch Syndrome (MMR-deficient)

This disease is the most frequent - autosomal dominant - cause of hereditary colorectal cancer. It is caused by a germline mutation in one of the MMR genes (MLH1, MSH2, MSH6, PMS2, and EPCAM), which leads to the loss of function of its protein and thus a defective MMR pathway [49,84]. Lynch

syndrome is known to be associated with a high lifetime risk of developing several types of tumors, including colorectal (20-70%), endometrial (15-70%), gastric (6-13%), and ovarian (4-12%) cancer [49]. Furthermore, its association with increased risk of urothelial carcinoma has been noted as well [85]. A deficient MMR pathway leads to a high mutational incidence in the repetitive DNA sequences, leading to microsatellite instability. It is important to note that 95% of Lynch syndrome-associated cancer present microsatellite instability [85,86].

Ataxia Telangiectasia (NHEJ, HR- deficient)

Ataxia telangiectasia is a single gene autosomal recessive disorder that is characterized by mutations of both alleles of the ATM (ataxia-telangiectasia mutated) gene. The ATM gene codes for the ATM serine/threonine kinase responsible for initiating cell cycle arrest and DNA repair in response to DSBs. ATM is considered to be the main regulator of the DDR as it is responsible for activating several downstream effectors through phosphorylation; those proteins include BRCA1, SMC1, Ch2, etc. ATM is also responsible for the phosphorylation of p53. As such, ATM function is associated with genome integrity [87,88]. Mutations in the ATM gene thus inevitably affect the DNA repair capacity of cells. In fact, individuals with Ataxia telangiectasia have a 50 to 150-fold increased risk of developing cancer [89].

Other Disorders: Two human syndromes are associated with mutations in genes encoding DNA helicases that play important roles in HR, NHEJ, or excision repair pathways. When mutated, these genes lead to a defective repair mechanism [90-95]. Werner Syndrome is an autosomal recessive disorder resulting from an inherited mutation in the WRN gene, which encodes for the WRN ATP-dependent helicase, a member of the RecQ helicase family, while Rothmund Thomson syndrome results from a germline mutation in the RECQL4 gene. Fanconi anemia is another autosomal recessive disorder resulting from a mutation in FA genes, the latter being involved in the HR pathway [96]. These three syndromes with different deficiencies in DNA repair pathways are also associated with increased risks of developing cancer [97-101].

DNA Repair and Cancer: The Link

Perhaps the best way to study the role of DNA repair pathways in tumorigenesis is to investigate the molecular bases of inherited genetic disorders associated with defects in genes encoding DNA repair factors. Many of these defects have indeed been shown to favor cancer development. In recent years, this relationship between DNA repair and cancer has gained a lot of attention, notably with the finding that defects in the MMR are the cause of hereditary non-polyposis colorectal cancer (HNPCC) and enhance cancer development [102]. However, recent studies have also revealed the complexity of this relationship. Depending on the disease stage and the DNA repair pathway, defects in DNA repair factors may either increase or decrease the rate of survival. Mutations in DNA repair genes can thus be considered as double-edged swords in the context of radio- and chemotherapy [103]. In the future, a better understanding of the molecular mechanisms underlying the functions of the DNA repair machinery will certainly facilitate the development of more targeted and personalized anti-cancer treatments to overcome these difficulties.

References

1. Huang R, Zhou PK. DNA damage repair: historical perspectives, mechanistic pathways and clinical translation for targeted cancer therapy. Signal Transduct Target Ther. 2021; 6: 254.
2. Chatterjee N, Walker GC. Mechanisms of DNA damage, repair and mutagenesis. Environ Mol Mutagen. 2017; 58: 235–263.
3. Fitzgerald DM, Rosenberg SM. What is mutation? A chapter in the series: How microbes “jeopardize” the modern synthesis. PLoS Genet. 2019; 15: e1007995.
4. Loewe L, Hill WG. The population genetics of mutations: good, bad and indifferent. Philos Trans R Soc Lond B Biol Sci. 2010; 365: 1153–1167.
5. Waxman D, Overall ADJ. Influence of Dominance and Drift on Lethal Mutations in Human Populations. Front Genet. 2020; 11: 267.
6. Jiang M. Alterations of DNA damage repair in cancer: from

mechanisms to applications. Ann Transl Med. 2020; 8: 1685.
7. Gerson SL. MGMT: its role in cancer aetiology and cancer therapeutics. Nat Rev Cancer. 2004; 4: 296–307.
8. Çağlayan M. The ligation of pol β mismatch insertion products governs the formation of promutagenic base excision DNA repair intermediates. Nucleic Acids Res. 2020; 48: 3708–3721.
9. Nakabeppu Y. Cellular Levels of 8-Oxoguanine in either DNA or the Nucleotide Pool Play Pivotal Roles in Carcinogenesis and Survival of Cancer Cells. Int J Mol Sci. 2014; 15: 12543–12557.
10. Schärer OD. Nucleotide Excision Repair in Eukaryotes. Cold Spring Harb Perspect Biol. 2013; 5: a012609.
11. Martin SA. Methotrexate induces oxidative DNA damage and is selectively lethal to tumour cells with defects in the DNA mismatch repair gene MSH2. EMBO Mol Med. 2009; 1: 323–337.
12. Lieber MR. The mechanism of double-strand DNA break repair by the nonhomologous DNA end-joining pathway. Annu Rev Biochem. 2010; 79: 181–211.
13. Boland CR, Yurgelun MB. Mutational cascades in cancer. Oncotarget. 2017; 8: 41784–41785.
14. Bernstein C, RA, Nfonsam V, Bernstei H. DNA Damage, DNA Repair and Cancer. In: Chen C, editor. New Research Directions in DNA Repair. London: InTech. 2013.
15. Loeb LA, Loeb KR, Anderson JP. Multiple mutations and cancer. Proc. Natl. Acad. Sci. U.S.A. 2003; 100: 776–781.
16. Hegan DC. Differing patterns of genetic instability in mice deficient in the mismatch repair genes Pms2, Mlh1, Msh2, Msh3 and Msh6. Carcinogenesis. 2006; 27: 2402–2408.
17. Narayanan L, Fritzell JA, Baker SM, Liskay RM, Glazer PM. Elevated levels of mutation in multiple tissues of mice deficient in the DNA mismatch repair gene Pms2. Proc Natl Acad Sci U S A. 1997; 94: 3122–3127.
18. Zhou J, Zhou XA, Zhang N, Wang J. Evolving insights: how DNA repair pathways impact cancer evolution. Cancer Biol Med. 2020; 17: 805–827.
19. Matsui A, Ihara T, Suda H, Mikami H, Semba K. Gene amplification: mechanisms and involvement in cancer. BioMolecular Concepts. 2013; 4: 567–582.

20. Ludmil B Alexandrov, Jaegil Kim, Nicholas J Haradhvala, Mi Ni Huang, Alvin Wei Tian Ng, et al. The repertoire of mutational signatures in human cancer. Nature. 2020; 578: 94–101.
21. Christopher D Steele, Ammal Abbasi, SM Ashiqul Islam, Amy L Bowes, Azhar Khandekar, et al. Signatures of copy number alterations in human cancer. Nature. 2022; 606: 984–991.
22. Hasty P, Montagna C. Chromosomal rearrangements in cancer. Mol Cell Oncol. 2004; 1: e29904.
23. Esteller M. Cancer epigenomics: DNA methylomes and histone-modification maps. Nat Rev Genet. 2007; 8: 286–298.
24. Ilango S, Paital B, Jayachandran P, Padma PR, Nirmaladevi R. Epigenetic alterations in cancer. Frontiers in Bioscience-Landmark. 2020; 25: 1058–1109.
25. Stratton MR, Campbell PJ, Futreal PA. The cancer genome. Nature. 2009; 458: 719–724.
26. Torgovnick A, Schumacher B. DNA repair mechanisms in cancer development and therapy. Front Genet. 2015; 6: 157.
27. Matos-Rodrigues G, Guirouilh-Barbat J, Martini E, Lopez BS. Homologous recombination, cancer and the 'RAD51 paradox'. NAR Cancer. 2021; 3: zcab016.
28. Roy R, Chun J, Powell SN. BRCA1 and BRCA2: different roles in a common pathway of genome protection. Nat Rev Cancer. 2011; 12: 68–78.
29. Greer JB, Whitcomb DC. Role of BRCA1 and BRCA2 mutations in pancreatic cancer. Gut. 2007; 56: 601–605.
30. Elizabeth C Page, Elizabeth K Bancroft, Mark N Brook, Melissa Assel, Mona Hassan Al Battat, et al. Interim Results from the IMPACT Study: Evidence for Prostate-specific Antigen Screening in BRCA2 Mutation Carriers. European Urology. 2019; 76: 831–842.
31. Daniel R Barnes, Valentina Silvestri, Goska Leslie, Lesley McGuffog, Joe Dennis, et al. Breast and Prostate Cancer Risks for Male BRCA1 and BRCA2 Pathogenic Variant Carriers Using Polygenic Risk Scores. JNCI: Journal of the National Cancer Institute. 2022; 114: 109–122.
32. Jordi Remon, Benjamin Besse, Alexandra Leary, Ivan Bièche, Bastien Job, et al. Somatic and Germline BRCA 1

and 2 Mutations in Advanced NSCLC From the SAFIR02-Lung Trial. JTO Clinical and Research Reports. 2020; 1: 100068.
33. Tommy Nyberg, Debra Frost, Daniel Barrowdale, D Gareth Evans, Elizabeth Bancroft, et al. Prostate Cancer Risks for Male BRCA1 and BRCA2 Mutation Carriers: A Prospective Cohort Study. Eur Urol. 2020; 77: 24–35.
34. Brentnall TA. Cancer surveillance of patients from familial pancreatic cancer kindreds. Medical Clinics of North America. 2000; 84: 707–718.
35. Kairupan C, Scott RJ. Base excision repair and the role of MUTYH. Hered Cancer Clin Pract. 2007; 5: 199–209.
36. Natalie Jones, Stefanie Vogt, Maartje Nielsen, Daria Christian, Petra A Wark, et al. Increased Colorectal Cancer Incidence in Obligate Carriers of Heterozygous Mutations in MUTYH. Gastroenterology. 2009; 137: 489-494.e1.
37. Aung Ko Win, Jeanette C Reece, James G Dowty, Daniel D Buchanan, Mark Clendenning, et al. Risk of extracolonic cancers for people with biallelic and monoallelic mutations in MUTYH. Int J Cancer. 2016; 139: 1557–1563.
38. Hutchcraft ML, Gallion HH, Kolesar JM. MUTYH as an Emerging Predictive Biomarker in Ovarian Cancer. Diagnostics. 2021; 11: 84.
39. Mehdi Touat, Tony Sourisseau, Nicolas Dorvault, Roman M Chabanon, Marlène Garrido, et al. DNA repair deficiency sensitizes lung cancer cells to NAD+ biosynthesis blockade. J Clin Invest. 2018; 128: 1671–1687.
40. Sophie Postel-Vinay, Elsa Vanhecke, Ken A Olaussen, Christopher J Lord, Alan Ashworth, et al. The potential of exploiting DNA-repair defects for optimizing lung cancer treatment. Nat Rev Clin Oncol. 2012; 9: 144–155.
41. Anouchka Guyon-Debast, Patricia Rossetti, Florence Charlot, Aline Epert, Jean-Marc Neuhaus, et al. The XPF-ERCC1 Complex Is Essential for Genome Stability and Is Involved in the Mechanism of Gene Targeting in Physcomitrella patens. Frontiers in Plant Science. 2019; 10.
42. McNeil EM, Melton DW. DNA repair endonuclease ERCC1–XPF as a novel therapeutic target to overcome chemoresistance in cancer therapy. Nucleic Acids Res. 2012; 40: 9990–10004.

43. Jaegil Kim, Kent W Mouw, Paz Polak, Lior Z Braunstein, Atanas Kamburov, et al. Somatic ERCC2 Mutations Are Associated with a Distinct Genomic Signature in Urothelial Tumors. Nat Genet. 2016; 48: 600–606.
44. Network TCGAR. Comprehensive molecular characterization of urothelial bladder carcinoma. Nature. 2014; 507: 315.
45. Mariana C Stern, Jie Lin, Jonine D Figueroa, Karl T Kelsey, Anne E Kiltie, et al. Polymorphisms in DNA repair genes, smoking, and bladder cancer risk: findings from the International Consortium of Bladder Cancer. Cancer Res. 2009; 69: 6857–6864.
46. Eliezer M Van Allen, Kent W Mouw, Philip Kim, Gopa Iyer, Nikhil Wagle, et al. Somatic ERCC2 mutations correlate with cisplatin sensitivity in muscle-invasive urothelial carcinoma. Cancer Discov. 2014; 4: 1140–1153.
47. Kenta Masuda, Kouji Banno, Megumi Yanokura, Yusuke Kobayashi, Iori Kisu, et al. Relationship between DNA Mismatch Repair Deficiency and Endometrial Cancer. Mol Biol Int. 2011; 2011: 256063.
48. Andrea Cercek, Gustavo Dos Santos Fernandes, Campbell S Roxburgh, Karuna Ganesh, Shu Ng, et al. Mismatch Repair–Deficient Rectal Cancer and Resistance to Neoadjuvant Chemotherapy. Clinical Cancer Research. 2020; 26: 3271–3279.
49. Duraturo F, Liccardo R, De Rosa M, Izzo P. Genetics, diagnosis and treatment of Lynch syndrome: Old lessons and current challenges (Review). Oncology Letters. 2019; 17: 3048–3054.
50. Peltomäki P. Role of DNA Mismatch Repair Defects in the Pathogenesis of Human Cancer. JCO. 2003; 21: 1174–1179.
51. Vasen HF. MSH2 Mutation Carriers Are at Higher Risk of Cancer Than MLH1 Mutation Carriers: A Study of Hereditary Nonpolyposis Colorectal Cancer Families. JCO. 2001; 19: 4074–4080.
52. Liu Y. Somatic mutations in genes associated with mismatch repair predict survival in patients with metastatic cancer receiving immune checkpoint inhibitors. Oncol Lett. 2020; 20: 27.
53. Emma J Crosbie, Neil A J Ryan, Rhona J McVey, Fiona

Lalloo, Naomi Bowers, et al. Assessment of mismatch repair deficiency in ovarian cancer. J Med Genet. 2021; 58: 687–691.
54. Xiao X, Melton DW, Gourley C. Mismatch repair deficiency in ovarian cancer — Molecular characteristics and clinical implications. Gynecologic Oncology. 2014; 132: 506–512.
55. Aysal A. Ovarian endometrioid adenocarcinoma: incidence and clinical significance of the morphologic and immunohistochemical markers of mismatch repair protein defects and tumor microsatellite instability. Am J Surg Pathol. 2012; 36: 163–172.
56. Sharma S. Role of MGMT in Tumor Development, Progression, Diagnosis, Treatment and Prognosis. Anticancer Research. 2009; 29: 3759–3768.
57. Lou L, Zhang W, Li J, Wang Y. Abnormal MGMT Promoter Methylation in Gastrointestinal Stromal Tumors: Genetic Susceptibility and Association with Clinical Outcome. Cancer Manag Res. 2020; 12: 9941–9952.
58. Asad Ur Rehman, Snigdha Saikia, Mohammad Askandar Iqbal, Istaq Ahmad,, Sadaf, et al. Decreased expression of MGMT in correlation with aberrant DNA methylation in esophageal cancer patients from North India. Tumour Biol. 2017; 39: 1010428317705770.
59. Ozaki T, Nakagawara A. Role of p53 in Cell Death and Human Cancers. Cancers (Basel). 2011; 3: 994–1013.
60. Williams AB, Schumacher B. p53 in the DNA-Damage-Repair Process. Cold Spring Harb Perspect Med. 2016; 6: a026070.
61. SJ Baker, ER Fearon, JM Nigro, SR Hamilton, AC Preisinger, et al. Chromosome 17 deletions and p53 gene mutations in colorectal carcinomas. Science. 1989; 244: 217–221.
62. K Vogan, M Bernstein, JM Leclerc, L Brisson, J Brossard, et al. Absence of p53 gene mutations in primary neuroblastomas. Cancer Res. 1993; 53: 5269–5273.
63. Milella M. PTEN: Multiple Functions in Human Malignant Tumors. Front Oncol. 2015; 5: 24.
64. Sansal I, Sellers WR. The biology and clinical relevance of the PTEN tumor suppressor pathway. J Clin Oncol. 2004; 22: 2954–2963.

65. Song MS, Salmena L, Pandolfi PP. The functions and regulation of the PTEN tumour suppressor. Nat Rev Mol Cell Biol. 2012; 13: 283–296.
66. Karimian A. Crosstalk between Phosphoinositide 3-kinase/Akt signaling pathway with DNA damage response and oxidative stress in cancer. Journal of Cellular Biochemistry. 2019; 120: 10248–10272.
67. Hlobilkova A. Cell cycle arrest by the PTEN tumor suppressor is target cell specific and may require protein phosphatase activity. Exp Cell Res. 2000; 256: 571–577.
68. Leslie NR, Foti M. Non-genomic loss of PTEN function in cancer: not in my genes. Trends Pharmacol Sci. 2011; 32: 131–140.
69. Ming M, He YY. PTEN in DNA damage repair. Cancer Lett. 2012; 319: 125–129.
70. Kim B, Kang SY, Kim D, Heo YJ, Kim KM. PTEN Protein Loss and Loss-of-Function Mutations in Gastric Cancers: The Relationship with Microsatellite Instability, EBV, HER2, and PD-L1 Expression. Cancers (Basel). 2020; 12: 1724.
71. Li S. Loss of PTEN expression in breast cancer: association with clinicopathological characteristics and prognosis. Oncotarget. 2017; 8: 32043–32054.
72. Molinari F, Frattini M. Functions and Regulation of the PTEN Gene in Colorectal Cancer. Frontiers in Oncology. 2014; 3.
73. Aguilera A, Gómez-González B. Genome instability: a mechanistic view of its causes and consequences. Nat Rev Genet. 2008; 9: 204–217.
74. Moon JJ, Lu A, Moon C. Role of genomic instability in human carcinogenesis. Exp Biol Med (Maywood). 2019; 244: 227–240.
75. Knoch J, Kamenisch Y, Kubisch C, Berneburg M. Rare hereditary diseases with defects in DNA-repair. Eur J Dermatol. 2012; 22: 443–455.
76. Cunniff C, Bassetti JA, Ellis NA. Bloom's Syndrome: Clinical Spectrum, Molecular Pathogenesis, and Cancer Predisposition. Mol Syndromol. 2017; 8: 4–23.
77. Tripathi V. MRN complex-dependent recruitment of ubiquitylated BLM helicase to DSBs negatively regulates

DNA repair pathways. Nat Commun. 2018; 9: 1016.
78. Davari P. Loss of Blm enhances basal cell carcinoma and rhabdomyosarcoma tumorigenesis in Ptch1+/- mice. Carcinogenesis. 2010; 31: 968–973.
79. Traverso G. Hyper-recombination and genetic instability in BLM-deficient epithelial cells. Cancer Res. 2003; 63: 8578–8581.
80. Kaur E, Agrawal R, Sengupta S. Functions of BLM Helicase in Cells: Is It Acting Like a Double-Edged Sword? Frontiers in Genetics. 2021; 12.
81. Menck CF, Munford V. DNA repair diseases: What do they tell us about cancer and aging? Genet Mol Biol. 2014; 37: 220–233.
82. Cleaver JE. Common pathways for ultraviolet skin carcinogenesis in the repair and replication defective groups of xeroderma pigmentosum. J Dermatol Sci. 2000; 23: 1–11.
83. Giglia G. p53 mutations in skin and internal tumors of xeroderma pigmentosum patients belonging to the complementation group C. Cancer Res. 1998; 58: 4402–4409.
84. Dabir PD. Microsatellite instability screening in colorectal adenomas to detect Lynch syndrome patients? A systematic review and meta-analysis. Eur J Hum Genet. 2020; 28: 277–286.
85. Lindner AK. Lynch Syndrome: Its Impact on Urothelial Carcinoma. Int J Mol Sci. 2021; 22: 531.
86. Idos G, Valle L. Lynch Syndrome. In: Adam MP, editors. GeneReviews®. University of Washington, Seattle. 1993.
87. Banin S. Enhanced phosphorylation of p53 by ATM in response to DNA damage. Science. 1998; 281: 1674–1677.
88. Shiloh Y. ATM and related protein kinases: safeguarding genome integrity. Nat Rev Cancer. 2003; 3: 155–168.
89. Olsen JH. Cancer in Patients With Ataxia-Telangiectasia and in Their Relatives in the Nordic Countries. JNCI: Journal of the National Cancer Institute. 2001; 93: 121–127.
90. Chen L. WRN, the protein deficient in Werner syndrome, plays a critical structural role in optimizing DNA repair. Aging Cell. 2003; 2: 191–199.
91. Saintigny Y, Makienko K, Swanson C, Emond MJ, Monnat RJ. Homologous Recombination Resolution Defect in

Werner Syndrome. Mol Cell Biol. 2002; 22: 6971–6978.
92. Monnat Jr RJ, Saintigny Y. Werner Syndrome Protein--Unwinding Function to Explain Disease. Science of Aging Knowledge Environment. 2004; 2004: re3–re3.
93. Lu H, Davis AJ. Human RecQ Helicases in DNA Double-Strand Break Repair. Frontiers in Cell and Developmental Biology. 2021; 9.
94. Vasseur E, Delaporte MT, Zabot F. Excision Repair Defect in Rothmund Thomson Syndrome. Acta Dermato-Venereologica. 1999; 79: 150–152.
95. Shamanna RA. WRN regulates pathway choice between classical and alternative non-homologous end joining. Nat Commun. 2016; 7: 13785.
96. Katsuki Y, Takata M. Defects in homologous recombination repair behind the human diseases: FA and HBOC. Endocr Relat Cancer. 2016; 23: T19-37.
97. Goto M, Miller RW, Ishikawa Y, Sugano H. Excess of rare cancers in Werner syndrome (adult progeria). Cancer Epidemiol Biomarkers Prev. 1996; 5: 239–246.
98. Chun SG. Pancreatic Adenocarcinoma Associated With Werner's Syndrome (Adult-Onset Progeria). Gastrointest Cancer Res. 2011; 4: 24–28.
99. MJ Moser, WL Bigbee, SG Grant, MJ Emond, RG Langlois, et al. Genetic Instability and Hematologic Disease Risk in Werner Syndrome Patients and Heterozygotes1. Cancer Research. 2000; 60: 2492–2496.
100. Sencen L. Rothmund-Thomson Syndrome. NORD (National Organization for Rare Disorders). Available online at: https://rarediseases.org/rare-diseases/rothmund-thomson-syndrome/.
101. Wang LL, Plon SE. Rothmund-Thomson Syndrome. In: Adam MP, editors. GeneReviews®. University of Washington, Seattle. 1993.
102. Tiwari V, Wilson DM. DNA Damage and Associated DNA Repair Defects in Disease and Premature Aging. Am J Hum Genet. 2019; 105: 237–257.
103. Kiwerska K, Szyfter K. DNA repair in cancer initiation, progression, and therapy-a double-edged sword. J Appl Genet. 2019; 60: 329–334.

Book Chapter

MAGE Genes, The Cancer Tested Antigens Targeted by Immunotherapy

Aline Radi* and Martin Kömhoff*

University Children's Hospital, Philipps University, Germany

***Corresponding Author:** Aline Radi, University Children's Hospital, Philipps University, 35043 Marburg, Germany

Martin Kömhoff, University Children's Hospital, Philipps University, 35043 Marburg, Germany

Published **December 13, 2022**

How to cite this book chapter: Aline Radi, Martin Kömhoff. MAGE Genes, The Cancer Tested Antigens Targeted by Immunotherapy. In: Hussein Fayyad Kazan, editor. Immunology and Cancer Biology. Hyderabad, India: Vide Leaf. 2022.

MAGE Genes: Introduction and Classification

Studying the immune system's ability to recognize and eliminate tumors may help in developing new therapies for cancer. In addition to the known mutated, overexpressed, fused, and oncoviral proteins, male germ cell–specific proteins were added to the list in 1991 when melanoma antigen 1 (MAGE-1) was identified in the melanoma cell line MZ2-MEL. A patient-derived MZ2-MEL cell line was created from a patient (MZ-2) who had, for 10 years, exhibited strong T-cell activity against autologous tumor cells in culture [1]. It is worth mentioning that

a patient survived without disease recurrence for more than 30 years after receiving autologous melanoma cell clones that had been mutagenized in vitro and lethally irradiated. However, all attempts to use MAGE-vaccines clinically have failed. In that sense, MAGE-A3 vaccine trials in Phase III trials were unsuccessful because they did not provide sufficient protection against melanoma, indicating that boosting T-cell responses to the MAGE-A3 protein is not sufficient to hinder the disease progression [2]. Still, MAGE proteins play an important role in tumor biology.

MAGE protein family consists of 10 subfamilies classified into two types based on their gene structures, chromosomal location, and expression patterns in specific tissues (Figure 1). MAGE type I genes (chromosome X-clustered genes), also called cancer-testis antigens (CTAs) are characterized by human leukocyte antigen epitope (HLA) in cancer cells and include MAGE-A, -B, and –C. In addition to cancer cells of diverse origins, germ-line cells in ovaries, testes, and placentas express these genes. However, they are not commonly expressed in adults' tissues [3]. Type II genes are involved in cell proliferation and apoptosis, including MAGE-D, -E, -F, -G, and -H. They are widely expressed in human and murine tissues and are not restricted to cancer tissues**.** In eutherian mammals, the MAGE family, which includes more than 50 related proteins, has expanded to protect the germline from environmental stress and help in stress adaptation. This stress tolerance may explain why MAGEs are abnormally expressed in many cancers where new studies showed a relation between stress and cancer growth [4].

MAGE protein family is a large and highly conserved group of proteins that possess a common domain; 180-amino acid domain known as the MAGE homology domain (MHD). Mammalians share 40% of amino acids in the MHD among all the MAGE subfamilies, but higher conservation is obvious at the subfamily level, where MAGE-D and MAGE-A subfamily members share 75 and 70% MHD residues, respectively. Long-term research into MAGE proteins has not yet revealed their diverse molecular functions. In line with the dynamic nature of the MHD structure, MAGE proteins exert their function through interactions with

diverse proteins. It has been shown that MAGEs cooperate with distinct E3 ligases to regulate ubiquitination of target proteins [5]. E3 ligases are enzymes that recognize and mediate the transfer of activated ubiquitin from the E2 enzyme to a specific target substrate. They are classified into four major classes: RING (really interesting new gene) finger, U- box, PHD finger, and HECT. Efforts were done to identify the function of MAGE proteins and led to a discovery that both type I and II MAGEs bind E3 ubiquitin ligases with RING domains and form MAGE-RING ligases (MRLs). Several distinct MRLs have been subsequently identified. MAGEs recognize and bind their E3 ligase partner through their MHDs [5].

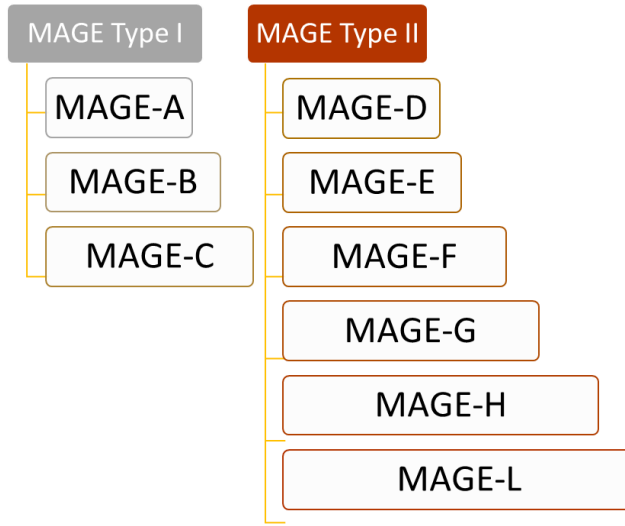

Figure 1: Main members of the MAGE family. Two main classes of MAGE genes, MAGE gene type I and type II which consist of different subfamilies.

Role of MAGE Genes in Cancer

Melanoma-associated antigen (MAGE) family members and specially class I are cancer/testis antigens. They are usually expressed in trophoblasts, germline cells, and a wide range of human cancer types such as melanoma, lung cancer, breast cancer, oral squamous cell carcinoma, esophageal carcinoma, urothelial malignancies and hematopoietic malignancies [6] [7]

[8] [9]. They drive tumor progression through various mechanisms, thereby resulting in tumor growth, metastasis, and recurrence. This common role in tumor progression has drawn research attention into focusing on MAGE's antigenicity and expression pattern in specific tissues to target them with cancer immunotherapy. Despite recent efforts to decipher the epigenetic regulation of certain MAGE family members, the transcriptional programs driving their abnormal expression remain poorly comprehended, and much remains to be discovered. The known tumor-related functions of MAGE family members are summarized in Table1. Additional mechanistical studies concerning MAGE function and regulation will provide some new alternative strategies targeting MAGEs in multiple types of cancers [10].

Table 1: The known tumor-related functions of MAGE family. MAGE genes have been classified as cancer related in various types of tumors with their related biological functions [10].

Type	Subtype	Gene name	Tumor type	Biological functions
MAGE-I	MAGE-A	MAGE-A1	Melanoma, gastric, endometrial, head and neck cancer	- Activating p-C-JUN - Repressing transcription - Recruiting HDAC1
		MAGE-A2	Glioma and breast cancer	- Degrading P53, MDM2 and MDM4 - Increasing ER signaling
		MAGE-A3	Non small lung cancer, hepatocellular carcinoma	- Degrading P53, and AMPKα1 - Enhancing TRIM28-dependent FBP1 degradation
		MAGE-A4	Hepatocellular carcinoma and lung cancer	- Inactivating the oncoprotein gankyrin
		MAGE-A6	Breast, colon, and lung cancer	- Degrading P53, and AMPKα1
		MAGE-A11	Breast cancer, esophageal squamous cell carcinoma, neck and prostate cancer	- Increasing Skp2-mediated degradation of cyclin A and P130 - Decreasing Skp2-mediated degradation of E2F1 - Increasing AR transcriptional activity
		MAGE-A12	Colorectal cancer, prostatic carcinoma , melanoma, bladder, lung, head and neck cancer	- Promoting P21 ubiquitination
	MAGE-C	MAGE-C2	Melanoma, breast, lung and hepatocellular carcinoma	- Enhancing TRIM28-dependent degradation of FBP1 - Inhibiting cyclin E degradation - Increasing KAP1-Ser824 phosphorylation
MAGE-II	MAGE-D	MAGE-D2	Melanoma, gastric, colorectal and hepatocellular carcinoma	- Suppressing TRAIL-induced apoptosis
	MAGE-H	MAGE-H1	Breast and colorectal cancer	- Upregulating mir-200 a/b expression via P73 association

Class I MAGE Genes

Class-I MAGE/cancer testes antigens include the MAGE-A, MAGE-B, and MAGE-C protein families, a group of highly homologous proteins whose expression is repressed in all normal tissues except developing sperm. Aberrant expression of class I MAGE proteins occurs in a wide range of cancer types. Thus, MAGE proteins have long been defined as tumor-specific targets; however, their functions have largely been unknown. Their role in cancer can be explained by the fact that Class I MAGE protein expression may suppress apoptosis by suppressing p53 and may actively contribute to the development of malignancies by promoting tumor survival. Since class I MAGE proteins expression is absent in normal tissues, inhibition of MAGE antigen expression or function represents a novel and specific treatment for melanoma and various malignancies [11].

MAGE-A

MAGE-A belongs to the type I melanoma antigen gene family, and it is associated with different cancer types. MAGE-A1 was the first identified human tumor antigen [12]. It interacts with transcriptional regulator SKIP, which in turn intervenes in signaling pathways involving Notch1-IC and TGF-β. SKIP can act as a transcription activator or repressor, it recruits a repression complex including HDAC. Therefore, MAGE-A1 aids in the setting of gene expression patterns for tumor cell growth [13]. Moreover, MAGE-*A expression is associated with low survival in* lung cancer patients [14], and it was also associated with malignant transformation in leukoplakia which is a precursor of oral and laryngeal squamous cell carcinoma despite the fact that it was not expressed in healthy oral mucosa [15]. MAGEA1-A3 and A12 have been shown to be expressed at an early stage in breast cancer [16].

MAGE-A3 is expressed in bladder cancer and represents a candidate for cancer immunotherapy, where it is thought to have an anti-oncogenic effect through diminishing proliferation and inducing apoptosis by regulating p21 and p53 [17]. MAGE-A4 is overexpressed in various cancers including non-small cell lung

carcinoma and it is widely used for cancer vaccine therapy. It was identified to inhibit apoptosis via caspase-3 and P53 interaction [18]. MAGE-A9 and MAGE-A11 are expressed in breast cancer and their expression was positively associated with estrogen receptors (ER) and HER2 expression [19].

As aforementioned, MAGE proteins proved to bind RING domain-containing proteins through its MHD (Melanoma Homology Domain). E3 ligase is a protein that recruits E2 ubiquitin conjugating enzyme that is linked to ubiquitin, which in turn will transfer the ubiquitin from E2 to a protein targeted for degradation. MAGE-A3/ 6-TRIM28 E3 ubiquitin ligase complex was found to degrade AMPKα1 resulting in downregulating AMPK signaling during tumorigenesis [20].

MAGE-A proteins were found to form complexes with RING domain proteins, such as MAGEA2/C2-TRIM28, MAGE-B18-LNX, and MAGE-G1-NSE1 complexes [21]. The RING domain is a cysteine-rich domain that normally forms a cross-brace structure that typically coordinates two zinc ions. RING domain proteins are proved to be a huge E3 ubiquitin ligase family, which bind to and localize E2 ubiquitin-conjugating enzymes to substrates for ubiquitination [22]. MAGE proteins regulate the ubiquitin ligase activity of RING domain proteins through binding them and acting as scaffold to their substrates.

MAGE-A2, -A3, -A6, and -C2 bound TRIM28 (also known as KAP1, TIF-1beta, or Krip125) were shown to downregulate the tumor suppressor protein p53 [23].

MAGE-B

MAGE-B belongs to type I MAGE genes forming a cluster of four human genes. The coding regions of the *MAGE-B* genes share about 75% nucleotide identity and about 60% identity with those of most *MAGE-A* genes. *MAGE-B2* is the most abundantly expressed member of the *MAGE-B* family. It has been shown to be overexpressed in a wide range of cancer types where it induces tumor growth and progression [24]. MAGE-B genes are expressed with relatively high frequency and specificity in

hepatocellular carcinoma HCC. Most HCC patients with positive expression of at least one member of the MAGE-B or MAGE-A gene family are adequate candidates to receive specific immunotherapy. Frequent co-expression of multiple members of MAGE-B and MAGE-A subfamilies provides the possibility of using polyvalent vaccines to achieve more effective immunotherapeutic results [25]. In light of its elevated expression in cancers, MAGEB2 is an appealing therapeutic target because it generates immunogenic peptides, making the cells susceptible to vaccination therapy in the same manner as MAGE-A genes. This would be particularly crucial in certain tumors that do not express any of the *MAGE-A* genes [26].

MAGE-C

MAGE-C melanoma antigen family belongs to type I MAGE genes. MAGE-C2 and MAGE-C3 have been shown to be cancer-related where MAGE-C2 binds KAP1, a heterochromatin protein that is robustly phosphorylated by ATM at Ser-824 in response to DNA damage. This binding increases the interaction between KAP1 and ATM and as a result increases KAP1 activation. Therefore, MAGE-C2 may enhance tumor growth through the enhancement of DNA damage repair [27].

MAGE-C3 was shown to be a potential prognostic marker and therapeutic target in cancer. It promotes tumor growth by enhancing epithelial-mesenchymal transition and protecting tumors from immune surveillance [28]. MAGE-C3 plays a role in regulating the cytokine secretion of T cells repressing antitumor immunity and protecting cancer cells. Mechanistically, MAGE-C3 fostered IFN-γ signaling and enhanced programmed cell death ligand 1 (PDL1) through binding IFN-γ receptor 1 (IFNGR1) and strengthening the interaction between IFNGR1 and the signal transducer and activator of transcription (STAT1) (Figure 2). Research was conducted to verify the immunosuppressive function of MAGE-C3, demonstrating that MAGE-C3 has a higher tumorigenic potential in immune-competent mice than in immune-deficient nude mice [29].

_MAGE-C2/CT10 promotes the growth of several tumors where it was shown to induce proliferation and metastasis in prostate cancer through the upregulation of c-Myc expression [30]. C-Myc the master regulator gene of cellular metabolism and proliferation.

MAGE- C1/CT7 is involved in the survival of myeloma cells where its knockdown has led to the apoptosis of malignant cells indicating that their expression is crucial for myeloma precursor's survival [31].

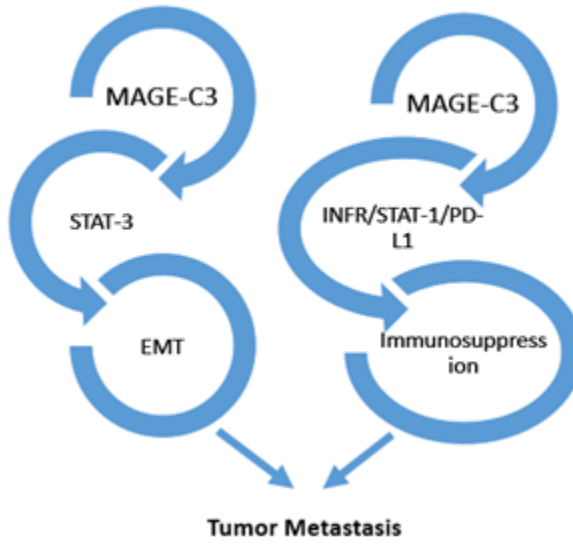

Figure 2: MAGE-C3 role in promotion of tumor metastasis. MAGE-C3 enhances EMT and tumor immunosuppression by activation of PD-L1 through INFR signaling.

MAGE-D2

Melanoma associated antigen D2. The function of MAGE-D2 remained unclear for a long time, but discovering its cellular localization provided the first insights into its biological role [32]. MAGE-D2 plays a role in the regulation, plasma membrane localization and function of the sodium chloride cotransporters SLC12A1 and SLC12A3 in the distal convoluted renal tubule. It

has also been shown that it plays a role in cell cycle regulation. In addition to these functions, MAGE-D2 proved to be closely related to cancer where it induces metastasis and cell adhesion of tumor cells and represents a promising biomarker in gastric tissues for malignancy of GC [33]. A significant subset of human tumors, such as neuroblastoma, breast and melanoma cancer have a low rate of p53 mutations and, thus, presumably, wild type p53 is inactivated via interactions with cellular negative regulators of p53, the p53-dissociators. Studies showed that MAGE-D2 interacts physically with p53 and impairs its transcriptional activity in human cancer cells [34], while a new study proved that MAGE-D2 inhibits MDM2 ligase activity under hypoxia [35]. This will secure P53 from Mdm2 in the presence of MAGE-D2. In that sense, more research should be done to investigate the connection between MAGE-D2 and P53 in malignancies. Furthermore, MAGE-D2 negatively regulates the expression of tumor necrosis factor-related apoptosis-inducing ligand (TRAIL) thereby protecting melanoma cells from TRAIL-induced apoptosis [36].

Therapeutic Approach: BiTEs, T cell Engagers Targeting MAGE-A

A therapeutic approach to attack cancer cells through targeting MAGE genes was developed by APO-T. APO-T is a biopharmaceutical company working on the development of new anti-cancer treatments in Netherlands. It is focusing on the development of a bispecific T cell engagers (BiTEs) that target MAGE-A cancer antigen. These engagers will attract the T cells to the cancer cells expressing MAGE-A protein in the tumor environment. Targeting MAGE-A family members specifically is based on their expression in a wide range of cancer types. The fact that MAGE-A is not expressed on the membrane like other cancer markers renders this approach more interesting. This will protect tissues like placenta and testes that express MAGE-A and not MHC-1 from being attacked by these T cell engagers. MAGE-A proteins are degraded by proteasomes and represented on cell surface by human leukocyte antigen as HLA/MAGE derived peptide complex. APO-T BiTEs act as a linker between T cells and cancer cells where it binds CD3 molecule presented

on T cell surface to HLA/MAGE on cancer cell surface. Thus, these engagers only help in the attraction of immune effector cells to cancer microenvironment (Figure3) [36].

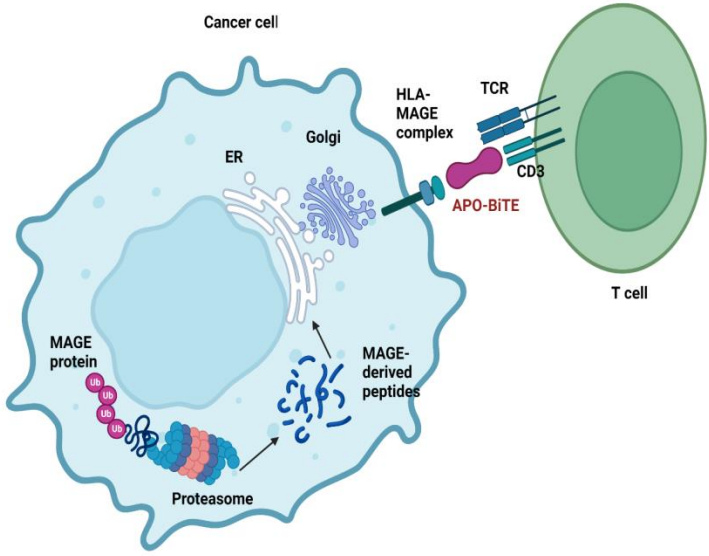

Figure 3: APO-T's BiTEs facilitate removal of cancer cells by immune cells. APO-BITE acts as a bridge between cancer cells and T lymphocytes through binding CD3 molecule to HLA-MAGE complex. Biorender.com

References

1. Whitehurst AW. Cause and Consequence of Cancer/Testis Antigen Activation in Cancer. Annu. Rev. Pharmacol. Toxicol. 2014; 54: 251–272.
2. Daud AI. Negative but not futile: MAGE-A3 immunotherapeutic for melanoma. The Lancet Oncology. 2018; 19: 852–853.
3. P Chomez, O De Backer, M Bertrand, E De Plaen, T Boon, et al. An overview of the MAGE gene family with the identification of all human members of the family. Cancer Res. 2001; 61: 5544–5551.
4. Rebecca R Florke Gee, Helen Chen, Anna K Lee, Christina A Daly, Benjamin A Wilander, et al. Emerging roles of the

MAGE protein family in stress response pathways. Journal of Biological Chemistry. 2020; 295: 16121–16155.
5. Weon JL, Potts PR. The MAGE protein family and cancer. Current Opinion in Cell Biology. 2015; 37: 1–8.
6. Achim A Jungbluth, Scott Ely, Maurizio DiLiberto, Ruben Niesvizky, Barbara Williamson, et al. The cancer-testis antigens CT7 (MAGE-C1) and MAGE-A3/6 are commonly expressed in multiple myeloma and correlate with plasma-cell proliferation. Blood. 2005; 106: 167–174.
7. TS Weiser, G A Ohnmacht, Z S Guo, M R Fischette, G A Chen, et al. Induction of MAGE-3 expression in lung and esophageal cancer cells. The Annals of Thoracic Surgery. 2001; 71: 295–302.
8. Alain Bergeron, Valérie Picard, Hélène LaRue, Francois Harel, Hélène Hovington, et al. High frequency of MAGE-A4 and MAGE-A9 expression in high-risk bladder cancer. Int. J. Cancer. 2009; 125: 1365–1371.
9. Simpson AJG, Caballero OL, Jungbluth A, Chen YT, Old LJ. Cancer/testis antigens, gametogenesis and cancer. Nat Rev Cancer. 2005; 5: 615–625.
10. Lian Y, Meng L, Ding P, Sang M. Epigenetic regulation of MAGE family in human cancer progression-DNA methylation, histone modification, and non-coding RNAs. Clin Epigenet. 2018; 10: 115.
11. Bing Yang, Sean M O'Herrin, Jianqiang Wu, Shannon Reagan-Shaw, Yongsheng Ma, et al. MAGE-A, mMage-b, and MAGE-C Proteins Form Complexes with KAP1 and Suppress p53-Dependent Apoptosis in MAGE-Positive Cell Lines. Cancer Research. 2007; 67: 9954–9962.
12. Zhao J, Wang Y, Mu C, Xu Y, Sang J. MAGEA1 interacts with FBXW7 and regulates ubiquitin ligase-mediated turnover of NICD1 in breast and ovarian cancer cells. Oncogene. 2017; 36: 5023–5034.
13. Laduron S. MAGE-A1 interacts with adaptor SKIP and the deacetylase HDAC1 to repress transcription. Nucleic Acids Research. 2004; 32: 4340–4350.
14. Lina Gu, Meixiang Sang, Danjing Yin, Fei Liu, Yunyan Wu, et al. MAGE-A gene expression in peripheral blood serves as a poor prognostic marker for patients with lung cancer:

MAGE-A related lung cancer prognosis. Thorac Cancer. 2018; 9: 431–438.
15. Christoph A Baran, Abbas Agaimy, Falk Wehrhan, Manuel Weber, Verena Hille, et al. MAGE-A expression in oral and laryngeal leukoplakia predicts malignant transformation. Mod Pathol. 2019; 32: 1068–1081.
16. Ayyoub M, Scarlata CM, Hamaï A, Pignon P, Valmori D. Expression of MAGE-A3/6 in Primary Breast Cancer is Associated With Hormone Receptor Negative Status, High Histologic Grade, and Poor Survival. Journal of Immunotherapy. 2014; 37: 73–76.
17. Zhou G. Expression and function of the tumor antigen MAGE-A3 in bladder cancer cell lines. 2020.
18. Aki Fujiwara-Kuroda, Tatsuya Kato, Takehiro Abiko, Takahiro Tsuchikawa, Noriaki Kyogoku, et al. Prognostic value of MAGEA4 in primary lung cancer depends on subcellular localization and p53 status. Int J Oncol. 2018; 53: 713-724.
19. Shu-Yun Hou, Mei-Xiang Sang, Cui-Zhi Geng, Wei-Hua Liu, Wei-Hua Lü, et al. Expressions of MAGE-A9 and MAGE-A11 in Breast Cancer and their Expression Mechanism. Archives of Medical Research. 2014; 45: 44–51.
20. Carlos T Pineda, Saumya Ramanathan, Klementina Fon Tacer, Jenny L Weon, Malia B Potts, et al. Degradation of AMPK by a Cancer-Specific Ubiquitin Ligase. Cell. 2015; 160: 715–728.
21. Doyle JM, Gao J, Wang J, Yang M, Potts PR. MAGE-RING Protein Complexes Comprise a Family of E3 Ubiquitin Ligases. Molecular Cell. 2010; 39: 963–974.
22. KL Lorick, J P Jensen, S Fang, AM Ong, S Hatakeyama, et al. RING fingers mediate ubiquitin-conjugating enzyme (E2)-dependent ubiquitination. Proc. Natl. Acad. Sci. U.S.A. 1999; 96: 11364–11369.
23. Doyle JM, Gao J, Wang J, Yang M, Potts PR. MAGE-RING Protein Complexes Comprise a Family of E3 Ubiquitin Ligases. Molecular Cell. 2010; 39: 963–974.
24. Rebecca R Florke Gee, Helen Chen, Anna K Lee, Christina A Daly, Benjamin A Wilander, et al. Emerging roles of the

MAGE protein family in stress response pathways. Journal of Biological Chemistry. 2020; 295: 16121–16155.
25. Mou D. Expression of MAGE-B genes in hepatocellular carcinoma. Zhonghua Zhong Liu Za Zhi. 2004; 26: 40–42.
26. Kavita M Pattani, Ethan Soudry, Chad A Glazer, Michael F Ochs, Hao Wang, et al. MAGEB2 is Activated by Promoter Demethylation in Head and Neck Squamous Cell Carcinoma. PLoS ONE. 2012; 7: e45534.
27. Neehar Bhatia, Tony Z Xiao, Kimberly A Rosenthal, Imtiaz A Siddiqui, Saravanan Thiyagarajan, et al. MAGE-C2 Promotes Growth and Tumorigenicity of Melanoma Cells, Phosphorylation of KAP1, and DNA Damage Repair. Journal of Investigative Dermatology. 2013; 133: 759–767.
28. Qingnan Wu, Weimin Zhang, Yan Wang, Qingjie Min, Hongyue Zhang, et al. MAGE-C3 promotes cancer metastasis by inducing epithelial-mesenchymal transition and immunosuppression in esophageal squamous cell carcinoma. Cancer Communications. 2021; 41: 1354–1372.
29. Qingnan Wu, Weimin Zhang, Yan Wang, Qingjie Min, Hongyue Zhang, et al. MAGE-C3 promotes cancer metastasis by inducing epithelial-mesenchymal transition and immunosuppression in esophageal squamous cell carcinoma. Cancer Communications. 2021; 41: 1354–1372.
30. Qiu J, Yang B. MAGE-C2/CT10 promotes growth and metastasis through upregulating c-Myc expression in prostate cancer. Mol Cell Biochem. 2021; 476: 1–10.
31. Djordje Atanackovic, York Hildebrandt, Adam Jadczak, Yanran Cao, Tim Luetkens, et al. Cancer-testis antigens MAGE-C1/CT7 and MAGE-A3 promote the survival of multiple myeloma cells. Haematologica. 2010; 95: 785–793.
32. Céline Pirlot, Marc Thiry, Charlotte Trussart, Emmanuel Di Valentin, Jacques Piette, et al. Melanoma antigen-D2: A nucleolar protein undergoing delocalization during cell cycle and after cellular stress. Biochimica et Biophysica Acta (BBA) - Molecular Cell Research. 2016; 1863: 581–595.
33. Mitsuro Kanda, Shuji Nomoto, Hisaharu Oya, Hideki Takami, Dai Shimizu, et al. The Expression of Melanoma-Associated Antigen D2 Both in Surgically Resected and Serum Samples Serves as Clinically Relevant Biomarker of

Gastric Cancer Progression. Ann Surg Oncol. 2016; 23: 214–221.
34. Rainer Brachmann, Jue Zeng, Robert Culverhouse, Wanghai Zhang, Howard McLeod et al. MAGED2: A novel p53-dissociator. Int J Oncol. 31: 1205-1211.
35. Elie Seaayfan, Sadiq Nasrah, Lea Quell, Maja Kleim, Stefanie Weber, et al. MAGED2 Is Required under Hypoxia for cAMP Signaling by Inhibiting MDM2-Dependent Endocytosis of G-Alpha-S. Cells. 2022; 11: 2546.
36. Hsin-Yi Tseng, Li Hua Chen, Yan Ye, Kwang Hong Tay, Chen Chen Jiang, et al. The melanoma-associated antigen MAGE-D2 suppresses TRAIL receptor 2 and protects against TRAIL-induced apoptosis in human melanoma cells. Carcinogenesis. 2021; 33: 1871–1881.
37. Available online at: https://www.nature.com/biopharmdeal

Book Chapter

Renal Involvement in Localized and Systemic Autoimmunity Diseases with Insights into the Ongoing Therapeutic Approaches

Aline Radi* and Sadiq Nasrah*

University Children's Hospital, Philipps University, Germany

***Corresponding Authors:** Aline Radi, University Children's Hospital, Philipps University, 35043 Marburg, Germany

Sadiq Nasrah, University Children's Hospital, Philipps University, 35043 Marburg, Germany

Published **December 13, 2022**

How to cite this book chapter: Aline Radi, Sadiq Nasrah. Renal Involvement in Localized and Systemic Autoimmunity Diseases with Insights into the Ongoing Therapeutic Approaches. In: Hussein Fayyad Kazan, editor. Immunology and Cancer Biology. Hyderabad, India: Vide Leaf. 2022.

Acknowledgments: Thanks to Martin Koemhoff and Elie Seaayfan for their proofreading.

Autoimmunity

Immune system is a complex network of organs, tissues, cells and components that protect our bodies from infections by differentiating self from non-self-antigens. Autoimmunity results from the loss of tolerance to self-antigens leading to the production of cytokines and antibodies reacting with endogenous components. A disease that results from this aberrant immune response is known as autoimmune disease that is usually caused by sequestered or hidden antigens, neo antigens, cessation of tolerance, cross reacting antigen or loss of immune-regulation and genetic mutations. Autoimmunity can be divided into three phases:

1. Initiation
2. Propagation
3. Resolution

It is initiated by a combination of environmental and genetic factors. The initiation phase is also known as the asymptomatic phase, followed by the propagation phase, which is characterized by inflammation and tissue damage due to cytokines production. Finally, the resolution phase results from persistent struggle between pathogenic effector responses and their regulation (Figure 1) [1].

Autoimmune diseases are classified mainly into localized and systemic reactions. Local diseases are specific to a particular tissue or organ, whereas systemic diseases consist of autoantibodies not specific to antigens found on certain tissues. Systemic autoimmune diseases encompass a broad spectrum of related diseases characterized by immune system dysregulation leading to an activation of immune cells, which in turn attack autoantigens and cause inappropriate inflammation and damage to various tissues [2].

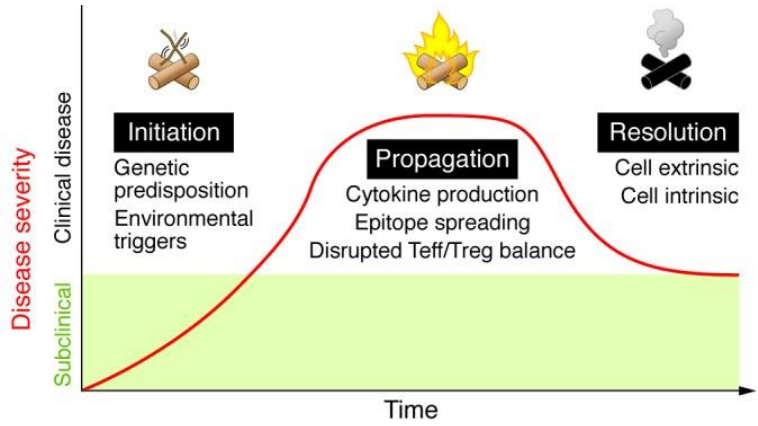

Figure 1: Three major phases of autoimmune disease. Initiation phase is usually triggered by genetic or environmental stimulus followed by propagation phase characterized by cytokine production. Then this is resolved by intrinsic or extrinsic pathways to restore the Teff/Treg balance [1].

Kidneys and Immune System

The kidneys are pairwise bean-shaped organs of the urinary system located retroperitoneal. The nephron, the functional unit of kidneys consists of the glomerulus and the attached tubule system. Kidneys have a variety of homoeostatic functions including the regulation of blood pressure, osmolality and pH. Kidneys also secrete some active compounds that contribute to immune homeostasis including calcitriol which regulates bone homeostasis and phagocyte function, erythropoietin which is induced in response to hypoxia for the purpose of regulating renin which in turn induces angiotensin and aldosterone that regulate blood pressure, electrolyte balance and extracellular osmolality. Thus, kidneys and immune system are closely related.

A number of chronic kidney diseases are caused by immunological diseases. These immune-mediated kidney diseases can be distinguished into two groups. First, direct immune-mediated kidney diseases are caused by direct autoantibodies against renal antigens, with the best-studied example being collagen IV. Indirect immune-mediated kidney

diseases can be the renal consequence of systemic, immune-complex-forming autoimmunity or can be caused by unregulated complement system activation. [3].

Kidneys are Frequent Targets of Autoimmunity

Several studies attempted to understand the reasons why kidneys are frequent targets for autoimmunity, especially to injury by altered antibodies, immune complexes and complement factors, which have helped in implementing new treatments in some cases.

Kidney's anatomy and physiology make it more susceptible to distinct forms of immune-mediated injury. The renal medulla of the kidney is characterized by high osmolality leading to crystal precipitation like uric acid which is sensed by the inflammasome that will in turn induce TH17 inflammatory response [4-5]. Renal autoimmunity is also triggered by antibody deposition or immune cell infiltration. Autoantigens are frequently of non-renal origin and accumulate in the kidney due to the physiological properties of the perm-selective high-flow and high-pressure filtration function of the glomeruli. Circulating autoantigens may be deposited in glomeruli as part of circulating immune complexes or may become "implantable" target antigens due to their physicochemical properties that promote their fixation in glomeruli [6]. After antibody deposition, the released Fc (crystalline fragment) regions of antibodies recruit and activate inflammatory cells and trigger complement activation. This process leads to further cell infiltration and secretion of inflammatory mediators by infiltrating and endogenous cells particularly neutrophils, T lymphocytes, and macrophages as well as platelets. The local response of renal cells plays an important role in determining the severity of inflammation. High severity and/or prolonged duration leads to fibrosis and eventually to organ failure. Genetic factors influence the intensity and severity of inflammation and fibrosis [7]. Glomerular, tubular and vascular structures of the kidney are all possible targets of the autoimmune disorder.

Direct Immune Mediated Renal Diseases

Anti-GBM Glomerular Basement Membrane Disease

Anti-GBM disease is a form of crescentic glomerulonephritis (GN), associated generally with acute kidney aberrations. The scaffold of the glomerular basement membrane is cooperatively formed by type IV collagen along with other macromolecular attributes such as entactin, laminin and heparan sulphate proteoglycans (HSPGs). The building units of type IV collagen consist of 6 distinct alpha chains separated into 3 domains each, the amino terminal 7S domain, the central triple-helical domain and the globular non-collagenous (NC)-1 domain at the carboxyl terminal. The assembly of the type IV collagen trimeric structure is initiated by 3 NC1 domains, where the triple helical molecules come together as combinations of α1.α1.α2, α3.α4.α5 and α5.α5.α6. The combination α3.α4.α5 is restricted to kidney, cochlea, lungs and testes. Circulating autoantibodies recognize the epitope (NC)1 domain of α3(IV)NC1 encompasses residues 198-233 as the primary interaction site which is normally hidden with the quaternary structure of type IV collagen [8-9-10]. Disclosing the epitope must be preceded by a conformational change which causes further conformational changes and the formation of antigen-antibody complex [11].

IgG primarily subtype 1 with few IgG4 are the major antibodies which together with the complement components harm the surrounding endothelial cells and podocytes, promoting immune cell infiltration inflammation and subsequently fibrosis (Figure1). Rarely, IgA or IgM will be present instead of IgG in anti-GBM patients [12].

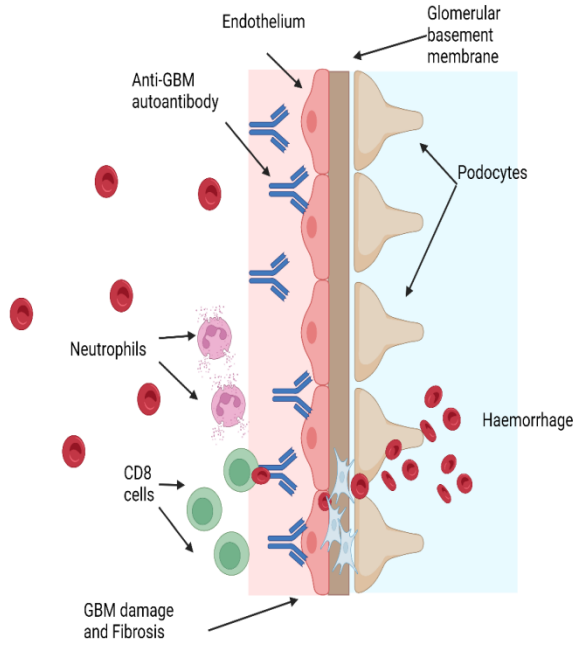

Figure 2: Anti-glomerular basement membrane disease pathogenesis at the molecular level. Anti-glomerular basement membrane Autoantibodies are produced in response to unknown stimulus. Antigen binding to the antibody activates the complement cascade, and further involvement of inflammatory cells leads to chronic inflammation and fibrosis [3]. Biorender.com.

Structural studies defined the role of the human leukocyte antigen (HLA) system mediating the risk/protection in immune renal diseases including anti-GBM. The difference between HLA DR1 and HLA DR15 of the major histocompatibility MHC class II resides in the fashion of introducing $\alpha 3_{135–145}$ to T cells, leading to different T cell populations. HLA DR1 produces high proportions of T regulatory cells which maintain tolerance in the periphery while HLA-DR15 expression ends in generating potentially damaging T helper cells observed in anti-GBM disease [13].

Patients presenting with severe alveolar haemorrhage are classified to have Good Pasture's Syndrome where autoantibodies target additionally the pulmonary epitope (NC)1

domain, in the alveolar basement membrane (ABM) [14]. Furthermore, the presence of ANCA-AAV (autoantibodies to neutrophil cytoplasmic antigens)-associated vasculitis was reported in 30% of anti-GBM cases [15-16].

Membranous Glomerulonephritis (MGN)

MGN denotes a diffuse thickening of the glomerular capillary wall by sub-epithelial immune deposits in which the autoantibodies target proteins normally expressed by podocytes in the glomerulus. A well-known target is (PLA_2R) the phospholipase A_2 receptor (75% of the cases) [17-18]. Another target is thrombospondin type-1 domain-containing 7A, which contributes to 8-14% of MGN cases [19].

Podocytes respond by modifying their cytoskeleton and extruding mediators of fibrosis and proinflammatory cytokines which in turn activate the classical complement pathway [17]. Glomerular podocytes are protected from cytotoxic T lymphocytes (CTLs) because they are located in immune-privileged sites. When the Bowman's capsule is destroyed in glomerulonephritis, podocytes become vulnerable to drainage of CTLs.

It is worth mentioning that MGN arises as well by immune complex deposition consequential to a primary disease such as systemic lupus nephritis (SLE), infections (Malaria, Hepatitis B) or malignancy. Immune complex deposition on the urinary side of the glomerular basement membrane is the major feature of MGN.

Anti-Tubular Basement Membrane (TBM) TIN Nephritis

TBM-TIN is a form of progressive tubulointerstitial nephritis (TIN) due to autoantibody deposition and activity of autoreactive T cells counter to 3M-1 membrane glycoprotein [20]. This antigen is a novel member of the basement membrane glycoproteins family whose expression is restricted to the renal proximal tubules, ileum and moderately to epidermal and corneal

basement membranes. It has a dose-related effect on the polymerization of Laminin and its predestined polymers while it does not intermeddle with the polymerization of type IV collagen. Studies showed that it elevates the adhesion of cultured renal tubular cells and aortic endothelial cells [21]. Interstitial inflammation with extensive fibrosis and small atrophic tubules are often revealed by renal biopsies [22].

TIN can also be seen in primary Sjögren's syndrome (pSS), a systemic autoimmune disease affecting glandular epithelium and eliciting glomerulonephritis as a result of circulating immune complexes deposition. Carbonic anhydrase and the hydrogen transporter H1-ATPase are the prospective self-antigens as they exist in both renal tubules and salivary glands [23]. Furthermore, TIN is present with linear deposition of IgG in TBM in 70% of anti-GBM GN patients [24].

Plasma Membranes of Tubular and Glomerular Epithelial Cells (Heymann Nephritis)

Two antigens were identified which associate with Heymann nephritis (the rat model of human membranous nephropathy). The main antigen, megalin is a ~600-kDa large molecule [25-26] located in the coated pits of tubular and glomerular epithelial cells and colocalizes with clathrin. It is also present in the Golgi apparatus, the endoplasmic reticulum, and in multivesicular bodies of glomerular visceral epithelial cells [27]. The interaction of circulating Abs with megalin leads to glomerular lesions manifested by proteinuria and nephrotic syndrome.

Another antigen is RAP (receptor associated protein) named after its ability to bind to LPR/α2-macroglobulin receptor. It is predominant in the ER and its assembly with megalin after biosynthesis was proved by trafficking studies. The assembly remains in the Golgi during the formation of the mature glycoprotein which in turn proceeds to the cell surface [28].

Indirect Immune Mediated Renal Disease

Renal disease is a bystander prey for a systemic dysregulation of the immune system originated by three major mechanisms:
-Circulating immune complex deposition
-Defects in the alternate complement system.
-Monoclonal immunoglobulins deposition
-Immune complexes of several antibodies bound to their antigens are formed not only after infection (e.g. Streptococcus, Hepatitis B) but following a systemic autoimmune disease as well, where the target antigen in this case is another antibody (rheumatoid factor) [29]. Due to their size and charge, the glomerulus is an attracting place for these complexes to settle and potentially clog the filtration barrier leading to glomerular damage [17]. As a result, circulating immune cells in addition to kidney cells expressing Fc receptors are activated leading to endothelial, epithelial and mesangial damage of the glomerulus induced by secreted cytokines and vasoactive substances. The latter create a proinflammatory environment and further activate the classical complement cascade causing damage to the surrounding cells and eliciting further pro-inflammatory signaling [30].

IgA nephritis for example occurs by IgA deposits, mainly subclass IgA1, in the mesangial area leading to recurrent hematuria and mesangioproliferative glomerulonephritis [31]. IgA is normally combined with C3 and to a lower degree with IgG and C4 causing hypercellularity and expansion of the mesangial matrix. Notably, IgA1 is deposited in glomeruli in many diverse diseases such as HIV, dermatitis herpetiformis and liver cirrhosis [32].

-The alternative pathway of complement activation is based on the spontaneous cleavage of C3 into C3a and C3b. Factor B in turn is cleaved by factor D, a serine plasma protease, to generate a small fragment called Bb which attaches to C3b generating the alternative short-lived C3bBb convertase. This pathway is regulated by soluble complement factor H (CHF), factor I and cell membrane associated cofactor protein (MCP or CD46) [33].

The complement pathway and its regulatory factors are closely involved in membranoproliferative glomerulonephritis MPGN pathogenesis [34]. MPGN is divided into three types based on the histological findings, both MPGN I (type1) and MPGN III (type3) are immunocomplex-mediated diseases symbolized by constant low C3 serum level and in some cases ~30% with the presence of nephritic factor (C3Nef). C3Nef extends C3bBb half-life and makes it less accessible to factor H and factor I responsible for its inactivation [35]. Other deficiencies are also reported involving factor H dysfunctions, dysfunctional C3 molecules and reduced factor B levels.

MPGN II (type 2) on the other hand has no association with immune complex deposition but is mainly triggered by the presence of C3NeF, or by defects of regulatory proteins, e.g. Factor H. Often low C3 levels are observed with normal C1q and C4 levels though. This disease is also known as dense-deposit disease (DDD) due to electron-dense deposits along the glomerular basement membrane GBM observed by EM [36].

MPGN causes morphological changes which can be seen by light microscopy represented by hypercellular glomeruli and proliferation of endothelial and mesangial cells evoking a lobular aspect of the capillary tuft.

The classical diarrhea related haemolytic uraemic syndrome HUS is typically incited by a toxin, assembled by *Shigella* and specific enterohaemorrhagic *E. coli* bacteria strains, called Shiga-toxin. Mutations in *CFH* gene encoding for complement Factor H develop atypical non diarrhea associated HUS. At the microscopic level, both classical and atypical HUS are characterized by thrombotic microangiopathy lesions [37]. CFH is a fluid phase complement regulatory protein which regulates the alternative pathway both in the fluid phase of the human body and on cell surfaces. Mutations in the N-terminal domain promotes C3 glomerulonephritis (C3GN) by disinhibiting activation of C3 in the fluid phase [38] while C-terminal mutations impose its ability to bind to endothelial cell surfaces leaving them vulnerable to complement mediated lysis and inducing microvascular thrombosis consequently as seen in

aHUS [37]. Microangiopathic hemolytic anemia, thrombocytopenia and renal failure are the diagnostic criteria of aHUS.

Similar lesions are present in 10% of primary anti-phospholipid syndrome APS [39] where the renal vascular tree is damaged due to loss of immune homeostasis. Circulating anti-phospholipid antibodies (aPLs) produce a procoagulant state, which turns into recurrent venous or arterial thrombosis in the presence of other prothrombotic factors [40].

Autoantibodies to neutrophil cytoplasmic antigens (ANCA) encompasses a collection of autoimmune diseases including GPA granulomatosis with polyangiitis _previously known as Wegener's granulomatosis (WG)_, MPA microscopic polyangiitis, EGPA eosinophilic granulomatosis with polyangiitis _formerly known as Churg-Strauss syndrome (CSS)_ and a renal limited form characterized specifically with necrotizing crescentic GN [41].

Two key antigens have been identified in the granules of neutrophils of the above-mentioned diseases: myeloperoxidase (MPO) a neutrophil cationic protein 146-kDa possesses an important role in the generation of oxygen radicals [42] and proteinase 3 (PR3) a 29-kDa glycoprotein, one of the three serine proteases existent in the azurophilic granules of monocytes and granulocytes [43]. MPO and PR3 antigens are distinguished by their immunofluorescence staining pattern: PR3 staining is cytoplasmic whereas MPO is perinuclear. Anti-PR3 antibodies are more common in GPA, while anti-MPO antibodies are strongly present in ANCA-GN and EGPA [44]. In normal subjects, neutrophils are activated to restore the tissue while in ANCA patients it turns to cause degranulation and extrusion of neutrophil extracellular traps (NETs). This extrusion into the glomerular capillaries releases ANCA associated antigens (MPO, PR3 and lysosome-associated membrane glycoprotein 2), which present attractive targets to circulating ANCA autoantibodies [29] that accordingly bind to cell surface-expressed ANCA antigens, resulting in subsequent neutrophil activation and inflammatory cascades that destructs the vascular endothelium.

Cross-linking of ANCA antigens present on the cell surface and Fc-gamma receptor signals were reported [45-46-47].

-Renal pathologies are also closely related to monoclonal gammopathies termed as monoclonal gammopathies of renal significance (MGRS) [48]. The deposit distribution of paraproteins in the kidney is consistently broader to include any compartment of the kidney in contradiction to immune-complex mediated disorders where the deposits are more exclusive to glomeruli and extra-glomerular regions. Based on the type and location of the monoclonal deposits, it affects one or more compartments such as glomeruli, renal vasculature, tubules and/or interstitium [49]. Light chain cast nephropathy is a well described pathology from this peer. Normally, the light chains of monoclonal immunoglobulin are filtered easily in the glomerulus. However, when high concentrations are present which surpass the reabsorption capacity of PCT proximal convoluted tubule, the light chains access the TAL thick ascending loop of Henle. This will be followed by attachment to uromodulin creating casts that obstruct the tubular lumen and incite acute loss of renal function. The light chains are capable of damaging the kidney at multiple levels originating vascular occlusion, glomerulonephritis and renal tubular pathologies such as Fanconi syndrome [49-50].

Therapeutic Approaches to Address Autoimmune Renal Diseases

Due to the fact that most GN are only partially curable nowadays, it is important to consider the role of autoimmunity, which is a major driver for chronic kidney diseases.

Current treatment is based on using a set of immunosuppressive drugs to govern autoimmunity such as mycophenolic acid, cyclophosphamide and rituximab (anti-CD20 monoclonal antibody) [51] in addition to corticosteroids [52]. This approach could be lifesaving but it comprises the risk of developing serious infections given that the healthy lymphocytes are impaired along the pathological ones on top of many undesirable

side effects [53]. Thus, novel targeted therapies are urgently necessitated.

- Immune antigen-antibody complexes are prominent in glomerular diseases and recent interventions address modifying/degrading the early components (IgG, IgA) of the inflammatory cascade.

Altering IgG crystallizable fragment (Fc) glycosylation, is an encouraging approach [54]. The heavy chain constant region Fc consists of CH2 and CH3 domains which carry its key functions [55]. CH2 domain contains the binding sites for C1q of the classical complement pathway as well as FcgR leukocyte Fc gamma receptors on monocytes or granulocytes. The latter is immensely affected by the presence and the variety of sugar moieties at Asn^{297} (asparagine) of CH2 domain [56]. This idea was developed by imitating how *Streptococcal pyogenes* escape the immune response by secreting the endoglycosidase S (EndoS) to resolve the sugar moieties from the N-glycan core on all IgG [57]. Recombinant EndoS was able to hydrolyze glycans of circulating IgG in animals and showed efficiency against ANCA MPO vasculitis [58].

IgG sialylation is an alternative model for IgG engineering that engages the binding of alpha2,6 sialic acid moieties to galactose residues on the core glycan [59]. This idea was derived from administering intravenous immunoglobulin (IVIG) in immune-deficient patients for its anti-inflammatory attributes where IVIG carries fully sialylated Fc. Engineering in vitro sialylated polyclonal or monoclonal IgG or Fc fragment multimers offers a considerable approach for neutralizing autoantibodies in autoimmune diseases [60-61]. Other studies revealed the possibility of bringing the terminal alpha2,6 sialic acid by an enzyme in the trans-Golgi sialyltransferase ST6GAL1 whose active form is also secreted by hepatocytes [62]. Based on that, fusion proteins consisting of B4GALT1 beta1,4 galactose transferase _to offer the sugar substrate for sialic_ and ST6GAL1 succeeded in sialylation of endogenous IgG deposited in kidneys [63].

IgG degradation is another strategy developed by mimicking the endopeptidase, called IdeS generated also by *Streptococcus pyogenes* [64] to dissociate F(ab')2 and Fc fragments of IgG at the hinge region and inactivate Fc-mediated functions. The treatment is effective, iso-specific for IgG2a and well tolerated. Its administration successfully enabled HLA incompatible kidney transplantation [65] highlighting the promising potential of this approach.

Following the same strategy to address IgA nephropathy, bacterial IgA proteases dissociate IgA similarly at the hinge region and iso-specific to IgA1. The aberrant glycosylated IgA1 in serum was successfully dissolved in human serum which opens a new path to target the prominence IGA1 depositions associated with IGA nephritis [66].

- Based on the fact that IgAN is directed by gut mucosal autoimmunity, a new study evaluated the efficiency of delivering a drug to the terminal ileum in a process called targeted-release formulation (TRF). Budesonide was designed to serve this purpose with less than 10% dose release in the circulation led to reduction in proteinurea for IGAN patients [67].
- Complement is activated by all three classical (C1q binding to Fc of immune globulin), alternative and the mannose binding lectin pathways which coincide at activating C5 component and thus making C5 an appealing target. Eculizumab is the first available high affinity humanized anti-C5 mAb which binds to C5 blocking its cleavage to prothrombotic C5a and the terminal C5b-9 complex [68]. It is of quite importance especially for aHUS patients who show intolerance for plasma fusions but the key limitations are its high cost, the need of intravenous infusions twice a month and the risk of facing terminal complement deficiency infections with encapsulated bacteria particularly *Neisseria meningitides*.

The C5 component normally recruits neutrophils, monocytes, and macrophages via the C5aR [69]. Inhibiting C5 receptor by administering a small antagonist CCX168 orally is a new

approach to suppress ANCA-associated vasculitis (AAV) [70]. The mechanism is derived from using another inhibitor for C1 esterase to block C1q-associated serine proteases C1s and C1r in the classic pathway, the consequent activation of C2, C4 in addition to C3 convertase generation [71].

- Other approaches concentrated on the lectin pathway since mannose binding lectin MBL was observed in many renal diseases like anti-GBM GN, IgA nephritis, MPGN, membranous nephropathy and lupus nephritis [72-73]. Circulating mannose binding lectin (MBL), ficolins and collectins bind to the carbohydrates on bacteria, yeast and other microbes promoting MBL associated serine proteases MASP 1,2 and/or 3 to cleave C4 [74] or directly C3 [72]. OMS721 is a novel MASP2 inhibitor reducing proteinurea in IgAN.
- A novel intervention to reduce the severity of autoimmune disease is the induction of antigen-specific tolerance established after identifying antigen-specific T cells and the possibility of augmentation of inhibitory immune cell populations such as regulatory T cells (Treg) [13] where protective HLA types secure a crucial layer of tolerance through the actions of antigen-specific Treg cells.
- An alternative mechanism to humoral immunity blockage is being tested for clinical application where B cells and plasma cells survival factors and/or a proliferation inducing ligands (APRIL) are to get blocked. Belimumab binding and inhibiting active soluble B cell activating factor (BAFF) is under inspection for clinical use in a variety of diseases, including membranous nephropathy, ANCA-AAV and has been approved in active SLE [75-76].
- Antigen-specific humoral responses and production of high affinity IgG are mediated mainly by the germinal center (GC) which increases in secondary lymphoid organs after antigen activation of T cells and B cells initiating differentiation to $CXCR5^+$ $ICOS^+$ $PD\text{-}1^+$ $CD4^+$ T follicular B helper cells (Tfh) and GC B cells [77-78]. Upon interaction of GC B cells and $CD4^+$ Tfh, a class switch of IgG isotypes is promoted in addition to memory B cell and plasma cell differentiation that yield high affinity IgG [79]. IL-21, a Tfh-

derived cytokine presented in high quantities and leads to GC B cell differentiation and IgG production [80-81] is the main target of immunotherapy. Blocking IL-21 activity by administering IL-21R-Fc fusion protein, anti-IL-21-receptor mAb or anti-IL-21 mAb managed to attenuate IgG autoantibody production and nephritis in murine lupus [82-83].

References

1. Rosenblum MD, Remedios KA, Abbas AK. Mechanisms of human autoimmunity. J. Clin. Invest. 2015; 125: 2228–2233.
2. Shi G, Zhang J, Zhang Z (Jason), Zhang, X. Systemic Autoimmune Diseases. Clinical and Developmental Immunology. 2013; 2013; 1–2.
3. Tecklenborg J, Clayton D, Siebert S, Coley SM. The role of the immune system in kidney disease. Clinical and Experimental Immunology. 2018; 192: 142–150.
4. Ip WKE, Medzhitov R. Macrophages monitor tissue osmolarity and induce inflammatory response through NLRP3 and NLRC4 inflammasome activation. Nat Commun. 2015; 6: 6931.
5. Ghaemi-Oskouie F, Shi Y. The Role of Uric Acid as an Endogenous Danger Signal in Immunity and Inflammation. Curr Rheumatol Rep. 2011; 13: 160–166.
6. Kettritz R. Autoimmunity in kidney diseases. Scandinavian Journal of Clinical and Laboratory Investigation. 2008; 68: 99–103.
7. Gorenjak M. Kidneys and Autoimmune Disease. EJIFCC. 2009; 20: 28–32.
8. Butkowski RJ, Langeveld JP, Wieslander J, Hamilton J, Hudson BG. Localization of the Goodpasture epitope to a novel chain of basement membrane collagen. Journal of Biological Chemistry. 1987; 262: 7874–7877.
9. S Gunwar, PA Bejarano, R Kalluri, JP Langeveld, BJ Wisdom Jr, et al. Alveolar Basement Membrane: Molecular Properties of the Noncollagenous Domain (Hexamer) of Collagen IV and its Reactivity with Goodpasture Autoantibodies. Am J Respir Cell Mol Biol. 1991; 5: 107–112.

10. BG Hudson, R Kalluri, S Gunwar, ME Noelken, M Mariyama, et al. Molecular characteristics of the Goodpasture autoantigen. Kidney International. 1993; 43: 135–139.
11. Vadim Pedchenko, Olga Bondar, Agnes B Fogo, Roberto Vanacore, Paul Voziyan, et al. Molecular Architecture of the Goodpasture Autoantigen in Anti-GBM Nephritis. N Engl J Med. 2010; 363: 343–354.
12. Lerner RA, Glassock RJ, Dixon FJ. The role of anti-glomerular basement membrane antibody in the pathogenesis of human glomerulonephritis. Journal of Experimental Medicine. 1987; 126: 989–1004.
13. Joshua D Ooi, Jan Petersen, Yu H Tan, Megan Huynh, Zoe J Willett, et al. Dominant protection from HLA-linked autoimmunity by antigen-specific regulatory T cells. Nature. 2017; 545: 243–247.
14. Rui Yang, Thomas Hellmark, Juan Zhao, Zhao Cui, Marten Segelmark, et al. Antigen and Epitope Specificity of Anti–Glomerular Basement Membrane Antibodies in Patients with Goodpasture Disease with or without Anti-Neutrophil Cytoplasmic Antibodies. JASN. 2007; 18: 1338–1343.
15. Levy JB, Hammad T, Coulthart A, Dougan T, Pusey CD. Clinical features and outcome of patients with both ANCA and anti-GBM antibodies. Kidney International. 2004; 66: 1535–1540.
16. Abraham Rutgers, Marjan Slot, Pieter van Paassen, Peter van Breda Vriesman, Peter Heeringa, et al. Coexistence of Anti-Glomerular Basement Membrane Antibodies and Myeloperoxidase-ANCAs in Crescentic Glomerulonephritis. American Journal of Kidney Diseases. 2005; 46: 253–262.
17. Sinico RA, Mezzina N, Trezzi B, Ghiggeri G, Radice A. Immunology of membranous nephropathy: from animal models to humans. Clinical and Experimental Immunology. 2016; 183: 157–165.
18. Laurence H Beck Jr, Ramon G B Bonegio, Gérard Lambeau, David M Beck, David W Powell, et al. M-Type Phospholipase A $_2$ Receptor as Target Antigen in Idiopathic Membranous Nephropathy. N Engl J Med. 2009; 361: 11–21.
19. Nicola M Tomas, Laurence H Beck Jr, Catherine Meyer-Schwesinger, Barbara Seitz-Polski, Hong Ma, et al.

Thrombospondin type-1 domain-containing 7A in idiopathic membranous nephropathy. N Engl J Med. 2014; 37: 2277–2287.
20. Neilson EG, Sun MJ, Kelly CJ. Molecular characterization of a major nephritogenic domain in the autoantigen of antitubular basement membrane disease. Proc Natl Acad Sci USA. 1991; 88: 2006–2010.
21. Kalfa TA. Thull JD, Butkowski RJ, Charonis AS. Tubulointerstitial nephritis antigen interacts with laminin and type IVcollagen and promotes cell adhesion. J Biol Chem. 1994; 269: 1654-1659.
22. Bonsib SM. Glomerular Diseases. in Atlas of Medical Renal Pathology. New York: Springer. 2013; 199–259.
23. Francois H, Mariette X. Renal involvement in primary Sjogren syndrome. Nat Rev Nephrol. 2016; 12: 82–93.
24. Singbartl K, Formeck CL, Kellum JA. Kidney-Immune System Crosstalk in AKI. Seminars in Nephrology. 2019; 39: 96–106.
25. Kerjaschki D, Farquhar MG. Identification of a membrane glycoprotein from kidney brush border as the pathogenic antigen of Heymann's nephritis. Proc Natl Acad Sci USA. 1982; 795557-5561.
26. Makker SP, Widstrom R, Huang J. Transcription and translation of gp600 and receptor-associated protein (RAP) in active Heymann nephritis. Am J Pathol. 1995; 146: 1481-1487.
27. Kerjaschki D, Farquhar MG. Immunocytochemical localization of the Heymann nephritis antigen (gp330) in glomerular epithelial cells of normal Lewis rats. J Exp Med. 1983; 157: 667486.
28. Abbate M, Bachinsky DR, McCluskey RT, Brown D. Expression of gp330 and gp330/a-macroglobulin receptor-associated protein in renal tubular differentiation. J Am SOC Nephrol. 1994; 4: 2003-2020.
29. Kurts C, Panzer U, Anders HJ, Rees AJ. The immune system and kidney disease: basic concepts and clinical implications. Nat Rev Immunol. 2013; 13: 738–753.
30. Nangaku M, Couser WG. Mechanisms of immune-deposit formation and the mediation of immune renal injury. Clin Exp Nephrol. 2005; 9: 183–191.

31. Tumlin JA, Madaio MP, Hennigar R. Idiopathic IgA nephropathy: pathogenesis, histopathology, and therapeutic options. Clin J Am Soc Nephrol. 2007; 2: 1054–1061.
32. Galla JH. IgA nephropathy. Kidney International. 1995; 47: 377–387.
33. Zipfel PF, Skerka C. Complement regulators and inhibitory proteins. Nat Rev Immunol. 2009; 9: 729–740.
34. Pickering MC, Cook HT. Translational mini-review series on complement factor H: renal diseases associated with complement factor H: novel insights from humans and animals. Clin Exp Immunol. 2008; 151: 210–230.
35. Berger SP, Daha MR. Complement in glomerular injury. Semin Immunopathol. 2007; 29: 375–384.
36. Walker PD. Dense deposit disease: new insights. Curr Opin Nephrol Hypertens. 2007; 16: 204–212.
37. Perez-Caballero D, Gonzalez-Rubio C, Gallardo ME. Clustering of missense mutations in the C-terminal region of factor H in atypical hemolytic uremic syndrome. Am J Hum Genet. 2001; 68: 478–484.
38. Pickering MC, Cook HT, Warren J. Uncontrolled C3 activation causes membranoproliferative glomerulonephritis in mice deficient in complement factor. Nat Genet. 2008; 31: 424–428.
39. Sinico RA, Cavazzana I, Nuzzo M. Renal involvement in primary antiphospholipid syndrome: retrospective analysis of 160 patients. Clin J Am Soc Nephrol. 2010; 5: 1211–1217.
40. Marcantoni C, Emmanuele C, Scolari F. Renal involvement in primary antiphospholipid syndrome. J Nephrol. 2016; 29: 507–515.
41. Bosch X, Guilabert A, Font J. Antineutrophil cytoplasmic antibodies. Lancet. 2006; 368: 404–418.
42. Weiss SJ. Tissue destruction by neutrophils. N Engl J Med. 1989; 320: 365-376.
43. Campanelli D, Melchior M, Fu Y, Nakata N, Shuman H, et al. Cloning of cDNA for proteinase 3: A serine protease, antibiotic, and autoantigen from human neutrophils. J Exp Med. 1990; 172: 1709-1715.
44. Kallenberg CGM, Brouwer E, Weening JJ, Cohen Tervaert JW. Anti-neutrophil cytoplasmic antibodies: Current

diagnostic and pathophysiological potential. Kidney Int. 1994; 46: 1-15.
45. Kettritz R, Jennette JC, Falk RJ. Crosslinking of ANCAantigens stimulates superoxide release by human neutrophils. J Am Soc Nephrol. 1997; 8: 386–394.
46. Ben-Smith A, Dove SK, Martin A, Wakelam MJ, Savage CO. Antineutrophil cytoplasm autoantibodies from patients with systemic vasculitis activate neutrophils through distinct signaling cascades: comparison with conventional Fcgamma receptor ligation. Blood. 2001; 98: 1448–1455.
47. Kettritz R, Choi M, Butt W, Madhavi Rane, Susanne Rolle, et al. Phosphatidylinositol 3- kinase controls antineutrophil cytoplasmic antibodies-induced respiratory burst in human neutrophils. J Am Soc Nephrol. 2002; 13: 1740–1749.
48. Leung N, Bridoux F, Hutchison CA, Samih H Nasr, Paul Cockwell, et al. Monoclonal gammopathy of renal significance: when MGUS is no longer undetermined or insignificant. Blood. 2012; 120: 4292–4295.
49. Al Hussain T, Hussein MH, Al Mana H, Akthar M. Renal involvement in monoclonal gammopathy. Adv Anat Pathol. 2015; 22: 121–134.
50. Frank Bridoux, Nelson Leung, Colin A Hutchison, Guy Touchard, Sanjeev Sethi, et al. Diagnosis of monoclonal gammopathy of renal significance. Kidney Int. 2015; 87: 698–711.
51. Kirsten De Groot, Niels Rasmussen, Paul A Bacon, Jan Willem Cohen Tervaert, Conleth Feighery, et al. Randomized trial of cyclophosphamide versus methotrexate for induction of remission in early systemic antineutrophil cytoplasmic antibody-associated vasculitis. Arthritis Rheum. 2005; 52: 2461–2469.
52. Ponticelli C, Locatelli F. Glucocorticoids in the Treatment of Glomerular Diseases: Pitfalls and Pearls. Clin J Am Soc Nephrol. 2018; 13: 815–822.
53. Jefferson JA. Complications of Immunosuppression in Glomerular Disease. Clin J Am Soc Nephrol. 2018; 13: 1264–1275.
54. Yusuke Mimura, Toshihiko Katoh, Radka Saldova, Roisin O'Flaherty, Tomonori Izumi, et al. Glycosylation engineering

of therapeutic IgG antibodies: challenges for the safety, functionality and efficacy. Protein Cell. 2018; 9: 47–62.
55. Schroeder HW, Cavacini L. Structure and function of immunoglobulins. J Allergy Clin Immunol. 2010; 125: S41-52.
56. Radaev S, Sun PD. Recognition of IgG by Fcgamma receptor. The role of Fc glycosylation and the binding of peptide inhibitors. J Biol Chem. 2001; 276: 16478–16483.
57. Collin M, Olsén A. EndoS, a novel secreted protein from Streptococcus pyogenes with endoglycosidase activity on human IgG. EMBO J. 2001; 20: 3046–3055.
58. Mirjan M van Timmeren, Betty S van der Veen, Coen A Stegeman, Arjen H Petersen, Thomas Hellmark, et al. IgG glycan hydrolysis attenuates ANCA-mediated glomerulonephritis. J Am Soc Nephrol. 2010; 21: 1103–1114.
59. Kaneko Y, Nimmerjahn F, Ravetch JV. Anti-inflammatory activity of immunoglobulin G resulting from Fc sialylation. Science. 2006; 313: 670–673.
60. Zuercher AW, Spirig R, Baz Morelli A, Käsermann F. IVIG in autoimmune disease - Potential next generation biologics. Autoimmun Rev. 2016; 15: 781–785.
61. Blundell PA, Le NPL, Allen J, Watanabe Y, Pleass RJ. Engineering the fragment crystallizable (Fc) region of human IgG1 multimers and monomers to fine-tune interactions with sialic acid-dependent receptors. Journal of Biological Chemistry. 2017; 292: 12994–13007.
62. Lu Meng, Farhad Forouhar, David Thieker, Zhongwei Gao, Annapoorani Ramiah, et al. Enzymatic basis for N-glycan sialylation: structure of rat α2,6-sialyltransferase (ST6GAL1) reveals conserved and unique features for glycan sialylation. J Biol Chem. 2013; 288: 34680–34698.
63. Pagan JD, Kitaoka M, Anthony RM. Engineered Sialylation of Pathogenic Antibodies In Vivo Attenuates Autoimmune Disease. Cell. 2018; 172: 564-577.e13.
64. von Pawel-Rammingen U, Johansson BP, Björck L. IdeS, a novel streptococcal cysteine proteinase with unique specificity for immunoglobulin G. EMBO J. 2002; 21: 1607–1615.

65. IgG Endopeptidase in Highly Sensitized Patients Undergoing Transplantation. N Engl J Med. 2017; 377: 1692–1694.
66. Li Wang, Xueying Li, Hongchun Shen, Nan Mao, Honglian Wang, et al. Bacterial IgA protease-mediated degradation of agIgA1 and agIgA1 immune complexes as a potential therapy for IgA Nephropathy. Sci Rep. 2016; 6: 30964.
67. Bengt C Fellström, Jonathan Barratt, Heather Cook, Rosanna Coppo, John Feehally, et al. Targeted-release budesonide versus placebo in patients with IgA nephropathy (NEFIGAN): a double-blind, randomised, placebo-controlled phase 2b trial. Lancet. 2017; 389: 2117–2127.
68. Rother RP, Rollins SA, Mojcik CF, Brodsky RA, Bell L. Discovery and development of the complement inhibitor eculizumab for the treatment of paroxysmal nocturnal hemoglobinuria. Nat Biotechnol. 2007; 25: 1256–1264.
69. Snyderman R, Phillips JK, Mergenhagen SE. Biological activity of complement in vivo. Journal of Experimental Medicine. 1971; 134: 1131–1143.
70. Hong Xiao, Daniel J Dairaghi, Jay P Powers, Linda S Ertl, Trageen Baumgart, et al. C5a receptor (CD88) blockade protects against MPO-ANCA GN. J Am Soc Nephrol. 2014; 25: 225–231.
71. M Cicardi, K Bork, T Caballero, T Craig, HH Li, et al. Evidence-based recommendations for the therapeutic management of angioedema owing to hereditary C1 inhibitor deficiency: consensus report of an International Working Group: HAE consensus report. Allergy. 2012; 67: 147–157.
72. Lhotta K, Würzner R, König P. Glomerular deposition of mannose-binding lectin in human glomerulonephritis. Nephrol Dial Transplant. 1999; 14: 881–886.
73. M Matsuda, K Shikata, J Wada, H Sugimoto, Y Shikata, et al. Deposition of Mannan Binding Protein and Mannan Binding Protein-Mediated Complement Activation in the Glomeruli of Patients with IgA Nephropathy. Nephron. 1998; 80: 408–413.
74. Matsushita M, Fujita T. Cleavage of the third component of complement (C3) by mannose-binding protein-associated serine protease (MASP) with subsequent complement activation. Immunobiology. 1995; 194: 443–448.

75. Schrezenmeier E, Jayne D, Dörner T. Targeting B Cells and Plasma Cells in Glomerular Diseases: Translational Perspectives. J Am Soc Nephrol. 2018; 29: 741–758.
76. Samy E, Wax S, Huard B, Hess H, Schneider P. Targeting BAFF and APRIL in systemic lupus erythematosus and other antibody-associated diseases. International Reviews of Immunology. 2017; 36: 3–19.
77. Victora GD, Nussenzweig MC. Germinal centers. Annu Rev Immunol. 2012; 30: 429–457.
78. Oliver M Steinmetz, Joachim Velden, Ursula Kneissler, Marlies Marx, Antje Klein, et al. Analysis and classification of B-cell infiltrates in lupus and ANCA-associated nephritis. Kidney International. 2008; 74: 448–457.
79. Lin Yan, Kitty de Leur, Rudi W Hendriks, Luc J W van der Laan, Yunying Shi, et al. T Follicular Helper Cells As a New Target for Immunosuppressive Therapies. Front Immunol. 2017; 8: 1510.
80. Vanessa L Bryant, Cindy S Ma, Danielle T Avery, Ying Li, Kim L Good, et al. Cytokine-mediated regulation of human B cell differentiation into Ig-secreting cells: predominant role of IL-21 produced by CXCR5+ T follicular helper cells. J Immunol. 2007; 179: 8180–8190.
81. Gensous N, Schmitt N, Richez C, Ueno H, Blanco PT. follicular helper cells, interleukin-21 and systemic lupus erythematosus. Rheumatology kew. 2016; 297.
82. Deborah Herber, Thomas P Brown, Spencer Liang, Deborah A Young, Mary Collins, et al. IL-21 Has a Pathogenic Role in a Lupus-Prone Mouse Model and Its Blockade with IL-21R.Fc Reduces Disease Progression. J Immunol. 2017; 178: 3822–3830.
83. Ming Zhang, Gang Yu, Brian Chan, Joshua T Pearson, Palaniswami Rathanaswami,et al. Interleukin-21 Receptor Blockade Inhibits Secondary Humoral Responses and Halts the Progression of Preestablished Disease in the (NZB × NZW)F1 Systemic Lupus Erythematosus Model: IL-21R blockade inhibits secondary responses and preestablished inflammation. Arthritis & Rheumatology. 2015; 67: 2723–2731.

Book Chapter

The Invadopodial Protein CRP2 in Breast Cancer: Molecular Pathology and Therapeutic Perspectives

Hady AL SHAMI[1#] and Fatima J BERRO[2#*]

[1]30, Faculté des Sciences de Montpellier, Place E. Bataillon, 34095 Montpellier, France
[2]Department of Earth and Life Sciences, Faculty of Sciences, Lebanese University, Beirut, Lebanon

[#]These authors contributed equally to this work.

***Corresponding Author:** Fatima J. Berro, Department of Earth and Life Sciences, Faculty of Sciences, Lebanese University, Beirut, Lebanon

Published **December 13, 2022**

How to cite this book chapter: Hady AL SHAMI, Fatima J BERRO. The Invadopodial Protein CRP2 in Breast Cancer: Molecular Pathology and Therapeutic Perspectives. In: Hussein Fayyad Kazan, editor. Immunology and Cancer Biology. Hyderabad, India: Vide Leaf. 2022.

Introduction

Cancer is an increasingly challenging global health concern. Out of the most commonly diagnosed cancer types in 2022, breast cancer, lung cancer and colorectal cancer account for 52 % of all

recent diagnoses in women in the United States. Breast cancer accounts for almost the third [1].

Breast cancer is still ahead of all causes of cancer-related deaths in women [2] despite the early diagnostic strategies and the refinement in treatment concepts [3,4]. This goes back to the fact that patients may eventually experience distant recurrence of the disease; a process called Metastasis [5]. Metastasis contributes to 90% of deaths from breast cancer, and no efficient treatment modality exists at the moment that can suppress or even prevent metastasis. As a consequence, a further investigation of the processes by which cancer cells leave the primary site of the tumor and spread to distant organs can likely lead to the development of tailored treatment options as well as the identification of novel prognostic biomarkers [6].

Activating invasion is an early step in the metastatic cascade where primary cancer cells breach the surrounding tissues (epithelial basement membrane and stromal connective tissue) and join the circulatory or the lymphatic system to facilitate their spread and colonization within the body [7,8]. In breast cancer like many other cancer types (melanoma, head & neck and prostate cancers) cancer cells form specialized membrane protrusions known as invadopodia to invade tissue barriers [9]. Invadopodia, first described by Chen in 1989, are rosette-like structures that develop at the basal surface of cancer cells and are active sites for extracellular matrix degradation [10].

Invadopodia, similar to podosomes in normal cells [11], are actin-based protrusions and "hotspots" where proteolytic, cytoskeletal and adhesion proteins converge with key signaling pathways [12]. Structurally, invadopodia are composed of a dense F-actin core surrounded by a protein ring [13]. The F-actin core consists of actin filaments assembled into thick bundles by actin-bundling proteins such as neural Wiskott–Aldrich syndrome protein (N-WASp), actin-related protein 2/3 (Arp2/3) complex, cofilin and cortactin around which a ring of adhesive and scaffolding molecules like integrins, vinculin, and phosphorylated paxillin is formed [13-18]. In addition to that, many signaling molecules synergize to promote invadopodia

formation such as Src family kinases, tyrosine kinase adaptor proteins, phosphatidylinositol, and small GTPases like cdc42 [19]. Invadopodia also constitute a repertoire of secreted and membrane-tethered matrix metalloproteases (MMPs), ADAM family members, the urokinase plasminogen activator receptor (uPAR) and membrane-bound serine proteases [20].

Cysteine and Glycine-Rich Protein 2 (CRP2) is a two-zinc binding LIM domain-containing protein that belongs to the cysteine-rich protein (CRP) family, a family of evolutionarily conserved proteins that mediate protein–protein interactions and are essential for cytoskeletal remodeling, development and transcription control [21]. In metastatic breast cancer, CRP2 is highly expressed, and it localizes along the protrusive actin core of formed invadopodium contributing to the invasiveness of breast cancer cells and to their spread to distant regions within the body [22]. In this review, we will be discussing the role of CRP2 in the human body and in specifically in breast cancer as an invadopodia actin bundling factor in addition to the possible therapeutic possibilities it offers.

CRP2, a Molecular Definition

CRP2 at Gene Level

CSRP2, the gene encoding the LIM domain protein CRP2, belongs to the *CSRP* multigene family. The three genes in this family were independently isolated: *CSRP1* gene was originally identified in human [23], CSRP2 in quail [24], and CSRP3 in rat and chicken [25]. In 1997, Weiskirchen et al. isolated the human CSRP2 (hCSRP2) homolog and determined its entire structural organization; hCSRP2 was mapped to the long arm of chromosome 12 (12q21.1) spanning a total of approximately 22 kb and consisting of six exons of which exons 2–6 defining the coding region of the gene. CSRP2P, a CSRP2-related pseudogene, was also identified and mapped to 3q21.1. hCSRP2 cDNA clone predicted the 193-amino-acid CRP2 protein that shared 96.4% amino acid sequence similarity with its avian homolog [26]. Additionally, CRP2 shares a high sequence identity with CRP1 and CRP3 but has a different spatial and

temporal expression pattern depending on the type of the tissue under consideration [27].

CRP2 at Protein Level

i. CRP2 as a LIM domain containing protein:

CRP2, a cysteine rich protein, belongs to the class of LIM domain proteins that have two tandemly arranged LIM domains, each linked to a short glycine-rich region but lack classical DNA-binding homeodomains [28,29]. A LIM domain (Linl-1, Isl-1 and Mec-3) is 50–60 amino acids in size and has two characteristic zinc finger domains which are separated by two amino acids [30]. Zinc fingers usually function as DNA binding sites, but research has shown that in the case of LIM domains, the zinc fingers function as sites for protein-protein interactions [30].

ii. CRP2 as an actin cytoskeleton binding and bundling protein

CRP2 is found to be present in both the nucleus and the cytoplasm. In the cytoplasm, CRP2 is associated with the actin cytoskeleton where it interacts with F-actin via its N-terminal LIM domain and glycine-rich region facilitating actin polymerization, crosslinking and clustering [31].

Furthermore, numerous actin-binding proteins, such as α-actinin and filamin, regulate the superstructure of F-actin where they form a variety of actin structures including meshworks and networks of thick bundles. Of these actin-binding proteins, CRP2 associates with α-actinin where a study showed that both molecules have close but different interacting positions with F-actin allowing them to act cooperatively to bundle and crosslink actin filaments [31].

iii. CRP2 as a regulator of the cytoarchitecture and migration of vascular smooth muscle cells:

Among the different CRPs, CRP2 is expressed mainly in vascular smooth muscle cells where, in addition to cytoplasmic roles, CRP2 has been reported to form complexes with serum response factor SRF and GATA transcription factors in the nucleus to facilitate vascular smooth muscle cell differentiation [32]. Normally, vascular smooth muscle cells exhibit a quiescent and differentiated phenotype and express proteins involved in the contractile functions such as smooth muscle α-actin, but after an

arterial injury, these cells de-differentiate and downregulate smooth muscle marker genes changing to a proliferative and migratory phenotype to manage the injury [33]. Studies showed that balloon or wire artery injury reduces CRP2 expression, and the lack of CRP2 enhanced vascular smooth muscle cell migration suggesting a critical role for CRP2 in the migration of vascular smooth muscle cells [34,35].

CRP2 and Human Cancers

CRP2 has been shown to play a role in the progression of various types of cancer. In hepatocarcinogenesis, early-stage hepatocellular carcinoma forms small nodules consisting of well-differentiated cancerous tissues. These tissues may occasionally give rise to less differentiated cancerous tissues within the well-differentiated tumor during its progression. Studies show that the upregulation of CRP2 is related to this dedifferentiation of hepatocellular carcinoma [36].

Another study proved that CRP2 is a downstream target of miR-27a which is a microRNA released by gastric cancer cells in exosomes. CRP2 expression is inversely proportional to that of miR-27a in gastric cancer and its downregulation can transform normal fibroblasts into cancer associated fibroblasts which accelerate the progression of the gastric cancer [37].

In colorectal cancer, the overexpression of CRP2 increased the levels of E-cadherin and decreased that of vimentin, β-catenin, and N-cadherin. This means that CRP2 inhibits epithelial-to-mesenchymal transition in these cells which is an important process in cancer invasion and metastasis. Thus, CRP2 has the potential to suppress the invasion and migration of colorectal cancer cells [38].

One study indicates that the knockdown of CRP2 promotes proliferation and cell cycle progression as well as drug resistance in acute myeloid leukemia (AML) cell lines. This knockdown promoted proliferation and cell cycle progression through the regulation of the AKT and CREB pathways. In addition to that, low CRP2 levels were correlated with a relatively higher

cumulative incidence of relapse rate and worse relapse-free survival rate in adults with AML [39].

CRP2 and Breast Cancer

Clinical Relevance of CRP2 in Human Breast Cancer

CRP2's function in crosslinking actin filaments suggests that it contributes to the assembly of the actin-based invadopodia. CRP2 knockdown significantly inhibits invadopodium formation in aggressive breast cancer cells supports that claim [40]. As proof of clinical relevance to human breast cancer, microarray data identified CRP2 in a cluster of 14 upregulated genes characteristic of the highly aggressive basal-like breast carcinoma subtype [41].

Expression and Regulation of CRP2 in Human Breast Cancer Cell Lines

Hypoxia is a common feature of solid tumors and the hypoxic tumor microenvironment is a strong driver of tumor aggressiveness and metastasis, and is highly associated with poor clinical outcomes in various cancers [42]. Hypoxia has recently been reported to promote the formation of the actin-rich membrane protrusions, invadopodia [43]. Furthermore, cis-regulatory elements, termed hypoxia responsive elements (HRE1 and HRE2) where identified two high-confidence HREs in the proximal promoter region of the gene coding for CRP2 [40]. These HREs are binding sites for HIF-1α which is activated by tumor cells in hypoxic conditions [44]. A study showed the effects of hypoxia on the expression of CRP2 in four breast cancer cell lines, including weakly invasive luminal/epithelial-like MCF-7 and T47D (ER+, PR+), and invasive mesenchymal-like MDA-MB-231 and Hs578T (ER−, PR−, HER2−, claudin-low) [40].

i. In normoxic conditions: CRP2 was expressed at significant levels in mesenchymal-like cells whereas it was absent or only weakly expressed in epithelial-like cells. In addition, invasive cells exhibited detectable amounts of HIF-1α under normoxia. This can be attributed to LINK-A37which works

on the stabilization of HIF-1α and activation of HIF-1 signaling in invasive breast cancer cells. This pathway may explain, at least to some extent, the normoxic expression of CSRP2 [40].

ii. In hypoxic conditions: there was a significant up-regulation of CSRP2 in all four cell lines with CRP2 protein levels increased by about ten times in epithelial-like cells and by about five times in mesenchymal-like cells, as compared to the respective normoxic conditions. Additionally, there was a significant and dramatic increase (>12 fold) in HIF-1α occupancy to both HREs compared to normoxic conditions [40]. Figure 1 shows the results from the study where HIF-1α and CRP2 levels were elevated in hypoxic conditions [40].

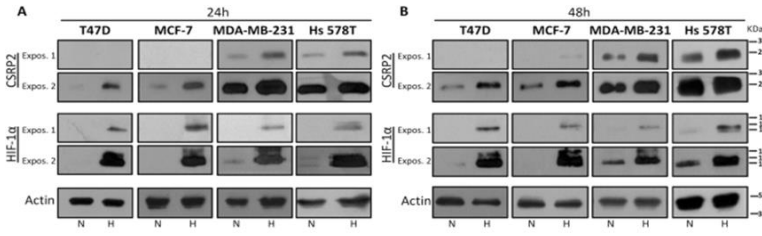

Figure 1: Western blot analysis of CSRP2 and HIF-1α protein levels in the 4 human breast cancer cells (T47D, MCF-7, MDA-MB-231, HS-578T) cultured for 24 h (A) or 48 h (B) in normoxic (N) or hypoxic (H) conditions. Short and long exposures for CSRP2 and HIF-1α blots are shown to better appreciate the differences between the cell lines ("Expos. 1" and "2", respectively) [40].

CRP2 Enhances the Metastatic Phenotype of Breast Cancer Cells by promoting the Biogenesis of Invadopodia

Invadopodia biogenesis largely relies on cytoskeletal rearrangements which are managed by a combination of lamellipodial and filopodial actin machineries [45]. The assembly of an actin core by the ARP2/3 complex and its associated regulators, such as N-WASP and cortactin, is a crucial step of invadopodium initiation. Invadopodium elongation is then promoted by the expansion of the actin core in both branched networks and unbranched bundles [16]. In the core,

actin filaments are cross-linked in thick bundles, which presumably focus actin polymerization-promoted force for protrusive activity, and stabilize invadopodia over long periods to optimize extracellular matrix degradation by metalloproteinases (MMPs) [22].

CRP2, being an actin -binding protein, plays a key role in invadopodia biogenesis where it can change actin polymerization from a randomly organized meshwork of fine actin filaments into reticulated network of thick and long actin bundles [22]. CRP2 has also been proven to localize with the actin fibers in the invadopodia of breast cancer [22].

In invasive breast cancer, hypoxia promoted invadopodia-mediated extracellular matrix degradation where studies showed that the percentage of active cells associated with local ECM degradation increased from about 50% in normoxia to about 70% in hypoxia. Additionally, hypoxia induced a 5-fold increase in the average surface of matrix degradation [40]. The stimulatory effects of hypoxia were inhibited by CSRP2 knockdown which decreased the percentage of active cells, the degradation index and the number of invadopodia per cell to values similar to those obtained for control cells in normoxia [40]. In support of this, the invasiveness of HIF-1α depleted invasive breast cancer cells was increased by CSRP2 forced expression under hypoxia [40].

Furthermore, even though weakly invasive breast cancer cells fail to promote extracellular matrix degradation, they were able to give rise to invadopodia precursors through CRP2 in hypoxic conditions [40].

CRP2 Transcriptionally Activates Pro-Metastatic Matrix Metalloproteinases (MMPs)

Extracellular matrix degradation is primarily mediated by metalloproteinases (MMPs) that are secreted at sites of invadopodia. And among secreted MMPs, the gelatinases MMP-2 and MMP-9 are repeatedly associated with breast cancer progression [22]. Invasive breast cancer cells, which secrete low

basal levels of MMP-2 and MMP-9, have been shown to respond to phorbol 12-myristate 13-acetate (PMA) by secreting MMP-9 [46]. Membrane type-1 MMP (MT1-MMP) is a membrane-tethered MMP that catalyzes MMP-2 activation by cleavage of its pro-domain34, and that MMP-2 contributes to MMP-9 activation [47]. In weakly invasive breast cancer which lacks MT1-MMP and can't perform extracellular matrix degradation, CRP2 gave rise to invadopodium precursors in hypoxic conditions with increased secretion of mostly inactive, high-molecular weight, forms of MMP-2 and MMP-9 suggesting that, although proteolytically inactive, these invadopodium precursors are mature enough for MMP secretion [40].

CRP2 as a Therapeutic Target in Breast Cancer

Use of MMPs Inhibitors: Failed in Clinical Trials

The extracellular matrix-degrading activities of MMPs in metastatic disease, especially in highly aggressive late-stage tumors with poor clinical outcome, made them an attractive cancer treatment target [48]. Preclinical studies testing the efficacy of MMP suppression in tumor models were so compelling that synthetic metalloproteinase inhibitors (MPIs) were rapidly developed and routed into human clinical trials [49].

Early phase I clinical trials revealed that prolonged treatment with MPIs caused musculoskeletal pain and inflammation, complications not seen in preclinical models. These side effects were reversible after taking breaks from the medication but they limited MPI dosages administered in subsequent trials [49].

Phase II trials which are designed to examine efficacy were problematic as well, since MPIs are not cytotoxic (cells are killed) but rather cytostatic (cells are growth-arrested but viable). This meant that conventional measures of efficacy such as reduction in tumor size could not be used to monitor drug activity [49]. As a consequence of these and other issues, phase I trials were followed immediately by phase II/III combination trials without the benefit of efficacy information from smaller studies [49].

Phase III trials are large-scale studies that evaluate efficacy in comparison to standard treatments. These trials examined the efficacy of the MPI alone versus that of cytotoxic drugs and the effect of an MPI, either in combination with or after treatment with cytotoxic drugs, compared with the effect of the cytotoxic drugs alone. The results of these trials have been disappointing and many investigators concluded that MPIs have no therapeutic benefit in human cancer [49].

Targeting Invadopodia as an Alternative for Blocking Breast Cancer Metastasis

The failure of MMP inhibitor-based strategies makes targeting invadopodia an attractive alternative [22]. In this context, CRP2 emerges as a new potential therapeutic target to treat metastatic breast cancers [22]. As mentioned before, studies have shown that CRP2 knockdown inhibits extracellular matrix degradation and MMP-9 expression and inhibits metastatic colonization [22]. In addition, one study found that mice lacking CRP2 are viable, fertile and only exhibit subtle alteration of cardiac ultrastructure [34]. This means that it is possible that targeting CRP2 in patients would only cause minor side effects [22].

References

1. RL Siegel, KD Miller, HE Fuchs, A Jemal. Cancer statistics, 2022, CA. Cancer J. Clin. 2022; 72: 7–33.
2. Overview of breast cancer - PubMed. Available Online at: https://pubmed.ncbi.nlm.nih.gov/31513033/
3. P Kumar, R Aggarwal. An overview of triple-negative breast cancer. Arch. Gynecol. Obstet. 2016; 293: 247–269.
4. L Wilkinson, T Gathani. Understanding breast cancer as a global health concern. Br. J. Radiol. 2022; 95: 20211033.
5. Targeting Breast Cancer Metastasis - Xin Jin, Ping Mu. 2015. Available Online at: https://journals.sagepub.com/doi/full/10.4137/BCBCR.S25460
6. T Meirson, H Gil-Henn. Targeting invadopodia for blocking breast cancer metastasis. Drug Resist. Updat. 2018; 39: 1–17.

7. AW Lambert, DR Pattabiraman, RA Weinberg. Emerging Biological Principles of Metastasis. Cell. 2017; 168: 670–691.
8. WP Schiemann. Introduction to this special issue 'Breast Cancer Metastasis.' J. Cancer Metastasis Treat. 2020; 6.
9. Pathological roles of invadopodia in cancer invasion and metastasis. Available Online at: https://pubmed.ncbi.nlm.nih.gov/22658792/
10. WT Chen. Proteolytic activity of specialized surface protrusions formed at rosette contact sites of transformed cells. J. Exp. Zool. 1989; 251: 167–185.
11. DA Murphy, SA Courtneidge. The 'ins' and 'outs' of podosomes and invadopodia: characteristics, formation and function. Nat. Rev. Mol. Cell Biol. 2011; 12: 413–426.
12. T Saha, H Gil-Henn. Invadopodia, a Kingdom of Non-Receptor Tyrosine Kinases. Cells. 2018; 10: 2037.
13. K Augoff, A Hryniewicz-Jankowska, R Tabola. Invadopodia: clearing the way for cancer cell invasion. Ann. Transl. Med. 2020; 8: 902.
14. O Tolde, D Rösel, P Veselý, P Folk, J Brábek. The structure of invadopodia in a complex 3D environment. Eur. J. Cell Biol. 2010; 89: 674–680.
15. Actin, microtubules, and vimentin intermediate filaments cooperate for elongation of invadopodia. Available Online at: https://pubmed.ncbi.nlm.nih.gov/20421424/
16. S Linder, C Wiesner, M Himmel. Degrading devices: invadosomes in proteolytic cell invasion. Annu. Rev. Cell Dev. Biol. 2011; 27: 185–211.
17. Stefan Linder, Christiane Wiesner. Tools of the trade: podosomes as multipurpose organelles of monocytic cells. Cell. Mol. Life Sci. CMLS. 2015; 72.
18. EK Paterson, SA Courtneidge. Invadosomes are coming: new insights into function and disease relevance. FEBS J. 2018; 285: 8–27.
19. AM Weaver. Invadopodia: Specialized cell structures for cancer invasion. Clin. Exp. Metastasis. 2006; 23: 97–105.
20. S Mrkonjic, O Destaing, C Albiges-Rizo. Mechanotransduction pulls the strings of matrix degradation at invadosome. Matrix Biol. 2017; 57–58: 190–203.

21. R Weiskirchen, K Günther. The CRP/MLP/TLP family of LIM domain proteins: Acting by connecting. BioEssays. 2003; 25: 152–162.
22. Céline Hoffmann, Xianqing Mao, Monika Dieterle, Flora Moreau, Antoun Al Absi, et al. CRP2, a new invadopodia actin bundling factor critically promotes breast cancer cell invasion and metastasis. Oncotarget. 2016; 7: 13688–13705.
23. SA Liebhaber, JG Emery, M Urbanek, X Wang, NE Cooke. Characterization of a human cDNA encoding a widely expressed and highly conserved cysteine-rich protein with an unusual zinc-finger motif. Nucleic Acids Res. 1990; 18: 3871–3879.
24. O002, Oncogene. 1993.
25. S Arber, G Haider. 1-S2.0-0092867494901929-Main. 1994; 79: 221–231.
26. R Weiskirchen, M Erdel, G Utermann, K Bister. Cloning, structural analysis, and chromosomal localization of the human CSRP2 gene encoding the LIM domain protein CRP2. Genomics. 1997; 44: 83–93.
27. HA Louis, JD Pino, KL Schmeichel, P Pomiès, MC Beckerle. Comparison of three members of the cysteine-rich protein family reveals functional conservation and divergent patterns of gene expression. J. Biol. Chem. 1997; 272: 27484–27491.
28. AW Crawford, JD Pino, MC Beckerle. Biochemical and molecular characterization of the chicken cysteine-rich protein, a developmentally regulated LIM-domain protein that is associated with the actin cytoskeleton. J. Cell Biol. 1994; 124: 117–127.
29. MA Karim, K Ohta, M Egashira, Y Jinno, N Niikawa, et al. Human ESP1/CRP2, a member of the LIM domain protein family: characterization of the cDNA and assignment of the gene locus to chromosome 14q32.3. Genomics. 1996; 31: 167–176.
30. Q Zheng, Y Zhao. The diverse biofunctions of LIM domain proteins: determined by subcellular localization and protein-protein interaction. Biol. Cell. 2007; 99: 489–502.
31. T Kihara, Y Sugimoto, S Shinohara, S Takaoka, J Miyake. Cysteine-rich protein 2 accelerates actin filament cluster formation. PloS One. 2017; 12: e0183085.

32. David F Chang, Narasimhaswamy S Belaguli, Dinakar Iyer, Wilmer B Roberts, San-Pin Wu, et al. Cysteine-rich LIM-only proteins CRP1 and CRP2 are potent smooth muscle differentiation cofactors. Dev. Cell. 2003; 4: 107–118.
33. GK Owens, MS Kumar, BR Wamhoff. Molecular regulation of vascular smooth muscle cell differentiation in development and disease. Physiol. Rev. 2004; 84: 767–801.
34. Jiao Wei, Terri E Gorman, Xiaoli Liu, Bonna Ith, Alan Tseng, et al. Increased neointima formation in cysteine-rich protein 2-deficient mice in response to vascular injury. Circ. Res. 2005; 97: 1323–1331.
35. MK Jain, KP Fujita, CM Hsieh, WO Endege, NE Sibinga, et al. Molecular cloning and characterization of SmLIM, a developmentally regulated LIM protein preferentially expressed in aortic smooth muscle cells. J. Biol. Chem. 1996; 271: 10194–10199.
36. Yutaka Midorikawa, Shuichi Tsutsumi, Hirokazu Taniguchi, Masami Ishii, Yuko Kobune, et al. Identification of genes associated with dedifferentiation of hepatocellular carcinoma with expression profiling analysis. Jpn. J. Cancer Res. Gann. 2002; 93: 636–643.
37. Jingya Wang, Xuwen Guan, Yue Zhang, Shaohua Ge, Le Zhang, et al. Exosomal miR-27a Derived from Gastric Cancer Cells Regulates the Transformation of Fibroblasts into Cancer-Associated Fibroblasts. Cell. Physiol. Biochem. Int. J. Exp. Cell. Physiol. Biochem. Pharmacol. 2018; 49: 869–883.
38. Lixia Chen, Xiaoli Long, Shiyu Duan, Xunhua Liu, Jianxiong Chen, et al. CSRP2 suppresses colorectal cancer progression via p130Cas/Rac1 axis-meditated ERK, PAK, and HIPPO signaling pathways. Theranostics. 2020; 10: 11063–11079.
39. Shujuan Wang, Yu Zhang, Yajun Liu, Ruyue Zheng, Zhenzhen Wu,et al. Inhibition of CSRP2 Promotes Leukemia Cell Proliferation and Correlates with Relapse in Adults with Acute Myeloid Leukemia. OncoTargets Ther. 2020; 13: 12549–12560.
40. Céline Hoffmann, Xianqing Mao, Joshua Brown-Clay, Flora Moreau, Antoun Al Absi, et al. Hypoxia promotes breast cancer cell invasion through HIF-1α-mediated up-regulation

of the invadopodial actin bundling protein CSRP2. Sci. Rep. 2018; 8: 10191.
41. Zhiyuan Hu, Cheng Fan, Daniel S Oh, J S Marron, Xiaping He, et al. The molecular portraits of breast tumors are conserved across microarray platforms. BMC Genomics. 2006; 7: 96.
42. DM Gilkes, GL Semenza, D Wirtz. Hypoxia and the extracellular matrix: drivers of tumour metastasis. Nat. Rev. Cancer. 2014; 14: 430–439.
43. CM Gould, SA Courtneidge. Regulation of invadopodia by the tumor microenvironment. Cell Adhes. Migr. 2014; 8: 226–235.
44. GL Semenza. Hypoxia-inducible factors: mediators of cancer progression and targets for cancer therapy. Trends Pharmacol. Sci. 2012; 33: 207–214.
45. C Albiges-Rizo, O Destaing, B Fourcade, E Planus, MR Block. Actin machinery and mechanosensitivity in invadopodia, podosomes and focal adhesions. J. Cell Sci. 2009; 122: 3037–3049.
46. MW Roomi, JC Monterrey, T Kalinovsky, M Rath, A Niedzwiecki. Patterns of MMP-2 and MMP-9 expression in human cancer cell lines. Oncol. Rep. 2009; 21: 1323–1333.
47. M Toth, I Chvyrkova, MM Bernardo, S Hernandez-Barrantes, R Fridman. Pro-MMP-9 activation by the MT1-MMP/MMP-2 axis and MMP-3: role of TIMP-2 and plasma membranes. Biochem. Biophys. Res. Commun. 2003; 308: 386–395.
48. CM Overall, O Kleifeld. Tumour microenvironment - opinion: validating matrix metalloproteinases as drug targets and anti-targets for cancer therapy. Nat. Rev. Cancer. 2006; 6: 227–239.
49. LM Coussens, B Fingleton, LM Matrisian. Matrix metalloproteinase inhibitors and cancer: trials and tribulations. Science. 2002; 295: 2387–2392.

Book Chapter

Gain-of-function Mutant P53 and Metabolomics in Lung Cancer: Novel Biomarkers for Early Detection

Hady AL SHAMI[1#] and Fatima J BERRO[2#]*

[1]30, Faculté des Sciences de Montpellier, Place E. Bataillon, 34095 Montpellier
[2]Department of Earth and Life Sciences, Faculty of Sciences, Lebanese University, Beirut, Lebanon

#These authors contributed equally to this work.

***Corresponding Author:** Fatima J Berro, Department of Earth and Life Sciences, Faculty of Sciences, Lebanese University, Beirut, Lebanon

Published **December 13, 2022**

How to cite this book chapter: Hady AL SHAMI, Fatima J BERRO. Gain-of-function Mutant P53 and Metabolomics in Lung Cancer: Novel Biomarkers for Early Detection. In: Hussein Fayyad Kazan, editor. Immunology and Cancer Biology. Hyderabad, India: Vide Leaf. 2022.

Introduction

According to the World Health organization, Cancer is an umbrella term that describes many diseases that can affect various part of the human body where normal cells transform into tumor cells in a multi-stage process that generally starts with

pre-cancerous lesions that may lead to a malignant tumor [1]. This transformation occurs due to the interaction between a person's genetic factors and external carcinogens which can be physical, chemical or biological [1]. Cancer is a leading cause of death worldwide with nearly 10 million deaths recorded in 2020 [1].

Lung cancer recorded 2.21 million cases in 2020 making it the second most common cancer after breast cancer (2.26 million cases). Even though lung cancer was the second most common cancer type in number of cases, it remains the leading cause of cancer related deaths worldwide with 1.8 million deaths recorded in 2020 alone [1]. Lung cancer has such a high mortality rate since it is often not diagnosed until advanced stages [2]. This is why early diagnosis is considered crucial for a better chance at surviving lung cancer, which mean screening in high-risk communities (e.g, smokers, exposure to fumes, oil fields, toxic occupational places, etc.) in addition to identifying novel biomarkers would prove to be key in combatting this disease [2].

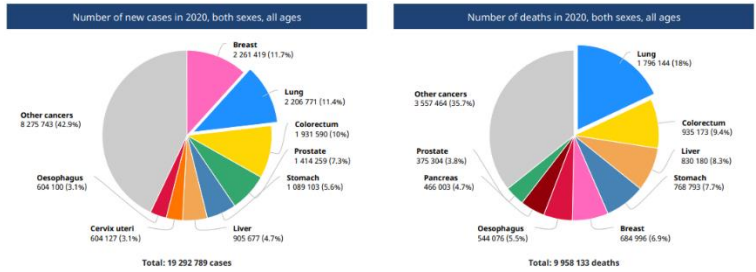

Figure 1: (A) distribution of new cancer cases in 2020 per different types of cancers with Lung cancer coming in second place. (B) Distribution of cancer-related deaths in 2020 with Lung cancer having the most deaths [3].

p53 is a transcription factor, encoded by tumor suppressor gene TP53, also known as "the guardian of the genome". In response to genomic stress, p53 stabilizes in the nucleus, triggering a transcriptional program of cell cycle arrest, DNA repair, senescence, autophagy and apoptosis [4]. The incidence of TP53 mutation in small-cell lung cancer is as high as 75-90% [5]. Mutation inhibits the normal transcriptional activity of p53 [5]. Most of TP53 mutations are point mutations that result from

single base substitutions with some mutations, called hotspots, having an extremely high frequency. In particular, Arg175, Gly245, Arg248, Arg273, and Arg282 in the p53 DNA-binding domain [4]. In this article we will be discussing the malignancy of Lung cancer and current diagnostic tools in addition to novel biomarkers as the future of lung cancer detection. We will also discuss p53 with its mutants as a potential biomarker and an influential factor in lung cancer malignancy.

Classification of Lung Cancer

A vast diversity of morphological appearances and genetic aberrations has been observed within the large group of lung cancers, proving that this is a heterogeneous disease. Hence, lung cancer has been classified into multiple subgroups, with the broadest division made between non-small-cell lung cancer (NSCLC) and small cell lung cancer (SCLC) [6].

Small Cell Lung Cancer (SCLC)

SCLCs are malignant tumors that account for approximately 15% of lung cancers and can be identified through their neuroendocrine features [6]. SCLC has been shown to have the rapid growth and a high tendency to metastasize to distant sites of the body at early stages in the disease. After its diagnosis, SCLC is most commonly classified as either limited stage disease (LD) or extensive stage disease (ED), depending on the absence or presence of distant metastases where around two-thirds of all SCLC patients are diagnosed with ED, with metastases commonly observed in the contralateral lung, liver, brain, and bones [6].

In spite of the late detection of SCLCs, it is shown to have good initial response to chemotherapy and radiotherapy, but this response doesn’t last where almost all patients relapse within 6–12 months with resistant disease [6]. Despite numerous clinical trials aimed to improve the therapeutic management for SCLC, the results didn’t lead to any positive outcomes, and, consequently, treatments have remained largely unchanged for the last 30 years [6].

Non-small Cell Lung Cancer (NSCLC)

NSCLC comprise about 80% to 85% of lung cancers and the main subtypes of are adenocarcinoma, squamous cell carcinoma, and large cell carcinoma. These subtypes, which arise from different cell types are grouped together as NSCLC because their treatment and prognoses are often similar [7]

Adenocarcinoma is the most common type of lung cancer which comprises around 40% of all lung cancers. They develop from small airway epithelial, type II alveolar cells, which secrete mucus and other substances [8]. Adenocarcinoma is the most common type of lung cancer in smokers and nonsmokers in men and women regardless of their age and it tends to occur as peripheral lesions in the lung. They tend to grow slower than other types of lung cancer and have a greater chance of being found before it has spread outside of the lungs [9].

Squamous Cell Carcinoma comprises 25–30% of all lung cancer cases and it arises from early versions of squamous cells in the airway epithelial cells in the bronchial tubes in the center of the lungs. It has been shown that this subtype is strongly correlated with smoking [9].

Large Cell Carcinoma shows no evidence of squamous or glandular maturation and as a result is often diagnosed by default through exclusion of other possibilities. It accounts for 5–10% of lung cancers and often begins in the central part of the lungs, sometimes moving into nearby lymph nodes and into the chest wall as well as distant organs [9].

Other Lung Cancer Types

Apart from the main groups of lung cancer, other types might occur. Lung carcinoid tumors are one type and they account for fewer than 5% of lung tumors. Other types of lung cancer such as adenoid cystic carcinomas, lymphomas, and sarcomas, as well as benign lung tumors such as hamartomas are rare but still might occur. And lastly, some tumors originate outside the respiratory system and then metastasize to the lungs. The last are

not lung cancer but rather another type of cancer that just moved to the lungs [7].

High Mortality Rate of Lung Cancer

In 2018, lung cancer caused an estimated 1.8 million deaths (1.2 million in men and 576,100 in women), accounting for 1 in 5 cancer deaths worldwide, which made lung cancer is the leading cause of cancer death in men and the second-leading cause in women worldwide [10]. This high mortality rate is not attributed to lung cancer being very common but rather because lung cancer is often not diagnosed until the cancer is at an advanced stage where survival rates are dismal [10]. The five-year relative survival rate for all lung cancers (non-small cell lung cancer [NSCLC] and small cell lung cancer combined) is 19% and the five-year survival is higher for non-small cell lung cancer (23%) than small cell lung cancer (6%) [10].

Current Diagnostic Tools for Lung Cancer

Imaging Studies

Many imaging techniques can be used to diagnose and stage lung cancer, and in reality a combination of several imaging tools are used to make an accurate diagnosis [11].

Chest CT is the most common noninvasive tool used for the screening and staging of lung cancer where it is especially useful to define the size, location, and characterization of lung lesions. In addition, a chest CT can assess mediastinal and hilar lymphadenopathy, pleural effusion, and metastasis in the liver, adrenal glands, bone, and other parts of the thoracic cavity [11].

A low-dose chest CT (LDCT) is now being adopted for diagnosing lung cancer as it is able to detect small lung nodules leading to an earlier detection of lung cancer in comparison to a normal chest CT [11].

Positron Emission Tomography-CT (PET) which uses the uptake of the radiolabeled glucose analogue [18F]-fluoro-2-doxyglucose by metabolically active cells, is a useful test for

staging lung cancer and thus deciding a treatment plan [11]. However, in cases of small lesions less than 1 cm in size and in tumors with low metabolic activity, such as in case of carcinoid tumors or bronchioloalveolar cell carcinoma, a false negative result may occur [11]. Additionally, false positives can also occur when inflammatory conditions, such as pneumonia or granulomatous disease, are present [11].

Brain Magnetic Resonance Imaging is used to diagnose brain metastases which are very common with lung cancer. Brain metastases can be detected as an early symptom in approximately 10% of diagnosed patients and associated with significant morbidity and limited survival and their presence is an important consideration in the selection of therapeutic agents and treatment modality [11].

Whole Body Bone Scintigraphy (WBBS) is useful for the detection of bone metastases which develop in approximately 30% to 40% of non-small cell lung cancer (NSCLC) patients leading to poorer prognosis and worsen quality of life during the remaining life [11]. It also has a high false positive rate due to trauma, inflammation and degenerative change of skeletal system and thus, the routine use of WBBS is not recommended by the National Comprehensive Cancer Network guidelines [11].

Biopsy Procedures

Biopsies have become indispensable for the diagnosis of lung cancer by confirming the presence of lung cancer cells and more recently for the selection of appropriate treatment by molecular genetic testing. Several tools for lung tissue biopsy are currently being used for diagnosis and staging of lung cancer, and the selection of the tool takes into account many factors including invasiveness and accuracy in addition to the location and characteristics of the lesion, the general condition of the patient, and the level of experience of the technician performing the examination [11].

Fiberoptic Bronchoscopy (FBS) is used to detect and biopsy lesions in the bronchi and up to the subsegmental bronchus since

FBS has a diameter of 6mm. The size and location, and visibility of lesion are important factors that influence the diagnostic yield as the diagnostic yield for FBS is low ranging from 20% to 60% [11]. A careful review of the patient's anatomy should be performed to determine the bronchial pathway leading to the target lesion and the location where the sampling will be performed [11].

Endobronchial Ultrasound-guided Transbronchial Needle Aspiration (EBUS-TBNA) was introduced to identify mediastinal lymph node metastasis of lung cancer, and is now widely used for the identification and biopsy of central lesions that cannot be reached by FBS. The EBUS-TBNA needle is typically inserted through the wall of the trachea into the mass or the lymph node with real-time ultrasound images being done to confirm the position of the target lesion [11]. The diagnostic yield for EBUS-TBNA is high with a sensitivity of 90% and a negative predictive value of 93% [11].

EBUS using a Guide Sheath is a tool where a radial EBUS probe is used to detect peripheral lung lesions while obtaining the image of radial-type EBUS using a guide sheath. Biopsy forceps and bronchial brushes can be placed using the guide sheath [11]. This method is superior to FBS or EBUS since it allows accessing small peripheral lung lesions. Until recently, the diagnostic yield and safety of EBUS-GS have not been fully evaluated, but a larger number of studies have now shown the good diagnostic yield of this tool and confirmed that it is a well-tolerated procedure [11].

Navigation Bronchoscopy is generally adopted for small peripheral lung lesions to increase diagnostic accuracy. This technique includes three stages where a CT scan is reconstructed and a virtual road map to the target is created as a first step. In the second step, an electromagnetic field is created around the body using sensors to overlap the virtual and the actual body which allows the navigation of the probe to guide it to the target site [11]. The diagnostic yield of this method has been found to range from 33% to 97% with an incidence of pneumothorax as the most frequent complication [11].

Transthoracic Needle Aspiration Biopsy with CT Guidance (CT-NAB) is one of the most commonly used tools to secure lung tissue, and its diagnostic yield is dependent on the size of the target lung lesion with lung nodules over 1 to 2 cm in size being good candidates for CT-NAB [11]. The diagnostic yield for CT-NAB ranged from 77% to 94%, but this technique is invasive and is associated with a risk of complications including pneumothorax and bleeding [11].

Gun Biopsy is one type of CT-NAB that uses automated core biopsy needles with a biopsy gun without causing crushing injuries. Specimens obtained from these core biopsies increase the rate of definite benign disease and allow for the characterization of different cell types [11]. The diagnostic yield of core biopsies is superior to that of CT-NAB particularly in benign disease and specimen obtained from core biopsy is more suitable for immunochemical and genetic variation test compared to that from fine needle aspiration which is used in a typical CT-NAB, but it has increased associated risk of complications including pneumothorax and pulmonary hemorrhage [11].

Laboratory Tests

With genomic alterations being an important cause of cancer initiation, growth, and progression, genomic analysis is needed to identify these genomic alterations and various technological advancements in cancer genomic analysis platforms have made that possible [11]. Some examples of genomic alterations that impact the therapeutic response in lung cancer are those that occur in various genetic factors such as EGFR, ALK, and ROS1 which are currently being used as targets for lung cancer treatment. In addition, data regarding mutations in genes such as BRAF, VEGF, KRAS, RET, and MET are also being used for cancer treatment, in addition to immunological markers such as programmed cell death (PD)-1 and PD ligand 1 (PD-L1) [11].

Polymerase Chain Reaction (PCR) based Tests are used to find driver mutations such as EGFR which aid in the diagnosis of lung cancer. This is largely due to PCR allowing us to amplify

large amounts of DNA in vitro. Modified methods, such as PCR-single-strand conformation polymorphism, TaqMan PCR, Cycleave PCR, and PCR-restriction length polymorphism among others are constantly being used and created to reach higher sensitivity than the original PCR technique [11].

Next Generation Sequencing (NGS) based Tests allow the quick decoding of large amounts of genetic information by breaking down a genome into numerous fragments, reading each fragment simultaneously, and finally combining the data obtained using bioinformatics techniques [11]. This is particularly needed in targeted NGS when in-depth reading is required and assay sensitivity is being evaluated. Targeted NGS panels, including those for EGFR, KRAS, BRAF, and MET, are widely used in lung cancer [11]. However, NGS can yield false negatives or positives, and therefore, additional tests such as fluorescence in situ hybridization or immunohistochemistry (IHC) for protein overexpression may improve the patients' diagnosis [11].

Transcriptome Analysis is performed using an RNA sequencing method called microarray, which separates mRNA, converts it into cDNA, and analyses its sequence using NGS. Whole transcriptome profiles can easily be obtained. Bang et al. [12] conducted transcriptome analyses for 10 NSCLC patients which reported that genes related to the cell cycle were highly upregulated in lung cancer. After validating their results with data from Gene Expression Omnibus (GEO) and The Cancer Genome Atlas (TCGA) they found that MFAP4 and AGER genes were significantly downregulated and the SPP1 gene was upregulated in NSCLC, and these genes were significantly associated with poorer prognoses [12].

Immunohistochemistry (IHC) Tests are used in the differential diagnosis of adenocarcinoma and squamous carcinoma; neuroendocrine marker identification; driver mutation assessment, including that for EGFR/ALK/ROS1 and PD-L1/PD-1 expression; and the differential diagnosis of lung cancer and mesothelioma [11].

Biomarkers: An Early Detection Tool

The demand for re-biopsy has been growing with the continuous development of new therapeutic modalities for lung cancer along with the increase in survival rates. Companion diagnostics, including immunochemical, genetic, and transcriptome analyses, for application of lung cancer therapeutic agent are associated with an increasing demand for a large amount of fresh tissue [11]. That said, performing additional invasive tests to obtain these fresh tissue is often not manageable, especially in patients who have experienced relapses during long-term anti-cancer treatment [11]. This is why the use of liquid biopsies like a simple blood draw is given high importance, as it could be used in lung cancer genetic, transcriptomic, and epigenetic screening biomarkers to determine potential high-risk subjects as a preliminary screening before the use of CT. Thus, early diagnostics using biomarkers could diagnose intermediate nodules identified by CT, leading to selecting subjects that need a surgical biopsy and saving others who do not need it [2]. For example, a number of single nucleotide polymorphisms (SNPs) have been proposed in this regard as potential biomarkers of constitutive genomic risk for a given individual which made them the focus of ongoing research when integrated with current clinical-epidemiological risk models for lung cancer [13].

The National Institutes of Health define a biomarker as “a characteristic that is objectively measured and evaluated as an indicator of normal biological processes, pathogenic processes, or pharmacologic responses to a therapeutic intervention” [13]. The benefit of clinical decisions influenced by biomarker true test results must outweigh the harms of decisions based on false positives or negatives. In the risk management setting, a biomarker should minimize harm and expense without leading to an increase in lung cancer deaths [13]. Biomarker performance and accuracy depends on the intended use and current alternatives. A successful biomarker must supersede the current standard of care, be cost effective, welcomed by the community, and eventually demonstrate cancer control if early detection is the goal [13].

Blood-based biomarkers provide an overview of the whole patient body, including the primary tumor, metastatic disease, immune response, and peri-tumoral stroma which makes blood an obvious first choice as the source of biomarker candidates for lung cancer screening [13]. However, sputum, bronchial lavage or aspirate samples, exhaled breath, or airway epithelium sampling are unique to lung and other respiratory tract cancers and can be used as potential sources of alternative biomarkers [13]. Figure 2 describes the different types of biomarkers and examples of each while also showing their phases of development according to a 2019 article [13]. Here are some of the most prominent groups of biomarkers:

Candidates	Biomarker	Target	Phase 1 Discovery, prediction	Phase 2 Assay validation	Phase 3 Retro/longitudinal	Phase 4 Clinical validation*	Phase 5 Clinical utility	References	Trial
SERUM/PLASMA									
Specific proteins/autoantibodies	Three proteins (CEA, CA-125, and CYFRA 21–1) and 1 AAb (NY-ESO-1)	RMS						39	
	Two proteins (LG3BP and C163A) and clinical features	DIPN						57	NCT01752114
	Seven AAbs (p53, NY-ESO-1, CAGE, GBU4-5, SOX2, HsD, and MAGE A4)	RMS						32,34	NCT01700257
		DIPN						37	
	Six proteins (CEA, CA-125, CEA 15-3, SCC, CYFRA 21–1, NSE, and proGRP)	DIPN						105,110	
	Complement fragment C4d	RMS						39	
		DIPN						41	
MiRNA	Ratios among 24 miRNAs	RMS						43,116	NCT02247453
		DIPN							
	Signature of 13 microRNA + 6 for normalization	RMS						117	COSMOS II trial
		DIPN							
	Signature of 2 microRNA	DIPN						118	
DNA methylation	SOX2 and PTGER4 methylation	RMS						119,120	
		DIPN							
Circulating tumor nucleic acids	Circulating tumor DNA; NGS technology	RMS						111	NCT02889978
	Circulating tumor DNA; NGS technology	DIPN						121	
	Circulating tumor DNA; Ion Torrent DNA Sequencing technology	DIPN						122	
	Circulating tumor DNA; TEC-Seq technology	RMS						123	
	Signature of 29 genes (RNA)	DIPN						124	
	ctDNA mutation and proteins (CA-125, CEA, CA19-9, PRL, HGF, OPN, MPO, and TIMP-1)	DIPN						110	
TUMOR/AIRWAY EPITHELIUM									
Chromosome aberrations	Chromosome regions copy number or fusions (FISH)	DIPN						125	
mRNA gene expression classifier	Twenty three gene classifier	DIPN							NCT01309087 NCT00746759
SNPs	12 SNPs for COPD and clinical features	RMS						101,126	
SPUTUM, BREATH AND URINE									
DNA methylation	SHOX2 and RASSF1A methylation	RMS						127	
MiRNA	Signature of 3 microRNA	DIPN						128	
Exhaled breath	VOC- Nanoparticle Biorretic Tagging (NBT)	DIPN							
	VOC- Field Asymmetric Ion Mobility Spectrometry (FAIMS)								NCT02612532
Tumor cells	>700 morphological features (by Cell CT)	RMS							
		DIPN							
	Buccal nanocytology	RMS						129	
	Porphyrin differential uptake by tumor cells	RMS						130	
Urine markers	Metabolites	RMS						93	

Figure 2: Various candidate biomarkers for lung cancer early detection from different origins and their phase of development [13].

Autoantibodies (AAbs) develop in response to an abnormal tumor antigen in some patients with lung cancer, often in the pre-clinical phase well before symptoms appear or imaging-based detection is possible. They have been identified in all histologic types and stages of lung cancer, but autoantibody panels are likely to be specific but not sensitive as they are usually absent or found in low titers in those without cancer, but also in many patients with the disease [13]. In a clinical validation study including all lung cancer histologies and stages the panel performed well with 93% specificity, but only 40% sensitivity

[14]. Autoantibodies may find a place in clinical practice by improving the overall test accuracy of hybrid panels featuring diverse biomarkers [13].

Complement Fragments like C4d which is a downstream split product of the classical complement pathway can be used as a lung cancer biomarker. This is due to lung cancer being able to activate the complement cascade via the classical complement pathway. Concentrations of C4d are increased in biological fluids from lung cancer patients which means testing for C4d levels could allow the early detection of lung cancer [13]. One study was able to link plasma C4d levels to increased lung cancer risk in a cohort of 190 asymptomatic individuals, including 32 patients with screening detected cancer [15].

Circulating MicroRNAs (miRNAs) reflecting tumor-host interactions, have emerged as potential biomarkers for cancer diagnosis and prognosis irrespective of tumor stage and mutational burden. Two studies were able to show that the use of the miRNA signature classifier (MSC) and the miR-Test resulted in a five- and four-fold reduction in the LDCT-false positive rate with comparable specificity (81-75%) and sensitivity (87-78%) [16,17].

Circulating Tumor DNA (ctDNA) is well established as a biomarker in advanced tumor stages, but its role in early lung cancer detection is still uncertain [18]. Abbosh et al. tested 96 stage I-III NSCLC patients and reported 48% overall sensitivity, setting a threshold of 2 single-nucleotide variants (SNVs) where sensitivity ranged from 15% for stage I adenocarcinomas to 100% for stage II-III squamous cell carcinomas [19]. Current efforts to develop NGS technologies in order to study ctDNA in the context of early detection may improve sensitivity in this context [13].

DNA Methylation can be used a biomarker since tumor tissue is characterized by global DNA hypomethylation together with hypermethylation of specific CpG islands in the promoter region of tumor-suppressor genes [13]. A study that performed methylation profiling of 230 tissue samples to learn cancer-

specific methylation patterns achieved a sensitivity of 92.7% and a specificity of 92.8% [20]. Additionally, when they compared the results to 118 samples from normal individuals, the model achieved a specificity of 93.2% [20].

Blood Protein Profiling where measurable serum antigens have been identified in lung cancer patients, and panels of serum cancer antigens have been developed to improve diagnostic accuracy [13]. One panel of 3 serum proteins (CEA, CA-125, CYFRA 21-1) and an autoantibody (NY-ESO-1) performed well in a high-risk cohort with 71% sensitivity and 88% specificity for lung cancer [21]. A clinical validation was later performed in a separate high-risk cohort (based on age and smoking history) and showed lower sensitivity (49%) but higher specificity (96%) [22].

Metabolomics as Biomarkers for Early Detection

Metabolomics aims to perform a comprehensive analysis of all metabolites in a biological system which reveals what exactly takes place inside organisms due to genetic modification, pathophysiologic stimuli, and environmental stress [23]. Endogenous metabolites have a good ability to provide information about physiological functions and pathological status in detail. This allowed metabolomics to become a promising tool in disease biomarker screening, pathological mechanism interpretation, and drug efficacy evaluation [23]. The two main tools for metabolic profiling are NMR spectroscopy and MS where their improved sensitivity and resolution, as well as the construction of efficient and large-scale metabolite annotation databases, have promoted the progress of metabolomics [23]. Current metabolomics studies of lung cancer mainly focus on early-stage detection, the differentiation between subtypes and biomarker discovery, metabolite alterations in different lung cancer stages, mechanism exploration, and the effective therapy evaluation of lung cancer [23].

Metabolic Alteration in Lung Cancer

Previous studies have shown that many metabolic disturbances occur in lung cancer patients. This information is helpful for defining potential biomarkers [23]. Figure 3 shows the main metabolic pathways in lung cancer, including the tricarboxylic acid cycle, glycolysis, fatty acid metabolism, and amino acid metabolism [23]. The findings in these pathways will be described below.

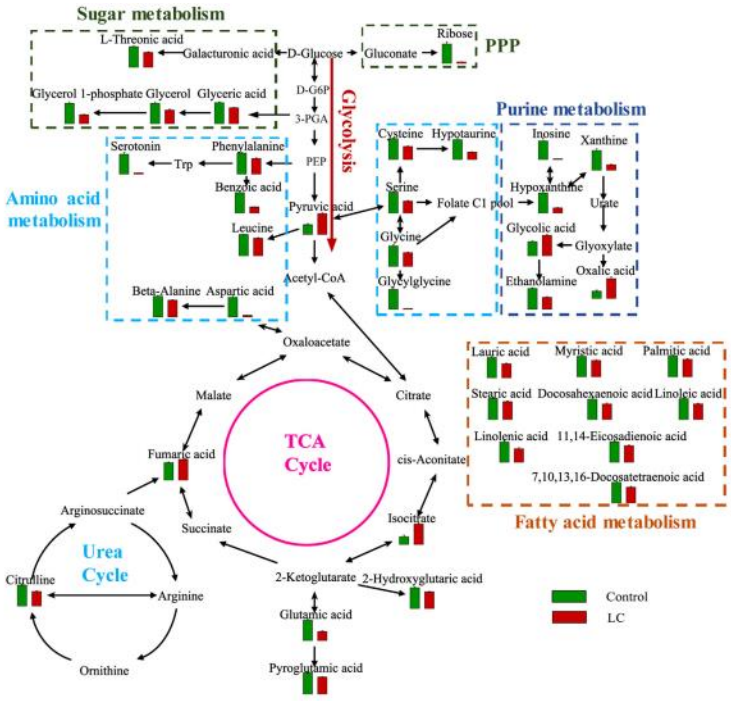

Figure 3: Map of the various pathways in lung cancer with significantly different metabolites[23] (lC: Lung Cancer).

Tricarboxylic Acid (TCA) Cycle and Glycolysis

The TCA cycle and glycolysis are central pathways that provide energy and essential metabolic substrates for cell biosynthesis and maintain redox balance in cells [23]. TCA cycle dysfunction is involved in a wide variety of cancer diseases, one example is

Fan et al. which found that ^{13}C enrichment in lactate, succinate, and citrate was higher in lung tumors, indicating that glycolysis and the TCA cycle were significantly changed in lung tumor tissues [24]. Another study, Davidson et al. performed metabolic flux analysis by using stable isotope tracing of [1,2-13C] glucose and [U-13C] glutamine to investigate whether glucose converts to lactate, and glutamine is the major source of the TCA cycle carbon in cancer tissue as found in cultured cell [25]. Their result showed that glucose converts to lactate and its contribution to the TCA cycle increased in lung cancer, which means that glucose is required for cancer formation. On the other hand, glutamine's utilization was insignificant in both sides. This lead the study to declare that nutrients and environment are very important for the determination of the metabolic phenotype of cancer cells [25].

The quantification of glycolytic metabolites revealed that the overexpression of pyruvate kinase isoform (M2) leads to an accumulation of glycolytic intermediates that are subsequently incorporated into the serine metabolism pathway. This shows that cancer cells offer higher concentrations of phosphoenolpyruvate and 3-phosphoglycerate [23]. In addition, Yang et al. reported that the activity of pyruvate carboxylase was upregulated in lung cancer which meant lung cancer cells have higher glycolysis [23].

Amino Acid Metabolism

Tumor growth and proliferation require fluctuations in amino acid concentrations and their biosynthetic pathways [23]. As proof, an analysis of the metabolome and proteome revealed that glycosylation, glutaminolysis, and polyamine biosynthesis were increased in lung adenocarcinoma [26]. Moreover, cysteine and glutamic acid, which are important components of glutathione, are significantly increased in lung adenocarcinoma compared to control tissue. Additionally, many enzymes related to glutathione biosynthesis, glutathione recycling, heterologous biological metabolism, and redox balance have increased significantly [26]. This would mean that amino acids and their derivatives could serve as candidate biomarkers as these molecules are closely related to disease occurrence [26].

Lipid Metabolism

Lipids include many different types of molecule classes and have many important biological functions including energy production, cell membrane composition and acting as signaling molecules. This means that disrupted lipid metabolism contributes to the occurrence and development of many diseases [23].

Abnormal lipid metabolism has been demonstrated in lung cancer where global lipidomics study was performed on early NSCLC, adenocarcinoma, and SCC patients and healthy controls. Their results suggested that some lipid species, including sphingomyelin, lysophosphatidylcholine (LPC), and fatty acid derivatives, were prominently changed and were associated with lung cancer progression [27]. Moreover, decreased choline levels in serum were observed in lung cancer; this is possibly related to the increased requirements of choline in cancer cells for proliferation due to its role as a building block for membrane phospholipids [28].

Lung cancer pathway analysis showed that the major alteration was in sphingolipid metabolism, and the ROC curve analysis showed that glycerophosphonarachidonoyl ethanolamine and sphingosine could be regarded as potential biomarkers for diagnosis and prognosis in lung cancer [29].

Dramatic alterations in lipid profiles were shown in NSCLC tumors, including increases in phosphatidylethanolamines (PEs) compared to healthy control tissue, which was shown in plasma of malignant nodules [23]. Moreover, the secretion of phosphatidylethanolamine-binding protein increased in lung adenocarcinoma and phosphatidylethanolamine-binding protein was found to be an important factor in the development and metastasis of cancer. PEs were found to be promising biomarkers for differentiation between benign and lung cancer samples [23].

Role of Gain of Function TP53 in Metabolic Regulation in Lung Cancer

The TP53 gene which is located on the short arm of chromosome 17, encodes the tumor suppressor protein p53 and is the most commonly mutated gene in human cancer [30]. Wild-type p53 is a tetrameric transcription factor typically found at very low levels with a short half-life until it is activated in cases such as DNA damage, oncogene activation, hypoxia, oxidative stress, ribonucleotide depletion or nutrient deprivation [30]. The phosphorylation and displacement of its negative regulators MDM2 and MDM4 allows p53 to bind to specific response elements and transcriptionally activate various target genes including CDKN1A, BAX and PUMA, which would lead to cell cycle arrest, senescence, or apoptosis, depending on the cellular context [30]. In addition to these crucial tumor suppressive functions, p53 may also regulate additional cellular processes including inhibiting metabolic reprogramming in cancer cells, promoting autophagy, preventing stem cell self-renewal, limiting accumulation of reactive oxygen species, and tumor microenvironment signaling [30].

The most common somatic mutations in TP53 are single nucleotide missense mutations that allow production of a full-length protein. In addition to losing their tumor suppressive function, some of these mutant p53 proteins can also acquire oncogenic gain-of-function (GOF) properties which include increased invasion, proliferation, and chemoresistance among others [30]. These mutated genes will give rise to mutated p53 proteins where the mutations can either be structural mutations, affecting the folding of the p53 protein, or DNA-contact mutations, which affect the transcriptional activity of p53 and regulation of target genes [31]. In most cases, p53 mutants lose the ability to bind canonical p53 elements leading to the interaction of mutant p53 proteins with non-canonical/different response elements which might induce an oncogenic response and the properties mentioned before [31].

Mutant p53 proteins are able to interact with other transcription factors to induce inhibitory responses such is the case of its

interaction with p63 transcription factors. Mutant p53 is found to interact with various isoforms of p63 thus inhibiting them [31]. Published data reported that mutant p53 increases the ability to develop spontaneous metastasis in mice by inhibiting p63 and p73 functions. This is due to the loss of p63 and/or p73 activities being linked to the development of spontaneous tumors and the capacity of cancer cells to invade other parts of the body [31].

Additionally, Mutant p53 targets other regulatory molecules including microRNAs such as miR-130b, miR-155 and miR-205. The binding of p53 to microRNAs has been associated with altering the stability of those molecules in addition to influencing crucial molecular pathways involved in invasion and metastasis through the modulation of transcripts such as ZEB1 and ZNF652 [31].

Not only do mutant p53 proteins interact with multiple transcription factors, it can also bind and regulate the function of other non-transcription factor proteins. Research showed that mutant p53 disrupts DNA-repair mechanisms by interacting with the DNA nuclease MRE11 [32]. Its interaction with other proteins involved in cell cycle regulation such as BTG2 modulates H-Ras, thereby enhancing oncogenic transformation [33].

Prominent p53 Gain of Function Mutants

As mentioned before, TP53 is highly mutated in cancer patients, and it has been shown that most TP53 mutations are located within the DNA binding domain (96–293 aa) and at several hotspots, such as R175, R248, R273, and R282 [34]. One of the reasons that could explain why there are hotspot mutations in the TP53 gene is that different mutations might have different levels of impact on the function of p53, either by altering the global protein structure or disrupting the p53–DNA interface [34]. Based on the crystal structure of the p53–DNA complex, these hotspots can be classified as contact mutants (R248 and R273) which make direct contact with DNA and structural mutants (R175, G245, R249, and R282) which maintain the structure of

the DNA binding interface [34]. Various hotspots of TP53 mutations will be discussed below:

TP53 R175H Mutant

The R175 hotspot is located at the zinc-binding site of tp53 near the DNA binding interface, which is very important to the maintenance of structural stability, which means that the p53-R175H mutation causes a change in the protein structure creating a defective DNA binding interface. The p53-R175H loses the transactivating function of the wild-type p53 due to this defective interface [34].

However, p53-R175H gains function by many kinds of mechanisms. Reports showed that p53-R175H can bind to some DNA sequences different from the wild-type p53 response element and transactivate those target genes. p53-R175H can also interact with numerous kinds of transcription factors to enhance or suppress the expression of their target genes [34]. In addition to the previous gained functions, p53-R175H has been proved to be more prone to aggregations in comparison to its wild counterpart as it exhibits a larger hydrophobic surface area and higher loop flexibility than the wild p53. This allows p53-R175H to induce coaggregation of wild-type p53 causing loss of function, in addition to inducing coaggregation of p63 and p73 to cause gain-of-functions [34].

P53-R175H has been found to promote tumor cell growth through inducing replication [35]. A study on lung adenocarcinoma has proved that this mutant p53 interacts with Myb, an oncogenic transcription factor, and transactivates replication-initiation-related genes CDC7 and DBF4, promoting the activity of CDC7/DBF4 complex [35]. Chromatin enrichment of replication initiation factors which leads to an increase in origin firing confirm increased CDC7-dependent replication initiation in mutant p53 cells. These findings confirm that high CDC7 expression significantly correlates with p53 mutational status and it predicts poor clinical outcome in lung adenocarcinoma patients [35].

This p53 mutant can also promote tumor migration, invasion, and metastasis [34]. Yeudall et al. reported that in lung cancer, among other cancer types, p53-R175H contribute to cancer cell migration by increasing the expression of several CXC-chemokines which are the inflammatory mediators that contribute to multiple aspects of tumorigenesis. This included CXCL5 which induces cell migration, CXCL8, and CXCL12 [36]. The study also proved that the knockdown of the mutant p53 in lung cancer reduced CXCL5 expression and cell migration [36].

Furthermore, several studies reported that many chemotherapy treatments have progressively become ineffective for patients with TP53 mutations [34]. Scian et al. showed that the overexpression of p53-R175H in p53-null human lung-carcinoma cells allowed the cells to become more resistant to common chemotherapy drug etoposide [37]. This mutant p53s can bind to the promoter of the NF-κB2 gene, which is involved in the antiapoptotic activity of cancer cells, and increase its expression [37]. Another study, Donzelli et al, also found that p53-R175H enhanced the expression of miR128-2 in lung-carcinoma cell lines H1299 and A549 through binding to the promoter of its host gene ARPP21 [38]. miR128-2 is known to inhibit E2F5 expression which in return increases the expression of p21, a E2F5 target gene. This would lead p21 protein to localize to the cytoplasmic compartment, where it exerts an anti-apoptotic effect by preventing pro-caspase-3 cleavage [38]. Therefore, p53-R175H confers lung-carcinoma cell resistance towards chemotherapy drugs doxorubicin, cisplatin, and 5-fluorouracil through the miR128-2/E2F5/p21 axis [34].

Lastly, p53-R175H mutants can also alter the metabolism of lung cancer cells among other cancer types. p53-R175H can induce the translocation of GLUT1 to the cell membrane through increasing the expression of small GTPases RhoA and ROCK, resulting in the stimulation of the Warburg effect, which means that these cancer cells generate energy by using aerobic glycolysis instead of oxidative phosphorylation [39].

TP53 R248Q Mutant

R248 is a mutation hotspot in the DNA binding domain (DBD) of p53, with mutations occurring in about 4% of all cancer patients [40]. This makes R248Q a contact mutation that prevents the proper binding of mutant p53 to its supposed DNA binding sites [34]. The site at which R248 resides is part of p53 that interacts with the small groove of the DNA it binds to, but the R248Q mutation causes changes in parts of DBD far from the mutation site preventing the mutant p53 from interacting with the major groove of DNA causing a loss of function of p53 [40].

Apart from preventing the normal functions of p53, the p53-R248Q mutant has been shown to enhance invasiveness of lung cancer cells [41]. A study compared 2 p53 mutations (R248Q and R248W) and found that they have similar growth activity p53 null lung cancer cells but p53-R248Q proved to promote invasiveness in lung cancer cells [41].

TP53 R273H Mutant

The p53-R273H is also classified as a contact mutant since the mutation occurs in the DNA binding district, this leads to loss of function of p53 as it prevents the mutant p53 from binding to its target genes [34]. In addition to the loss of function, this mutant p53 expression can promote invasion, loss of directionality of migration due to this mutant's ability to promote recycling of integrins and EGFR in a way that is dependent on n Rab-coupling protein [42].

P53-R273H has been shown to have similar actions as the p53-R175H mutant. The first is its ability to promote lung cancer cell growth through inducing the activation of replication-initiation-related genes CDC7 and DBF4 leading to increased CDC7-dependent replication [35]. this mutant p53 have been shown to promote chemoresistance in lung cancer much like the p53-R273H where its overexpression in human lung-carcinoma cells allowed the cells to become more resistant to common chemotherapy drug etoposide [37].

TP53 R282W Mutant

While other hotspots of mutations have been intensively studied, studies concerning p53-R282W have been relatively limited (in this case, R282W designates an arginine mutated to a tryptophan at position 282 in the p53 protein) [43]. P53-R282 is a structural mutant as the position of R282 plays a role in maintaining the structural integrity of the DNA-binding surface [43].

In regards to lung cancer, p53-R282W mutant has been shown to exert drug-resistance function through the proteasome degradation pathway. Normally, wild-type p53 binds to the promoter of proteasome activator gene REGγ recruiting a corepressor SMAD3 to repress its expression but this mutant p53 binds to the promoter of REGγ preventing SMAD3 binding, thus upregulating REGγ expression and causing the degradation of several tumor suppressors including p53, p21, and p16, leading to cell proliferation and drug resistance [44].

Conclusion

Lung cancer has proven to be a highly malignant cancer due to multiple reasons and extensive research is still needed to help introduce new tools and biomarkers that would aid in the early detection of this cancer, decreasing its mortality rate. P53 has also shown the significant role it plays in cancer progression but this would open doors to new tools that can help combat lung cancer by using p53 as a biomarker and target for future therapies.

References

1. Cancer. Available Online at: https://www.who.int/news-room/fact-sheets/detail/cancer.
2. Nooreldeen R, Bach H. Current and Future Development in Lung Cancer Diagnosis. Int. J. Mol. Sci. 2021; 22: 8661.
3. Cancer today. Available Online at: http://gco.iarc.fr/today/home.
4. Seitaro Nakazawa, Ken-Ichiro Sakata, Shanshan Liang, Kazuhito Yoshikawa, Hisashi Iizasa, et al. Dominant-

negative p53 mutant R248Q increases the motile and invasive activities of oral squamous cell carcinoma cells. Biomed. Res. Tokyo Jpn. 2019; 40: 37–49.
5. Xinyu Tang Yang Li Long Liu Rui Guo Ping Zhang, et al. Sirtuin 3 induces apoptosis and necroptosis by regulating mutant p53 expression in small-cell lung cancer. Oncol. Rep. 2020; 43: 591–600.
6. Semenova EA, Nagel R, Berns A. Origins, genetic landscape, and emerging therapies of small cell lung cancer. Genes Dev. 2015; 29: 1447–1462.
7. What Is Lung Cancer? | Types of Lung Cancer. Available Online at: https://www.cancer.org/cancer/lung-cancer/about/what-is.html.
8. Denisenko TV, Budkevich IN, Zhivotovsky B. Cell death-based treatment of lung adenocarcinoma. Cell Death Dis. 2018; 9: 117.
9. Zappa C, Mousa S. A. Non-small cell lung cancer: current treatment and future advances. Transl. Lung Cancer Res. 2016; 5: 288–300.
10. Schabath MB, Cote ML. Cancer Progress and Priorities: Lung Cancer. Cancer Epidemiol. Biomark. Prev. Publ. Am. Assoc. Cancer Res. Cosponsored Am. Soc. Prev. Oncol. 2019; 28: 1563–1579.
11. Park HJ, Lee SH, Chang YS. Recent advances in diagnostic technologies in lung cancer. Korean J. Intern. Med. 2020; 35: 257–268.
12. Man Seok Bang, Keunsoo Kang, Jung-ju Lee, Yea-Jin Lee, Jin Eun Choi, et al. Transcriptome analysis of non-small cell lung cancer and genetically matched adjacent normal tissues identifies novel prognostic marker genes. Genes Genomics. 2017; 39: 277–284.
13. Luis M Seijo, Nir Peled, Daniel Ajona, Mattia Boeri, John K Field, et al. Biomarkers in Lung Cancer Screening: Achievements, Promises, and Challenges. J. Thorac. Oncol. Off. Publ. Int. Assoc. Study Lung Cancer. 2019; 14: 343–357.
14. P Boyle, CJ Chapman, S Holdenrieder, A Murray, C Robertson, et al. Clinical validation of an autoantibody test for lung cancer. Ann. Oncol. 2011; 22: 383–389.

15. Daniel Ajona, María J Pajares, Leticia Corrales, Jose L Perez-Gracia, Jackeline Agorreta, et al. Investigation of complement activation product c4d as a diagnostic and prognostic biomarker for lung cancer. J. Natl. Cancer Inst. 2013; 105: 1385–1393.
16. Francesca Montani, Matteo Jacopo Marzi, Fabio Dezi, Elisa Dama, Rose Mary Carletti, et al. miR-Test: a blood test for lung cancer early detection. J. Natl. Cancer Inst. 2015; 107: djv063.
17. Gabriella Sozzi, Mattia Boeri, Marta Rossi, Carla Verri, Paola Suatoni, et al. Clinical utility of a plasma-based miRNA signature classifier within computed tomography lung cancer screening: a correlative MILD trial study. J. Clin. Oncol. Off. J. Am. Soc. Clin. Oncol. 2014; 32: 768–773.
18. Jason D Merker, Geoffrey R Oxnard, Carolyn Compton, Maximilian Diehn, Patricia Hurley, et al. Circulating Tumor DNA Analysis in Patients With Cancer: American Society of Clinical Oncology and College of American Pathologists Joint Review. J. Clin. Oncol. J. Clin. Oncol. Off. J. Am. Soc. Clin. Oncol. 2018; 36: 1631–1641.
19. Christopher Abbosh, Nicolai J Birkbak, Gareth A Wilson, Mariam Jamal-Hanjani, Tudor Constantin, et al. Phylogenetic ctDNA analysis depicts early-stage lung cancer evolution. Nature. 2017; 545: 446–451.
20. Wenhua Liang, Yue Zhao, Weizhe Huang, Yangbin Gao, Weihong Xu,et al. Non-invasive diagnosis of early-stage lung cancer using high-throughput targeted DNA methylation sequencing of circulating tumor DNA (ctDNA). Theranostics. 2019; 9: 2056–2070.
21. Doseeva V, Colpitts T, Gao G, Woodcock J, Knezevic V. Performance of a multiplexed dual analyte immunoassay for the early detection of non-small cell lung cancer. J. Transl. Med. 2015; 13: 55.
22. Peter J Mazzone, Xiao-Feng Wang, Xiaozhen Han, Humberto Choi, Meredith Seeley, et al. Evaluation of a Serum Lung Cancer Biomarker Panel. Biomark. Insights. 2018; 13: 1177271917751608.

23. Noreldeen HAA, Liu X, Xu G. Metabolomics of lung cancer: Analytical platforms and their applications. J. Sep. Sci. 2020; 43: 120–133.
24. Teresa WM Fan, Andrew N Lane, Richard M Higashi, Mohamed A Farag, Hong Gao, et al. Altered regulation of metabolic pathways in human lung cancer discerned by (13)C stable isotope-resolved metabolomics (SIRM). Mol. Cancer. 2009; 8: 41.
25. Shawn M Davidson, Thales Papagiannakopoulos, Benjamin A Olenchock, Julia E Heyman, Mark A Keibler, et al. Environment Impacts the Metabolic Dependencies of Ras-Driven Non-Small Cell Lung Cancer. Cell Metab. 2016; 23: 517–528.
26. Johannes F Fahrmann, Dmitry D Grapov, Kwanjeera Wanichthanarak, Brian C DeFelice, Michelle R Salemi, et al. Integrated Metabolomics and Proteomics Highlight Altered Nicotinamide- and Polyamine Pathways in Lung Adenocarcinoma. Carcinogenesis. 2017; 38: 271–280.
27. Zongtao Yu, Hankui Chen, Junmei Ai, Yong Zhu, Yan Li, et al. Global lipidomics identified plasma lipids as novel biomarkers for early detection of lung cancer. Oncotarget. 2017; 8: 107899–107906.
28. Leonor Puchades-Carrasco, Eloisa Jantus-Lewintre, Clara Pérez-Rambla, Francisco García-García, Rut Lucas, et al. Serum metabolomic profiling facilitates the non-invasive identification of metabolic biomarkers associated with the onset and progression of non-small cell lung cancer. Oncotarget. 2016; 7: 12904–12916.
29. Yingrong Chen, Zhihong Ma, Lishan Min, Hongwei Li, Bin Wang, et al. Biomarker identification and pathway analysis by serum metabolomics of lung cancer. BioMed Res. Int. 2015; 2015: 183624.
30. Barta JA, Pauley K, Kossenkov AV, McMahon SB. The lung-enriched p53 mutants V157F and R158L/P regulate a gain of function transcriptome in lung cancer. Carcinogenesis. 2020; 41: 67–77.
31. Hany E Marei, Asmaa Althani, Nahla Afifi, Anwarul Hasan, Thomas Caceci, et al. p53 signaling in cancer progression and therapy. Cancer Cell Int. 2021; 21: 703.

32. Song H, Hollstein M, Xu Y. p53 gain-of-function cancer mutants induce genetic instability by inactivating ATM. Nat. Cell Biol. 2007; 9: 573–580.
33. Hilla Solomon, Yosef Buganim, Ira Kogan-Sakin, Leslie Pomeraniec, Yael Assia, et al. Various p53 mutant proteins differently regulate the Ras circuit to induce a cancer-related gene signature. J. Cell Sci. 2012; 125: 3144–3152.
34. Yen-Ting Chiang, Yi-Chung Chien, Yu-Heng Lin, Hui-Hsuan Wu, Dung-Fang Lee, et al. The Function of the Mutant p53-R175H in Cancer. Cancers. 2021; 13: 4088.
35. Arindam Datta, Dishari Ghatak, Sumit Das, Taraswi Banerjee, Anindita Paul, et al. p53 gain-of-function mutations increase Cdc7-dependent replication initiation. EMBO Rep. 2017; 18: 2030–2050.
36. W Andrew Yeudall, Catherine A Vaughan, Hiroshi Miyazaki, Mahesh Ramamoorthy, Mi-Yon Choi, et al. Gain-of-function mutant p53 upregulates CXC chemokines and enhances cell migration. Carcinogenesis. 2012; 33: 442–451.
37. Mariano J Scian, Katherine E R Stagliano, Michelle A E Anderson, Sajida Hassan, Melissa Bowman, et al. Tumor-derived p53 mutants induce NF-kappaB2 gene expression. Mol. Cell. Biol. 2005; 25: 10097–10110.
38. S Donzelli, G Fontemaggi, F Fazi, S Di Agostino, F Padula, et al. MicroRNA-128-2 targets the transcriptional repressor E2F5 enhancing mutant p53 gain of function. Cell Death Differ. 2012; 19: 1038–1048.
39. Cen Zhang, Juan Liu, Yingjian Liang, Rui Wu, Yuhan Zhao, et al. Tumour-associated mutant p53 drives the Warburg effect. Nat. Commun. 2013; 4: 2935.
40. Jeremy W K Ng, Dilraj Lama, Suryani Lukman, David P Lane, Chandra S Verma, et al. R248Q mutation--Beyond p53-DNA binding. Proteins. 2015; 83: 2240–2250.
41. Kazuhito Yoshikawa, Jun-ichi Hamada, Mitsuhiro Tada, Takeshi Kameyama, Koji Nakagawa, et al. Mutant p53 R248Q but not R248W enhances in vitro invasiveness of human lung cancer NCI-H1299 cells. Biomed. Res. Tokyo Jpn. 2010; 31: 401–411.
42. Patricia AJ Muller, Patrick T Caswell, Brendan Doyle, Marcin P Iwanicki, Ee H Tan, et al. Mutant p53 drives

invasion by promoting integrin recycling. Cell. 2009; 139: 1327–1341.
43. Zhang Y, Coillie SV, Fang JY, Xu J. Gain of function of mutant p53: R282W on the peak? Oncogenesis. 2016; 5: e196.
44. Amjad Ali, Zhuo Wang, Junjiang Fu, Lei Ji, Jiang Liu, et al. Differential regulation of the REGγ-proteasome pathway by p53/TGF-β signalling and mutant p53 in cancer cells. Nat. Commun. 2013; 4: 2667.

Book Chapter

Inflammasomes: Key Players in the Development of Cancer

Aline Radi[1]* and Hussein Fayyad-Kazan[2]*

[1]University Children's Hospital, Philipps University, Germany
[2]Laboratory of Cancer Biology and Molecular Immunology, Faculty of Sciences -I, Lebanese University Hadath-Beirut, Lebanon

***Corresponding Authors:** Aline Radi, University Children's Hospital, Philipps University, 35043 Marburg, Germany

Hussein Fayyad-Kazan, Laboratory of Cancer Biology and Molecular Immunology, Faculty of Sciences -I, Lebanese University Hadath-Beirut, Lebanon

Published **December 13, 2022**

How to cite this book chapter: Aline Radi, Hussein Fayyad-Kazan. Inflammasomes: Key Players in the Development of Cancer. In: Hussein Fayyad Kazan, editor. Immunology and Cancer Biology. Hyderabad, India: Vide Leaf. 2022.

Innate Immune Response

Immunity refers to the resistance of the body against pathogenic microbes, their toxins, or other kinds of foreign substances through the ability to distinguish self from non-self. Immune responses can be broadly divided into innate and adaptive [1]. Innate immunity represents the first line of host defense against

pathogens. Effectors of innate immune responses include epithelial barriers in the skin and mucosae, their secretion of antimicrobial proteins, mucus and enzymes (e.g., lysozyme in tears), as well as phagocytes (monocytes, macrophages and neutrophils) and the complement system [2]. As a result of the activation of cell receptors specific for microorganism molecular patterns, innate immune cells are able to recognize diverse microorganisms such as bacteria, viruses, and fungi. This set of germline-encoded pattern recognition receptors (PRRs) has evolved to detect the presence of non-self through the binding of highly conserved microbial molecular features known as pathogen associated molecular patterns (PAMPs), which are essential for the survival of microorganisms and therefore difficult for the microorganism to alter. PRRs also recognize molecules released by damaged cells, so called danger associated molecular patterns (DAMPs), or perturbations induced by pathogens (patterns of pathogenicity) such as bacterial pore-forming toxins, perturbations of the cytoskeleton, and various types of cell stress. The engagement of PRRs leads to the activation of various inflammatory pathways that contribute to host defense. PRRs are expressed by several cell types involved in innate immune responses, such as monocytes, macrophages, dendritic cells (DCs), neutrophils and epithelial cells [3]. PRRs include Toll-like receptors (TLRs: transmembrane receptors), Nod-like receptors (NLRs: cytoplasmic sensors), RIG-I-like receptors (RLRs: cytoplasmic RNA helicases), and C-type lectin receptors (CLRs: transmembrane receptors) [2].

Inflammation is a normal physiological process which involves a well-organized cascade of changes within the living tissue in response to injury. Based on visual observation, inflammation is characterized by five main signs which are heat, redness, pain, swelling, and loss of function. These signs reflect increased blood flow, elevated cellular metabolism, vasodilation, release of soluble mediators, extravasation of fluids and cellular influx. Inflammation is a process that protects the host from invading pathogens or injury. The process dissipates after a short or long period of time, resulting in acute or chronic inflammation, respectively [4]. Inflammation requires a great amount of metabolic energy and can result in tissue damage and

destruction. Therefore, control mechanisms over the termination of inflammation are required [5]. Chronic inflammation is usually caused by persistent infections such as the microbes difficult-to-eradicate like Mycobacterium tuberculosis and Treponema pallidum, prolonged exposure to potentially toxic agents like silica, and monogenic and polygenic immune-mediated inflammatory diseases. Systemic chronic inflammation leads to disease complications such as diabetes mellitus, chronic kidney disease, autoimmune disorders and cancer [6].

A key signaling pathway that leads to acute and chronic inflammation is through the activation of the caspase-1 inflammasome which is assembled upon activation of certain nucleotide-binding domain, leucine-rich repeat containing proteins (NLRs), a cytoplasmic multimeric protein that causes the activation and the secretion of interleukins mainly Il-1b and Il-18 after being exposed to a stimulus [7].

Inflammasomes

Inflammasomes orchestrate pathogen defense and the repair process by activating the inflammatory response. They are formed after the detection of DAMPs and PAMPs by NLRs. Inflammasomes correspond to multi-protein complexes usually formed of two NLRs leading to the cleavage of the 17kDA pro-inflammatory cytokine IL-1b, from its 31kDa precursor, pro-IL-1B, via caspase 1 (Figure 1). This process also leads to activation of the IL-1 family member IL-18. Activation of the inflammasome is also associated with the onset of a form of cell death termed pyroptosis [8].

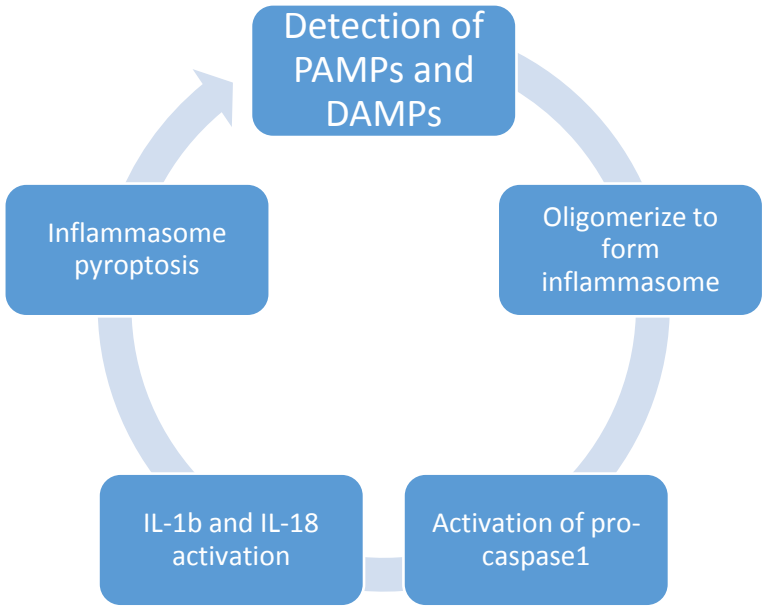

Figure 1: Pathway for inflammasomes activation after its stimulation. Once PAMPs and DAMPs are detected, inflammasomes are formed that in turns lead to pro-caspase1 activation. This results in IL-1b and IL-18 secretion and pyroptosis cell death.

The name inflammasome comes from the word inflammation, which reflects the function of the complex, and "some", which is from the Greek word for body, *soma*. The name also reflects similarities with the apoptosome, which triggers apoptosis (Zou et al., 1999). The inflammasome can recognize a wide variety of dangers, both internal and external. Endogenous signals that are known to activate the inflammasome include uric acid, ATP and potassium efflux [9]. On the other hand, external signals include stressors derived from a diverse range of conserved molecular motifs that are unique to bacteria, viruses and parasites, exogenous chemicals and ultraviolet light. The mechanism by which these signals are detected has yet to be fully elucidated for the majority of inflammasomes. The core structure of all inflammasomes is caspase-1, a variety of other proteins co-assemble with procaspase-1 to bring about its activation. Many, but not at all inflammasomes, have a member of the nucleotide-binding domain and leucine-rich repeat containing (NLR) gene

23 Like Family [10]. The production of IL-1B and IL-18 by the inflammasome is one of the first lines of defense against tissue damage and pathogen invasion. The inflammasome clinical importance exceeds infectious diseases, where its deregulation can lead to numerous inflammatory disorders [11]. Examples of diseases associated with inflammasome deregulation include Multiple Sclerosis, Alzheimer's disease, Parkinson's disease, Atherosclerosis and type2 Diabetes (Guo et al., 2015).

NLRPs

Nucleotide-binding domain leucine-rich repeat-containing receptors (NLRs) regulate innate immunity by activating inflammatory responses in a variety of biological systems following the recognition of pathogen- or disease-associated molecular patterns in the cell cytoplasm. Twenty-two NLRs have been identified in humans which presents the NLR family as a major class of intracellular PRRs. NLRs possess three different domains, an N-terminal death-fold domain that directly or indirectly engages caspase-1, a central nucleotide-binding or NACHT domain, and a C-terminal leucine-rich repeat (LRR) domain [8]. NLRs are classified based on their N-terminal domain. Once activated, NLRs induce a number of signaling pathways such as the pro-inflammatory NF-kB (for NOD1 and NOD2) and the caspase-1 inflammasome (for NLRC4, NLRP3 and NLRP1) pathways in addition to the induction of autophagy (NOD1, NOD2, and NLRC4) and cell death (NLRC4, NLRP3, and NLRP1). NLRs detect various DAMPs and PAMPs, where Nod1 and Nod2 recognize bacterial peptidoglycan specific structures, NLRC4 detects bacterial flagellin, and NLRP3 (inflammasome triggering protein) detects molecules like ATP, muramyl dipeptide (MDP) bacterial toxins, viral nucleic acids, b-amyloid fibrils and potassium efflux. Following the detection of PAMPs and DAMPs. NLRs activation leads to inflammasome assembly, through the recruitment of ASC adaptor protein (apoptosis-associated speck-like protein containing a CARD), ASC, that contains a pyrin domain (PYD) and a caspase activation and recruitment domain (CARD) allowing to bridge either a PYD or a CARD domain from the activated NLR and the CARD domain of pro-caspase-1 (pro-CASP1). Next, pro-

CASP1 undergoes proximity-induced auto-proteolysis to form an active enzyme (CASP1) that leads to the cleavage and activation of inflammatory cytokines (example: IL-1β and IL-18) and gasdermin D (GSDMD), the N-terminal resulting from this cleavage induces a pro-inflammatory form of programmed cell death known as pyroptosis [12].

IL-18 and IL-1b

Interleukin-1B (IL-1B) also known as catabolin, is a member of the interleukin 1 cytokine family of ligands, which also includes IL-1a, IL-18 and IL- 33. IL-1B is a pleiotropic cytokine that is involved in inflammation, cell growth, and tissue repair [13]. IL-1B is produced by blood monocytes but also by macrophages, dendritic cells and a variety of other cells in the body. IL-1B participates in the generation of systemic and local responses to infection and injury by generating fever, activating lymphocytes and promoting leukocyte infiltration at sites of infection or injury. IL-1B is believed to be the major mediator of inflammation in the periodic fever syndromes caused by mutations in NLRP family genes. It has been shown that treatment of the patients with an IL-1 receptor antagonist (IL-1Ra) or with anti-IL-1b neutralizing antibodies can improve their symptoms [14]. IL-18 induces IFN-b production and contributes to T-helper 1 (Th1) cell polarization. IL-18 also regulates Th2 and Th17 cell responses, in-addition to the activity of CD8 cytotoxic cells and neutrophils, in a host microenvironment-dependent manner and also boosts expression and production of certain cytokines, chemokines, and adhesion molecules (Wawrocki et al., 2016).

NLRP1

NLRP1 (nucleotide-binding domain leucine-rich repeat pyrin domain containing 1) was the first discovered PRR to form an inflammasome and with 1473 amino acids, human NLRP1 is the largest member of the family. NLPRs family members share three characteristic domains, the N-terminal death-fold domain or pyrin domain “PYD” that directly or indirectly engages caspase-1; the central nucleotide-binding or NACHT domain

made of "NAIP, CIITA, HET-E and TP-1" and the C-terminal leucine rich repeat LRR domain (Figure 2). NLRP1 also possesses two additional domains: (1) FIIND "function-to-find domain" that consists of ZU5 and UPA, which auto-processes NLRP1 into two polypeptide chains remaining non-covalently associated; (2) a C-terminal CARD domain signaling toward caspase-1 activation. Binding to a ligand causes NLRP1 self-oligomerization in a manner that is dependent on auto-proteolytic cleavage within the FIIND domain. Due to the poor conservation between mice and human, the molecular mechanisms for its activation and the resulting downstream events are still poorly understood. NLRP1 inflammasome stimuli can be divided into "direct activators" such as Anthrax lethal toxin and Shigella Flexneri that directly cause NLRP1 activation through degradation of the N-terminal PYD domain, and "indirect activators" such as Toxoplasma gondii and VbP the DPP8/9 inhibitor that cause disturbances within the cell that can be detected by NLRP1 [15]. It is worth to mention also that NLRP1 acts as sensor for virus infection by being stimulated by long dsRNA through binding it through its LRR domain [8]. NLRP1 is expressed mainly by keratinocytes and fibroblasts, and it is the only detectable inflammasome sensor in the human skin. Importantly, keratinocytes but not fibroblasts express a functional NLRP1 inflammasome. In that sense, not only do keratinocytes form the outer barrier of the skin but also play a role of immune cells by expressing molecules and peptides involved in immune responses. NLRP1 is regarded as the principal inflammasome sensor in human keratinocytes and UVB radiation induces its activation, which is believed to underlie the induction of sunburn. Moreover, gain-of-function mutations of ***NLRP1*** cause inflammatory skin syndromes. Thus, the detection of stress factors in the skin can lead to inflammation after NLRP1 activation and pro-inflammatory cytokine secretion. In addition, gain-of-function mutations lead to various skin disorders and increased risk for skin cancer. Therefore, pharmacological targeting of NLRP1 in epidermal keratinocytes represents a promising strategy for the treatment of patients suffering from NLRP1-dependent inflammatory skin disorders and cancer [16].

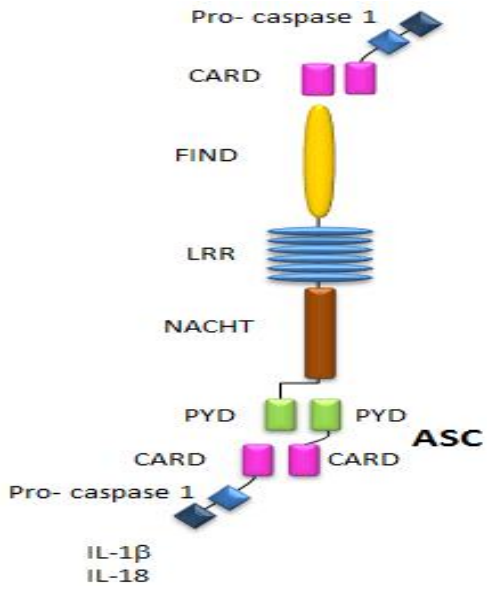

Figure 2: Schematic representation for the different domains of NLRP1. NLRP1 has three characteristic domains (PYD, NACHT and LRR) in addition to FIND and CARD domains.

NLRP1 Mutation

NLRP1 PYD domain interacts with the LRR domain to maintain NLRP1 as an inactive monomer. In some cases, a gain-of-function mutation on NLRP1 domains can lead to permanent activation and continuous secretion of interleukins in the absence of stimuli, thus leading to systemic chronic inflammation. When PYD or LRR domains are mutated, the auto-inhibitory mechanism is lost and NLRP1 becomes spontaneously activated triggering inflammasome assembly and thereby leading to pyroptotic cell death and IL-1 release from the initiating cells (Figure 3).

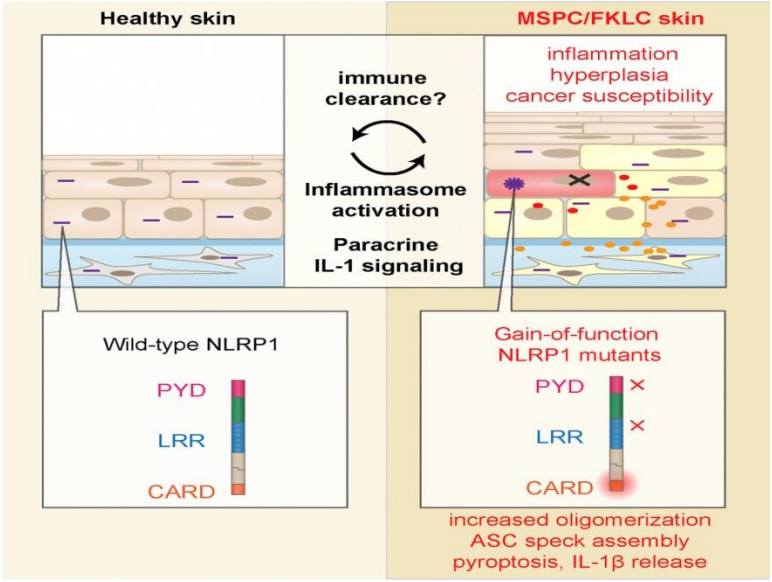

Figure 3: Gain-of-function mutations in the inflammasome sensor NLRP1 increase susceptibility to skin cancer and unmask unique regulatory auto-inhibition in the inflammasome [17].

IL-1 triggers the release of other inflammatory cytokines and growth factors such as TNFα and KGF from surrounding cells including neighboring keratinocytes and fibroblasts. A paracrine pro-inflammatory environment is created triggering epidermal hyperplasia and keratoacanthoma formation. Unresolved inflammation over years facilitates acquisition of additional oncogenic mutations and promotes malignant transformation toward SCC development. These gain-of-function mutations in Nod like receptors (NLRs) which activate inflammasomes leading to cytokine secretion cause systemic auto-inflammatory diseases. This has shed the light into the use of targeted anti-cytokine treatments that block interleukin signaling and help in the development of medicine in auto-inflammation [17]. The two most well-known skin disorders linked to NLRP1 mutations are MSPC "Multiple self-healing palmoplantar carcinoma" and the FKLC "Familial keratosis lichenoides chronica". The PYD domain is mutated in case of MSPC and the LRR domain is mutated in case of FKLC (Figure 4).

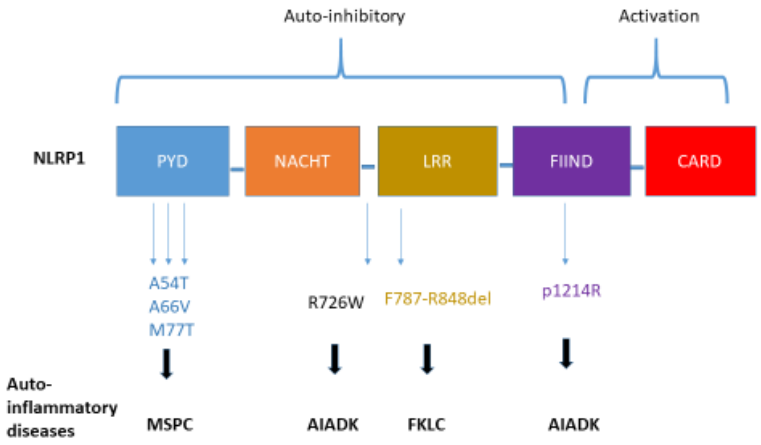

Figure 4: Different skin disorders associated with different mutations in different domains of NLRP1. Each domain of NLRP1 has a unique function and its mutation lead to different auto-inflammatory disease.

Inflammasomes and Cancer

During inflammation tissues become damaged and chemicals are released, causing white blood cells to secrete substances that stimulate cell growth resulting in wound repair. Inflammation ceases once the injury has healed, because it is a response to a stimulus and the removal of a stimulus should result in its abatement. In chronic inflammation, the inflammatory process may start even if there is no injury and persist for prolonged periods. Gain-of-function mutations on some of NLRP1 domains can lead to permanent activation of inflammasomes resulting in continuous secretion of interleukins especially IL-1β even in the absence of a stimulus as in the case of systemic chronic inflammation. Chronic inflammation is one of the most known hallmarks of carcinogenesis, allowing tumor growth and invasion. In contrast to NLRP3, NLRP1 has not been precisely analyzed. It plays a role as negative regulator of malignant melanoma cells apoptosis, where it binds caspase 1 and 9 in melanoma preventing their activation by other proteins and as result inhibiting their mediated apoptotic pathway. In that sense, NLRP1 overexpression promotes melanoma progression. In recent years, therapies targeting inflammasomes have been

widely improved to overcome human diseases such as cancer, where much attention has been paid to the development of compounds that inhibit the IL-1β signaling pathways as another approach for inflammasome inhibition in cancer treatment. Using IL-1 receptor antagonist (IL-1Ra) inhibits these effects thereby inhibiting the proliferation of skin carcinomas [18]. For example, Anakinra is a recombinant human IL-1 receptor antagonist and is regarded as a biological agent that blocks the inflammatory effects of IL-1 [19]. It was observed that its administration causes a dramatic improvement in hyperkeratosis which suggests that this treatment may regulate IL-1-induced keratinocyte hyperplasia and potentially reduce the risk of skin carcinomas in patients. Other examples of available treatments are Nidanilimab the ILR antibody, xilonix the IL-1α blocker and canakinumab the IL -1b blocker (Figure 5) [20]. It is also worth mentioning that some melanoma cancer cells gain drug resistance through a complex mechanism, in which nuclear factor-κB (NF-κB) and interleukin-1β (IL-1β) are critical contributors. Because NACHT, LRR and PYD domains-containing protein (NLRP) inflammasomes mediate IL-1β maturation and NF-κB activation, the role of inflammasome sensor NLRP1 in acquired drug resistance to temozolomide (TMZ) in melanoma was investigated [21]. Inflammasomes remain poorly understood with regards to their role in cancer development. Better understanding of their signaling regulation may help pave the way for future improvements in cancer prevention and treatment.

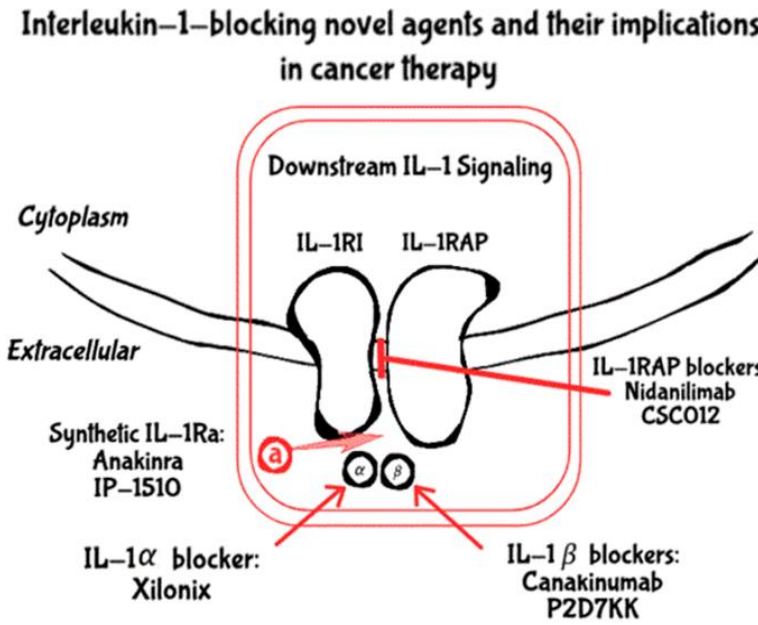

Figure 5: Novel IL-1 blockers used in clinical trails for cancer therapy. Xilonix and Canakinumab are IL-1 α monoclonal antibodies that bind to specific regions on their targets and prevent agonists binding to IL-1RI, thus inhibiting downstream signaling pathways. Nidanilimab and CSC012 are antibodies that prevent IL-1RAP from forming the heterotrimeric complex [20].

References

1. Chaplin DD. Overview of the immune response. Journal of Allergy and Clinical Immunology. 2010; 125: S3–S23.
2. Hoffmann J, Akira S. Innate immunity. Current Opinion in Immunology. 2013; 25: 1–3.
3. Martinon F, Mayor A, Tschopp J. The Inflammasomes: Guardians of the Body. Annu. Rev. Immunol. 2009; 27: 229–265.
4. Ferrero-Miliani L, Nielsen OH, Andersen PS, Girardin SE. Chronic inflammation: importance of NOD2 and NALP3 in interleukin-1? Generation. Clin Exp Immunol. 2006; 061127015327006.
5. Barton GM. A calculated response: control of inflammation by the innate immune system. J. Clin. Invest. 2008; 118: 413–420.

6. David Furman, Judith Campisi, Eric Verdin, Pedro Carrera-Bastos, Sasha Targ, et al. Chronic inflammation in the etiology of disease across the life span. Nat Med. 2019; 25: 1822–1832.
7. Karki R, Man SM, Kanneganti TD. Inflammasomes and Cancer. Cancer Immunol Res. 2017; 5: 94–99.
8. Bauernfried S, Scherr MJ, Pichlmair A, Duderstadt KE, Hornung V. Human NLRP1 is a sensor for double-stranded RNA. Science. 2021; 371: eabd0811.
9. Kahlenberg JM, Dubyak GR. Mechanisms of caspase-1 activation by $P2X_7$ receptor-mediated K^+ release. American Journal of Physiology-Cell Physiology. 2004; 286: C1100–C1108.
10. Irving C Allen, Margaret A Scull, Chris B Moore, Eda K Holl, Erin McElvania-TeKippe, et al. The NLRP3 Inflammasome Mediates In Vivo Innate Immunity to Influenza A Virus through Recognition of Viral RNA. Immunity. 2009; 30: 556–565.
11. Broz P, Dixit VM. Inflammasomes: mechanism of assembly, regulation and signalling. Nat Rev Immunol. 2016; 16: 407–420.
12. Taabazuing CY, Griswold AR, Bachovchin DA. The NLRP1 and CARD8 inflammasomes. Immunol Rev. 2020; 297: 13–25.
13. Molgora M, Barajon I, Mantovani A, Garlanda C. Regulatory Role of IL-1R8 in Immunity and Disease. Front. Immunol. 2016; 7.
14. Dinarello CA. Interleukin-1 in the pathogenesis and treatment of inflammatory diseases. Blood. 2011; 117: 3720–3732.
15. Taabazuing CY, Griswold AR, Bachovchin DA. The NLRP1 and CARD8 inflammasomes. Immunol Rev. 2020; 297: 13–25.
16. Fenini G, Karakaya T, Hennig P, Di Filippo M, Beer HD. The NLRP1 Inflammasome in Human Skin and Beyond. IJMS. 2020; 21: 4788.
17. Franklin L Zhong, Ons Mamaï, Lorenzo Sborgi, Lobna Boussofara, Richard Hopkins, et al. Germline NLRP1 Mutations Cause Skin Inflammatory and Cancer

Susceptibility Syndromes via Inflammasome Activation. Cell. 2016; 167: 187-202.e17.
18. La E, Rundhaug JE, Fischer SM. Role of intracellular interleukin-1 receptor antagonist in skin carcinogenesis: IL-1 Receptor Antagonist and Skin Tumor Cell Growth. Mol. Carcinog. 2001; 30: 218–223.
19. Roy M Fleischmann, Joy Schechtman, Ralph Bennett, Malcolm L Handel, Gerd-Rudiger Burmester, et al. Anakinra, a recombinant human interleukin-1 receptor antagonist (r-metHuIL-1ra), in patients with rheumatoid arthritis: A large, international, multicenter, placebo-controlled trial. Arthritis & Rheumatism. 2003; 48: 927–934.
20. Litmanovich A, Khazim K, Cohen I. The Role of Interleukin-1 in the Pathogenesis of Cancer and its Potential as a Therapeutic Target in Clinical Practice. Oncol Ther. 2018; 6: 109–127.
21. Zili Zhai, Jenny Mae Samson, Takeshi Yamauchi, Prasanna K Vaddi, Yuko Matsumoto, et al. Inflammasome Sensor NLRP1 Confers Acquired Drug Resistance to Temozolomide in Human Melanoma. Cancers. 2020; 12: 2518.
22. Philpott DJ, Girardin SE. Nod-like receptors: sentinels at host membranes. Current Opinion in Immunology. 2010; 22: 428–434.
23. Kozuch O, Mayer V. Pig kidney epithelial (PS) cells: a perfect tool for the study of flaviviruses and some other arboviruses. Acta Virol. 1975; 19: 498.
24. Coussens LM, Werb Z. Inflammation and cancer. Nature. 2002; 420: 860–867.

Book Chapter

Tumor Associated Macrophages (TAMs) Contribution in Melanoma Progression: Potential Molecular Pathways and Proposed Therapies

Alaa Skeyni[1]*, Hady Al Shami[2] and Hussein Fayyad-Kazan[3]*

[1]Centre de Recherche d'Immunologie et d'Hématologie, Inserm U-1109, Université de Strasbourg, France
[2]Faculté des Sciences de Montpellier, France
[3]Laboratory of Cancer Biology and Molecular Immunology, Faculty of Science, Lebanese University, Lebanon

***Corresponding Authors:** Alaa Skeyni, Centre de Recherche d'Immunologie et d'Hématologie, Inserm U-1109, Université de Strasbourg, Strasbourg, France

Hussein Fayyad-Kazan, Laboratory of Cancer Biology and Molecular Immunology, Faculty of Science, Lebanese University, Hadath-Beirut, Lebanon

Published **January 04, 2023**

How to cite this book chapter: Alaa Skeyni, Hady Al Shami, Hussein Fayyad-Kazan. Tumor Associated Macrophages (TAMs) Contribution in Melanoma Progression: Potential Molecular Pathways and Proposed Therapies. In: Hussein Fayyad Kazan, editor. Immunology and Cancer Biology. Hyderabad, India: Vide Leaf. 2023.

Abstract

The incidence of melanoma continues to escalate worldwide. Its ethology is related to cumulative genetic and environmental factors. However, despite the fact that various genetic mutations were found in metastatic and malignant melanoma, predispositions do not occur equally often. Mutations in BRAF, MAPK, and ERK were observed as landmarks for treatment approaches. Although a global improvement was attained, patients relapsed after a short period and were then diagnosed with a late stage of metastatic melanoma. The need to better understand the tumor microenvironment TME of melanoma became heavily crucial. Out of the cells exhibiting an immunosuppressive phenotype in the tumor microenvironment TME, are tumor-associated macrophages TAMs. The latter result from defects in several pathways, such as JAK/STAT network causing an imbalance between macrophages promoting tumor progression and those suppressing the tumor hence aiding the immune response. Comprehending the link between TAMs and the molecular pathways promoting its aggressive phenotype offers a new avenue to personalized medicine.

Introduction

According to US assessments, skin cancer is the most frequent malignancy among Caucasian populations, with about one in every five Americans contracting some kind of skin cancer [1]. Melanoma is cancer that originates from melanocytes and is the deadliest skin cancer that predominantly affects younger and middle-aged people [2]. It doesn't always emerge on the skin; it can also develop in the eyes, vagina, anus, sinus, and oropharynx, whereas only 5% of melanoma incidence occurs at these sites [2]. Cutaneous melanomas are characterized as either superficial spreading, lentigo malignant, or nodular and acral lentiginous [2]. Malignant melanoma is the most aggressive form of skin cancer, comprising 4% of all skin cancer occurrences but contributing to 80% of vast skin cancer mortality [3]. Globally, it affected 324,600 individuals in 2020, resulting in 57,000 deaths [4].

According to annual cancer status reports issued in the United States in 2020, the incidence of melanoma is steadily growing, regardless of gender [5]. Current therapies, including immune checkpoint treatment, targeted therapy, radiotherapy, and chemotherapy, have resulted in a sustained reduction in the death rates of melanoma (6.1% annually) [5], nonetheless treatments of melanoma still keep room for advancement due to drug resistance [6]. Various studies showed that melanoma has a large tumor mutational burden protecting it from immunity invasion [7,8]. Understanding the precise mechanism of immunosuppression in melanoma has indeed become crucially influential.

The tumor microenvironment (TME) is the complex ecosystem in which tumor cells reside and interact with various types of cells [9]. The former comprises a significant role in tumor progression and drug resistance [10]. Many cells, including fibroblasts, adipocytes, and migratory hematopoietic cells, particularly macrophages, thrive in the tumor microenvironment. Evidence shows that macrophages aid in tumor progression and metastasis. In the tumor microenvironment, macrophages are educated to exhibit a restorative role that induces angiogenesis, matrix breakdown, and tumor-cell motility. TAMs have a focal role in tumor progression and metastasis [9].

A network of signaling molecules, transcription factors, epigenetic mechanisms, and post-transcriptional regulators underly the distinct forms of macrophages' activation. A candidate activator is the canonical JAK-STAT signaling pathway. Upon activation, it drifts macrophages' function toward the M1 phenotype or towards the M2 phenotype according to the transcription activated [10].

While the role of myeloid cells in innate and adaptive immunity has been known for over 100 years, leukocyte detection in tumors goes back to the middle of the nineteenth century. Macrophage's role in tumors was only examined recently, despite the fact that many malignancies are inundated with these cells. Normally, upon tissue damage, cells express various chemokines and growth factors to recruit circulating monocytes

to the site of impairment. Macrophages serve as an immune system mediator to kill pathogens and aid tissue repair. TAMs, on the other hand, are lured by tumor cells, and a specific stimulus repurposes their innate immune activity to guard against tumor progression. As the presence of TAMs in human cancers is concomitant with poor prognosis in more than 80% of studies, we further explore the role of TAMs in melanoma and their distinct stimulating molecular networks [11]. Here, we describe skin melanoma disease and focus on mechanisms that induce the immunosuppressive phenotype of TAMs and their effect on tumor progression and dissemination depending on emerging data.

Skin Melanoma

Biology of Melanoma

Melanoma is the deadliest form of skin cancer. Melanocytes are neural crest-derived cells and can be found mainly in the basal epidermis and hair follicles, in addition to mucosal surfaces, meninges, and the choroidal layer of the eye [12]. Skin keratinocytes produce melanocyte-stimulating hormone (MSH), as a response to UV-induced DNA damage, which binds to the melanocortin receptor 1 (MC1R) on melanocytes, prompting them to generate and release melanin. The melanin pigment ultimately operates as a shield from UV radiation, thus preventing further DNA alteration [13]. However, melanin has a complex of anti-oxidant and pro-oxidant properties [14], and the conversion of melanin from an antioxidant to a pro-oxidant agent under the influence of various etiological factors such as UV radiation, heavy metals, and herbicides, marks a critical pathogenetic event that initiates carcinogenesis. Melanin's pro-oxidant action causes a rise in the quantities of intracellular oxygen radicals, which results in damage to the melanocyte's DNA molecule. These mutations would result in excessive activation of various cell signaling pathways leading to uncontrolled proliferation and cancer [15].

Risk Factors

The risk factors for the development of melanoma are related to both the human body and the environment.

Exposure to ultraviolet radiation is the leading risk factor for the development of melanoma where both natural sunlight and artificial lighting systems are ultraviolet radiation sources [16]. The UVB wavelength between 290 and 320 nm is by far the most carcinogenic to the skin [17]. Those UVB waves are mostly absorbed by the nuclear proteins and acids of melanocytes leading to oxidative stress, which disrupts the latter [18]. Recent studies concluded that intermittent exposure to sunlight is one of the major risk determinants for melanoma [19].

Environmental factors contribute to a variation in melanoma incidence globally. The etiology arises from the fact that people residing at lower latitude are at higher risk of melanoma, where Australia and New Zealand record the highest incidence [20]. Scandinavia and Northern Europe record the highest incidence in Europe whereas the lowest incidence of melanoma there is in Eastern and Southern Europe [21]. Socioeconomic status and occupation impact melanoma development in individuals, coming from the fact that sun exposure acts as a major risk factor. Individuals receiving immunosuppressive treatments, and patients diagnosed with immunodeficiency syndrome are more susceptible to melanoma progression [22].

Genetic factors highly contribute to melanoma occurrence, as a family history of melanoma accounts for high-risk probability of malignancy. Mutations in various genes are the main driving force in melanoma as they initiate cell proliferation and cessation of apoptosis as a normal response to DNA damage [23].

Autosomal dominant alleles were present in the familial inheritance of melanoma and exceeded the first generation [19]. NRAS is one example of genes that are particularly altered in 15–20% of melanoma cases [24]. Another mutation is the BRAF gene, which occurs in about 50% of melanoma cases. BRAF kinase plays a role in the regulation of the signaling pathway

between mitogen-activated protein kinase and extracellular signal-regulated kinase (MAP/ERK), which controls cell division and differentiation. As a result, this mutation causes uncontrollable division of melanocytes, which culminates in the onset of melanoma [25]. Individuals with predispositions are demonstrated to develop melanoma at a younger age (40 years old) [22], and in such situations, medical surveillance at a young age might assist better prognosis.

Diagnosis

Physical examination requires general skin inspection. Moles described as the ugly ducklings exhibit a phenotype distinctive from other moles and are further inspected following a criteria covering the asymmetry, border, color, diameter, and evolution (ABCDEs) [26].

A biopsy from the suspected skin lesion is fundamental for melanoma diagnosis confirmation. It's typically performed with local anesthesia using 1 of 3 techniques: saucerization shave biopsy, punch biopsy, or narrow excision with 2-mm margins. The sample should assess the invasion depth (Breslow thickness) covering the surrounding healthy tissue as well [27].

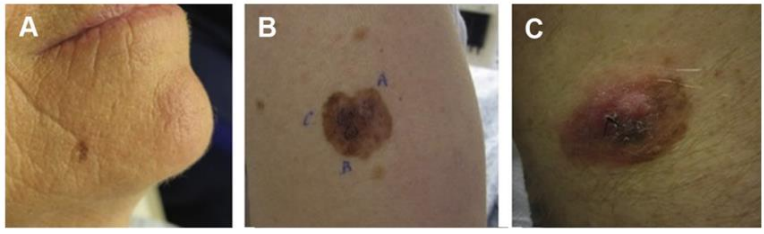

Figure 1: Clinical illustartion of melanoma where (A) Melanoma in situ on sun damaged skin can exhibit few features except for irregularity of pigmentation and early dermato-scopy signs. (B) T1 melanomas can develop a prominent radial growth phase, initially growing outward, but careful examination demonstrates gray stippling in the area marked "C" as evidence of early invasion. (C) Late-stage tumors, such as this T3 lesion, have developed a vertical growth phase and developed a nodule in this preexisting nevus. Vertical growth phase and nodular components of melanomas can grow rapidly and are more likely to be amelanotic [26].

Treatment

The majority of newly diagnosed melanoma patients have an early-stage illness, for which surgical excision is the therapy of choice. Such therapy is curative in the vast majority of instances. [28]. However, some patients will later relapse with metastasis dissemination, while approximately 10% of melanoma cases are diagnosed at an advanced stage and are unresectable or already metastatic. Approximately one-third of stage IV cancers had visceral and brain involvement at diagnosis, which is consistent with a poor prognosis and a reduced likelihood of a sustained response to treatment [29].

In the second line of defense comes drug therapy. In cases of metastatic melanoma, the most efficient choice would be chemotherapy. Until recently, dacarbazine remains to be the traditional chemotherapy used with a survival rate of only 27% in one year. The invention of novel medications with high efficacy and minimal toxicity is one of the limitations of chemotherapeutic development.

Several targeted therapies are selected to deal with melanoma mutations. The most promising targeted drugs are BRAF inhibitors, which permit excellent efficacy in patients with BRAF mutations. Yet, 50% of patients relapse due to secondary resistance only shortly after receiving the treatment. Several underlying mechanisms, including tumor suppressor gene PTEN loss, cyclin D amplification, MEK mutations, NF1 loss, and others, drive tumor cells to become resilient to BRAF inhibitors.

The fact that many sufferers still are diagnosed at a late stage of the illness necessitates the development of innovative treatments for advanced melanoma. Melanoma cells can bypass and avoid the immune response attributed to their profoundly mutagenic nature. Tumor cells in melanoma can diminish MHC1 expression, reducing antigen recognition by TCR on T cells. In addition, immune inhibitory substances such as suppressive cytokines, TGF-, and PGE2 are emitted [11].

Another trick melanoma cells use to evade the immune response, is to express programmed cell protein PD1 that inhibits the activity of T cells hence promoting self-tolerance [11].

Three Prominent types of immune-based treatments exist: cancer vaccines, adoptive cell therapies, and immunomodulatory strategies.

Cancer vaccines are administered to patients in the late stages of melanoma. It includes sensitization of the immune system against tumor antigens. The tumor's capacity to evade the immune response is the strategy's only drawback. In light of this, no melanoma vaccination is authorized for clinical use [30].

Immune therapies including the administration of interleukin-2 to promote tumor T-cells proliferation, elicited limited response in patients with high toxicity.

Nowadays, immunotherapies showing curative effects are immune checkpoint inhibitors. Nivolumab and ipilimumab are antibodies against PD-1 and CTLA4 respectively, that can block the checkpoint-manipulating virulence that melanoma exhibits. Treatment with antibodies blocks the binding to respective ligands and consecutive signals that promote immune tolerance. Treatment with these drugs has already shown durable survival for up to 10 years in 20% of patients with stage IV melanoma. Though these tactics demonstrate remarkable progress, they have pitfalls such as encouraging self-tolerance, which frequently causes inflammation in the gastrointestinal tract, skin, and endocrine organs [31].

Despite the breakthrough, immunotherapeutic drugs have been recorded in melanoma treatment, a considerable number of patients still don’t benefit efficiently or develop secondary resistance. Conducting further research would help understand why patients acquire resistance after benefiting from a certain treatment, are there specific biomarkers that aid in choosing the most efficient treatment and reducing the severe side effects? There is no magic potion for treating melanoma, hence prioritizing personalized treatment. Such a treatment is initiated

with thorough research on tumor environment residents and molecular networks involved.

Molecular defects in Melanoma

Somatic mutations in melanoma don't occur at the same frequency, but often rearise in signaling pathways responsible for cell proliferation, growth and metabolic, cell cycle control, cell identity, replicative life span, as well as those controlling resistance to apoptosis [32].

Staring BRAF mutations in cancers lead to further interest in the subsequent molecular pathways. Mitogen-activated protein kinase (MAPK) signal transduction pathway gained focus lately because of the major role BRAF plays in its activation. Additionally, NRAS, MEK1/2, and ERK. Mutations in the G protein subunit alpha 11 (GNA 11) are activating, leading to the production of an overactive Gα11 protein that stimulates uncontrolled proliferation of the pigment-producing cells (melanocytes) in the uvea or the skin. As in cancerous tumors, the G protein subunit alpha q (GNAQ) gene mutations in uveal melanoma result in an overactive protein, which leads to excessive signaling. This abnormal signaling likely contributes to the overgrowth of cells and tumor formation [33].

As previously mentioned, despite using inhibitors of aberrant proteins implicated in cell cycle control, numerous melanoma patients still exhibit resistance against therapy. One of the ubiquitous features of such cases is the presence of cells promoting tumor growth and suppressing the immune response such as tumor-associated macrophages.

Macrophages and Tumor Microenvironment

TAMs (Tumor-Associated Macrophages) are critical to the development, maintenance, and eradication of cancer cells. In general, macrophages in the tumor microenvironment can be polarized into two functional states M1 and M2 macrophages. Classically activated macrophages, or M1 polarized macrophages, are those that emit pro-inflammatory and immune-

stimulatory cytokines like interleukin 12 and 23, after being aroused by cytokines like interferon-gamma. M1 macrophages can have anti-tumoral properties, by scavenging and destroying phagocytosed tumor cells and stimulating helper cell type 1 responses. M2 polarized macrophages, also known as alternatively activated macrophages, are activated by Interleukin 4, 10 and 13. Most TAMs are thought to resemble M2 macrophages. These cells play an important role in connecting inflammation with cancer. Expressing high levels of anti-inflammatory cytokines, scavenging receptors, angiogenic factors, and proteases compared to M1 type counterparts. TAMs can reprogram the immunosuppressive microenvironment and promote the proliferation, invasion, and metastasis of tumor cells. They can stimulate tumor angiogenesis, and inhibit anti-tumor immune responses mediated by T cells [34].

As TAMs are mostly similar to M2 macrophages in their phenotypic traits, studies have demonstrated that the presence of TAMs is associated with poor survival in various tumor types [35,36]. Nevertheless, the TME is observed to contain a variety of macrophage subtypes, reflecting its intricacy [37]. TAMs participate in tumor progression by interacting with both tumor and other stromal cells where these tumor cells reverse the function of macrophages making them an adjunct to the tumor. This allows TAMs to promote tumor proliferation, angiogenesis, immune evasion, invasion, and metastasis [38].

TAMs in Melanoma

Tumors are known to contain varying numbers of macrophages. In melanoma, the macrophage content ranges from 0 to 30% of the total cells of the tumor. Metastasizing melanomas, as well as metastatic lesions, all contain <10% of macrophages, whereas non-metastasizing tumors have widely varying numbers of macrophages [39]. The two categories of TAMs, M1 and M2, have opposing tumor-promoting and tumor-suppressing roles, this leads TAMs to playing a dual role on tumor proliferation, invasion and metastasis, angiogenesis, and resistance to treatment.

Regulating Tumor Proliferation, Invasion and Metastasis

Studies showed that the increased number of M2 macrophages promotes melanoma growth [40], whereas the M1 polarization of macrophages inhibits the proliferation of melanoma [41]. Several reasons might lead to the polarization of one type of macrophage over the other. One example is macrophages deficient in integrin β3 inducing the polarization of the M2 macrophage phenotype [42]. The survival analysis of melanoma patients treated with isolated hepatic perfusion showed that M1 polarization was associated with higher overall survival of patients, due to M1 macrophage inhibitory effects on melanoma proliferation [43].

The increased expression of Connexin 43 which is a vital gap junction protein in the TME has been reported to induce M1 polarization, which in return inhibited the invasion and migration of melanoma cells in vitro [44]. On the other hand, M2 macrophages that lack tripartite motif 59 (TRIM59), which belongs to the TRIM family of proteins, promote the expression of Matrix metallopeptidase 9 (MMP-9) and mucosal vascular addressing cell adhesion molecule 1 (MAdCAM-1). Being mentioned, they are implicated in tumor migration and invasion [45].

The ability of TAMs to communicate with other immune cells in the TME is intriguing [46]. For example, the nuclear factor of activated T cells (NFAT1) is a transcription factor that can bind to IL-2 and regulate its expression promoting T cell activation. It has also been proved to increase the infiltration of M2 macrophages, thus promoting TAM-mediated growth and metastasis in melanoma [47].

Angiogenesis Alteration in Melanoma

A vital process in the preparation of lymph nodes for melanoma metastasis would be angiogenesis [48]. Studies showed that M1 TAMs trigger immune responses and normalize irregular tumor vascular networks, which sensitize cancer cells to chemotherapy and radiotherapy thus suppressing tumor growth [49]. On the

other hand, increased M2 polarization of TAMs stimulates tumor angiogenesis, leading to tumor progression in return [50]. This is attributed to the induction of endothelial cells by melanoma exosomes promoting the expression of Granulocyte-macrophage colony-stimulating factor (GM-CSF). This enhances the activity of hypoxia-inducible factor-2α (HIF-2α) in M2-like TAMs, which attenuates vascular endothelial growth factor (VEGF) activity by inducing the production of soluble VEGFR-1, promoting improved tissue and vasculature patency [48].

Resistance to Melanoma Treatment

Recent studies indicate that macrophages serve a role in melanoma resistance, where the different phenotypes of macrophages either promote resistance in melanoma or improve the efficacy of drugs in the treatment of melanoma [51]. An approach that achieved durable responses hand in hand with immunotherapy, is targeting immune checkpoint molecules such as programmed cell death protein 1 (PD-1) [52], but 25% of patients with melanoma who have shown an objective response to PD-1 blockers also develop resistance [53]. This resistance is due to increased frequencies of M2-polarization TAMs, which link to the high levels of IL-34 induced by PD-1 inhibitors [54]. In addition, blocking the binding of G protein-coupled receptor 4 (GPCR4) on TAMs to its ligand R-spondin 1-4 can reduce the polarization of M2 macrophages on one hand, and promote the polarization of M1 macrophages, on the other hand, further enhancing the efficacy of PD-1 immunotherapy in melanoma treatment [55].

JAK-STAT Pathway and TAMs

A wide range of processes required for homeostasis and development in mammals are mediated by the Signal transducer and activator of transcription (STAT) signaling [56]. It is shown that STAT activation induces a myriad of cytokines and growth factors that drive events as varied as hematopoiesis, immune fitness, inflammation, tissue repair, adipogenesis, and apoptosis [57]. It should come as no surprise that any STAT signaling flaws that cause either global deregulation or overactivation cause the

disease to manifest and worsen [58]. . Additionally, the STAT family, to a large extent, regulates the distinction between immune responses that inhibit and those that promote cancer [59].

The extracellular binding of numerous cytokines and other ligands with their corresponding transmembrane receptors results in the activation of receptor-bound Janus kinases (JAKs). The latter eventually stimulates the phosphorylation and subsequent homo- or heterodimerization of resting STAT monomers in the cytoplasm.

This Cascade of events accounts for STAT activation. Activated STAT dimers would translocate to the nucleus and bind to specific target genes inducing their activation and further modulation of downstream targets [60]. The JAK family involves four kinases JAK1, JAK2, JAK3, and TYK2 [61], whereas the STAT protein family consists of seven members: STAT1, STAT2, STAT3, STAT4, STAT5A, STAT5B, and STAT6 [61]. Several STAT members including STAT3 and STAT5 are linked to tumor initiation and progression while others (STAT1 and STAT2) are integral in antitumor defense and in maintaining an effective and long-term immune response [56]. The STAT family proved to have a central role in the polarization of myeloid cell functions as well as in tumor progression and the alteration of immune response to cancer. STAT1, STAT3, and STAT6 orchestrate a massive role in transmitting polarizing signals to the nucleus and have distinct roles in macrophage polarization [62].

Available data suggest that STAT1 acts as a tumor suppressor and negative regulator of tumors. Its activity is essential for the antiproliferative effects of interferons. In most patients with resistant human melanoma, the loss of STAT1 activity was detected [63]. The STAT1 transcription factor is essential for mediating melanoma cell sensitivity to various pro-apoptotic stimuli. One example is the ability of STAT1 to regulate the expression of death-receptor-4 (DR4) expression on melanoma cells, which could affect (TNF-related apoptosis-inducing ligand) TRAIL sensitivity [63]. The major event required for

recruiting M1- macrophages is the participation of NF-KB and STAT1 along with interferon regulatory factor IRF9, P53. Disruption in this corporation leads to M1phenotype conversion towards the immunosuppressive phenotype of TAMs [10]. Evidence indicates that STAT1 activation is essential for immune surveillance against tumors [64]. One study showed that mice deficient in either the IFN-γ receptor (signaling that activates STAT1) or STAT1 displayed enhanced resistance to the induction of tumors by methylcholanthrene [65].

As it promotes distinct transcriptional patterns in response to a range of growth factors, cytokines, hormones, and oncogenes (e.g., IL6, leptin, IL12, IFNs, IL10, GCSF, prolactin, growth hormone, EGF, HGF, bFGF, v-Src, v-Fps, and v-Sis), the STAT3 transcription factor is critical in this context [63]. In malignant cells where STAT3 activation is constitutive, this protein is a key mediator in promoting cell proliferation, angiogenesis, and apoptosis inhibition. It also activates the transcription of genes important for invasion and metastasis [63]. This malignant profile of STAT3 is exhibited by its ability to activate various genes responsible for tumor progressions such as c-myc and cyclin D1. As well as one that inhibits apoptosis (Bcl-xL, survivin), and promotes metastasis (matrix metalloproteinases) [63]. It is shown that STAT3 is constitutively activated in diverse tumor-infiltrating immune cells, including TAMs and its activation is associated with M2 macrophage polarization [10]. STAT3 directly induces the expression of the M2 marker CD163, both in macrophages and tumor cells [66]. Additionally, IL6 inhibition of M-CSF-induced colony formation observed in animals is abolished in mice mutated for the gp130-STAT1/3 signaling, suggesting that the IL6/STAT3 pathway could regulate macrophage homeostasis [67].

TAM-Targeting Therapies in Melanoma

Given the vital role of macrophages in melanoma progression and several other tumors, targeting macrophages is considered a promising potential therapeutic strategy. This would give rise to two primary approaches to melanoma treatment: Conventional therapies, including surgery, chemotherapy, radiotherapy and

targeted therapy with reduced side effects on one hand, and reducing or reprogramming TAMs on the other [68]. The current TAM-related approaches for melanoma treatment include:

Reducing the Number of TAMs in Melanoma: Deleting or Recruitment Inhibition

Direct deletion of TAMs poses an attractive alternative to improve the prognosis of a patient with melanoma. One example is the colony-stimulating factor 1 receptor (CSF1R) which can control the differentiation, proliferation, and survival of macrophages [69]. It is present in the vast majority of macrophages and targeting it seems to be an effective method for depleting TAMs in tumors. Clinical trials have shown that targeting CSF1R or combining it with other therapies, can result in improved treatment outcomes for patients [68].

Another approach would be reducing the number of TAMs in the TME by inhibiting their recruitment. One way would be inhibiting CCL2 which is involved in recruiting monocytes and giving rise to TAM expansion. This method was able to delay tumor progression in several experimental tumor models, including melanoma. Since there is a lack of evidence on thisstrategy, more research is recommended [70].

Activating Macrophages in Melanoma

It is proven that some TAMs have antitumor effects and suppress tumor growth by activating immune responses while other TAMs promote tumors [71]. This suggests that TAMs are flexible, and reprogramming them to treat tumors would be a reasonable therapeutic approach. It was demonstrated that melanoma cells can block macrophage activation by suppressing toll-like receptor (TLR) signaling [72], hence, a clinical study tested the efficiency and safety of TLR7 ligands (852A) in the treatment of melanoma and found that combining an agonist of TLR (3M-052 for TLR7/8), which polarizes macrophages towards a pro-inflammatory phenotype, with a checkpoint blockade is more efficient than a checkpoint blockade alone in the treatment of B16-F10 melanomas [73].

Adoptive Macrophage Therapy

Adoptive cellular therapy and chimeric antigen receptor (CAR) T cells have achieved marked success in the treatment of lymphoma and leukemia, among others [74], which allows the possibility of using adoptive transfer of engineered active macrophages as a treatment for melanoma. The technique uses the artificial administration of special drugs, cytokines, and even gene editing to promote macrophages that are cytotoxic to tumor cells [75]. Chen et al [76] have reported that CAR-macrophages could be utilized as a novel immunotherapy candidate against solid tumors. However, this technique is far from any clinical application as the mechanism of action of adoptive macrophage therapy is not fully understood.

Furthermore, the current successful trials of the monoclonal antibodies (mAb) acting as checkpoints inhibitors are coming to the surface. A recent study shows that the expression of (macrophage receptor with collagenous structure) MACRO which is a pattern recognition receptor of the class A scavenger receptor family, was shown to be overexpressed in TME in cancers with poor prognosis [34]. Expression of MACRO was identified in TAMs in murine melanoma TME. The former is promoted by the tumor and M2-polarizing cytokines [77]. Secondly, MACRO expression correlates to M2 TAM and EMT-metastasis driving gene profile in human metastatic melanoma. Providentially, immunotherapy targeting MACRO arrested tumor growth and metastasis and increased TME immunogenicity [77]. Overall, employing mAb to rewire TAMs is a viable method of treating melanoma.

Conclusion

In summary, melanoma is the deadliest form of skin cancer, showing a high risk of metastasis and resistance to available therapies. Seeking new prognostic markers to recognize patients at high risk of developing metastases became imperative. Exhibiting a tumor-promoting phenotype, TAMs appear to be a target for novel therapies. Clarifying the link between malignant tumors and TAMs proposes novel biomarkers for prognosis,

diagnosis, and therapy. Meanwhile, clear differentiation between M1 and M2 polarized macrophages is essential. The two types of macrophages exist as two extremes upon a continuum, with the balance being tipped one way or the other by higher or lower levels of cytokines in the tumor environment. Macrophages are plastic, therefore M1 macrophages give the respective stimuli in the right environment and can become more M2-like, and vice versa. Dissecting networks like JAK-STAT, MAPK, and the role of PD-1 expression could open a new window toward safe and subtle therapeutics against melanoma. Mechanistically, enhancing TME's immunogenicity by antibodies that target Tams specifically will liberate T cells to fight the cancer onslaught, which may also be helped by anti-CTLA4 therapy. These therapies elucidated the role performed by the immune system in the cancer battle.

References

1. Non-Surgical Treatment of Keratinocyte Skin Cancer | Springer Link. Available online at: https://link.springer.com/book/10.1007/978-3-540-79341-0
2. WP Coleman, PR Loria, RJ Reed, ET Krementz. Acral lentiginous melanoma, Arch. Dermatol. 1980; 116: 773–776.
3. S Kuphal, A Bosserhoff. Recent progress in understanding the pathology of malignant melanoma. J. Pathol. 2009; 219: 400–409.
4. H Wang, L Yang, D Wang, Q Zhang, L Zhang. Pro-tumor activities of macrophages in the progression of melanoma. Hum. Vaccines Immunother. 2017; 13: 1556–1562.
5. Annual report to the nation on the status of cancer, part I: National cancer statistics - Available online at: https://pubmed.ncbi.nlm.nih.gov/32162336/
6. M Mandalà, C Voit. Targeting BRAF in melanoma: biological and clinical challenges. Crit. Rev. Oncol. Hematol. 2013; 87: 239–255.
7. Y Fu, S Liu, S Zeng, H Shen. From bench to bed: the tumor immune microenvironment and current immunotherapeutic strategies for hepatocellular carcinoma. J. Exp. Clin. Cancer Res. CR. 2019; 38: 396.

8. M Marzagalli, ND Ebelt, ER Manuel. Unraveling the crosstalk between melanoma and immune cells in the tumor microenvironment. Semin. Cancer Biol. 2019; 59: 236–250.
9. R Noy, JW Pollard. Tumor-Associated Macrophages: From Mechanisms to Therapy. Immunity. 2014; 41: 866.
10. JJ O'Shea, M Pesu, DC Borie, PS Changelian. A new modality for immunosuppression: targeting the JAK/STAT pathway. Nat. Rev. Drug Discov. 2004; 3: 555–564.
11. Sydney R Gordon, Roy L Maute, Ben W Dulken, Gregor Hutter, Benson M George, et al. PD-1 expression by tumour-associated macrophages inhibits phagocytosis and tumour immunity. Nature. 2017; 545: 495–499.
12. Anatomy, histology and immunohistochemistry of normal human skin. Available online at: https://pubmed.ncbi.nlm.nih.gov/12095893/
13. JY Lin, DE Fisher. Melanocyte biology and skin pigmentation. Nature. 2007; 445: 843–850.
14. A Nemmar, S Al-Salam, S Beegam, P Yuvaraju, BH Ali. Waterpipe Smoke Exposure Triggers Lung Injury and Functional Decline in Mice: Protective Effect of Gum Arabic. Oxid. Med. Cell. Longev. 2019; 2019.
15. FL Meyskens, PJ Farmer, H Anton-Culver. Etiologic pathogenesis of melanoma: a unifying hypothesis for the missing attributable risk. Clin. Cancer Res. Off. J. Am. Assoc. Cancer Res. 2004; 10: 2581–2583.
16. S Kozmin, G Slezak, A Reynaud-Angelin, C Elie, Y de Rycke, et al. UVA radiation is highly mutagenic in cells that are unable to repair 7,8-dihydro-8-oxoguanine in Saccharomyces cerevisiae. Proc. Natl. Acad. Sci. U. S. A. 2005; 102.
17. M Ichihashi, M Ueda, A Budiyanto, T Bito, M Oka, et al. UV-induced skin damage, Toxicology, vol. 189, no. 1–2, pp. 21–39, Jul. 2003, doi: 10.1016/s0300-483x(03)00150-1.
18. E Obrador, F Liu-Smith, RW Dellinger, R Salvador, FL Meyskens, et al. Oxidative stress and antioxidants in the pathophysiology of malignant melanoma. Biol. Chem. 2019; 400: 589–612.
19. Sara Gandini, Francesco Sera, Maria Sofia Cattaruzza, Paolo Pasquini, Orietta Picconi, et al. Meta-analysis of risk factors

for cutaneous melanoma: II. Sun exposure. Eur. J. Cancer. 2005; 41: 45–60.
20. C Karimkhani, AC Green, T Nijsten, MA Weinstock, RP Dellavalle,et al. The global burden of melanoma: results from the Global Burden of Disease Study 2015. Br. J. Dermatol. 2017; 177: 134–140.
21. E de Vries, FI Bray, JWW Coebergh, DM Parkin. Changing epidemiology of malignant cutaneous melanoma in Europe 1953-1997: rising trends in incidence and mortality but recent stabilizations in western Europe and decreases in Scandinavia. Int. J. Cancer. 2003; 107: 119–126.
22. Svetomir N Markovic, Lori A Erickson, Ravi D Rao, Roger H Weenig, Barbara A Pockaj, et al. Malignant Melanoma in the 21st Century, Part 1: Epidemiology, Risk Factors, Screening, Prevention, and Diagnosis. Mayo Clin. Proc. 2007; 82: 364–380.
23. C Dahl, P Guldberg. The genome and epigenome of malignant melanoma. APMIS Acta Pathol. Microbiol. Immunol. Scand. 2007; 115: 1161–1176.
24. E Muñoz-Couselo, EZ Adelantado, C Ortiz, JS García, J Perez-Garcia. NRAS-mutant melanoma: current challenges and future prospect. OncoTargets Ther. 2017; 10: 3941–3947.
25. M Pons, M Quintanilla. Molecular biology of malignant melanoma and other cutaneous tumors. Clin. Transl. Oncol. Off. Publ. Fed. Span. Oncol. Soc. Natl. Cancer Inst. Mex. 2006; 8: 466–474.
26. RI Hartman, JY Lin. Cutaneous Melanoma-A Review in Detection, Staging, and Management. Hematol. Oncol. Clin. North Am. 2019; 33: 25–38.
27. Jeffrey E Gershenwald, Richard A Scolyer, Kenneth R Hess, Vernon K Sondak, Georgina V Long, et al. Melanoma staging: Evidence-based changes in the American Joint Committee on Cancer eighth edition cancer staging manual. CA. Cancer J. Clin. 2017; 67: 472–492.
28. MI Ross, JE Gershenwald. Evidence-based treatment of early-stage melanoma. J. Surg. Oncol. 2011; 104: 341–353.
29. JJ Luke, KT Flaherty, A Ribas, GV Long. Targeted agents and immunotherapies: optimizing outcomes in melanoma. Nat. Rev. Clin. Oncol. 2017; 14: 463–482.

30. BD Curti, MB Faries. Recent Advances in the Treatment of Melanoma. N. Engl. J. Med. 2021; 384: 2229–2240.
31. A Rotte. Combination of CTLA-4 and PD-1 blockers for treatment of cancer. J. Exp. Clin. Cancer Res. 2019; 38: 255.
32. BY Reddy, DM Miller, H Tsao. Somatic driver mutations in melanoma: Somatic Driver Mutations in Melanoma. Cancer. 2017; 123: 2104–2117.
33. M Raman, W Chen, MH Cobb. Differential regulation and properties of MAPKs. Oncogene. 2007; 26: 3100–3112.
34. Peter J Murray, Judith E Allen, Subhra K Biswas, Edward A Fisher, Derek W Gilroy, et al. Macrophage activation and polarization: nomenclature and experimental guidelines. Immunity. 2014; 41: 14–20.
35. Qiong-wen Zhang, Lei Liu, Chang-yang Gong, Hua-shan Shi, Yun-hui Zeng, et al. Prognostic significance of tumor-associated macrophages in solid tumor: a meta-analysis of the literature. PloS One. 2012; 7: e50946.
36. Andrew J Gentles, Aaron M Newman, Chih Long Liu, Scott V Bratman, Weiguo Feng, et al. The prognostic landscape of genes and infiltrating immune cells across human cancers. Nat. Med. 2015; 21: 938–945.
37. DM Mosser, JP Edwards. Exploring the full spectrum of macrophage activation. Nat. Rev. Immunol. 2008; 8: 958–969.
38. Targeting Tumor-Associated Macrophages in Cancer. Available online at: https://pubmed.ncbi.nlm.nih.gov/30890304/
39. MR Hussein. Tumour-associated macrophages and melanoma tumourigenesis: integrating the complexity. Int. J. Exp. Pathol. 2006; 87: 163–176.
40. Luciana R Muniz-Bongers, Christopher B McClain, Mansi Saxena, Gerold Bongers, Miriam Merad, et al. MMP2 and TLRs modulate immune responses in the tumor microenvironment. JCI Insight. 2021; 6.
41. H Guo, L Zhou, J Guo, X Huang, J Gu. Endostatin inhibits the proliferation and migration of B16 cells by inducing macrophage polarity to M1-type. Mol. Med. Rep. 2021; 24: 841.
42. Xinming Su, Alison K Esser, Sarah R Amend, Jingyu Xiang, Yalin Xu, et al. Antagonizing Integrin β3 Increases

Immunosuppression in Cancer, Cancer Res. vol. 76, no. 12, pp. 3484–3495, Jun. 2016, doi: 10.1158/0008-5472.CAN-15-2663.
43. Junko Johansson, Jan Siarov, Roberta Kiffin, Johan Mölne, Jan Mattsson, et al. Presence of tumor-infiltrating CD8+ T cells and macrophages correlates to longer overall survival in patients undergoing isolated hepatic perfusion for uveal melanoma liver metastasis. Oncoimmunology. 2020; 9: 1854519.
44. Yu Kou, Liyan Ji, Haojia Wang, Wensheng Wang, Hongming Zheng, et al. Connexin 43 upregulation by dioscin inhibits melanoma progression via suppressing malignancy and inducing M1 polarization. Int. J. Cancer. 2017; 141: 1690–1703.
45. Yuan Tian, Yantong Guo, Pei Zhu, Dongxu Zhang, Shanshan Liu,et al. TRIM59 loss in M2 macrophages promotes melanoma migration and invasion by upregulating MMP-9 and Madcam1. Aging. 2019; 11: 8623–8641.
46. Y Shu, P Cheng. Targeting tumor-associated macrophages for cancer immunotherapy. Biochim. Biophys. Acta Rev. Cancer. 2020; 1874: 188434.
47. H Liu, L Yang, M Qi, J Zhang. NFAT1 enhances the effects of tumor-associated macrophages on promoting malignant melanoma growth and metastasis. Biosci. Rep. 2018; 38: BSR20181604.
48. JL Hood. Melanoma exosome induction of endothelial cell GM-CSF in pre-metastatic lymph nodes may result in different M1 and M2 macrophage mediated angiogenic processes. Med. Hypotheses. 2016; 94: 118–122.
49. Magdalena Jarosz-Biej, Natalia Kamińska, Sybilla Matuszczak, Tomasz Cichoń, Jolanta Pamuła-Piłat, et al. M1-like macrophages change tumor blood vessels and microenvironment in murine melanoma. PloS One. 2018; 13: e0191012.
50. Kazuya Yamada, Akihiko Uchiyama, Akihito Uehara, Buddhini Perera, Sachiko Ogino, et al. MFG-E8 Drives Melanoma Growth by Stimulating Mesenchymal Stromal Cell-Induced Angiogenesis and M2 Polarization of Tumor-Associated Macrophages. Cancer Res. 2016; 76: 4283–4292.

51. B Ruffell, LM Coussens. Macrophages and therapeutic resistance in cancer. Cancer Cell. 2015; 27: 462–472.
52. Omid Hamid, Caroline Robert, Adil Daud, F Stephen Hodi, Wen-Jen Hwu, et al. Safety and tumor responses with lambrolizumab (anti-PD-1) in melanoma. N. Engl. J. Med. 2013; 369: 134–144.
53. Antoni Ribas, Omid Hamid, Adil Daud, F Stephen Hodi, Jedd D Wolchok, et al. Association of Pembrolizumab With Tumor Response and Survival Among Patients With Advanced Melanoma. JAMA. 2016; 315: 1600–1609.
54. Nanumi Han, Muhammad Baghdadi, Kozo Ishikawa, Hiraku Endo, Takuto Kobayashi, et al. Enhanced IL-34 expression in Nivolumab-resistant metastatic melanoma. Inflamm. Regen. 2018; 38: 3.
55. Binghe Tan, Xiujuan Shi, Jie Zhang, Juliang Qin, Na Zhang, et al. Inhibition of Rspo-Lgr4 Facilitates Checkpoint Blockade Therapy by Switching Macrophage Polarization. Cancer Res. 2018; 78: 4929–4942.
56. SJ Thomas, JA Snowden, MP Zeidler, SJ Danson. The role of JAK/STAT signalling in the pathogenesis, prognosis and treatment of solid tumours. Br. J. Cancer. 2015; 113: 365–371.
57. B Groner, V von Manstein. Jak Stat signaling and cancer: Opportunities, benefits and side effects of targeted inhibition. Mol. Cell. Endocrinol. 2017; 451: 1–14.
58. STAT3 Establishes an Immunosuppressive Microenvironment during the Early Stages of Breast Carcinogenesis to Promote Tumor Growth and Metastasis. Available online at: https://pubmed.ncbi.nlm.nih.gov/26719528/
59. K Takeda, S Akira. STAT family of transcription factors in cytokine-mediated biological responses. Cytokine Growth Factor Rev. 2000; 11: 199–207.
60. C Schindler, DE Levy, T Decker. JAK-STAT signaling: from interferons to cytokines. J. Biol. Chem. 2007; 282: 20059–20063.
61. H Yu, R Jove. The STATs of cancer--new molecular targets come of age. Nat. Rev. Cancer. 2004; 4: 97–105.
62. A Yoshimura. Signal transduction of inflammatory cytokines and tumor development. Cancer Sci. 2006; 97: 439–447.

63. C Nicholas, GB Lesinski, C Nicholas, GB Lesinski. The Jak-STAT Signal Transduction Pathway in Melanoma. IntechOpen. 2011.
64. GP Dunn, CM Koebel, RD Schreiber. Interferons, immunity and cancer immunoediting. Nat. Rev. Immunol. 2006; 6: 836–848.
65. DH Kaplan, V Shankaran, AS Dighe, E Stockert, M Aguet, et al. Demonstration of an interferon gamma-dependent tumor surveillance system in immunocompetent mice. Proc. Natl. Acad. Sci. U. S. A. 1998; 95: 7556–7561.
66. CD163 as a novel target gene of STAT3 is a potential therapeutic target for gastric cancer. Available online at: https://pubmed.ncbi.nlm.nih.gov/29152078/
67. Brendan J Jenkins, Dianne Grail, Melissa Inglese, Cathy Quilici, Steven Bozinovski, et al. Imbalanced gp130-dependent signaling in macrophages alters macrophage colony-stimulating factor responsiveness via regulation of c-fms expression. Mol. Cell. Biol. 2004; 24: 1453–1463.
68. L Cassetta, JW Pollard. Targeting macrophages: therapeutic approaches in cancer. Nat. Rev. Drug Discov. 2008; 17: 887–904.
69. CSF-1 receptor signaling in myeloid cells. Available online at: https://pubmed.ncbi.nlm.nih.gov/24890514/
70. Targeted gene silencing of CCL2 inhibits triple negative breast cancer progression by blocking cancer stem cell renewal and M2 macrophage recruitment. Available online at: https://pubmed.ncbi.nlm.nih.gov/27283985/
71. CE Lewis, JW Pollard. Distinct role of macrophages in different tumor microenvironments. Cancer Res. 2006; 66: 605–612.
72. Graham Thomas, Luca Micci, Wenjing Yang, Joseph Katakowski, Cecilia Oderup, et al. Intra-Tumoral Activation of Endosomal TLR Pathways Reveals a Distinct Role for TLR3 Agonist Dependent Type-1 Interferons in Shaping the Tumor Immune Microenvironment. Front. Oncol. 2021; 11: 711673.
73. Manisha Singh, Hiep Khong, Zhimin Dai, Xue-Fei Huang, Jennifer A Wargo, et al. Effective innate and adaptive antimelanoma immunity through localized TLR7/8

activation. J. Immunol. Baltim. Md 1950. 2014; 193: 4722–4731.
74. AK Singh, JP McGuirk. CAR T cells: continuation in a revolution of immunotherapy. Lancet Oncol. 2020; 21: e168–e178.
75. C Sloas, S Gill, M Klichinsky. Engineered CAR-Macrophages as Adoptive Immunotherapies for Solid Tumors. Front. Immunol. 2021; 12: 783305.
76. Yizhao Chen, Zhiying Yu, Xuewen Tan, Haifeng Jiang, Zhen Xu, et al. CAR-macrophage: A new immunotherapy candidate against solid tumors, Biomed. Pharmacother. Biomedecine Pharmacother. 2021; 139: 111605.
77. Anna-Maria Georgoudaki, Kajsa E Prokopec, Vanessa F Boura, Eva Hellqvist, Silke Sohn, et al. Reprogramming Tumor-Associated Macrophages by Antibody Targeting Inhibits Cancer Progression and Metastasis. Cell Rep. 2016; 15: 2000–2011.

Book Chapter

Liquid Biopsy in Non-Small Cell Lung Cancer (NSCLC): State of the Art and the Next Opportunity

Carl KHAWLY

Cancer Research Center of Toulouse (CRCT), France

***Corresponding Author:** Carl KHAWLY, Cancer Research Center of Toulouse (CRCT), France

Published **December 13, 2022**

How to cite this book chapter: Carl KHAWLY. Liquid Biopsy in Non-Small Cell Lung Cancer (NSCLC): State of the Art and the Next Opportunity. In: Hussein Fayyad Kazan, editor. Immunology and Cancer Biology. Hyderabad, India: Vide Leaf. 2022.

Abstract

With lung cancer maintaining alarming mortality rates, the clinic calls for sensitive cancer screening tools. This need is dire for the nine-out-of-ten patients experiencing the non-small cell variant (NSCLC) that deploys high rates of drug resistance. The concept of liquid biopsy is nothing short of a breakthrough in precision oncology. Not only did recent advancements demonstrate the competence of liquid biopsy technologies but also showed that this new paradigm is here to stay. Based on peer-reviewed journals and publicly available information from the industry leaders, this chapter depicts the state of the art of liquid biopsy in

NSCLC patient monitoring, the different clinical and academic uses, an objective view of the field, and the advancements we can expect to see in the coming years that will push the boundaries of precision medicine.

Introduction

Lung cancer leads cancer lethality rates causing nearly two out of every ten cancer deaths [2]. Non-small-cell lung cancer (NSCLC) presents exceptional cellular heterogeneity and a broad spectrum of resistance mechanisms [3]. An added problem is that the tumor does not relinquish reliable biomarkers that facilitate detection or gauge treatment efficiency. A few parameters can make or break patient outcomes, including detection sensitivity and the ability to obtain a tumor profile. But lung cancer poses problems in the clinic as well. The difficulty of performing tissue biopsy for lung cancer patients and the percentage of tumors that could go below the radar of imaging techniques are worrying. Meanwhile, doctors would still be pressed for a decision – even amid such uncertainty. This is when the fifteen minutes of liquid biopsy started. The need for biomarkers, the difficulty of obtaining tissue biopsy, and the inferior sensitivity of CT scans [4] all primed liquid biopsy to be the next gold standard. Liquid biopsy has the potential to coin the term ‘precision medicine.’ It has the power to transform the clinical workflow by circumventing the hurdles of traditional protocols, all the while improving patient outcomes, alleviating the stress and uncertainty of decision-making, and improving the quality of patient care. The past decade witnessed technical advancements in PCR and sequencing methods and trial output. This enhanced the reliability of liquid biopsy as the preferred method of analysis for some clinical settings and a complement to tissue analysis in others. But the march to the clinic is not over, and we are yet to see the best of liquid biopsy. This chapter depicts the recent advancements in liquid biopsy for NSCLC and highlights opportunities to push the boundaries of the field.

Liquid biopsy is the analysis of body fluids for information about the pathological state (Figure 1). It is used in cancer as an alternative to tissue (solid) sampling to diagnose or follow

disease progression using tumor components present in body fluids – mainly blood. Liquid biopsy relies on the isolation and enrichment of tumor components from the rest of the blood, like isolating ctDNA from the pool of cell-free DNA (cfDNA). Despite tissue sampling being the gold standard for tumor profiling, and CT scans being the standard for detection, liquid biopsy has clear advantages. Compared to tissue sampling, liquid biopsy is non-to-minimally invasive, repeatable, requires a small sample volume, and provides information from all locations as opposed to a single locus provided by tissue biopsy. Compared to CT scans, it is radiation-free and more sensitive [4]. A growing list of tumor components can be isolated from patient blood, including circulating tumor DNA (ctDNA), circulating tumor cells (CTCs), platelets, vesicles, and RNA. Different isolation, enrichment, and analysis techniques are developed, and different outputs are drawn from each.

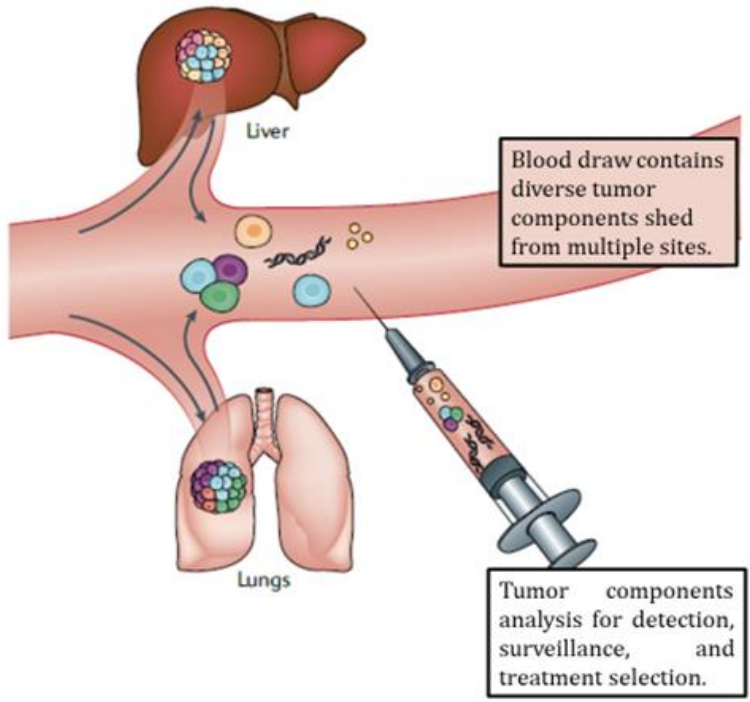

Figure 1: Liquid biopsy illustration, adapted from Ignatiadis and colleagues [1].

Circulating Tumor DNA (ctDNA)

CtDNA analysis is the flagship product of liquid biopsy. Being the most established component of the tumor, sequencing and PCR-based assays are witnessing improvement and a high number of ongoing trials to demonstrate the competence of this parameter. Tumor DNA represents a fraction of the pool of cell-free DNA (cfDNA) in plasma, often referred to as mutant-allele fraction (MAF). This fraction strikingly ranges between 0.01 and 90% [5]. Although this proportion is parallel to the tumor load, patients with the same cancer type can show different MAF [6]. The half-life of ctDNA is just shy of two hours, making it a real-time snapshot of the tumor profile. CtDNA is analyzed using one of two methodologies: polymerase chain reaction (PCR) or next generation sequencing (NGS) – each having its merits. PCR-based technologies (ddPCR, BEAMing) partition the sample and allow high sensitivity of detection that can reach 0.01% MAF [7,8]. However, PCR can only detect known mutations and is not suitable for high-throughput analyses nor for detecting new mutations. Contrarily, NGS sacrifices sensitivity for a more comprehensive tumor profile. NGS allows the discovery of new mutations in the blood of patients and high throughput screening of samples. Recent advancements in NGS technology allowed it to compete in sensitivity with PCR [24]. However, price is still an issue. NGS runs cost anywhere in the four-digit ballpark. Both approaches have clinical employment, and the choice depends on the clinical application. The best-case scenario would be having a highly sensitive, cost-effective, and fast NGS platform that would be one fit for all.

Circulating Tumor Cells CTCs

CTCs hold a versatile edge over ctDNA. With tumor cells at hand, both genetic and biological assessments are possible. The ability to capture CTCs opened more possibilities, like CTC-derived xenografts, by expanding CTCs from patients to immune-compromised mice [9]. Immunohistochemical staining and FISH can be done on CTCs [10]. NSCLC is also known for the ALK rearrangements that are difficult to detect via ctDNA, making CTCs staining an efficient alternative [10]. Monitoring

patients' CTCs is a booming field with plenty of room for imagination. This is evident from the capital pouring in and the innovation in detection, capture, enrichment, and analyses performed on tumor cells. Peculiarities of CTCs can be combined with ctDNA profiling – potentially giving birth to a comprehensive approach for patient monitoring, i.e., eradicating the need for validation using tissue biopsy. Tumor DNA and cell analysis holds promise for the future but is facing technical hurdles on its way to the clinic. Meanwhile, new players are emerging with the potential to complement the shortcomings of DNA and circulating cells.

Tumor-Educated Platelets TEPs

Platelets serve as a warehouse of high-quality tumor RNA molecules. They give direct insight into the exome of the tumor. Platelets are the second-most abundant cell type in blood. Robust isolation and purification protocols are already established. The tumor 'educates' blood platelets by an influx of information via vesicles that contain RNA [11]. Platelets are also proven to collude with CTCs: information exchange, protecting CTCs from the shearing forces in the blood circulation, and immune protection by transferring MHC I molecules to the surface of CTCs allowing their escape from NK cell recognition [11]. The relationship with tumors positions platelets as subjects for clinical investigation and further investment.

Extracellular vesicles (Exosomes)

Another way tumors thrive – and give up information – is by exosomal secretion. By carrying a plethora of tumor cargo (DNA, RNA, and proteins), vesicles provide genomic and metabolomic insight into tumor biology. Exosome secretion is exaggerated in tumors [12]. They are involved in angiogenesis, EMT, invasion, metastasis, immune escape, drug resistance, and other aspects of resistance and survival of tumors and are hot prospects in liquid biopsy [12,13]. Exosomes shelter their components and allow for supplementary ctDNA and RNA/miRNA analyses. Accumulating evidence in the literature

backs exosomes for being diagnostic, prognostic, and predictive biomarkers and another potential versatile tool in the clinic [34].

RNA Tumor Components

Amid the genetic mesh, what makes the difference inside tumors is what is being expressed – or what is not. RNA adds this dimension to the clinical tumor analysis. Aside from mRNA, non-coding RNA molecules are slowly taking the limelight. New players include miRNA, circRNA, and lncRNA. MicroRNA (miRNA) interferes in gene expression by binding mRNA and preventing it from being translated into protein. Tumors avail miRNAs that target tumor-suppressor genes [14]. Detecting miRNA fragments in plasma depicts epigenetic regulation inside the tumor cell. Circular RNA (circRNA) audits miRNA activity by acting as a sponge against miRNA. Pro-tumor circRNAs are up-regulated in cancers to dampen miRNAs that target oncogenic proteins [15]. Long non-coding RNAs (lncRNAs) are also regulatory molecules that act on nucleic-acid binding proteins (e.g., histones) [16]. All three non-coding forms of RNA are proven to be biomarker material for lung cancers as well as therapeutic vehicles (circRNA and lncRNA) [17]. The performance of RNA molecules hinted at possible future employment in the early detection of lung cancers [18].

Post-enrichment sample analysis uses a variety of multidisciplinary technologies and platforms. For ctDNA and RNA, analysis requires either polymerase chain reaction or sequencing technologies. CTCs, platelets, and vesicles are versatile and can be utilized for genomic (DNA, RNA) analyses, morphological (shape and size), metabolomic (protein composition), and biological (functionality) ones [19].

Employment of liquid biopsy spans all stages of disease development. It can be used for the detection of the disease, following progression upon treatment (longitudinal follow-up), testing for minimal residual disease (MRD), and screening for resistance mechanisms and alternative drug targets [20]. Numerous tests and kits for ctDNA and CTCs monitoring have been approved by the FDA for certain cancer types. Those

endorsements include: Cobas, Guardant360 CDx, FoundationOne CDx (ctDNA), CancerSEEK (ctDNA and protein biomarkers), CellSearch (CTCs), and more! [21].

NSCLC Cooperativeness

To detect tumor components in blood samples, they must break free from the tumor and enter the circulation. What constitutes 'cooperativeness' is how efficiently the tumor debris makes it to the blood stream. Wide discrepancies in MAF are observed among patients [22]. This phenomenon is governed by biological parameters including the location of the tumor relative to the bloodstream, the rate of cell death, and ctDNA suppression by treatment. A pan-cancer study combining samples from 10,000 patients demonstrated that both variants of lung cancer (NSCLC and SCLC) and pancreatic cancer showed relatively high detectability of ctDNA in patient blood samples [23]. Contrary to what was seen in more introverted tumors like renal, breast, and brain. Another study in a smaller cohort showed a promising 100% detectability of ctDNA across NSCLC patients in stages II-IV. The sensitivity of NSCLC ctDNA detection was shown to be correlated to tumor size. NSCLC also exhibits detectability, although variable, in earlier tumor stages [24]. Concordance between liquid and tissue biopsy is commonly used as a reference [23]. The literature suggests that NGS results between plasma and tumor are reproducible. Therefore, discrepancies predominantly stem from additional information ctDNA uncovers – which gives plasma analysis an edge over tissue samples, as mentioned earlier. Gauging such numbers, especially in earlier stages, is crucial before pushing the diverse areas of employment for liquid biopsy approaches like early detection and minimal residual disease follow-up.

State of the Art

Early Detection

Nothing holds more promise for the future of cancer diagnosis than a robust early detection system. Catching NSCLC in the 'controllable' stages is key to improving patient outcomes. A 2018 study used a multi-analyte test called Cancer SEEK on a

cohort of 1,005 patients of various cancer types. Cancer SEEK attempted detection of resectable cancers using both ctDNA and protein biomarkers. The scientists at Johns Hopkins were able to detect cancers with an overall 99% specificity and a 69-98% sensitivity. Cancer SEEK is an FDA-approved test as of 2019 [25]. But perhaps the most promising results in NSCLC were delivered at Stanford University using Cancer Personalized Profiling by deep Sequencing (CAPP-Seq), where 100% of NSCLC tumors in stages II-IV were detected [24]. Like the Cancer SEEK blood test, combinatorial approaches add a sense of certainty to the test, which manifests in higher sensitivities. CTC analysis had a 100% concordance with tissue biopsy when analyzed for mutations using PCR, cell count, and single-cell-level gene expression for molecular characterization. A combination of genomic and expression level analyses on CTCs holds the potential for circumventing the lack of biomarkers in NSCLC. Positioning platelets and miRNAs as predictive biomarkers in NSCLC is showing encouraging returns. The best result was obtained in a cohort of 283 patients. Platelet-derived RNA-Seq was able to distinguish the 55 healthy individuals from the 228 patients with 96% accuracy [26]. Two other studies on NSCLC cohorts attempted to detect early-stage disease using miRNAs. The studies showed sensitivities and specificities in the 80-90% ballpark, seemingly outperforming ctDNA in the early stages [27,28]. In the two ctDNA studies, NSCLC stage I tumors went undetected in nearly half the cases (50-60% sensitivity). Judging by results from two different approaches, this talks more about the biology of NSCLC tumors in early stages – Stage I NSCLC could be invisible to plasma analysis. This stimulates the search for other tumor components that improve detectability. But even when early detection falls short, longitudinal monitoring constantly reports significantly better prognosis and survival in patients with undetected ctDNA in the early stages compared with those who flash signs of the disease early [29]. Such correlation adds value to liquid biopsy by positioning tumor components as prognostic factors.

Prognosis

Physicians encounter a plethora of drug resistance mechanisms, relapse in nearly 100% of patients, and an overwhelming number of options and combinations of therapeutics [30]. Predictive and prognostic values are capable of alleviating the stress of decision-making. Collecting data to establish the best therapeutic options has been one area of employment for liquid biopsy. This is achieved by demonstrating the outcomes of therapeutic choices and establishing a consensus for each case. All ctDNA assessments report better prognosis and higher survival for patients with undetected ctDNA. This can extend to establishing the predictive value of mutations. A study attempted to map the effect of somatic copy number variation (SCNV) on the therapeutic outcome using ddPCR and shallow NGS. It was proven that SCNV in resistance-related genes had significantly lower progression-free survival, overall survival, and response rate to Osimertinib [31]. Additionally, the EURTAC intended to compare the efficiency of erlotinib to chemotherapy as a first-line treatment in NSCLC. By analyzing the cfDNA of participants using PCR, the trial pointed out that the presence of the L858R mutation marked a reduction of overall survival by half (13.7 vs. 27.7 months) [32]. In a cohort of NSCLC patients stages III to IV, the presence of fewer than 5 CTCs per blood sample (7.5 ml) correlated to a 2-3-fold increase in progression-free and overall survival. CTCs were also the strongest predictor of overall survival in multivariate analysis [33]. Besides ctDNA and CTCs, smaller tumor components carry a predictive value of their own. Exosome-derived miRNA has been proven to induce resistance to cisplatin (DDP) in A549 cell lines (a lung adenocarcinoma cell line). A different miRNA molecule was shown to desensitize cells to the same chemotherapy [34]. Choosing chemotherapy is a tough call to make. This showcases an opportunity to test for either plasma exosomes or miRNA as prognostic factors prior to chemotherapy treatment. Extrapolation of such *in vitro* studies on patient cohorts could prove valuable for the prognosis of this option.

Tracking Changes in Tumor Profile

Longitudinal follow-up is one of the most widely – and rapidly – adopted uses of liquid biopsy. Endorsement of plasma analysis is accelerating, especially in lung cancer. A liquid biopsy allows for baseline measurement of the tumor mutational status. This occurs during diagnosis and before any treatment is administered. One approved use of NGS is screening for EGFR mutations which select patients for first-line TKI treatment. Initial screening allows for the selection of drugs according to the tumor profile provided by NGS. However, this does not guarantee a relapse-free journey. As mentioned earlier, NSCLC tumors switch between resistance mechanisms to survive the pressure of treatment, and relapse is almost inevitable in NSCLC – rendering the first line of treatment inefficient. A successful selection of the second-line treatment warrants tracking ctDNA mutations and anticipating resistance mechanisms early by a repetitive follow-up of the tumor profile. But taking repetitive tissue biopsies to analyze how the tumor evolves is not feasible for lung cancer, and CT scans provide no genetic and molecular information. Meanwhile, the repeatability of liquid biopsies allows for constant patient surveillance. The residual disease is detectable in ctDNA months before light patches are visible on the X-ray [4,35,36]. Liquid biopsy has demonstrated its superiority to CT imaging in terms of sensitivity. Plasma analysis is now the preferred choice for clinicians for longitudinal follow-up of patients. Longitudinal follow-up not only anticipates relapse but also depicts the tumor profile and which mutations will amplify after the first line of treatment. Another example of how liquid biopsy can hedge against guesswork and aid decision-making is in the case of ALK rearrangements. Similar to EGFR, ALK is another tyrosine kinase driver of NSCLC. But unlike EGFR, ALK can be activated in two ways: an activating mutation or a rearrangement in the receptor. The problem with ALK rearrangements is that there are no solid criteria to select the proper TKI treatment for ALK-positive patients. Using NGS can identify and quantify ALK rearrangements and mutations and narrow down the options for a better selection of therapeutics

[37]. Approval for using NGS for ALK-positive NSCLC has been granted [38].

Platelets are another prominent element in NSCLC research. Monitoring plasma mutations using RT-qPCR on platelet-derived RNA isolated from advanced NSCLC patients surpassed the gold-standard FISH technique in terms of sensitivity, specificity, and accuracy in detecting ALK rearrangements [39].

Beyond mutations, ctDNA analysis in NSCLC can also assess gene changes such as loss of heterozygosity, microsatellite instability, and gene methylation [40-42]. All pivotal intra-tumor events inform clinicians about cancer behavior and allow for other therapy options. But perhaps the most appealing use of NGS is uncovering new druggable targets. This benefit was demonstrated in 53 patients with difficulty in tissue sampling who were assessed using Guradant360 NGS genotyping. Actionable mutations appeared in 12 patients who then received corresponding therapies and had significant clinical benefits [43]. As time passes, repetitive monitoring of patients by liquid biopsy adds value to precision oncology by default. One hidden benefit that liquid biopsy trials are accumulating is uncovering molecular patterns of resistance. Depending on the patient's mutational status at baseline, the physician might prescribe Osimertinib as a first-line treatment or leave it to a possible second line (in case resistance emerges). One striking phenomenon observed in NSCLC is that frequencies of resistance mechanisms are different when Osimertinib is chosen for first-line therapy instead of a second-line – despite being the same drug [44]. Evaluating the molecular profile allows for observing a pattern in resistance mechanisms resulting from each choice. One example is the AURA3 trial. Researchers utilized the Guardant360 NGS platform to track mutational profile evolution as a function of Osimertinib treatment. 15% of the cohort in the trial acquired EGFR mutations (mainly C797S), while 19% showed MET receptor amplification [44]. Another study used ddPCR to find that the ratio of the amount of the T790M mutation to the EGFR activating mutation correlated with the response to Osimertinib [45].

Without a doubt, liquid biopsy clears the fog and narrows down imprecision on different fronts. The field promises to cover tumor biology blind spots, enhance patient outcomes, and improve the quality of life for cancer patients. But the race to the clinic is far from over. Plenty of building blocks still need to be laid – and plenty of opportunity still exists.

The Next Opportunity

Both academia and the industry report an influx of innovation in the field, meaning liquid biopsy is shaping up by the day. However, the uses mentioned in Section IV are only seen in research and trials and not yet in the clinic. New technology needs more than a proof of concept to make it to the clinical routine. Despite being approved for several uses, especially in the niche of longitudinal follow-up, liquid biopsy clinical use is currently restricted to only a few specific cases. The IASLC surveyed 2537 health professionals from Asia, Europe, the US and Canada, Latin America, and the rest of the world [46]. The survey showed that cost is the main barrier to the adoption of ctDNA analysis (Figure 2). Money is one of many concerns of thought leaders in the field as liquid biopsy's journey to the clinic warrants multidisciplinary efforts – and a wealth of opportunity. Here are some aspects of liquid biopsy that will be groomed in the coming years.

Technology Transfer

For a new paradigm to leap to the clinic, it will be molded and polished into a more practical form that fits the day-to-day clinical work. A process termed technology transfer. Technology transfer guarantees (1) a user-friendly interface that shortcuts the complexities of the academic bench work, (2) reproducibility of the results observed in the academic literature in the absence of academic expertise, (3) agile modes of operation with minimal training required, and (4) standard pre-analytical and analytical procedures. The leap to the clinic allows all user interface and commercialization experts in the life sciences industries to help push this forward. However, a prerequisite for technology

transfer is consensus about the protocols and workflow followed in the field, which is another box to check.

Standardization of Procedures

Discrepancies between platforms are a cause for concern. Two commercially available NGS platforms could yield different results for the same population of patients [47]. This could be attributed to the sample preparation process that alters the sample. For liquid biopsy to be reliable, it has to be reproducible. Hence the importance of agreement on the optimal conditions and best practices in all phases of sample and data processing. Modern healthcare still suffers from a high percentage of pre-analytical errors to the total laboratory testing errors (62-68%) [48]. Blood samples are susceptible to bad storage, DNA degradation, and blood cells lysis diluting the pool ctDNA with more unwanted healthy genetic material. Such hurdles pushed standardizing sample handling and processing procedures to the top of the agenda of thought leaders. BloodPAC is an American initiative specialized in information transfer among stakeholders: academia, industry, regulatory authorities, and the public media. BloodPAC aims at galvanizing liquid biopsy assay adoption for improved patient outcomes. SPIDIA4P and SPIDIA European consortia address handling samples before *in vitro* diagnosis involving 10 European countries. CANCER-ID consortium specializes in standardizing protocols for blood-based biomarkers and involves partners from 13 European countries. The international association for the study of lung cancer (IASLC) is also placing liquid biopsy high on its agenda. In 2021 the IASLC released a consensus statement with a list of the recommended practices for sample treatment prior to cfDNA analysis [49]. The practices include the recommended volume of the sample, favoring plasma over serum, and rapid blood treatment after extraction. Such attempts to standardize the practice are crucial. Performing optimization and quality control experiments would complement those efforts and boost the regulatory process. As analysis techniques increase by the day, quality control needs to catch up by providing the optimal conditions for each workflow and each tumor component.

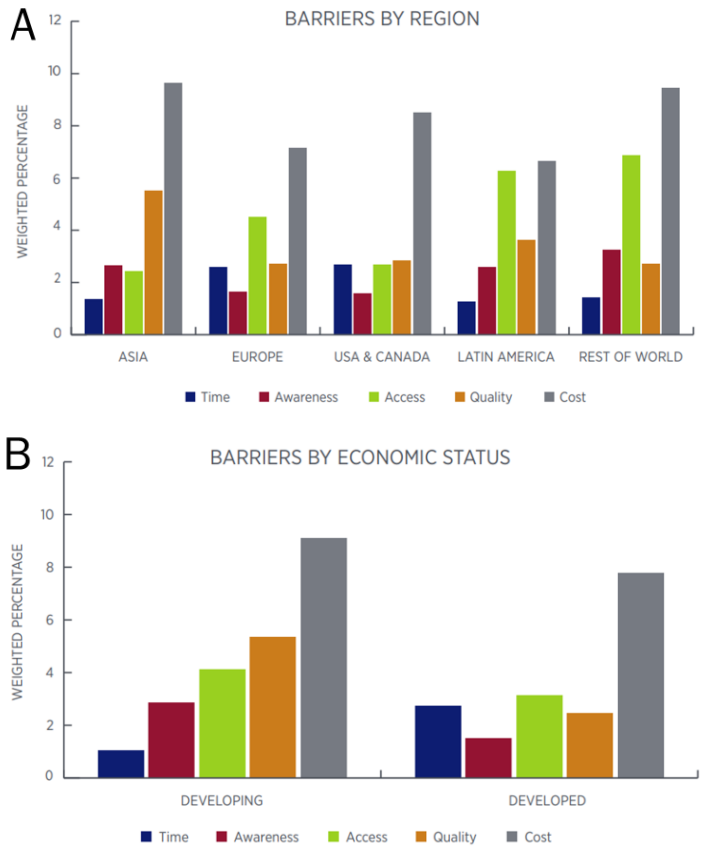

Figure 2: Most frequently reported barriers to molecular testing by (A) region of the world and (B) the economic status of the respondents' countries. Adopted from the IASLC global survey on molecular testing in lung cancer [46]. The survey clearly shows that cost is the major barrier regardless of the economic status of the population.

Clinical Validation

Liquid biopsy detects earlier, is more sensitive, and is more convenient. But is it tangibly helping? Clinical validation is simply demonstrating the added value of liquid biopsy, i.e., will the adoption of liquid biopsy indeed lead to statistical improvements in clinical outcomes and precision healthcare? One example is the additional mutations observed in plasma analysis. That could be justified by the fact that plasma

represents the mutations from different areas in the body and not just a single location like in the case of a tumor, which is more comprehensive and accurate. However, it is unclear whether acting on those mutations is of added value to the patient. The clinical utility of plasma analysis is to be demonstrated. Another example is improved sensitivity. Liquid biopsy can detect changes months before they appear on CT scans [4,35,36]. One of the next outlooks for thought leaders is capitalizing on this superpower for early detection and MRD, even in the absence of previous pathological diagnoses. But this presents another area where clinical utility needs to be showcased: will early detection lead to improved patient survival statistics? Will tumors be more 'controllable' if detected earlier? Lead time bias is one of the arguments against the benefit of earlier detection (Figure 3). Lead time bias refers to when patients appear to have longer survival only because detection was done earlier [50]. Finally, plasma DNA analysis allows us to deduce the density of unique mutations inside the cancer cell's coding genome - a parameter called tumor mutational burden (TMB). TMB measures the tumor's neo antigenic and neoplastic power [51]. A tumor with a higher frequency of mutations tends to grow more aggressively and express more surface proteins. TMB can be obtained from both tissue (tTMB) and blood (bTMB) samples. Because of such a correlation to the antigenic profile of a tumor cell, one could reason about a predictive role of TMB in patient response to immune checkpoint inhibitors (ICI) that assist the immune system in recognizing the tumor. Retrospective analysis of bTMB has shown that bTMB indeed predicted the outcome of patients treated with ICIs and combination treatments [52]. The technical difficulty in extracting tTMB could be circumvented shortly by the predictive power of bTMB, and exploiting this biological parameter definitely will have its place in the clinic with the surge in ICIs. bTMB "harmonization" experiments to assess reproducibility between different methodologies are expected soon [51-54]. Clinical utility is demonstrated by clinical trials using liquid biopsy techniques that go hand in hand with discovering new therapeutic molecules and technological improvement in analytical power.

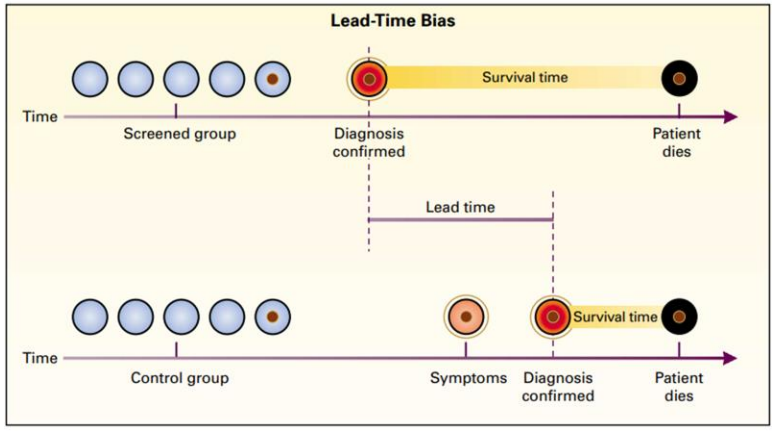

Figure 3: Lead time bias as illustrated by Patz and colleagues [50]. Disease diagnosis is done earlier in the screened group, resulting in an apparent increase in survival time (lead-time bias), although the time of death is the same in both groups.

Technical Hurdles

The most obvious need for improvement can be found in the technicalities of pre- and analytical procedures. CTCs, TEPs, exosomes, and RNAs are extremely interesting components. Each has its advantage over ctDNA analysis. However, complicated purification, capture, enrichment, and analysis protocols call for expertise on the bench and delay their arrival in the clinic. The biggest hurdle in CTCs is enrichment. The number of CTCs per ml of patient blood is a single digit. More sensitive enrichment methods are needed to more efficiently sort out and count CTCs and draw out more conclusions about tumors. TEPs and Exosomes face the same problems. Exosomes are showing the potential for high versatility in terms of analysis. However, their richness in the plasma is the bottleneck. Cost and efficiency are also limiting factors to be addressed. TEPs' promising attributes have their bottlenecks. TEPs adoption into the clinical routine demands validation using studies on larger cohorts of patients to demonstrate the potency of analyzing TEPs. Additionally, a round of simplifying the pre-analytical procedures is necessary for clinical incorporation. MicroRNAs have shown appealing results, except for normalization and

specificity. miRNA lacks a reliable normal to which we refer when analyzing [55]. Additionally, miRNA conservation among different tumors diminishes their biomarker status because they are not specific to tumor types. What can be improved for RNAs is validating the reliability of the pre-analytical procedures [55,56]. Despite being the most developed component, ctDNA analysis presents room for improvement. The spectrum of ctDNA analysis technologies ranges from PCR with high sensitivity but low throughput to NGS with high throughput and high cost. Finding alternatives that would bring costs down would revolutionize and field and spark the adoption of NGS technologies. Another dent in the reliability of ctDNA analysis is a phenomenon called clonal hematopoiesis of indeterminate potential (CHIP). Mutations detected in the pool of cfDNA could originate from this natural event that occurs in blood cells and are not of tumor origin. This spikes the pool of ctDNA and presents indistinguishable false positives [57]. The CHIP problem was mitigated in a large pan-cancer study by separately sequencing WBC [23]. This approach might rule out some biases. However, our best bet is to cross-validate ctDNA results with other parameters – like sequencing CTCs. Finally, it is notable that all ctDNA analysis techniques favor specificity over sensitivity. Therefore, the rate of false negatives trumps false positives [49]. Then when a negative result comes up, this result has to be validated by a tissue biopsy, as the negative predictive value of ctDNA is higher. Another window of opportunity is establishing complementarity between ctDNA, and CTCs analyses independent of tissue biopsy. That would circumvent the CHIP bias (as CTCs do not bear hematopoietic mutations), double-check the negative results of ctDNA, and drop the need for tissue biopsy to validate results.

A.I.

Machine learning is where countless opportunities hide. And because liquid biopsy is a relatively new approach, artificial intelligence did not have the time to fully catch up. One can see plenty of employment opportunities for artificial intelligence. Raw data coming from blood samples is noisy and hard to interpret manually. Machines would lift the weight of

interpreting, storing, and retrieving data. In addition, deducing patterns is complementary to mere data storage. With large volumes of trial results and longitudinal follow-ups, computers are good at drawing out tumor behavior patterns for the different types of therapy. Such patterns include the frequency by which mutations and resistance mechanisms arise in response to each drug. This data will be of high value once established, as it would point out patterns of emergence of mutations or resistance mechanisms. Finally, selecting drugs based on data can be daunting for the physician. Artificial intelligence can boost decision-making by narrowing down therapy options as well as present outcomes of previous trials, giving clinicians a landscape of scenarios of what to expect after every decision. Armed with data and outcomes of each drug option and biopsy results, A.I. would help deliver the right drug to the right patient, at the right time.

A Word to Academia

The contribution of fundamental research will be valuable in layering the rationale and credibility for using liquid biopsy. Many questions regarding the biology of tumors, shedding, and interaction between tumors and tumor components remain unanswered. The biology of TEPs' interaction with the tumor is not well established. This gap makes it natural to argue against the 'representativeness' of platelets to the tumor's actual exome. The interest in platelets calls for a clearer understanding of how the tumor exchanges information with those components and how reliable this mechanism is in TEPs as biomarkers. More clinical trials, proof of utility and mechanistic studies could place TEPs high in the clinical hierarchy. Exosomes and their miRNA cargo showed pivotal roles in tumor survival, communication, and overall biology [58,59]. Mechanistic insight into these roles would solidify such tumor derivatives as biomarker candidates. Investigating the tumor-tumor component relationship will undoubtedly be of added value to our reliance on plasma analysis. Finally, the resilience of NSCLC and the plethora of resistance mechanisms make it hard to ignore. Numerous explanations have surfaced on how the tumor develops resistance and whether it follows Darwinian selection or a more

Lamarckian model (Figure 4). A 2022 review highlighted the role of drug-tolerant persistent (DTP) cells that act as reservoirs of resistance mechanisms that are induced according to the stress in the medium [30]. The presence of such engines of resistance spikes interest in targeting them therapeutically or utilizing them as biomarkers. DTPCs present an opportunity for a leap in our understanding of cancer biology.

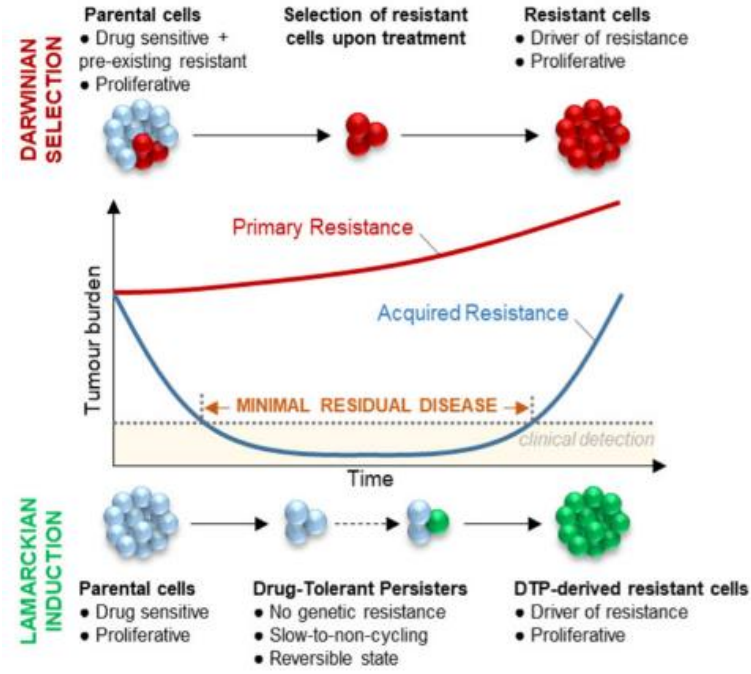

Figure 4: The two different models of clinical response to treatment in NSCLC. Primary resistance that resembles the Darwinian selection (red) exhibits very little initial response as the resistant clone is amplified. Meanwhile, the Lamarckian-like, DTP-derived resistant clones (green) are induced after a strong response to therapy and clearance of the tumor. Adapted from Delahaye et al [30].

Conclusion

What the market needs could turn out to be radically different from the initial purpose of the technology. Historically, before endorsing a new technology on a full scale, it has to go through

an ‘amorphous’ and uncertain phase. This phase lasts until the technology is molded to match the market needs and its most convenient uses are demonstrated. Liquid biopsy gave birth to a diversity of uses. It is not yet the gold standard for diagnosis and monitoring but is certainly shaping out of the uncertain introduction phase. A few years ago, the literature presented data with a dose of constraint. Today, we see a more optimistic presentation of trial results and a broader endorsement of new technologies. We see a clear trend in the scientific literature: liquid biopsy has already started to take shape. According to the director of the Thoracic Medical Oncology and the Early Clinical Trials Departments at the University of Maryland, Professor Christian Rolfo, there are two major obstacles: first is the price of liquid biopsy – especially for NGS assays that falls in the $1,000-$7,000 ballpark per run. The second big obstacle is false negative results for non-shedding patients, despite such assays being awaited eagerly. Until the field improves and achieves higher sensitivity, institutes should strive to respect standards, and boards should keep the use of NGS in check to avoid misinterpretation of NGS results. Efforts on the academic end are anticipated. High trial output, proof of clinical utility, and studies on tumor biology will clear out uncertainties and give the clinic a confidence interval to operate within. Standardizing workflows, sensitivity, and false negatives are still to be handled. One solution is to improve those aspects of the technology. But a more creative approach would be designing a new workflow that paves the way around these obstacles. Emerging new technologies are circumventing the pre-analytical hurdles. Electric field-induced release and measurement – or EFIRM – strikingly detected two major lung tumor mutations from the saliva of NSCLC patients with little to no sample preparation procedure [60]. EFIRM is still far from the market, but it promises to skip the pre-analytical impediment and provide a 100% non-invasive approach. The new ‘fragmentomics’ approach developed by Delfi Diagnostics is an example of novel technologies that made it to the market. By discerning ctDNA from healthy cfDNA using its differential fragmentation pattern, Delfi promises to skip the sequencing bottleneck and reduce the cost of ctDNA analysis compared to NGS by nearly 10-fold [61]. A few boxes need to be checked before we see liquid

biopsy as the gold standard for NSCLC patient care. But despite the rough patches, the clinical value of liquid biopsy is undeniable. Innovation is picking up, and capital is pouring into the startups. What we have at hand shows glimpses of its power. Papers present their 'Discussion' section with a tone of encouragement. We can see a continual influx of new trends and ideas – we can even predict upcoming ways the clinic will avail liquid biopsy. Such tendencies can only tell a few things: liquid biopsy is here to stay, and an accelerated endorsement is expected.

References

1. Ignatiadis M, Sledge GW, Jeffrey SS. Liquid biopsy enters the clinic - implementation issues and future challenges. Nature reviews. Clinical oncology. 2021; 18: 297–312.
2. World Health Organization (WHO). Available online at: who.int/news-room/fact-sheets/detail/cancer
3. Morgillo F, Della Corte CM, Fasano M, Ciardiello F. Mechanisms of resistance to EGFR-targeted drugs: lung cancer. ESMO open. 2016; 1: e000060.
4. Dawson SJ, Tsui DW, Murtaza M, Biggs H, Rueda OM, et al. Analysis of circulating tumor DNA to monitor metastatic breast cancer. The New England journal of medicine. 2013; 368: 1199–1209.
5. Diehl F, Schmidt K, Choti MA, Romans K, Goodman S, et al. Circulating mutant DNA to assess tumor dynamics. Nature medicine. 2008; 14: 985–990.
6. Shen S, Wei Y, Zhang R, Du M, Duan W, et al. Mutant-allele fraction heterogeneity is associated with non-small cell lung cancer patient survival. Oncology letters. 2018; 15: 795–802.
7. Li H, Jing C, Wu J, Ni J, Sha H, et al. Circulating tumor DNA detection: A potential tool for colorectal cancer management. Oncology letters. 2019; 17: 1409–1416.
8. Huang A, Zhang X, Zhou SL, Cao Y, Huang XW, et al. Detecting Circulating Tumor DNA in Hepatocellular Carcinoma Patients Using Droplet Digital PCR Is Feasible and Reflects Intratumoral Heterogeneity. Journal of Cancer. 2016; 7: 1907–1914.

9. Vasseur A, Kiavue N, Bidard FC, Pierga JY, Cabel L. Clinical utility of circulating tumor cells: an update. Molecular oncology. 2021; 15: 1647–1666.
10. Kulasinghe A, Lim Y, Kapeleris J, Warkiani M, O'Byrne K, et al. The Use of Three-Dimensional DNA Fluorescent In Situ Hybridization (3D DNA FISH) for the Detection of Anaplastic Lymphoma Kinase (ALK) in Non-Small Cell Lung Cancer (NSCLC) Circulating Tumor Cells. Cells. 2020; 9: 1465.
11. Varkey J, Nicolaides T. Tumor-Educated Platelets: A Review of Current and Potential Applications in Solid Tumors. Cureus. 2021; 13: e19189.
12. Whiteside TL. Tumor-Derived Exosomes and Their Role in Cancer Progression. Advances in clinical chemistry. 2016; 74: 103–141.
13. Osaki M, Okada F. Exosomes and Their Role in Cancer Progression. Yonago acta medica. 2019; 62: 182–190.
14. Peng Y, Croce CM. The role of MicroRNAs in human cancer. Signal transduction and targeted therapy. 2016; 1: 15004.
15. Chen L, Shan G. CircRNA in cancer: Fundamental mechanism and clinical potential. Cancer letters. 2021; 505: 49–57.
16. Hu D, Lou X, Meng N, Li Z, Teng Y, et al. Peripheral Blood-Based DNA Methylation of Long Non-Coding RNA H19 and Metastasis-Associated Lung Adenocarcinoma Transcript 1 Promoters are Potential Non-Invasive Biomarkers for Gastric Cancer Detection. Cancer control: journal of the Moffitt Cancer Center. 2021; 28: 10732748211043667.
17. Zhang L, Li C, Su X. Emerging impact of the long noncoding RNA MIR22HG on proliferation and apoptosis in multiple human cancers. Journal of experimental & clinical cancer research: CR. 2020; 39: 271.
18. Li W, Liu JB, Hou LK, Yu F, Zhang J, et al. Liquid biopsy in lung cancer: significance in diagnostics, prediction, and treatment monitoring. Molecular cancer. 2022; 21: 25.
19. Lim M, Park J, Lowe AC, Jeong HO, Lee S, et al. A lab-on-a-disc platform enables serial monitoring of individual CTCs associated with tumor progression during EGFR-targeted

therapy for patients with NSCLC. Theranostics. 2020; 10: 5181–5194.
20. Adashek JJ, Janku F, Kurzrock R. Signed in Blood: Circulating Tumor DNA in Cancer Diagnosis, Treatment and Screening. Cancers. 2021; 13: 3600.
21. Available online at: Food and Drug Adminitration: fda.gov/medical-devices/in-vitro-diagnostics/list-cleared-or-approved-companion-diagnostic-devices-in-vitro-and-imaging-tools.
22. Shen S, Wei Y, Zhang R, Du M, Duan W, et al. Mutant-allele fraction heterogeneity is associated with non-small cell lung cancer patient survival. Oncology letters. 2018; 15: 795–802.
23. Zhang Y, Yao Y, Xu Y, Li L, Gong Y, et al. Pan-cancer circulating tumor DNA detection in over 10,000 Chinese patients. Nature communications. 2021; 12: 11.
24. Newman AM, Bratman SV, To J, Wynne JF, Eclov NC, et al. An ultrasensitive method for quantitating circulating tumor DNA with broad patient coverage. Nature medicine. 2014; 20: 548–554.
25. Cohen JD, Li L, Wang Y, Thoburn C, Afsari B, et al. Detection and localization of surgically resectable cancers with a multi-analyte blood test. Science (New York, N.Y.). 2018; 359: 926–930.
26. Best MG, Sol N, Kooi I, Tannous J, Westerman BA, et al. RNA-Seq of Tumor-Educated Platelets Enables Blood-Based Pan-Cancer, Multiclass, and Molecular Pathway Cancer Diagnostics. Cancer cell. 2015; 28: 666–676.
27. Shen J, Todd NW, Zhang H, Yu L, Lingxiao X, et al. Plasma microRNAs as potential biomarkers for non-small-cell lung cancer. Laboratory investigation; a journal of technical methods and pathology. 2011; 91: 579–587.
28. Sozzi G, Boeri M, Rossi M, Verri C, Suatoni P, et al. Clinical utility of a plasma-based miRNA signature classifier within computed tomography lung cancer screening: a correlative MILD trial study. Journal of clinical oncology: official journal of the American Society of Clinical Oncology. 2014; 32: 768–773.
29. Seremet T, Jansen Y, Planken S, Njimi H, Delaunoy M, et al. Undetectable circulating tumor DNA (ctDNA) levels

correlate with favorable outcome in metastatic melanoma patients treated with anti-PD1 therapy. Journal of translational medicine. 2019; 17: 303.
30. Delahaye C, Figurearol S, Pradines A, Favre G, Mazieres J, et al. Early Steps of Resistance to Targeted Therapies in Non-Small-Cell Lung Cancer. Cancers. 2022; 14: 2613.
31. Buder A, Heitzer E, Waldispühl-Geigl J, Weber S, Moser T, et al. Somatic Copy-Number Alterations in Plasma Circulating Tumor DNA from Advanced EGFR-Mutated Lung Adenocarcinoma Patients. Biomolecules. 2021; 11: 618.
32. Karachaliou N, Mayo-de las Casas C, Queralt C, de Aguirre I, Melloni B, et al. Association of EGFR L858R Mutation in Circulating Free DNA With Survival in the EURTAC Trial. JAMA oncology. 2015; 1: 149–157.
33. Krebs MG, Sloane R, Priest L, Lancashire L, Hou JM, et al. Evaluation and prognostic significance of circulating tumor cells in patients with non-small-cell lung cancer. Journal of clinical oncology: official journal of the American Society of Clinical Oncology. 2011; 29: 1556–1563.
34. Wu H, Mu X, Liu L, Wu H, Hu X, et al. Bone marrow mesenchymal stem cells-derived exosomal microRNA-193a reduces cisplatin resistance of non-small cell lung cancer cells via targeting LRRC1. Cell death & disease. 2020; 11: 801.
35. Campos-Carrillo A, Weitzel JN, Sahoo P, Rockne R, Mokhnatkin JV, et al. Circulating tumor DNA as an early cancer detection tool. Pharmacology & therapeutics. 2020; 207: 107458.
36. Diaz LA, Jr, Bardelli A. Liquid biopsies: genotyping circulating tumor DNA. Journal of clinical oncology: official journal of the American Society of Clinical Oncology. 2014; 32: 579–586.
37. NGS for ALK rearrangements and mutations: Dagogo-Jack I, Shaw AT. Screening for ALK Rearrangements in Lung Cancer: Time for a New Generation of Diagnostics? The oncologist. 2016; 21: 662–663.
38. Available online at: NGS approval granted by FDA: https://www.fda.gov/drugs/resources-information-approved-

drugs/fda-approves-liquid-biopsy-ngs-companion-diagnostic-test-multiple-cancers-and-biomarkers.
39. Park CK, Kim JE, Kim MS, Kho BG, Park HY, et al. Feasibility of liquid biopsy using plasma and platelets for detection of anaplastic lymphoma kinase rearrangements in non-small cell lung cancer. Journal of cancer research and clinical oncology. 2019; 145: 2071–2082.
40. Palanca-Ballester C, Rodriguez-Casanova A, Torres S, Calabuig-Fariñas S, Exposito F, et al. Cancer Epigenetic Biomarkers in Liquid Biopsy for High Incidence Malignancies. Cancers. 2021; 13: 3016.
41. Boldrin E, Nardo G, Zulato E, Bonanno L, Polo V, et al. Detection of Loss of Heterozygosity in cfDNA of Advanced EGFR- or KRAS-Mutated Non-Small-Cell Lung Cancer Patients. International journal of molecular sciences. 2019; 21: 66.
42. Tieng F, Abu N, Lee LH, Ab Mutalib NS. Microsatellite Instability in Colorectal Cancer Liquid Biopsy-Current Updates on Its Potential in Non-Invasive Detection, Prognosis and as a Predictive Marker. Diagnostics (Basel, Switzerland). 2021; 11: 544.
43. Zugazagoitia J, Ramos I, Trigo JM, Palka M, Gómez-Rueda A, et al. Clinical utility of plasma-based digital next-generation sequencing in patients with advance-stage lung adenocarcinomas with insufficient tumor samples for tissue genotyping. Annals of oncology : official journal of the European Society for Medical Oncology. 2019; 30: 290–296.
44. Papadimitrakopoulou VA, Han JY, Ahn MJ, Ramalingam SS, Delmonte A, et al. Epidermal growth factor receptor mutation analysis in tissue and plasma from the AURA3 trial: Osimertinib versus platinum-pemetrexed for T790M mutation-positive advanced non-small cell lung cancer. Cancer. 2020; 126: 373–380.
45. Ariyasu R, Nishikawa S, Uchibori K, Oh-Hara T, Yoshizawa T, et al. High ratio of T790M to EGFR activating mutations correlate with the osimertinib response in non-small-cell lung cancer. Lung cancer (Amsterdam, Netherlands). 2018; 117: 1–6.
46. Smeltzer MP, Wynes MW, Lantuejoul S, Soo R, Ramalingam SS, et al. The International Association for the

Study of Lung Cancer Global Survey on Molecular Testing in Lung Cancer. Journal of thoracic oncology: official publication of the International Association for the Study of Lung Cancer. 2020; 15: 1434–1448.
47. Kuderer NM, Burton KA, Blau S, Rose AL, Parker S, et al. Comparison of 2 Commercially Available Next-Generation Sequencing Platforms in Oncology. JAMA oncology. 2017; 3: 996–998.
48. Mrazek C, Lippi G, Keppel MH, Felder TK, Oberkofler H, et al. Errors within the total laboratory testing process, from test selection to medical decision-making - A review of causes, consequences, surveillance and solutions. Biochemia medica. 2020; 30: 020502.
49. Rolfo C, Mack P, Scagliotti GV, Aggarwal C, Arcila ME, et al. Liquid Biopsy for Advanced NSCLC: A Consensus Statement From the International Association for the Study of Lung Cancer. Journal of thoracic oncology: official publication of the International Association for the Study of Lung Cancer. 2021; 16: 1647–1662.
50. Patz EF, Jr, Goodman PC, Bepler G. Screening for lung cancer. The New England journal of medicine. 2000; 343: 1627–1633.
51. Samstein RM, Lee CH, Shoushtari AN, Hellmann MD, Shen R, et al. Tumor mutational load predicts survival after immunotherapy across multiple cancer types. Nature genetics. 2019; 51: 202–206.
52. Bonanno L, Dal Maso A, Pavan A, Zulato E, Calvetti L, et al. Liquid biopsy and non-small cell lung cancer: are we looking at the tip of the iceberg?. British journal of cancer. 2022; 127: 383–393.
53. Carbone DP, Reck M, Paz-Ares L, Creelan B, Horn L, et al. First-Line Nivolumab in Stage IV or Recurrent Non-Small-Cell Lung Cancer. The New England journal of medicine. 2016; 376: 2415–2426.
54. Brueckl WM, Ficker JH, Zeitler G. Clinically relevant prognostic and predictive markers for immune-checkpoint-inhibitor (ICI) therapy in non-small cell lung cancer (NSCLC). BMC cancer. 2020; 20: 1185.
55. Vandesompele J, De Preter K, Pattyn F, Poppe B, Van Roy N, et al. Accurate normalization of real-time quantitative

RT-PCR data by geometric averaging of multiple internal control genes. 2002; 3.
56. Farazi TA, Hoell JI, Morozov P, Tuschl T. MicroRNAs in human cancer. Advances in experimental medicine and biology. 2013; 774: 1–20.
57. Yaung SJ, Fuhlbrück F, Peterson M, Zou W, Palma JF, et al. Clonal Hematopoiesis in Late-Stage Non-Small-Cell Lung Cancer and Its Impact on Targeted Panel Next-Generation Sequencing. JCO precision oncology. 2002; 4: 1271–1279.
58. Padda J, Khalid K, Khedr A, Patel V, Al-Ewaidat OA, et al. Exosome-Derived microRNA: Efficacy in Cancer. Cureus. 2021; 13: e17441.
59. Li C, Zhou T, Chen J, Li R, Chen H, et al. The role of Exosomal miRNAs in cancer. Journal of translational medicine. 2002; 20: 6.
60. Tu M, Wei F, Yang J, Wong D. Detection of exosomal biomarker by electric field-induced release and measurement (EFIRM). Journal of visualized experiments: JoVE. 2015; 95: 52439.
61. Cristiano S, Leal A, Phallen J, Fiksel J, Adleff V, et al. Genome-wide cell-free DNA fragmentation in patients with cancer. Nature. 2019; 570: 385–389.

Book Chapter

Central and Peripheral Neuroinflammation: A Focus on the Macrophage

Zeina MSHEIK

University of Limoges, NeurIT UR 20218, Faculties of Medicine and Pharmacy, France

***Corresponding Author:** Zeina MSHEIK, University of Limoges, NeurIT UR 20218, Faculties of Medicine and Pharmacy, Limoges, France

Published **February 14, 2023**

How to cite this book chapter: Zeina MSHEIK. Central and Peripheral Neuroinflammation: A Focus on the Macrophage. In: Hussein Fayyad Kazan, editor. Immunology and Cancer Biology. Hyderabad, India: Vide Leaf. 2023.

Graphical Abstract

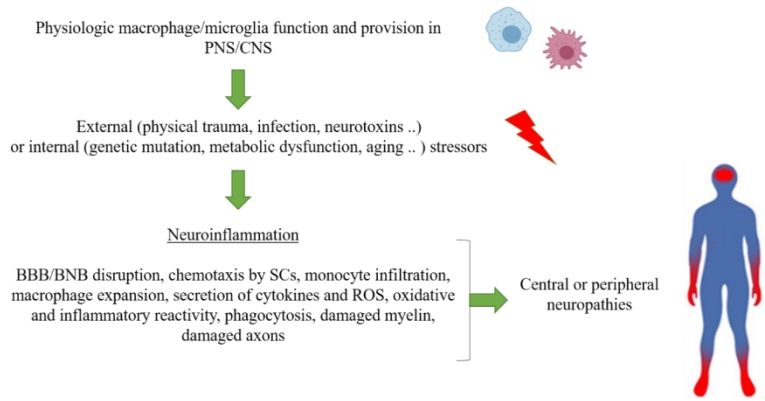

BBB: blood-brain-barrier, BNB: blood-nerve-barrier, ROS: reactive oxygen species, SCs: Schwann cells

Abstract

Central and peripheral neuropathies are widespread nowadays. Symptoms range from cognitive problems to sensori-motor disabilities. On the physiopathological side, inflammation is currently recognized as a pillar of the initiation and progression of these diseases. Indeed, the roles of individual cells in the pathological process was largely unknown. The advent of new techniques such as fate mapping and single-cell transcriptomics and their synergistic use has permitted the fine characterization of cellular traits and the degree of their implication in health and in disease states. Interestingly, macrophages have gained increasing attention over the last years. These techniques have allowed a better understanding of their functions from simple homeostatic supervisors to chief regulators in central and peripheral neuropathies. In this chapter, we summarize the latest knowledge about tissue macrophage and microglial ontogeny, function and tissue identity, as well as their interaction with reactive oxygen species under physiological and pathological conditions. Finally, we review these processes in light of internal and external insults to the nervous system, the involvement of

macrophages and the potential benefit of the targeting of specific macrophages for the alleviation of functional defects.

Keywords

Central Nervous System; Peripheral Nervous System; Neuroinflammation; Oxidative Stress; Macrophage

Introduction

The majority of the body's tissues include macrophages that are resident in tissues, thus called tissue-resident macrophages. These play a crucial roles in regulating tissue homeostasis and host defence. These cells have been identified as tissue phagocytes deriving from blood monocytes, but their heterogeneity is receiving high attention. Despite some unresolved issues, it is now largely understood that key tissue-resident macrophage populations emerge during embryonic development. It is therefore hypothesized that two mechanisms contribute to the daily maintenance and homeostasis of the resident macrophage pool: (i) proliferation of initially resident macrophages and (ii) blood monocyte infiltration and engraftment [1]. In order to control their surroundings in an active feedback loop, macrophages adapt their metabolism and polarize their phenotype/function in response to environmental inputs. These cells produce a large number of cytokines, nerve growth factor (NGF), and reactive oxygen species (ROS), as well as control the extracellular matrix (ECM) composition [2-6]. It is well known that several non-neuronal cells, primarily Schwann cells (SC) and immune cells such macrophages and fibroblasts, function at the site of injury in the case of injury such as trauma or infection [7,8]. For example, in both the central and peripheral nervous system (CNS and PNS, respectively), tissue injury and degeneration as well as later in the resolution of inflammation and tissue repair, microglia/macrophages play an orchestrating function. Indeed, pro-inflammatory versus anti-inflammatory macrophage phenotype may influence the success of regeneration [9]. It is true that adequate neuroinflammation aids in healing and remyelination through the synthesis of a number of neurotrophic factors by all immune cell types, the

suppression of immunological hyperactivity by immune cell-produced growth factors, the phagocytic clearance of inhibitory myelin debris and toxic chemicals, and the elimination of chondroitin sulphate proteoglycans that impede remyelination and axonal regeneration [10]. In contrast, persistent and exaggerated neuroinflammation, can harm neuron structure and, as a result, nerve function. In rodent PNS axon regeneration models, the local environment is regenerative-friendly for up to 4–8 weeks following damage before becoming less trophic or atrophic due to changes in the ECM [4]. There is some evidence that suggests that PNS axons may be able to repair and resume normal function following damage. However, following an injury, nerve regeneration and clinical functionality are probably not as good, therefore in this case the tern "repair", rather than regeneration, is preferred.

Indeed, studying nerve-associated macrophages is a hotly debated topic with significant challenges. In this chapter, we will discuss the most recent research on nerve-resident macrophages, our understanding of the mechanisms underlying their self-maintenance and imprinting, as well as the mechanisms governing monocyte entry into the macrophage niche. We describe both the PNS and CNS-resident macrophages, while also considering the significance of the nerve-blood barrier in this process. Finally, we go over the major PNS and CNS disorders, paying particular attention to how neuroinflammation and oxidative stress affect the development and course of these diseases. Indeed, new methods are improving our comprehension of the role of macrophages in immunity and immunopathology and giving precise insights on macrophage commitment to tissue niches and their behaviour in case of external or internal insults, albeit many concerns still need to be adequately handled. It is believed that this would open the door to targeting certain macrophages for treating nerve damage brought on by peripheral neuropathies. In this regard, cytokines, chemicals, and nano-carriers are being under research as potential therapeutic approaches [11] to modulate macrophage polarization.

Our Current Knowledge about Macrophage Origin

"A macrophage is merely a monocyte in a more active metabolic condition" [12]. Since 1926, the prevailing theory has been that blood-circulating monocytes descended from bone marrow-based progenitors continuously replenish tissue macrophages. The mononuclear phagocyte system (MPS), which was proposed in the early seventies, is a classification system for both monocytes, macrophages, and their precursors. Based on their origin, shape, function, and dynamics, scientists from all over the world described this family of cells [13]. In fact, Purine-rich Box-1 (PU.1) and other transcriptional regulators are used by both monocytes and macrophages, and both cells express a number of surface markers, most notably colony stimulating factor-1 (CSF1) receptor [14].

This viewpoint, however, has been altered over the past ten years as a result of several breakthrough publications. Macrophage ontology provided compelling evidence that some tissue-resident macrophages are first seeded during embryonic haematopoiesis without monocyte intermediates and are maintained over the course of the individual's life. As a result, they are capable of local self-maintenance without blood monocyte input [15-17]. Given the high degree of conservation of haematopoiesis between Drosophila and vertebrates, research on Drosophila larvae revealed that the only "white blood cells" produced by primitive haematopoiesis in the yolk sac are erythroid cells and macrophage progenitors. Numerous varieties of tissue-resident macrophages are descended from these primordial macrophages [18]. Embryonic macrophage ontogeny demonstrated that three distinct waves of haematopoiesis occur during development [17]. Primitive haematopoiesis is the name given to the initial phase, which occurs in the extraembryonic yolk sac and results in the maturation of macrophages. The erythro-myeloid progenitors (EMP), which move to the foetal liver and give birth to maturing monocyte/macrophages, are the source of the second wave, which is intraembryonic. The third wave emerges from the haemogenic endothelium and produces immature haemopoietic stem cells (HSCs), which invade the foetus's liver and bone

marrow. Over time, mature HSC's commitment to adult haematopoiesis occurs in the bone marrow [17,19]. It is remarkable that numerous adult tissue-resident macrophages have been linked to embryonic genesis, independent of bone marrow supply. For example, microglia and CNS-associated macrophages (CAMs) are originally derived from EMPs [20]. Then this gives rise to immature A1 macrophage progenitors that further differentiate into A2 pre-macrophage progenitors in the CNS [21].

Which of these, local macrophages or haemogenic is preferred under either physiological or pathological circumstances? It is still an open question. According to the evidence that is now available, it is doubtful that these two pathways act independently during local macrophage proliferation [22]. It is well acknowledged that at steady state (i) adult monocyte-derived macrophages (ii) embryonic macrophages (ii) adult monocyte-derived macrophages' daughter cells act collectively. Furthermore, in inflamed tissue (iv) recruited adult monocyte-derived cells are added to the existing varied population [17]. It is currently unknown, though, how various macrophage lineages and subtypes contribute to these activities in a given tissue.

Complex methods (such fate mapping) are being developed and used to distinguish resident from invading macrophages in order to answer this question. Recently, adult tissues were categorized into three groups: those with fast steady-state monocyte recruitment (dermis and gut), those with delayed steady-state input (pancreas and heart), and those with exclusively yolk-sac-derived macrophages (brain, lung, liver, and epidermis) [17]. These tissue macrophage pools can become depleted by long-term, low-grade metabolic, oxidative, or mechanical stress (such as that caused by physiological aging). These circumstances could therefore promote homeostatic monocyte supply to refill tissue-macrophage pools in a manner resembling inflammatory patterns.

Macrophage Function: Is the M1/M2 Dichotomy Exact?

The remarkable plasticity of macrophages and their ability to change their phenotype in response to microenvironmental signals are collectively referred to as "macrophage polarization" [23]. Recruited monocytes and tissue-resident macrophages multiply in response to injury and experience noticeable changes in cell surface markers and function, which control inflammation and, ultimately, tissue repair or fibrosis [24]. Activated macrophages can be broadly classified into two subtypes based on *in vitro* induction experiments: M1-like macrophages and M2-like macrophages. The M1/M2 nomenclature was developed in a similar fashion to the Th1/Th2 dichotomy. High antigen-presenting capacity and activation of the polarized type 1 response are characteristics of “classical” macrophage activation (therefore M1) [25]. Indeed, pro-inflammatory markers such Nos2, Arg1, Ccl2, Ccl7, Il1 and Alox15 are expressed by M1 macrophages [26]. Additionally, when stimulated by pathogen- or damage-associated molecular patterns (PAMPs or DAMPs, respectively), they exhibit enhanced reactive oxygen and nitrogen species (ROS and RNS, respectively) production [23,25]. The M2 family, on the other hand, is referred to be “alternately activated”/”deactivated” macrophages that acquire an anti-inflammatory phenotype. M2 macrophages can be further subdivided into M2a (where "a" refers for alternative), which is induced by interleukin (IL)-4 or IL-13; M2b, which is triggered by immune complexes and agonists of Toll-like receptors (TLRs) or IL-1R; and M2c that is induced by IL-10 and glucocorticoids [25], and M2d, induced by TLR antagonists to secrete IL-10 and vascular endothelial growth factor (VEGF) [27]. PPARγ, a nuclear transcription factor, regulates macrophage polarization by favouring the M2 cell phenotype and inhibiting the transition to an M1 phenotype. In contrast, activation of the NF-κB signaling pathway promotes M1 macrophage polarization, whereas its blocking favours M2 phenotype [11].

In fact, macrophage populations are far from being stable subsets, but rather cells that actively modulate their phenotypes

in response to precise physical, chemical, and cell-to-cell cues [28,29]. Currently, fully polarized "mature" M1 and M2 macrophages -similar to M1 and M2 microglia- in their various versions seem to be the extreme ends of a continuum. Additionally, several investigators find it difficult to apply the *in vitro* M1/M2 classification *in vivo* [29-31]. Thus, it becomes more crucial to employ specialized and complementary approaches, such as single-cell transcriptomics, proteomics, fate mapping, and imaging, for studying complicated macrophage populations [29,32]. When analysing the results, it's also important to consider the variety of markers employed to identify macrophages, *in vivo/in vitro* variations, and interspecies variability. Indeed, M1/M2 paradigm is simplified for academic and research purposes but one should keep in mind that the story is much more complex.

Macrophage Tissue Identity

In fact, macrophages are not alike. They adopt tissue-specific roles such as Kupffer cells in the liver, microglia in the brain, and nerve-associated macrophages in the PNS. The PNS, however, is unique in that it innervates diverse tissue types and is geographically spread throughout the entire body. A description of nerve-associated macrophages in several tissues was reviewed and summarized [33]. Although there is some controversy as to whether these macrophages have a PNS-specific identity or rather a host tissue-signature, it is expected that both organ- and nerve-specific inputs would affect resident macrophage identity. Multiple populations of macrophage-like cells co-exist in adult tissue and carry out timely activities [16,32,34,35]. Microenvironmental cues, such as trophic factors, ECM scaffolds, stromal cells, and the vasculature, are well recognized to tightly govern the development and homeostasis of all cell types in addition to ontogeny. Consequently, according to the niche theory, macrophages' identity is modulated by the tissue environment in which they are found [36]. Specifically, Different macrophage precursors compete for a finite number of niches despite having nearly comparable ability to mature into resident macrophages. When the niche is crowded, monocytes cannot differentiate into macrophages; nevertheless, when the niche is

empty, these cells can differentiate into macrophages with high efficiency.

On the other hand, mechanisms such as DNA methylation, histone modification, and chromatin structure control these tissue-specific activities [37]. The microglia, Kupffer cells, spleen, lung, peritoneal, ileal, and colonic macrophage populations, which are representative of all tissue macrophage populations, were shown to share less than 2% of these characteristics [38]. Interestingly, the expression profile of fully differentiated macrophages was reprogrammed when they were transplanted into a different tissue [35,38]. As a result, the tissue identity of macrophages is shaped through epigenetic regulation that is controlled by both tissue- and lineage-specific transcription factors. In fact, cell survival and function cannot be divorced from their microenvironment. It is also noteworthy that there are many similarities and striking differences between human and rodent cells. For instance, Gosselin and colleagues [39], have shown tissue signature similarities and differences between human and mouse CNS microglia, as well as between *ex vivo* and *in vitro* microglia. Thus, gene signature of these cells is highly dependent on the correct microenvironment.

Central Nervous System Macrophages: The Microglia

The CNS, which includes the brain and spinal cord, is made up of billions of neuroectodermal cells such neurons, astrocytes, and oligodendrocytes in addition to resident immune cells, which make up 10% of the overall CNS cells [40]. The CNS has two types of tissue macrophages: microglia, which are found in the parenchyma and get their name from their tiny (7–10 µm) cell bodies, and CNS-associated macrophages (CAMs), which are present in CNS interfaces like the meninges, perivascular space, and choroid plexus [40]. Perivascular macrophages, subdural leptomeningeal macrophages, and choroid plexus macrophages are all examples of CAMs, also known as border-associated macrophages (BAMs) [41,42]. Contrary to perivascular microglia, which are located between two basal laminae formed by the glia limitans and endothelial cells, respectively,

perivascular macrophages have a distinctly defined position [43]. The retinal, corneal, and ciliary body macrophages in the eye and the endoneurial and epineurial macrophages in the peripheral nervous system are further neural-associated macrophages. While T and B cells, dendritic cells, monocytes, and natural killer cells are all found at the CNS borders, such as the meninges (leptomeninges, dura), and in the choroid plexus, microglia are the only immune cells identified in the CNS parenchyma in close proximity to neurons [43].

In vivo imaging techniques, which revealed microglial activities in the brain milieu, high throughput gene expression analyses, which distinguished microglia from their myeloid relatives and other brain cells, and advances in genetic tools, which enabled specific fate mapping of microglia, have all aided the rapid progress towards unravelling the multiple facets of microglia in shaping brain development and maintaining homeostasis throughout an organism's lifetime [44]. Recently, microglia were morphologically defined and genetically profiled in a variety of animals, concluding that microglia have undergone little change during evolution [45]. Astonishingly, the fundamental transcriptional microglial profile was preserved, showing that microglial cells function similarly in all species. Additionally, microglial density was consistent across over 33 species of vertebrates [46].

Unlike circulating monocytes with haematogeneous myeloid lineages, microglia and most tissue macrophages emerge exclusively from erythromyeloid progenitors in the yolk sac that differentiate into YS macrophages during embryonic development [47]. Precursor macrophages migrate to/and colonize the CNS parenchyma prior to the maturation of the blood–brain barrier and subsequently differentiate to microglia [48,49]. The seeding of the CNS by yolk sac macrophages requires healthy blood circulation. Microglia and maybe CAMs in mice arise from c-Kit+ non-committed EMPs that begin at embryonic day 7.25 (E7.25) in the yolk sac. These cells are similar to other embryonic tissue macrophages in mice [50]. Studies on chickens and zebrafish have provided more evidence confirming that microglia form during development [47,51,52].

The transcription factor c-Myb is not required for the development of microglia or CAMs by EMPs [52,53]. A1 and A2 c-Kit CX3CR1+ maturing macrophages are produced by c-Kit+ CX3CR1+ EMPs in an IRF-8-dependent manner, and they have been demonstrated to enter the brain anlage at E9.5 through the bloodstream without a monocyte intermediary [21,54]. However, the majority of other tissue macrophages are descended from EMPs that were produced later and were c-Myb dependent which move to the foetal liver, where they give rise to monocyte intermediates [55].

Regarding the prenatal origin of CAMs, there has recently been speculation that they share a considerable ontogenetic overlap with the brain's microglia, in a mouse model. CAMs are currently understood to be prenatal lineage cells that lack the c-Myb and CCR2 receptors [53]. This has been supported by a number of investigations in mice [56,57]. The choroid plexus macrophages are the only outliers to this norm, as they are partially replaced and maintained by monocytes as opposed to perivascular macrophages and subdural leptomeningeal macrophages. This is most likely because the choroid plexus contains fenestrated capillaries [53]. Microglia and CAMs have separate yolk sac progenitors, which suggests that their cell fate is decided before they invade, infiltrate, or seed the developing brain [58]. Other regions of the CNS and head, including the retina have similar prenatal origins of tissue macrophages [20,59,60].

It is currently unknown how microglia and CAMs migrate to the brain throughout development or which cues direct them to their predetermined final location. Microglial movement across the developing CNS appears to be dependent on chemokine-derived signals, such as the CXCL2/CXCR4 axis [20] and extracellular matrix proteins regulated by matrix metalloproteinases [21]. Admitting the “niche theory”, however, little is known about the start and stop signals governing the replenishment of the microglia niche. Fundamental issues about the cell cycle dynamics of microglia still exist despite the exponential rise in studies on their origin over the previous five years [40].

Peripheral Nerve-Associated Macrophages

PNS-resident macrophages, in stark contrast to CNS microglia, are one of the least well-researched subpopulations. Their cellular origin, ability to maintain themselves, and gene signature are all poorly understood. The majority of research is focused on understanding CNS pathogenic processes, where macrophages play crucial roles. In addition, recent findings suggest that PNS is a pertinent disease target in many CNS neurodegenerative illnesses, particularly Multiple Sclerosis [61]. This may restructure research to focus on systemic involvement in neurological diseases.

Axons are normally contained in an endoneural compartment consisting of fibroblasts and collagenous connective tissue [62]. The collagenous epineurium matrix that encloses axon fascicles, also contains macrophages, tiny arteries, and veins [63,64]. Studies have also revealed the presence of macrophages in the endoneurium, in the spaces between myelin sheaths, and in close proximity to axons [63,65,66]. These macrophages often continuously scan the surrounding environment for dangers and aid in the removal of cellular debris.

Single-cell RNA sequencing was recently employed to identify nerve-associated macrophages in mouse skin [32]. These cells can be distinguished from other dermal macrophages by having higher levels of the CX3CR1 marker ($CX3CR1^{hi}$). In terms of their transcriptome and axon-scanning behaviour, $CX3CR1^{hi}$ nerve-associated macrophages intimately interact with sensory nerves. By using fate mapping techniques, it was discovered that these cells develop from either $CX3CR1^{hi}$ prenatal progenitors, which are the primary source in homeostasis, or from $CX3CR1^{lo}$ pro-inflammatory monocyte-derived macrophages in the event of tissue injury [67]. These findings allow for the differentiation of the two different origins of these nerve macrophages. These cells expand in a mouse ear-punch model and aid in myelin breakdown, nerve regeneration, and wound healing [32]. It is yet unclear how CX3CR1 interacts with these highly committed peripheral nerve macrophages. CXCR1 ligand CX3CL1, also known as fractalkine FKN, has been shown to activate ROS

generation in CX3CR1 macrophages and monocyte infiltration in sciatic nerves in mouse models [68]. Additionally, it has been demonstrated that the chemokine FKN mediates the neural/microglial relationship in rat neuropathic pain [69].

A recent study in mice thoroughly characterized sciatic nerve macrophages [31]. Sciatic-nerve macrophages had a tissue-specific gene signature that distinguished them from other tissue macrophages and CNS microglia (in the optic nerve, liver, lung, spleen, and peritoneum). Unique genes such as Adam19, Cbr2, Cd209d, Foxred2, Fxyd2, Mgl2, Mmp9, Il1rl1, Kmo, and Tslp were all found in the sciatic nerve macrophage profile. Single-cell analysis revealed two distinct types of sciatic nerve macrophages: Relm+Mgl1+ cells in the epineurium and Relm-Mgl1- cells in the endoneurium. By fate mapping technique, the authors discovered that sciatic nerve macrophages do not originate from early embryonic precursors colonizing the CNS, but rather from late embryonic precursors that are gradually replaced by bone marrow-derived macrophages. Finally following injury, unlike the CNS where the macrophage family is replenished by local cells, the PNS macrophage pool is replenished by monocyte-derived macrophages. Although few studies have been published recently regarding PNS macrophages, they have made significant contributions to our understanding of macrophages' remarkable functional plasticity and their potential role in peripheral neuropathies. The investigation of peripheral nerve immune responses in conditional knockout transgenic animals has added to our understanding of the physiological/pathological crosstalk between the systemic immune system and the peripheral nerve compartment. Figure 1 represents a simplistic comparison between CNS microglia and PNS macrophages regarding their origin, morphology, function and gene signature. It is noteworthy that little information are available on PNS macrophages as compared to microglia.

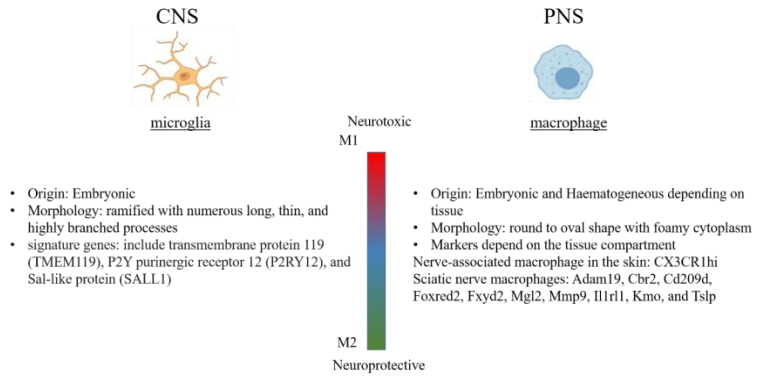

Figure 1: A schematic representation of CNS microglia and PNS macrophages. They are compared according to their origin, morphology, and tissue signature. For both macrophages and microglia, classification based on M1/M2 criteria is proposed.

Neuroinflammation and Blood-Nerve Barrier

After nerve insult, monocytes and macrophages are drawn to the injury site by factors produced by repair SCs that produce chemo-attractants, such as CCL2, TNF□, IL-1, and IL-1 [70]. Macrophages are among the first and most abundant cells to infiltrate the injury site. In turn, the main chemokine produced by monocytes and macrophages is CCL2. It binds to the CCR2 receptor with high affinity, which is primarily expressed by monocytes and macrophages [71] as well as by sensory neurons after damage [72]. It is known that normal axonal conduction is dependent on the endoneurial microenvironment, which includes cells or cell parts (axon, myelin sheath, fibroblasts, and macrophages) and connective tissue. Thus, active functional and anatomical relationship exists between this area of high metabolic demand and the vascular compartment [73]. Endoneurial microvascular endothelia form tight junctions that control ion, solute, water, nutrient, macromolecule, and leukocyte movement between the bloodstream and the endoneurium. According to classic *in situ* permeability studies, the blood-nerve barrier (BNB) is the second most restrictive vascular system after the blood-brain barrier (BBB) [64]. Passage across the BNB is hampered by lower levels of P-

glycoprotein transporter activity than the BBB, limiting the efficiency of xenobiotic and neurotoxin removal [74]. Furthermore, structural changes in endoneurial microvessels or interactions with haematogenous immune cells have been described in several human peripheral neuropathies. Neuroinflammation, which is now recognized as a defining feature of nearly all neurological disorders [10], increases vascular permeability and disrupts both the BBB [75] and BNB [76]. Furthermore, oxidative stress causes a decrease in the expression of tight and adherens junction proteins [77]. As a result, neurotoxins, endotoxins, and inflammatory cells can infiltrate. Moreover, our understanding of the mechanisms of haematogenous leukocyte trafficking at the human BBB and BNB remains limited due to phenotypic and functional differences between endothelial cells from different tissues and species [64]. Nonetheless, macrophages appear to interact closely with vascular compartments to drive the inflammatory process. Indeed, macrophages at the site of injury detect local hypoxia and secrete VEGF to polarize the surrounding vasculature [70]. Furthermore, all infiltrating monocytes express VEGF to help guide vascular sprouting. Blood vessels guide the migrating cords of SCs, which essentially guide regrowing axons [31]. Besides, ECM proteins such as collagen VI influence cellular changes at the injury site. Both local macrophages and SCs with a repair phenotype create collagen VI, which not only works as a chemoattractant for monocytes and macrophages but also controls the production of other substances. Moreover, macrophages, which are well-known for their powerful phagocytic activity, are essential for removing inhibiting myelin detritus and enabling regeneration [7,9]. In conclusion, SCs and macrophages collaborate to control each other's function. The secretion and synthesis of numerous cytokines, chemokines, regeneration factors, ROS, and ECM molecules, which all contribute to the milieu of degeneration/regeneration adaptation processes, mediates all of these cellular alterations and interactions.

It is unclear how peripheral nerve disorders affect changes in vascular permeability. On one hand, increasing BBB and BNB permeability suggests increased monocyte infiltration, which

intensifies the immunological response. The polarizing effects of macrophage secretions, on the other hand, might help the regeneration of damaged nerves. In fact, there is growing interest in their role in neurological illnesses, and targeted treatments are being considered for neuropathies and other pathologies related with macrophages.

Neuroinflammation and Oxidative Stress

It is well-known that monocyte/macrophage surveillance in tissue homeostasis and first-line defence depends on the release of ROS and RNS. Under healthy settings, oxidative phosphorylation in the mitochondria generates around 90% of endogenous ROS [78], with the remaining 10% coming from plasma membrane proteins, lipid metabolism, and the action of cytosolic enzymes [79]. Normal physiological ROS generation is "balanced" by the body's countervailing defence mechanism, which includes substances like glutathione and cytochrome p450. However, there is a persistent low level of oxidative damage, and the balance between ROS formation and the antioxidant system is somewhat in favour of ROS [80]. In turn, after being exposed to a variety of signals, such as pathogen-derived molecular patterns (PAMPs, e.g. lipopolysaccharide), damage-associated molecular patterns (DAMPs, e.g. high-mobility box 1 protein (HMGB-1), nucleotides, and DNA), cytokines (e.g., tumour necrosis factor-α (TNFα)), interferon-γ, metabolic stress (e.g., hyperglycaemia, advanced glycation end products, oxidized lipoproteins), endoplasmic reticulum stress, unfolded/misfolded protein accumulation, and some nanoparticles; activated circulating monocytes and M1 macrophages increase ROS and RNS production [81]. Monocytes and macrophages are both susceptible to oxidative damage brought on by their own release of reactive species, although macrophages are more resilient than monocytes [82]. The FOXO pathway and the Nrf2 pathway, in particular, are part of a network of defence mechanisms that macrophages have access to in order to survive and continue to operate in such a hostile oxidative and inflammatory environment [81]. This variation could be explained by the modulatory action of macrophages, which destroy extra monocytes in response to an

inflammatory reaction. It is important, nonetheless, that the method by which macrophages (and other cells) detect ROS is not fully understood. Despite this benefit of being shielded from oxidative damage, macrophages are nevertheless not completely immune to the deleterious effects of ROS. Long-term oxidative stress causes macrophages to accumulate large amounts of oxidized proteins and lipids, which causes metabolic malfunction, phenotypic changes, and cell death. This is especially important for human disorders where excessive ROS production occurs, such as inflammatory, autoimmune, neoplastic, vascular, respiratory, and neurological diseases [79]. Additionally, when cellular damage accumulates over time, natural repair systems become increasingly sluggish and eventually ineffective, leading the organisms to lose physiological integrity and causing age-related illnesses.

Oxidative stress is almost always present in conjunction with neurodegeneration [83]. High quantities of ROS are produced by dying cells and degenerating axons and are subsequently discharged into the extracellular compartment. Because myelin is high in lipids and excessive ROS production is harmful to cells, SCs are especially vulnerable to lipoperoxidation. Inflammation and other internal and external stresses upset the equilibrium between pro- and anti-oxidant mechanisms, causing an oxidative burst (82). Sciatic nerves from CMT1A rats [85], diabetic mice [86], and sciatic nerves following crush injury [87] were all observed to have higher ROS levels. Additionally, sciatic nerves subjected to non-freezing cold stress displayed increased ROS generation linked to reperfusion damage [88]. Evidence has shown that certain environmental toxins and endogenous proteins cause the CNS microglia to excessively release ROS that cause brain damage [89]. According to Hervera and colleagues [90], inflammatory cells must be recruited by the CX3CR1 receptor in order for ROS to be produced in the injured sciatic nerve and DRG. Inflammatory cells including monocytes [91] and macrophages [92] are attracted as a result of injury-induced ROS and chemokines released by SC. By interfering with epigenetic (re)programming and favouring the development of pro-inflammatory M1 macrophages, ROS changes macrophage differentiation [93]. As a result of the stimulation

provided by FKN generated from endothelial cells, macrophages release ROS. The pain response is then triggered by the activation of TRPA1 channels on sensory neurons by ROS [94].

Macrophage and Neuropathies

In 2003, the role of CNS microglia in neuropathic pain was initially demonstrated [95]. More proof later emerged that immune cells are active participants in the onset and/or development of neuropathies rather than passive observers of the nervous system. In particular, macrophage activation causes the release of powerful pro-inflammatory mediators as TNFα, IL-1, MCP-1, NGF, nitric oxide (NO), and prostanoids, which are associated with experimental neuropathic pain states [96]. Furthermore, neuropathic pain is induced by peripheral nerve damage and is related with an increase in CSF1 in the DRG and spinal cord [97].

One of the most typical rodent models of peripheral nerve injury and regeneration is the sciatic nerve crush model [98]. Importantly, this model has been a useful tool for researching macrophage participation in the inflammatory and regenerative responses to nerve injury. Pro-inflammatory mediators including IL-1, Cox2, and TNFα are rapidly produced after sciatic nerve axonotmesis in mice (within 5–10 hours) [5], along with chemokines like MIP-1 and monocyte chemoattractant protein 1 (MCP-1) (peaking at 24 hours) [6]. Additionally, two days after an acute peripheral nerve damage, pro-inflammatory cytokine expression was shown to rebound to baseline levels. Arginase-1, Ym1, and Trem2 were strongly up-regulated, demonstrating that M2-like macrophages were activated. This limited the attack of the pro-inflammatory surge, creating a neuroprotective milieu. Endoneurial macrophages living nearby were discovered to be the key cells responding to the damage. They responded quickly, within a few of days of the crush, with blood-originating macrophages beginning to show up on day four [63]. After sciatic nerve crush in mouse, Relm+Mgl1+ macrophages did not change their gene expression profile in the distal portion of the sciatic nerve, whereas Relm-Mgl1- cells did so quickly [31]. Indeed, Relm-Mgl1- endoneurial cells responded to injury

as they were discovered to be in greater contact with the damaged axon and transdifferentiating repair SCs. These cells then phagocytose the debris in damage site and aid in the degradation of the downstream axons.
On the other hand, there are various causes for neurodegenerative diseases where macrophage plays a key role. For example, rare monogenetic abnormalities that alter microglial cell functioning can cause severe CNS pathologies. Rademakers and colleagues [99] have first reported that microgliopathy, an autosomal dominant disease brought on by different sequence variants in the gene locus encoding the tyrosine-kinase domain of the cytokine receptor CSF-1R, is a monogenetic disease affecting CNS microglia. Patients who carry this allelic mutation show alterations in the white matter, as well as a variety of clinical symptoms, such as Parkinsonism, dementia, depression, and seizures. The underlying disease is characterized by neurofilament-positive axonal spheroids, extensive demyelination, astrocyte activation, and neuronal damage.

Although there are many different causes for neurodegenerative diseases, they all have some common characteristics, including decreased mitochondrial function, elevated levels of oxidative stress and ROS production, inflammatory responses, the formation of protein aggregates, and excito-toxicity. Whether an axon is preserved or self-destructs depends on the opposing impacts of axonal survival against axonal degeneration components. These occurrences create a vicious loop that, in the setting of a disease, results in neuronal death [100]. In the next section, disease states where inflammatory activity directly contributes to common neuropathies are covered. We shall find that oxidative stress traits almost always coexist with neuroinflammation, maintaining or aggravating the condition. Based on the published data that is now available, the interaction between macrophages and other cells in the initiation, maintenance, or correction of the disease milieu will also be explored.

Microglia in Brain Aging

Aging has a significant impact on how well the brain functions and is a primary risk factor for the majority of neurodegenerative diseases, such as dementia and Alzheimer's disease. Reduced cognitive ability is a hallmark of brain aging, even in non-pathological settings, and may be caused by hampered synaptic plasticity [101]. Research in this field has revealed that microglia play a crucial function in maintaining synaptic plasticity in both the developing and adult body [102]. Microglial aging was first detected in the brains of elderly people by immunohistochemistry and morphology [103]. Age causes a considerable slowdown in microglial activities, which results in decreased tissue scanning, diminished synaptic contact, and subpar damage repair. The "inflammaging" state of primed microglia is characterized by alterations in activation and density, shape, and phenotype, as well as altered cytokine expression, phagocytosis, and ROS generation [101]. An accumulation of lipofuscin, a by-product of phagocytosis, occurs in microglia as the brain ages. A dystrophic appearance, as seen by an increased soma volume, anomalies in the cytoplasmic structure, retracted, fragmented processes, and an uneven tissue distribution, is another difference between old and activated microglia [104]. As they age, microglia experience cytoplasmic fragmentation, loss of process ramification, and process anomalies. They exhibit elevated ferritin expression and storage of iron. Neurons are more vulnerable because of their increased production of poisons that are harmful to the nervous system and their diminished capacity to phagocytose waste and toxic protein aggregates (reviewed in [101]). In addition, aged microglia promote greater inflammation in the aging nervous system, which raises the possibility that they contribute to the genetic instability observed in aging neurons [105].

Recent research using single cell RNA-sequencing further demonstrated the intricacy of microglia, which exhibit a wide range of abnormalities both during normal development and as we age. Particularly, the microglia states in adult, elderly, and early postnatal brains all differ significantly from one another [106-108]. For example, the greatest microglia heterogeneity

was found in developing, aged and injured brains [106]. Moreover, Neurodegenerative and demyelinating disorders induced context-dependent subgroups of microglia with unique molecular characteristics and varied cellular dynamics [108].

Multiple Sclerosis (MS)

Multiple sclerosis (MS) lesions that do not resolve in the months after they form harbour ongoing demyelination and axon degeneration, and are identifiable in vivo by their paramagnetic rims on MRI scans [109]. In the onset and remission of CNS inflammation, such as in MS and its animal counterpart, experimental autoimmune encephalomyelitis (EAE), macrophages, monocytes, dendrocytes, and maybe CAMs play crucial roles [40]. Although numerous cell types are implicated in the pathogenesis of MS, self-reactive T lymphocytes that settle in the CNS and launch an immunological attack against the myelin sheaths that cover neurons are thought to be the primary culprit [110]. In this setting, myeloid cells are very dynamic and interact with a variety of cell types, including CNS-resident astrocytes, oligodendrocytes, and neurons, as well as T cells that have been recruited from the CNS. Monocytes that are pro-inflammatory are crucial in the development of EAE and maybe MS. The recruitment of classical proinflammatory CCR2+ Ly-6Chi monocytes is an important characteristic of the EAE model [111], and consistent with the current pathological criteria for lesion classification in MS [112]. In MS patients and EAE mouse brains, resident microglia were marked, and specific subpopulations of microglia were similarly present. These were predominantly *Ccl4*+ cells in MS lesions [106].

Indeed, high-dimensional single-cell technologies have made it possible to classify myeloid cells in great detail and have never-before-seen access to them in the CNS and surrounding regions. The CNS myeloid compartment, comprising the brain parenchyma and meninges, was examined in a thorough set of single-cell mass spectrometry and flow cytometry investigations in homeostasis and EAE [56]. Researchers found that MHC-II, CD44, CD11c, and PDL1 traditional pathways were all activated in brain-associated myeloid cells during CNS inflammation.

Single-nucleus RNA sequencing guided by MRI was used to characterize demyelinated white matter lesions at different phases of inflammation in MS. Researchers found significant glial and immunological cell variety, particularly around the border of the chronically inflamed lesion. Interestingly, transcriptional profile of inflamed microglia in MS overlaps with that of microglia in other neurodegenerative diseases, indicating that primary and secondary neurodegeneration may have similar underlying processes and respond to comparable treatment strategies [109]. Moreover, the observation that microglia ablation with a Csf1 inhibitor during EAE progression worsens clinical impairment suggests that the functions of microglia are likely to change during the course of the disease [113].

Guillain-Barré Syndrome (GBS)

Guillain-Barré syndrome is a simple illustration of a disease state where aberrant immune activation is the principal driver of pathological processes in peripheral nerves (GBS). Following a bacterial or viral infection, molecular mimicry is thought to be the cause of GBS, an autoimmune illness [114]. GBS refers to a spectrum of acute immune-mediated illnesses that are limited to peripheral nerves and nerve roots and is the most frequent cause of acute neuromuscular weakness and paralysis worldwide. Changes in BNB permeability, macrophage infiltration, and macrophage-associated demyelination have all been observed in GBS [115], however the precise involvement of macrophages in this disease is still unclear. The complement cascade mechanism is activated by auto-antibodies against SCs and axonal plasma membranes, which further draws macrophages to the damage site [116]. Additionally, Th1 cells release TNFα, which boosts the production of MCP-1 and ICAM-1, aiding macrophage infiltration, SC identification, and ultimately myelin phagocytosis [117]. The development and progression of GBS and its animal model were both demonstrated to be significantly influenced by the macrophage migration inhibitory factor (MIF) [118]. Recently, it was shown that GBS patients had macrophage cytoplasmic processes that had invaded the internodes and nodal regions of the sural nerves. These locations had a link to demyelination brought on by macrophages [119]. In

comparison to healthy persons, human GBS patients have been found to have higher median amounts of inflammatory mediators such IL-8 and IL-1ra, as well as CCL2-7-9, CXCL9-10-12, and VEGF in their CSF fluid [120].

Chemotherapy-Induced Peripheral Neuropathy (CIPN)

With a prevalence ranging from 19% to over 85%, chemotherapy-induced peripheral neuropathy (CIPN) is one of the most common adverse effects brought on by antineoplastic medications [121]. Following therapies with vinca alkaloids, such as vincristine, platinum compounds, such as cisplatin and oxaliplatin, and taxanes, CIPN develops (e.g. paclitaxel). Importantly, pathological alterations and symptoms are primarily sensory, including pain, tingling, and numbness, and they depend on the dose, frequency, and physicochemical qualities of the medication [122]. Peripheral sensitization brought on by inflammation and oxidative stress have been suggested as probable causes of CIPN, despite the fact that the underlying mechanisms are not fully understood. In dorsal root ganglia (DRG) sensory neurons, CIPN is linked to mitochondrial changes, elevated intracellular ROS, and elevated inflammatory cytokines [123,124]. Paclitaxel has been demonstrated to increase neuronal ROS in mouse models, and this has been proven to activate the endogenous expression of the antioxidant enzyme superoxide dismutase-1 (SOD1) [125]. Additionally, it is well known that chemotherapeutic drugs promote the immune system's participation in the anti-cancer action in both animal models and human patients [126]. Given that there is occasionally only a minimal association between CIPN and neuronal injury, both in human patients and animal models, the role of non-neuronal cells, notably leukocytes, in CIPN is particularly significant [127]. Numerous studies using paclitaxel-induced animal models of CIPN show that symptoms are accompanied by innate immune signals, particularly macrophages in the DRG and sciatic nerves [128-130]. This is because TLR4 signaling is activated, and the expression of MCP-1 is enhanced [130]. The breakdown of the BNB by matrix metalloproteinases (MMPs), some of which are induced by

chemotherapy medications, can worsen the entry of poisons and leukocytes through the BNB. When monoclonal anti-MMP9 antibodies are administered, the expression of IL-6 and TNFα is greatly reduced. These two proinflammatory cytokines have been linked to paclitaxel-induced CIPN [131]. Oxaliplatin was found to activate MMP-9, increase tissue factor (TF) and HSP70 expression in macrophages, and stimulate the hypoxia signaling pathway through HIF-1 in a murine CIPN model, all of which result in circulatory disturbances caused by thrombosis in the sciatic nerve microenvironment [132]. More recently, it was discovered that oxaliplatin increased the release of high-mobility group box-1 (HMGB-1) from neurons and macrophages, which in turn caused the release of MMP-9 in neurons and macrophages, accelerating the course of CIPN in mice [133].

Diabetic PolyNeuropathy (DPN)

The existence of the diabetic milieu is well known to result from the activation of inflammatory and oxidative stress pathways by hyperglycaemia. These two axes interact at various levels of cell signalling, which over time results in diabetic polyneuropathy (DPN), a condition marked by peripheral nerve dysfunction and microvascular consequences [134-136]. Advanced glycation end products (AGEs), polyol, protein kinase C (PKC), and hexosamine pathways are among the metabolic pathways that are activated by unchecked chronic hyperglycaemia and change the cellular metabolic state. AGEs induce the production of cytokines such IL-1, IL-6, IL-17, TNFα, C reactive protein, and chemokines like CCL-2 and CXC by macrophages and microglia [93]. Additionally, cells that are hyperglycaemia-sensitive, like endothelial cells, react by producing more mitochondrial ROS and RNS and creating more vascular adhesion molecules. Persistent hyperglycaemia also alters the glycosylation of myelin proteins and, as a result, their antigenicity, leading to increased infiltration and activation of neutrophils, macrophages, and monocytes as well as the formation of ROS. Metabolically generated ROS emission in diabetic leukocytes is more impulsive and dysregulated than ROS generation in the anti-microbial response, which is well-regulated. Oedema, inflammation, and cell necrosis are caused by macrophage

infiltration, which also exacerbates damage to the myelin sheath and raises axon excitability. [93,134,135]. The Nrf-2 pathway has been demonstrated to be repressed in these circumstances, which results in a downregulation of the expression of antioxidant genes [135]. Therefore, prolonged high glucose levels trigger a vicious cycle of neuroinflammation, oxidative stress, and microvasculitis at nerve sites, damaging peripheral nerves and resulting in a wide spectrum of sensori-motor symptoms.

Charcot-Marie-Tooth Disease (CMT)

The most prevalent hereditary disorder of the PNS is the heterogeneous set of illnesses known as Charcot-Marie-Tooth (CMT) disease. Lesions in the myelin (CMT1) or axons (CMT2) are the signs of genetic alterations, which can also cause sensory disturbances and distal muscular weakening [137]. There have been reports of the presence of neuroinflammation in both demyelinating and axonal CMT. Myelin gene mutations associated with CMT1 cause SC cytotoxicity, impaired myelination, and ultimately nerve pathology. It's interesting to note that research using CMT1X, CMT1A, and CMT1B mouse models revealed that mutant SC express MCP-1/CCL2 via the MEK-ERK signalling pathway, which directs pathogenic macrophage invasion. The CSF-1-expressing fibroblasts and endoneurial macrophages in the sick nerve were also found to make significant cell-cell connections, which raised greater concerns about the intricate cellular and molecular interactions in peripheral nerves [138]. On the other hand, axonal CMT is brought on by mutations in the gene for the mitochondrial protein GDAP1 (Ganglioside-induced differentiation-associated protein 1), which is also linked to elevated levels of inflammatory mediators and ROS [139]. Additionally, oxidative stress has been mentioned in relation to CMT1A patients [140] and the rat model [85], raising the possibility that it contributes to the disease process. However, in the case of CMT disease, the connection between oxidative stress and macrophages has not yet been proven.

Macrophages in Therapy

What about the therapeutic potential of macrophages and microglia? Indeed monocyte/macrophage modulation has therapeutic potential for treating a variety of pathologies, including cancer, metabolic, autoimmune, and neuroinflammatory illnesses, as well as for regenerative medicine, thanks to the divergence in these phenotypes. This strategy has already been the focus of in-depth research. Indeed, targeting the CNS microglia is much more advanced than that of PNS macrophages. Many preclinical studies have been very promising and have led to a relatively big number of completed or recruiting clinical trials [141]. Diagnostic and therapeutic trials regarding the implication of microglia in MS, Alzheimer's disease, and traumatic brain injury are being carried out (clinicaltrials.gov).

On the other hand, cell therapy using *ex vivo*-activated macrophages or the administration of chemicals and biomaterials to modify the accumulation and behaviour of endogenous macrophages are two potential therapeutic approaches [142]. By modifying the action of inflammatory cytokines and transcription factors, attempts have also been made to promote an anti-inflammatory M2-like phenotype or inhibit a pro-inflammatory M1-like phenotype. Anti-IL-1 antibodies have been demonstrated to enhance the M2-like phenotype and downregulate the M1-like phenotype in diabetic rats, enhancing wound healing [143]. Similar to this, topical administration of PPAR-agonists—which are known to encourage an M2-like phenotype [77]—improved wound healing in diabetic mice [144]. Similar results have been observed in rats with spinal cord injuries treated with systemic M-CSF treatment [145]. Similarly, implanting dental pulp stem cells reduced diabetic polyneuropathy and reduced inflammation in rat sciatic nerves by encouraging macrophage polarization toward an anti-inflammatory phenotype [146].

In CMT1A mouse model (C61 mouse), macrophage ablation by treatment with inhibitor of CSF-1R, PLX5622, failed to mitigate neuropathological changes when treatment started at 3 months of

age [147]. However, genetic inactivation of CSF-1 in these mice resulted in lower endoneurial macrophage numbers and alleviated the neuropathy. Afterwards, lactating mothers of CMT1A mice were treated with chow containing PLX5622, followed by treatment of the respective new-borns after weaning until the age of 6 months by PLX5622. The authors [148] found out that CMT1A symptoms were substantially alleviated after early postnatal treatment, leading to preserved motor function in CMT1A mice. Additionally, macrophage reduction had an impact on the changed phenotype of Schwann cell differentiation.

Data from the PNS are currently insufficient in a clinical setting. However, some clinical information has been gathered through tests in several organ systems. In both animal and human investigations, novel therapeutic approaches based on one or more targets in this network (e.g., inhibiting microglia/macrophage activity, reducing oxidative stress, blocking MMPs, and anticoagulants) showed promise in preventing or lessening the symptoms of CIPN [149]. By changing the polarization of macrophages from an M1 to an M2 profile, for instance, niacin therapy in Parkinson's disease patients was associated with an enhanced quality of life [150]. Additionally, it has been demonstrated that patients suffering from heart failure or stroke benefit from receiving ex vivo-activated autologous M2 macrophages [151,152]. Although clinical trials are currently lacking, numerous experimental and clinical studies have demonstrated a protective function for MIF in GBS [118]. Many clinical trials have utilized macrophage-related variables as primary or secondary clinical outcomes or biomarkers, such as cytokine secretion (for example NCT03321955).

Conclusion and Discussion

The fact that many tissue-resident macrophages do not directly derive from monocytes is now widely acknowledged. In fact, a portion of the tissue-resident macrophage pool, which is seeded during pregnancy, is contributed by the provision of monocytes during homeostasis [153]. But regardless of where macrophages

come from, the tissue-specific local environment is now understood to be the most effective regulator of their phenotype. The daily function, maintenance, population density, and interaction with the surrounding microenvironment (or niche) are some of the concepts put out to explain macrophage differentiation [1]. These arguments highlight the intricacy and diversity of these immune cells in tissue. For instance, macrophage heterogeneity within a single tissue may be understated in part as a result of the difficulties in examining small cell subsets and the potential for sample contamination by other cells. These restrictions are currently being overcome by new sophisticated single-cell sequencing and destiny mapping techniques, which are making a significant contribution to the field.

Peripheral nerve injuries result in the recruitment of monocytes to the area of injury and the activation of local macrophages. Neuroinflammation refers to a group of processes that can either improve or impair nerve function. Although PNS axons have the ability to regenerate damaged tissue, clinical experience attests to pathological tissue remodelling and unsatisfactory functional recovery. These results are a result of the intricate interactions between SCs, the axon, macrophages, and endoneurial fibroblasts. It's possible to mistakenly believe that nerve regeneration in the PNS is less invasively needed than in the CNS [9]. However, the age of the patient, the length of time before treatment, the type, location, and severity of the damage, as well as the recruitment of non-neuronal cells are all local factors that affect PNS regeneration. Several studies are being carried out on how to use neuroinflammation to our advantage by polarizing macrophages into their regulatory/anti-inflammatory phenotype or by promoting the removal of debris. In addition, it is important to note that the interactions between the four local cell types previously discussed appear to be vital in both healthy and pathological circumstances, making them a promising but difficult target for possible therapies. In the future, by focusing on both neuroinflammatory and oxidative stress pathways, study into the manipulation of macrophage phenotype may provide strategies to reduce and reverse damages to peripheral nerves or brain.

Finally, neuroinflammation seems to be a crucial landmark in both central and peripheral neuropathies. Applying the newest research methods (single cell analysis, fate mapping) to the PNS will undoubtedly yield useful data about the geographical, temporal, and functional distribution of tissue macrophages, despite their current limitations in comparison to their more extensive use in the research of CNS cells. In the setting of a pathological condition, these traits are anticipated to be considerably more complicated. As there is a paucity of information on this subject, further research into macrophage recruitment and origin in diseased situations is an intriguing topic. Furthermore, more research is needed to confirm the current hypothesis that macrophages regulate inflammatory responses and pain signals through interactions with primary sensory neurons in peripheral tissues and the DRG. The widespread distribution of peripheral nerves across different tissue compartments presents another difficulty in investigating macrophages connected to the PNS; as a result, nerve-associated macrophages are exposed to varied environmental signals. In fact, epigenetic imprinting cannot be detected using transcriptomic or proteomic methods, making it necessary to combine several methods to determine the state of the chromatin.

References

1. Guilliams M, Thierry GR, Bonnardel J, Bajenoff M. Establishment and Maintenance of the Macrophage Niche. Immunity. 2020; 52: 434–451.
2. Heumann, R, Korsching S, Bandtlow C, Thoenen H. Changes of nerve growth factor synthesis in nonneuronal cells in response to sciatic nerve transection. J Cell Biol. 1987; 104: 1623–1631.
3. La Fleur M, Underwood JL, Rappolee DA, Werb Z. Basement membrane and repair of injury to peripheral nerve: defining a potential role for macrophages, matrix metalloproteinases, and tissue inhibitor of metalloproteinases-1. J Exp Med. 1996; 184: 2311–2326.
4. Sulaiman OA, Gordon T. Effects of short- and long-term Schwann cell denervation on peripheral nerve regeneration, myelination, and size. Glia. 2000; 32: 234–246.

5. Shamash S, Reichert F, Rotshenker S. The cytokine network of Wallerian degeneration: tumor necrosis factor-alpha, interleukin-1alpha, and interleukin-1beta. J Neurosci Off J Soc Neurosci. 2002; 22: 3052–3060.
6. Perrin FE, Lacroix S, Avilés-Trigueros M, David S. Involvement of monocyte chemoattractant protein-1, macrophage inflammatory protein-1alpha and interleukin-1beta in Wallerian degeneration. Brain J Neurol. 2005; 128: 854–866.
7. Chen P, Piao X, Bonaldo P. Role of macrophages in Wallerian degeneration and axonal regeneration after peripheral nerve injury. Acta Neuropathol (Berl). 2015; 130: 605–618.
8. Caillaud M, Richard L, Vallat JM, Desmoulière A, Billet F. Peripheral nerve regeneration and intraneural revascularization. Neural Regen Res. 2019; 14: 24–33.
9. Scheib J, Höke A. Advances in peripheral nerve regeneration. Nat Rev Neurol. 2013; 9: 668–676.
10. Yong HYF, Rawji KS, Ghorbani S, Xue M, Yong VW. The benefits of neuroinflammation for the repair of the injured central nervous system. Cell Mol Immunol. 2019; 16: 540–546.
11. Yunna C, Mengru H, Lei W, Weidong C. Macrophage M1/M2 polarization. Eur J Pharmacol. 2020; 877: 173090.
12. Carrel A, Ebeling AH. The fundamental properties of the fibroblast and the macrophage: II. The macrophage. J Exp Med. 1926; 44: 285–305.
13. van Furth R, Cohn ZA, Hirsch JG, Humphrey JH, Spector WG, et al. The mononuclear phagocyte system: a new classification of macrophages, monocytes, and their precursor cells. Bull World Health Organ. 1972; 46: 845–852.
14. Rojo R, Pridans C, Langlais D, Hume DA. Transcriptional mechanisms that control expression of the macrophage colony-stimulating factor receptor locus. Clin Sci Lond Engl 1979. 2017; 131: 2161–2182.
15. Hashimoto D, Chow A, Noizat C, Teo P, Beasley MB, et al. Tissue-resident macrophages self-maintain locally throughout adult life with minimal contribution from circulating monocytes. Immunity. 2013; 38: 792–804.

16. Epelman S, Lavine KJ, Beaudin AE, Sojka DK, Carrero JA, et al. Embryonic and adult-derived resident cardiac macrophages are maintained through distinct mechanisms at steady state and during inflammation. Immunity. 2014; 40: 91–104.
17. Ginhoux F, Guilliams M. Tissue-Resident Macrophage Ontogeny and Homeostasis. Immunity. 2016; 44: 439–449.
18. Makhijani K, Brückner K. Of blood cells and the nervous system: hematopoiesis in the Drosophila larva. Fly (Austin). 2012; 6: 254–260.
19. Gomez Perdiguero E, Klapproth K, Schulz C, Busch K, Azzoni E, et al. Tissue-resident macrophages originate from yolk-sac-derived erythro-myeloid progenitors. Nature. 2015; 518: 547–551.
20. Kierdorf K, Masuda T, Jordão MJC, Prinz M. Macrophages at CNS interfaces: ontogeny and function in health and disease. Nat Rev Neurosci. 2019; 20: 547–562.
21. Kierdorf K, Erny D, Goldmann T, Sander V, Schulz C, et al. Microglia emerge from erythromyeloid precursors via Pu.1- and Irf8-dependent pathways. Nat Neurosci. 2013; 16: 273–280.
22. Epelman S, Lavine KJ, Randolph GJ. Origin and functions of tissue macrophages. Immunity. 2014; 41: 21–35.
23. Weigert A, von Knethen A, Fuhrmann D, Dehne N, Brüne B. Redox-signals and macrophage biology. Mol Aspects Med. 2018; 63: 70–87.
24. Wynn TA, Vannella KM. Macrophages in Tissue Repair, Regeneration, and Fibrosis. Immunity. 2016; 44: 450–462.
25. Mantovani A, Sica A, Sozzani S, Allavena P, Vecchi A, et al. The chemokine system in diverse forms of macrophage activation and polarization. Trends Immunol. 2004; 25: 677–686.
26. Tomlinson JE, Žygelytė E, Grenier JK, Edwards MG, Cheetham J. Temporal changes in macrophage phenotype after peripheral nerve injury. J Neuroinflammation. 2018; 15: 185.
27. Yao Y, Xu XH, Jin L. Macrophage Polarization in Physiological and Pathological Pregnancy. Front Immunol. 2019; 10: 792.
28. Sica A, Mantovani A. Macrophage plasticity and

polarization: In vivo veritas. J Clin Invest. 2012; 122: 787–795.
29. Martinez FO, Gordon S. The M1 and M2 paradigm of macrophage activation: Time for reassessment. F1000Prime Rep. 2014; 6.
30. Xue J, Schmidt SV, Sander J, Draffehn A, Krebs W, et al. Transcriptome-based network analysis reveals a spectrum model of human macrophage activation. Immunity. 2014; 40: 274–288.
31. Ydens E, Amann L, Asselbergh B, Scott CL, Martens L, et al. Profiling peripheral nerve macrophages reveals two macrophage subsets with distinct localization, transcriptome and response to injury. Nat Neurosci. 2020; 23: 676–689.
32. Kolter J, Feuerstein R, Zeis P, Hagemeyer N, Paterson N, et al. A Subset of Skin Macrophages Contributes to the Surveillance and Regeneration of Local Nerves. Immunity. 2019; 50: 1482-1497.e7.
33. Kolter J, Kierdorf K, Henneke P. Origin and Differentiation of Nerve-Associated Macrophages. J Immunol Baltim Md 1950. 2020; 204: 271–279.
34. Lech M, Anders HJ. Macrophages and fibrosis: How resident and infiltrating mononuclear phagocytes orchestrate all phases of tissue injury and repair. Biochim Biophys Acta. 2013; 1832: 989–997.
35. Okabe Y, Medzhitov R. Tissue-specific signals control reversible program of localization and functional polarization of macrophages. Cell. 2014; 157: 832–844.
36. Guilliams M, Scott CL. Does niche competition determine the origin of tissue-resident macrophages? Nat Rev Immunol. 2017; 17: 451–460.
37. Chen S, Yang J, Wei Y, Wei X. Epigenetic regulation of macrophages: from homeostasis maintenance to host defense. Cell Mol Immunol. 2020; 17: 36–49.
38. Lavin Y, Winter D, Blecher-Gonen R, David E, Keren-Shaul H, et al. Tissue-resident macrophage enhancer landscapes are shaped by the local microenvironment. Cell. 2014; 159: 1312–1326.
39. Gosselin D, Skola D, Coufal NG, Holtman IR, Schlachetzki JCM, et al. An environment-dependent transcriptional network specifies human microglia identity. Science. 2017;

356: eaal3222.
40. Prinz M, Masuda T, Wheeler MA, Quintana FJ. Microglia and Central Nervous System–Associated Macrophages—From Origin to Disease Modulation. Annu Rev Immunol. 2021; 39: 251–277.
41. Ransohoff RM, Cardona AE. The myeloid cells of the central nervous system parenchyma. Nature. 2010; 468: 253–262.
42. Herz J, Filiano AJ, Smith A, Yogev N, Kipnis J. Myeloid Cells in the Central Nervous System. Immunity. 2017; 46: 943–956.
43. Prinz M, Priller J. The role of peripheral immune cells in the CNS in steady state and disease. Nat Neurosci. 2017; 20: 136–144.
44. Tay TL, Savage JC, Hui CW, Bisht K, Tremblay MÈ. Microglia across the lifespan: from origin to function in brain development, plasticity and cognition. J Physiol. 2017; 595: 1929–1945.
45. Geirsdottir L, David E, Keren-Shaul H, Weiner A, Bohlen SC, et al. Cross-Species Single-Cell Analysis Reveals Divergence of the Primate Microglia Program. Cell. 2019; 179: 1609-1622.e16.
46. Dos Santos SE, Medeiros M, Porfirio J, Tavares W, Pessôa L, et al. Similar Microglial Cell Densities across Brain Structures and Mammalian Species: Implications for Brain Tissue Function. J Neurosci Off J Soc Neurosci. 2020; 40: 4622–4643.
47. Alliot F, Godin I, Pessac B. Microglia derive from progenitors, originating from the yolk sac, and which proliferate in the brain. Brain Res Dev Brain Res. 1999; 117: 145–152.
48. Ginhoux F, Greter M, Leboeuf M, Nandi S, See P, et al. Fate mapping analysis reveals that adult microglia derive from primitive macrophages. Science. 2010; 330: 841–845.
49. Goldmann T, Wieghofer P, Jordão MJC, Prutek F, Hagemeyer N, et al. Origin, fate and dynamics of macrophages at central nervous system interfaces. Nat Immunol. 2016; 17: 797–805.
50. Ginhoux F, Greter M, Leboeuf M, Nandi S, See P, et al. Fate mapping analysis reveals that adult microglia derive from primitive macrophages. Science. 2010; 330: 841–545.

51. Herbomel P, Thisse B, Thisse C. Zebrafish early macrophages colonize cephalic mesenchyme and developing brain, retina, and epidermis through a M-CSF receptor-dependent invasive process. Dev Biol. 2001; 238: 274–288.
52. Schulz C, Gomez Perdiguero E, Chorro L, Szabo-Rogers H, Cagnard N, et al. A lineage of myeloid cells independent of Myb and hematopoietic stem cells. Science. 2012; 336: 86–90.
53. Goldmann T, Wieghofer P, Jordão MJC, Prutek F, Hagemeyer N, et al. Origin, fate and dynamics of macrophages at central nervous system interfaces. Nat Immunol. 2016; 17: 797–805.
54. Stremmel C, Schuchert R, Wagner F, Thaler R, Weinberger T, et al. Yolk sac macrophage progenitors traffic to the embryo during defined stages of development. Nat Commun. 2018; 9: 75.
55. Hoeffel G, Chen J, Lavin Y, Low D, Almeida FF, et al. C-Myb+ Erythro-Myeloid Progenitor-Derived Fetal Monocytes Give Rise to Adult Tissue-Resident Macrophages. Immunity. 2015; 42: 665–678.
56. Mrdjen D, Pavlovic A, Hartmann FJ, Schreiner B, Utz SG, et al. High-Dimensional Single-Cell Mapping of Central Nervous System Immune Cells Reveals Distinct Myeloid Subsets in Health, Aging, and Disease. Immunity. 2018; 48: 380-395.e6.
57. Van Hove H, Martens L, Scheyltjens I, De Vlaminck K, Pombo Antunes AR, et al. A single-cell atlas of mouse brain macrophages reveals unique transcriptional identities shaped by ontogeny and tissue environment. Nat Neurosci. 2019; 22: 1021–1035.
58. Utz SG, See P, Mildenberger W, Thion MS, Silvin A, et al. Early Fate Defines Microglia and Non-parenchymal Brain Macrophage Development. Cell. 2020; 181: 557-573.e18.
59. O'Koren EG, Yu C, Klingeborn M, Wong AYW, Prigge CL, et al. Microglial Function Is Distinct in Different Anatomical Locations during Retinal Homeostasis and Degeneration. Immunity. 2019; 50: 723-737.e7.
60. Wieghofer P, Hagemeyer N, Sankowski R, Schlecht A, Staszewski O, et al. Mapping the origin and fate of myeloid cells in distinct compartments of the eye by single-cell

profiling. EMBO J. 2021; 40: e105123.
61. Oudejans E, Luchicchi A, Strijbis EMM, Geurts JJG, Dam AM van. Is MS affecting the CNS only? Lessons from clinic to myelin pathophysiology. Neurol - Neuroimmunol Neuroinflammation. 2021; 8. Available online at: https://nn.neurology.org/content/8/1/e914
62. Richard L, Védrenne N, Vallat JM, Funalot B. Characterization of Endoneurial Fibroblast-like Cells from Human and Rat Peripheral Nerves. J Histochem Cytochem. 2014; 62: 424–435.
63. Mueller M, Leonhard C, Wacker K, Ringelstein EB, Okabe M, et al. Macrophage Response to Peripheral Nerve Injury: The Quantitative Contribution of Resident and Hematogenous Macrophages. Lab Invest. 2003; 83: 175–185.
64. Ubogu EE. Biology of the human blood-nerve barrier in health and disease. Exp Neurol. 2020; 328: 113272.
65. Oldfors A. Macrophages in peripheral nerves. An ultrastructural and enzyme histochemical study on rats. Acta Neuropathol (Berl). 1980; 49: 43–49.
66. Griffin JW, George R, Ho T. Macrophage systems in peripheral nerves. A review. J Neuropathol Exp Neurol. 1993; 52: 553–560.
67. Yang J, Zhang L, Yu C, Yang XF, Wang H. Monocyte and macrophage differentiation: circulation inflammatory monocyte as biomarker for inflammatory diseases. Biomark Res. 2014; 2: 1.
68. Old EA, Nadkarni S, Grist J, Gentry C, Bevan S, et al. Monocytes expressing CX3CR1 orchestrate the development of vincristine-induced pain. J Clin Invest. 2014; 124: 2023–2036.
69. Zhuang ZY, Kawasaki Y, Tan PH, Wen YR, Huang J, et al. Role of the CX3CR1/p38 MAPK pathway in spinal microglia for the development of neuropathic pain following nerve injury-induced cleavage of fractalkine. Brain Behav Immun. 2007; 21: 642–651.
70. Cattin AL, Burden JJ, Van Emmenis L, Mackenzie FE, Hoving JJA, et al. Macrophage-Induced Blood Vessels Guide Schwann Cell-Mediated Regeneration of Peripheral Nerves. Cell. 2015; 162: 1127–1139.

71. Abbadie C, Lindia JA, Cumiskey AM, Peterson LB, Mudgett JS, et al. Impaired neuropathic pain responses in mice lacking the chemokine receptor CCR2. Proc Natl Acad Sci U S A. 2003; 100: 7947–7952.
72. Jung H, Toth PT, White FA, Miller RJ. Monocyte chemoattractant protein-1 functions as a neuromodulator in dorsal root ganglia neurons. J Neurochem. 2008; 104: 254–263.
73. Makita T. Nerve Control of Blood Vessel Patterning. Dev Cell. 2013; 24: 340–341.
74. Balayssac D, Cayre A, Authier N, Bourdu S, Penault-Llorca F, et al. Patterns of P-glycoprotein activity in the nervous system during vincristine-induced neuropathy in rats. J Peripher Nerv Syst JPNS. 2005; 10: 301–310.
75. Yang C, Hawkins KE, Doré S, Candelario-Jalil E. Neuroinflammatory mechanisms of blood-brain barrier damage in ischemic stroke. Am J Physiol Cell Physiol. 2019; 316: C135–153.
76. Skaper SD. Impact of Inflammation on the Blood-Neural Barrier and Blood-Nerve Interface: From Review to Therapeutic Preview. Int Rev Neurobiol. 2017; 137: 29–45.
77. Krizbai IA, Bauer H, Bresgen N, Eckl PM, Farkas A, et al. Effect of oxidative stress on the junctional proteins of cultured cerebral endothelial cells. Cell Mol Neurobiol. 2005; 25: 129–139.
78. Lambert AJ, Brand MD. Reactive oxygen species production by mitochondria. Methods Mol Biol Clifton NJ. 2009; 554: 165–181.
79. Checa J, Aran JM. Reactive Oxygen Species: Drivers of Physiological and Pathological Processes. J Inflamm Res. 2020; 13: 1057–1073.
80. Poljsak B, Šuput D, Milisav I. Achieving the balance between ROS and antioxidants: when to use the synthetic antioxidants. Oxid Med Cell Longev. 2013; 2013: 956792.
81. Virág L, Jaén RI, Regdon Z, Boscá L, Prieto P. Self-defense of macrophages against oxidative injury: Fighting for their own survival. Redox Biol. 2019; 26: 101261.
82. Ponath V, Kaina B. Death of Monocytes through Oxidative Burst of Macrophages and Neutrophils: Killing in Trans. PLOS ONE. 2017; 12: e0170347.

83. Halliwell B. Oxidative stress and neurodegeneration: where are we now? J Neurochem. 2006; 97: 1634–1658.
84. Knight JA. Diseases related to oxygen-derived free radicals. Ann Clin Lab Sci. 1995; 25: 111–121.
85. Caillaud M, Msheik Z, Ndong-Ntoutoume GMA, Vignaud L, Richard L, et al. Curcumin-cyclodextrin/cellulose Nanocrystals Improve the Phenotype of Charcot-Marie-Tooth-1A Transgenic Rats Through the Reduction of Oxidative Stress. Free Radic Biol Med. 2020; 161: 246-262.
86. Eid SA, El Massry M, Hichor M, Haddad M, Grenier J, et al. Targeting the NADPH Oxidase-4 and Liver X Receptor Pathway Preserves Schwann Cell Integrity in Diabetic Mice. Diabetes. 2020; 69: 448–464.
87. Caillaud M, Chantemargue B, Richard L, Vignaud L, Favreau F, et al. Local low dose curcumin treatment improves functional recovery and remyelination in a rat model of sciatic nerve crush through inhibition of oxidative stress. Neuropharmacology. 2018; 139: 98–116.
88. Geng Z, Tong X, Jia H. Reactive oxygen species (ROS) mediates non-freezing cold injury of rat sciatic nerve. Int J Clin Exp Med. 2015; 8: 15700–15707.
89. Block ML, Zecca L, Hong JS. Microglia-mediated neurotoxicity: uncovering the molecular mechanisms. Nat Rev Neurosci. 2007; 8: 57–69.
90. Hervera A, De Virgiliis F, Palmisano I, Zhou L, Tantardini E, et al. Reactive oxygen species regulate axonal regeneration through the release of exosomal NADPH oxidase 2 complexes into injured axons. Nat Cell Biol. 2018; 20: 307–319.
91. Hackel D, Pflücke D, Neumann A, Viebahn J, Mousa S, et al. The connection of monocytes and reactive oxygen species in pain. PloS One. 2013; 8: e63564.
92. W Tian, T Czopka, H López-Schier. Systemic loss of Sarm1 protects Schwann cells from chemotoxicity by delaying axon degeneration. Commun. Biol. 2020; 3: 1–14.
93. Rendra E, Riabov V, Mossel DM, Sevastyanova T, Harmsen MC, et al. Reactive oxygen species (ROS) in macrophage activation and function in diabetes. Immunobiology. 2019; 224: 242–253.
94. Yang H, Li S. Transient Receptor Potential Ankyrin 1

(TRPA1) Channel and Neurogenic Inflammation in Pathogenesis of Asthma. Med Sci Monit Int Med J Exp Clin Res. 2016; 22: 2917–2923.
95. Tsuda M, Shigemoto-Mogami Y, Koizumi S, Mizokoshi A, Kohsaka S, et al. P2X4 receptors induced in spinal microglia gate tactile allodynia after nerve injury. Nature. 2003; 424: 778–783.
96. Scholz J, Woolf CJ. The neuropathic pain triad: neurons, immune cells and glia. Nat Neurosci. 2007; 10: 1361–1368.
97. Okubo M, Yamanaka H, Kobayashi K, Dai Y, Kanda H, et al. Macrophage-Colony Stimulating Factor Derived from Injured Primary Afferent Induces Proliferation of Spinal Microglia and Neuropathic Pain in Rats. PloS One. 2016; 11: e0153375.
98. Bauder AR, Ferguson TA. Reproducible Mouse Sciatic Nerve Crush and Subsequent Assessment of Regeneration by Whole Mount Muscle Analysis. J Vis Exp JoVE. 2012; 60: 3606.
99. Rademakers R, Baker M, Nicholson AM, Rutherford NJ, Finch N, et al. Mutations in the colony stimulating factor 1 receptor (CSF1R) gene cause hereditary diffuse leukoencephalopathy with spheroids. Nat Genet. 2011; 44: 200–205.
100. Halliwell B. Oxidative stress and neurodegeneration: where are we now? J Neurochem. 2006; 97: 1634–1658.
101. Angelova DM, Brown DR. Microglia and the aging brain: are senescent microglia the key to neurodegeneration? J Neurochem. 2019; 151: 676–688.
102. Z Wu, S Wang, I Wu, M Mata, DJ Fink. Activation of TLR-4 to produce tumour necrosis factor-α in neuropathic pain caused by paclitaxel. Eur. J. Pain Lond. Engl. 2015; 19: 7.
103. Streit WJ, Sammons NW, Kuhns AJ, Sparks DL. Dystrophic microglia in the aging human brain. Glia. 2004; 45: 208–212.
104. Galloway DA, Phillips AEM, Owen DRJ, Moore CS. Phagocytosis in the Brain: Homeostasis and Disease. Front Immunol. 2019; 10: 790.
105. Burhans WC, Weinberger M. DNA replication stress, genome instability and aging. Nucleic Acids Res. 2007; 35:

7545–7556.
106. Hammond TR, Dufort C, Dissing-Olesen L, Giera S, Young A, et al. Single cell RNA sequencing of microglia throughout the mouse lifespan and in the injured brain reveals complex cell-state changes. Immunity. 2019; 50: 253-271.e6.
107. Li Q, Cheng Z, Zhou L, Darmanis S, Neff NF, et al. Developmental heterogeneity of microglia and brain myeloid cells revealed by deep single-cell RNA sequencing. Neuron. 2019; 101: 207-223.e10.
108. Masuda T, Sankowski R, Staszewski O, Böttcher C, Amann L, et al. Spatial and temporal heterogeneity of mouse and human microglia at single-cell resolution. Nature. 2019; 566: 388–392.
109. Absinta M, Maric D, Gharagozloo M, Garton T, Smith MD, et al. A lymphocyte-microglia-astrocyte axis in chronic active multiple sclerosis. Nature. 2021; 597: 709–714.
110. Reich DS, Lucchinetti CF, Calabresi PA. Multiple Sclerosis. N Engl J Med. 2018; 378: 169–180.
111. Mildner A, Mack M, Schmidt H, Brück W, Djukic M, et al. CCR2+Ly-6Chi monocytes are crucial for the effector phase of autoimmunity in the central nervous system. Brain J Neurol. 2009; 132: 2487–2500.
112. Polman CH, Reingold SC, Banwell B, Clanet M, Cohen JA, et al. Diagnostic criteria for multiple sclerosis: 2010 revisions to the McDonald criteria. Ann Neurol. 2011; 69: 292–302.
113. Tanabe S, Saitoh S, Miyajima H, Itokazu T, Yamashita T. Microglia suppress the secondary progression of autoimmune encephalomyelitis. Glia. 2019; 67: 1694–1704.
114. Liu S, Dong C, Ubogu EE. Immunotherapy of Guillain-Barré syndrome. Hum Vaccines Immunother. 2018; 14: 2568–2579.
115. Yosef N, Ubogu EE. α(M)β(2)-integrin-intercellular adhesion molecule-1 interactions drive the flow-dependent trafficking of Guillain-Barré syndrome patient derived mononuclear leukocytes at the blood-nerve barrier in vitro. J Cell Physiol. 2012; 227: 3857–3875.
116. Martini R, Willison H. Neuroinflammation in the peripheral nerve: Cause, modulator, or bystander in

peripheral neuropathies? Glia. 2016; 64: 475–486.
117. Langert KA, Von Zee CL, Stubbs EB. Tumour necrosis factor α enhances CCL2 and ICAM-1 expression in peripheral nerve microvascular endoneurial endothelial cells. ASN Neuro. 2013; 5: e00104.
118. Shen D, Lang Y, Chu F, Wu X, Wang Y, et al. Roles of macrophage migration inhibitory factor in Guillain-Barré syndrome and experimental autoimmune neuritis: beneficial or harmful? Expert Opin Ther Targets. 2018; 22: 567–577.
119. Koike H, Fukami Y, Nishi R, Kawagashira Y, Iijima M, et al. Ultrastructural mechanisms of macrophage-induced demyelination in Guillain-Barré syndrome. J Neurol Neurosurg Psychiatry. 2020; 91: 650–659.
120. Sainaghi PP, Collimedaglia L, Alciato F, Leone MA, Naldi P, et al. The expression pattern of inflammatory mediators in cerebrospinal fluid differentiates Guillain-Barré syndrome from chronic inflammatory demyelinating polyneuropathy. Cytokine. 2010; 51: 138–143.
121. Zajączkowska R, Kocot-Kępska M, Leppert W, Wrzosek A, Mika J, et al. Mechanisms of Chemotherapy-Induced Peripheral Neuropathy. Int J Mol Sci. 2019; 20: E1451.
122. Bouchenaki H, Danigo A, Sturtz F, Hajj R, Magy L, Demiot C. An overview of ongoing clinical trials assessing pharmacological therapeutic strategies to manage chemotherapy-induced peripheral neuropathy, based on preclinical studies in rodent models. Fundam Clin Pharmacol. 2021; 35: 506–523.
123. Boyette-Davis JA, Walters ET, Dougherty PM. Mechanisms involved in the development of chemotherapy-induced neuropathy. Pain Manag. 2015; 5: 285–296.
124. Carozzi VA, Canta A, Chiorazzi A. Chemotherapy-induced peripheral neuropathy: What do we know about mechanisms? Neurosci Lett. 2015; 596: 90–107.
125. Duggett NA, Griffiths LA, McKenna OE, de Santis V, Yongsanguanchai N, et al. Oxidative stress in the development, maintenance and resolution of paclitaxel-induced painful neuropathy. Neuroscience. 2016; 333: 13–26.
126. Zitvogel L, Apetoh L, Ghiringhelli F, Kroemer G. Immunological aspects of cancer chemotherapy. Nat Rev

Immunol. 2008; 8: 59–73.
127. Montague K, Malcangio M. The Therapeutic Potential of Monocyte/Macrophage Manipulation in the Treatment of Chemotherapy-Induced Painful Neuropathy. Front Mol Neurosci. 2017; 10: 397.
128. Peters CM, Jimenez-Andrade JM, Jonas BM, Sevcik MA, Koewler NJ, et al. Intravenous paclitaxel administration in the rat induces a peripheral sensory neuropathy characterized by macrophage infiltration and injury to sensory neurons and their supporting cells. Exp Neurol. 2007; 203: 42–54.
129. Liu CC, Lu N, Cui Y, Yang T, Zhao ZQ, et al. Prevention of paclitaxel-induced allodynia by minocycline: Effect on loss of peripheral nerve fibers and infiltration of macrophages in rats. Mol Pain. 2010; 6: 76.
130. Zhang H, Li Y, de Carvalho-Barbosa M, Kavelaars A, Heijnen CJ, et al. Dorsal Root Ganglion Infiltration by Macrophages Contributes to Paclitaxel Chemotherapy-Induced Peripheral Neuropathy. J Pain. 2016; 17: 775–786.
131. Tonello R, Lee SH, Berta T. Monoclonal Antibody Targeting the Matrix Metalloproteinase 9 Prevents and Reverses Paclitaxel-Induced Peripheral Neuropathy in Mice. J Pain. 2019; 20: 515–527.
132. Yang Y, Hu L, Wang C, Yang X, Song L, et al. p38/TF/HIF-α Signaling Pathway Participates in the Progression of CIPN in Mice. BioMed Res Int. 2019; 2019: 5347804.
133. Gu H, Wang C, Li J, Yang Y, Sun W, et al. High mobility group box-1-toll-like receptor 4-phosphatidylinositol 3-kinase/protein kinase B-mediated generation of matrix metalloproteinase-9 in the dorsal root ganglion promotes chemotherapy-induced peripheral neuropathy. Int J Cancer. 2020; 146: 2810–2821.
134. Tesch GH. Role of macrophages in complications of type 2 diabetes. Clin Exp Pharmacol Physiol. 2007; 34: 1016–1019.
135. Sandireddy R, Yerra VG, Areti A, Komirishetty P, Kumar A. Neuroinflammation and oxidative stress in diabetic neuropathy: futuristic strategies based on these targets. Int J Endocrinol. 2014; 2014: 674987.

136. Román-Pintos LM, Villegas-Rivera G, Rodríguez-Carrizalez AD, Miranda-Díaz AG, Cardona-Muñoz EG. Diabetic Polyneuropathy in Type 2 Diabetes Mellitus: Inflammation, Oxidative Stress, and Mitochondrial Function. J Diabetes Res. 2016; 2016: 3425617.
137. Morena J, Gupta A, Hoyle JC. Charcot-Marie-Tooth: From Molecules to Therapy. Int J Mol Sci [Internet]. 2019; 20. Available online at: https://www.ncbi.nlm.nih.gov/pmc/articles/PMC6679156/
138. Groh J, Weis J, Zieger H, Stanley ER, Heuer H, et al. Colony-stimulating factor-1 mediates macrophage-related neural damage in a model for Charcot-Marie-Tooth disease type 1X. Brain J Neurol. 2012; 135: 88–104.
139. Fernandez-Lizarbe S, Civera-Tregón A, Cantarero L, Herrer I, Juarez P, et al. Neuroinflammation in the pathogenesis of axonal Charcot-Marie-Tooth disease caused by lack of GDAP1. Exp Neurol. 2019; 320: 113004.
140. Chahbouni M, López MDS, Molina-Carballo A, de Haro T, Muñoz-Hoyos A, et al. Melatonin Treatment Reduces Oxidative Damage and Normalizes Plasma Pro-Inflammatory Cytokines in Patients Suffering from Charcot-Marie-Tooth Neuropathy: A Pilot Study in Three Children. Mol Basel Switz. 2017; 22: E1728.
141. Kwon HS, Koh SH. Neuroinflammation in neurodegenerative disorders: the roles of microglia and astrocytes. Transl Neurodegener. 2020; 9: 42.
142. Spiller KL, Koh TJ. Macrophage-based therapeutic strategies in regenerative medicine. Adv Drug Deliv Rev. 2017; 122: 74–83.
143. Mirza RE, Fang MM, Weinheimer-Haus EM, Ennis WJ, Koh TJ. Sustained inflammasome activity in macrophages impairs wound healing in type 2 diabetic humans and mice. Diabetes. 2014; 63: 1103–1114.
144. Mirza RE, Fang MM, Novak ML, Urao N, Sui A, et al. Macrophage PPARγ and impaired wound healing in type 2 diabetes. J Pathol. 2015; 236: 433–444.
145. Döring A, Sloka S, Lau L, Mishra M, van Minnen J, et al. Stimulation of monocytes, macrophages, and microglia by amphotericin B and macrophage colony-stimulating factor promotes remyelination. J Neurosci Off J Soc

Neurosci. 2015; 35: 1136–1148.
146. Omi M, Hata M, Nakamura N, Miyabe M, Kobayashi Y, et al. Transplantation of dental pulp stem cells suppressed inflammation in sciatic nerves by promoting macrophage polarization towards anti-inflammation phenotypes and ameliorated diabetic polyneuropathy. J Diabetes Investig. 2016; 7: 485–496.
147. Huxley C, Passage E, Robertson AM, Youl B, Huston S, et al. Correlation between varying levels of PMP22 expression and the degree of demyelination and reduction in nerve conduction velocity in transgenic mice. Hum Mol Genet. 1998; 7: 449–458.
148. Klein D, Groh J, Yuan X, Berve K, Stassart R, et al. Early targeting of endoneurial macrophages alleviates the neuropathy and affects abnormal Schwann cell differentiation in a mouse model of Charcot-Marie-Tooth 1A. Glia. 2022; 70: 1100–1116.
149. Hu LY, Mi WL, Wu GC, Wang YQ, Mao-Ying QL. Prevention and Treatment for Chemotherapy-Induced Peripheral Neuropathy: Therapies Based on CIPN Mechanisms. Curr Neuropharmacol. 2019; 17: 184–196.
150. Wakade C, Giri B, Malik A, Khodadadi H, Morgan JC, et al. Niacin modulates macrophage polarization in Parkinson's disease. J Neuroimmunol. 2018; 320: 76–79.
151. Bartel RL, Cramer C, Ledford K, Longcore A, Parrish C, et al. The Aastrom experience. Stem Cell Res Ther. 2012; 3: 26.
152. Chernykh ER, Shevela EY, Starostina NM, Morozov SA, Davydova MN, et al. Safety and Therapeutic Potential of M2 Macrophages in Stroke Treatment. Cell Transplant. 2016; 25: 1461–1471.
153. Yona S, Kim KW, Wolf Y, Mildner A, Varol D, et al. Fate mapping reveals origins and dynamics of monocytes and tissue macrophages under homeostasis. Immunity. 2013; 38: 79–91.

Book Chapter

The Secreted Glycoprotein PAMR1: A New Potential Tumor Suppressor in Cancer

Layla Haymour, Abderrahman Maftah and Sébastien Legardinier*

Univ. Limoges, LABCiS, UR 22722, F-87000 Limoges, France

***Corresponding Author:** Sébastien Legardinier, Univ. Limoges, LABCiS, UR 22722, F-87000 Limoges, France

Published **March 15, 2023**

This Book Chapter is partly adapted from a pre-published paper by Layla Hamour et al. at BioRXive (Haymour, L., Chaunavel, A., Diab-Assaf, M., Maftah, A. and Legardinier, S. PAMR1 negatively impacts cell proliferation and migration of Human Colon Cancer HT29 Cell Line. BioRXive, posted September 8, 2022. https://doi.org/10.1101/2022.09.07.506931)

How to cite this book chapter: Layla Haymour, Abderrahman Maftah, Sébastien Legardinier. The Secreted Glycoprotein PAMR1: A New Potential Tumor Suppressor in Cancer. In: Hussein Fayyad Kazan, editor. Immunology and Cancer Biology. Hyderabad, India: Vide Leaf. 2023.

Competing Interests: The authors declare that they have no competing interests.

Acknowledgements: The authors gratefully acknowledge the financial support of the “Ligue contre le Cancer”, France.

Introduction

This chapter focuses on PAMR1 (Peptidase domain containing Associated with Muscle Regeneration 1), a secreted multi-domain protein, which was first considered as a putative tumor suppressor in breast cancer in 2015 [1]. It was formerly named RAMP (Regenerative Associated Muscle Protease), because of its C-terminal trypsin-like domain and increased expression during muscle regeneration of injured muscles in mice [2]. After a structural description of PAMR1 (protein structure, isoforms and glycosylation), we will focus on its expression, role and potential mechanisms of action in cancer. We also will consider point mutations found in cancer and affecting all potential glycosylation sites of human PAMR1.

PAMR1: A Multidomain Protein

PAMR1 is a secreted multi-domain glycoprotein formed of five domains: an N-terminal Cubilin domain referred to as CUB (Complement C1r/C1s, Uegf, Bmp1), a unique EGF-like domain (Epidermal growth factor-like domains or ELD), two Sushi domains (Sushi 1 and 2) and C-terminal Peptidase S1 domain (Figure 1).

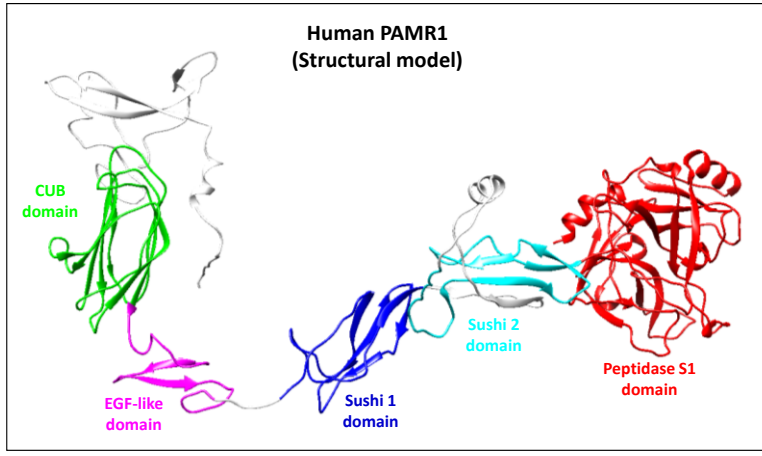

Figure 1: Predicted structural model of human PAMR1 canonical isoform 1 (AF-Q6UX9-F1-MODEL_V4.PDB) using AlphaFold (https://alphafold.ebi.ac.uk/). Boundaries of each colored protein domain were defined according information found in Uniprot database (https://www.uniprot.org/).

The CUB domain is a 110 residue-long extracellular domain, which is found in plasma-membrane and extracellular proteins. CUB-containing-proteins are involved in various functions (complement activation, tissue repair, cell signaling...) and also in tumor suppression [3,4], such as SCUBE2 (Signal peptide, CUB, and EGF-like domain-containing protein 2) [5]. In addition to a CUB domain, PAMR1 and SCUBE2 contain one and nine EGF-like domains respectively. EGF-like domains, which usually comprise about 30 to 40 amino-acid residues and are stabilized by three disulfide bonds, are often involved in protein-protein interactions [6], such as for those between NOTCH receptors and their ligands [7]. Indeed, CUB and EGF-like domains were shown to be involved in tumor suppressor activity of SCUBE2, through protein interactions with Bone Morphogenetic Proteins (BMPs) and E-cadherin respectively [8].

Sushi domains exist in a wide variety of complement and adhesion proteins but are also found in potential tumor suppressors such as SUSD4 (Sushi domain-containing protein 4) [9] and CSMD1 (CUB and Sushi Multiple Domains 1) [10].

The peptidase S1 domain is predominately found in serine proteases. Using Swiss-model server (https://swissmodel.expasy.org/), we found that this domain within human PAMR1 isoform 1 shared 26.53% identity with thrombin heavy chain, which is a serine protease composed of a “catalytic triad” in its active site. The structural model built with thrombin as a template for the peptide S1 domain of human PAMR1 shows a potential catalytic triad (Figure 2) with three key residues very close in space, namely a histidine at position 504, an aspartic acid at position 560 and a threonine (instead of serine as found in thrombin at this position) at position 665.

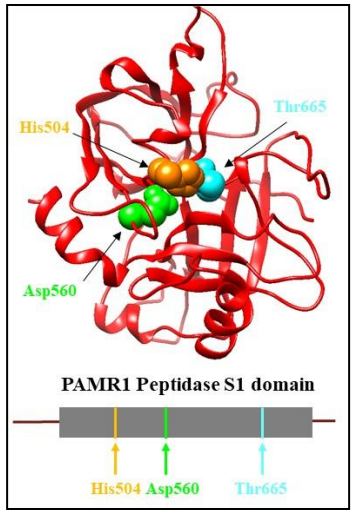

Figure 2: Predicted structure of human PAMR1 trypsin-like domain. The peptidase S1 domain of human PAMR1 (445-720) was built using Swiss-model Server with the X-ray structure of human thrombin (PDB 7SR9) used as a template. The three residues (H^{504}, D^{560}, T^{665}) are spatially close and at the same locations as residues composing the catalytic triad (H^{57}, D^{102}, S^{195}) of thrombin.

Although related to peptidase S1 family, PAMR1 might have no protease activity due to the presence of a threonine residue at position 665 instead of the conserved serine residue. However, some proteins like TSP50, which is homologous to serine proteases, have also a threonine in their catalytic triad [11]. This threonine catalytic site was shown to be essential for TSP protease activity [11] and its function in cell proliferation [12]. Although the threonine residue is known to be substantially less nucleophilic than a serine residue, it might be interesting to determine whether or not PAMR1 might have a protease activity. No evidence in the literature supports this hypothesis.

PAMR1 and Isoforms

There are several human PAMR1 transcripts coding for different isoforms (ENSEMBL database), some of which are well described, and others are predicted. By referring to the UniProt database, three human PAMR1 isoforms (named Iso 1-3) were described and obtained by alternative splicing (Figure 3).

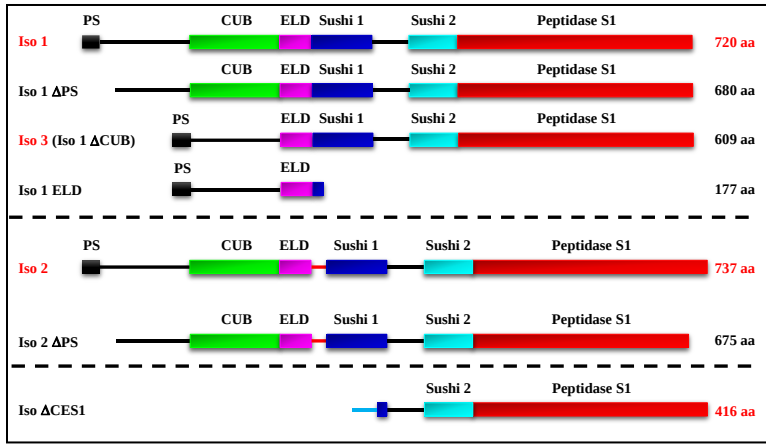

Figure 3: Representation at scale of human PAMR1 isoforms, according to data available in the Uniprot (www.uniprot.org/) and Ensembl (www.ensembl.org/) databases. Three main protein isoforms are described: Iso 1 (canonical isoform), Iso 2 and Iso 3 (named Iso1 ΔCUB). Iso 2 is distinguished from Iso 1 by the presence of 17 additional residues (red line) between the EGF-like domain (ELD) and Sushi 1 domains. The 4 other potential isoforms are: Iso 1 ΔPS (without signal peptide), Iso1 ELD (only ELD is present), Iso 2 ΔPS (without signal peptide) and Iso ΔCES1 (without the CUB, ELD and Sushi1 domains).

Isoform 1 (Iso 1) is considered as the canonical form with a non-mature 720 amino acid (aa) sequence. After cleavage of its signal peptide (21 aa), Iso 1 does not have more than 699 amino acid residues and its theoretical molecular weight (MW) is 77849.95 Da. Isoform 2 (Iso 2) differs from Iso 1 by the presence of 17 additional aa at position 274 (737 aa) following the EGF-like domain (ELD). Iso 2 is therefore composed of 716 aa after cleavage of its signal peptide and its theoretical MW is 79593.93 Da. Isoform 3 (Iso 3) differs from Iso 1 by lacking the CUB domain (Iso1 ΔCUB), it is of 609 aa and 67541 Da of MW. Other described or potential isoforms exist, Iso 1 without signal peptide (Iso 1 ΔSP) or with only the EGF-like domain called ELD (Iso 1 ELD). For Iso 2, there would also be an isoform without signal peptide (Iso2 ΔSP). Finally, there would be an isoform with only the Sushi 2 and peptidase S1 domains (Iso ΔCES1). If the Iso 1 ΔSP and Iso 2 ΔSP isoforms are indeed expressed by cells, it can be expected that they would encode non-secreted isoforms of PAMR1 due to the absence of a signal

peptide. We can wonder what would be the exact location and role of these intracellular isoforms.

PAMR1 is a Glycoprotein with *N*- and *O*-glycans

Human PAMR1 possesses several potential *N*- and *O*-glycosylation sites, as predicted by NetNGlyc, NetOGlyc databases and the presence of consensus sequences of *O*-glycosylation within its EGF-like domain (Figure 4).

Although possessing five *N*-glycosylation consensus sequences of the type Asn-Xaa-(Ser/Thr), only four sites are predicted by the NetNGlyc server [13] to be occupied by *N*-glycans on asparagine residues at positions 96, 279, 451 and 614. Except Asn 96, the three others are located within domains of PAMR1, namely Sushi and Peptidase S1 domain. In humans, *N*-glycans are mainly sialylated and fucosylated complex-type *N*-glycans as shown in Figure 4, with two, three or four antennae. Although PNGase F treatment showed the presence of *N*-glycans on PAMR1, we have not determined yet the number nor the structure of these *N*-glycans. The presence of these *N*-glycans could be required for PAMR1 folding and/or secretion.

Different types of *O*-glycosylation are predicted for human PAMR1. Concerning secreted glycoproteins like PAMR1, the most common *O*-glycosylation is mucin-type *O*-GalNAc glycosylation, for which there is no defined consensus sequence yet but which can be predicted using NetOGlyc [13]. For human PAMR1, 18 sites are predicted with most of them within Sushi 2 and inter-Sushi region (Figure 4) but the occupation of these glyco-sites must be experimentally demonstrated. However, the most relevant predicted *O*-GalNAc glyco-sites are those between the two Sushi domains because mucin-type *O*-glycosylation is often found in not structured proline-rich protein regions. The simplest form of mucin *O*-glycans is formed of attached GalNAc to the serine or threonine. This *O*-GalNAc can be extended by various sugar moieties (galactose, N-acetylglucosamine and sialic acid), forming different “core” structures that are counted to be 8 cores [14]. An example: Galβ1-3GalNAc- is the most common *O*-GalNAc and is referred to as core 1.

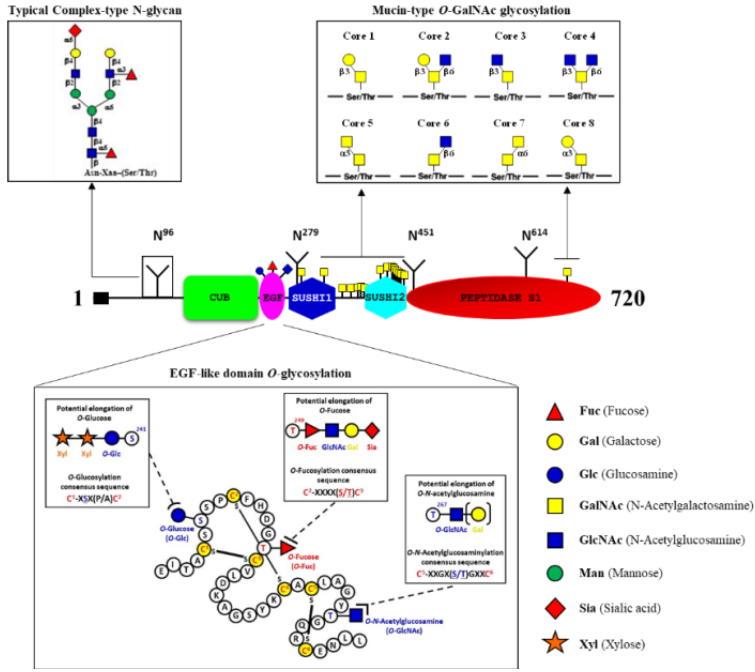

Figure 4: Representation at scale of multi-domain human PAMR1 and its potential *N*- and *O*-glycosylation sites, predicted according to NetNGlyc-1.0 and NetOGlyc-4.0 databases or linked to presence of consensus sequences. An example of sialylated and fucosylated complex-type *N*-glycan with two antennae found in human glycoproteins is shown. Among the eight structures known for *O*-GalNAc mucin-type glycosylation, Core 1-4 are the most abundant ones and can be elongated and terminated with fucoses and/or sialic acids. The EGF-like domain of human PAMR1 exhibits three consensus sequences, for specific addition of *O*-Glucose, *O*-Fucose and *O*-GlcNAc. As shown in inserts, these *O*-linked monosaccharides can be elongated or not by other monosaccharides.

Despite a prediction of one *O*-GalNAc site in the EGF-like domain (see Table I), it is unlikely that a residue would actually be attached as this has never been shown for Notch receptors having 29-36 EGF-like repeats [15]. However, other rare *O*-glycosylations with well-defined consensus sequences can be found in EGF-like domains such as *O*-Glucose, *O*-Fucose and *O*-GlcNAc type glycosylations. Human PAMR1 exhibits the three consensus sequences within its EGF-like domain.

O-Glucosylation is less familiar than most *O*-linked glycosylation, it refers to the attachment of *O*-Glucose to Epidermal growth factors repeats (EGF-like) of proteins, especially NOTCH receptors. It is mediated by *O*-Glucosyltransferases, including POGLUT1 known to add *O*-Glucose on serine of consensus sequence C^1-X-S-X-(P/A)-C^2 of EGF-like domain. *O*-Glucosylation is crucial for the regulation of NOTCH trafficking [16]. Human PAMR1 exhibits a potential *O*-Glucosylation site within its EGF-like domain at Serine 241 between C1 and C2 (Figure 4) but doesn't possess the consensus sequence for specific addition of Glc between C3 and C4 of the EGF-like domain, mediated by ER (endoplasmic reticulum)-resident POGLUT2/3 [17]. In some cases, *O*-Glucose can be elongated by xylose residues [18].

O-Fucose can be added on consensus sequences of EGF-like repeats and Thrombospondin Type 1 Repeats (TSRs) in properly folded proteins, following specific action of ER-resident Protein *O*-Fucosyltransferase 1 (POFUT1 or FUT12) [19,20] and Protein *O*-Fucosyltransferase 2 (POFUT2 or FUT13) [21,22] respectively [23]. POFUT1-mediated *O*-Fucosylation occurs on serine and threonine of the following consensus sequence C^2-XXXX-(S/T)-C^3 of an EGF-like domain, as it is the case for human PAMR1 which possesses a potential *O*-Fucosylation site at threonine 249 (Figure 4). This *O*-Fucose can be elongated, in some cases, by successive additions of GlcNAc, Gal and sialic acid to form a sialylated tetrasaccharide *O*-Fucosylglycan [24]. It is well known that *O*-Fucose added by POFUT1 car modulate protein-protein interactions. Indeed, the *O*-Fucosylation of EGF-like repeats within the extracellular domains of NOTCH receptors modulates the receptor–ligand interactions, which are essential for activation of NOTCH signaling [25].

Another *O*-linked glycosylation found in EGF like domains of glycoproteins is *O*-N-Acetylglucosamine (*O*-GlcNAc) added by ER-resident EGF-domain specific *O*-GlcNAc transferase (EOGT). The *O*-GlcNAc added on NOTCH1 by EOGT was shown to promote Notch signaling by enhancing its interaction with mammalian DLL ligands [26]. EOGT mediated *O*-GlcNAc addition occurs on serine or threonine of the consensus sequence

$C^5XXGX(S/T)GXXC^6$ [27] of an EGF-like domain. As shown in Figure 4, the threonine 267 of human PAMR1 exhibiting the sequence $C^5LAGYTGQRC^6$ is thus a potential *O*-GlcNAcylation site. Interestingly, the occupation of this threonine 267 by an *O*-GlcNAc was experimentally demonstrated by mass spectrometry [28].

By Copper-catalyzed Azide-Alkyne Cycloaddition referred to as click chemistry and target mass spectrometry, we demonstrated that mouse PAMR1 (homolog to human PAMR1 isoform 1) was, as expected, composed of a unique triple-modified EGF-like domain with *O*-Glucose, *O*-Fucose and *O*-GlcNAc [29].

The role of all these glycosylations is not known but they could be important for the folding and the secretion of PAMR1 but also for its interactions with other protein partners. It is therefore interesting to know whether these different potential or proven glycosylation sites could be affected in cancer.

Alteration of the Glycosylation Sites of Human PAMR1 in Cancer

BioMuta database (BioMuta v4.0), which is a single-nucleotide variation and disease association database, contains non-synonymous single-nucleotide variations associated with cancer. All alterations of the glycosylation sites of human PAMR1 occurring in cancer, either by change of keys residues (Asn, Ser, Thr) or change of keys residues in consensus sequences, are presented in the following table.

Table I: Point mutations found in cancer, affecting *N*- and *O*-glycosylation sites found in human PAMR1 or key residues in consensus sequences of glycosylation.

Type of glycosylation	Predicted Occupation	Location	Ref. residue	Position	Alt. residue	Variation	Cancer type	Functional predictions
N-glycan	Yes ($\underline{N}^{96}$GS)		Asn	96		none		
O-Glc	Yes (CS$\underline{S}^{241}$SPC)	EGF-like	Ser	241		none		
O-Fuc	Yes (CFHDG$\underline{T}^{249}$C)	EGF-like	Thr	249	Lys	**T249K**	Liver cancer	probably damaging
O-Fuc	Yes (CFHDG$\underline{T}^{249}$C)	EGF-like	Thr	249	Met	**T249M**	Melanoma	probably damaging
O-GalNAc	Never detected in EGF-like	EGF-like	Ser	257		none		
O-GlcNAc	Yes (CXXG$\underline{X}^{267}$GXXC)*	EGF-like	Thr	267		none		
	No	EGF-like	Gly	265	Cys	**G265C**	Uterine cancer	probably damaging
N-glycan	Yes ($\underline{N}^{279}$CS)	Sushi 1	Asn	279		none		
O-GalNAc	Yes (T^{294}, NetOGlyc)	Sushi 1	Thr	294		none		
N-glycan	**No** (N^{316}NS)	Sushi 1	Asn	316		none		
O-GalNAc	Yes (T^{328}, NetOGlyc)	Sushi 1	Thr	328		none		
O-GalNAc	Yes (S^{352}, NetOGlyc)		Ser	352	Leu	**S352L**	Melanoma	probably damaging
O-GalNAc	Yes (S^{366}, NetOGlyc)		Ser	366		none		
O-GalNAc	Yes (S^{376}, NetOGlyc)		Ser	376		none		
O-GalNAc	Yes (S^{380}, NetOGlyc)		Ser	380		none		
O-GalNAc	Yes (S^{386}, NetOGlyc)		Ser	386		none		
O-GalNAc	Yes (T^{389}, NetOGlyc)	Sushi 2	Thr	389		none		
O-GalNAc	Yes (T^{408}, NetOGlyc)	Sushi 2	Thr	408	Ala	**T408A**	Kidney cancer	probably damaging
O-GalNAc	Yes (S^{416}, NetOGlyc)	Sushi 2	Ser	416		none		
O-GalNAc	Yes (S^{424}, NetOGlyc)	Sushi 2	Ser	424		none		
O-GalNAc	Yes (S^{425}, NetOGlyc)	Sushi 2	Ser	425	Arg	**S425R**	Sarcoma	probably damaging
O-GalNAc	Yes (T^{428}, NetOGlyc)	Sushi 2	Thr	428		none		
O-GalNAc	Yes (T^{432}, NetOGlyc)	Sushi 2	Thr	432		none		
O-GalNAc	Yes (S^{436}, NetOGlyc)	Sushi 2	Ser	436		none		
O-GalNAc	Yes (S^{441}, NetOGlyc)	Sushi 2	Ser	441		none		
N-glycan	Yes ($\underline{N}^{451}$IT)	Peptidase S1	Asn	451		none		
	No	Peptidase S1	Thr	453	Ala	**T453A**	Uterine cancer	benign**
N-glycan	Yes ($\underline{N}^{614}$DT)	Peptidase S1	Asn	614		none		
O-GalNAc	Yes (S^{672}, NetOGlyc)	Peptidase S1	Ser	672		none		
*** demonstrated experimentally (Alfaro et al., 2012)**								
**** functional prediction according the change of Thr into Ala**								

There is no variation listed in the Biomuta database concerning the asparagine residues potentially bearing *N*-glycans, namely N^{96}, N^{279}, N^{451} and N^{614}. On the other hand, the T453A mutation causes the loss of the *N*-glycosylation site $\underline{N}^{451}$IT in uterine cancer. This variation is predicted to be benign by BioMuta. However, if we consider that this asparagine $\underline{N}^{451}$, located in the peptidase S1 domain, is really occupied, it is possible that the loss of the *N*-glycan at this position impacts the folding and/or the secretion of the protein or even its activity.

Concerning mucin-type *O*-GalNAc glycosylation, only the sites with scores higher than 0.5, predicted as glycosylated by NetOGlyc, are listed in the table. Occupancy of these *O*-glycosylation sites can change *in vivo*, depending on the cells expressing the protein. In addition, some local regions in a protein are more likely to carry *O*-GalNAc than others. By example, the presence of *O*-GalNAc site is predicted within the EGF-like domain of human PAMR1 at S^{257}. Regarding NOTCH

receptor, which contains a large number of EGF-like repeats (29-36), mucin-type *O*-glycosylation can be present but always outside the EGF-like repeats [15].

The regions most likely to carry this type of modification are destructured and prolin-rich regions such as that between the two Sushi domains (region 345-386) of human PAMR1. This region matches the sequence below and contains 5 serine residues with each of them predicted as an *O*-GalNAc site, 3 proline residues and unpredicted threonine T^{369}.

ACRE**P**KIS^{352}DLVRRRVL**P**MQVQS^{366}RET**P**LHQLYS^{376}AAF S^{380}KQKLQS^{386}

The S352L mutation found in melanoma, probably damaging, could thus lead to the elimination of *O*-GalNAc or extended *O*-GalNAc glycan important for the secretion and/or activity of human PAMR1.

If taking account the nine predicted *O*-GalNAc sites in the Sushi 2 domain and predicted structure of human PAMR1 by Alphafold (Figure 1), seven of them are relevant since located in unstructured regions, without periodic secondary structures including T^{408} and S^{425}, for which there is variation in cancer (T408A in kidney cancer and S425R in sarcoma).

Human PAMR1 also contains an EGF-like domain, which is a protein domain often involved in protein-protein interactions and which potentially bears three *O*-linked monosaccharides (*O*-Glucose, *O*-Fucose and *O*-GlcNAc) like mouse PAMR1 [29] or corresponding extended *O*-glycosylglycans capable of modulating these interactions. The T249K and T249M mutations found in liver cancer and melanoma, respectively, target the potential *O*-Fucosylation site, while the G265C mutation found in uterine cancer affects the consensus sequence for the addition of an *O*-GlcNAc. Besides the amino acid change, the loss of *O*-Fucose or *O*-GlcNAc on the EGF-like domain is probably damaging for PAMR1 function.

Expression of PAMR1 in Normal and Cancer Tissues

Little is known about the expression of PAMR1 in normal and malignant/cancerous tissues, as well as its role in different tissues/cell lines. PAMR1 is a low-tissue-specific protein. It is known to be overexpressed in cervical and endocervical tissues at its mRNA level. It is recorded to be highly present in the serum and gallbladder at its protein level (Gene card database). The analysis of Lo et al, to 27 normal tissues, showed that the highest expression of PAMR1 transcriptome is found in brain, bladder, aorta, and colon tissues, with lower expression in breast and skeletal tissues of both isoforms 1 and 2 [1]. On the other hand, no data are available concerning PAMR1 expression in embryonic and stem cells.

RNA Seq data concerning PAMR1 expression in tumoral tissues from patients *versus* normal ones can be found in the Firebrowse database (Figure 5).

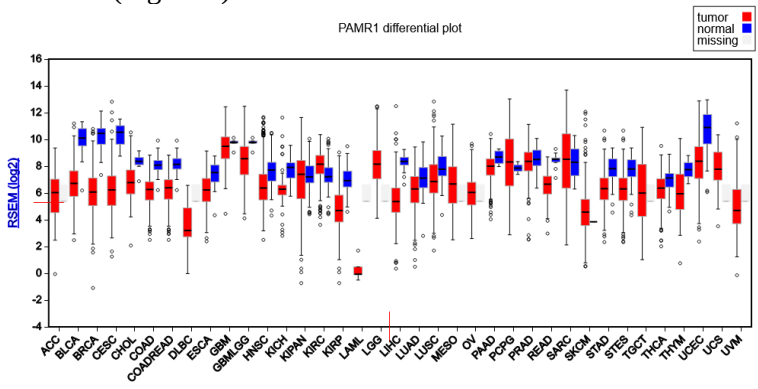

Figure 5: Expression of PAMR1 in normal and tumoral cancer samples from TCGA Firebrowse database (http://firebrowse.org/). PAMR1's expression is downregulated in many cancers such as breast invasive carcinoma (BRCA), Cervical and Endocervical Cancers (CESC), Colon Adenocarcinoma (COAD), Colorectal Adenocarcinoma (COADREAD) and Rectal Adenocarcinoma (READ).

According to data from Firebrowse, PAMR1 is downregulated in tumoral tissues of several cancers including BRCA (Breast invasive carcinoma), CESC (Cervical and Endocervical

carcinoma), LIHC (Liver hepatocellular carcinoma) confirming earlier research on breast [1], cervical [30], hepatocellular [31] cancers, as well as for cutaneous squamous cell carcinoma [32]. Recently, we also confirmed PAMR1 downexpression in colorectal cancer [33], consistent with public data from Firebrowse concerning COAD (Colon Adenocarcinoma), READ (Rectal Adenocarcinoma) and COADREAD (Colorectal Adenocarcinoma).

PAMR1 could be, as well, overexpressed in some/exceptional tumoral tissues such as the case of KIRC (Kidney renal clear cell carcinoma), PCPG (Pheochromocytoma, and Paraganglioma), and SKCM (Skin Cutaneous Melanoma), and also meningioma. On the other hand, data is missing for PAMR1's expression in the following cancers: ACC (Adrenocortical Carcinoma), DLBC (Lymphoid Neoplasm Diffuse Large B-cell Lymphoma), LAML (Acute Myeloid Leukemia), LGG (Brain Lower Grade Glioma), MESO (Mesothelioma), OV (Ovarian Serous Cystadenocarcinoma), TGCT (Testicular Germ cell Tumors), UCS (Uterine Carcinosarcoma), and UVM (Uveal Melanoma). All these differences of PAMR1 expression according to the considered cancer type could be correlated to potentially different roles of this glycoprotein in normal different cell types before their malign transformation.

PAMR1 as a Potential Tumor Suppressor

Recent studies showed a reduced expression of PAMR1 in breast [1] and cervical [30] cancers. Different mechanisms could explain this very low expression of PAMR1 in cancer such as epigenetic silencing. Indeed, PAMR1 was shown to be down-expressed by promoter hypermethylation in breast cancer, such as other tumor-suppressor genes including APC, BRCA1, p16, P21 and TIMP3 [1].

Since a long time, DNA methyltransferase inhibitors such as 5-aza-2' deoxycytidine (also named decitabine [34]) are used for DNA demethylation inducing reactivation of epigenetically silenced tumor suppressor genes. In addition, the use of decitabine was shown to lead to cell cycle arrest (G2/M phase)

and apoptosis in human cancer cells [35]. Due to its anti-cancer properties, decitabine was thus used in cancer chemotherapy in different cancers such as lung cancer [36], leukemia [37] and gastric cancer [38]; sometimes in combination of inhibitors of deacetylation [39]. In gastric cancer, decitabine led to inhibition of tumor cell proliferation and up-regulation of E-cadherin [38].

Due to its recovered expression by decitabine and its suppressor role of cancer cell growth, PAMR1 was regarded as a potential tumor suppressor gene in breast cancer [1]. PAMR1 was also shown to be downregulated in cervical cancer and correlated with favorable prognosis [30]. In this latter study, cervical cancer cell proliferation, migration, and invasion were shown to be increased after PAMR1 knockdown by siRNA in HeLa and Me180 cells and on the contrary decreased following its overexpression. These data, in addition to more recent data on colorectal cancer [33], reinforce the idea that PAMR1 is indeed a tumor suppressor gene.

PAMR1 Inhibits Myc and mTORC1 Signaling Pathways

Cancer's molecular alterations are intricate and induce alteration in numerous signaling pathways. Recently, it was revealed by Yang et al. that PAMR1 could be involved in the suppression of MYC and mTOR signaling pathways [30]. MYC is a proto-oncogene activated among others by the MAPK pathway, which plays a role in favoring proliferation, migration, apoptotic resistance, and angiogenesis. MYC has many properties: it can regulate the transcription of other genes and stabilize mRNA and proteins [40]. When it is positively deregulated, it will activate the transcription of target genes which will have a favorable effect on tumorigenesis and tumor progression [41]. mTOR, a serine/threonine kinase protein, is activated by the PI3K/AKT pathway involved in the same biological processes as the MAPK pathway [30]. mTOR is known also to activate the metastatic cascade in cancers. SIN1 and MLST8 are two subunits of mTORC1 and mTORC2 that promote cell migration and invasion. The regulation of ULK1 by PAMR1, a mTORC1

negative regulator, as well as SIN1 and MLST8, could suppress cell migration and invasion in cervical cancer.

Conclusion

PAMR1 is a secreted multi-domain *N*- and *O*-linked glycoprotein, which was initially discovered as a potential actor in muscle regeneration [2] and later as a potential tumor suppressor in breast cancer, where its expression was epigenetically silenced by promoter hypermethylation [1]. In addition of an anti-proliferative role in breast [1] and colorectal [33] cancer, PAMR1 exhibited a negative effect on migration and invasion of cervical cancer cell lines [30]. Although PAMR1 was able to inhibit Myc and mTORC1 signaling pathways, the precise molecular mechanism by which PAMR1 exerts its action is still unclear. Among its potential roles, PAMR1 might have an anti-protease activity due to the presence a threonine (less nucleophile than serine) at position 665 in its C-terminal trypsin-like domain, instead of serine residue usually found in the catalytic triad at this position. If PAMR1 indeed possesses even weak proteolytic activity, one can wonder about its protein targets.

To exert its specific action on proliferation and other cell properties, PAMR1 might be involved in protein-protein interactions with extracellular and/or membrane protein partners via its CUB and EGF-like domains. By analogy with the SCUBE2 protein, which contains CUB and EGF-like domains and also exhibits anti-tumor activity toward breast cancer cells [42], PAMR1 could interact with a surface membrane protein such as E-cadherin [5] and affect signaling pathways as mentioned above. However, the protein partners of PAMR1 are not known and remain to be discovered depending on the tumor context.

References

1. Paulisally Hau Yi Lo, Chizu Tanikawa, Toyomasa Katagiri, Yusuke Nakamura, Koichi Matsuda. Identification of novel epigenetically inactivated gene PAMR1 in breast carcinoma. Oncol Rep. 2015; 33: 267-273.
2. Yuki Nakayama, Noriko Nara, Yukiko Kawakita, Yasuhiro Takeshima, Masayuki Arakawa, et al. Cloning of cDNA encoding a regeneration-associated muscle protease whose expression is attenuated in cell lines derived from Duchenne muscular dystrophy patients. Am J Pathol. 2004; 164: 1773-1782.
3. Sara E Perry, Philip Robinson, Alan Melcher, Philip Quirke, Hans-Jörg Bühring, et al. Expression of the CUB domain containing protein 1 (CDCP1) gene in colorectal tumour cells. FEBS Lett. 2007; 581: 1137-1142.
4. Kumar S, KS Prajapati, S Gupta. The Multifaceted Role of Signal Peptide-CUB-EGF Domain-Containing Protein (SCUBE) in Cancer. Int J Mol Sci. 2022; 23.
5. Yuh-Charn Lin, Yi-Ching Lee, Ling-Hui Li, Chien-Jui Cheng, Ruey-Bing Yang. Tumor suppressor SCUBE2 inhibits breast-cancer cell migration and invasion through the reversal of epithelial-mesenchymal transition. J Cell Sci. 2014; 127: 85-100.
6. Z Rao, P Handford, M Mayhew, V Knott, G G Brownlee, et al. The structure of a Ca(2+)-binding epidermal growth factor-like domain: its role in protein-protein interactions. Cell. 1995; 82: 131-141.
7. MD Rand, A Lindblom, J Carlson, BO Villoutreix, J Stenflo. Calcium binding to tandem repeats of EGF-like modules. Expression and characterization of the EGF-like modules of human Notch-1 implicated in receptor-ligand interactions. Protein Sci. 1997; 6: 2059-2071.
8. Yuh-Charn Lin, Chun-Chuan Chen, Chien-Jui Cheng, Ruey-Bing Yang. Domain and functional analysis of a novel breast tumor suppressor protein, SCUBE2. J Biol Chem. 2011; 286: 27039-27047.
9. Konstantinos S Papadakos, Alexander Ekström, Piotr Slipek, Eleni Skourti, Steven Reid, et al. Sushi domain-

containing protein 4 binds to epithelial growth factor receptor and initiates autophagy in an EGFR phosphorylation independent manner. J Exp Clin Cancer Res. 2022; 41: 363.
10. Ermis Akyuz E, SM Bell. The Diverse Role of CUB and Sushi Multiple Domains 1 (CSMD1) in Human Diseases. Genes (Basel). 2022; 13.
11. Haopeng Xu, Jidong Shan, Vladimir Jurukovski, Liming Yuan, Jianhua Li, et al. TSP50 encodes a testis-specific protease and is negatively regulated by p53. Cancer Res. 2007; 67: 1239-1245.
12. Yu-Yin Li, Yong-Li Bao, Zhen-Bo Song, Lu-Guo Sun, Ping Wu, et al. The threonine protease activity of testes-specific protease 50 (TSP50) is essential for its function in cell proliferation. PLoS One. 2012; 7: e35030.
13. Gupta R, S Brunak. Prediction of glycosylation across the human proteome and the correlation to protein function. Pac Symp Biocomput. 2002; 310-322.
14. Inka Brockhausen, Hans H Wandall, Kelly G Ten Hagen, Pamela Stanley. O-GalNAc Glycans. In: Varki A, Cummings RD, Esko JD, editors. Essentials of Glycobiology. Cold Spring Harbor: Cold Spring Harbor Laboratory Press. 2022; 117-128.
15. Wang W, T Okajima, H Takeuchi. Significant Roles of Notch O-Glycosylation in Cancer. Molecules. 2022; 27.
16. Yu H, H Takeuchi. Protein *O*-glucosylation: another essential role of glucose in biology. Curr Opin Struct Biol. 2019; 56: 64-71.
17. Hideyuki Takeuchi, Michael Schneider, Daniel B Williamson, Atsuko Ito, Megumi Takeuchi, et al. Two novel protein O-glucosyltransferases that modify sites distinct from POGLUT1 and affect Notch trafficking and signaling. Proc Natl Acad Sci U S A. 2018; 115: E8395-E8402.
18. Maya K Sethi, Falk FR Buettner, Vadim B Krylov, Hideyuki Takeuchi, Nikolay E Nifantiev, et al. Identification of glycosyltransferase 8 family members as xylosyltransferases acting on O-glucosylated notch epidermal growth factor repeats. J Biol Chem. 2010; 285: 1582-1586.

19. Brian J McMillan, Brandon Zimmerman, Emily D Egan, Michael Lofgren, Xiang Xu, et al. Structure of human POFUT1, its requirement in ligand-independent oncogenic Notch signaling, and functional effects of Dowling-Degos mutations. Glycobiology. 2017; 27: 777-786.
20. Y Wang, L Shao, S Shi, RJ Harris, MW Spellman, et al. Modification of epidermal growth factor-like repeats with O-fucose. Molecular cloning and expression of a novel GDP-fucose protein O-fucosyltransferase. J Biol Chem. 2001; 276: 40338-40345.
21. J Hofsteenge, KG Huwiler, B Macek, D Hess, J Lawler, et al. C-mannosylation and O-fucosylation of the thrombospondin type 1 module. J Biol Chem. 2001; 276: 6485-6498.
22. Chun-I Chen, Jeremy J Keusch, Dominique Klein, Daniel Hess, Jan Hofsteenge, et al. Structure of human POFUT2: insights into thrombospondin type 1 repeat fold and O-fucosylation. EMBO J. 2012; 31: 3183-3197.
23. Holdener BC, RS Haltiwanger. Protein O-fucosylation: structure and function. Curr Opin Struct Biol. 2019; 56: 78-86.
24. Takeuchi H, RS Haltiwanger. Significance of glycosylation in Notch signaling. Biochem Biophys Res Commun. 2014; 453: 235-242.
25. Stanley P. Regulation of Notch signaling by glycosylation. Curr Opin Struct Biol. 2007; 17: 530-535.
26. Shogo Sawaguchi, Shweta Varshney, Mitsutaka Ogawa, Yuta Sakaidani, Hirokazu Yagi, et al. O-GlcNAc on NOTCH1 EGF repeats regulates ligand-induced Notch signaling and vascular development in mammals. Elife. 2017; 6.
27. Mitsutaka Ogawa, Yuya Senoo, Kazutaka Ikeda, Hideyuki Takeuchi, Tetsuya Okajima. Structural Divergence in O-GlcNAc Glycans Displayed on Epidermal Growth Factor-like Repeats of Mammalian Notch1. Molecules. 2018; 23.
28. Joshua F Alfaro, Cheng-Xin Gong, Matthew E Monroe, Joshua T Aldrich, Therese R W Clauss, et al. Tandem mass spectrometry identifies many mouse brain O-

GlcNAcylated proteins including EGF domain-specific O-GlcNAc transferase targets. Proc Natl Acad Sci U S A. 2012; 109: 7280-7285.
29. Florian Pennarubia, Agnès Germot, Emilie Pinault, Abderrahman Maftah, Sébastien Legardinier. The single EGF-like domain of mouse PAMR1 is modified by O-Glucose, O-Fucose and O-GlcNAc. Glycobiology. 2021; 31: 55-68.
30. Rui Yang, Mingjun Ma, Sihui Yu, Xi Li, Jiawen Zhang, et al. High Expression of PAMR1 Predicts Favorable Prognosis and Inhibits Proliferation, Invasion, and Migration in Cervical Cancer. Front Oncol. 2021; 11: 742017.
31. Fuqiang Yin, Lipei Shu, Xia Liu, Ting Li, Tao Peng, et al. Microarray-based identification of genes associated with cancer progression and prognosis in hepatocellular carcinoma. J Exp Clin Cancer Res. 2016; 35: 127.
32. Wei Wei, Yan Chen, Jie Xu, Yu Zhou, Xinping Bai, et al. Identification of Biomarker for Cutaneous Squamous Cell Carcinoma Using Microarray Data Analysis. J Cancer. 2018; 9: 400-406.
33. Layla Haymour, Alain Chaunavel, Mona Diab Assaf, Abderrahman Maftah, Sébastien Legardinier. PAMR1 negatively impacts cell proliferation and migration of Human Colon Cancer HT29 Cell line. BioRXiv (The Preprint Server For Biology). 2022.
34. Hackanson B, M Daskalakis. Decitabine. Recent Results Cancer Res. 2014; 201: 269-297.
35. Dong Yeok Shin, Ho Sung Kang, Gi-Young Kim, Wun-Jae Kim, Young Hyun Yoo, et al. Decitabine, a DNA methyltransferases inhibitor, induces cell cycle arrest at G2/M phase through p53-independent pathway in human cancer cells. Biomed Pharmacother. 2013; 67: 305-311.
36. RL Momparler, DY Bouffard, LF Momparler, J Dionne, K Belanger, et al. Pilot phase I-II study on 5-aza-2'-deoxycytidine (Decitabine) in patients with metastatic lung cancer. Anticancer Drugs. 1997; 8: 358-368.
37. Momparler RL, S Cote, N Eliopoulos. Pharmacological approach for optimization of the dose schedule of 5-Aza-2'-deoxycytidine (Decitabine) for the therapy of

leukemia. Leukemia. 1997; 11: S1-6.
38. Munetaka Nakamura, Jun Nishikawa, Mari Saito, Kouhei Sakai, Sho Sasaki, et al. Decitabine inhibits tumor cell proliferation and up-regulates e-cadherin expression in Epstein-Barr virus-associated gastric cancer. J Med Virol. 2017; 89: 508-517.
39. Richard L Momparler, Sylvie Côté, Louise F Momparler, Youssef Idaghdour. Epigenetic therapy of acute myeloid leukemia using 5-aza-2'-deoxycytidine (decitabine) in combination with inhibitors of histone methylation and deacetylation. Clin Epigenetics. 2014; 6: 19.
40. Kress TR, A Sabo, B Amati. MYC: connecting selective transcriptional control to global RNA production. Nat Rev Cancer. 2015; 15: 593-607.
41. Corey Lourenco, Diana Resetca, Cornelia Redel, Peter Lin, Alannah S. MacDonald, et al. MYC protein interactors in gene transcription and cancer. Nat Rev Cancer. 2021; 21: 579-591.
42. Chien-Jui Cheng, Yuh-Charn Lin, Ming-Tzu Tsai, Ching-Shyang Chen, Mao-Chih Hsieh, et al. SCUBE2 suppresses breast tumor cell proliferation and confers a favorable prognosis in invasive breast cancer. Cancer Res. 2009; 69: 3634-3641.

Book Chapter

Role of Extracellular Vesicles in Cancer Progression

Bailasan Haidar[#]*, Batul Kamar[#], Farah A Farran, Karen Moghabghab, Rayan A Assaf and Hussein Fayyad-Kazan*

Laboratory of Cancer Biology and Molecular Immunology, Faculty of Sciences I, Lebanese University, Lebanon

[#]Both authors contributed equally to this work

***Corresponding Authors:** Bailasan Haidar, Laboratory of Cancer Biology and Molecular Immunology, Faculty of Sciences I, Lebanese University, Hadath-Beirut, Lebanon

Hussein Fayyad-Kazan, Laboratory of Cancer Biology and Molecular Immunology, Faculty of Sciences I, Lebanese University, Hadath-Beirut, Lebanon

Published **May 16, 2023**

How to cite this book chapter: Bailasan Haidar, Batul Kamar, Farah A Farran, Karen Moghabghab, Rayan A Assaf, Hussein Fayyad-Kazan. Role of Extracellular Vesicles in Cancer Progression. In: Hussein Fayyad Kazan, editor. Immunology and Cancer Biology. Hyderabad, India: Vide Leaf. 2023.

Abstract

Extracellular vesicles (EVs) are lipid-bound vesicles that contain proteins, receptors, and nucleic acids from their cells of origin. EVs have emerged as key players in intercellular communication and are involved in several physiological and pathological processes including cancer. Cancer cells secrete EVs, which promote cell growth and survival, angiogenesis, metastasis, and immunosuppression, thereby contributing to cancer progression. EVs also serve as diagnostic biomarkers for cancer development and treatment efficacy. Additionally, EVs can be harnessed as drug delivery systems because of their ability to target specific cells and tissues. This review provides an overview of the current understanding of the role of EVs in cancer progression, and highlights their potential as diagnostic and therapeutic tools for cancer treatment.

Introduction: Extracellular Vesicles Definition and History

Extracellular vesicles (EVs) are lipid-bound vesicles that are secreted by all cells into the extracellular space [1,2]. They do not contain a functional nucleus, and therefore cannot replicate [3]. Although EVs were not recognized for their enzymatic and functional potential until the 1980s and 1990s [4], what we refer to now as EVs, have been observed before that time and in different physiological settings, especially in the field of platelet biology where they were referred to as “platelet dust” in 1967 [5]. In 1993, Lee et al. described the phenomenon of elevated microparticles in transient brain ischemia and other infarctions. The same phenomena have been discovered in multiple other diseases, such as angina and Crohn's disease. Such discoveries increased the interest in EVs, and more research involving their role in different diseases immerged [4].

In 1996, Raposo et al. showed that EV released from immune cells can present antigens [6], which sparked further interest and research in the field of EV, where they were shown to have functional roles in biological processes, the potential to be used as biomarkers, and potential in therapeutics [4]. With the recent discovery in 2006-2007 that EVs contain mRNA and

microRNA, they have gained new interest as mediators of cell-to-cell communication [5].

Data have shown that the contents, size ranging from 30 to 10000 nm in diameter, and membrane composition of EVs are heterogeneous and differ depending on the cell source and environmental conditions. Currently, there are three defined types of EVs: (a) apoptotic bodies, (b) cellular microvesicles, and (c) exosomes [7,8]. As such, the primary focus of this review will be on the different types of EVs and their roles in tumor development and therapeutics.

Extracellular Vesicles Subtypes

EVs are lipid vesicles with a spheroidal shape, containing membrane and cytosolic proteins, receptors, and nucleic acids originating from their cells of origin [9]. EVs are typically released by all cell types and play a major role in cell-to-cell communication by transferring biological information between cells. In general, cells release different EVs, with the most common subtypes being exosomes, microvesicles, and apoptotic bodies; they differ in size, biogenesis, release pathways, biophysical properties, and biological functions [1,8].

Exosomes

Exosomes, also known as intraluminal vesicles (ILVs), are enclosed by a single outer membrane and secreted by all cell types. Their sizes range between 30 nm – 100 nm, and they are characterized by protein biomarkers, including CD63, CD81, and CD9 [10]. They typically appear as cup-shaped entities by transmission electron microscopy, whilst they appear as round-shaped vesicles by cryoelectronic microscopy [11,12].

Exosomes in the extracellular space were first identified in the 1980s. Previously, exosomes were believed to be “waste vesicles” containing cellular waste from cell damage or homeostasis by-products that do not affect surrounding cells [2].

However, in recent years, it was discovered that these exosomes carry proteins, lipids, and nucleic acids that allow them to play a significant role in intracellular communication and affect cellular

processes, such as immune response, signal transduction, and antigen presentation. Depending on their cells of origin, exosomes carry different cargo and thus provide prognostic information for a variety of diseases, such as chronic inflammation, cardiovascular and renal diseases, and tumors [2,13-15]. Exosomes isolated from various body fluids exhibit a significant degree of morphological variation, suggesting the existence of exosome subpopulations with distinct roles and biochemical compositions. Furthermore, Zabeo et al. showed that even exosomes originating from the same cell type exhibit variations in their morphology [12,16].

Exosome Biogenesis

Several mechanisms have been identified for exosome formation. However, the most recognized and understood pathway is the endosome pathway. First, endocytosis causes the formation of endocytic vesicles in the lipid raft domain of the plasma membrane, which in turn causes the formation of early endosomes. Through the Golgi complex, early endosomes become late endosomes and intraluminal vesicles (ILVs) accumulate in their lumen during this process. The molecules in the early endosome can be recycled back into the plasma membrane or incorporated into ILVs [12,17]. Cargo sorting into ILVs is mediated by endosomal sorting complexes required for transport (ESCRT)-dependent and -independent mechanisms [18,19]. It is worth noting that most ESCRT-independent mechanisms occur under hypoxic conditions in the tumor microenvironment [20]. Later, by inward budding of the early endosomal membrane and cytosol sequestration, these vesicles aggregate in late endosomes, altering endosomes into multivesicular bodies (MVBs) [21]. These MVBs then fuse with either lysosomes, causing their degradation, or the plasma membrane, resulting in the release of their internal vesicles into the extracellular space. These vesicles are called exosomes [22,23]. The mechanisms by which the MVB move and fuse with the cell membrane are regulated by Rab guanosine triphosphatase (GTPase) proteins and are coordinated with cytoskeletal and molecular motor activities [24,25].

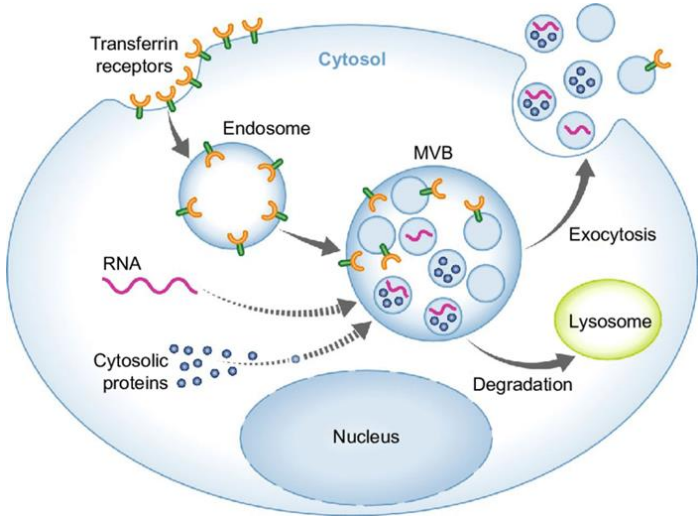

Figure 1: Exosome Biogenesis [26].

Exosome Uptake and Function

To understand their functions, we must examine how exosomes are selected and taken up by recipient cells. According to previous studies, this occurs through three main mechanisms including receptor-ligand interactions, direct membrane fusion, and endocytosis/ phagocytosis (Figure 2) [27].

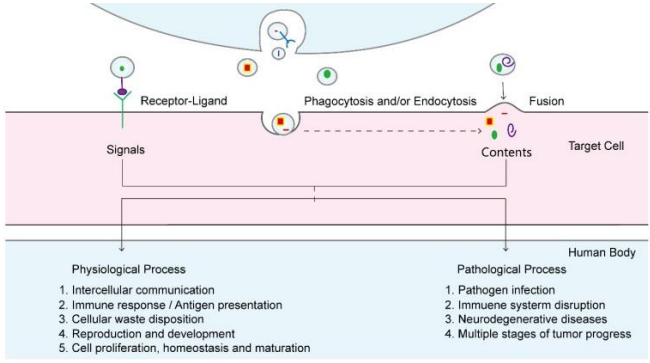

Figure 2: Exosome Uptake and Downstream Function in Recipient Cells [27].

Receptor-Ligand Interactions

Ligands present on the exosomal surface can bind directly to the surface receptors on target/recipient cells and activate the downstream signaling cascade. This route is common for mediating immunomodulatory and apoptotic functions [27]. For instance, exosomes released from dendritic cells activate T lymphocytes through the MHC-peptide complex [28] and bind to Toll-like receptor ligands on the bacterial surface to activate bystander dendritic cells and enhance immune responses [29]. Furthermore, it has been shown that umbilical cord blood-derived exosomes expressing tumor antigens such as MHC-I, MHC-II, CD34, or CD80 can stimulate T cell proliferation to produce antitumor activity [30]. Moreover, exosomes released from dendritic cells and expressing ligands, such as tumor necrosis factor (TNF), Fas ligand (FasL), and TNF related apoptosis inducing ligand (TRAIL), can bind to TNF receptors on tumor cells [31].

Direct Membrane Fusion

Alternatively, exosomes can fuse with the plasma membrane and release their content directly into the cytosol. This occurs through the formation of a hemi-fusion stalk between the hydrophobic lipid bilayers of the exosome and the recipient cell, where the two membranes then form a consistent structure. This fusion is believed to be mediated by families of SNARE and Rab proteins [32]. Lipid raft-like domains, integrins, and adhesion molecules present on the surface of exosomes play a role in mediating interaction, attachment, and membrane fusion with the recipient cell [27].

This uptake mechanism has been observed in dendritic and tumor cells [33,34]. Research suggests that this mechanism is weak; however, low pH in the tumor microenvironment could facilitate exosome fusion by increasing rigidity and sphingomyelin. Therefore, this route is speculated to be adopted by tumor cells [35].

Internalization (Endocytosis/Phagocytosis)

Endocytosis of exosomes by macropinocytosis or receptor- or raft-mediated mechanisms always results in the delivery of the vesicular cargo to the endosomal pathway. These pathways ultimately lead exosomes to fuse with lysosomes, whilst some proteins and fluids may be redirected back to the plasma membrane through recycling endosomes. However, some exosomes may escape degradation by the trans-Golgi network [36]. Similarly, phagocytosis results in the fusion of phagosomes with lysosomes; however, this method of internalization leads to the degradation of exosome content [36].

Several studies have suggested that internalization is the primary method of exosome uptake [37]. However, under certain conditions such as low temperatures, this mechanism may be inhibited [38]. Studies indicate that internalization is highly dependent on cell type and exosomal surface proteins such as CD9, CD81, and ICAM-1. Moreover, the size of exosomes affects their internalization, with smaller exosomes usually preferred by cells [12].

Microvesicles

Microvesicles (MV) are membrane-derived vesicles that are structurally similar to exosomes but differ in size (ranging from 100 nm to 1μm in diameter), lipid composition, content, and cellular origin [39,40]. MVs are released by cells under physiological conditions such as cell growth [41]. However, their shedding increases in response to changes in the physiological state and microenvironment, such as proinflammatory stimulants, hypoxia, oxidative stress, and shear stress [39,42].

MVs are characterized by the high surface expression of tubulin and low expression of exosome CD9 and CD81 markers. Furthermore, depending on their cellular origin, MVs exhibit different markers. For instance, platelet-derived MVs express CD62P and leukocyte-derived MVs express CD45 [43]. In regard to their composition, they mainly contain endoplasmic

reticulum, proteasome, mitochondrial proteins, and lipids including ceramide and sphingomyelin [44].
Similar to exosomes, they were first believed to contain cellular waste. However, recent studies have shown that they play a significant role in cell-cell communication between local and distant cells [45].

Microvesicle Biogenesis

The biogenesis of MVs starts with the budding of the plasma membrane, followed by their release from the cell surface. MV biogenesis is a calcium-dependent process [46]. It is triggered by several events, with the main events leading to MV formation being cell growth and reorganization of the cytoskeleton. This means that proteins associated with the plasma membrane break down via two different pathways: the calpain-dependent pathway and the Caspase-3-dependent pathway [17,46].

First, the calpain-dependent pathway stimulates intracellular calcium flow via an agonist. This causes the activation of thiol protease and calpain in the cytoplasm, causing them to move to the cell membrane, which then bind to phosphate esters on the membrane, thus generating calmodulin by calcium-regulated conformational change. Activated calmodulin then cleaves the α-actin and talin filaments, allowing cytoskeletal proteins to be separated, thus causing MVs release. Besides that, Caspase-3 cleaves the *C*-linked domain of Rho-associated protein kinase 1 (ROCK-1) thereby activating the phosphorylated myosin light chain (MLC) of ROCK-1, resulting in myosin interaction. A member of the GTPase protein in the Rho family, RhoA, also plays a role in MV biogenesis through its ability to activate Rock (RhoA kinase), stimulate LIM kinase, inhibit fibroin, reorganize the donor cell actin cytoskeleton, and finally cause the release of MVs [17,47].

Microvesicle Uptake and Function

Although the biogenesis of different types of EVs has been well researched and understood, the mechanisms of their uptake have received less attention. Most research on their uptake focuses on

the functional changes that occur in target cells rather than on the mechanism of fusion or uptake. Furthermore, most of these studies have focused on exosomes [33,48].

The mechanisms by which cellular uptake occurs vary depending on the contents or cargo of the vesicle, the cellular microenvironment, the type of recipient cell, its physiological state, and the recognition of ligands or receptors [37]. For instance, vesicles secreted from platelets interact with monocytes and endothelial cells but not with neutrophils [49,50]. The uptake mechanisms of MVs are similar to those of exosomes, where internalization (endocytosis) is the most common mechanism [5]. Direct membrane fusion is another MV uptake mechanism that is enhanced in an acidic microenvironment [35,46]. Similar to exosomes, MVs play a role in transporting proteins to neighboring or distant cells and affecting target cells. Therefore, they are involved in cell-to-cell communication. Depending on their cells of origin, the target cells differ, and the consequent effects on target cells differ [46]. Furthermore, MVs can affect their microenvironment; for instance, lipids in platelet microvesicles play a role in increasing adhesion between endothelial cells and monocytes [51].

Apoptotic Bodies

As their name indicates, apoptotic bodies (ApoBDs) are vesicular bodies that are released from dying cells [52]. Their sizes range from 500 nm to 2 μm. Depending on the microenvironment and conditions, ApoBDs can be more abundant than exosomes or MVs; they come in various sizes, structures, and compositions [17,53].

Apoptotic Bodies: Biogenesis

ApoBDs are a byproduct of apoptotic cells; they are formed through the separation of the cell's plasma membrane from the cytoskeleton as a result of increased hydrostatic pressure after cell contraction. They carry cellular contents such as micronuclei, chromatin remnants, cytosol portions, degraded

proteins, DNA fragments, or even intact organelles, and prevent them from leaking [1,53].

Apoptotic Bodies: Uptake and Function

After their release into the extracellular space, ApoBDs are phagocytosed by macrophages, parenchymal cells, or neoplastic cells and degraded within phagolysosomes [54]. Because they are quickly phagocytosed by surrounding cells and because they prevent the leakage of cellular components, ApoBDs prevent secondary necrosis and inflammatory reactions due to apoptosis [55,56]. ApoBD is believed to have significant effects on their recipient cells. However, little is known about their functions in intercellular communication [53].

Extracellular Vesicles' Role in Cancer Progression

Cancer cells adapt to their microenvironment to escape the immune system and metastasize. With evidence that cancer cells are being able to secrete EVs and with their presence in the surrounding environment, it is important to look at the role they play in cancer progression. In this section of the review, we will discuss the influence of EVs on cancer progression.

It wasn't until 2008 that the role of EV in cancer progression was uncovered by the work of Nedawi et al. and Skog et al., who showed that glioma cells actively release EVs containing EGFRvIII proteins and mRNA transcripts. EGFRvIII is a highly oncogenic EGF receptor, and upon its transfer to recipient cells it triggers pathways that activate survival proteins, promote cell growth via AKT and ERK pathways as well as enhance the cells' ability to grow when cultured under anchorage independent conditions [57,58].

After these ground-breaking discoveries, several laboratories reported similar findings regarding the role of EVs in cancer progression. For instance, it was shown that the MVs released by the aggressive breast cancer MDA-MB-231 cell line, and the U87-MG glioma cell line play a significant role in promoting the

survival and growth of non-transformed cells, both of which are characteristics of transformed cells [59,60]. Further research on EVs' role in cancer has proven that other EV subtypes, such as exosomes released from cancer and transformed cells can also promote survival in both cancer and normal cells [59,61]. In addition to their role in promoting survival, EVs released by cancer cells promote angiogenesis through VEGF release, which binds to their respective endothelial cell receptors, thus recruiting them to the tumor microenvironment and inducing angiogenesis [62,63].

EVs have also been associated with cancer metastasis. To begin with, EVs from cancer cells have been shown to play a role in the epithelial-to-mesenchymal transition (EMT) needed for cancer cell migration by downregulating epithelial markers such as α-, β-, γ-catenin, and E-cadherin, and enhancing the expression of mesenchymal markers such as N-cadherin, fibronectin, and vimentin [64]. Moreover, EVs released by cancer cells were shown to be enriched with matrix metalloproteases (MMPs), a disintegrin and metalloproteinases (ADAMs), and ADAMs with thrombospondin motifs (ADAMTS) that break down and remodel the extracellular matrix to create a path for cancer cells in the primary tumor to migrate through and intravasate into the bloodstream [65]. Increasing evidence has also shown that metastatic cancer cells often release exosomes expressing integrins that allow them to migrate and accumulate at future sites of metastasis [66].

The cancer microenvironment is known to be immunosuppressive. Recent evidence has demonstrated that EVs contribute to the formation of such microenvironments. Perhaps one of the most understood mechanisms of immunosuppression is through the interaction between programmed death-ligand 1 (PD-L1) on the surfaces of cancer cells and programmed death 1 (PD-1) receptor on the surface of immune cells, specifically CD8+ T cells (i.e., cytotoxic T cells). The interaction between PD-L1 and PD-1 activates a signaling cascade that inhibits both the growth and function of immune cells [67,68]. Recent evidence has shown that exosomes released by various cancer cell types such as melanoma, prostate cancer, colorectal cancer,

head and neck cancer, and glioblastoma, express PD-L1 and suppress CD8+ T cell growth and immune activity [69-72].

Moreover, exosomes released by cancer cells were found to influence the extracellular levels of adenosine by expressing the adenosine-regulating ectonucleotidases CD39 and CD73. CD39 and CD73 function by catalyzing the hydrolysis of ATP to AMP and dephosphorylating AMP to adenosine, respectively. Adenosine then binds to the A_{2A} or A_{2B} adenosine receptor subtypes expressed in immune cells, thus activating signaling proteins that stimulate the biosynthesis of cyclic AMP (cAMP), whose buildup causes the inhibition of immune cells [73,74]. As such, EVs are believed to provide an extra layer of protection for tumor cells.

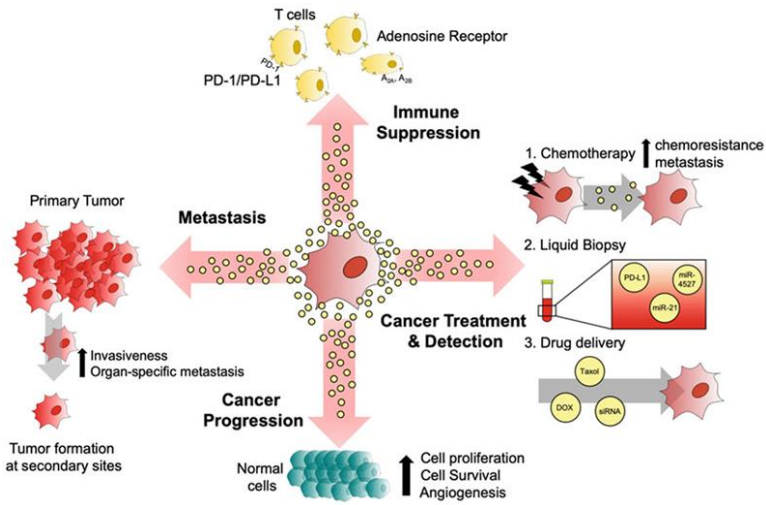

Figure 3: EVs Role in Cancer Progression [75].

Extracellular Vesicles and their Clinical Application

EVs released from cancer cells contain biological material that reflects the physiology and developmental stage of their cells of origin. Therefore, they can be used as sources of diagnostic information. EVs can be obtained through liquid biopsies, which

are painless and non-invasive methods. By exploring their content and looking for markers such as PD-L1, CD39, and CD73, information about cancer developmental stage and treatment effectiveness can be deduced [69,76]. Furthermore, EVs can reflect prognosis, where the expression of certain microRNAs such as miR-21 and miR-4527 in non–small cell lung cancers (NSCLC) could be linked to worse prognosis [77].

Another approach for EVs could be to utilize them as drug delivery systems. Since EVs are produced by cells, they would resolve issues that other engineered materials pose (such as inflammation and cytotoxicity). Furthermore, their protein surface composition can be easily manipulated and modified to efficiently and effectively target certain tissues and cells. Such an approach has been taken by Raghu Kalluri (MD Anderson Cancer Center) and colleagues, who targeted the k-RAS gene responsible for tumor growth in pancreatic cells by targeting exosomes containing k-RAS siRNA to cancer cells [78].

Conclusion

Although EV research has increased in the past years, there are still a lot of details and information to be uncovered. Of course, with EVs playing a critical role in cancer biology, they have gained extra interest from clinicians and researchers around the world. However, the more we uncover the more questions we obtain. How is the loading of specific proteins and nucleic acids into EVs controlled? What controls the rate of secretion of EVs? Are EVs functionally complementary or redundant with soluble factors from the same cell? Understanding such questions and EV biology will put us one step closer to perfecting their use in clinical settings.

References

1. Laura M Doyle, Michael Zhuo Wang. Wang, Overview of Extracellular Vesicles, Their Origin, Composition, Purpose, and Methods for Exosome Isolation and Analysis. Cells. 2019; 8.
2. Yokoi A, T Ochiya. Exosomes and extracellular vesicles: Rethinking the essential values in cancer biology. Seminars

in Cancer Biology. 2021; 74: 79-91.
3. Erica Bazzan, Mariaenrica Tinè, Alvise Casara, Davide Biondini, Umberto Semenzato, et al. Critical Review of the Evolution of Extracellular Vesicles' Knowledge: From 1946 to Today. Int J Mol Sci. 2021; 22.
4. Yvonne Couch, Edit I Buzàs, Dolores Di Vizio, Yong Song Gho, Paul Harrison, et al. A brief history of nearly EV-erything – The rise and rise of extracellular vesicles. Journal of Extracellular Vesicles. 2021; 10.
5. María Yáñez-Mó, Pia R-M Siljander, Zoraida Andreu, Apolonija Bedina Zavec, Francesc E Borràs, et al. Biological properties of extracellular vesicles and their physiological functions. J Extracell Vesicles. 2015; 4: 27066.
6. G Raposo, HW Nijman, W Stoorvogel, R Liejendekker, CV Harding, et al. B lymphocytes secrete antigen-presenting vesicles. J Exp Med. 1996; 183: 1161-1172.
7. Colombo M, G Raposo, C Théry. Biogenesis, secretion, and intercellular interactions of exosomes and other extracellular vesicles. Annu Rev Cell Dev Biol. 2014; 30: 255-289.
8. Eduard Willms, Carlos Cabañas, Imre Mäger, Matthew JA Wood, Pieter Vader. Extracellular Vesicle Heterogeneity: Subpopulations, Isolation Techniques, and Diverse Functions in Cancer Progression. Front Immunol. 2018; 9: 738.
9. Artur Słomka, Sabine Katharina Urban, Veronika Lukacs-Kornek, Ewa Żekanowska, Miroslaw Kornek. Large Extracellular Vesicles: Have We Found the Holy Grail of Inflammation? Front Immunol. 2018; 9: 2723.
10. McAndrews KM, R Kalluri. Mechanisms associated with biogenesis of exosomes in cancer. Molecular Cancer. 2019; 18: 52.
11. Yuana Yuana, Roman I Koning, Maxim E Kuil, Patrick CN Rensen, Abraham J Koster, et al. Cryo-electron microscopy of extracellular vesicles in fresh plasma. J Extracell Vesicles. 2013; 2.
12. Chuanjiang He, Shu Zheng, Yan Luo, Ben Wang. Exosome Theranostics: Biology and Translational Medicine. Theranostics. 2018; 8: 237-255.
13. Richard J Simpson, Justin We Lim, Robert L Moritz, Suresh Mathivanan. Exosomes: proteomic insights and diagnostic potential. Expert Review of Proteomics. 2009; 6: 267-283.

14. David W Greening, Shashi K Gopal, Rong Xu, Richard J Simpson, Weisan Chen. Exosomes and their roles in immune regulation and cancer. Seminars in Cell & Developmental Biology. 2015; 40: 72-81.
15. Salem KZ. Exosomes in Tumor Angiogenesis. In: D Ribatti, editor. Tumor Angiogenesis Assays: Methods and Protocols. New York: Springer New York. 2016; 25-34.
16. Davide Zabeo, Aleksander Cvjetkovic, Cecilia Lässer, Martin Schorb, Jan Lötvall, et al. Exosomes purified from a single cell type have diverse morphology. J Extracell Vesicles. 2017; 6: 1329476.
17. Yuanxin Xu, Kuanhan Feng, Huacong Zhao, Liuqing Di, Lei Wang, et al. Tumor-derived extracellular vesicles as messengers of natural products in cancer treatment. Theranostics. 2022; 12: 1683-1714.
18. Aude de Gassart, Charles Géminard, Dick Hoekstra, Michel Vidal. Exosome secretion: the art of reutilizing nonrecycled proteins? Traffic. 2004; 5: 896-903.
19. Katarina Trajkovic, Chieh Hsu, Salvatore Chiantia, Lawrence Rajendran, Dirk Wenzel, et al. Ceramide triggers budding of exosome vesicles into multivesicular endosomes. Science. 2008; 319: 1244-1247.
20. Kumar A, G Deep. Hypoxia in tumor microenvironment regulates exosome biogenesis: Molecular mechanisms and translational opportunities. Cancer Lett. 2020; 479: 23-30.
21. Susmita Sahoo, Ekaterina Klychko, Tina Thorne, Sol Misener, Kathryn M Schultz, et al. Exosomes from human CD34(+) stem cells mediate their proangiogenic paracrine activity. Circ Res. 2011; 109: 724-728.
22. Simons M, G Raposo. Exosomes--vesicular carriers for intercellular communication. Curr Opin Cell Biol. 2009; 21: 575-81.
23. RJ Advani, B Yang, R Prekeris, KC Lee, J Klumperman, et al. VAMP-7 mediates vesicular transport from endosomes to lysosomes. J Cell Biol. 1999; 146: 765-776.
24. Héctor Peinado, Maša Alečković, Simon Lavotshkin, Irina Matei, Bruno Costa-Silva, et al. Melanoma exosomes educate bone marrow progenitor cells toward a pro-metastatic phenotype through MET. Nat Med. 2012; 18: 883-891.

25. Matias Ostrowski, Nuno B Carmo, Sophie Krumeich, Isabelle Fanget, Graça Raposo, et al. Rab27a and Rab27b control different steps of the exosome secretion pathway. Nat Cell Biol. 2010; 12: 19-30; sup pp 1-13.
26. Jeffrey S Schorey, Yong Cheng, Prachi P Singh, Victoria L Smith. Exosomes and other extracellular vesicles in host-pathogen interactions. EMBO Rep. 2015; 16: 24-43.
27. Sonam Gurung, Dany Perocheau, Loukia Touramanidou, Julien Baruteau. The exosome journey: from biogenesis to uptake and intracellular signalling. Cell Communication and Signaling. 2021; 19: 47.
28. Mercedes Tkach, Joanna Kowal, Andres E Zucchetti, Lotte Enserink, Mabel Jouve, et al. Qualitative differences in T-cell activation by dendritic cell-derived extracellular vesicle subtypes. Embo j. 2017; 36: 3012-3028.
29. Sobo-Vujanovic A, S Munich, NL Vujanovic. Dendritic-cell exosomes cross-present Toll-like receptor-ligands and activate bystander dendritic cells. Cell Immunol. 2014; 289: 119-127.
30. Shasha Guan, Qianru Li, Pingping Liu, Xiaoyan Xuan, Ying Du. Umbilical cord blood-derived dendritic cells loaded with BGC823 tumor antigens and DC-derived exosomes stimulate efficient cytotoxic T-lymphocyte responses and antitumor immunity in vitro and in vivo. Cent Eur J Immunol. 2014; 39: 142-51.
31. Stephan Munich, Andrea Sobo-Vujanovic, William J Buchser, Donna Beer-Stolz, Nikola L Vujanovic. Dendritic cell exosomes directly kill tumor cells and activate natural killer cells via TNF superfamily ligands. Oncoimmunology. 2012; 1: 1074-1083.
32. Chernomordik LV, GB Melikyan, YA Chizmadzhev. Biomembrane fusion: a new concept derived from model studies using two interacting planar lipid bilayers. Biochim Biophys Acta. 1987; 906: 309-352.
33. Angela Montecalvo, Adriana T Larregina, William J Shufesky, Donna Beer Stolz, Mara LG Sullivan, et al. Mechanism of transfer of functional microRNAs between mouse dendritic cells via exosomes. Blood. 2012; 119: 756-766.
34. Yongjiang Zheng, Chenggong Tu, Jingwen Zhang, Jinheng

Wang. Inhibition of multiple myeloma-derived exosomes uptake suppresses the functional response in bone marrow stromal cell. Int J Oncol. 2019; 54: 1061-1070.
35. Isabella Parolini, Cristina Federici, Carla Raggi, Luana Lugini, Simonetta Palleschi, et al. Microenvironmental pH is a key factor for exosome traffic in tumor cells. J Biol Chem. 2009; 284: 34211-34222.
36. Kelly J McKelvey, Katie L Powell, Anthony W Ashton, Jonathan M Morris, Sharon A McCracken. Exosomes: Mechanisms of Uptake. J Circ Biomark. 2015; 4: 7.
37. Mulcahy LA, RC Pink, DR Carter. Routes and mechanisms of extracellular vesicle uptake. J Extracell Vesicles. 2014; 3.
38. Aled Clayton, Atilla Turkes, Sharon Dewitt, Robert Steadman, Malcolm D Mason, et al. Adhesion and signaling by B cell-derived exosomes: the role of integrins. Faseb j. 2004; 18: 977-979.
39. MikoŁaj P Zaborowski, Leonora Balaj, Xandra O Breakefiel, Charles P Lai et al. Extracellular Vesicles: Composition, Biological Relevance, and Methods of Study. Bioscience. 2015; 65: 783-797.
40. Giovanni Camussi, Maria C Deregibus, Stefania Bruno, Vincenzo Cantaluppi, Luigi Biancone et al. Exosomes/microvesicles as a mechanism of cell-to-cell communication. Kidney Int. 2010; 78: 838-848.
41. J Ratajczak, M Wysoczynski, F Hayek, A Janowska-Wieczorek, MZ Ratajczak. Membrane-derived microvesicles: important and underappreciated mediators of cell-to-cell communication. Leukemia. 2006; 20: 1487-1495.
42. Bénédicte Hugel, M Carmen Martínez, Corinne Kunzelmann, Jean-Marie Freyssinet et al. Membrane microparticles: two sides of the coin. Physiology (Bethesda). 2005; 20: 22-27.
43. Kerstin Menck, Annalen Bleckmann, Matthias Schulz, Lena Ries, Claudia Binder et al. Isolation and Characterization of Microvesicles from Peripheral Blood. J Vis Exp. 2017(119).
44. Laberge A, S Arif, VJ Moulin. Microvesicles: Intercellular messengers in cutaneous wound healing. J Cell Physiol. 2018; 233: 5550-5563.
45. Ian J White, Lorna M Bailey, Minoo Razi Aghakhani, Stephen E Moss, Clare E Futter et al. EGF stimulates

annexin 1-dependent inward vesiculation in a multivesicular endosome subpopulation. Embo j. 2006; 25: 1-12.
46. Anne-Lie Ståhl, Karl Johansson, Maria Mossberg, Robin Kahn, Diana Karpman et al. Exosomes and microvesicles in normal physiology, pathophysiology, and renal diseases. Pediatr Nephrol. 2019; 34: 11-30.
47. Huijun Dai, Suisui Zhang, Xueke Du, Weikang Zhang, Ren Jing, et al. RhoA inhibitor suppresses the production of microvesicles and rescues high ventilation induced lung injury. Int Immunopharmacol. 2019; 72: 74-81.
48. Valapala M, JK Vishwanatha. Lipid raft endocytosis and exosomal transport facilitate extracellular trafficking of annexin A2. J Biol Chem. 2011; 286: 30911-30925.
49. Wolfgang Lösche, Thomas Scholz, Uta Temmler, Volker Oberle, Ralf A Claus. Platelet-derived microvesicles transfer tissue factor to monocytes but not to neutrophils. Platelets. 2004; 15: 109-115.
50. Anne-lie Ståhl, Ida Arvidsson, Karl E Johansson, Milan Chromek, Johan Rebetz, et al. A novel mechanism of bacterial toxin transfer within host blood cell-derived microvesicles. PLoS Pathog. 2015; 11: e1004619.
51. OP Barry, D Praticò, RC Savani, GA FitzGerald. Modulation of monocyte-endothelial cell interactions by platelet microparticles. J Clin Invest. 1998; 102: 136-44.
52. T Ihara, T Yamamoto, M Sugamata, H Okumura, Y Ueno. The process of ultrastructural changes from nuclei to apoptotic body. Virchows Arch. 1998; 433: 443-447.
53. Battistelli M, E Falcieri. Apoptotic Bodies: Particular Extracellular Vesicles Involved in Intercellular Communication. Biology (Basel). 2020; 9.
54. Blander JM. The many ways tissue phagocytes respond to dying cells. Immunol Rev. 2017; 277: 158-173.
55. Ivan K H Poon, Christopher D Lucas, Adriano G Rossi, Kodi S Ravichandran. Apoptotic cell clearance: basic biology and therapeutic potential. Nat Rev Immunol. 2014; 14: 166-180.
56. F Renò, S Burattini, S Rossi, F Luchetti, M Columbaro, S Santi, et al. Phospholipid rearrangement of apoptotic membrane does not depend on nuclear activity. Histochem Cell Biol. 1998; 110: 467-476.
57. Johan Skog, Tom Würdinger, Sjoerd van Rijn, Dimphna H

Meijer, Laura Gainche, et al. Glioblastoma microvesicles transport RNA and proteins that promote tumour growth and provide diagnostic biomarkers. Nat Cell Biol. 2008; 10: 1470-1476.
58. Khalid Al-Nedawi, Brian Meehan, Johann Micallef, Vladimir Lhotak, Linda May, et al. Intercellular transfer of the oncogenic receptor EGFRvIII by microvesicles derived from tumour cells. Nat Cell Biol. 2008; 10: 619-624.
59. Arash Latifkar, Lu Ling, Amrit Hingorani, Eric Johansen, Amdiel Clement, et al. Loss of Sirtuin 1 Alters the Secretome of Breast Cancer Cells by Impairing Lysosomal Integrity. Dev Cell. 2019; 49: 393-408.e7.
60. Bridget T Kreger, Andrew L Dougherty, Kai Su Greene, Richard A Cerione, Marc A Antonyak. Microvesicle Cargo and Function Changes upon Induction of Cellular Transformation. J Biol Chem. 2016; 291: 19774-19785.
61. Bridget T Kreger, Eric R Johansen, Richard A Cerione, Marc A Antonyak. The Enrichment of Survivin in Exosomes from Breast Cancer Cells Treated with Paclitaxel Promotes Cell Survival and Chemoresistance. Cancers (Basel). 2016; 8.
62. Qiyu Feng, Chengliang Zhang, David Lum, Joseph E Druso, Bryant Blank, et al. A class of extracellular vesicles from breast cancer cells activates VEGF receptors and tumour angiogenesis. Nat Commun. 2017; 8: 14450.
63. Khalid Al-Nedawi, Brian Meehan, Robert S Kerbel, Anthony C Allison, Janusz Rak. Endothelial expression of autocrine VEGF upon the uptake of tumor-derived microvesicles containing oncogenic EGFR. Proc Natl Acad Sci U S A. 2009; 106: 3794-3799.
64. Kalluri R, RA Weinberg. The basics of epithelial-mesenchymal transition. J Clin Invest. 2009; 119: 1420-1428.
65. Bow J Tauro, Rommel A Mathias, David W Greening, Shashi K Gopal, Hong Ji, et al. Oncogenic H-ras reprograms Madin-Darby canine kidney (MDCK) cell-derived exosomal proteins following epithelial-mesenchymal transition. Mol Cell Proteomics. 2013; 12: 2148-2159.
66. Ayuko Hoshino, Bruno Costa-Silva, Tang-Long Shen, Goncalo Rodrigues, Ayako Hashimoto, et al. Tumour exosome integrins determine organotropic metastasis.

Nature. 2015; 527: 329-335.
67. Gavin P Dunn, Allen T Bruce, Hiroaki Ikeda, Lloyd J Old, Robert D Schreiber. Cancer immunoediting: from immunosurveillance to tumor escape. Nat Immunol. 2002; 3: 991-998.
68. Schreiber RD, LJ Old, MJ Smyth. Cancer immunoediting: integrating immunity's roles in cancer suppression and promotion. Science. 2011; 331: 1565-1570.
69. Gang Chen, Alexander C Huang, Wei Zhang, Gao Zhang, Min Wu, et al. Exosomal PD-L1 contributes to immunosuppression and is associated with anti-PD-1 response. Nature. 2018; 560: 382-386.
70. Mauro Poggio, Tianyi Hu, Chien-Chun Pai, Brandon Chu, Cassandra D Belair, et al. Suppression of Exosomal PD-L1 Induces Systemic Anti-tumor Immunity and Memory. Cell. 2019; 177: 414-427.e13.
71. Franz L Ricklefs, Quazim Alayo, Harald Krenzlin, Ahmad B Mahmoud, Maria C Speranza, et al. Immune evasion mediated by PD-L1 on glioblastoma-derived extracellular vesicles. Sci Adv. 2018; 4: eaar2766.
72. Marie-Nicole Theodoraki, Saigopalakrishna S Yerneni, Thomas K Hoffmann, William E Gooding, Theresa L Whiteside. Clinical Significance of PD-L1(+) Exosomes in Plasma of Head and Neck Cancer Patients. Clin Cancer Res. 2018; 24: 896-905.
73. Dipti Vijayan, Arabella Young, Michele WL Teng, Mark J Smyth. Targeting immunosuppressive adenosine in cancer. Nat Rev Cancer. 2017; 17: 709-724.
74. van Calker D, M Müller, B Hamprecht. Adenosine regulates via two different types of receptors, the accumulation of cyclic AMP in cultured brain cells. J Neurochem. 1979; 33: 999-1005.
75. Chang WH, RA Cerione, MA Antonyak. Extracellular Vesicles and Their Roles in Cancer Progression. Methods Mol Biol. 2021; 2174: 143-170.
76. Johnny C Akers, Valya Ramakrishnan, Ryan Kim, Johan Skog, Ichiro Nakano, et al. MiR-21 in the extracellular vesicles (EVs) of cerebrospinal fluid (CSF): a platform for glioblastoma biomarker development. PLoS One. 2013; 8: e78115.

77. Hitoshi Dejima, Hisae Iinuma, Rie Kanaoka, Noriyuki Matsutani, Masafumi Kawamura et al. Exosomal microRNA in plasma as a non-invasive biomarker for the recurrence of non-small cell lung cancer. Oncol Lett. 2017; 13: 1256-1263.
78. Warsame R, A Grothey. Treatment options for advanced pancreatic cancer: a review. Expert Rev Anticancer Ther. 2012; 12: 1327-1336.

Book Chapter

An iTRAQ Quantitative Proteomic Study to Reveal How Hypoxia in Tumor Micro-Environment Regulates Metabolic Reprogramming in A549 KRAS-Mutant Non-Small Cell Lung Cancer Cells upon Lysine Deacetylases Inhibitor Treatments to propose Machine-Learning-Based Drug Repositioning

Alfonso Martín-Bernabé[1,2,3,4†], Josep Tarragó-Celada[3†], Valérie Cunin[1,2], Sylvie Michelland[1,2], Roldán Cortés[3,5], Johann Poignant[6], Cyril Boyault[6], Walid Rachidi[7,8], Sandrine Bourgoin-Voillard[1,2], Marta Cascante[3,5,9*†] and Michel Seve[1,2*]

[1]LBFA et BEeSy, Université Grenoble Alpes, Inserm, U1055, CHU Grenoble Alpes, PROMETHEE Proteomic Platform, France
[2]PROMETHEE Proteomic Platform, TIMC-IMAG, Université Grenoble Alpes, CNRS, Grenoble INP, CHU Grenoble Alpes, France
[3]Department of Biochemistry and Molecular Biomedicine, Institute of Biomedicine of Universitat de Barcelona, Faculty of Biology, Universitat de Barcelona, Spain
[4]Department of Oncology-Pathology, BioClinicum, Karolinska Institutet, Sweden
[5]Centro de Investigación Biomédica en Red de Enfermedades Hepáticas y Digestivas (CIBEREHD), Instituto de Salud Carlos III (ISCIII), Spain
[6]Reckonect, Institute for Advanced Biosciences—IAB, Université Grenoble Alpes, Inserm, UMR_S 1209/CNRS UMR 5309, France
[7]SyMMES/CIBEST, Université Grenoble Alpes, UMR 5819 UGA-CNRS-CEA, France
[8]BIG-BGE, Université Grenoble Alpes, CEA, Inserm, U1038, France

[9]Metabolomics Node at Spanish National Bioinformatics Institute (INB-ISCIII-ES-ELIXIR), Institute of Health Carlos III (ISCIII), Spain

[†]These authors contributed equally to this work.

***Corresponding Authors:** Michel Seve, LBFA et BEeSy, Université Grenoble Alpes, Inserm, U1055, CHU Grenoble Alpes, PROMETHEE Proteomic Platform, 38000 Grenoble, France

Marta Cascante, Department of Biochemistry and Molecular Biomedicine, Institute of Biomedicine of Universitat de Barcelona, Faculty of Biology, Universitat de Barcelona, 08028 Barcelona, Spain

Published **January 20, 2023**

This Book Chapter is a republication of an article published by Michel Seve, et al. at International Journal of Molecular Sciences in March 2021. (Martín-Bernabé, A.; Tarragó-Celada, J.; Cunin, V.; Michelland, S.; Cortés, R.; Poignant, J.; Boyault, C.; Rachidi, W.; Bourgoin-Voillard, S.; Cascante, M.; Seve, M. Quantitative Proteomic Approach Reveals Altered Metabolic Pathways in Response to the Inhibition of Lysine Deacetylases in A549 Cells under Normoxia and Hypoxia. Int. J. Mol. Sci. 2021, 22, 3378. https://doi.org/10.3390/ijms22073378)

How to cite this book chapter: Alfonso Martín-Bernabé, Josep Tarragó-Celada, Valérie Cunin, Sylvie Michelland, Roldán Cortés, Johann Poignant, Cyril Boyault, Walid Rachidi, Sandrine Bourgoin-Voillard, Marta Cascante, Michel Seve. An iTRAQ Quantitative Proteomic Study to Reveal How Hypoxia in Tumor Micro-Environment Regulates Metabolic Reprogramming in A549 KRAS-Mutant Non-Small Cell Lung Cancer Cells upon Lysine Deacetylases Inhibitor Treatments to propose Machine-Learning-Based Drug Repositioning. In: Hussein Fayyad Kazan, editor. Immunology and Cancer Biology. Hyderabad, India: Vide Leaf. 2023.

Author Contributions: Conceptualization, A.M.-B., J.T.-C., S.B.-V., M.C., and M.S.; methodology, A.M.-B., J.T.-C., V.C., S.M., J.P., and C.B.; software, J.P., C.B., and M.C.; validation, A.M.-B. and J.T.-C.; formal analysis, A.M.-B., J.T.-C., and S.B.-V.; investigation, A.M.-B., J.T.-C., S.B.-V., M.C., and M.S.; resources, S.B.-V., M.C., and M.S; data curation, A.M.-B., J.T.-C., and S.B.-V.; writing—original draft preparation, A.M.-B., J.T.-C., and S.B.-V.; writing—review and editing, A.M.-B., J.T.-C., V.C., S.M., J.P., C.B., W.R., S.B.-V., M.C., M.S., and S.B.-V.; visualization, A.M.-B., J.T.-C., and S.B.-V.; supervision, S.B.-V., M.C., and M.S.; project administration, A.M.-B., J.T.-C., and S.B.-V.; funding acquisition, S.B.-V., M.C., and M.S. All authors have read and agreed to the published version of the manuscript.

Data Availability Statement: The proteomic data were deposited to the ProteomeXchange Consortium with the MassIVE identifier MSV000083174 (http://massive.ucsd.edu (accessed on 23 March 2021)) and ProteomeXchange identifier PXD011900 (http://www.proteomexchange.org (accessed on 23 March 2021)).

Funding: This work was supported by grants to M.C. from the "Agència de Gestio' d'Ajuts Universitaris i de Recerca (AGAUR)"—Generalitat de Catalunya, (2017SGR1033), ICREA Foundation (ICREA Academia), MCIU/AEI/FEDER, UE (SAF2017-89673-R), MINECO/FEDER, UE (SAF2015-70270-REDT) and Instituto de Salud Carlos III (CIBEREHD, CB17/04/00023). J.T.-C. was supported by grants of the "Ministerio de Educación y Formación Profesional" (FPU14-05992) and the Biohealth Computing Schools. A.M.-B. was supported by grants of the "Ministère de l'Enseignement supérieur et de la Recherche" from the French Government and The Coordinating Action Systems Medicine (CASyM).

Acknowledgments: The authors thank Catherine Guette and Damien Besson from the Institut de Cancerologie de l'Ouest (ICO) -Université Nantes Angers- Centre de Lutte Contre le Cancer Paul Papin (Angers, France) for sharing their expertise in the optimization of the modified FASP/iTRAQ protocol.

Data Availability Statement: The data presented in this study are openly available in [ProteomeXchange Consortium (http://proteomecentral.proteomexchange.org)], reference number [PXD011900] and [MassIVE ((http://massive.ucsd.edu)], reference number [MSV000083174].

Conflicts of Interest: The authors declare no conflict of interest.

Abstract

Growing evidence is showing that acetylation plays an essential role in cancer, but studies on the impact of KDAC inhibition (KDACi) on the metabolic profile are still in their infancy. Here, we report the study that was published by our teams in the International Journal of Molecular Sciences [1]. In this study, we analyzed, by using an iTRAQ-based quantitative proteomics approach, the changes in the proteome of *KRAS*-mutated non-small cell lung cancer (NSCLC) A549 cells in response to trichostatin-A (TSA) and nicotinamide (NAM) under normoxia and hypoxia. Part of this response was further validated by molecular and biochemical analyses and correlated with the proliferation rates, apoptotic cell death, and activation of ROS scavenging mechanisms in opposition to the ROS production. Despite the differences among the KDAC inhibitors, up-regulation of glycolysis, TCA cycle, oxidative phosphorylation and fatty acid synthesis emerged as a common metabolic response underlying KDACi. We also observed that some of the KDACi effects at metabolic levels are enhanced under hypoxia. Furthermore, we used a drug repositioning machine learning approach to list candidate metabolic therapeutic agents for *KRAS* mutated NSCLC. Together, these results allow us to better understand the metabolic regulations underlying KDACi in NSCLC, taking into account the microenvironment of tumors

related to hypoxia, and bring new insights for the future rational design of new therapies.

[1] A. Martín-Bernabé, J. Tarragó-Celada, V. Cunin, S. Michelland, R. Cortés, J. Poignant, C. Boyault, W. Rachidi, S. Bourgoin-Voillard, M. Cascante *, Michel Seve *. Quantitative Proteomic Approach Reveals Altered Metabolic Pathways in Response to the Inhibition of Lysine Deacetylases in A549 Cells under Normoxia and Hypoxia, Int. J. Mol. Sci. 2021, 22(7), 3378. https://doi.org/10.3390/ijms22073378.

Keywords

Cancer Metabolism; Lysine Deacetylase Inhibitors; Hypoxia; NSCLC

Abbreviations

AcCoA- Acetyl-CoA; ACSL3- Long-Chain-Fatty-Acid-CoA Ligase 3; ALDC- Fructose-bisphosphate Aldolase C; ALDH10- Fatty Aldehyde Dehydrogenase; ALK- Anaplastic Lymphoma Kinase; CID- Collision-Induced Dissociation; COX6A1- Cytochrome c Oxidase Subunit 6A1; COX2- Cytochrome c Oxidase Subunit 2; EGFR- Epidermal Growth Factor Receptor; ENO1- Alpha-enolase; ER- Estrogen Receptor; FDR- False Discovery Rate; GAPDH- Glyceraldehyde-3-Phosphate dehydrogenase; Glc- Glucose; Gln- Glutamine; GLS- Glutaminase; GLS1- Glutaminase 1; GO- Gene Ontology; GPI- Glucose-6-phosphate Isomerase; HIF- Hypoxia-Inducible Factor; HK- Hexokinase; IPG- Immobilized pH Gradient; ITRAQ- Isobaric Tags for Relative and Absolute Quantitation; KDAC- Lysine deacetylase; KDAC6- Lysine deacetylase 6; KDACI- Lysine deacetylase Inhibitor; Lac- Lactate; LC- Liquid Chromatography; LDH- Lactate dehydrogenase; NAM- Nicotinamide; NSCLC- Non-Small Cell Lung Cancer; MMTS- Methylmethanethiosulfate; OAT- Ornithine Aminotransferase; OGDH-2-oxoglutarate dehydrogenase; OXPHOS- Oxidative Phosphorylation; PFK1- ATP-dependent 6-phosphofructokinase; PDHE- Pyruvate dehydrogenase Subunit E; PGI- Glucose-6-Phosphate Isomerase; Pyr- Pyruvate; pI- Isoelectric Point; PI-

Propidium Iodide; PIR- Protein Information Resource; PPP- Pentose Phosphate Pathway; PRDX1- Peroxiredoxin-1; PRDX4- Peroxiredoxin-4; PSME1- Proteasome Activator Complex Subunit 1; PSME2- Proteasome Activator Complex Subunit 2; ROS- Reactive Oxygen Species; SAHA- Suberoylanilide Hydroxamic Acid

Introduction

Herein, we report a proteomic study combined to a machine learning analysis we published in the International Journal of Molecular Sciences in 2021 [1] to reveal how hypoxia in tumor micro-environment regulates metabolic reprogramming in A549 *KRAS*-mutant non-small cell lung cancer cells upon deacetylases inhibitor (KDACI) treatments to propose a drug repositioning miming the effects of those KDACI treatments.

Lung cancer is the leading cause of cancer-related death worldwide, with an estimated upward trend of 2.1 million new cases and 1.8 million deaths per year (approximately 18.4% of total cancer deaths) in 2018 [2]. Non-small cell lung cancer (NSCLC) represents about 80–85% of all lung cancer cases, with an overall 5-year survival rate of 19% [3]. Traditional therapies in NSCLC such as radiotherapy and platinum-based chemotherapy lack specificity and often cause severe side effects as they affect healthy cells [4]. To address this problem, targeted therapies and immunotherapies have emerged as a way to specifically target cancer cells. However, the therapeutic response may be limited as tumors are often heterogeneous, and some cell populations within the tumor can be resistant to the inhibition of the selected target [5]. Thus, targeted therapies and immunotherapies will not benefit patients harboring other molecular driver gene mutations, such as patients whose tumors harbor activating *KRAS* mutation that leads to constitutively active RAS signaling independent of upstream signals [6]. To date, clinical approaches targeting mutated *KRAS* have been unsuccessful [7]. Several studies have shown that mutations in *KRAS* play a critical role in metabolic reprogramming in multiple cancers, including lung cancer [8,9].

Generally, in cancer cells, metabolic reprogramming is considered to be one of the hallmarks of cancer disease allowing them to produce enough energy, reducing power and precursors required for growth and proliferation [10,11]. The general metabolic phenotype of cancer cells consists of elevated glycolysis and lactate production even under aerobic conditions; a phenomenon called the "Warburg effect" [12]. This switch in metabolism allows cancer cells to survive with a limited oxygen supply characteristic of the tumor microenvironment as they become less dependent on oxidative phosphorylation (OXPHOS) [13]. Furthermore, an enhanced glucose uptake favors the pentose phosphate pathway (PPP) flux to generate enough reducing power for antioxidant defense and intermediates for nucleotide synthesis [14,15]. Additionally, a higher glutamine uptake is also considered a major component of the general metabolic phenotype of tumor cells, providing an additional advantage in synthesizing amino acids, nucleotides, and lipids [16]. Although many cancers share similar metabolic adaptations, cancer cells rewire their metabolic programs in response to changes in the tumor microenvironment and oncogenic signals such as an activating *KRAS* mutation. Indeed, *KRAS* mutated NSCLC A549 cell line, which exhibits high resistance to current treatments, is characterized by specific metabolic adaptations that rely on glycolysis and PPP [17].

Multiple studies have demonstrated that the hypoxic tumor microenvironment plays a critical role in cancer progression and drug resistance [18–21]. Under hypoxia, cancer cells engage metabolic adaptation strategies to survive and growth by activating a relevant gene expression program through HIF-1α. The HIF-1α-dependent gene program involves the up-regulation of genes associated with increased glycolysis and lactate production, such as glucose transporters, glycolytic enzymes, and LDH-A [22]. Interestingly, HIF-1α is regulated by acetylation and deacetylation processes: The transcriptional activity of HIF-1α is repressed by KDAC activity, and also sirtuins have emerged as regulators of HIF-1α [18,20–23].

On the other hand, and given the increasing importance of the post-translational modifications in cancer and metabolism, the

inhibition of lysine deacetylases (KDAC) has emerged in recent years as another promising therapeutic strategy in cancer [24–26]. Lysine deacetylase inhibitors (KDACIs) are used clinically to treat hematological malignancies [27] but have not demonstrated clinical benefit in solid tumors [28]. Current research focuses on developing new KDACIs and prospects for therapeutic application in cancer and other pathological conditions. Additionally, even though the use of KDACIs in NSCLC is less established, several studies using them either as monotherapy or in combination with other inhibitors has created a new therapeutic scenario offering the possibility to improve the effectiveness reducing resistance to current treatments [29–32].

KDACIs target different classes of KDACs, suggesting that they may have a different effect on gene expression, affecting key cellular processes that ultimately can lead to apoptotic cell death. The use of KDACIs such as trichostatin A (TSA), an inhibitor of classes I, II, and IV KDAC enzymes, and nicotinamide (NAM), an inhibitor of class III KDACs (also known as sirtuins), has been shown to exhibit significant antitumor activity in terms of cell proliferation, viability and apoptosis in cell models of lung cancer [33,34]. However, their impact on cancer metabolism has not been addressed in detail in these studies although acetylation is known to play a critical role in regulating metabolism [35]. Herein, we investigated the effect of inhibition of KDAC by using TSA and NAM on the global proteome of the active *KRAS*-mutant NSCLC A549 cell line, which exhibits high resistance to current therapies. The inhibition of KDAC allowed us to explore how protein acetylation status affects the metabolic profile, thus better elucidating the link between acetylation and metabolic reprogramming in cancer.

Several studies have demonstrated the utility of isobaric Tags for Relative and Absolute Quantitation (iTRAQ)-based quantitative proteomic approaches for global in-depth profiling of proteomes by measuring the relative protein abundance in cancer samples. The evaluation of the differences between proteomes from cancer samples cultured under different culture conditions might identify specific proteome signatures associated with tumor growth and survival [36]. One of such culture conditions is

certainly hypoxia exposure, which has been shown to induce a substantial shift in the proteome supporting metabolic processes when oxygen is limiting [37–42].

In this study, we performed a quantitative iTRAQ-based proteomic experiment coupled with two-dimensional (2D) fractionation (OFFGEL/RP-nano-LC) and mass spectrometry (MS) analysis together with other metabolic measurements and enzyme activity assays. Furthermore, we used a drug repositioning strategy to identify potential therapeutic opportunities for existing drugs targeting the metabolic reprogramming induced by KDAC inhibition and hypoxia. Our results explored new mechanisms of metabolic adaptations that lead to a deeper understanding of the regulation of lung cancer metabolism under KDACIs and hypoxic conditions, which may contribute to the development and design of new cancer therapies.

Results

KDAC Inhibition Leads to Reduced Cell Proliferation by Inducing Apoptosis, Cell Cycle Arrest, and Oxidative Stress in A549 Cells

The overall proliferation of A549 cells varied among the different KDACI treatments (Figure 1A). Both TSA and TSA/NAM double-treated cells inhibited cell proliferation, and decreased cell viability, which correlates with the significantly increased cell death by apoptosis (Figure 1B). NAM-treated cells, instead, exhibited a lower growth rate than control cells, also accompanied by a significant increase in apoptosis. The TSA/NAM double treatment further induced apoptotic cell death by approximately 2-fold compared with TSA single treatment. Finally, the hypoxic treatment only limited cell proliferation, and KDACI-treated cells under hypoxia followed a similar cell proliferative and apoptosis pattern to treated cells under normoxia.

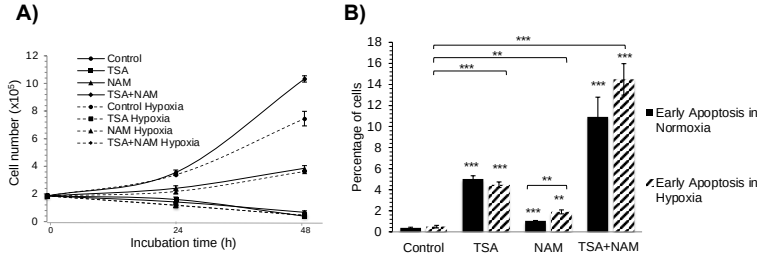

Figure 1: (**A**) Effect of trichostatin-A (TSA) and nicotinamide (NAM) treatments on A549 cell proliferation. A549 cells treated with 1 μM TSA, 20 mM NAM, or both 1 μM TSA and 20 mM NAM for 24 h and 48 h of incubation under normoxia or hypoxia. Dots represent means ± standard deviations of three independent experiments. (**B**) Apoptosis analysis of KDACI-treated A549 cells under normoxia and hypoxia. Apoptosis was measured after 24 h of incubation. Cells in the stage of early apoptosis are represented as the percentage with respect to total cells. A549 cells were treated with 1 μM TSA, 20 mM NAM or both 1 μM TSA and 20 mM NAM for 24 h under normoxia or hypoxia. Bars represent the means ± standard error of the mean of three independent experiments. The asterisks above bars indicate statistically significant differences compared to normoxic control cells. Asterisks above curly brackets indicate statistically significant differences between hypoxic and normoxic treatments and between hypoxic treatments and hypoxic control cells. Statistical significance was assessed by a two-tailed Student's *t*-test. **, $p \leq 0.01$; ***, $p \leq 0.001$.

TSA-treated cells exhibited a high percentage of cells at G2/M phase, while NAM-treated cells showed a delayed progression through the G1 phase. The combination of TSA and NAM treatment led to a drastic cell cycle arrest at the G2/M phase and decreased S phase. A similar trend was observed in KDACI treatments under hypoxia (Figure S1). ROS generation increased substantially in A549 cells under KDAC inhibition (Figure S2) and was enhanced under hypoxia. These elevated ROS levels could be associated with the dysregulation of the antioxidant defense system, a possibility that is further explored below.

KDAC Inhibition Modulates the Tumor Phenotype through Changes in the Metabolic Profile

The TSA treatment did not significantly alter the glucose consumption and lactate production under normoxia (Figures 2A,B). In contrast, both the NAM and TSA/NAM double

treatments showed a significantly decreased glucose uptake and lactate production compared with the control cells. Under hypoxia, the glucose consumption and lactate production rates were significantly different in the TSA, NAM, and TSA/NAM treatments with respect to control cells under normoxia (Figures 2A,B). The glutamine uptake was significantly increased only under the TSA treatment in both contexts of normoxia and hypoxia (Figure 2C).

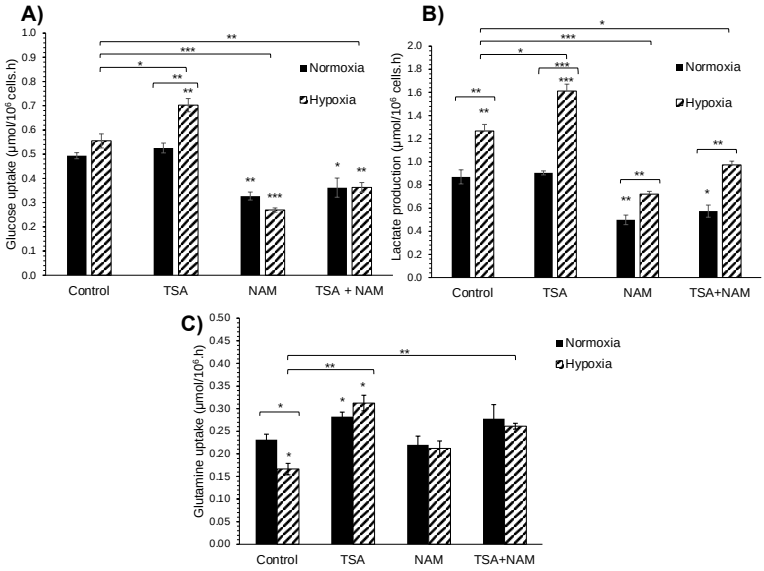

Figure 2: Extracellular metabolite quantitation of KDACI-treated A549 cells under normoxia and hypoxia. The glucose uptake (**A**), lactate production (**B**), and glutamine uptake (**C**) were measured in the beginning and at the end of the 24 h-incubation, and the metabolite consumption/production rates were normalized by the number of cells in each condition. (**A**–**C**) A549 cells were treated with 1 µM TSA, 20 mM NAM, or both 1 µM TSA and 20 mM NAM for 24 h under normoxia or hypoxia. Bars represent the means ± standard error of the mean of three independent experiments. The asterisks above bars indicate statistically significant differences compared to normoxic control cells. The asterisks above curly brackets indicate statistically significant differences between hypoxic and normoxic treatments and between hypoxic treatments and hypoxic control cells. Statistical significance was assessed by a two-tailed Student's *t*-test. *, $p \leq 0.05$; **, $p \leq 0.01$; ***, $p \leq 0.001$.

The iTRAQ-based quantitative proteomic analysis was performed using a 4800 MALDI-TOF/TOF mass spectrometer

(Sciex, Les Ulis, France) and allowed the quantification of 834 proteins from 2710 peptides. This analysis evidenced dysregulation of several proteins related to metabolism upon the different KDACI treatments (Figure 3). The Gene Ontology (GO) enrichment analysis of the dysregulated proteins allowed us to decipher the biological processes (Figure 3B) and the protein information resource (PIR) keywords (Table S1) related to these treatments. Overall, proteins related to the generation of energy and intracellular transport were up-regulated (Figure 3B), while the transcription and RNA processing were generally down-regulated. Furthermore, according to the PIR keywords enrichment analysis, approximately 60–70% of the proteins that were dysregulated in all the treatments were proteins modified by acetylation, phosphorylation, or both post-translational modifications (Table S1).

A)

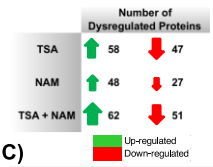

B)

Gene ontology analysis	TSA		NAM		TSA + NAM	
Biological process term	% of proteins	*p*-value	% of proteins	*p*-value	% of proteins	*p*-value
Generation of precursor metabolites and energy	14	<0.001	13	0.002	11	0.003
Intracellular transport	14	0.012	19	<0.001	20	<0.001
Nuclear transport	7	0.023	11	0.001	8	0.005
Nucleocytoplasmic transport	7	0.022	11	0.001	8	0.005
Translation	26	<0.001	30	<0.001	26	<0.001
Translational elongation	21	<0.001	22	<0.001	20	<0.001
RNA processing	21	<0.001	19	0.019	20	<0.001
RNA splicing	17	<0.001	15	0.017	14	<0.001
mRNA metabolic process	15	0.001	15	0.033	16	<0.001
mRNA processing	15	<0.001	15	0.023	14	0.001

C)

Enzyme name	Accesion	TSA		NAM		TSA + NAM	
Glycolysis/Gluconeogenesis (K00010)	Number	Ratio	*p*-value	Ratio	*p*-value	Ratio	*p*-value
Glucose-6-phosphate isomerase, GPI	P06744	0.77	0.186	0.95	0.392	0.69	0.155
ATP-dep 6-phosphofructokinase, liver type, PFK1	P17858	**1.48**	**0.029**	**1.56**	**0.015**	1.97	0.059
Fructose-bisphosphate aldolase C, ALDC	P09972	**2.00**	**0.038**	0.79	0.319	**1.99**	**<0.001**
Glyceraldehyde-3-Ph dehydrogenase, GAPDH	P04406	1.06	0.437	1.13	0.361	1.11	0.406
Phosphoglycerate mutase 1, PGAM1	P18669	0.82	0.277	1.04	0.449	0.89	0.182
Alpha-enolase, ENO1	P06733	1.39	0.175	**1.78**	**0.032**	1.50	0.093
L-lactate dehydrogenase A chain, LDHA	P00338	0.89	0.382	1.10	0.396	0.93	0.401
L-lactate dehydrogenase B chain, LDHB	P07195	**0.67**	**0.013**	0.80	0.213	**0.58**	**<0.001**
Pyruvate dehydrogenase E1, PDHE	P11177	1.17	0.299	1.26	0.097	0.91	0.355
Krebs Cycle (K00020)							
2-oxoglutarate dehydrogenase, mitochondrial, OGDH	Q02218	**1.89**	**0.002**	1.41	0.237	1.68	0.253
Succinate dehydrogenase, mitochondrial, SDHA	P31040	1.47	0.222	1.12	0.318	1.49	0.194
Oxidative phosphorylation (K00190)							
Cytochrome c oxidase, COX subunit 6A1	P12074	2.49	0.119	3.13	0.065	1.94	0.195
Cytochrome c oxidase, COX subunit 2	P00403	1.09	0.458	0.90	0.335	1.64	0.085
Fatty acid metabolism (K01212)							
Long-chain-fatty-acid--CoA ligase 3, ACSL3	O95573	**2.15**	**0.010**	1.27	0.197	1.68	0.065
Very-long-chain enoyl-CoA reductase, TECR	Q9NZ01	**1.77**	**0.001**	**1.83**	**0.001**	1.21	0.289
Fatty aldehyde dehydrogenase, ALDH10	P51648	**0.69**	**0.033**	0.93	0.344	0.72	0.093
Other pathways							
Glutaminase kidney isoform, mitochondrial, GLS1	O94925	1.23	0.173	0.86	0.307	**1.53**	**0.017**
Ornithine aminotransferase, mitochondrial, OAT	P04181	1.45	0.228	1.03	0.452	**2.03**	**0.047**
Peroxiredoxin-1	Q06830	0.86	0.201	0.93	0.346	0.89	0.317
Peroxiredoxin-4	Q13162	0.95	0.467	1.72	0.200	2.30	0.092
Spermidine synthase, SRM	P19623	**0.31**	**0.034**	0.60	0.171	**0.29**	**0.020**
Thioredoxin domain-containing protein 5	Q8NBS9	0.99	0.442	1.00	0.489	**1.28**	**0.010**
Thioredoxin domain-containing protein 17	Q9BRA2	**1.95**	**0.022**	1.36	0.164	**2.01**	0.000

Figure 3: Effect of KDAC inhibition on the global proteome and metabolic enzymes compared to control A549 cells. Quantitative proteomic analysis of differentially expressed proteins in A549 cells treated with 1 μM of TSA, 20 mM of NAM or both 1 μM TSA, and 20 mM NAM for 24 h under normoxic conditions. (**A**) The number of up-regulated and down-regulated proteins (isobaric Tags for Relative and Absolute Quantitation (iTRAQ) ratio < 1 and > 1, respectively) showing significant (p-value ≤ 0.05) differences between TSA, NAM and TSA/NAM treatments with respect to control cells. (**B**) GO

enrichment analysis of the Biological process term for each condition shown as the percentage of proteins related to each process. All biological processes are shown as significantly (p-value ≤ 0.05) up-regulated or down-regulated. (**C**) Quantitative measurement of the main metabolic enzymes identified using the iTRAQ approach for the different conditions compared to untreated control cells. Significantly up-regulated enzymes (iTRAQ ratio < 1 and p-value ≤ 0.05) are represented in green and significantly down-regulated enzymes (iTRAQ ratio > 1 and p-value ≤ 0.05) are represented in red. Non-significantly up-regulated, and down-regulated enzymes are represented in gray.

Our iTRAQ analysis confirmed a metabolic reprogramming in A549 cells treated with KDACIs (Figure 3C). Upon TSA treatment, enzymes from glycolysis (fructose-bisphosphate aldolase C, ALDC and phosphofructokinase 1, PFK1), TCA cycle (2-oxoglutarate dehydrogenase, OGDH) were found to be significantly up-regulated, while lactate dehydrogenase B (LDH-B) was down-regulated. This pattern was confirmed by Western blot and enzyme activity analysis (Figure 4), although glucose uptake and lactate production were not altered. Furthermore, some enzymes involved in the synthesis of fatty acids were significantly up-regulated after TSA treatment (very-long-chain enoyl-CoA reductase, TECR, and long-chain-fatty-acid-CoA ligase, ACSL3), whereas the fatty aldehyde dehydrogenase (ALDH10) involved in fatty acid β-oxidation was down-regulated (Figure 3C). Interestingly, the spermidine synthase (SRM) levels, which catalyzes the synthesis of the polyamine spermidine, were strongly down-regulated (Figure 3C).

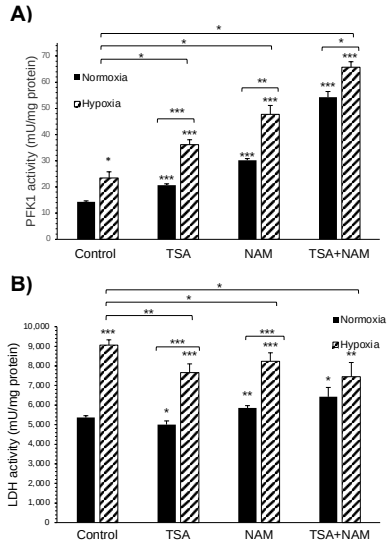

D)

	Normoxia						Hypoxia					
	TSA		NAM		TSA + NAM		Control		TSA		NAM		TSA + NAM	
	WB ratio	iTRAQ ratio	WB ratio	iTRAQ ratio	WB ratio	iTRAQ ratio	WB ratio	iTRAQ ratio	WB ratio	iTRAQ ratio	WB ratio	iTRAQ ratio	WB ratio	iTRAQ ratio
GPI	0.95 ± 0.10	0.77	1.08 ± 0.02	0.95	1.00 ± 0.07	0.69	1.57 ± 0.10***	1.74*	1.18 ± 0.08**	1.23	1.02 ± 0.03	0.89	0.93 ± 0.09	1.04
PFK1	1.32 ± 0.65	1.48*	1.93 ± 0.66	1.56*	1.89 ± 0.61	1.97	2.37 ± 1.07	1.75*	1.97 ± 0.88	2.09*	2.02 ± 0.62	2.29*	1.61 ± 0.48	1.54
ALDC	1.05 ± 0.02	2.00*	1.01 ± 0.05	0.79	1.10 ± 0.06	1.99*	1.95 ± 0.40*	1.23	2.74 ± 0.73	5.19*	1.39 ± 0.07*	1.35	1.69 ± 0.06**	3.04*
GAPDH	1.36 ± 0.18	1.06	1.34 ± 0.32	1.13	1.63 ± 0.21	1.11	1.31 ± 0.19	1.36	1.75 ± 0.33	1.32	1.21 ± 0.27	1.21	1.28 ± 0.20	1.20
ENO1	0.87 ± 0.20	1.39	1.23 ± 0.16*	1.78*	1.36 ± 0.29	1.50	1.46 ± 0.22	1.41	1.35 ± 0.32	1.71*	1.22 ± 0.18	1.66	1.34 ± 0.31	1.59
LDH-A	0.93 ± 0.09	0.89	1.10 ± 0.11	1.10	1.05 ± 0.10	0.93	1.40 ± 0.17	1.71	1.31 ± 0.18	1.31	1.16 ± 0.11	1.19	1.28 ± 0.08	1.17
LDH-B	0.87 ± 0.03	0.67*	1.19 ± 0.12	0.80	1.04 ± 0.19	0.58*	1.64 ± 0.21	0.80	1.26 ± 0.11	0.62	1.21 ± 0.07	0.63*	0.89 ± 0.48	0.79*
OGDH	1.52 ± 0.06*	1.89*	1.13 ± 0.18	1.41	1.73 ± 0.34	1.68	1.32 ± 0.17	1.11	2.00 ± 0.31*	1.81	1.20 ± 0.13	1.40	1.62 ± 0.39	1.69

Figure 4: Effect of KDAC inhibition on enzyme activities in A549 cells under normoxia and hypoxia. A and B. The ATP- dependent 6-phosphofructokinase (PFK1) (**A**) and lactate dehydrogenase (LDH) (**B**) enzymatic activities were measured after 24 h of incubation, and activities were normalized to intracellular protein content in each condition. A549 cells were treated with 1 μM of TSA, 20 mM of NAM, and both 1 μM TSA and 20 mM NAM for 24 h of incubation under normoxia and hypoxia. Cells incubated in medium without KDACIs served as control. Bars represent the means ± standard error of the mean of three independent experiments. The asterisks above bars indicate statistically significant differences compared to normoxic control cells. The asterisks above curly brackets indicate statistically significant differences between hypoxic and normoxic treatments and between hypoxic treatments and hypoxic control cells. Statistical significance was assessed by a two-tailed Student's *t*-test. *, $p \leq 0.05$; **, $p \leq 0.01$; ***, $p \leq 0.001$. (**C**) Western blot images of HIF-1α and selected metabolic enzymes identified by iTRAQ. A549 cells were treated with 1 μM of TSA, 20 mM of NAM and both 1 μM TSA and 20 mM NAM for 24 h of incubation under normoxia and hypoxia. Cells incubated in medium without KDACIs served as control. Immunoblotting of hypoxia-inducible factor-1α (HIF-1α), glucose-6-phosphate isomerase (GPI), phosphofructokinase-1 (PFK1), fructose-bisphosphate aldolase C (ALDC), glyceraldehyde-3-phosphate dehydrogenase (GAPDH), alpha-enolase (ENO1),

lactate dehydrogenase A (LDH-A), lactate dehydrogenase B (LDH-B) and 2-oxoglutarate dehydrogenase (OGDH). β-actin was used as the loading control. (**D**) Densitometry analysis of selected metabolic enzymes shown in C. The ratios of the Western blot bands (WB ratios) of KDACI-treated cells to control cells under normoxia after normalization to β-actin. Densitometric values are presented as mean ± standard deviation. Asterisks indicate significant differences compared to untreated normoxic control cells assessed by two-tailed Student's *t*-test in WB ratios and R software package Isobar (iTRAQ ratios) *, $p \leq 0.05$; **, $p \leq 0.01$; ***, $p \leq 0.001$.

In the NAM treatment, the glycolytic enzymes PFK1 and alpha-enolase (ENO1) were significantly increased, together with TECR (Figures 3C and 4A). A similar pattern to the TSA treatment was also found in the TSA/NAM combined treatment (Figure 3C). Although in this case, enzymes involved in glutamine metabolism such as glutaminase 1 (GLS1) and ornithine aminotransferase (OAT) were significantly up-regulated. Additionally, SRM was again strongly down-regulated in the double treatment at similar levels than in the TSA treatment.

The Metabolic Changes Observed in KDAC Inhibition Are Enhanced under Hypoxia

As expected, in all the treatments under hypoxia, the HIF-1α factor appeared to be overexpressed compared to normoxia (Figure 4C). The KDAC inhibition under hypoxia showed a similar behavior to the one observed in normoxia, although the metabolic changes resulted in a larger magnitude (Figure 5A). Similarly, as the analysis performed in normoxic conditions, the GO enrichment analysis on biological processes showed that proteins related to the generation of energy and intracellular transport were significantly enriched when cells were treated with TSA, NAM, and both compounds under hypoxia (Figure 5B). In contrast, proteins involved in transcription and translation processes were down-regulated. The PIR keywords enrichment analysis also showed that 60–70% of the dysregulated proteins were acetylated or phosphorylated (Table S1).

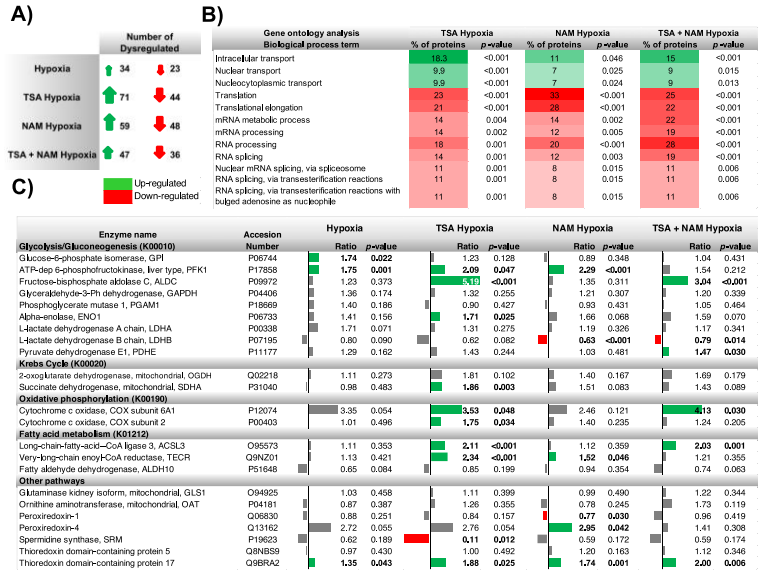

Figure 5: Effect of KDAC inhibition and hypoxia on the global proteome and metabolic enzymes compared to control A549 cells under normoxia. Quantitative proteomic analysis of differentially expressed proteins in A549 cells treated with 1 μM of TSA, 20 mM of NAM, and both 1 μM TSA and 20 mM NAM for 24 h under hypoxic conditions. (**A**) The number of up-regulated and down-regulated proteins (iTRAQ ratio < 1 and > 1, respectively) showing significant (p-value ≤ 0.05) differences between TSA, NAM, and TSA/NAM treatments under hypoxia with respect to control cells under normoxia. (**B**) GO enrichment analysis of the Biological process term for each condition shown as the percentage of proteins related to each process. All biological processes are shown as significantly (p-value ≤ 0.05) up-regulated or down-regulated. (**C**) Quantitative measurement of the main metabolic enzymes identified using the iTRAQ approach for the different conditions compared to untreated control cells under normoxia. Significantly up-regulated enzymes (iTRAQ ratio < 1 and p-value ≤ 0.05) are represented in green and significantly down-regulated enzymes (iTRAQ ratio > 1 and p-value ≤ 0.05) are represented in red. Non-significantly up-regulated and down-regulated enzymes are represented in gray.

Regarding the changes in the abundance of metabolic enzymes, the inhibition of TSA under hypoxia had similar effects as control cells under normoxia, although in this case, hypoxia elicited a different metabolic response affecting both glycolysis and mitochondrial respiration. Upon TSA treatment, glycolytic enzymes and mitochondrial enzymes such as succinate dehydrogenase complex subunit A (SDHA), which is part of the

mitochondrial respiratory complex II, and cytochrome c oxidase subunits 6A1 and 2 (COX6A1 and COX2) of mitochondrial complex IV were significantly up-regulated (Figures 4C,D and 5C). Fatty acid metabolism was also altered, and SRM was strongly down-regulated (Figure 5C). The sirtuin inhibition by NAM treatment under hypoxia showed few significant effects on metabolic enzymes. Similar to the TSA treatment, in the TSA/NAM double treatment under hypoxia, the levels of ALDC, pyruvate dehydrogenase subunit E1 (PDHE), COX6A1, and ACSL3 were significantly up-regulated, whereas LDH-B was significantly down-regulated (Figure 5C).

Furthermore, concerning the oxidative stress results reported above, the proteomic analysis showed the dysregulation of some enzymes related to the antioxidant defense system (Figures 3C and 5C). The expression of thioredoxin domain-containing protein 17 (TXNDC17) was significantly up-regulated in all the KDACI treatments except for TSA under normoxia. Thioredoxin domain-containing protein 5 (TXNDC5) was also up-regulated by TSA/NAM treatment under normoxia. In addition, the expression of peroxiredoxin -1 (PRDX1) and -4 (PRDX4) resulted altered upon NAM treatment and hypoxia.

Chemicals Targeting Proteins Affected by KDAC Inhibition under Hypoxia

Machine learning based on the integration of large-scale omics data is an emerging approach for identifying new therapeutic targets, new molecules, and repurposing existing drugs [42–44]. We applied this approach to our proteomic data to reveal which chemicals are known to target proteins revealed, in our study, affected by KDAC inhibition under hypoxia in *KRAS* mutated NSCLC A549 cells. We classified 500 chemicals according to their link to lung cancer and our network enriched in the following cell metabolism processes: ATP metabolic process (GO:0046034), oxidation–reduction process (GO:0055114), carbohydrate metabolic process (GO:0005975), lipid metabolic process (GO:0006629), and cellular protein metabolic process (GO:0044267). Chemicals with higher scores target our network more, while chemicals in lower ranks were more reported to

have a connection with lung cancer (especially MESH: D002282 pulmonary adenocarcinoma) in the literature, clinical trials, or clinical care. In Figure 6, we selected the top 70 chemicals targeting the protein dysregulation network when KDACi treatment favored A549 cell apoptosis (i.e., for combined KDACi (TSA and NAM) treatment in hypoxia conditions). Each chemical's score was higher than 100 confirming a substantial connection with our protein network and metabolic processes. Among the 70 chemicals that our machine learning approach proposed for targeting protein adaptation network of KDAC inhibitors (TSA and NAM) upon hypoxia, we found drugs used as anti-cancer agents for NSCLC and other cancers or known for some anti-cancer properties in NSCLC (such as metformin, gemcitabine, 5-Fluorouracil, paclitaxel, imatinib, doxorubincin, and tamoxifen) target similar protein network in KDAC inhibitors (TSA and NAM) under hypoxia and normoxia.

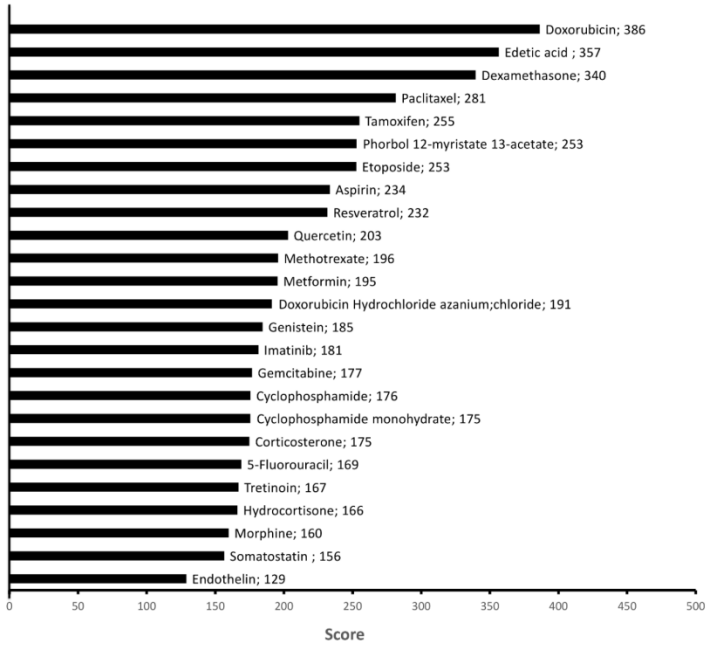

Figure 6: Classification of drugs targeting metabolic protein networks modulated by TSA and NAM in hypoxia conditions. The classification of chemicals is done through a deep machine learning according to their link to bronco-alveolar adenocarcinoma and cell metabolism processes (ATP metabolic process (GO:0046034), oxidation–reduction process (GO:0055114),

carbohydrate metabolic process (GO:0005975), lipid metabolic process (GO:0006629), and cellular protein metabolic process (GO:0044267)). Five hundred chemicals were classified. A high score symbolized a high link of the chemical with the cell metabolism process and our protein network. The classification presented here was obtained by extracting drugs obtained by our machine learning analysis in the top 70 rank of chemicals related to MESH: D002282 pulmonary adenocarcinoma with exclusion of chemicals/metabolites. The top 70 rank ensures a high link between the chemical and data reported on these chemicals in the literature in broncho-alveolar adenocarcinoma (MESH: D002282 pulmonary adenocarcinoma).

Discussion

In recent years, increasing evidence has demonstrated the involvement of acetylation in the metabolic reprogramming of cancer cells, which mediates tumorigenesis, tumor progression, and resistance to cancer therapies. The aberrant expression and activity of KDACs are postulated to be one of the drivers of this metabolic reprogramming [46].

KDACIs exhibit multiple antitumor activities, including tumor cell differentiation, growth arrest, autophagy, and apoptosis in various NSCLC cancer cell lines and tumor xenografts [33,34,47–49]. The activation of either the extrinsic or intrinsic apoptotic pathway is a key event involved in the antitumor activity of KDACIs, although many aspects of their mechanisms of action remain conflicting and unclear [50]. Consistent with previous studies, our results confirmed increased apoptosis and cell cycle arrest under the inhibition of KDAC activity in adenocarcinoma A549 cells [51–54]. Furthermore, a remarkable synergistic apoptotic response and cell cycle arrest were observed following the TSA and NAM combined treatment.

The inhibition of KDAC induces a general increase in the level of acetylated proteins [55]. The exposure of cells to KDACIs not only induces hyperacetylation of histones, which is typically associated with a general increase of transcriptional activity but also targets other proteins from different subcellular compartments that regulate the proteome through the transcriptome. Wu et al. reported that the increased acetylation level in A549 cells under suberoylanilide hydroxamic acid (SAHA) treatment is positively correlated with the down-

regulation of the global proteome expression level due to the crosstalk between acetylation and ubiquitination [56]. Indeed, protein acetylation and ubiquitination sites have now been considered cancer driver mechanisms per se [57]. In our study, proteins involved in the proteasome activity such as the proteasome activator complex subunits 1 and 2 (PSME1 and PSME2) and the ubiquitin-like modifier-activating enzyme 1 (UBA1) were significantly up-regulated under both TSA and NAM treatments, suggesting a higher protein degradation. On the other hand, both transcription and translation processes were down-regulated in KDACI treatments according to the DAVID functional annotation analysis. Therefore, both TSA and NAM treatments might cause general protein degradation in A549 cells, which also correlates with the low-proliferative phenotype reported here. Previous studies indicated that KDACs, especially KDAC6, play an essential role in protein quality control mechanisms [58]. Thus, the inhibition of KDAC to maintain proteostasis has been proposed to have therapeutic potential in cancer [59]. Indeed, several studies have demonstrated the potential therapeutic value of combining proteostasis regulators such as KDACIs and proteasome inhibitors in cancer [60,61].

Mitochondrial function and ROS production, have been reported to be altered during *KRAS*-driven malignant transformation [62–64]. KDACIs have also been shown to generate ROS in cancer [65–67]. The excessive production of ROS results in cellular oxidative damage and ultimately cell death [68]. For that reason, tumor cells usually have an enhanced antioxidant capacity to combat ROS. In addition to the classical antioxidant enzymes, thiol-containing redox enzymes such as the family of thioredoxins (TRXs) are also expressed in human lungs [69]. In our proteomic approach, we identified significant alterations in several enzymes involved in the antioxidant defense system. Interestingly, the expression of TXNDC17 has been recently associated with paclitaxel resistance in ovarian and colorectal cancer [70,71]. The activation of the antioxidant defense requires the coordinated action of a number of sirtuins that work together with ROS scavenging and generating pathways to maintain ROS homeostasis. Altogether, the iTRAQ results indicate that activation of ROS scavenging mechanisms, most likely in

response to increased ROS levels is involved in the KDAC inhibition response.

The inhibition of KDAC may increase the acetylation level of metabolic enzymes, thereby affecting their catalytic activity, substrate accessibility, or amount of enzyme [72]. Besides, fluctuations of acetyl-CoA levels due to the changes in protein acetylation can affect metabolic processes as acetyl-CoA is required for the TCA cycle and fatty acid biosynthesis [73]. The changes in the levels of metabolic enzymes found in the current study suggest a switch in the metabolic profile of A549 cells towards a higher capacity of mitochondrial OXPHOS. This metabolic change correlates with the proliferation rates and apoptotic cell death reported here and with the impaired antioxidant defense and increased ROS production, which was previously described in KDACIs treatment of *KRAS*-driven cancers [65–67].

As most cancer cell lines, NSCLC A549 cells tend to exhibit the Warburg effect by relying on both an enhanced glycolysis and production of lactate together with an enhanced mitochondrial metabolism relying on other sources such as glutamine [74,75]. In our analysis, inhibition of KDAC classes I, II, and IV showed a significant overexpression and increased activity of several glycolytic enzymes. However, this glycolytic response did not induce a proportional increase in lactate production, whereas LDH-B was down-regulated. Therefore, the conversion from pyruvate and lactate seems to be impaired by TSA, which implies that the inhibition of Zn^{2+}-dependent KDAC classes could compromise not only the Warburg effect but also other cancer metabolic adaptations related to LDH-B such as mTOR hyperactivation or lysosome acidification and autophagy [76,77]. Furthermore, the higher levels of TCA cycle enzymes are consistent with the hypothesis that a low lactate production would favor oxidation of pyruvate from glycolysis to acetyl-CoA for entry into the TCA cycle under TSA treatment. Furthermore, the up-regulation of ACSL3, which has recently demonstrated to be essential for tumorigenesis in *KRAS*-driven lung cancer [78,79], may also be involved in activating mitochondrial respiration from fatty acids. On the other hand, sirtuin inhibition

exhibited a lower effect on metabolic enzymes than the other classes of KDAC inhibition, where it seems that only the glycolytic pathway was affected. Although the up-regulation of PFK1 and ENO1, the observed net decrease of glucose uptake and lactate production supports the hypothesis that NAM treatment may inhibit glycolysis most likely by the inactivation of the AMPK/SIRT1 pathway, impairing the Warburg effect even more than TSA treatment. AMPK plays a critical role in stimulating glucose uptake, and the link between AMPK and SIRT1 has been described in various studies [23,80,81]. Some of the metabolic changes observed in TSA or NAM treatment alone were particularly acute in the double treatment, suggesting that the effect of targeting both Zn^{2+}-dependent KDAC classes and sirtuins on metabolic enzymes was stronger than only inhibiting Zn^{2+}-dependent KDAC classes.

The up-regulation of glycolytic enzymes in cancer cells under hypoxic conditions were consistent with previous comparative proteomic studies [38–40]. However, while a switch from OXPHOS to glycolysis for ATP production is considered a major cancer cell adaptation to hypoxia, it has been suggested as well that low oxygen concentration in hypoxic regions of tumors may not be limiting OXPHOS [82–84]. Thus, A549 cells under hypoxia may still retain the function of OXPHOS to generate ATP. Our study confirmed the overexpression of HIF-1α among all the treatments except TSA single treatments whose expression was down-regulated. It has been previously demonstrated that KDACIs such as TSA can degrade HIF-1α stimulated by hypoxia with variable efficiency in different tumor cell lines [84]. Interestingly, we found increased iTRAQ ratios of TCA cycle enzymes under KDAC classes I/II and IV inhibition in hypoxia compared with normoxia. Since the mitochondrial function is usually attenuated in response to HIF-1α and hypoxia, we assume that A549 cells may activate mitochondrial metabolism as an adaptive response to KDACIs. This is supported by the fact that TSA treatments repressed the induction of HIF-1α, probably allowing mitochondrial respiration. In contrast, we suggest that sirtuin inhibition may enhance HIF-1α response, which agrees with the activation of HIF-1α through acetylation by SIRT1 [86–88]. Therefore, the

metabolic adaptation of cancer cells to hypoxia could be less affected by NAM treatment than by TSA treatment. Finally, the TSA and NAM double treatment under hypoxia might cause a controversial scenario where HIF-1α may be stimulated and repressed simultaneously at different levels. Interestingly, we found LDH-B significantly down-regulated, while pyruvate dehydrogenase (PDHE) resulted significantly up-regulated. Such evidence confirms our precedent interpretation where residual production and release of lactate is enough to maintain an increased glycolytic flux, meanwhile it allows the entry of pyruvate in the TCA cycle under KDAC inhibition and hypoxia, thus equally impairing the Warburg effect as in normoxia. In addition, COX2 and COX6A1 were highly probably increased to enhance OXPHOS and ROS level, even though the limited oxygen availability.

Our machine learning analysis revealed a list of chemotherapeutic agents, including doxorubicin, paclitaxel, etoposide, tamoxifen, bortezomib, 5-fluorouracil, methotrexate, imatinib, gemcitabine, and metformin that may target proteins affected by KDAC inhibition under hypoxia in *KRAS* mutated NSCLC A549 cells.

Doxorubicin induces cell death by regulating oxidative stress mediated through the formation of mitochondrial ROS [89–91]. In contrast, paclitaxel and etoposide trigger cell death by engaging the intrinsic mitochondrial pathway of apoptosis [92]. Tamoxifen is a selective estrogen receptor (ER) modulator used as a hormonal therapeutic agent to treat ER-positive breast cancer. Several ER-independent mechanisms that modulate metabolic pathways have been reported; for example, an AMPK activation induced by tamoxifen through inhibition of mitochondrial complex I leading to a glycolysis activation, alteration of fatty acid metabolism, and inhibition of the mTOR pathway and translation [93]. In ER-positive NSCLC, tamoxifen was found to play a negative role in the growth of ER-positive NSCLC alone [94] or used as an adjuvant EGFR-TKI treatment [95,96].

It should be noted that previous studies have demonstrated that hypoxia protects tumor cells from apoptosis induced by chemotherapeutic agents. For instance, it leads chemoresistance to doxorubicin and tamoxifen in NSCLC cells, including A549 cells, through the HIF pathway [20,97], thus limiting chances of successful treatment. However, hypoxia may have no effect on apoptosis triggered by etoposide in A549 cells, suggesting a cell type-specific effect to trigger apoptosis under hypoxia by different chemotherapeutic agents [98].

Bortezomib is a protease inhibitor currently approved to treat multiple myeloma and mantle cell lymphoma that has been studied in preclinical and clinical settings of lung cancer, showing potential benefit in combination therapies [99].
Our analysis also identified therapeutic agents that interfere with DNA synthesis, such as nucleoside analogs 5-fluorouracil and gemcitabine, and the nucleotide biosynthesis inhibitor methotrexate. Gemcitabine has been used to treat NSCLC, either in combination with cisplatin or carboplatin or as a single drug adjuvant treatment. By contrast, 5-fluorouracil and methotrexate have shown limited therapeutic benefit in NSCLC [100].

Imatinib is a TKI with clinical activity in the treatment of chronic myeloid leukemia and gastrointestinal stromal tumors [101]. In lung cancer models, several studies have shown that imatinib has indirect antitumor activity through the inhibitory effects on lung cancer-associated fibroblasts [102–104]. Interestingly, imatinib resistance can be mediated by a metabolic shift characterized by an up-regulation of OXPHOS but also in part by HIF1α-dependent up-regulation of glycolysis [105–108]. Therefore, the use of OXPHOS inhibitors may reverse imatinib resistance.

The standard antidiabetic agent metformin has already been investigated for NSCLC repositioning drugs in clinical trials for non-diabetic NSCLC treatment patients [ClinicalTrial.gov identifier: NCT02285855] as it decreases lung cancer incidence and mortality [108]. It also improved the progression-free survival of diabetic patients chemoradiotherapy for NSCLC [110]. Metformin has been reported to sensitize EGFR-TKI–

resistant NSCLC through the inhibition of IL-6 or AMP-activated kinase signaling [111,112] and increase the radiosensitivity of NSCLC through ATM and AMPK [113]. In addition to its repressive effects on IGF-1R and PI3K/AKT/mTOR pathways, inhibition of tumor angiogenesis, aerobic glycolysis, DNA repair, activation of the antitumoral immunity, metformin showed benefic effects on cancer cells by inhibiting mitochondrial complex I and lipid/protein synthesis, regulating glycolysis, glucose level uptake and insulin/insulin-like growth factor signaling availability for tumor cells.

Additionally, synergistic antitumor interactions of KDAC inhibitors with the proposed drugs have been identified in different cancer types, including NSCLC, representing novel approaches potentially exploitable in therapy [114–116]. The anti-cancer properties in NSCLC treatments, their role in metabolic reprogramming, and the synergistic effects with KDAC inhibitors of these chemical agents support the purpose of considering the drugs proposed by our machine learning approach for targeting metabolic reprogramming of *KRAS*-mutated NSCLC treatment upon hypoxia conditions.

In our study, we comprehensively investigated the regulation of metabolic enzymes of the NSCLC A549 cell line under the effects of the KDAC inhibitors (TSA and NAM) in normoxic and hypoxic conditions by using an iTRAQ-based quantitative proteomic approach. A549 cells, which present mutation in *KRAS* and display the Warburg phenotype, are resistant to current lung cancer therapies. Besides the low proliferation behavior under KDAC inhibition, we found altered expression patterns in metabolic enzymes, which were exacerbated by hypoxia (Figure 7). This allowed profiling the metabolic heterogeneity of the NSCLC A549 cell line according to the oxygen level. Under KDAC classes I/II and IV inhibition, we observed that A549 cells stimulate oxidative metabolism and oxidative stress while glycolysis is increased, but lactate production is decreased. Sirtuin inhibition impaired both glucose uptake and lactate production, although the up-regulation of some glycolytic enzymes.

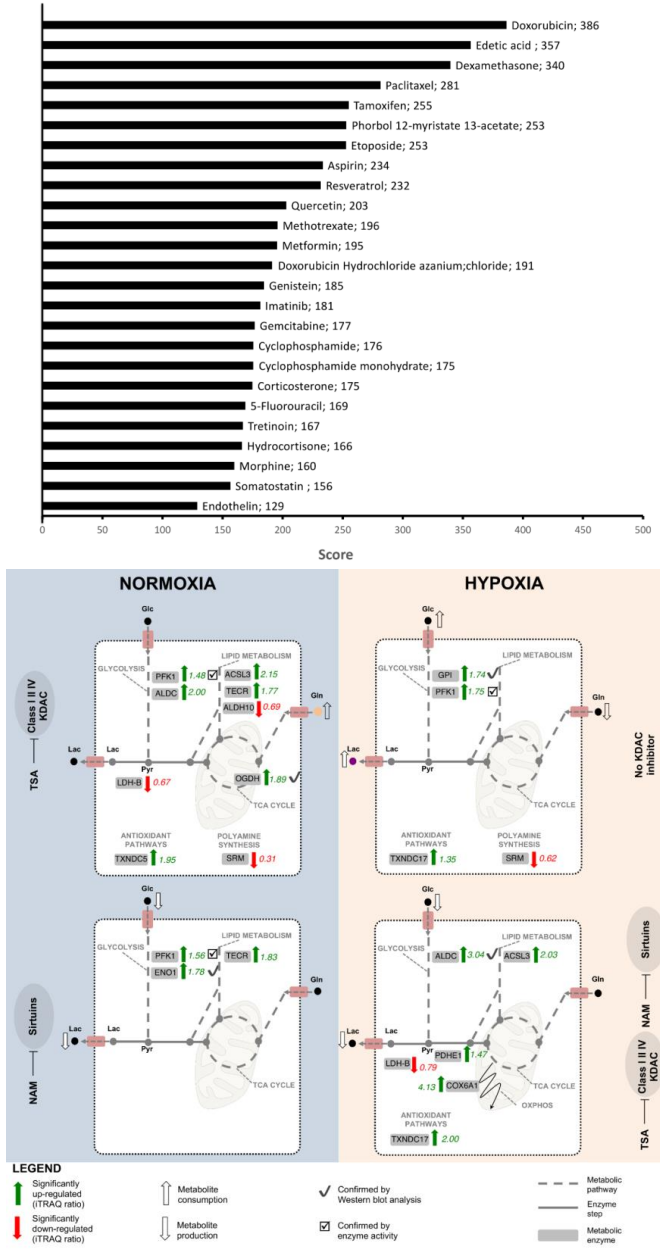

Figure 7: Schematic representation of the dysregulation of metabolic enzymes triggered by TSA and NAM under normoxia and hypoxia in A549 cells.

Metabolic pathways are represented with dysregulated enzymes quantified by iTRAQ. Significantly up-regulated enzymes (iTRAQ ratio < 1 and *p*-value ≤ 0.05) are represented by green arrows. Significantly down-regulated enzymes (iTRAQ ratio > 1 and a *p*-value ≤ 0.05) are represented by red arrows. Non-significantly dysregulated enzymes are represented by grey arrows. Metabolic dysregulations confirmed by enzyme activities and Western blot analyses are represented by check box and check marks, respectively. Downward and upward white arrows indicate significant changes in metabolite consumption and production rates. (**A**) Metabolic enzyme profile in A549 cells under inhibition of classes I/II/IV KDAC by 1 μM of TSA for 24 h incubation under normoxic conditions. (**B**) Metabolic enzymes regulation in A549 cells under sirtuin inhibition by 20 mM NAM for 24 h incubation under normoxic conditions. (**C**) Metabolic enzymes regulation in A549 cells under hypoxic conditions for 24 h incubation. D. Metabolic enzymes regulation in A549 cells under inhibition of both classes I/II/IV KDAC and sirtuins by 1 μM TSA and 20 mM NAM for 24 h incubation under hypoxic conditions. AcCoA: Acetyl-CoA; ACSL3: Long-chain-fatty-acid-CoA ligase 3; ALDC: Fructose-bisphosphate aldolase C; ALDH10: Fatty aldehyde dehydrogenase; COX6A1: Cytochrome c oxidase subunit 6A1; ENO1: Alpha-enolase; Glc: Glucose; Gln: Glutamine; KDAC: Lysine deacetylases; Lac: Lactate; LDH-B: Lactate dehydrogenase B; NAM: Nicotinamide; OGDH: 2-oxoglutarate dehydrogenase, mitochondrial; OXPHOS: Oxidative Phosphorylation; Pyr: Pyruvate; PDHE: Pyruvate dehydrogenase E1; PFK1: ATP-dependent 6-phosphofructokinase 1, liver type; Pyr: Pyruvate; SIRT: Sirtuins; SRM: Spermidine synthase; TCA: tricarboxylic acid; TECR: Very-long-chain enoyl-CoA reductase; TSA: Trichostatin A; TXNDC17: Thioredoxin domain-containing protein 17; TXNDC5: Thioredoxin domain-containing protein Our machine learning analysis revealed a list of chemotherapeutic agents, including doxorubicin, paclitaxel, etoposide, tamoxifen, bortezomib, 5-fluorouracil, methotrexate, imatinib, gemcitabine and metformin that may target proteins affected by KDAC inhibition under hypoxia in *KRAS* mutated NSCLC A549 cells.

Therefore, we propose the inhibition of both KDAC classes I/II/IV and sirtuins as a valid strategy to explore cancer metabolic reprogramming, as their inhibition provides new insights into the metabolic adaptations of the A549 cell line that may help design new and more effective therapies. Moreover, our machine learning approach revealed which chemicals may target the metabolic adaptations observed by KDAC inhibition under hypoxia when apoptosis was favored. These chemicals should be further explored to evaluate the therapeutic efficacy in *KRAS* mutated NSCLC under hypoxia conditions Although this study brings new insights to elucidate the effects of hypoxic response upon KDACi treatments on metabolic reprogramming, it is important to mention that the present study did not assess

whether wild-type *KRAS* cells undergo distinct metabolic reprogramming events upon KDAC inhibition. Thus, we certainly cannot claim that the metabolic reprogramming observed in the study is a common response among *KRAS* mutant NSCLC cells and differs from wild-type *KRAS* NSCLC cells. Further studies involving wild-type and *KRAS* mutant NSCLC cells might help understand the impact of *KRAS* mutation on the metabolic reprogramming upon KDAC inhibition.

Materials and Methods

Cell Culture

Human lung adenocarcinoma epithelial cell line A549 was obtained from American Type Culture Collection and cultured in Dulbecco's modified Eagle's medium (DMEM; Gibco) containing 10 mM glucose, 10% fetal bovine serum (Gibco 10270), 0.5% penicillin (50 U mL^{-1}) and streptomycin (50 µg mL^{-1}). Cells were seeded and incubated for 24 h at 37 °C in a humidified 5% CO_2 incubator. After 24 h, A549 cells were treated with $^{24\ h}IC_{20}$ concentrations of 1 µM TSA (Sigma-Aldrich), 20 mM NAM (Sigma-Aldrich) and its combination (1 µM TSA and 20 mM NAM). A549 cells were either maintained in normoxia or placed into hypoxia for 24 h of treatment. Cells incubated in medium without KDACIs served as control. Hypoxia was achieved by placing cells in a Whitley H35 Hypoxystation (Don Whitley Scientific, UK) hypoxic incubator flushed with 5% CO_2 and 95% N_2 until the O_2 content reached 1%.

Cell Viability Assay

Viability tests of both KDACIs (TSA and NAM) were performed at 24 h to determine the respective $^{24\ h}IC_{50}$ values (Figure S1). A549 cells were cultured on 96-well plates in the aforementioned culture conditions, adding TSA or NAM at different concentrations in six replicates for 24 h. The cell viability was determined by the MTT colorimetric assay [117] after 1 h of incubation with 0.5 mg mL^{-1} of MTT.

Cell Proliferation Assay

A549 cells were seeded in 6-well plates at the density of 6×10^3 cells mL^{-1}. Once cells were attached, they were treated with 1 µM TSA, 20 mM NAM separately and in combination under both normoxia and hypoxia for 24 h and 48 h. Untreated cells cultured under both normoxia and hypoxia were used as controls. After the incubations, cells were washed with PBS, trypsinized, centrifuged and resuspended in PBS. Cell proliferation was determined by direct cell counting with Scepter™ 2.0 Handheld Automated Cell Counter (Millipore, Burlington, MA, USA).

Apoptosis Assay

Apoptosis was tested by fluorescence-activated cell sorting (FACS) analysis using Annexin V and propidium iodide (PI) staining to differentiate non-apoptotic cells (Annexin V^-, PI^-) and late apoptotic/necrotic cells (Annexin V^+, PI^+) from early apoptotic cells (Annexin V^+, PI^-) [117]. A549 cells were seeded in 6-well plates at the density of 6 x 10^3 cells mL^{-1} and treated as described above. After the incubation, cells were trypsinized, centrifuged and resuspended in binding buffer (10 mM HEPES/NaOH, pH 7.4, 140 mM NaCl and 2.5 mM $CaCl_2$). Annexin V conjugated to fluorescein isothiocyanate (FITC) was added to each sample and incubated for 30 min in darkness. Following PI addition, cells were analyzed by a flow cytometer (Gallios, Beckman Coulter, Brea, CA, USA) using FlowJo software.

Cell Cycle Analysis

Cell cycle analysis was assayed by flow cytometry using FACS after treatments described above. Following 24 h of incubation, adherent cells were collected by centrifugation after trypsinization, washed with PBS, resuspended in 0.5 mL of PBS and fixed by dropwise addition of 4.5 mL ice-cold 70% (v/v) ethanol. Cells were fixed for at least 4 h at −20 °C. Then, cells were centrifuged, washed with ice-cold PBS and incubated in PBS containing 50 µg mL^{-1} propidium iodide (PI, Sigma–Aldrich), 20 µg mL^{-1} DNase-free RNase A (Roche) for 1 h at

room temperature. FACS analysis was carried out in a flow cytometer (Gallios, Beckman Coulter, Brea, CA, USA) and data were analyzed using FlowJo software.

Measurement of Extracellular Metabolites

The concentration of glucose, glutamine, and lactate in media was determined spectrophotometrically [118–120]. The media were collected at the beginning and end of incubations and measured using a Cobas Mira Plus chemistry analyzer (Horiba ABX, Montpellier, France) by monitoring the production of NADPH in the specific reactions at 340 nm. Glucose concentration was measured using the hexokinase (HK) and glucose-6-phosphate dehydrogenase (G6PDH) coupled enzymatic reactions (ABX PentraTM Glucose HK CP; A11A01667). Lactate concentration was determined based on the lactate dehydrogenase (LDH) reaction. Glutamine concentration was measured by means of the conversion of glutamate via the glutaminase (GLS) reaction and glutamate, in turn, was determined using the glutamate dehydrogenase reaction. The metabolite consumption/production rates were normalized according to the cell proliferation. Metabolite concentrations were expressed as $\mu mol\ mL^{-1} \times 10^6$ cells h^{-1}.

Determination of Intracellular ROS levels

Total intracellular reactive oxygen species (ROS) levels were determined using flow cytometry after treatments with TSA (1 μM) and NAM (20 mM) alone or in combination using 2′-7′-dichlorodihydrofluorescein diacetate (H_2DCFDA, Invitrogen) probe. A549 cells were incubated with 5 μM H_2DCFA in PBS supplemented with 5.5 mM glucose for 30 min at 37 °C. Next, PBS was replaced with DMEM supplemented with 10% FBS and incubated for 45 min at 37 °C. After incubation, cells were trypsinized and resuspended in a solution consisted of 50 mM H_2DCFDA with 20 μg ml^{-1} propidium iodide (PI, Sigma–Aldrich) for flow cytometry analysis (Cyan ADP analyzer, Dako Cytomation, Agilent Technologies, Santa Clara, CA, USA). Cells positive only for PI were considered as necrotic and

excluded from the analysis. Data analysis was performed using FlowJo software.

Proteomic Analysis

The overall workflow of our quantitative proteomic approach for the study is illustrated in Figure 8. Briefly, our approach included a filter-aided sample preparation (FASP) step prior iTRAQ labeling of peptides, followed by a two-step fractionation of labeled peptides (OFFGEL IEF/RP-nano-LC), MALDI-MS/MS analysis, database search and quantitative iTRAQ analysis as already published [122,123].

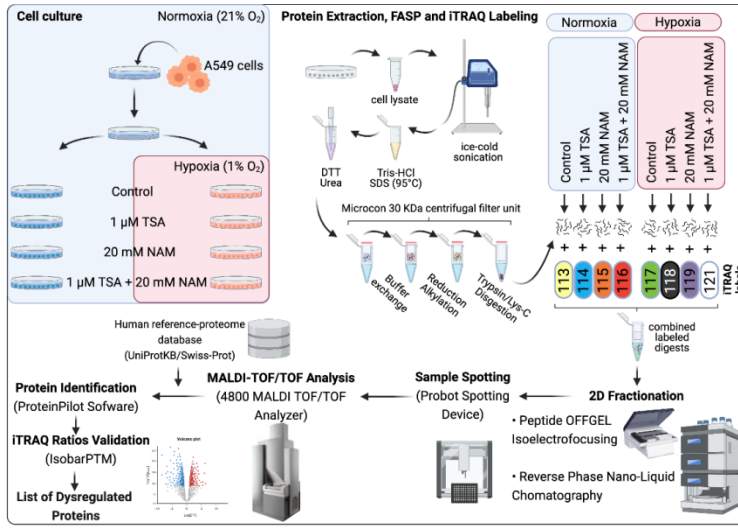

Figure 8: Schematic workflow of the proteomic approach used in the present study. A549 cells were treated with 1 µM of TSA, 20 mM of NAM and both 1 µM TSA and 20 mM NAM for 24 h under normoxia and hypoxia. Cells incubated in medium without KDACIs served as control. Cell lysates were processed according to the filter-aided sample preparation (FASP) protocol. Digested peptides of each treatment group were labeled with iTRAQ tags and separated in a 2-step fractionation. Fraction peptides were spotted on MALDI plates using a spotting system. Mass spectrometer 4800 MALDI TOF/TOF analyzer was used to collect MS and MS/MS data for identify and quantify proteins. iTRAQ ratios were quantified and validated. Proteins with iTRAQ ratios <1 and a p-value ≤ 0.05 were considered to be significantly increased whereas proteins with iTRAQ ratios >1 and a p-value ≤ 0.05 were considered to be significantly decreased.

Filter-Aided Sample Preparation for iTRAQ Quantitation

Following 24 h of treatment, A549 cells were washed twice with PBS, frozen in liquid nitrogen and stored at -80 °C. For protein extraction, cells were scraped off the plates and incubated for 10 min at 4 °C using lysis buffer (0.1 M Tris-HCl pH 7.5 and 4% sodium dodecyl sulfate) containing protease inhibitors (1X Halt Protease Inhibitor Cocktail, Thermo Scientific), phosphatase inhibitors (1X Phosphatase Inhibitor Cocktail, Sigma-Aldrich) and KDACIs (2.5 µM TSA and 20 mM NAM). Lysates were sonicated at 4 °C and centrifuged at 14,000× g for 10 min at room temperature. Protein concentration was determined using the bicinchoninic acid (BCA) method (Thermo Fisher Scientific) according to the manufacturer's instructions. An equal amount of protein for each condition (1 mg) was digested using a filter-aided sample preparation (FASP) protocol [124] modified for iTRAQ-OFFGEL-LC-MS/MS analysis as proposed by Campone, *et al.* [125]. Briefly, protein samples were boiled for 5 min at 95 °C with 0.1 M dithiothreitol (DTT) in the lysis buffer described previously. Then, the buffer was changed to 8 M urea in 0.1 M Tris-HCl pH 8.5 using a Microcon® 30 kDa filter (Millipore). Samples were incubated with 12 mM of methylmethanethiosulfate (MMTS) for 30 min at room temperature. Afterwards, the buffer was changed to 0.5 M triethylammonium bicarbonate (TEAB) pH 8. Digestion was performed in the same filter device using trypsin/lysine C mix (Promega) in a 1:40 (w/w) protease-to-protein ratio and incubated on a shaker for 16 h at 37 °C. Peptides eluted after digestion on the filter device were purified and desalted using Pierce® C-18 Spin Columns (Thermo-Scientific) according to the manufacturer's instructions. Peptides were washed with 1% acetonitrile (ACN), 0.1% trifluoroacetic acid (TFA) and eluted with 80% ACN and 0.1% TFA in HPLC grade water before vacuum-drying samples using a Speed-vac (Eppendorf, Hamburg, Germany). The amount of peptides was measured using the BCA method at appropriate dilutions.

iTRAQ Labeling

The use of iTRAQ allows to differentially quantify the proteins from each sample in the mass spectrometry analysis [126]. Samples were labeled using the 8-plex iTRAQ Reagent Kit (Sciex, Les Ulis, France) following the manufacturer's instructions. Equal amounts (100 µg) of peptides from each sample were labeled with each iTRAQ reagent as follows: The iTRAQ reporter ions of *m/z* 113.1 for control cells in normoxia, the *m/z* 114.1 for TSA treated cells in normoxia, the *m/z* 115.1 for NAM treated cells in normoxia, the *m/z* 116.1 for TSA/NAM double-treated cells in normoxia, the *m/z* 117.1 for control cells in hypoxia, the *m/z* 118.1 for TSA treated cells in hypoxia, the *m/z* 119.1 for NAM treated cells in hypoxia and the *m/z* 121.1 for double-treated cells in hypoxia. Then, all the samples were pooled, and the labeling reaction was stopped by evaporation in a vacuum concentrator before the 2D fractionation.

Two-dimensional (2D) fractionation: Peptide OFFGEL Isoelectrofocusing and Reversed Phase Nano-liquid Chromatography

Peptide fractionation was performed in two dimensions: OFFGEL isoelectrofocusing for pI-based peptide separation followed with reverse phase nano-liquid chromatography (RP-nano-LC) for further separation based on peptide hydrophobicity. The peptide OFFGEL fractionation was performed on a 3100 OFFGEL Fractionator using the 24-well OFFGEL Kit linear pH 3–10 (Agilent Technologies, Les Ulis, France) according to the manufacturer's instructions. The pooled samples (containing in total 800 µg of peptides) were resuspended in 3.6 mL of focusing OFFGEL buffer and loaded in each of the 24 wells. The IPG gel strip was rehydrated and 150 µL of sample was loaded into each well. Peptides were focused with a maximum voltage of 8000 V, 50 µA, and 200 W until 50 kVh was reached. Afterwards, the 24 fractions were collected into individual tubes, dried in a vacuum concentrator and stored at −20 °C. Previous to the RP-nano-LC fractionation, OFFGEL fractions were purified and desalted using C18 ZipTip® columns (Merck Millipore, Molsheim, France),

vacuum-dried and then resuspended in 2% (v/v) ACN and 0.05% (v/v) TFA loading buffer. The peptides were separated according to their hydrophobicity on Ultimate 3000 nano-HPLC system controlled by Chromeleon 7 software (Dionex/Thermo Scientific, The Netherlands). For each sample, peptides were trapped on a µ-Precolumn (300 µm i.d. x 5 mm, C18 PepMap100, 5 µm, 100 Å pore size; Thermo Scientific) in 2% (v/v) ACN and 0.05% (v/v) at a flow rate of 20 µL min^{-1} for 3 min. Afterwards, peptides were separated in the reversed phase nano-HPLC column (Acclaim PepMap300 75 µm, 15 cm, nanoViper C18, 2 µm, 100 Å pore size; Thermo Scientific) in a binary gradient of buffer A (0.05% (v/v) TFA) and buffer B (80% (v/v) ACN and 0.05% (v/v) TFA) at a flow rate of 0.3 µL min^{-1}. The entire run last for 60 min and the nano-LC gradient was performed during 5–40 min (5–35 min, 12–46% of buffer B; 35–40 min, 46–62% of buffer B). Finally, the column was washed with buffer B at 40 min (62–94%), 40–50 min (94%) and re-equilibrated at 50 min (94–4%). The nano-HPLC eluted peptides of each OFFGEL fraction were spotted by a PROBOT MALDI spotting device controlled by the µCarrier 2.0 software (Dionex/Thermo Scientific/LC Packings, The Netherlands) onto a MALDI sample plate, with a spot collection time of 15 s resulting in 200 spots per fraction. Samples were spotted on MALDI plates in duplicates. The matrix (α-Cyano-4-hydroxycinnamic acid, HCCA, 2 mg mL^{-1} in 70% ACN and 0.1% TFA) was continuously added at a dosage speed of 0.9 µL min^{-1}.

MALDI-TOF/TOF Analysis

RP-nano-LC-MS/MS analysis of spotted peptides was performed by using a 4800 MALDI-TOF/TOF mass spectrometer (Sciex, Les Ulis, France) controlled by the 4000 Series Data Explorer software (V.3.5.3, Sciex, Les Ulis, France). The mass spectrometer was operated in positive ion reflector mode externally calibrated by using the Peptide Calibration Standard II (Bruker Daltonics, Champs sur Marne, France) with 50 ppm of mass tolerance. Each spectrum was recorded in the mass range of 700–4000 *m/z*. Up to 40 of the most intense ions per spot characterized by a signal/noise ratio ≥ 40 were considered for

MS/MS analysis. Selected ions for MS/MS analysis were activated using CID (collision-induced dissociation) activation mode.

Database Search and Quantitative iTRAQ Analysis

MS and MS/MS raw data were processed using ProteinPilot software (version 4.5, Sciex, Les Ulis, France) with the Paragon Algorithm (Sciex, Les Ulis, France). The analysis was performed using the human reference-proteome database UniProtKB/Swiss-Prot (release 2015_06; 20,206 protein entries; European Bioinformatics Institute, Hinxton, United Kingdom). After the identification and quantification of peptides, a statistical analysis with the R software package Isobar [127] was used to relatively quantify the levels of proteins present in the different conditions. Only proteins with high confidence identification (≥95% of peptide confidence level), positive "used score" of 1 and global False Discovery Rate (FDR) cutoff of 1%, were considered for the Isobar analysis. iTRAQ ratios and *p*-values were calculated by Isobar estimating both technical and biological variability using a Cauchy distribution. iTRAQ ratios of the different treatments were normalized to the control cells under normoxia (114:113; 115:113; 116:113; 117:113; 118:113; 119:113; 121:113). The level of proteins with iTRAQ ratios <1 and a *p*-value ≤ 0.05 was considered to be significantly increased whereas the level of proteins with iTRAQ ratios >1 and a *p*-value ≤ 0.05 was considered to be significantly decreased.

Gene Ontology Enrichment Analysis

The Database for Annotation, Visualization, and Integrated Discovery was used to explore the functional annotation of significantly dysregulated proteins. The corresponding UniProtKB accession numbers of these proteins were imported into the Gene Functional Annotation Tool of DAVID bioinformatics resources v6.7 (https://david.ncifcrf.gov/) [128,129]. The human genome was set as background. The functional category Protein Information Resource (PIR) Keywords and the Biological Process (BP) term were taken into consideration.

Western Blot Analysis

Equal amounts of protein lysates (35 μg) were separated by 12% SDS polyacrylamide gel electrophoresis (SDS-PAGE) and transferred to a nitrocellulose membrane (0.45 μm pore size, Bio-Rad) in transfer buffer (25 mM Tris-HCl, 192 mM glycine and 20% (v/v) ethanol) using the Mini Trans-Blot Electrophoretic Transfer Cell (Bio-Rad) at 45 V for 2 h. Membranes were blocked with PBS-0.1% (w/v) Tween 20 containing 5% (w/v) nonfat dry milk for 1 h at room temperature. Primary and secondary antibodies were diluted in the same solution. After primary and secondary antibody incubations, the blots were washed three times with PBS-0.1% (w/v) Tween 20. Membranes were blotted with primary antibodies overnight at 4 °C. Primary antibodies used include rabbit anti-β-actin (PA1-183, Thermo Fisher Scientific, 1:500), rabbit anti-PGI (SAB 2100894, Sigma-Aldrich, 1:500), rabbit anti-PFK1 (AB170868, Abcam, 1:1000), rabbit anti-ALDC (PA5-27659, Thermo Fisher Scientific, 1:500), rabbit anti-GAPDH (SAB 2100894, Sigma-Aldrich, 1:500), rabbit anti-ENO1 (PA5-29660, Thermo Fisher Scientific, 1:500), rabbit anti-LDH-A (SAB 1100050, Sigma-Aldrich, 1:500) and rabbit anti-LDH-B (PA5-27505, Thermo Fisher Scientific, 1:500), rabbit anti-OGDH (PA5-28195, Thermo Fisher Scientific, 1:1000) and anti-HIF1α (clone 28B, sc-13515, Santa Cruz Biotechnology, 1:200). HRP labeled anti-mouse IgG (A8924, Sigma- Aldrich, 1:3000) and anti-rabbit IgG (7074, Cell signaling, 1:2000) were used as secondary antibodies. Horseradish peroxidase (HRP) activity was assessed with the Clarity Western ECL substrate (Bio-Rad Laboratories, Inc.) and visualized with ChemidocTM XRS+ system (Bio-Rad Laboratories, Inc.), except for HIF-1α, which was analyzed by film detection of chemiluminescence. The levels of proteins were normalized and relatively quantified according to β-actin levels in at least three independent experiments. Western blot ratios (WB ratios) of the different metabolic enzymes amongst treatments were normalized to untreated A549 control cells under normoxia. Image analysis and quantification by densitometric scanning of replicate blots were performed using

Image LabTM software (version 4.1, Bio-Rad Laboratories, Hercules, CA, USA).

Enzyme Activities

A549 cells were rinsed with ice-cold PBS and scraped with lysis buffer 20 mM Tris-HCl pH 7.5 containing 1 mM DTT, 1 mM EDTA, 0.2% (v/v) Triton, 0.02% (v/v) sodium deoxycholate and supplemented with a protease inhibitor cocktail (Sigma-Aldrich). Cell lysates were disrupted by sonication using a titanium probe (Vibra-Cell^{TM}, Sonics & Materials, Newtown, CO, USA) and immediately centrifuged at 12,000× *g* for 20 min at 4 ºC. The supernatant was used for the determination of specific LDH and PFK-1 enzyme activities using a Cobas Mira Plus chemistry analyzer (Roche) in two independent experiments performed in triplicate. LDH activity in the forward reaction was measured in 100 mM KH_2PO_4/K_2HPO_4 (pH 7.4) containing 0.2 mM pyruvate and 0.2 mM NADH, and the mixture was incubated at 37 ºC. PKF1 activity was measured in 62.5 mM Tris-HCl (pH 8.0) containing 94 mM KCl, 1.85 mM DTT, 0.24 mM ATP, 0.60 mM $MgSO_4$, 0.24 mM fructose-6-phosphate, 43.2 U mL^{-1} aldolase, 15.6 U mL^{-1} triosephosphate isomerase and 2.4 U mL^{-1} glyceraldehyde 3-phosphate dehydrogenase. The mixture was incubated at 37 ºC. The enzyme activities were normalized by protein content using BCA method (Thermo Fisher Scientific). Enzyme activities are expressed as milliunits per milligram (mU mg^{-1}) of protein.

Network Analysis by Node Embeddings

Protein-protein interaction signaling networks were modelized throughout Reckonect process based on the machine learning algorithm node2vec [130]. This process produces for each protein of the network a vector in an embedding space. These vectors can be compared via a cosine distance to predict their proximity. To predict the proximity between two groups of proteins, we sum of the cosine distance (exceeding a threshold set at 0.5 in this article) in the cosine similarity matrix of the nodes embedding of all proteins of the 2 groups. We model a disease (or a chemical) through proteins co-cited with the disease

(or the chemical) in the scientific literature (bioassays and scientific articles). The more a protein is co-cited with the disease (or the chemical), more important its embedding vector will have in the representation of the disease (or the chemical). Finally, the proximity of a group of proteins and a disease (or chemical) can be predicted by comparing the embedding vectors of the protein group to the embedding vectors of the proteins co-cited in the literature with the disease (or the chemical) by considering the number of co-citations has a weight of the vectors.

Altogether, this machine learning method produces a proximity score that we used to rank therapeutic candidates. It should be distinguished from restricted enrichment methodologies. Noteworthy, it uses the recurrence frequency of therapeutic association with proteins, and learns a model in an unsupervised dependent manner. As a machine learning method, it relies on previously described statistical methods [130].

This process uses several databases of protein-protein interactions as well as databases of relationships between chemicals, diseases, biological processes and proteins. (ChEMBL [130], PubChem [132], PUBMED/MEDLINE, CTD [133], DGIdb [134], SIGNOR [135], UniProt [136], BioGRID [137], Complex Portal [138], IntAct [139], mentha [140], MINT [141], Reactome [142], and STRING [143]).

In our analysis, we took into account only proteins extracted by proteomic analysis that are involved in cell metabolism processes (ATP metabolic process (GO:0046034), oxidation–reduction process (GO:0055114), carbohydrate metabolic process (GO:0005975), lipid metabolic process (GO:0006629) and cellular protein metabolic process (GO:0044267)). We compared the different sets of proteins extracted by proteomic analysis with bronchoalveolar adenocarcinoma (MESH: D002282 pulmonary adenocarcinoma). Drug repositioning was performed for each condition with phase 4 used drugs targeting each network of deregulated proteins upon TSA, NAM under hypoxic and normoxic treatments.

Experimental Design and Statistical Rationale

Three biological replicates were used in all experiments except for the proteomic analysis. The statistical analysis of the proteomic data described above in "Database search and quantitative iTRAQ analysis" was based on one experiment setup prior to confirm the dysregulation of eight proteins by three biological replicates through Western blot analysis. Statistical significance of differences between treatments was calculated by Student's *t*-test.

References

1. A Martín-Bernabé, J Tarragó-Celada, V Cunin, S Michelland, R Cortés, et al. Quantitative Proteomic Approach Reveals Altered Metabolic Pathways in Response to the Inhibition of Lysine Deacetylases in A549 Cells under Normoxia and Hypoxia, Int. J. Mol. Sci. 2021; 22: 3378.
2. Bray F, Ferlay J, Soerjomataram I, Siegel RL, Torre LA, et al. Global Cancer Statistics 2018: GLOBOCAN Estimates of Incidence and Mortality Worldwide for 36 Cancers in 185 Countries. CA Cancer J. Clin. 2018; 68: 394–424.
3. Siegel RL, Miller KD, Jemal A. Cancer statistics. CA Cancer J. Clin. 2020; 70: 7–30.
4. Dasari S, Tchounwou, P.B. Cisplatin in cancer therapy: Molecular mechanisms of action. *Eur. J. Pharmacol.* **2014**; *740*: 364–378.
5. Lim ZF, Ma PC. Emerging insights of tumor heterogeneity and drug resistance mechanisms in lung cancer targeted therapy. J. Hematol. Oncol. 2019; 12: 1–18.
6. Jeannot V, Busser B, Brambilla E, Wislez M, Robin B, et al. The PI3K/AKT pathway promotes gefitinib resistance in mutant KRAS lung adenocarcinoma by a deacetylase-dependent mechanism. Int. J. Cancer. 2013; 134: 2560–2571.
7. Saliani M, Jalal R, Ahmadian MR. From basic researches to new achievements in therapeutic strategies of KRAS-driven cancers. Cancer Biol. Med. 2019; 16: 435–461.
8. Kerr EM, Martins CP. Metabolic rewiring in mutant Kras lung cancer. FEBS J. 2018; 285: 28–41.

9. Pupo E, Avanzato D, Middonti E, Bussolino F, Lanzetti L. KRAS-Driven Metabolic Rewiring Reveals Novel Actionable Targets in Cancer. Front. Oncol. 2019; 9: 848.
10. Hanahan D, Weinberg RA. Hallmarks of Cancer: The Next Generation. *Cell*. **2011**; *144*: 646–674.
11. Bober P, Alexovič M, Tomková Z, Kilík R, Sabo J. RHOA and mDia1 promotes apoptosis of breast cancer cells via a high dose of doxorubicin treatment. Open Life Sci. 2019; 14: 619–627.
12. Warburg O, Wind F, Negelein E. THE METABOLISM OF TUMORS IN THE BODY. J. Gen. Physiol. 1927; 8: 519–530.
13. Kroemer G, Pouyssegur J. Tumor cell metabolism: Cancer's Achilles' heel. Cancer Cell. 2008; 13: 472-482.
14. Benito A, Diaz-Moralli S, Coy JF, Centelles JJ, Cascante M. Role of the Pentose Phosphate Pathway in Tumour Metabolism. In: Sybille Mazurek, Maria Shoshan, editors. Tumor Cell Metabolism: Pathways, Regulation and Biology. Vienna: Springer. 2015; 143–163.
15. Jiang P, Du W, Wu M. Regulation of the pentose phosphate pathway in cancer. Protein Cell. 2014; 5: 592–602.
16. Cluntun AA, Lukey MJ, Cerione RA, Locasale JW. Glutamine Metabolism in Cancer: Understanding the Heterogeneity. Trends Cancer. 2017; 3: 169–180.
17. Martín-Bernabé A, Cortés R, Lehmann SG, Seve M, Cascante M, et al. Quantitative Proteomic Approach to Understand Metabolic Adaptation in Non-Small Cell Lung Cancer. J. Proteome Res. 2014; 13: 4695–4704.
18. Minakata K, Takahashi F, Nara T, Hashimoto M, Tajima K, et al. Hypoxia induces gefitinib resistance in non-small-cell lung cancer with both mutant and wild-type epidermal growth factor receptors. Cancer Sci. 2012; 103: 1946–1954.
19. Jing X, Yang F, Shao C, Wei K, Xie M, et al. Role of hypoxia in cancer therapy by regulating the tumor microenvironment. Mol. Cancer. 2019; 18: 1–15.
20. Song X, Liu X, Chi W, Liu Y, Wei L, et al. Hypoxia-induced resistance to cisplatin and doxorubicin in non-small cell lung cancer is inhibited by silencing of HIF-1α gene. Cancer Chemother. Pharmacol. 2006; 58: 776–784.

21. Wu HM, Jiang ZF, Ding PS, Shao LJ, Liu RY. Hypoxia-induced autophagy mediates cisplatin resistance in lung cancer cells. Sci. Rep. 2015; 5: 12291.
22. Semenza GL. HIF-1 mediates metabolic responses to intratumoral hypoxia and oncogenic mutations. J. Clin. Investig. 2013; 123: 3664–3671.
23. Price NL, Gomes AP, Ling AJ, Duarte FV, Martin-Montalvo A, et al. SIRT1 Is Required for AMPK Activation and the Beneficial Effects of Resveratrol on Mitochondrial Function. Cell Metab. 2012; 15: 675–690.
24. Marks PA, Xu WS. Histone deacetylase inhibitors: Potential in cancer therapy. J. Cell. Biochem. 2009; 107: 600–608.
25. Verza FA, Das U, Fachin AL, Dimmock JR, Marins M. Roles of Histone Deacetylases and Inhibitors in Anticancer Therapy. Cancers. 2020; 12: 1664.
26. Martín-Bernabé A, Balcells C, Tarragó-Celada J, Foguet C, Bourgoin-Voillard S, et al. The importance of post-translational modifications in systems biology approaches to identify therapeutic targets in cancer metabolism. Curr. Opin. Syst. Biol. 2017; 3: 161–169.
27. Huang M, Geng M. Exploiting histone deacetylases for cancer therapy: from hematological malignancies to solid tumors. Sci. China Life Sci. 2016; 60: 94–97.
28. Suraweera A, O'Byrne KJ, Richard DJ. Combination Therapy With Histone Deacetylase Inhibitors (HDACi) for the Treatment of Cancer: Achieving the Full Therapeutic Potential of HDACi. Front. Oncol. 2018; 8: 92.
29. Damaskos C, Tomos I, Garmpis N, Karakatsani A, Dimitroulis D, et al. Histone Deacetylase Inhibitors as a Novel Targeted Therapy Against Non-small Cell Lung Cancer: Where Are We Now and What Should We Expect? Anticancer. Res. 2018; 38: 37–43.
30. Neal JW, Sequist LV. Complex Role of Histone Deacetylase Inhibitors in the Treatment of Non–Small-Cell Lung Cancer. J. Clin. Oncol. 2012; 30: 2280–2282.
31. Wang L, Li H, Ren Y, Zou S, Fang W, et al. Targeting HDAC with a novel inhibitor effectively reverses paclitaxel resistance in non-small cell lung cancer via multiple mechanisms. Cell Death Dis. 2016; 7: e2063.

32. Witta S. Histone Deacetylase Inhibitors in Non–Small-Cell Lung Cancer. J. Thorac. Oncol. 2012; 7: S404–S406.
33. Mukhopadhyay NK, Weisberg E, Gilchrist D, Bueno R, Sugarbaker DJ, et al. Effectiveness of Trichostatin A as a Potential Candidate for Anticancer Therapy in Non–Small-Cell Lung Cancer. Ann. Thorac. Surg. 2006; 81: 1034–1042.
34. Tang Y, Zhao W, Chen Y, Zhao Y, Gu W. Acetylation Is Indispensable for p53 Activation. Cell. 2008; 133: 612–626.
35. Guan KL, Xiong Y. Regulation of intermediary metabolism by protein acetylation. Trends Biochem. Sci. 2011; 36: 108–116.
36. Cheung CHY, Juan HF. Quantitative proteomics in lung cancer. J. Biomed. Sci. 2017; 24: 1–11.
37. Vinaiphat A, Low JK, Yeoh KW, Chng WJ, Sze SK. Application of Advanced Mass Spectrometry-Based Proteomics to Study Hypoxia Driven Cancer Progression. Front. Oncol. 2021; 11: 98.
38. Bush JT, Chan MC, Mohammed S, Schofield CJ. Quantitative MS-Based Proteomics: Comparing the MCF-7 Cellular Response to Hypoxia and a 2-Oxoglutarate Analogue. ChemBioChem. 2020; 21: 1647–1655.
39. Song Z, Pearce MC, Jiang Y, Yang L, Goodall C, et al. Delineation of hypoxia-induced proteome shifts in osteosarcoma cells with different metastatic propensities. Sci. Rep. 2020; 10: 1–17.
40. Zhang K, Xu P, Sowers JL, Machuca DF, Mirfattah B, et al. Proteome Analysis of Hypoxic Glioblastoma Cells Reveals Sequential Metabolic Adaptation of One-Carbon Metabolic Pathways. Mol. Cell. Proteom. 2017; 16: 1906–1921.
41. Djidja MC, Chang J, Hadjiprocopis A, Schmich F, Sinclair J, et al. Identification of Hypoxia-Regulated Proteins Using MALDI-Mass Spectrometry Imaging Combined with Quantitative Proteomics. J. Proteome Res. 2014; 13: 2297–2313.
42. Bousquet PA, Sandvik JA, Arntzen MØ, Edin NFJ, Christoffersen S, et al. Hypoxia Strongly Affects Mitochondrial Ribosomal Proteins and Translocases, as Shown by Quantitative Proteomics of HeLa Cells. Int. J. Proteom. 2015; 2015: 1–9.

43. Napolitano F, Zhao Y, Moreira VM, Tagliaferri R, Kere J, et al. Drug repositioning: a machine-learning approach through data integration. J. Chemin. 2013; 5: 30.
44. Aliper A, Plis S, Artemov A, Ulloa A, Mamoshina P, et al. Deep Learning Applications for Predicting Pharmacological Properties of Drugs and Drug Repurposing Using Transcriptomic Data. Mol. Pharm. 2016; 13: 2524–2530.
45. Ekins S, Puhl AC, Zorn KM, Lane TR, Russo DP, e al. Exploiting machine learning for end-to-end drug discovery and development. Nat. Mater. 2019; 18: 435–441.
46. Zhao D, Li FL, Cheng ZL, Lei QY. Impact of acetylation on tumor metabolism. Mol. Cell. Oncol. 2014; 1: e963452.
47. Cantor JP, Iliopoulos D, Rao AS, Druck T, Semba S, et al. Epigenetic modulation of endogenous tumor suppressor expression in lung cancer xenografts suppresses tumorigenicity. Int. J. Cancer. 2006; 120: 24–31.
48. Chang J, Varghese DS, Gillam MC, Peyton M, Modi B, et al. Differential response of cancer cells to HDAC inhibitors trichostatin A and depsipeptide. Br. J. Cancer. 2011; 106: 116–125.
49. Miyanaga A, Gemma A, Noro R, Kataoka K, Matsuda K, et al. Antitumor activity of histone deacetylase inhibitors in non-small cell lung cancer cells: development of a molecular predictive model. Mol. Cancer Ther. 2008; 7: 1923–1930.
50. Rosato RR, A Almenara J, Dai Y, Grant S. Simultaneous activation of the intrinsic and extrinsic pathways by histone deacetylase (HDAC) inhibitors and tumor necrosis factor-related apoptosis-inducing ligand (TRAIL) synergistically induces mitochondrial damage and apoptosis in human leukemia cells. Mol. Cancer Ther. 2003; 2: 1273–1284.
51. Amoedo ND, Rodrigues MF, Pezzuto P, Galina A, Da Costa RM, et al. Energy Metabolism in H460 Lung Cancer Cells: Effects of Histone Deacetylase Inhibitors. PLoS ONE. 2011; 6: e22264.
52. Choi YH. Induction of apoptosis by trichostatin A, a histone deacetylase inhibitor, is associated with inhibition of cyclooxygenase-2 activity in human non-small cell lung cancer cells. Int. J. Oncol. 2005; 27: 473–479.
53. Liu X, Shao K, Sun T. SIRT1 Regulates the Human Alveolar Epithelial A549 Cell Apoptosis Induced byPseudomonas

AeruginosaLipopolysaccharide. Cell. Physiol. Biochem. 2013; 31: 92–101.
54. Platta CS, Greenblatt DY, Kunnimalaiyaan M, Chen H. The HDAC Inhibitor Trichostatin A Inhibits Growth of Small Cell Lung Cancer Cells. J. Surg. Res. 2007; 142: 219–226.
55. Zhao S, Xu W, Jiang W, Yu W, Lin Y, et al. Regulation of Cellular Metabolism by Protein Lysine Acetylation. *Science.* **2010**; *327*: 1000–1004.
56. Wu Q, Cheng Z, Zhu J, Xu W, Peng X, et al. Suberoylanilide Hydroxamic Acid Treatment Reveals Crosstalks among Proteome, Ubiquitylome and Acetylome in Non-Small Cell Lung Cancer A549 Cell Line. Sci. Rep. 2015; 5: 9520.
57. Narayan S, Bader GD, Reimand J. Frequent mutations in acetylation and ubiquitination sites suggest novel driver mechanisms of cancer. Genome Med. 2016; 8: 55.
58. Li Y, Shin D, Kwon SH. Histone deacetylase 6 plays a role as a distinct regulator of diverse cellular processes. FEBS J. 2012; 280: 775–793.
59. Kulka LAM, Fangmann PV, Panfilova D, Olzscha H. Impact of HDAC Inhibitors on Protein Quality Control Systems: Consequences for Precision Medicine in Malignant Disease. Front. Cell Dev. Biol. 2020; 8: 425.
60. Heider U, Rademacher J, Lamottke B, Mieth M, Moebs M, et al. Synergistic interaction of the histone deacetylase inhibitor SAHA with the proteasome inhibitor bortezomib in cutaneous T cell lymphoma. Eur. J. Haematol. 2009; 82: 440–449.
61. Laporte AN, Poulin NM, Barrott JJ, Wang XQ, Lorzadeh A, et al. Death by HDAC Inhibition in Synovial Sarcoma Cells. Mol. Cancer Ther. 2017; 16: 2656–2667.
62. Park MT, Kim MJ, Suh Y, Kim RK, Kim H, et al. Novel signaling axis for ROS generation during K-Ras-induced cellular transformation. Cell Death Differ. 2014; 21: 1185–1197.
63. Ralph SJ, Rodríguez-Enríquez S, Neuzil J, Saavedra E, Moreno-Sánchez R. The causes of cancer revisited: “Mitochondrial malignancy” and ROS-induced oncogenic transformation – Why mitochondria are targets for cancer therapy. Mol. Asp. Med. 2010; 31: 145–170.

64. Weinberg F, Hamanaka R, Wheaton WW, Weinberg S, Joseph J, et al. Mitochondrial metabolism and ROS generation are essential for Kras-mediated tumorigenicity. Proc. Natl. Acad. Sci. USA. 2010; 107: 8788–8793.
65. Gong K, Xie J, Yi H, Li W. CS055 (Chidamide/HBI-8000), a novel histone deacetylase inhibitor, induces G1 arrest, ROS-dependent apoptosis and differentiation in human leukaemia cells. Biochem. J. 2012; 443: 735–746.
66. Rosato RR, Almenara JA, Maggio SC, Coe S, Atadja P, et al. Role of histone deacetylase inhibitor-induced reactive oxygen species and DNA damage in LAQ-824/fludarabine antileukemic interactions. Mol. Cancer Ther. 2008; 7: 3285–3297.
67. You BR, Park WH. Trichostatin A induces apoptotic cell death of HeLa cells in a Bcl-2 and oxidative stress-dependent manner. Int. J. Oncol. 2012; 42: 359–366.
68. Liou GY, Storz P. Reactive oxygen species in cancer. *Free Radic. Res.* **2010**; *44*: 479–496.
69. Kinnula VL, Pääkkö P, Soini Y. Antioxidant enzymes and redox regulating thiol proteins in malignancies of human lung. FEBS Lett. 2004; 569: 1–6.
70. Zhang SF, Wang XY, Fu ZQ, Peng QH, Zhang JY, et al. TXNDC17 promotes paclitaxel resistance via inducing autophagy in ovarian cancer. Autophagy. 2015; 11: 225–238.
71. Zhang Z, Wang A, Li H, Zhi H, Lu F. RETRACTED: STAT3-dependent TXNDC17 expression mediates Taxol resistance through inducing autophagy in human colorectal cancer cells. Gene. 2016; 584: 75–82.
72. Xiong Y, Guan KL. Mechanistic insights into the regulation of metabolic enzymes by acetylation. J. Cell Biol. 2012; 198: 155–164.
73. Guarente L. The Logic Linking Protein Acetylation and Metabolism. Cell Metab. 2011; 14: 151–153.
74. Smith B, Schafer XL, Ambeskovic A, Spencer CM, Land H, et al. Addiction to Coupling of the Warburg Effect with Glutamine Catabolism in Cancer Cells. Cell Rep. 2016; 17: 821–836.

75. Liberti MV, Locasale JW. The Warburg Effect: How Does it Benefit Cancer Cells? Trends Biochem. Sci. 2016; 41: 211–218.
76. Zha X, Wang F, Wang Y, He S, Jing Y, et al. Lactate Dehydrogenase B Is Critical for Hyperactive mTOR-Mediated Tumorigenesis. Cancer Res. 2011; 71:13.
77. Brisson L, Bański P, Sboarina M, Dethier C, Danhier P, et al. Lactate Dehydrogenase B Controls Lysosome Activity and Autophagy in Cancer. Cancer Cell. 2016; 30: 418–431.
78. Padanad MS, Konstantinidou G, Venkateswaran N, Melegari M, Rindhe S, et al. Fatty Acid Oxidation Mediated by Acyl-CoA Synthetase Long Chain 3 Is Required for Mutant KRAS Lung Tumorigenesis. Cell Rep. 2016; 16: 1614–1628.
79. Saliakoura M, Reynoso-Moreno I, Pozzato C, Sebastiano MR, Galié M, et al. The ACSL3-LPIAT1 signaling drives prostaglandin synthesis in non-small cell lung cancer. Oncogene. 2020; 39: 2948–2960.
80. Cantó C, Gerhart-Hines Z, Feige JN, Lagouge M, Noriega L, et al. AMPK regulates energy expenditure by modulating NAD+ metabolism and SIRT1 activity. Nat. Cell Biol. 2009; 458: 1056–1060.
81. Hardie DG. Energy sensing by the AMP-activated protein kinase and its effects on muscle metabolism. Proc. Nutr. Soc. 2010; 70: 92–99.
82. Moreno-Sánchez R, Rodriguez-Enriquez S, Saavedra E, Marin-Hernandez A, Gallardo-Perez JC. The bioenergetics of cancer: is glycolysis the main ATP supplier in all tumor cells? BioFactors. 2009; 35: 209–225.
83. Li P, Zhang D, Shen L, Dong K, Wu M, et al. Redox homeostasis protects mitochondria through accelerating ROS conversion to enhance hypoxia resistance in cancer cells. Sci. Rep. 2016; 6: 22831.
84. Zheng J. Energy metabolism of cancer: Glycolysis versus oxidative phosphorylation (Review). Oncol. Lett. 2012; 4: 1151–1157.
85. Kong X, Lin Z, Liang D, Fath D, Sang N, et al. Histone Deacetylase Inhibitors Induce VHL and Ubiquitin-Independent Proteasomal Degradation of Hypoxia-Inducible Factor 1α. Mol. Cell. Biol. 2006; 26: 2019–2028.

86. Bell EL, Emerling BM, Ricoult SJH, Guarente LP. SirT3 suppresses hypoxia inducible factor 1α and tumor growth by inhibiting mitochondrial ROS production. Oncogene. 2011; 30: 2986–2996.
87. Lim JH, Lee YM, Chun YS, Chen J, Kim JE, et al. Sirtuin 1 Modulates Cellular Responses to Hypoxia by Deacetylating Hypoxia-Inducible Factor 1α. Mol. Cell. 2010; 38: 864–878.
88. Zhong L, D'Urso A, Toiber D, Sebastian C, Henry RE, et al. The Histone Deacetylase Sirt6 Regulates Glucose Homeostasis via Hif1α. Cell. 2010; 140: 280–293.
89. Faraji A, Manshadi HRD, Mobaraki M, Zare M, Houshmand M. Association of ABCB1 and SLC22A16 Gene Polymorphisms with Incidence of Doxorubicin-Induced Febrile Neutropenia: A Survey of Iranian Breast Cancer Patients. PLoS ONE. 2016; 11: e0168519.
90. Aniogo EC, George BPA, Abrahamse H. Phthalocyanine induced phototherapy coupled with Doxorubicin, a promising novel treatment for breast cancer. Expert Rev. Anticancer. Ther. 2017; 17: 693–702.
91. Nitiss KC, Nitiss JL. Twisting and Ironing: Doxorubicin Cardiotoxicity by Mitochondrial DNA Damage. Clin. Cancer Res. 2014; 20: 4737–4739.
92. Sermeus A, Genin M, Maincent A, Fransolet M, Notte A, et al. Hypoxia-Induced Modulation of Apoptosis and BCL-2 Family Proteins in Different Cancer Cell Types. PLoS ONE. 2012; 7: e47519.
93. Daurio NA, Tuttle SW, Worth AJ, Song EY, Davis JM, et al. AMPK Activation and Metabolic Reprogramming by Tamoxifen through Estrogen Receptor–Independent Mechanisms Suggests New Uses for This Therapeutic Modality in Cancer Treatment. Cancer Res. 2016; 76: 3295–3306.
94. Niikawa H, Suzuki T, Miki Y, Suzuki S, Nagasaki S, et al. Intratumoral Estrogens and Estrogen Receptors in Human Non–Small Cell Lung Carcinoma. Clin. Cancer Res. 2008; 14: 4417–4426.
95. Ko JC, Chiu HC, Syu JJ, Jian YJ, Chen CY, et al. Tamoxifen enhances erlotinib-induced cytotoxicity through down-regulating AKT-mediated thymidine phosphorylase

expression in human non-small-cell lung cancer cells. Biochem. Pharmacol. 2014; 88: 119–127.
96. Shen H, Yuan Y, Sun J, Gao W, Shu YQ. Combined tamoxifen and gefitinib in non-small cell lung cancer shows antiproliferative effects. Biomed. Pharmacother. 2010; 64: 88–92.
97. Zeng L, Kizaka-Kondoh S, Itasaka S, Xie X, Inoue M, et al. Hypoxia inducible factor-1 influences sensitivity to paclitaxel of human lung cancer cell lines under normoxic conditions. Cancer Sci. 2007; 98: 1394–1401.
98. Cosse JP, Sermeus A, Vannuvel K, Ninane N, Raes M, et al. Differential effects of hypoxia on etoposide-induced apoptosis according to the cancer cell lines. Mol. Cancer. 2007; 6: 61.
99. Ahmed ZSO, Dou QP. Updated Review and Perspective on 20S Proteasome Inhibitors in the Treatment of Lung Cancer. Curr. Cancer Drug Targets. 2020; 20: 392–409.
100. García-Fernández C, Fornaguera C, Borrós S. Nanomedicine in Non-Small Cell Lung Cancer: From Conventional Treatments to Immunotherapy. Cancers. 2020; 12: 1609.
101. Duffaud F, Le Cesne A. Imatinib in the treatment of solid tumours. Target. Oncol. 2009; 4: 45–56.
102. Kinoshita K, Nakagawa K, Hamada JI, Hida Y, Tada M, et al. Imatinib mesylate inhibits the proliferation-stimulating effect of human lung cancer-associated stromal fibroblasts on lung cancer cells. Int. J. Oncol. 2010; 37: 869–877.
103. Aono Y, Nishioka Y, Inayama M, Ugai M, Kishi J, et al. Imatinib as a Novel Antifibrotic Agent in Bleomycin-induced Pulmonary Fibrosis in Mice. Am. J. Respir. Crit. Care Med. 2005; 171: 1279–1285.
104. Abdollahi A, Li M, Ping G, Plathow C, Domhan S, et al. Inhibition of platelet-derived growth factor signaling attenuates pulmonary fibrosis. J. Exp. Med. 2005; 201: 925–935.
105. Vitiello GA, Medina BD, Zeng S, Bowler TG, Zhang JQ, et al. Mitochondrial Inhibition Augments the Efficacy of Imatinib by Resetting the Metabolic Phenotype of Gastrointestinal Stromal Tumor. Clin. Cancer Res. 2017; 24: 972–984.

106. Alvarez-Calderon F, Gregory MA, Pham-Danis C, DeRyckere D, Stevens BM, et al. Tyrosine Kinase Inhibition in Leukemia Induces an Altered Metabolic State Sensitive to Mitochondrial Perturbations. Clin. Cancer Res. 2015; 21: 1360–1372.
107. Zhao F, A Mancuso A, Bui TV, Tong X, Gruber JJ, et al. Imatinib resistance associated with BCR-ABL upregulation is dependent on HIF-1α-induced metabolic reprograming. Oncogene. 2010; 29: 2962–2972.
108. Kluza J, Jendoubi M, Ballot C, Dammak A, Jonneaux A, et al. Exploiting Mitochondrial Dysfunction for Effective Elimination of Imatinib-Resistant Leukemic Cells. PLOS ONE. 2011; 6: e21924.
109. Levy A, Doyen J. Metformin for non-small cell lung cancer patients: Opportunities and pitfalls. Crit. Rev. Oncol. 2018; 125: 41–47.
110. Wink KCJ, Belderbos JSA, Dieleman EMT, Rossi M, Rasch CRN, et al. Improved progression free survival for patients with diabetes and locally advanced non-small cell lung cancer (NSCLC) using metformin during concurrent chemoradiotherapy. Radiother. Oncol. 2016; 118: 453–459.
111. Li L, Han R, Xiao H, Lin C, Wang Y, Liu H, et al. Metformin Sensitizes EGFR-TKI–Resistant Human Lung Cancer Cells &lt,em&gt,In Vitro and In Vivo through Inhibition of IL-6 Signaling and EMT Reversal. Clin. Cancer Res. 2014; 20: 2714.
112. Troncone M, Cargnelli SM, Villani LA, Isfahanian N, Broadfield LA, et al. Targeting metabolism and AMP-activated kinase with metformin to sensitize non-small cell lung cancer (NSCLC) to cytotoxic therapy: translational biology and rationale for current clinical trials. Oncotarget. 2017; 8: 57733–57754.
113. Storozhuk Y, Hopmans SN, Sanli T, Barron CC, Tsiani E, et al. Metformin inhibits growth and enhances radiation response of non-small cell lung cancer (NSCLC) through ATM and AMPK. Br. J. Cancer. 2013; 108: 2021–2032.
114. Lee BB, Kim Y, Kim D, Cho EY, Han J, et al. Metformin and tenovin-6 synergistically induces apoptosis through LKB1-independent SIRT1 down-regulation in non-small cell lung cancer cells. J. Cell. Mol. Med. 2019; 23: 2872–2889.

115. Zhang S, Zhang QC, Jiang SJ. Effect of trichostatin A and paclitaxel on the proliferation and apoptosis of lung adenocarcinoma cells. Chin. Med J. 2013; 126: 129–134.
116. Hontecillas-Prieto L, Flores-Campos R, Silver A, De Álava E, Hajji N, et al. Synergistic Enhancement of Cancer Therapy Using HDAC Inhibitors: Opportunity for Clinical Trials. Front. Genet. 2020; 11: 1113.
117. Mosmann T. Rapid colorimetric assay for cellular growth and survival: Application to proliferation and cytotoxicity assays. J. Immunol. Methods. 1983; 65: 55–63.
118. Vermes I, Haanen C, Steffens-Nakken H, Reutellingsperger C. A novel assay for apoptosis Flow cytometric detection of phosphatidylserine expression on early apoptotic cells using fluorescein labelled Annexin V. J. Immunol. Methods. 1995; 184: 39–51.
119. Gutmann I. L-Lactate. Determination with lactate dehydrogenase and NAD. In: Bergmeyer H, editors. Methods of Enzymatic Analysis, 2nd ed. Cambridge: Academic Press. 1963; 1464–1468.
120. Kunst A, Draeger B, Ziegenhorn J. UV methods with hexokinase and glucose-6-phosphate dehydrogenase. In Methods in Enzymatic Analysis. Verlag Chemie: H.U. Bergmeyer. 1984; 162–172.
121. Tarrado-Castellarnau M, de Atauri P, Tarrago-Celada J, Perarnau, J, Yuneva, M, Thomson, T.M, Cascante, M. De novo MYC addiction as an adaptive response of cancer cells to CDK4/6 inhibition. Mol. Syst. Biol. 2017; 13.
122. Lehmann SG, Seve M, VanWonterghem L, Michelland S, Cunin V, et al. A large scale proteome analysis of the gefitinib primary resistance overcome by KDAC inhibition in KRAS mutated adenocarcinoma cells overexpressing amphiregulin. J. Proteom. 2019; 195: 114–124.
123. Askri D, Cunin V, Béal D, Berthier S, Chovelon B, et al. Investigating the toxic effects induced by iron oxide nanoparticles on neuroblastoma cell line: an integrative study combining cytotoxic, genotoxic and proteomic tools. Nanotoxicology. 2019; 13: 1021–1040.
124. Wiśniewski JR, Zougman A, Nagaraj N, Mann M. Universal sample preparation method for proteome analysis. Nat. Methods. 2009; 6: 359–362.

125. Campone M, Valo I, Jézéquel P, Moreau M, Boissard A, et al. Prediction of Recurrence and Survival for Triple-Negative Breast Cancer (TNBC) by a Protein Signature in Tissue Samples. Mol. Cell. Proteom. 2015; 14: 2936–2946.
126. Unwin RD, Griffiths JR, Whetton AD. Simultaneous analysis of relative protein expression levels across multiple samples using iTRAQ isobaric tags with 2D nano LC–MS/MS. Nat. Protoc. 2010; 5: 1574–1582.
127. Breitwieser FP, Müller A, Dayon L, Köcher T, Hainard A, et al. General Statistical Modeling of Data from Protein Relative Expression Isobaric Tags. J. Proteome Res. 2011; 10: 2758–2766.
128. Huang DW, Sherman BT, Lempicki RA. Systematic and integrative analysis of large gene lists using DAVID bioinformatics resources. Nat. Protoc. 2009; 4: 44–57.
129. Huang DW, Sherman BT, Lempicki RA. Bioinformatics enrichment tools: paths toward the comprehensive functional analysis of large gene lists. *Nucleic Acids Res.* **2009**; *37*: 1–13.
130. Grover A, Leskovec J. node2vec: Scalable Feature Learning for Networks. In Proceedings of the 22nd ACM SIGKDD International Conference on Knowledge Discovery and Data Mining, Association for Computing Machinery. San Francisco, CA, USA. 2016; 855–864.
131. Gaulton A, Hersey A, Nowotka M, Bento AP, Chambers J, et al. The ChEMBL database in 2017. Nucleic Acids Res. 2017; 45: D945–D954.
132. Fu G, Batchelor C, Dumontier M, Hastings J, Willighagen E, et al. PubChemRDF: towards the semantic annotation of PubChem compound and substance databases. J. Chemin. 2015; 7: 34.
133. Davis AP, Grondin CJ, Johnson RJ, Sciaky D, Wiegers J, et al. Comparative Toxicogenomics Database (CTD): update 2021. Nucleic Acids Res. 2021; 49: D1138–D1143.
134. Freshour SL, Kiwala S, Cotto KC, Coffman AC, McMichael JF, et al. Integration of the Drug–Gene Interaction Database (DGIdb 4.0) with open crowdsource efforts. Nucleic Acids Res. 2021; 49: D1144–D1151.

135. Licata L, Surdo PL, Iannuccelli M, Palma A, Micarelli E, et al. SIGNOR 2.0, the SIGnaling Network Open Resource 2.0: 2019 update. Nucleic Acids Res. 2019; 48: D504–D510.
136. The UniProt Consortium. UniProt: the universal protein knowledgebase in 2021. Nucleic Acids Res. 2021; 49: D480–D489.
137. Oughtred R, Stark C, Breitkreutz BJ, Rust J, Boucher L, et al. The BioGRID interaction database: 2019 update. Nucleic Acids Res. 2019; 47: D529–D541.
138. Meldal BHM, Bye-A-Jee H, Gajdoš L, Hammerová Z, Horáčková A, et al. Complex Portal 2018: extended content and enhanced visualization tools for macromolecular complexes. Nucleic Acids Res. 2019; 47: D550–D558.
139. Orchard S, Ammari M, Aranda B, Breuza L, Briganti L, et al. The MIntAct project—IntAct as a common curation platform for 11 molecular interaction databases. Nucleic Acids Res. 2014; 42: D358–D363.
140. Calderone A, Castagnoli L, Cesareni G. mentha: a resource for browsing integrated protein-interaction networks. Nat. Methods. 2013; 10: 690–691.
141. Calderone A, Iannuccelli M, Peluso D, Licata L. Using the MINT Database to Search Protein Interactions. Curr. Protoc. Bioinform. 2020; 69: e93.
142. Jassal B, Matthews L, Viteri G, Gong C, Lorente P, et al. The reactome pathway knowledgebase. Nucleic Acids Res. 2020; *48*: D498–D503.
143. Szklarczyk D, Gable AL, Lyon D, Junge A, Wyder S, et al. STRING v11: protein–protein association networks with increased coverage, supporting functional discovery in genome-wide experimental datasets. Nucleic Acids Res. 2019; *47*: D607–D613.

Supplementary Data

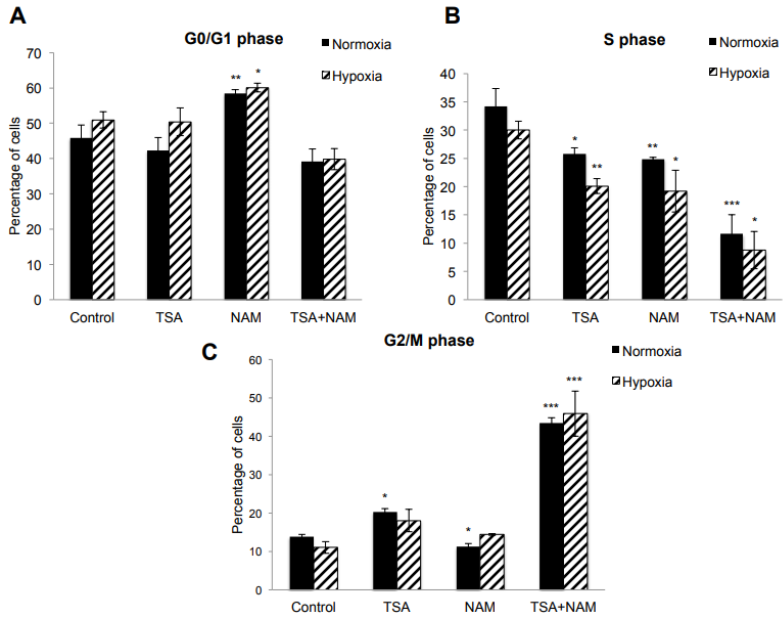

Figure S1: Cell cycle analysis of KDACI-treated cells under normoxia and hypoxia. A, B and C. A549 cells were treated with 1 μM of TSA, 20 mM of NAM and both 1 μM TSA and 20 mM NAM for 24 h of incubation under normoxia and hypoxia. Cells incubated in medium without KDACIs served as control. Bars represent the means ± standard error of the mean of three independent experiments. The asterisks above bars indicate statistically significant differences compared to normoxic control cells. The ssterisks above curly brackets indicate statistically significant differences between hypoxic and normoxic treatments and between hypoxic treatments and hypoxic control cells. Statistical significance was assessed by a two-tailed Student's t-test. *, $p \leq 0.05$; **, $p \leq 0.01$; ***, $p \leq 0.001$.

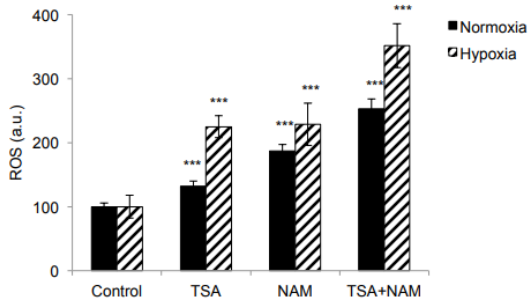

Figure S2: Intracellular ROS levels of KDACI-treated A549 cells under normoxia and hypoxia. A549 cells were treated with 1 μM TSA, 20 mM NAM and both 1 μM TSA and 20 mM NAM under normoxia and hypoxia. Cells incubated in medium without KDACIs served as control. Bars represent the means ± standard error of the mean of three independent experiments. The asterisks above curly brackets indicate statistically significant differences between normoxic treatments and normoxic control cells and between hypoxic treatments and hypoxic control cells. Statistical significance was assessed by a two-tailed Student's t-test. ***, $p \leq 0.001$.; a. u., arbitrary units.

Table S1: Gene ontology enrichment analysis on PIR keywords. A549 cells were treated with 1 μM TSA, 20 mM NAM and both 1 μM TSA and 20 mM NAM under normoxia and hypoxia. Cells incubated in medium without KDACIs served as controls. GO enrichment analysis of the Protein Information Resource (PIR) keywords is shown for TSA treatment under normoxia, NAM treatment under normoxia, TSA/NAM treatment under normoxia, control cells under hypoxia, TSA treatment under hypoxia, NAM treatment under hypoxia and TSA/NAM treatment under hypoxia with respect to control cells under normoxia. The list of the PIR keyword is presented with the percentage of proteins and the p-value related to each keyword for each treatment. Significantly (p-value ≤ 0.05) enriched processes are colored in blue.

	TSA Normoxia		**NAM Normoxia**		**TSA + NAM Normoxia**		**Hypoxia**		**TSA Hypoxia**		**NAM Hypoxia**		**TSA + NAM Hypoxia**	
Keywords	% of proteins	p-value	% of proteins	p-value	% of proteins	p-value	% of proteins	p-value	% of proteins	p-value	% of proteins	p-value	% of proteins	p-value
Acetylation	70	<0.001	76	<0.001	63	<0.001	61	<0.001	68	<0.001	66	<0.001	64	<0.001
Ribosome	12	<0.001	4	0.031	1	<0.001	5	0.019	8	<0.001	14	<0.001	10	<0.001
Protein Biosynthesis	16	<0.001	15	<0.001	17	<0.001	14	<0.001	11	<0.001	19	<0.001	16	<0.001
Ribonucleoprotein	16	<0.001			16	<0.001	14	<0.001	11	<0.001	20	<0.001	12	<0.001
Ribosomal protein	13	<0.001	7	0.005	12	<0.001	11	<0.001	10	<0.001	16	<0.001	10	<0.001
Phosphoprotein	74	<0.001	61	<0.001	65	<0.001	68	<0.001	68	<0.001	64	<0.001	72	<0.001
Cytoplasm	42	<0.001	34	<0.001	35	<0.001	43	<0.001	37	<0.001	4	<0.001	4	<0.001
RNA-binding	13	<0.001	12	<0.001	13	<0.001	13	0.004	9	0.005	12	<0.001	15	<0.001
mRNA splicing	9	<0.001	10	<0.001	8	<0.001	7	0.020	8	<0.001	7	<0.001	10	<0.001
mRNA procesing	9	<0.001	10	<0.001			5	0.019	8	<0.001	7	<0.001	10	<0.001
Methylation	8	<0.001	8	0.002	6	0.003					7	<0.001	6	0.020
Blocked amino end	5	0.002	5	0.005	6	<0.001	5	0.029	4	0.002	4	0.002	6	<0.001
NADP	6	0.002												
Glycolysis	4	0.002							3	0.028			4	0.015
Actin-binding	7	0.004							7	<0.001				
Oxidoreductase	9	0.004	8	0.062							7	0.046		
Spliceosome	5	0.006	4	0.076	6	<0.001	5	0.046			4	0.005	7	<0.001
Mitochondrion	11	0.008	10	0.096	11	0.004	13	0.031	17	<0.001	10	0.025	15	<0.001

Book Chapter

Adoptive T-cell Therapy in Cancer

Else Marit Inderberg

Translational Research Unit, Section for Cellular Therapy, Department of Oncology, Oslo University Hospital, Norway

***Corresponding Author:** Else Marit Inderberg, Translational Research Unit, Section for Cellular Therapy, Department of Oncology, Oslo University Hospital, Oslo, Norway

Published **May 30, 2023**

How to cite this book chapter: Else Marit Inderberg. Adoptive T-cell Therapy in Cancer. In: Hussein Fayyad Kazan, editor. Immunology and Cancer Biology. Hyderabad, India: Vide Leaf. 2023.

Abstract

During the last decade, T-cell therapies, and particularly chimeric antigen receptors (CAR) T-cell therapies, have established themselves as a treatment modality in haematological malignancies. Their success in solid cancer is still not evident due to several factors, including the challenge of an immunosuppressive tumour microenvironment (TME). This chapter will discuss the development of adoptive T-cell therapies, and the genetic modification of T cells with CAR and T cell receptors (TCR) providing a powerful approach to engineer an anti-tumour reactive T-cell repertoire when the endogenous repertoire is insufficient. Extending the success of T

cell therapies to other patient populations requires novel strategies to overcome immunosuppression and logistical manufacturing challenges.

Adoptive Cell Therapy

Ideally, efficient tumour-specific effectors and memory T cells can be induced spontaneously or by therapeutic vaccination. Nevertheless, in certain cases, active immunization is difficult due to the lack of an effective endogenous T-cell repertoire against targeted tumour antigens.

Adoptive T cell-mediated therapy started with bone marrow transplantations in leukaemia patients around 1980 [1,2] and in 1985 came the first report of adoptive transfer of lymphokine-activated killer (LAK) cells in metastatic cancer patients [3]. LAK cells are CD3+ CD8+, but distinct from NK and T cells, and are generated from PBMCs grown in high concentrations of IL-2. As their name indicates, they can mediate lysis of fresh, non-cultured tumour cells. Donor leukocyte infusion (DLI) has become an established treatment for relapsed haematological malignancies [4]. It was first performed in chronic myelogenous leukaemia (CML) patients [5] for which high response rates are limited. DLI often has major complications like acute and chronic graft-versus-host disease (GVHD) [6]. These initial treatments were followed by a series of T cell transfers to limit toxicity. One of the most effective strategies is to generate tumour-specific T cells. The adoptive transfer of selected tumour-reactive T cells has so far proven efficacious in patients suffering from Epstein-Barr virus (EBV)-associated lymphomas and solid tumours [7-10]. The infusion of tumour-infiltrating lymphocytes (TILs) in melanoma patients was pioneered by Steven Rosenberg's group [11] and has also been tested for the treatment of other types of cancers [12-15]. Combining TIL transfer with intensive preconditioning of the patient results in high response rates, occasionally durable [16]. However, TILs can only be reliably grown from patients with a very limited number of cancer types, mainly melanoma. TIL therapy was introduced prior to the immune checkpoint inhibitor (ICI) era; however, most melanoma patients progress within the first 5

years of therapy. Hence, there is still a significant unmet clinical need [17].Therefore, there are ongoing clinical trials and treatments offered of TIL therapy [18]. Recently, a phase III trial, M14TIL (NCT02278887) showed ground-breaking results [19]. The trial randomised 168 patients with unresectable stage IIIC-IV melanoma to receive immunotherapy with the anti-CTLA-4 antibody ipilimumab or TIL treatment. Most patients had failed previous treatment with anti-PD-1 antibodies. TIL-treated patients had a significantly longer median progression-free survival (7.2 months) compared to those receiving ipilimumab (3.1 months). The overall response rate to TILs was 49% versus 21% for ipilimumab; median overall survival was 25.8 months versus 18.9 months.

When cancer patients are exposed to high levels of tumour antigen expression over a longer period of time, this may result in profound immune tolerance. Additionally, the expression of many tumour-associated antigens, including cancer germline antigens like NY-ESO-1 and MAGE, has been detected in medullary thymic epithelial cells and is involved in the induction of central tolerance [20]. In the absence of an adequate level of endogenous tumour-reactive T-cell response, recent clinical studies have shown that it is feasible to compensate for this by engineering a tumour-specific T cell repertoire [21].

Redirected T cells – Promise and Pitfalls

T cells can be retargeted against tumour cells through the transfer of genes encoding T cell receptors (TCR) or chimeric antigen receptors (CAR) (Figure 1). The latter receptor is normally derived from the variable chain of an antibody recognizing extracellular proteins that are tumour- or cell-type-specific, and the intracellular domain of CAR comes from TCR co-signalling moieties [22-25]. Most CARs combine the benefits of high-affinity antibodies with T cell effector functions. The first CAR prototype was published by Kuwana and colleagues [22] where they showed that a chimeric construct of immunoglobulin-derived V regions and TCR-derived C regions could signal when recognizing its target. Another early construct was produced by Zelig Eshar's group who showed that a similar

chimeric construct could kill target cells with the specificity of the antibody from which the CAR was built [23]. The end goal of T-cell therapy is to achieve both long-term persistence and durable remission.

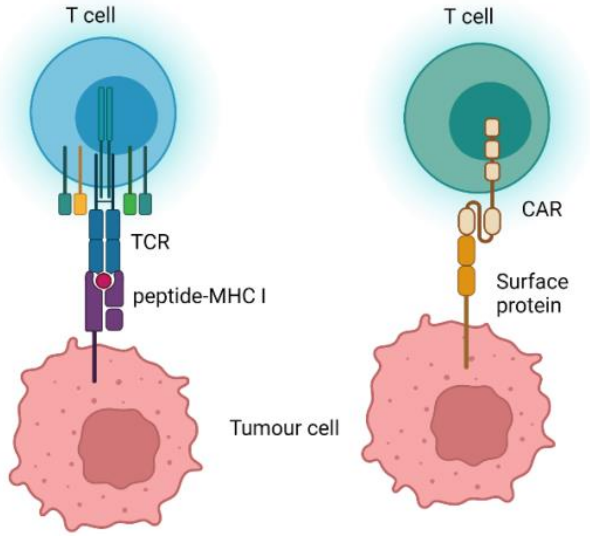

Figure 1: TCR and CAR T cell recognition of tumour cells. Created using BioRender.com.

However, some early experiences have shown that the potency of this treatment may also lead to unexpected toxicity caused by reactivity against normal tissues expressing low levels of the antigen. In melanoma trials, this toxicity has mainly consisted of "on-target" toxicity against pigmented cells in the eye and inner ear, side effects that have been manageable. In a clinical trial of metastatic renal cell carcinoma (RCC), patients were treated with increasing doses of T-cells transduced with CAR specific for carboxy-anhydrase-IX (CAIX) [26]. The initial T-cell infusions were well tolerated, but after 4-5 infusions, severe liver toxicity occurred, most likely due to CAIX expression in bile duct epithelial cells. Another patient participating in a trial at the National Cancer Institute, US, employing a CAR targeting Her2/neu, died after experiencing sudden respiratory toxicity [27]. Infused T cells were localized non-specifically in the lung and liver after infusion, and the effect in the above clinical trial

was thought to be due to low-level expression of Her-2/neu in the lung, causing massive T-cell infiltration and cytokine release. To prevent these effects, fewer T cells are infused and lymphodepletion regimens are adjusted. The potency of engineered T cells highlights the need for the careful selection of target antigens based on their expression profiles.

CAR in the Clinic

CAR-based T-cell therapies have been very successful in haematological malignancies where they have led to durable clinical responses. The overall response rate across numerous trials in patients with leukaemia, lymphoma, and myeloma is 50-90% [28]. Currently, six CAR-T products have been approved by the US Food and Drug Administration (FDA) and European Medicines Agency (EMA) (Table 1). In haematological malignancies, cancer cells are generally more accessible to CAR T cells, which can be targeted against B-cell lineage antigens (CD19 and BCMA) without acceptable toxicity. In contrast, solid tumour CAR T-cell therapies have limited efficacy and are still under development. Several hundred clinical trials are ongoing; however, to date, no solid cancer CAR has been approved by the FDA or EMA.

Table 1: FDA- and EMA-approved CAR-T products since 2017.

Target	Disease	Patient Population	Brand Name	Company
CD19	B-cell acute lymphoblastic Leukaemia (B-ALL), B-cell Non-Hodgkin Lymphoma (NHL)	Children or young adults with refractory or relapsed B-ALL. Adults with refractory or relapsed B-cell NHL.	Kymriah	Novartis
CD19	B-cell Non-Hodgkin Lymphoma (NHL), Follicular Lymphoma (FL)	Adults with refractory or relapsed B-cell NHL, Adults with refractory or relapsed FL	Yescarta	Kite, a Gilead Company
CD19	B-cell acute	Adults with	Tecartus	Kite

	lymphoblastic Leukaemia (B-ALL), Mantle cell lymphoma (ML)	refractory or relapsed B-ALL, Adults with refractory or relapsed ML.		Pharma, Inc.
CD19	B-cell Non-Hodgkin Lymphoma (NHL)	Adults with refractory or relapsed B-cell NHL	Breyanzi	Juno Therapeutics Inc. (Bristol Meyers Squibb)
BCMA	Multiple myeloma (MM)	Adults with relapsed or refractory MM	Abecma	Bristol Meyers Squibb
BCMA	Multiple myeloma (MM)	Adults with relapsed or refractory MM	Carvykti*	Janssen Pharmaceu-tical (Johnson & Johnson)

*Conditional marketing authorization by EMA May 2022.

TCR in the Clinic

Selecting TCRs that target true tumour-specific antigens offers the possibility of selective tumour eradication without serious adverse autoimmune effects.

Results from the first clinical trial using retroviral transfection of an αβ TCR specific for a tumour-associated antigen (MART-1) demonstrated that conferring T-cell-mediated immunity by this approach can be used to obtain important clinical results. Regression of metastatic lesions and prolonged persistence of CTLs in two out of fifteen patients has been reported [21].

The potential risk of toxicity in TCR gene therapy is α/β-chain mispairing, which leads to off-target autoimmune reactivity. When a new TCR is introduced by gene transfer, the native α or β chains can cross-pair with the reciprocal transgenic chains to produce a new hybrid TCR giving rise to TCRs with neo-reactivities. To date, this has not been reported in clinical trials, but in vitro systems and animal models have demonstrated potential risks [29]. Several approaches have been developed to

prevent such TCR cross-pairing and generate predictable TCR transgenic T cells in clinical studies (175). One approach to obtain preferential pairing of TCR chains is the introduction of cysteines in the constant domains of the α and β chains [30]. This also increased the surface expression of the TCR. Specific silencing of endogenous TCR by small interfering RNA (siRNA) incorporated in the viral vector encoding the novel TCR is another strategy to reduce the expression of endogenous TCR and thereby the risk of mispairing [31]. One of the challenges in TCR gene therapy is to increase the functional avidity of T cells as TCRs, in contrast to antibodies that do not undergo somatic hypermutation to enhance their affinity for the recognized antigen.

Very high-affinity TCRs specific for self-peptides are generally not present due to tolerance towards self-antigens, although some autoreactive T cell clones probably escape deletion during negative selection in the thymus [32]. One strategy to generate high-affinity TCRs is the *in vitro* affinity maturation of TCRs. Several reports indicate that enhancing TCR affinity beyond a certain threshold does not improve T cell function [33] and can lead to the loss of target cell specificity [34]. Even when peptide specificity is retained, very high affinity TCRs mediate accelerated T-cell responses, but interestingly lead to an inability to recognize a low density of MHC/peptide antigen [35].

A limitation of using transferred TCRs that do not apply to CARs is their HLA-dependence. The TCR is restricted to binding to a certain HLA molecule. However, certain HLA molecules are widely expressed, such as HLA-A2 and HLA-A3 for HLA class I, together covering 75% of the Caucasian population, or HLA-DP4 for HLA class II, which is present in 76% of the Caucasian population [36]. This approach is both laborious and costly and therefore, likely to be restricted to patients with common HLA types.

To date, no TCR has been approved for use in T cell therapy for cancer. However, recently, the bispecific T-cell engager tebentafusp, which targets the melanoma-associated antigen (gp100) was approved by the FDA for the treatment of

unresectable/metastatic uveal melanoma [37]. Unfortunately, TCR-based therapy lags behind the CAR-based therapy clinically, but could be more efficient than CARs against solid tumour [38]. The number of targetable tumour antigens is largely increased for TCR compared to CAR therapy, as it includes all proteins present on the cell surface in the context of MHC, requires a lower abundance of the target antigen, and reduces the risk of cross-reactivity with healthy cells [39,40]. The number of clinical trials testing different TCRs is steadily increasing [41]. Several of these trials have shown very encouraging clinical results [42-44].

Transient versus Stable CAR and TCR Expression

The main approach used for CAR and TCR transfer in clinical trials is transduction with lentiviral (LV) or retroviral (RV) vectors, which give stable expression of the receptor of interest. The main difference between the two types of viral vectors is that RV vectors only infect dividing cells, whereas LV vectors can infect non-activated resting cells. LV vectors can also accommodate larger genetic cargo than RV vectors [45]. The viral vector life cycle involves cell entry, reverse transcription of the RNA genome into complementary (c)DNA and integration of the latter into the host genome.

The RV vector should not continue to spread after the initial infection and by replacing most of the coding regions of the retrovirus with the transgene of interest, the vector itself cannot produce the proteins required for subsequent replication. The viral proteins required for initial infection can be produced in a retroviral packaging cell line that has gag, pol, and env genes integrated separately in its genome [46].

T cell manufacturing using viral vectors is costly and time-consuming, leaving a logistical bottleneck, and there are therefore ongoing efforts to reduce production time and avoid activation of T cells leading to differentiation [47]. Pre-clinical results are encouraging but will have to be clinically validated.

Additionally, novel methods for gene editing are becoming increasingly available, including CRISPR-Cas systems, which can be scaled up with high precision, allowing precise insertion of receptors into defined genomic loci, as well as combinatorial gene knock-ins and knockouts. The technology has already made its way to the clinic [48,49] and could provide a more sustainable production method than viral vector technology in the long term due to the lower costs of material [50,51]. The clinical proof-of-concept demonstrated the feasibility and safety of CRISPR engineering of T cells for the treatment of cancer.

Another alternative non-viral method for gene transfer is the Sleeping Beauty (SB) transposon technology. SB transposase is introduced into a cell in the form of DNA (expression plasmid), mRNA, or recombinant protein together with donor DNA containing the transposon to be mobilized. SB transposon technology was first tested clinically for CD19CAR-T production from autologous or donor-derived T cells in acute lymphoblastic leukaemia (ALL) and Non-Hodgkin Lymphoma (NHL) [52].

These trials met their clinical endpoints in terms of safety, feasibility, and efficacy.

There have been a limited number of clinical studies, but this technology has been proven to be safe and feasible for the treatment of ALL with CAR-modified donor-derived cytokine-induced killer (CIK) cells [53]. In this study, a dose-dependent clinical response was observed. The first clinical trial using this technology for CAR-T therapy in multiple myeloma is ongoing [54].

Insertional mutagenesis has been a concern associated with the use of viral vectors for the modification of haematopoietic stem cells, but mature T cells have been shown to be much less prone to oncogene transformation in both clinical [55] and pre-clinical [56] settings. To enable the destruction of stably transfected T cells misbehaving in vivo, the strategy of transferring suicide genes along with TCR genes has been explored and is already in late-phase clinical trials [57].

To eliminate the potential risks of T cell transformation and long-term toxicity, mRNA-engineered T cells with transient TCR and CAR expression can be used [58-60]. This strategy enables the fast screening of TCRs candidates for clinical use. Although long-term TCR expression is not achieved by mRNA electroporation, this could be partially compensated for by multiple infusions, as recently demonstrated in a mesothelioma mouse model with the adoptive transfer of T cells electroporated with mRNA encoding CAR [61]. Furthermore, another advantage offered by this approach is the possibility of co-electroporation of T cells with RNA encoding homing receptors or other molecules [62-64]. Clinically, transient CAR expression was first used to treat pancreatic cancer patients with mesothelin-specific CAR in order to avoid off-target toxicity [60]. The treatment was shown to be safe and feasible, with mesothelin CAR-T cells migrating to primary and metastatic tumour sites. There was also evidence of the therapeutic potential of the transiently modified CAR T cells, with a mixed metabolic tumour response in one patient [60,65]. A c-Met-specific CAR was also tested in a trasneint approach in metastatic breast cancer patients in a phase 0 clinical trial with a single intratumoural injection producing local inflammatory responses and tumour necrosis [66].

The transient approach is also gaining momentum in other solid tumours where the risk for uncontrollable off-tumor toxicities is of particular concern such as glioblastoma. Preclinical testing of NKG2D-based CAR T cells co-expressing interleukin-12 (IL-12) and interferon alpha2 (IFN-α2) in orthotopic immunocompetent mouse models demonstrated increased anti-glioma activity and provided a rationale for clinical studies with mRNA-based CAR T cell treatment of brain tumours [67]. For TCR, this approach has so far mainly been tested pre-clinically [59,68-71], but the approach has been used clinically in colorectal cancer (NCT03431311). Furthermore, a recent study in patients with recurrent hepatitis B virus (HBV)-related hepatocellular carcinoma showed that multiple infusions of mRNA-electroporated T cells expressing HBV-specific TCR was well-tolerated [72]. Due to the concomitant use of immunosuppressive drugs after liver transplantation in these

patients, TCR-modified T-cell anti-tumour reactivity was not detected.

The Optimal T-cell Subset for ACT

Both the adoptive transfer of tumour-reactive TILs and TCR engineered T cells require *ex vivo* expansion of T cells. Several studies have demonstrated that multiple rounds of stimulation result in full differentiation, loss of homing receptors and potential exhaustion of the expanded T cells and reduced *in vivo* persistence [73,74]. *In vivo* persistence of modified T cells has been correlated with clinical response [75]. CD8+ T cells are divided into different subsets based on their multi-parameter phenotype and function [76,77]. The expression of CD27 and CD28 is associated with increased proliferative capacity of T cells as well as the ability of T cells to survive following activation. This has also been linked to the upregulation of anti-apoptosis molecules like Bcl-x upon stimulation through CD27 [78]. A lack of telomerase activity and the consequent shortening of chromosomal telomeres are associated with the differentiation of T cells to an end-stage effector cell with limited proliferative capacity [79]. Great variation in *in vitro* culture protocols used for activation and expansion of tumour-specific T cells and results in variable T-cell differentiation. These differences most likely have major implications for *in vivo* T-cell persistence and the success of the treatment [80,81]. The main focus of T-cell therapy development has been on finding tumour targets and improving the genetic modifications of the immune cells while less effort has been made to efficiently produce the optimal cell subset. The present *ex vivo* T-cell manufacturing (Figure 2) is very different from physiological T-cell expansions occurring *in vivo* when T cells encounter antigen and does not generate the T-cell subsets that provide long term optimal therapeutic efficacy in solid cancers. After the patient has undergone leukapheresis, the T cells are isolated and activated, transduced by viral vectors encoding for the CAR or TCR, expanded and cryopreserved before they are infused back into the patient

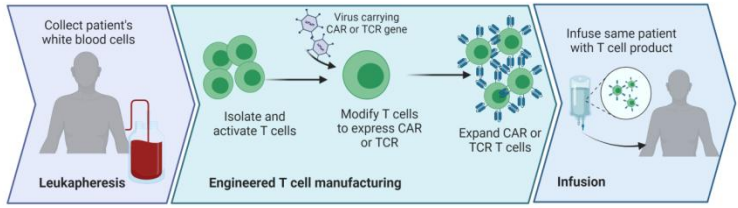

Figure 2: CAR- and TCR-modified T cell manufacturing. Created using BioRender.com.

The T cells are generally stimulated with CTS™ Dynabeads™ CD3/CD28 or with MACS® GMP T Cell TransAct™ beads coated with CD3 and CD28 antibodies that mimic the interaction between T cells and antigen presenting cells *in vivo* and have been used for expansion of large numbers of T cells for T-cell based therapies [82]. Most current protocols generate a heterogeneous population of mainly so-called effector memory T cells (T_{EM}). It is now clear that the quality, efficacy, and longevity of T-cell immunity depend on the differentiation of naïve T cells (T_N) into phenotypically distinct subsets with specific roles in protective immunity. These include memory stem-like (T_{SCM}), central memory (T_{CM}), effector memory (T_{EM}), and highly differentiated effector (T_E) T cells. Less differentiated cells like T_{CM} and T_{SCM} were shown to respond more persistently against cancer cells [83,84]. Indeed, the hostile milieu where cancer cells proliferate inhibits killing and growth of non-optimal, fragile effector T cells, whereas T_{CM} and T_{SCM} better withstand the immunosuppressive environment. Preclinical mouse models have shown that engineering T cells selected from more naïve (T_N) and central memory (T_{CM}) subsets (or their intermediates), or expanding T_N *ex vivo* in the presence of molecules that inhibit T cell differentiation, provide cell products with superior engraftment, proliferation and anti-tumour effects after adoptive transfer [85,86]. Efforts have been made to produce larger numbers of T_{CM} which are less differentiated and persist for longer using combinations of cytokines including IL-2, IL-4, IL-7, IL-15 and IL-21 and varying stimulation times and transduction time points [87,88]. Cellular products with a higher percentage of central memory phenotype T cells showed high *in vitro* efficacy in 2D and 3D cultures. There is also several

ongoing efforts to produce T_{SCM} which have been shown to give rise to T_{CM} [89,90]. The presence of these cells have been shown to correlate with higher efficacy in response vaccination, immune checkpoint therapy, and CAR-T therapy, both pre-clinically and clinically [83,91-94].

Allogeneic Approaches

The production of patient autologous T cell products is complex and expensive and remains a bottleneck for the wider distribution of this therapy. To provide increased availability of T-cell therapy to patients, allogeneic approaches are promising solutions. The number of patients that can be treated from one batch of allogeneic immune cells will depend on the production methods and yield of efficient and persistent CAR- or TCR modified cells. An important obstacle to the production of allogeneic CAR T cells is the requirement for human leukocyte antigen (HLA)-matching to avoid rejection of the infused T cells or Graft versus Host Disease (GvHD). To remedy this, genome-editing has been used to disrupt the endogenous TCR generating universal CAR T cells. Clinical studies have shown proof of concept of allogeneic CAR T cells inducing remissions in leukemia patients, with a few cases of mild GvHD [95].

Another alternative would be to use Natural Killer (NK) cells for allogeneic CAR- or TCR- therapy as these cells generally do not cause GvHD. In a recent phase I/II study CD19CAR NK cells produced from cord blood showed clinical efficacy in B-cell lymphoma and –leukaemia patients [96]. A concern using NK cells is their persistence, however, in this study the infused CAR-NK cells could be detected at low levels for at least 12 months. Further clinical studies using allogeneic approaches are warranted to investigate clinical efficacy.

The Tumour Microenvironment and Resistance Mechanisms

T-cell therapy has shown signs of activity in solid tumours, but consistent durable response rates have so far been disappointing [97,98]. The tumour microenvironment (TME) plays an

important role in the response to therapy and can inhibit anti-tumour T cell responses in several ways. The TME impairs trafficking to the tumour site using physical barriers such as dysregulated tumour vasculature and dense fibrogenic extracellular matrix (ECM), or the presence of immunosuppressive cells including myeloid-derived suppressor cells (MDSC), regulatory T cells (Treg), and cancer-associated fibroblasts (CAF). These cells produce immunosuppressive cytokines and chemokines, attracting more immunosuppressive cells, and express inhibitory enzymes and immune checkpoint molecules that further dampen the anti-tumour response [97]. In solid tumours there is also extensive competition for nutrition and metabolic fuel between proliferative cancer cells and activated T cells, both relying on glycolysis as their primary means of energy metabolism [99].

Ways of counteracting this is to produce more metabolically fit therapeutic T cells, use intra-tumoural or locoregional delivery of T cells, or use combination therapies to induce acute inflammation in the TME. Brain tumours have a very challenging TME and a challenging route to reach the tumour after intravenous administration. Several clinical trials have demonstrated safety and efficacy of locoregional infusion of CAR T cells into the central nervous system [100-102].

Combination Therapies

Another way to enhance the efficacy of T cell therapy in a hostile TME is to combine the therapy with other therapeutic approaches to enhance the efficacy. In patients with malignant pleural disease (including metastatic lung cancer and breast cancer), mesothelin CAR T cells were administered into the pleura in combination with anti-PD-1 blockade [103]. Stable disease was obtained for ≥6 months in 8/27 patients, and 2 patients exhibited complete metabolic response on PET scan.

In addition to immune checkpoint blockade, CAR T cell therapies have been tested in combination with chemotherapy, radiotherapy, oncolytic viruses, cancer vaccines, cytokines, Bi-specific T-cell engagers (BiTEs), immunomodulatory agents,

haematopoietic stem cell transplantation (HSCT), and metabolic inhibitors (recently reviewed in [104]). Personalising such strategies for patients will most likely be necessary to improve current response rates to T-cell therapies in advanced solid tumours.

Conclusion

Adoptive T-cell therapy is well established as an effective therapeutic modality in cancer. Progress has been made in understanding the mechanism of action of engineered T cells and major therapeutic resistance mechanisms. Modifications to CAR- and TCR-engineered T cells or combination with other therapies can increase their potency; however, logistical challenges in manufacturing and delivery are required for increased availability and their broader use. Current viral vector production is complex and expensive, and we see alternative methods including mRNA, CRISPR-Cas, and transposon technologies which are already in early clinical trials. Allogeneic immune cell approaches are also a field of intense research, but further studies are needed to improve therapeutic immune cell safety, efficacy, and persistence.

Finally, the success of these therapies in solid cancer is still very limited and combination therapies to address the challenges of the TME and increase tumour infiltration are essential to enhance therapeutic efficacy.

References

1. Marmont AM. Transplantation haemopoiesis. Morphological bone marrow studies after allogeneic marrow transplantation in man for severe aplastic anaemia and acute leukaemia. Nouv Rev Fr Hematol. 1979; 21: 133–148.
2. Islam A, Catovsky D, Goldman JM, Galton D. A. Histological study of the bone marrow in chronic granulocytic leukaemia in blast transformation. I. Serial observations before and after autografting. Histopathology. 1981; 5: 339–351.
3. SA Rosenberg, MT Lotze, LM Muul, S Leitman, AE Chang,

et al. Observations on the systemic administration of autologous lymphokine-activated killer cells and recombinant interleukin-2 to patients with metastatic cancer. N Engl J Med. 1985; 313: 1485–1492.
4. Tomblyn M, Lazarus HM. Donor lymphocyte infusions: the long and winding road: how should it be traveled? Bone Marrow Transplant. 2008; 42: 569–579.
5. HJ Kolb, J Mittermüller, C Clemm, E Holler, G Ledderose, et al. Donor leukocyte transfusions for treatment of recurrent chronic myelogenous leukemia in marrow transplant patients. Blood. 1990; 76: 2462–2465.
6. Porter D, Levine JE. Graft-versus-host disease and graft-versus-leukemia after donor leukocyte infusion. Semin Hematol. 2006; 43: 53–61.
7. Heslop HE, Brenner MK, Rooney CM. Donor T cells to treat EBV-associated lymphoma. N Engl J Med. 1994; 331: 679–680.
8. Mark E Dudley, John R Wunderlich, Paul F Robbins, James C Yang, Patrick Hwu, et al. Cancer regression and autoimmunity in patients after clonal repopulation with antitumor lymphocytes. Science. 2002; 298: 850–854.
9. C Yee, JA Thompson, D Byrd, SR Riddell, P Roche, et al. Adoptive T cell therapy using antigen-specific CD8+ T cell clones for the treatment of patients with metastatic melanoma: in vivo persistence, migration, and antitumor effect of transferred T cells. Proceedings of the National Academy of Sciences of the United States of America. 2002; 99: 16168–16173.
10. Houssem Benlalam, Virginie Vignard, Amir Khammari, Annabelle Bonnin, Yann Godet, et al. Infusion of Melan-A/Mart-1 specific tumor-infiltrating lymphocytes enhanced relapse-free survival of melanoma patients. Cancer immunology, immunotherapy : CII. 2007; 56: 515–526.
11. SA Rosenberg, JR Yannelli, JC Yang, SL Topalian, DJ Schwartzentruber,et al. Treatment of patients with metastatic melanoma with autologous tumor-infiltrating lymphocytes and interleukin 2. J Natl Cancer Inst. 1994; 86: 1159–1166.
12. RS Freedman, CL Edwards, JJ Kavanagh, AP Kudelka, RL Katz, et al. Intraperitoneal adoptive immunotherapy of ovarian carcinoma with tumor-infiltrating lymphocytes and

low-dose recombinant interleukin-2: a pilot trial. J Immunother Emphasis Tumor Immunol. 1994; 16: 198–210.
13. K Fujita, H Ikarashi, K Takakuwa, S Kodama, A Tokunaga, et al. Prolonged disease-free period in patients with advanced epithelial ovarian cancer after adoptive transfer of tumor-infiltrating lymphocytes. Clin Cancer. 1995; 1: 501–507.
14. Niels Junker, Mads Hald Andersen, Lynn Wenandy, Sarah Louise Dombernowsky, Katalin Kiss, et al. Bimodal ex vivo expansion of T cells from patients with head and neck squamous cell carcinoma: a prerequisite for adoptive cell transfer. Cytotherapy. 2011; 13: 822-834.
15. Magnus Pedersen, Marie Christine Wulff Westergaard, Katy Milne, Morten Nielsen, Troels Holz Borch, et al. Adoptive cell therapy with tumor-infiltrating lymphocytes in patients with metastatic ovarian cancer: a pilot study. OncoImmunology. 2018; 7: e1502905.
16. Mark E Dudley, James C Yang, Richard Sherry, Marybeth S Hughes, Richard Royal, et al. Adoptive cell therapy for patients with metastatic melanoma: evaluation of intensive myeloablative chemoradiation preparative regimens. J Clin Oncol. 2008; 26: 5233–5239.
17. James Larkin, Vanna Chiarion-Sileni, Rene Gonzalez, Jean-Jacques Grob, Piotr Rutkowski, et al. Five-Year Survival with Combined Nivolumab and Ipilimumab in Advanced Melanoma. N Engl J Med. 2019; 381: 1535–1546.
18. Joachim Stoltenborg Granhøj, Agnete Witness Præst Jensen, Mario Presti, Özcan Met, Inge Marie Svane, et al. Tumor-infiltrating lymphocytes for adoptive cell therapy: recent advances, challenges, and future directions. Expert Opinion on Biological Therapy. 2022; 22: 627–641.
19. Maartje W Rohaan, Troels H Borch, Joost H van den Berg, Özcan Met, Rob Kessels, et al. Tumor-Infiltrating Lymphocyte Therapy or Ipilimumab in Advanced Melanoma. N Engl J Med. 2022; 387: 2113–2125.
20. Derbinski J, Schulte A, Kyewski B, Klein L. Promiscuous gene expression in medullary thymic epithelial cells mirrors the peripheral self. Nat Immunol. 2001; 2: 1032–1039.
21. Richard A Morgan, Mark E Dudley, John R Wunderlich, Marybeth S Hughes, James C Yang, et al. Cancer regression

in patients after transfer of genetically engineered lymphocytes. Science. 2006; 314: 126–129.
22. Y Kuwana, Y Asakura, N Utsunomiya, M Nakanishi, Y Arata, et al. Expression of chimeric receptor composed of immunoglobulin-derived V resions and T-cell receptor-derived C regions. Biochemical and Biophysical Research Communications. 1987; 149: 960–968.
23. Gross G, Waks T, Eshhar Z. Expression of immunoglobulin-T-cell receptor chimeric molecules as functional receptors with antibody-type specificity. Proceedings of the National Academy of Sciences of the United States of America. 1989; 86: 10024–10028.
24. Eshhar Z, Waks T, Gross G, Schindler DG. Specific activation and targeting of cytotoxic lymphocytes through chimeric single chains consisting of antibody-binding domains and the gamma or zeta subunits of the immunoglobulin and T-cell receptors. Proceedings of the National Academy of Sciences of the United States of America. 1993; 90: 720–724.
25. Jena B, Dotti G, Cooper LJ. Redirecting T-cell specificity by introducing a tumor-specific chimeric antigen receptor. Blood. 2010; 116: 1035–1044.
26. Cor HJ Lamers, Stefan Sleijfer, Arnold G Vulto, Wim HJ Kruit, Mike Kliffen, et al. Treatment of metastatic renal cell carcinoma with autologous T-lymphocytes genetically retargeted against carbonic anhydrase IX: first clinical experience. J Clin Oncol. 2006; 24: e20-22.
27. Richard A Morgan, James C Yang, Mio Kitano, Mark E Dudley, Carolyn M Laurencot,et al. Case report of a serious adverse event following the administration of T cells transduced with a chimeric antigen receptor recognizing ERBB2. Mol Ther. 2010; 18: 843–851.
28. June CH, O'Connor RS, Kawalekar OU, Ghassemi S, Milone MC. CAR T cell immunotherapy for human cancer. Science. 2018; 359: 1361–1365.
29. Gavin M Bendle, Carsten Linnemann, Anna I Hooijkaas, Laura Bies, Moniek A de Witte, et al. Lethal graft-versus-host disease in mouse models of T cell receptor gene therapy. Nature medicine. 2010; 16: 565–570, 1p following 570.
30. Jürgen Kuball, Michelle L Dossett, Matthias Wolfl, William

Y Ho, Ralf-Holger Voss, et al. Facilitating matched pairing and expression of TCR chains introduced into human T cells. Blood. 2007; 109: 2331–2338.
31. Sachiko Okamoto, Junichi Mineno, Hiroaki Ikeda, Hiroshi Fujiwara, Masaki Yasukawa, et al. Improved expression and reactivity of transduced tumor-specific TCRs in human lymphocytes by specific silencing of endogenous TCR. Cancer Research. 2009; 69: 9003–9011.
32. Yin Y, Li Y, Kerzic MC, Martin R, Mariuzza RA. Structure of a TCR with high affinity for self-antigen reveals basis for escape from negative selection. Embo J. 2011; 30: 1137–1148.
33. Daphné A Schmid, Melita B Irving, Vilmos Posevitz, Michael Hebeisen, Anita Posevitz-Fejfar, et al. Evidence for a TCR affinity threshold delimiting maximal CD8 T cell function. Journal of immunology (Baltimore, Md. : 1950). 2010; 184: 4936–4946.
34. Yangbing Zhao, Alan D Bennett, Zhili Zheng, Qiong J Wang, Paul F Robbins, et al. High-affinity TCRs generated by phage display provide CD4+ T cells with the ability to recognize and kill tumor cell lines. Journal of immunology (Baltimore, Md. : 1950). 2007; 179: 5845–5854.
35. Sharyn Thomas, Shao-An Xue, Charles RM Bangham, Bent K Jakobsen, Emma C Morris, et al. Human T cells expressing affinity-matured TCR display accelerated responses but fail to recognize low density of MHC-peptide antigen. Blood. 2011; 118: 319–329.
36. Florence A Castelli, Cécile Buhot, Alain Sanson, Hassane Zarour, Sandra Pouvelle-Moratille, et al. HLA-DP4, the most frequent HLA II molecule, defines a new supertype of peptide-binding specificity. Journal of immunology (Baltimore, Md. : 1950). 2002; 169: 6928–6934.
37. Mark R Middleton, Cheryl McAlpine, Victoria K Woodcock, Pippa Corrie, Jeffrey R Infante, et al. Tebentafusp, A TCR/Anti-CD3 Bispecific Fusion Protein Targeting gp100, Potently Activated Antitumor Immune Responses in Patients with Metastatic Melanoma. Clin Cancer Res. 2020; 6: 5869–5878.
38. Garber K. Driving T-cell immunotherapy to solid tumors. Nat Biotechnol. 2018; 36: 215–219.

39. Jun Huang, Mario Brameshuber, Xun Zeng, Jianming Xie, Qi-jing Li, et al. A single peptide-major histocompatibility complex ligand triggers digital cytokine secretion in CD4(+) T cells. Immunity. 2013; 39: 846–857.
40. Chandran SS, Klebanoff CA. T cell receptor-based cancer immunotherapy: Emerging efficacy and pathways of resistance. Immunol Rev. 2019; 290: 127–147.
41. Shafer P, Kelly LM, Hoyos V. Cancer Therapy With TCR-Engineered T Cells: Current Strategies, Challenges, and Prospects. Front Immunol. 2022; 13: 835762.
42. Tran E. T-Cell Transfer Therapy Targeting Mutant KRAS in Cancer. N Engl J Med. 2016; 375: 2255–2262.
43. Veatch JR. Tumor-infiltrating BRAFV600E-specific CD4+ T cells correlated with complete clinical response in melanoma. J Clin Invest. 2018; 128: 1563–1568.
44. David S Hong, Brian A Van Tine, Swethajit Biswas, Cheryl McAlpine, Melissa L Johnson, et al. Autologous T cell therapy for MAGE-A4+ solid cancers in HLA-A*02+ patients: a phase 1 trial. Nat Med. 2023; 29: 104–114.
45. Labbé RP, Vessillier S, Rafiq Q. A. Lentiviral Vectors for T Cell Engineering: Clinical Applications, Bioprocessing and Future Perspectives. Viruses. 2021; 13: 1528.
46. Strayer DS. Viral gene delivery. Expert Opin Investig Drugs. 1999; 8: 2159–2172.
47. Ghassemi S. Rapid manufacturing of non-activated potent CAR T cells. Nat Biomed Eng. 2022; 6: 118–128.
48. Stadtmauer EA. CRISPR-engineered T cells in patients with refractory cancer. Science. 2020; 367: eaba7365.
49. Susan P Foy, Kyle Jacoby, Daniela A Bota, Theresa Hunter, Zheng Pan, et al. Non-viral precision T cell receptor replacement for personalized cell therapy. Nature. 2023; 615: 687–696.
50. Wagner DL, Koehl U, Chmielewski M, Scheid C, Stripecke R. Review: Sustainable Clinical Development of CAR-T Cells - Switching From Viral Transduction Towards CRISPR-Cas Gene Editing. Front Immunol. 2022; 13: 865424.
51. Jonas Kath, Weijie Du, Alina Pruene, Tobias Braun, Bernice Thommandru, et al. Pharmacological interventions enhance virus-free generation of TRAC-replaced CAR T cells. Mol

Ther Methods Clin Dev. 2022; 25: 311–330.
52. Partow Kebriaei, Harjeet Singh, M Helen Huls, Matthew J Figliola, Roland Bassett, et al. Phase I trials using Sleeping Beauty to generate CD19-specific CAR T cells. J Clin Invest. 2016; 126: 3363–3376.
53. Chiara F Magnani, Giuseppe Gaipa, Federico Lussana, Daniela Belotti, Giuseppe Gritti, et al. Sleeping Beauty-engineered CAR T cells achieve antileukemic activity without severe toxicities. J Clin Invest. 2020; 130: 6021–6033.
54. Sabrina Prommersberger, Michael Reiser, Julia Beckmann, Sophia Danhof, Maximilian Amberger, et al. CARAMBA: a first-in-human clinical trial with SLAMF7 CAR-T cells prepared by virus-free Sleeping Beauty gene transfer to treat multiple myeloma. Gene Ther. 2021; 28: 560–571.
55. C Bonini, M Grez, C Traversari, F Ciceri, S Marktel, et al. Safety of retroviral gene marking with a truncated NGF receptor. Nature medicine. 2003; 9: 367–369.
56. Sebastian Newrzela, Kerstin Cornils, Zhixiong Li, Christopher Baum, Martijn H Brugman, et al. Resistance of mature T cells to oncogene transformation. Blood. 2008; 112: 2278–2286.
57. Fabio Ciceri, Chiara Bonini, Maria Teresa Lupo Stanghellini, Attilio Bondanza, Catia Traversari, et al. Infusion of suicide-gene-engineered donor lymphocytes after family haploidentical haemopoietic stem-cell transplantation for leukaemia (the TK007 trial): a non-randomised phase I-II study. Lancet Oncol. 2009; 10: 489–500.
58. K Birkholz, A Hombach, C Krug, S Reuter, M Kershaw, et al. Transfer of mRNA encoding recombinant immunoreceptors reprograms CD4+ and CD8+ T cells for use in the adoptive immunotherapy of cancer. Gene Ther. 2009; 16: 596–604.
59. Niels Schaft, Jan Dörrie, Ina Müller, Verena Beck, Stefanie Baumann, et al. A new way to generate cytolytic tumor-specific T cells: electroporation of RNA coding for a T cell receptor into T lymphocytes. Cancer immunology, immunotherapy : CII. 2006; 55: 1132–1141.
60. Gregory L Beatty, Andrew R Haas, Marcela V Maus, Drew A Torigian, Michael C Soulen, et al. Mesothelin-specific

chimeric antigen receptor mRNA-engineered T cells induce anti-tumor activity in solid malignancies. Cancer Immunol Res. 2014; 2: 112–120.

61. Yangbing Zhao, Edmund Moon, Carmine Carpenito, Chrystal M Paulos, Xiaojun Liu, et al. Multiple injections of electroporated autologous T cells expressing a chimeric antigen receptor mediate regression of human disseminated tumor. Cancer Research. 2010; 70: 9053–9061.
62. Antonio Di Stasi, Biagio De Angelis, Cliona M Rooney, Lan Zhang, Aruna Mahendravada, et al. T lymphocytes coexpressing CCR4 and a chimeric antigen receptor targeting CD30 have improved homing and antitumor activity in a Hodgkin tumor model. Blood. 2009; 113: 6392–6402.
63. Weiyi Peng, Yang Ye, Brian A Rabinovich, Chengwen Liu, Yanyan Lou, et al. Transduction of tumor-specific T cells with CXCR2 chemokine receptor improves migration to tumor and antitumor immune responses. Clin Cancer Res. 2010; 16: 5458–5468.
64. Hilde Almåsbak, Edith Rian, Hanna Julie Hoel, Martin Pulè, Sébastien Wälchli, et al. Transiently redirected T cells for adoptive transfer. Cytotherapy. 2011; 13: 629–640.
65. Gregory L Beatty, Mark H O'Hara, Simon F Lacey, Drew A Torigian, Farzana Nazimuddin, et al. Activity of Mesothelin-specific Chimeric Antigen Receptor T Cells Against Pancreatic Carcinoma Metastases in a Phase 1 Trial. Gastroenterology. 2018; 155: 29-32.
66. Julia Tchou, Yangbing Zhao, Bruce L Levine, Paul J Zhang, Megan M Davis, et al. Safety and Efficacy of Intratumoral Injections of Chimeric Antigen Receptor (CAR) T Cells in Metastatic Breast Cancer. Cancer Immunol Res. 2017; 5: 1152–1161.
67. Hanna Meister, Thomas Look, Patrick Roth, Steve Pascolo, Ugur Sahin, et al. Multifunctional mRNA-Based CAR T Cells Display Promising Antitumor Activity Against Glioblastoma. Clinical Cancer Research. 2022; 28: 4747–4756.
68. Yangbing Zhao, Zhili Zheng, Paul F Robbins, Hung T Khong, Steven A Rosenberg, et al. Primary human lymphocytes transduced with NY-ESO-1 antigen-specific

TCR genes recognize and kill diverse human tumor cell lines. J Immunol. 2005; 174: 4415–4423.
69. Nadia Mensali, Marit Renée Myhre, Pierre Dillard, Sylvie Pollmann, Gustav Gaudernack, et al. Preclinical assessment of transiently TCR redirected T cells for solid tumour immunotherapy. Cancer Immunol. Immunother. 2019; 68: 1235–1243.
70. Diana Campillo-Davo, Fumihiro Fujiki, Johan MJ Van den Bergh, Hans De Reu, Evelien LJM Smits, et al. Efficient and Non-genotoxic RNA-Based Engineering of Human T Cells Using Tumor-Specific T Cell Receptors With Minimal TCR Mispairing. Front Immunol. 2018; 9: 2503.
71. Sólrún Melkorka Maggadóttir, Gunnar Kvalheim, Patrik Wernhoff, Stein Sæbøe-Larssen, Mona-Elisabeth Revheim,et al. A phase I/II escalation trial design T-RAD: Treatment of metastatic lung cancer with mRNA-engineered T cells expressing a T cell receptor targeting human telomerase reverse transcriptase (hTERT). Frontiers in Oncology. 2022; 12.
72. Fan Yang, Xiaofang Zheng, Sarene Koh, Jianxi Lu, Jintao Cheng, et al. Messenger RNA electroporated hepatitis B virus (HBV) antigen-specific T cell receptor (TCR) redirected T cell therapy is well-tolerated in patients with recurrent HBV-related hepatocellular carcinoma post-liver transplantation: results from a phase I trial. Hepatol Int. 2023.
73. Paul F Robbins, Mark E Dudley, John Wunderlich, Mona El-Gamil, Yong F Li, et al. Cutting edge: persistence of transferred lymphocyte clonotypes correlates with cancer regression in patients receiving cell transfer therapy. Journal of immunology (Baltimore, Md. : 1950). 2004; 173: 7125–7130.
74. Michael H Kershaw, Jennifer A Westwood, Linda L Parker, Gang Wang, Zelig Eshhar, et al. A phase I study on adoptive immunotherapy using gene-modified T cells for ovarian cancer. Clin Cancer Res. 2006; 12: 6106–6115.
75. Jianping Huang, Hung T Khong, Mark E Dudley, Mona El-Gamil, Yong F Li, et al. Survival, persistence, and progressive differentiation of adoptively transferred tumor-reactive T cells associated with tumor regression. J

Immunother. 2005; 28: 258–267.
76. Victor Appay, John J Zaunders, Laura Papagno, Julian Sutton, Angel Jaramillo, et al. Characterization of CD4(+) CTLs ex vivo. Journal of immunology (Baltimore, Md. : 1950). 2002; 168: 5954–5958.
77. Pedro Romero, Alfred Zippelius, Isabel Kurth, Mikaël J Pittet, Cédric Touvrey, et al. Four functionally distinct populations of human effector-memory CD8+ T lymphocytes. Journal of immunology (Baltimore, Md. : 1950). 2007; 178: 4112–4119.
78. Peperzak V, Veraar EA, Keller AM, Xiao Y, Borst J. The Pim kinase pathway contributes to survival signaling in primed CD8+ T cells upon CD27 costimulation. Journal of immunology (Baltimore, Md. : 1950). 2010; 185: 6670–6678.
79. Xinglei Shen, Juhua Zhou, Karen S Hathcock, Paul Robbins, Daniel J Powell, Jr, et al. Persistence of tumor infiltrating lymphocytes in adoptive immunotherapy correlates with telomere length. J Immunother. 2007; 30: 123–129.
80. Daniel Hollyman, Jolanta Stefanski, Mark Przybylowski, Shirley Bartido, Oriana Borquez-Ojeda, et al. Manufacturing validation of biologically functional T cells targeted to CD19 antigen for autologous adoptive cell therapy. J Immunother. 2009; 32: 169–180.
81. Donald B Kohn, Gianpietro Dotti, Renier Brentjens, Barbara Savoldo, Michael Jensen, et al. CARs on track in the clinic. Mol Ther. 2011; 19: 432–438.
82. David L Porter, Bruce L Levine, Nancy Bunin, Edward A Stadtmauer, Selina M Luger, et al. A phase 1 trial of donor lymphocyte infusions expanded and activated ex vivo via CD3/CD28 costimulation. Blood. 2006; 107: 1325–1331.
83. Gattinoni L, Speiser DE, Lichterfeld M, Bonini C. T memory stem cells in health and disease. Nat. Med. 2017; 23: 18–27.
84. McLellan AD, Ali Hosseini Rad SM. Chimeric antigen receptor T cell persistence and memory cell formation. Immunol. Cell Biol. 2019; 97: 664–674.
85. Gattinoni L, Klebanoff CA, Restifo NP. Paths to stemness: building the ultimate antitumour T cell. Nat. Rev. Cancer. 2012; 12: 671–684.
86. Hannah M Knochelmann, Connor J Dwyer, Stefanie R

Bailey, Sierra M Amaya, Dirk M Elston, et al. When worlds collide: Th17 and Treg cells in cancer and autoimmunity. Cell. Mol. Immunol. 2018; 15: 458–469.
87. Jiali Sun, Leslie E Huye, Natalia Lapteva, Maksim Mamonkin, Manasa Hiregange,et al. Early transduction produces highly functional chimeric antigen receptor-modified virus-specific T-cells with central memory markers: a Production Assistant for Cell Therapy (PACT) translational application. J Immunother Cancer. 2015; 3: 5.
88. Daniela Nascimento Silva, Michael Chrobok, Giulia Rovesti, Katie Healy, Arnika Kathleen Wagner, et al. Process Development for Adoptive Cell Therapy in Academia: A Pipeline for Clinical-Scale Manufacturing of Multiple TCR-T Cell Products. Front Immunol. 2022; 13: 896242.
89. Nicoletta Cieri, Barbara Camisa, Fabienne Cocchiarella, Mattia Forcato, Giacomo Oliveira, et al. IL-7 and IL-15 instruct the generation of human memory stem T cells from naive precursors. Blood. 2013; 121: 573–584.
90. Daniela Pais Ferreira, Joana Gomes Silva, Tania Wyss, Silvia A Fuertes Marraco, Léonardo Scarpellino, et al. Central memory CD8+ T cells derive from stem-like Tcf7hi effector cells in the absence of cytotoxic differentiation. Immunity. 2020; 53: 985-1000.e11.
91. Philippe O Gannon, Petra Baumgaertner, Alexandre Huber, Emanuela M Iancu, Laurène Cagnon, et al. Rapid and Continued T-Cell Differentiation into Long-term Effector and Memory Stem Cells in Vaccinated Melanoma Patients. Clin Cancer Res. 2017; 23: 3285–3296.
92. Imran Siddiqui, Karin Schaeuble, Vijaykumar Chennupati, Silvia A Fuertes Marraco, Sandra Calderon-Copete, et al. Intratumoral Tcf1+PD-1+CD8+ T Cells with Stem-like Properties Promote Tumor Control in Response to Vaccination and Checkpoint Blockade Immunotherapy. Immunity. 2019; 50: 195-211.e10.
93. Luca Biasco, Natalia Izotova, Christine Rivat, Sara Ghorashian, Rachel Richardson, et al. Clonal expansion of T memory stem cells determines early anti-leukemic responses and long-term CAR T cell persistence in patients. Nat Cancer. 2021; 2: 629–642.
94. Deborah Meyran, Joe Jiang Zhu, Jeanne Butler, Daniela

Tantalo, Sean MacDonald, et al. TSTEM-like CAR-T cells exhibit improved persistence and tumor control compared with conventional CAR-T cells in preclinical models. Sci Transl Med. 2023; 15: eabk1900.

95. Reuben Benjamin, Charlotte Graham, Deborah Yallop, Agnieszka Jozwik, Oana C Mirci-Danicar, et al. Genome-edited, donor-derived allogeneic anti-CD19 chimeric antigen receptor T cells in paediatric and adult B-cell acute lymphoblastic leukaemia: results of two phase 1 studies. The Lancet. 2020; 396: 1885–1894.
96. Enli Liu, David Marin, Pinaki Banerjee, Homer A Macapinlac, Philip Thompson, et al. Use of CAR-Transduced Natural Killer Cells in CD19-Positive Lymphoid Tumors. N Engl J Med. 2020; 382: 545–553.
97. Kankeu Fonkoua LA, Sirpilla O, Sakemura R, Siegler EL, Kenderian SS. CAR T cell therapy and the tumor microenvironment: Current challenges and opportunities. Mol Ther Oncolytics. 2022; 25: 69–77.
98. Labanieh L, Mackall CL. CAR immune cells: design principles, resistance and the next generation. Nature. 2023; 614: 635–648.
99. Heintzman DR, Fisher EL, Rathmell JC. Microenvironmental influences on T cell immunity in cancer and inflammation. Cell Mol Immunol. 2022; 19: 316–326.
100. Christine E Brown, Darya Alizadeh, Renate Starr, Lihong Weng, Jamie R Wagner, et al. Regression of Glioblastoma after Chimeric Antigen Receptor T-Cell Therapy. N Engl J Med. 2016; 375: 2561–2569.
101. Nicholas A Vitanza, Adam J Johnson, Ashley L Wilson, Christopher Brown, Jason K Yokoyama, et al. Locoregional infusion of HER2-specific CAR T cells in children and young adults with recurrent or refractory CNS tumors: an interim analysis. Nat Med. 2021; 27: 1544–1552.
102. Robbie G Majzner, Sneha Ramakrishna, Kristen W Yeom, Shabnum Patel, Harshini Chinnasamy, et al. GD2-CAR T cell therapy for H3K27M-mutated diffuse midline gliomas. Nature. 2022; 603: 934–941.
103. Prasad S Adusumilli, Marjorie G Zauderer, Isabelle Rivière, Stephen B Solomon, Valerie W Rusch,et al. A Phase I Trial of Regional Mesothelin-Targeted CAR T-cell Therapy

in Patients with Malignant Pleural Disease, in Combination with the Anti-PD-1 Agent Pembrolizumab. Cancer Discov. 2021; 11: 2748–2763.

104. Maysoon Al-Haideri, Santalia Banne Tondok, Salar Hozhabri Safa, Ali Heidarnejad Maleki, Samaneh Rostami, et al. CAR-T cell combination therapy: the next revolution in cancer treatment. Cancer Cell International. 2022; 22: 365.

Book Chapter

Therapeutic Cancer Vaccines

Else Marit Inderberg

Translational Research Unit, Section for Cellular Therapy, Department of Oncology, Oslo University Hospital, Norway

***Corresponding Author:** Else Marit Inderberg, Translational Research Unit, Section for Cellular Therapy, Department of Oncology, Oslo University Hospital, Oslo, Norway

Published **May 30, 2023**

How to cite this book chapter: Else Marit Inderberg. Therapeutic Cancer Vaccines. In: Hussein Fayyad Kazan, editor. Immunology and Cancer Biology. Hyderabad, India: Vide Leaf. 2023.

Abstract

Therapeutic cancer vaccines were first tested clinically around three decades ago but failed to provide sufficient clinical benefits. These vaccines have undergone revival in recent years, particularly with the introduction of immune checkpoint inhibitor therapy. Their goal is to induce *de novo* immune responses or boost those already existing against cancer antigens to establish a long-term specific immunological memory. Ideally, this would be sufficient to eradicate the disease, which may occur in cases with a low tumour burden or high risk of relapse. With a higher tumour burden, therapeutic vaccines can stabilize the disease or, if combined with other therapies, induce

tumour regression and elimination. Here, we review different types of cancer vaccine platforms, types of target antigens and mechanisms that can lead to reduced efficacy, including both tumour-intrinsic and -extrinsic factors. Lastly, we will demonstrate how strategies for combining cancer vaccines with other immunomodulatory therapies may surmount tumour resistance mechanisms and improve clinical efficacy.

The Beginning of Immunotherapy

Non-specific immunotherapy dates back to at least 1774, when Dupré de Lisle, a Parisian physician, found that the cancer regressed as the infection became more severe after injecting pus into the leg of a patient with inoperable breast cancer [1]. Over a century later William Coley, a bone surgeon, noted that a sarcoma patient showed regression of his tumour after developing erysipelas, a superficial bacterial infection of the skin that is most often caused by *Streptococcus.* During the next 40 years, Coley treated numerous patients with a heat-killed bacterial vaccine containing extracts from *Streptococcus* and *Serratia.* Approximately half of the patients treated with "Coley's toxin" showed a good clinical responses [2]. Nonetheless, immunotherapy targeting tumour antigens is a preferred choice to limit toxicity to normal tissue>

There is an important distinction between preventive (prophylactic) and therapeutic cancer vaccines. Examples of preventive vaccines include the Human Papilloma virus (HPV) and the Hepatitis B virus (HBV) vaccines. These vaccines are designed to prevent the infection itself and thereby associated cervical or hepatocellular cancers, respectively (reviewed in [3]). Preventive vaccines will not be treated here; however, there are also therapeutic cancer vaccines that target viral or bacterial antigens in these cancers. The first preventive vaccine approved for cancer therapy was the Bacillus Calmette-Guérin (BCG, TheraCys®, TICE®) vaccine. Originally used for the prevention of tuberculosis, and therefore based on a live attenuated strain of *Mycobacterium bovis*, the vaccine replaced cystectomy as the treatment of choice for *in situ* bladder carcinoma in the mid-1980s. The BCG vaccine has been shown to reduce the risk of

recurrence, and maintenance therapy reduces the risk of progression in non–muscle invasive bladder cancer [4,5].

The Mechanism of Action of Therapeutic Cancer Vaccines

The immune response against cancer depends on T cells that can recognise antigens, peptides, or degraded proteins from cancer cells, which differ from or are overexpressed compared to in normal cells. Cancer cells are characterized by genetic alterations and abnormal cell growth [6].

These genetic alterations give rise to neoantigens and expression of differentiation antigens or cancer germline antigens, which can be degraded into peptides presented on major histocompatibility complex (MHC) class I molecules on the surface of cancer cells.

Boon and colleagues showed that these were recognised by CD8 T cells in cancer patients [7,8]. However, this antitumour immunity was mostly insufficient to control the tumours. Cancer immune editing demonstrates how cancer cells evolve to escape the immune system by downregulating the expression of T cell targets or MHC class I molecules [9,10].

Therapeutic cancer vaccines aim to generate de novo responses against such antigens or boost pre-existing anti-tumour reactive T cell responses. For a successful antitumour response, a series of events must occur, also termed the cancer immunity cycle [11]. Cancer cell antigens are released due to cancer cell death and can be captured by dendritic cells (DC), which are optimal antigen presenting cells (APC). These, in turn, process and present antigens to both CD8+ T cells on MHC class I and CD4+ T cells on MHC class II in the lymph nodes, leading to increased frequencies of specific T cells. These tumour-reactive T cells will then leave the lymph nodes and circulate to infiltrate the tumour elsewhere in the body. The killing of new cancer cells by these T cells will in turn create a second wave of immunity, with the release of new cancer antigens and a broadening of the immune system which can recognise a larger repertoire of

antigens, a process called epitope or determinant spreading [12–14]. In cancer patients, this process is not optimal due to the numerous resistance mechanisms. However, vaccination can enhance the priming and activation of tumour-specific T cells, providing replenishment of tumour-specific T cells, which can boost the cancer immune cycle.

The first vaccines approved were Oncophage (Vitespen) in Russia in 2008, a personalised cancer vaccine for renal cell carcinoma based on the autologous tumour-derived gp96 heat shock protein-peptide complex (HSPPC-96) [15], and Provenge. Provenge (sipuleucel-T) is an autologous cellular immunotherapy indicated for the treatment of asymptomatic or minimally symptomatic metastatic castrate-resistant (hormone-refractory) prostate cancer and was the first FDA-approved therapeutic cancer vaccine in 2010 [16].

Tumour Specificity and Target Antigens

A vaccine antigen should ideally be expressed exclusively in cancer cells, be essential for cancer cell survival, and be highly immunogenic. Target tumour antigens include a variety of mutated antigens and shared non-mutated, but aberrantly expressed, self-antigens (Table 1). Neoantigens or mutated antigens are generated due to the inherent genomic instability of a cancer which can harbour over 20 000 mutations [17]. These neoantigens are often unique, that is, they are expressed by a particular cancer cell in a particular patient and are therefore not easily defined or targeted. There are, however, "hotspots" for mutations, leading to neoantigens being expressed by a large number of tumours. These hotspots represent the key regulatory genes that are important in carcinogenesis. In microsatellite instable (MSI) tumours, as in the case of Lynch syndrome, patients have hereditary defects in DNA mismatch repair genes and early onset of a variety of cancers, such as colon adenocarcinoma. In MSI-positive colon cancer genes, transforming growth factor beta receptor II (TGFβRII) harbors frameshift mutations in approximately 90% of patients [18–20]. The immune system has generally not developed tolerance against these neoantigens as they are different from "self".

Nevertheless, as human tumours generally take years to develop to the stage where they clinically manifest, the patient's immune system will have been exposed to these neoantigens for several years and could become tolerant.

Differentiation antigens are expressed in both normal and malignant cells but are often overexpressed in tumour cells. These antigens are generally shared between patients and have been targets of cancer vaccination due to their broad applicability. Examples include the melanocyte antigens Melan-A/MART-1, tyrosinase first identified by Boon and colleagues [21,22] and gp100, identified by Bakker *et al* [23]. The repertoire of T cells specific for these antigens is often weak due to established tolerance, which, if broken, could cause autoimmunity [24].

Cancer germline or cancer testis (CT) antigens are antigens whose expression is essentially restricted to malignant cells, apart from the testis, placenta, and occasionally ovaries. Many CT antigens have been discovered through the identification of specific T cells from patients or screening for autoantibodies in patient sera using the SEREX (serological identification of antigens by recombinant expression cloning) technology [25], implying that there must be an interaction between APCs, antibody-producing B cells, and T cells. The MAGE family [26–28], SSX [29] and NY-ESO-1 [30,31] are well-known examples of these types of antigens.

Overexpressed antigens are those whose expression exists in normal tissue, but their expression is restricted to some tissues and is generally low or transient in these tissues. As these are self-antigens, immunological tolerance to these antigens is normally high, but they are expressed at high frequency. One example is the reverse transcriptase subunit of telomerase (hTERT), which is overexpressed in 85-90% of human tumours [32–34] and absent in most normal adult tissues except stem cells, germ cells, and transiently in proliferating lymphocytes [35,36]. There is immunological tolerance against these overexpressed antigens, but this has been shown to be easily

broken naturally, as evidenced by spontaneous immunity or vaccination [37–39].

Additionally, molecules present on the tumour cell surface can carry posttranslational modifications to proteins that differ from normal cells, such as aberrantly glycosylated or phosphorylated antigens that can be recognized by the immune system and have now reached clinical trials [40–42].

It has been known for many decades that infectious agents can be present in tumours and involved in tumourigenesis [43,44]. Many preventive vaccines have been developed against these infectious agents; however, some are also targeted by therapeutic vaccines. One of the best-known examples is vaccines targeting Human Papilloma virus (HPV) in cervical cancer [45,46]. These antigens are truly foreign to the immune system and are, thus, excellent targets for vaccination.

Table 1:

Antigen type	Antigens	Targets for vaccination	Type of therapeutic vaccine
Overexpressed antigens	hTERT, survivin, HER2, MUC1, mesothelin	Yes	Peptide vaccine, DC-based vaccines
Differentiation antigens	gp100, MART1, tyrosinase, PSA, PAP	Yes	Peptide vaccine, DC-based vaccines
Cancer germline/CT antigens	MAGEA1–4, NY-ESO-1, PRAME, SSX2	Yes	Peptide vaccine, DC-based vaccines, protein
Neoantigens	KRAS, EGFR variant III, TGFβRII, private/unique antigens	Yes	Peptides, protein, DC-based vaccines, mRNA
Post-translationally modified (e.g glyco- or phosphopeptides)	phosphorylated BCAR3 peptide, O-GlcNAc peptides	Yes	Peptide vaccines
Viral/bacterial antigens	HPV, HBV, CMV, BCG	Yes	Peptide vaccines, DC-based vaccines, DNA vaccines

An ideal target antigen for a vaccine should be indispensable to tumour cells and be expressed at a relatively high frequency in the patient population. This implies that the target antigen has an essential role in tumour growth, survival, or progression and that if antigen loss variants occur, the tumour cells would have markedly impaired tumorigenic potential [47].

Vaccine Platforms

A number of improvements to vaccine platforms, adjuvants, and delivery systems have been made in recent years. A basic overview of vaccine strategies is shown in Figure 1. For vaccine efficacy, it is essential to ensure the delivery of vaccine antigens to the right compartment and in the right context.

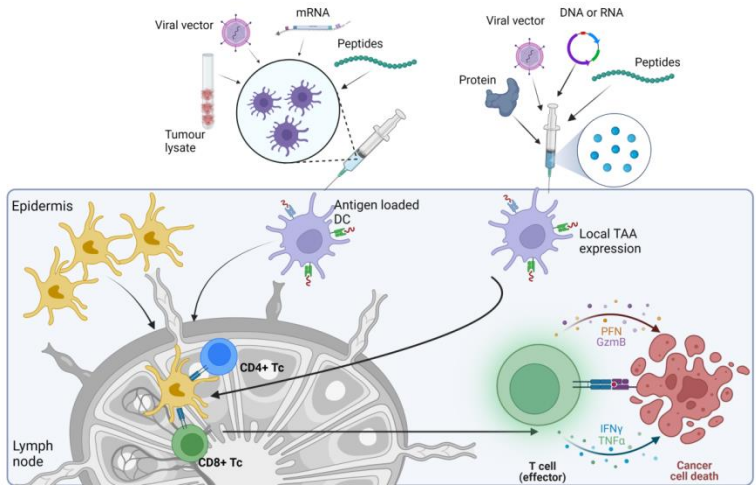

Figure 1: Strategies for cancer vaccination. Created using BioRender.

Peptide Vaccines

The first peptide vaccine against cancer was tested clinically in the 1990s. One of the first vaccines against mutant p21 ras in five pancreatic adenocarcinoma patients induced detectable T-cell responses in 2/5 patients [48]. The patients were vaccinated with autologous PBMCs loaded overnight with a long synthetic

Ras peptide containing a mutation corresponding to that identified in their tumour. However, the T-cell responses seen in peripheral blood were transient. Peptides are generally easy to synthesize, produce clinical-grade, safe, and can be combined with a vaccine adjuvant. Short peptides (typically 8-10 amino acids) bind MHC class I molecules and induce CD8+ T cell responses, whereas longer peptides (typically 12-15 amino acids) can bind MHC class II molecules on antigen-presenting cells and induce CD4 T cell responses [49]. Numerous clinical trials of therapeutic vaccination have been conducted but gave clinical benefits only in a minority of patients. Most of the early trials used minimal T cell epitopes binding MHC class I molecules, however, this was also shown to lead to immunotolerance against vaccine peptides [50,51]. Short peptides can bind exogenously to MHC I molecules on all nucleated cells that express these molecules. In preclinical experiments this was found to cause general antigen presentation without proper co-stimulation or adjuvant stimuli. In comparison, synthetic long peptides (SLP) (typically [25-35] amino acids long) must be taken up by antigen presenting cells and processed before they can be presented on MHC class I and MHC class II molecules. This can only be performed by professional antigen-presenting cells like dendritic cells (DC), which can ensure optimal peptide presentation and T-cell stimulation [52–54].

SLP vaccines have demonstrated efficacy in HPV-16-induced cancers [55].

Vaccination-Site Sequestration

A non-persisting vaccine formulation shifted T cell localization toward tumors, inducing superior antitumor activity, while reducing systemic T-cell dysfunction, and promoting memory formation. These data show that persisting vaccine depots can induce specific T cell sequestration, dysfunction, and deletion at vaccination sites [56]. Hailemichael and colleagues suggested the use of adjuvants such as Granulocyte-Macrophage Colony-stimulating factor (GM-CSF) or poly-ICLC (Hiltonol®) not creating the depot effect for short peptides could avoid this sequestration of CD8 T cells. However, this has only been

demonstrated in mouse models and others have shown detectable circulating and tumour-infiltrating vaccine-specific T cells after vaccination protocols [57,58].

DNA and RNA Vaccines

DNA vaccines are plasmids encoding TAAs that induce de novo or increasing T-cell responses against cancer cells carrying the same TAAs. DNA vaccines can also stimulate innate immune responses through DNA-sensing pathways in the cytosol of transfected cells because of their CpG motifs and double-stranded structures. They are perceived by the immune system as "danger signals" (reviewed in [59]). Examples of more advanced DNA-based cancer vaccines are: 1) the therapeutic antigen-presenting cell-targeting DNA vaccine VB10.16 tested in patients with HPV16-positive high-grade cervical intraepithelial neoplasia [60]. The vaccine induced strong HPV-16 specific T cell responses and the IFN-γ response, and the lesion size reduction was correlated. 2) Another DNA vaccine encoding rhesus prostate-specific antigen was delivered by intradermal electroporation in patients with relapsed prostate cancer [61]. The vaccine was immunogenic; however, no clinical response was observed. 3) VXM01 is a cancer vaccine based on live attenuated Salmonella bacteria carrying an expression plasmid, encoding VEGFR-2 and has been tested in advanced pancreatic cancer. Vaccine-specific T cell responses significantly are correlated with reduced tumour perfusion and high levels of pre-existing VEGFR2-specific T cells [62]. The vaccine was also tested in progressive glioblastoma patients [63]. The vaccine was shown to be safe, and specific immune responses in blood, as well as an increased CD8/Treg ratio in tumour tissue after vaccination could be detected. One out of fourteen patients had an objective response. VXM01 is currently being tested in combination with anti-PD-L1 in the same patient group (NCT03750071) [64]. 4) Finally, a telomerase-based DNA vaccine, INVAC-1, was recently tested in patients with relapsed or refractory solid tumors [65]. The vaccine was safe and immunogenic, inducing both CD4+ and CD8+ T-cell responses, and nearly 60% of the patients experienced disease stabilisation.

RNA used on its own or packaged into liposomes has been in development for numerous years but has not been extensively used until relatively recently under the SARS-CoV2 pandemic when they were distributed at a very large scale [66,67]. RNA vaccines have been used in combination with immune checkpoint inhibitors (ICI) and have been shown to reverse ICI resistance in melanoma patients [68]. This will definitely be seen in future clinical testing of therapeutic cancer vaccines.

Cellular Vaccines

Modified whole tumour cell vaccines have been used for cancer vaccination. Their advantage is that these cells are a source of all potential tumour antigens, not only one or a handful of selected tumour antigens [69]. Cancer cells modified to secrete GM-CSF is one approach tested in numerous cancer types, in both preclinical models and patients. Recently, a phase II clinical study with this type of vaccine, GVAX, was performed in mismatch repair proficient colorectal cancer patients, in combination with chemotherapy and the immune checkpoint inhibitor anti- Programmed cell death protein 1(PD-1) [70]. No objective clinical responses were seen, but a subset of patients demonstrated biochemical responses (decrease in plasma carcinoembryonic antigen (CEA) levels) indicating that the vaccine modulated the anti-tumour immune response.

The production of dendritic cell (DC) vaccines entails personalised vaccine production [71]. DCs are the optimal antigen presenting cells and therefore essential in inducing immunity against cancer [72].

Cellular vaccines use either killed/modified cancer cells or autologous antigen presenting cells (APCs) that have been loaded with cancer antigens in the form of peptides, mRNA or viral constructs [73–76]. Dendritic cell (DC) vaccines have been shown to induce strong immune responses in several cancers, but are more effective in and adjuvant setting, preventing relapse or in patients with low tumour burden (Figure 2) [77–79].

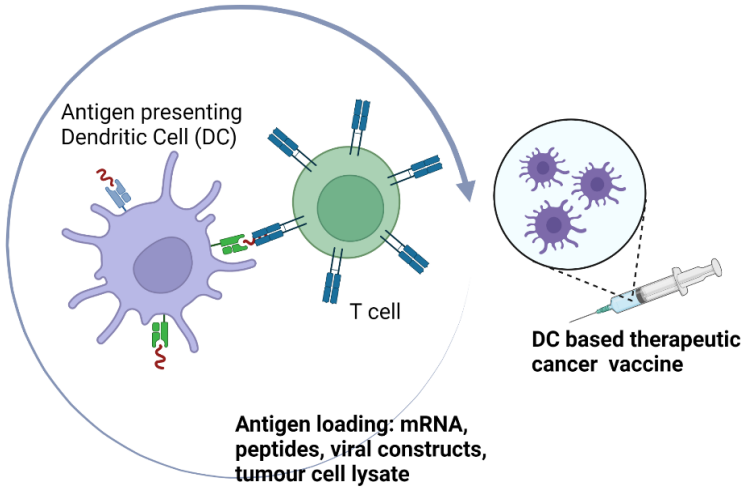

Figure 2: Dendritic cells (DC) are the optimal antigen presenting cells. Created using BioRender.

Provenge (Sipuleucel-T) was the first US Food and Drug administration (FDA) - and European Medicines Agency (EMA)-approved therapeutic cancer vaccine in 2010. The vaccine, consisting of monocyte-derived, matured DCs modified to express prostate acid phosphatase (PAP) and GM-CSF, was approved after demonstrating a modest, but significantly survival advantage of 4.1 months in metastatic castrate-resistant prostate cancer patients compared to the placebo group [80]. However, logistically the vaccine is hard to produce and administer to the patient and is not in use at a large scale. If a vaccine can be produced and several batches frozen down for future vaccination, the logistics are easier. However, a certain infrastructure is still required for storage and thawing for administration of these cell-based vaccines.

Recently, DC vaccines have also been used for prophylactic vaccine treatment of Lynch syndrome carriers who due to deficiency in the DNA mismatch repair mechanisms have a very high risk of developing cancer [81]. In an ongoing trial (NCT01885702), Lynch syndrome carriers are vaccinated, with autologous DCs loaded with a CD8 T cell epitope from the frameshift mutated transforming growth factor beta receptor II

(TGFβRII). The clinical results will take time to collect as the aim is cancer prevention, however, the vaccine seems safe and efficient at inducing immune responses in healthy carriers [82].

Novel Platforms and Adjuvants

Effective vaccines are normally dependent on good adjuvants. These are not required for administration with DC vaccines, as the DCs should have been matured often using some of the same danger signals and are optimal APCs.

Nucleic acid based vaccines can provide danger signals of their own, e,g. through the stimulator of interferon genes (STING pathway) for DNA sensing and can provide deep remodelling of the TME [83,84]. Several novel agents for stimulating this important pathway are in preclinical and clinical development [85]. Examples are the direct linkage of peptide vaccines with Toll-like receptor (TLR) ligand 1/2 as adjuvants [86–89]. A multipeptide melanoma vaccine was found to be more efficient when administered with the TLR7 agonist imiquimod than without, but also caused increased systemic toxicity [90].

Vaccines can be packed into nanoparticles and targeted to specific sites like the lymph nodes where they can be taken up by DCs which will stimulate T cell responses [91,92]. Further developments in this field could lead to more controlled and targeted vaccination strategies.

Finally, cellular vaccines are costly and time-consuming to manufacture. Instead, the use of nanosized, artificial APCs of biodegradable polymers has been pioneered [93]. In addition to easier manufacturing, artificial APCs may be influenced by the TME and signalling moieties may present on their surface in contrast to natural, cellular APCs. The artificial presentation of antigens enables more defined systems with improved control over the signals presented, but on the other hand artificial APCs are not equipped to actively migrate into tissues and will need the addition of targeting moieties. It was recently shown that their topology (size and shape, functionality, and ligand density) determine optimal artificial APC-T cell interaction and

subsequent T cell activation [94]. Further development is required for the optimal artificial APC, but this is a highly promising approach.

Personalized Treatment

Recent technological advances in sequencing and bioinformatics have made highly personalized cancer vaccines available which are customized to each patient's cancer. This is still resource- and time-demanding and can only be achieved in very institutes. Furthermore, numerous tumours have low TMB and less suitable for neoantigen vaccines [95]. For patients in this category vaccines targeting shared antigens may be a better option. Vaccines could also be combined with other treatments. Recently an mRNA vaccine targeting four shared TAAs combined with immune checkpoint blockade (ICB) therapy (anti-PD-L1) in ICB-refractory melanoma patients demonstrated the induction of type I IFN resulting in T cell recruitment, vaccine-specific T cell responses and reversal of ICB resistance [68].

Other groups combine shared antigen and neoantigen approaches and shown successful induction of immune responses, but as some of these early trials have been in advanced, hard-to-treat-cancers like glioblastoma, clinical responses have been difficult to obtain [96–100]. This type of vaccine requires efficient and extensive logistics, but may be feasible at a larger scale with new technology [101].

Importance of both MHC class I and II Epitopes

As mentioned previously, initial vaccines focused on CD8 T cell epitopes. However, CD4+ cells play a critical role in both initiation and maintenance of the cytotoxic response of CD8 T cells (reviewed in [102]). The cancer vaccine should therefore incorporate T helper epitopes as well as cytotoxic T cell epitope for the induction of a strong and durable T cell response [103–105].

Vaccination with cytotoxic T-cell epitopes have been shown to be more effective if the vaccine includes helper epitopes from the same protein(s) as for the CD8 T cell target rather than against a non-specific helper epitope [106]. Recent evidence has underlined the importance of CD4 T cells by demonstrating that immune checkpoint inhibitors work better if the tumour intrinsically expresses MHC class II [107].

TME and Resistance Mechanisms

The TME can vary from one cancer to another; however, the TME in established solid cancer is generally immunosuppressive. The tumour recruits cells to support its growth and escape the immune response. Despite the induction of an immune response in the periphery and even an initial clinical response to vaccination, the TME may tip the balance in the favour of the tumour and inhibit the ongoing immune response (Figure 3). Tumour cells can downregulate HLA class I as an escape mechanism, becoming invisible to CD8 T cells [108,109]. By doing so they become more sensitive to NK cell attack, however, the TME has also been found to contain corrupted, immunosuppressive NK cells.

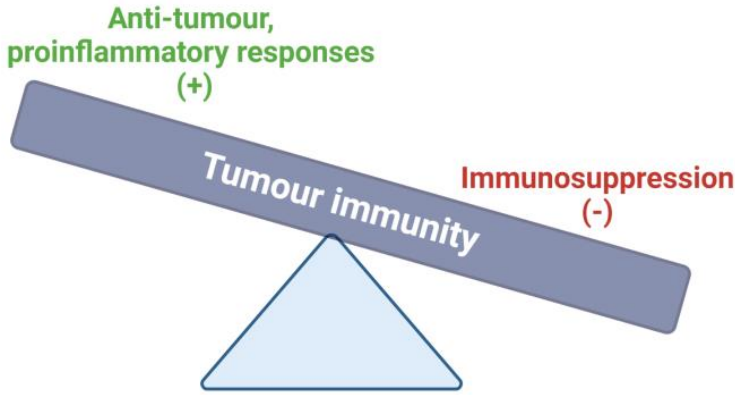

Figure 3: Anti-tumour immunity and immunosuppression. Created using BioRender.

Tumour cells interact closely with non-malignant cells, creating a complex and dynamic interplay in the local environment in which the tumour develops and grows. Myeloid cells, in particular tumour-associated macrophages (TAMs), are often abundant in the TME. Most TAMs are infiltrating immune cells that originate from monocytes. Other myeloid-derived cells are represented by infiltrating DCs, monocytes, neutrophils, and the less defined myeloid-derived suppressor cells (MDSCs). Tumour-infiltrating MDSCs promote tumour growth and suppression of lymphocytes through the expression of several molecules, such as programmed death-ligand 1(PD-L1), indoleamine 2, 3-dioxygenase (IDO), arginase 1 (ARG1), nitric oxide (NO), reactive oxygen species (ROS), IL-10 and TGF-β [110]. Elevated MDSC infiltration has been shown to correlate with poor OS and PFS in patients with solid tumours [111].

Tumour-specific CD8 cytotoxic T cells (CTLs) and CD4 helper T cells (Th); are important, but a variable proportion of CD4 T cells can be regulatory (Treg) and contribute to tumour cell growth.

The TME is an extremely complex ecosystem where tumour cells and other non-malignant cells interact and can have both anti-tumoural and pro-tumoural effects. They influence each other through the release of cytokines, chemokines, growth factors, metabolites and soluble factors, which continuously remodel the TME and create an immunosuppressive and dynamic milieu that supports tumour growth, adaption, and invasion. This contributes to tumour escape and therapy resistance.

Extracellular Matrix (ECM) and Cancer-Associated Fibroblasts (CAF)

Solid cancers consist not only of tumour cells, but are complex structures of stromal cells, immune cells, vasculature, and ECM. The ECM regulates the tumour cell growth and response to therapy.

In many tumours, the ECM can make up 60% of the tumour mass and produce high levels of proteins including collagens, fibronectin, elastin, and laminins (reviewed in [112]). Source of these ECM molecules are the tumour cells themselves, but to an even larger extent also cancer-associated fibroblasts (CAFs) which often take on a pro-tumorigenic role, but their defined function is still largely unknown (reviewed in [113]). Further knowledge about the ECM and CAFs could facilitate the development of novel diagnostic and therapeutic approaches to increase clinical responses in solid tumour.

The increased focus on and understanding of the biology of the TME and the relatively low clinical response rates for cancer vaccines in advanced cancer has led to a number of cancer vaccines being tested in combination with other types of conventional treatment or immunotherapy.

Combination Therapies

Whilst cancer vaccines have a place in cancer treatment, we have now learnt that they are not very efficacious as monotherapy in advances cancers but can be applied early in treatment to prevent relapse or in combination with other therapies that will increase clinical efficacy. In the landmark study of anti-CTLA4 treatment in melanoma, one patient cohort received ipililumab in combination with a gp100 peptide vaccine [114]. The combination treatment showed no improvement; the patients fared worse than in the group that received ipilimumab monotherapy. This may have been due to either the vaccination schedule, immunogenicity of the vaccine, or the use of short epitope in Montanide™, giving the vaccine depot effect and sequestration of antigen-specific T cells. Later studies have shown that this combination can be effective, albeit so far in relatively low patient numbers [68,115].

The efficacy shown in a phase I trial [115] and an ongoing phase I/II study (NCT03538314) recently led to an FDA fast track approval for the combination of the telomerase peptide vaccine UV1 in combination with anti-PD-1 (Pembrolizumab) or anti-

Cytotoxic T-lymphocyte antigen 4 (CTLA-4) (Ipilimumab) in metastatic melanoma.

Furthermore, a recent trial by Kjeldsen and colleagues showed an impressive clinical response response to anti-PD-1 in malignant melanoma patients when combining the ICI with a peptide vaccine targeting PD-L1 and indoleamine-pyrrole 2,3-dioxygenase 1 (IDO1) [116].

Conclusion

The impressive speed with which vaccine development was carried out under the coronavirus pandemic relied to a large extent on infrastructure and technology developed for producing cancer vaccines. Now that the platforms have been shown useful the pandemic may give a boost to further development of cancer vaccines.

After their initial development, cancer vaccines have had a poor reputation of not being effective. This has largely been due to i) testing vaccines in very advanced cancer patients which are no longer able to mount an immune response sufficiently fast and strong to overcome their cancer disease, and ii) earlier cancer vaccines that quite often consisted of short epitopes only aiming at inducing a CD8 T cell response. Recent research has shown that cancer vaccines can be effective if introduced much earlier during the disease course, or in combination with ICI treatment. Adoptive T-cell therapy may be a more appropriate immunotherapy for vey advanced cancer compared to cancer vaccines which require time to induce an endogenous immune response. However, a major problem with T-cell based therapies is the in vivo persistence of the infused cells. Preliminary data has shown that vaccines may be useful to maintain these T cells *in vivo*.

References

1. Dupré de Lisle. Traité sur le vice cancéreux par M. Dupré de Lisle,... (Couturier fils, 1774).
2. Starnes CO. Coley's toxins in perspective. Nature. 1992 ; 357 : 11–12.
3. Finn OJ. The dawn of vaccines for cancer prevention. Nat Rev Immunol. 2018; 18: 183–194.
4. DL Lamm, BA Blumenstein, ED Crawford, JE Montie, P Scardino, et al. A randomized trial of intravesical doxorubicin and immunotherapy with bacille Calmette-Guérin for transitional-cell carcinoma of the bladder. N Engl J Med. 1991; 325: 1205–1209.
5. Sylvester RJ, van der MEIJDEN APM, Lamm DL. Intravesical bacillus Calmette-Guerin reduces the risk of progression in patients with superficial bladder cancer: a meta-analysis of the published results of randomized clinical trials. J Urol. 2002; 168: 1964–1970.
6. Hanahan D, Weinberg RA. The Hallmarks of Cancer. Cell. 2000; 100: 57–70.
7. C Traversari, P van der Bruggen, IF Luescher, C Lurquin, P Chomez, et al. A nonapeptide encoded by human gene MAGE-1 is recognized on HLA-A1 by cytolytic T lymphocytes directed against tumor antigen MZ2-E. J Exp Med. 1992; 176: 1453–1457.
8. Boon T, Cerottini JC, Van den Eynde B, van der Bruggen P, Van Pel A. Tumor antigens recognized by T lymphocytes. Annu Rev Immunol. 1994; 12: 337–365.
9. Dunn GP, Bruce AT, Ikeda H, Old LJ, Schreiber RD. Cancer immunoediting: from immunosurveillance to tumor escape. Nat Immunol. 2002; 3: 991–998.
10. T Cabrera, M Angustias Fernandez, A Sierra, A Garrido, A Herruzo, et al. High frequency of altered HLA class I phenotypes in invasive breast carcinomas. Hum Immunol. 1996; 50: 127–134.
11. Chen DS, Mellman I. Oncology Meets Immunology: The Cancer-Immunity Cycle. Immunity. 2013; 39: 1–10.
12. Vanderlugt CL, Miller SD. Epitope spreading in immune-mediated diseases: implications for immunotherapy. Nat Rev Immunol. 2002; 2: 85–95.

13. Lisa H Butterfield, Antoni Ribas, Vivian B Dissette, Saral N Amarnani, Huong T Vu, et al. Determinant spreading associated with clinical response in dendritic cell-based immunotherapy for malignant melanoma. Clin Cancer Res. 2003; 9: 998–1008.
14. Ribas A, Timmerman JM, Butterfield LH, Economou JS. Determinant spreading and tumor responses after peptide-based cancer immunotherapy. Trends in Immunology. 2003; 24: 58–61.
15. Christopher Wood, Pramod Srivastava, Ronald Bukowski, Louis Lacombe, Andrei I Gorelov, et al. An adjuvant autologous therapeutic vaccine (HSPPC-96; vitespen) versus observation alone for patients at high risk of recurrence after nephrectomy for renal cell carcinoma: a multicentre, open-label, randomised phase III trial. Lancet. 2008; 372: 145–154.
16. Cheever MA, Higano CS. PROVENGE (Sipuleucel-T) in Prostate Cancer: The First FDA-Approved Therapeutic Cancer Vaccine. Clin Cancer Res. 2011; 17: 3520–3526.
17. Erin D Pleasance, Philip J Stephens, Sarah O'Meara, David J McBride, Alison Meynert, et al. A small-cell lung cancer genome with complex signatures of tobacco exposure. Nature. 2010; 463: 184–190.
18. R Parsons, LL Myeroff, B Liu, JK Willson, SD Markowitz, et al. Microsatellite instability and mutations of the transforming growth factor beta type II receptor gene in colorectal cancer. Cancer Research. 1995; 55: 5548–5550.
19. Manuela Pinheiro, Terje Ahlquist, Stine A Danielsen, Guro E Lind, Isabel Veiga, et al. Colorectal carcinomas with microsatellite instability display a different pattern of target gene mutations according to large bowel site of origin. BMC Cancer. 2010; 10: 587.
20. Swati Biswas, Patricia Trobridge, Judith Romero-Gallo, Dean Billheimer, Lois L Myeroff, et al. Mutational inactivation of TGFBR2 in microsatellite unstable colon cancer arises from the cooperation of genomic instability and the clonal outgrowth of transforming growth factor beta resistant cells. Genes Chromosomes Cancer. 2008; 47: 95–106.

21. V Brichard, A Van Pel, T Wölfel, C Wölfel, E De Plaen, et al. The tyrosinase gene codes for an antigen recognized by autologous cytolytic T lymphocytes on HLA-A2 melanomas. J Exp Med. 1993; 178: 489–495.
22. PG Coulie, V Brichard, A Van Pel, T Wölfel, J Schneider, et al. A new gene coding for a differentiation antigen recognized by autologous cytolytic T lymphocytes on HLA-A2 melanomas. J Exp Med. 1994; 180: 35–42.
23. AB Bakker, MW Schreurs, AJ de Boer, Y Kawakami, SA Rosenberg, et al. Melanocyte lineage-specific antigen gp100 is recognized by melanoma-derived tumor-infiltrating lymphocytes. J Exp Med. 1994; 179: 1005–1009.
24. Steven Yeh, Neel K Karne, Sid P Kerkar, Charles K Heller, Douglas C Palmer, et al. Ocular and systemic autoimmunity after successful tumor-infiltrating lymphocyte immunotherapy for recurrent, metastatic melanoma. Ophthalmology. 2009; 116: 981-989 e1.
25. U Sahin, O Türeci, H Schmitt, B Cochlovius, T Johannes, et al. Human neoplasms elicit multiple specific immune responses in the autologous host. Proceedings of the National Academy of Sciences of the United States of America. 1995; 92: 11810–11813.
26. YT Chen, E Stockert, Y Chen, P Garin-Chesa, WJ Rettig, et al. Identification of the MAGE-1 gene product by monoclonal and polyclonal antibodies. Proceedings of the National Academy of Sciences of the United States of America. 1994; 91: 1004–1008.
27. B Gaugler, B Van den Eynde, P van der Bruggen, P Romero, JJ Gaforio, et al. Human gene MAGE-3 codes for an antigen recognized on a melanoma by autologous cytolytic T lymphocytes. J Exp Med. 1994; 179: 921–930.
28. C De Smet, C Lurquin, P van der Bruggen, E De Plaen, F Brasseur, et al. Sequence and expression pattern of the human MAGE2 gene. Immunogenetics. 1994; 39: 121–129.
29. AO Gure, O Türeci, U Sahin, S Tsang, MJ Scanlan, et al. SSX: a multigene family with several members transcribed in normal testis and human cancer. Int J Cancer. 1997; 72: 965–971.
30. YT Chen, AD Boyer, CS Viars, S Tsang, LJ Old,et al. Genomic cloning and localization of CTAG, a gene

encoding an autoimmunogenic cancer-testis antigen NY-ESO-1, to human chromosome Xq28. Cytogenet Cell Genet. 1997; 79: 237–240.
31. Elke Jäger, Yao-Tseng Chen, Jan W Drijfhout, Julia Karbach, Mark Ringhoffer, et al. Simultaneous Humoral and Cellular Immune Response against Cancer–Testis Antigen NY-ESO-1: Definition of Human Histocompatibility Leukocyte Antigen (HLA)-A2–binding Peptide Epitopes. The Journal of Experimental Medicine. 1998; 187: 265–270.
32. NW Kim, MA Piatyszek, KR Prowse, CB Harley, MD West, et al. Specific association of human telomerase activity with immortal cells and cancer. Science. 1994; 266: 2011–2015.
33. CB Harley, NW Kim, KR Prowse, SL Weinrich, KS Hirsch, et al. Telomerase, cell immortality, and cancer. Cold Spring Harb Symp Quant Biol. 1994; 59: 307–315.
34. Shay JW. Telomerase in human development and cancer. J Cell Physiol. 1997; 173: 266–270.
35. Broccoli D, Young JW, de Lange T. Telomerase activity in normal and malignant hematopoietic cells. Proceedings of the National Academy of Sciences of the United States of America. 1995; 92: 9082–9086.
36. K Hiyama, Y Hirai, S Kyoizumi, M Akiyama, E Hiyama, et al. Activation of telomerase in human lymphocytes and hematopoietic progenitor cells. Journal of immunology (Baltimore, Md. : 1950). 1995; 155: 3711–3715.
37. Zanetti M, Hernandez X, Langlade-Demoyen P. Telomerase reverse transcriptase as target for anti-tumor T cell responses in humans. Springer Semin Immun. 2005; 27: 87–104.
38. Nagorsen D, Scheibenbogen C, Marincola FM, Letsch A, Keilholz U. Natural T cell immunity against cancer. Clin Cancer Res. 2003; 9: 4296–4303.
39. Magalie Dosset, Yann Godet, Charline Vauchy, Laurent Beziaud, Yu Chun Lone, et al. Universal cancer peptide-based therapeutic vaccine breaks tolerance against telomerase and eradicates established tumor. Clin Cancer Res. 2012; 18: 6284–6295.
40. Angela L Zarling, Rebecca C Obeng, A Nicole Desch, Joel Pinczewski, Kara L Cummings, et al. MHC-Restricted Phosphopeptides from Insulin Receptor Substrate-2 and

CDC25b Offer Broad-Based Immunotherapeutic Agents for Cancer. Cancer Res. 2014; 74: 6784–6795.
41. Victor H Engelhard, Rebecca C Obeng, Kara L Cummings, Gina R Petroni, Angela L Ambakhutwala, et al. MHC-restricted phosphopeptide antigens: preclinical validation and first-in-humans clinical trial in participants with high-risk melanoma. J Immunother Cancer. 2020; 8: e000262.
42. Stacy A Malaker, Sarah A Penny, Lora G Steadman, Paisley T Myers, Justin C Loke, et al. Identification of Glycopeptides as Posttranslationally Modified Neoantigens in Leukemia. Cancer Immunol Res. 2017; 5: 376–384.
43. zur Hausen H, Henle W, Hummeler K, Diehl V, Henle G. Comparative study of cultured Burkitt tumor cells by immunofluorescence, autoradiography, and electron microscopy. J Virol. 1967; 1: 830–837.
44. zur Hausen H. The Search for Infectious Causes of Human Cancers: Where and Why (Nobel Lecture). Angewandte Chemie International Edition. 2009; 48: 5798–5808.
45. WJ van Driel, ME Ressing, RM Brandt, RE Toes, GJ Fleuren, et al. The current status of therapeutic HPV vaccine. Ann Med. 1996; 28: 471–477.
46. Erminia Massarelli, William William, Faye Johnson, Merrill Kies, Renata Ferrarotto, et al. Combining Immune Checkpoint Blockade and Tumor-Specific Vaccine for Patients With Incurable Human Papillomavirus 16-Related Cancer: A Phase 2 Clinical Trial. JAMA Oncol. 2019; 5: 67–73.
47. Hollingsworth RE, Jansen K. Turning the corner on therapeutic cancer vaccines. NPJ Vaccines. 2019; 4: 7.
48. MK Gjertsen, A Bakka, J Breivik, I Saeterdal, BG Solheim, et al. Vaccination with mutant ras peptides and induction of T-cell responsiveness in pancreatic carcinoma patients carrying the corresponding RAS mutation. Lancet (London, England). 1995; 346: 1399–1400.
49. Slingluff CL. The Present and Future of Peptide Vaccines for Cancer: Single or Multiple, Long or Short, Alone or in Combination? Cancer J. 2011; 17: 343–350.
50. Melief CJ, van der Burg SH. Immunotherapy of established (pre)malignant disease by synthetic long peptide vaccines. Nat Rev Cancer. 2008; 8: 351–360.

51. Hailemichael Y, Overwijk WW. Cancer vaccines: Trafficking of tumor-specific T cells to tumor after therapeutic vaccination. Int J Biochem Cell Biol. 2014; 53: 46–50.
52. Martijn S Bijker, Susan JF van den Eeden, Kees L Franken, Cornelis JM Melief, Rienk Offringa, et al. CD8 CTL priming by exact peptide epitopes in incomplete Freund's adjuvant induces a vanishing CTL response, whereas long peptides induce sustained CTL reactivity. Journal of immunology (Baltimore, Md. : 1950). 2007; 179: 5033–5040.
53. Martijn S Bijker, Susan JF van den Eeden, Kees L Franken, Cornelis JM Melief, Sjoerd H van der Burg, et al. Superior induction of anti-tumor CTL immunity by extended peptide vaccines involves prolonged, DC-focused antigen presentation. European Journal of Immunology. 2008; 38: 1033–1042.
54. Rodney A Rosalia, Esther D Quakkelaar, Anke Redeker, Selina Khan, Marcel Camps, et al. Dendritic cells process synthetic long peptides better than whole protein, improving antigen presentation and T-cell activation. European Journal of Immunology. 2013; 43: 2554–2565.
55. Luana Guimaraes de Sousa, Kimal Rajapakshe, Jaime Rodriguez Canales, Renee L Chin, Lei Feng, et al. ISA101 and nivolumab for HPV-16+ cancer: updated clinical efficacy and immune correlates of response. J Immunother Cancer. 2022; 10: e004232
56. Yared Hailemichael, Zhimin Dai, Nina Jaffarzad, Yang Ye, Miguel A Medina, et al. Persistent antigen at vaccination sites induces tumor-specific CD8 T cell sequestration, dysfunction and deletion. Nat Med. 2013; 19: 465–472.
57. Lynn T Dengel, Allison G Norrod, Briana L Gregory, Eleanor Clancy-Thompson, Marie D Burdick, et al. Interferons Induce CXCR3-cognate Chemokine Production by Human Metastatic Melanoma. Journal of Immunotherapy. 2010; 33: 965–974.
58. Sapna P Patel, Gina R Petroni, Jason Roszik, Walter C Olson, Nolan A Wages, et al. Phase I/II trial of a long peptide vaccine (LPV7) plus toll-like receptor (TLR) agonists with or without incomplete Freund's adjuvant (IFA)

for resected high-risk melanoma. J Immunother Cancer. 2021; 9: e003220.
59. Cai X, Chiu YH, Chen Z J. The cGAS-cGAMP-STING Pathway of Cytosolic DNA Sensing and Signaling. Molecular Cell. 2014; 54: 289–296.
60. Peter Hillemanns, Agnieszka Denecke, Linn Woelber, Gerd Böhmer, Matthias Jentschke, et al. A therapeutic antigen-presenting cell-targeting DNA vaccine VB10.16 in HPV16-positive high-grade cervical intraepithelial neoplasia: results from a phase 1/2a trial. Clin Cancer Res CCR-22-1927. 2022.
61. Eriksson F, Tötterman T, Maltais AK, Pisa P, Yachnin J. DNA vaccine coding for the rhesus prostate specific antigen delivered by intradermal electroporation in patients with relapsed prostate cancer. Vaccine. 2013; 31: 3843–3848.
62. Friedrich H Schmitz-Winnenthal, Nicolas Hohmann, Andreas G Niethammer, Tobias Friedrich, Heinz Lubenau, et al. Anti-angiogenic activity of VXM01, an oral T-cell vaccine against VEGF receptor 2, in patients with advanced pancreatic cancer: A randomized, placebo-controlled, phase 1 trial. Oncoimmunology. 2015; 4: e1001217.
63. Wolfgang Wick, Antje Wick, Felix Sahm, Dennis Riehl, Andreas von Deimling, et al. VXM01 phase I study in patients with progressive glioblastoma: Final results. JCO. 2018; 36: 2017–2017.
64. Kelly WJ, Giles AJ, Gilbert M. T lymphocyte-targeted immune checkpoint modulation in glioma. J Immunother Cancer. 2020; 8: e000379.
65. Luis Teixeira, Jacques Medioni, Julie Garibal, Olivier Adotevi, Ludovic Doucet, et al. A First-in-Human Phase I Study of INVAC-1, an Optimized Human Telomerase DNA Vaccine in Patients with Advanced Solid Tumors. Clin Cancer Res. 2020; 26: 588-597.
66. Benjamin Weide, Jean-Philippe Carralot, Anne Reese, Birgit Scheel, Thomas Kurt Eigentler, et al. Results of the first phase I/II clinical vaccination trial with direct injection of mRNA. J Immunother. 2008; 31: 180–188.
67. Karl-Josef Kallen, Regina Heidenreich, Margit Schnee, Benjamin Petsch, Thomas Schlake, et al. A novel, disruptive

vaccination technology: self-adjuvanted RNActive(®) vaccines. Hum Vaccin Immunother. 2013; 9: 2263–2276.
68. Ugur Sahin, Petra Oehm, Evelyna Derhovanessian, Robert A Jabulowsky, Mathias Vormehr, et al. An RNA vaccine drives immunity in checkpoint-inhibitor-treated melanoma. Nature. 2020; 585: 107–112.
69. Keenan BP, Jaffee EM. Whole cell vaccines--past progress and future strategies. Semin Oncol. 2012; 39: 276–286.
70. Mark Yarchoan, Chiung-Yu Huang, Qingfeng Zhu, Anna K Ferguson, Jennifer N Durham, et al. A phase 2 study of GVAX colon vaccine with cyclophosphamide and pembrolizumab in patients with mismatch repair proficient advanced colorectal cancer. Cancer Medicine. 2020; 9: 1485–1494.
71. Palucka K, Banchereau J. Cancer immunotherapy via dendritic cells. Nat Rev Cancer. 2012; 12: 265–277.
72. Palucka AK, Ueno H, Fay J, Banchereau J. Dendritic cells: a critical player in cancer therapy? J Immunother. 2008; 31: 793–805.
73. BS Sundarasetty, L Chan, D Darling, G Giunti, F Farzaneh, et al. Lentivirus-induced 'Smart' dendritic cells: Pharmacodynamics and GMP-compliant production for immunotherapy against TRP2-positive melanoma. Gene Ther. 2015; 22: 707–720.
74. Ann Van Driessche, Ann L R Van de Velde, Griet Nijs, Tessa Braeckman, Barbara Stein, et al. Clinical-grade manufacturing of autologous mature mRNA-electroporated dendritic cells and safety testing in acute myeloid leukemia patients in a phase I dose-escalation clinical trial. Cytotherapy. 2009; 11: 653–668.
75. JA Kyte, L Mu, S Aamdal, G Kvalheim, S Dueland, et al. Phase I/II trial of melanoma therapy with dendritic cells transfected with autologous tumor-mRNA. Cancer Gene Ther. 20096; 13: 905–918.
76. Smita K Nair, Michael Morse, David Boczkowski, R Ian Cumming, Ljiljana Vasovic, et al. Induction of tumor-specific cytotoxic T lymphocytes in cancer patients by autologous tumor RNA-transfected dendritic cells. Ann Surg. 2002; 235: 540–549.

77. Yanina Jansen, Vibeke Kruse, Jurgen Corthals, Kelly Schats, Pieter-Jan van Dam,et al. A randomized controlled phase II clinical trial on mRNA electroporated autologous monocyte-derived dendritic cells (TriMixDC-MEL) as adjuvant treatment for stage III/IV melanoma patients who are disease-free following the resection of macrometastases. Cancer Immunol Immunother. 2020; 69: 2589–2598.
78. Anne MA Tryggestad, Karol Axcrona, Ulrika Axcrona, Iris Bigalke, Bjørn Brennhovd, et al. Long-term first-in-man Phase I/II study of an adjuvant dendritic cell vaccine in patients with high-risk prostate cancer after radical prostatectomy. Prostate. 2022; 82: 245–253.
79. Raquel S Laureano, Jenny Sprooten, Isaure Vanmeerbeerk, Daniel M Borras, Jannes Govaerts, et al. Trial watch: Dendritic cell (DC)-based immunotherapy for cancer. Oncoimmunology. 2022; 11: 2096363.
80. Paweł Kawalec, Anna Paszulewicz, Przemysław Holko, Andrzej Pilc. Sipuleucel-T immunotherapy for castration-resistant prostate cancer. N Engl J Med. 2011; 363: 411–422.
81. Lynch HT, de la Chapelle A. Hereditary colorectal cancer. N Engl J Med. 2003; 348: 919–932.
82. Asima Abidi, Harm Westdorp, Mark AJ Gorris, Blanca Scheijen, Anna-Lena Boller, et al. Dendritic cells to prevent cancer: Immune responses against neoantigens after dendritic cell vaccination of Lynch Syndrome patients. The Journal of Immunology. 2022; 208: 178.03-178.03.
83. Vanpouille-Box C, Hoffmann JA, Galluzzi L. Pharmacological modulation of nucleic acid sensors — therapeutic potential and persisting obstacles. Nat Rev Drug Discov. 2019; 18: 845–867.
84. Fyrstenberg Laursen M, Kofod-Olsen E, Agger R. Activation of dendritic cells by targeted DNA: a potential addition to the armamentarium for anti-cancer immunotherapy. Cancer Immunol Immunother. 2019; 68: 1875–1880.
85. Gilles Berger, Erik H Knelson, Jorge L Jimenez-Macias, Michal O Nowicki, Saemi Han, et al. STING activation promotes robust immune response and NK cell-mediated tumor regression in glioblastoma models. Proc Natl Acad Sci U S A. 2022; 119: e2111003119.

86. Gijs G Zom, Marian MJHP Willems, Selina Khan, Tetje C van der Sluis, Jan Willem Kleinovink, et al. Novel TLR2-binding adjuvant induces enhanced T cell responses and tumor eradication. j. immunotherapy cancer. 2018; 6: 146.
87. Hans-Georg Rammensee, Karl-Heinz Wiesmüller, P Anoop Chandran, Henning Zelba, Elisa Rusch, et al. A new synthetic toll-like receptor 1/2 ligand is an efficient adjuvant for peptide vaccination in a human volunteer. J Immunother Cancer. 2019; 7: 307.
88. Gijs G Zom, Selina Khan, Cedrik M Britten, Vinod Sommandas, Marcel G M Camps, et al. Efficient Induction of Antitumor Immunity by Synthetic Toll-like Receptor Ligand–Peptide Conjugates. Cancer Immunology Research. 2014; 2: 756–764.
89. Victoria A Brentville, Rachael L Metheringham, Ian Daniels, Suha Atabani, Peter Symonds, et al. Combination vaccine based on citrullinated vimentin and enolase peptides induces potent CD4-mediated anti-tumor responses. J Immunother Cancer. 2020; 8: e000560.
90. Max O Meneveau, Gina R Petroni, Elise P Salerno, Kevin T Lynch, Mark Smolkin, et al. Immunogenicity in humans of a transdermal multipeptide melanoma vaccine administered with or without a TLR7 agonist. J Immunother Cancer. 2021; 9: e002214.
91. Jan D Beck, Daniel Reidenbach, Nadja Salomon, Ugur Sahin, Özlem Türeci, et al. mRNA therapeutics in cancer immunotherapy. Molecular Cancer. 2021; 20: 69.
92. Qiu Wang, Zhe Wang, Xinxin Sun, Qikun Jiang, Bingjun Sun, et al. Lymph node-targeting nanovaccines for cancer immunotherapy. Journal of Controlled Release. 2022; 351: 102–122.
93. Eggermont LJ, Paulis LE, Tel J, Figdor CG. Towards efficient cancer immunotherapy: advances in developing artificial antigen-presenting cells. Trends Biotechnol. 2014; 32: 456–465.
94. Annelies C Wauters , Jari F Scheerstra, Irma G Vermeijlen, Roel Hammink, Marjolein Schluck, et al. Artificial Antigen-Presenting Cell Topology Dictates T Cell Activation. ACS Nano (2022) doi:10.1021/acsnano.2c06211.

95. Ludmil B Alexandrov, Serena Nik-Zainal, David C Wedge, Samuel AJR Aparicio, Sam Behjati, et al. Signatures of mutational processes in human cancer. Nature. 2013; 500: 415–421.
96. Derin B Keskin, Annabelle J Anandappa, Jing Sun, Itay Tirosh, Nathan D Mathewson, et al. Neoantigen vaccine generates intratumoral T cell responses in phase Ib glioblastoma trial. Nature. 2019; 565: 234–239.
97. Norbert Hilf, Sabrina Kuttruff-Coqui, Katrin Frenzel, Valesca Bukur, Stefan Stevanović, et al. Actively personalized vaccination trial for newly diagnosed glioblastoma. Nature. 2019; 565: 240–245.
98. Patrick A Ott, Siwen Hu-Lieskovan, Bartosz Chmielowski, Ramaswamy Govindan, Aung Naing, et al. A Phase Ib Trial of Personalized Neoantigen Therapy Plus Anti-PD-1 in Patients with Advanced Melanoma, Non-small Cell Lung Cancer, or Bladder Cancer. Cell. 2020; 183: 347-362.e24.
99. Michael Platten, Lukas Bunse, Antje Wick, Theresa Bunse, Lucian Le Cornet, et al. A vaccine targeting mutant IDH1 in newly diagnosed glioma. Nature. 2021; 592: 463–468.
100. Zhuting Hu, Donna E Leet, Rosa L Allesøe, Giacomo Oliveira, Shuqiang Li, et al. Personal neoantigen vaccines induce persistent memory T cell responses and epitope spreading in patients with melanoma. Nat Med. 2021; 27: 515–525.
101. Hu Z, Ott PA, Wu CJ. Towards personalized, tumour-specific, therapeutic vaccines for cancer. Nat Rev Immunol. 2018; 18: 168–182.
102. Borst J, Ahrends T, Babala N, Melief CJM, Kastenmuller W. CD4(+) T cell help in cancer immunology and immunotherapy. Nat Rev Immunol. 2018; 18: 635–647.
103. Michael Reiser, Andreas Wieland, Bodo Plachter, Thomas Mertens, Jochen Greiner, et al. The Immunodominant CD8 T Cell Response to the Human Cytomegalovirus Tegument Phosphoprotein pp65495–503 Epitope Critically Depends on CD4 T Cell Help in Vaccinated HLA-A*0201 Transgenic Mice. The Journal of Immunology. 2011; 187: 2172–2180.
104. Yusuke Tomita, Akira Yuno, Hirotake Tsukamoto, Satoru Senju, Yasuhiro Kuroda, et al. Identification of

Promiscuous KIF20A Long Peptides Bearing Both CD4 and CD8 T-cell Epitopes: KIF20A-Specific CD4 T-cell Immunity in Patients with Malignant Tumor. Clinical Cancer Research. 2013; 19: 4508–4520.

105. Yusuke Tomita, Akira Yuno, Hirotake Tsukamoto, Satoru Senju, Sachiko Yoshimura, et al. Identification of CDCA1-derived long peptides bearing both CD4 and CD8 T-cell epitopes: CDCA1-specific CD4 T-cell immunity in cancer patients. International Journal of Cancer. 2014; 134: 352–366.
106. Pardoll DM, Topalian SL. The role of CD4 T cell responses in antitumor immunity. Current Opinion in Immunology. 1998; 10: 588–594.
107. Amber M Johnson, Bonnie L Bullock, Alexander J Neuwelt, Joanna M Poczobutt, Rachael E Kaspar, et al. Cancer Cell–Intrinsic Expression of MHC Class II Regulates the Immune Microenvironment and Response to Anti–PD-1 Therapy in Lung Adenocarcinoma. The Journal of Immunology. 2020; 204: 2295–2307.
108. Garrido F, Cabrera T, Aptsiauri N. 'Hard' and 'soft' lesions underlying the HLA class I alterations in cancer cells: implications for immunotherapy. Int J Cancer. 2010; 127: 249–256.
109. Seliger B. Molecular mechanisms of MHC class I abnormalities and APM components in human tumors. Cancer immunology, immunotherapy : CII. 2008; 57: 1719–1726.
110. Lakshmanachetty S, Cruz-Cruz J, Hoffmeyer E, Cole AP, Mitra SS. New Insights into the Multifaceted Role of Myeloid-Derived Suppressor Cells (MDSCs) in High-Grade Gliomas: From Metabolic Reprograming, Immunosuppression, and Therapeutic Resistance to Current Strategies for Targeting MDSCs. Cells. 2021; 10: 893.
111. Diaz-Montero CM, Finke J, Montero AJ. Myeloid-derived suppressor cells in cancer: therapeutic, predictive, and prognostic implications. Semin Oncol. 2014; 41: 174–184.
112. Henke E, Nandigama R, Ergün S. Extracellular Matrix in the Tumor Microenvironment and Its Impact on Cancer Therapy. Frontiers in Molecular Biosciences. 2020; 6.

113. Chen Y, McAndrews KM, Kalluri R. Clinical and therapeutic relevance of cancer-associated fibroblasts. Nat Rev Clin Oncol. 2021; 18: 792–804.
114. F Stephen Hodi, Steven J O'Day, David F McDermott, Robert W Weber, Jeffrey A Sosman, et al. Improved survival with ipilimumab in patients with metastatic melanoma. N Engl J Med. 2010; 363: 711–723.
115. Elin Aamdal, Else Marit Inderberg, Espen Basmo Ellingsen, Wenche Rasch, Paal Fredrik Brunsvig, et al. Combining a Universal Telomerase Based Cancer Vaccine With Ipilimumab in Patients With Metastatic Melanoma - Five-Year Follow Up of a Phase I/IIa Trial. Front Immunol. 2021; 12: 663865.
116. Julie Westerlin Kjeldsen, Cathrine Lund Lorentzen, Evelina Martinenaite, Eva Ellebaek, Marco Donia, et al. A phase 1/2 trial of an immune-modulatory vaccine against IDO/PD-L1 in combination with nivolumab in metastatic melanoma. Nat Med. 2021; 27: 2212–2223.

Book Chapter

Role of Tumor Cell Metabolism and Immune Cells in Tumor Progression

Zeinab El Rashed[1]*, Mariangela Petito[1], Silvia Ravera[2] and Ulrich Pfeffer[1]

[1]IRCCS Ospedale Policlinico San Martino, Largo Rosanna Benzi, Italy
[2]Department of Experimental Medicine, Human Anatomy, University of Genoa, Italy

***Corresponding Author:** Zeinab El Rashed, IRCCS Ospedale Policlinico San Martino, Largo Rosanna Benzi, 10, 16132 Genova, Italy

Published **July 24, 2023**

How to cite this book chapter: Zeinab El Rashed, Mariangela Petito, Silvia Ravera, Ulrich Pfeffer. Role of Tumor Cell Metabolism and Immune Cells in Tumor Progression. In: Hussein Fayyad Kazan, editor. Immunology and Cancer Biology. Hyderabad, India: Vide Leaf. 2023.

Acknowledgments: ZER was a fellow of the Fondazione Umberto Veronesi. The work was partially supported by the association “Per il sorriso di Ilaria di Montebruno”.

Abstract

Understanding the biological characteristics of cancer cells is critical to demonstrate that these highly proliferating cells are remarkably different from normal cells in terms of morphology, function, signaling pathways, mutations, microenvironment, and, especially, metabolism. Recently metabolic reprogramming has been significantly targeted therapeutically to inhibit cancer cell growth. This promising approach is based on the initial recognition of metabolic alterations in cancer cells by Otto Warburg about a hundred years ago. The Warburg effect can be defined as a combination of elevated levels of glycolysis, glutaminolysis, and induced pentose phosphate pathways in cancer cells compared to normal cells, which cause an enhancement in building-blocks synthesis and energy metabolism, promoting cell proliferation and tumor survival. Furthermore, cancer is considered a "tumor ecosystem" in which a tumor cell interacts with other tumor cells, stromal cells, and all types of immune cells to form an immunosuppressive tumor microenvironment, thus being a principal barrier for cancer therapy. On the other hand, in tumor immunology and medical oncology, it is established that studying the tumor microenvironment is the key to understanding tumor immunity. Altogether, this is leading to new and increasingly targeted therapeutic strategy development.

Keywords

Cancer Metabolism; Warburg Effect; Glycolysis; Lactic Acid; Glutaminolysis; Tumor Microenvironment; Immunology

Cancer Cell versus Normal Cell (*Morphology*, *Physiology*, and *Metabolism*)

Usually, under normal physiological conditions, the same type of cells show similar morphological features; by contrast, cancer cells exhibit variations in size and shape. For example, whereas the nucleus in normal cells appears smooth and spheroid, cancer cells have a larger nucleus, with a blebbing membrane that could

be due to the imbalance in the proteins that constitute the nuclear lamina.

In addition, cancer cells show other features such as tumor-induced angiogenesis, increased and uncontrolled proliferation rate, metastatic potential, and, especially, altered metabolism, as reported by Alibert et al [1].

Apoptosis has an essential role in both physiological and pathological processes, particularly crucial for oncogenesis, cancer progression, and even treatment. A main feature of cancer cells is the loss of apoptotic regulation, which enhances cell survival and allows more time for the accumulation of mutations that can increase invasiveness during tumor progression, induce angiogenesis, deregulate cell proliferation, and interfere with differentiation [2].

Vascularization is crucial for the growth and evolution of normal tissue, and it plays an essential role in the development of tumor tissue's alert rhythm as well as in the spread and metastasis of cancerous cells. The amount of blood vessels present in tumor tissue is closely correlated with the frequency of metastases. Furthermore, tumor cell mutations can result in the development of cell clones with angiogenetic properties [3].

Hypoxia and Tumor

In physiological conditions and normal oxygen levels (normoxia), oxidative phosphorylation (OxPhos) is the principal pathway involved in cellular energy production. However, in the case of many solid tumors, their rapid growth and impaired blood flow are accompanied by an abnormally insufficient amount of oxygen, known as tumor hypoxia [4].

The hypoxic response is controlled mainly by a specific mediator known as a hypoxia-inducible transcription factor (HIF). HIF is composed of two subunits; HIF1β, which is constitutively expressed, and HIF1α, whose expression depends on the oxygen concentration. Whereas, in normoxia, HIF1α is rapidly degraded by the ubiquitin-proteasome system, under hypoxic conditions,

HIF1α is more stable and subsequently translocates into the nucleus binding the HIF1β subunit, activating the expression of genes involved in cell survival, proliferation, cell migration, angiogenesis, and glucose metabolism [5,6].

Among the upregulated genes induced by hypoxia and HIF activation, some **encoding** glucose transporters (Glut-1 and 3) and glycolytic enzymes such as aldolase, enolase, or lactate dehydrogenase (LDH-A), suggesting that the tumor cells respond to hypoxia by increasing glucose uptake and the anaerobic glycolysis rate. Furthermore, HIF positively regulates the bifunctional glycolytic regulatory enzymes 6-phospho-2-kinase/fructose2 and 6-biphosphatase (PFKFB1-4), which in turn control the activity of phosphofructokinase-1 (PFK1); an enzyme that catalyzes a rate-limiting step in the glycolytic pathway by the phosphorylation of fructose-6-phosphate to fructose-1,6-bisphosphate [7].

In addition, hypoxic conditions trigger the activation of the AMP-activated protein kinase (AMPK) signaling pathway in tumor cells. AMPK is considered a sensor and indicator for cellular energy status, which is activated in response to increased AMP/ATP and ADP/ATP ratios, such as an attempt to replenish ATP levels and restore the cellular energy balance. AMPK activation has been shown to cause inducible phosphofructokinase-2 phosphorylation, increasing fructose 2,6-bisphosphate level, which, in turn, activates fructose 6-phosphate 1-phosphotransferase, inducing glycolysis. Therefore, AMPK activation under hypoxic conditions may be essential for cell survival and proliferation [8].

However, despite the hypoxic condition creating a slowdown in aerobic metabolism, mitochondria maintain their importance in sustaining the proliferation and aggressiveness of cancer cells [9,10]. For example, in some tumors, mitochondria shift their metabolic dependence towards more energy-efficient substrates, such as fatty acids [11]; in other cases, they modulate the processes of fusion and fission, modifying the shape and organization of their network and inducing greater or lesser energy efficiency [9].

In addition, a slight uncoupling between oxygen consumption and ATP synthesis leads to limited production of reactive oxygen species that represent a pro-proliferative stimulus for tumor cells [12].

Tumor Microenvironment

Understanding the underlying mechanisms in tumors at the cellular and molecular level has been considered a challenge to identify therapeutic targets for cancer treatment. It should be noticed that a tumor is not only a group of highly proliferating cells but rather several components forming a diverse and heterogeneous collection of secreted factors, infiltrating and resident host cells, stromal cells such as fibroblasts, immune cells (including T and B lymphocytes, and natural killer cells), and the extracellular matrix [13], altogether, known as the tumor microenvironment (TME).

The TME diversity promotes several interactions between cancer cells and the cellular and structural components of TME, enhancing tumor survival, proliferation, and invasion from the primary site to distant locations. Furthermore, a principal feature of TME is the hypoxic conditions that, as mentioned above, trigger tumor progression by enhancing proliferation, angiogenesis, metabolism, and the tumor immune response [14].

The cellular components of TME contribute to a critical role in modulating cancer metastasis, inducing angiogenesis, and stimulating tumor cells to release matrix metalloproteinases (MMPs) which degrade matrix barriers, thus favoring cancer progression [15]. In addition to the importance of mesenchymal stem cells, cancer-associated fibroblasts, and endothelial cells in secreting signaling molecules that attract cancer cells to the metastatic site facilitating tumor progression [16].

The non-cellular component of the TME known as the extracellular matrix (ECM), is defined as a three-dimensional network of extracellular proteins and other macromolecules, including collagen, fibronectin, integrins, microfibrillar proteins, and proteoglycans that provide structural and biochemical

support to the tissue. Normally, ECM under tumorigenic conditions functions as a biological barrier restraining tumor cells from proliferating and metastasizing. However, ECM is transformed into a metastasis-promoting microenvironment during tumor progression [17].

Due to the overall complexity of dividing cancer cells and their associated microenvironment, it has been a challenge to develop effective anti-cancer therapies. Thus, several systems have been described as potential targets of anti-cancer treatments, such as cancer cell metabolism, tumor suppressor system, inflammation, immunotherapy, and, recently, the TME. In a previous study, it has been shown that TME may be a target of cancer therapy by different strategies such as inhibiting macrophages recruitment and differentiation, targeting the extracellular matrix, targeting tumor cell-derived exosomes, targeting chronic inflammation, activating anti-tumoral activity of the immune system, targeting hypoxia, and avoiding neovascularization [18].

Furthermore, it has been demonstrated that pH 6-6.5 in the tumor microenvironment is associated with metastasis, angiogenesis, and therapy resistance, a phenotype common in more aggressive tumors [19]. Metastatic dissemination is a malignant feature of cancer with significant clinical implications because the metastatic disease causes the majority of cancer-related deaths rather than primary tumors [20].

Cancer Cell Altered Metabolism

Cellular metabolism is an energy-producing process consisting of a complex of controlled catabolic and anabolic biochemical reactions that provide a basal energy level through ATP production to maintain cellular homeostasis in resting cells. However, proliferating cells require further energy to satisfy increased anabolic demands illustrated by macromolecular biosynthesis (nucleotides, proteins, and lipids) [21,22].

Cancer cells alter their metabolism as a response to promote growth, proliferation, and long-term survival [23]. The switch in core metabolism is directly influenced by enhanced key

metabolic pathways such as glucose, lipids, and amino acid metabolism caused by a series of activated mutated oncogenes, tumor suppressor genes' loss of function, and further epigenetic post-translational modifications [24].

Mutations in genes encoding metabolic enzymes are directly implicated in cellular metabolic pathways or can indirectly trigger and promote cancer cell transformation [24,25]. Normal cells have complex signaling networks that are orchestrated by key control enzymes, sensing environmental cues and running metabolic engines to provide enough energy for survival in a perfectly controlled manner [26]. Normal cells activate metabolic pathways during proliferation to satisfy increased adenosine triphosphate (ATP) consumption for cell reproduction [21].

The hallmark of tumor metabolic transformation includes metabolic features such as a switch to aerobic glycolysis, known as the *Warburg effect*, pentose phosphate pathway (PPP) enhancement, mitochondrial reprogramming, and the deregulation of lipid metabolism [27]. It is noteworthy to mention that inflammation within the tumor microenvironment is known to influence cancer cell metabolism. Considering that metabolic rewiring is critical for understanding the essential mechanisms of tumorigenesis and discovering novel, therapeutically utilizable liabilities of malignant cells. We will describe the key aspects of cancer cell metabolic transformation.

The Warburg Effect: A Hallmark of Cancer Cell Metabolism

The Warburg effect is a cancer hallmark that refers to cancer cells' preference to metabolize glucose anaerobically rather than aerobically, even under normoxia (with completely functioning mitochondria) [28]. Based on Warburg's hypothesis, cancer cells prefer aerobic glycolysis over the more efficient oxidative phosphorylation as the primary pathway of glucose metabolism. The inefficient aerobic glycolysis produces only two ATP molecules per glucose molecule, thus highly proliferating cancer cells search to increase glucose uptake from the

microenvironment to meet energy requirements and consequently secrete more lactic acids to the microenvironment to maintain cellular environment homeostasis [29]. The glucose transport across a plasma membrane by the glucose transporter/solute carrier (GLUT/SLC2A) family facilitates glucose uptake from the microenvironment into the cytoplasm. Cancer cells frequently overexpress GLUTs in hypoxia, particularly GLUT1 and GLUT3 [30]. The hypoxic condition of the tumor microenvironment induces the upregulation of the hypoxia-inducible factors (HIFs) containing HIF-1α [31]. HIF-1 has been identified as an oxygen sensor that regulates GLUT1 expression [32]. Hypoxia activated an enhancer element located 5′ to the Glut-1 gene, and a distinct cis-acting sequence was discovered as a HIF-1 binding site to increase GLUT1 expression [33]. Since GLUT1 has a high affinity for glucose (Km = 6.9 mM) [34], cancer cells can efficiently plunder glucose, lowering the glucose concentration in the tumor microenvironment and, consequently, influencing the function of infiltrated immune cells.

Aerobic glycolysis is an inefficient method to produce ATP compared to mitochondrial respiration [35]. However, the rate of glucose metabolism via aerobic glycolysis is faster, with lactate produced 10-100 times faster than the complete oxidation of glucose in the mitochondria [28]. When either form of glucose metabolism is used, the amount of ATP synthesized over any given period is comparable [36]. Cells with a higher rate but lower yield of ATP production have been shown to have a selective advantage when competing for shared and limited energy resources [37]. Indeed, tumor microenvironments have limited glucose availability and compete for nutrients with stromal cells and the immune compartment [38]. A recent study found that when changes to the cellular environment were induced to significantly increase ATP demand by changing the demand of ATP-dependent membrane pumps, aerobic glycolysis increased rapidly while oxidative phosphorylation remained constant [39]. This discovery adds to the evidence that the Warburg Effect supports the quick production of ATP, which can be swiftly tuned to meet the demand for ATP synthesis.

Regarding cell intrinsic actions of the Warburg effect, the regeneration of NAD^+ from NADH in the pyruvate to lactate step that completes aerobic glycolysis is one proposed mechanism to account for the biosynthetic function of the Warburg Effect. To keep glycolysis active, NADH produced by glyceraldehyde phosphate dehydrogenase (GAPDH) must be consumed to regenerate NAD^+. This high rate of glycolysis allows supply lines to remain open, allowing 3-phosphoglycerate (3PG) to be siphoned to serine for one-carbon metabolism-mediated production of NADPH and nucleotides [21]. In addition to the important role of NAD^+ in influencing key cellular functions where it functions as a substrate for lysine deacetylases, ADP-ribosylating enzymes, DNA ligase, glycolysis, metabolic signaling, and cellular biosynthesis.

Together, the above-mentioned proposals suggest that the Warburg effect provides a metabolic environment that promotes cancer cell proliferation, not only at the level of ATP compensation but, importantly, also by providing intermediate molecules that are essentially required as building blocks in cellular biosynthesis.

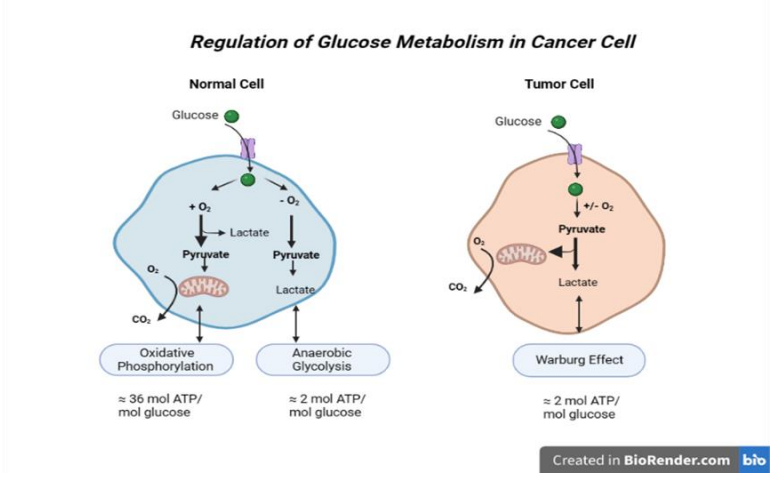

Figure 1: Regulation of Glucose metabolism in normal and cancer cells.

Lactate Production and Cancer Progression: A Consequence of Cancer Cell Altered Metabolism

Lactate, a hypoxic waste product, is both a powerful fuel and a signaling molecule. In healthy conditions, physiological lactate concentration is between 1.5-3 mM; however, in cancer tissues, this concentration can increase to 10-30 mM [40]. A study using nuclear magnetic resonance to examine [3-13C]-lactate metabolism in vitro and in vivo observed that lactate could be transported into and oxidized by breast cancer cells [41].

Since tumor cells preferentially and frequently utilize glucose for their metabolic needs, its consumption is high, and its level is extremely low, favoring intracellular amino acid accumulation except for glutamine [42]. However, even if breast cancer-derived cells produce high lactate levels when grown in various glucose concentrations, they switch from lactate producers to consumers when glucose is limited [43]. On the other hand, the metabolic approach shows that cancer cells can use the compound lactate to fuel biochemical reactions and generate other compounds required for cell growth, such as lipids to build new cellular membranes [44]. Whether lactate is secreted and then taken up by cancer cells requires further investigation.

Lactate can now be incorporated into the tricarboxylic acid (TCA) cycle and act as an energy source and an oncometabolite with some signaling properties [45]. While it has been demonstrated that lactate can be used as a fuel source when glucose is scarce, scientists disagree on whether it enters the TCA cycle directly or must first be converted to glucose via gluconeogenesis [46]. More research is needed to determine its role in cancer, specifically which metabolic pathway is preferred and whether it is dependent on tumor metabolism.

According to Walenta et al., intratumor lactate levels can be used as a prognostic factor and a biomarker of therapy response [47]. High lactate concentrations in biopsies of cervical, lung, head and neck, colorectal, and breast cancers have been linked to an increased risk of metastasis, indicating a poor prognosis for survival in cancer patients [40]. Furthermore, lactate

concentrations were significantly higher in cervical tumors with metastatic spread when imaging bioluminescence from primary cryo-tumor sections of human cancers [47].

Lactate's role in therapy resistance has also been demonstrated using in vivo and in vitro models. Lactate has been identified as a key molecule involved in resistance to tyrosine kinase inhibitor (TKI)-based therapy in NSCLC lung cancer, specifically with the c-MET receptor tyrosine kinase inhibitor JNJ-605 and the epidermal growth factor receptor (EGFR) inhibitor erlotinib [48]. The authors demonstrated that prolonged treatment with these TKIs induces tumor cells to produce lactate, which, in turn, stimulates hepatocyte growth factor (HGF) production by TME cells, reinforcing drug resistance and tumor progression.

Targeting tumor lactate metabolism was enough to overcome resistance, demonstrating the causative role of lactate in therapy resistance. Due to the previously mentioned role of lactate in tumor initiation and metastatic spread, an alteration of lactate homeostasis has proved to be such a promising approach for cancer therapy that it has been implemented in several preclinical and clinical studies, although to establish a synergy between lactate inhibitors and other adjuvant therapies should be critical.

Regulation of Pentose Phosphate Pathway and the Warburg Effect in Cancer

Historically, much less emphasis has been placed on the importance of the pentose phosphate pathway (PPP) in cancer growth, ans its alterations in cancer cells have been poorly understood. Recent research has shown that the PPP, in conjunction with glycolysis, coordinates glucose flux and supports cellular macromolecule biogenesis and energy production [49]. The PPP is a principal glucose catabolic pathway that connects glucose metabolism to ribose nucleotide precursor biosynthesis and NADPH production [50]. This latter process is required for antioxidant defense and reductive biosynthesis, such as lipid synthesis. Glycolysis provides energy to cells for biogenesis; however, large amounts of lipids,

nucleotide precursors and other building blocks are required to support cancer cell proliferation [51].

PPP is an essential metabolic pathway, parallel to glycolysis, considered the principal source of NADPH, and ribose 5-phosphate, as NADPH plays a pivotal role in reductive biosyntheses, such as cholesterol, fatty acids, and nucleotide biosynthesis, and ribose 5-phosphate is necessary for the biosynthesis of nucleic acids. Altogether, PPP is critical in regulating DNA damage response, metabolism, and cell proliferation enhancing cancer progression [50].

Cancer cells are metabolically reprogrammed to direct glucose flux into the PPP in order to meet these biosynthetic demands [49]. Indeed, evidence suggests that, like glycolysis, higher PPP flux is present in many human cancers and that PPP is connected to glycolysis [52]. Cancer cells will shut down the glycolytic pathway during oxidative stress, increasing glucose flux through the PPP to produce more NADPH for antioxidant defense [53]. The finding that PPP flux is higher in some human cancer cells lends credence to the notion that the PPP may play a pivotal role in meeting the bioenergetic burden of cancer cell proliferation and contribute to the Warburg effect. The activation of glycolysis in cancer cells may be accompanied by a boost in PPP activity for biosynthesis.

Interestingly, P53 is one of the most often mutated genes, known as a tumor suppressor gene that codes for a protein that has a key role in controlling cell proliferation, as p53 mutations or loss of function increase glycolytic and PPP flux [53]. Furthermore, PPP is suppressed by p53 by directly binding to G6PD and inhibiting its enzyme activity [51].

Another study showed that p53 deficiency reduces TP53-induced glycolysis and apoptosis regulator (TIGAR) expression suppresses glycolysis, reducing intracellular levels of fructose-2,6-bisphosphate (F-2,6-P2). F-2,6-P2 is a potent allosteric activator of phosphofructokinase-1 (PFK1), and its deficiency reduces PFK1 activity and glycolytic flux [53]. Thus, it might be that p53 mutations in cancer cells liberate G6PD and activate

PFK1, resulting in increased PPP flux and glycolysis. On the other hand, the regulation of key oncoproteins and tumor suppressors influences glycolysis and PPP since some signaling pathways or mutations frequently activated in cancers, such as PI3K and K-ras G12D, positively regulate glycolysis and PPP.

Inactivation of tumor suppressors such as p53 and PTEN (phosphatase and tensin homolog: another tumor suppressor gene involved in the regulation of cell cycle, PTEN is frequently mutated in many cancers, specifically glioblastoma, lung cancer, breast cancer, and prostate cancer) consistently increases glycolysis and PPP flux and promotes cell proliferation [54].

Furthermore, activation of the metabolic regulatory network downstream of mTORC1 known as the mammalian target of rapamycin complex 1 (or mechanistic target of rapamycin complex 1), has been shown to result in reprogramming of key metabolic pathways such as glycolysis, glutaminolysis, and the PPP [21]. Moreover, the mTORC1 signaling pathway plays a key role in tumor metabolism, in addition to the regulation of gene transcription and protein synthesis involved in cell proliferation and immune cell differentiation. In detail, mTORC1 activation increases glycolysis and PPP metabolite levels by inducing the expression of glycolytic genes and G6PD [21]. It is worth noting that mTORC1 induction of G6PD is dependent on the SREBP (sterol regulatory element-binding protein) transcription factors [55].

Glutaminolysis in the Milieu of Cancer

Glutaminolysis is a metabolic pathway based on a series of biochemical reactions in which glutamine is transported into the cell by specific transporters, such as SLC1A5 and SLC7A5, and converted to glutamate and further to alpha-ketoglutarate (α-KG) to enable ATP production through the TCA cycle and to provide biosynthetic precursors such as nitrogen, carbon, and sulfur for cell growth [56].

Tumor cells require at least ten times the amount of glutamine as any other amino acid in culture. In the mitochondrion, glutamine

is deaminated to glutamate by glutaminase (GLS), and then -ketoglutarate is generated by the enzyme glutamate dehydrogenase (GDH), which is then incorporated into the TCA cycle to generate malate by fumarase enzyme because -ketoglutarate is the principal anaplerotic source for the TCA cycle [57]. Malate is transported to the cytosol and converted to pyruvate by the malic enzyme before being converted to lactate by LDHA. Tumor cells have a higher flux of mitochondrial enzymes involved in glutamine/glutamate oxidation than normal cells [58,59]. Glutaminolysis promotes tumor growth in two distinct but linked ways: it promotes cell proliferation and inhibits cell death [60]. The primary function of glutaminolysis is to provide intermediary metabolites for cell growth in the TCA cycle [61]. Glutamine is necessary for nucleotide biosynthesis because it is a nitrogen source for purines and pyrimidines synthesis. Furthermore, glutamine is involved in the biosynthesis of hexosamine and other non-essential amino acids [62]. As a result, glutamine is essential for cell proliferation because it provides nitrogen and carbon skeletons for macromolecule biosynthesis [63].

It has been reported that glutamine flux regulates mTOR activation to coordinate cell growth and proliferation [64]. Furthermore, glutaminolysis promotes lysosomal translocation and subsequent mTORC1 activation. These findings collectively broaden the role of glutaminolysis in metabolic rewiring to support cancer cell proliferation and tumor growth. Moreover, glutaminolysis is involved in many metabolic processes and signaling pathways that prevent cell death. Most glutamine transporters are overexpressed in cancer cells, and some oncogenes or tumor suppressors have been shown to regulate their expression. SLC1A5 (ASCT2), Na+-coupled glutamine, alanine, serine, and cysteine transporter, is shown to be upregulated by Myc oncogene (which contributes to altered cellular metabolism by regulating glucose and glutamine metabolism, thus promoting cell proliferation in many human cancers) [64], while SLC1A5 is downregulated by the tumor suppressor retinoblastoma protein (Rb) [65].

Furthermore, hypoxia-inducible factor 2α (HIF-2α) and Myc upregulate SLC7A5 (LAT1), a bidirectional transporter that regulates the simultaneous efflux of glutamine out of cells and the influx of leucine into cells, inducing tumor growth. SLC7A5 is highly expressed in renal cell carcinoma and prostate cancer [66,64].

These findings indicate a functional link between oncogenes and glutamine uptake, which promotes glutaminolysis and tumor growth. Indeed, Nicklin *et al.* discovered that SLC1A5 acts together with SLC7A5 to activate mTOR signaling. Glutamine enters the cells via SLC1A5, and its efflux out of the cells via SLC7A5 is coupled to the entry of leucine, which activates mTOR signaling and coordinates cell proliferation and growth [67]. On the other hand, cancer cell proliferation *in vitro* and tumor growth *in vivo* are suppressed by targeting SLC1A5 with RNAi or small molecule inhibitors, benzylserine and l—glutamyl-p-nitroanilide [68].

Thus, the fact that the expression of glutamine transporters links inversely with cancer patient prognosis indicates glutamine transporters' potential as a prognostic biomarker and therapeutic target for cancer treatment.

An Emerging Aspect of Metabolic Transformation in Cancer is Fatty Acid Oxidation

Rapidly dividing cancer cells require increased de novo fatty acid synthesis from acetyl-CoA and reducing power (NADPH) for membrane biogenesis. The function of mitochondrial fatty acid -oxidation (FAO) in cancer is less clear than that of the lipogenic phenotype. Most previous studies regarding cancer bioenergetics focused on the Warburg effect, even if FAO is considered one of the principal sources of ATP production [21].

The cytosolic NADPH, which has the reducing power to support biosynthesis and combat oxidative stress, is produced by FAO in addition to ATP. Many FAO enzymes, including a cluster of differentiation 36 (CD36) and carnitine palmitoyl transferase (such as CPT1A, CPT1B, CPT1C, CPT-2), carnitine transporter

(CT2), and acyl-CoA synthetase long-chain 3, are overexpressed in various cancers compared to their healthy counterparts, according to several studies.

Most previous findings linking ASR to oncogenesis were supported by pharmacological suppression of CPT1. CPT-1 is involved in the long-chain fatty acyl-CoA conversion to acylcarnitines and is an enzyme that limits the transport of long-chain fatty acids rate from the cytoplasm to the mitochondrial matrix.

Poor patient outcomes for cancer, such as acute myeloid leukemia (AML) and ovarian cancer, are highly correlated with overexpression of particular FAO enzymes, such as CPT1A [69]. Myeloid leukemia, ovarian cancer [70], hepatocellular carcinoma, prostate cancer [71], and glioma cell lines' proliferation and/or viability were inhibited by CPT1 inhibitors. Mechanistically, FAO appears to be a crucial ATP source for the rapid growth of several cancer types [72]. CPT1 inhibition in ovarian cancer decreased cellular ATP levels and activated AMP-activated protein kinase (AMPK), which was linked to cell cycle arrest at the G1/G0 stage [70], suggesting that FAO is significantly correlated to ATP production and regulation of cellular metabolism.

More recent research on colon and breast cancer indicates that cancer cells prefer to spread to tissues rich in adipocytes [73-74]. Cancer cells' uptake of fatty acids from nearby adipocytes facilitated FAO [75]. In addition to its effect on cell proliferation, FAO inhibition was also associated with the induction of apoptosis or decreased viability in cell lines of myeloid leukemia, glioma, and hepatocellular carcinoma [76-78].

In a previous study, it was observed that the antiproliferative effect of FAO inhibition was linked with the disruption of NADPH homeostasis, reactive oxidative species (ROS) production, mitochondrial damage, and apoptosis induction [78].

Through its potential involvement in cancer stem cell regulation, FAO may also contribute to the emergence of the metastatic phenotype. According to Ito *et al.*, the hematopoietic stem cell's asymmetric division depends on promyelocytic leukemia (PML)–peroxisome proliferator-activated receptor δ (PPAR-δ)–fatty-acid oxidation (FAO), in which they observed that mitochondrial FAO inhibition or loss of PPAR-δ leads to loss of HSC maintenance [79]. Another study revealed that the supply of fatty acids reduction or CPT1A silencing resulted in abnormalities that lowered the number of neural stem cells in the mouse embryonic neocortex. Trimethyllysine hydroxylase is a crucial enzyme in carnitine production, the CPT1 substrate [80], suggesting that active FAO promotes phenotypic maintenance in normal tissue stem cells. The difference between CD36-positive and CD36-negative leukemic stem cells in terms of FAO activity and treatment resistance suggests that FAO activity influences the characteristics of cancer stem cells [74].

Metabolic Reprogramming by Frequently Activated Cancer Cell Signaling Pathways

There has been a resurgence of interest in understanding how metabolism is altered in cancer cells over the last decade. Evidence suggests that signaling pathways involving oncogenes and tumor suppressors, in addition to their well-known functions in inducing aberrant cell proliferation or attenuating apoptosis, play a direct role in promoting the conversion of energy metabolism to aerobic glycolysis [81]. Outstandingly, physiological cellular signaling mechanisms normally tightly control cells' ability to access and consume nutrients, posing a basic barrier to transformation [82]. This barrier is frequently overcome by cellular signaling abnormalities that force tumor pathogenesis by allowing cancer cells to make critical cellular fates in a cell-autonomous manner.

The PI3K/AKT/mTOR signal transduction pathway and the Ras/MAPK pathway, in particular, are frequently activated or mutated in cancer [83]. The PI3K-Akt-mTOR pathway coordinates the uptake and utilization of multiple nutrients, including glucose, glutamine, nucleotides, and lipids, in a

manner best suited for supporting cancer cell growth and proliferation through both post-translational regulation and transcriptional program induction [84]. Aerobic glycolysis is observed in immortalized hematopoietic cells transformed by a constitutively active Akt mutant, showing higher rates of glycolysis without affecting the rate of oxidative phosphorylation [85]. The same results have been observed in human glioblastoma cells with constitutive Akt activity. Notably, because they are more susceptible to cell death after glucose withdrawal, these cells are dependent on aerobic glycolysis for growth and survival. These findings suggest that PI3K-Akt-mTOR signaling is sufficient to trigger the switch to aerobic glycolysis. As mentioned earlier, aerobic glycolysis is linked with increased glucose uptake. Under normal physiological conditions, the PI3K-Akt-mTOR signaling pathway regulates glucose uptake via post-translational and transcriptional mechanisms [86]. Glucose uptake is primarily stimulated at the post-translational level by regulating glucose transporter trafficking. Although the regulation of GLUT4 by Akt has received considerable attention, it is important to remember that GLUT4 is a muscle- and fat-cell-specific glucose transporter [87]. In other words, most cancer cells express the embryonic glucose transporter isoform, GLUT1, rather than GLUT4 [88]. Particularly, GLUT1 has a high affinity for glucose and may be chosen by cancer cells to increase the efficiency of glucose transport [89]. It has also been proposed that PI3K-Akt signaling regulates GLUT1 trafficking to the plasma membrane [90]. However, the specific mechanisms by which such regulation occurs remain an open question. The transcriptional level of glucose transporters is also regulated by PI3K-Akt-mTOR signaling. Continuous Akt activation increases GLUT1, but not GLUT4, mRNA and protein levels [91]. The upregulation of HIF1a levels and activity by mTORC1 is required for increased GLUT1 expression [92]. c-Myc can also promote the transcription of GLUT1 [93], which is located downstream of PI3K. These mechanisms work together to strongly stimulate glucose uptake in cancer cells, providing them with enough substrate for aerobic glycolysis. An early study revealed that Akt and S6K phosphorylate the bifunctional enzyme PFK-2/FBPase-2 (PFK2) in vitro, which increased Phosphofructokinase-2 (PFK-

2) activity [94]. PFK2 regulates glycolysis by producing fructose 2,6-bisphosphate, the most potent allosteric activator of PFK1, a glycolysis rate-limiting enzyme [95]. Akt activation has also been linked to an increase in the hexokinase (HK) activity, which is a key mediator of aerobic glycolysis, increased cell proliferation, and therapeutic resistance [96]. By phosphorylating glucose to form glucose 6-phosphate, HK catalyzes the first and rate-limiting step of glycolysis (G6P) [90]. The PI3K-Akt-mTOR signaling pathway also regulates the expression of glycolytic genes by upregulating the HIF1 transcription factor. The upregulation of HIF1a by mTORC1 increases the expression of GLUT1 and GLUT3 as well as almost all glycolysis-related genes [55].

Members of the mitogen-activated protein kinase (MAPK) family are among the many signaling pathways that respond to oncogenic mutational events and regulate proliferation, apoptosis, and aerobic glycolysis. Among the well-studied MAPK subfamilies in mammals are the extracellular signal-regulated kinases (ERKs) and the c-Jun N-terminal kinases (JNKs), which have recently been shown to regulate the redirection of energy harvest to glycolysis in both malignant and highly proliferative cells by influencing the activity of key metabolic regulators. Indeed, constitutive activation of ERK1 and ERK2 signaling is common in human cancers caused by mutations in RTK, RAS, BRAF, CRAF, MEK1, and MEK2 genes [97]. These mutations promote BRAF kinase's active structural conformation, resulting in constitutive activation of the ERK1/2 pathway, which then turns on proliferative programs and induces the aerobic glycolytic phenotype through the initiation of transcriptional regulators of glycolysis, the TCA cycle, and macromolecular biosynthesis [98].

Competition for Nutrients between Tumor Cells and Immune Cells

Recently, many studies have shown that tumor metabolism is also involved in the regulation of the anti-tumor immune response through the release of several metabolites that influence immune system function, as well as playing a crucial role in

cancer signaling in support of tumorigenesis and cell survival [100]. Emerging evidence indicates that cancer cells suppress the anti-tumor immune response by competing with essential nutrients by depleting them or otherwise reducing the metabolic intermediates available to immune cells. This energetic interaction between tumor and immune cells leads to metabolic reprogramming of immune cells during their process of proliferation, differentiation, and execution of effector functions causing them to become tolerogenic and inefficient in eradicating tumor cells [101,102].

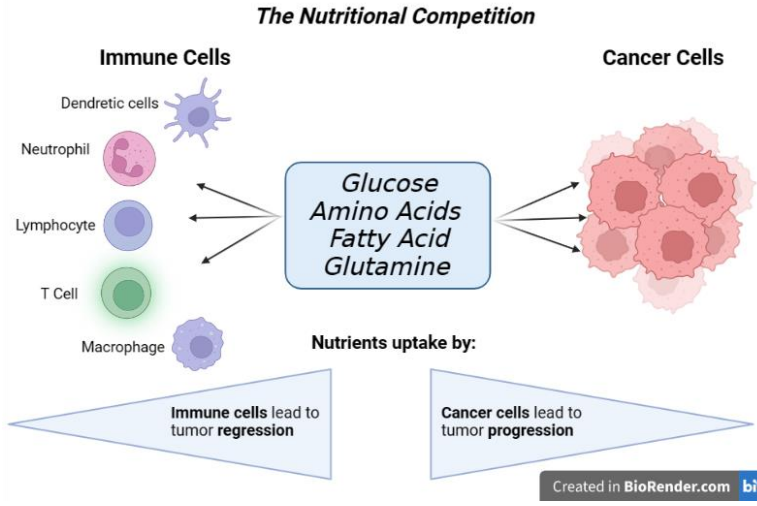

Figure 2: The nutritional competition between cancer and immune cells.

The Metabolism of the Immune Cells

Innate and adaptive immune systems have well-established roles in host defense against tumors through various mechanisms. The innate immune system consists of diverse cell populations, including macrophages, neutrophils, monocytes, eosinophils, basophils, and natural killer cells that are responsible for innate immunity against pathogens to maintain host homeostasis [102,99]. Acquired immunity intervenes only when other defense lines have failed to effectively counteract the pathogen, overlapping with innate immunity, and enhancing the immune response. Antigen-presenting cells (APCs) and T- and B-

lymphocytes are the cells mainly involved in establishing acquired immunity.

Generally, cells depend on a variety of nutrients and undergo various biochemical processes that support growth and division; during tumor initiation and progression, every cellular component in the cancer niche undergoes dramatic metabolic reprogramming, including the immune cells. As previously said, glucose, fatty acids, and amino acids are three major building blocks of cellular metabolism. Thus, the study of nutrient metabolism by immune cells is urgently needed. Disruption of such metabolic pathways collectively contributes to a highly acidic, nutrient-deficient, and hypoxic TME that further aggravates metabolic reprogramming processes in tumor cells and the tumor niche immunocytes [103,104].

Immune Cells and Glucose Restriction

Immune system cells are at rest when the body is in a steady state and will be rapidly activated and respond when the body is stimulated by infection, inflammation, or other external substances. Furthermore, the diverse levels of immune cell activation are accompanied by different metabolic patterns [105].

In neutrophils, M1 macrophages, dendritic cells, naive T cells, and effector T cells, glycolysis is the primary metabolic process [106]. For instance, CD8T cells, a crucial part of the adaptive immune response, require a high glycolytic metabolism to proliferate and expand their population of activated CD8T cells [107]. More critically, glycolysis can control the inflammatory response linked to macrophages; in fact, cellular glycolysis is elevated when the M1-type stimulating factor IFN- and LPS co-stimulate mouse bone marrow-derived macrophages [108]. Thus, glycolysis can regulate tumor immunity as it regulates many important functions of neutrophils, activated NK cells, and DC cells [109].

Lactic Acid Metabolism and Immune Cells

The metabolites produced by tumor cells as a result of metabolic reprogramming can have a profound effect on microenvironment immune cells [110]. For instance, lactate, a byproduct of increased aerobic glycolysis in tumor cells, causes naive T cells from ovarian cancer patients and mice models to undergo apoptosis [111]. Because of this anomaly in the glycolytic pathway, we now know that cancer cells use a lot of glucose and generate a lot of lactic acids, even in the presence of sufficient oxygen amounts [99]. Monocarboxylate transporters (MCTs), specifically monocarboxylate transporter 4 (MCT4), are activated at the cell membrane to move lactic acid from cells to the extracellular environment, where it accumulates and eventually creates an acidic TME [112]. The low pH of TME is beneficial for the selection of more aggressive tumor cells and suppresses tumor immunity to promote tumor progression [113].

It is shown that lactic acid can impact NK cell performance, and, therefore, impairs IFN-γ secretion. An excessive intake of pathologically high levels of lactic acid by NK cells can lead to intracellular acidification and inhibit the up-regulation of the nuclear factor of activated T cells (NFAT) signal, which lowers the amount of NFAT-regulated IFN-γ produced and ultimately induced apoptosis in those cells. More significantly, elevated lactate levels can be found in both human and rat melanoma. When lactic acid generation is reduced in immune-competent mice, the ability of CD8+ cells to form tumors is slowed, and the infiltration of T cells and NK cells that secrete IFN- in the tumor is markedly increased [114,115].

Another analysis revealed low variation in tumorigenic potential between the low lactate group and the control group in mice lacking lymphocytes and NK cells. It's interesting to note that a recent study found that the tumor microenvironment's lactate production by tumor cells' glycolysis activates the mTOR pathway and promotes cell survival and proliferation [116].

Amino Acid Metabolism and Immune Cells

One of the fundamental building blocks of the body's immune system is amino acids. The release of cytokines and the control of immune responses are both influenced by amino acids, in addition to their role in the development of immune organs and the proliferation and differentiation of immune cells. A lack of amino acids can cause dysfunction of immune cells [117,99].

One essential component of cancer cell metabolism is the overall metabolism of glutamine. The synthesis of nucleotides, the generation of amino acids, redox equilibrium, glycosylation, the development of extracellular matrix, autophagy, and epigenetics are all dependent on glutamine, knowing that glutamine is crucial for both healthy and cancer cell development [118,119]. In case of nutritional deficiencies, cancer cells can obtain glutamine by breaking down large molecules. For instance, high oncogene RAS activation might induce endocytosis, allowing cancer cells to remove extracellular proteins and break them down into amino acids like glutamine, which feeds the cancer cells [120].

In addition to tumor cells, lymphocytes, macrophages, and neutrophils are immune cells characterized by a high rate of glutamine use to enable cell fate determination and immunological responses. According to the study, glutamine deprivation can reduce the generation of cytokines and T-cell proliferation. Moreover, neutrophils and macrophages both use glutamine very efficiently. The rate of immune cell death decreased significantly with increased use of glutamine [121,122].

For instance, glutamine inhibits the production of the pro-apoptotic proteins Bax and Bcl-xs, hence lowering neutrophil apoptosis [123]. The availability of glutamine also influences the synthesis and release of pro-inflammatory cytokines (IL-6, IL-1, and TNF) by macrophages. As a result, the activation of a macrophage is regulated by and supported synergistically by the metabolism of glutamine [124].

Additionally, by preventing the glutamine pathway in cancer cells, the number of amino acids in the tumor microenvironment will accumulate, enhancing the ability of immune cells to target the tumor cells. The immunological escape of tumors can be stopped by inhibiting glutamine, according to research by Jonathan D. Powell and his team. It implies that a revolutionary approach to treating cancer will involve focusing on glutamine metabolism [125].

Conclusion

In conclusion, we can confirm that cancer is a complex and multifactorial disease because several factors are involved in its progression and aggressiveness, such as metabolic changes, the extracellular tumor microenvironment, and associated immune cells. Studying and understanding all the processes implicated in cancerogenesis is essential to identify therapeutic approaches targeting cancer cells at different levels. In this chapter, we tried to explain how the metabolic alterations in cancer cells favor cell growth and proliferation and how the TME and their immune cells trigger tumor pathogenesis.

References

1. Alibert C, Goud B, Manneville JB. Are cancer cells softer than normal cells? Biol Cell. 2017; 109: 167-189.
2. Wong RS. Apoptosis in cancer: from pathogenesis to treatment. J Exp Clin Cancer Res. 2011; 30: 87.
3. Baba AI, Câtoi C. Comparative Oncology. Bucharest: The Publishing House of the Romanian Academy. 2007.
4. Bartrons R, Caro, J. Hypoxia, glucose metabolism and the Warburg's effect. J Bioenerg Biomembr. 2007; 39: 223–229.
5. Scholz, Carsten & Taylor, Cormac. Hydroxylase-dependent regulation of the NF-κB pathway. Biological chemistry. 2013; 394.
6. Wilson, Robert. Hypoxia, cytokines and stromal recruitment: Parallels between pathophysiology of encapsulating peritoneal sclerosis, endometriosis and peritoneal metastasis. Pleura and Peritoneum. 2018; 3.
7. Minchenko O, Opentanova I, Caro J. Hypoxic regulation of

the 6-phosphofructo-2-kinase/fructose-2,6-bisphosphatase gene family (PFKFB-1-4) expression in vivo. FEBS Lett. 2003; 554: 264-270.
8. Atsumi T, Nishio T, Niwa H, Takeuchi J, Bando H, et al. Expression of inducible 6-phosphofructo-2-kinase/fructose-2,6-bisphosphatase/PFKFB3 isoforms in adipocytes and their potential role in glycolytic regulation. Diabetes. 2005; 54: 3349-3357.
9. Gundamaraju R, Lu W, Manikam R. Revisiting Mitochondria Scored Cancer Progression and Metastasis. Cancers (Basel). 2021; 13: 432.
10. Zong WX, Rabinowitz JD, White E. Mitochondria and Cancer. Mol Cell. 2016; 61: 667-676.
11. Koundouros N, Poulogiannis G. Reprogramming of fatty acid metabolism in cancer. Br J Cancer. 2020; 122: 4-22.
12. Arfin S, Jha NK, Jha SK, Kesari KK, Ruokolainen J, et al. Oxidative Stress in Cancer Cell Metabolism. Antioxidants (Basel). 2021; 10: 642.
13. Anderson NM, Simon MC. The tumor microenvironment. Curr Biol. 2020; 30: R921-R925.
14. Li Y, Zhao L, Li XF. Hypoxia and the Tumor Microenvironment. Technol Cancer Res Treat. 2021; 20: 15330338211036304.
15. Singh S, Mehta N, Lilan J, Budhthoki MB, Chao F, et al. Initiative action of tumor-associated macrophage during tumor metastasis. Biochim Open. 2017; 4: 8-18: 29450136.
16. Neophytou CM, Panagi M, Stylianopoulos T, Papageorgis P. The Role of Tumor Microenvironment in Cancer Metastasis: Molecular Mechanisms and Therapeutic Opportunities. Cancers (Basel). 2021; 13: 2053.
17. Xiao Y, Yu D. Tumor microenvironment as a therapeutic target in cancer. Pharmacol Ther. 2021; 221: 107753.
18. Roma-Rodrigues C, Mendes R, Baptista PV, Fernandes AR. Targeting Tumor Microenvironment for Cancer Therapy. Int J Mol Sci. 2019; 20: 840.
19. García-Cañaveras, Juan C, Li Chen, Joshua D. Rabinowitz. "The Tumor Metabolic Microenvironment: Lessons from Lactate The Tumor Metabolic Microenvironment: Lessons from Lactate." Cancer research 79. 2013; 13: 3155-3162.
20. Seyfried, Thomas N. "Cancer as a metabolic disease:

implications for novel therapeutics." Carcinogenesis. 2014; 35: 515-527.
21. Vander Heiden MG, Cantley LC, Thompson CB. Understanding the Warburg effect: the metabolic requirements of cell proliferation. Science. 2009; 324: 1029–1033.
22. Zhu J, Thompson CB. Metabolic regulation of cell growth and proliferation. Nat Rev Mol Cell Biol. 2019; 20: 436-450.
23. Liberti MV, Dai Z, Wardell SE, Baccile JA, Liu X, et al. A Predictive Model for Selective Targeting of the Warburg Effect through GAPDH Inhibition with a Natural Product. Cell Metab. 2017; 26: 648-659.e8.
24. Tarrado-Castellarnau M, de Atauri P, Cascante M. Oncogenic regulation of tumor metabolic reprogramming. Oncotarget. 2016; 7: 62726-62753.
25. Pavlova NN, Thompson CB. The Emerging Hallmarks of Cancer Metabolism. Cell Metab. 2016; 23: 27–47.
26. Wang Y, Xu X, Maglic D, Dill MT, Mojumdar K, et al. Cancer Genome Atlas Research Network, Camargo F, Liang H. Comprehensive Molecular Characterization of the Hippo Signaling Pathway in Cancer. Cell Rep. 2018; 25: 1304-1317.e5.
27. Schiliro C, Firestein BL. Mechanisms of Metabolic Reprogramming in Cancer Cells Supporting Enhanced Growth and Proliferation. Cells. 2021; 10: 1056. Erratum in: Cells. 2022; 11.
28. Liberti MV, Locasale JW. The Warburg Effect: How Does it Benefit Cancer Cells? Trends Biochem Sci. 2016; 41: 211-218. Erratum in: Trends Biochem Sci. 2016; 41: 287. Erratum in: Trends Biochem Sci. 2016; 41: 287.
29. Jiang B. Aerobic glycolysis and high level of lactate in cancer metabolism and microenvironment. Genes Dis. 2017; 4: 25-27.
30. Ancey, Pierre-Benoit. “Glucose transporters in cancer - from tumor cells to the tumor microenvironment.” The FEBS journal. 2018; 285: 2926-2943.
31. Li X, Yang Y, Huang Q, Deng Y, Guo F, et al. Crosstalk Between the Tumor Microenvironment and Cancer Cells: A Promising Predictive Biomarker for Immune Checkpoint Inhibitors. Front Cell Dev Biol. 2021; 9: 738373.

32. Masoud GN, Li W. HIF-1α pathway: role, regulation and intervention for cancer therapy. Acta Pharm Sin B. 2015; 5: 378-389.
33. Ebert BL, Firth JD, Ratcliffe PJ. Hypoxia and mitochondrial inhibitors regulate expression of glucose transporter-1 via distinct Cis-acting sequences. J Biol Chem. 1995; 270: 29083-29089.
34. Shepherd PR, Barbara BK. "Glucose transporters and insulin action—implications for insulin resistance and diabetes mellitus." New England journal of medicine. 1999; 341: 248-257.
35. Luengo A, Li Z, Gui DY, Sullivan LB, Zagorulya M, et al. Increased demand for NAD+ relative to ATP drives aerobic glycolysis. Mol Cell. 2021; 81: 691-707.e6.
36. Shestov AA, Liu X, Ser Z, Cluntun AA, Hung YP, et al. Quantitative determinants of aerobic glycolysis identify flux through the enzyme GAPDH as a limiting step. Elife. 2014; 3: e03342.
37. Pfeiffer T, Schuster S, Bonhoeffer S. Cooperation and competition in the evolution of ATP-producing pathways. Science. 2001; 292: 504-507. Erratum in: Science. 2001; 293:1436.
38. Chang C, Su H, Zhang D, Wang Y, Shen Q, et al. AMPK-Dependent Phosphorylation of GAPDH Triggers Sirt1 Activation and Is Necessary for Autophagy upon Glucose Starvation. Mol Cell. 2015; 60: 930-940.
39. Epstein T, Xu L, Gillies RJ, Gatenby RA. Separation of metabolic supply and demand: aerobic glycolysis as a normal physiological response to fluctuating energetic demands in the membrane. Cancer Metab. 2014; 2: 7.
40. Brizel DM, Clough RW, Dewhirst MW, Schroeder T, Walenta S, et al. Elevated tumor lactate concentrations predict for an increased risk of metastases in head-and-neck cancer. Int J Radiat Oncol Biol Phys. 2001; 51: 349–353.
41. Kennedy KM, Scarbrough PM, Ribeiro A, Richardson R, Yuan H, et al. Catabolism of exogenous lactate reveals it as a legitimate metabolic substrate in breast cancer. PLoS One. 2013; 8: e75154.
42. Hirayama A, Kami K, Sugimoto M, Sugawara M, Toki N, et al. Quantitative metabolome profiling of colon and stomach

cancer microenvironment by capillary electrophoresis time-of-flight mass spectrometry. Cancer Res. 2009; 69: 4918-4925.
43. Park S, Chang CY, Safi R, Liu X, Baldi R, et al. ERRα-Regulated Lactate Metabolism Contributes to Resistance to Targeted Therapies in Breast Cancer. Cell Rep. 2016; 15: 323-335.
44. Schmidt DR, Patel R, Kirsch DG, Lewis CA, Vander Heiden MG, et al. Metabolomics in cancer research and emerging applications in clinical oncology. CA Cancer J Clin. 2021; 71: 333-358.
45. Dhup S, Dadhich RK, Porporato PE, Sonveaux P. Multiple biological activities of lactic acid in cancer: influences on tumor growth, angiogenesis and metastasis. Curr Pharm Des. 2012; 18: 1319-1330.
46. Leithner K, Hrzenjak A, Trötzmüller M, Moustafa T, Köfeler HC, et al. PCK2 activation mediates an adaptive response to glucose depletion in lung cancer. Oncogene. 2015; 34: 1044-1050.
47. Walenta S, Wetterling M, Lehrke M, Schwickert G, Sundfør K, et al. High lactate levels predict likelihood of metastases, tumor recurrence, and restricted patient survival in human cervical cancers. Cancer Res. 2000; 60: 916-921.
48. Apicella M, Giannoni E, Fiore S, Ferrari KJ, Fernández-Pérez D, et al. Increased Lactate Secretion by Cancer Cells Sustains Non-cell-autonomous Adaptive Resistance to MET and EGFR Targeted Therapies. Cell Metab. 2018; 28: 848-865.e6.
49. Jiang P, Du W, Wu M. Regulation of the pentose phosphate pathway in cancer. Protein Cell. 2014; 5: 592-602.
50. Ge T, Yang J, Zhou S, Wang Y, Li Y, et al. The Role of the Pentose Phosphate Pathway in Diabetes and Cancer. Front Endocrinol (Lausanne). 2020; 11: 365.
51. Jiang P, Du W, Wang X, Mancuso A, Gao X, et al. p53 regulates biosynthesis through direct inactivation of glucose-6-phosphate dehydrogenase. Nat Cell Biol. 2011; 13: 310-316.
52. Cho ES, Cha YH, Kim HS, Kim NH, Yook JI. The Pentose Phosphate Pathway as a Potential Target for Cancer Therapy. Biomol Ther (Seoul). 2018; 26: 29-38.

53. Bensaad K, Tsuruta A, Selak MA, Vidal MN, Nakano K, et al. TIGAR, a p53-inducible regulator of glycolysis and apoptosis. Cell. 2006; 126: 107-120.
54. Aquila S, Santoro M, Caputo A, Panno ML, Pezzi V, et al. The Tumor Suppressor PTEN as Molecular Switch Node Regulating Cell Metabolism and Autophagy: Implications in Immune System and Tumor Microenvironment. Cells. 2020; 9: 1725.
55. Düvel K, Yecies JL, Menon S, Raman P, Lipovsky AI, et al. Activation of a metabolic gene regulatory network downstream of mTOR complex 1. Mol Cell. 2010; 39: 171-183.
56. Jin L, Alesi GN, Kang S. Glutaminolysis as a target for cancer therapy. Oncogene. 2016; 35: 3619-3625.
57. Zhang J, Pavlova NN, Thompson CB. Cancer cell metabolism: the essential role of the nonessential amino acid, glutamine. EMBO J. 2017; 36: 1302-1315.
58. Ying M, You D, Zhu X, Cai L, Zeng S, et al. Lactate and glutamine support NADPH generation in cancer cells under glucose deprived conditions. Redox Biol. 2021; 46: 102065.
59. Friday E, Oliver R, Welbourne T, Turturro F. Glutaminolysis and glycolysis regulation by troglitazone in breast cancer cells: relationship to mitochondrial membrane potential. J Cell Physiol. 2011; 226: 511–519.
60. Medina MA, Núñez de Castro I. Glutaminolysis and glycolysis interactions in proliferant cells. Int J Biochem. 1990; 22: 681-683.
61. Reitzer LJ, Wice BM, Kennell D. Evidence that glutamine, not sugar, is the major energy source for cultured HeLa cells. J Biol Chem. 1979; 254: 2669-2676.
62. Hensley CT, Wasti AT, DeBerardinis RJ. Glutamine and cancer: cell biology, physiology, and clinical opportunities. J Clin Invest. 2013; 123: 3678-3684.
63. Dang CV. Glutaminolysis: supplying carbon or nitrogen or both for cancer cells? Cell Cycle. 2010; 9: 3884-3886.
64. Dang CV. MYC, microRNAs and glutamine addiction in cancers. Cell Cycle. 2009; 8: 3243-3245.
65. Reynolds MR, Lane AN, Robertson B, Kemp S, Liu Y, et al. Control of glutamine metabolism by the tumor suppressor Rb. Oncogene. 2014; 33: 556-566.

66. Elorza A, Soro-Arnáiz I, Meléndez-Rodríguez F, Rodríguez-Vaello V, Marsboom G, et al. HIF2α acts as an mTORC1 activator through the amino acid carrier SLC7A5. Mol Cell. 2012; 48: 681-691.
67. Nicklin P, Bergman P, Zhang B, Triantafellow E, Wang H, et al. Bidirectional transport of amino acids regulates mTOR and autophagy. Cell. 2009; 136: 521-534.
68. Hassanein M, Hoeksema MD, Shiota M, Qian J, Harris BK, et al. SLC1A5 mediates glutamine transport required for lung cancer cell growth and survival. Clin Cancer Res. 2013; 19: 560-570.
69. Shi J, Fu H, Jia Z, He K, Fu L, et al. High Expression of CPT1A Predicts Adverse Outcomes: A Potential Therapeutic Target for Acute Myeloid Leukemia. EBioMedicine. 2016; 14: 55-64.
70. Shao H, Mohamed EM, Xu GG, Waters M, Jing K, et al. Carnitine palmitoyltransferase 1A functions to repress FoxO transcription factors to allow cell cycle progression in ovarian cancer. Oncotarget. 2016; 7: 3832-3846.
71. Schlaepfer IR, Rider L, Rodrigues LU, Gijón MA, Pac CT, et al. Lipid catabolism via CPT1 as a therapeutic target for prostate cancer. Mol Cancer Ther. 2014; 13: 2361-2371.
72. Pike LS, Smift AL, Croteau NJ, Ferrick DA, Wu M. Inhibition of fatty acid oxidation by etomoxir impairs NADPH production and increases reactive oxygen species resulting in ATP depletion and cell death in human glioblastoma cells. Biochim Biophys Acta. 2011; 1807: 726-734.
73. Wen YA, Xing X, Harris JW, Zaytseva YY, Mitov MI, et al. Adipocytes activate mitochondrial fatty acid oxidation and autophagy to promote tumor growth in colon cancer. Cell Death Dis. 2017; 8: e2593.
74. Wang YY, Attané C, Milhas D, Dirat B, Dauvillier S, et al. Mammary adipocytes stimulate breast cancer invasion through metabolic remodeling of tumor cells. JCI Insight. 2017; 2: e87489.
75. Lazar I, Clement E, Dauvillier S, Milhas D, Ducoux-Petit M, et al. Adipocyte exosomes promote melanoma aggressiveness through fatty acid oxidation: a novel mechanism linking obesity and cancer. Can Res. 2016; 76:

4051–4057.
76. Qu Q, Zeng F, Liu X, Wang QJ, Deng F. Fatty acid oxidation and carnitine palmitoyltransferase I: emerging therapeutic targets in cancer. Cell Death Dis. 2016; 7: e2226.
77. Lin H, Patel S, Affleck VS, Wilson I, Turnbull DM, et al. Fatty acid oxidation is required for the respiration and proliferation of malignant glioma cells. Neuro Oncol. 2017; 19: 43-54.
78. Samudio I, Harmancey R, Fiegl M, Kantarjian H, Konopleva M, et al. Pharmacologic inhibition of fatty acid oxidation sensitizes human leukemia cells to apoptosis induction. J. Clin. Invest. 2010; 120: 142–156.
79. Ito K, Carracedo A, Weiss D, Arai F, Ala U, et al. A PML–PPAR-δ pathway for fatty acid oxidation regulates hematopoietic stem cell maintenance. Nat Med. 2012; 18: 1350-1358.
80. Xie Z, Jones A, Deeney JT, Hur SK, Bankaitis VA. Inborn Errors of Long-Chain Fatty Acid β-Oxidation Link Neural Stem Cell Self-Renewal to Autism. Cell Rep. 2016; 14: 991-999.
81. Kroemer G, Pouyssegur J. Tumor cell metabolism: cancer's Achilles' heel. Cancer Cell. 2008;13: 472-482.
82. Nash SH, Till C, Song X, Lucia MS, Parnes HL, et al. Serum Retinol and Carotenoid Concentrations and Prostate Cancer Risk: Results from the Prostate Cancer Prevention Trial. Cancer Epidemiol Biomarkers Prev. 2015; 24: 1507-1515.
83. Asati V, Bharti SK, Mahapatra DK. Mutant B-Raf Kinase Inhibitors as Anticancer Agents. Anticancer Agents Med Chem. 2016; 16: 1558-1575.
84. Hoxhaj G, Manning BD. The PI3K-AKT network at the interface of oncogenic signalling and cancer metabolism. Nat Rev Cancer. 2020; 20: 74-88.
85. Elstrom RL, Bauer DE, Buzzai M, Karnauskas R, Harris MH, Plas DR. et al. Akt stimulates aerobic glycolysis in cancer cells. Cancer Res. 2004; 64: 3892-3899.
86. Stine ZE, Walton ZE, Altman BJ, Hsieh AL, Dang CV. MYC, Metabolism, and Cancer. Cancer Discov. 2015; 5: 1024-1039.
87. Olson AL. Regulation of GLUT4 and Insulin-Dependent Glucose Flux. ISRN Mol Biol. 2012; 2012: 856987.

88. Adekola K, Rosen ST, Shanmugam M. Glucose transporters in cancer metabolism. Curr Opin Oncol. 2012; 24: 650-654.
89. Ganapathy V, Thangaraju M, Prasad PD. Nutrient transporters in cancer: relevance to Warburg hypothesis and beyond. Pharmacol Ther. 2009; 121: 29-40.
90. Rathmell JC, Fox CJ, Plas DR, Hammerman PS, Cinalli RM, et al. Akt-directed glucose metabolism can prevent Bax conformation change and promote growth factor-independent survival. Mol Cell Biol. 2003; 23: 7315-7328.
91. Kohn AD, Summers SA, Birnbaum MJ, Roth RA. Expression of a constitutively active Akt Ser/Thr kinase in 3T3-L1 adipocytes stimulates glucose uptake and glucose transporter 4 translocation. J Biol Chem. 1996; 271: 31372-31378.
92. Wieman HL, Wofford JA, Rathmell JC. Cytokine stimulation promotes glucose uptake via phosphatidylinositol-3 kinase/Akt regulation of Glut1 activity and trafficking. Mol Biol Cell. 2007; 18: 1437-1446.
93. Osthus RC, Shim H, Kim S, Li Q, Reddy R, et al. Deregulation of glucose transporter 1 and glycolytic gene expression by c-Myc. J Biol Chem. 2000; 275: 21797-21800.
94. Deprez J, Vertommen D, Alessi DR, Hue L, Rider MH. Phosphorylation and activation of heart 6-phosphofructo-2-kinase by protein kinase B and other protein kinases of the insulin signaling cascades. J Biol Chem. 1997; 272: 17269-17275.
95. Kotowski K, Rosik J, Machaj F, Supplitt S, Wiczew D, et al. Role of PFKFB3 and PFKFB4 in Cancer: Genetic Basis, Impact on Disease Development/Progression, and Potential as Therapeutic Targets. Cancers (Basel). 2021; 13: 909.
96. Pastorino JG, Hoek JB, Shulga N. Activation of glycogen synthase kinase 3beta disrupts the binding of hexokinase II to mitochondria by phosphorylating voltage-dependent anion channel and potentiates chemotherapy-induced cytotoxicity. Cancer Res. 2005; 65: 10545-10554.
97. Raman M, Chen W, Cobb MH. Differential regulation and properties of MAPKs. Oncogene. 2007; 26: 3100-3112.
98. Parmenter TJ, Kleinschmidt M, Kinross KM, Bond ST, Li J, et al. Response of BRAF-mutant melanoma to BRAF inhibition is mediated by a network of transcriptional

regulators of glycolysis. Cancer Discov. 2014; 4: 423-433.
99. Xia L, Oyang L, Lin J, Tan S, Han Y, et al. The cancer metabolic reprogramming and immune response. Mol Cancer. 2021; 20: 28.
100. Hurley HJ, Dewald H, Rothkopf ZS, Singh S, Jenkins F, et al. Frontline Science: AMPK regulates metabolic reprogramming necessary for interferon production in human plasmacytoid dendritic cells. J Leukoc Biol. 2021; 299-308.
101. Guerra L, Bonetti L, Brenner D. Metabolic Modulation of Immunity: A New Concept in Cancer Immunotherapy. Cell Rep. 2020; 32: 107848.
102. Cicco S, Cicco G, Racanelli V, Vacca A. Neutrophil Extracellular Traps (NETs) and Damage-Associated Molecular Patterns (DAMPs): Two Potential Targets for COVID-19 Treatment. Mediators Inflamm. 2020; Article ID 7527953.
103. Zheng Y, Delgoffe GM, Meyer CF, Chan W, Powell JD. Anergic T cells are metabolically anergic. J Immunol. 2009; 183: 6095-6101.
104. Lian X, Yang K, Li R, Li M, Zuo J, et al. Immunometabolic rewiring in tumorigenesis and anti-tumor immunotherapy. Mol Cancer. 2022; 21: 27.
105. Hao S, Yan KK, Ding L, Qian C, Chi H, et al. Network Approaches for Dissecting the Immune System. iScience. 2020; 23: 101354.
106. Tan S, Li S, Min Y, Gisterå A, Moruzzi N, et al. Platelet factor 4 enhances $CD4^+$ T effector memory cell responses via Akt-PGC1α-TFAM signaling-mediated mitochondrial biogenesis. J Thromb Haemost. 2020; 18: 2685-2700.
107. Sohrabi Y, Lagache SMM, Voges VC, Semo D, Sonntag G, et al. OxLDL-mediated immunologic memory in endothelial cells. J Mol Cell Cardiol. 2020; 146: 121-132.
108. Sun L, Yang X, Yuan Z, Wang H. Metabolic Reprogramming in Immune Response and Tissue Inflammation. Arterioscler Thromb Vasc Biol. 2020; 40: 1990-2001.
109. Tan SY, Kelkar Y, Hadjipanayis A, Shipstone A, Wynn TA, et al. Metformin and 2-Deoxyglucose Collaboratively Suppress Human CD4(+) T Cell Effector Functions and

Activation-Induced Metabolic Reprogramming. J Immunol. 2020; 205: 957-967.

110. Harmon C, O'Farrelly C, Robinson MW. The Immune Consequences of Lactate in the Tumor Microenvironment. Adv Exp Med Biol. 2020; 1259: 113-124.

111. Wei H, Guan JL. Pro-tumorigenic function of autophagy in mammary oncogenesis. Autophagy. 2012; 8: 129-131.

112. Halestrap AP. The monocarboxylate transporter family--Structure and functional characterization. IUBMB Life. 2012; 64: 1-9.

113. Huang Z, Gan J, Long Z, Guo G, Shi X, et al. Targeted delivery of let-7b to reprogramme tumor-associated macrophages and tumor infiltrating dendritic cells for tumor rejection. Biomaterials. 2016; 90: 72–84.

114. Dodard G, Tata A, Erick TK, Jaime D, Miah SMS, et al. Inflammation-Induced Lactate Leads to Rapid Loss of Hepatic Tissue-Resident NK Cells. Cell Rep. 2020; 32: 107855.

115. Brand A, Singer K, Koehl GE, Kolitzus M, Schoenhammer G, et al. LDHA-Associated Lactic Acid Production Blunts Tumor Immunosurveillance by T and NK Cells. Cell Metab. 2016; 24: 657–671.

116. Liu N, Luo J, Kuang D, Xu S, Duan Y, et al. Lactate inhibits ATP6V0d2 expression in tumor-associated macrophages to promote HIF-2alpha-mediated tumor progression. J Clin Invest. 2019; 129: 631–646.

117. Nielsen JP, Foged NT, Sørensen V, Barfod K, Bording A, et al. Vaccination against progressive atrophic rhinitis with a recombinant Pasteurella multocida toxin derivative. Can J Vet Res. 1991; 55: 128-138.

118. Fan SJ, Kroeger B, Marie PP, Bridges EM, Mason JD, et al. Glutamine deprivation alters the origin and function of cancer cell exosomes. EMBO J. 2020; 39: e103009.

119. Caiola E, Colombo M, Sestito G, Lupi M, Marabese M, et al. Glutaminase Inhibition on NSCLC Depends on Extracellular Alanine Exploitation. Cells. 2020; 9:1766.

120. Cohen AS, Geng L, Zhao P, Fu A, Schulte ML, et al. Combined blockade of EGFR and glutamine metabolism in preclinical models of colorectal cancer. Transl Oncol. 2020; 13: 100828.

121. Carr EL, Kelman A, Wu GS, Gopaul R, Senkevitch E, et al. Glutamine uptake and metabolism are coordinately regulated by ERK/MAPK during T lymphocyte activation. Journal of Immunol. 2010; 185: 1037–1044.
122. Püschel F, Favaro F, Redondo-Pedraza J, Lucendo E, Iurlaro R, et al. Starvation and antimetabolic therapy promote cytokine release and recruitment of immune cells. Proc Natl Acad Sci U S A. 2020; 117: 9932-9941.
123. Lagranha CJ, Senna SM, de Lima TM, Silva E, Doi SQ, et al. Beneficial effect of glutamine on exercise-induced apoptosis of rat neutrophils. Med Sci Sports Exerc. 2004; 36: 210–217.
124. Shah AM, Wang Z, Ma J. Glutamine Metabolism and Its Role in Immunity, a Comprehensive Review. Animals (Basel). 2020; 10: 326. Retraction in: Animals (Basel). 2021; 11.
125. Leone RD, Zhao L, Englert JM, Sun IM, Oh MH, et al. Glutamine blockade induces divergent metabolic programs to overcome tumor immune evasion. Science. 2019; 366: 1013–1021.

Book Chapter

A Practical Introduction to Single-Cell RNA-seq in Immuno-Oncology

Benoît Aliaga*, Matthieu Genais and Vera Pancaldi

Centre de Recherches en Cancérologie de Toulouse, Université de Toulouse, Inserm, CNRS, Université Toulouse III-Paul Sabatier, France

***Corresponding Author:** Benoît Aliaga, Centre de Recherches en Cancérologie de Toulouse, Université de Toulouse, Inserm, CNRS, Université Toulouse III-Paul Sabatier, Toulouse, France

Published **October 31, 2023**

How to cite this book chapter: Benoît Aliaga, Matthieu Genais, Vera Pancaldi. A Practical Introduction to Single-Cell RNA-seq in Immuno-Oncology. In: Hussein Fayyad Kazan, editor. Immunology and Cancer Biology. Hyderabad, India: Vide Leaf. 2023.

Acknowledgment: We thank Chloé Bessière, and Malvina Marku for providing interesting comments and improvements to this manuscript.

Abstract

Single-cell approaches are a major revolution in biology. With this technology, it becomes possible to sequence a tumor's transcriptome and dissect tumor heterogeneity. Studying the interaction between heterogeneous cancer and immune cells beyond population averages becomes accessible. This approach

is promising to improve immuno-oncology treatments for patients. To exploit its full potential, biologists need to understand the steps needed to perform these experiments, the main scRNA-seq analysis pipeline components, and the frequently used tools available in the literature for further computational downstream analysis and interpretation. Throughout the chapter, we will guide the reader to several available libraries and packages that can be used to perform these analyses. Inference of intercellular communication will be further explored in the context of immuno-oncology at the end of the chapter.

Introduction

Since the birth of DNA sequencing, first performed by Fred Sanger and his group in 1977, sequencing technologies have been revolutionized several times [1]. The first technology (Sanger sequencing) uses the chain termination method, which generates DNA fragments that elongate at different points using dye-dideoxynucleotides. Electrophoresis is employed to separate DNA based on size. A laser scanner will provide an electropherogram, from which we can read the DNA sequence. This technique was widely used, and it remains frequently used nowadays. However, this method has some limitations. Indeed, it can only sequence short pieces of DNA (300 to 1000 bp), and the sequence quality degrades after 700 to 900 bases. Moreover, it has major limitations in cost and time. The second generation of sequencing, called “Next Generation Sequencing (NGS) Technologies” appeared at the beginning of the 2000s. With these new sequencers, it became possible to generate millions of short reads in parallel; sequencing was quicker than the Sanger method, could be achieved at a lower cost, and could be performed on smaller quantities of DNA. NGS opened new opportunities to decipher the genomes and to study the transcriptomes, which had up to then been studied using array-based technologies, limiting the quantification of transcripts only based on specific sequence probes distributed along the genome. Even the NGS technologies have some limitations: it is necessary to prepare amplified sequencing libraries before sequencing amplified DNA clones, with these steps being time-consuming and amplification libraries being expensive.

Moreover, there are still unresolved issues in sequencing complex genomes with many repetitive regions, due to the difficulty of assembling short reads. For these reasons, new sequencers came to the market with a new technology that aimed to further reduce the price of sequencing, and simplify the library preparation. These sequencers employ Single Molecule Sequencing Technology [2]. A few years ago, single-cell technologies slowly emerged [1], making it possible to sequence the transcriptome at the single-cell level and allowing us to study tissues in unprecedented detail. Tissue heterogeneity, detection of rare subpopulations, trajectory inference, gene regulatory network inference, and cell-cell communication inference are examples of what we can do with this technology [3].

Cancer involves uncontrolled proliferation of specific cells but it has become apparent that this process involves a complex ecological system of interacting cells. The tumor is composed of several cell types including normal cells, fibroblasts, immune cells, endothelial cells, adipocytes, and cancer cells, which interact in a surrounding environment rich in signaling molecules, and the extracellular matrix. During oncogenesis, cells are fed by the blood vessels, which give them the necessary nutrients for their growth. Intercellular communication has a fundamental role in homeostasis and also in cancer. This communication allows the recruitment and modulation of the stromal and immune cells, cell fate decisions, proliferation, and migration. This crosstalk inside the tumor and in the surrounding environment will promote angiogenesis, immune-escape, pre-metastatic niche formation, metastasis, and drug resistance [4,5]. Cell-cell communication (CCC) can occur either through direct cell interactions, mediated by gap junctions, cell adhesion, and intercellular bridges (tunnel nanotubes), or indirectly via the release of soluble factors, such as cytokines, growth factors, and chemokines. Extracellular vesicles are an important mode of communication between cancer cells and the tumor microenvironment (TME). The immune cells in the TME are abundant, varied in types, phenotypes, and states (CD4 and CD8 T lymphocytes, naive T lymphocytes, B lymphocytes, macrophages, NK cells, etc.). In fact, it was observed that tumor-infiltrating lymphocytes are tightly related to tumor growth and patient prognosis [6–9].

Tumor heterogeneity and the composition of its microenvironment are major causes of treatment failure and cancer resistance. For example, immune checkpoint blockers only work in at most 30% of the patients (and very often much less), and understanding how to predict patients' responses has become a real priority [10]. Relapse can be explained by the acquired resistance mechanisms present in the subclones, which have self-renewing characteristics. They will stay quiescent until the selective pressure of treatment or immune response is gone.

Descriptions of the TME have therefore become essential, and they can be obtained by either bulk technologies combined with deconvolution approaches or, more recently, by applying single-cell approaches. Single-cell technology allows us to study tumor heterogeneity, as well as cell-cell communication involving all the cells in the TME.

Single-cell sequencing technologies provide a large amount of data and require bioinformatic skills and knowledge to design scRNA-seq experiments and analyze them appropriately. The raw data produced are not exploitable immediately and need to be pre-processed before being used to address biological questions. This chapter will give an overview of different aspects of computational analysis of single-cell RNA-seq datasets. We will describe the different steps from designing scRNA-seq experiments to pre-processing and analysis of the data, mentioning which tools are available for the different steps of the analysis. The list of methods and tools will not be exhaustive, as this is a field in constant expansion and new ones are frequently produced, but we hope this chapter will serve as a helpful introduction to the topic and allow interested researchers to identify more complete resources to acquire deeper knowledge or more detailed information.

Designing Single-Cell Experiments and Choosing the Best Single-Cell Technologies

Before performing single-cell sequencing, it is necessary to carefully design the experiment in a way that will ensure that data analysis will generate robust and trustworthy results. This part is crucial to reduce the technical noise and to objectively measure the biological effect that we want to study.

Firstly, it is important to make a clear plan considering the following points:

- The project's goal
- The biological question and its hypothesis
- The budget and time allocated to the project
- The tissue under study
- The number of samples, replicates, and cells that we expect to consider in our experiment
- Whether we are interested in studying gene expression, alternative splicing, or also in identifying rare cell subpopulations

Secondly, it is important to choose the right technology to answer the biological question, and sometimes, this can be difficult because several technologies have been developed (table 1). Currently, two main technologies are used in scRNA-seq: plate-based and droplet-based.

- For the plate-based, fluorescence-activated cell sorting (FACS) is necessary to deposit one cell in each well (plate 96 or 384) containing a hypotonic lysis buffer Triton-X100 where mRNA is separated [11]. After that, cell barcodes are added to each well, and libraries are made. The major advantage of these methods is that they can sequence full-length transcripts, so they can be used to study structural variations such as RNA fusion, mutations in transcripts, and detection of pseudogenes and splice variants at the single-cell level [12]. Smart-seq techniques are the most used plate based method.
- Droplet-based methods use microfluidics which allows the fabrication of devices with microchannels handling very small quantities of liquid in micro volumes. In scRNA-seq, isolated cells encapsulate both barcode-containing beads/hydrogels, and unique molecular identifiers (UMIs), such that after pooling, and sequencing, each read can be mapped back to its cell of origin. Drop-seq and Chromium by 10X are examples of these methods.

Several studies compared the two technologies and showed that plate-based methods allow more detection of genes per cell if we

compare them with the droplet method. But these last methods quantified mRNA levels with less amplification noise due to the use of UMI [13]. In addition, Chromium detects more cell clusters than Smart-seq2, which on the other side detects more genes than Chromium [14]. A comparison of droplet methods like Chromium and drop-seq showed that Chromium has higher molecular sensitivity, and precision, and less technical noise [15].

In conclusion, plate-based methods must be considered if the main aim is to identify rare cell subpopulations or structural variation. On the contrary, if the goal is to study the heterogeneity of the tissue, Chromium is adequate.

Thirdly, we can start designing the experiment to ensure that we reduce the technical noise, which could have several origins, also depending on the single-cell technology used (batch effect, amplification bias, dropout, etc). This noise can confound downstream analysis and can be dealt with using two approaches:

- If we do a **balanced design**, samples, and replicates are sequenced in the same lanes on the flow cell (same conditions). Thus, it becomes possible to compare them and to be sure of the origin of the variation [16,17]. However, it is not always possible to do a balanced design, and in some cases, we do not have the choice to do a confounded design.
- In a **confounded design**, the samples and replicates are separated from the others (different lanes and flow cells), thus when we compare the measure between them, it becomes difficult to identify the source of the biological variation. In this case, several statistical methods exist to correct batch effects.

Table 1: the different single-cell technologies.

Technology	Isolation	Capacity (# of cells)	Coverage	UMI or spike-in	Advantages	Disadvantages	Year	Reference
Smart-seq	FACS	96 plates or 384 plates	Full-length	spike-in			2012	[18]
Smart-seq2	FACS	96 plates or 384 plates	Full-length	spike-in	● detect more genes ● alternative splicing	● capture a high proportion of mitochondrial genes ● cost	2013	[11,19]
Drop-seq	FACS		3’	UMI	● most cost-effective ● customizable		2015	[20]
Chromium	Droplet-based	1,000-10,000 cells	3’ or 5’	UMI	● cost	● Higher noise for mRNA with low expression levels ● dropout problem	2016	[21]

Data Analysis Pipeline Overview

Once the sequencing has been performed, a thorough data analysis will be key to extract biological information. This analysis will be divided into 3 steps (figure 1). The two first steps are common, and the third depends on the analysis goals defined in the experimental design.

- **Step 1:** *pre-processing*. In this stage, the sequence quality needs to be checked, and if it is not good, the sequences need to be trimmed. After that, the sequences will be aligned with the genome reference; if the mapping score is good, the analysis will follow step 2.
- **Step 2:** *main analysis*. This step is crucially dependent on the experimental design and can be divided into several subsets. For example, if it is a balanced or confounded design, it is necessary to correct the batch effects. The final result will be biased if an appropriate statistical method is not applied. This stage will close by the clustering, revealing the different subpopulations in the tissue/tumor.
- **Step 3:** can be denoted as *functional analysis*, depending on the biological question. It involves studying expression profiles at the gene or cell level. At the gene level, it is possible to study differential gene expression in different conditions (treated or not, for example) or use various tools for inferring the gene regulatory networks and identify pathways that are differentially enriched (through functional enrichment analysis). The trajectory inference (or pseudo-time) and the cell-cell interaction inference are examples of common analysis at the cell level.

In the following, we will provide an overview of different software frequently used for carrying out these steps.

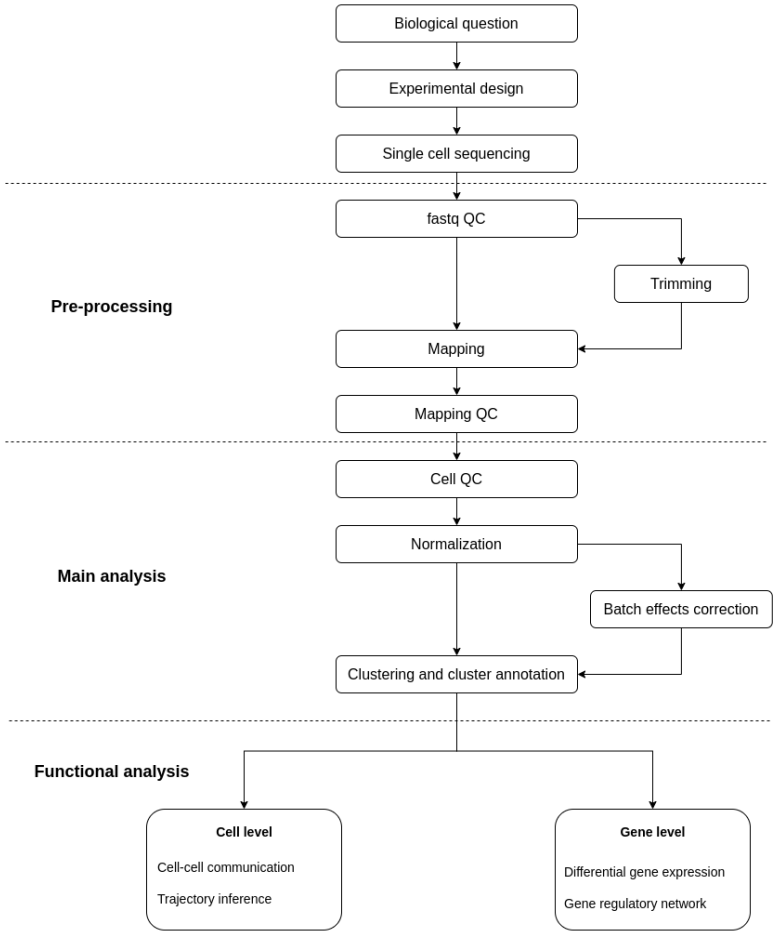

Figure 1: the different steps of single-cell analysis.

Pre-Processing

Raw Quality Check & Trimming

As for bulk RNA-seq, the scRNA-seq analysis starts by checking the quality of the raw sequences. Several phenomena, like sequencing errors, PCR artifacts, and contaminations, can

degrade the final sequencing result during the wet lab part and sequencing. To detect them, tools will check the presence of adaptors, the GC content, duplicated reads, and overrepresented k-mers (explained in the mapping and quality check paragraph). It is well known that the sequencing quality decreases at the 3' end of the reads. Thus, these bases must be removed to improve the mappability. FastQC is the most used tool for this part, and it computes some statistics about the composition and quality of raw sequences [22]. These statistics include the following:

- Summary statistics
- Distribution of per-base sequence quality
- Distribution of quality scores per sequence
- Distribution of per-base N content
- Sequence length distribution
- Sequence duplication
- Distribution of overrepresented sequences

With an automated pipeline, it will become easy to run FASTQC on a large number of samples. But, the FASTQC reports are not easy to compare between them. With MultiQC, it becomes easier to compare the FASTQC reports and interpret them [23]. Moreover, MultiQC will generate an HTML file report. Several tools, such as Trimmomatic [24] and Cutadapt [25], exist to discard the low-quality reads, trim adaptor sequences, and detect contamination, and poor-quality bases.

Mapping and Quality Check

After doing the raw quality check and adaptor trimming, mapping is the next step. By definition, read mapping assigns each read to a specific location in the genome. As explained in the different *single-cell technologies*, in Chromium and droplet technology, we have three important objects, (i) a cDNA fragment that identifies an RNA transcript, (ii) a cell barcode for each cell, and (iii) a unique molecular identifier (UMI). Mapping of reads includes four steps:

- Aligning the reads to a reference genome
- Assigning reads to genes
- Cell barcode demultiplexing (allocate each read to a specific cell)

- UMI deduplication (count the number of unique RNA molecules)

These four steps will produce a cell expression matrix, which contains the counts of RNA molecules in each cell for each gene. Several tools have been developed for bulk and single cell RNA-seq. Thus, it is not easy to choose a good aligner for the analysis, and benchmarking studies could be helpful. Here, we will present the main read mapping software used in scRNA-seq, which could be useful in immuno-oncology projects.

Two main approaches exist for alignment. The first tools use splice-aware aligner algorithms. Genes in the human genome contain a lot of introns, and coding sequences are short. Thus, it becomes difficult to properly align reads to the genome. For example, reads can be mapped entirely within an exon or can be spanning two or more exons [26–28]. To overcome this difficulty, splice-aware aligners have been developed. They used the annotation file (GFF/GTF). In this way, STAR can detect the splice junctions and correctly map the read to the reference genome. HISAT2 [29], STARsolo [30], and CellRanger (10X read mapping software) are the most used splice-aware alignment tools in scRNA-seq.

The other methods are based on pseudo-alignment algorithms, which include four steps. Firstly, the reference transcriptome will be split into *k*-mers, and a De Bruijn graph will be constructed. *k*-mers are unique length *k* subsequences of a sequence. A De Bruijn graph is a directed graph in which vertices are *k*-mers, and edges represent overlaps between the *k*-mers. Through the graph, a path represents a sequence [31]. Secondly, the RNA-seq reads will be converted into *k*-mers. Thirdly, the software will use the *k*-mers to assign reads to a transcript or several transcripts. Finally, the reads will be counted for each transcript or for each gene. In single-cell two common tools use pseudo-alignment strategy: kallisto/BUStools [32] and Salmon/Alevin/Alevin-fry [33].

In bulk RNA-seq, STAR is one of the top-performing read mapping tools [26,34]. When 10X developed their technology, they also wrote a read mapping software derived from STAR, CellRanger, which is one of the most used software in the

literature. This software uses STAR to perform the alignment while the transcript quantification part is done by the 10X proprietary algorithms. Alexander Dobin, the STAR's developer, decided to develop an extension of STAR, called STARsolo. CellRanger and STARsolo produce similar results [30]. Unlike CellRanger, STARSolo can take into account multi-gene reads (transcripts that align well to two or more genes), which is important to detect different classes of biologically important genes (e.g. paralogs) [30]. As written above, STARSolo uses the annotation file to recognize the splice junctions and to detect the spliced/unspliced transcripts. This information is important to perform RNA velocity studies to reconstruct pseudo-temporal trajectories of cell phenotypes starting from a cell mixture. STAR showed a better alignment rate and measured more abundance of the gene compared to Kallisto/BUStools [34]. By comparing 10x PBMC 3K data clustering results (annotation of cell types), the pipeline which used STAR and Kallisto annotated the same cell types but one cell type was lacking with Kallisto [34]. Kallisto has the advantage of being 4 times faster than STARSolo and the memory usage is 7.7 times less than the previous one [34].

Alignment files (bam) can contain biases, which are introduced during sequencing, sample preparation, and/or mapping algorithm. Thus, checking the quality of the read alignment is an important step. Thus, we will have an idea about the read alignment to the human genome and if the data fit with the expected outcome. The percentage of reads mapped to the reference genome (human) is a global indicator of the overall sequencing accuracy. A percentage above 90% in all samples indicates a very good mapping rate. Usually, we expect between 70 and 90% of reads mapped on the human genome. We also expect a small fraction of reads to map to multiple regions in the genome (multi-mapping reads). After these first read mapping quality statistics, we check to see where the reads are mapped. We expect more than 60% of reads in the exonic regions and between 20-30% in the intronic regions. If an equal distribution of reads mapping to intronic, exonic, and intergenic regions is present, this could be a sign of DNA contamination since mRNA from introns is normally quickly degraded.

Table 2: the different mapper frequently used in single-cell analysis.

Aligner	Strategy	Advantage	Disadvantage	References
STARsolo	Splice-aware	Precise	Slow	[30]
HISAT2	Splice-aware	Fast		[29]
CellRanger	Splice-aware	User-friendly	Proprietary software	No publication
Kallisto/BUStools	Pseudoalignment	Fast		[32]
Salmon/Alevin/Alevin-fry	Pseudoalignment	Fast		[33]

Main Analysis

Cell Quality Check

After ensuring that mapping quality is good, it is important to remove low-quality cells which can bias the analysis. In single-cell data, some metrics are used for quality control:

- the number of UMIs per cell, which represents the number of transcripts per cell
- the number of *features,* which represents the number of detected genes per cell
- the mitochondrial ratio, giving the percentage of reads coming from mitochondrial genes per cell (representing the living status of the cell)

In the literature, researchers use thresholds to filter the low-quality cells. The number of UMIs should be above 500 to have enough transcripts per cell and at least 250 genes must be detected per cell.

Traditionally, we see a high mitochondrial ratio in low UMIs and a low number of genes in cells, showing dying/damaged cells. A threshold <0.2 for this ratio is used to remove top damaged cells (except if high mitochondrial gene expression is expected in the experiment).

This first step of quality control was for cells, but more quality checks must be performed at the gene level. For example, we can remove genes that are expressed in less than 10 cells. This way we will keep living cells and expressed genes. Some literature is available to understand these thresholds [35,36]. Some data-driven methods exist to avoid choosing thresholds as they are often arbitrarily chosen [38]. Some code in R is available to be guided through the steps of quality control for single-cell experiments [1].

A possible additional step for quality control would be to remove doublets from the experiment. Technically, doublets are generated when two cells merge due to errors in cell sorting or capture, more often in droplet-based experiments. A benchmark

for doublet detection was performed identifying DoubletFinder as the best in detection accuracy and also in computational efficiency (memory usage+time) [38].

Normalization

As written in the introduction, the experimental design and the sequencing can generate several technical biases. The variability in sequencing depth might be increased by technical factors like sequencing depth, amplification, gene length, and GC content. But they are not the only source of unwanted variation. The amount of RNA per cell can vary between cell cycle stages [39,40]. Hence, it becomes difficult to untangle the biological differences from the technical ones between samples. The goal of the normalization is to eliminate/reduce these technical biases so that we can preserve the biological signal in our transcriptomic data. Bulk RNA-seq developed normalization methods. However, these methods are not suitable for single cell transcriptomics. Indeed, scRNA-seq generates abundant zero-expression values [41]. If bulk normalization methods are used in scRNA-seq, it may be a source of overcorrection for lowly expressed genes [42,43]. To avoid this problem, specific normalization methods for scRNA-seq have been developed. They are based on the scRNA-seq technologies that have been developed: plate based which uses spike-ins and droplet technology which uses UMIs. Using a technology that uses UMI can reduce technical biases.

scRNA-seq normalization methods are divided into two steps: scaling and transformation. The aim of scaling is to apply a size factor to scale data. In other words, all counts for each cell are divided by a cell-specific factor. The main hypothesis is that the bias affects all genes equally with the expected mean count for that cell. By dividing the counts by the size factor, we can remove the bias. To conclude, the size factor for each cell represents the estimate of the relative bias [44]. Then, the number of counts becomes comparable across cells and is less related to technical variation. The goal of transformation is to reduce the skewness in the distribution of the normalized values. Log transformation is often used for this step.

The first method of normalization is LogNorm which is the default method in the Seurat package for scRNA-seq analysis [45]. The idea of this method is to measure the gene expression for each cell is normalized over the total expression. Thus, we can eliminate the effect of the sequencing depth variation between cells. Firstly, we compute the normalized gene expression value (x_i) of gene X in cell *i* (Eq. 1). The transformation is performed by the log (Eq. 2). scRNAseq has a lot of zero-expression data values and to avoid zero counts, in Eq. 2, we add 1.

$$x_i = \frac{The\ read\ count\ of\ gene\ X\ in\ cell\ i}{Total\ of\ counts\ of\ cell\ i} \times 10^4 \quad \text{(Eq. 1)}$$

$$f(x_i) = ln(x_i + 1) \quad \text{(Eq. 2)}$$

The LogNorm method is a global scale factor because it is applied on all genes. However, if this is not the case, these methods may fail to detect true differential expressed genes. Genes with weak to moderate expression tend to get overcorrected, while genes with high expression get undercorrected. To avoid this problem, two other methods have been developed.

SCnorm is a method [46] that uses quantile regression to estimate the dependence of transcript expression on sequencing depth for every gene. Genes with similar dependence are then grouped, and a second quantile regression is used to estimate scale factors within each group. Within-group adjustment for sequencing depth is then performed using the estimated scale factors to provide normalized estimates of expression. However, this method has a major problem. As written above scRNA-seq has a lot of zero-expression values and this issue is not taken into account by this method.

As for LogNorm, sctransform is a method developed in the Seurat package [47]. The authors proposed a novel statistical approach for the modeling, normalization, and variance stabilization of UMI count data for scRNA-seq. They observed a linear relationship between UMI counts and the number of genes detected in a cell. They showed that different groups of genes

cannot be normalized by the same constant factor, representing an intrinsic challenge for scaling-factor-based normalization schemes, regardless of how the factors themselves are calculated. This method has three steps. Firstly, sctransform fits a generalized linear model (GLM) for each gene with UMI counts as the response variable and sequencing depth as the explanatory variable. This model describes the influence of technical noise on UMI counts. Secondly, sctransform uses the model parameter values and gene mean to learn global trends in the data. Thus, it is possible to perform independent regularizations for all parameters. Thirdly, the regularized regression parameters are used to define an affine function that transforms UMI counts into Pearson residuals. These residuals will inform us on how much the count is far from the true mean expression.

Batch Effect Correction & Integration

Very often people confuse normalization, batch effect, and data integration. These notions are different steps of pre-processing, but they are essentially different. To clarify, the goal of normalization is to target the variance from sequencing, like library preparation, amplification bias caused by gene length, GC content, *etc* [48]. Normalization is applied to the count matrix. This step does not correct the other sources of unwanted variation, which could stem from experimental design (sequencing platforms, sequencing lane, timing, reagents for example) and should be removed with batch effect correction [49]. We must distinguish three cases. Firstly, the correction of the samples from the same experiment. Secondly and thirdly, the correction between experiments performed in the same laboratory or between datasets from different laboratories. For the last two, we will need to perform data integration, which combines data from different sources and provides users with a unified view of them [50].

Several software has been developed to correct batch effects and to integrate data and it is based on three broad strategies:

- Regression-based correction
- Joint dimensionality reduction
- Joint dimensionality reduction and graph-based joint clustering

The first strategy uses regression-based correction. ComBat is a software that uses this strategy and it was the first method written to correct batch effects in microarray and bulk RNA-seq [51]. At the beginning of single-cell analysis, ComBat was used, but quickly, three main pitfalls were detected. Firstly, it does not account for differences in population composition. Secondly, it assumes the batch effect is additive. Thirdly, it is prone to overcorrection (in case of partial confounding). This method works well in small-medium datasets like microarray with similar cell type composition. Otherwise, it will fail in a large dataset with a complex mixture of cell types [49,50,52]. Another method must be used to correct the batch effect in scRNA-seq.

The second strategy uses joint dimensionality reduction (jDR). By definition, dimensionality reduction includes numerous methods for transforming a high-dimensional space, with a lot of variables or features, into a low-dimensional one, with few variables or features. This transformation will preserve the characteristic and/or structure of the data. These methods are applied to a dataset individually. In bioinformatics, we can have several datasets in our experiments. Joint dimensionality reduction will allow us to transform several data sets in a low dimensional space while preserving the specificities of each dataset. In other words, jDR methods use existing dimensionality reduction methods to apply multiple data sets [53,54].

Harmony is an example of a tool that uses the jDR strategy [55]. Firstly, Harmony will perform a Principal Component Analysis (PCA) to integrate the cells in low dimensional space and assign them to clusters. Secondly, the algorithm will compute the cluster centroids for each dataset. Thirdly it will apply a correction factor for each cluster. Finally, cells are rearranged into the cluster from the last correction. This workflow will be repeated until convergence is obtained, meaning that additional training will not improve batch correction. Mutual Nearest Neighbors (MNN) is an algorithm to correct batch effects with jDR strategy.

The MNN algorithm is inspired by the idea of K-Nearest Neighbors (KNN). This algorithm has 2 main assumptions [49].

Firstly, there is at least one cell population that is present in both batches. Secondly, the batch effect variation is much smaller than the biological effect variation between different cell types. The method tries to find the most similar cells (mutual neighbors) between the batches. Then, the algorithm will measure the difference between batches to quantify how strong the batch effect is. This information is used to scale the counts for the rest of the cells in the batches.

Seurat uses Canonical Correlation Analysis (CCA) [56]. In this method, the data from the batches are projected into a low-dimensional space. The algorithm maximizes correlation (or covariance) between the data sets from different batches. The dataset projections are correlated but they do not overlap well in low dimensional space. This problem is fixed with the Dynamic Time Warping (DTW) algorithm, which compares the similarity or calculates the distance between two or more arrays with different lengths. CCA data projection will be stretched and squeezed to align well between them.

These tools are frequently used in scRNA-seq analysis in immuno-oncology. Several studies compared and evaluated their efficiency. By testing different tools with five scenarios of batch effect correction and several datasets, Tran *et al*, showed that Harmony, and Seurat achieved good scores. On the other hand, Combat was the worst-performing method [57].

Feature Selection & Dimensionality Reduction

In data science, we often work with high-dimensional data. The dimension of a dataset corresponds to the number of attributes/features that exist in a dataset. For example, a table with 2 columns is a 2-dimensional dataset, which can be represented by a 2D plot. If we add another dimension, we will obtain a 3-dimensional space and a 3D plot. We can add as many dimensions as we want. High-dimensional datasets are common in genomics [58–61]. Having a high dimensional dataset leads to difficulties during analyses and visualization, leading to what is currently referred to as the ‘Curse of Dimensionality’. In scRNA-seq, the datasets have a high-dimensional space with *N*

(tens to hundreds normally) samples, *M (thousands)* genes, and *P (thousands)* cells. This requires a lot of computational time, while some algorithms struggle with many dimensions. Dimensionality reduction (DR) describes the techniques that transform the data from a high-dimensional space into a low-dimensional space to overcome these difficulties. They are divided into two different groups: (i) linear and (ii) non-linear. In linear methods, the output (low dimension) of the system is proportional to the input (high dimension). This proportionality is achieved by the linear projection of the original data onto a low-dimensional space. In the case of non-linear methods, the output of the system is not proportional to the input. In scRNA-seq, we can use both methods.

Principal Component Analysis (PCA) is a linear method, which is a commonly used DR method. The PCA algorithm will find the first principal component with the largest variance in the data. Thus, it will seek the second component with the largest variance which is not correlated to the first component. This process will be repeated until the component reaches a threshold defined by the users.

The *t*-Stochastic Neighborhood Embedding (*t*-SNE) algorithm is a non-linear method for DR [62]. This algorithm is divided into 3 steps. Firstly, the algorithm will convert the Euclidean distances of a high dimensional space into a conditional probability that represents similarities. Secondly, the algorithm will create a low-dimensional space where the data will be represented, but on which we do not know the coordinates of our points. We are therefore going to randomly distribute the points over this new space. The rest is quite similar to the first step, we calculate the similarities of the points in the newly created space, but using a t-Student distribution and not Gaussian. Thirdly, to faithfully represent the points in the lower dimensional space, we would ideally like the similarity measures in the two spaces to be consistent. We, therefore, need to compare the similarities of points in the two spaces using the Kullback-Leibler (KL) measure.

The Uniform Manifold Approximation and Projection (UMAP) algorithm is based on three assumptions about the data. Firstly, the data are uniformly distributed on the Riemannian manifold. Secondly, the Riemannian metric is locally constant, and finally, the manifold is locally connected. According to these assumptions, the manifold with fuzzy topology can be modeled. The UMAP algorithm has two main stages. The first stage involves constructing a weighted graph that encodes the local structure of the data. This is done by selecting a set of "landmark" points in the high-dimensional space and then calculating the distances between each point and its nearest neighbors. The distances are used to construct a weighted graph, where the nodes represent the data points and the edges represent the distances between them. The second stage involves finding a low-dimensional representation of the data that preserves the global structure of the graph. This is done by minimizing a cost function that measures the difference between the distances in the original high-dimensional space and the distances in the low-dimensional space. This optimization problem is solved using a technique called "stochastic gradient descent," which involves iteratively updating the low-dimensional representation in a way that reduces the cost function. UMAP has superior run-time performance compared with the *t*-SNE [63,64].

Clustering and Cell Type Annotation

These methods presented previously gather a set of learning algorithms whose goal is to group unlabeled data with similar properties. Thus, we obtain a cluster of different groups of cells whose cell types are unknown. We then need to assign cell types for each group. This step is a critical feature of scRNA-seq. Several tools Seurat [45], Monocle 3 [65], SCENIC [66] perform clustering with DR methods (t-SNE, UMAP) and cell type identification. In this step, we can identify rare cell types or subpopulations. In order to improve this identification, new tools, like scClassify [67], SingleCellNet [68], and Sincell [69] have been developed. Once the cell type assignment is done, we can start the downstream analysis, like cell trajectories or cell-cell communication inference.

An Example of Downstream Analysis: Cell-Cell Communication Inference and Analysis in TME

After clustering annotation, the *downstream analysis* will allow us to extract biological insights from the scRNA-seq data. As written in *Data analysis pipeline overview*, this analysis can be divided into two parts, which are cell- and gene-level. The cell-level analysis will use methods to characterize cellular structure like trajectory inference and cell-cell communication, while gene-level with differential gene expression and gene regulatory network will investigate molecular signals in the data. At the gene-level, with the differential gene expression approach ask the question is whether any genes are differentially expressed between two experimental conditions. Gene regulatory networks with scRNA-seq is the second method that we could perform at this level and it will be explained in the next chapter. At the cell-level, the clustering annotation cannot describe the whole cellular diversity. The observed heterogeneity is under continuous biological processes. By using trajectory inference methods, which use dynamic models of gene expression, it becomes possible to capture transitions between cell identities, and branching differentiation processes for example. Cell-cell communication (CCC) is the second type of analysis that can be performed at this level and as explained in the introduction, the rise of tools for inference of cell-cell communication from scRNA-seq has advanced the development of cancer immunotherapies. Here, we will explore more deeply CCC analysis with scRNA-seq data.

Cell-cell communication, also known as cell-cell interaction or intercellular communication, is essential for the development of multicellular systems [70]. Cells are able to receive and process many signals simultaneously which are from their immediate environment. But cells also send out messages to other cells close or far away. This intercellular communication requires coordination by soluble factors, associated membrane proteins, exosomes, and gap junction channels, for example. In the past, researchers thought that CCC was lost in cancer because cancer cells are disconnected from healthy cells but it is likely that communication is changed but is not lost. For example, in

melanoma, malignant cells can deliver exosomes that create an environment for tumor cells to survive [71]. With scRNA-seq it's possible to infer CCC between TME, immune, and cancer cells. Several tools have been developed to infer CCC from scRNA-seq data and it can be difficult to choose a tool for our analysis. In this paragraph, we will explain the main ideas behind these tools, and after we will compare some of them.

All these CCC inference tools share a common input, the count matrix, which contains the transcript levels of each gene across different samples and cells. At the same time, the known interacting protein or ligand-receptor pairs in specialized databases like KEGG and Reactome are collected. This information is used to filter the count matrix, which will contain only the genes associated with the interacting proteins. This filtered table will be used for the CCC analysis which is divided into three steps [72]. Firstly, the expression levels of ligand-receptors pairs are used as inputs to compute a communication score by using a scoring function (function f(L, R), where L and R are the expression values of the ligand and the receptor). Secondly, an aggregation function will compute the communication scores between samples or cells. In the third step, the communication and aggregation scores are used to generate different graphics, like hierarchical and circle plots or network visualizations, which will facilitate the interpretation of the results. In this chapter, we do not explain the mathematical methods to compute the computation and aggregation score, but we refer the reader to a comprehensive review [73].

The inference of cell-cell communication from scRNA-seq data can help us understand the signaling alterations provoked by immune checkpoint blockers in the TME [74]. For example, CellPhoneDB was the first tool developed for this aim and became one of the most used tools in CCC [75,76]. In hepatocarcinoma and esophageal squamous carcinoma, CellPhoneDB found a potential reprogramming interaction from tumor cells to macrophages by the SPP1-CD44 axis [77,78]. This axis is involved in an immune checkpoint. Several studies with patients used CellPhoneDB to characterize CCC in ICB resistance and response. They identified enhanced signaling of

HAVCR3-LGALS9 (TIM3-Galectin9) in CD8+ T cells in non-responding and resistant patients [79–81]. CellPhoneDB is able to highlight the intercellular communication between immune cells and cancer cells, but it has some limitations. Indeed, CellPhoneDB takes into account only ligands and receptors, while it is known that some signaling cofactors in the sender or receiver cells can influence intracellular pathways. Alternative software, like CellChat, and NicheNet was developed to take this point into account. CellChat was used and showed promising results in different immunotherapy signaling studies [77,82–84]. NicheNet [85] is widely used when researchers want to investigate intercellular communication in the TME [74].

Conclusion: The Future of scRNA-seq in Immuno-Oncology

Single-cell RNA-seq is revolutionizing our perspective on the tumor microenvironment and driving innovative approaches in immuno-oncology research [86–88]. In this chapter, we have described the main parts of the computational analysis and given examples of downstream analysis. Understanding the different steps of this analysis is important for generating valuable experiments and trustworthy results. Unfortunately, single-cell analysis requires statistical knowledge and programming skills and can be difficult for biologists. In order to make scRNA-seq more accessible to a broader community of researchers and/or clinicians, some pipelines have been developed. scAmpi and Bullito are automated, flexible, and parallelizable pipelines [89,90]. These pipelines include all the steps and software described above. The main difference between the two is that scAmpi has been developed for clinical applications. pipeCom is a flexible R framework for pipeline comparison, which then chooses the best among the various tools [91].

As with everything, there are some limitations of these approaches that should be considered. For example, isolation of cells from solid tissues can introduce biases on the number of cells of each type that is captured and included in the data, so it is not advisable to assume that cell numbers obtained in scRNAseq experiments are directly proportional to those

effectively present in the tissue. Also, defining cell types can be done based on expression of proteins on cell surfaces, which are not necessarily strongly correlated to the levels of the corresponding mRNAs. For this reason, additional technologies such as CITEseq [92] and INs-Seq [93] provide a multi-omic view of cells, detecting both cell surface proteins and transcripts on each cell. Similarly, the combination of transcriptomics with the identification of open chromatin regions can currently be performed on the same cell, like NEAT-seq [94] and smart3-seq [95]. It is also possible to perform genome and transcriptome single-cell approaches like G&T-seq [96] and scTrio-seq [97].

In conclusion, single-cell approaches can be helpful to study the TME, but the spatial information and context of the cells are lost. Recently the development of spatial omics techniques at the single-cell level and computational methods to analyze them are revolutionizing biology once again [98]. Nowadays, it is possible to combine spatial transcriptomics with scRNA-seq datasets to infer spatial cell-cell communication [99–102]. With the progress of machine learning, new computational methods will be developed to integrate these datasets to understand how cell-cell communication influences the fate of cells in tumors.

References

1. Heather JM, Chain B. The sequence of sequencers: The history of sequencing DNA. Genomics. 2016; 107: 1–8.
2. Bleidorn C. Third generation sequencing: technology and its potential impact on evolutionary biodiversity research. Syst. Biodivers. 2016; 14: 1–8.
3. Dal Molin A, Di Camillo B. How to design a single-cell RNA-sequencing experiment: pitfalls, challenges and perspectives. Brief. Bioinform. 2018; 1–11.
4. Roghayyeh Baghban, Leila Roshangar, Rana Jahanban-Esfahlan, Khaled Seidi, Abbas Ebrahimi-Kalan, et al. Tumor microenvironment complexity and therapeutic implications at a glance. Cell Commun. Signal. 2020; 18: 59.
5. Salemme V, Centonze G, Cavallo F, Defilippi P, Conti L. The Crosstalk Between Tumor Cells and the Immune Microenvironment in Breast Cancer: Implications for

Immunotherapy. Front. Oncol. 2021; 11: 610303.
6. Brummel K, Eerkens AL, De Bruyn M, Nijman HW. Tumour-infiltrating lymphocytes: from prognosis to treatment selection. Br. J. Cancer. 2023; 128: 451–458.
7. Fridman WH, Pagès F, Sautès-Fridman C, Galon J. The immune contexture in human tumours: impact on clinical outcome. Nat. Rev. Cancer. 2012; 12: 298–306.
8. F Pagès, J Galon, MC Dieu-Nosjean, E Tartour, C Sautès-Fridman, et al. Immune infiltration in human tumors: a prognostic factor that should not be ignored. Oncogene. 2010; 29: 1093–1102.
9. Zhu N, Hou J. Assessing immune infiltration and the tumor microenvironment for the diagnosis and prognosis of sarcoma. Cancer Cell Int. 2020; 20: 577.
10. L Castelo-Branco, G Morgan, A Prelaj, M Scheffler, H Canhão, et al. Challenges and knowledge gaps with immune checkpoint inhibitors monotherapy in the management of patients with non-small-cell lung cancer: a survey of oncologist perceptions. ESMO Open. 2023; 8: 100764.
11. Simone Picelli, Omid R Faridani, Åsa K Björklund, Gösta Winberg, Sven Sagasser, et al. Full-length RNA-seq from single cells using Smart-seq2. Nat. Protoc. 2014; 9: 171–181.
12. Victoria Probst, Arman Simonyan, Felix Pacheco, Yuliu Guo, Finn Cilius Nielsen, et al. Benchmarking full-length transcript single cell mRNA sequencing protocols. BMC Genomics. 2022; 23: 860.
13. Christoph Ziegenhain, Beate Vieth, Swati Parekh, Björn Reinius, Amy Guillaumet-Adkins, et al. Comparative Analysis of Single-Cell RNA Sequencing Methods. Mol. Cell. 2017; 65: 631-643.e4.
14. Wang X, He Y, Zhang Q, Ren X, Zhang Z. Direct Comparative Analyses of 10X Genomics Chromium and Smart-seq2. Genomics Proteomics Bioinformatics. 2021; 19: 253-266.
15. Xiannian Zhang, Tianqi Li, Feng Liu, Yaqi Chen, Jiacheng Yao, et al. Comparative Analysis of Droplet-Based Ultra-High-Throughput Single-Cell RNA-Seq Systems. Mol. Cell. 2019; 73: 130-142.e5.
16. Baran-Gale J, Chandra T, Kirschner K. Experimental design

for single-cell RNA sequencing. Brief. Funct. Genomics. 2018; 17: 233–239.
17. Hicks SC, Teng M, Irizarry RA. Missing data and technical variability in single-cell RNA-sequencing experiments. Biostatistics. 2018; 562–578.
18. Goetz JJ, Trimarchi JM. Transcriptome sequencing of single cells with Smart-Seq. Nat. Biotechnol. 2012; 30: 763–765.
19. Simone Picelli, Åsa K Björklund, Omid R Faridani, Sven Sagasser, Gösta Winberg, et al. Smart-seq2 for sensitive full-length transcriptome profiling in single cells. Nat. Methods. 2013; 10: 1096–1098.
20. Evan Z Macosko, Anindita Basu, Rahul Satija, James Nemesh, Karthik Shekhar, et al. Highly parallel genome-wide expression profiling of individual cells using nanoliter droplets. Cell. 2015; 161: 1202–1214.
21. Grace XY Zheng, Jessica M Terry, Phillip Belgrader, Paul Ryvkin, Zachary W Bent, et al. Massively parallel digital transcriptional profiling of single cells. Nat. Commun. 2017; 8.
22. Andrews S. FastQC. 2012.
23. Ewels P, Magnusson M, Lundin S, Käller M. MultiQC: summarize analysis results for multiple tools and samples in a single report. Bioinformatics. 2016; 32: 3047–3048.
24. Bolger AM, Lohse M, Usadel B. Trimmomatic: a flexible trimmer for Illumina sequence data. Bioinformatics. 2014; 30: 2114–2120.
25. Martin M. Cutadapt removes adapter sequences from high-throughput sequencing reads. EMBnet.journal. 2011; 17: 10.
26. Giacomo Baruzzo, Katharina E Hayer, Eun Ji Kim, Barbara Di Camillo, Garret A FitzGerald, et al. Simulation-based comprehensive benchmarking of RNA-seq aligners. Nat. Methods. 2017; 14: 135–139.
27. Leonard D Goldstein, Yi Cao, Gregoire Pau, Michael Lawrence,Thomas D Wu, et al. Prediction and Quantification of Splice Events from RNA-Seq Data. PLOS ONE. 2016; 11: e0156132.
28. Pär G Engström, Tamara Steijger, Botond Sipos, Gregory R Grant, André Kahles, et al. Systematic evaluation of spliced alignment programs for RNA-seq data. Nat. Methods. 2013; 10: 1185–1191.

29. Kim D, Paggi JM, Park C, Bennett C, Salzberg SL. Graph-based genome alignment and genotyping with HISAT2 and HISAT-genotype. Nat. Biotechnol. 2019; 37: 907–915.
30. Kaminow B, Yunusov D, Dobin A, Spring C. STARsolo : accurate , fast and versatile mapping / quantification of single-cell and single-nucleus RNA-seq data. 2021; 1–35.
31. Compeau PEC, Pevzner PA, Tesler G. How to apply de Bruijn graphs to genome assembly. Nat. Biotechnol. 2011; 29: 987–991.
32. Páll Melsted, A. Sina Booeshaghi, Lauren Liu, Fan Gao, Lambda Lu, et al. Modular, efficient and constant-memory single-cell RNA-seq preprocessing. Nat. Biotechnol. 2021; 39: 813–818.
33. Srivastava A, Malik L, Sarkar H, Patro R. A Bayesian framework for inter-cellular information sharing improves dscRNA-seq quantification. Bioinformatics. 2020; 36: i292–i299.
34. Du Y, Huang Q, Arisdakessian C, Garmire LX. Evaluation of STAR and kallisto on single cell RNA-seq data alignment. G3 Genes Genomes Genet. 2020; 10: 1775–1783.
35. Imad Abugessaisa, Akira Hasegawa, Shuhei Noguchi, Melissa Cardon, Kazuhide Watanabe, et al. SkewC: Identifying cells with skewed gene body coverage in single-cell RNA sequencing data. iScience. 2022; 25: 103777.
36. Tomislav Ilicic, Jong Kyoung Kim, Aleksandra A Kolodziejczyk, Frederik Otzen Bagger, Davis James, et al. Classification of low quality cells from single-cell RNA-seq data. Genome Biol. 2016; 17: 1–15.
37. Ariel A Hippen, Matias M Falco, Lukas M Weber, Erdogan Pekcan Erkan, Kaiyang Zhang, et al. miQC: An adaptive probabilistic framework for quality control of single-cell RNA-sequencing data. PLOS Comput. Biol. 2021; 17: e1009290.
38. Xi NM, Li JJ. Benchmarking Computational Doublet-Detection Methods for Single-Cell RNA Sequencing Data. Cell Syst. 2021; 12: 176-194.e6.
39. Georgi K Marinov, Brian A Williams, Ken McCue, Gary P Schroth, Jason Gertz, et al. From single-cell to cell-pool transcriptomes: Stochasticity in gene expression and RNA splicing. Genome Res. 2014; 24: 496–510.

40. Andrews TS, Kiselev VY, McCarthy D, Hemberg M. Tutorial: guidelines for the computational analysis of single-cell RNA sequencing data. Nat. Protoc. 2020; 16: 1–9.
41. Bacher R, Kendziorski C. Design and computational analysis of single-cell RNA-sequencing experiments. Genome Biol. 2016; 17: 1–14.
42. Vallejos CA, Risso D, Scialdone A, Dudoit S, Marioni JC. Normalizing single-cell RNA sequencing data: challenges and opportunities. Nat. Methods. 2017; 14: 565–571.
43. Chen G, Ning B, Shi T. Single-cell RNA-seq technologies and related computational data analysis. Front. Genet. 2019; 10: 1–13.
44. Anders S, Huber W. Differential expression analysis for sequence count data. Genome Biol. 2010; 11: R106.
45. Satija R, Farrell JA, Gennert D, Schier AF, Regev A. Spatial reconstruction of single-cell gene expression data. Nat. Biotechnol. 2015; 33: 495–502.
46. Rhonda Bacher, Li-Fang Chu, Ning Leng, Audrey P Gasch, James A Thomson, et al. SCnorm: robust normalization of single-cell RNA-seq data. Nat. Methods. 2017; 14: 584–586.
47. Hafemeister C, Satija R. Normalization and variance stabilization of single-cell RNA-seq data using regularized negative binomial regression. Genome Biol. 2019; 20: 296.
48. Cheng Jia, Yu Hu, Derek Kelly, Junhyong Kim, Mingyao Li, et al. Accounting for technical noise in differential expression analysis of single-cell RNA sequencing data. Nucleic Acids Res. 2017; 45: 10978–10988.
49. Haghverdi L, Lun ATL, Morgan MD, Marioni JC. Batch effects in single-cell RNA-sequencing data are corrected by matching mutual nearest neighbors. Nat. Biotechnol. 2018; 36: 421–427.
50. Luecken MD, Theis FJ. Current best practices in single-cell RNA-seq analysis: a tutorial. Mol. Syst. Biol. 2019; 15.
51. Johnson WE, Li C, Rabinovic A. Adjusting batch effects in microarray expression data using empirical Bayes methods. Biostatistics. 2007; 8: 118–127.
52. Hoa Thi Nhu Tran, Kok Siong Ang, Marion Chevrier, Xiaomeng Zhang, Nicole Yee Shin Lee, et al. A benchmark of batch-effect correction methods for single-cell RNA sequencing data. Genome Biol. 2020; 21: 12.

53. Laura Cantini, Pooya Zakeri, Celine Hernandez, Aurelien Naldi, Denis Thieffry, et al. Benchmarking joint multi-omics dimensionality reduction approaches for the study of cancer. Nat. Commun. 2021; 12: 124.
54. Wei Liu, Xu Liao, Yi Yang, Huazhen Lin, Joe Yeong, et al. Joint dimension reduction and clustering analysis of single-cell RNA-seq and spatial transcriptomics data. Nucleic Acids Res. 2022; 50: e72–e72.
55. Ilya Korsunsky, Nghia Millard, Jean Fan, Kamil Slowikowski, Fan Zhang, et al. Fast, sensitive and accurate integration of single-cell data with Harmony. Nat. Methods. 2019; 16: 1289–1296.
56. Butler A, Hoffman P, Smibert P, Papalexi E, Satija R. Integrating single-cell transcriptomic data across different conditions, technologies, and species. Nat. Biotechnol. 2018; 36: 411–420.
57. Chazarra-Gil R, van Dongen S, Kiselev VY, Hemberg M. Flexible comparison of batch correction methods for single-cell RNA-seq using BatchBench. Nucleic Acids Res. 2012; 49: e42–e42.
58. Ding J, Condon A, Shah SP. Interpretable dimensionality reduction of single cell transcriptome data with deep generative models. Nat. Commun. 2018; 9.
59. Huang H, Wang Y, Rudin C, Browne EP. Towards a comprehensive evaluation of dimension reduction methods for transcriptomic data visualization. Commun. Biol. 2022; 5: 719.
60. Chen Meng, Oana A Zeleznik, Gerhard G Thallinger, Bernhard Kuster, Amin M Gholami, et al. Dimension reduction techniques for the integrative analysis of multi-omics data. Brief. Bioinform. 2016; 17: 628–641.
61. Quackenbush J. Extracting biology from high-dimensional biological data. J. Exp. Biol. 2007; 210: 1507–1517.
62. Maaten L. van der & Hinton, G. Visualizing Data using t-SNE. J. Mach. Learn. Res. 2008; 9: 2579–2605.
63. Kobak D, Berens P. The art of using t-SNE for single-cell transcriptomics. Nat. Commun. 2019; 10.
64. McInnes L, Healy J, Melville J. UMAP: Uniform manifold approximation and projection for dimension reduction. arXiv 2018.

65. Junyue Cao, Malte Spielmann, Xiaojie Qiu, Xingfan Huang, Daniel M Ibrahim, et al. The single-cell transcriptional landscape of mammalian organogenesis. Nature. 2019; 566: 496–502.
66. Sara Aibar, Carmen Bravo González-Blas, Thomas Moerman, Vân Anh Huynh-Thu, Hana Imrichova, et al. SCENIC: single-cell regulatory network inference and clustering. Nat. Methods. 2017; 14: 1083–1086.
67. Yingxin Lin, Yue Cao, Hani Jieun Kim, Agus Salim, Terence P Speed, et al. scClassify: sample size estimation and multiscale classification of cells using single and multiple reference. Mol. Syst. Biol. 2020; 16.
68. Tan Y, Cahan P. SingleCellNet: A Computational Tool to Classify Single Cell RNA-Seq Data Across Platforms and Across Species. Cell Syst. 2019; 9: 207-213.e2.
69. Juliá M, Telenti A, Rausell A. Sincell: an R/Bioconductor package for statistical assessment of cell-state hierarchies from single-cell RNA-seq. Bioinformatics. 2015; 31: 3380–3382.
70. Singer SJ. Intercellular Communication and Cell-Cell Adhesion. Science. 1992; 255: 1671–1677.
71. Cassidy L Bland, Christina N Byrne-Hoffman, Audry Fernandez, Stephanie L Rellick, Wentao Deng, et al. Exosomes derived from B16F0 melanoma cells alter the transcriptome of cytotoxic T cells that impacts mitochondrial respiration. FEBS J. 2018; 285: 1033–1050.
72. Armingol E, Officer A, Harismendy O, Lewis NE. Deciphering cell–cell interactions and communication from gene expression. Nat. Rev. Genet. 2021; 22: 71–88.
73. Lihong Peng, Feixiang Wang, Zhao Wang, Jingwei Tan, Li Huang, et al. Cell–cell communication inference and analysis in the tumour microenvironments from single-cell transcriptomics: data resources and computational strategies. Brief. Bioinform. 2022; 23: bbac234.
74. Bridges K, Miller-Jensen K. Mapping and Validation of scRNA-Seq-Derived Cell-Cell Communication Networks in the Tumor Microenvironment. Front. Immunol. 2022; 13: 885267.
75. Efremova M, Vento-Tormo M, Teichmann SA, Vento-Tormo R. CellPhoneDB: inferring cell–cell communication

from combined expression of multi-subunit ligand–receptor complexes. Nat. Protoc. 2020; 15: 1484–1506.
76. Roser Vento-Tormo, Mirjana Efremova, Rachel A Botting, Margherita Y Turco, Miquel Vento-Tormo, et al. Single-cell reconstruction of the early maternal–fetal interface in humans. Nature. 2018; 563: 347–353.
77. Zhencong Chen, Mengnan Zhao, Jiaqi Liang, Zhengyang Hu, Yiwei Huang, et al. Dissecting the single-cell transcriptome network underlying esophagus non-malignant tissues and esophageal squamous cell carcinoma. eBioMedicine. 2021; 69: 103459.
78. Lulu Liu, Ruyi Zhang, Jingwen Deng, Xiaomeng Dai, Xudong Zhu, et al. Construction of TME and Identification of crosstalk between malignant cells and macrophages by SPP1 in hepatocellular carcinoma. Cancer Immunol. Immunother. 2022; 71: 121–136.
79. Ayse Bassez, Hanne Vos, Laurien Van Dyck, Giuseppe Floris, Ingrid Arijs, et al. A single-cell map of intratumoral changes during anti-PD1 treatment of patients with breast cancer. Nat. Med. 2021; 27: 820–832.
80. Kevin Bi, Meng Xiao He, Ziad Bakouny, Abhay Kanodia, Sara Napolitano, et al. Tumor and immune reprogramming during immunotherapy in advanced renal cell carcinoma. Cancer Cell. 2021; 39: 649-661.e5.
81. Yi-Quan Jiang, Zi-Xian Wang, Ming Zhong, Lu-Jun Shen, Xue Han, et al. Investigating Mechanisms of Response or Resistance to Immune Checkpoint Inhibitors by Analyzing Cell-Cell Communications in Tumors Before and After Programmed Cell Death-1 (PD-1) Targeted Therapy: An Integrative Analysis Using Single-cell RNA and Bulk-RNA Sequencing Data. OncoImmunology. 2021; 10: 1908010.
82. Alexander H Lee, Lu Sun, Aaron Y Mochizuki, Jeremy G Reynoso, Joey Orpilla, et al. Neoadjuvant PD-1 blockade induces T cell and cDC1 activation but fails to overcome the immunosuppressive tumor associated macrophages in recurrent glioblastoma. Nat. Commun. 2021; 12: 6938.
83. Park Y, Jeong J, Seong S, Kim W. In Silico Evaluation of Natural Compounds for an Acidic Extracellular Environment in Human Breast Cancer. Cells. 2021; 10: 2673.
84. Honghao Yin, Rui Guo, Huanyu Zhang, Songyi Liu, Yuehua

Gong, et al. A Dynamic Transcriptome Map of Different Tissue Microenvironment Cells Identified During Gastric Cancer Development Using Single-Cell RNA Sequencing. Front. Immunol. 2021; 12: 728169.
85. Browaeys R, Saelens W, Saeys Y. NicheNet: modeling intercellular communication by linking ligands to target genes. Nat. Methods. 2020; 17: 159–162.
86. Bai Z, Su G, Fan R. Single-cell Analysis Technologies for Immuno-oncology Research: from Mechanistic Delineation to Biomarker Discovery. Genomics Proteomics Bioinformatics. 2021; 19: 191–207.
87. Ma A, Xin G, Ma Q. The use of single-cell multi-omics in immuno-oncology. Nat. Commun. 2022; 13: 2728.
88. Fatima Valdes-Mora, Kristina Handler, Andrew M K Law, Robert Salomon, Samantha R Oakes, et al. Single-cell transcriptomics in cancer immunobiology: The future of precision oncology. Front. Immunol. 2018; 9.
89. Anne Bertolini, Michael Prummer, Mustafa Anil Tuncel, Ulrike Menzel, María Lourdes Rosano-González, et al. scAmpi—A versatile pipeline for single-cell RNA-seq analysis from basics to clinics. PLOS Comput. Biol. 2022; 18: e1010097.
90. Luis García-Jimeno, Coral Fustero-Torre, María José Jiménez-Santos, Gonzalo Gómez-López, Tomás Di Domenico, et al. bollito: a flexible pipeline for comprehensive single-cell RNA-seq analyses. Bioinformatics. 2022; 38: 1155–1156.
91. Germain PL, Sonrel A, Robinson MD. pipeComp, a general framework for the evaluation of computational pipelines, reveals performant single cell RNA-seq preprocessing tools. Genome Biol. 2020; 21: 227.
92. Marlon Stoeckius, Christoph Hafemeister, William Stephenson, Brian Houck-Loomis, Pratip K Chattopadhyay, et al. Simultaneous epitope and transcriptome measurement in single cells. Nat. Methods. 2017; 14: 865–868.
93. Yonatan Katzenelenbogen, Fadi Sheban, Adam Yalin, Ido Yofe, Dmitry Svetlichnyy, et al. Coupled scRNA-Seq and Intracellular Protein Activity Reveal an Immunosuppressive Role of TREM2 in Cancer. Cell. 2020; 182: 872-885.e19.
94. Amy F Chen, Benjamin Parks, Arwa S Kathiria, Benjamin

Ober-Reynolds, Jorg J Goronzy, et al. NEAT-seq: simultaneous profiling of intra-nuclear proteins, chromatin accessibility and gene expression in single cells. Nat. Methods. 2022; 19: 547–553.
95. Cheng H. Smart3-ATAC: a highly sensitive method for joint accessibility and full-length transcriptome analysis in single cells. 2021. Available online at: http://biorxiv.org/lookup/doi/10.1101/2021.12.02.470912
96. Iain C Macaulay, Wilfried Haerty, Parveen Kumar, Yang I Li, Tim Xiaoming Hu, et al. G&T-seq: parallel sequencing of single-cell genomes and transcriptomes. Nat. Methods. 2015; 12: 519–522.
97. Yu Hou, Huahu Guo, Chen Cao, Xianlong Li, Boqiang Hu, et al. Single-cell triple omics sequencing reveals genetic, epigenetic, and transcriptomic heterogeneity in hepatocellular carcinomas. Cell Res. 2016; 26: 304–319.
98. Marx V. Method of the Year: spatially resolved transcriptomics. Nat. Methods. 2021; 18: 9–14.
99. Chiara Baccin, Jude Al-Sabah, Lars Velten, Patrick M Helbling, Florian Grünschläger, et al. Combined single-cell and spatial transcriptomics reveal the molecular, cellular and spatial bone marrow niche organization. Nat. Cell Biol. 2020; 22: 38–48.
100. Cang Z, Nie Q. Inferring spatial and signaling relationships between cells from single cell transcriptomic data. Nat. Commun. 2020; 11: 1–13.
101. Bin Li, Wen Zhang, Chuang Guo, Hao Xu, Longfei Li, et al. Benchmarking spatial and single-cell transcriptomics integration methods for transcript distribution prediction and cell type deconvolution. Nat. Methods. 2022; 19: 662–670.
102. Yan L, Sun X. Benchmarking and integration of methods for deconvoluting spatial transcriptomic data. Bioinformatics. 2023; 39: btac805.

Book Chapter

Dissecting Cellular Phenotypes in the Tumour Microenvironment through Gene Regulatory Networks: Inference, Analysis and Dynamical Modelling

Malvina Marku[1]*, Hugo Chenel[1,2] and Vera Pancaldi[1,3]

[1]Université de Toulouse, Inserm, CNRS, Université Toulouse III-Paul Sabatier, Centre de Recherches en Cancérologie de Toulouse, France
[2]Evotec, France
[3]Barcelona Supercomputing Center, Spain

***Corresponding Author:** Malvina Marku, Université de Toulouse, Inserm, CNRS, Université Toulouse III-Paul Sabatier, Centre de Recherches en Cancérologie de Toulouse, Toulouse, France

Published **October 31, 2023**

How to cite this book chapter: Malvina Marku, Hugo Chenel, Vera Pancaldi. Dissecting Cellular Phenotypes in the Tumour Microenvironment through Gene Regulatory Networks: Inference, Analysis and Dynamical Modelling. In: Hussein Fayyad Kazan, editor. Immunology and Cancer Biology. Hyderabad, India: Vide Leaf. 2023.

Abstract

Gene regulatory networks (GRNs) and mathematical modelling are critical for understanding the complex regulatory mechanisms that underlie tumour development and progression, providing insights into the molecular mechanisms that drive cancer, including the identification of key driver genes/pathways, and novel therapeutic targets. In the context of the tumour microenvironment (TME), the complex interactions between immune and cancer cells give rise to a cascade of regulatory processes at different levels, defining the cellular behaviour and response to external or internal stimuli. It has been shown that, in the presence of cancer cells, several immune cells including macrophages, neutrophils or T cells undergo cell-state transitions toward pro-tumoral phenotypes or exhaustion. Therefore, the detailed molecular description of cancer cells' and immune cells' behaviour, and cell-state transitions in response to their interactions, particularly at the molecular level, remain crucial to cancer research. In this chapter, we give an overview of mathematical modelling of cancer systems through gene regulatory networks, and give a step-by-step tutorial of how to build them from gene expression data, to analyse and study their temporal behaviour through dynamical modelling.

Introduction

In various subjects, including cancer research, the term "*complex*" is usually mistaken to define "*complicated*", or non-trivial problem-solving tasks. However, the theory of complex systems provides a more precise definition of what a complex system is, and its properties. A system is considered *complex* if certain properties, such as emergent behaviour, nonlinearity, feedback loops and adaptation, emerge from the collective behaviour between the system components and the surrounding environment. From this definition, all biological systems, including the tumour microenvironment (TME), are inherently complex, and their global structure and temporal behaviour (in different scales, from molecular to cellular level) cannot be straightforwardly inferred from the local properties of their interacting components. To facilitate the study of these systems,

the intracellular interacting components can be best represented as a network, commonly visualised as a graph of *nodes (vertices)* connected by *edges (links)* (Figure 1). Depending on the types of nodes and edges, different molecular networks exist, like protein-protein networks (PPI) [1,2], gene regulatory networks (GRN) [3,4], signal transduction networks [5,6], etc. This representation enables the application of the mathematical toolbox of graph theory to study the structural properties of these networks and, furthermore, of dynamical models to study their temporal behaviour under different environmental conditions, effect of drugs, or intracellular mutations. In particular, building these networks using various sources of information constitutes an important reverse engineering process, referred to as *network inference*, and requires the combination of both a thorough biological understanding of the system, and the application of accurate and advanced computational inference methods [7]. Notably, the advanced technological improvements in measuring gene expression and the ever increasing interest in clinical applications of genomics, confer data-driven GRN inference methods with high importance and relevance to get more precise insights on gene regulation, drug action, pathway perturbation, etc.

Thanks to the technological developments of the last 20 years, inference methods have also evolved from inference based on bulk gene expression data [8–11] to single-cell transcriptomics [12–17], and extending to time-series and/or pseudotime of transcriptomics, with which more accurate knowledge on gene-gene interaction can be inferred [15,18,19].

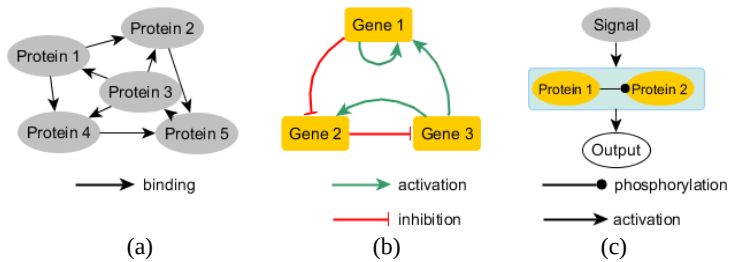

Figure 1: A simplified example of (a) protein-protein (PPI) network, (b) gene regulatory network, (c) signal transduction network.

The importance of performing such calculations relies on using these networks for getting relevant insights on the biology underlying them, aiming to make new discoveries on molecular interactions, drug targets, mechanisms of action, etc. [3]. For example, performing *in silico* experiments and verifying how a perturbation in one of the molecular pathways, genes or interactions might affect the downstream network components helps understanding which are the key intracellular mechanisms, regulators and processes that drive the appearance of particular cell phenotypes or cell states. Experimentally, we can then compare the gene abundance in the perturbed and unperturbed cells and, potentially, identify putative target genes that determine cellular dynamics.

In this chapter, we follow a *horizontal approach*, giving a description of GRNs and their topological features, describing the algorithm behind some available methods on network inference from experimental data, and giving an introduction to dynamical modelling of GRN, as a promising perspective toward bridging the computational methods to the biology of GRNs. This chapter is intended to give biologists and researchers in cancer research an overview of how to use the network approach, and the information it provides to answer their biological questions, aims and research goals. Throughout the text, we direct the readers with a higher mathematical background to consult the recommended literature, for more detailed mathematical and algorithmic details. Thus, the goals for this chapter are as follows:

- give a description of GRNs as simplified representation of regulatory interactions between molecular entities and explain the type of information provided by performing structural analysis on the GRNs;
- describe the algorithm and list some available methods on network inference from public databases and experimental data;
- give an introduction to dynamical modelling of GRNs and describe the basic principles of Boolean modelling;
- list some computational tools to simulate and analyse Boolean models, and describe some recent work on the application of Boolean modelling in cancer research.

Like other similar works, this chapter provides a partial glimpse into the domain of research that is constantly evolving. Considering the substantial amount of ongoing research in this field, it is evident that significant advancements can be expected in the coming years.

Gene Maps: Network Representation of Gene Regulation

Although a single definition of GRN does not exist, we define GRNs as topological maps representing the connection between regulatory proteins (e.g. transcription factors (TFs), RNA binding proteins) that control the expression level of a gene. These interactions can be represented as directed graphs of *nodes* and *edges*. Notably, the directionality of the edges (defining the source and the target in the interaction) represents an important feature in the case of regulatory networks, defining the direction of information flow. For example, in a GRN or metabolic network a TF can regulate the expression of a gene, or a protein can contribute to the production of another protein indirectly, but not vice versa [20]. In these networks, additional information is added by indicating specific types of interactions, represented by signed edges (Figure 1, b). In the simplest case, the interactions are categorised as *activations and inhibitions*, represented as *positive and negative edges* accordingly. GRNs are composed of *regulatory nodes* (*source/cause nodes*) and *regulated nodes* (*target/effect nodes*), generally mapped as TF-target gene networks. The structure of the network enables the calculation of various quantities that capture different features of the network topology, and reveal important information on the underlying biology of the system. In the following sections, we describe some of these features and their biological implication in the network structural organisation. We direct the reader to [21–24] for a complete overview of the topological analysis of networks, whereas a list of the basic parameters and their definition is given in Table 1.

Table 1: A list of basic network parameters.

Parameter		Definition
n	total number of nodes	
m	total number of edges	
k	degree of a node	The number of incoming and outgoing edges connected to the node
z	mean degree	The average of node degree, calculated among all the nodes in the network
l	mean distance	The average shortest path between two nodes, calculated among all the nodes in the network
λ	scale coefficient	The exponent of degree distribution if the distribution follows a power law
r	degree correlation coefficient	The Pearson correlation coefficient between the degrees found at the two end of the same link
d	diameter of the network	The shortest distance between the two most distant nodes in the network
C	clustering coefficient	The level to which nodes in a graph tend to cluster together

Basic Concepts of Networks

First, let's describe the concept of *centrality*, as a measure for identifying the most important or central nodes in the network. Notably, what defines a node as important is relative to the type of centrality measure, therefore several nodes can be identified as such. Further analysis (such as TF activity estimation) can help validate the results.

The basic mathematical presentation of a network, either directed or undirected, is the adjacency matrix. By definition, the adjacency matrix is a $n \times n, n - number\ of\ nodes$ matrix, whose elements take values

$$A_{ij} = \begin{cases} 1 & \text{if there exists an edge between node } i \text{ and node } j \\ 0 & \text{otherwise} \end{cases} \quad (1)$$

From its definition, it is important to note that in directed networks, such as GRNs, the adjacency matrix is not symmetric. For example, the adjacency matrices of the small networks in Figure 2 (a),(b), are going to be

$$A = \begin{pmatrix} 0 & 1 & 1 & 0 \\ 0 & 0 & 1 & 0 \\ 0 & 1 & 0 & 0 \\ 1 & 0 & 1 & 0 \end{pmatrix}$$
$$B = \begin{pmatrix} 0 & 1 & 1 & 1 \\ 1 & 0 & 1 & 0 \\ 1 & 1 & 0 & 1 \\ 1 & 0 & 1 & 0 \end{pmatrix} \quad (2)$$

Additionally, we notice the binary nature of the adjacency matrix ($A_{ij} \in \{0,1\}$); however, in many cases, as well as in GRNs, the elements of the adjacency matrix can take non-binary values, representing the strength or weight of the interaction between two nodes. We refer to these networks as *weighted networks*. For example, in a GRN, the weights might indicate the strength of the interaction or regulation of a TF on a gene, or the effect that a protein might have in regulating the expression of another gene.

Notably, the weights are usually positive numbers, but in regulatory networks they can also take negative values, indicating the *type* of the interaction. The positive values would then denote positive regulation (activation), and the negative values would indicate negative regulation (inhibition).

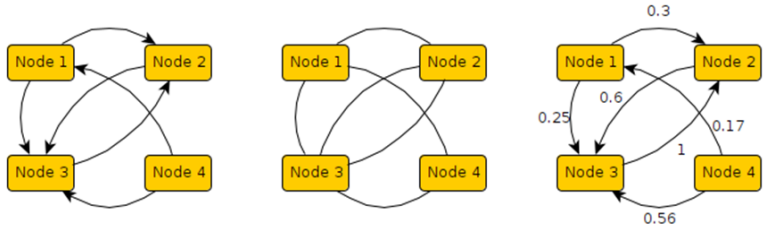

(a) (b) (c)

Figure 2. An example of a regulatory network composed of 4 nodes. (a) directed network, (b) undirected network, (c) directed weighted network.

Degree Centrality

Given a network, the *degree k* of a node is defined as the number of links connected to it. The term degree centrality is usually used to emphasise the usage of the degree as a centrality measure. In directed networks, such as GRNs, nodes can have both incoming and outgoing edges, therefore we distinguish between *in-degree* (k_{in}) and *out-degree* (k_{out}) of a node. In large networks, the degree distribution $P(k)$ defined as the fraction of nodes having degree *k* might be highly informative on the network organisation, identification of network *hubs* as nodes with particularly high degree, its connectivity, etc.
Given the definition of the adjacency matrix, the degree of node i can be simply calculated as the sum of the i^{th} row in undirected networks, or the sum of the i^{th} row plus the sum of the i^{th} column in directed networks.

Eigenvector Centrality

Eigenvector centrality can be defined as an extension of degree centrality. In principle, it measures the connectivity of *important nodes* with each other: considering a node connected with several neighbouring nodes and their downstream networks, we can note that not all the nodes are equivalently significant, and the node's importance is increased either by having many connections or by it being connected with other important nodes, or both. The eigenvector centrality score is therefore proportional to the sum of the centralities of its j neighbouring nodes:

$$x_i = \sum_j A_{ij} x_j \qquad i = 1,2,\dots n \tag{3}$$

It can be proven that the limiting vector of centralities is proportional to the largest eigenvector λ_{max} of A_{ij}, from which it takes the name [23]. It is important to note that the eigenvector centrality scores are all non-negative values, obtained from the multiplication of a positively defined matrix with a positively defined vector. Careful attention should be paid in the case of directed networks, where the asymmetry in the adjacency matrix

raises additional questions. The asymmetric nature of A_{ij} gives two leading eigenvectors, defined as *left* and *right* eigenvectors, representing the *outgoing* and the *incoming* edges respectively. Generally, the centrality score is defined from the right eigenvector - however, this might affect the calculation of eigenvector scores for the other nodes. For example, in the network of Figure 2 (a), Node 4 does not have any incoming edges, therefore its score is equal to zero. Node 1 however has an incoming edge from Node 4 and 2 outgoing edges, but since Node 4 has a score equal to zero, from Eq. 4 Node 2 will also have a score equal to zero. By following this logic, many nodes will be defined by an eigenvector centrality score equal to zero, and only the nodes with a large in-degree will be distinguished by a non-zero score.

PageRank

From the definition of eigenvector centrality, we see that a node with high centrality score increases the centrality of all the nodes it points to. Consequently, if a high-centrality node points to many other nodes, all the nodes will have a high centrality too, and the effect might be distributed throughout the network. To avoid this effect, *PageRank* calculates the centrality of a node as proportional to the centrality of its neighbouring nodes, divided by their out-degree. In this way, nodes pointing to many other nodes have a small contribution to the centrality of the nodes they are pointing to. The mathematical formula of PageRank is thus written as

$$x_i = \alpha \sum_j A_{ij} \frac{x_j}{{k_j}^{out}} + \beta_i, \quad i = 1,2,\dots n \tag{4}$$

where α and β are positive constants, representing a normalising factor and the centrality of the node with zero in-degree respectively. Importantly, β_i enables the zero in-degree nodes to have a non-zero centrality, therefore the nodes they point to derive some advantage from being pointed to. Eq. 5 however raises a problem if ${k_j}^{out} = 0$. In this case, the easier solution is to set ${k_j}^{out} = 1$, as the nodes without-degree equal to zero should not contribute to the centrality of other nodes.

Betweenness Centrality

Comparably from the measures represented above, *betweenness centrality* is a measure of the extent to which a node is located on the path connecting other nodes. Therefore, betweenness centrality might be an important measure to identify the nodes with the highest influence in the network, by quantifying their control on the spread of information. Consider, for example, a GRN with a perturbation applied on one node. We can think of the perturbation being an "information" flow, diffused from node to node by cascades of interactions. In the long term, we can suppose that the information has reached every node in the network, and define the betweenness centrality as *the number of times a node lies in the information flow path between other nodes*. Mathematically, letting ${l^i}_{j\to m} = 1$ if node i lies in path between j and m, and 0 otherwise, the betweenness centrality is calculated as

$$x_i = \sum_{j,m,j\neq m}^{n} {l^i}_{j\to m} \qquad i = 1,2,\dots n \tag{5}$$

Importantly, contrary to the other measures presented above, betweenness centrality is not always an indicator of the connectivity of a node. For example, a node connecting two clusters of nodes might have a small degree but it is essential for transmitting the information from one cluster to another and will thus have high betweenness centrality). The interpretation and generalisation of betweenness centrality however depends on the definition of information flow along the edges and the type of the network itself.

We refer the reader to [23] for a broader description of betweenness measures.

Computational Tools for Structural Network Analysis

Numerous computational tools for performing structural and topological analysis of networks have been developed and are available in different programming languages. Here, we mention some of them, focusing on the main libraries used for the

analysis of biological networks. In Table 2 we list the tools, altogether with their features and computational characteristics.

Table 2: A list of network analysis tools and their features.

Tool	Language	Features
Cytoscape [25]	Java	● Finding a set of differentially expressed genes ● Retrieving relevant networks from public databases ● Integration and visualisation of experimental data ● Topological network analysis ● Network functional enrichment analysis ● Exporting network visualisations ● Extensions according to a long list of available apps, including community detection, etc.
igraph [26]	Python and R packages Code written in C and C++	● Creating graphs from scratch or generating graphs ● Setting and retrieving attributes ● Calculating various structural properties of graphs ● Querying vertices and edges based on attributes ● Treating a graph as an adjacency matrix ● Plotting and visualisation
NetworkX [27]	Python Code written in C, C++, and FORTRAN	● Studying structure and dynamics of social, biological, and infrastructure networks ● Standard programming interface and graph implementation that is suitable for many

		applications • Rapid development environment for collaborative and multidisciplinary projects • Optimal for large datasets
gephi [28]	Java	• Intuition-oriented analysis by network manipulations in real time • Revealing the underlying structures of associations between objects • Representing patterns of biological data
R packages Tidygraph ggraph network visNetwork networkD3 WGCNA	R	• Node and edge list • Creating network objects • Centrality measures analysis • Graph exploration • Network layouts • Highlighting aspects of the network, specific nodes or links • Interactive and animated network visualisation

Gene Regulatory Network Inference

By definition, the process of building the network structure of a biological system through a reverse engineering process is referred to as GRN inference, usually describing the use of experimental data to predict the causal relationships between molecular entities. More precisely, GRN inference involves various forms of reasoning and use of evidence from different sources, including literature, public repositories of experimental data, etc. In this way, the GRN inference approaches can be classified in two groups[1]: (1) *bottom-up approach*, and (2) *top-*

[1] This classification of approaches is usually used when building Boolean models of interacting genes, which we will discuss more in detail in section 3.1. In this case the two approaches are used not only to infer the causal interactions between genes, but also the Boolean formalism governing these interactions.

down approach. The first category, also known as knowledge-driven approach, consists of an extensive literature evaluation and the use of biological pathway databases and text-mining algorithms to build the functional networks of genes of interest. The second category, known as data-driven approach, identifies differentially expressed molecular entities from 'omics-based analyses and bioinformatics tools to perform functional annotation and biological pathway mapping. Each approach has limitations that can result in the omission of important nodes and pathways within the biological system of interest. Literature-based networks may overlook crucial features or require choosing between conflicting information. On the other side, data-driven approaches can fail to identify differentially expressed components depending on experimental design, statistical methods, timing, and biological variability. Ideally, a hybrid approach that combines knowledge and data-driven methods should be employed to construct interaction networks. We will discuss more on the current challenges of each approach in the following sections.

Inference from Databases

A common approach to build a GRN is to exploit TF-target interactions annotated in public databases, which can be of different kinds, depending on the type of information they contain [29–31]. Some databases will provide information on functional interactions, that is evidence that two genes/proteins, in this case a TF-target pair, can be related based on a any type of link between them, evidenced by gene expression correlation, co-evolution of the genes, co-mention in scientific abstracts etc. These functional interactions can be found in databases such as String [32], Reactome (the functional interaction network [33], TRRUST [34] or RegNetwork [35], the latest selecting information from around 25 databases. Moreover, there are efforts to map more specific TF-target interactions based on experimental evidence, either collecting results of CHIP-seq experiments, which show in which target gene promoters the binding peak of the TF can be found, or also combining these experimental results with a crosscheck of the presence of the TF binding motif in the peak regions. Among the databases

including these interactions we mention ChEA [36] or ReMap [37]. Additionally, other databases, generally used when GRN inference is performed on single-cell RNAseq datasets, the validation of inferred interactions is performed on data on the same or similar cell types. Databases providing such information include ENCODE [38], ESCAPE [39], or CHIP-Atlas [40].

Inference from Expression Datasets

Based on input data used, data–driven GRN inference methods can be categorised in two types: (i) *steady state gene expression*, and (ii) *time-series gene expression* inference methods. In the first category, gene regulatory network (GRN) inference typically involves perturbing the system or studying different instances to estimate gene expression levels once the system reaches equilibrium. In the second category, the input data consists of gene expression measurements taken at multiple time points following a perturbation, enabling the observation of the temporal evolution of expression profiles. As a result, time-series inference methods can provide more comprehensive information compared to static data, allowing for the inference of gene functionalities, interactions, causal relationships, and potential clinical implications based on the dynamics of gene expression [41]. However, both methods have limitations due to technical issues inherent in experimental protocols, such as limited sampling time points, cost constraints, difficulties stemming from lack of cell-cycle synchronisation, and sparsity of gene expression data (in the case of single-cell RNAseq). To address these limitations, various computational methods have been developed that combine steady-state and time-series approaches. Moreover, the emergence of single-cell transcriptomics technology has prompted the development of inference methods specifically tailored to single-cell data analysis [42].

Problem Definition

Let's define the dataset as D_S, a matrix with dimensions $N \times S$, where N is the number of genes and S is the number of samples in which their expression is measured:

$$D_S = \{\boldsymbol{X^1}, \boldsymbol{X^2}, \ldots, \boldsymbol{X^S}\} \quad (6)$$

where $\boldsymbol{X^s}, s = 1,2,\ldots,S$ is a vector of $\boldsymbol{N}$ genes with their expression for each sample s. A similar problem definition follows in the case of time-series transcriptomics, in which case the expression dataset D_S is given as a function of expression levels at different time points [43]. The main goal of inference methods is to assign a weight $w_{j,i} \geq 0, i, j = 1,2,\ldots,N$ to any putative interaction between gene i (target) and j (source), representing a regulatory interaction in the biological system. To this purpose, different inference methods use various regression tools to model the expression of a gene as a function of its regulators. Independent of the method chosen, the goal is to reconstruct the GRN that would produce the observed profile of expression, in the form of a directed graph, in which each edge is associated with its characteristic weight.

Based on the inference model they use, inference methods can be grouped into 7 categories, namely (i) mutual information (MI), (ii) dynamical Bayesian, (iii) Granger causality, (iv) Boolean, (v) ordinary differential equation (ODE), (vi) graphical Gaussian and (vii) regression. Importantly, many methods apply a combination of different models and approaches in order to increase the accuracy to gain more insights from the inferred network. We refer the reader to [43] for a mathematical description of these inference algorithms based on bulk and single-cell RNAseq time-series.

Validation of the inferred network is a crucial step in the GRN inference process. It is important to have a validation protocol that can assess the quality of each proposed model, enabling the selection of the optimal inference procedure from the available algorithms. Despite progress in this area, evaluating the effectiveness of inference methods remains challenging, primarily due to limitations in ground truth or gold standard datasets. Existing repositories of experimental data provide reference data for only a limited number of interactions, thereby restricting validation to a subset of the inferred network. Consequently, interactions without reference data are often considered non-existent, raising questions about potential biases

and the ability to infer novel interactions and regulators. Relying solely on prior knowledge for validation may hinder the identification of new regulatory pathways within the system under investigation, especially when gold standard references with high scores are absent or scarce.

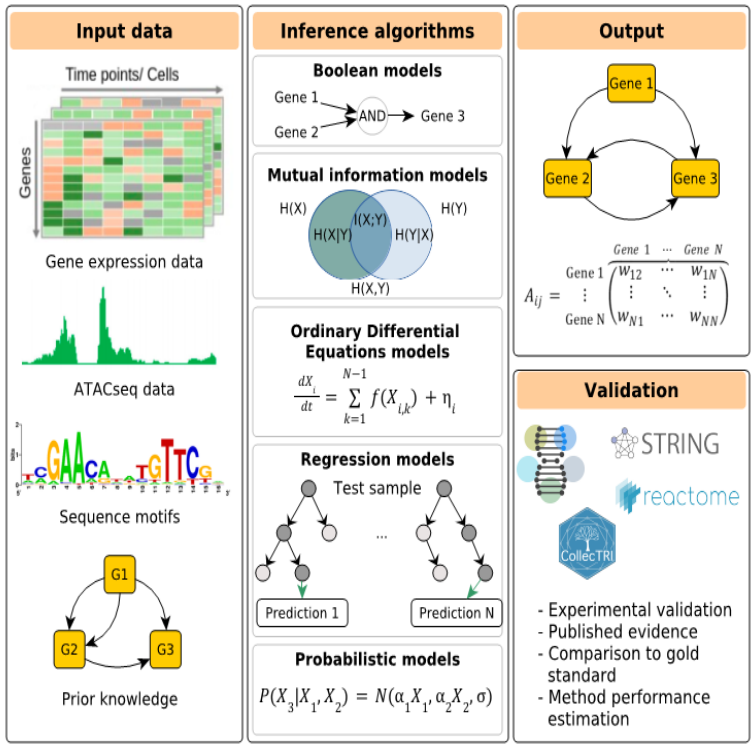

Figure 3: General schema of network inference from expression datasets.

Another possibility for network validation comes from using simulated data, which can be engineered to include several conditions and measurements [9] - yet the extent of coverage of the inferred interactions remains limited to small network size. Other than validating the inferred network with a gold-standard one, another important point in GRN inference is comparison between networks obtained by the different inference methods, on the same dataset, which can provide an estimate of the "robustness" of the inferred network. Additionally, one may

perform this benchmark analysis in order to choose the algorithm/method that best suits a given dataset.

Quantitatively, the algorithm's performance can be evaluated as for any prediction by two metrics typically used in prediction tests: (i) area under precision-recall curve for estimating the performance of a certain algorithm, and (ii) area under receiver operating characteristics curve for comparing the GRN inferred by the algorithm against a gold standard network.

Computational Tools for GRN Inference from Expression Data

When performing GRN inference, the scope is to deduce which are the key molecular entities, whose interactions determine and explain a cell state (phenotype), or a cell type (in differentiation processes). Therefore, depending on the type, and amount of data available, the focus of GRN inference can be either to build a general GRN (i.e., covering all the possible scenarios of cell states/types), or a cell-state/type specific GRN (i.e. a specific GRN for each of the cell states/types identified during the experiment).

Bulk transcriptomics, either steady-state or time-series, come as a low cost sequencing solution compared to single-cell RNAseq, but comes with limitations, such as providing only an average gene expression level at a given time, estimated from a population of cells of different states/types. Nonetheless, this type of data can be more adapted when the focus is to build a general GRN of cell fate decisions. This evolving field has resulted in the development of various algorithms and computation approaches, from sparse candidate models, module networks, ensembles of networks, and furthermore methods that combine prior knowledge and TF activity estimation with data-driven network inference [30,44].

For some biological processes, like cell differentiation or phenotypic reprogramming, a higher resolution of the temporal dynamics of gene expression is necessary to identify major phenotypic transitions in complex tissues while characterising

the phenotypic spectrum of individual cells. In this regard, single-cell RNA-sequencing technology enables deeper investigation of the molecular interactions and identification of novel molecular mechanisms that orchestrate biological processes at the single cell level. Computationally, this technological revolution has led to the development of several algorithms to analyse single-cell RNA-seq, and - as a part of it - inference of GRNs. Intuitively, a single-cell resolution of genes' dynamics would lead to an increased accuracy in inferring the functional interactions between genes that define the biological process. However, due to the limitations in some of the most widely available single-cell technologies, the heterogeneity and sparsity of single-cell data lead to limitations and challenges for GRN inference methods and put reliability of these approaches in question.

An important limitation in using single-cell RNA-seq data for GRN inference is usually the lack of time-resolved expression measurements. Instead, many inference methods exploit the multiplicity of RNAseq profiles at one single time point across cells as a proxy for temporal evolution of the phenotype, assuming ergodicity of this system, as is the case for trajectory inference based on pseudo-time ordering of the cells [45]. In this process, the pseudo-temporal trajectory is generated by linearly ordering the single-cell profiles from a specific time point based on their transcriptional similarity, thus enabling the identification of gene patterns along the developmental trajectory of continuously ordered cells [46]. Subsequently, to extract discrete time-points from pseudo-temporal ordering, different techniques can be followed: cell cluster time-point assignment (Slingshot [47], TSCAN [48] or Palantir [49]), partition of pseudo-temporal trajectories into discrete time-points or differential gene expression time-point assignment (Monocle [50]). However, it is important to note that the temporal representation obtained from pseudo-temporal analysis in single-cell lacks the equivalence between pseudo-time and real time. In addition, this pseudo-temporal representation is better suited in developmental systems, in which cells undergo differentiation processes recognised by the presence of bifurcation points in the pseudo-temporal trajectory. This is not always the case, in which

occasion the trajectory inference may lead to inaccurate results. Nonetheless, this representation helps implement the GRN inference algorithms in modelling the expression levels at a given (pseudo)time-point as a function of gene expression at the previous (pseudo)time-point(s). Accordingly, a subset of the inference methods require specific information about the pseudo-temporal ordering of the cells, having a significant difference in performance when such information is not available. Other methods, like GENIE3 [51], GRNBoost2 [52], or PPCOR [53] do not require a temporal ordering of the cells as input and have relatively good performance when tested on some published curated models [54]. However, the incomplete equivalence between bulk gene expression time courses and pseudo-time time-series implies that these two types of inference cannot always be performed by the same tools.

Several benchmarking papers on the performance of single-cell RNA-seq inference methods have been published, facilitating the comparison of different inference methods. We refer the reader to [12,13,16,55] for an extensive review and comparison of single-cell RNA-seq inference methods, [14,54,56] for some benchmarking libraries and to [43,57,58] for an algorithmic review. For a user, the choice between all the different inference methods will depend primarily on the type of data available, the methods' overall performance, the type and amount of information they require, and the type of reconstructed network they provide.

Some of the inference methods to use for bulk and single-cell RNAseq are recapitulated in Table 3. We note that this list is not exhaustive and many other methods are mentioned in the benchmarking and review references mentioned above.

Table 3: List of some GRN inference methods for bulk and single-cell RNAseq datasets.

	Method	**Source**	**Reference**
Bulk transcriptomics	ARACNE TimeDelay ARACNE	https://github.com/califano-lab/ARACNe-AP	[59]

	Method	Source	Reference
	Minet CLR, MRNET		[60] [61]
	GRENITS	https://bioconductor.org/packages/release/bioc/html/GRENITS.html	[62]
	GeneNet	https://strimmerlab.github.io/software/genenet/	[63]
	Inferelator 3.0	https://github.com/flatironinstitute/inferelator	[64]
	TSNI		[65]
	GENIE3 dynGENIE3	https://github.com/vahuynh/GENIE3 https://github.com/vahuynh/dynGENIE3	[51] [19]
	Jump3	https://github.com/vahuynh/Jump3	[58]
	SWING	https://github.com/bagherilab/SWING	[66]
	CellNet	https://github.com/pcahan1/CellNet	[67]
	TIGRESS	https://github.com/jpvert/tigress	[68]
Single cell transcriptomics	SINCERITIES	https://github.com/CABSEL/SINCERITIES	[69]
	SCODE	https://github.com/hmatsu1226/SCODE	[15]
	GRISLI	https://github.com/	[18]

	Method	Source	Reference
		PCAubin/GRISLI	
	SCENIC	https://github.com/aertslab/SCENIC	[45]
	WASABI	https://github.com/eliasventre/cardamom	[70,71]
	CARDAMON	https://github.com/ulysseherbach/harissa	[72]
	CellOracle	https://github.com/morris-lab/CellOracle	[73]
	Pando	https://github.com/quadbiolab/Pando	[74]
	SCRIBE	https://github.com/cole-trapnell-lab/Scribe	[75]
	PAGA - partition-based graph abstraction	https://github.com/theislab/paga	[76]

It is important to note that, although inferring regulatory networks is a trending topic and despite the multitude of different algorithms available, data-driven GRN inference methods struggle to reach a high performance in real-world studies, on both bulk and single-cell RNA-seq data, as reported in [42]. Therefore, their application to biologically relevant datasets remain limited. Nevertheless, different applications of inferring GRNs for novel discoveries in biology have been presented in most of the cited works on GRN inference methods, including studies on cancer, cell development, and cell fate decision. Importantly, combining information from multiple data sources to improve predictions is a current challenge in several research areas. Several recent papers have addressed this issue, including [77,78], where gene expression data are combined with

DNA methylation, copy number variation, or genome-wide binding data. As a consequence, many inference methods introduced above combine multiple data sources to improve the predictions of GRN inference and provide more insightful results on the regulatory processes. For example, in SCENIC [45], results of a GRN analysis are combined with transcription factor binding motif information from RcisTarget to identify a subset of high-confidence interactions. In CellOracle [73] and Pando [74], single-cell RNAseq time-series is combined with ATACseq data. These papers illustrate diverse strategies for integrating multiple data sources to enhance predictions and gain a deeper understanding of complex biological systems.

In cancer research, special focus has been set onto identifying driver genes in cancer progression, and drug resistance. For example, in [79] the authors perform GRN inference from time-series RNAseq in gliomas to build sensitive and resistant networks, found to exhibit significant differences with respect to network topology, local entropy and gene expression dynamics. Based on the node importance score, they developed a differential regulatory network-based biomarker model to identify the most influential genes in the differential network for predicting and controlling drug resistance. Going a step further, [80] use time-series of single-cell RNAseq to study epithelial–to–mesenchymal transition, following a multi-layer network approach, and linking the intracellular gene regulation to cell-cell communications in ovarian cancer cell lines. Other applications of GRN inference to cancer research focused on identifying putative key regulators and gene modules in PDAC disease progression [81], building cancer cell expression networks in liver hepatocellular carcinoma and bladder urothelial carcinoma (BLCA) [82], analysing the functional components by extracting subnetworks and investigating the local landscape of prostate cancer genes [83], etc.

Other applications have been focusing on differentiation processes, like cell differentiation and development [45,70]. In addition, research efforts have been directed towards integration of different layers of information in GRN inference. For example, in [84] time-series of RNAseq data is combined with

ATACseq data to derive dynamic gene regulatory networks for human myeloid differentiation, specifically promyelocytes differentiating into macrophages, neutrophils, monocytes, and monocyte-derived macrophages. In Bocci et al [85], single-cell transcriptomics is fed with mRNA splicing data to identify the key molecular drivers leading to different final states when starting from a common initial state during pancreas endocrinogenesis and epithelial/mesenchymal state transition. In another application, Thorne [86] used public time-series datasets from recount2 database [87] to infer the GRN of neural progenitor cell differentiation. Applying structural analysis on the inferred GRN, they identified key genes which were experimentally observed to influence neuronal differentiation. In another approach, Kamimoto et al [73] used single-cell RNAseq and ATACseq datasets to infer cell state-specific GRNs that emerge during the differentiation process of fibroblasts. In this way, analysing the changes in the GRNs during cell reprogramming or development can help understanding how the TF interactions regulate and define cell identity. In cell fate decision studies, Fleck et al [74] used multi-omics datasets including RNAseq and ATACseq combined with transcription factor binding sites analysis to infer a GRN describing brain organoid developments, leading to the identification of key regulators of cell fate.

Some applications include building molecular disease maps [88,89], phenotypic characterization of a cell in a given microenvironment [90,91], identifying predictive or prognostic biomarkers [92], performing extensive studies on performance of the available methods on different datasets/conditions [17,93,94], and many more.

Despite the exciting progress in the application of data-driven GRN inference methods in biological research, significant challenges remain, as discussed in [43]. Gene expression is a process determined from different levels of regulation, from chromatin to post-translational modifications and signal transduction levels, and including all these levels consist of a non-trivial computational and conceptual task. In addition, these networks are highly context-specific (to a given cell type, tissue, condition, and furthermore to each individual), for which, in

most of the cases, the GRN is unknown. Another major challenge lies in accurately modelling the non-linear dynamics and stochastic nature of gene regulation. Similarly, inferring causality in gene-gene interactions remains a difficult problem to solve due to the observational nature of the data.

Moving forward, a promising direction is the integration of multi-omics data, such as combining transcriptomic, proteomic, and epigenomic information, for a more comprehensive understanding of cellular mechanisms. Transitioning into the realm of artificial intelligence, these computational tools are progressively enhancing our capacity to interpret intricate biological data, especially in the realm of GRNs.

Dynamical Modelling

In addition to the types of analysis represented in the previous sessions that one can perform on the inferred GRNs, dynamical modelling plays a crucial role in analysing the system's behaviour with temporal resolution and across various conditions. For example, having performed GRN inference and validation, one can study what is going to be the *state* (a vector of gene expression of the nodes composing the GRN) of the GRN after multiple time steps, when starting from a certain initial condition (gene expression at the initial time). Dynamical modelling of gene regulatory networks is a computational approach used in systems biology to study the complex interactions between genes and their targets (proteins and RNAs) with the primary goal of understanding how these GRNs evolve over time in response to various internal/external stimuli, predicting their dynamic responses, and gaining insights into the underlying biological processes.

Methods for dynamical models of GRNs cover a spectrum of approaches as wide as the GRN inference methods do, ranging from continuous quantitative ordinary differential equation (ODE) models to discrete logic qualitative models). In continuous models, the temporal evolution of the state X_i of gene i $(i = 1,2,\ldots,N)$ in the network is given by continuous mathematical functions of its regulators, such as ODEs,

stochastic differential equations, etc. and the regulatory interactions between genes are usually modelled as chemical reactions, or species interactions in ecological models [95,96]. In this way, the temporal evolution of the system is described at the level of individual reactions. However, their usage in dynamical modelling of GRN remains limited because of the detailed and complete mathematical and parametric description they require. On the other side of the spectrum, in discrete models, such as multivariate logic models [97], Petri nets [98], or Boolean models [99,100], a discrete logic of interactions is applied and the temporal evolution of expression of each gene is given by a discrete (and often logic) function of their regulators (example given below). Contrary to continuous models, discrete models can be applied with no or considerably fewer parameters and fragmented mechanistic description, making them suitable for large networks. However, the system behaviour is only described (semi)quantitatively. In the following section, we will elaborate more in detail on the basic principles of Boolean modelling of GRNs.

For a modeller, the type of questions being asked about the system, the type of description of the system dynamics available (quantitative or qualitative), the type and amount of available data, prior knowledge, etc. will all influence the modelling approach to use. The basic objective, regardless of the dynamical model employed, is to pinpoint the phenotypic alterations that occur in a cell in response to medications, specific extracellular environmental factors, cellular interactions in the microenvironment, or experimental knockout/overexpression. According to Shah et al. [101], these phenotypic changes may be represented graphically as the system's steady states or attractors, which are states (a vector of expression values for each gene) that remain constant despite perturbations. A GRN often has numerous attractors, each of which represents a potential phenotype or state that may be attained given a set of initial conditions. In this situation, extra analysis must be done to examine the attractors' stability, biological significance, or their classification into biologically interpretable phenotypes.

Boolean Model Formalism of Gene Regulatory Networks

To study the temporal behaviour of this system, it is necessary to associate each gene with a dynamical function, which will explain how its *state* (expression, activity state) will change with *time*, given the types of interactions with its regulators. Boolean networks, referring to Boolean modelling of regulatory networks, were first introduced by Kauffman [102] and Thomas [103] to model the metabolic stability of epigenetics networks, displaying a *sigmoidal* behaviour, which could then be approximated to a switch-like behaviour. For example, let us consider the production of mRNA of a gene (X) as a function of the concentration of a transcription factor (A), usually described with a Hill function: $\frac{dX}{dt} = T_{max} \frac{[A]^n}{K^n + [A]^n}$ [104,105], where T_{max} is the maximal transcription rate, n is the Hill exponent, and K is the concentration of transcription factor at which the synthesis of mRNA of X is at half maximal rate). If the Hill coefficient is high, the synthesis term can be approximated by a Boolean step function, $[X] = 0$ if $[A] \leq threshold$, and $[X] = 0$ if $[A] > threshold$ (Figure 4).

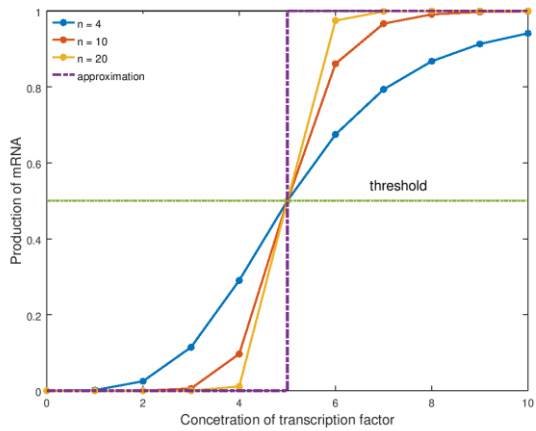

Figure 4: Illustration of the transition between a continuous and a Boolean description of a process through which transcription factor A positively regulates the mRNA production of gene X. If the Hill coefficient is high, the mRNA synthesis can be approximated by a Boolean function, $[X] = 0$ if $[X] \leq 0.5$, and $[X] = 0$ if $[X] > 0.5$.

In this formalism the interactions between the nodes are represented by *Boolean transition functions (Boolean rules)*, usually expressed via the logic operators: AND and OR for positive interactions, and NOT for the negative ones. Special care should be put on the choice between AND and OR operators, as they indicate a simultaneous synchronisation of the expression of the regulators of a certain target gene, or an independent regulation of two or more regulators on the target gene (see example below). In Boolean modelling *time is implicit* and *discrete* and each function at a given time point will take as input the variables' expressions at the previous time point. Most importantly, as mentioned above, the state of each node in a GRN will be characterised by discrete values (1 - expressed or 0 - not expressed), there will therefore be *finite combinations of possible states of the system* ($2^N, N$- number of nodes in the GRN) (binary vectors, each element of which representing the state of a node in the GRN, for example $state\{0,0,1\} \equiv \{G1\ (not\ expressed), G2\ (not\ expressed), G3\ (expressed)\}$). As a consequence, the system will eventually fall in one of the states it has previously been to, usually referred to as *stable states*, *fixed points* or *attractors*. Graphically, the set of all system's states and their possible transitions (defined by the Boolean rules) can be represented in the form of a *state transition graph* (special care should be taken to distinguish between the GRN and the state transition graph, where nodes are not genes but states of the entire system described by vectors of 0/1 values), in which the fixed-point attractors are usually identified by the presence of self-loops.

While the transition functions of a Boolean model specify the rules for calculating the future states of the nodes in the GRN (usually referred to as update), the order in which the updates are performed needs to be specified. In this context, various update methods can be implemented, which are broadly classified into *synchronous* and *asynchronous*. In the synchronous method, the states of all nodes in the GRN are updated simultaneously considering the state of the system at the previous time step, implicitly assuming that the time-scales of all biological events in the system are similar and that the state transitions of all the different components are synchronised. To avoid this

assumption, which is rarely biologically relevant, different asynchronous methods were developed to account for timescale diversity of biological processes by updating the nodes in an asynchronous or probabilistic manner. In this case all nodes are updated according to a random sequence or with a given probability [106], or one randomly selected node is updated at each time step [107,108]. Afterwards, multiple simulations can be performed to mitigate the effect of random updates, thus considering numerous updating sequences. Most importantly, the fixed-point attractors are time-invariant, implying that the same fixed points will be obtained independent of the updating method. Therefore, choosing between the updating methods will depend mostly on the computational question a modeller wants to answer, and other aspects, such as the size of the GRN (the size of the state transition graph increasing exponentially with the number of nodes), the availability of additional information regarding the *timing* of specific interactions in the GRN, the interest in following the system's dynamics before reaching the fixed points, etc.

Example: Let's consider the GRN in Figure 5, (a) as being the output of a given inference method, either from following a data-driven approach or provided from the available public databases. We can imagine it as the network illustration of a cell, whose behaviour is represented by the interactions of these 3 genes. Here, Gene 2 (G2) is positively regulated by Gene 1 (G1) and negatively regulated by Gene 3 (G3), thus the state of G2 can be a result either of a cooperation of G1 with G3 (AND operator), or each of these genes can regulate the expression of G2 independently (OR operator). In these cases, additional experimental or biological information will be necessary to determine the Boolean operators to be used.

Let's write the Boolean functions for each node, as in Figure 5. (b). Finding the system's attractors implies solving the system of Boolean equations by considering all the possible combinations of the states of the nodes ($2^3 = 8$ states) and calculating their future states, which can be represented as a *truth table*. In our case, the system displays a single fixed-point attractor (110, Figure 5, (c)), in which G1 and G2 are both expressed, and G3 is

not expressed. What is the biological meaning of this? Here the attractor will represent a phenotype of this virtual cell, or a cell state, characterised by the repression of G3.

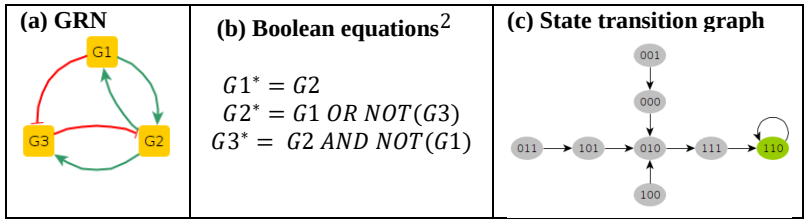

Figure 5: A toy example of a Boolean model of a GRN. Starting from a GRN (a), the next step consists of building the Boolean equations (b), by taking into consideration all the regulatory interactions and their nature (positive or negative interactions). Afterwards, the solution of the system of Boolean equations can be represented as a state transition graph. The attractors of the system can be identified by self-loops (in the case of fixed point attractors), or loops involving a subset of nodes (in the case of limit cycles). In this example, the system has only one fixed point attractor (110), coloured in green.

It is understandable that, for larger networks, solving the system of Boolean equations with the truth table quickly becomes challenging and impractical. For this reason, various computational tools have been developed to run Boolean models of hundreds of nodes (we will discuss more on these methods in the following section).

The example given above was intentionally chosen to point out that a system can display more than one attractor; in fact, the higher N, the most likely the system can display multistability (multiple possible attractors). We can imagine these different attractors being various states of a cell (e.g. a differentiating cell, a tumour cell entering apoptosis, proliferation, migration, etc.), each of which is defined by a combination of gene expression levels/states. We will discuss more on analysis of large networks and attractor classification in the following section.

[2] In these equations, the asterisk (*) indicates the expression of each gene at the next time point (i.e, *t+1*) as a Boolean function of the regulators at the current time point (i.e, *t*). Note that time is *implicit*, and is not involved as a variable when solving the system of the Boolean equations.

Beyond identifying the attractors of the system, the Boolean model can be further used to simulate internal or external perturbations on the states of the nodes, e.g. overexpression (OE - a node or a group of nodes forced into state 1) or knock-out (KO - a node or a group of nodes forced into state 0), thus mimicking the effect of a change in the system's internal or external environment (e.g. the action of a drug, a change in the extracellular stimuli, etc.). In this scope, special interest has been focused on the opposite analysis: given the possible stable states the system can have, identifying which nodes should be perturbed (either OE or KO) in order to prevent the system from reaching certain states. For example, if we consider the GRN in Figure 5, (a) to represent a cancer cell and the fixed point attractor to be a proliferative state of the cell, the interest is to find which gene or combination of genes should be ONE or KO in order to completely repress this attractor. One way to do this is to use the prior biological knowledge on the role of each gene in the GRN and perform multiple simulations with various combinations of perturbations. Alternatively, some computational tools have incorporated functions to perform this analysis, as we will see in the following chapter.

Boolean Model Inference: Applications

As mentioned in section 2, the same classification of approaches applies for Boolean model inference as for GRN inference, I,e. using the available evidence to build the Boolean functions reflecting the functional regulations between the molecular entities in the GRN. In addition to public databases mentioned in section 2.1, other databases such as Signor [109], BioModels [110], Minerva [111], NaviCell [112], etc. provide curated Boolean models, which can be further modified according to the system of interest.

In the data-driven approach, similar to using expression data for GRN inference, the information in the changes of the genes' expression is also used to infer the Boolean rules that govern these changes [113–119], which can then be studied using several available tools, integrated in the Consortium for Logical Models and Tools (CoLoMoTo) [120].

Despite the oversimplified representation of biological events in the Boolean formalism, predictions on cancer evolution and immuno-oncology, descriptions of signalling pathways activated in specific cell types (different tumour types such as bladder [121], breast [122], gastric [123], to name a few, but also T cells [124,125], macrophages [126,127], etc.), suggestions of patient-specific treatments [128,129], have flourished over the past decades [130]. More recently, patient-specific Boolean models have been developed to design targeted therapy strategies for patients based on their ‘omics profile [131]. Importantly, these intracellular models can be further integrated with other cell population models, like agent-based models or metabolic models, thus providing a multilevel description of the system dynamics, including mechanistic functionalities like cell motility, cytokine diffusion, tissue expansion and spatial organisation, etc. [132–134]. This combined approach enables addressing more complex questions, like drug design, or therapy action from the cell to the tissue scale [135–138]. For example, in [135] the intracellular Boolean models of cancer cells, stellate cells, macrophages, CD4+ and CD8+ T cells were implemented into an agent-based model of pancreatic ductal adenocarcinoma, thus describing cell type–specific molecular interactions and cytokine-mediated cell-cell communications. From model simulations, the authors suggest that the autocrine loop involving EGF signalling is a key interaction modulator between pancreatic cancer and stellate cells, and that reducing bFGF secretion by stellate cells will have a positive impact on cancer apoptosis.

Conclusions

The applications of GRNs in representation and modelling of regulatory systems has reached a mature stage in methodological research, with its applications in cancer research expanding and gaining popularity. In this chapter, we have endeavoured to provide a general overview of the field, emphasising the biological motivations behind it and the technological advancements in data collection that have boosted its recent growth. Additionally, we have presented a high-level perspective

on the statistical principles that underlie several widely used methodologies for GRN inference. Our main focus has been on establishing a foundational understanding, covering broad concepts in GRN analysis, inference and dynamical modelling. It is important to note that numerous significant contributions in developing methods in GRN inference, dynamical modelling and structural analysis exist, and we could not cover them all into this simplified summary.

Naturally, attempting to cover such a vast and diverse research area in a brief chapter is a challenging task. Our intention here is to equip the reader with the fundamentals of system biology, and its great potential to study diverse biological systems. We have endeavoured to make this chapter as self-contained as possible, hoping that it will also serve as a valuable introduction for new researchers to the field.

The technicalities of GRN inference and modelling of regulatory systems are the key motivating forces behind the surge of interdisciplinary collaborations. The intersection of bioinformatics, molecular biology, clinical research, computer science, physics and other disciplines is the core upon which these applications are built and expanded. Specialists in bioinformatics and artificial intelligence, for instance, are continuously developing powerful algorithms for network inference. However, these computational platforms should be firmly grounded in the rich experimental data provided by molecular biologists. Any given computational algorithm's outputs need to be decoded and interpreted within the correct biological context to bring meaningful insights. This process underscores the critical role of effective collaboration with biologists and clinicians. By embracing a multidisciplinary approach that merges computational methodologies with experimental validation, the aim is to unravel the complexity of biological systems. Furthermore, this synergistic approach is key to translating computational and theoretical findings into clinical applications.

References

1. Koh GCKW, Porras P, Aranda B, Hermjakob H, Orchard SE. Analyzing Protein–Protein Interaction Networks. Journal of Proteome Research. 2012; 11: 2014–2031.
2. Pellegrini M, Haynor D, Johnson JM. Protein Interaction Networks. Expert Review of Proteomics. 2004; 1: 239–249.
3. Emmert-Streib F, Dehmer M, Haibe-Kains B. Gene regulatory networks and their applications: Understanding biological and medical problems in terms of networks. Frontiers in Cell and Developmental Biology. 2014; 2.
4. Vijesh N, Chakrabarti SK, Sreekumar J. Modeling of gene regulatory networks: A review. Journal of Biomedical Science and Engineering. 2013; 06, Article 02.
5. Hu Y, Peng T, Gao L, Tan K. CytoTalk: De novo construction of signal transduction networks using single-cell transcriptomic data. Science Advances. 2021; 7: eabf1356.
6. Kolch W, Halasz M, Granovskaya M, Kholodenko BN. The dynamic control of signal transduction networks in cancer cells. Nature Reviews Cancer. 2015; 15: Article 9.
7. Angelin-Bonnet O, Biggs PJ, Vignes M. Gene Regulatory Networks: A Primer in Biological Processes and Statistical Modelling. Methods in Molecular Biology (Clifton, N.J.). 2019; 1883: 347–383.
8. Barabási AL, Gulbahce N, Loscalzo J. Network medicine: A network-based approach to human disease. Nature Reviews Genetics. 2011; 12, Article 1.
9. Marbach D, Costello JC, Küffner R, Vega N, Prill RJ, et al. Wisdom of crowds for robust gene network inference. Nature Methods. 2012; 9: 796–804.
10. Silverman EK, Schmidt HHHW, Anastasiadou E, Altucci L, Angelini M, et al. Molecular networks in Network Medicine: Development and applications. Wiley Interdisciplinary Reviews. Systems Biology and Medicine. 2020; 12: e1489.
11. Sonawane AR, Weiss ST, Glass K, Sharma A. Network Medicine in the Age of Biomedical Big Data. Frontiers in Genetics. 2019; 10.
12. Blencowe M, Arneson D, Ding J, Chen YW, Saleem Z, et al. Network modeling of single-cell omics data: Challenges,

opportunities, and progresses. Emerging Topics in Life Sciences. 2019; 3: 379–398.
13. Fiers MWEJ, Minnoye L, Aibar S, Bravo González-Blas C, Kalender Atak Z, et al. Mapping gene regulatory networks from single-cell omics data. Briefings in Functional Genomics. 2018; 17: 246–254.
14. Kang Y, Thieffry D, Cantini L. Evaluating the Reproducibility of Single-Cell Gene Regulatory Network Inference Algorithms. Frontiers in Genetics. 2021; 12.
15. Matsumoto H, Kiryu H, Furusawa C, Ko MSH, Ko SBH, et al. SCODE: An efficient regulatory network inference algorithm from single-cell RNA-Seq during differentiation. Bioinformatics. 2017; 33: 2314–2321.
16. Nguyen H, Tran D, Tran B, Pehlivan B, Nguyen T. A comprehensive survey of regulatory network inference methods using single cell RNA sequencing data. Briefings in Bioinformatics. 2021; 22: bbaa190.
17. Raharinirina NA, Peppert F, von Kleist M, Schütte C, Sunkara V. Inferring gene regulatory networks from single-cell RNA-seq temporal snapshot data requires higher-order moments. Patterns. 2021; 2: 100332.
18. Aubin-Frankowski PC, Vert JP. Gene regulation inference from single-cell RNA-seq data with linear differential equations and velocity inference. Bioinformatics. 2020; 36: 4774–4780.
19. Huynh-Thu VA, Geurts P. dynGENIE3: Dynamical GENIE3 for the inference of gene networks from time series expression data. Scientific Reports. 2018; 8: 3384.
20. Ouma WZ, Pogacar K, Grotewold E. Topological and statistical analyses of gene regulatory networks reveal unifying yet quantitatively different emergent properties. PLOS Computational Biology. 2018; 14: e1006098.
21. Ashtiani M, Mirzaie M, Jafari M. CINNA: An R/CRAN package to decipher Central Informative Nodes in Network Analysis. Bioinformatics. 2019; 35: 1436–1437.
22. Cohen R, Havlin S. Complex Networks: Structure, Robustness and Function. Cambridge: Cambridge University Press. 2010.
23. Newman M. Networks: An Introduction. Oxford: Oxford University Press. 2010.

24. Newman M, Barabási AL, Watts DJ. The Structure and Dynamics of Networks. Princeton: Princeton University Press. 2006.
25. Shannon P, Markiel A, Ozier O, Baliga NS, Wang JT, et al. Cytoscape: A Software Environment for Integrated Models of Biomolecular Interaction Networks. Genome Research. 2003; 13: 2498–2504.
26. Csardi G, Nepusz T. The Igraph Software Package for Complex Network Research. InterJournal, Complex Systems. 2005; 1695.
27. Hagberg A, Swart P, S Chult D. Exploring network structure, dynamics, and function using networkx (LA-UR-08-05495; LA-UR-08-5495). Los Alamos National Lab. (LANL), Los Alamos, NM (United States). 2008.
28. Bastian M, Heymann S, Jacomy M. Gephi: An Open Source Software for Exploring and Manipulating Networks. Proceedings of the International AAAI Conference on Web and Social Media. 2009; 3: Article 1.
29. Garcia-Alonso L, Holland CH, Ibrahim MM, Turei D, Saez-Rodriguez J. Benchmark and integration of resources for the estimation of human transcription factor activities. Genome Research. 2019; 29: 1363–1375.
30. Mercatelli D, Scalambra L, Triboli L, Ray F, Giorgi FM. Gene regulatory network inference resources: A practical overview. Biochimica et Biophysica Acta (BBA) - Gene Regulatory Mechanisms. 2020; 1863: 194430.
31. Müller-Dott S, Tsirvouli E, Vázquez M, Flores ROR, Badia-i-Mompel P, et al. Expanding the coverage of regulons from high-confidence prior knowledge for accurate estimation of transcription factor activities (p. 2023.03.30.534849). bioRxiv. 2023.
32. Mering, C von, Huynen M, Jaeggi D, Schmidt S, Bork P, et al. STRING: A database of predicted functional associations between proteins. Nucleic Acids Research. 2003; 31: 258–261.
33. Fabregat A, Jupe S, Matthews L, Sidiropoulos K, Gillespie M, et al. The Reactome Pathway Knowledgebase. Nucleic Acids Research. 2018; 46: D649–D655.
34. Han H, Cho JW, Lee S, Yun A, Kim H, et al. TRRUST v2: An expanded reference database of human and mouse

transcriptional regulatory interactions. Nucleic Acids Research. 2018; 46: D380–D386.
35. Liu ZP, Wu C, Miao H, Wu H. RegNetwork: An integrated database of transcriptional and post-transcriptional regulatory networks in human and mouse. Database. 2015; 2015: bav095.
36. Lachmann A, Xu H, Krishnan J, Berger SI, Mazloom AR, et al. ChEA: Transcription factor regulation inferred from integrating genome-wide ChIP-X experiments. Bioinformatics. 2010; 26: 2438–2444.
37. Chèneby J, Gheorghe M, Artufel M, Mathelier A, Ballester B. ReMap 2018: An updated atlas of regulatory regions from an integrative analysis of DNA-binding ChIP-seq experiments. Nucleic Acids Research. 2018; 46: D267–D275.
38. Davis CA, Hitz BC, Sloan CA, Chan ET, Davidson JM, et al. The Encyclopedia of DNA elements (ENCODE): Data portal update. Nucleic Acids Research. 2018; 46: D794–D801.
39. Xu H, Baroukh C, Dannenfelser R, Chen EY, Tan CM, et al. ESCAPE: Database for integrating high-content published data collected from human and mouse embryonic stem cells. Database. 2018; 2013: bat045.
40. Oki S, Ohta T, Shioi G, Hatanaka H, Ogasawara O, et al. ChIP-Atlas: A data-mining suite powered by full integration of public ChIP-seq data. EMBO Reports. 2018; 19: e46255.
41. Bar-Joseph Z, Gitter A, Simon I. Studying and modelling dynamic biological processes using time-series gene expression data. Nature Reviews Genetics. 2012; 13: Article 8.
42. Chen S, Mar JC. Evaluating methods of inferring gene regulatory networks highlights their lack of performance for single cell gene expression data. BMC Bioinformatics. 2018; 19: 232.
43. Marku M, Pancaldi V. From time-series transcriptomics to gene regulatory networks: A review on inference methods. PLOS Computational Biology. 2023; 19: e1011254.
44. Barbosa S, Niebel B, Wolf S, Mauch K, Takors R. A guide to gene regulatory network inference for obtaining predictive solutions: Underlying assumptions and fundamental

biological and data constraints. Biosystems. 2018; 174: 37–48.
45. Aibar S, González-Blas CB, Moerman T, Huynh-Thu VA, Imrichova H, et al. SCENIC: Single-cell regulatory network inference and clustering. Nature Methods. 2017; 14: 1083–1086.
46. Lange M, Bergen V, Klein M, Setty M, Reuter B, et al. CellRank for directed single-cell fate mapping. Nature Methods. 2022; 19: 159–170.
47. Street K, Risso D, Fletcher RB, Das D, Ngai J, et al. Slingshot: Cell lineage and pseudotime inference for single-cell transcriptomics. BMC Genomics. 2018; 19: 477.
48. Ji Z, Ji H. TSCAN: Pseudo-time reconstruction and evaluation in single-cell RNA-seq analysis. Nucleic Acids Research. 2016; 44: e117.
49. Setty M, Kiseliovas V, Levine J, Gayoso A, Mazutis L, et al. Characterization of cell fate probabilities in single-cell data with Palantir. Nature Biotechnology. 2019; 37: Article 4.
50. Trapnell C, Cacchiarelli D, Grimsby J, Pokharel P, Li S, et al. The dynamics and regulators of cell fate decisions are revealed by pseudotemporal ordering of single cells. Nature Biotechnology. 2014; 32: Article 4.
51. Huynh-Thu VA, Irrthum A, Wehenkel L, Geurts P. Inferring Regulatory Networks from Expression Data Using Tree-Based Methods. PLOS ONE. 2010; 5: e12776.
52. Moerman T, Aibar Santos S, Bravo González-Blas C, Simm J, Moreau Y, et al. GRNBoost2 and Arboreto: Efficient and scalable inference of gene regulatory networks. Bioinformatics. 2019; 35: 2159–2161.
53. Kim S. ppcor: An R Package for a Fast Calculation to Semi-partial Correlation Coefficients. Communications for Statistical Applications and Methods. 2015; 22: 665–674.
54. Pratapa A, Jalihal AP, Law JN, Bharadwaj A, Murali TM. Benchmarking algorithms for gene regulatory network inference from single-cell transcriptomic data. Nature Methods. 2020; 17: Article 2.
55. Zhao M, He W, Tang J, Zou Q, Guo F. A comprehensive overview and critical evaluation of gene regulatory network inference technologies. Briefings in Bioinformatics. 2021; 22: bbab009.

56. Bellot P, Olsen C, Salembier P, Oliveras-Vergés A, Meyer PE. NetBenchmark: A bioconductor package for reproducible benchmarks of gene regulatory network inference. BMC Bioinformatics. 2015; 16: 312.
57. Androulakis IP, Yang E, Almon RR. Analysis of Time-Series Gene Expression Data: Methods, Challenges, and Opportunities. Annual Review of Biomedical Engineering. 2007; 9: 205–228.
58. Huynh-Thu VA, Sanguinetti G. Combining tree-based and dynamical systems for the inference of gene regulatory networks. Bioinformatics (Oxford, England). 2015; 31: 1614–1622.
59. Zoppoli P, Morganella S, Ceccarelli M. TimeDelay-ARACNE: Reverse engineering of gene networks from time-course data by an information theoretic approach. BMC Bioinformatics. 2015; 11: 154.
60. Faith JJ, Hayete B, Thaden JT, Mogno I, Wierzbowski J, et al. Large-Scale Mapping and Validation of Escherichia coli Transcriptional Regulation from a Compendium of Expression Profiles. PLOS Biology. 2007; 5: e8.
61. Liu W, Zhu W, Liao B, Chen H, Ren S, et al. Improving gene regulatory network structure using redundancy reduction in the MRNET algorithm. RSC Advances. 2017; 7: 23222–23233.
62. Morrissey ER. Gene Regulatory Network Inference Using Time Series. 2016.
63. Schäfer J, Opgen-Rhein R. Reverse Engineering Genetic Networks using the GeneNet Package. 2006; 6.
64. Skok Gibbs C, Jackson CA, Saldi GA, Tjärnberg A, Shah A, et al. High-performance single-cell gene regulatory network inference at scale: The Inferelator 3.0. Bioinformatics. 2022; 38: 2519–2528.
65. Bansal M, Gatta GD, di Bernardo D. Inference of gene regulatory networks and compound mode of action from time course gene expression profiles. Bioinformatics. 2006; 22: 815–822.
66. Finkle JD, Wu JJ, Bagheri N. Windowed Granger causal inference strategy improves discovery of gene regulatory networks. Proceedings of the National Academy of Sciences. 2018; 115: 2252–2257.

67. Cahan P, Li H, Morris SA, Lummertz da Rocha E, Daley GQ, et al. CellNet: Network Biology Applied to Stem Cell Engineering. Cell. 2014; 158: 903–915.
68. Haury AC, Mordelet F, Vera-Licona P, Vert JP. TIGRESS: Trustful Inference of Gene REgulation using Stability Selection. BMC Systems Biology. 2012; 6: 145.
69. Papili Gao N, Ud-Dean SMM, Gandrillon O, Gunawan R. SINCERITIES: Inferring gene regulatory networks from time-stamped single cell transcriptional expression profiles. Bioinformatics. 2018; 34: 258–266.
70. Bonnaffoux A, Herbach U, Richard A, Guillemin A, Gonin-Giraud S, et al. WASABI: A dynamic iterative framework for gene regulatory network inference. BMC Bioinformatics. 2009; 20: 220.
71. Herbach U, Bonnaffoux A, Espinasse T, Gandrillon O. Inferring gene regulatory networks from single-cell data: A mechanistic approach. BMC Systems Biology. 2017; 11: 105.
72. Ventre E, Herbach U, Espinasse T, Benoit G, Gandrillon O. One model fits all: Combining inference and simulation of gene regulatory networks [Preprint]. Systems Biology. 2022.
73. Kamimoto K, Stringa B, Hoffmann CM, Jindal K, Solnica-Krezel L, et al. Dissecting cell identity via network inference and in silico gene perturbation. Nature. 2023; 1–10.
74. Fleck JS, Jansen SMJ, Wollny D, Zenk F, Seimiya M, et al. Inferring and perturbing cell fate regulomes in human brain organoids. Nature. 2022; 1–8.
75. Qiu X, Rahimzamani A, Wang L, Ren B, Mao Q, et al. Inferring Causal Gene Regulatory Networks from Coupled Single-Cell Expression Dynamics Using Scribe. Cell Systems. 2020; 10: 265-274.e11.
76. Wolf FA, Hamey FK, Plass M, Solana J, Dahlin JS, et al. PAGA: Graph abstraction reconciles clustering with trajectory inference through a topology preserving map of single cells. Genome Biology. 2019; 20: 59.
77. Liang X, Young WC, Hung LH, Raftery AE, Yeung KY. Integration of Multiple Data Sources for Gene Network Inference using Genetic Perturbation Data: Extended Abstract. Proceedings of the 2018 ACM International

Conference on Bioinformatics, Computational Biology, and Health Informatics. 2018; 601–602.
78. Yuan L, Guo LH, Yuan CA, Zhang Y, Han K, et al. Integration of Multi-Omics Data for Gene Regulatory Network Inference and Application to Breast Cancer. IEEE/ACM Transactions on Computational Biology and Bioinformatics. 2019; 16: 782–791.
79. Zhang J, Zhu W, Wang Q, Gu J, Huang LF, et al. Differential regulatory network-based quantification and prioritization of key genes underlying cancer drug resistance based on time-course RNA-seq data. PLOS Computational Biology. 2019; 15: e1007435.
80. Sha Y, Wang S, Bocci F, Zhou P, Nie Q. Inference of Intercellular Communications and Multilayer Gene-Regulations of Epithelial–Mesenchymal Transition From Single-Cell Transcriptomic Data. Frontiers in Genetics. 2021; 11.
81. Hossain SMM, Halsana AA, Khatun L, Ray S, Mukhopadhyay A. Discovering key transcriptomic regulators in pancreatic ductal adenocarcinoma using Dirichlet process Gaussian mixture model. Scientific Reports. 2021; 11: 7853.
82. Zhang Y, Chang X, Liu X. Inference of gene regulatory networks using pseudo-time series data. Bioinformatics. 2021; 37: 2423–2431.
83. Moore D, de Matos Simoes R, Dehmer M, Emmert-Streib F. Prostate Cancer Gene Regulatory Network Inferred from RNA-Seq Data. Current Genomics. 2019; 20: 38–48.
84. Ramirez RN, El-Ali NC, Mager MA, Wyman D, Conesa A, et al. Dynamic Gene Regulatory Networks of Human Myeloid Differentiation. Cell Systems. 2017; 4: 416-429.e3.
85. Bocci F, Zhou P, Nie Q. spliceJAC: Transition genes and state-specific gene regulation from single-cell transcriptome data. Molecular Systems Biology. 2022; 18: e11176.
86. Thorne T. Approximate inference of gene regulatory network models from RNA-Seq time series data. BMC Bioinformatics. 2018; 19: 127.
87. Collado-Torres L, Nellore A, Kammers K, Ellis SE, Taub MA, et al. Reproducible RNA-seq analysis using recount2. Nature Biotechnology. 2017; 35: Article 4.

88. Janssens J, Aibar S, Taskiran II, Ismail JN, Gomez AE, et al. Decoding gene regulation in the fly brain. Nature. 2022; 601: Article 7894.
89. Van Hove H, Martens L, Scheyltjens I, De Vlaminck K, Pombo Antunes AR, et al. A single-cell atlas of mouse brain macrophages reveals unique transcriptional identities shaped by ontogeny and tissue environment. Nature Neuroscience. 2019; 22: 1021–1035.
90. Lambrechts D, Wauters E, Boeckx B, Aibar S, Nittner D, et al. Phenotype molding of stromal cells in the lung tumor microenvironment. Nature Medicine. 2018; 24: 1277–1289.
91. Patsalos A, Halasz L, Medina-Serpas MA, Berger WK, Daniel B, et al. A growth factor–expressing macrophage subpopulation orchestrates regenerative inflammation via GDF-15. The Journal of Experimental Medicine. 2021; 219: e20210420.
92. Lu J, Dumitrascu B, McDowell IC, Jo B, Barrera A, et al. Causal network inference from gene transcriptional time-series response to glucocorticoids. PLOS Computational Biology. 2021; 17: e1008223.
93. Duren Z, Lu WS, Arthur JG, Shah P, Xin J, et al. Sc-compReg enables the comparison of gene regulatory networks between conditions using single-cell data. Nature Communications. 2021; 12: Article 1.
94. Jackson CA, Castro DM, Saldi GA, Bonneau R, Gresham D. Gene regulatory network reconstruction using single-cell RNA sequencing of barcoded genotypes in diverse environments. Elife. 2020; 9: e51254.
95. Polynikis A, Hogan SJ, di Bernardo M. Comparing different ODE modelling approaches for gene regulatory networks. Journal of Theoretical Biology. 2009; 261: 511–530.
96. Takeuchi Y. Global Dynamical Properties of Lotka-volterra Systems. Singapore: World Scientific. 1996.
97. Aldridge BB, Saez-Rodriguez J, Muhlich JL, Sorger PK, Lauffenburger DA. Fuzzy Logic Analysis of Kinase Pathway Crosstalk in TNF/EGF/Insulin-Induced Signaling. PLOS Computational Biology. 2009; 5: e1000340.
98. Murata T. Petri nets: Properties, analysis and applications. Proceedings of the IEEE. 1989; 77: 541–580.

99. Glass L, Kauffman SA. The logical analysis of continuous, non-linear biochemical control networks. Journal of Theoretical Biology. 1973; 39: 103–129.
100. Kauffman SA, Kauffman M. of the S. F. I. and P. of B. S. A. The Origins of Order: Self-organization and Selection in Evolution. Oxford: Oxford University Press.1993.
101. Shah OS, Chaudhary MFA, Awan HA, Fatima F, Arshad Z, et al. ATLANTIS - Attractor Landscape Analysis Toolbox for Cell Fate Discovery and Reprogramming. Scientific Reports. 2018; 8: Article 1.
102. Kauffman SA. Metabolic stability and epigenesis in randomly constructed genetic nets. Journal of Theoretical Biology. 1969; 22: 437–467.
103. Thomas R, D'Ari R. Biological Feedback. Boca Raton: CRC Press. 1990.
104. Albert R, Thakar J. Boolean modeling: A logic-based dynamic approach for understanding signaling and regulatory networks and for making useful predictions. WIREs Systems Biology and Medicine. 2014; 6: 353–369.
105. Davidich M, Bornholdt S. The transition from differential equations to Boolean networks: A case study in simplifying a regulatory network model. Journal of Theoretical Biology. 2008; 255: 269–277.
106. Shmulevich I, Dougherty ER, Kim S, Zhang W. Probabilistic Boolean networks: A rule-based uncertainty model for gene regulatory networks. Bioinformatics. 2022; 18: 261–274.
107. Albert R, Robeva R. Chapter 4 - Signaling Networks: Asynchronous Boolean Models. In: RS Robeva, editor. Algebraic and Discrete Mathematical Methods for Modern Biology. Cambridge: Academic Press. 2015; 65–91.
108. Paulevé L, Sené S. Boolean Networks and Their Dynamics: The Impact of Updates. In E. De Maria (Ed.), Systems Biology Modelling and Analysis 1st ed. Hoboken: Wiley. 2022; 173–250.
109. Licata L, Lo Surdo P, Iannuccelli M, Palma A, Micarelli E, et al. SIGNOR 2.0, the SIGnaling Network Open Resource 2.0: 2019 update. Nucleic Acids Research. 2020; 48: D504–D510.

110. Li C, Donizelli M, Rodriguez N, Dharuri H, Endler L, et al. BioModels Database: An enhanced, curated and annotated resource for published quantitative kinetic models. BMC Systems Biology. 2010; 4: 92.
111. Gawron P, Ostaszewski M, Satagopam V, Gebel S, Mazein A, et al. MINERVA—a platform for visualization and curation of molecular interaction networks. Npj Systems Biology and Applications. 2016; 2: Article 1.
112. Kuperstein I, Cohen DP, Pook S, Viara E, Calzone L, et al. NaviCell: A web-based environment for navigation, curation and maintenance of large molecular interaction maps. BMC Systems Biology. 2013; 7: 100.
113. Barman S, Kwon YK. A Boolean network inference from time-series gene expression data using a genetic algorithm. Bioinformatics. 2018; 34: i927–i933.
114. Gjerga E, Trairatphisan P, Gabor A, Koch H, Chevalier C, et al. Converting networks to predictive logic models from perturbation signalling data with CellNOpt. Bioinformatics. 2020; 36: 4523–4524.
115. Hall, Niarakis. Data integration in logic-based models of biological mechanisms | Elsevier Enhanced Reader. 2021.
116. Henao JD, Lauber M, Azevedo M, Grekova A, List M, et al. Multi-Omics Regulatory Network Inference in the Presence of Missing Data [Preprint]. Systems Biology. 2022.
117. Ostrowski M, Paulevé L, Schaub T, Siegel A, Guziolowski C. Boolean network identification from perturbation time series data combining dynamics abstraction and logic programming. Biosystems. 2016; 149: 139–153.
118. Paulevé L, Kolčák J, Chatain T, Haar S. Reconciling qualitative, abstract, and scalable modeling of biological networks. Nature Communications. 2020; 11: Article 1.
119. Razzaq M, Paulevé L, Siegel A, Saez-Rodriguez J, Bourdon J, et al. Computational discovery of dynamic cell line specific Boolean networks from multiplex time-course data. PLOS Computational Biology. 2018; 14: e1006538.
120. Naldi A, Hernandez C, Levy N, Stoll G, Monteiro PT, et al. The CoLoMoTo Interactive Notebook: Accessible and Reproducible Computational Analyses for Qualitative Biological Networks. Frontiers in Physiology. 2018; 9.

121. Remy E, Rebouissou S, Chaouiya C, Zinovyev A, Radvanyi F, et al. A Modeling Approach to Explain Mutually Exclusive and Co-Occurring Genetic Alterations in Bladder Tumorigenesis. Cancer Research. 2015; 75: 4042–4052.
122. Gómez Tejeda Zañudo J, Scaltriti M, Albert R. A network modeling approach to elucidate drug resistance mechanisms and predict combinatorial drug treatments in breast cancer. Cancer Convergence. 2017; 1: 5.
123. Flobak Å, Baudot A, Remy E, Thommesen L, Thieffry D, et al. Discovery of Drug Synergies in Gastric Cancer Cells Predicted by Logical Modeling. PLOS Computational Biology. 2015; 11: e1004426.
124. Cacace E, Collombet S, Thieffry D. Chapter Seven—Logical modeling of cell fate specification—Application to T cell commitment. In I. S. Peter (Ed.), Current Topics in Developmental Biology (Vol. 139). Cambridge: Academic Press. 2020; 205–238.
125. Kondratova M, Barillot E, Zinovyev A, Calzone L. Modelling of Immune Checkpoint Network Explains Synergistic Effects of Combined Immune Checkpoint Inhibitor Therapy and the Impact of Cytokines in Patient Response. Cancers. 2020; 12: Article 12.
126. Marku M, Verstraete N, Raynal F, Madrid-Mencía M, Domagala M, et al. Insights on TAM Formation from a Boolean Model of Macrophage Polarization Based on In Vitro Studies. Cancers. 2020; 12: Article 12.
127. Palma A, Jarrah AS, Tieri, P, Cesareni G, Castiglione F. Gene Regulatory Network Modeling of Macrophage Differentiation Corroborates the Continuum Hypothesis of Polarization States. Frontiers in Physiology. 2018; 9.
128. Eduati F, Jaaks P, Wappler J, Cramer T, Merten CA, et al. Patient-specific logic models of signaling pathways from screenings on cancer biopsies to prioritize personalized combination therapies. Molecular Systems Biology. 2020; 16: e8664.
129. Béal J, Montagud A, Traynard P, Barillot E, Calzone L. Personalization of Logical Models with Multi-Omics Data Allows Clinical Stratification of Patients. Frontiers in Physiology. 2019; 9.

130. Sherekar S, Viswanathan GA. Boolean dynamic modeling of cancer signaling networks: Prognosis, progression, and therapeutics. Computational and Systems Oncology. 2021; 1: e1017.
131. Montagud A, Béal J, Tobalina L, Traynard P, Subramanian V, et al. Patient-specific Boolean models of signalling networks guide personalised treatments. Elife. 2022; 11: e72626.
132. Letort G, Montagud A, Stoll G, Heiland R, Barillot E, et al. PhysiBoSS: A multi-scale agent-based modelling framework integrating physical dimension and cell signalling. Bioinformatics. 2019; 35: 1188–1196.
133. Stoll G, Naldi A, Noël V, Viara E, Barillot E, et al. UPMaBoSS: A Novel Framework for Dynamic Cell Population Modeling. Frontiers in Molecular Biosciences. 2022; 9.
134. Swat MH, Thomas GL, Belmonte JM, Shirinifard A, Hmeljak D, et al. Chapter 13—Multi-Scale Modeling of Tissues Using CompuCell3D. In: AR Asthagiri, AP Arkin, editors. Methods in Cell Biology (Vol. 110). Cambridge: Academic Press. 2012; 325–366.
135. Aguilar B, Gibbs DL, Reiss DJ, McConnell M, Danziger SA, et al. A generalizable data-driven multicellular model of pancreatic ductal adenocarcinoma. GigaScience. 2020; 9: giaa075.
136. Prokopiou SA, Barbarroux L, Bernard S, Mafille J, Leverrier Y, et al. Multiscale Modeling of the Early CD8 T-Cell Immune Response in Lymph Nodes: An Integrative Study. Computation. 2014; 2: Article 4.
137. Roy M, Finley SD. Metabolic reprogramming dynamics in tumor spheroids: Insights from a multicellular, multiscale model. PLOS Computational Biology. 2019; 15: e1007053.
138. Wertheim KY, Puniya BL, Fleur AL, Shah AR, Barberis M, et al. A multi-approach and multi-scale platform to model CD4+ T cells responding to infections. PLOS Computational Biology. 2021; 17: e1009209.

Book Chapter

The Dualistic Role of Macrophages in Aortic Valve Calcification

Nervana Issa[1], Alexandre Candellier[1,2], Cédric Boudot[1], Saïd Kamel[1,3] and Lucie Hénaut[1]*

[1]UR UPJV 7517 MP3CV, CURS, France
[2]Department of Nephrology, Amiens University Hospital, France
[3]Department of Biochemistry, Amiens University Hospital, France

***Corresponding Author:** Lucie Hénaut, UR UPJV 7517, MP3CV, CURS, Université de Picardie Jules Verne, Avenue René Laennec, 80054, Amiens, France, Tel: +33322825425; Email: lucie.henaut@u-picardie.fr

Published **November 10, 2023**

How to cite this book chapter: Nervana Issa, Alexandre Candellier, Cédric Boudot, Saïd Kamel, Lucie Hénaut. The Dualistic Role of Macrophages in Aortic Valve Calcification. In: Hussein Fayyad Kazan, editor. Immunology and Cancer Biology. Hyderabad, India: Vide Leaf. 2023.

Acknowledgements: The authors are grateful to the French government's *Investissements d'Avenir* program (reference: ANR-16-RHUS-0003_STOP-AS, managed by the French National Research Agency), the *Fédération Hospitalo-Universitaire* program "CArdiac Research Network on Aortic VAlve and heart failure" (reference: GCS G4 FHU CARNAVAL), the Fédération Hospitalo-Universitaire program

"Early Markers of Cardiovascular Remodeling in Valvulopathy and Heart Failure" (reference: GCS G4 FHU REMOD VHF) and the Hauts-de-France Regional Council for their support in this research topic.

Abstract

Calcific aortic valve stenosis (CAS) is the most common valvular heart disease worldwide, associated with cardiovascular morbidity and mortality. This pathology results from fibro-calcific degeneration of the aortic valve leaflets, causing major cardiovascular complications. To date**,** drug therapies have been ineffective in preventing the progression of CAS and aortic valve replacement remains the mainstay of management for patients with symptomatic CAS. Unfortunately, not all patients are eligible for this procedure, which is associated with a greater risk of mortality for subjects presenting comorbidities. A better understanding of the mechanisms responsible for CAS pathogenesis is therefore of crucial importance to develop new therapeutic strategies. Inflammation is a key driver of aortic valve fibrosis and calcification. Macrophages, which play critical roles in the induction and resolution of sterile inflammation, may therefore represent interesting therapeutic targets. Once infiltrated within the aortic leaflet, these dynamic cells can adopt a pro-inflammatory M1 phenotype or switch toward an alternatively activated M2 phenotype, resulting in wound healing and anti-inflammatory activities. This plasticity complicates the efforts to understand their role in the initiation and progression of CAS. This book chapter aims to summarize our current knowledge regarding the role played by macrophage subsets on aortic valve remodelling.

Keywords

Macrophages, Valvular Interstitial Cell, Inflammation, Calcific Aortic Valve Stenosis

Introduction

Calcific aortic valve stenosis (CAS) is the most prevalent valvular heart disease worldwide [1]. This pathology is characterized by slowly progressive fibro-calcific remodelling of the valve leaflets. Over the years, the disease evolves to severe valve calcification with impaired leaflet motion and vast blood flow obstruction, which leads to ventricular hypertrophy. Untreated, symptomatic CAS is associated with a dismal prognosis. Aortic valve replacement is the only treatment shown to improve survival for selected and eligible patients. Before symptoms occur, aortic stenosis is preceded by a silent, latent phase characterized by a slow progression at the molecular, cellular, and tissue levels. A better understanding of the pathophysiology of this latent phase of CAS is needed to develop new therapeutic strategies that would slow disease progression.

A growing body of evidence indicates that a close association exists between inflammation and CAS and that immune signalling, in particular that linked to infiltrated macrophages, may be a viable target for therapeutic intervention. Macrophages are present in healthy valves as a central component of the immune surveillance cell system. Once infiltrated, these dynamic cells play critical roles in the induction and resolution of sterile inflammation. Macrophages exhibit a considerable degree of plasticity depending on signals from the extracellular environment. Indeed, they can adopt a pro-inflammatory M1 phenotype in response to TH1 cytokines and switch toward an alternatively activated M2 phenotype when meeting Th2 cytokines, resulting in wound healing and anti-inflammatory activities. Macrophages' polarization is quickly reversible. Indeed, it takes less than 24 hours for macrophages cultured *in vitro* to switch from one phenotype to another in response to appropriate cytokines [2]**.** Infiltration of macrophages is enhanced in the human calcified aortic valves [3]. In this context, the recent observation that both pro-inflammatory M1 and anti-inflammatory M2 cytokines are upregulated in samples of calcified aortic valves compared with that in non-calcified valves, suggests that both M1 and M2 phenotypes may influence CAS. This book chapter aims to summarize our current

knowledge regarding the role played by macrophage subsets on aortic valve remodelling.

Pathophysiology of CAS

The human aortic valve is composed of three thin and flexible leaflets. Each leaflet is composed of three layers of extracellular matrix, named fibrosa, spongiosa, and ventricularis [4]**,** covered by an outer layer of valvular endothelial cells (VECs) (Figure 1). The entire structure of each leaflet is less than 1 mm thick. The three layers composing the leaflets are principally populated with quiescent valvular interstitial cells (qVICs) [5]. The trilaminar structure of the leaflets determines the biomechanical properties of the aortic valve. Located on the aortic side of the valve, the lamina fibrosa is rich in circumferentially oriented type I and type III collagen fibrils. This composition helps to maintain structural integrity and transfer pressure load to the aortic root. The lamina ventricularis, which is located on the ventricular side of the leaflet, contains radially aligned collagen and elastin fibers. This composition provides more compliance, allowing the valve to expand under pressure [6]. The spongiosa, which has a high proteoglycan content, is located between the fibrosa and ventricularis [7].

During the cardiac cycle, the mechanical stresses applied to the aortic valve can disrupt the endothelial layer, allowing the infiltration of oxidized lipids (ox-LDL) and immune cells [8,9]. Monocytes and lymphocytes are the main cells that adhere and infiltrate the sub-endothelium. Once infiltrated, they differentiate into macrophages and activated T cells able to release growth factors and pro-inflammatory cytokines such as TGF-β, IL-1β, IL-6 and TNF-α. In response to TGFβ, qVICs differentiate into activated VICs (aVICs), displaying a myofibroblastic phenotype, characterized by the expression of α-smooth muscle actin (α-SMA). The concomitant exposure to pro-inflammatory cytokines promotes their proliferation and release of matrix metalloproteinases, inducing fibrosis, thickening and increased valvular stiffness [9-11]. This phenomenon is generally associated with a process of biomineralization during which aVICs differentiate toward osteoblast-like phenotype (obVICs).

During this process, aVICs downregulate their expression of α-SMA and acquire the capacity to express key osteogenic markers such as alkaline phosphatase (ALP), bone morphogenetic protein 2 (BMP2), Runt-related transcription factor 2 (RUNX2, a marker of terminal osteoblastic differentiation) and osteopontin (OPN) [12,13]**.** Through this phenomenon, they acquire the capacity to secrete a bone-like matrix able to calcify. The progressive calcification reduces the elasticity of aortic valve leaflets and over time narrows the aortic valve opening. Symptoms generally occur when the narrowing of the valve is severe.

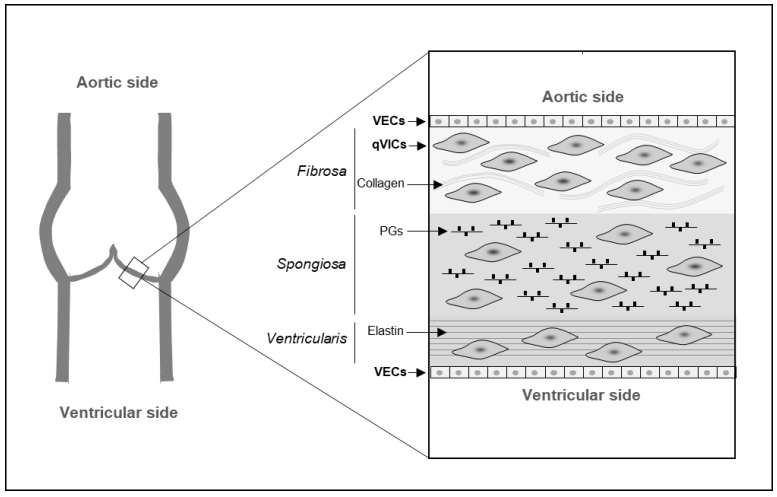

Figure 1: Structure and composition of aortic valve leaflets. PGs: proteoglycans, qVICs: quiescent valvular interstitial cells, VECs: valvular endothelial cells.

Macrophages Plasticity

Once infiltrated within the leaflet, macrophages can acquire distinct functional phenotypes as a reaction to specific micro-environmental stimuli. In response to Th1 cytokines, such as interferon-gamma (IFN-γ), they usually take a classically activated M1 phenotype. Macrophages with an M1 phenotype display cytotoxic and tissue-damaging pro-inflammatory functions after the release of pro-inflammatory mediators such as IL-1β, IL-6, TNFα or reactive oxygen species. Major markers for

the identification of the M1 phenotype are CD11c, CD80, CD86, CD64, CD16, CD32 and nitric oxide synthase (iNOS). In response to Th2 cytokines (e.g, IL-4 and IL-13) they can adopt an alternatively activated M2 phenotype. Macrophages with a M2 phenotype display the ability to secrete anti-inflammatory cytokines such as IL-1 receptor antagonist (IL1ra), IL-10, CCL22 or TGF-β1. Their activity is usually associated with wound healing and anti-inflammatory properties [14]. Major markers for the identification of the M2 phenotype are CD163 and CD206. The next chapter provides a summary of the most recent experimental data evaluating the influence of M1 and M2 macrophages on the calcification of the resident cells of the aortic valve (Figure 2).

M1 Macrophages and Aortic Valve Calcification

Inflammation is a potent driver of aortic valve calcification [15]. Indeed, the exposure *in vitro* to recombinant TNF-α, IL-6, IL-1β or IL-8 has been repeatedly reported to favour the osteogenic differentiation and calcification of primary human VICs (hVICs) [16-20]. These observations have led to a general hypothesis that M1 macrophages may promote VIC-to-osteoblast differentiation and subsequent valve calcification via paracrine pro-inflammatory signalling.

Confirming this hypothesis, in 2017 Li *et al.* reported that conditioned medium (CM) from M1 macrophages (M1-CM) enhances VICs expression of several osteoblastic markers, including BMP2, ALP, and OPN as compared to exposure to CM from unpolarised macrophages (M0-CM) [3]. The fact that neutralizing antibodies against TNF-α or IL-6 blocked hVICs osteogenic differentiation and mineralization, indicated that the procalcific effects of M1-CM are mediated, at least in part, by TNF-α and IL-6. These data were confirmed in 2020 when Grim *et al.* further described that TNF-α and IL-1β in M1-CM indeed deactivate aVIC, as evidenced by a robust reduction of αSMA expression and promote their proliferation, while IL-6 in M1-CM subsequently triggers their differentiation toward obVICs able to express RUNX2 and OPN [21]. These data indicate that

inflammatory M1 macrophages may be responsible for the switch from fibrosis to calcification during aortic valve stenosis progression through their ability to drive VICs myofibroblast-to-osteogenic transition.

Interestingly, M1-polarized macrophages not only communicate with VICs through the secretion of cytokines but also by releasing extracellular vesicles (EVs). In 2022, Xia *et al.* reported that the internalization of EVs produced by M1 macrophages (M1-EVs) increased calcium nodule formation and expression of osteogenesis-related genes in VICs, including RUNX2, BMP2 and OPN, compared with EVs from control macrophage [22]. In this study, the expression of α-SMA and collagen I in VICs was significantly increased in response to M1-EVs, suggesting that M1-EVs promote both the osteogenic and fibrotic processes of VICs. The authors identified that tsRNA-5006c, a novel type of noncoding RNA cleaved from tRNA (tsRNAs), was significantly up-regulated in M1-EVs and that its deletion reduced VICs osteogenic and fibrotic markers as well as nodule formation, indicating that M1-EVs promote VICs mineralization by delivering tsRNA-5006c. In addition, incubation of M1-EVs with tsRNA-5006c inhibitor led to a significant reduction in the expression of markers of autophagy/mitophagy activation, suggesting that the enhanced osteogenic differentiation capacity of M1-EVs tsRNA-5006c may be linked to autophagy/mitophagy. The data are in line with previous studies showing that excessive mitophagy/autophagy exacerbates CAS progression [23].

In 2016, Li et al reported that M1-polarization in CAS correlates with the upregulation of miR-214, a miRNA which expression is essential for M1-directed polarization [24]. Upregulation of miR-214 in aortic valve samples is generally associated with decreased expression of its target gene TWIST-1, a transcription factor that prevents hVICs osteoblastic differentiation by functionally antagonizing RUNX2 [25]. From this observation, Li et al. hypothesized that the release of miR-214 by macrophages may promote CAS development. They confirmed that the co-culture with M1 macrophages or M1-EVs decreased TWIST-1 expression in VICs and favoured their osteogenic

transition as evidenced by the elevation of ALP activity. In line with these data, TWIST1 expression was higher, while ALP activity was lower, in VICs exposed to EVs from miR-214-silenced M1 macrophages compared to those exposed to M1-EVs. These effects were abrogated in VICs silenced for TWIST1. Intravenous injections of a miR-214 inhibitor in hypercholesterolemic apoE-/- mice upregulated valvular TWIST-1 expression and reduced aortic valve calcification. These findings suggest that M1 macrophages' EVs can promote aortic valve calcification by delivering miR-214 to VICs.

It is interesting to note that physical interactions between macrophages and VICs promote the calcification process induced by macrophages' procalcific secretions [26]**.** Indeed, in a study published in 2020, Raddatz and colleagues showed that the direct co-culture with macrophages promoted VICs osteogenic transition (evidenced by the elevation of RUNX2 expression) as compared to a co-culture in transwell systems (no physical contact). In this study, the physical contact of macrophages with VICs was associated with a marked decrease in VICs expression of STAT3β, an alternative splice product of the STAT3 gene**,** displaying the ability to bind and inhibit RUNX2 activity [27]**.** Interestingly, treatment of VICs monoculture with an inhibitor of STAT3 phosphorylation increased RUNX2 transcription, suggesting that STAT3 mediates the connection between macrophage-secreted factors and RUNX2 expression. In line with these data**,** in calcified regions of diseased aortic valves, the elevation of RUNX2 expression negatively correlated with that of STAT3β. Further investigation of STAT3 and macrophage-driven inflammation as therapeutic targets in CAS is warranted.

M2 macrophages and aortic valve calcification

In 2023, Wu et al. reported that the exposure of qVICs to CM from M2 macrophages (M2-CM) promotes their differentiation toward myofibroblasts (aVICs) as evidenced by the elevation α-SMA expression but has no impact on VICs RUNX2 expression [28]. This observation suggests that although M2 macrophages secretions may promote myofibroblast activation, they may not directly contribute to osteogenesis induction. In line with these

data, areas staining positive for the M2 marker CD163 correlated with α-SMA expression in histological samples of CAS.

M2 macrophages are known to facilitate the resolution of inflammation and tissue reconstruction via secreting IL-10 and TGF-β [29,30]. Aortic valve inflammation and degeneration negatively correlate with plasma levels of IL-10 [31] and single nucleotide polymorphisms (SNPs) of IL-10 associated with CAS. Interestingly, cusps from CAS patients also contain higher levels of TGF-β1 than noncalcified normal cusps [32]. Transforming growth factor-β is a well-known fibrosis stimulative factor involved in tissue-repairing processes and immune homeostasis regulation [33]. *In vitro*, the exposure to recombinant TGF-β promotes qVICs differentiation toward myofibroblastic aVICs [34]**.** The addition of TGF-β1 to primary VICs also promotes VICs mobility, aggregation, formation of nodules enriched in ALP, and subsequent mineralization of these nodules [32]. In this model, blockade of TGF-β1-induced apoptosis with a caspase inhibitor significantly inhibits the calcification but has no effect on nodule formation. By contrast, the exposure to an actin-depolymerizing agent named cytochalasin D inhibits nodule formation but has no impact on calcification. Together these data indicate that strategies aiming at blocking M2-derived TGF-β activity may protect the valve from fibro-calcic remodelling.

In 2016, Villa-Bellosta and colleagues elegantly demonstrated that macrophages polarized *in vitro* toward a M2 phenotype are better able to trigger the synthesis of pyrophosphate (PPi) than M1 macrophages [2]. PPi is a calcification inhibitor that is produced after adenosine triphosphate (ATP) hydrolysis by ectoenzyme nucleotide pyrophosphatase/phosphodiesterase-1 (eNPP1) and is then degraded to Pi by tissue non-specific alkaline phosphatase. In Villa-Bellosta et al.'s study, alternatively activated M2 macrophages increased extracellular PPi levels *in vitro* through increased ATP release and eNPP1 overexpression. If this effect was shown to protect vascular smooth muscle cells cultured in the presence of M2 macrophages from calcification, its impact on VICs calcification remains to be demonstrated.

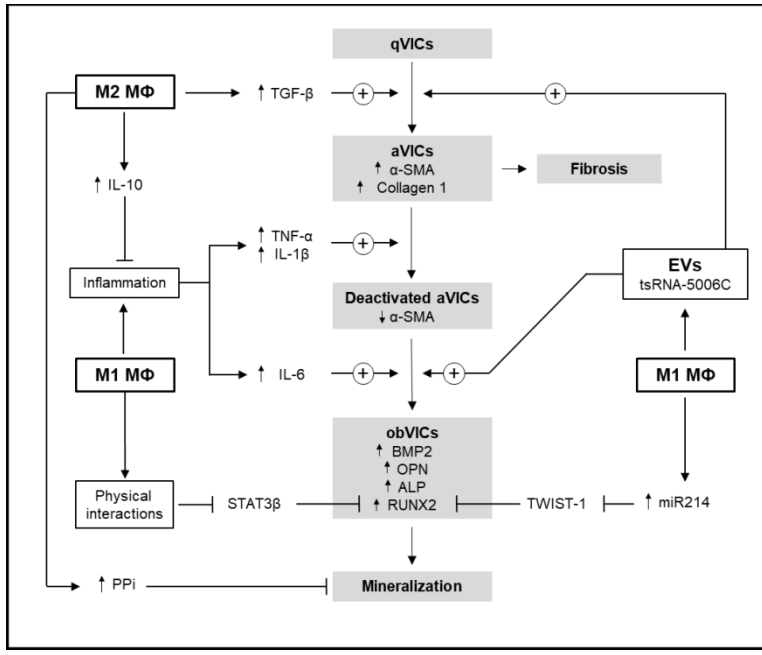

Figure 2: Dualistic role of macrophages in aortic valve calcification: A schematic representation. ALP: alkaline phosphatase, aVICs: activated VICs, α-SMA: α-smooth muscle actin, BMP2: bone morphogenetic protein 2, EVs: extracellular vesicles, IL-1β: interleukin 1β, IL-6: interleukin 6, IL-10: interleukin 10, M1 MΦ: classically-activated M1 macrophages, M2 MΦ: alternatively-activated M2 macrophages, obVICs: osteogenic VICs, OPN: osteopontin, PPi: pyrophosphate, qVICs: quiescent VICs, RUNX2: Runt-related transcription factor 2, TGF-β: transforming growth factor β, TNF-α: tumor necrosis factor α.

Targeting the M1/M2 Balance to prevent CAS

Over the last decade, our understanding of monocytes/macrophages's roles in CAS has improved considerably. In this regard, the therapeutic potential of approaches targeting macrophage recruitment and polarization to prevent the onset or progression of CAS is now being explored. Data from *in vitro* and *ex vivo* experiments have already identified several promising therapeutic targets, such as AFAP1-AS1 [35] and NLR family pyrin domain-containing 3 (NLRP3) [36].

AFAP1-AS1 is a long non-coding RNA (lncRNA) which overexpression in macrophages promotes the M1 but inhibits the M2 polarization [35]. *In vitro***,** exposure to CM from AFAP1-AS1-overexpressing macrophages, which display a M1-like phenotype, promotes VICs osteogenic transition and calcification**.** By contrast, exposure to conditioned medium from AFAP1-AS1-depleted macrophages, which display a M2-like phenotype, inhibits VICs osteogenic differentiation and calcification**.** Future studies should determine whether targeting AFAP1-AS1 is a feasible strategy to reduce CAS.

The pro-inflammatory NLRP3 inflammasome pathway is activated in circulating monocytes of CAS patients [37]. *In ApoE* $^{-/-}$ mice fed a high-fat diet, inhibition of NLRP3 activity thanks to an intraperitoneal injection of 2.5 mg/kg/day of the NLRP3 inhibitor CY-09 prevented the shift of macrophages towards the M1 phenotype, downregulated the levels of the pro-inflammatory factors IL-6 and TNF-α and reduced aortic valve calcification [36]. This study offers a proof-of-concept that pharmacological inhibition of the NLRP3 inflammasome is a feasible strategy for modulating macrophage polarization in order to alleviate CAS.

Conclusion

Over the last decade, it became clear that the diversity of macrophage subtypes complicates our understanding of the pathogenesis of CAS, a disorder for which effective treatments are still lacking. M1 macrophages' secretion of pro-inflammatory cytokines favours the onset and progression of both fibrosis and calcification, while the capacity of M2 macrophages to resolve inflammation may help to prevent CAS. These observations, together with the epidemiological data linking CAS to systemic inflammation, suggest that targeting inflammation may help to slow down CAS progression. However, despite the widespread use of biologicals targeting inflammatory cytokines for a variety of inflammatory conditions, there is yet no information available on these drugs on CAS in humans. In this regard, observational studies of CAS in patients treated with biologicals targeting inflammation for other reasons

may provide valuable information that may help to design an adequately powered concept clinical trial with CAS as a primary endpoint. For instance, it is estimated that over 2 million patients suffering from rheumatoid arthritis are treated every year with biologicals targeting TNF-α, and additional patients receive biologicals targeting IL-1β, and IL-6. The age range of these patients at initiation of therapy may allow studying the impact on CAS.

In recent years, an increasing number of experimental studies evaluated the therapeutic potential of approaches targeting macrophages recruitment and polarization to prevent the onset or progression of CAS. Data from these studies identified AFAP1-AS1 and NLRP3 as potential therapeutic targets able to reduce the pro-calcific M1 polarization. In this context, it is interesting to note that according to the most recent literature M2 macrophages may display dualistic actions on CAS. On the one hand, they may promote the fibrocalcic remodelling of the aortic valve by secreting high level of TGF-β, while on the other hand, their capacity to secrete high levels of IL-10 and PPi may help to prevent CAS. Therefore, to date, it is not clear whether increasing the M2 polarization should be a goal to achieve. Further studies are warranted to evaluate this aspect.

References

1. Alan S Go, Dariush Mozaffarian, Véronique L Roger, Emelia J. Benjamin, Jarett D Berry, et al. Executive Summary: Heart Disease and Stroke Statistics—2013 Update. Circulation. 2013; 127: 143–152.
2. Villa-Bellosta R, Hamczyk MR, Andrés V. Alternatively activated macrophages exhibit an anticalcifying activity dependent on extracellular ATP/pyrophosphate metabolism. Am. J. Physiol.-Cell Physiol. 2016; 310: C788–C799.
3. Geng Li, Weihua Qiao, Wenjing Zhang, Fei Li, Jiawei Shi, et al. The shift of macrophages toward M1 phenotype promotes aortic valvular calcification. J. Thorac. Cardiovasc. Surg. 2017; 153: 1318-1327.
4. Leopold JA. Cellular Mechanisms of Aortic Valve Calcification. Circ. Cardiovasc. Interv. 2012; 5: 605–614.

5. Huang Y. Comparison of Rapidly Proliferating, Multipotent Aortic Valve-Derived Stromal Cells and Valve Interstitial Cells in the Human Aortic Valve. Stem Cells Int. 2019; 2019: e7671638.
6. Hadji F. Altered DNA Methylation of Long Noncoding RNA H19 in Calcific Aortic Valve Disease Promotes Mineralization by Silencing NOTCH1. Circulation. 2016; 134: 1848–1862.
7. Buchanan RM, Sacks MS. Interlayer micromechanics of the aortic heart valve leaflet. Biomech. Model. Mechanobiol. 2014; 13: 813–826.
8. KD O'Brien, DD Reichenbach, SM Marcovina, J Kuusisto, CE Alpers, et al. Apolipoproteins B, (a), and E Accumulate in the Morphologically Early Lesion of 'Degenerative' Valvular Aortic Stenosis. Arterioscler. Thromb. Vasc. Biol. 1996; 16: 523–532.
9. Dania Mohty, Philippe Pibarot, Jean-Pierre Després, Claude Côté, Benoit Arsenault, et al. Association Between Plasma LDL Particle Size, Valvular Accumulation of Oxidized LDL, and Inflammation in Patients With Aortic Stenosis. Arterioscler. Thromb. Vasc. Biol. 2008; 28: 187–193.
10. Philip Roger Goody, Mohammed Rabiul Hosen, Dominik Christmann, Sven Thomas Niepmann, Andreas Zietzer, et al. Aortic Valve Stenosis. Arterioscler. Thromb. Vasc. Biol. 2020; 40: 885–900.
11. V Parisi, D Leosco, G Ferro, A Bevilacqua, G Pagano, et al. The lipid theory in the pathogenesis of calcific aortic stenosis. Nutr. Metab. Cardiovasc. Dis. 2015; 25: 519–525.
12. Xiaoping Yang, Xianzhong Meng, Xin Su, David C Mauchley, Lihua Ao, et al. Bone morphogenic protein 2 induces Runx2 and osteopontin expression in human aortic valve interstitial cells: Role of Smad1 and extracellular signal-regulated kinase 1/2. J. Thorac. Cardiovasc. Surg. 2009; 138: 1008-1015.e1.
13. Liu AC, Joag VR, Gotlieb AI. The Emerging Role of Valve Interstitial Cell Phenotypes in Regulating Heart Valve Pathobiology. Am. J. Pathol. 2007; 171: 1407–1418.
14. Wang N, Liang H, Zen K. Molecular Mechanisms That Influence the Macrophage M1–M2 Polarization Balance. Front. Immunol. 2014; 5.

15. Cho KI, Sakuma I, Sohn IS, Jo SH, Koh KK. Inflammatory and metabolic mechanisms underlying the calcific aortic valve disease. Atherosclerosis. 2018; 277: 60–65.
16. Jens J Kaden, Refika Kiliç, Aslihan Sarikoç, Siegfried Hagl, Siegfried Lang, et al. Tumor necrosis factor alpha promotes an osteoblast-like phenotype in human aortic valve myofibroblasts: A potential regulatory mechanism of valvular calcification. Int. J. Mol. Med. 2005; 16: 869–872.
17. Zaiqiang Yu, Kazuhiko Seya, Kazuyuki Daitoku, Shigeru Motomura, Ikuo Fukuda, et al. Tumor Necrosis Factor-α Accelerates the Calcification of Human Aortic Valve Interstitial Cells Obtained from Patients with Calcific Aortic Valve Stenosis via the BMP2-Dlx5 Pathway. J. Pharmacol. Exp. Ther. 2011; 337: 16–23.
18. Diala El Husseini, Marie-Chloé Boulanger, Ablajan Mahmut, Rihab Bouchareb, Marie-Hélène Laflamme, et al. P2Y2 receptor represses IL-6 expression by valve interstitial cells through Akt: Implication for calcific aortic valve disease. J. Mol. Cell. Cardiol. 2014; 72: 146–156.
19. Isoda K, Matsuki T, Kondo H, Iwakura Y, Ohsuzu F. Deficiency of Interleukin-1 Receptor Antagonist Induces Aortic Valve Disease in BALB/c Mice. Arterioscler. Thromb. Vasc. Biol. 2010; 30: 708–715.
20. Kawthar Dhayni, Yuthiline Chabry, Lucie Hénaut, Carine Avondo, Cedric Boudot, et al. Aortic valve calcification is promoted by interleukin-8 and restricted through antagonizing CXC motif chemokine receptor 2. Cardiovasc. Res. cvad117. 2023.
21. Joseph C Grim, Brian A Aguado, Brandon J Vogt, Dilara Batan, Cassidy L Andrichik, et al. Secreted Factors from Proinflammatory Macrophages Promote an Osteoblast-Like Phenotype in Valvular Interstitial Cells. Arterioscler. Thromb. Vasc. Biol. 2020; 40: e296–e308.
22. Hao Xia, Mingjian Gao, Jun Chen, Guanshen Huang, Xiuting Xiang, et al. M1 macrophage-derived extracellular vesicle containing tsRNA-5006c promotes osteogenic differentiation of aortic valve interstitial cells through regulating mitophagy. PeerJ. 2022; 10: e14307.
23. Giampaolo Morciano, Simone Patergnani, Gaia Pedriali, Paolo Cimaglia, Elisa Mikus, et al. Impairment of mitophagy

and autophagy accompanies calcific aortic valve stenosis favouring cell death and the severity of disease. Cardiovasc. Res. 2022; 118: 2548–2559.
24. Lu S, Gao Y, Huang X, Wang X. Cantharidin Exerts Anti-Hepatocellular Carcinoma by Mir-214 Modulating Macrophage Polarization. Int. J. Biol. Sci. 2014; 10: 415–425.
25. Zhang XW. Twist-related protein 1 negatively regulated osteoblastic transdifferentiation of human aortic valve interstitial cells by directly inhibiting runt-related transcription factor 2. J. Thorac. Cardiovasc. Surg. 2014; 148: 1700-1708.e1.
26. Raddatz MA. Macrophages Promote Aortic Valve Cell Calcification and Alter STAT3 Splicing. Arterioscler. Thromb. Vasc. Biol. 2020; 40: e153–e165.
27. Ziros PG, Georgakopoulos T, Habeos I, Basdra EK, Papavassiliou AG. Growth Hormone Attenuates the Transcriptional Activity of Runx2 by Facilitating Its Physical Association with Stat3β. J. Bone Miner. Res. 2004; 19: 1892–1904.
28. Wu L. Crosstalk between myofibroblasts and macrophages: A regulative factor of valvular fibrosis in calcific aortic valve disease. Cell Biol. Int. 2003; 47: 754–767.
29. Frantz S, Nahrendorf M. Cardiac macrophages and their role in ischaemic heart disease. Cardiovasc. Res. 2014; 102: 240–248.
30. Kessler B. Interleukin 10 inhibits pro-inflammatory cytokine responses and killing of Burkholderia pseudomallei. Sci. Rep. 2017; 7: 42791.
31. Yong An, Yong-Tao Wang, Yi-Tong Ma, Muhuyati Wulasihan, Ying Huang, et al. IL-10 Genetic Polymorphisms Were Associated with Valvular Calcification in Han, Uygur and Kazak Populations in Xinjiang, China. PLOS ONE 10, e0128965 (2015).
32. Jian B, Narula N, Li Q, Mohler ER, Levy RJ. Progression of aortic valve stenosis: TGF-β1 is present in calcified aortic valve cusps and promotes aortic valve interstitial cell calcification via apoptosis. Ann. Thorac. Surg. 2003; 75: 457–465.
33. Eming SA, Wynn TA, Martin P. Inflammation and

metabolism in tissue repair and regeneration. Science. 2017; 356: 1026–1030.
34. Li C, Gotlieb AI. Transforming Growth Factor-β Regulates the Growth of Valve Interstitial Cells in Vitro. Am. J. Pathol. 2011; 179: 1746–1755.
35. He W. LncRNA AFAP1-AS1 promotes M1 polarization of macrophages and osteogenic differentiation of valve interstitial cells. J. Physiol. Biochem. 2021; 77: 461–468.
36. Lu J, Xie S, Deng Y, Xie X, Liu Y. Blocking the NLRP3 inflammasome reduces osteogenic calcification and M1 macrophage polarization in a mouse model of calcified aortic valve stenosis. Atherosclerosis. 2022; 347: 28–38.
37. Wesley Tyler Abplanalp, Silvia Mas-Peiro, Sebastian Cremer, David John, Stefanie Dimmeler, et al. Association of Clonal Hematopoiesis of Indeterminate Potential with Inflammatory Gene Expression in Patients With Severe Degenerative Aortic Valve Stenosis or Chronic Postischemic Heart Failure. JAMA Cardiol. 2020; 5: 1170–1175.

Book Chapter

Skin Cancer Metabolism

Ferial KHALIFE and Hamid-Reza REZVANI*

Univ. Bordeaux, Inserm, BRIC, UMR 1312, F-33076 Bordeaux, France.

***Corresponding Author:** Hamid-Reza REZVANI, Univ. Bordeaux, Inserm, BRIC, UMR 1312, F-33076 Bordeaux, France

Published **June 12, 2024**

How to cite this book chapter: Ferial KHALIFE, Hamid-Reza REZVANI. Skin Cancer Metabolism. In: Hussein Fayyad Kazan, editor. Immunology and Cancer Biology. Hyderabad, India: Vide Leaf. 2024.

Abstract

Skin cancer, the most common form of malignancy globally, encompasses different types such as basal cell carcinoma, squamous cell carcinoma, and melanoma. These cancers exhibit unique biological behaviors and metabolic demands, necessitating a deeper understanding of their metabolic reprogramming to develop effective therapies. Metabolic reprogramming in cancer cells involves a shift from oxidative phosphorylation to aerobic glycolysis, known as the Warburg effect. However, recent studies have demonstrated that metabolic reprograming can also be distinguished by a shift to the oxidative phosphorylation pathway. In skin cancer, the metabolic

landscape is further complicated by the interplay of UV radiation-induced DNA damage, inflammation, and the tumor microenvironment. Recent research has highlighted potential therapeutic targets within these reprogrammed metabolic pathways. Understanding the intricate relationship between metabolic reprogramming and skin cancer progression is crucial for developing innovative treatments. In this review, we provide a comprehensive overview of the link between skin cancer and metabolic reprogramming, emphasizing the potential for novel therapeutic strategies based on these insights.

Keywords

Skin Cancer; Metabolism; Metabolic Reprogramming; Cancer Therapy

Introduction

Skin cancer is one of the most common cancer types in humans, affecting millions worldwide, particularly in the United States. The incidence of common skin cancers, including melanoma, cutaneous basal cell carcinoma (cBCC) and cutaneous squamous cell carcinoma (cSCC), is increasing each year, posing significant global health concern [1]. Non-melanoma skin cancer (NMSC), encompassing cSCC and cBCC and also referred to as keratinocyte carcinomas, constitutes approximately 95% of all skin cancer cases. Notably, cBCC alone makes up 80% of NMSC, rendering it the most prevalent cutaneous malignancy [2]. Additionally, rare skin cancers like Merkel cell carcinomas, adnexal carcinomas of the skin, and skin sarcomas are classified under NMSC [3]. On the other hand, melanomas account for the remaining 5%, despite being the most lethal form of skin cancer and responsible for the majority of mortality cases [4]. Apart from the genetic factors, that are the main starting point for the formation of cancer, UV light is directly related to skin cancer. Despite being a crucial risk factor affecting skin cancer, UV exposure is a modifiable factor [5]. In that respect, prevention in this type of cancer is highly featured, and highlights the importance of sun prevention by minimizing sun exposure, use of sunscreen, wear UV-protective clothing and many more [6].

Skin cancer treatment include localized therapies such as surgery and radiation, and systemic therapies like chemotherapies. Evolution in targeted therapies help in overcoming chemo-resistance and the cytotoxic effect of the chemotherapy, while this latter become less frequently used. Early detections, and the development of potential biomarkers will lead to a better outcome in cancer treatment, taking into consideration the genetic and molecular modifications in cancer cells [7]. Generally, in cancer, genetic modifications cluster a large landscape of mutations, that are still undefined; specifically, in skin cancer, cells have from 5 to 15% times higher modification rate than those found is non-cutaneous cancer cells, caused by UV exposure [8]. Recently, several studies have highlighted the key role of energy metabolism in skin cancer initiation and progression. Mitochondrial functions are essential for cancer cells, and different types of cancer undergo different bioenergetic alterations [9]. In this chapter, we will highlight the different metabolic modifications in the different types of skin cancer, and how they can serve as potential biomarkers for diagnosis and treatment.

Overview of Metabolic Modifications in Cancer

The metabolism of cancer cells has been a focal point of research and continues to be extensively studied to this day. Nearly a century ago, Otto Warburg was the first to identify the phenomenon of "aerobic glycolysis" in cancer cells, wherein cells produce excessive lactate even in the presence of oxygen [10,11]. Cancer cells employ various strategies to meet their energy demands. For instance, while some cancer cells exhibit enhanced glycolysis and impaired oxidative phosphorylation (OXPHOS), others display distinct profiles by upregulating OXPHOS components for their anabolism and energy production [12,13]. This latter profile has been found in metastasis and certain subclasses of diffuse B cell lymphomas and lung adenocarcinoma [14-16]. Ultimately, the main objective of metabolic reprogramming in cancer cells is to sustain anabolism and ensure efficient energy provision to fuel cell proliferation [17].

Several factors are able to affect the energy metabolism in cancer cells, with mitochondria playing a central role in orchestrating the chemical reactions necessary to meet the cells' energy demands. Consequently, any alterations in mitochondrial enzymes can profoundly impact the energy metabolism of cancer cells. The following mechanisms have been identified thus far to explain the metabolic alterations in cancer cells: somatic mutations in mitochondrial DNA (mtDNA), increased oxidative stress, adaptation to chronic environmental hypoxia, and activation of oncogenes or inactivation of tumor suppressors that influence metabolic shifts (e.g., TP53, HIF-1α, c-MYC, and PI3K).

Studies have revealed that several cancers exhibit inherent reductions in mitochondrial function, often attributed to mutations in mitochondrial DNA (mtDNA). Indeed, mtDNA possesses a high mutation rate, attributed to factors such as damage accumulation during replication and oxidative stress. Furthermore, certain nuclear genome-encoded mitochondrial enzymes, such as succinate dehydrogenase (SDH) and fumarate hydratase (FH), have been identified as tumor suppressors [18]. Therefore, mutations in both mtDNA and nuclear-encoded mitochondrial enzymes contribute to the etiology of cancer [19].

Oxidative stress, besides its mutagenic effect on mtDNA, directly influences cellular energy metabolism by either activating or inactivating specific metabolic enzymes. Elevated levels of reactive oxygen species (ROS) trigger the activation of proteins, such as HIF-1α, AKT, and oncogenes RAS, SRC, and MYC, which, in turn, regulate the expression of enzymes involved in glycolysis. Additionally, ROS induce oxidation and inactivation of protein tyrosine phosphatases like phosphatase and tensin homolog (PTEN) [20]. Furthermore, various signaling pathways are activated in response to oxidative stress to mitigate the effects of elevated ROS. The elevated ROS levels activate K-Ras, B-Raf, and Myc, which subsequently promote the basal NRF2 (Nuclear factor erythroid 2-related factor 2) antioxidant program. This program regulates NRF2 at the transcriptional level [21].

Another mechanism through which metabolic rewiring occurs in cancer cells is hypoxia. The hyperplastic growth in tumors induces significant hypoxia, which in turn compels cells to rely on glycolysis through the stabilization of the hypoxia-inducible transcription factor HIF-1α [22]. This metabolic adaptation to hypoxia leads to acidification of the tumor environment, resulting in low extracellular pH and a neutral to alkaline intracellular pH (pHi) [23]. Enhanced activity of pHi-regulating systems serves as a beneficial adaptation for cancer cells, promoting cell survival and invasion [24].

Activation of oncogenes and/or inactivation of tumor suppressor genes have a huge impact on the cellular energy metabolism [25]. The activation of c-MYC, PI3K, AKT, and HIF, or the loss of p53, are among the most commonly observed alterations in human cancers. c-MYC is a proto-oncogene that stimulate the transcription of PDK1 and LDH, consequently it positively modulates the glycolysis pathway [25]. HIF-1α is responsible for the transcription of GLUT-1, HK-2, LDH and PDK-1. The expression of PDK1 leads to the inactivation of PDH, therefore to a decreased conversion of pyruvate to acetyl-coA and eventually the reduction of the OXPHOS pathway [25]. The deregulation of the PI3K pathway in cancer, occurs through various mechanisms, including activating mutations in AKT and mTOR and the loss of PTEN. The deregulation of the PI3K pathway causes alteration in metabolic pathways through various mechanisms [26]. TP53, a tumor suppressor gene, is mutated in the majority of human cancers, affecting energy metabolism at various levels. For example, TIGAR (TP53-induced glycolysis and apoptosis regulator) is an enzyme induced by p53, which reduces the activity of PFK-1, thereby inhibiting glycolysis. Conversely, loss of TP53 leads to the opposite effect [27].

Overview of Metabolic Modifications in Skin Cancers

Metabolic Modifications in Melanoma

Melanoma, deriving from melanocytes, is the most aggressive type of skin cancer. Several genes mutations are reported in melanomas: N-RAS, BRAF, PTEN, MEK1, KIT, CTNNB1,

GNA11, GNAQ, etc... (http://www.mycancergenome.org/content/disease/melanoma/)[28,29].

Mutations in BRAF oncogenes are usually detected in early stages and in approximately ~50% of cutaneous melanoma [30]. It leads to the activation of BRAF protein kinase. This latter phosphorylates MEK1/2 to finally activate the MAPK/ERK pathway, which in turn promote the expression of HIF1α. Also, BRAF mutations are responsible for the upregulation of GLUT1. These findings explain why melanomas manifest increased glucose uptake and enhanced glycolytic rate [31]. On the other hand, BRAF mutations inhibits MITF and PGC-1α, and consequently leads to the inhibition of OXPHOS [32]. Contrariwise, treating BRAF-mutated melanoma with BRAF inhibitors will render them dependent on OXPHOS [33].

N-RAS mutations exist in approximately ~13-25% of skin melanoma [28] and was from the first oncogenes identified in melanoma skin cancer. It has been demonstrated that melanoma harboring N-RAS activating mutations have either activated MAPK or PI3K pathway [34]. PI3K/AKT/mTOR activation is also associated with an increased glycolysis through the expression of GLUT1, PFKFB2, PGC-1α, PEPCK, TIGAR, MnSOD and HIF-1α [35-37]. However, a small group of melanoma with mutation in BRAF and N-RAS exhibit an increase OXPHOS due an activation of MITF/PGC1α pathway [38].

PTEN is a tumor suppressor gene detected in approximately ~19% of skin melanoma. Melanoma cancer cells with PTEN mutation express high levels of OXPHOS and low levels of glycolysis. This status could take place either through expression of PGC1α, or instability of PFKFB [29,39].

Studying the mtDNA variability in melanoma, research has shown that D-loop mtDNA instability was widely found in numerous melanoma cells, on the contradictory to the point mutations that were rarely found in malignant melanoma [40-42]. Nonetheless, mtDNA D-loop alteration and 4977 bp

deletions were detected in blood samples of melanoma patients [42,43].

Metabolic Modifications in cBCC

Cutaneous BCC is a type of the NMSCs that originate from the deepest part of the epidermis, in particular from the basal keratinocytes. cBCC is highly curable and treatment could vary from a simple topical treatment to radiation and excisional surgeries for more severe cases [44].

Aberrant activation of hedgehog (Hh) signaling is a pathognomonic feature of cBCC and has been reported in approximately ~90% [45]. The hedgehog signaling pathway is essential for transmitting information to embryonic cells for a proper cell differentiation, whilst in adults malfunction in this pathway plays an essential role in tumorigenesis in addition to other disorders [46]. Mutations in this pathway regroup activating mutations of SMO and inactivating mutations of tumor suppressor gene PTCH [47]. The Gli family of transcription factors is responsible for the transcription of hedgehog targeted genes, and it activated by SMO; while PTCH possess an inhibitory effect on SMO [48]. Presently, it has been confirmed that hedgehog pathway has an impact on the energy metabolism of the cell. It has been demonstrated that accumulation of Gli promotes HIF-1α expression, which in turn promotes glycolysis [49]. SMO activity can be influenced by intracellular lipids such as PI4P [50]. Moreover, intracellular and extracellular sterols have impact on SMO activity, and can react to sterol-sensing domain of PTCH [51]. In the same line, it has been demonstrated that treating cells with SMO smoothened agonist (SAG) induces Warburg-like metabolic reprogramming by modulating PDHA1, AMPK and PKM1/2 [52].

Among the genetic alterations of cBCC is the TP53 gene mutations, which has been reported in approximately ~60% of BCC [53]. As we mentioned before, TP53 is proved to alter energy metabolism even though there's no concrete evidence of it reprogramming metabolism in cBCC. TP53 enhances OXPHOS and inhibits glycolysis through several mechanisms. It

is responsible for the activation of several proteins such as SCO2, COX1, COX2 and p52R2 [54-56]. On the other hand, TP53 is able to down-regulate the transcriptional expression of GLUT1, GLUT4, and GLUT3 through the inhibition of IKK, which in turn leads to the reduction of glycolysis [57,58]. TP53 also influences glucose flux by regulating PGM and TIGAR, a protein that regulates fructose 2,6-biphosphate levels and glycolytic rate [59-61].

A smaller number of cBCC were identified for mutations in members of the RAS genes [62]. The RAS GTPase family, gathering H-RAS, N-RAS and K-RAS, is oncogenic and commonly activated in human cancers. While concrete data regarding the role of RAS in the metabolic reprogramming of cBCC is lacking, there is emerging evidence, suggesting that RAS could potentially impact cancer cell metabolism more broadly. Zheng *et al.* have demonstrated that H-RAS mutations lead to an increased glycolytic metabolism. In this state, an increased expression of glycolytic enzymes take place including PGK-1, PKM-1, LDH-A and PDK-1. On the other hand, a reduction in the Krebs cycle has been demonstrated through a decrease activity of PDH and mitochondrial complex 1 [63]. Additionally, oncogenic mutation of K-RAS was demonstrated to induce glycolysis through upregulation of GLUT1, HK-1, HK-2, PFK-1 and LDH-A [64,65]. Also, it was found to affect glutamine metabolism [66], and glycolysis rate through the activation of the non-oxidative arm of the pentose phosphate pathway (PPP) to promote the production of nucleotides [67].

Metabolic Modifications in cSCC

Cutaneous SCC derives from keratinocytes cells of the epidermis and can metastases to distant regions from the origin [2]. Different mutated genes have been identified in cSCC including mostly CDKN2A, TP53 and H-RAS [68,69]. As it was mentioned before, TP53 and H-RAS surely have a huge effect on the energy metabolism in cells despite of our limited understanding of the metabolic reprogramming in this type of skin cancer. However, several lines of proof propose a

substantial role of metabolism in cSCC initiation and progression.

CDKN2A gene, that provide instruction for making several proteins, encodes for $p16^{INK4a}$ and $p14^{ARF}$ tumor suppressor genes. Studies showed that $p16^{INK4a}$ positively regulates cyclin D1-CDK4 which inhibits PGC-1α and suppress gluconeogenesis [70]. Furthermore, $p16^{INK4a}$ deficiency causes phosphorylation of PKA leading to the activation of PKA-CREB-PGC1α pathway. The consequence of this process is stimulation of the expression of genes involved in gluconeogenesis [71].

UV exposure, in addition of being a curious risk factor in cSCC, affect mtDNA integrity. This latter is shown to affect cell invasion and tumor progression [72,73]. UV-radiation was proved to affect D-loop mtDNA in a 260 bp mtDNA tandem duplication and mtDNA deletions specially 4977 bp and 3895 bp deletion in a study performed on sun-exposed skin and NMSCs [74-77]. Being useful biomarkers for photoaging and skin cancers, mtDNA mutations are able to affect energy metabolism as its common deletions affect regions encoding for ATPase8, ATPase6, COXIII, ND3, ND4, ND4L and ND5 [78].

DNA damage response (DDR) pathway promotes altered energy metabolism. DDR network is induced by DNA damage, like that resulting from UV radiations, and refers to the process by which the cell maintains the integrity of the genome after a damage. This pathway comprises DNA repair and cell-cycle checkpoint pathways to finally define cell fate [79]. A failure in this response is associated with cancer development. Recently, a link between genomic mutations and metabolic alterations in keratinocyte cells was explored. From the variety of proteins belonging to the DDR network, we studied the role of xeroderma pigmentosum type C (XPC) protein on metabolic reprogramming in human keratinocytes. XPC plays an important role in recognition of DNA damage in nucleotide excision repair. XP-C patients have higher incidence of skin cancer and other malignancies [80]. In this study, we showed that silencing of XPC resulted in the activation of AKT1 and NADPH oxidase-1 (NOX1), accumulation of ROS and specific deletions in mtDNA

[81]. Nonetheless, XPC knockdown in human keratinocytes escalated glycolysis with a reduction in OXPHOS. Implanted into immunodeficient mice, XPC-deficient cells with mtDNA deletions were capable of forming SCC. However, inactivation of AKT or NOX in these cells blocked neoplastic transformation [82]. In another study, using a multistage model of UVB-induced skin cancer, we discovered that cSCC formation is conditional to a certain cellular energy metabolism, that once rewired cancer formation will be inhibited [83-85]. It was demonstrated that at a very early stage of photo-carcinogenesis glycolysis, TCA cycle and fatty acid β-oxidation were decreased, while the distal part of the electron transport chain (ETC) were upregulated. These specific metabolic modifications that precede primary skin tumor formation, were accompanied with activated DHODH and glutamine metabolism. DHODH activity is essential for maintaining an increased ETC activity. Mice with decreased DHODH activity or impaired ETC failed to develop pre-malignant or malignant lesions, concluding that DHODH create a major link between DNA repair efficiency and bioenergetic pattering during skin carcinogenesis [83,84].

Energy Metabolism in Skin Cancer Therapy

Profiling cellular energy metabolism in cancer is beneficial for prognosis and diagnosis. As it has been demonstrated, metabolic status is substantial in carcinogenesis, and certainly every cancer cell has altered energy metabolism. In fact, disorders related to cellular metabolism, such as obesity, hyperglycemia, hyperlipidemia and insulin resistance, are associated to an increased risk of developing several types of cancer, increased tumor progression and poor clinical outcome [86,87]. However, metformin (medication used principally for the treatment of type 2 diabetes) and statins (lipid-lowering medication) are associated with reduced incidence of cancer in patients receiving any of these drugs [88]. In addition, genomic alteration and cellular energy metabolism, affecting each other, communicate and influence carcinogenesis and tumor progression. As noted, mutations in oncogenes and tumor suppressor genes influence metabolic reprogramming in cancer [25,27,89]. As well, a continuous presence of a oncogene can stimulate a cancer cell to

shift from highly glycolytic to highly oxidative metabolism during tumor development [90]. Owing to the fact that UV-induced genomic alteration alone cannot account for the origin of cancer, as we recently demonstrated in the XPC knockout normal human keratinocytes and *Tfam* knockout keratinocytes, we can assure that the role of mitochondria and metabolic status is pivotal in skin carcinogenesis and further used for preventative and curative objectives [81,83]. However, the lack of evidence that support the role of energy metabolism in the initiation and progression of cancer drive us to do further research to understand the bioenergetic profiling in cancer and how it can be useful in treatment and prevention. While studying a multi-stage model of UVB-induced skin cancer, we found that leflunomide, which is an FDA-approved inhibitor of DHODH, completely inhibited the UVB-induced pre-malignant and malignant lesions, suggesting the importance of early modifications of energy metabolism in the initiation on cSCC {Formatting Citation}. Accordingly, targeting energy metabolism could be reasonably anticipated as anti-cancer strategy. Likewise, activation of BRAF in melanoma or Hh pathway in cBCC are associated with the induction of Warburg like metabolic reprogramming that can be targeted for an anticancer therapy [91-93].

Targeting energy metabolism could not only be studied for prevention or first-hand treatment, but it surely can be used in combination therapies. Cancer treatment faces various difficulties like drug resistance and drug toxicity, that's when combination therapies are adopted to overcome these obstacles. In addition, it is evidence that cellular energy metabolism plays an important role in the emergence of resistant cells. Using drugs that target energy metabolism in combination targeted therapies contribute to prominent results. For instance, vemurafenib-resistant BRAF-mutant melanoma cells, which rely on OXPHOS, have been shown to become sensitive to mitochondrial uncouplers or OXPHOS inhibitors [32]. Additionally, using anti-diabetic metformin, that inhibits complex 1 of ETC, significantly increased the effect of $BRAF^{V600E}$ inhibition *in vitro* and in murine models [94,95]. Besides relying on OXPHOS, other resistant BRAF-mutant cells have upregulated glutaminase (GLS) and increased glutamine

uptake. Treatment with BPTES, which is a GLS inhibitor, re-sensitizes resistant cells to BRAF inhibition [96]. Furthermore, Hosseini *et al.* have demonstrated that DHODH could not only be targeted for the prevention from skin cancer, but also used in combination therapy for the treatment of cSCC. Leflunomide (LFN), which is an FDA-approved drug for the treatment of rheumatoid arthritis and an inhibitor of DHODH, was used in a combination therapy with 5-fluorouracil (5-FU), a genotoxic agent, on human tumor xenograft model. Results showed a reduction in tumor growth for both SCC-15 and A431 tumor transplants, which suggest that DHODH is a promising target for chemoprevention and combination therapy of UVB-induced cSCC [84]. Considering the promising outcomes of targeting metabolism in enhancing the efficacy of cancer therapy, further research is justified to investigate the potential of targeting energy metabolism in skin cancers as a promising approach for both prevention and therapy of this cancer type.

Conclusion

Findings from studies using melanoma, cBCC, and cSCC models and cells indicate a significant involvement of metabolism in various stages of skin cancer progression. Furthermore, targeting metabolism has shown promising outcomes for the prevention and treatment of skin cancers in certain models. Nevertheless, further in-depth studies are necessary to elucidate the molecular mechanisms underlying metabolic rewiring at different cancer stages, thus paving the way for establishing novel strategies for skin cancer treatment and prevention. Additionally, such research efforts could determine whether metabolic profiling holds potential as a biomarker for prognosis and diagnosis in skin cancer.

References

1. Gordon R. Skin Cancer: An Overview of Epidemiology and Risk Factors. Seminars in Oncology Nursing. 2013; 29: 160–169.
2. Gandhi SA, Kampp J. Skin Cancer Epidemiology, Detection, and Management. Medical Clinics of North America. 2015;

99: 1323–1335.
3. Brandt MG, Moore CC. Nonmelanoma Skin Cancer. Facial Plastic Surgery Clinics of North America. 2019; 27: 1–13.
4. Linares MA, Zakaria A, Nizran P. Skin Cancer. Primary Care: Clinics in Office Practice. 2015; 42: 645–659.
5. Watson M, Holman DM, Maguire-Eisen M. Ultraviolet Radiation Exposure and Its Impact on Skin Cancer Risk. Seminars in Oncology Nursing. 2016; 32: 241–254.
6. Kornek T, Augustin M. Skin cancer prevention: CME Article. JDDG: Journal Der Deutschen Dermatologischen Gesellschaft. 2013; 11: 283–298.
7. South AP, Purdie KJ, Watt SA, Haldenby S, den Breems NY, et al. NOTCH1 Mutations Occur Early during Cutaneous Squamous Cell Carcinogenesis. Journal of Investigative Dermatology. 2014; 134: 2630–2638.
8. Hodis E, Watson IR, Kryukov GV, Arold ST, Imielinski M, et al. A Landscape of Driver Mutations in Melanoma. Cell. 2012; 150: 251–263.
9. Vyas S, Zaganjor E, Haigis MC. Mitochondria and Cancer. Cell. 2016; 166: 555–566.
10. Warburg O. On the Origin of Cancer Cells. Science. 1956; 123: 309–314.
11. Warburg O, Wind F, Negelein E. THE METABOLISM OF TUMORS IN THE BODY. Journal of General Physiology. 1927; 8: 519–530.
12. Jose C, Bellance N, Rossignol R. Choosing between glycolysis and oxidative phosphorylation: A tumor's dilemma? Biochimica et Biophysica Acta (BBA) – Bioenergetics. 2011; 1807: 552–561.
13. Smolková K, Plecitá-Hlavatá L, Bellance N, Benard G, Rossignol R, et al. Waves of gene regulation suppress and then restore oxidative phosphorylation in cancer cells. The International Journal of Biochemistry & Cell Biology. 2011; 43: 950–968.
14. Amoedo ND, Sarlak S, Obre E, Esteves P, Bégueret H, et al. Targeting the mitochondrial trifunctional protein restrains tumor growth in oxidative lung carcinomas. Journal of Clinical Investigation. 2021; 131.
15. Caro P, Kishan AU, Norberg E, Stanley IA, Chapuy B, et al. Metabolic Signatures Uncover Distinct Targets in Molecular

Subsets of Diffuse Large B Cell Lymphoma. Cancer Cell. 2012; 22: 547–560.
16. Porporato PE, Payen VL, Pérez-Escuredo J, De Saedeleer CJ, Danhier P, et al. A Mitochondrial Switch Promotes Tumor Metastasis. Cell Reports. 2014; 8: 754–766.
17. Vander Heiden MG, Cantley LC, Thompson CB. Understanding the Warburg Effect: The Metabolic Requirements of Cell Proliferation. Science. 2009; 324: 1029–1033.
18. Gottlieb E, Tomlinson IPM. Mitochondrial tumour suppressors: A genetic and biochemical update. Nature Reviews Cancer. 2005; 5: 857–866.
19. Brandon M, Baldi P, Wallace DC. Mitochondrial mutations in cancer. Oncogene. 2006; 25: 4647–4662.
20. Panieri E, Santoro MM. ROS homeostasis and metabolism: A dangerous liason in cancer cells. Cell Death & Disease. 2016; 7: e2253–e2253.
21. DeNicola GM, Karreth FA, Humpton TJ, Gopinathan A, Wei C, et al. Oncogene-induced Nrf2 transcription promotes ROS detoxification and tumorigenesis. Nature. 2011; 475: 106–109.
22. Peppicelli S, Bianchini F, Calorini L. Extracellular acidity, a "reappreciated" trait of tumor environment driving malignancy: Perspectives in diagnosis and therapy. Cancer and Metastasis Reviews. 2014; 33: 823–832.
23. Alfarouk KO, Verduzco D, Rauch C, Muddathir AK, Bashir AHH, et al. Glycolysis, tumor metabolism, cancer growth and dissemination. A new pH-based etiopathogenic perspective and therapeutic approach to an old cancer question. Oncoscience. 2014; 1: 777–802.
24. Chiche J, Brahimi-Horn MC, Pouysségur J. Tumour hypoxia induces a metabolic shift causing acidosis: A common feature in cancer. Journal of Cellular and Molecular Medicine. 2010; 14: 771–794.
25. Yeung SJ, Pan J, Lee MH. Roles of p53, Myc and HIF-1 in Regulating Glycolysis—The Seventh Hallmark of Cancer. Cellular and Molecular Life Sciences. 2008; 65: 3981–3999.
26. Jia S, Liu Z, Zhang S, Liu P, Zhang L, et al. Essential roles of PI(3)K–p110β in cell growth, metabolism and tumorigenesis. Nature. 2008; 454: 776–779.

27. Bensaad K, Vousden KH. p53: New roles in metabolism. Trends in Cell Biology. 2007; 17: 286–291.
28. Ball NJ, Yohn JJ, Morelli JG, Norris DA, Golitz LE, et al. RAS Mutations in Human Melanoma: A Marker of Malignant Progression. Journal of Investigative Dermatology. 1994; 102: 285–290.
29. Goel VK, Lazar AJF, Warneke CL, Redston MS, Haluska FG. Examination of Mutations in BRAF, NRAS, and PTEN in Primary Cutaneous Melanoma. Journal of Investigative Dermatology. 2006; 126: 154–160.
30. Maldonado JL, Fridlyand J, Patel H, Jain AN, Busam K, et al. Determinants of BRAF Mutations in Primary Melanomas. JNCI Journal of the National Cancer Institute. 2003; 95: 1878–1890.
31. McArthur GA, Puzanov I, Amaravadi R, Ribas A, Chapman P, et al. Marked, Homogeneous, and Early [18 F]Fluorodeoxyglucose–Positron Emission Tomography Responses to Vemurafenib in BRAF -Mutant Advanced Melanoma. Journal of Clinical Oncology. 2012; 30: 1628–1634.
32. Haq R, Shoag J, Andreu-Perez P, Yokoyama S, Edelman H, et al. Oncogenic BRAF Regulates Oxidative Metabolism via PGC1α and MITF. Cancer Cell. 2013; 23: 302–315.
33. Corazao-Rozas P, Guerreschi P, Jendoubi M, André F, Jonneaux A, et al. Mitochondrial oxidative stress is the achille's heel of melanoma cells resistant to Braf-mutant inhibitor. Oncotarget. 2013; 4: 1986–1998.
34. Posch C, Moslehi H, Feeney L, Green GA, Ebaee A, et al. Combined targeting of MEK and PI3K/mTOR effector pathways is necessary to effectively inhibit NRAS mutant melanoma in vitro and in vivo. Proceedings of the National Academy of Sciences. 2013; 110: 4015–4020.
35. Bhatt AP, Jacobs SR, Freemerman AJ, Makowski L, Rathmell JC, et al. Dysregulation of fatty acid synthesis and glycolysis in non-Hodgkin lymphoma. Proceedings of the National Academy of Sciences. 2012; 109: 11818–11823.
36. Ersahin T, Tuncbag N, Cetin-Atalay R. The PI3K/AKT/mTOR interactive pathway. Molecular BioSystems. 2015; 11: 1946–1954.
37. Huang SW, Kao JK, Wu CY, Wang ST, Lee HC, et al.

Targeting Aerobic Glycolysis and HIF-1` Expression Enhance Imiquimod-induced Apoptosis in Cancer Cells. 2014; 5: 1363-1381.
38. Gopal YNV, Rizos H, Chen G, Deng W, Frederick DT, et al. Inhibition of mTORC1/2 Overcomes Resistance to MAPK Pathway Inhibitors Mediated by PGC1α and Oxidative Phosphorylation in Melanoma. Cancer Research. 2014; 74: 7037–7047.
39. Ortega-Molina A, Serrano M. PTEN in cancer, metabolism, and aging. Trends in Endocrinology & Metabolism. 2013; 24: 184–189.
40. Deichmann M, Kahle B, Benner A, Thome M, Helmke B, et al. Somatic mitochondrial mutations in melanoma resection specimens. International Journal of Oncology. 2004; 24: 137-141.
41. Poetsch M, Petersmann A, Lignitz E, Kleist B. Relationship Between Mitochondrial DNA Instability, Mitochondrial DNA Large Deletions, and Nuclear Microsatellite Instability in Head and Neck Squamous Cell Carcinomas: Diagnostic Molecular Pathology. 2004; 13: 26–32.
42. Takeuchi H, Fujimoto A, Hoon DSB. Detection of Mitochondrial DNA Alterations in Plasma of Malignant Melanoma Patients. Annals of the New York Academy of Sciences. 2004; 1022: 50–54.
43. Shen J, Wan J, Huff C, Fang S, Lee JE, et al. Mitochondrial DNA 4977-base pair common deletion in blood leukocytes and melanoma risk. Pigment Cell & Melanoma Research. 2016; 29: 372–378.
44. Kasper M, Jaks V, Hohl D, Toftgård R. Basal cell carcinoma—Molecular biology and potential new therapies. Journal of Clinical Investigation. 2012; 122: 455–463.
45. Geeraert P, Williams JS, Brownell I. Targeting the hedgehog pathway to treat basal cell carcinoma. Journal of Drugs in Dermatology: JDD. 2013; 12: 519–523.
46. Robbins DJ, Fei DL, Riobo NA. The Hedgehog Signal Transduction Network. Science Signaling. 2013; 5.
47. Wang XD, Inzunza H, Chang H, Qi Z, Hu B, et al. Mutations in the Hedgehog Pathway Genes SMO and PTCH1 in Human Gastric Tumors. PLoS ONE. 2013; 8: e54415.
48. Athar M, Li C, Kim AL, Spiegelman VS, Bickers DR. Sonic

Hedgehog Signaling in Basal Cell Nevus Syndrome. Cancer Research. 2014; 74: 4967–4975.
49. Chen Y, Choi SS, Michelotti GA, Chan IS, Swiderska-Syn M, et al. Hedgehog Controls Hepatic Stellate Cell Fate by Regulating Metabolism. Gastroenterology. 2012; 143: 1319-1329.e11.
50. Yavari A, Nagaraj R, Owusu-Ansah E, Folick A, Ngo K, et al. Role of Lipid Metabolism in Smoothened Derepression in Hedgehog Signaling. Developmental Cell. 2010; 19: 54–65.
51. Teperino R, Aberger F, Esterbauer H, Riobo N, Pospisilik JA. Canonical and non-canonical Hedgehog signalling and the control of metabolism. Seminars in Cell & Developmental Biology. 2014; 33: 81–92.
52. Teperino R, Amann S, Bayer M, McGee SL, Loipetzberger A, et al. Hedgehog Partial Agonism Drives Warburg-like Metabolism in Muscle and Brown Fat. Cell. 2012; 151: 414–426.
53. Kim M. Mutations of the p53 and PTCH gene in basal cell carcinomas: UV mutation signature and strand bias. Journal of Dermatological Science. 2002; 29: 1–9.
54. Bourdon A, Minai L, Serre V, Jais JP, Sarzi E, et al. Mutation of RRM2B, encoding p53-controlled ribonucleotide reductase (p53R2), causes severe mitochondrial DNA depletion. Nature Genetics. 2007; 39: 776–780.
55. Matoba S, Kang JG, Patino WD, Wragg A, Boehm M, et al. P53 Regulates Mitochondrial Respiration. Science. 2006; 312: 1650–1653.
56. Zhou S. Mitochondrial impairment in p53-deficient human cancer cells. Mutagenesis. 2003; 18: 287–292.
57. Kawauchi K, Araki K, Tobiume K, Tanaka N. P53 regulates glucose metabolism through an IKK-NF-κB pathway and inhibits cell transformation. Nature Cell Biology. 2008; 10: 611–618.
58. Schwartzenberg-Bar-Yoseph F, Armoni M, Karnieli E. The Tumor Suppressor p53 Down-Regulates Glucose Transporters GLUT1 and GLUT4 Gene Expression. Cancer Research. 2004; 64: 2627–2633.
59. Bensaad K, Tsuruta A, Selak MA, Vidal MNC, Nakano K, et al. TIGAR, a p53-Inducible Regulator of Glycolysis and Apoptosis. Cell. 2006; 126: 107–120.

60. Gottlieb E, Vousden KH. P53 Regulation of Metabolic Pathways. Cold Spring Harbor Perspectives in Biology. 2010; 2: a001040–a001040.
61. Li H, Jogl G. Structural and Biochemical Studies of TIGAR (TP53-induced Glycolysis and Apoptosis Regulator). Journal of Biological Chemistry. 2009; 284: 1748–1754.
62. Bonilla X, Parmentier L, King B, Bezrukov F, Kaya G, et al. Genomic analysis identifies new drivers and progression pathways in skin basal cell carcinoma. Nature Genetics. 2016; 48: 398–406.
63. Zheng W, Tayyari F, Gowda GAN, Raftery D, McLamore ES, et al. Altered glucose metabolism in Harvey- ras transformed MCF10A cells: ALTERED GLUCOSE METABOLISM IN HARVEY-ras TRANSFORMED CELLS. Molecular Carcinogenesis. 2015; 54: 111–120.
64. Sasaki H. Overexpression of GLUT1 correlates with Kras mutations in lung carcinomas. Molecular Medicine Reports. 2011.
65. Yun J, Rago C, Cheong I, Pagliarini R, Angenendt P, et al. Glucose Deprivation Contributes to the Development of KRAS Pathway Mutations in Tumor Cells. Science. 2009; 325: 1555–1559.
66. Son J, Lyssiotis CA, Ying H, Wang X, Hua S, et al. Glutamine supports pancreatic cancer growth through a KRAS-regulated metabolic pathway. Nature. 2013; 496: 101–105.
67. Ying H, Kimmelman AC, Lyssiotis CA, Hua S, Chu GC, et al. Oncogenic Kras maintains pancreatic tumors through regulation of anabolic glucose metabolism. Cell. 2012; 149: 656–670.
68. Ping XL, Ratner D, Zhang H, Wu XL, Zhang MJ, et al. PTCH Mutations in Squamous Cell Carcinoma of the Skin. Journal of Investigative Dermatology. 2001; 116: 614–616.
69. Uribe P, Gonzalez S. Epidermal growth factor receptor (EGFR) and squamous cell carcinoma of the skin: Molecular bases for EGFR-targeted therapy. Pathology - Research and Practice. 2011; 207: 337–342.
70. Lee Y, Dominy JE, Choi YJ, Jurczak M, Tolliday N, et al. Cyclin D1–Cdk4 controls glucose metabolism independently of cell cycle progression. Nature. 2014; 510: 547–551.

71. Bantubungi K, Hannou SA, Caron-Houde S, Vallez E, Baron M, et al. Cdkn2a/p16Ink4a Regulates Fasting-Induced Hepatic Gluconeogenesis Through the PKA-CREB-PGC1a Pathway. 2014; 63: 11.
72. Amuthan G, Biswas G, Ananadatheerthavarada HK, Vijayasarathy C, Shephard HM, et al. Mitochondrial stress-induced calcium signaling, phenotypic changes and invasive behavior in human lung carcinoma A549 cells. Oncogene. 2002; 21: 7839–7849.
73. Petros JA, Baumann AK, Ruiz-Pesini E, Amin MB, Sun CQ, et al. MtDNA mutations increase tumorigenicity in prostate cancer. Proceedings of the National Academy of Sciences. 2005; 102: 719–724.
74. Harbottle A, Birch-Machin MA. Real-time PCR analysis of a 3895 bp mitochondrial DNA deletion in nonmelanoma skin cancer and its use as a quantitative marker for sunlight exposure in human skin. British Journal of Cancer. 2006; 94: 1887–1893.
75. Krishnan KJ, Harbottle A, Birch-Machin MA. The Use of a 3895 bp Mitochondrial DNA Deletion as a Marker for Sunlight Exposure in Human Skin. Journal of Investigative Dermatology. 2004; 123: 1020–1024.
76. Krishnan KJ, Birch-Machin MA. The Incidence of Both Tandem Duplications and the Common Deletion in mtDNA from Three Distinct Categories of Sun-Exposed Human Skin and in Prolonged Culture of Fibroblasts. Journal of Investigative Dermatology. 2006; 126: 408–415.
77. Powers JM, Murphy G, Ralph N, O'Gorman SM, Murphy JEJ. Mitochondrial DNA deletion percentage in sun exposed and non sun exposed skin. Journal of Photochemistry and Photobiology B: Biology. 2016; 165: 277–282.
78. Russell O, Turnbull D. Mitochondrial DNA disease—Molecular insights and potential routes to a cure. Experimental Cell Research. 2014; 325: 38–43.
79. Branzei D, Foiani M. Regulation of DNA repair throughout the cell cycle. Nature Reviews Molecular Cell Biology. 2008; 9: 297–308.
80. Hosseini M, Ezzedine K, Taieb A, Rezvani HR. Oxidative and energy metabolism as potential clues for clinical heterogeneity in nucleotide excision repair disorders. The

Journal of Investigative Dermatology. 2015; 135: 341–351.
81. Rezvani HR, Rossignol R, Ali N, Benard G, Tang X, et al. XPC silencing in normal human keratinocytes triggers metabolic alterations through NOX-1 activation-mediated reactive oxygen species. Biochimica et Biophysica Acta (BBA) – Bioenergetics. 2011; 1807: 609–619.
82. Rezvani HR, Kim AL, Rossignol R, Ali N, Daly M, et al. XPC silencing in normal human keratinocytes triggers metabolic alterations that drive the formation of squamous cell carcinomas. Journal of Clinical Investigation. 2011; 121: 195–211.
83. Hosseini M, Dousset L, Mahfouf W, Serrano-Sanchez M, Redonnet-Vernhet I, et al. Energy Metabolism Rewiring Precedes UVB-Induced Primary Skin Tumor Formation. Cell Reports. 2018; 23: 3621–3634.
84. Hosseini M, Dousset L, Michon P, Mahfouf W, Muzotte E, et al. UVB-induced DHODH upregulation, which is driven by STAT3, is a promising target for chemoprevention and combination therapy of photocarcinogenesis. Oncogenesis. 2019; 8: 52.
85. Mahfouf W, Muzotte E, Dousset L, Moisan F, Taieb A, et al. Hypoxia-inducible factor-1 alpha play a critical role in UVB-induced tumorigenesis by affecting DNA repair capacity and oxidative stress. Journal of Investigative Dermatology. 2019; 139: S294.
86. Khandekar MJ, Cohen P, Spiegelman BM. Molecular mechanisms of cancer development in obesity. Nature Reviews Cancer. 2011; 11: 886–895.
87. Pollak M. The insulin and insulin-like growth factor receptor family in neoplasia: An update. Nature Reviews Cancer. 2012; 12: 159–169.
88. Gronich N, Rennert G. Beyond aspirin—Cancer prevention with statins, metformin and bisphosphonates. Nature Reviews Clinical Oncology. 2013; 10: 625–642.
89. Ward PS, Thompson CB. Metabolic Reprogramming: A Cancer Hallmark Even Warburg Did Not Anticipate. Cancer Cell. 2012; 21: 297–308.
90. Hu S, Balakrishnan A, Bok RA, Anderton B, Larson PEZ, et al. 13C-Pyruvate Imaging Reveals Alterations in Glycolysis that Precede c-Myc-Induced Tumor Formation and

Regression. Cell Metabolism. 2011; 14: 131–142.
91. Ferecatu I, Bergeaud M, Rodríguez-Enfedaque A, Le Floch N, Oliver L, et al. Mitochondrial localization of the low level p53 protein in proliferative cells. Biochemical and Biophysical Research Communications. 2009; 387: 772–777.
92. Filipp FV, Ratnikov B, De Ingeniis J, Smith JW, Osterman AL, et al. Glutamine-fueled mitochondrial metabolism is decoupled from glycolysis in melanoma: Exploring the metabolic landscape of melanoma. Pigment Cell & Melanoma Research. 2012; 25: 732–739.
93. Parmenter TJ, Kleinschmidt M, Kinross KM, Bond ST, Li J, et al. Response of BRAF -Mutant Melanoma to BRAF Inhibition Is Mediated by a Network of Transcriptional Regulators of Glycolysis. Cancer Discovery. 2014; 4: 423–433.
94. Roesch A, Vultur A, Bogeski I, Wang H, Zimmermann KM, et al. Overcoming Intrinsic Multidrug Resistance in Melanoma by Blocking the Mitochondrial Respiratory Chain of Slow-Cycling JARID1Bhigh Cells. Cancer Cell. 2013; 23: 811–825.
95. Yuan P, Ito K, Perez-Lorenzo R, Del Guzzo C, Lee JH, et al. Phenformin enhances the therapeutic benefit of BRAF V600E inhibition in melanoma. Proceedings of the National Academy of Sciences. 2013; 110: 18226–18231.
96. Baenke F, Chaneton B, Smith M, Van Den Broek N, Hogan K, et al. Resistance to BRAF inhibitors induces glutamine dependency in melanoma cells. Molecular Oncology. 2016; 10: 73–84.

Book Chapter

Breast Cancer Stem Cells: A Key for Breast Cancer Treatment

Rania El Majzoub[1#], Jana Doghman[2#], Zeinab Al Dirani[2#], Rawan Issa[2#], Mohammad Fayyad-Kazan[3], Chourouk Joumaa[2], Ali Hamade[4], Farah A. Farran[2], Berlant Shakra[2], Samah Al Zein[2], Mona Al Jamal[2], Fatima Soufan[2], Katia Smeha[2], Jana Zaraket[2], Jana Kourani[2], Mariam Hamze[2], Mohamad El Saheli[5], Sana Dheini[2], Fatima Fakih[2], Zahraa Fakih[2], Alaa Bishkar[2], Ritaj Fakih[2], Amal Al Kadi[2], Khalid Omama[2], Afaf El Joubaei[2], Douaa Khreis[2†], Fatima Dandash[2†], Fatima Berro[2†], Hussein Fayyad-Kazan[2†]

[1]Department of Biomedical Sciences, School of Pharmacy, Lebanese International University, Beirut, Lebanon
[2]Lebanese University, Faculty of Science (I), Biology and Biochemistry Departments, Hadath, Beirut, Lebanon
[3]Department of Natural and Applied Sciences, College of Arts and Sciences, The American University of Iraq-Baghdad (AUIB), Baghdad 10001, Iraq
[4]School of Arts and Sciences, Lebanese American University, Lebanon
[5]Department of Biological Sciences, Faculty of Science, Beirut Arab University, Debbieh, Lebanon

[#]Contributed equally to this work
[†]Joint senior co-authors

***Corresponding Author:** Hussein Fayyad-Kazan, Biology Department, Lebanese University, Faculty of Science (I), Hadath, Beirut, Lebanon

Published **September 02, 2024**

How to cite this book chapter: Rania El Majzoub, Jana Doghman, Zeinab Al Dirani, Rawan Issa, Chourouk Joumaa, Farah A. Farran, Berlant Shakra, Samah Al Zein, Mona Al Jamal, Fatima Soufan, Katia Smeha, Jana Zaraket, Jana Kourani, Mariam Hamze, Sana Dheini, Fatima Fakih, Zahraa Fakih, Alaa Bishkar, Ritaj Fakih, Amal Al Kadi, Khalid Omama, Afaf El Joubaei, Douaa Khreis, Fatima Dandash, Fatima Berro, Hussein Fayyad-Kazan. Breast Cancer Stem Cells: A Key for Breast Cancer Treatment. In: Immunology and Cancer Biology. Hyderabad, India: Vide Leaf. 2024.

Abstract

Breast cancer, a predominant health concern for women worldwide, is frequently distinguished by its stubborn resistance to traditional treatments and a high likelihood of recurrence. Breast Cancer Stem Cells (BCSC), a specific subset of cells within the disease, are thought to be responsible for these challenges. These cells possess distinct abilities for self-renewal and differentiation, enabling them to elude standard therapeutic approaches. Researchers are increasingly acknowledging the crucial role BCSC play in the persistence and recurrence of breast cancer, making them a promising target for more effective treatment strategies. However, successfully neutralizing BCSC requires a comprehensive understanding of their biological nature and proliferation mechanisms. In this review, we explore the intricacies of breast cancer and its various subtypes before focusing on BCSC, offering a detailed examination of their defining characteristics and their involvement in drug resistance, recurrence, and metastasis. By illuminating the elusive nature of these cells, we aspire to pave the way for innovative strategies to eliminate them, ultimately improving the efficacy of breast cancer treatment.

Keywords

Breast Cancer; Breast Cancer Stem Cells (BCSC); Resistance; Recurrence; Treatment Strategies

Introduction

Female breast cancer is the most commonly diagnosed cancer worldwide, according to GLOBOCAN 2020 global estimates of cancer incidence and mortality by the International Agency for Research on Cancer. In 2020 alone, there were 2.3 million new cases, representing 11.7% of all cancer cases. Despite its prevalence, it is the fifth leading cause of cancer mortality worldwide, with 685,000 deaths accounting for 6.9% of all cancer deaths [1].

Interestingly, incidence rates are higher in transitioned countries than in transitioning countries. However, transitioning countries face higher mortality rates. By 2040, breast cancer is projected to cause more than 3 million new cases and 1 million deaths [2].

Focusing on the United States, the American Cancer Society estimates that around 287,850 new cases of invasive breast cancer will be diagnosed in women in 2022, with 43,250 women expected to succumb to the disease [3].

Breast Cancer Risk Factors

Some risk factors for breast cancer are unchangeable, such as age or inherited gene changes. These increase the chance of developing breast cancer. Other risk factors are lifestyle-related and are changeable, and some have unclear effects on the likelihood of developing the disease or are disproven or debatable risk factors [4].

Ageing is a main risk factor for breast cancer. The American Cancer Society reports that 1 in 8 invasive breast tumors occur in women under the age of 45 and invasive breast cancer affects women over the age of 55 in about 2 out of 3 cases [4]. Ageing increases genetic mutations and decreases the ability to repair damage.

Family history is another risk factor occurring in over a quarter of all breast cancer cases. Women with two or more first-degree family members are 2.5 times more likely to develop the disease

[5]. The mutations in breast cancer-related genes, such as BRCA1 and BRCA2, are mainly responsible for this hereditary risk [6]. Additionally, the female's reproductive history is a risk factor. Beginning menstruation before the age of 12 and menopause after the age of 55 expose women to hormones for a longer length of time, increasing their risk of breast cancer [7].

Lifestyle, such as diet and physical activity, are linked to certain breast cancer risk factors. Other lifestyle-related risk factors include having children and taking hormone-containing medications. Women who have just given birth have a short-term increase in breast cancer risk, which disappears after roughly ten years. The cause of this transient rise is unknown, however some experts believe it may be linked to the influence of high hormone levels on cancer development or to the fast expansion of breast cells during pregnancy [8]. Moreover, women who used diethylstilbestrol (DES) during their pregnancy may be at a slightly increased risk of getting breast cancer than women who did not use DES during their pregnancy. DES is an artificial form of estrogen that was used to prevent miscarriages and other pregnancy complications between the early 1940s and 1971 [9].

The risk of breast cancer can be raised by variables associated with modern lifestyles, such as excessive alcohol intake, smoking, and dietary fat consumption [10]. Alcohol consumption is linked to a slight increase in the risk of breast cancer. The influence of the ADH1C genotype on this link, along with the relationship between alcohol consumption and increased breast density, provide additional evidence supporting a causal effect [11]. Moreover, the relative risk of breast cancer linked with smoking was much higher for women with a family history of the disease. Smoking is related to a moderate but significantly elevated risk of breast cancer, particularly among those who started at teenage or peri-menarcheal ages [12]. Additionally, a link likely exists between the prevalence of breast cancer and total dietary fat consumption. Breast cancer incidence rises over time in correlation with increasing fat content, according to research by Bjarnason et al. among the Icelandic population [13]. So, a woman's chance of developing breast cancer is increased if she is physically inactive. Furthermore, Breast cancer risk is

linked to estrogens, including both endogenous and exogenous estrogens. In women before menopause, the ovary normally generates endogenous estrogen, therefore ovarian excision can lessen the risk of breast cancer [14].

Some factors may pose a risk for breast cancer, but their influence is unclear. Research is being conducted to understand potential environmental effects on breast cancer risk. A special attention should be paid to environmental chemicals with estrogen-like characteristics. Examples of compounds that appear to have these qualities include those found in some plastics, specific cosmetics and personal care items, insecticides, and PCBs (polychlorinated biphenyls) [15]. These may have an impact on the risk of breast cancer. Although it is challenging to explore such effects in humans, research to date has not clearly linked exposure to these drugs to an increased risk of breast cancer. In this area, more research is required.

Breast Cancer Subtypes

Breast Cancer is molecularly classified according to the presence of certain biomarkers that are usually hormone receptors. Those hormonal Receptors include estrogen receptor (ER) and progesterone receptor (PR).

Luminal Subtypes

One of the first and most widely utilized BC biomarkers is ER. A pooled data set from numerous cohorts and cooperative studies indicate that roughly 80% of all BC are ER-positive (ER+). Compared to ER-negative (ER-) BC, ER-positive (ER+) BC is generally well-differentiated, less aggressive, and has a better prognosis [16].

The ER-positive type is further classified into subtypes A and B according to gene expression profiles of more than 500 genes: Luminal A and B subtypes. In contrast to the luminal B subtype, a higher expression of luminal genes and ER+ associated genes (such as PR) in the luminal-A subtype. Additionally, compared to the luminal-B subtype, the luminal A subtype shows a better

prognosis and overall survival. Poor response to luminal-B subtype endocrine treatments is frequently associated with low ER/PR expression, high Ki-67 expression, and atypical overexpression of HER2 according to numerous studies. As a result, the proliferative biomarker Ki-67 is also recommended as a second clinical biomarker to help distinguish between luminal-A and luminal-B subtypes [16].

HER2-Positive Breast Cancer

The Human Epidermal Receptors is a family of 4 members. The orphan tyrosine kinase receptor, also called human epidermal growth factor receptor 2 (HER2), is a member of the family. HER2 does not have a ligand, yet it either homo or hetero dimerizes with one of the 3 three other human epidermal factors. Thus, results in the activation of downstream tyrosine kinase signaling cascades, which leads to the promotion of cell growth, migration, invasion, and survival. In 15% of breast carcinomas, HER2 is amplified, resulting to HER2 overexpression [17]. The extracellular domain of HER2 is targeted by the monoclonal antibody trastuzumab along with chemotherapy, which alters the normal tyrosine kinase signaling. While on the one hand this mechanism confers a poor prognosis (due to the effect on cell proliferation, migration, invasion, and survival, all key aspects of cancer), on the other hand, it offers the unique possibility to use a targeted treatment approach [17].

Immunohistochemistry (IHC), which evaluates the levels of HER2 protein expression, and in situ hybridization (ISH), which determines the status of the *HER2* gene, are the only two methods with established clinical relevance. They are frequently used to determine the HER2 status in diagnostic pathology [17].

Triple Negative Breast Cancer

TNBC is a type of Breast Cancer where estrogen receptor ER, progesterone receptor PR, and human epidermal growth factor receptor 2 HER2 are not immunohistochemically expressed in triple-negative breast cancer (TNBC). It represents around 12–20% of all occurrences of breast cancer and is the most aggressive subtype. TNBC is linked to an earlier age of onset,

increased risk of metastasis, more relapses, and higher mortality rates [17].

TNBC usually appears in younger women and has a 40% mortality rate in advanced stages during the first 5 years following diagnosis compared to other types of Breast Cancer. Despite the development of novel biological and targeted medicines, cytotoxic chemotherapy remains the cornerstone of treatment for TNBC [17].

Breast Cancer Stem Cells

Breast Cancer Stem Cells and Relapse

Tumor recurrence and therapy failure are common outcomes in patients with breast cancer. Despite advances in diagnosis and treatment, therapeutic strategies have shown limited efficacy in patients with metastatic breast cancer. Therefore, it is essential to investigate the processes underlying this phenomenon to provide effective strategies for its treatment [18].

Breast cancer stem cells (BCSCs) are a minor cell population with plasticity and multipotent differentiation capabilities observed in breast tumors and are considered to be a factor contributing to the heterogeneity of primary tumors. BCSCs can originate from various sources, including normal stem cells that have acquired aberrations, or through the de-differentiation of malignant cells triggered by environmental elements in their surroundings. Although BCSCs represent a minor fraction of tumor cells, they are shown to have a critical role in the initiation, progression, and metastasis of breast cancer [20]. BCSCs can exist in various forms, each possessing resistance to severe environmental circumstances, anticancer therapies, and the immune system. BCSCs retain their plasticity and are potent shifters. The tumor microenvironment plays a significant role in shaping cancer stem cells. Importantly, it controls the fluctuation of cancer stem cells between a mesenchymal state with quiescent properties responsible for epithelial mesenchymal transition (EMT) and an epithelial state with proliferative traits required for mesenchymal epithelial transition (MET). EMT is a biological process involving the loss of strong cell-to-cell

adhesion and polarization in epithelial cells and the development of mesenchymal features including mobility and invasiveness [20]. MET is the term used to describe a reversal of EMT, where cells lose their mesenchymal characteristics and regain epithelial features. The conversion between EMT and MET is mediated by a series of transcriptional and epigenetic modifications. In fact, it has been postulated that EMT and MET are the two main processes indispensable for the metastatic spread of malignancy. Cells adopting the EMT phenotype will eventually reach the circulation and travel either as individual cancer circulating cells or in a cluster. Then, the MET program will be initiated to ensure the invasion of premetastatic sites. These cells can remain for up to two decades as disseminated tumor cells (DTCs) [20].

Characteristics of BCSCs

Tumorigenicity of BCSCs and Self-Renewal

Cancer stem cells (CSCs) are a heterogeneous population of cells that have been known to be particularly aggressive and tumorigenic. The ability of malignant stem cells to self-renew, similar to somatic cells, allows them to survive and multiply. A relatively small number of CSCs have been shown to initiate tumor growth in xenografts, demonstrating their tumorigenic nature. The great majority of these cells are dormant, which has been identified as critical for minimizing the incidence of replication errors and oxygen free radicals in CSCs. BCSCs also demonstrated the potential to withstand extreme environmental conditions, avoid anticancer therapies, and evade the immune system [4].

Surface Markers

CD44 is an important membrane glycoprotein that controls cell-extracellular matrix communication. It is abundant in BCSCs and is the most frequent recognition and classification marker for them. Remarkably, it is linked to the preservation of stem cell properties, epithelial-mesenchymal transition and tumor stem cell profiling [21,22] In addition, CD44 promotes tumor stem cell self-renewal and increases tumor stem cell invasion and dissemination by increasing growth factor and cytokine

signalling in the tumor microenvironment [21,22]. Downregulating CD44 overcomes BCSC treatment resistance and impairs self-renewal. In addition, CD44 is a receptor for both growth factors, the epidermal (EGF) and hepatocyte (HGF). Thus, it functions in cancer stem cell signaling. Furthermore, CD44 is a hyaluronic acid receptor that collaborates with HA to establish a matrix that governs cell adhesion and migration. The CD44- Hyaluronic acid interaction advocates malignant cell metastasis and infiltration into target tissues [21,22].

ALDH are a group of enzymes known as aldehyde dehydrogenases, which are primarily elevated in breast cancer [23]. ALDH is a marker used to detect and isolate BCSCs. It is closely linked to the survival of cancer stem cells and the maintenance of their stem-like properties. Furthermore, studies have demonstrated that specifically knocking out the Aldehyde Dehydrogenase 1 Family Member A1 (ALDH1A1) gene diminishes the production of stem biomarkers and the potential of cancer stem cells to develop into tumor [23]. Interestingly, ALDHs can stimulate cancer stem cell growth by neutralizing and removing toxic chemicals so as to escape oxidative stress. As a result, ALDH is critical in the proliferation and differentiation of tumor stem cells [23].

CD133 has been discovered to be a malignant marker for BCSCs. CD133 is a transmembrane glycoprotein expressed on the surface of hematopoietic stem cells and progenitor cells [21]. It is frequently associated with poor prognosis and limited metastasis survival in various types of breast tumors, such as Estrogen receptor positive (ER+) and human epidermal growth factor receptor 2 positive (HER2) [21].

The prevalence of cells expressing CD55 is associated with oncogenesis and tumor recurrence, indicating that CD55 is linked to a poor prognosis in breast cancer [24]. Yet, it isn’t validated whether CD55 can be used as a marker of BCSCs [24].

Ganglioside (GD2) represents a small fraction of BCSCs. It has been identified as a novel marker of BCSCs and is prevalent in cells actively undergoing EMT [20].

Drug Resistance

Drug resistance is a protective feature of BCSCs that contributes to their malignant nature. Because of their extended dormant phase, BCSCs are a challenging target to chemotherapy [25,26]. Similarly, the ABC transporters are a superfamily of integral membrane proteins that are upregulated on the surface of cancer stem cells and are responsible for the efflux of wide range of substances along the membrane including anti-cancer drugs. ALDHs, on the other hand, are a class of enzymes that are abundant in BCSCs and are responsible for the oxidation of aldehydes. ALDHs can either inactivate anti-cancer treatments or aid in their excretion, keeping malignant stem cells free of oxidative stress [25,26]. BCSCs also display superior DNA repair activity upon radiotherapy and generate lower levels of reactive oxygen species than their non-stem cell counterparts due to their enhanced expression of free radical scavenging mechanisms [25,26].

Furthermore, several studies have also connected autophagy to therapeutic resistance in cancer cells and BCSCs. Autophagy was previously defined as a catabolic mechanism involved in the control of cell viability and senescence, preserving energy expenditure in the face of limited nutrition, stress, or oxygen deprivation [25,26]. In breast cancer, autophagy has been demonstrated to be critical for BCSCs tumorigenicity and a key element of BCSC survival, particularly in the presence of harsh microenvironments. Because dispersed breast cancer stem cells can survive for decades before resurfacing as aggressive secondary tumors, autophagy is especially important in the premetastatic contex [25,26].

Plasticity

Cancer stem cells are also very plastic, allowing them to switch between several developmental programs. They have been linked to cancer metastasis, which is a sequential process of (EMT) and MET [27-29]. EMT is the molecular process that converts adherent epithelial cells into individual mesenchymal cells with the ability to migrate and penetrate neighboring regions. The

stimulation of EMT causes an increase in the expression of genes linked with "stemness" and is also characterized by the loss of cell connections and the decrease in E cadherin expression which compromises cellular integrity [27-29]. Furthermore, the cytoskeleton shifts from keratin to vimentin and cellular polarity of the epithelial cells is disrupted, leading to a mesenchymal phenotype. During tumorigenesis, this process is reactivated in BCSCs, allowing them to traverse the basement membrane and extravasate into the vasculature [27-29]. The EMT-BCSCs are in quiescent- mesenchymal-like states defined by their capacity for migration and resistance to chemotherapy, seen near the tumor front and are characterized by having CD24− CD44+ surface markers [27-29].

When the cancerous cells reach a distal tissue, they adopt a MET phenotype, the inverse process of EMT. MET-BCSCs thus exhibit an increased E- cadherin expression and reduced vimentin expression. These cells are present near the core of the tumor, express aldehyde dehydrogenase (ALDH+), and feature characteristics of self-renewal and proliferation. The CD24+ BCSCs and ALDH+ BCSCs populations intertwine and are convertible to some extent [27-29].

Cytotoxic chemotherapy and radiation treatment are highly ineffective against EMT BCSCs. Furthermore, previous research has associated ALDH1 expression in BCSCs to a poor prognosis, suggesting that ALDH+ MET-BCSCs share features with EMT-BCSCs in terms of relapse and therapeutic resistance [27-29].

The growing evidence of BCSCs plasticity define this population as a flexible entity, prone to transition between EMT and MET developmental programs, and extremely influenced by the surrounding tumor microenvironment (Figure 1). BCSCs' plasticity is also demonstrated with the ability of non-breast cancer stem cells to convert into BCSCs, a process called de-differentiation [27-29].

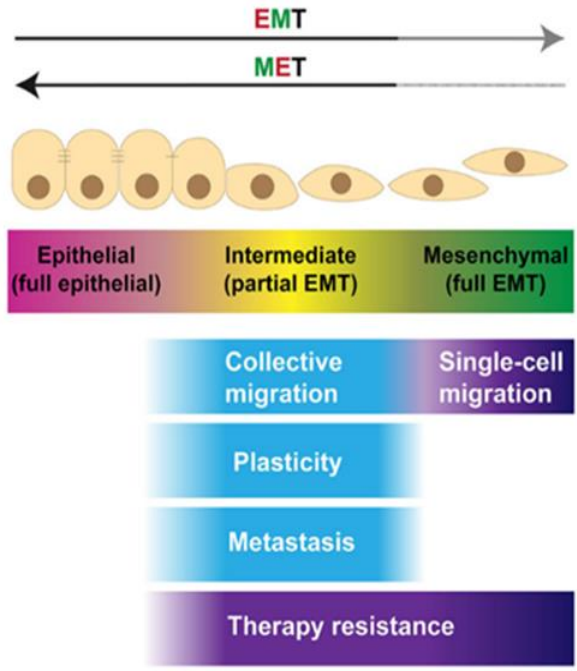

Figure 1: Characteristics of breast cancer stem cells. This figure illustrates the progression of Epithelial-Mesenchymal Transition (EMT) and Mesenchymal-Epithelial Transition (MET) stages. It captures the transformation of cells from a rounded form (representing full epithelial) to an elongated form (indicating full mesenchymal). Key characteristics associated with these transitions, such as migration, plasticity, metastasis, and therapy resistance, are also emphasized [30].

Interaction with Tumor Microenvironment (TME)

The microenvironment encompasses the extracellular matrix (ECM); soluble substances such as growth factors, hormones, and cytokines; and cellular components including cancer-associated fibroblasts, macrophages, endothelial cells, and immune cells. The collagen content of the ECM and its mechanical properties such as matrix stiffness have a substantial impact on cancer stemness [31]. In addition, the physiological properties of the TME, such as the oxygen level, acidity and nutrient status have been shown to influence the stemness and viciousness of breast cancers. The quiescence of CSCs in primary breast cancer and other malignancies is significantly

prevalent in regions of hypoxia, necrosis, and acidity [32]. Such unfavourable conditions have been indeed discovered to promote stemness, quiescence, and migration. Acidity in premetastatic locations provides a safe and nurturing environment for quiescent cancer cells, promoting dispersed malignant cell persistence and ultimately cancer progression. Several studies have revealed the impact of the tumor microenvironment on the modulation of EMT and MET states of BCSCs in response to a number of signalling molecules. For instance, it is evident that the EMT switchover stimulates various transcription factors in cancer stem cells under the influence of external stimuli [27].

Penetrating immune cells and activated fibroblasts, known as cancer associated fibroblasts (CAFs), induce inflammation in the tumor microenvironment, releasing cytokines, chemokines, and growth factors to which the tumor adjusts. It has been proposed that inflammation plays a critical role in tumorigenesis, angiogenesis, and dissemination. Tumor growth and metastasis are enhanced by IL-1, IL-6, IL-11, and transforming growth factor (TGF-β). TGF-β has two major roles in tumorigenesis. It acts as a tumor suppressor in the early stages of carcinogenesis; however, tumor cells in later stages evade this impact and advance in response to TGF-β signalling [33,34]. It also promotes EMT and the ability of BCSCs to initiate cancer. CAFs in breast cancer environment also produce IL-6, which promotes proliferation and tumorigenesis. IL-6 regulates self-renewal and initiates EMT in BCSCs. The activation of NF-κB by proinflammatory stimuli results in the conversion of normal cells to have a persistent malignant morphology with no alteration in Genomic DNA [33,34].

Cellular crosstalk in the TME is fundamental for cancer progression. As a matter of fact, BCSCs boost cancer progression by controlling immune cells and establishing an immunosuppressive environment thus minimizing cancer cell susceptibility and promoting resistance [4]. In particular, a range of chemokines released by BCSCs stimulates the recruitment of tumor-associated macrophages (TAMs) that help build the BCSC niche and promote immunological tolerance. They inhibit immune cells by secreting cytokines and growth factors, as well

as inducing the secretion of immunosuppressives found naturally in T cells [4]. In addition, macrophages secrete epidermal growth factor (EGF), which enhances the migration and invasion of malignant cells. Another molecule, the vascular endothelial growth factor (VEGF), induces vascularization and ECM remodeling. Macrophages also stimulate an increase in the expression of sex determining region Y-box 2 (SOX2), a transcription factor that correlates with stemness [35]. Cancer-associated fibroblasts (CAFs) are ubiquitous in connective tissues and one of the most frequent tumor microenvironment cells in all tumor types [36]. CAFs promote uncontrolled growth, vascularization, invasion, dissemination, and resistance to therapy in BCSCs. CAFs have also been shown to stimulate vascularization in breast cancer by attracting endothelial progenitor cells (EPCs) [37].

Similarly, cell-cell interactions of BCSCs with CD8 T lymphocytes in the microenvironment exhaust immune cells and induce immunological tolerance. This interaction occurs between PDL1, a T-cell suppressive molecule prevalent on the surface of BCSCs, and the PD1 receptor present on T-cells. Notably, PD-L1 also stimulates multidrug resistance and BCSC stemness by triggering the PI3K/Akt and ERK1/2 signalling pathways (Figure 2). In addition, ECM protects BCSCs from treatment pressure and promotes their metastatic development [38,39].

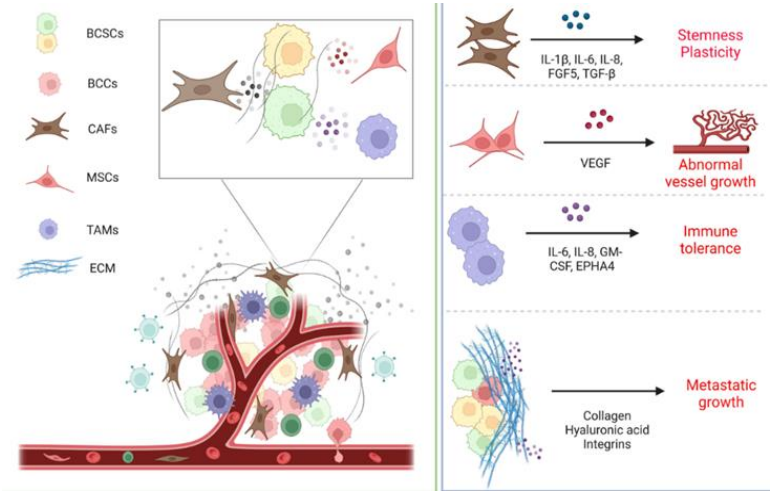

Figure 2: Interaction between tumor cell and the microenvironment. The biological activities of BCSCs are controlled by their microenvironment through direct interaction, the extracellular matrix (ECM), and signaling molecules. Cancer-associated fibroblasts (CAFs) release cytokines like IL-6, IL-8, and IL-1β, which enhance the stem-like properties and adaptability of BCSCs. Mesenchymal stem cells (MSCs) produce VEGF that nourishes BCSCs, resulting in irregular blood vessel formation. Similarly, macrophages emit a variety of cytokines that create a supportive environment for BCSCs and induce immune system tolerance. The ECM provides a shield for BCSCs against therapeutic stress and ensures their metastatic expansion [20].

Mechanisms of Relapse and Metastasis in BCSCs

Tumor metastasis is an intricate cascade involving a set of characteristics that should be adopted by metastatic tumor cells. These cells should be able to evacuate from the blood vessel walls by extravasation, withstand prolonged durations of mechanical stress in circulation, invade novel tissues, and multiply in target organs [40,41]. Despite the common misconception regarding metastasis as a latent event, malignant cells disseminate from primary tumors as an early event in oncogenesis. Recent findings indicate that 60- 70% of patients have already started the metastatic process by the time they are diagnosed. These data demonstrate that cancer growth and metastasis occur simultaneously. Gene expression studies in breast cancer demonstrate unique genetic modifications occurring in primary tumors and metastatic cells, providing

importance to the hypothesis of early metastatic spread [40,41]. Approximately half of the metastatic cells isolated from bone marrow of breast cancer patients contained fewer chromosomal abnormalities than the initial tumors, indicating that they disseminated prior to genomic instability events. These data imply that BCSCs have a metastatic potential [40,41].

A subset of breast cancer cells with characteristics such as self-renewal, quiescence, and strong metastasis and invasion capabilities reside in the circulation of patients with breast cancer who are undergoing or have completed treatment. These findings show that BCSCs have the capacity to migrate to distant organs and spread tumors to new locations [42] (Figure 3).

EMT promotes malignant cell dissemination, whereas MET promotes metastatic cell invasion. As previously stated, the tumor microenvironment influences cancer stem cells to upregulate transcription factors, such as Slug, Zebl, Zeb2, Snail, Twist, FOXC1, FOXC2, bHLH proteins, and TCF3 [43,44]. This provokes the synthesis of N-cadherin, vimentin, fibronectin, α-SMA, urging the shift to mesenchymal phenotype. EMT BCSCs in breast cancer promote tumor migration into the basal membrane, neighboring tissues, and even into the circulation where they survive because of their acquired quiescence and immunity to treatment [43,44].

Recent investigations on circulating tumor cells (CTCs) and disseminated tumor cells, both of which demonstrate EMT and sternness, support the involvement of EMT in tumor cell dissemination. In fact, tumors release thousands of cells into the circulation daily; however, only a minority of them cause secondary tumors to emerge. Metastasis-initiating cells (MICs) are a subpopulation of CTCs capable of generating clonal metastatic growth in distant organs [45] Clinically, the presence of five or more CTCs in 7.5 ml of blood plasma is a sign of tumor progression. The number of CTCs in patients with metastatic breast cancer is a stronger predictor of cancer outcome than other diagnostic methods. Recent research on CTCs from breast cancer patients has found a link between mesenchymal CTCs and tumor progression [45]. CTCs can exist as single cells

or multicellular clusters and they have been shown to display recognized mesenchymal markers and EMT markers such as the transforming growth factor beta (TGFB) signalling pathway and the transcription factor FOXC1. As a result, CTCs can withstand mechanical stress accompanied during their migration to distal organs through blood [45].

Upon extravasation from the vasculature, these EMT BCSCs produce micro metastasis in target organs. Although BCSCs derived from primary cancer tissues and CTCs have been demonstrated to exhibit typical EMT characteristics, the majority of metastatic cancers exhibit an epithelial architecture indicating that the reversal of the EMT program is required for dissemination [46]. (MET) is induced at pre-metastatic locations, resulting in the establishment of substantial macro-metastatic populations at remote sites. Indeed, the interaction between EMT and MET transition is the main driving mechanism of metastasis [46].

Recent studies have also revealed that stimulating MET with miRNA regulatory networks, particularly the miR-200 group, can facilitate breast cancer metastatic proliferation. In another study, selective activation of the Id1 gene in EMT-induced breast cancer cells induced MET via Twist1 inhibition, and this shift was essential for metastatic proliferation in the lung [46].

Given that primary cancerous masses discharge a significant proportion of malignant cells to circulate the bloodstream, only a small proportion of these cells (2%) are capable of initiating another tumor as a micro metastasis, and only 0.02% of CTCs are expected to become substantial macro metastases at distant sites [45].

Some secondary cancers could include CSCs with EMT and MET features. The presence of invasive and proliferative CSCs in a single tumor mass may contribute to a particularly aggressive subtype of breast cancer [45].

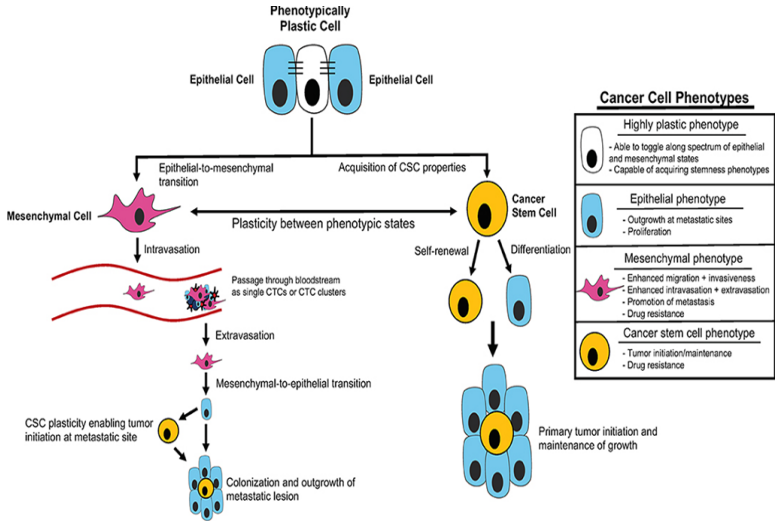

Figure 3: Tumor metastasis and cancer cell phenotypes. The versatility of cancer cells during the onset of a tumor and the metastatic process is discussed. This includes the role of epithelial-mesenchymal plasticity (EMP) and the development of cancer stem cell (CSC) traits in starting a tumor and elements of the metastatic process, such as entering and exiting blood vessels, and the colonization and expansion of metastases. Each stage is associated with unique cell phenotypes and features [47].

Conclusion

In conclusion, this review highlights the critical role of BCSCs in breast cancer's persistence, recurrence, and metastasis. BCSCs' distinct characteristics, drug resistance, and interaction with the tumor environment have been explored. Their metastatic potential challenges the traditional view of metastasis as a late-stage event, emphasizing the need for early targeting. The tumorigenicity, self-renewal, and surface markers of BCSCs, along with their plasticity and ability to transition between states, add complexity to our understanding. The significance of BCSCs in early tumor dissemination and the role of EMT and MET processes in malignant cell dissemination and invasion are discussed. Recent studies on circulating tumor cells (CTCs) and metastasis-initiating cells (MICs) support the involvement of EMT in tumor cell dissemination. The heterogeneity within breast cancer subtypes is underscored by the potential role of CSCs with EMT and MET features in secondary cancers.

References

1. Sung H, Ferlay J, Siegel RL, Laversanne M, Soerjomataram I, et al. Global Cancer Statistics 2020: GLOBOCAN Estimates of Incidence and Mortality Worldwide for 36 Cancers in 185 Countries. CA A Cancer J Clin. 2021; 71: 209–249.
2. Arnold M, Morgan E, Rumgay H, Mafra A, Singh D, et al. Current and future burden of breast cancer: Global statistics for 2020 and 2040. The Breast. 2022; 66: 15–23.
3. Giaquinto AN, Sung H, Miller KD, Kramer JL, Newman LA, et al. Breast Cancer Statistics, 2022. CA A Cancer J Clinicians. 2022; 72: 524–541.
4. Wang L, Jin Z, Master RP, Maharjan CK, Carelock ME, et al. Breast Cancer Stem Cells: Signaling Pathways, Cellular Interactions, and Therapeutic Implications. Cancers. 2022; 14: 3287.
5. Brewer HR, Jones ME, Schoemaker MJ, Ashworth A, Swerdlow AJ. Family history and risk of breast cancer: an analysis accounting for family structure. Breast Cancer Res Treat. 2017; 165: 193–200.
6. Paluch-Shimon S, Cardoso F, Sessa C, Balmana J, Cardoso MJ, et al. Prevention and screening in BRCA mutation carriers and other breast/ovarian hereditary cancer syndromes: ESMO Clinical Practice Guidelines for cancer prevention and screening. Ann Oncol. 2016; 27: v103–10.
7. Titus-Ernstoff L, Hatch EE, Hoover RN, Palmer J, Greenberg ER, et al. Long-term cancer risk in women given diethylstilbestrol (DES) during pregnancy. Br J Cancer. 2001; 84: 126–133.
8. Knight JA, Fan J, Malone KE, John EM, Lynch CF, et al. Alcohol consumption and cigarette smoking in combination: A predictor of contralateral breast cancer risk in the WECARE study. Int J Cancer. 2017; 141: 916–924.
9. McDonald JAK, Schroeter K, Fuentes S, Heikamp-Dejong I, Khursigara CM, et al. Evaluation of microbial community reproducibility, stability and composition in a human distal gut chemostat model. J Microbiol Methods. 2013; 95: 167–174.
10. Jones ME, Schoemaker MJ, Wright LB, Ashworth A,

Swerdlow AJ. Smoking and risk of breast cancer in the Generations Study cohort. Breast Cancer Res. 2017; 19: 118.
11. Tremblay A, Plourde G, Despres JP, Bouchard C. Impact of dietary fat content and fat oxidation on energy intake in humans. Am J Clin Nutr. 1989; 49: 799–805.
12. Key T, Appleby P, Barnes I, Reeves G, Endogenous Hormones and Breast Cancer Collaborative Group. Endogenous sex hormones and breast cancer in postmenopausal women: reanalysis of nine prospective studies. J Natl Cancer Inst. 2002; 94: 606–616.
13. Calaf GM, Ponce-Cusi R, Aguayo F, Muñoz JP, Bleak TC. Endocrine disruptors from the environment affecting breast cancer. Oncol Lett. 2020; 20: 19–32.
14. Bhushan A, Gonsalves A, Menon JU. Current State of Breast Cancer Diagnosis, Treatment, and Theranostics. Pharmaceutics. 2021; 13: 723.
15. Khalkhali I, Mena I, Diggles L. Review of imaging techniques for the diagnosis of breast cancer: a new role of prone scintimammography using technetium-99m sestamibi. Eur J Nucl Med. 1994; 21: 357–362.
16. Marchiò C, Annaratone L, Marques A, Casorzo L, Berrino E, et al. Evolving concepts in HER2 evaluation in breast cancer: Heterogeneity, HER2-low carcinomas and beyond. Semin Cancer Biol. 2021; 72: 123–135.
17. Bou Zerdan M, Ghorayeb T, Saliba F, Allam S, Bou Zerdan M, et al. Triple Negative Breast Cancer: Updates on Classification and Treatment in 2021. Cancers. 2022; 14: 1253.
18. Courtney D, Davey MG, Moloney BM, Barry MK, Sweeney K, et al. Breast cancer recurrence: factors impacting occurrence and survival. Ir J Med Sci. 2022; 191: 2501–2510.
19. Zhang T, Zhou H, Wang K, Wang X, Wang M, et al. Role, molecular mechanism and the potential target of breast cancer stem cells in breast cancer development. Biomedicine & Pharmacotherapy. 2022; 147: 112616.
20. Xu H, Zhang F, Gao X, Zhou Q, Zhu L. Fate decisions of breast cancer stem cells in cancer progression. Frontiers in Oncology [Internet]. 2022; 12. Available online at: https://www.frontiersin.org/articles/10.3389/fonc.2022.9683

06
21. Song K, Farzaneh M. Signaling pathways governing breast cancer stem cells behavior. Stem Cell Research & Therapy. 2021; 12: 245.
22. Yousefnia S, Seyed Forootan F, Seyed Forootan S, Nasr Esfahani MH, Gure AO, et al. Mechanistic Pathways of Malignancy in Breast Cancer Stem Cells. Frontiers in Oncology [Internet]. 2020; 10. Available online at: https://www.frontiersin.org/articles/10.3389/fonc.2020.00452
23. Chen W, Zhang L, Liu S, Chen C. Advances in Biomarkers and Endogenous Regulation of Breast Cancer Stem Cells. Cells. 2022; 11: 2941.
24. Geller A, Yan J. The Role of Membrane Bound Complement Regulatory Proteins in Tumor Development and Cancer Immunotherapy. Frontiers in Immunology [Internet]. 2019; 10. Available online at: https://www.frontiersin.org/articles/10.3389/fimmu.2019.01074
25. Zheng Q, Zhang M, Zhou F, Zhang L, Meng X. The Breast Cancer Stem Cells Traits and Drug Resistance. Frontiers in Pharmacology [Internet]. 2021; 11. Available online at: https://www.frontiersin.org/articles/10.3389/fphar.2020.599965
26. Saha T, Lukong KE. Breast Cancer Stem-Like Cells in Drug Resistance: A Review of Mechanisms and Novel Therapeutic Strategies to Overcome Drug Resistance. Frontiers in Oncology [Internet]. 2022; 12. Available online at: https://www.frontiersin.org/articles/10.3389/fonc.2022.856974
27. Zheng X, Dai F, Feng L, Zou H, Feng L, et al. Communication Between Epithelial–Mesenchymal Plasticity and Cancer Stem Cells: New Insights Into Cancer Progression. Frontiers in Oncology [Internet]. 2021; 11. Available online at: https://www.frontiersin.org/articles/10.3389/fonc.2021.617597
28. Akhmetkaliyev A, Alibrahim N, Shafiee D, Tulchinsky E. EMT/MET plasticity in cancer and Go-or-Grow decisions in quiescence: the two sides of the same coin? Molecular

Cancer. 2023; 22: 90.
29. Baram T, Rubinstein-Achiasaf L, Ben-Yaakov H, Ben-Baruch A. Inflammation-Driven Breast Tumor Cell Plasticity: Stemness/EMT, Therapy Resistance and Dormancy. Frontiers in Oncology [Internet]. 2021; 10. Available online at: https://www.frontiersin.org/articles/10.3389/fonc.2020.614468
30. Lüönd F, Sugiyama N, Bill R, Bornes L, Hager C, et al. Distinct contributions of partial and full EMT to breast cancer malignancy. Developmental Cell. 2021; 56: 3203-3221.e11.
31. Shah L, Latif A, Williams KJ, Tirella A. Role of stiffness and physico-chemical properties of tumour microenvironment on breast cancer cell stemness. Acta Biomater. 2022; 152: 273–289.
32. Sistigu A, Musella M, Galassi C, Vitale I, De Maria R. Tuning Cancer Fate: Tumor Microenvironment's Role in Cancer Stem Cell Quiescence and Reawakening. Frontiers in Immunology [Internet]. 2020; 11. Available online at: https://www.frontiersin.org/articles/10.3389/fimmu.2020.02166
33. Nallasamy P, Nimmakayala RK, Parte S, Are AC, Batra SK, et al. Tumor microenvironment enriches the stemness features: the architectural event of therapy resistance and metastasis. Molecular Cancer. 2022; 21: 225.
34. Henke E, Nandigama R, Ergün S. Extracellular Matrix in the Tumor Microenvironment and Its Impact on Cancer Therapy. Frontiers in Molecular Biosciences [Internet]. 2020; 6. Available online at: https://www.frontiersin.org/articles/10.3389/fmolb.2019.00160
35. Wang J, Zeng H, Li H, Zhang J, Wang S. Roles of sex-determining region Y-box 2 in cell pluripotency and tumor-related signaling pathways (Review). Molecular and Clinical Oncology. 2015; 3: 1203–1207.
36. Wang G, Zhang H, Shen X, Jin W, Wang X, et al. Characterization of cancer-associated fibroblasts (CAFs) and development of a CAF-based risk model for triple-negative breast cancer. Cancer Cell International. 2023; 23: 294.

37. Chen K, Li Y, Xu L, Qian Y, Liu N, et al. Comprehensive insight into endothelial progenitor cell-derived extracellular vesicles as a promising candidate for disease treatment. Stem Cell Research & Therapy. 2022; 13: 238.
38. Wang S, Ma L, Wang Z, He H, Chen H, et al. Lactate Dehydrogenase-A (LDH-A) Preserves Cancer Stemness and Recruitment of Tumor-Associated Macrophages to Promote Breast Cancer Progression. Frontiers in Oncology [Internet]. 2021; 11. Available online at: https://www.frontiersin.org/articles/10.3389/fonc.2021.654452
39. Akhtar M, Rashid S, Al-Bozom IA. PD−L1 immunostaining: what pathologists need to know. Diagnostic Pathology. 2021; 16: 94.
40. Majidpoor J, Mortezaee K. Steps in metastasis: an updated review. Med Oncol. 2021; 38: 3.
41. Springer [Internet]. Cancer and Metastasis Reviews. 2023. Available online at: https://www.springer.com/journal/10555
42. He L, Wick N, Germans SK, Peng Y. The Role of Breast Cancer Stem Cells in Chemoresistance and Metastasis in Triple-Negative Breast Cancer. Cancers. 2021; 13: 6209.
43. Liu F, Gu LN, Shan BE, Geng CZ, Sang MX. Biomarkers for EMT and MET in breast cancer: An update (Review). Oncology Letters. 2016; 12: 4869–4876.
44. Lai X, Li Q, Wu F, Lin J, Chen J, et al. Epithelial-Mesenchymal Transition and Metabolic Switching in Cancer: Lessons From Somatic Cell Reprogramming. Frontiers in Cell and Developmental Biology [Internet]. 2020; 8. Available online at: https://www.frontiersin.org/articles/10.3389/fcell.2020.00760
45. Papadaki MA, Stoupis G, Theodoropoulos PA, Mavroudis D, Georgoulias V, et al. Circulating Tumor Cells with Stemness and Epithelial-to-Mesenchymal Transition Features Are Chemoresistant and Predictive of Poor Outcome in Metastatic Breast Cancer. Molecular Cancer Therapeutics. 2019; 18: 437–447.
46. Drago-García D, Espinal-Enríquez J, Hernández-Lemus E. Network analysis of EMT and MET micro-RNA regulation in breast cancer. Sci Rep. 2017; 7: 13534.

47. Kong D, Hughes C, Ford H. Cellular Plasticity in Breast Cancer Progression and Therapy. Frontiers in Molecular Biosciences. 2020; 7: 72.

Book Chapter

Current Breast Cancer Treatment Strategies and Resistance Mechanisms

Rania El Majzoub[1#], Zeinab Al Dirani[2#], Rawan Issa[2#], Samah Al Zein[2#], Mohammad Fayyad-Kazan[3], Zahra Farroukh[2], Sana Dheini[2], Mona Al Jamal[2], Ali Hamade[4], Mohamad El Saheli[5], Leen Fadlallah[2], Mona Sahmarani[2], Jana Zaraket[2], Fatima Shaalan[2], Chourouk Joumaa[2], Ali Al Khatib[6], Belal Osman[6], Mariam Hamze[2], Jana Kourani[2], Farah A. Farran[2], Berlant Shakra[2], Katia Smeha[2], Khalid Omama[2], Dima Dagher[2], Aya El Hage Ali[2], Douaa Khreis[2†], Fatima Dandash[2†], Fatima Berro[2†], Hussein Fayyad-Kazan[2†]

[1]Department of Biomedical Sciences, School of Pharmacy, Lebanese International University, Beirut, Lebanon
[2]Lebanese University, Faculty of Science (I), Biology and Biochemistry Departments, Hadath, Beirut, Lebanon
[3]Department of Natural and Applied Sciences, College of Arts and Sciences, The American University of Iraq-Baghdad (AUIB), Baghdad 10001, Iraq
[4]School of Arts and Sciences, Lebanese American University, Lebanon
[5]Department of Biological Sciences, Faculty of Science, Beirut Arab University, Debbieh, Lebanon
[6]American University of Beirut, Faculty of Medicine, Beirut, Lebanon

[#]Contributed equally to this work
[†]Joint senior co-authors

***Corresponding Author:** Hussein Fayyad-Kazan, Lebanese University, Faculty of Science (I), Biology and Biochemistry Departments, Hadath, Beirut, Lebanon

Published **September 02, 2024**

How to cite this book chapter: Rania El Majzoub, Zeinab Al Dirani, Rawan Issa, Samah Al Zein, Zahra Farroukh, Sana Dheini, Mona Al Jamal, Leen Fadlallah, Mona Sahmarani, Jana Zaraket, Fatima Shaalan, Chourouk Joumaa, Ali Al Khatib, Belal Osman, Mariam Hamze, Jana Kourani, Farah A. Farran, Berlant Shakra, Katia Smeha, Khalid Omama, Dima Dagher, Aya El Hage Ali, Douaa Khreis, Fatima Dandash, Fatima Berro, Hussein Fayyad-Kazan. Current Breast Cancer Treatment Strategies and Resistance Mechanisms. In: Immunology and Cancer Biology. Hyderabad, India: Vide Leaf. 2024.

Abstract

Breast cancer, characterized by diverse subtypes and intricate molecular landscapes, poses persistent challenges in treatment. A nuanced understanding of current therapies and resistance mechanisms is essential. Subdivision based on hormonal receptors and HER2 expression yields four distinct subtypes with varying prognosis and treatments. Despite initial success in clinics, concerns arise due to patients developing resistance mechanisms over time. This review comprehensively explores evolving breast cancer treatment strategies, focusing on molecular landscapes and challenges associated with targeted therapies. It covers endocrine therapy, receptor roles, and emerging resistance strategies. Approved inhibitors' mechanisms and the importance of comprehending signaling pathway interplay are discussed. The review connects the themes by examining resistance strategies against inhibitors and advocating for combination therapies. Current and evolving treatment strategies are scrutinized, encompassing established and investigational modalities. The review aims to provide valuable insights for researchers, clinicians, and policymakers to advance therapeutic strategies and enhance patient outcomes.

Keywords

Breast Cancer; Resistance Mechanisms; Targeted Therapies; Combination Therapies

Introduction

Breast cancer develops when some breast cells begin to grow uncontrollably. Treatments for breast cancer include surgery, radiation therapy, chemotherapy, hormonal therapy, targeted therapy, and immunotherapy [1]. Most breast cancers are hormone receptor positive, meaning that they depend on hormones to grow and spread. Hormone therapy works by blocking the cancer cells from receiving the natural hormones that they crave. Targeted therapy uses specifically designed drugs such as monoclonal antibodies that act on specific tumor antigens (neoantigens), or those found in the tumor microenvironment [2]. Typically, when it comes to targeted therapy and biological therapy, the treatment is based on the molecular subtype of breast cancer that is in turn based on the genes the cancer cells express, which control how cells behave [3]. Herein, we will cover the current treatments and possible mechanisms of resistance against such options in the context of the most common breast cancer molecular subtypes, namely being luminal breast cancer, HER2-enriched breast cancer, and triple negative or basal-like breast cancer.

Luminal Breast Cancer Treatment Options

Luminal breast tumors, so-called estrogen receptor (ER) - positive (ER+) tumors represent around two-thirds of all breast cancers. This subtype is further divided into luminal A, luminal B, and B-like breast cancers. Hormonal therapy is well thought-out as an indispensable part of the management of patients with ER+ breast cancer [4].

Hormonal Therapy of Luminal Breast Cancer Subtype: Special Focus on ER Modulation-based Therapy

Endocrinal therapies that either disrupt the production of estrogens or hamper estrogen-mediated signaling pathways have become an important part of the management of hormone-dependent breast cancer [5]. Existing drugs for adjuvant

endocrine therapy can be separated into three classes: selective estrogen receptor modulators (SERMs), aromatase inhibitors (AIs), and selective estrogen receptor down regulators (SERDs) [5]. The most used class of estrogen receptor modulators is Tamoxifen (TAM), in both pre- and post-menopausal women. The antitumor attributes of TAM are reflected to be a result of its anti-estrogenic action, mediated by completive inhibition of estrogen binding to ER, where TAM belongs to SERMs. Prior to entering breast cancer cell, TAM is metabolized in the liver into 2 active metabolites, endoxifen and 4-hydroxytamoxifen (4-OHT) [5]. When these metabolites enter the cell, they bind to the cytosolic ERs, thereby blocking the binding of estrogen. TAM-bound ERs dimerize, translocate to the nucleus, and bind to the estrogen response element (ERE) in the promoter region of estrogen-induced genes. The ER-TAM complex, however, does not recruit the essential coactivators; as a result, TAM inhibits the expression of estrogen-induced genes, including growth factors and angiogenic factors secreted by the tumor, which may stimulate growth via autocrine or paracrine mechanisms [5]. As a result, the G1 phase of the cell cycle is stalled and cell proliferation is slowed. Because of the altered balance between cell proliferation and ongoing cell loss, tumors may regress [5].

Figure 1: Diagrammatic illustration of how fulvestrant works. AF1 and AF2 are known as activation functions 1 and 2, respectively. ER stands for estrogen receptor, and ERE is an acronym for estrogen receptor response element. F represents fulvestrant, and RNA POL II is short for ribonucleic acid polymerase II [6].

TAM has a partial ER-agonistic effect versus fulvestrant, which has an almost entirely antagonistic effect. Furthermore, TAM only affects the ER's AF2 domain, whereas fulvestrant affects

both activating function 1 (AF1) and activating function 2 (AF2) [7] (Figure 1).

There exist other options for hormonal therapy of ER-positive breast cancer such as Toremifene, used to treat metastatic breast cancer. It is structurally and pharmacologically similar to TAM, differing only by a single chlorine atom [7]. The major difference between the two compounds is in the preclinical activity. Fulvestrant, a SERD, is used to treat progressed breast cancer in postmenopausal women. When fulvestrant binds to estrogen receptor monomers it hinders receptor dimerization, AF1 and AF2 are thus left inactive, translocation of receptor to the nucleus is abridged, and degradation of the estrogen receptor is augmented [7]. While the medicines indicated above work by preventing hormones from binding to cancer cells, other medications work by preventing the body from producing estrogen after menopause. This comprises AIs, a class of medicines that lessen the quantity of estrogen in the body, depriving breast cancer cells of the hormones they need to grow. AIs are only utilized in women who have experienced menopause [7]. They cannot be used unless the body is in natural menopause or menopause triggered by medications or the elimination of the ovaries. Mechanism-based AIs are steroidal inhibitors that imitate the substrate and are transformed by the fat tissue enzyme aromatase to a reactive intermediate, causing the inactivation of aromatase. These different types of endocrine therapies have been used effectively to cause a momentous decline in cancer recurrence and death [7].

Resistance Strategies of Endocrine Therapy

Although existing endocrine therapies for women with ER+ breast cancer have resulted in significant improvements in outcomes, not all patients with ER+ tumors respond to endocrine treatment (de novo or primary resistance). Besides, ER+ patients, who at first, respond may later become non-responsive to the therapy (acquired resistance) [8]. Acknowledging the ultimate origins of treatment resistance has therefore been the interest of several studies to tackle this paramount clinical dilemma. The intricate crosstalk, both genomic and non-genomic, between

estrogen receptors and growth factors was well thought out to be a critical issue contributing to endocrine resistance (Figure 2). ERs refer to a family of nuclear transcriptional regulators that engage in an essential role in the progress of breast cancer [8]. ERs are classified into two isoforms: ER-α and ER-β. Because the role of ER-β in endocrine resistance is still debated, and because ER-α expression is higher in breast tumors than ER-β, it is the target of therapeutic intervention. Here, we will limit our discussion to ' ER-α ' which will be referred to as 'ER' in the following sections. Nuclear ER and membrane ER both act through genomic (nuclear) and non-genomic (membrane) pathways [8]. In general, one of the main features of the apparatus of ER-mediated antiestrogen treatment resistance is the loss of ER expression [9]. The fact is that nearly all primary ER+ patients will develop endocrine resistance, implying that some distorted pathways may affect ER expression and functions. For instance, ER loss has been linked to unusual methylation of CpG islands in the ER gene's 5′ regulatory regions. This in turn could result in transcriptional inactivation of the ER gene and lead to hormone resistance in various human breast cancers. Furthermore, 50% of patients with ER+ breast tumors express PR [9]. The increased resistance of ER+ breast tumors to SERMs could be because estrogen has a higher affinity to ER compared to SERMs. Numerous clinical studies have exposed that ER+/PR+ tumors are quicker to respond to SERMs therapy than ER+/PR- tumors. Indeed, two trials concerning the function of progesterone receptor (PR) in response to AIs revealed an improved response to endocrine therapy in PR+ tumors than PR- tumors [9] Multiple studies described that many growth factors of breast cancer could ultimately reduce PR levels through the PI3K/Akt/mTOR pathway and downregulate ER expression level and action. Sian Tovey et al. found that PR and HER2 status could help predict early decline in ER+ tamoxifen-treated breast cancer patients [9]. Furthermore, the status of expression of both HER-1 (EGFR) and HER-2 was drastically elevated in the ER+/PR- patients than in that of ER+/PR+ patients, despite recent clinical recommendations that such elevated levels of HER-1 and HER-2 were associated with TAM resistance [10]. It is noteworthy that treating HER2-positive breast cancer patients with TAM has resulted in weak outcomes.

A more extensive understanding of the function of HER2 in endocrine resistance sheds light on the crosstalk among HER2 and ER signaling tracks. It is notable that TAM, through membrane ER, is competent in activating HER2, which in turn causes ER and A1B1 (an essential ER co-activator) phosphorylation. Benz and colleagues discovered that transfecting HER2 in MCF-7 cells, which are hormone-dependent breast cancer cell lines, can result in TAM resistance [10]. Another in vitro study found that MCF-7 developed resistant clones to TAM; these clones were found to have increased levels of phosphorylated EGFR and HER2. Estrogen and TAM seem to turn on EGFR and HER2 signaling pathways through on-genomic mechanisms in HER2 overexpressing tumors. It should be noted that some downstream kinases, such as AKT, can phosphorylate ER and activate A1B1, resulting in a crosstalk between the nuclear TAM-ER complex and its co-activators that promote cell survival and proliferation [10]. Interestingly, the role of miRNAs in encouraging endocrine resistance is represented by, but not restricted to, their participation in controlling ERα. MiR-221 and miR-222, for example, are overexpressed in TAM-resistant and even ER-negative breast cancer cell lines and tumors. It is important to note that the 3′UTR of ERα is a straight target of miR-221/222 lessening ERα protein expression [11]. An experiment attempting to transiently overexpress miR-221/222 in TAM-sensitive MCF-7 cells led to TAM resistance whilst downregulation of miR-221/222 in ERα negative/TAM-resistant MDA-MB-468 cells brought back ERα expression and cells became susceptible to TAM-induced cell cycle arrest and apoptosis. However, miR-873 has been revealed to be reduced in TAM-resistant MCF-7 compared to TAM-sensitive and in breast tumors compared to usual tissues [11]. It is a target of cyclin-dependent kinase 3 (CDK3) for downregulation, where CDK3-mediated ERα phosphorylation enhances ERα function [11]. Lately, miR-519a was demonstrated as a new onco-miRNA via enhancing cell viability and cell cycle succession. MiR-519a level was elevated in TAM- resistant MCF-7 cells as compared with TAM-sensitive MCF-7 cells. Upregulated levels of miR-519a in primary breast tumors were linked with abridged disease-free survival in ERα+ breast cancer patients and thus

miR-519a was recommended as a possible contributor to TAM resistance. This is supported by the fact that miR-519a knockdown in TAM-resistant MCF-7 cells made the cells susceptible to TAM growth inhibition. In contrast, overexpressing miR-519a in TAM-sensitive MCF-7 cells desensitized the cells to TAM by averting growth inhibition while encouraging caspase action and apoptosis [11]. It is noteworthy that tumor suppressor genes (TSGs) involved in PI3K signaling p21, RB1, and PTEN, were reported to be actual targets of miR-519a, even though the function of such targets in causing TAM-resistance has not been discovered yet [12]. Thereby, it is critical to gain a more complete understanding of the underlying resistance mechanisms and elucidate targets for therapeutic intervention and by combining endocrine therapy with various molecularly targeted agents and signal transduction inhibitors, some success has been achieved in overcoming and modulating endocrine resistance in Hormone-positive breast cancer. Established strategies include selective ER modulators, anti-HER2 agents, mTOR inhibitors and inhibitors of PI3K are not at present a treatment alternative for women with ER+ breast cancer outside the milieu of clinical trials [12].

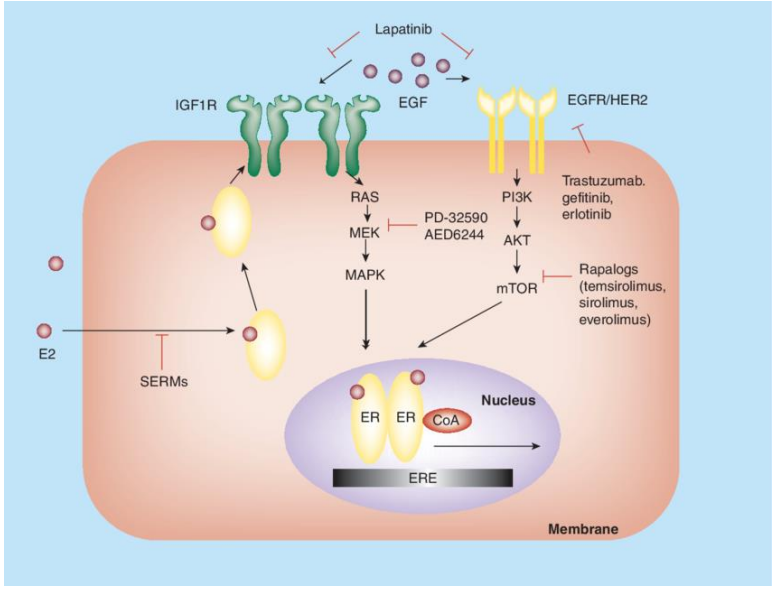

Figure 2: Molecular changes in endocrine-resistant breast cancer. This scientific diagram represents cellular signaling pathways involving IGF1R, EGF, and EGFR/HER2 receptors. It illustrates the roles and interactions of various molecules and inhibitors within these pathways, including Lapatinib, Trastuzumab, PD-32590, and AED6244. The diagram also depicts the internal cellular components like RAS, MEK, MAPK, and the AKT pathway leading to mTOR. The nucleus with ER, CoA indicating a complex formation at ERE is also shown [13].

It is demonstrated that resistance to TAM could be due to the activation of mER leading to the increase in HER2 expression levels, consequently, elevating HER2-mediated signaling pathways including PI3K/AKT/mTOR pathway. Additionally, the change in expression levels of certain miRNAs upon endocrine resistance implies a role of RNA interference in this mechanism which requires further investigation [12].

HER2-Enriched Breast Cancer Treatment Options

HER2-enriched breast cancer is ER-, PR-, and HER2+. HER2-enriched cancers are likely to develop quicker than luminal

cancers and can have poorer prognosis but are typically effectively treated with therapies targeting HER2 [14]. Its attributes are due to HER2-mediated activation of oncogenic pathways that force the different cancer cell traits, such as the Mitogen Activated Protein Kinase (MAPK) and the PI3K/AKT/mTOR cascades [14]. At present, specific monoclonal antibodies (mAbs) and tyrosine kinase inhibitors (TKIs) are the two HER2 targeting approaches that have effectually boosted the prognosis of patients with HER2+ breast cancer. Anti-HER2 therapies (also referred to as HER2 inhibitors or HER2-targeted therapies) are a set of medicines used to treat all stages of HER2+ breast cancer and HER2-low breast cancers. In addition, small molecule TKIs are an alternative for patients with early phase or progressive HER2 + breast cancer [14].

Anti-HER2 Mechanisms of Approved HER2 Inhibitors

HER2 is a transmembrane tyrosine kinase receptor and has a unique feature that differentiates it from the other members of the family in the absence of a known ligand. HER2 is overexpressed in 25 to 30% of human breast cancers and has been determined to be an adverse prognostic factor [10,15]. Since the level of HER2 in human cancer cells is with membrane overexpression than in normal adult tissue, they are potentially more sensitive to the toxicity of HER2 sensitive drugs. HER2 overexpression is typically found in both the primary tumor and at the metastatic sites which provides the rational for the effectiveness of anti-HER2 at all disease sites [10,15]. Research thus focused heavily on HER2 inhibitors as anticancer agents. Trastuzumab is the first of such agents which was registered for use in patients with HER2 overexpressing breast cancer. Trastuzumab is a recombinant monoclonal antibody (mAb) directed against the extracellular domain of the tyrosine kinase receptor, HER2. It is known to bind to domain 4 [10,15]. It has shown clinical activity in HER2 overexpressing breast cancers and is currently approved in patients in both metastatic and adjuvant settings. Although still subjects of discussion, different mechanisms of action have been attributed to its anti-HER2 activity: (i) antibody-dependent cell mediated cytotoxicity, (ii)

prevention of HER2 truncated membrane bound fragment following HER2 overexpression and (iii) HER2 receptor downregulation [16]. The binding of trastuzumab to HER2 receptor with high affinity and specificity prevents the formation of HER2-HER2 homodimers and HER2-HER3 heterodimers. This subsequently inhibits HER2-mediated signal transduction pathways, hence it is thought to be the main mechanism of action of trastuzumab [16]. Additionally, the binding of trastuzumab to HER2 on cancer cell membranes is documented by Fcɤ receptors expressed by cells of the innate immune system, including natural killer (NK) cells, antigen-presenting cells (APCs) as well as effector immune cells; this results in the clearance of T-bound cancer cells either through antibody-dependent cellular cytotoxicity (ADCC) and complement-dependent cytotoxicity (CDC). Pertuzumab is a novel fully humanized mAB that binds to domain 2, a portion of the extracellular domain essential for dimerization [16]. While trastuzumab is known to bind to domain 4. This binding of pertuzumab efficiently sterically blocks ligand-induced homodimerization and importantly HER2-HER3 heterodimerization that is known to activate downstream survival signaling pathways such as PI3K/AKT, whereas trastuzumab has only a minor effect in the presence of a ligand [17]. Pertuzumab was approved in mid-2012 for use in combination with trastuzumab and Docetaxel to treat patients with metastatic or locally recurrent unresectable HER2 positive breast cancer who have not received previous anti-HER2 therapy or chemotherapy for their metastatic disease. To increase the potency of antibody directed therapy, the specificity of the antigen binding site has been combined with a wide variety of effector agents including toxins [17]. This led to the development of antibody-drug conjugate (ADC) Ado-trastuzumab emtansine (T-DM1). T-DM1 is comprised of the anti-HER2 antibody trastuzumab bound to the potent antimicrotubule cytotoxic agent maytansine (DM1) by a thioether linker. T-DM1 uses trastuzumab to specifically localize the highly active chemotherapy to HER2 positive tumor cells. Trastuzumab and DM1 are degraded by the lysosome leading to cell cycle arrest and apoptosis [17]. It was initially approved in 2013 for metastatic patients. In 2020, trastuzumab deruxtecan (T-DXd) was the second approved ADC for patients who had

received at least 2 lines of anti-HER2-based therapy in the metastatic setting [17]. Like T-DM1, it is made of a mAb backbone of trastuzumab, its cytotoxic payload, obtained from exatecan, is a powerful topoisomerase I inhibitor rather than a microtubule inhibitor [18]. Moreover, T-Dxd comprises a cleavable linker where cathepsins, lysosomal enzymes upregulated in numerous cancer cells, are thought to act on [18]. The payload is membrane permeable and, thus is able to perform the bystander effect, supposedly enabling action even in tumors with varied or low expression of HER2, a property not noticed with T-DM1. All these attributes could clarify the anticancer activity of T-DXd in tumors that are intractable to T-DM1 [18].

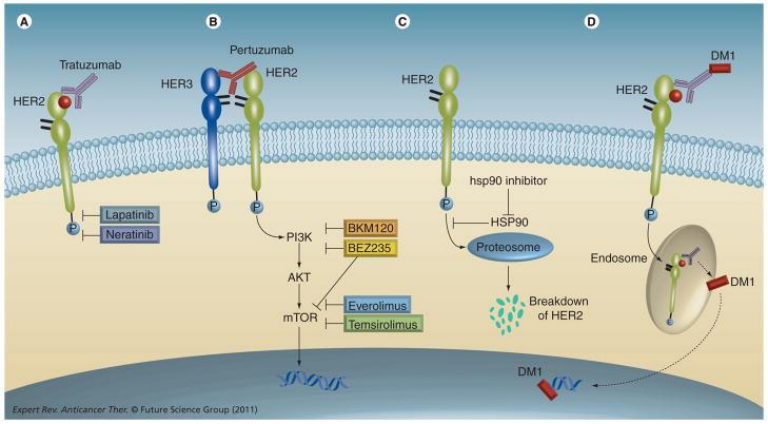

Figure 3: Novel therapeutic agents' points of intervention for HER2-enhanced breast cancer. (A) Lapatinib, a dual inhibitor of EGF receptor (EGFR)/HER2 tyrosine kinase, is sanctioned for use in patients resistant to trastuzumab. Neratinib, on the other hand, is an irreversible inhibitor of the tyrosine kinase of EGFR/HER2. (B) Pertuzumab, a monoclonal antibody for HER2, attaches to a unique epitope on HER2, distinct from the binding site of trastuzumab, and inhibits ligand-induced heterodimerization with HER3. The PI3K–AKT–mTOR pathway, when dysregulated, can lead to resistance to trastuzumab, and therapies targeting the direct inhibition of PI3K, AKT, and mTOR are under development. © Inhibitors of HSP90 facilitate the degradation of HER2 by impeding the function of HSP90, a chaperone protein that safeguards HER2 from proteasomal degradation. (D) TDM-1, a conjugate of the antibody–drug of trastuzumab and maytansine, enables the selective delivery of a potent microtubule inhibitor into cells overexpressing HER2 [18].

The HER2 extracellular domain has no known ligand and is activated by the formation of homo or heterodimers. These dimers lead to the phosphorylation of tyrosine kinase residues in the cytoplasmic domain which function as docking sites for proteins that activate the PI3K and MAPK signaling pathways downstream leading to cell cycle progression and proliferation. Both trastuzumab and pertuzumab work by binding to the extracellular region of HER2 at domains 4 and 2, respectively. Trastuzumab binding to HER2 on breast cancer cells enhances their clearance by innate immune cells [18] (Figure 3).

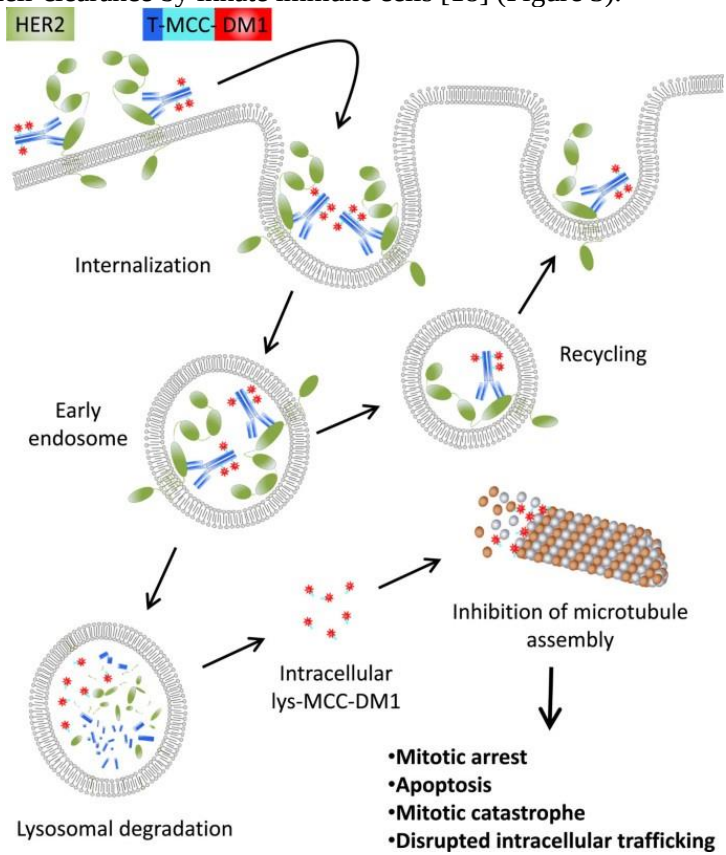

Figure 4: The internal movement and processing of trastuzumab emtansine (T-DM1) within a cell. The T-DM1 compound binds to the human epidermal growth factor receptor-2 (HER2) located on the plasma membrane, leading to the formation of a HER2-T-DM1 complex that enters the cell through receptor-mediated endocytosis. This process results in the formation of early endosomes

from the internalized endocytic vesicles. The contents of these early endosomes can either be recycled back to the cell membrane or the endosome can mature into a lysosome. The DM1 component is released following the proteolytic degradation of the antibody portion of T-DM1 in the lysosomes. The intracellular lysine (lys)-MCC-DM1 then inhibits the assembly of microtubules, leading to mitotic arrest, apoptosis, mitotic catastrophe, and disruption of intracellular trafficking. MCC refers to a non-reducible thioether linker [19].

T-DM1 is a next-generation ADC that merges the anti-HER2 outcome of trastuzumab with the cytotoxicity of the anti-microtubule agent DM1. In order to target HER2+ breast cancer cells, T-DM1 must bind HER2 on the plasma membrane, in which the HER2-T-DM1 complex must be internalized via receptor-mediated endocytosis. DM1 is then freed into lysosomes due to proteolytic degradation of the antibody part of the complex, where the Lys-MCC-DM1 metabolite of DM1 acts as a microtubule inhibitor of assembly and inhibiting cell cycle progression through mitosis [19] (Figure 4).

Small TKIs Mechanisms of Approved TKIs against HER2-Positive Breast Cancer

Small TKI molecules have many benefits over monoclonal antibody therapies, such as the aptitude to target several family members concurrently, to act straight at the level of the intracellular signaling cascade, and to possibly cross the blood brain barrier (BBB). Two small molecule TKIs, lapatinib and neratinib, have been officially approved for HER2 breast cancer management [20]. Herein we will focus on the mechanism of action of these TKIs. TKI refers to certain oral small molecular drugs dynamic in encouraging apoptosis and hindering the proliferation of cancer cells. It competitively binds intracellular adenosine triphosphate (ATP) binding domains of the HER family owing to the homological organization of the ATP, inhibiting tyrosine kinase phosphorylation, and thereby blocking downstream signals [20]. In the context of brain metastasis cancer management, the effectiveness of monoclonal antibodies can be inadequate in crossing BBB, whilst small molecule TKIs, such as lapatinib, are considered to have permeability through the BBB. Both lapatinib and neratinib bind to inactive

conformation of HER family members, thereby limiting ligand-induced activation. Lapatinib reduces the phosphorylation of HER1 and HER2 to promote apoptosis [20]. However, Neratinib is an irreversible TKI of HER1, HER2, and HER 4. Neratinib was accepted by the FDA in 2017 as an unlimited adjuvant management for patients with early-stage HER2 overexpressing breast cancer following surgery and trastuzumab-based adjuvant management [20]. It acts by preventing phosphorylation of the ErbB family and downstream pathways comprising ERK and Akt, via its covalent combination with cysteine residues Cys-773 and Cys-805 of the ATP-binding domain of HER1, HER2, and HER4. Downstream signal transduction inhibition following neratinib treatment results in abridged cyclin D1 expression, thereby arresting the G1-S phase transition, ultimately leading to a reduction of cell proliferation. Furthermore, neratinib can also induce ubiquitylation and endocytic degradation and reduction in HER2 expression in a process involving HSP90 dissociation [21]. Besides, neratinib has been shown to hinder ATP-binding cassette transporter and subsequently overturn the multidrug resistance of cancer cells [21].

By reversibly and irreversibly inhibiting HER2 phosphorylation via Laptinib and neratinib respectively, HER2-mediated signaling pathways PI3K/AKT/mTOR and MAPK signaling cascades are hindered, thus reducing cell proliferation and cancer progression. Neratinib can also cause ubiquitylation, endocytic degradation, and a decrease in HER2 expression through a process involving HSP90 dissociation [21].

Resistance Strategies to Single HER2 Inhibitors

Regardless of the fact that in the last years, the introduction of mAbs, TKIs, and ADCs targeting HER2 notably improved patient prognosis in all disease stages, not all patients with limited-stage disease are cured and HER2+ metastatic breast cancer is still roughly considered a deadly disease. Primary or acquired resistance to anti-HER2 therapies is accountable for the majority of treatment failures. Lately, several resistance mechanisms have been recognized, such as ongoing activation of signaling pathways similar to or downstream of HER2, altered

binding of anti-HER2 agents to HER2, and abridged immune system activation. Even though trastuzumab noticeably enhanced the prognosis of HER2+ breast cancer patients, many patients still progress within 12 months from the start of trastuzumab treatment [22]. One way of resistance to trastuzumab could be due to its impaired binding to HER2 because of intratumor heterogeneity of HER2 expression which has been shown to be linked with abridged activity of Trastuzumab-based treatments [23]. This indicates the presence of some breast cancer clones with low expression levels of HER2 that may gradually become presiding throughout trastuzumab exposure. Additionally, some HER2 splicing variants can also affect the aptitude of trastuzumab to bind HER2. New studies involving breast cancer cell lines recognized a splicing variant of HER2 missing exon-16, which forms HER2 dimers in an SRC-dependent way and which has been shown to associate with in vitro resistance to trastuzumab [23]. Furthermore, the expression of specific molecules by the cancer cells themselves or even other cells within the surrounding microenvironment can affect trastuzumab binding to HER2 ectodomain could be a way of resistance to this treatment. One way of this is through the expression of membrane-associated mucin 4 (MUC4) which hides the trastuzumab binding site on HER2, thereby trastuzumab binding and inhibiting HER2 could be altered, however, this needs further evaluation [23]. Moreover, it is not surprising that mutations in genes encoding players in the PI3K/AKT/mTOR signaling cascade associated with the ongoing activation of such a pathway could account for the resistance to trastuzumab. Two activating mutations, namely E545K and H1047R, residing within PI3K catalytic subunit alpha, were linked with trastuzumab resistance in HER2+ breast cancers [23]. Comparable observations appeared in tumors expressing small levels of PTEN that are acknowledged to oppose PI3K-induced phosphorylation of inositide lipids. This could be further backed by the observation that the inhibition of PIK3CA or mTOR sensitizes cancer cell lines to trastuzumab [24]. Knowing that the tyrosine kinase SRC acts downstream of HER2, one possible mechanism of resistance to trastuzumab is the abnormal activation of SRC. Inhibition of SRC has been shown to re-establish sensitivity to trastuzumab both in vitro and in vivo [24].

Even though trastuzumab averts HER2 homodimerization and restrains its driven signaling, diverse RTKs, such as EGFR, HER1, and HER3, are capable of heterodimerizing with HER2, and trigger downstream signaling cascades in the same way as HER2 homodimers. This enables tumor cells to utilize a small number of HER2 molecules that are not trastuzumab-bound and thus reactivate the HER2 signaling cascade. It has also been demonstrated that the escape from ADCC could induce resistance to trastuzumab [24]. This is consistent with the observation that mice deficient in CD16A have altered ADCC-mediated lysis of cancer cells, and HER2+ve tumors developing in these animals are resistant to trastuzumab. Particularly, trastuzumab binding to the inhibitory receptor CD32B: FcγRIIB on myeloid cells averts ADCC. While recent data propose that T-DM1 could eliminate HER2+ tumor clones that are resistant to trastuzumab, resistance to T-DM1 limits the anticancer effectiveness of T-DM1 in the metastatic situation [24]. Resistance mechanisms to T-DM1 comprise besides altered binding of T-MD1 to HER2, an altered HER2-T-DM1 complex internalization, faulty lysosomal function that hinders DM1 release, and efflux pumps concerned in DM1 export [15,24]. In vitro and in vivo studies revealed that altered lysosomal acidification and degradation of the antibody part of T-DM1, or abridged export of lys-MCC-DM1 from the lysosome into the cytoplasm via SLC46A3 transporter, lead to an earned resistance to T-DM1 [15,24]. MDR1, a plasma membrane transporter, can promote T-DM1 resistance by inducing extracellular DM1 efflux, further backed up by the fact that MDR1 inhibitors might re-establish sensitivity to T-DM1. On the other hand, even though several tumors are initially resistant to lapatinib, HER2+ tumors obtain resistance following a median time of 6 months following lapatinib treatment [15,24]. Various HER2 amino acid substitution mutations have been shown to be linked with lapatinib resistance, with the HER2 L755S and T798I mutations accounting for the uppermost levels of resistance. However, neratinib has been shown to have an anticancer action in patients with metastatic breast cancer nurturing mutations in the HER2 tyrosine kinase domain separately from HER2 levels of expression [15,24]. Additionally, parallel signaling pathways to HER2 activation can be activated in a process involving elevated

expression of RTK ligands by tumor cells of nearby cells. For example, overexpression of neuregulin-1 (NRG1), the major HER3 ligand, turns on the EGFR-HER3-PI3K-PDK1 signaling cascade, thereby overcoming lapatinib-induced reversion of HER2/EGFR [15,24]. Likewise, the binding of HGF to MET as well leads to lapatinib resistance via PI3K/AKT/mTOR pathway reactivation throughout HER2 inhibition therapy. Interestingly, Lapatinib-induced inactivation of HER2 promotes adjusting PI3K/AKT elevation of HER3 expression [25], therefore encouraging HER2-HER3 heterodimerization. In the cases of trastuzumab and lapatinib, the enhanced activation of cyclin D1-CDK4/6 cascade seems to be linked to the resistance to these therapies as revealed in HER2+ breast cancer cell lines. This is consistent with the reversion of such resistance following pharmacological inhibition of CDK4/6 [25]. In terms of neratinib, Breslin et al. established that improved activity of the metabolism enzyme cytochrome P4503A4 results in neratinib resistance and cross-resistance to trastuzumab and lapatinib. Additionally, Seyhan et al. had acknowledged a set of genes linked to neratinib resistance by means of a genome-wide RNAi screen coupled with a lethal amount of neratinib, such as oncogenesis, transcription factors, protein ubiquitination, cell cycle, and genes recognized to cooperate with breast cancer-coupled genes [25]. The expression of RB1CC1, ERBB3, and FOXO3a has been shown to be elevated in HER2 TKI-sensitive breast cancer cell lines following management with lapatinib and neratinib. A study by Takeda et al demonstrated that the activation of YES1, being an SRC family member, has been shown to be upregulated in two neratinib resistant breast cancer cell lines [25]. This study showed that the knockdown of YES1 via siRNA made YES1 amplified cancer cell lines sensitive to neratinib. The authors revealed that YES1 interacts with and activates HER2 [25].

Numerous possible resistance mechanisms to anti-HER2 agents have been recognized. The majority of them engage genetic or epigenetic alterations causing either overexpression or ongoing activation of HER2/HER3/HER4 or other plasma membrane kinases (e.g. FGFR1) or downstream effectors. Regardless of the exact mechanism, reactivation of the PI3K/AKT/mTOR cascade

looks critical to promote and uphold resistance to anti-HER2 therapies. Regarding T-DM1 resistance, mechanisms including its internalization or lysosomal role might as well have an outstanding role [25]. Taken together, it is of use to assess the possibility of combining anti-HER2 mAbs/TKIs with the parallel players in the resistance to HER2 including PI3K inhibitor, AKT inhibitor, mTOR inhibitor, CDK4/6 inhibitor, and YES1 inhibitor among others.

Triple Negative Breast Cancer Treatment Strategies

Triple-negative breast cancer (TNBC) does not express ER and PR and doesn't overexpress HER2 (81). Since tumor cells do not have these proteins, hormone therapy and HER2 targeted therapy are not supportive; consequently chemotherapy (chemo) is the major systemic treatment alternative [26]. Nevertheless, TNBC regularly responds splendidly to chemotherapy and tends to relapse more often than other breast cancers. However, for women with TNBC who have a BRCA mutation and whose cancer no longer responds to ordinary breast cancer chemo drugs, targeted drugs called Poly ADP-ribose polymerases (PARP) inhibitors may be considered. Furthermore, in favor of advanced TNBC in which the cancer cells have the PD-L1 protein, the primary treatment may be immunotherapy besides chemo [26]. Also, antibody-drug conjugates (ADCs) like SG and T-DXd, as well as additional ADCs in later phases of research with alternative targets, will revolutionize the therapy landscape for BC and other cancer types. The PD-L1 protein is detected in around 1 out of 5 TNBCs [26].

Chemotherapy in the Context of TNBC

The goal of chemotherapy is to eliminate cancer cells in the original tumor and any sites of metastasis [26,27]. In addition to being a primary cancer treatment option in the case of TNBC, chemotherapy can also act as a secondary treatment before, during, and after other primary cancer treatments such as radiation therapy or surgical excision of a tumor. In most cases, several chemotherapy drugs could be administered to increase

their effectiveness [26,27]. This allows the body to recover and kills as many cancer cells as possible. Anthracycline/taxane-based chemotherapy is considered the standard of care for patients with TNBC, whether in the neoadjuvant or adjuvant setting. Both Paclitaxel and Docetaxel are anti-cancer chemotherapies. They are considered "plant alkaloids," "taxane" and "anti-microtubule agents. The main manne of paclitaxel's action is the hyper-stabilization of microtubules (a constituent of the cytoskeleton) made of repeating subunits of α- and β-tubulin vital for numerous cellular behaviors [26,27]. Paclitaxel binds to the N-terminal amino acids of the β-tubulin subunit and lowers the threshold concentration of purified tubulin subunits required for in vitro polymerization into microtubules while increasing the fraction of tubulin subunits that assemble [26,27]. Paclitaxel also interacts directly with microtubules, preventing depolymerization by cold and calcium [28]. As a result, cancer cells treated with the drug enter metaphase on bipolar spindles, and their growth is halted. The activation of the spindle assembly checkpoint prevents the progression of the cell cycle, specifically the separation of the chromosomes due to the presence of kinetochores that do not have a solid attachment to microtubules [28]. Cancer cells exposed to the drug exhibit decreased inner mitochondrial membrane potential, which causes the permeability transition pore channel to open and the release of cytochrome c and apoptosis-inducing factor. Apoptotic death is thereby carried out by activated effectory caspases. At the same time, docetaxel has been found to be twice as effective as paclitaxel in inhibiting microtubule depolymerization. Paclitaxel and docetaxel are both commonly used to treat a variety of tumors [28]. Other common chemo drugs used in TNBC include Anthracyclines. Its mode of action within cancer cells is based on growth arrest and programmed cell death by poisoning topoisomerase, a critical enzyme for unwinding DNA for replication and synthesis. One of the most promising new cytotoxic agents is gemcitabine, a pyrimidine nucleoside antimetabolite. The drug has been approved for the treatment of breast cancer and has shown activity in a variety of solid tumors. The most imperative mode of action of gemcitabine is DNA synthesis inhibition [28]. When gemcitabine triphosphate (dFdCTP) is incorporated into DNA, it is followed by a single

deoxynucleotide, preventing chain elongation. The chemo drugs mentioned above can be either used alone or in combination [29]. Unfortunately, chemotherapy drugs cannot tell the difference between fast growing normal cells and cancer cells; as a result, these drugs also damage or irritate some of the fast-growing normal cells such as those in the bone marrow, digestive system, and hair follicles. Death, irritation, or damage of these cells produces side-effects such as a weakened immune system, nausea, and hair loss [29].

BRCAness and PARP Inhibitors as a TNBC Treatment Option

A germline BRCA1 or BRCA2 mutation is present in 25% of patients with triple negative breast cancer [26,30]. BRCAness is defined as a set of traits in which BRCA1 dysfunction, caused by gene mutation, methylation, or deletion, results in a lack of DNA repair. Sometimes TNBCs seem to have BRCAness, and these tumors share clinicopathological features with BRCA1-mutated tumors. A better understanding of TNBC and the presence of BRCAness may have implications for both hereditary breast cancer screening and treatment of these tumors [26,30]. Tumors with BRCAness are thought to be extremely sensitive to chemotherapy. However, targeted drugs called poly (ADP-ribose) polymerase (PARP) inhibitors, like olaparib [Lynparza] or talazoparib [Talzenna] may be considered for women with TNBC who have a BRCA mutation and whose tumor no longer responds to common breast cancer chemo drugs. PARP1, which was discovered about 50 years ago, is involved in gene transcription, DNA repair, and cell death [26,30]. PARP inhibitor therapy is not currently approved by the FDA for patients with TNBC who do not have a germline BRCA mutation [31]. PARP is a major protein that is involved in DNA repair pathways, base excision repair (BER) mechanisms, homologous recombination (HR), and NEJ deficiency-based repair mechanisms. DNA damage repair deficiencies increase the likelihood of tumor formation. DNA DSB repair is inadequate in cancer cells affected by harmful mutations in the breast cancer susceptibility genes BRCA 1 and BRCA2 [31]. In fact, the homologous recombination repair (HRR) pathway relies heavily

on both BRCA1 and BRCA2. BRCA 1 is a multifunctional enzyme with a direct role in HRR. In conjunction with CHK2, it is initially in charge of signal transduction; following that, ATM and ATR detect DNA double strand damage. It then works by establishing a structure that arranges the repair proteins at the DNA repair site. On the other hand, BRCA 2 brings in RAD51, a recombinase, at the DNA repair site [31]. Therefore, if additional occurrences that could hinder DNA damage repair take place, the damage could result in a gradual accumulation of DNA changes that could eventually result in apoptosis [32,33]. The first clinically approved synthetic lethality-exploiting drug, PARPib, has demonstrated promising activity in patients with BRCA-deficient tumors. It has been shown that PARPib primarily works by blocking the PARylation mechanism, which causes DNA damage to be trapped at the site of the damage, activating effector genes, and ultimately interrupting the replication fork by causing DSB damage with a cytotoxic effect [32,33]. Preclinical models thus demonstrated that DNA trapping on PARP may be a more potent means of inducing cell death than catalytic enzyme alone. Thus, the current inhibition of PARP enzymes results in the accumulation of unpaired damages in tumors harboring a defect in the HRR pathway, which ultimately results in tumor cell death. Contrarily, patients with BRCA 1 or 2 mutations may benefit clinically because healthy cells may be spared. Olaparib and talazopirib are the only two PARPibs that have currently been authorized for the treatment of patients with metastatic TNBC [32,33]. Olaparib is a small molecule that was initially thought to be an inhibitor of PARP-1 and PARP-2 but data revealed that it is also a potent inhibitor of PARP-3. On the other hand, talazoparib is a powerful PARP inhibitor with both a strong catalytic inhibition and a potential for trapping PARP [34,35].

PDL1 Inhibitors

Recent years have seen an increase in the relevance of research on PD-L1 expression in breast cancer, particularly in triple-negative breast cancer (TNBC). When compared to other breast cancer subtypes, TNBC has been reported to have higher rates of cell surface PD-L1 expression, and higher PD-L1 expression

implies a greater potential benefit from using PD-1/PD-L1 targeted immunotherapy in this population of patients [36,37]. It has been discovered that the PD-1 receptor of Treg cells enhances the de novo conversion of naïve CD4+ T cells to Treg cells in the presence of CD3 and TGF-, therefore attenuating immunological responses. Through blocking the mTOR-Akt signaling cascade, this conversion promotes the production of Treg and the immunological suppressive activity of CD4+ T cells [36,37]. As a result, PD-1 expression not only inhibits effector T-cell activity but also promotes the conversion of the population of immunosuppressive Treg cells. Although PD-1 has been extensively investigated in T-cells, its roles in B-cells for tumor immunosuppression have also come to light. However, PD-1 levels are negligible in pro-B cells, an early stage of the mature B cell, and rise with B cell development. It has been shown that PD-1 expression is heavily controlled during B cell differentiation [36,37]. PD-1 is a novel regulator of human B-cell activation. Additionally, PD-1 activated toll-like receptor 9 (TLR9) agonists can greatly improve B-cell maturation [38]. It has been demonstrated that inhibiting PD-1 activity on B cells improves antigen-specific antibody responses, proving that PD-1 suppresses B cell-mediated T-cell activation. Monoclonal antibodies (mAbs) are a kind of checkpoint inhibitor that inhibits the interaction of PD-1 and PD-L1 and thereby overcomes the drawbacks of traditional anticancer treatment [38]. mAbs can considerably reduce toxicity while shrinking solid tumors, suppressing advanced malignancies and metastasis, and improving overall patient survival. Interferon gamma (IFN)-induced increase of PD-L1 expression on tumor cell surfaces is one way of regulation. This is probably a way by which tumor cells avoid being destroyed by T lymphocytes that are specifically designed to fight tumors. Oncogenic signaling is a second pathway [38]. The FDA recently approved various anti-PD-1 and PD-L1 mAbs that target a variety of human malignancies. The clinical efficacy of anti-PD-1 and PD-L1 mAbs show promise in targeting PD-1 and PD-L1 immune checkpoints, consequently considerably improving patient conditions [39]. Atezolizumab (Tecentriq®), the first PD-1/PD-L1 immune checkpoint inhibitor for metastatic triple-negative breast cancer, was FDA approved in March 2019 as a treatment

for advanced TNBC. A monoclonal immunoglobulin-G1 (IgG1) antibody called atezolizumab is Fc-engineered, non-glycosylated, and humanized. It binds to PD-L1 and prevents it from interacting with PD-1 and B7.1 (CD80) receptors [39]. Tumor-infiltrating immune cells and/or tumor-associated tumor cells may both express PD-L1. Cytotoxic T-cell activity, T-cell proliferation, and cytokine production are suppressed when PD-L1 binds with PD-1 and B7.1 receptors on T-cells and antigen-presenting cells, preventing the anti-tumor immune response in the tumor microenvironment [39].

Other FDA Approved

TNBC patients who relapse soon after (neo) adjuvant treatment like chemotherapy have more severe conditions. Patients with TNBC who relapse within a year of following (neo) adjuvant chemotherapy have either primary resistance or early acquired resistance to cytotoxic chemotherapy. Shortened disease-free intervals in such cases are linked with a poor prognosis for successive lines of therapy [40]. Therefore, patients with TNBC chemotherapy resistance require improved therapies. Trop-2 is a protein that is over-expressed in more than 80% of TNBC. Sacituzumab govitecan (SG) is an antibody-drug conjugate (ADC) made of a humanized trophoblast cell-surface antigen-2 (Trop-2) antibody linked to an SN-38 payload, the active form of the metabolite topoisomerase 1 inhibitor Irinotecan (a chemotherapeutic medication), through a unique, hydrolyzable linker [40,41]. Breast cancer cells are immediately treated with chemotherapy when the antibody attaches to them. The high drug-to-antibody ratio of 7.6:1, the fact that internalization and enzymatic cleavage of SG by tumor cells are not necessary for SN-38 release from the antibody, and its bystander impact in tumor microenvironment make SG a unique Trop-2-directed ADC [42].

Breast Cancer Treatments Currently Evaluated in Clinical Trials

Intense research allowed a better understanding of the pathophysiology of breast cancer and led to the identification of

more effective, safe, and individualized novel drugs. Currently, many promising clinical trials targeting all the subtypes of breast cancer are in progress. This significant breakthrough changed the outlook of breast cancer therapy as it increased treatment options, reduced the risk of recurrence and progression, improved overall survival, and enhanced patient prognosis, especially for late-stage advanced breast cancer. Novel breast cancer therapies are numerous with diverse characteristics and different modes of action. Such therapies include PARP inhibitors, gene therapy, and immunotherapy [43].

PARP Inhibitors

Veliparib

Veliparib is a selective, oral inhibitor of PARP1 and PARP2. A phase 3 study showed that Veliparib enhanced the effect of platinum-based chemotherapy (Carboplatin/Paclitaxel) and it is considered a new treatment option for patients with HER2-negative, gBRCA-mutated metastatic or locally advanced breast cancer. It demonstrated promising anti-tumor activity with a tolerable safety profile as a single agent and in combination with carboplatin and paclitaxel in patients with BRCA mutation-associated breast cancer [44,45].

Recently, a phase II trial compared the outcomes in patients with different genomic characteristics treated with Cisplatin alone and in combination with Veliparib. 323 patients were classified into three groups: patients with a germline BRCA mutation, patients with a BRCA-like mutation in HR genes, and non-BRCA-like mutation. In addition, there was an unclassified group due to missing biomarker information. The studied endpoints were progression-free survival (PFS), objective response rate (ORR), overall survival (OS), and toxicity [44,45].

In the group of patients having a germline BRCA mutation, the results of PFS were not statistically significant. However, in the BRCA-like group, PFS with Veliparib treatment was enhanced compared to placebo (5.7 versus 4.3 months respectively). Besides in the same group OS (13.7 versus 12.1 months) and ORR (45% versus 35%). The patients in the non-BRCA-like

group and the unclassified group didn't benefit from Veliparib as the variation of PFS was not significant. Regarding toxicity, Grade 3/4 neutropenia (46% versus 19%) and anemia (23% versus 7%) occurred at a higher rate in the Veliparib arm compared to placebo. Consequently, the combination of Veliparib with Cisplatin was successful as it significantly improved PFS and OS for BRCA-like advanced TNBC. Biomarkers used in this study allowed the identification of a subgroup of BRCAwt TNBC that benefited from the addition of PARP inhibitors to cisplatin. This combination is promising and should be studied further in BRCA-like TNBC [44,45].

Rucaparib

Rucaparib is a PARP inhibitor that targets PARP1 and PARP2. It can also target PARP3 which is involved in chromosomal DNA double-strand break repair. Rucaparib is currently under a phase-II trial done on 78 patients with BRCA1/2-mutated advanced breast or ovarian cancers. This trial includes two cohorts with different treatment administration routes. The first cohort receives oral treatment while the second cohort receives intravenous treatment. In both cohorts, the first step of the study included a dose-escalation phase by which the best dose with the least side effects was determined. No objective response was observed in breast cancer patients of the two cohorts. However, 20% of patients in the oral cohort and 44% of patients in the intravenous cohort exhibited disease stabilization over 12 weeks. This means that the treatment can impede the spread of cancer. So, as a monotherapy, Rucaparib was well tolerated as the most adverse events were fatigue and nausea [46,47].

Another phase-II trial was done on patients with TNBC with residual disease after neoadjuvant therapy. These patients have a high risk of cancer recurrence. A total of 128 patients were recruited in the study, with 22% of them carrying a BRCA1/2 germline mutation. Rucaparib was administered in combination with cisplatin. This combination didn't impact the toxicity of cisplatin, and it didn't improve disease-free survival. Probably this is due to the dose of Rucaparib used in this study, as it was substantially less than the current phase II monotherapy dose,

and it may not have been sufficient to inhibit PARP activity. So, dose escalation may be required to check whether this combination is successful [48].

Immunotherapy

Various populations of immune cells are present in the breast stroma at different stages of development and maturation like post-natal development, puberty, and pregnancy. So, breast cancer is considered a moderately immunogenic cancer, with HER2-positive and TNBC subtypes, being the most immunogenic. Immune cells have a crucial role in the early detection and eradication of BC [49].

However, some breast cancer cells are less immunogenic as they have the capability to evade the immune system through different mechanisms. Tumor cells can reduce the expression of the major histocompatibility complex (MHC) that can decrease immune recognition and immune cell activation. This contributes to the development of low immunogenic tumor cells that can escape immune system surveillance. So, due to the importance of the immune system in breast cancer, immunotherapy emerged as a promising treatment option with fewer adverse reactions, strong specificity, and favorable clinical application. Immunotherapy boosts the immune system's ability to recognize, target, and eliminate cancer cells. The most important immunotherapies in breast cancer are immune checkpoint inhibitors, cytokine therapy, and cell-based immunotherapy (CAR-T cell therapy) [49].

Immune checkpoints negatively control immunity by induction of anergy or apoptosis of immune cells. The most important immune checkpoints are programmed cell death-1 (PD-1), programmed cell death ligand-1 (PD-L1), and cytotoxic T-lymphocyte antigen-4 (CTLA-4). Some tumors exploit the function of immune checkpoints to escape from immune surveillance. PD-1, a protein expressed on the surface of T lymphocytes, interacts with its ligand (PD-L1) expressed on tumor cells to inhibit T cells' proliferation and reduce their survival and cytotoxic abilities. CTLA-4, expressed on

regulatory T cells, weakens the immune response against tumor cells by inhibiting the interaction between T cells and antigen-presenting cells (APCs). It also inhibits the function of CD28, a protein that acts as a co-stimulator essential for T cell activation and survival [50,51]. The fact that immune checkpoints' function is triggered by ligand-receptor interactions makes it easy to develop inhibitors that can reverse the immunosuppressive state caused by such checkpoints. These inhibitors are mostly monoclonal antibodies that are currently in different stages of clinical trials; for example, anti-PD-1 mAbs (Nivolumab), anti-PDL-1 mAbs (Durvalumab, Avelumab), and anti-CTLA4 (Ipilimumab). Two mAbs are FDA-approved: Pembrolizumab against PD-1 for the treatment of patients with unresectable or metastatic solid tumors, and Atezolizumab in combination with nab-paclitaxel (a chemotherapy drug) against PD-L1 for the treatment of locally advanced/ metastatic TNBC [50,51].

Conclusion

To put it briefly, this comprehensive review has provided a detailed exploration of the current and evolving treatment strategies for breast cancer. It has elucidated the intricate molecular mechanisms underlying hormone receptor-positive (HR+), HER2-enriched, and triple-negative breast cancers (TNBC), shedding light on the challenges and therapeutic strategies associated with each subtype. The review has underscored the need for a personalized and multifaceted approach to breast cancer treatment, emphasizing the importance of understanding the dynamic interplay between various receptors, growth factors, and microRNAs, and the development of combination therapies to improve patient outcomes. The exploration of resistance strategies against single HER2 inhibitors and the advent of targeted therapies, notably PARP inhibitors and immunotherapy have broadened treatment options and introduced personalized dimensions to breast cancer management. The ongoing clinical trials and FDA-approved interventions present a tapestry of opportunities for enhanced patient outcomes. As the scientific community navigates this intricate landscape, collaborative efforts, rigorous research, and

an unwavering commitment to understanding breast cancer at its molecular core will be paramount for advancing the field and ultimately, enhancing the well-being of individuals impacted by this formidable ailment.

References

1. Yang K, Kim H, Choi DH, Park W, Noh JM, et al. Optimal radiotherapy for patients with internal mammary lymph node metastasis from breast cancer. Radiation Oncology. 2020; 15: 16.
2. Drăgănescu M, Carmocan C. Hormone Therapy in Breast Cancer. Chirurgia. 2017; 112: 413.
3. Kersh AE, Ng S, Chang YM, Sasaki M, Thomas SN, et al. Targeted Therapies: Immunologic Effects and Potential Applications Outside of Cancer. Journal of Clinical Pharmacology. 2018; 58: 7–24.
4. Pellegrino B, Hlavata Z, Migali C, De Silva P, Aiello M, et al. Luminal Breast Cancer: Risk of Recurrence and Tumor-Associated Immune Suppression. Mol Diagn Ther. 2021; 25: 409–424.
5. Ziyeh S, Wong L, Basho RK. Advances in Endocrine Therapy for Hormone Receptor-Positive Advanced Breast Cancer. Curr Oncol Rep. 2023; 25: 689–698.
6. Li J, Wang Z, Shao Z. Fulvestrant in the treatment of hormone receptor-positive/human epidermal growth factor receptor 2-negative advanced breast cancer: A review. Cancer Medicine. 2019; 8: 1943–1957.
7. Buzdar AU, Hortobagyi GN. Tamoxifen and toremifene in breast cancer: comparison of safety and efficacy. JCO. 1998; 16: 348–353.
8. Saatci O, Huynh-Dam KT, Sahin O. Endocrine resistance in breast cancer: from molecular mechanisms to therapeutic strategies. J Mol Med. 2021; 99: 1691–1710.
9. Ozyurt R, Ozpolat B. Molecular Mechanisms of Anti-Estrogen Therapy Resistance and Novel Targeted Therapies. Cancers. 2022; 14: 5206.
10. Rahem SM, Epsi NJ, Coffman FD, Mitrofanova A. Genome-wide analysis of therapeutic response uncovers molecular pathways governing tamoxifen resistance in ER+ breast

cancer. EBioMedicine. 2020; 61: 103047.
11. Muluhngwi P, Klinge CM. Roles for miRNAs in endocrine resistance in breast cancer. Endocrine-Related Cancer. 2015; 22: R279–300.
12. Glaviano A, Foo ASC, Lam HY, Yap KCH, Jacot W, et al. PI3K/AKT/mTOR signaling transduction pathway and targeted therapies in cancer. Molecular Cancer. 2023; 22: 138.
13. Fan W, J C, fu P. Endocrine therapy resistance in breast cancer: current status, possible mechanisms and overcoming strategies. Future medicinal chemistry. 2015; 7: 1511–1519.
14. Kang I, Dong S, Lu J, Xia B. Recent Developments in HER2-Directed Therapy in Breast Cancer. Curr Breast Cancer Rep. 2019; 11: 311–325.
15. Thaper A, Tran J, Ali A. Current Updates in Management of HER2-Positive and HER2-Low Breast Cancer. Curr Breast Cancer Rep. 2023; 15: 135–141.
16. Xing F, Gao H, Chen G, Sun L, Sun J, et al. CMTM6 overexpression confers trastuzumab resistance in HER2-positive breast cancer. Molecular Cancer. 2023; 22: 6.
17. Omarini C, Piacentini F, Sperduti I, Cerma K, Barbolini M, et al. T-DM1 efficacy in trastuzumab-pertuzumab pre-treated HER2 positive metastatic breast cancer patients: a meta-analysis. BMC Cancer. 2022; 22: 623.
18. Gajria D, Chandarlapaty S. HER2-amplified breast cancer: mechanisms of trastuzumab resistance and novel targeted therapies. Expert Rev Anticancer Ther. 2011; 11: 263–275.
19. Barok M, Joensuu H, Isola J. Trastuzumab emtansine: mechanisms of action and drug resistance. Breast Cancer Research. 2014; 16: 209.
20. Cunningham N, Shepherd S, Mohammed K, Lee KA, Allen M, et al. Neratinib in advanced HER2-positive breast cancer: experience from the Royal Marsden hospital. Breast Cancer Res Treat. 2022; 195: 333–340.
21. Martin M, Holmes FA, Ejlertsen B, Delaloge S, Moy B, et al. Neratinib after trastuzumab-based adjuvant therapy in HER2-positive breast cancer (ExteNET): 5-year analysis of a randomized, double-blind, placebo-controlled, phase 3 trial. The Lancet Oncology. 2017; 18: 1688–1700.
22. Earl HM, Hiller L, Vallier AL, Loi S, McAdam K, et al. 6

versus 12 months of adjuvant trastuzumab for HER2-positive early breast cancer (PERSEPHONE): 4-year disease-free survival results of a randomized phase 3 non-inferiority trial. Lancet. 2019; 393: 2599–2612.
23. Wang ZH, Zheng ZQ, Jia SC, Liu SN, Xiao XF, et al. Trastuzumab resistance in HER2-positive breast cancer: Mechanisms, emerging biomarkers and targeting agents. Front Oncol. 2022; 12: 1006429.
24. Hunter FW, Barker HR, Lipert B, Rothé F, Gebhart G, et al. Mechanisms of resistance to trastuzumab emtansine (T-DM1) in HER2-positive breast cancer. Br J Cancer. 2020; 122: 603–612.
25. Takeda T, Yamamoto H, Suzawa K, Tomida S, Miyauchi S, et al. YES1 activation induces acquired resistance to neratinib in HER2-amplified breast and lung cancers. Cancer Sci. 2020; 111: 849–856.
26. Leon-Ferre RA, Goetz MP. Advances in systemic therapies for triple negative breast cancer. BMJ. 2023; 381: e071674.
27. Lafanechère L. The microtubule cytoskeleton: An old validated target for novel therapeutic drugs. Frontiers in Pharmacology [Internet]. 2022; 13. Available online at: https://www.frontiersin.org/articles/10.3389/fphar.2022.969183
28. Zhang Z, Wang G, Li Y, Lei D, Xiang J, et al. Recent progress in DNA methyltransferase inhibitors as anticancer agents. Frontiers in Pharmacology [Internet]. 2022; 13. Available online at: https://www.frontiersin.org/articles/10.3389/fphar.2022.1072651
29. Das M, Li J, Bao M, Huang L. Nano-delivery of Gemcitabine Derivative as a Therapeutic Strategy in a Desmoplastic KRAS Mutant Pancreatic Cancer. AAPS J. 2020; 22: 88.
30. Barchiesi G, Roberto M, Verrico M, Vici P, Tomao S, et al. Emerging Role of PARP Inhibitors in Metastatic Triple Negative Breast Cancer. Current Scenario and Future Perspectives. Frontiers in Oncology [Internet]. 2021; 11. Available online at: https://www.frontiersin.org/articles/10.3389/fonc.2021.769280

31. Cortesi L, Rugo HS, Jackisch C. An Overview of PARP Inhibitors for the Treatment of Breast Cancer. Targ Oncol. 2021; 16: 255–282.
32. Kaur SD, Chellappan DK, Aljabali AA, Tambuwala M, Dua K, et al. Recent advances in cancer therapy using PARP inhibitors. Med Oncol. 2022; 39: 241.
33. Rose M, Burgess JT, O'Byrne K, Richard DJ, Bolderson E. PARP Inhibitors: Clinical Relevance, Mechanisms of Action and Tumor Resistance. Frontiers in Cell and Developmental Biology [Internet]. 2020; 8. Available online at: https://www.frontiersin.org/articles/10.3389/fcell.2020.564601
34. Boussios S, Abson C, Moschetta M, Rassy E, Karathanasi A, et al. Poly (ADP-Ribose) Polymerase Inhibitors: Talazoparib in Ovarian Cancer and Beyond. Drugs R D. 2020; 20: 55–73.
35. Bruin MAC, Sonke GS, Beijnen JH, Huitema ADR. Pharmacokinetics and Pharmacodynamics of PARP Inhibitors in Oncology. Clin Pharmacokinet. 2022; 61: 1649–1675.
36. Oner G, Önder S, Karatay H, Ak N, Tükenmez M, et al. Clinical impact of PD-L1 expression in triple-negative breast cancer patients with residual tumor burden after neoadjuvant chemotherapy. World Journal of Surgical Oncology. 2021; 19: 264.
37. Dong Y, Han Y, Huang Y, Jiang S, Huang Z, et al. PD-L1 Is Expressed and Promotes the Expansion of Regulatory T Cells in Acute Myeloid Leukemia. Frontiers in Immunology [Internet]. 2020; 11. Available online at: https://www.frontiersin.org/articles/10.3389/fimmu.2020.01710
38. Thibult ML, Mamessier E, Gertner-Dardenne J, Pastor S, Just-Landi S, et al. PD-1 is a novel regulator of human B-cell activation. International Immunology. 2013; 25: 129–137.
39. Twomey JD, Zhang B. Cancer Immunotherapy Update: FDA-Approved Checkpoint Inhibitors and Companion Diagnostics. AAPS J. 2021; 23: 39.
40. Yin L, Duan JJ, Bian XW, Yu S cang. Triple-negative breast cancer molecular subtyping and treatment progress. Breast Cancer Research. 2020; 22: 61.
41. Bardia A, Hurvitz SA, Tolaney SM, Loirat D, Punie K, et al.

Sacituzumab Govitecan in Metastatic Triple-Negative Breast Cancer. N Engl J Med. 2021; 384: 1529–1541.
42. Syed YY. Sacituzumab Govitecan: First Approval. Drugs. 2020; 80: 1019–1025.
43. Advances in Breast Cancer Research - NCI [Internet]. 2019. Available online at: https://www.cancer.gov/types/breast/research
44. Diéras V, Han HS, Kaufman B, Wildiers H, Friedlander M, et al. Veliparib with carboplatin and paclitaxel in BRCA-mutated advanced breast cancer (BROCADE3): a randomized, double-blind, placebo-controlled, phase 3 trial. The Lancet Oncology. 2020; 21: 1269–1282.
45. Rodler E, Sharma P, Barlow WE, Gralow JR, Puhalla SL, et al. Cisplatin with veliparib or placebo in metastatic triple-negative breast cancer and BRCA mutation-associated breast cancer (S1416): a randomized, double-blind, placebo-controlled, phase 2 trial. The Lancet Oncology. 2023; 24: 162–174.
46. Curtin N. Phase 2 multicentre trial investigating intermittent and continuous dosing schedules of the poly(ADP-ribose) polymerase inhibitor rucaparib in germline BRCA mutation carriers with advanced ovarian and breast cancer. British Journal of Cancer [Internet]. 2016. Available online at: https://www.academia.edu/94587776/Phase_2_multicentre_trial_investigating_intermittent_and_continuous_dosing_schedules_of_the_poly_ADP_ribose_polymerase_inhibitor_rucaparib_in_germline_BRCA_mutation_carriers_with_advanced_ovarian_and_breast_cancer
47. Michela P, Tedaldi G, Sirico M, Virga A, Ulivi P, et al. Moving Beyond PARP Inhibition: Current State and Future Perspectives in Breast Cancer. International Journal of Molecular Sciences. 2021; 22: 7884.
48. Kalra M, Tong Y, Jones DR, Walsh T, Danso MA, et al. Cisplatin +/- rucaparib after preoperative chemotherapy in patients with triple-negative or BRCA mutated breast cancer. NPJ Breast Cancer. 2021; 7: 29.
49. Li Y, Miao W, He D, Wang S, Lou J, et al. Recent Progress on Immunotherapy for Breast Cancer: Tumor Microenvironment, Nanotechnology and More. Frontiers in Bioengineering and Biotechnology [Internet]. 2021; 9.

Available online at: https://www.frontiersin.org/articles/10.3389/fbioe.2021.680315

50. Yi H, Li Y, Tan Y, Fu S, Tang F, et al. Immune Checkpoint Inhibition for Triple-Negative Breast Cancer: Current Landscape and Future Perspectives. Frontiers in Oncology [Internet]. 2021; 11. Available online at: https://www.frontiersin.org/articles/10.3389/fonc.2021.648139
51. Zhang W, Kong X, Ai B, Wang Z, Wang X, et al. Research Progresses in Immunological Checkpoint Inhibitors for Breast Cancer Immunotherapy. Frontiers in Oncology [Internet]. 2021; 11. Available online at: https://www.frontiersin.org/articles/10.3389/fonc.2021.582664

Book Chapter

Breast Cancer Treatment in the Modern Era: A Focus on Drug Combinations

Rania El Majzoub[1#], Zeinab Al Dirani[2#], Chourouk Joumaa[2#], Rawan Issa[2#], Mohammad Fayyad-Kazan[3], Dima Dagher[2], Mariam Hamze[2], Samah Al Zein[2], Ali Bannout[2], Katia Smeha[2], Jana Zaraket[2], Aya El Hage Ali[2], Fatima Shaalan[2], Belal Osman[4], Ali Al Khatib[4], Mohamad El Saheli[5], Jana Mahmoud-Haidar[2], Ghinwa Itani[2], Ghida Temraz[2], Samer Krayan[2], Khalid Omama[2], Somaya Al Hallak[2], Mona Sahmarani[2], Dima Obeid[2], Douaa Khreis[2†], Fatima Dandash[2†], Fatima Berro[2†], Hussein Fayyad-Kazan[2†]

[1]Department of Biomedical Sciences, School of Pharmacy, Lebanese International University, Beirut, Lebanon
[2]Lebanese University, Faculty of Science (I), Biology and Biochemistry Departments, Hadath, Beirut, Lebanon
[3]Department of Natural and Applied Sciences, College of Arts and Sciences, The American University of Iraq-Baghdad (AUIB), Baghdad 10001, Iraq
[4]American University of Beirut, Faculty of Medicine, Beirut, Lebanon
[5]Department of Biological Sciences, Faculty of Science, Beirut Arab University, Debbieh, Lebanon

#: Contributed equally to this work
†: Joint senior co-authors

***Corresponding Author:** Ángel Manteca, Área de Microbiología, Departamento de Biología Funcional, IUOPA and ISPA, Facultad de Medicina, Universidad de Oviedo, 33006 Oviedo, Spain

Published **September 02, 2024**

How to cite this book chapter: Rania El Majzoub, Zeinab Al Dirani, Chourouk Joumaa, Rawan Issa, Dima Dagher, Mariam Hamze, Samah Al Zein, Ali Bannout, Katia Smeha, Jana Zaraket, Aya El Hage Ali, Fatima Shaalan, Jana Mahmoud-Haidar, Ghinwa Itani, Ghida Temraz, Samer Krayan, Khalid Omama, Somaya Al Hallak, Mona Sahmarani, Dima Obeid, Douaa Khreis, Fatima Dandash, Fatima Berro, Hussein Fayyad-Kazan. Breast Cancer Treatment in the Modern Era: A Focus on Drug Combinations. In: Immunology and Cancer Biology. Hyderabad, India: Vide Leaf. 2024.

Abstract

Breast cancer, a complex oncological challenge, requires a nuanced treatment approach. Despite effective treatments, drug-resistant tumors contribute to the majority of mortalities. The focus has shifted to combining drugs, such as chemotherapy, immunotherapy, and gene therapy, to enhance efficacy and reduce toxicities. This chapter offers a detailed exploration of the present landscape of breast cancer therapeutics, emphasizing the shift from traditional single-drug treatments to more sophisticated combination strategies. It delves into the realm of combination therapies, where diverse treatment methods such as chemotherapy, immunotherapy, Hormone therapy, and gene therapy are strategically blended to address the intricate nature of breast cancer biology. The goal is to achieve a balanced approach, maximizing effectiveness while minimizing toxicity. Ongoing research aims to diversify treatment options, envisioning a future with more personalized and comprehensive care for breast cancer patients.

Keywords

Breast Cancer; Drug-Resistant Tumors; Combination Therapies; Chemotherapy; Immunotherapy; Hormone Therapy; Gene Therapy

Introduction

Breast cancer treatments include surgery, radiation, neoadjuvant chemotherapy, adjuvant chemotherapy, immunotherapy, and endocrine or hormone therapy. Maximum therapeutic efficacy combined with a minimum of side effects is necessary for breast cancer treatment to maintain patients' lives [1].

Because the majority of anticancer drugs do not distinguish well between cancerous and normal cells, systemic toxicity and undesirable effects of chemotherapeutics significantly reduce treatment efficacy. Additionally, acquired drug resistance may further reduce chemotherapy and other adjuvant medicines' ability to treat cancer. Although patients receiving high doses of chemotherapy may be able to overcome drug resistance, the overall survival rate did not improve due to increased treatment toxicity. In addition, the effectiveness of cancer treatment is also limited by the heterogeneity of breast cancer [2].

Furthermore, cancer patients may experience unfavorable side effects from monotherapies, which do not usually work well for them, especially in the case of metastatic cancers [3]. It has been noted that the tumor contains a variety of cell types, from them the breast cancer stem cells (BCSCs) that contribute to the aggressiveness of metastatic lesions [4]. When a tumor has been successfully treated, some cells are left behind and contribute to the tumor's recurrence. These characteristics make treating cancer patients only with monotherapy challenging [5].

Towards Combinatorial Therapies

A new and promising approach is combining cancer therapies to see whether they can complement one another in a way that lessens side effects and gets beyond the resistance of tumor cells. This has built up an efficient way to handle some of these problems by specifically targeting cancer-inducing or cell-sustaining pathways Combinatorial therapy may involve combining two distinct modalities, such as radio-immunotherapy and radio-chemotherapy, or it may involve combining two or

more therapeutic agents, such as chemotherapy medicines or other types of therapies [6,7].

Combination chemotherapy provides benefits such as improved efficacy, decreased toxicity, and a slowed or delayed formation of drug resistance since it necessitates a lower therapeutic dosage of each medicine alone. Because of these advantages, combined chemotherapy is now the most widely used technique in clinical practice [8].

Drug combinations are typically based on the following general principles: (a) without overlapping toxicities so that each drug can be administered at the appropriate dose (b) with different therapeutic mechanisms and minimal cross-resistance to suppress broad-spectrum drug resistance (c) with optimized dose ratios for synergistic or additive therapeutic effects (d) with similar solubility and permeation to ensure adequate delivery and high intracellular levels [8].

Chemotherapeutic Drugs Combination

Combination chemotherapy (or polychemotherapy) has traditionally been used to treat breast cancer to lower the risk of recurrence and improve overall response. A common regimen for breast cancer is combining an alkylating agent like cyclophosphamide with antimetabolites such as methotrexate and 5-FU. Other combinations between chemotherapies were assessed in clinical trials for breast cancer treatment and some of these combinations are approved by the Food and Drug Administration (FDA) [9].

Numerous combination therapies, including those based on paclitaxel (PTX), methotrexate (MTX), and anthracycline, have been developed throughout the years to treat various cancers. Liposomes, polymers, dendrimers, hybrid nanoparticles, inorganic nanoframes, and nanogels are just a few of the diverse nanocarriers that have been used to carry different drugs together for combination chemotherapy [10].

Currently, administering a physical mixture of two or more anticancer drugs is the only option for combination regimens for metastatic breast cancer that are available in clinics. Clinically employed combination regimens can be broadly categorized based on their mechanisms of action, including (a) nonspecific small molecule chemotherapeutic agents that can be given singly or in combination; (b) combinations of target-specific biologic agents and small molecule chemotherapeutic agents; and (c) combinations of target-specific biologic agents [11] (Table 1).

Small-molecule chemotherapeutic agents can appear in many active combination chemotherapy regimens in metastatic breast cancer. Anthracycline-based regimens, often known as anthracycline antibiotics, are a class of widely used and researched medications used in cancer chemotherapy [12]. They are derived from the Streptomyces bacteria. Anthracyclines work by three different mechanisms: (1) intercalating between base pairs of the DNA/RNA strand to inhibit DNA and RNA synthesis, which stops the replication of quickly proliferating cancer cells; (2) inhibiting topoisomerase II to prevent the relaxing of supercoiled DNA, which stops DNA transcription and replication; and (3) producing iron-mediated free oxygen radicals to harm DNA and cell membranes [12,13].

To improve the anti-cancer activity, anthracycline combinations were made, such as doxorubicin or epirubicin with cyclophosphamide; doxorubicin, cyclophosphamide, and fluorouracil; and epirubicin with cyclophosphamide and fluorouracil. In comparison to single-agent regimens or combinations not based on anthracyclines, these regimens are both more active and toxic [9].

In addition, taxane-based regimens, which include paclitaxel (Taxol) and docetaxel (Taxotere), disrupt the microtubules' functions which are essential for cell division, so they are known as mitotic inhibitors. As compared to anthracyclines, taxanes have reduced bioavailability [14].

Taxanes and anthracyclines typically do not produce overlapping toxicities with existing therapies. An anthracycline/taxane

combination's overall increased toxicity may be compensated by its significantly higher therapeutic benefits [15].

Additionally, in multidrug-resistant (MDR) tumors, some multidrug regimens without anthracyclines or taxanes show high response rates. For instance, combining the nontaxane Ixabepilone with capecitabine leads to a longer progression-free survival than capecitabine by itself. For the treatment of metastatic breast cancer, another combination regimen is cyclophosphamide, methotrexate, and fluorouracil [16-18].

Table 1: Mixtures of non-specific small molecule drugs used in chemotherapy. OS stands for overall survival, PFS is an acronym for progression-free survival, RFS represents replace-free survival, RR is short for response rate, and TTP denotes time to progression [11].

Classes	Combination	Advantages	Disadvantages
Anthracycline-based	Doxorubicin or epirubicin + Cyclophosphamide Doxorubicin or epirubicin + Fluorouracil	Improved RR	No significant difference in time to progression or survival
Taxane-based	Doxorubicin or Gemcitabin + Paclitaxel Doxorubicin or Capecitabin + Docetaxel	Improved RR, PFS, TTP, and OS	More hematologic and non-hematologic toxicity, cardiotoxicity
Other combinations	Ixabepilone + Capecitabine Cyclophosphamide + Methotrexate + Fluorouracil	Improved RR and TTP in heavily pretreated patients Improved RR, RFS, and OS	Peripheral neuropathy Rapid bone loss

Immunotherapy Combinations

Another effective therapy for cancer treatment is immunotherapy. Although immunotherapy has been used to treat a variety of tumors such as multiple myeloma, pancreatic, ovarian, and skin cancer, it is less frequently utilized than

standard therapies and surgery. Though immunotherapy is sometimes effective, not all patients benefit from it [19].

Recently, the combined drug therapy (CDT) strategy has been widely used for immunotherapy checkpoint inhibitors to effectively target triple-negative breast cancer (TNBC) [19]. According to a study, the combination of the doxorubicin-loaded cyclic octapeptide liposomes and the mTOR inhibitor rapamycin prevented the production of hypoxia-inducible factor-1 alpha (HIF-1α) in TNBC cells [20]. The progression-free survival (PFS) of TNBC patients significantly improved when chemotherapy and phosphoinositide 3-kinase (PI3K)/AKT/mTOR inhibition were combined [21]. Another study revealed that TNBC cells' ability to activate tumor-infiltrating T lymphocytes was significantly boosted by the combination of suppression of cyclin-dependent kinase 4/6 (CDK4/6) and PI3Kα [22] (Figure 1).

Figure 1: The figure illustrates the various phases of the cancer immunity cycle, our body's innate defense mechanism against cancer. The cycle initiates

with the release of tumor antigens from cancer cells. Dendritic cells capture these antigens and journey to the lymph nodes to present them to T cells. Upon antigen presentation, T cells activate and return to the tumor to eliminate cancer cells. The figure also highlights potential disruptions to the cancer immunity cycle, such as loss of tumor antigens, diminished MHC presentation, an immunosuppressive tumor microenvironment (TME), and immune cell dysfunction. Furthermore, the diagram outlines potential therapeutic strategies to enhance the immune response against cancer. These include cancer vaccines, anti-PD1/PD-L1 therapy, and adoptive cell transfer [23].

Chemo-Immunotherapy Combinations

The combination of chemotherapy and immunotherapy (chemo-immunotherapy) explores the hypothesis that combination therapy may act synergistically against different cancers. Immunotherapy's ability to elicit particular immune responses has a significant prognostic and predictive impact on cancer patients receiving chemotherapy in these combination systems. While this is happening, chemotherapy can improve immunotherapy by increasing tumor cells' susceptibility to the cytotoxic effects of T-lymphocytes (CTLs) and decreasing immunosuppression by removing regulatory T cells (Tregs) and myeloid-derived suppressor cells (MDSCs) [24].

According to a number of results from clinical trials, atezolizumab (programmed cell death-ligand 1 (PD-L1) antibody) and pembrolizumab (PD-1 antibody) are both promising immunotherapies when used in conjunction with chemotherapy as a treatment for metastatic and advanced TNBC [25-30].

Immunotherapy-Hormone Therapy Combinations

Also, according to a few studies, the combination of immunotherapy with endocrine or hormone therapy appears promising. In a recent trial, two patients with metastatic HR-positive breast cancer benefited from the combination of antiestrogen medications (letrozole or tamoxifen) plus immunotherapy (pembrolizumab) [31]. The patients displayed greater T-cell receptor diversity following treatment, which is

reportedly associated with a better prognosis after immunotherapy. Although the study was modest and the research is still in its early phases, larger sample sizes are needed to corroborate these findings [31].

In patients with estrogen receptor (ER)-positive metastatic breast cancer, first-line salvage hormone treatment (HT) is combined with recombinant interferon-beta/interleukin-2 as immunotherapy. Multiple types of solid and hematological cancers have been treated with recombinant interleukin-2 (IL-2), which can boost lymphocytes (mainly natural killer cells) and lymphokine-activated killer (LAK) cells [32-34].

Moreover, previous studies in which aromatase inhibitors (Letrozole or Anastrozole) or Fulvestrant were used as endocrine therapy combined with CDK 4/6 inhibitors (such as Palbociclib or Abemaciclib) were proven to increase endocrine sensitivity in patients with HR+, HER2-advanced, or metastatic breast cancer. This combination is more effective than endocrine therapy alone; however, not all are successful [35].

Gene Therapy-Chemotherapy Combinations

Gene therapy, which involves delivering functional DNA or RNA to suppress undesirable gene expression or downregulate disordered genes, has recently been used to supplement chemotherapy in the treatment of cancer. Due to their dissimilar physicochemical characteristics, co-administration of a medication and gene is extremely difficult. Plasmid DNA (pDNA), small interfering RNA (siRNA), and microRNA (miRNA) have been added to these combinational systems to mix with chemotherapy medicines [10].

Chemotherapy combined with siRNA-based gene therapy has the potential to significantly improve cancer treatment over chemotherapy alone. The effect of siRNA in sequence-specific gene silencing has a synergetic apoptotic effect with chemotherapy. For example, using cationic micelles, co-delivery of SN-38 and human vascular endothelial growth factor (VEGF)-targeted siRNA (siVEGF) was accomplished [36]. Before

complexing with a drug-loaded micelle, the siVEGF was attached to a Polyethylene Glycol (PEG) chain to produce siRNA-PEG to increase the stability and lengthen the retention duration of siRNA in the blood circulation. The SN-38-loaded siRNA-PEG micelleplex provided synergistic therapeutic effects by passively targeting the tumor while simultaneously facilitating VEGF silencing and chemotherapy [36].

Due to the increased therapeutic results, miRNA-based gene therapy combined with chemotherapy is currently the subject of extensive research. Apoptosis induction, blocking of autophagy, reversal of the epithelial-to-mesenchymal transition (EMT), inhibition of tumor angiogenesis, and downregulation of ATP-binding cassette (ABC) transporters are all benefits of this therapy [10]. One method of miRNA-based cancer therapy involves using miRNA mimics to directly upregulate tumor-suppressive miRNAs, which have the potential to reprogram cancer cells by building RNA-induced silencing complexes.

Conclusion

In conclusion, the multifaceted landscape of breast cancer treatment demands innovative approaches to optimize therapeutic outcomes while minimizing toxicity and recurrence. The exploration of drug combinations, spanning traditional chemotherapy, immunotherapy, and gene therapy, unveils a promising horizon for tailored interventions. Combinatorial strategies, such as anthracycline and taxane regimens, showcase enhanced efficacy, while immunotherapy combinations and chemo-immunotherapy unveil novel synergies against metastatic breast cancer. Furthermore, the integration of gene therapy, employing siRNA and miRNA, underscores the potential for sequence-specific gene silencing and apoptosis induction. This comprehensive overview underscores the evolving paradigm in breast cancer treatment, emphasizing the pivotal role of combination therapies in shaping more effective, individualized, and less toxic interventions for diverse stages and subtypes of the disease. As challenges persist, continuous refinement of drug utilization and administration remains paramount for advancing the field and realizing the potential of personalized treatments in the future.

References

1. Burguin A, Diorio C, Durocher F. Breast Cancer Treatments: Updates and New Challenges. J Pers Med. 2021; 11: 808.
2. Guo L, Kong D, Liu J, Zhan L, Luo L, et al. Breast cancer heterogeneity and its implication in personalized precision therapy. Experimental Hematology & Oncology. 2023; 12: 3.
3. Castelo-Branco L, Morgan G, Prelaj A, Scheffler M, Canhão H, et al. Challenges and knowledge gaps with immune checkpoint inhibitors monotherapy in the management of patients with non-small-cell lung cancer: a survey of oncologist perceptions. ESMO Open. 2023; 8: 100764.
4. Song K, Farzaneh M. Signaling pathways governing breast cancer stem cells behavior. Stem Cell Research & Therapy. 2021; 12: 245.
5. Sambi M, Bagheri L, Szewczuk MR. Current Challenges in Cancer Immunotherapy: Multimodal Approaches to Improve Efficacy and Patient Response Rates. Journal of Oncology. 2019; 2019: e4508794.
6. Combinatorial Approaches for Cancer Treatment: from Basic to Translational Research | Frontiers Research Topic [Internet]. 2023. Available online at: https://www.frontiersin.org/research-topics/16925/combinatorial-approaches-for-cancer-treatment-from-basic-to-translational-research
7. Cerrato A, Mattheolabakis G, Spano D. Editorial: Combinatorial Approaches for Cancer Treatment: From Basic to Translational Research. Frontiers in Oncology [Internet]. 2022; 12. Available online at: https://www.frontiersin.org/articles/10.3389/fonc.2022.842114
8. Bayat Mokhtari R, Homayouni TS, Baluch N, Morgatskaya E, Kumar S, et al. Combination therapy in combating cancer. Oncotarget. 2017; 8: 38022–38043.
9. Fisusi FA, Akala EO. Drug Combinations in Breast Cancer Therapy. Pharm Nanotechnol. 2019; 7: 3–23.
10. Qin SY, Cheng YJ, Lei Q, Zhang AQ, Zhang XZ. Combinational strategy for high-performance cancer chemotherapy. Biomaterials. 2018; 171: 178–197.
11. Lee JH, Nan A. Combination Drug Delivery Approaches in

Metastatic Breast Cancer. Journal of Drug Delivery. 2012; 2012: e915375.
12. Avendaño López C, Menendez JC. DNA Intercalators and Topoisomerase Inhibitors. In: Medicinal Chemistry of Anticancer Drugs. 2008; 199–228.
13. Yaqub F. Mechanism of action of anthracycline drugs. The Lancet Oncology. 2013; 14: e296.
14. Lai JI, Chao TC, Liu CY, Huang CC, Tseng LM. A systemic review of taxanes and their side effects in metastatic breast cancer. Frontiers in Oncology [Internet]. 2022; 12. Available online at: https://www.frontiersin.org/articles/10.3389/fonc.2022.940239
15. Radaideh SM, Sledge GW. Taxane vs. taxane: is the duel at an end? A commentary on a phase-III trial of doxorubicin and docetaxel versus doxorubicin and paclitaxel in metastatic breast cancer: results of the ERASME 3 study. Breast Cancer Res Treat. 2008; 111: 203–208.
16. Roché H, Conte P, Perez EA, Sparano JA, Xu B, et al. Ixabepilone plus capecitabine in metastatic breast cancer patients with reduced performance status previously treated with anthracyclines and taxanes: a pooled analysis by performance status of efficacy and safety data from 2 phase III studies. Breast Cancer Res Treat. 2011; 125: 755–765.
17. Khan M, Torchilin V. Recent Trends in Nanomedicine-Based Strategies to Overcome Multidrug Resistance in Tumors. Cancers. 2022; 14: 4123.
18. Thomas ES, Gomez HL, Li RK, Chung HC, Fein LE, et al. Ixabepilone Plus Capecitabine for Metastatic Breast Cancer Progressing After Anthracycline and Taxane Treatment. Journal of Clinical Oncology [Internet]. 2016. Available online at: https://ascopubs.org/doi/pdf/10.1200/JCO.2007.12.6557
19. Wang Y, Minden A. Current Molecular Combination Therapies Used for the Treatment of Breast Cancer. International Journal of Molecular Sciences. 2022; 23: 11046.
20. Dai W, Yang F, Ma L, Fan Y, He B, et al. Combined mTOR inhibitor rapamycin and doxorubicin-loaded cyclic octapeptide modified liposomes for targeting integrin α3 in

triple-negative breast cancer. Biomaterials. 2014; 35: 5347–5358.
21. Ganesan P, Moulder S, Lee JJ, Janku F, Valero V, et al. Triple-negative breast cancer patients treated at MD Anderson Cancer Center in phase I trials: improved outcomes with combination chemotherapy and targeted agents. Mol Cancer Ther. 2014; 13: 3175–3184.
22. Teo ZL, Versaci S, Dushyanthen S, Caramia F, Savas P, et al. Combined CDK4/6 and PI3Kα Inhibition Is Synergistic and Immunogenic in Triple-Negative Breast Cancer. Cancer Res. 2017; 77: 6340–6352.
23. Zhu S, Zhang T, Zheng L, Liu H, Song W, et al. Combination strategies to maximize the benefits of cancer immunotherapy. J Hematol Oncol. 2021; 14: 1–33.
24. Bailly C, Thuru X, Quesnel B. Combined cytotoxic chemotherapy and immunotherapy of cancer: modern times. NAR Cancer. 2020; 2: zcaa002.
25. Schmid P, Cortes J, Dent R, Pusztai L, McArthur H, et al. Event-free Survival with Pembrolizumab in Early Triple-Negative Breast Cancer. N Engl J Med. 2022; 386: 556–567.
26. Cortes J, Rugo HS, Guo Z, Karantza V, Schmid P. Pembrolizumab plus chemotherapy in triple-negative breast cancer - Authors' reply. Lancet. 2021; 398: 24–25.
27. Schmid P, Salgado R, Park YH, Muñoz-Couselo E, Kim SB, et al. Pembrolizumab plus chemotherapy as neoadjuvant treatment of high-risk, early-stage triple-negative breast cancer: results from the phase 1b open-label, multicohort KEYNOTE-173 study. Ann Oncol. 2020; 31: 569–581.
28. Cortes J, Cescon DW, Rugo HS, Nowecki Z, Im SA, et al. Pembrolizumab plus chemotherapy versus placebo plus chemotherapy for previously untreated locally recurrent inoperable or metastatic triple-negative breast cancer (KEYNOTE-355): a randomised, placebo-controlled, double-blind, phase 3 clinical trial. The Lancet. 2020; 396: 1817–1828.
29. Schmid P, Adams S, Rugo HS, Schneeweiss A, Barrios CH, et al. Atezolizumab and Nab-Paclitaxel in Advanced Triple-Negative Breast Cancer. N Engl J Med. 2018; 379: 2108–2121.
30. Mittendorf EA, Zhang H, Barrios CH, Saji S, Jung KH, et al.

Neoadjuvant atezolizumab in combination with sequential nab-paclitaxel and anthracycline-based chemotherapy versus placebo and chemotherapy in patients with early-stage triple-negative breast cancer (IMpassion031): a randomised, double-blind, phase 3 trial. Lancet. 2020; 396: 1090–1100.

31. Wu D, Tang S, Ye R, Li D, Gu D, et al. Case Report: Long-Term Response to Pembrolizumab Combined With Endocrine Therapy in Metastatic Breast Cancer Patients With Hormone Receptor Expression. Front Immunol. 2021; 12: 610149.
32. Nicolini A, Rossi G, Ferrari P, Morganti R, Carpi A. A new immunotherapy schedule in addition to first-line hormone therapy for metastatic breast cancer patients in a state of clinical benefit during hormone therapy. J Mol Med (Berl). 2020; 98: 375–382.
33. Nicolini A, Carpi A, Ferrari P, Biava PM, Rossi G. Immunotherapy and Hormone-therapy in Metastatic Breast Cancer: A Review and an Update. Curr Drug Targets. 2016; 17: 1127–1139.
34. Albertini MR, Gibson DF, Robinson SP, Howard SP, Tans KJ, et al. Influence of estradiol and tamoxifen on susceptibility of human breast cancer cell lines to lysis by lymphokine-activated killer cells. J Immunother (1991). 1992; 11: 30–39.
35. Gao JJ, Cheng J, Bloomquist E, Sanchez J, Wedam SB, et al. CDK4/6 inhibitor treatment for patients with hormone receptor-positive, HER2-negative, advanced or metastatic breast cancer: a US Food and Drug Administration pooled analysis. Lancet Oncol. 2020; 21: 250–260.
36. Lee SY, Yang CY, Peng CL, Wei MF, Chen KC, et al. A theranostic micelleplex co-delivering SN-38 and VEGF siRNA for colorectal cancer therapy. Biomaterials. 2016; 86: 92–105.

Book Chapter

Targeting Signaling Pathways for TNBC Treatment

Zeinab El Dor[1#], Berlant Shakra[1#], Zeinab Al Dirani[1#], Zahraa Salhab[1#], Mohammad Fayyad-Kazan[2], Rawan Issa[1], Farah A. Farran[1], Mariam Hamze[1], Chourouk Joumaa[1], Mohamad El Saheli[3], Ghinwa Osman[1], Samah Al Zein[1], Ali Bannout[1], Ritaj Fakih[1], Katia Smeha[1], Jana Zaraket[1], Zahra Farroukh[1], Leen Fadlallah[1], Ghida Temraz[1], Ali Al Khatib[4], Belal Osman[4], Ghinwa Itani[1], Marwa Bazzi[1], Khalid Omama[1], Diana El Hosni[1], Mohammad Shkeir[1], Malak El Itawi[1], Malak AlMazbouh[1], Douaa Khreis[1†], Fatima Dandash[1†], Hussein Fayyad-Kazan[1†]

[1]Lebanese University, Faculty of Science (I), Biology and Biochemistry Departments, Hadath, Beirut, Lebanon
[2]Department of Natural and Applied Sciences, College of Arts and Sciences, The American University of Iraq-Baghdad (AUIB), Baghdad 10001, Iraq
[3]Department of Biological Sciences, Faculty of Science, Beirut Arab University, Debbieh, Lebanon
[4]American University of Beirut, Faculty of Medicine, Beirut, Lebanon

[#]Contributed equally to this work
[†]Joint senior co-authors

***Corresponding Author:** Hussein Fayyad-Kazan, Lebanese University, Faculty of Science (I), Biology and Biochemistry Departments, Hadath, Beirut, Lebanon

Published **September 02, 2024**

How to cite this book chapter: Zeinab El Dor, Berlant Shakra, Zeinab Al Dirani, Zahraa Salhab, Mohammad Fayyad-Kazan, Rawan Issa, Farah A. Farran, Mariam Hamze, Chourouk Joumaa, Mohamad El Saheli, Ghinwa Osman, Samah Al Zein, Ali Bannout, Ritaj Fakih, Katia Smeha, Jana Zaraket, Zahra

Farroukh, Leen Fadlallah, Ghida Temraz, Ali Al Khatib, Belal Osman, Ghinwa Itani, Marwa Bazzi, Khalid Omama, Diana El Hosni, Mohammad Shkeir, Malak El Itawi, Malak AlMazbouh, Douaa Khreis, Fatima Dandash, Hussein Fayyad-Kazan. Targeting Signaling Pathways for TNBC Treatment. In: Immunology and Cancer Biology. Hyderabad, India: Vide Leaf. 2024.

Abstract

Triple negative breast cancer (TNBC) is the breast cancer subtype with the poorest prognosis, mainly affecting women of smaller age. It is characterized by high heterogeneity, reflected by the presence of different TNBC subtypes that show distinct tumor grade and treatment sensitivity. To date, chemotherapies remain a primary treatment option for TNBC patients, however, patients usually develop resistance to the treatment and are prone to relapse less than 5 years following the initial diagnosis. Cell survival and proliferation signaling pathways like the PI3K/AKT/mTOR, NFκB, Wnt, and EGFR are activated in TNBC. In this chapter, we provide a comprehensive analysis of the signaling pathways aberrantly activated in TNBC and their targeting strategies, either alone or in combination with other targeted- or chemo-therapies.

Keywords

TNBC; Chemotherapy Resistance; Relapse; Signaling Pathways; Targeted Therapies

Introduction

Breast cancer refers to an abnormal condition in the breast tissues and is mostly formed in the milk ducts or lobules. Ductal carcinoma refers to cancer developed in the ducts, while lobular carcinoma is formed in the mammary lobules [1,2]. According to the World Health Organization, at the end of 2020, 7.8 million females contracted breast cancer within the previous five-year period, establishing it as the most widespread form of cancer in females on a global scale. This affliction manifests across all nations, affecting females of all ages after the onset of puberty, albeit with a greater propensity for occurrence in advanced stages of life [3,4].

Triple-negative breast cancer (TNBC) is an aggressive form of breast cancer that lacks estrogen and progesterone receptors (ER and PR) expression, and does not carry an amplification of human growth factor receptor 2 (HER2) gene [5]. TNBC accounts for approximately 12–17% of all breast cancers and demonstrates high recurrence rates [6]. TNBC exhibits a more aggressive clinical behavior compared to other breast cancer subtypes. They have distinct metastatic patterns and are associated with a poor prognosis [7]. TNBC accounts for about 24% of newly diagnosed breast cancers, and their incidence continues to rise [8]. In 2018 alone, there were approximately 2,088,849 reported cases of TNBC globally, making it a prevalent cancer among women [9]. TNBC 5-year survival rate is around 65% for regional tumors and only 11% for cases of metastatic disease [10].

TNBC Prognosis

Patients with TNBC have a poor prognosis [11]. Unlike other subtypes, TNBC is more commonly observed in pre-menopausal women during early life. Furthermore, TNBC exhibits a more aggressive expression profile, characterized by high levels of p54 and Ki67, as well as low Bcl-2 expression. Tumors are often large and have a high nuclear mitotic grade [12]. Numerous studies have shown that TNBC patients have lower recurrence-free survival rates compared to non-TNBC patients. For instance,

the 4-year survival rate for TNBC patients is 85.5%, whereas it is 94.2% for non-TNBC patients [12]. Additionally, tumor recurrence tends to occur earlier in TNBC patients compared to non-TNBC patients, with an average time of 1.2 years. Additionally, TNBC patients have a higher risk of tumor recurrence and death compared to other subtypes. In fact, the hazard ratio for developing TNBC tumor recurrence is 4.2 in comparison to other cancers [13]. For triple-positive breast cancer, the 5-year survival rate is 91%, while for TNBC and HR-positive/HER2-negative cancers, it is 81% and 94%, respectively [14].

TNBC Risk Factors

The exact causes of TNBC are not fully understood; however, several risk factors have been identified [15,16]. These risk factors can be divided into modifiable and non-modifiable risk factors [16].

Modifiable Risk Factors

The most common modifiable risk factors are alcohol intake and obesity [16,17].

Alcohol Intake

Although alcohol is an established breast cancer risk factor, the underlying mechanisms remain unclear [18]. Biological mechanisms and a causal relationship between alcohol consumption and the development of cancer have been reported for laryngeal, pharyngeal, esophageal, liver, colorectal, and breast cancer [17]. Alcohol increased the risk of TNBC by 7-10% per each unit of alcohol consumed daily. This association between alcohol consumption and the development of BC is modified by the body mass index (BMI) [17]. Moreover, alcohol promotes TNBC cell proliferation, migration, and invasion through the induction of oxidative stress and the activation of NF-κB signaling [18].

Obesity

According to several epidemiological studies, obesity is a potential risk factor for TNBC, especially in premenopausal women. Women older than 50 years of age with higher BMI are at an increased risk of TNBC and lymph node metastasis than those with low BMI [16,19]. Obesity also increases breast cancer invasion, and migration, as well as cancer, stem cell enrichment, and mesenchymal stem cell dysregulation in the tumor microenvironment, which increases the risk of TNBC [20].

Drugs

Prolonged use of hormonal replacement therapy for more than 5-7 years and the use of certain selective antidepressants, such as paroxetine, tricyclic, and serotonin inhibitors, have been linked to an increased risk of breast cancer [21]. The antibiotic tetracycline has also been reported to raise the risk of breast cancer [22].

Non-Modifiable Risk Factors

Age [SSH]

According to Donepudi *et al*, more than 50% of breast cancers affect individuals over 50 years old. According to Ukasiewicz *et al*, the cancer risk rises with age as follows: 1.5% risk at age 40, 3% risk at age 50, and more than 4% risk at age 70. Additionally, there is a connection between age and cancer subtype. For instance, TNBC is typically diagnosed in patients under the age of 40, while the luminal subtype is more frequent in patients aged 70 and above [16].

Gender

Women are much more likely than men to develop TNBC. TNBC represents just 1% of males who develop breast cancer overall, as opposed to 11% of women [24].

Ethnicity

In comparison to women of other ethnicities, African American women have a higher incidence rate and a worse prognosis of TNBC than women of other ethnicities. Furthermore, women of Hispanic/Latin descent, when compared to non-Hispanic white women, have a greater incidence and worse prognosis of TNBC. Asian women experience a lower incidence of TNBC than women from other racial or ethnic groups [25,26].

Genetic Factors

Genetic mutations play a significant role in TNBC, particularly in genes such as *BRCA1* and *BRCA2* [27]. Other mutations, including TP53, CDH1, PTEN, STK11, and XRCC2, are associated with both breast cancer and TNBC [28-30]. Interestingly, BRCA1 mutated tumors exhibit similarities to the TNBC subtype, while BRCA2 mutations are more closely aligned with luminal-like breast cancers, specifically the Luminal B subtype [31]. Estimates of the probability of TNBC in women with BRCA1 mutations range from 50 to 80% [6,32].

Family History

A family history of breast cancer is one of the major risk factors for developing the disease, including TNBC. Approximately 13-19% of diagnosed breast cancer patients have a close relative who has also had breast cancer [33]. Having a family history of ovarian cancer, particularly with BRCA1 and BRCA2 mutations, also increases the risk [34].

TNBC Subtypes

TNBC is a heterogeneous disease that can be classified into distinct molecular subtypes based on gene expression profiling (Figure 1). The identification and characterization of TNBC subtypes have important implications for prognosis, treatment selection, and the development of targeted therapies.

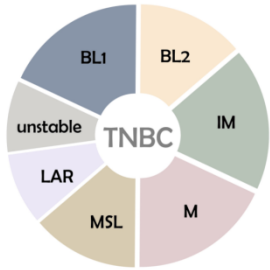

Types	Characteristics	Cell lines
BL1	Cellular proliferation, cell cycle, DNA repair	HCC2157, MDA-MB-468, HCC38, HCC1937
BL2	Growth factor, myoepithelial markers	HCC1806, SUM149PT, CAL851
IM	Immune mediated signaling	HCC1187, DU4475
M	EMT and differentiation	BT549, CAL51, CAL-120
MSL	MET, angiogenesis, differentiation and stemness	MDA-MB-157, MDA-MB-436, MDA-MB-231, SUM159
LAR	Hormone signaling, luminal gene up-regulation	MDA-MB-453, SUM185, CAL148, MFM223

Figure 1: TNBC subtypes and cell line models. TNBC gene expression subtypes are linked to distinct molecular features. TNBC subtypes include BL1 (basal-like 1), BL2 (basal-like 2), IM (immunomodulatory), ML (mesenchymal-like), MSL (mesenchymal stem-like), and LAR (luminal androgen receptor) [35].

Lehmann et al proposed a classification system based on gene expression patterns. Initially, they identified six molecular subtypes: basal-like 1 (BL1), basal-like 2 (BL2), immunomodulatory (IM), mesenchymal (M), mesenchymal stem-like (MSL), and luminal androgen receptor (LAR) [36]. The classification was then refined and excluded the MSL and IM subtypes [37].

Basal-like 1

The BL1 subtype is associated with a high proliferation rate and a more aggressive clinical phenotype [38]. BL1 tumors exhibit high expression of genes associated with cell proliferation and DNA repair pathways [39]. Studies have shown that BL1 tumors have a higher likelihood of responding to chemotherapy. This subtype is often associated with a better response to neoadjuvant chemotherapy and a higher rate of pathological complete response (pCR) [38]. However, BL1 tumors may also have a higher risk of relapse and metastasis [38].

Basal-like 2

The BL2 subtype is associated with more aggressive clinical behavior and poorer prognosis compared to other TNBC subtypes [40]. BL2 tumors often have high histological grades,

frequent nodal metastases, and a higher risk of recurrence and metastasis [40]. These tumors are typically characterized by a high proliferation rate and exhibit gene expression patterns associated with cell proliferation and DNA repair pathways [40]. In addition, the BL2 subtype has been associated with specific immunologic features. Studies have shown that TNBC, including the BL2 subtype, exhibits strong immunogenicity and enrichment of immune cell activities and pathways [41]. This suggests that immunotherapy may be a promising strategy for treating BL2 tumors, given the limited therapeutic options currently available for TNBC [41].

Mesenchymal Subtype

The mesenchymal subtype of TNBC is characterized by the expression of genes associated with mesenchymal features, such as extracellular matrix remodeling, cell migration, and invasion [37,42,43]. This subtype is often associated with a poor prognosis and resistance to chemotherapy [37,42]. It has been shown to have a low pathological complete response (pCR) rate to neoadjuvant chemotherapy [42].

LAR Subtype

The LAR subtype is defined by the expression of androgen receptor (AR) [44]. It is characterized by the expression of luminal markers, such as AR and luminal cytokeratins, despite being ER-negative [45]. It is associated with older age at diagnosis, lower histologic grade, lower tumor stage, and lower proliferation index [44]. It has also been shown to have a higher mutational burden, with enriched mutations in genes such as PIK3CA, AKT1, and CDH1 [46]. Additionally, the LAR subtype has been associated with a worse prognosis compared to other TNBC subtypes [46]. In terms of treatment response, the LAR subtype has a differential response to neoadjuvant chemotherapy. Combined analysis of TNBC patients demonstrated that the LAR subtype had a lower rate of pCR compared to other subtypes [37]. However, the LAR subtype has been found to be sensitive to androgen receptor-targeted therapies, suggesting potential therapeutic options [44].

Signaling Pathways Deregulated in TNBC

NF-κB Pathway

NF-κB is a transcription factor that is critical for the control of inflammation, cell proliferation, and cell line survival [47-51] (Figure 2). The NF-kB superfamily of TFs was identified in 1986 and consists of NF-κB1 (p50), NF-κB (p52), ReIA (p65), ReIB, and C-ReI [52-54]. The N-terminus contains ReI, which binds DNA, whereas the C-terminus interacts with other TFs [55, 56]. By complexing with inhibitor subunits IKB-α, -β, and -γ, NF-κB exists in the cytoplasm as an inactive form [57-59].

Cell survival, stress response, proliferation, differentiation, and apoptosis are all regulated by the NF-κB signaling pathway [60-64]. The IκB kinases IKKα, IKKβ, and IkKε mediate NF-κB activation, which leads to nuclear localization of NF-κB and consequent transcriptional activation [65]. The NF-κB pathway allows for the tight regulation of a variety of biological activities through the operation of both canonical and non-canonical pathways [66]. NF-κB can be activated by a variety of stimuli and interacts with other signaling pathways [53,65,67-69]. NF-kB promotes transcription of multiple cytokines (e.g, TNF-α, IL-1b, IL-6, IL2), chemokines (IL-8), macrophage inflammatory protein-1a (MIP-1a), cell adhesion molecules (e.g, B. E-selectin, ICAM-1, VCAM-1) and inducible pro-inflammatory enzymes such as NO synthase II and cyclooxygenase-2. Furthermore, increased NF-kB activity is associated with improved cancer cell survival by inhibiting apoptosis in breast and pancreatic cancer [70], through transcriptional regulation of anti-apoptotic proteins (IAPs, FLIP, and Bcl-XL) and cyclin D1 [71].

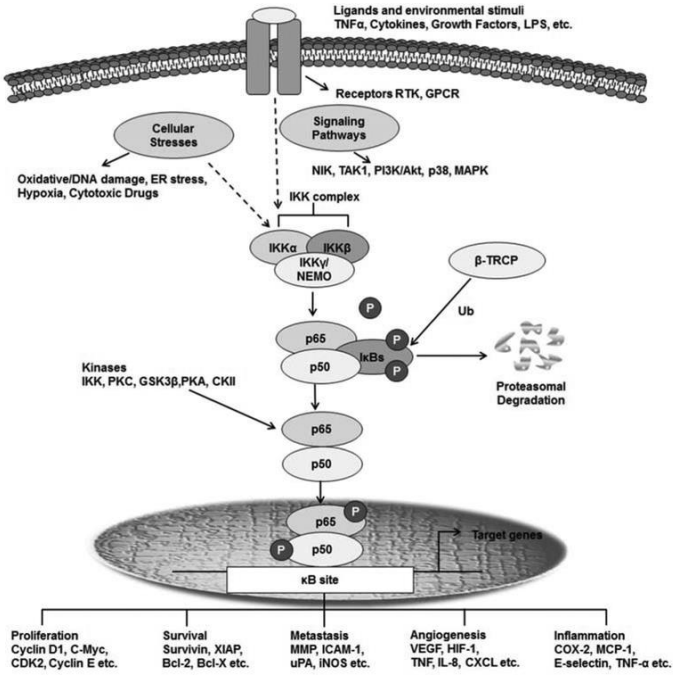

Figure 2: Diagram illustrating the upstream physiological and pathological stimuli and kinases responsible for NFκB activation in the cytoplasm, along with representative transcriptional activities in the nucleus [72].

TNF-α stimulates the CS pathway, which is activated by IκB proteins (IκBα, IκBβ, IκBε, or IκBγ) in response to UV radiation, cytokines, growth factors, bacteria, and mitogens [73]. The binding of TNFα to its receptor TNFR1 recruits a series of proteins including TRAF2, TRADD, and RIP. TRAF2 binds the complex IKKα, IKKβ, and NEMO to connect with TNFR1 and activates IKKβ, resulting in IκBα phosphorylation [74,75]. The consequent ubiquitination of IκBα frees NF-κB (p50-p65 heterodimer) in the cytoplasm leading to its translocation to the nucleus, where it binds to NF-κB sites on DNA and triggers IL-6 and chemokine production. The NCS route, on the other hand, is activated by growth factors, viruses, stress stimuli, and lipopolysaccharides. CD40, a TNF receptor, activates RelB/NF-κB 2, which subsequently recruits TRAF2-TRAF3, connects c-IAP to NIK, and causes NIK phosphorylation followed by destruction via c-IAP. NIK stimulates IKKα and degrades p100,

releasing p52 and RelB, which move to the nucleus and promote chemokine gene expression [76,77].

NF-κB has primarily been associated with the production of many pro-inflammatory proteins such as cytokines, chemokines, and adhesion molecules thus involving in the regulation of inflammatory response. Tumors can boost NF-κB activity by enhancing the production of cytokines from stromal cells and fibroblasts in the tumor microenvironment [78,79].

NF-κB is a key contributor to cancer development and chemoresistance, according to numerous studies [66,80-82]. Several studies report the aberrant constitutive expression of NF-κB subunits in breast tumors [83-85]. It has been shown that NF-κB activation promotes the growth and spread of breast cancer [86-88]. TNBC is characterized by NF-κB overexpression at the protein level [78,79], and shows an elevated level of permanently active NF-κB signaling [89]. It has been shown that NF-κB is important for cell survival and proliferation in the TNBC [90].

The majority of cytokines responsible for anchorage-independent cell growth are synthesized by activating NF-κB. In addition, acetyltransferase p300 recruitment and NF-κB acetylation via RelA modification prolong NF-κB retention in the nucleus, increasing its tumorigenicity. NF-κB increases IL-6 production and results in the maintenance of this positive loop, exacerbating the problem [91].

Analysis of TNBC tissue expression in comparison to nearby normal breast tissue revealed that NF-κB is a critical regulator of the molecular TNBC phenotype [92]. Moreover, in an immune-activated subtype of TNBC, Ikkε in conjunction with Jak/Stat signaling may increase cytokine activation and carcinogenesis. In various situations, Ikkε collaborates with either MEK or non-canonical NF-κB to drive the growth of TNBC cells [93].

PI3K/AKT Pathway and Its Activation in TNBC

The PI3-kinase (PI3K) signaling pathway in breast cancer plays a crucial role in relating receptor tyrosine kinase (RTK) signaling to the control of cell growth and survival, and its molecular mechanisms [94]. Protein kinase B (commonly known as AKT) and mammalian target of rapamycin (mTOR) are the most important effectors downstream of PI3K. Multiple phosphatases, including phosphatase and tensin homologue (PTEN) and inositol polyphosphate-4-phosphatase type II B (INPP4B), control the pathway. This pathway has a critical oncogenic function in cancer, interacting extensively with other canonical signaling pathways to induce tumor progression and resistance against treatments [95]. Activating events in oncogenes PIK3CA, AKT, and MTOR, as well as inactivating events in tumor suppressor genes PIK3R1, INPP4B, PTEN, TSC1, TSC2, and LKB1, all contribute to a hyperactivated PI3K pathway [96]. In TNBC, PIK3CA is the second most commonly mutated gene after TP53, with additional inactivating changes in PTEN [97] and activating mutations in AKT1. Pathway mutations/alterations are seen in 25% of primary TNBC and probably at a greater frequency in metastatic TNBC [98].

PI3KCA Activating Mutations

Phosphoinositide-3 kinases (PI3Ks) are intracellular signaling enzymes that phosphorylate the free 3-hydroxyl of phosphoinositides in the cell membrane. The various PI3Ks are typically classified into classes, with class I PI3K being the most often changed in cancer, and consisting of a heterodimer comprised of a regulatory (p85) and a catalytic (p110) subunit. The regulatory subunits (p85a and p85b) and catalytic subunits (p110a, b, c, and d) have numerous paralogues [99]. The most common activating mutations in TNBC occur in the p110a (alpha subunit encoded by PIK3CA), which is mutated in 9% of primary TNBC cases [100]. PIK3CA mutations activate alpha PI3K, resulting in increased phosphorylation and accumulation of PtdIns-3,4,5-P3 and/or PtdIns-3,4-P2 in the membrane, hence activating downstream pathways [98].

AKT1 Activating Mutations

AKT1 mutations are observed in a variety of tumor types, including breast cancer, with 2.5% of cases having a mutation leading to a single amino acid change, E17K [101]. The AKT family, which consists of three distinct isoforms (AKT1, AKT2, and AKT3), forms a node downstream of PI3K [102]. AKT signaling plays several roles including survival, cell proliferation, cell cycle control, and metabolism. An antiapoptotic function was previously demonstrated by phosphorylation and inhibition of antiapoptotic proteins such as BAD and BAX (both involved in the caspase pathway) as well as NF-kB acting as a transcriptional factor for antiapoptotic gene expression), which are turned on in response to stress and resulting in cell death [103].

Increased expression of AKT1 has been demonstrated to influence cell proliferation via S6 and cyclin D1, whereas AKT2 controls cytoskeleton components [104]. Moreover, the AKT3 isoform has been found to be notably overexpressed in TNBC at both the protein and mRNA levels, promoting cell proliferation and tumor development but not invasiveness [105]. AKT phosphorylation is greatly elevated in TNBC relative to luminal breast cancer, which is a hallmark of AKT activation in TNBC [100]. Alternative AKT activation genetic events are unknown outside of the AKT1 E17K activating mutation. Although AKT1 L52R, Q79K, and D323Hnd are uncommon mutations, they have been shown to increase AKT1 activity in comparison to the wild-type [106]. AKT2 [107] and AKT3 [108] have both been found to carry the E17K mutation. Except for AKT1 E17K, all genetic changes that activate AKT are uncommon in TNBC.

mTOR Activating Mutations

The mammalian target of rapamycin (mTOR) can give rise to two complexes mTORC1 and mTORC2. mTOR mutations are detected in just 1.8% of TCGA primary breast cancer patients, with a tiny proportion identified as probable drivers [109]. Other rare mTOR activating mutations have been discovered, such as mutations in the tumor suppressor LKB1, which upregulates mTOR and promotes downstream pathway activation [109], and mutations in the TSC1-TSC2 complex, which acts as an inhibitor

of mTORC1 and enhances mTORC2 activation [110]. Unlike genetic activation, PI3K and MAPK signaling both activate mTOR [111].

PTEN Inactivating Mutations

The Cancer Genome Atlas Networks of the comprehensive molecular landscape of breast cancer revealed that *PTEN* mutation/loss of expression affects up to 35% of basal-like TNBC. The PTEN protein functions as a tumor suppressor by dephosphorylating phosphatidylinositol (3,4,5)-trisphosphate (PIP3), which inhibits AKT and the remaining signaling cascade [112]. Lack of PTEN activates PI3K, in particular the PI3K beta (PIK3CB) isoform via its lipid kinase domain [113, 114]. Lack of PTEN at the genetic or proteomic level is associated with a higher risk of breast cancer and is related to a poor prognosis, reduced estrogen receptor expression, and overall negative phenotypes [115-117]. TNBC was related to PTEN loss in the TNBC subgroup of an African American and Hispanic/Latina women research comprising 318 patients [118]. The loss of PTEN was also related to increased tumor size, high grade, recurrence, and triple-negative phenotype in a tissue microarray of 1000 primary breast tumors from Middle Eastern ethnicity using immunohistochemistry (IHC) and fluorescence in situ hybridization [119]. PTEN mutations are common in TNBC, with 15% experiencing genetically driven loss of function [100]. Detecting which *PTEN* alterations bestow significant loss of function to be targetable and the best approach for recognizing this loss of function remains a big difficulty. Truncating and frameshift mutations, as well as homozygous deletion, are examples of targetable inactivating mutations. Single nucleotide variations, on the other hand, are often of unknown pathogenicity, with many probable passenger mutations. However, several hotspot mutations such as R130X, R233X, and R335X are also likely pathogenic [120,121].

Silencing mutations in a single wild-type allele may result in haploinsufficiency because PTEN mutants heterodimerize with the wild-type protein, creating a hypofunctional PTEN protein [122]. Epigenetic control of the promoter via methylation has also been found [123], which may inactivate the wild-type allele

in heterozygous situations, rendering PTEN activity completely inert.

INPP4B Loss

INPP4B is another phosphatase in the PI3K pathway and its knockdown leads to a boosted AKT pathway. Decreased INPP4B level, which is rarely caused by chromosomal events, is most common in basal-like breast cancer [124,125]. Instead of PIP3 dephosphorylation by PTEN, INPP4B dephosphorylates phosphatidylinositol (3,4)-bisphosphate (PIP2) [126].

The Epidermal Growth Factor Receptor (EGFR)

The epidermal growth factor receptor (EGFR) is a member of the receptor tyrosine kinase (RTK) class of cell surface receptors. The EGFR family includes four tyrosine kinase receptors (EGFR/HER1, HER2, HER3, and HER4). Following its activation upon ligand binding, EGFR forms homo- or hetero-dimers and undergoes autophosphorylation at tyrosine residues in its intracellular catalytic domains. The activation of EGFR leads to cellular proliferation, survival, angiogenesis, invasion, and metastasis. The abnormal expression of EGFR has been associated with the causation of numerous human epithelial malignancies, including breast cancer, head and neck squamous cell carcinoma, non-small cell lung cancer, colorectal cancer, pancreatic cancer, and brain cancer [127]. EGFR is overexpressed in more than 50% of TNBC patients [128]. The elevated copy number and surface expression of EGFR seem to be a prognostic predictor of poor overall survival (OS) and disease-free survival (DFS) in TNBC [129].

Targeting Signaling Pathways for TNBC Treatment

Targeting the PI3K/AKT Pathway

The mTOR pathway is aberrantly expressed in individuals with TNBC and associated with poor prognosis [130]. The PI3K/Akt/mTOR pathway contributes to cancer cell growth, proliferation, and vasculature through the initiation of a cascade of phosphorylation reactions (Figure 3). Overexpression of AKT has also been attributed to tumor metastasis and invasion [131].

The PI3K/Akt pathway culminates in the mTOR signaling cascade, which consists of two functionally different complexes, mTORC1 and mTORC2. The mTORC1 pathway increases mRNA translocation and phosphorylates various substrates necessary for anabolic activity. There are six categories of inhibitors of the PI3K/AKT/mTOR network: Pan-class I (PI3K inhibitor), isoform-selective (PI3K inhibitor), rapamycin analogs (also known as rapalogs, which include Everolimus, Temsirolimus, and Deforolimus), active site (mTOR inhibitor), Pan-PI3K/mTOR inhibitor, and AKT inhibitors [132]. In certain situations, tackling both mTOR and a specific PI3K isoform simultaneously may result in better therapeutic efficacy compared to PI3K inhibition alone.

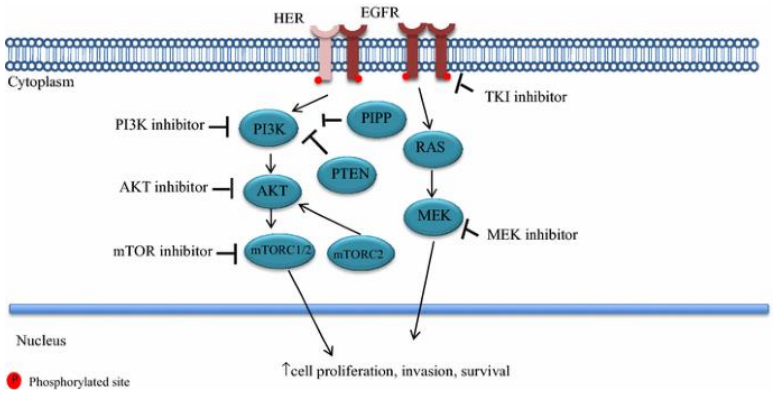

Figure 3: Possible druggable targets in the PI3K/AKT/mTOR pathway in TNBC. Activation of PI3K in the cytoplasm results from activating mutations in the α catalytic unit and/or loss of PTEN and/or PIPP. Alternatively, receptor tyrosine kinase activation occurs through homodimerization or heterodimerization with other HER family members, such as HER2. Activated EGFR initiates downstream signaling via the PI3K/AKT/mTOR and RAS-MEK pathways, promoting cell proliferation and survival. Lines with wider ends indicate the inhibitory activity of targeted therapies, while lines with arrowheads indicate the stimulatory activity of upstream molecules. ADC: for Antibody Drug Conjugate, EGFR: epidermal growth factor receptor, HER: human epidermal receptor, mTORC: mechanistic target of rapamycin complex, PTEN: for phosphatase and tensin homolog, PIPP: proline-rich inositol polyphosphate, TKI: tyrosine kinase inhibitor *[133]*.

Rapamycin and paclitaxel both affect the PI3K/AKT/mTOR pathway, thereby serving as crucial components of TNBC therapy. Despite a shortage of data supporting synergy between anti-EGFR and mTOR inhibitors, the combination of mTOR antibodies and EGFR inhibitors has shown enhanced efficacy compared with anti-mTOR treatment alone in breast cancer [134]. In TNBC patients, an innovative oral AKT inhibitor, ipatasertib, has been demonstrated to promote progression-free survival while triggering the PI3K/AKT pathway [135]. Nonetheless, novel inhibitors that can effectively target the PI3K/Akt/mTOR pathway for TNBC treatment are urgently required [136].

Targeting the NF-κB Pathway

Panepoxydone (PP)

Panepoxydone (PP), a compound isolated from Lentinus crinitus (edible mushroom), disrupts NF-kB-mediated signaling by inhibiting IkB phosphorylation [137]. The antitumor effect of PP appeared to be related to its ability to inhibit IkBa phosphorylation, with an accumulation of NF-kB in the cytoplasm. PP treatment also reduced FOXM1, vimentin, zeb1, and slug expression while increasing E-cadherin expression, like what is observed following NF-kB silencing.

NF-kB has been shown to be overexpressed in TNBC tumors and may be responsible for the tumor's aggressiveness. NF-kB plays an important role in many signaling pathways, including those involved in cancer development and progression [138]. PP shows strong anti-tumor effects on all breast cancer cells in a dose- and time-dependent manner. The mechanism of action of PP seems to involve NF-kB, which is evident through the movement of NF-kB from the nucleus to the cytoplasm. This shift is associated with a decrease in pIkB and an increase in total IkB expression across all cell lines [139].

PP treatment reduces the expression of cyclinD1 and survival, a member of the Inhibitor of Apoptosis (IAP) family that is highly expressed in most human tumors, including breast cancer [140]. Taken together, these results demonstrate the mechanisms by

which PP exerts its antitumor effects, specifically via modulation of apoptotic-related proteins and modulation of DNA repair via PARP cleavage.

Results indicate that treatment with PP has a direct effect on aggressive features of breast tumors, such as cell migration and invasion, however, as in the cytotoxicity experiments, there is differential efficacy across cell lines. PP treatment inhibited TNBC cell lines' invasiveness differently. A significant reduction in migration and invasion was observed in all TNBC cell lines [141]. Interestingly, NF-kB silencing reduces expression of FOXM1, like PP treatment, which is associated with upregulation of E-cadherin expression and downregulation of Vimentin, Slug, and Zeb1. These results indicate the potential of PP to downregulate FOXM1 and well-established mesenchymal markers as well as to induce expression of the epithelial marker E-cadherin in breast cancer cells. Taken together, these findings show that PP-induced EMT reversal occurs in breast cancer cells via FOXM1 inhibition [141].

Rh1

Studies have shown that bioactive substances can prevent BC metastasis by targeting several signaling pathways, such as EGFR and STAT, as well as regulating the production of ROS [142]. One of the minor ginsenosides and metabolites produced by the gut microbiota by Re and Rg1 is Rh1 [143]. Rh1 has several pharmacological actions, such as anti-inflammatory, anti-cancer, and antibacterial properties [144].

According to reports, STAT3 activation promotes cell invasion and migration and is associated with the upregulation of MMP2 and MMP9 or interleukin-22 expression [145]. Through phosphorylation of NF-kB p65 and forming connections with it, STAT3 facilitates the advancement of TNBC by activating a signalling pathway associated with the activation of genes linked to cancer or immune cell metastasis [146]. MMPs' gene expression was boosted by the activation of the NF-kB or STAT3 promoter, whose signals cause cancer to metastasize [147].

In line with earlier studies, it was shown that Rh1 therapy greatly reduced p-STAT3 nuclear accumulation and altered the nuclear localization and promoter activity of NF-B p65. Rh1 therapies reduced NF-B p65 phosphorylation, which was lowered by STAT3 activity inhibition caused by static treatments. Additionally, Rh1 inhibited phosphorylated p65 nuclear translocation, but STAT3 inhibition inhibited phosphorylated p65 nuclear translocation just as effectively as BAY, a particular inhibitor of NF-B activation. Additionally, static or BAY administration totally reversed the effects of Rh1-inhibited NF-B-Luc activity. The regulation of cell metastatic functions through NF-B transcriptional targets, MMP2, and MMP9 expression was achieved in this process by Rh1-induced mtROS generation, which was also engaged in the inhibition of STAT3 and NF-B activation [148].

Targeting the EGFR Pathway

EGFR is an attractive candidate for targeted therapy for TNBC, as aberrant cellular responses have been reported in 89% of TNBC patients [149]. Such dysregulation in EGFR signal transduction, which has been described in numerous cancer types, is governed by multiple molecular mechanisms, namely overexpression either due to gene amplification or epigenetic events [150] (Figure 4). EGFR overexpression has been implicated in tumour proliferation, angiogenesis, and metastasis [151]. For TNBC targeted therapy, EGFR is currently targeted using two classes of inhibitors: monoclonal antibodies (mAbs) and small-molecule tyrosine kinase inhibitors (TKIs). TKIs target the intracellular domain (ICD) of EGFR, while its extracellular domain (ECD) is targeted by mAbs [150, 151]. The latter can trigger an immune reaction in the host against the tumor, thereby enhancing the efficiency of the drug [152].

Gefitinib, an EGFR inhibitor, has been evaluated due to its potential to reduce cancer cell proliferation. Additionally, combining gefitinib with carboplatin and docetaxel has been investigated to enhance the cytotoxic effects of these chemotherapeutic agents [151]. Furthermore, clinical trials for TNBC treatment evaluated other EGFR inhibitors such as

erlotinib and lapatinib, which belong to the class of TKI, and cetuximab and panitumumab (monoclonal antibodies). However, such single-agent therapeutics have failed to yield satisfactory outcomes, urging researchers to explore combination therapy [150]. When compared to individual treatments, the combination of cetuximab with the chemotherapies carboplatin or cisplatin demonstrated better therapeutic responses in advanced TNBC cases [153]. Similarly, a tri-inhibitor combination, including gefitinib, carboplatin, and docetaxel, revealed synergistic effects, which led to improved cytotoxicity against TNBC cells [154].

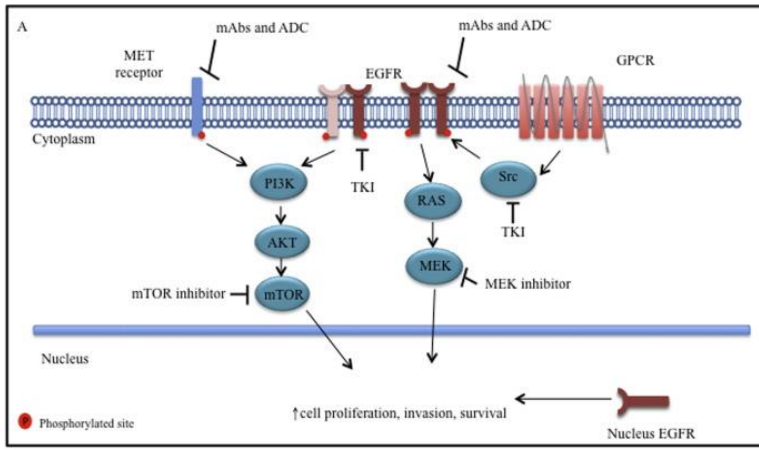

Figure 4: EGFR signal transduction pathway. The activation of the receptor tyrosine kinase happens through homodimerization or heterodimerization with other HER family members, such as HER2. Once activated, EGFR initiates downstream signaling through the PI3K–AKT–mTOR and RAS-MEK pathways, fostering cell proliferation and survival. The alternative cytoplasmic activation of the EGFR kinase domain by GPCR and the nuclear activity of EGFR is also illustrated. Lines with flat ends signify the inhibitory activity of targeted therapies, while lines with arrowheads represent the stimulatory activity of upstream molecules. Abbreviations include Antibody Drug Conjugate (ADC), Epidermal Growth Factor Receptor (EGFR), G-Protein Coupled Receptor (GPCR), Human Epidermal Receptor (HER), monoclonal antibodies (mAbs), triple-negative breast cancer (TNBC), and tyrosine kinase inhibitor (TKI) *[155]*.

Combination Therapy in TNBC

Pembrolizumab Combination with Chemotherapy

Pembrolizumab, an immune checkpoint inhibitor, has received FDA approval for the treatment of high-risk, early-stage TNBC [156]. In combination with chemotherapy, it is approved as a neoadjuvant treatment before surgery and can be continued as a single agent for adjuvant treatment after surgery. Additionally, pembrolizumab, in combination with chemotherapy, has gained regular FDA approval for locally recurrent unresectable or metastatic TNBC, specifically in tumors expressing PD-L1 (Combined Positive Score [CPS] ≥10), as determined by an FDA-approved test (Figure 5). These approvals are based on positive results from the KEYNOTE-522 trial, highlighting the efficacy of pembrolizumab in improving outcomes for TNBC patients in both early and advanced stages. This signifies pembrolizumab as a significant therapeutic option, particularly in the neoadjuvant and adjuvant settings, offering new possibilities for the treatment of TNBC [156].

Platinum/PARP Inhibitor

The first developed PARP inhibitor, nicotinamide, naturally exists in cells [157] and forms a core pharmacophore binding to the nicotinamide pocket of PARP-1 [158]. The synthetic PARP inhibitor, 3-AB, designed to mimic nicotinamide, displayed synergistic effects with genotoxic agents but had limited clinical use due to low potency (IC50=30 μM) and selectivity [159]. Multiple generations of PARP inhibitors have since been developed to enhance potency and selectivity. As of now, the Food and Drug Administration has approved three PARP inhibitors for clinical use: niraparib, rucaparib, and olaparib. Other candidates like veliparib, talazoparib, and iniparib are undergoing evaluation in preclinical studies and clinical trials [160].

Platinum compounds, widely used in chemotherapy for various cancers, create intra-strand DNA adducts, causing replication fork collapse and DNA breaks. The primary DNA lesions, intra-strand DNA crosslinks induced by platinum, are predominantly

repaired through the PARP/BER DNA repair pathway. Platinum resistance is closely associated with DNA repair pathway activity [161]. Combining a PARP inhibitor with platinum therapy has been investigated in preclinical studies across cancer types (Figure 5). Early research demonstrated that 3-AB overcame cisplatin resistance, enhancing cell cycle arrest and apoptosis [162]. Similarly, the PARP inhibitor PJ34, in combination with platinum, suppressed TNBC and hepatocellular carcinoma both in vitro and in vivo [163].

TME Targeting for Neoadjuvant Treatment

The tumor microenvironment (TME) in TNBC is implicated in immune suppression, evasion from immune surveillance, and the development of drug resistance. Recognizing the potential of TME as a treatment target for TNBC, active investigation into TME-targeted therapies is underway [164]. Tumor-associated macrophages (TAMs) play a role in promoting TNBC progression and metastasis by releasing inhibitory cytokines, diminishing the functions of tumor-infiltrating lymphocytes (TILs), favoring regulatory T-cells (TREG), and modulating PD-1/PD-L1 expression in TME [165].

Clinical trials are exploring TME-targeted therapies in combination treatment, and one such combination involves cabiralizumab, an antibody inhibiting the colony-stimulating factor-1 receptor (CSF1R). Cabiralizumab works by blocking the activation and survival of macrophages. Combining cabiralizumab with immune checkpoint inhibitors and neoadjuvant chemotherapy is proposed to enhance efficacy by reducing TAMs and increasing TILs in early-stage TNBC [166]. An ongoing clinical trial (NCT04331067) is investigating the use of cabiralizumab in combination with nivolumab and neoadjuvant chemotherapy in patients with localized TNBC. This approach represents a novel strategy to modulate the TME and enhance the effectiveness of TNBC treatment [164].

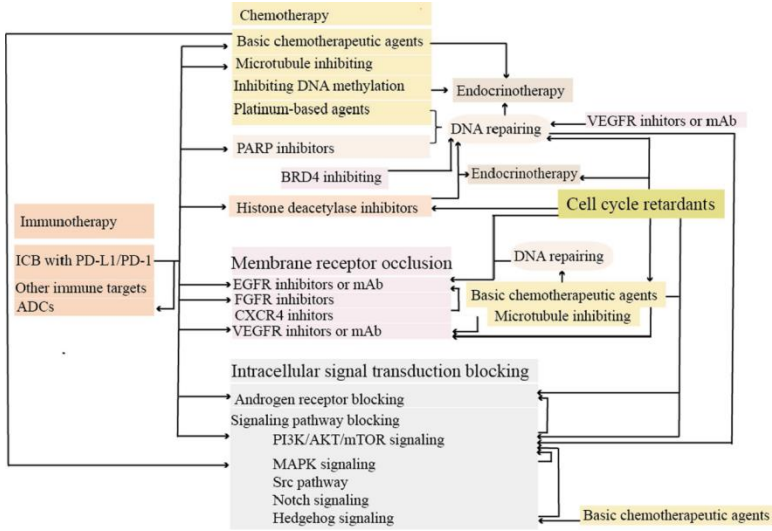

Figure 5: An overview of the current combinations being evaluated in clinical trials for the treatment of TNBC. These treatment approaches encompass immunotherapy as well as a range of molecular targeted therapies, which consist of inhibitors targeting intracellular pathways, cell cycle control, and androgen receptor (AR). Notable among these are antibody-drug conjugates (ADCs), bromodomain-containing 4 (BRD4) inhibitors, immune checkpoint blockade (ICB), monoclonal antibodies (mAb), and poly-adenosine diphosphate ribose polymerase (PARP) inhibitors [167].

Conclusion

In conclusion, understanding the intricate molecular pathways in triple-negative breast cancer (TNBC), including the pivotal roles of NF-κB, PI3K/AKT, and EGFR, unveils potential targets for therapeutic interventions. As we delve into targeted treatments, the promise of combination therapies, such as pembrolizumab with chemotherapy, platinum/PARP inhibitor combinations, and TME-targeted approaches, emerges. Ongoing clinical trials signify a dynamic landscape of advancements, offering hope for more effective and personalized strategies in the management of TNBC, a challenging and aggressive subtype of breast cancer. The integration of molecular insights with evolving treatment modalities holds promise for improving outcomes and transforming the clinical landscape for TNBC patients.

References

1. Mauricio A. Medina, Goldie Oza, Ashutosh Sharma, L.G. Arriaga, José Manuel Hernández Hernández, et al. Triple-Negative Breast Cancer: A Review of Conventional and Advanced Therapeutic Strategies. Int J Environ Res Public Health. 2020; 17.
2. Iqra Muneer, Muhammad T Ul Qamar, Kishver Tusleem, Sadaf Abdul Rauf, Hafiz M J Hussain, et al. Discovery of selective inhibitors for cyclic AMP response element-binding protein: a combined ligand and structure-based resources pipeline. Anticancer Drugs. 2019; 30: 363-373.
3. Ghoncheh M, Z Pournamdar, H Salehiniya. Incidence and Mortality and Epidemiology of Breast Cancer in the World. Asian Pac J Cancer Prev. 2016; 17: 43-46.
4. Muhammad Suleman, Muhammad Tahir ul Qamar, Shoaib Saleem, Sajjad Ahmad, Syed Shujait Ali, et al. Mutational Landscape of Pirin and Elucidation of the Impact of Most Detrimental Missense Variants That Accelerate the Breast Cancer Pathways: A Computational Modelling Study. Front Mol Biosci. 2021; 8: 692835.
5. Giampaolo Bianchini, Justin M Balko, Ingrid A Mayer, Melinda E Sanders, Luca Gianni. Triple-negative breast cancer: challenges and opportunities of a heterogeneous disease. Nat Rev Clin Oncol. 2016; 13: 674-690.
6. Foulkes WD, IE Smith, JS Reis-Filho. Triple-negative breast cancer. N Engl J Med. 2010; 363: 1938-1948.
7. Rebecca Dent, Maureen Trudeau, Kathleen I Pritchard, Wedad M Hanna, Harriet K Kahn, et al. Triple-negative breast cancer: clinical features and patterns of recurrence. Clin Cancer Res. 2007; 13: 4429-4434.
8. Jacqueline Tsai, Danielle Bertoni, Tina Hernandez-Boussard, Melinda L Telli, Irene L Wapnir. Lymph Node Ratio Analysis After Neoadjuvant Chemotherapy is Prognostic in Hormone Receptor-Positive and Triple-Negative Breast Cancer. Ann Surg Oncol. 2016; 23: 3310-3316.
9. Sima Singh, Arshid Numan, Balaji Maddiboyina, Saahil Arora, Yassine Riadi, et al. The emerging role of immune checkpoint inhibitors in the treatment of triple-negative breast cancer. Drug Discov Today. 2021; 26: 1721-1727.

10. Betsy A Kohler, Recinda L Sherman, Nadia Howlader, Ahmedin Jemal, A Blythe Ryerson, et al. Annual Report to the Nation on the Status of Cancer, 1975-2011, Featuring Incidence of Breast Cancer Subtypes by Race/Ethnicity, Poverty, and State. J Natl Cancer Inst. 2015; 107: djv048.
11. Sharon Nofech-Mozes, Maureen Trudeau, Harriet K Kahn, Rebecca Dent, Ellen Rawlinson, et al. Patterns of recurrence in the basal and non-basal subtypes of triple-negative breast cancers. Breast Cancer Res Treat. 2009; 118: 131-127.
12. Jiyoung Rhee, Sae-Won Han, Do-Youn Oh, Jee Hyun Kim, Seock-Ah Im, et al. The clinicopathologic characteristics and prognostic significance of triple-negativity in node-negative breast cancer. BMC Cancer. 2008; 8: 307.
13. Hakan Mersin, Emin Yildirim, Ugur Berberoglu, Kaptan Gülben. The prognostic importance of triple negative breast carcinoma. Breast. 2008; 17: 341-346.
14. Kaplan HG, JA Malmgren. Impact of triple negative phenotype on breast cancer prognosis. Breast J. 2008; 14: 456-463.
15. Qingli Jiao, Aiguo Wu, Guoli Shao, Haoyu Peng, Mengchuan Wang, et al. The latest progress in research on triple negative breast cancer (TNBC): risk factors, possible therapeutic targets and prognostic markers. J Thorac Dis. 2014; 6: 1329-1335.
16. Almansour NM. Triple-Negative Breast Cancer: A Brief Review About Epidemiology, Risk Factors, Signaling Pathways, Treatment and Role of Artificial Intelligence. Front Mol Biosci. 2022; 9: 836417.
17. Dagmar Horakova, Katerina Bouchalova, Karel Cwiertka, Ladislav Stepanek, Jana Vlckova, et al. Risks and protective factors for triple negative breast cancer with a focus on micronutrients and infections. Biomed Pap Med Fac Univ Palacky Olomouc Czech Repub. 2018; 162: 83-89.
18. Ming Zhao, Erin W Howard, Amanda B Parris, Zhiying Guo, Qingxia Zhao, et al. Alcohol promotes migration and invasion of triple-negative breast cancer cells through activation of p38 MAPK and JNK. Mol Carcinog. 2017; 56: 849-862.
19. Devericks Emily N, Carson Meredith S, McCullough Lauren E, Coleman Michael F, Hursting Stephen D. The obesity-

breast cancer link: a multidisciplinary perspective. Cancer Metastasis Rev. 2022; 41: 607-625.
20. Dietze EC, TA Chavez, VL Seewaldt. Obesity and Triple-Negative Breast Cancer: Disparities, Controversies, and Biology. Am J Pathol. 2018; 188: 280-290.
21. Dong Niu, Chenchen Li, Xiaoyu Yan, Haoran Qu, Yuling Zheng. Antidepressant medication use and breast cancer risk. Am J Epidemiol. 2000; 151: 951-957.
22. Gary D Friedman, Nina Oestreicher, James Chan, Charles P Quesenberry Jr, Natalia Udaltsova, et al. Antibiotics and risk of breast cancer: up to 9 years of follow-up of 2.1 million women. Cancer Epidemiol Biomarkers Prev. 2006; 15: 2102-2106.
23. Andrew McGuire, James AL Brown, Carmel Malone, Ray McLaughlin, Michael J Kerin. Effects of age on the detection and management of breast cancer. Cancers (Basel). 2015; 7: 908-929.
24. Ayca Gucalp, Tiffany A Traina, Joel R Eisner, Joel S Parker, Sara R Selitsky, et al. Male breast cancer: a disease distinct from female breast cancer. Breast Cancer Res Treat. 2019; 173: 37-48.
25. Deirdre A Hill, Eric R Prossnitz, Melanie Royce, Andrea Nibbe. Temporal trends in breast cancer survival by race and ethnicity: A population-based cohort study. PLoS One. 2019; 14: e0224064.
26. Carol E DeSantis, Stacey A Fedewa, Ann Goding Sauer, Joan L Kramer, Robert A Smith, et al. Breast cancer statistics, 2015: Convergence of incidence rates between black and white women. CA Cancer J Clin. 2016; 66: 31-42.
27. Shiovitz S, LA Korde. Genetics of breast cancer: a topic in evolution. Ann Oncol. 2015; 26: 1291-1299.
28. Giovanni Corso, Paolo Veronesi, Virgilio Sacchini, Viviana Galimberti. Prognosis and outcome in CDH1-mutant lobular breast cancer. Eur J Cancer Prev. 2018; 27: 237-238.
29. Shahbandi A, HD Nguyen, JG Jackson. TP53 Mutations and Outcomes in Breast Cancer: Reading beyond the Headlines. Trends Cancer. 2020; 6: 98-110.
30. Wojciech Kluźniak, Dominika Wokołorczyk, Bogna Rusak, Tomasz Huzarski, Jacek Gronwald, et al. Inherited variants

in XRCC2 and the risk of breast cancer. Breast Cancer Res Treat. 2019; 178: 657-663.
31. Lorena Incorvaia, Daniele Fanale, Marco Bono, Valentina Calò, Alessia Fiorino, et al. BRCA1/2 pathogenic variants in triple-negative versus luminal-like breast cancers: genotype-phenotype correlation in a cohort of 531 patients. Ther Adv Med Oncol. 2020; 12: 1758835920975326.
32. Hermela Shimelis, Holly LaDuca, Chunling Hu, Steven N Hart, Jie Na, et al. Triple-Negative Breast Cancer Risk Genes Identified by Multigene Hereditary Cancer Panel Testing. J Natl Cancer Inst. 2018; 110: 855-862.
33. Cuzick J. Epidemiology of breast cancer--selected highlights. Breast. 2003; 12: 405-411.
34. Hui-Chen Wu, Catherine Do, Irene L Andrulis, Esther M John, Mary B Daly, et al. Breast cancer family history and allele-specific DNA methylation in the legacy girls study. Epigenetics. 2018; 13: 240-250.
35. Chia-Jung Li, Yen-Dun Tony Tzeng, Yi-Han Chiu, Hung-Yu Lin, Ming-Feng Hou, et al. Pathogenesis and Potential Therapeutic Targets for Triple-Negative Breast Cancer. Cancers. 2021; 13: 2978.
36. Brian D Lehmann, Joshua A Bauer, Xi Chen, Melinda E Sanders, A Bapsi, et al. Identification of human triple-negative breast cancer subtypes and preclinical models for selection of targeted therapies. J Clin Invest. 2011; 121: 2750-2767.
37. Brian D Lehmann, Bojana Jovanović, Xi Chen, Monica V Estrada, Kimberly N Johnson, et al. Refinement of Triple-Negative Breast Cancer Molecular Subtypes: Implications for Neoadjuvant Chemotherapy Selection. PLoS One. 2016; 11: e0157368.
38. Miller K, J Kremer, T Ballinger. Triple Negative Breast Cancer—Review of Current and Emerging Therapeutic Strategies. Oncology & Hematology Review (US). 2016; 12.
39. Lorenzo Melchor, Gemma Molyneux, Alan Mackay, Fiona-Ann Magnay, María Atienza, et al. Identification of cellular and genetic drivers of breast cancer heterogeneity in genetically engineered mouse tumour models. J Pathol. 2014; 233: 124-137.

40. Aye Aye Thike, Poh Yian Cheok, Ana Richelia Jara-Lazaro, Benita Tan, Patrick Tan, et al. Triple-negative breast cancer: clinicopathological characteristics and relationship with basal-like breast cancer. Mod Pathol. 2010; 23: 123-133.
41. Zhixian Liu, Mengyuan Li, Zehang Jiang, Xiaosheng Wang. A Comprehensive Immunologic Portrait of Triple-Negative Breast Cancer. Transl Oncol. 2018; 11: 311-329.
42. Hiroko Masuda, Keith A Baggerly, Ying Wang, Ya Zhang, Ana Maria Gonzalez-Angulo, et al. Differential response to neoadjuvant chemotherapy among 7 triple-negative breast cancer molecular subtypes. Clin Cancer Res. 2013; 19: 5533-5540.
43. Sandeep Kumar, Amanjit Bal, Ashim Das, Shalmoli Bhattacharyya, Ishita Laroiya, et al. Molecular Subtyping of Triple Negative Breast Cancer by Surrogate Immunohistochemistry Markers. Appl Immunohistochem Mol Morphol. 2021; 29: 251-257.
44. Kristine Astvatsaturyan, Yong Yue, Ann E Walts, Shikha Bose. Androgen receptor positive triple negative breast cancer: Clinicopathologic, prognostic, and predictive features. PLoS One. 2018; 13: e0197827.
45. Valerie N Barton, Nicholas C D'Amato, Michael A Gordon, Hanne T Lind, Nicole S Spoelstra, et al. Multiple molecular subtypes of triple-negative breast cancer critically rely on androgen receptor and respond to enzalutamide in vivo. Mol Cancer Ther. 2015; 14: 769-778.
46. Y Bareche, D Venet, M Ignatiadis, P Aftimos, M Piccart, et al. Unravelling triple-negative breast cancer molecular heterogeneity using an integrative multiomic analysis. Ann Oncol. 2018; 29: 895-902.
47. Zihan Lin, Lijuan Liao, Shengchao Zhao, Wei Gu, Guanzhen Wang, et al. Corylin inhibits the progression of Non-small cell lung cancer cells by regulating NF-κB signaling pathway via targeting p65. Phytomedicine. 2023; 110: 154627.
48. Xudong Cheng, Fei Wang, Yu Qiao, Ting Chen, Ling Fan, et al. Honokiol inhibits interleukin-induced angiogenesis in the NSCLC microenvironment through the NF-κB signaling pathway. Chem Biol Interact. 2023; 370: 110295.

49. Dongwen Que, Feimei Kuang, Rui Kang, Daolin Tang, Jiao Liu. ACSS2-mediated NF-κB activation promotes alkaliptosis in human pancreatic cancer cells. Sci Rep. 2023; 13: 1483.
50. Zhiwen Qian, Lingyan Chen, Jiayu Liu, Ying Jiang, Yan Zhang. The emerging role of PPAR-alpha in breast cancer. Biomed Pharmacother. 2023; 161: 114420.
51. Lioba Koerner, Marcel Schmiel, Tsun-Po Yang, Martin Peifer, Reinhard Buettner, et al. NEMO- and RelA-dependent NF-κB signaling promotes small cell lung cancer. Cell Death Differ. 2023; 30: 938-951.
52. Akansha Chauhan, Asim Ul Islam, Hridayesh Prakash, Sandhya Singh. Phytochemicals targeting NF-κB signaling: Potential anti-cancer interventions. J Pharm Anal. 2022; 12: 394-405.
53. Perkins ND. The diverse and complex roles of NF-κB subunits in cancer. Nat Rev Cancer. 2012; 12: 121-132.
54. Malla RR, P Kiran. Tumor microenvironment pathways: Cross regulation in breast cancer metastasis. Genes Dis. 2022; 9: 310-324.
55. Ke Yang, Xin Wang, Hongmei Zhang, Zhongliang Wang, Guoxin Nan, et al. The evolving roles of canonical WNT signaling in stem cells and tumorigenesis: implications in targeted cancer therapies. Lab Invest. 2016; 96: 116-136.
56. SA Piha-Paul, PN Munster, A Hollebecque, G Argilés, O Dajani, et al. Results of a phase 1 trial combining ridaforolimus and MK-0752 in patients with advanced solid tumours. Eur J Cancer. 2015; 51: 1865-1873.
57. Gilmore TD.The Re1/NF-kappa B/I kappa B signal transduction pathway and cancer. Cancer Treat Res. 2003; 115: 241-265.
58. Noritaka Yamaguchi, Taku Ito, Sakura Azuma, Emi Ito, Reiko Honma, et al. Constitutive activation of nuclear factor-kappaB is preferentially involved in the proliferation of basal-like subtype breast cancer cell lines. Cancer Sci. 2009; 100: 1668-1674.
59. Mahmoud Darweesh, Shady Younis, Zamaneh Hajikhezri, Arwa Ali, Chuan Jin, et al. ZC3H11A loss of function enhances NF-κB signaling through defective IκBα protein expression. Front Immunol. 2022; 13: 1002823.

60. Sen R, D Baltimore. Inducibility of kappa immunoglobulin enhancer-binding protein Nf-kappa B by a posttranslational mechanism. Cell. 1986; 47: 921-928.
61. Duckett CS. Apoptosis and NF-kappa B: the FADD connection. J Clin Invest. 2002; 109: 579-580.
62. DC Guttridge, C Albanese, JY Reuther, RG Pestell, AS Baldwin Jr. NF-kappaB controls cell growth and differentiation through transcriptional regulation of cyclin D1. Mol Cell Biol. 1999; 19: 5785-5799.
63. La Rosa FA, JW Pierce, GE Sonenshein. Differential regulation of the c-myc oncogene promoter by the NF-kappa B rel family of transcription factors. Mol Cell Biol. 1994; 14: 1039-1044.
64. Eli Pikarsky, Rinnat M Porat, Ilan Stein, Rinat Abramovitch, Sharon Amit, et al. NF-kappaB functions as a tumour promoter in inflammation-associated cancer. Nature. 2004; 431: 461-466.
65. Hayden MS, S Ghosh. Signaling to NF-kappaB. Genes Dev. 2004; 18: 2195-2224.
66. Carrie D House, Elizabeth Jordan, Lidia Hernandez, Michelle Ozaki, Jana M James, et al. NFκB Promotes Ovarian Tumorigenesis via Classical Pathways That Support Proliferative Cancer Cells and Alternative Pathways That Support ALDH(+) Cancer Stem-like Cells. Cancer Res. 2017; 77: 6927-6940.
67. Oeckinghaus A, MS Hayden, S Ghosh. Crosstalk in NF-κB signaling pathways. Nat Immunol. 2011; 12: 695-708.
68. Jérôme Kucharczak, Matthew J Simmons, Yongjun Fan, Céline Gélinas. To be, or not to be: NF-kappaB is the answer--role of Rel/NF-kappaB in the regulation of apoptosis. Oncogene. 2003; 22: 8961-8982.
69. Jesse S Boehm, Jean J Zhao, Jun Yao, So Young Kim, Ron Firestein, et al. Integrative genomic approaches identify IKBKE as a breast cancer oncogene. Cell. 2007; 129: 1065-1079.
70. R Romieu-Mourez, E Landesman-Bollag, DC Seldin, AM Traish, F Mercurio, et al. Roles of IKK kinases and protein kinase CK2 in activation of nuclear factor-kappaB in breast cancer. Cancer Res. 2001; 61: 3810-3818.

71. Chen F, V Castranova, X Shi. New insights into the role of nuclear factor-kappaB in cell growth regulation. Am J Pathol. 2001; 159: 387-397.
72. Wang W, SA Nag, R Zhang. Targeting the NFκB signaling pathways for breast cancer prevention and therapy. Curr Med Chem. 2015; 22: 264-289.
73. Manran Liu, Toshiyuki Sakamaki, Mathew C Casimiro, Nicole Willmarth, Andrew A Quong, et al. The canonical NF-kappaB pathway governs mammary tumorigenesis in transgenic mice and tumor stem cell expansion. Cancer Res. 2010; 70: 10464-10473.
74. Mingjian Du, Chee-Kwee Ea, Yan Fang, Zhijian J Chen. Liquid phase separation of NEMO induced by polyubiquitin chains activates NF-κB. Mol Cell. 2022; 82: 2415-2426.e5.
75. Yuchun Liu, Kunpeng Liu, Yingqi Huang, Meng Sun, Qingnan Tian, et al. TRIM25 Promotes TNF-α-Induced NF-κB Activation through Potentiating the K63-Linked Ubiquitination of TRAF2. J Immunol. 2020; 204: 1499-1507.
76. Razani B, AD Reichardt, G Cheng. Non-canonical NF-κB signaling activation and regulation: principles and perspectives. Immunol Rev. 2011; 244: 44-54.
77. Fernando J Velloso, Arthur FR Bianco, Jessica O Farias, Nadia EC Torres, Pault YM Ferruzo, et al. The crossroads of breast cancer progression: insights into the modulation of major signaling pathways. Onco Targets Ther. 2017; 10: 5491-5524.
78. Connie I Diakos, Kellie A Charles, Donald C McMillan, Stephen J Clarke. Cancer-related inflammation and treatment effectiveness. Lancet Oncol. 2014; 15: e493-503.
79. Sandra Kraljevic Pavelic, Mirela Sedic, Hrvojka Bosnjak, Sime Spaventi, Kresimir Pavelic. Metastasis: new perspectives on an old problem. Mol Cancer. 2011; 10: 22.
80. Whitney Barham, Lianyi Chen, Oleg Tikhomirov, Halina Onishko, Linda Gleaves, et al. Aberrant activation of NF-κB signaling in mammary epithelium leads to abnormal growth and ductal carcinoma in situ. BMC Cancer. 2015; 15: 647.
81. Christina M Annunziata, Helene Tuft Stavnes, Lilach Kleinberg, Aasmund Berner, Lidia F Hernandez, et al. Nuclear factor kappaB transcription factors are coexpressed

and convey a poor outcome in ovarian cancer. Cancer. 2010; 116: 3276-3284.
82. Sarah Hsu, Marianne Kim, Lidia Hernandez, Valentina Grajales, Anne Noonan, et al. IKK-ε coordinates invasion and metastasis of ovarian cancer. Cancer Res. 2012; 72: 5494-504.
83. PC Cogswell, DC Guttridge, WK Funkhouser, AS Baldwin Jr. Selective activation of NF-kappa B subunits in human breast cancer: potential roles for NF-kappa B2/p52 and for Bcl-3. Oncogene. 2000; 19: 1123-1131.
84. H Nakshatri, P Bhat-Nakshatri, DA Martin, RJ Goulet, Jr, GW Sledge, Jr. Constitutive activation of NF-kappaB during progression of breast cancer to hormone-independent growth. Mol Cell Biol. 1997; 17: 3629-3639.
85. MA Sovak, RE Bellas, DW Kim, GJ Zanieski, AE Rogers, et al. Aberrant nuclear factor-kappaB/Rel expression and the pathogenesis of breast cancer. J Clin Invest. 1997; 100: 2952-2960.
86. Raphaëlle Romieu-Mourez, Dong W Kim, Sang Min Shin, Elizabeth G Demicco, Esther Landesman-Bollag, et al. Mouse mammary tumor virus c-rel transgenic mice develop mammary tumors. Mol Cell Biol. 2003; 23: 5738-5754.
87. Elizabeth G Demicco, Kathryn T Kavanagh, Raphaëlle Romieu-Mourez, Xiaobo Wang, Sangmin R Shin, et al. RelB/p52 NF-kappaB complexes rescue an early delay in mammary gland development in transgenic mice with targeted superrepressor IkappaB-alpha expression and promote carcinogenesis of the mammary gland. Mol Cell Biol. 2005; 25: 10136-10147.
88. Sunil Srivastava, Manabu Matsuda, Zhaoyuan Hou, Jason P Bailey, Riko Kitazawa, et al. Receptor activator of NF-kappaB ligand induction via Jak2 and Stat5a in mammary epithelial cells. J Biol Chem. 2003; 278: 46171-46178.
89. Peddi PF, MJ Ellis, C Ma. Molecular basis of triple negative breast cancer and implications for therapy. Int J Breast Cancer. 2012; 2012: 217185.
90. Hoesel B, JA Schmid. The complexity of NF-κB signaling in inflammation and cancer. Mol Cancer. 2013; 12: 86.
91. Zachary C Hartman, Graham M Poage, Petra den Hollander, Anna Tsimelzon, Jamal Hill, et al. Growth of triple-negative

breast cancer cells relies upon coordinate autocrine expression of the proinflammatory cytokines IL-6 and IL-8. Cancer Res. 2013; 73: 3470-3480.
92. Valeria Ossovskaya, Yipeng Wang, Adam Budoff, Qiang Xu, Alexander Lituev, et al. Exploring molecular pathways of triple-negative breast cancer. Genes Cancer. 2011; 2: 870-879.
93. Carrie D House, Valentina Grajales, Michelle Ozaki, Elizabeth Jordan, Helmae Wubneh, et al. IKKε cooperates with either MEK or non-canonical NF-kB driving growth of triple-negative breast cancer cells in different contexts. BMC Cancer. 2018; 18: 595.
94. Cantley LC. The phosphoinositide 3-kinase pathway. Science. 2002; 296: 1655-1657.
95. LoRusso PM. Inhibition of the PI3K/AKT/mTOR Pathway in Solid Tumors. J Clin Oncol. 2016; 34: 3803-3815.
96. Baselga J. Targeting the phosphoinositide-3 (PI3) kinase pathway in breast cancer. Oncologist. 2011; 16: 12-19.
97. Sohrab P Shah, Andrew Roth, Rodrigo Goya, Arusha Oloumi, Gavin Ha, et al. The clonal and mutational evolution spectrum of primary triple-negative breast cancers. Nature. 2012; 486: 395-399.
98. Pascual J, NC Turner. Targeting the PI3-kinase pathway in triple-negative breast cancer. Ann Oncol. 2019; 30: 1051-1060.
99. David A Fruman, Honyin Chiu, Benjamin D Hopkins, Shubha Bagrodia, Lewis C Cantley, et al. The PI3K Pathway in Human Disease. Cell, 2017. 170(4): p. 605-635.
100. Comprehensive molecular portraits of human breast tumours. Nature. 2012; 490: 61-70.
101. John D Carpten, Andrew L Faber, Candice Horn, Gregory P Donoho, Stephen L Briggs, et al. A transforming mutation in the pleckstrin homology domain of AKT1 in cancer. Nature. 2007; 448: 439-444.
102. Hanna Y Irie, Rachel V Pearline, Dorre Grueneberg, Maximilian Hsia, Preethi Ravichandran, et al. Distinct roles of Akt1 and Akt2 in regulating cell migration and epithelial-mesenchymal transition. J Cell Biol. 2005; 171: 1023-1034.
103. Ng SSW, MS Tsao, S Chow, DW Hedley. Inhibition of phosphatidylinositide 3-kinase enhances gemcitabine-

induced apoptosis in human pancreatic cancer cells. Cancer Res. 2000; 60: 5451-5455.
104. Marina Riggio, María C Perrone, María L Polo, María J Rodriguez, María May, et al. AKT1 and AKT2 isoforms play distinct roles during breast cancer progression through the regulation of specific downstream proteins. Sci Rep. 2017; 7: 44244.
105. Y Rebecca Chin, Taku Yoshida, Andriy Marusyk, Andrew H Beck, Kornelia Polyak, et al. Targeting Akt3 signaling in triple-negative breast cancer. Cancer Res. 2014; 74: 964-973.
106. Yi KH, J Lauring. Recurrent AKT mutations in human cancers: functional consequences and effects on drug sensitivity. Oncotarget. 2016; 7: 4241-4251.
107. Hussain K. An activating mutation of AKT2 and human hypoglycemia. Science. 2011; 334: 474.
108. Poggio F. Platinum-based neoadjuvant chemotherapy in triple-negative breast cancer: a systematic review and meta-analysis. Ann Oncol. 2018; 29: 1497-1508.
109. Shaw RJ. The LKB1 tumor suppressor negatively regulates mTOR signaling. Cancer Cell. 2004; 6: 91-99.
110. Huang J. The TSC1-TSC2 complex is required for proper activation of mTOR complex 2. Mol Cell Biol. 2008; 28: 4104-4115.
111. José Baselga, Mario Campone, Martine Piccart, Howard A Burris, Hope S Rugo, et al. Everolimus in postmenopausal hormone-receptor-positive advanced breast cancer. N Engl J Med. 2012; 366: 520-529.
112. Wen Hong Shen, Adayabalam S Balajee, Jianli Wang, Hong Wu, Charis Eng, et al. Essential role for nuclear PTEN in maintaining chromosomal integrity. Cell. 2007; 128: 157-170.
113. Shidong Jia, Zhenning Liu, Sen Zhang, Pixu Liu, Lei Zhang, et al. Essential roles of PI(3)K-p110beta in cell growth, metabolism and tumorigenesis. Nature. 2008; 454: 776-779.
114. Susan Wee, Dmitri Wiederschain, Sauveur-Michel Maira, Alice Loo, Christine Miller, et al. PTEN-deficient cancers depend on PIK3CB. Proc Natl Acad Sci U S A. 2008; 105: 13057-13062.

115. JM Garcia, JM Silva, G Dominguez, R Gonzalez, A Navarro, et al. Allelic loss of the PTEN region (10q23) in breast carcinomas of poor pathophenotype. Breast Cancer Res Treat. 1999; 57: 237-243.
116. S Bose, SI Wang, MB Terry, H Hibshoosh, R Parsons. Allelic loss of chromosome 10q23 is associated with tumor progression in breast carcinomas. Oncogene. 1998; 17: 123-127.
117. Li S. Loss of PTEN expression in breast cancer: association with clinicopathological characteristics and prognosis. Oncotarget. 2017; 8: 32043-32054.
118. Wu Y. Triple negative breast tumors in African-American and Hispanic/Latina women are high in CD44+, low in CD24+, and have loss of PTEN. PLoS One. 2013; 8: e78259.
119. Beg S. Loss of PTEN expression is associated with aggressive behavior and poor prognosis in Middle Eastern triple-negative breast cancer. Breast Cancer Res Treat. 2015; 151: 541-553.
120. Song MS, L Salmena, PP Pandolfi. The functions and regulation of the PTEN tumour suppressor. Nat Rev Mol Cell Biol. 2012; 13: 283-296.
121. Marcus G Pezzolesi, Petra Platzer, Kristin A Waite, Charis Eng. Differential expression of PTEN-targeting microRNAs miR-19a and miR-21 in Cowden syndrome. Am J Hum Genet. 2008; 82: 1141-1149.
122. Antonella Papa, Lixin Wan, Massimo Bonora, Leonardo Salmena, Min Sup Song, et al. Cancer-associated PTEN mutants act in a dominant-negative manner to suppress PTEN protein function. Cell. 2014; 157: 595-610.
123. Hollander MC, GM Blumenthal, PA Dennis. PTEN loss in the continuum of common cancers, rare syndromes and mouse models. Nat Rev Cancer. 2011; 11: 289-301.
124. Christina Gewinner, Zhigang C Wang, Andrea Richardson, Julie Teruya-Feldstein, Dariush Etemadmoghadam, et al. Evidence that inositol polyphosphate 4-phosphatase type II is a tumor suppressor that inhibits PI3K signaling. Cancer Cell. 2009; 16: 115-125.
125. Clare G Fedele, Lisa M Ooms, Miriel Ho, Jessica Vieusseux, Sandra A O'Toole, et al. Inositol polyphosphate

4-phosphatase II regulates PI3K/Akt signaling and is lost in human basal-like breast cancers. Proc Natl Acad Sci U S A. 2010; 107: 22231-22236.
126. Satoshi Kofuji, Hirotaka Kimura, Hiroki Nakanishi, Hiroshi Nanjo, Shunsuke Takasuga, et al. INPP4B Is a PtdIns(3,4,5)P3 Phosphatase That Can Act as a Tumor Suppressor. Cancer Discov. 2015; 5: 730-739.
127. Toni M Brand, Mari Iida, Chunrong Li, Deric L Wheeler. The nuclear epidermal growth factor receptor signaling network and its role in cancer. Discov Med. 2011; 12: 419-432.
128. Masuda H. Role of epidermal growth factor receptor in breast cancer. Breast Cancer Res Treat. 2012; 136: 331-345.
129. Ogden A. Combined HER3-EGFR score in triple-negative breast cancer provides prognostic and predictive significance superior to individual biomarkers. Scientific Reports. 2020; 10: 3009.
130. Fruman DA, C Rommel. PI3K and cancer: lessons, challenges and opportunities. Nat Rev Drug Discov. 2014; 13: 140-156.
131. Arcaro A, AS Guerreiro. The phosphoinositide 3-kinase pathway in human cancer: genetic alterations and therapeutic implications. Curr Genomics. 2007; 8: 271-306.
132. Zaytseva YY. mTOR inhibitors in cancer therapy. Cancer Lett. 2012; 319: 1-7.
133. Costa RLB, HS Han, WJ Gradishar. Targeting the PI3K/AKT/mTOR pathway in triple-negative breast cancer: a review. Breast Cancer Research and Treatment. 2018; 169: 397-406.
134. Ali R, MK Wendt. The paradoxical functions of EGFR during breast cancer progression. Signal Transduct Target Ther. 2017; 2: 16042.
135. Chan JJ, TJY Tan, RA Dent. Novel therapeutic avenues in triple-negative breast cancer: PI3K/AKT inhibition, androgen receptor blockade, and beyond. Ther Adv Med Oncol. 2019; 11: 1758835919880429.
136. Blanco E. Colocalized delivery of rapamycin and paclitaxel to tumors enhances synergistic targeting of the PI3K/Akt/mTOR pathway. Mol Ther. 2014; 22: 1310-1319.

137. Erkel G, T Anke, O Sterner. Inhibition of NF-kappa B activation by panepoxydone. Biochem Biophys Res Commun. 1996; 226: 214-221.
138. Karin M, Y Ben-Neriah. Phosphorylation Meets Ubiquitination: The Control of NF-κB Activity. Annual Review of Immunology. 2000; 18: 621-663.
139. Li X. Sulindac inhibits tumor cell invasion by suppressing NF-κB-mediated transcription of microRNAs. Oncogene. 2012; 31: 4979-4986.
140. Blanc-Brude OP. Therapeutic targeting of the survivin pathway in cancer: initiation of mitochondrial apoptosis and suppression of tumor-associated angiogenesis. Clin Cancer Res. 2003; 9: 2683-2692.
141. Ritu Arora, Clayton Yates, Bernard D Gary, Steven McClellan, Ming Tan, et al. Panepoxydone targets NF-kB and FOXM1 to inhibit proliferation, induce apoptosis and reverse epithelial to mesenchymal transition in breast cancer. PLoS One. 2014; 9: e98370.
142. Yali Li, Cailing Gan, Yange Zhang, Yan Yu, Chen Fan, et al. Inhibition of Stat3 Signaling Pathway by Natural Product Pectolinarigenin Attenuates Breast Cancer Metastasis. Front Pharmacol. 2019; 10: 1195.
143. Yoon JH, YJ Choi, SG Lee. Ginsenoside Rh1 suppresses matrix metalloproteinase-1 expression through inhibition of activator protein-1 and mitogen-activated protein kinase signaling pathway in human hepatocellular carcinoma cells. Eur J Pharmacol. 2012; 679: 24-33.
144. Diem Thi Ngoc Huynh, Yujin Jin, Chang-Seon Myung, Kyung-Sun Heo. Ginsenoside Rh1 Induces MCF-7 Cell Apoptosis and Autophagic Cell Death through ROS-Mediated Akt Signaling. Cancers (Basel). 2021; 13.
145. Jiang-Jiang Qin, Li Yan, Jia Zhang, Wei-Dong Zhang. STAT3 as a potential therapeutic target in triple negative breast cancer: a systematic review. J Exp Clin Cancer Res. 2019; 38: 195.
146. Heehyoung Lee, Andreas Herrmann, Jie-Hui Deng, Maciej Kujawski, Guilian Niu, et al. Persistently activated Stat3 maintains constitutive NF-kappaB activity in tumors. Cancer Cell. 2009; 15: 283-293.

147. Dawei Yang, Qinglong Guo, Yin Liang, Yue Zhao, Xiaoyu Tian, et al. Wogonin induces cellular senescence in breast cancer via suppressing TXNRD2 expression. Arch Toxicol. 2020; 94: 3433-3447.
148. Jin Y. Ginsenoside Rh1 Prevents Migration and Invasion through Mitochondrial ROS-Mediated Inhibition of STAT3/NF-κB Signaling in MDA-MB-231 Cells. Int J Mol Sci. 2021; 22.
149. Sobande F. EGFR in triple negative breast carcinoma: significance of protein expression and high gene copy number. Cesk Patol. 2015; 51: 80-86.
150. Eccles SA. The epidermal growth factor receptor/Erb-B/HER family in normal and malignant breast biology. Int J Dev Biol. 2011; 55: 685-696.
151. Burness ML, TA Grushko, OI Olopade. Epidermal growth factor receptor in triple-negative and basal-like breast cancer: promising clinical target or only a marker? Cancer J. 2010; 16: 23-32.
152. Julie M Roda, Trupti Joshi, Jonathan P Butchar, Jaclyn W McAlees, Amy Lehman, et al. The activation of natural killer cell effector functions by cetuximab-coated, epidermal growth factor receptor positive tumor cells is enhanced by cytokines. Clin Cancer Res. 2007; 13: 6419-6428.
153. José Baselga, Patricia Gómez, Richard Greil, Sofia Braga, Miguel A Climent, et al. Randomized phase II study of the anti-epidermal growth factor receptor monoclonal antibody cetuximab with cisplatin versus cisplatin alone in patients with metastatic triple-negative breast cancer. J Clin Oncol. 2013; 31: 2586-2592.
154. B Corkery, J Crown, M Clynes, N O'Donovan. Epidermal growth factor receptor as a potential therapeutic target in triple-negative breast cancer. Ann Oncol. 2009; 20: 862-867.
155. Ricardo Costa, Ami N Shah, Cesar A Santa-Maria, Marcelo R Cruz, Devalingam Mahalingam, et al. Targeting Epidermal Growth Factor Receptor in triple negative breast cancer: New discoveries and practical insights for drug development. Cancer treatment reviews. 2017; 53: 111-119.
156. Winstead E. Pembrolizumab Improves Survival in Advanced Triple-Negative Breast Cancer. 2022; 2022.

157. Rankin GO. Renal and hepatic toxicity of N-arylsuccinimides in Fischer 344 rats. J Appl Toxicol. 1989; 9: 223-228.
158. Ruf A, G de Murcia, GE Schulz. Inhibitor and NAD+ binding to poly(ADP-ribose) polymerase as derived from crystal structures and homology modeling. Biochemistry. 1998; 37: 3893-900.
159. Kehe K. Inhibition of poly(ADP-ribose) polymerase (PARP) influences the mode of sulfur mustard (SM)-induced cell death in HaCaT cells. Arch Toxicol. 2008; 82: 461-470.
160. Lu Y. Double-barreled gun: Combination of PARP inhibitor with conventional chemotherapy. Pharmacol Ther. 2018; 188: 168-175.
161. McKeage MJ, JD Higgins, LR Kelland. Platinum and other metal coordination compounds in cancer chemotherapy. A commentary on the sixth international symposium: San Diego, California, 23-26th January 1991. Br J Cancer. 1991; 64: 788-792.
162. Paul A Nguewa, Miguel A Fuertes, Victoria Cepeda, Carlos Alonso, Celia Quevedo, et al. Poly(ADP-ribose) polymerase-1 inhibitor 3-aminobenzamide enhances apoptosis induction by platinum complexes in cisplatin-resistant tumor cells. Med Chem. 2006; 2: 47-53.
163. Hastak K, E Alli, JM Ford. Synergistic chemosensitivity of triple-negative breast cancer cell lines to poly(ADP-Ribose) polymerase inhibition, gemcitabine, and cisplatin. Cancer Res. 2010; 70: 7970-7980.
164. Deepak KGK. Tumor microenvironment: Challenges and opportunities in targeting metastasis of triple negative breast cancer. Pharmacol Res. 2020; 153: 104683.
165. Matteo Santoni, Emanuela Romagnoli, Tiziana Saladino, Laura Foghini, Stefania Guarino, et al. Triple negative breast cancer: Key role of Tumor-Associated Macrophages in regulating the activity of anti-PD-1/PD-L1 agents. Biochim Biophys Acta Rev Cancer. 2018; 1869: 78-84.
166. Michael A Cannarile, Martin Weisser, Wolfgang Jacob, Anna-Maria Jegg, Carola H Ries, et al. Colony-stimulating factor 1 receptor (CSF1R) inhibitors in cancer therapy. J Immunother Cancer. 2017; 5: 53.

167. Shuangli Zhu, Yuze Wu, Bin Song, Ming Yi, Yuheng Yan, et al. Recent advances in targeted strategies for triple-negative breast cancer. Journal of Hematology & Oncology. 2023; 16: 100.

Book Chapter

Novel Therapies Based on Synthetic Biology to Cure a Range of Ailments

Fatima Fakih[1#], Ghoson Albahri[1#], Zeinab Al Dirani[1#], Dima Dagher[1#], Rawan Issa[1], Mohammad Fayyad-Kazan[2], Aya El Hage Ali[1], Fatima Shaalan[1], Mariam Hamze[1], Zahra Farroukh[1], Mona Al Jamal[1], Leen Fadlallah[1], Marwa Bazzi[1], Samer Krayan[1], Khalid Omama[1], Belal Osman[3], Mohamad El Saheli[4], Ali Hamade[5], Soumaya Al Hallak[1], Samah Al Zein[1], Jana Doghman[1], Ritaj Fakih[1], Jana Mahmoud-Haidar[1], Ghinwa Itani[1], Ghida Temraz[1], Aisha Al Sousi[1], Jana Zaraket[1], Katia Smeha[1], Douaa Khreis[1†], Fatima Dandash[1†], Hussein Fayyad-Kazan[1†]

[1]Lebanese University, Faculty of Science (I), Biology and Biochemistry Departments, Hadath, Beirut, Lebanon
[2]Department of Natural and Applied Sciences, College of Arts and Sciences, The American University of Iraq-Baghdad (AUIB), Baghdad 10001, Iraq
[3]American University of Beirut, Faculty of Medicine, Beirut, Lebanon
[4]Department of Biological Sciences, Faculty of Science, Beirut Arab University, Debbieh, Lebanon
[5]School of Arts and Sciences, Lebanese American University, Lebanon

[#]Contributed equally to this work
[†]Joint senior co-authors

***Corresponding Author:** Hussein Fayyad-Kazan, Lebanese University, Faculty of Science (I), Biology and Biochemistry Departments, Hadath, Beirut, Lebanon

Published **September 02, 2024**

How to cite this book chapter: Fatima Fakih, Ghoson Albahri, Zeinab Al Dirani, Dima Dagher, Rawan Issa, Mohammad Fayyad-Kazan, Aya El Hage Ali, Fatima Shaalan, Mariam Hamze, Zahra Farroukh, Mona Al Jamal, Leen Fadlallah, Marwa Bazzi, Samer Krayan, Khalid Omama1, Belal Osman, Mohamad El Saheli, Ali Hamade, Soumaya Al Hallak, Samah Al Zein, Jana Doghman, Ritaj Fakih, Jana Mahmoud-Haidar, Ghinwa Itani, Ghida Temraz, Aisha Al Sousi, Jana Zaraket, Katia Smeha, Douaa Khreis, Fatima Dandash, Hussein Fayyad-Kazan. Novel Therapies Based on Synthetic Biology to Cure a Range of Ailments. In: Immunology and Cancer Biology. Hyderabad, India: Vide Leaf. 2024.

Abstract

Synthetic biology is a multidisciplinary field of study that tries to develop new biological components, devices, and systems, as well as remodel existing systems found in nature. It is created when engineering science meets biological science, it combines biology and engineering to create new biological systems which currently do not exist in nature. As the immune system serves as the first line of defense against infections and plays a crucial role in chronic diseases, the development of immune-based therapy involves manipulating the immune system both endogenously and exogenously. Now, synthetic biology can be used in the context of medicine, to engineer biological systems with structures and functions not found in nature to process information, maintain cell environment, even enhance human health, and discover new therapeutic targets for the treatment of various diseases so that methods based on this platform enable the design of new strategies for the treatment and diagnosis of cancer, immune diseases, metabolic disorders, and infectious diseases. However, challenges loom at every stage of the process in synthetic biology, from part characterization to system design and assembly. Herein, we will describe the recent synthetic biology-based developments as novel therapeutics for cancer, bacterial drug resistance, natural drug synthesis, autoimmunity, neurodegenerative, and infectious diseases, highlighting the challenges faced in immune based therapies and synthetic biology.

Keywords

Synthetic Biology; Therapeutic Agents; Medical Applications; Various Disorders

Introduction

Everything living or nonliving is just chemicals made from atoms. Fish are just potages of atoms, but what makes the fish alive is how the atoms are structured, by a special kind of molecule, the DNA. Every living creature has a code that makes it develop, reproduce, and converge. 20 years ago, scientists learned to read a creature's entire genome. As biologists got better at this, as Stanford professor Drew Endy, a new kind of science was born, called "Synthetic Biology" [1]. Some of the most challenging global health issues require novel, technology-enabled alternatives to traditional approaches for developing novel human health solutions, where solutions must combine ground-breaking science with being useful, affordable, and accessible to those in need [2]. Synthetic biology is a recent field that is currently growing quickly. This prompts the query of what distinct contributions synthetic biology makes that cannot be met by other means. A synthetic biology method tries to solve issues through the creation of new models rather than only through research and observation, which sets it apart from a purely biological approach. By combining biology, chemistry, and engineering, this method offers a fresh viewpoint on several long-standing biological issues.

Building and simulating biological systems aids in a deeper comprehension of pertinent biological phenomena and paves the way for the creation of more accurate, predictable methods of biological manipulation in the fields of agriculture, bioenergy production, and medicines (Figure 1). Contributing to the development of biomedical breakthroughs is one of the goals of synthetic biology. Among these difficulties is the escalating bacterial antibiotic resistance [3], the rapid introduction of novel infectious diseases [4], and the evolving cancer medication resistance [5]. Synthetic biology anticipates the creation of specially crafted, easily controlled, and secure devices that would support human immune systems and correct metabolic anomalies to solve these issues. This review focuses on current synthetic biology based potential treatments as promising future disease therapies. We will go through several synthetic biology techniques that have recently been applied to research into disease mechanisms.

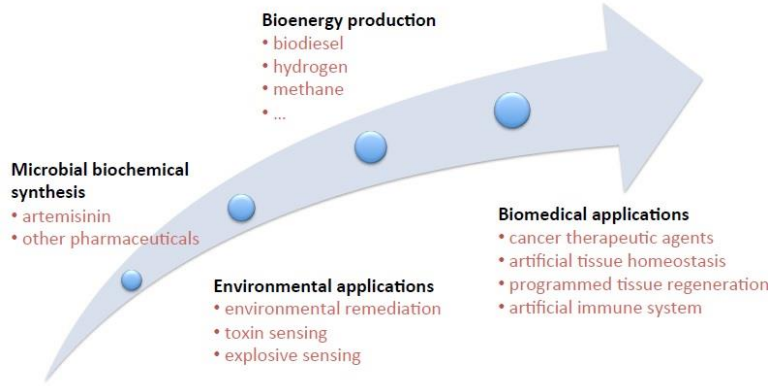

Figure 1: Synthetic biology applications. The figure is segmented into three distinct areas: Bioenergy Production, Biomedical Applications, and Environmental Applications. Bioenergy Production encompasses the generation of biodiesel, hydrogen, and methane. Biomedical Applications involve the production of pharmaceuticals such as artemisinin and cancer therapeutic agents, and the process of tissue engineering for artificial tissue homeostasis and programmed tissue regeneration. Environmental Applications focus on environmental remediation, toxin sensing, and explosive sensing, highlighting the diverse applications of the depicted processes [6].

Synthetic Biology Meets Medicine: Applications of Synthetic Biology in Developing Diagnostics and Therapeutics

Current global pandemics demonstrate that the approach to disease diagnosis, treatment, and prevention necessitates the organized and efficient use of ever-increasing amounts of biological data and bioengineering techniques to maximize responsiveness and to be prepared for future threats to human health [7]. Over the last two decades, synthetic biology has offered enormous potential in a wide range of applications. For instance, the primary goal of synthetic biology is to genetically change cells and redesign/synthesize regulatory systems to aid in disease diagnosis and treatment [8].

In the context of diagnostics, the vital first step in treating a disease is determining if it is present or not, making diagnostics a

vital component of public health. The primary goal of diagnostics development is to improve clinical performance, such as increased sensitivity, specificity, and quantification accuracy, as well as assay characteristics, such as shorter time to results, lower cost, greater portability, simplified workflow, and contaminant resistance [7]. For that synthetic biologists have begun to direct their bio-molecular engineering approaches toward this goal, yielding promising results that could lead to the development of new classes of low-cost, easily accessible diagnostics [9].

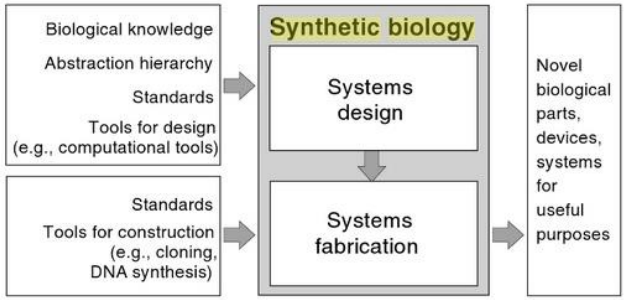

Figure 2: Synthetic Biology: Infusing Engineering Principles into Bioengineering. Synthetic biology encompasses systems design and fabrication. Each part has its specific prerequisites and inputs. Ultimately, synthetic biology delivers novel biological entities with improved functionality [6].

Synthetic biologists are applying rational engineering principles to the development of novel biosensing devices, which include a sensor that detects desired signal(s) from *in vitro* or *in vivo* environments, a processor that is a simple or multiplex synthetic circuit capable of processing received signals, integrating them with medical knowledge, and classifying patient conditions into clinical categories, and a reporter that displays assay results as chemical, biological, electronic, or a combination of these (Figure 2). These synthetic systems can be developed in a variety of ways, either as standalone diagnostic or diagnostic-therapeutic assays/devices or as components of conventional assays/devices. For instance, *in vitro* assays are made up of synthetic genes and oligonucleotides, synthetic multifunctional antibodies, or multiepitope and chimeric antigens that are printed on paper or

integrated into traditional testing platforms for probing or detection. For example, Geraldi et al. highlighted two synthetic biology-based In Vitro Diagnostics (IVD) systems, synthetic RNA-CRISPR/Cas-based biosensors that have been shown to detect and report various nucleic acid biomarkers from pathogens with high accuracy and sensitivity, relatively simple logistics, and low development and operational costs [10]. In another example, fluoromycobacteriophages are genetically altered phages that have been produced for phage-based diagnostics to identify pathogens such as Staphylococcus aureus, Listeria, E. coli, and Bacillus anthracis [11]. Moreover, Ye et al., for example, created a synthetic insulin-sensitive mammalian transcription circuit capable of detecting and correcting insulin resistance *in vivo* [12].

On the other hand, it is vital not only to detect an illness but also to employ the proper treatment. However, there are certain biomedical challenges such as increasing bacterial antibiotic resistance [3], the rapid emergence of new infectious diseases [4], and the evolution of cancer treatment resistance [13]. To overcome such challenges, synthetic biology envisions the development of specially made, easily controlled, safe devices that would support human immune system and solve metabolic disorders [14].

In this context, an example of synthetic biology-based therapeutics is the use of modified T cells, such as chimeric antigen receptor T cell immunotherapy (CAR-T), which is used to treat leukemia. Tisagenlecleucel was the first CAR-T treatment authorized by the FDA to treat cell acute lymphoblastic leukemia (ALL), a cancer that affects B lymphocytes (or B cells) in the immune system [15]. Another successful examples have been the manufacture of terpenoid chemicals in E. coli [16] and Saccharomyces cerevisiae [17] that can be employed in the manufacturing of anti-malaria medication, and synthetic mammalian gene circuit was utilized to find novel antituberculosis drugs [16]. Also, synthetic biology can be used in the design and modification of viruses to efficiently deliver healthy genes to the target tissue, facilitating precise recombination and integration of synthetic genes with the

existing genome [18]. Furthermore, it aids in the understanding of the complex traits of a disease, which paves the way to address these difficulties through personalized medicine [19].

Thus, synthetic biotics, like many other medical therapies under clinical trials, hold great promise for preventing, diagnosing, and treating diseases, as well as lowering future mortality and morbidity rates. Synthetic biology has the potential to boost the availability and efficacy of treatments as well as supply rapid diagnostic testing for bacterial illnesses. The risk of incorrect use, on the other hand, needs controls to prevent potential chemical and biological risks and ensure that this technology helps the greater good. If these novel medicines are effective in the market in the future years, they will contribute to the transformation of modern medicine.

Immunology-Related Applications of Synthetic Biology: Promising Cures for Autoimmune Disorders

The primary functions of the immune system lie in protecting the body against foreign antigens and activating repair systems to heal damaged tissues. Unfortunately, immune malfunctions can occur in several conditions, thus being a root cause of diseases in the body. Autoimmune disorders are one of the immune malfunctions where the immune system fails to distinguish between self and non-self; as a result, immune cells will attack self-antigens and destroy them [20]. Both aspects of the immune system, innate and adaptive immunity, take part in the contribute to autoimmune disorders [21]. This state of self-intolerance induces the production of autoantibodies and autoreactive T cells against self-bodies. Over 80 types of autoimmune disorders are diagnosed worldwide including multiple sclerosis (MS), systemic lupus erythematosus (SLE), type 1 diabetes (T1D), etc.. [22].

Defects in the production of mature B and T cells remain a leading etiology for the development of self-intolerance status [23]. This made B and T lymphocytes targets for therapeutic approaches against autoimmune disorders, and thus cellular

immunotherapy became a breakthrough in the treatment of autoimmunity. Immune cells are engineered to eliminate autoreactive immune effectors [24]. Monoclonal antibodies are one of the approaches for treating B cell-mediated autoimmunity, such as in the case of Rheumatoid Arthritis (RA) [25]. Rituximab is an anti-CD20 chimeric monoclonal antibody, designed against B-cells expressing CD20 antigens. It causes depletion of pre-B cells and mature B cells expressing CD20 via several mechanisms including B cell apoptosis, antibody-dependent cellular toxicity, and complement-dependent cellular toxicity [26]. This approach showed significant improvement in patients with RA [25]. Moreover, chimeric antibodies have been studied as a treatment for Systemic Lupus erythematosus. These chimeric antibodies were able to selectively target double stranded DNA-specific B cells at early stages of differentiation, causing their silencing and inactivation [27].

Equipped with chimeric antigen receptor (CAR), engineered T cells showed significant success in treating B-cell malignancies and leading to lasting remission periods [28]. This paved the way for directing CAR-T cell therapy toward B-cell mediated autoimmune diseases. CARs are synthetic receptors, having fragments of the single chain variable fragment (scFv) from the antibody, and instruct the immune cells to attack specific targets. Thus, allows taking further advantage of the specificity of autoantigens as tools for designing autoimmune therapies [29]. To study the efficacy of cell-based therapy against SLE, CD19 targeted CAR T-cells were administered to SLE mice models. Results showed depletion of CD19+ B cells, effective elimination of autoantibodies, reduction in lupus manifestations, and increased lifespan of the mice [30]. This approach helped overcome limitations seen in the course of treating SLE by monoclonal antibody technology and highlighted the superiority of CAR-T cell therapy [30]. However, depletion of B cells can raise risks of hypogammaglobulinemia, thus requiring a more pathogenic B cells specific approach [31]. Chimeric Autoantibody Receptor (CAAR) T cell therapy helped in targeting autoreactive B-cells through B cell receptor (BCR) specificity, and this technique showed promising results in cases of Pemphigus vulgaris (PV) autoimmune disease [32]. During

PV, autoantibodies are secreted against the keratinocyte adhesion protein desmoglein 3 (Dsg3). Accordingly, T-cells were engineered to express Dsg3-specific CAAR, enabling these T-cells to specifically target and destroy B-cells expressing anti-Dsg3 BCR [32]. CAAR-T cell therapy has been also applied in approaches to treat Myasthenia gravis (MG) disease, an autoimmune disorder where autoantibodies are secreted against muscle-specific tyrosine kinase (MuSK) [33]. *In vivo* results in mice showed the efficacy of MuSk CAAR T-cells in depleting B cells bearing anti-MuSK BCR [33].

CAR T-cell therapy has shown promising results in terms of efficacy and safety; however, a set of roadblocks exist. Limitations include HLA compatibility with donors, cytotoxicity, and the sophisticated manufacturing process [28]. Similarly, the production of CAAR T-cells is also difficult to standardize [34]. Thus, CAR engineering has gone beyond T cells, where other immune cells have been studied, including Natural Killer (NK) cells [35]. CAR-NK cell therapy administration in B-cell cancer patients showed significant clinical response to the treatment without adverse side effects [35]. Eventually, CAAR-NK cell therapy has been studied in the battle against autoimmune diseases. Autoantibodies against La/SSB are detected in patients with several immune diseases including Systemic Lupus Erythematosus (SLE) and Sjögren's syndrome (SS) [34]. NK92MI cell line was used to engineer La/SSB CAAR NK-cells and then co-cultured with anti-La/SSB autoantibody positive whole blood samples from SLE and SS patients. *In vitro* results showed selective killing of B-cells expressing anti-La/SSB BCR, indicating promising results for this technology [34].

The aforementioned techniques are based on the engineering of effector T cells, which can end up in critical complications in case of an askew [36]. As an alternative, regulatory T cells (Tregs) are approached as key players in the CAR technology against autoimmune diseases [36]. Tregs possess an immunosuppressive power to control autoimmunity, such as in the case of RA. Patients with RA have the citrullinated vimentin (CV) protein abundantly expressed in the extracellular matrix of

their inflamed joints, in consistency with the presence of anti-citrullinated protein antibodies (ACPA) [37].

Current therapies adopted against autoimmune diseases rely on immunosuppressive and anti-inflammatory agents, along with synthesized biologics like monoclonal antibodies. Nevertheless, cell-based therapy has shown promising treatment approaches in cancer patients, and within existing experiments against autoimmune diseases [38]. Indeed, the application of this technology in autoimmune diseases will pave the way for a new potential therapeutic option [38].

Synthetic Biology Approaches for The Degenerating Brain: Novel Treatments for Neurodegenerative Diseases

The central nervous system (CNS) is susceptible to a wide range of neurodegenerative diseases that impair neural connection and communication, which are crucial for sensory, motor, and cognitive functions like vision, hearing, movement, speech and language, memory, and others. Neurodegenerative disorders, including Alzheimer's disease (AD), Huntington's disease (HD), Parkinson's disease (PD), and amyotrophic lateral sclerosis (ALS), impact the brain tissue, resulting in diverse symptoms. Although the etiology, severity, and rate of progression of each neurodegenerative disease are unique, common molecular changes and mechanisms can be identified, providing potential directions for research into a variety of diseases [39].

Synthetic biology has the potential to advance therapies for neurodegenerative illnesses by introducing new tools and methods. Synthetic biology will particularly aid in the design of small molecules, proteins, gene networks, and vectors to target disease-related genes. Combining protection and repair methods will lead to the development of novel therapies, including the use of medication, the promotion of neurotrophic factor synthesis, and gene targeting [40]. Due to their master regulatory function in several signal transduction cascades in the neuroscience field, protein kinases (PKs) have come to be identified as CNS disease-relevant targets. In the context of neurodegeneration,

GSK-3, FYN, and DYRK1A are particularly important, and the deregulation of all three PKs has been connected to a variety of CNS disorders [41]. Since Alzheimer's disease (AD) has a complex etiology and a dynamic progression from preclinical to clinical stages, it poses a unique therapeutic challenge. In more than two thousand clinical trials, several prospective treatment targets and approaches for AD were investigated. Recent breakthroughs in technical developments in the design, manufacturing, and targeting of brain mRNA and microRNA with synthetic antisense oligonucleotides (ASOs) appear to present opportunities to address the problems of AD therapy. Given that over 70% of human miRNAs are expressed in the brain and that many of these miRNAs play a role in the regulation of neuroinflammation and other important pathomechanisms of AD, this novel idea of targeting entire signaling cascades using miRNA-based ASOs is further validated [42]. By targeting the mRNA for APP or its amyloidogenic processing enzymes, several ASOs attempted to reduce the amounts of toxic amyloid. ASO OL-1 was created to specifically target the 17-30 amino acid region of the APP mRNA. Two AD mouse models, transgenic Tg2576 (APPswe) and SAMP8 mice that spontaneously generate Aβ plaques with aging, both had their APP expression levels reduced by OL-1 in the brain. Despite worries caused by the observed shift towards soluble Aβ, OL-1 treated mice were characterized by enhanced cognitive function and decreased neuroinflammation [43]. In older SAMP8 mice, ASO aimed at APP processing PS1 reduced Aβ-mediated brain oxidative stress and enhanced learning and memory. Another ASO downregulated BACE1 mRNA and protein levels in the HEK293 cell line by 90% and 45%, respectively [44]. After giving ASO intracerebroventricularly to SAMP8 mice, tau phosphorylation and oxidative stress were reduced, and learning and memory were also improved [45].Using an ASO intended to promote exon 19 inclusion in ApoER2 mRNA enhanced synaptic function, memory, and learning in mice [46]. Huntington's disease (HD) is an autosomal-dominant neurological disease brought on by CAG expansion in huntingtin (HTT) exon 1. Because the mutant huntingtin (mHTT) protein is the underlying cause of Huntington's disease, oligonucleotide-based therapeutic methods

using siRNAs and antisense oligonucleotides created to specifically silence mHTT may be cutting-edge treatment options [47]. A genetic circuit for the cytomegalovirus promoter that codes for both mHTTsiRNA and a rabies virus glycoprotein tag that targets neurons was created. This circuit was able to reprogram hepatocytes to transcribe and self-assemble mHTTsiRNA into rabies virus glycoprotein-tagged exosomes after being taken up by mouse livers following intravenous injection. A rabies virus glycoprotein tag is used to direct the mHTTsiRNA to the cortex and striatum during subsequent delivery via the exosome-circulating mechanism. As a result, the amounts of mHTT protein and toxic aggregates were successfully decreased in the cortex of three mouse models of Huntington's disease that were treated with this circuit. These findings established an efficient method for siRNA self-assembly *in vivo* that could have a considerable therapeutic advantage for Huntington's disease [48]. Parkinson's disease (PD) is a multi-factorial degenerative illness that causes tremors, gait rigidity, and hypokinesia, making daily life difficult. Because this disease is typically detected in its later stages, when neurons have completely degenerated, cure is on hold, eventually leading to death due to a lack of early diagnostic techniques. As a result, biomarkers are required to diagnose the disease early on when prevention is viable [49]. The GPR55 receptor is abundantly expressed in the brain, particularly in the striatum, implying that it may have a role in motor function. Indeed, mice lacking GPR55 have impaired motor behavior, as well as dampened inflammatory responses. Abnormal-cannabidiol (AbnCBD), a synthetic cannabidiol (CBD) isomer, is a GPR55 agonist that may be used to treat inflammatory illnesses. Abn-CBD had an anti-cataleptic effect that was reversed by CBD and PSB1216, a recently synthesized GPR55 antagonist, and two other GPR55 agonists (CID1792197 and CID2440433) also had anti-cataleptic effects. These findings show, for the first time, that activating GPR55 may be beneficial in the treatment of Parkinson's disease [50]. ALS is a fatal neurological disease that causes specific degeneration of motor neurons, resulting in muscular atrophy, eventual respiratory failure, and death. A well-known variant of the disease (fALS) is linked to point mutations. The most prevalent is an extension of the C9orf72

gene's noncoding GGGGCC hexanucleotide repeat on chromosome 9p21. Chemical chaperones (CSs) are a traditional technique for discovering treatments for protein aggregation-related disorders. The FDA has approved a CS treatment for such complication in ALS; 4-phenylbutyric acid (4-PBA). However, its high active concentration dosage prevents it from being used as an effective therapeutic agent for a long time. Hence, selective targeting of 4-PBA to specific cellular compartments such as lysosomes and ER is needed to limit its effective concentration. The 4-PBA derivatives were synthesized using organic chemistry synthetic techniques and solid-phase peptide synthesis (SPPS). The effect of these derivatives was evaluated on the eye of an ALS Drosophila model expressing C9orf72 repeat expansion. Several 4-PBA derivatives had a significant biological effect on eye degeneration. They inhibited neurodegeneration in the retina at various efficacy levels. Compound 9, a peptide derivative that was ER-targeted, was the most active CS [51]. Novel CSs surpassed 4-PBA in terms of efficacy, suggesting that they could be employed as a new class of therapeutic candidates to treat ALS [52].

Synthetic Biology-Based Cancer Therapies

By manipulating the behavior of living organisms, synthetic biology tries to apply engineering ideas to biology. An emerging application of this field is the genetic modification of bacteria to program therapeutic, safety, and specificity features as a cancer therapy [53]. Bacteria can naturally localize to tumors by entering through the vast vascular of the tumor. Once inside, they can colonize the necrotic core, an immune-privileged environment that protects them from macrophages and neutrophils. This natural colonization process has the potential to be enhanced by the addition of targeting or directing mechanisms, which can potentially lower the likelihood of off-target colonization. One approach is engineering bacteria to express tumor-homing proteins or peptides on the outer membrane. Affibodies (proteins engineered to bind targets such as upregulated receptors in cancer cells (e.g., HER2)), synthetic adhesion molecules that mimic immunoglobulin fragments and identify antigen receptors, and recognized tumor-targeting

peptides such as RGD, have all been employed as targeting motifs [54]. A magnetotactic bacterium strain was developed to transport drug-loaded nanoliposomes. After injecting grafted tumors in mice. The introduction of a magnetic field was applied in the tumor-guided bacteria. after injection of grafted tumors in mice. Enhancing tumor localization, whether through creating targeted or remotely guidable bacteria, has the potential to enhance colonization efficiency and off-target effects, and may have a significant impact on attaining effective clinical usage of these medicines [55]. Animal tumor model injected with Salmonella typhimurium harboring a promoter library generating GFP, were able to discover tumor-specific promoters by sorting and sequencing GFP-expressing bacteria. In a subsequent study, these promoters were modified, and hypoxia-detecting regions were added to create a synthetic tumor-specific hypoxic promoter [56]. Recently, *in vivo*, delivery of S. typhimurium producing flagellin B, a structural component of the flagellum from Vibrio Vulnificus, resulted in macrophage mobilization and tumor regression, possibly via activation of the toll-like receptor pathways [57]. research has employed bacteria as carriers for standard chemotherapies, such as "bacteriobots" and "nanoswimmers" loaded with doxorubicin liposomes and nano-particles, respectively [58]. A bacterium that has been genetically modified, Escherichia coli MG1655, is engineered with NDH-2 enzyme (respiratory chain enzyme II) overexpression (Ec-pE), having the ability to infiltrate tumors and increase localized H2O2 production. As a result, magnetic Fe3O4 nanoparticles bond covalently to the bacteria, serving as a catalyst for a Fenton like reaction. This reaction transforms H2O2 into hazardous hydroxyl radicals for tumor therapy. The Fenton-like reaction happens in this bioreactor using sustainably generated H2O2 generated by the engineered bacteria, and thus the produced poison causes tumor death (Figure 3). These findings demonstrate that this bioreactor can achieve effective tumor colonization as well as a self-supplied therapeutic Fenton-like reaction without the use of additional H2O2 [59]. Using engineered cells to monitor long-term blood calcium concentration, detect the onset of mild hypercalcemia, and respond via subcutaneous accumulation of the black pigment melanin to form a visible tattoo, a synthetic biology-inspired

biomedical tattoo was developed. Cells, engineered to express ectopically generated calcium-sensing receptors rewired to a synthetic signaling cascade, stimulate the production of transgenic tyrosinase, which creates melanin in response to persistently elevated blood Ca2+. Tattoos were seen in all animals implanted with hypercalcemic breast and colon adenocarcinoma cells, but not in mice inoculated with normocalcemic tumor cells. Recent scientific developments have enabled the identification of tumor-specific mutations as well as the development of personalized therapeutic cancer vaccines tailored to target tumor cells rather than normal cells in individual patients, greatly enabling targeted cancer therapy [60]. Cancer vaccines, which are important components of immunotherapy, attempt to induce long-lasting antigen-specific immunity to kill tumor cells and prevent recurrence. Many cancer vaccines have been developed in the past using tumor cells, immune cells, and live attenuated or inactivated bacteria and viruses. Two examples of cancer vaccines are KLH, a glycoprotein produced from giant keyhole limpets and employed in pre-clinical investigations, and DT, a formaldehyde-inactivated diphtheria toxoid. TT is another formaldehyde-inactivated neurotoxin commonly utilized as a vaccine carrier due to its accessibility from Clostridium tetani cultures and its well-established safety profile. CRM197, derived from the Corynebacterium diphtheriae C7(197)tox- strain, is now frequently used in clinical vaccines because of its low toxicity and large-scale manufacturability. It results from a single amino acid mutation and offers a high-purity protein [61]. Synthetic mRNA is an interesting cancer vaccine technique that can be used to execute successful cancer immunotherapy. A lipid-polyethylene glycol (lipid-PEG) shelled adjuvant-pulsed mRNA vaccination nanoparticle (NP) consisted of an ovalbumin-coded mRNA and a palmitic acid-modified TLR7/8 agonist R848 (C16-R848). This mRNA vaccine NP formulation retained the adjuvant activity of encapsulated C16-R848 while also significantly improving mRNA transfection efficacy (>95%) and subsequent MHC class I presentation of OVA mRNA derived antigen in antigen-presenting cells. In comparison to the mRNA vaccine NP without adjuvant, the C16-R848 adjuvant-pulsed mRNA vaccine NP approach created an effective adaptive

immune response by significantly enhancing the expansion of OVA-specific CD8+ T cells and infiltration of these cells into the tumor bed *in vivo*. The approach resulted in effective anti-tumor immunity against OVA-expressing syngeneic allograft mouse models of lymphoma and prostate cancer, resulting in significant tumor growth prevention [62]. PRAD (prostate adenocarcinoma) is the main cause of death among males [63]. K LHL17, CPT1B, IQGAP3, LIME1, YJEFN3, KIAA1529, MSH5, and CELSR3 were identified as overexpressed and mutant tumor antigens with poor prognostic value in PRAD. The relationship between these genes and antigen-presenting immune cells was investigated. PIS1 had greater survival and immune cell infiltration, but PIS2 and PIS3 had cold tumor characteristics, a worse prognosis, and more tumor genetic instability. Furthermore, these immune subtypes were associated with immune checkpoints, immunogenic cell death modulators, and PRAD prognostic factors. These findings indicated that KLHL17, CPT1B, IQGAP3, LIME1, YJEFN3, KIAA1529, MSH5, and CELSR3 are possible antigens for PRAD mRNA vaccine development, and that patients in the PIS2 and PIS3 groups are better candidates for immunization [64].

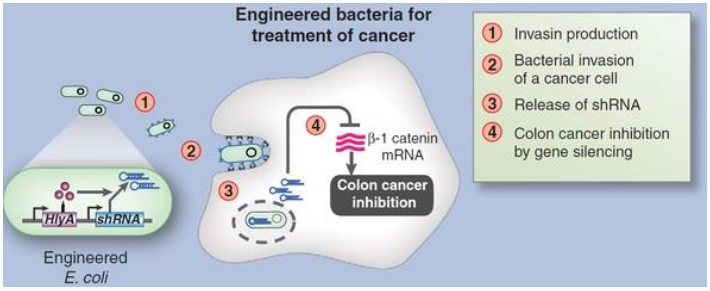

Figure 3: Engineered bacteria for treatment for cancer. A research team at UCSF engineered E. coli to penetrate mammalian cells in low-oxygen conditions, a crude indicator of a tumor. Another study enhanced this approach by programming the infiltrating E. coli to suppress a colon cancer gene (CTNNB1), thereby curbing tumor expansion. The E. coli produce a tiny RNA molecule that attaches to the CTNNB1 mRNA, signaling its breakdown. By injecting the modified E. coli, human colon cancer cells implanted beneath the skin of laboratory mice were successfully targeted, marking a fascinating initial progress [6].

Synthetic Biology in The Battle Against Infectious Diseases

Infectious diseases are a major public health concern and continue to be a leading cause of morbidity and mortality worldwide. These diseases are caused by microorganisms such as bacteria, viruses, fungi, and parasites. They can spread from person to person, through contact with infected animals or contaminated surfaces, or air [65]. Strategies for preventing the spread of infectious diseases include vaccination, proper hand hygiene, use of personal protective equipment, quarantine and isolation measures, and public health education [65]. Treatment may include antibiotics, antivirals, antifungal medications, and other targeted therapies [65]. However, a set of obstacles including late diagnosis and drug resistance prevent effective control over these diseases. Nevertheless, synthetic biology plays a significant role in disease control by providing tools for disease diagnosis and treatment [66].

If the identification of bacterial infection is delayed in diagnosing a disease, it can cause ineffective antibiotic treatment and result in early death, especially from sepsis [67]. Remarkably, the mortality rate is high, up to 30-39%, with inappropriate antibiotic treatment, whereas appropriate treatment can reduce it to 12-28%. Typically, it takes 24-48 hours or more to culture bacteria and enable appropriate antibiotic treatment [67]. Synthetic biology diagnostics can provide fast and precise identification of bacterial infections, reducing the time to diagnose [68]. For example, phages, or bacteriophages, are viruses that can eliminate bacteria. To diagnose pathogens like Staphylococcus aureus (S. aureus), Listeria, Escherichia coli (E. coli), and Bacillus anthracis, genetically engineered phages known as fluoromycobacteriophages are developed [69]. This phage-based diagnostic method can detect pathogens much faster than traditional methods, significantly reducing detection time [69]. By using this new approach, tuberculosis (TB) diagnosis, which usually takes up to 10 weeks to culture, can now be completed in as little as 24 hours [69]. The commercially available phage-based diagnostic platforms, FastPlaque TB and FastPlaque-Response assays, can diagnose TB and determine

rifampicin resistance with a sensitivity of 95% and specificity of 97% [70]. KeyPath is an FDA-approved blood culture test for methicillin-resistant S. aureus (MRSA)/methicillin-susceptible S. aureus (MSSA), which can identify S. aureus and distinguish MRSA in only 5.5 hours [71]. This is much faster than current methods of culturing S. aureus, which typically require more than 48 hours. The sensitivity and specificity of the KeyPath test are 91.8% and 98.3%, respectively. Eventually, having S. aureus as the leading sepsis etiology, the risks of sepsis are predicted to drop with this technology [71]. Moreover, a novel and affordable diagnostic tool has been created to quickly detect the Zika virus. This tool employs toehold switches, a type of RNA engineering designed for medical diagnosis, to identify the RNA genome of the Zika virus on a paper-based platform that has been freeze-dried [72]. This technique consists of a short segment of RNA that acts as a trigger (the toehold) and a larger segment of RNA that functions as the responder. When the toehold switch encounters a specific target RNA sequence, it undergoes a conformational change that activates the responder segment, allowing it to carry out the desired function, such as generating signal to indicate the presence of the target RNA [73]. Diagnostic tests based on synthetic biology are being developed to rapidly detect infectious diseases such as fungal sepsis and pneumonia, in a faster manner than traditional techniques [68].

As potential alternatives to antibiotics amid antibiotic-resistant crises, bacteriophages have been investigated as a potential therapy for bacterial infections since their initial identification as a means of treating Shigella dysenteriae in 1919 [74]. While phage therapy has been effective against a number of bacterial infections including cholera, diabetic foot ulcers, and chronic otitis, it is hindered by various limitations such as the inability of phages to penetrate cell walls, the limited host range of phages, and the development of bacterial resistance [74]. Fortunately, synthetic biology provides solutions to the limitations of phage therapy by modifying or engineering phages, which can make them safer and more effective for use in therapy [75]. One way this is accomplished is by engineering the tail component of phages to recognize multiple host strains, thus expanding the host range [76]. Using a yeast-based phage engineering system,

researchers were able to modify the host range of E. coli phages (T7, T3) by engineering the phage tail components to target Yersinia and Klebsiella bacteria. This approach succeeded in eliminating the targeted bacteria [76]. Moreover, phages have been engineered to inhibit biofilm production by expressing enzymes that degrade the biofilm matrix or by blocking communication between bacteria, which in turn leads to biofilm inhibition [76]. This strategy is highly valuable since biofilm production is a key element in disease development, as it makes bacteria resistant to drug treatment and the immune system [66]. Quorum sensing is the process through which bacteria communicate and coordinate biofilm formation. The main component of this cellular signaling is acyl-homoserine lactones (AHL), and lactonase is a molecule known for its ability to quench this quorum sensing process [77]. Based on this, scientists have developed phages that can prevent biofilm formation by quenching quorum sensing. They engineered the T7 bacteriophage to produce the AiiA lactonase enzyme upon infection, which can degrade the AHLs. As a result, the T7 phage expressing AiiAlactonase efficiently inhibited biofilm production [77].

To add more, one of the most high-profile breakthroughs in medicine from synthetic biology research is the creation of a precursor to anti-malarial drugs, artemisinic acid, from yeast [78]. Artemisinic acid can be sourced from Artemisia annua (sweet wormwood) using an extraction process, which before this discovery was in a crisis state due to unrelenting demand and limited supplies of the plant. Now, instead of relying on natural sources, scientists can produce artemisinin-based therapies (ACTs), ranked as the most effective anti-malarial treatment, which is cheaper and more reliable [78].

During the Coronavirus disease 2019 (COVID-19) pandemic, synthetic biology provided lifesaving tools for disease diagnosis, treatment, and prevention [66]. Development of several diagnostic platforms such as specific high sensitivity enzymatic reporter unlocking (SHERLOCK), DNA endonuclease-targeted CRISPR trans reporter (DETECTR), and 1 h low-cost multipurpose highly efficient system (HOLMES) helped detect

disease biomarkers with high sensitivity and efficiency [79]. Additionally, programmable toehold switch sensors have been developed to isolate viral RNA from patients' swab samples and detect SARS-CoV-2-specific genomic regions, producing a fluorescent signal [80].

As a therapeutic approach, a synthetic biology drug called carrimycin has been approved by the FDA for a Phase III trial to treat bacterial infections associated with COVID-19 [81]. This is a newly developed drug with anti-bacterial and anti-inflammatory properties, which is created through genetic engineering of Streptomyces spiramyceticus by adding a 4″-O-isovaleryltransferase gene from Streptomyces thermotolerant [81]. This modification allowed carrimycin to possess stronger antibacterial properties, where studies have demonstrated that carrimycin can effectively inhibit viral RNA synthesis, particularly post-entry replication events, without causing any major adverse effects in the treatment of severe COVID-19 cases [81].

As preventive measures, synthetic biology enabled the creation of vaccines that contain only the nucleic acid building blocks of an antigen, addressing several safety concerns [82]. This technology has been instrumental during the COVID-19 pandemic, as it has allowed for the rapid development and distribution of DNA and RNA vaccines at an unparalleled rate [83].

Finally, synthetic biology presents a promising potential to improve future rates of morbidity and mortality caused by infectious diseases through preventive, diagnostic, and therapeutic synthetic biotics (Figure 4).

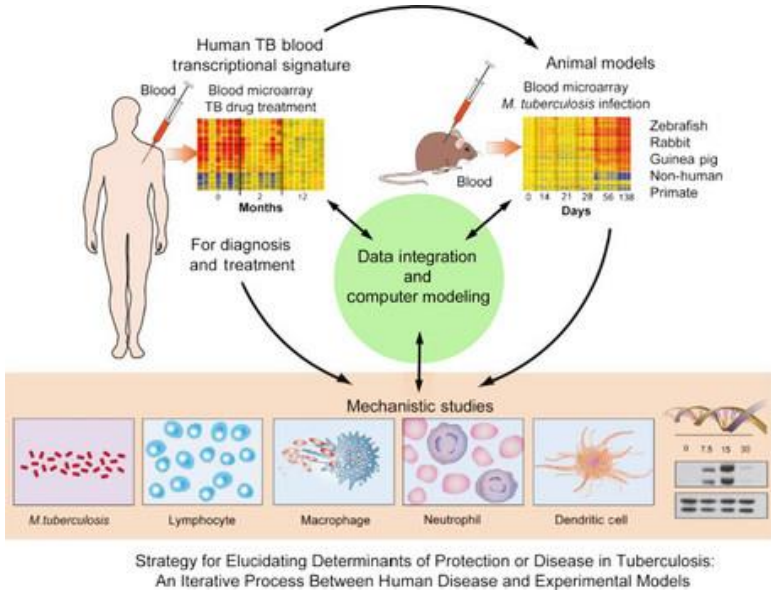

Figure 4: Employing a systems biology methodology in the study of infectious diseases, the figure outlines the strategy for uncovering factors that either protect against or contribute to tuberculosis. This involves a cyclical process alternating between human disease investigation and experimental model testing [84].

Tackling Bacterial Drug Resistance Utilizing Synthetic Antibiotics Assortment

The emergence and spread of bacteria resistant to the majority of known medicines increases fears of a worldwide infectious disease crisis [85]. Any solution relies on the development of novel medicines that are efficient against current bacterial diseases, although opinions differ on what methods are most effective for achieving these discoveries [86]. For decades, natural products served as both conceptual and material starting points for antibiotic discovery. However, making specific chemical modifications to structurally complex natural products (that is, semisynthesis) is inherently difficult, and the pace of drug discovery via this route has slowed significantly [87]. In an alternative approach, the development of fully synthetic platforms for the construction of tetracycline [88], macrolide

[89] group (A) streptogramin [90], and arylomycin [91] antibiotics has enabled deep structural modifications not possible with semisynthetic drugs. These tools enable chemists to imagine and evaluate an infinite number of design possibilities.

We employ component-based chemical synthesis to achieve a significant re-scaffolding of lincosamide antibiotics, yielding a broad-spectrum agent effective against a broad spectrum of multidrug-resistant bacterial infections. Lincosamides are one of the numerous ribosome-targeting groups that have proven crucial to current pharmacopeia [92]. The first member of the family, lincomycin, was discovered in 1963 from a streptomycete found in Nebraskan soil [93] and found immediate application in the management of staphylococcal, pneumococcal, and streptococcal infections. An early semisynthetic modification led to the antibiotic now known as clindamycin, a molecule with optimized pharmacokinetic properties and an expanded spectrum of activity [94] that has mainly replaced lincomycin in human medicine [94]. Considering the US Food and Drug Administration accepted clindamycin in 1970, semisynthetic and fully synthetic methods of lincosamide discovery have been investigated, leading to candidates with six- and seven-membered aminoacyl residues, each with an expanded spectrum of activity [95]. More recently, reports of changes in the aminosugar residue through semisynthesis have been made, extending coverage to some Gram-positive bacteria that are multidrug resistant [96].

Clindamycin-resistant bacteria are globally distributed and are commonly acquired through N6-dimethylation of 23S ribosomal RNA (rRNA) residue A2058 [97]. The US Centers for Disease Control and Prevention (CDC) have identified three major resistance mechanisms among its most pressing threats in their 2019 report (1): a distinct rRNA methyltransferase, Cfr (encoded by the horizontally transferrable gene CFR) [98], methylates C8 of the 23S rRNA residue A2503 and confers resistance to phenicol, lincosamide, oxazolidinone, pleuromutilin and streptogramin A [98]. (PhLOPSA) antibiotics as well as 16-membered macrolides [99]. Additionally, recent studies have elucidated a third major resistance mechanism affecting lincosamides, whereby target-protection proteins (e.g. LsaA)

bind to antibiotic-inhibited ribosomes, evicting the drug and restoring protein synthesis [100]. The prevalence of erm genes among clinical streptococcal and staphylococcal isolates has led to the rise of Clostridium difficile colitis, which challenges the continued utility of this antibiotic in patients.

To counteract the possibility of bacterial resistance, phytochemicals are thought to have a crucial role in reducing bacterial virulence. It's interesting to note that these processes allow natural phytocompounds to display their antibacterial activity through their chemical makeup and physical characteristics [101]. Because of their antimicrobial activity, bioactive-rich compounds like alkaloids, phenols, flavonoids, and terpenoids, among others, must be isolated and profiled to be used in the creation of novel and natural antimicrobial drugs. These compounds also have a specific clinical significance because of their bioactivity, which does not result in resistance. These bioactive substances are often divided into five categories: polyphenolics, alkaloids, tannins, glycosides, and steroids. Among them, polyphenols have antibacterial properties that are effective against a variety of pathogens. Polyphenolic compounds, especially flavanol and phenolic acids, have been shown to have the highest activity for a variety of scientific reasons, including attenuating bacterial virulence factors such as enzymes and toxins, decreasing extracellular polysaccharide activity, and acting as extracellular polysaccharide inhibitors. Much scientific research has clearly demonstrated that increasing the number of compounds stimulated pathogen inhibition potential [102].

Alkaloids, such as quinolone, dictamnine [103], and kokusagine [104], are a cluster of heterocyclic compounds with antimicrobial potential. These compounds show suitable antibacterial activity against a wide range of bacterial pathogens, including B. cereus, S. aureus, and K. pneumonia [105]. Piperine, which was isolated from Piper nigrum and ciprofloxacin, has been shown to inhibit type II topoisomerase enzyme and reduce the consumption of O2 against bacteria. Diterpenoid alkaloids belonging to Ranunculaceae have antimicrobial properties. The mechanism of action of quaternary

alkaloids, such as berberine and harmane, is accomplished by their ability to interpolate with DNA, leading to impairment in cell division and cell death. These compounds have antimicrobial potential against bacteria, fungi, protozoa, and even viruses by aiming at DNA intercalation, affecting RNA polymerase, gyrase, and topoisomerase, and by inhibiting cell division [106]. Comparably berberine has potent antimicrobial activity against bacteria, fungi, protozoa, and even viruses by intercalating DNA, affecting RNA polymerase, gyrase, and topoisomerase, and inhibiting cell division [107]. Berberis spp., a phytochemical substance, decreased E. coli development by inhibiting cell division, protein, and DNA synthesis [106]. The antimicrobial chemical chanoclavine, derived from Ipomoea muricata, had synergistic efficacy when combined with tetracycline, which appears to block EP and was described as efficacious and ATPase dependent [108].

Plasmid, a self-replicating, circular DNA coding for multiple gene groups, is resistant to antibiotics in bacteria. Certain phytochemicals were reported to target such plasmids [109]. 8-Epidiosbulbin-E-acetate, derived from Dioscorea bulbifera, has been shown to effectively cure antibiotic-resistant R-plasmids in clinical isolates of E. faecalis, E. coli, Shigella sonnei, and P. aeruginosa [110]. Tomatidine, a Solanaceous plant derivative, has been shown to have antibacterial action against Listeria, Bacillus, and Staphylococcus spp. Tomatidine's probable mode of action is as an ATP synthase inhibitor [111].

P. aeruginosa and S. epidermidis are resistant to allicin, an organosulfur molecule derived from Allium sativum. Allicin's antibacterial action mechanism involves the suppression of DNA synthesis, protein synthesis, and sulfhydryl-dependent enzymes [112]. The antibacterial activity of ajoene from A. sativum inhibits the sulfhydryl-dependent enzyme inhibitor of Campylobacter jejuni [113]. The application of Diplotaxis harra-derived sulforaphane as an ATP synthase inhibitor and DNA/protein synthesis inhibitor was investigated, and the results demonstrated that this molecule successfully inhibits E. coli growth. Furthermore, this compound has been shown to destroy the target pathogen's membrane [114].

Terpenes, also known as isoprenoids, are the most abundant family of substances found in essential oils and are composed of isoprene molecules [115]. Essential oils (EOs) are made up of a variety of phytochemicals and are well known for their antibacterial properties. Furthermore, because they are considered safe to consume and necessary for host tissues, they have been used as a traditional medicinal treatment to combat antibiotic resistance [116]. EOs produced from Melaleuca alternifolia improved bacterial membrane permeability [117]. Farnesol, an essential oil phytochemical, suppressed S. aureus development by damaging the cell membrane [118].

Plant flavonoids are phenolic compounds with a 2-phenyl-benzo-γ-pyrane nucleus and two benzene rings with potent antimicrobial activities. Flavonoids such as flavanols, flavanones, isoflavonoids, chalcones, and dihydrochalcones have been reported to exhibit antimicrobial properties [119]. Catechin causes membrane disruption in MRSA, leading to the accumulation of bacterial cells and increased permeability of pathogenic S. aureus and E. faecalis [120].

Numerous plant-derived bioactive substances (phytochemicals) have been studied for their ability to reverse antibiotics and kill bacteria. The bioactive potentials of such phytochemicals have been found to inhibit important virulence factors linked to resistance development, such as cell permeability, efflux pumps, DNA replication mechanisms, and other bacterial virulence-related processes, such as biofilm formation and quorum sensing. Furthermore, the synergistic effects of these phytochemicals in combination with conventional antibiotics were found to be extremely effective against antibiotic-resistant pathogenic bacteria.

Synthetic Biology Related Advances for Natural Drugs Synthesis

Synthetic biology blends classical metabolic engineering and ideas from systems biology. Recent developments in synthetic biology have strongly influenced research on herbal remedies. The characteristics of optimized and altered organisms include

reduced carbon emissions, environmental friendliness, and economic effectiveness. They can constantly and effectively synthesize specified target molecules with high yields. New biosynthetic pathways can be devised to produce numerous natural medications and analogs, eliminating the need to rely solely on conventional discovery and separation or difficult synthetic chemistry to acquire a small number of natural pharmaceuticals and analogs [121].

Plant extraction is now a way of producing natural pharmaceuticals from plants; nevertheless, traditional methods of preparing natural chemicals that rely on plant extraction have several drawbacks. Most natural plant medicines have extremely low content in the host; for example, 3 kg of bark from a 100-year-old Pacific yew may contain just 300 mg of paclitaxel, accounting for 0.01% of the bark's dry weight [122]. The first and most widely publicized application of synthetic biology for the industrial production of an important drug is the case of semi-synthetic artemisinin. This antimalarial drug was originally obtained from plant sources but can now be produced in large quantities in heterologous hosts, including Saccharomyces cerevisiae [123]. Malaria is one of the world's worst parasite infections. Malaria infected about 214 million people in 2015, killing 438,000 individuals, most of whom were children under the age of five. WHO presently considers artemisinin-based combination therapy to be the most effective technique for treating malaria [124]. Due to the unstable structure of artemisinin and the complexity of the method of purification, the manufacturing cost of artemisinin is expensive, hampering efforts to meet market needs. As a result, identifying a more efficient way to produce artemisinin is critical. The advancement of high-throughput sequencing and molecular technology has resulted in the elucidation of the artemisinin biosynthesis route, and the genes of certain essential enzymes in the artemisinin biosynthetic pathway have been cloned and described [125]. The methylerythritol-4-phosphate route (MEP) in plastids and the mevalonate pathway (MVA) in the cytoplasm of A. annua are the two pathways that give rise to the universal 5-carbon precursor isopentenyl pyrophosphate (IPP) and its double-bond isomer dimethylallyl pyrophosphate (DMAPP) [126]. The

artemisinin precursor farnesyl diphosphate (FPP) was discovered to be involved in the synthesis of different isoprenoids (artemisinin, aristolochene, caryophyllene, farnesene, and sterols) by combining two IPP molecules with a single DMAPP molecule. In artemisinin-producing organisms, farnesyl diphosphate synthase (FPS) catalyzes the synthesis of FPP [127]. The first unique sesquiterpenoid precursor of the artemisinin biosynthesis pathway, amorpha-4,11-diene (AD), is generated by cyclization of FPP catalyzed by amorpha-4,11-diene synthase (ADS) [128]. The Keasling group cloned the amorpha-4,11-diene oxidase gene CYP71AV1 from A. annua glandular hairs and inserted ADS, CYP71AV1, and CPR into Saccharomyces cerevisiae at the same time [17]. This yeast cell factory produced more than 100 mg/L of artemisinic acid. Semi-chemical synthesis can effectively and cheaply convert artemisinin acid to artemisinin. All FPP synthesis-related genes in S. cerevisiae CEN.PK2 was overexpressed in order to increase the yield of artemisinic acid [129]. These genes included ERG10, ERG13, tHMG1, ERG12, ERG8, ERG19, IDI1, and ERG20. Additionally, three copies of tHMG1 were integrated to achieve the 40 g/L fermentation level of the artemisinin. The highest concentration of artemisinic acid (25 g/L) was produced by the Keasling group [130] by combining the expression of the cytochrome b5 gene, NAD alcohol dehydrogenase, and NAD acetaldehyde dehydrogenase genes. It is still unknown whether A. annua converts dihydroartemisinic acid to artemisinin by enzymatic or nonenzymatic means during the last stages of artemisinin production. It is understood that spontaneous autoxidation, a non-enzymatic process, can transform dihydroartemisinic acid into artemisinin [131]. RNA interference technology is used for inserting antisense strands of cDNA into A. annua to downregulate the expression levels of β-farnesyl pyrophosphate synthase, β-caryophyllene synthase (CPS), and squalene synthase to block the effects of the pathways that compete with artemisinin biosynthesis [132]. The production of artemisinin in all transgenic A. annua plants rose by 70% as compared to control plants. Furthermore, because the organism is a complex membrane structure system, compartmentalization of the secondary metabolite biosynthetic process not only allows enzymes to be aggregated as functional units but also separates

the pathway from the rest of the cell. Certain types of selective advantages can be expected from the co-compartmentalization of biosynthetic enzymes. The closeness of continuous enzymes in the secondary metabolite biosynthesis pathway might increase route efficiency. This is especially critical if the products and intermediates are potentially harmful to the manufacturing cell [133].

Salvia miltiorrhiza Bunge (Danshen) is a Lamiaceae-family medicinal herb. Because the hydrophilic phenolic acids and lipophilic constituents of these roots are pharmaceutically active components, dried roots of this plant have been used in traditional Chinese medicine (TCM) for a long time [134]. Tanshinone I (TS I), TS IIA, and crypto tanshinone (CTS), which make up the majority of the lipophilic constituents, have a variety of pharmacological activities, including anticancer [135] and antibacterial effects [136], and can be effectively used to treat cardiovascular diseases [137]. The enzymes diterpene synthase copalyldiphosphate synthase (SmCPS) and kaurene synthase-like (SmKSL) cyclize GGPP, the tanshinone precursor in the cytosolic MVA pathway and plastid-localized MEP pathway, to produce miltiradiene [138], a crucial precursor for the biosynthesis of tanshinone. A mutagenesis cassette encoding SMCPS, SMKSL, ERG-20, BTS1, and HMG1 was constructed using the modularized pathway engineering methodologies, and a high yield of miltiradiene (365 mg/L) was produced in yeast [138]. Miltiradiene production was increased to 488 mg/L thanks to pathway optimization in a yeast expression system [139]. A high-yielding GGPP chassis line was created by deleting the distant genetic loci YPL062w and YJL064w and knocking out the transcriptional regulator Rox1 (repressor of hypoxia). Next, two high-efficiency catalytic enzymes (CfTPS1 and SmKSL1) were combined to create a fusion protein that can most efficiently convert GGPP to miltiradiene in yeast. Finally, miltiradiene production was increased [140].

The first-line medicine for the treatment of breast cancer and ovarian cancer is paclitaxel, a diterpenoid anticancer agent derived from Chinese yew. Yew has little paclitaxel in it, and there are not many T. chinensis plants around. The complicated and expensive complete chemical synthesis of paclitaxel makes

semichemical synthesis a significant approach for the commercial manufacturing of paclitaxel [141]. The primary pathway for paclitaxel's biosynthesis has been established, and most of the enzymes have been acquired and functionally assigned. Currently, 14 of the 19 enzymes needed for the biosynthesis of paclitaxel have been discovered; however, the sequence in which most of these enzymes, particularly P450 enzymes, engage in the pathway has not yet been established [142]. The most promising ways for producing paclitaxel right now are semisynthesis and microbial synthesis of its precursors. These technologies are expected to address the market's issues with unaffordable prices and insufficient supply of paclitaxel. The endangered T. chinensis must also be protected [143]. The basic biosynthetic pathway includes the cyclization of GGPP to taxa-4(5),11(12) diene by taxadiene synthase [144]; hydroxylation of taxane skeleton at C5, C10, C13, C2, C9, C7, and C1 by cytochrome P450 monooxygenase to generate oxetane; the creation of epoxypropane D-ring at C4 and C5; and then CoA acylation to synthesize the essential intermediate baccatin III [145]. Taxol's C13 side chain is the essential component for its anticancer properties. The side chains of baccatin III and phenylisoserine are joined at position C13, and the side chains are subsequently hydroxylated and benzoylated at positions C2 and C3 to produce paclitaxel [146]. Engels and colleagues overexpressed the genes for taxadiene synthesis, geranylgeranyl diphosphate (GGPP) synthase, HMG1 reductase (thmgr), and the transcription factor UPC2-1 in S. cerevisiae [147]. The modified microbe produced 8.7 0.85 mg/L of taxa-4(5), 11(12)-diene, and up to 33.1 5.6 mg/L of geranylgeraniol accumulated. The Scott team introduced four genes to engineer E. coli to produce taxadiene, which was a breakthrough in paclitaxel synthesis. Two P450 enzymes and an acetyltransferase enzyme were introduced into yeast to obtain taxadien-5-acetate-10-ol yield of 1 mg/L [138].

Challenges in Synthetic Biology

Despite advances in many aspects of synthetic biology, this field is facing various challenges. Challenges loom at every stage of the process in synthetic biology, from part characterization to system design and assembly. Synthetic biology aims to assemble

or build novel functions that do not exist in nature. In this regard, standard components such as amino acids, nucleotides, and other chemical concerns will be used where a biological component can range from a DNA sequence that encodes a specific protein to a promoter, which is a region that facilitates gene expression. It also takes standard parts, computer design, and software, and understanding to put together a functional system. Besides, the issue is that many sections have not been well defined. They have not always been studied to prove what they do, and even when they have, their performance might vary depending on cell type or laboratory settings. Furthermore, the full promise of synthetic biology has yet to be realized [148], primarily due to challenges associated with its integration. This integration is impeded by debates surrounding genetically modified organisms (GMOs), their potential environmental effects, and the accompanying containment and regulation problems [149]. Additionally, while cell-free systems, which mimic life-like functioning outside living cells, offer promise, debates over GMOs have influenced their adoption. However, despite these challenges, cell-free systems have demonstrated success in manufacturing essential bio-molecules, including medicines [150]. The inherent lack of understanding of fundamental biological processes is the key constraint in synthetic biology in general, not simply scaling already proven technology. Much metabolic engineering research now focuses on "mutagenesis" and "directed evolution," which involves messing with a cell's DNA and hoping for the best. So one issue is getting proteins (which are encoded by DNA) to do the exact function that we want [151]. One of the many exciting potentials that synthetic biology provides for medicine is the creation of theranostic cell lines capable of sensing disease states and producing an appropriate therapeutic response [152]. To achieve this goal, several obstacles need to be addressed. First, we must broaden the range of molecules that can be recognized as inputs by cellular "sensors," and second, we must better understand the genetic control factors that regulate gene expression in space and time so that we can engineer better activator systems. Furthermore, the circuitry is erratic. Even though the function of each element is known, the pieces may not perform as predicted when assembled. Synthetic biologists are frequently stuck in a

lengthy trial-and-error process, in contrast to the more predictable design techniques used in other modern engineering fields. Synthetic genetic circuits, once built and implanted in cells, can have unforeseen consequences for their host. For example, we can't predict how protein-DNA interactions change DNA structure, how a specific protein-DNA structure affects gene expression, how supercoiling occurs as a result of genetic circuit layout, how DNA-encoded modules perform due to the possibility of mechanical interactions, and how the location of a gene on the genome affects gene expression [153]. Even if one could mimic the entire designed cell using known software tools, the information obtained would be useless for design and verification. In truth, there is a wealth of experimental data and computational tools available to define some of these effects individually, but there is a lack of a design-oriented mathematical framework to explain these effects and their relationships. Also, our inability to address the preceding issue is primarily due to our lack of understanding of modularity and compositionality in natural biological systems. Natural biological systems, such as (unfortunately) cancer pathways, are exceedingly resistant to parameter uncertainty and external perturbations [154]. Synthetic biologists must also verify that circuits work dependably. Molecular processes inside cells are subject to random oscillations or noise, where its propagation can deteriorate circuit performance or even lead to complete circuit failure [155].

Variations in growing conditions can also influence behavior and eventually, randomly occurring genetic mutations might completely disable a circuit's function. Addressing these robustness issues may need a shift away from conventional fundamental processes in synthetic biology, such as gene expression and gene control, and toward new types of processes, such as protein-protein interactions and CRISPR/Cas-based systems. These biological tools are currently ignored, even though they may allow for faster reactions and a simpler tuning approach [156]. However, how to do circuit design employing these key techniques to obtain a desired functionality remains unknown. Moreover, synthetic biology is an example of a dual-use technology: it has many promising uses, yet it may also be harmful [157].

Conclusion

We have reached a watershed moment in the history of modified immune cell cancer therapies. The emerging field of synthetic immunology is assembling a large resource of tools that can be used to enhance or reprogram T cell function in various ways and overcome the fundamental problems in cancer treatment, how to recognize the tumor and distinguish it from normal cells, and how to mount a potent cytotoxic response that overcomes the local immunosuppression that is common in many solid tumors. Although we have concentrated on CAR T cells as an engineering T cell therapy for cancer, many of the techniques and tactics apply to other disorders such as autoimmune ones. It is also feasible that modified immune cells will become beneficial as a research tool. An immune cell with the ability to identify user-defined antigen signatures and change the microenvironment, like an antibody or medication, would enable a novel and customized form of targeted disruption. A precision-engineered cell that can participate as an active yet controlled node within the complex, *in vivo* networks would be a great tool as we learn more about the fundamental principles of tissues and systems composed of numerous cell types. In order to overcome some of the apparent drawbacks of current biological molecules, an intriguing new generation of biologics that not only disrupt the immune response but also use autologous immune cells to treat illnesses is now being developed. In conclusion, although synthetic immunology is young, it has a promising future. In preclinical and clinical trials, fascinating new treatment ideas for modifying the immune response, as well as innovative technical techniques that alter the function, activity, or Immune cell targeting are currently being developed. Modulation of the immune response based on the principles of synthetic biology has enormous potential since immune cells are implicated in the pathogenesis of a range of disorders. Synthetic biology will contribute to innovative technologies by introducing therapeutic systems based on a synthetic genome, employing an enlarged genetic code, and built for precisely tailored medication manufacturing as well as transport and activation by a pathological signal.

References

1. Rabinow P, Bennett ÆG. Synthetic biology: ethical ramifications. 2009; 2009: 99–108.
2. Andrianantoandro E, Basu S, Karig DK, Weiss R. Synthetic biology : new engineering rules for an emerging discipline. 2006; 1–14.
3. Bassetti M, Merelli M, Temperoni C, Astilean A. New antibiotics for bad bugs : where are we ? Annals of Clinical Microbiology and Antimicrobials. 2013; 12: 1.
4. Jones KE, Patel NG, Levy MA, Storeygard A, Balk D, et al. Global trends in emerging infectious diseases. 2008; 451: 990–994.
5. Yan X, Liu X, Zhao C, Chen GQ. Applications of synthetic biology in medical and pharmaceutical fields. Sig Transduct Target Ther. 2023; 8: 1–33.
6. SYNTHETIC BIOLOGY (SYNBIO) – Dr Rajiv Desai [Internet]. 2023. Available online at: https://drrajivdesaimd.com/2017/05/07/synthetic-biology-synbio/
7. Tan X, Letendre JH, Collins JJ, Wong WW, Hospital MG. HHS Public Access. 2022; 184: 881–898.
8. Zhao N, Song Y, Xie X, Zhu Z, Duan C, et al. Synthetic biology-inspired cell engineering in diagnosis, treatment , and drug development. 2023.
9. Slomovic S, Pardee K, Collins JJ. Synthetic biology devices for in vitro and in vivo diagnostics. 2015; 112: 14429–14435.
10. Geraldi A, Giri-rachman EA. Synthetic biology-based portable in vitro diagnostic platforms. Alexandria Journal of Medicine. 2020; 54: 423–428.
11. Meile S, Sarbach A, Du J, Schuppler M, Saez C. crossm Engineered Reporter Phages for Rapid Bioluminescence-Based Detection and Differentiation of Viable Listeria Cells. 2020; 86: 1–14.
12. Ye H, Xie M, Xue S, Hamri GC el, Yin J. Europe PMC Funders Group Self-adjusting synthetic gene circuit for correcting insulin resistance. 2017; 1: 1–21.
13. Holohan C, Schaeybroeck S Van, Longley DB, Johnston PG. Cancer drug resistance : an evolving paradigm. Nature

Publishing Group. 2013; 13: 714–726.
14. Abil Z, Xiong X, Zhao H. Synthetic Biology for Therapeutic Applications. 2015.
15. Grupp SA, Maude SL, Teachey DT. Tisagenlecleucel for the treatment of B-cell acute lymphoblastic leukemia. 2022; 18: 959–971.
16. Weber W, Schoenmakers R, Keller B, Gitzinger M, Grau T, et al. A synthetic mammalian gene circuit reveals antituberculosis compounds. 2008; 105.
17. Ro D kyun, Paradise EM, Ouellet M, Fisher KJ, Newman KL, et al. Production of the antimalarial drug precursor artemisinic acid in engineered yeast. 2006; 440: 3–6.
18. Wagner HJ, Weber W, Fussenegger M. Synthetic Biology : Emerging Concepts to Design and Advance Adeno-Associated Viral Vectors for Gene Therapy. 2021; 2004018: 1–22.
19. Jain KK. Synthetic Biology and Personalized. 2013; 209–219.
20. Wang L, Wang F sheng, Gershwin ME. Human autoimmune diseases : a comprehensive update. 2015; 369–395.
21. Zhernakova A, Diemen CC Van, Wijmenga C. Detecting shared pathogenesis from the shared genetics of immune-related diseases. 2009; 10.
22. Habibi MA, Nezhad Shamohammadi F, Rajaei T, Namdari H, Pashaei MR, et al. Immunopathogenesis of viral infections in neurological autoimmune disease. BMC Neurology. 2023; 23: 201.
23. Rosenblum MD, Remedios KA, Abbas AK. Mechanisms of human autoimmunity. 2015; 125.
24. Brenner MJ, Cho JH, Wong NML, Wong WW. Synthetic Biology : Immunotherapy by Design. 2018; 95–118.
25. Ph D, Shaw T, Sc B. Efficacy of B-Cell–Targeted Therapy with Rituximab in Patients with Rheumatoid Arthritis. 2004; 2572–2581.
26. Pescovitz MD, Pescovitz MD. Rituximab, an Anti-CD20 Monoclonal Antibody : History and Mechanism of Action. American Journal of Transplantation. 2006; 6: 859–866.
27. Tchorbanov AI, Voynova EN, Mihaylova NM, Todorov TA, Nikolova M, et al. Selective silencing of DNA-specific B lymphocytes delays lupus activity in MRL / lpr mice. 2007;

3587–3596.
28. Chen R, Jing J, Siwko S, Huang Y, Zhou Y. ScienceDirect Intelligent cell-based therapies for cancer and autoimmune disorders. Current Opinion in Biotechnology. 2020; 66: 207–216.
29. Caliendo F, Dukhinova M, Siciliano V. Engineered Cell-Based Therapeutics : Synthetic Biology Meets Immunology. 2019; 7: 1–8.
30. Ghani M, Ghani Q ul ain, Balazs L, Beranova-giorgianni S, Giorgianni F, et al. highly effective treatment for murine lupus. 2021; 11: 1–28.
31. Rafiq S, Hackett CS, Brentjens RJ. therapy. Nature Reviews Clinical Oncology. 2020; 17.
32. Ellebrecht CT, Bhoj VG, Nace A, Choi EJ, Mao X, et al. therapy of autoimmune disease. 2017; 353: 179–184.
33. Oh S, Connor KCO, Payne AS. MuSK chimeric autoantibody receptor (CAAR) T cells for antigen-specific cellular immunotherapy of myasthenia gravis antibodies NMJ Autoreactive B cells produce antibodies. 2012.
34. Meng H, Sun X, Song Y, Zou J, An G. La/SSB chimeric autoantibody receptor modified NK92MI cells for targeted therapy of autoimmune disease. Clinical Immunology. 2018.
35. Tumors L. HHS Public Access. 2020; 382: 545–553.
36. Haddadi M hossein, Hajizadeh-saffar E, Khosravi-maharlooei M, Basiri M, Negahdari B, et al. Jo ur l P of. Blood Reviews. 2019; 100645.
37. Steendam K Van, Tilleman K, Ceuleneer M De, Keyser F De, Elewaut D, et al. Citrullinated vimentin as an important antigen in immune complexes from synovial fluid of rheumatoid arthritis patients with antibodies against citrullinated proteins. 2010.
38. Nezhad MS, Seifalian A, Bagheri N, Yaghoubi S. Chimeric Antigen Receptor Based Therapy as a Potential Approach in Autoimmune Diseases : How Close Are We to the Treatment ? 2020; 11: 1–12.
39. Wareham LK, Liddelow SA, Temple S, Benowitz LI, Polo A Di, et al. Solving neurodegeneration : common mechanisms and strategies for new treatments. Molecular Neurodegeneration. 2022; 1–29.
40. Agust C. Prospects & Overviews Synthetic biology and

therapeutic strategies for the degenerating brain. 2014; 979–990.
41. Demuro S, Martino RMC Di, Ortega JA, Cavalli A. GSK-3 β, FYN, and DYRK1A: Master Regulators in Neurodegenerative Pathways. 2021.
42. Grabowska-pyrzewicz W, Want A, Leszek J, Wojda U. EBioMedicine Antisense oligonucleotides for Alzheimer ' s disease therapy : from the mRNA to miRNA paradigm. 2021; 74.
43. Medical A, Louis S. Peripheral Administration of Antisense Oligonucleotides Targeting the Amyloid- ␣ Protein Precursor Reverses A ␣ PP and LRP-1 Overexpression in the Aged SAMP8 Mouse. 2012; 28: 951–960.
44. Chakravarthy M, Veedu RN. BACE1 Inhibition Using 2' - OMePS Steric Blocking Antisense Oligonucleotides. 2019; 1–12.
45. Farr SA, Ripley JL, Sultana R, Zhang Z, Michael L, et al. Implications for Alzheimer Disease. 2015; 387–395.
46. Hinrich AJ, Jodelka FM, Chang JL, Brutman D, Bruno AM, et al. Therapeutic correction of ApoER 2 splicing in Alzheimer' s disease mice using antisense oligonucleotides. 2016; 8: 328–345.
47. Sathasivam K, Neueder A, Gipson TA, Landles C, Benjamin AC, et al. Aberrant splicing of HTT generates the pathogenic exon 1 protein in Huntington disease. 2012.
48. Zhang L, Wu T, Shan Y, Li G, Ni X, et al. Therapeutic reversal of Huntington' s disease by in vivo self-assembled siRNAs. 2021.
49. Lotankar S, Prabhavalkar KS, Bhatt LK. Biomarkers for Parkinson' s Disease: Recent Advancement. Neuroscience Bulletin. 2017; 33: 585–597.
50. Celorrio M, Rojo-bustamante E, Fernández-suárez D, Sáez E, Mendoza AE hermoso De, et al. SC. Neuropharmacology. 2017.
51. Mathis S, Goizet C, Soulages A. PT SC. Journal of the Neurological Sciences. 2019.
52. Azoulay S, Michela G, Salvio D, Weitman M, Afri M, et al. Chemical chaperones targeted to the endoplasmic reticulum (ER) and lysosome prevented neurodegeneration in a C9orf72 repeat expansion drosophila amyotrophic lateral

sclerosis (ALS) model. Pharmacological Reports. 2021; 73: 536–550.
53. Siuti P, Yazbek J, Lu TK. letters Synthetic circuits integrating logic and memory in living cells. Nature Biotechnology. 2013; 31: 448–452.
54. Ferna R, Cuesta AM, Luis A, Luis A. Programming Controlled Adhesion of E. coli to Target Surfaces, Cells, and Tumors with Synthetic Adhesins. 2014.
55. Felfoul O, Mohammadi M, Taherkhani S, Lanauze D De, Xu YZ, et al. Magneto-aerotactic bacteria deliver drug-containing nanoliposomes to tumour hypoxic regions. 2016.
56. Deyneko I V, Kasnitz N, Leschner S, Weiss S. Composing a Tumor Specific Bacterial Promoter. 2016; 1–17.
57. Zheng JH, Nguyen VH, Jiang S nan, Park S hwan, Tan W, et al. Two-step enhanced cancer immunotherapy with engineered Salmonella typhimurium secreting heterologous flagellin. 2017; 9537: 1–11.
58. Park S. Ac ce p te us cr t. Sensors & Actuators: B Chemical. 2015.
59. Fan J xuan, Peng M yun, Wang H, Zheng H ran, Liu Z lin, et al. Engineered Bacterial Bioreactor for Tumor Therapy via Fenton-Like Reaction with Localized H 2 O 2 Generation. 2019; 1808278: 1–8.
60. Blass E, Ott PA. Advances in the development of personalized neoantigen-based therapeutic cancer vaccines. Nature Reviews Clinical Oncology. 2021; 18: 215-229.
61. Xiong A wen, Fang J min, Ren S xiang, Li W, Wang J, et al. Therapeutic Cancer Vaccine , Recombinant EGF-CRM197 , in Patients With Advanced Solid Tumors : A Phase I Clinical Study. 2021; 11: 1–10.
62. Islam MA, Rice J, Reesor E, Zope H, Tao W, et al. Jo ur na l P re of. Biomaterials. 2020; 120431.
63. Sung H, Ferlay J, Siegel RL, Laversanne M, Soerjomataram I, et al. Global Cancer Statistics 2020 : GLOBOCAN Estimates of Incidence and Mortality Worldwide for 36 Cancers in 185 Countries. 2021; 71: 209–249.
64. Zheng X, Xu H, Yi X, Zhang T, Wei Q, et al. Tumor-antigens and immune landscapes identification for prostate adenocarcinoma mRNA vaccine. Molecular Cancer. 2021; 1–7.

65. Watkins K. Emerging Infectious Diseases : a Review. 2018; 86–93.
66. Khan A, Ostaku J, Aras E, Ozgur U, Seker S. Combating Infectious Diseases with Synthetic Biology. 2022.
67. Carrigan SD, Scott G, Tabrizian M. Toward Resolving the Challenges of Sepsis Diagnosis. 2004; 1314: 1301–1314.
68. Wei T yen, Cheng C min. Minireview Diagnostics for Infectious Disease Minireview. Cell Chemical Biology. 2016; 23: 1056–1066.
69. Piuri M, Jr WRJ, Hatfull GF. Fluoromycobacteriophages for Rapid, Specific , and Sensitive Antibiotic Susceptibility Testing of Mycobacterium tuberculosis. 2009; 4.
70. Albert H, Trollip A, Seaman T, Mole RJ. Simple, phage-based (FASTPlaque) technology to determine rifampicin resistance of Mycobacterium tuberculosis directly from sputum. The International Journal of Tuberculosis and Lung Disease. 2004; 8: 1114–1119.
71. Sullivan KV, Turner NN, Roundtree SS, Mcgowan KL. Rapid Detection of Methicillin-Resistant Staphylococcus Staphylococcus aureus (MSSA) Using the KeyPath MRSA / MSSA Blood Culture Test and the BacT / ALERT System in a Pediatric Population. 2013; 137.
72. Pardee K, Green AA, Takahashi MK, Connor DHO, Gehrke L, et al. Rapid, Low-Cost Detection of Zika Virus Using Programmable Biomolecular Components Resource Rapid, Low-Cost Detection of Zika Virus Using Programmable Biomolecular Components. Cell. 2016; 1–12.
73. Hoang Trung Chau T, Hoang Anh Mai D, Ngoc Pham D, Thi Quynh Le H, Yeol Lee E. Developments of Riboswitches and Toehold Switches for Molecular Detection—Biosensing and Molecular Diagnostics. International Journal of Molecular Sciences. 2020; 21: 3192.
74. Principi N, Silvestri E, Esposito S. Advantages and Limitations of Bacteriophages for the Treatment of Bacterial Infections. 2019; 10: 1–9.
75. Lin DM, Koskella B, Lin HC, Lin DM, Lin HC, et al. Phage therapy: An alternative to antibiotics in the age of multi-drug resistance. 2017; 8: 162–173.
76. Usman SS, Uba AI, Christina E. Bacteriophage genome engineering for phage therapy to combat bacterial

antimicrobial resistance as an alternative to antibiotics. Mol Biol Rep. 2023; 50: 7055–7067.
77. Pei R, Lamas-samanamud GR. Inhibition of Biofilm Formation by T7 Bacteriophages Producing Quorum-Quenching Enzymes. 2014; 80: 5340–5348.
78. Hale V, Keasling JD, Renninger N, Diagana TT. Microbially Derived Artemisinin: A Biotechnology Solution to the Global Problem of Access to Affordable Antimalarial Drugs. 2007; 77: 198–202.
79. Huang Z, Tian D, Liu Y, Lin Z, Lyon CJ, et al. Since January 2020 Elsevier has created a COVID-19 resource centre with free information in English and Mandarin on the novel coronavirus COVID- 19. The COVID-19 resource centre is hosted on Elsevier Connect, the company's public news and information. 2020.
80. Ahan RE, Dinc B. SARS-CoV - 2 Detection with De Novo-Designed Synthetic Riboregulators. 2021.
81. Yan H, Sun J, Wang K, Wang H, Wu S, et al. Repurposing carrimycin as an antiviral agent against human coronaviruses, including the currently pandemic SARS-CoV-2. 2021; 11: 2850–2858.
82. Chung YH, Beiss V, Fiering SN, Steinmetz NF. COVID-19 Vaccine Frontrunners and Their Nanotechnology Design. 2020.
83. Therapeutics T, Pharmacology S, Therapeutics T, Therapeutics T. The Coming of Age of Nucleic Acid Vaccines during COVID-19. 2023.
84. Cliff J, Kaufmann S, McShane H, Helden P, O'Garra A. The human immune response to tuberculosis and its treatment: A view from the blood. Immunological Reviews. 2015; 264.
85. Centers US, Control D. Antibiotic Resistance Threats in the United States, 2019. 2019.
86. Pew T, Trusts C. Roadmap for Antibiotic Discovery. 2016.
87. Role TE, Synthesis C, Discovery AD. HHS Public Access. 2015; 53: 8840–8869.
88. Charest MG, Charest MG, Lerner CD, Brubaker JD, Siegel DR, et al. A Convergent Enantioselective Route to Structurally Diverse 6-Deoxytetracycline Antibiotics. 2012; 395.
89. Seiple IB, Zhang Z, Jakubec P, Langlois-mercier A, Peter M,

et al. HHS Public Access. 2019; 533: 338–345.
90. Li Q, Pellegrino J, Lee DJ, Tran AA, Chaires HA, et al. Synthetic group A streptogramin antibiotics that overcome Vat resistance. 2020.
91. Smith PA, Koehler MFT, Girgis HS, Yan D, Chen Y, et al. Optimized arylomycins are a new class of Gram-negative antibiotics. Nature. 2018.
92. Wilson DN. Ribosome-targeting antibiotics and mechanisms of bacterial resistance. Nature Publishing Group. 2014; 12: 35–48.
93. Schaffer L, Finkelstein J, Hohn A, Djerassi I. LINCOMYCIN--A NEW ANTIBIOTIC. Clin Pediatr (Phila). 1963: 2: 642-645.
94. Landauer R, Tonge EL, Wiley A, Rein RB, Wiley A, et al. Lincomycin. XI. Synthesis and structure of clindamycin. A potent antibacterial agent. J. Med. Chem. 1970; 13: 616–619.
95. Birkenmeyer RD, Kroll SJ, Lewis C, Stern KF, Zurenko GE. Synthesis and Antimicrobial Activity of Clindamycin Analogues: Pirlimycin,'p2 a Potent Antibacterial Agent. 1984; 216–223.
96. Hirai Y, Maebashi K, Yamada K, Wakiyama Y, Kumura K, et al. Characterization of compound A, a novel lincomycin derivative active against methicillin-resistant Staphylococcus aureus. The Journal of Antibiotics. 2020.
97. Mitcheltree MJ, Pisipati A, Syroegin EA, Silvestre KJ, Klepacki D, et al. A synthetic antibiotic class overcoming bacterial multidrug resistance. 2021; 599.
98. Toh S ming, Xiong L, Arias CA, Villegas M V, Lolans K, et al. Acquisition of a natural resistance gene renders a clinical strain of methicillin-resistant Staphylococcus aureus resistant to the synthetic antibiotic linezolid. 2007; 64: 1506–1514.
99. Smith LK, Mankin AS. Transcriptional and Translational Control of the mlr Operon, Which Confers Resistance to Seven Classes of Protein Synthesis Inhibitors . 2008; 52: 1703–1712.
100. Crowe-mcauliffe C, Murina V, Turnbull KJ, Kasari M, Mohamad M, et al. Structural basis of ABCF-mediated resistance to. Nature Communications. 2021.
101. Khameneh B, Iranshahy M, Ghandadi M, Atashbeyk DG. Investigation of the antibacterial activity and efflux

pump inhibitory effect of co-loaded piperine and gentamicin nanoliposomes in methicillin-resistant Staphylococcus aureus. 2014; 9045: 1–6.
102. Sedigheh B, Bazzaz F, Khameneh B, Reza M, Ostad Z, et al. In vitro evaluation of antibacterial activity of verbascoside, lemon verbena extract and caffeine in combination with gentamicin against drug- resistant Staphylococcus aureus and Escherichia coli clinical isolates. 2018; 8: 246–253.
103. Siriwong S, Thumanu K, Hengpratom T, Eumkeb G. Synergy and Mode of Action of Ceftazidime plus Quercetin or Luteolin on Streptococcus pyogenes. 2015; 2015.
104. Yan Y, Li X, Zhang C, Lv L, Gao B, et al. Research Progress on Antibacterial Activities and Mechanisms of Natural Alkaloids: A Review. 2021.
105. Porras G, Lyles JT, Marquez L, Dettweiler M, Salam AM, et al. Ethnobotany and the Role of Plant Natural Products in Antibiotic Drug Discovery. Chem. Rev. 2021; 121: 3495–3560.
106. Boberek JM, Stach J, Good L. Genetic Evidence for Inhibition of Bacterial Division Protein FtsZ by Berberine. 2010; 5: 1–9.
107. Yi Z biao, Yu Y, Liang Y zeng, Zeng B. Evaluation of the antimicrobial mode of berberine by LC / ESI-MS combined with principal component analysis. 2007; 44: 301–304.
108. Dwivedi GR, Maurya A, Yadav DK. Synergy of clavine alkaloid ‘ chanoclavine ’ with tetracycline against multi drug resistant E . coli Synergy of clavine alkaloid ‘ chanoclavine ’ with tetracycline against multi drug resistant E . coli. Vol. 1102, Journal of Biomolecular Structure and Dynamics. Oxfordshire: Taylor & Francis. 2018; 1–47.
109. Buckner MMC, Ciusa ML, Piddock LJ V. Strategies to combat antimicrobial resistance: anti-plasmid and plasmid curing. 2018.
110. Shriram V, Jahagirdar S, Latha C, Kumar V, Puranik V, et al. International Journal of Antimicrobial Agents A potential plasmid-curing agent, 8-epidiosbulbin E acetate, from Dioscorea bulbifera L. against multidrug-resistant bacteria. 2008; 32: 405–410.
111. Guay I, Boulanger S, Isabelle C, Brouillette E, Chagnon

F, et al. Tomatidine and analog FC04 – 100 possess bactericidal activities against Listeria, Bacillus and Staphylococcus spp. 2018; 1–12.
112. Reiter J, Levina N, Linden M Van Der, Gruhlke M, Martin C, et al. Diallylthiosulfinate (Allicin), a Volatile Antimicrobial from Garlic (Allium sativum), Kills Human Lung Pathogenic Bacteria, Including MDR Strains, as a Vapor. 2017; 22: 1–14.
113. J Sharifi-Rad, Sm Hoseini Alfatemi, M Sharifi Rad, M Iriti. Antimicrobial Synergic Effect of Allicin and Silver Nanoparticles on Skin Infection Caused by Methicillin - Resistant Staphylococcus aureus spp. Ann Med Health Sci Res. 2014; 4: 863-868.
114. Li J, Koh J jie, Liu S, Lakshminarayanan R, Conlon JM. Membrane Active Antimicrobial Peptides: Translating Mechanistic Insights to Design. 2017; 11: 1–18.
115. Perveen S. Introductory Introductory Chapter: Chapter: Terpenes Terpenes and and Terpenoids Terpenoids. 2018; 1–12.
116. Yu Z, Tang J, Khare T, Kumar V. The alarming antimicrobial resistance in ESKAPEE pathogens: Can essential oils come to the rescue? Fitoterapia. 2019; 104433.
117. Cox SD, Mann CM, Markham JL, Bell HC, Gustafson JE, et al. The mode of antimicrobial action of the essential oil of Melaleuca alternifolia (tea tree oil). 2000; 170–175.
118. Taylor P, Togashi N, Hamashima H. Antibacterial Activities Against Staphylococcus aureus of Terpene Alcohols With Aliphatic Carbon Antibacterial Activities Against Staphylococcus aureus of Terpene Alcohols With Aliphatic Carbon Chains. 2010; 37–41.
119. Jarosław B. Comprehensive review of antimicrobial activities of plant flavonoids. 2018.
120. Budzy A, Ró M, Karolczak W. Synthetic 3-Arylidenefl avanones as Inhibitors of the Initial Stages of Biofi lm Formation by Staphylococcus aureus and Enterococcus faecalis. 2011.
121. Interests CF. Synergies between synthetic biology and metabolic engineering. 2011; 29.
122. Nadeem M, Rikhari HC, Kumar A, Palni LMS, Nandi SK. Taxol content in the bark of Himalayan Yew in relation

to tree age and sex. Phytochemistry. 2002; 60: 627–631.
123. Paddon CJ, Westfall PJ, Pitera DJ, Benjamin K, Fisher K, et al. High-level semi-synthetic production of the potent antimalarial artemisinin. Nature. 2013; 496: 528–532.
124. Banek K, Lalani M, Staedke SG, Chandramohan D. Adherence to artemisinin-based combination therapy for the treatment of malaria: a systematic review of the evidence Adherence to artemisinin-based combination therapy for the treatment of malaria: a systematic review of the evidence. 2014.
125. Lu X, Shen Q, Zhang L, Zhang F, Jiang W, et al. Promotion of artemisinin biosynthesis in transgenic Artemisia annua by overexpressing ADS, CYP71AV1 and CPR genes. 2013; 49: 380–385.
126. Ma D ming, Wang Z, Wang L, Alejos-gonzales F, Sun M an, et al. SC. MOLECULAR PLANT. 2015.
127. Zainul M, Pravej A. Genetic engineering of artemisinin biosynthesis: prospects to improve its production. 2015; 37.
128. Mannan A, Liu C, Arsenault P, Towler M, Vail D, et al. DMSO triggers the generation of ROS leading to an increase in artemisinin and dihydroartemisinic acid in Artemisia annua shoot cultures. Plant cell reports. 2010; 29: 143–152.
129. Westfall PJ, Pitera DJ, Lenihan JR, Eng D, Woolard FX, et al. Production of amorphadiene in yeast , and its conversion to dihydroartemisinic acid , precursor to the antimalarial agent artemisinin. 2012; 109: 111–118.
130. Table S. High-level semi-synthetic production of the potent antimalarial artemisinin. 2010.
131. Sy L king, Brown GD. The mechanism of the spontaneous autoxidation of dihydroartemisinic acid. 2002; 58.
132. Lv Z, Zhang F, Pan Q, Fu X, Jiang W, et al. Branch Pathway Blocking in Artemisia annua is a Useful Method for Obtaining High Yield Artemisinin. 2016; 1–15.
133. Kistler HC, Broz K, Schäfer W. Cellular compartmentalization of secondary metabolism. 2015; 6: 1–11.
134. Wang B qing. Salvia miltiorrhiza : Chemical and pharmacological review of a medicinal plant. Journal of Medicinal Plants Research. 2010; 4: 2813–2820.

135. Munagala R, Aqil F, Jeyabalan J, Gupta RC. apoptosis and inhibition of cervical cancer. Cancer Letters. 2014.
136. Yu Q, Chen H, Sheng L, Liang Y, Li Q. International Immunopharmacology Sodium tanshinone IIA sulfonate prolongs the survival of skin allografts by inhibiting inflammatory cell in fi ltration and T cell proliferation. International Immunopharmacology. 2014; 22: 277–284.
137. Wang H, Zhong L, Mi S, Song N, Zhang W, et al. Tanshinone IIA prevents platelet activation and down-regulates CD36 and MKK4/JNK2 signaling pathway. BMC Cardiovascular Disorders. 2020; 20: 81.
138. Zhou YJ, Gao W, Rong Q, Jin G, Chu H, et al. Modular Pathway Engineering of Diterpenoid Synthases and the Mevalonic Acid Pathway for Miltiradiene Production. 2012.
139. Dai Z, Liu Y, Huang L, Zhang X. Production of Miltiradiene by Metabolically Engineered Saccharomyces cerevisiae. 2012; 100: 1–9.
140. Hu T, Zhou J, Tong Y, Su P, Li X, et al. Engineering chimeric diterpene synthases and isoprenoid biosynthetic pathways enables high-level production of miltiradiene in yeast. Metabolic Engineering. 2020.
141. Li Y, Zhang G, Pfeifer BA. Current and Emerging Options for Taxol Production. 2014.
142. Schoendorf A, Rithner CD, Williams RM, Croteau RB. Molecular cloning of a cytochrome P450 taxane 10 ␣ - hydroxylase cDNA from Taxus and functional expression in yeast. 2001; 98: 10–15.
143. Liu WC, Gong T, Zhu P. RSC Advances Advances in exploring alternative Taxol sources. RSC Advances. 2016; 6: 48800–48809.
144. Jin Y, Coates RM, Croteau R, Christianson DW, Ko M. Taxadiene synthase structure and evolution of modular architecture in terpene biosynthesis. 2011.
145. Croteau R, Ketchum REB, Long RM, Wildung MR. Taxol biosynthesis and molecular genetics. 2006; 75–97.
146. Howat S, Park B, Oh IS, Jin Y woo, Lee E kyong, Loake GJ. Paclitaxel: biosynthesis, production and future prospects. New BIOTECHNOLOGY. 2014; 31: 242–245.
147. Engels B, Dahm P, Jennewein S. Metabolic engineering of taxadiene biosynthesis in yeast as a first step towards

Taxol (Paclitaxel) production. 2008; 10: 201–206.
148. Gallup O, Ming H, Ellis T. Ten future challenges for synthetic biology. Engineering Biology. 2021; 5: 51–59.
149. Keatley KL. controversy over genetically modified organisms: the governing laws and regulations organisms: the governing laws and. 2016; 9411.
150. Sheahan T, Wieden H joachim. Emerging regulatory challenges of next-generation synthetic. 2021; 771: 766–771.
151. Hecko S, Schiefer A, Badenhorst CPS, Fink MJ, Mihovilovic MD, et al. Enlightening the Path to Protein Engineering: Chemoselective Turn- On Probes for High-Throughput Screening of Enzymatic Activity. 2023.
152. Teixeira AP, Fussenegger M. ScienceDirect Engineering mammalian cells for disease diagnosis and treatment. Current Opinion in Biotechnology. 2019; 55: 87–94.
153. Cardinale S, Arkin AP. Contextualizing context for synthetic biology – identifying causes of failure of synthetic biological systems. Biotechnology Journal. 2012.
154. Hanahan D, Weinberg RA. Review Hallmarks of Cancer: The Next Generation. Cell. 2011; 144: 646–674.
155. Hooshangi S, Thiberge S, Weiss R. Ultrasensitivity and noise propagation in a synthetic transcriptional cascade. 2005; 2005: 1–6.
156. Potvin-trottier L, Lord ND, Vinnicombe G, Paulsson J, Biology C. HHS Public Access. 2017; 538: 514–517.
157. Karoui M El, Hoyos-flight M, Fletcher L. Future Trends in Synthetic Biology — A Report. 2019; 7: 1–8.

The book Immunology and Cancer Biology cover topics from different fields in Immunology and Cancer.

VIDE LEAF

E-book Available
@
www.videleaf.com